SECOND EDITION

CAPNOGRAPHY

EDITED BY
J. S. Gravenstein
Michael B. Jaffe
Nikolaus Gravenstein
David A. Paulus

CAMBRIDGE Medicine

CAMBRIDGE www.cambridge.org/9780521514781

This page intentionally left blank

Capnography

Second Edition

Capnography

Second Edition

Edited by

J. S. Gravenstein, MD
Formerly Graduate Research Professor, Emeritus, Department of Anesthesiology, University of Florida College of Medicine, Gainesville, FL, USA

Michael B. Jaffe, PhD
Biomedical Engineer, Advanced Development, Philips Healthcare, Wallingford, CT, USA

Nikolaus Gravenstein, MD
Jerome H. Modell Professor of Anesthesiology and Professor of Neurosurgery, Department of Anesthesiology, University of Florida College of Medicine, Gainesville, FL, USA

David A. Paulus, MD
Professor, Department of Anesthesiology, University of Florida College of Medicine; Professor, Department of Mechanical Engineering, University of Florida College of Engineering, Gainesville, FL, USA

CAMBRIDGE
UNIVERSITY PRESS

CAMBRIDGE UNIVERSITY PRESS
Cambridge, New York, Melbourne, Madrid, Cape Town,
Singapore, São Paulo, Delhi, Tokyo, Mexico City

Cambridge University Press
The Edinburgh Building, Cambridge CB2 8RU, UK

Published in the United States of America by Cambridge University Press, New York

www.cambridge.org
Information on this title: www.cambridge.org/9780521514781

© Cambridge University Press 2004, 2011

This publication is in copyright. Subject to statutory exception
and to the provisions of relevant collective licensing agreements,
no reproduction of any part may take place without the written
permission of Cambridge University Press.

First Edition published by Cambridge University Press 2004
Second Edition published 2011

Printed in the United Kingdom at the University Press, Cambridge

A catalog record for this publication is available from the British Library

Library of Congress Cataloging in Publication data
Capnography / [edited by] J.S. Gravenstein ... [et al.]. – 2nd ed.
p. ; cm.
Includes bibliographical references and index.
ISBN 978-0-521-51478-1 (hardback)
1. Respiratory gas monitoring. 2. Capnography. I. Gravenstein, J. S. II. Title.
[DNLM: 1. Capnography. 2. Anesthesia. 3. Carbon Dioxide – physiology.
4. Respiration, Artificial. WF 141.5.C2]
RD52.R47C36 2011
617.9′62–dc22 2010042839

ISBN 978-0-521-514781 Hardback

Cambridge University Press has no responsibility for the persistence or
accuracy of URLs for external or third-party internet websites referred to in
this publication, and does not guarantee that any content on such websites is,
or will remain, accurate or appropriate.

Every effort has been made in preparing this book to provide accurate and up-to-date
information which is in accord with accepted standards and practice at the time of publication.
Although case histories are drawn from actual cases, every effort has been made to disguise the
identities of the individuals involved. Nevertheless, the authors, editors, and publishers can make no
warranties that the information contained herein is totally free from error, not least because clinical
standards are constantly changing through research and regulation. The authors, editors, and
publishers therefore disclaim all liability for direct or consequential damages resulting from the use
of material contained in this book. Readers are strongly advised to pay careful attention
to information provided by the manufacturer of any drugs or equipment that they plan to use.

Contents

List of contributors *page* ix
Preface xiii
Commonly used abbreviations xiv

1 **Clinical perspectives** 1
J. S. Gravenstein

Section 1 Ventilation

2 **Capnography and respiratory assessment outside of the operating room** 11
R. R. Kirby

3 **Airway management in the out-of-hospital setting** 19
C. C. Zuver, G. A. Ralls, S. Silvestri, and J. L. Falk

4 **Airway management in the hospital setting** 32
A. G. Vinayak and J. D. Truwit

5 **Airway management in the operating room** 37
D. G. Bjoraker

6 **Capnography during anesthesia** 43
Y. G. Peng, D. A. Paulus, and J. S. Gravenstein

7 **Monitoring during mechanical ventilation** 54
J. Thompson and N. Craig

8 **Capnography during transport of patients (inter/intrahospital)** 63
M. A. Frakes

9 **Capnography as a guide to ventilation in the field** 72
D. P. Davis

10 **Neonatal monitoring** 80
G. Schmalisch

11 **Capnography in sleep medicine** 96
P. Troy and G. Gilmartin

12 **Conscious sedation** 102
E. A. Bowe and E. F. Klein, Jr.

13 **Capnometry monitoring in high- and low-pressure environments** 115
C. W. Peters, G. H. Adkisson, M. S. Ozcan, and T. J. Gallagher

14 **Biofeedback** 127
A. E. Meuret

15 **Capnography in non-invasive positive pressure ventilation** 135
J. A. Orr, M. B. Jaffe, and A. Seiver

16 **End-tidal carbon dioxide monitoring in postoperative ventilator weaning** 145
J. Varon and P. E. Marik

17 **Optimizing the use of mechanical ventilation and minimizing its requirement with capnography** 148
I. M. Cheifetz and D. Hamel

18 **Volumetric capnography for monitoring lung recruitment and PEEP titration** 160
G. Tusman, S. H. Böhm, and F. Suarez-Sipmann

19 **Capnography and adjuncts of mechanical ventilation** 169
U. Lucangelo, F. Bernabè, and L. Blanch

Section 2 Circulation, metabolism, and organ effects

20 Cardiopulmonary resuscitation 185
D. C. Cone, J. C. Cahill, and M. A. Wayne

21 Capnography and pulmonary embolism 195
J. T. Anderson

22 Non-invasive cardiac output via pulmonary blood flow 208
R. Dueck

23 $PaCO_2$, $P_{ET}CO_2$, and gradient 225
J. B. Downs

24 The physiologic basis for capnometric monitoring in shock 231
K. R. Ward

25 Carbon dioxide production, metabolism, and anesthesia 239
D. Willner and C. Weissman

26 Tissue- and organ-specific effects of carbon dioxide 250
O. Akça

Section 3 Special environments/ populations

27 Atmospheric monitoring outside the healthcare environment and within enclosed environments: a historical perspective 261
G. H. Adkisson and D. A. Paulus

28 Capnography in veterinary medicine 272
R. M. Bednarski and W. Muir

Section 4 Physiologic perspectives

29 Carbon dioxide pathophysiology 283
T. E. Morey

30 Acid–base balance and diagnosis of disorders 295
P. G. Boysen and A. V. Isenberg

31 Ventilation/perfusion abnormalities and capnography 313
N. Al Rawas, A. J. Layon, and A. Gabrielli

32 Capnographic measures 329
U. Lucangelo, A. Gullo, F. Bernabè, and L. Blanch

33 Improving the analysis of volumetric capnograms 340
G. Tusman, A. G. Scandurra, E. Maldonado, and L. I. Passoni

34 Capnography and the single-path model applied to cardiac output recovery and airway structure and function 347
P. W. Scherer, J. W. Huang, and K. Zhao

35 Carbon dioxide and the control of breathing: a quantitative approach 360
M. C. K. Khoo

Section 5 Technical perspectives

36 Technical specifications and standards 373
D. E. Supkis

37 Carbon dioxide measurement 381
M. B. Jaffe

38 Gas flow measurement 397
M. B. Jaffe

39 Combining flow and carbon dioxide 407
J. A. Orr and M. B. Jaffe

Section 6 Historical perspectives

40 Brief history of time and volumetric capnography 415
M. B. Jaffe

41 The first years of clinical capnography 430
B. Smalhout

42 The early days of volumetric capnography 457
R. Fletcher

Appendix: Patterns of time-based capnograms 461
Index 466

Contributors

Gregory H. Adkisson, MD
(Capt USN MC Retired)
Assistant Professor of Anesthesiology, New York Medical College; Director of Perioperative Services, Westchester Medical Center and Maria Fareri Children's Hospital, Valhalla, NY, USA

Ozan Akça, MD
Director of Research and Associate Professor, Department of Anesthesiology and Perioperative Medicine, Neuroscience and Anesthesia ICU, University of Louisville and Outcomes Research Consortium, Louisville, KY, USA

Nawar Al-Rawas, MD
Clinical Research Fellow, Department of Anesthesiology, Division of Critical Care Medicine, University of Florida College of Medicine, Gainesville, FL, USA

John T. Anderson, MD
Clinical Professor of Surgery, Department of Surgery, University of California–Davis, Medical Center, Sacramento, CA, USA

Richard M. Bednarski, DVM, MS, Dipl. ACVA
Associate Professor, Department of Veterinary Clinical Sciences, The Ohio State University Veterinary Medical Center, Columbus, OH, USA

Francesca Bernabè, MD
Medical Doctor in Anesthesia and Intensive Care, Department of Perioperative Medicine, Intensive Care and Emergency Medicine, Trieste University School of Medicine, Italy

David G. Bjoraker, MD
Associate Professor of Anesthesiology, University of Florida College of Medicine, Gainesville, FL, USA

Lluis Blanch, MD, PhD
Senior, Critical Care Center, Hospital de Sabadell, Sabadell, Spain

Stephan H. Böhm, MD
Medical Director, Medical Sensors, Research Centre for Nanomedicine, CSEM Nanomedicine Division, Landquart, Switzerland

Edwin A. Bowe, MD
Professor and Chair, Department of Anesthesiology, University of Kentucky College of Medicine, Lexington, KY, USA

Philip G. Boysen, MD, MBA, FACP, FCCP, FCCM
Professor of Anesthesiology and Medicine; Executive Associate Dean for Graduate Medical Education, UNC School of Medicine, The University of North Carolina at Chapel Hill, NC, USA

Justin C. Cahill, MD, FACEP
Emergency Services, Bridgeport Hospital, Bridgeport, CT, USA

Ira M. Cheifetz, MD, FCCM, FAARC
Professor of Pediatrics; Chief, Pediatric Critical Care Medicine; Medical Director, Pediatric Intensive Care Unit; Medical Director, Pediatric Respiratory Care and ECMO Program; Fellowship Director, Pediatric Critical Care Medicine, Duke Children's Hospital, Durham, NC, USA

David C. Cone, MD
EMS Section Chief, Yale Emergency Medicine, Yale University School of Medicine, New Haven CT, USA; Editor-in-Chief, *Academic Emergency Medicine*, Des Plains, IL, USA

Nancy Craig, RRT
Supervisor, Respiratory Care, Children's Hospital, Boston, MA, USA

Daniel P. Davis, MD
Professor of Clinical Medicine, Department of Emergency Medicine, University of California–San Diego, San Diego, CA, USA

John B. Downs, MD
Professor of Anesthesiology, University of Florida College of Medicine, Gainesville, FL, USA; Professor Emeritus of Anesthesiology and Critical Care Medicine, University of South Florida, Tampa, FL, USA

Ronald Dueck, MD
Clinical Professor of Anesthesiology, University of California–San Diego and Veterans Affairs San Diego Healthcare System, San Diego, CA, USA

Jay L. Falk, MD, FCCM, FACEP
Vice President, Medical Education, Orlando Health; Clinical Professor, Clinical Sciences, University of Central Florida College of Medicine, Orlando, and Florida State University College of Medicine, Tallahassee; Clinical Professor, Medicine and Emergency Medicine, University of Florida College of Medicine, Gainesville, FL, USA

Roger Fletcher, MD, FRCA
Former Honorary Lecturer, Department of Anaesthesia, University Hospital, Lund, Sweden; Formerly at the Department of Anaesthesia, Manchester Royal Infirmary, Manchester, England

Michael A. Frakes, APRN, MS, CCNS, CFRN, EMTP
Clinical Nurse Specialist, Boston MedFlight, Bedford, MA, USA

Andrea Gabrielli, MD, FCCM
Professor of Anesthesiology and Surgery, Division of Critical Care Medicine; Section Head, NeuroCritical Care, University of Florida College of Medicine; Medical Director, Cardiopulmonary Service and Hyperbaric Medicine, Shands Hospital at the University of Florida, Gainesville, FL, USA

Thomas J. Gallagher, MD
Professor, Departments of Anesthesiology and Surgery, University of Florida College of Medicine, Gainesville, FL, USA

Geoff Gilmartin, MD
Instructor in Medicine, Harvard Medical School; Clinical Director, Sleep Disorders Center, Department of Medicine, Division of Pulmonary, Critical Care, and Sleep Medicine, Beth Israel Deaconess Medical Center, Boston, MA, USA

J. S. Gravenstein, MD
Formerly Graduate Research Professor, Emeritus, Department of Anesthesiology, University of Florida College of Medicine, Gainesville, FL, USA

Antonino Gullo, MD
Full Professor in Intensive Care; Head, Department and School of Anesthesia and Intensive Care, Catania University Hospital, Catania, Italy

Donna Hamel, RRT, RCP, FCCM, FAARC
Clinical Research Coordinator, Duke Clinical Research Unit, Duke University Medical Center, Durham, North Carolina, USA

John W. Huang, PhD
Hillsborough, CA, USA; formerly with Draeger Medical Systems

Amy V. Isenberg, MD
Anesthesiology Specialist, Wilmington, NC, USA

Michael B. Jaffe, PhD
Biomedical Engineer, Advanced Development, Philips Healthcare, Wallingford, CT, USA

Michael C. K. Khoo, PhD
Professor of Biomedical Engineering and Pediatrics, Dwight C. and Hildagarde E. Baum Chair of Biomedical Engineering, University of Southern California, Los Angeles, CA, USA

Robert R. Kirby, MD
Professor Emeritus of Anesthesiology, University of Florida College of Medicine, Gainesville, FL, USA

E. F. Klein, Jr., MD, FCCM
Professor Emeritus, Department of Anesthesiology, University of Arkansas for Medical Sciences, Little Rock, AR, USA

A. Joseph Layon, MD, FACP
Professor of Anesthesiology, Surgery, and Medicine and Chief, Division of Critical Care Medicine, University of Florida College of Medicine; Medical Director, Gainesville Fire Rescue Service, Gainesville, FL, USA

Umberto Lucangelo, MD
Assistant Professor in Anesthesia and Intensive Care, Dipartimento di Medicina Perioperatoria, Terapia, Intensiva ed Emergenza, Ospedale di Cattinara, Trieste, Italy; Critical Care Center, CIBER Enfermedades Respiratorias, Hospital de Sabadell, Corporacio Parc Tauli, Institut Universitari Fundacio Parc Tauli, Universitat Autónoma de Barcelona, Sabadell, Spain

Emilio Maldonado, Eng
Bioengineering Laboratory, Department of Electronics, Mar del Plata University, Mar del Plata, Argentina

Paul E. Marik, MD
Chief of Pulmonary and Critical Care Medicine, Eastern Virginia Medical School, Norfolk, VA, USA

Alicia E. Meuret, PhD
Assistant Professor of Psychology, Department of Psychology, Southern Methodist University, Dallas, TX, USA

Timothy E. Morey, MD
Professor of Anesthesiology and Executive Associate Chair, Department of Anesthesiology, University of Florida College of Medicine, Gainesville, FL, USA

William Muir, DVM, PhD, ACVA, ACVECC
Chief Medical Officer, The Animal Medical Center, New York, NY, USA

Joseph A. Orr, PhD
Research Associate Professor, Department of Anesthesiology, University of Utah, School of Medicine, Salt Lake City, UT, USA

Mehmet S. Ozcan
Department of Anesthesiology, University of Oklahoma College of Medicine, Oklahoma, OK, USA

Lucía Isabel Passoni, PhD, Eng
Associate Professor, Bioengineering Laboratory, Department of Electronics, National University of Mar del Plata, Buenos Aires, Argentina

David A. Paulus, MD
Professor, Department of Anesthesiology, University of Florida College of Medicine; Professor, Department of Mechanical Engineering, University of Florida College of Engineering, Gainesville, FL, USA

Yong G. Peng, MD, PhD
Associate Professor of Anesthesiology and Surgery and Director, Cardiothoracic Anesthesia Fellowship Program and Perioperative Transesophageal Echocardiography, Shands Hospital at the University of Florida, Gainesville, FL, USA

Carl W. Peters, MD
Clinical Associate Professor of Anesthesiology and Surgery, Department of Anesthesiology, University of Florida College of Medicine, Gainesville, FL, USA

George A. Ralls, MD, FACEP
Director, Orange County Health Services; Medical Director, Orange County EMS System, Orlando, FL, USA

Adriana G. Scandurra, Eng
Assistant Professor, Bioengineering Laboratory, Department of Electronics, National University of Mar del Plata, Buenos Aires, Argentina

Peter W. Scherer, MD, PhD
Emeritus Professor of Bioengineering; Member, Monell Chemical Senses Center, University of Pennsylvania, School of Engineering and Applied Science, Philadelphia, PA, USA

Gerd Schmalisch, Priv.-Doz., Dr. sc.nat., PhD
Clinic of Neonatology, Charité-Universitätsmedizin Berlin, Berlin, Germany

Adam Seiver, MD, PhD, MBA
Senior Director and Chief Medical Officer, Hospital Respiratory Care, Philips Healthcare; Consulting Associate Professor of Management Science and Engineering, Stanford University, Stanford, CA, USA; Medical Director, Critical Care Telemedicine Program, Sutter Health System, Sacramento, CA, USA

Salvatore Silvestri, MD, FACEP
Program Director, Emergency Medicine Residency, Orlando Regional Medical Center; Associate Professor, Emergency Medicine, University of Central Florida College of Medicine, Orlando, FL, USA; Associate EMS Medical Director, Orange County EMS System, Orlando, FL, USA

Bob Smalhout, MD, PhD
Anaesthesiologist–bronchoscopist, medical adviser/airway problems, Bosch en Duin, Holland

Fernando Suarez-Sipmann, MD, PhD
Department of Critical Care, Servicio de Medicina Intensiva, Fundación Jiménez Díaz-UTE, Madrid, Spain

Daniel E. Supkis, MD
Medical Director, Anesthesia Preoperative Evaluation Clinic, The Methodist Hospital, Houston, TX, USA

John Thompson, RRT, FAARC
Director of Clinical Technology, Children's Hospital, Boston; Associate in Anesthesia, Harvard Medical School, Boston, MA, USA

Patrick Troy, MD
Pulmonary and Critical Care Unit, Department of Medicine, Division of Pulmonary and Critical Care, Massachusetts General Hospital, Boston, MA, USA

Jonathon D. Truwit, MD, MBA
E. Cato Drash Associate Professor; Senior Associate Dean for Clinical Affairs; Chief Medical Officer; Chief, Pulmonary and Critical Care Medicine, University of Virginia Health Systems, Charlottesville, VA, USA

Gerardo Tusman, MD
Department of Anesthesiology, Hospital Privado de Comunidad, Mar del Plata, Buenos Aires, Argentina

Joseph Varon, MD, FACP, FCCP, FCCM
Clinical Professor of Medicine, The University of Texas Health Science Center, Houston;
Clinical Professor of Medicine, The University of Texas Medical Branch at Galveston; Professor of Acute and Continuing Care, The University of Texas, Houston, TX, USA

Ajeet G. Vinayak, MD
Assistant Professor of Medicine, Georgetown University Hospital, Washington, DC, USA

Kevin R. Ward, MD
Associate Professor of Emergency Medicine, Physiology, and Biochemistry;
Director of Research, Department of Emergency Medicine; Senior Fellow, VCURES, Virginia Commonwealth University, Richmond, VA, USA

Marvin A. Wayne, MD, FACEP, FAAEM
Associate Clinical Professor, University of Washington School of Medicine; EMS Medical Program Director, Bellingham/Whatcom County; Attending Physician, Emergency Department, St. Joseph Hospital, Bellingham, WA, USA

Charles Weissman, MD
Professor and Chairman, Department of Anesthesiology and Critical Care Medicine, Hadassah-Hebrew University Medical Centers, Hebrew University-Hadassah School of Medicine, Jerusalem, Israel

Dafna Willner, MD
Attending, Department of Anesthesiology and Critical Care Medicine, Hassadah-Hebrew University Medical Center; Instructor, Hebrew University-Hassadah School of Medicine, Jerusalem, Israel

Kai Zhao, PhD
Assistant Member, Monell Chemical Senses Center; Adjunct Assistant Professor of Otolaryngology, Thomas Jefferson University Medical College, Philadelphia, PA, USA

Christian C. Zuver, MD
Medical Director, Dane County ALS System; Assistant Professor of Medicine, Division of Emergency Medicine, University of Wisconsin School of Medicine and Public Health, Madison, WI, USA

Preface

This book explores carbon dioxide physiology, monitoring, and its operative as well as non-operative applications. In this text, we have considered both applications in which capnography has gained a foothold, and is fast becoming a standard of care, and its use in newer, emerging applications. The diversity contained within this edition calls for wide-ranging expertise. We were fortunate to have persuaded over 40 specialists to chronicle their findings in utilizing capnography in essays that we believe could each stand as independent reports. As a consequence, this book may seem, in some respects, more of a symposium than a textbook on the application of capnography in healthcare. For the reader's comfort, we have accepted some overlap and repetition. Differences in perspectives, inherent in the backgrounds of the contributing authors, have also been allowed. We are particularly pleased with the historical section of the book, in which unique contributions from some of the pioneers of capnography offer personal accounts and experiences.

In the last few years since the publication of the first edition, we have seen expansion in the recognition of capnography's value and its applications. For the second edition, we have endeavored to update the first edition to reflect this evolution. Most chapters have been revised, and several have been completely rewritten. We have also added chapters to fill gaps identified in the first edition and to explore additional emerging and noteworthy applications. The basic organization of the text remains the same as envisioned by J. S. Gravenstein who passed away after an extended illness during the preparation of this edition. While the first edition was being generated, he explained how he viewed carbon dioxide in such a clear and wonderful context that we readily adopted that organization for the clinical section of the text.

> *CO_2 has four stories to tell: The first, starting from the outside, deals with the adequacy of breathing (and the occasional problem of rebreathing), that is, with the transport of the gas from within the body to the outside. The next story has to do with transport of CO_2 in the body, bringing the gas to the lungs, which is dealing with the circulation and particularly with pulmonary blood flow. It includes the business of how CO_2 is transported in the blood. The third story has to do with the production of CO_2, which has to do with metabolism and temperature. The fourth story deals with the effects of CO_2 itself on the body, where it not only drives the respiratory system, but can produce mischief by changing the pH, blood flow to the brain, and affecting the lungs.*

We will always remember J. S. for his wisdom, insightful advice, humor, and, most of all, his friendship.

M. B. Jaffe
N. Gravenstein
D. A. Paulus

We would like to express our gratitude to Hope Olivo, Editor in the Department of Anesthesiology at the University of Florida College of Medicine, whose invaluable assistance allowed the editors and contributors to complete this second edition in a timely manner.

Commonly used abbreviations

CaO_2	Oxygen concentration, arterial
C_L	Lung compliance
F_ECO_2	Fractional concentration of carbon dioxide in expired gas
FEV	Forced expiratory volume
FEV_1	Forced expiratory volume in 1 second; forced expiratory volume in the first second
FiO_2	Fraction of inspired oxygen
FRC	Functional residual capacity
FVC	Forced vital capacity
$PaCO_2$	Partial pressure of carbon dioxide in arterial blood
P_ACO_2	Partial pressure of carbon dioxide in alveolar gas
P_AO_2	Partial pressure of oxygen in the alveoli
$P_AO_2–PaO_2$	Alveolar–arterial difference in partial pressure of oxygen
P_B	Barometric pressure
$P_{E_{max}}$	Maximum expiratory pressure
$P_{ET}CO_2$	Partial pressure of carbon dioxide at end-tidal
$P_{I_{max}}$	Maximum inspiratory pressure
$P\bar{v}O_2$	Partial pressure of oxygen, mixed venous
R_{aw}	Airway resistance
TLC	Total lung capacity
V_A	Alveolar ventilation
VC	Vital capacity
$\dot{V}_E$	Expired volume per unit time
$\dot{V}O_2$	Oxygen consumption per unit time
$\dot{V}O_{2max}$	Maximum oxygen consumption
V_T	Tidal volume
$\dot{V}/\dot{Q}$	Ventilation–perfusion ratio

Chapter 1

Clinical perspectives

J. S. Gravenstein

Introduction

Unless you are on cardiopulmonary bypass or in deep hypothermia, you must breathe, that is, you must ventilate your lungs to pick up oxygen and deliver carbon dioxide (CO_2) from the lungs to the outside. The detection – breath after breath – of appropriate volumes of gas and concentrations of CO_2 in the exhaled gas (it is no longer air!) proves, in one stroke, several important facts:

- CO_2 is being generated by metabolic processes during which the body utilizes oxygen.
- Venous blood brings the CO_2 from the periphery to the heart.
- The heart pumps blood through the lungs.
- Ventilation of the lungs – spontaneous, manual, or mechanical – conveys the CO_2 and other gases to the outside. As long as no contrivance, such as a ventilator, is attached to the patient, the journey of CO_2 ends here as far as we are concerned.

Subsequent chapters in this book will deal in detail with CO_2 production, transport, and analysis. In this chapter, we will examine different time- and volume-based capnograms, and invite the reader to analyze them with a clinical eye, with a special focus on problems related to ventilation – by far the most common clinical application of capnography.

First a word of caution: a capnogram, whether time- or volume-based, presents only a snapshot. Even a trend plot running over several minutes represents but a brief episode in a phase of a patient's disease. More often than not, capnography is recruited to help with the diagnosis and interpretation of an acute process (intubation, embolism, bronchospasm, adjustment of ventilation, bicarbonate infusion, etc.). The body has uncounted mechanisms to compensate for disturbances. These corrective efforts overlap, and are accomplished at different speeds, some taking a few breaths and others days to reach a new equilibrium. They can affect cardiac output, pulmonary blood flow, ventilation, acid–base balance, and renal physiology. When capnographic data during such unsteady states are observed, we must be aware of the fact that capnography can tell only a small part of the story and that the data in front of us are likely to change until a new steady state has been reached.

The normal time-based capnogram

For many years, the only widely available capnographic display plotted PCO_2 along a time axis. The phases were labeled in different ways, as shown in Figures AP1 and AP2 (page 462).

Time-based capnography can use either an on-airway (or "mainstream") method, which uses a cuvette containing a cell in which the concentration of CO_2 is assessed, or a sidestream system, which relies on aspirating gas close to the patient's face and transfering it via a long capillary tube to the gas analyzer.

Difficulties arise when we try to determine when in the respiratory cycle the phases were recorded. Figure 1.1 shows tracings obtained during mechanical ventilation of an anesthetized patient. The time plots represent top to bottom: flow, mainstream capnogram, sidestream capnogram, and airway pressure.

Observe that the mainstream capnogram precedes the sidestream capnogram by the transport time of gas in the capillary connecting the sampling port (usually on the "Y" of the breathing circuit close to the patient's mouth) to the gas analyzer. At the end of inspiration, the deadspace of the patient will be filled with air. Thus, the first exhaled gas (about 150 mL for the average adult) of anatomic deadspace without CO_2 will not be recognized by the capnograph. Phase I (without CO_2) of the capnogram, therefore, contains a little exhaled

Capnography, Second Edition, ed. J. S. Gravenstein, Michael B. Jaffe, Nikolaus Gravenstein, and David A. Paulus. Published by Cambridge University Press. © Cambridge University Press 2011.

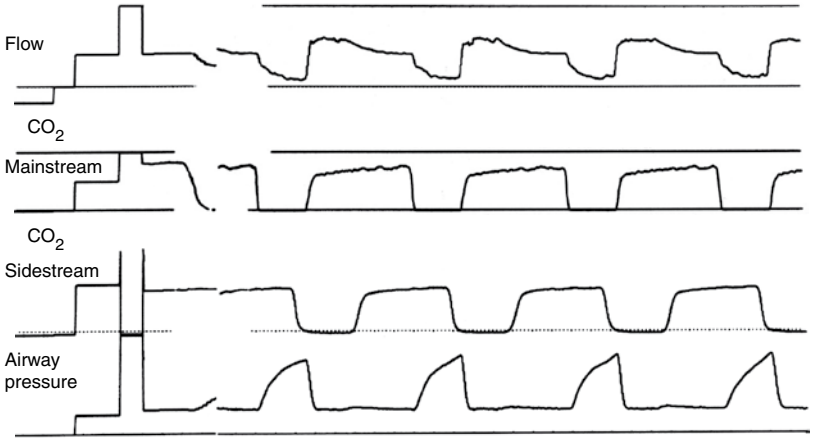

Figure 1.1 Tracing from a patient during controlled ventilation using a circle breathing system. Tracings (from top to bottom) are flow, mainstream capnogram, sidestream capnogram, and airway pressure. Observe that flow and pressure show relatively short fluctuations with inspiration and expiration, and that the sidestream capnogram is out of phase. With sidestream analyzers, the gas has to be carried from the patient to the analyzer through a capillary. Inspiration and expiration on the pressure and flow recording are not simultaneous with inspiration and expiration on the capnogram. The plateaus of the capnograms extend into the respiratory pause and last until the next inspiration arrives.

gas. Finally, a respiratory pause at the end of expiration will leave stagnant gas in the cuvette of the mainstream analyzer or under the sampling port of the sidestream analyzer. Hence, time-based capnograms show the end of exhalation only when end-tidal values are abruptly interrupted by an incoming fresh breath that washes away the CO_2. If phase III of a time-based capnogram is horizontal, we cannot separate the end-expiratory portion that may represent a respiratory pause from an ongoing exhalation delivering a steady level of CO_2. Indeed, should the patient be in respiratory arrest, for example, the plateau would eventually slowly decay as the sidestream (gas aspirating) analyzer continues to aspirate air (or gas from the breathing circuit).

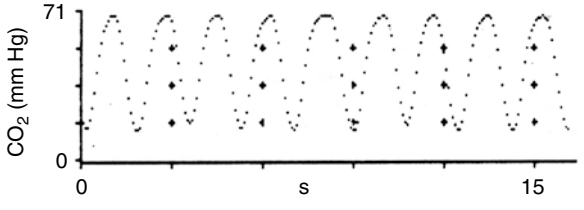

Figure 1.2 A capnogram without a well-defined plateau does not enable end-tidal partial pressure of CO_2 ($P_{ET}CO_2$) to be deduced. End-tidal values are reported to be 70.5 mm Hg; however, they are likely to be much higher in this tachypneic child. Observe that the inspired values show a PCO_2 of 14.9 even though no rebreathing occurred. The respiratory rate exceeded the capnograph's power of resolution. A capnogram without a plateau in phase III may not give meaningful end-tidal values for any other gas exhaled by the patient. Inspect the capnogram before accepting the data presented by the instrument as valid.

Artifacts

Before interpreting the capnogram, we must ascertain that artifacts have not distorted the tracing. Two sources of distortions can be recognized as detailed below.

Mechanical artifacts

Improper calibration of the gas analyzer can be a cause of a distorted tracing, as discussed in the chapter dealing with technical specifications and standards (Chapter 36: Technical specifications and standards). A leak in the sampling tube of a sidestream gas analyzer can allow air to be aspirated and, thus, dilutes the sampled CO_2. Obstruction of the sampling catheter will cause the capnogram to be dampened, slurring the up- and down-slopes of the capnogram and causing falsely high inspired and falsely low end-expired CO_2 values.

Observe that the sidestream capnograms are a little more rounded than the on-airway capnograms (Figure 1.1); this indicates that the sidestream capnographic signals have undergone some damping brought about when the front of the gas column traveling in the long capillary tube undergoes some mixing with adjoining gas. This damping problem becomes more troublesome with rapid respiration, as shown in Figure 1.2. With rapid ventilation, as encountered in pediatric anesthesia, the system might not have sufficient time to reach 100% of the required response, thus displaying higher than actual inspired and lower than actual expired CO_2 values. The response time of capnographs are discussed in the chapter dealing with technical specifications and standards (Chapter 36: Technical specifications and standards).

A water trap with a large internal volume (Figure 1.3) can also introduce artifacts when high

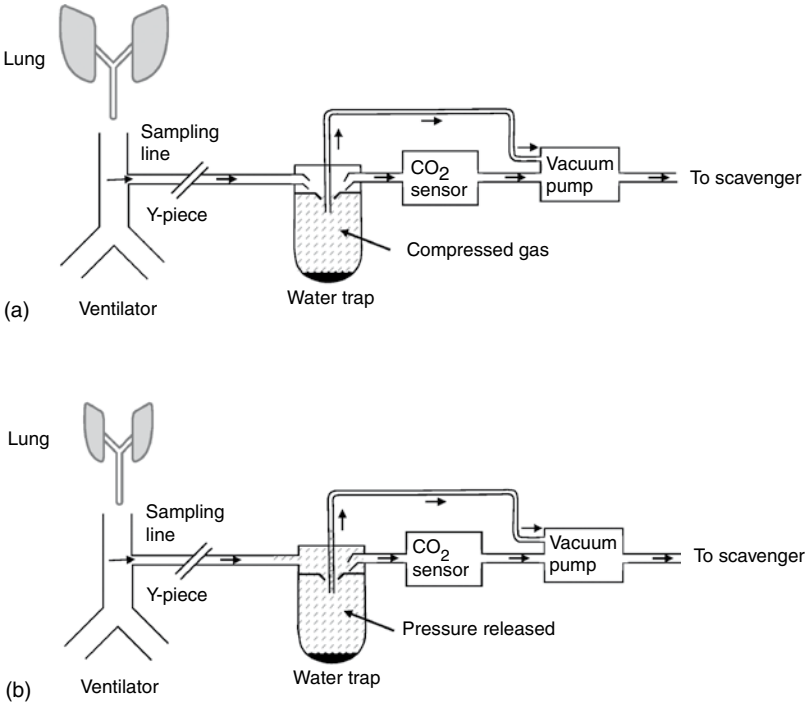

Figure 1.3 Capnogram artifact and water traps. Large water traps (10 mL) produce artifact, which has its origin in the phase of respiration and whose appearance depends on respiratory rate. (a) At the end of inspiration, the system is pressurized at peak airway pressure (P_{aw}) and filled with fresh gas, except for the lower part of the water trap, which holds a gas mixture containing CO_2 (shaded). (b) At the beginning of expiration, P_{aw} decreases to baseline. The pressurized gas mixture in the lower part of the water trap expands and some flows into the sampling tube, the CO_2 content of which is eventually detected by the capnograph. Its appearance on the capnograph depends on what part of an earlier breath is moving through the water trap when the P_{aw} drops to baseline. With constant sampling, flow, and tube length, it depends on respiratory rate. [Modified from: van Genderingen HR, Gravenstein N. Capnogram artifact during high airway pressures caused by a water trap. *Anesth Analg* 1987; **66**: 185–7.]

airway pressures during inspiration compress gas in the trap [1]. This gas expands during expiration and enters the gas stream to be analyzed, thereby introducing an artifact [2]. Modern sidestream capnographs therefore use small water traps and/or filters.

Clinical artifacts

The smooth outline of the capnogram might be dented by the patient taking a breath while undergoing mechanical ventilation (see examples – Figures 9 and 10 in the Appendix). Pattern #10 has been baptized a "curare cleft," an unfortunate appellation. Calling it a curare cleft implies that not enough muscle-relaxant drugs were given so that the patient was capable of initiating a breath. Instead of focusing on incomplete relaxation, the clinician should ask why the patient attempts to breathe while being mechanically ventilated. The answer may be that the patient's partial pressure of CO_2 in arterial blood ($PaCO_2$) exceeds the physiological limits and that in the face of partial paralysis, a troubled respiratory center attempts to correct hypercarbia. Increasing the minute ventilation would be a better measure than deepening the muscle relaxation. An alternative explanation might be that the patient, unable to signal pain because of almost complete paralysis, gasps in desperation. Rather than blocking the response with deeper muscle paralysis, the patient should be better anesthetized. Finally, a "curare cleft," can be generated by pushing on the patient's chest, as might well happen when the surgeon leans on the chest during an operation. Only if the clinician is persuaded that none of these explanations apply and that a hiccup, for example, must be held responsible for the "curare cleft", and that the brief inspiratory efforts interfere with the surgical procedure, should the degree of muscle relaxation be increased.

Finally, cardiogenic oscillations may ripple the down-slope of the capnogram (Figure 13 in the Appendix). These interesting, heart-rate-synchronous, small inspirations and expirations provide evidence that cardiac contractions and relaxations in the chest cause fluctuations of the lung volume with tidal volumes of about 10 mL, the recording of which generates a pneumocardiogram [2]. Evidence of these cardiogenic tidal volumes can also be seen in the movement of the inspiratory and expiratory valves of an anesthesia breathing system. During the respiratory pause in mechanical ventilation, the valves can be seen to flutter synchronously with the heartbeat.

In summary, a capnogram should have four well-defined phases. Figure 1.4 lists points to be considered

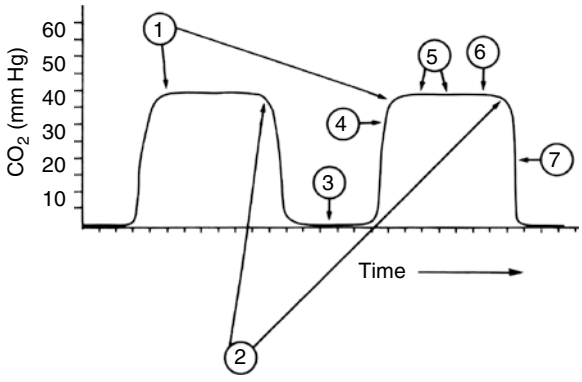

Figure 1.4 (1) *Plateau/onset* – Is there a pattern demonstrating that the patient is being ventilated? (2) *Plateau/end* – Are peak values appropriate? Are the ventilator settings and the patient's respiratory pattern consistent with the capnogram and capnographic findings? (3) *Baseline* – Is the inspired CO_2 tension zero (normal baseline), or is there evidence for rebreathing (elevated baseline)? (4) *Upstroke* – Is there evidence for slow exhalation (slanted upstroke)? (5) *Plateau/horizontal* – Is there evidence of uneven emptying of lungs? (6) *Plateau/smooth* – Is expiration interrupted by inspiratory efforts? (7) *Downstroke* – Is the downstroke steep, or is there evidence of slow inspiration or partial rebreathing?

when deciding whether or not to accept a capnogram of a quality sufficient for clinical interpretation.

Interpreting an artifact-free, time-based capnogram

Cardiovascular issues

The presence of a capnogram signifies that the patient's lungs are perfused. In cardiac arrest, the lungs will not be perfused, but with successful resuscitation, CO_2 will appear in the exhaled gas (as discussed in greater detail in Chapter 20: Cardiopulmonary resuscitation). In general, the capnogram will give evidence of acutely reduced pulmonary perfusion coincident with a drop in cardiac output. Figure 1.5 shows an example of momentarily induced ventricular fibrillation as practiced during implantation of a pacemaker/defibrillator. This will produce a typical pattern of decreasing capnographic tracings. During the first seconds of arrest without pulmonary perfusion, the lung yields quickly decreasing amounts of CO_2 from the stagnant blood or from lung tissue. With successful defibrillation and re-establishment of pulmonary perfusion, CO_2 once again appears in the exhaled breath. Of course, with continued cessation of pulmonary blood flow and continued ventilation, the capnogram will eventually show zero CO_2. If ventilation is stopped during cardiac arrest, a time-based sidestream capnogram will gradually reach zero values as the system continues to aspirate gas (with many devices about 200 mL/min), thus eventually aspirating breathing circuit gas. An on-airway (mainstream) system might show steady values (high or low) if the gas in the cuvette of the system remained stationary.

Some changes in end-tidal values develop slowly, and are thus more readily recognized in trend plots. For example, showers of air emboli can produce areas of alveolar deadspace (ventilated but not perfused alveoli), perhaps associated with a decrease in cardiac output. Shortly thereafter, the air bubbles either pass through the lungs or make it into the alveoli to be exhaled. This process causes the tell-tale transient dip in end-tidal CO_2 values as shown in Figure 1.6. This capnogram is from a patient undergoing a posterior fossa operation in the sitting position and suffering from a typical shower of air emboli. Such ventilation/perfusion $\dot{V}/\dot{Q}$ abnormalities are discussed in greater detail in Chapter 31 (Ventilation/perfusion abnormalities and capnography).

Pulmonary issues

The most important use of capnography in the field, in the intensive care unit, and in the operating room comes with the establishment of an artificial airway. Intubation of the esophagus instead of the trachea still kills people who depend on a tracheal tube for ventilation. Capnography indicates whether or not the tube is in the esophagus. Details of this essential application of capnography in different settings are discussed in considerable detail in several subsequent chapters.

In an artifact-free capnogram, normal end-tidal CO_2 values (between 35 and 45 mm Hg) suggest normal ventilation. However, because a $\dot{V}/\dot{Q}$ mismatch (see Chapter 31: Ventilation/perfusion abnormalities and capnography) can cause the end-tidal values to appear normal while arterial values are high, the clinician will consider other evidence to confirm adequate ventilation. First, the clinician will need to assess the minute volume in the light of the patient's age and weight. We are reassured if the patient's end-tidal CO_2 values are within the normal range and tidal volume and minute ventilation fall within the ranges given in Table 1.1. However, observe that the adult range of minute ventilation covers a wide span. In general, recumbent patients under anesthesia requiring mechanical ventilation

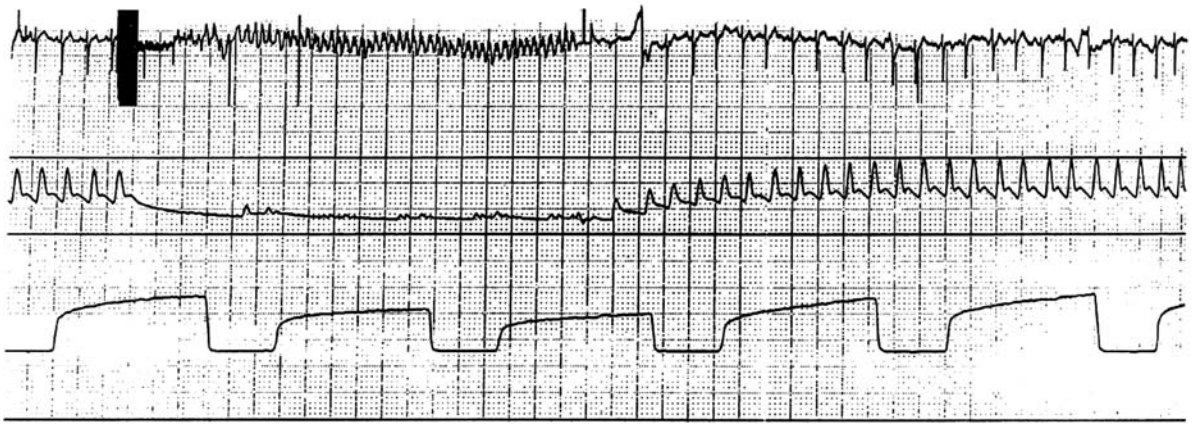

Figure 1.5 A patient undergoing the implantation of an automatic internal cardiac defibrillator was monitored with electrocardiogram (ECG) (top), radial arterial pressure (middle), and mainstream capnography (bottom). Induced ventricular fibrillation (black areas in ECG) and defibrillation are apparent in the ECG tracing. Observe decay of arterial pressure. During absent pulmonary blood flow, the patient's lungs were ventilated, and, with two breaths, the $P_{ET}CO_2$ decreased from 35 mm Hg before fibrillation to 22 mm Hg before defibrillation.

Figure 1.6 The capnogram shows a trend of slow decrease in peak expiratory CO_2 from about 34 to a low of 22 mm Hg, and then an increase to 35 mm Hg. Inspiratory values remained normal. This trend is compatible with a brief shower of air emboli in a patient undergoing a posterior fossa craniectomy in the sitting position.

Table 1.1 Average respiratory values for resting, healthy patients

Parameter	Adult range	Neonatal range
Respiratory rate	10–15 breaths/min	30–40 breaths/min
Tidal volume	6–10 mL/kg	5–7 mL/kg
Minute ventilation	4–10 L/min	200–300 mL/kg/min

need larger tidal volumes to maintain normal blood gas values than spontaneously breathing patients sitting upright. The selection of the optimal minute ventilation must also take into account the deadspace ventilation. Every tidal volume ventilates deadspace as well as the alveoli. If we wish to double the minute ventilation, we *might* double the respiratory rate. However, if we increase the respiratory rate without changing the tidal volume, deadspace ventilation is increased in parallel with alveolar ventilation. If the beginning tidal volume is small enough to tolerate, then increasing the tidal volume instead of changing the respiratory rate would greatly improve alveolar ventilation without increasing deadspace ventilation.

Figure 12 in the Appendix shows a capnogram from an asthmatic patient. The reported end-tidal CO_2 pressure of 42 mm Hg is likely to be distinctly lower than the $PaCO_2$ of this patient, as the patient does not show a plateau of phase III, and the still-rising values were interrupted by the next inspiration.

If the plateau of the capnogram (phase III) does not become almost horizontal before the next breath brings the transition to phase IV, we must wonder how long the CO_2 levels would have continued to rise had an inspiration not interrupted exhalation. Patients with obstructive lung disease, such as asthma, will often show such a sloping phase III. The end-tidal partial pressure of CO_2 ($P_{ET}CO_2$) will then faithfully fail to represent $PaCO_2$. Asthmatic patients exhibiting such a sloping phase III of the capnogram often respond to the inhalation of bronchodilators with improvement of their capnogram and rising $P_{ET}CO_2$ until the improved gas exchange has corrected the problem.

Small tidal volumes will represent relatively low effective alveolar ventilation; that is, with shallow breathing, deadspace will make up more than the usual 30% of tidal volume. In such circumstances, the end-tidal CO_2 values might appear normal, and the

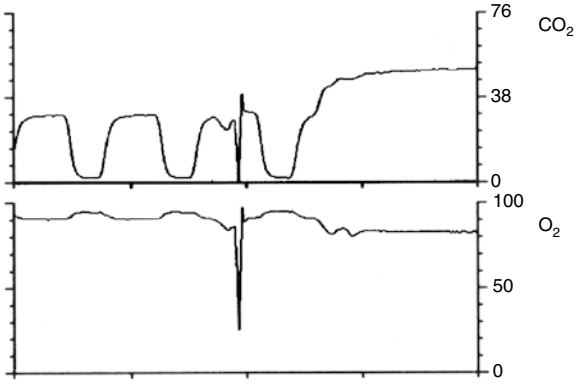

	O_2	N_2O	ISOFL
End-tidal %	91	0	0.40
Inspired %	94	0	0.50

Figure 1.7 A patient undergoing thoracotomy was intubated with an endotracheal tube that enables the blocking of one mainstem bronchus while collecting gas from the blocked lung as well as the ventilated lung. The left part of the capnogram is produced by the ventilated lung, showing a $P_{ET}CO_2$ of 29 mm Hg. The $PaCO_2$ was 46 mm Hg. The right part of the capnogram represents gas sampled distal to the blocker in the right lung showing a PCO_2 of 48 mm Hg. The PCO_2 of the mixed venous blood sampling through a pulmonary arterial catheter was 49 mm Hg.

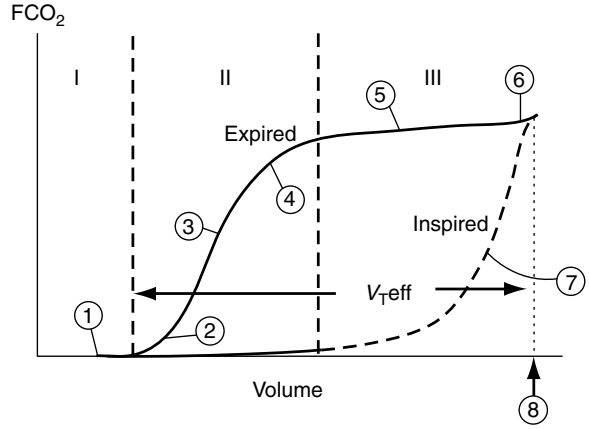

Figure 1.8 A solid line denotes the expiratory portion; the inspiratory portion, if shown, is denoted by a dashed line. The three phases are "denoted" by I, II, and III. (Numbers 1–8 represent the checklist and comments below.) (1) *Phase I* – Is the inspired CO_2 tension zero (normal baseline), or is there evidence of rebreathing (elevated baseline)? Does the volume of phase I reasonably reflect the anatomical and apparatus deadspace (in addition to possibly compressed volume if the program does not subtract this)? Please note that the vertical interrupted line for phase I does not intersect the abscissa at the deadspace volume. (2) *Angle between phases I and II* – Is the transition clearly defined? (3) *Slope of phase II* – Is there evidence for slow exhalation (slanted up-slope)? When the transition to phase III is slurred, consider obstructive pulmonary disease. (4) *Angle between phases II and III* – Is the transition clearly defined? (5) *Slope of phase III* – Is the slope almost level (children and young adults), or is there a clear gradient (i.e., evidence of uneven emptying in patients with lung disease)? (6) *End of phase III* – What is the final value? Is expiration interrupted by inspiratory efforts? Are peak values appropriate? The area under the expiratory limb represents the volume of expired CO_2. (7) *Down-slope (if inspiratory limb shown)* – Is the down-slope steep, or is there evidence of partial rebreathing? The area under the inspiratory limb represents the volume of inspired CO_2; the area between the curves represents the volume of CO_2 eliminated. (8) *Exhaled volume and exhaled CO_2 volume* – Are the values consistent with the expected value and ventilator settings?

capnogram can look quite unremarkable. Yet, an interposed large tidal volume can reveal a $P_{ET}CO_2$ much higher than expected.

Intubation of a mainstem bronchus will result in relative hyperventilation of the intubated lung, producing low $P_{ET}CO_2$ values. Once both lungs are ventilated without changing the tidal volume, the end-tidal values will normalize. In the unventilated airways, CO_2 will equilibrate with venous blood as seen in Figure 1.7.

In the discussion of time-based capnography, the question of the adequacy of ventilation – that is, the adequacy of CO_2 elimination and deadspace ventilation – pops up repeatedly. Thus, it would be nice to be able to view deadspace ventilation as it relates to tidal volume. Enter volume-based capnography.

The normal volume-based capnogram

An individual tracing of the time-based capnogram left a number of questions unanswered, which the single breath volume-based capnogram provides. In Figure 1.8, the solid line denotes the expiratory portion, and the inspiratory portion (not always shown) is denoted by a dashed line. In general, the data offered by the volume-based capnogram refine the information offered by time-based capnography. Again, we ask for an artifact-free tracing, and we consider ventilation and circulation. The phases of the capnogram can then be scanned for detailed information; the questions to be raised for each phase are numbered and enumerated in Figure 1.8. Our most important question is: is there evidence that the lungs are being ventilated? If they are not, is the endotracheal tube in the esophagus, or is the patient in cardiac arrest? Once we are reassured, we proceed to examine the details. The inspired CO_2 tension

should be zero; if not, this is evidence of rebreathed CO_2, as discussed in Chapter 6 (Capnography during anesthesia). A normal deadspace is assumed to occupy about 1 mL/pound (0.5 mL/kg) or, for the average adult, about 150 mL, or approximately one-third of the tidal volume. The volume-based capnogram provides a convenient opportunity to confirm this fact. A larger than normal deadspace points to either an equipment deadspace (see Chapter 6: Capnography during anesthesia), exhausted CO_2 absorber, or ventilation of unperfused lung segments (see Chapter 31: Ventilation/perfusion abnormalities and capnography). Ideally, the transition from phase I to II should be abrupt, although it usually is not because as alveolar gas passes through the deadspace, it first mixes with the deadspace gas and then rapidly displaces it. This process should result in a steep rise of the capnogram in phase II. If the alveoli empty grossly unevenly, as in severe emphysematous or obstructive lung disease, the slope will be slanted. The angle between the up-slope and the plateau indicates that the addition of CO_2 from the alveoli is now beginning to become homogeneous. A lazy up-slope and a slurred transition again indicate a troubled lung that empties its CO_2 unevenly. A horizontal (or nearly so) plateau shows a lung that fairly prodigiously adds CO_2 to every milliliter of exhaled gas. Healthy children and young adults often show nearly horizontal plateaus. Cardiogenic oscillations, as described above, can put heartbeat-synchronous ripples on the plateau. At the end of the plateau, we expect to read the true end-tidal value for CO_2, which, as already mentioned, should be between 35 and 45 mm Hg:

- If the inspiratory limb is inscribed, we would expect a steep fall of CO_2 in the inspired gas, soon reaching zero, unless the patient is rebreathing CO_2, as discussed above. The area under the inspiratory limb is the volume of inspired CO_2; and the area between the curves represents the volume of CO_2 eliminated.
- Since we have plotted the tidal volume on the abscissa, we can check the exhaled volume and compare it with the expected value for the patient. Remember that inspired and expired volumes are often not identical either because the respiratory quotient is less than 1 (more oxygen consumed than CO_2 exhaled), or because the uptake or elimination of anesthetic gases causes a discrepancy. During anesthesia, nitrous oxide is often the culprit because we may give it in relatively high concentrations (up to 70%). Its solubility coefficient of 0.47 for blood at body temperature predicts that many liters will go into solution in the body and will at the end of anesthesia again appear in the exhaled gas.

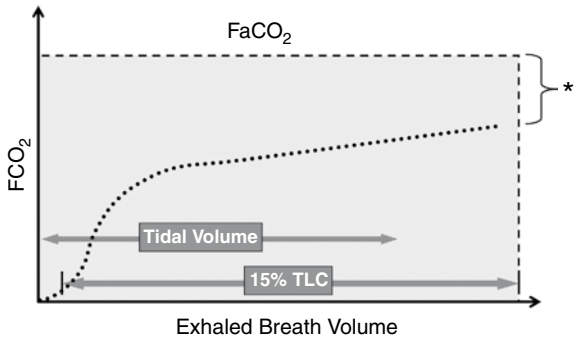

Figure 1.9 Volume-based capnogram from a patient with pulmonary embolism. Observe the large difference between end-tidal and arterial CO_2 tension. The asterisk shows the size of the alveolar deadspace at end-expiration. [Modified from: Anderson JT, Owings JT, Goodnight JE. Bedside non-invasive detection of acute pulmonary embolism in critically ill surgical patients. *Arch Surg* 1999; **134**: 869–74.]

The gas inhaled last will fill the patient's deadspace; it will be the gas exhaled first and should be free of CO_2. If it is not, the patient is rebreathing exhaled CO_2, which may be linked to the type of equipment in use or an equipment malfunction, or CO_2 is being added to the inspired gas. For example, at the end of anesthesia, some anesthetists like to add CO_2 so as to allow hyperventilation for the elimination of anesthetic gases without causing the patient to develop a respiratory alkalosis.

Figure 1.9 is from a patient who suffered a pulmonary embolism. Conditions that increase deadspace ventilation (ventilated but not perfused alveoli), such as emboli (tumor, gas, clot) or right-to-left shunts, will stand out clearly in the volume-based capnogram that shows the large deadspace. With a decrease in cardiac output, the volume of CO_2 delivered to the lungs will also decrease. As the volume-based capnogram enables the calculation of the exhaled CO_2, we can quantify the change better than with time-based capnography, which only reports the end-tidal values.

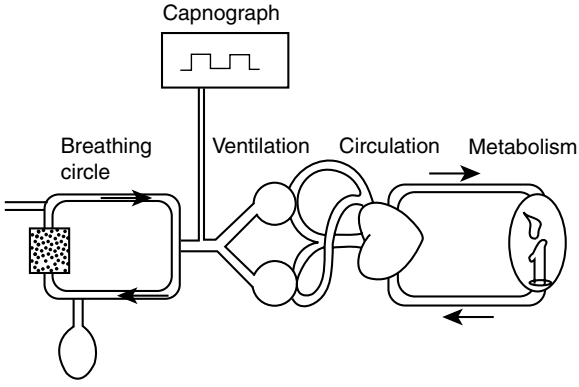

Figure 1.10 End-tidal values can be affected by a number of mechanisms, starting with the generation of CO_2 in the cell (candle), the transport of venous blood to the heart (cardiac output), the pulmonary blood flow (part of which may be shunted past ventilated alveoli), ventilation (part of which may be blocked from perfused alveoli), the breathing system (which may cause rebreathing, hyperventilation, or hypoventilation), and ending with the capnograph (which may fail because of artifacts or incorrect calibration).

Summary

Whether using time- or volume-based capnography, many questions will confront the clinician when abnormal capnographic data call for an analysis. Figure 1.10 recapitulates the fact that many components of the system can cause trouble, starting with cellular metabolism (remember malignant hyperthermia) to mechanical problems related to the airway, ventilation, and monitors. These topics, buttressed by exhaustive references, will be discussed in detail in subsequent chapters.

References

1. van Genderingen HR, Gravenstein N. Capnogram artifact during high airway pressures caused by a water trap. *Anesth Analg* 1987; **66:** 185–7.
2. Bijaoui E, Baconnier PF, Bates JHT. Mechanical output impedance of the lung determined from cardiogenic oscillations. *J Appl Physiol* 2001; **91**: 859–65.

Section 1

Ventilation

Section 1
Chapter
2

Ventilation

Capnography and respiratory assessment outside of the operating room

R. R. Kirby

Introduction

Since gas exchange is a primordial function of the lungs and the conductive airways, respiratory assessment is of paramount importance. Clinicians evaluate this function by visual observation of chest expansion, depth and rate of ventilation, use of accessory respiratory muscles, and auscultation of the quality and quantity of breath sounds. Quantitative information is obtained by determining thoracic/pulmonary compliance (change of volume related to change in pressure) and airways resistance. Other more complex techniques involve measurement of lung volumes and capacities with spirometry, which also evaluates airway patency and lung/thorax expansion. Factors that affect these measurements include pain, fatigue, and poor understanding by the patients and clinicians of how the test is to be carried out. As a result, assessment of airway obstruction or lung restriction is reliable only insofar as the patient's ability to perform the tests is optimal and unimpaired.

Perhaps the ultimate test for adequate ventilation is invasive determination of arterial CO_2 partial pressure ($PaCO_2$). In general, an elevation in $PaCO_2$ (hypercapnia) represents a decreased respiratory rate, depth, or both; inefficient alveolar ventilation (ventilation/perfusion [$\dot{V}/\dot{Q}$] inequalities); or production of CO_2 in excess of the patient's ability to excrete it. A reduction in $PaCO_2$ (hypocapnia) results from excessive alveolar ventilation in relation to CO_2 production. Measurement of $PaCO_2$, although a true reflection of ventilatory efficacy, is far from ideal since it is invasive and intermittent.

Capnography has been utilized in surgical patients for over three decades to confirm tracheal intubation and assess ventilation. Measurement of exhaled CO_2, particularly the end-tidal PCO_2 ($PETCO_2$), is an established standard of care in patient monitoring [1]. In conjunction with $PaCO_2$, capnography provides a semiquantitative assessment of $\dot{V}/\dot{Q}$ mismatch by changes in the $PaCO_2$–$PETCO_2$ gradient (normal ≤5 mm Hg). Capnograms are of three types, depending on whether the concentration of CO_2 is plotted against (1) expired volume, otherwise known as *volumetric capnogram*, (2) single breath time concentration CO_2 curve [2], or (3) time during a respiratory cycle. The latter technique is more practical for clinical use.

Capnography is increasingly employed outside the operating room as a non-invasive, continuous trend monitor of $PaCO_2$ and airway dynamics. It is of value in assessing the efficacy of cardiopulmonary resuscitation during low perfusion states or cardiac arrest, and is considered a standard of care by the American Heart Association [3]. Colorimetric capnometry is fast, convenient, and useful to verify tracheal intubation in nonoperating room settings. However, it can present problems, as was indicated by Puntervoll *et al.* [4]. They compared colorimetric methodology with mainstream capnography, and found that in emergency situations in which CO_2 containing air may be present in the esophagus, mainstream capnography should be the preferred method of verifying tracheal – and not esophageal – intubation. The colorimetric CO_2 indicator is very sensitive to low CO_2 values, and may falsely indicate correct tracheal intubation, even when the tube is in the esophagus.

As the use of capnography increases and the interpretation of abnormalities becomes more complex, categorization into useful and meaningful diagnostic and therapeutic modes is of value. The data have been classified in a simplified manner (Table 2.1) [5]. Some redundancy is noted among categories, since capnography is applicable in numerous clinical settings.

Capnography, Second Edition, ed. J. S. Gravenstein, Michael B. Jaffe, Nikolaus Gravenstein, and David A. Paulus. Published by Cambridge University Press. © Cambridge University Press 2011.

Table 2.1 Clinical uses of capnography

Airway	Breathing	Circulation	Anesthetic delivery apparatus	Homeostasis	Outside the operating room
Confirm intubation	Detect spontaneous breathing	Infer cardiac output	Adequacy of manual or mechanical ventilation	Malignant hyperthermia	Confirm intubation
Endotracheal tube blockage or obstruction	Onset and offset of neuromuscular blockade	Cyanotic heart disease and central shunts	Adequacy of fresh gas inflow during spontaneous ventilation	Carbon dioxide retention	Acid–base monitoring
Double-lumen tube insertion	One-lung ventilation	Pulmonary embolization	Circuit disconnects and leaks	Absorption of CO_2 during laparoscopy	Respiratory failure
Fiberoptic or blind nasal endotracheal tube insertion	Distal airway obstruction and bronchospasm	Acid–base changes	Functional analysis of rebreathing	Seizures	Apnea, respiratory monitoring
Monitor during sedation/ analgesia	Airway collapse/ atelectasis	Effectiveness of cardiopulmonary resuscitation	Soda lime exhaustion	Venous thromboembolism	Nasogastric tube insertion
–	–	Nontraditional forms of ventilation	Inspiratory/ expiratory valve malfunction	–	Neonatal ventilation

Source: Modified from: Eipe N, Tarshis J. A system of classification for the clinical applications of capnography. *J Clin Monit Comp* 2007; **21**: 341–4.

Capnography and lung volumes

The traditional determination of lung volumes and ventilation incorporates the analysis of the expired concentration of a trace gas, such as nitrogen or helium, during a single breath ("washout") against exhaled volume. Nitrogen washout provides an estimate of functional residual capacity, total lung volume, deadspace volume, and alveolar volume. If one substitutes CO_2 for nitrogen or helium, a similar washout curve is generated [2]. This technique is known as *single breath capnography* (SBT-CO_2) (Figure 2.1), which is divided into three phases. Phase I consists of anatomical deadspace which contains little to no CO_2. This phase is followed by a steep increase in CO_2 concentration as gas from the conductive airways is mixed with alveolar gas (phase II). A plateau follows (phase III) in which there is no change in exhaled CO_2 concentration; phase III represents alveolar emptying. Occasionally, a terminal upswing is seen (phase IV), particularly in obese or pregnant individuals. Factors such as uneven or delayed alveolar emptying (from slow compartments) contribute to this aberrancy.

Uses of time capnography

Clinicians typically utilize exhaled CO_2 concentration against time during a respiratory cycle. A number of applications are available in and out of the operating room.

Trend monitoring of alveolar ventilation

Capnography can be used as a continuous monitor of alveolar ventilation in patients with lung disease or hemodynamic instability. Although such use does not replace arterial blood gas analysis, it may decrease the required frequency [6]. In stable patients with body temperature that remains constant, the $PaCO_2$ and $P_{ET}CO_2$ can be used as surrogates, because their difference is 1 to 5 mm Hg in normal individuals [7,8]. When changes in temperature, cardiovascular function, and CO_2 production occur, capnography used

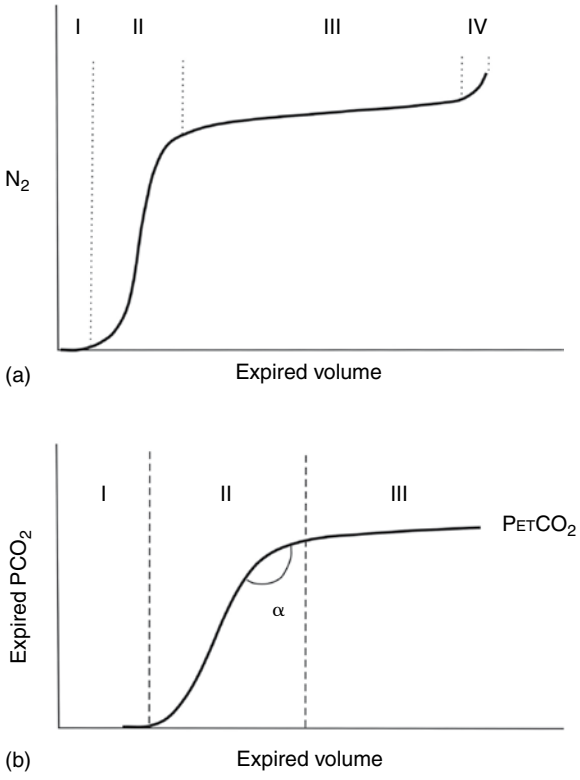

Figure 2.1 Curves of exhaled nitrogen (a) and CO_2 (b) concentration versus expired volume during a single breath "washout" test. Both show the traditional division into phases I–IV (for full explanation, see text). N_2, nitrogen.

alone to trend $PaCO_2$ can be misleading. The primary reason capnography has not replaced arterial blood gas analysis to determine $PaCO_2$ is related to the variability in the three physiological parameters that determine $P_{ET}CO_2$: (1) production of CO_2; (2) delivery of CO_2 via pulmonary blood flow; and (3) elimination of CO_2.

Trend monitoring of deadspace ventilation

Components of a time capnogram are similar to those of a SBT-CO_2 capnogram (Figure 2.2)[9,10], and consist of a square wave in which phase I represents the CO_2-free gas from the airways (anatomical and physiologic deadspace). Phase II consists of a rapid S-shaped upswing on the tracing, due to mixture of deadspace gas with alveolar gas. Phase III represents the alveolar plateau (CO_2-rich gas from the alveoli). Unlike SBT-CO_2, a descending limb results from the inspiratory phase during which the fraction of inspired CO_2 decreases to zero.

The capnograph also exhibits two angles [10]: the alpha angle between phases II and III, and the beta angle between the end of phase III and the beginning of inspiration. The alpha angle is about 110°, and increases as the slope of phase III increases. The slope of phase III is dependent on $\dot{V}/\dot{Q}$ relationships within the lungs. Alpha angle values are important in assessing airway obstruction. Other factors that can produce changes in the alpha angle include equipment-related characteristics, capnometer response time, and the patient's respiratory cycle time. The beta angle can be used to assess the extent of rebreathing. During rebreathing of CO_2, an increase in the angle from the normal 90° occurs, since the descending slope becomes less vertical in the presence of inspired CO_2.

Assessment and monitoring of patients with airway obstruction

Capnography may represent a useful alternative to spirometry in the evaluation of patients with asthma or chronic obstructive lung disease. The normal rectangular shape of the capnograph is affected by various degrees of airway obstruction (Figure 2.3) [11–13]. Parameters used to assess airway obstruction include: (1) slope of the alveolar plateau, which can be related to end-tidal CO_2; (2) radius of minimal curvature of the alpha angle; (3) time necessary to pass from 25% to 75% of the $P_{ET}CO_2$; and (4) the beta angle. Several studies have shown significant correlation between these capnographic indices and spirometric measures in stable patients. You *et al.* [12] found a good correlation in asthmatic patients between the end-tidal slope (phase III) obtained by the capnograph and the forced expiratory volume in 1 s.

Capnography in patients with reactive airway disease does not require the patient's cooperation or wakefulness. Therefore, it can be used continuously in a number of clinical situations. Limitations result from several factors, particularly the analyzer's dynamic characteristics; expiratory flow rate; duration of the expiratory phase; and artifacts derived from the upper airway, such as nasal obstruction and pulsatile waves of carotid origin. These factors require criteria for adequate use, interpretation, and assessment of airway patency.

Assessment of sleep disorders

Capnography has been used to detect disorders of central regulation of breathing during sleep. In 57 patients

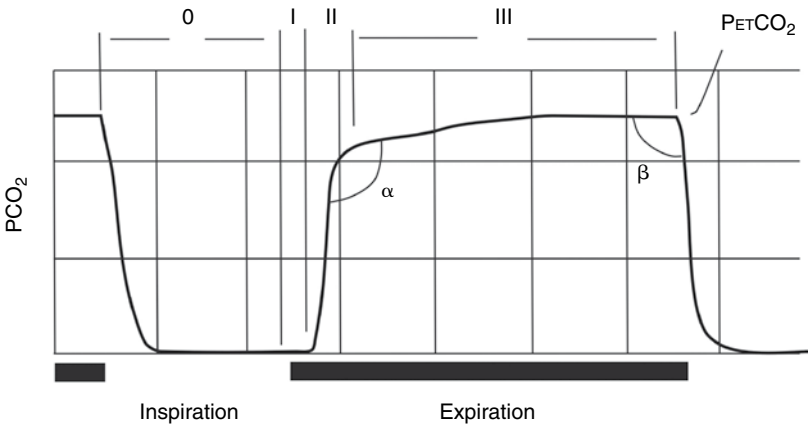

Figure 2.2 Time capnogram showing exhaled PCO_2 versus time. All three phases are shown. Alpha (*α*) angle: angle between phases II and III; beta (*β*) angle: angle between phase III and inspiratory limb (phase 0). [From: Bhavani-Shankar K, Kumar AY, Moseley HSL, Ahyee-Hallsworth R. Terminology and the current limitations of time capnography: a brief review. *J Clin Monit* 1995; **11**: 175–82.]

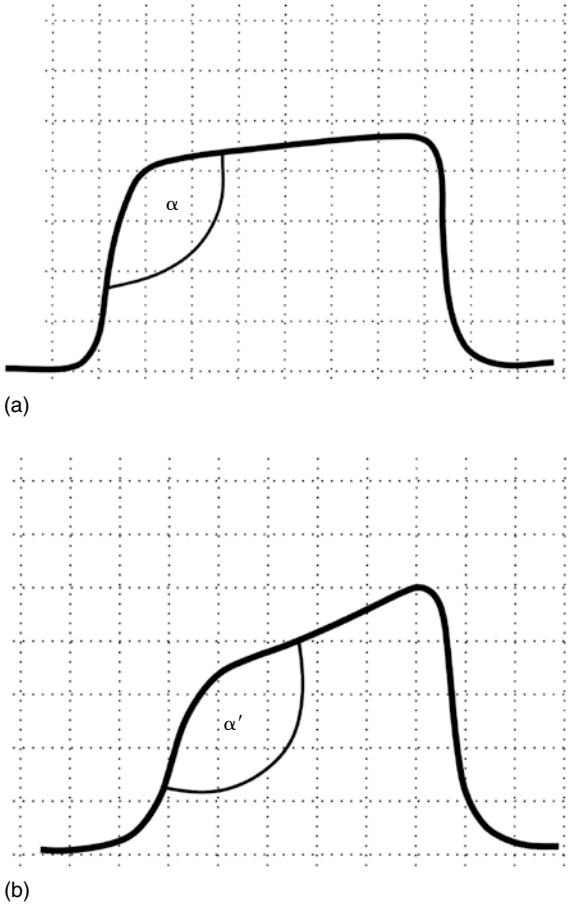

Figure 2.3 (a) Normal capnogram showing alpha (*α*) angle of 105°. (b) Capnogram during acute bronchospasm showing an alpha (*α′*) angle of 140°.

evaluated for sleep-disordered breathing, the $PaCO_2$ (38.8 ± 4.1 mm Hg) was not significantly different from the $PETCO_2$ (38.1 ± 4.3 mm Hg) [14]. The investigators concluded that the continuous non-invasive attribute of capnography may be useful to assess ventilation in patients with suspected sleep-related breathing disorders.

Giner and Casan [15] demonstrated that capnography and pulse oximetry have a role in lung-function laboratories. They utilized $PETCO_2$ and SpO_2 from pulse oximetry in 57 patients and compared these values to blood-gas partial pressure and direct measurement of oxygen saturation (SaO_2). The mean difference between the SpO_2 and SaO_2 was 0.08 ± 1.46% and between the $PETCO_2$ and $PaCO_2$ was 2.7 ± 2.9 mm Hg. The investigators concluded that these non-invasive monitors were useful when ventilation and oxyhemoglobin saturation monitoring are the objectives.

Evaluation of non-intubated patients

Capnography has been utilized in emergency departments to evaluate patients with respiratory distress. Plewa *et al.* [16] evaluated 29 patients with symptoms of dyspnea and a respiratory rate greater than 16/min in a level 1 trauma center/community hospital emergency department. Their primary goal was to assess the ability of $PETCO_2$ to predict $PaCO_2$. Although there was a significant correlation with $PaCO_2$, they found that within two standard deviations, $PETCO_2$ underestimated $PaCO_2$ by as much as 16 mm Hg and overestimated it by up to 5 mm Hg. Values of $PETCO_2$ correlated reasonably well with $PaCO_2$ only in patients who were able to provide a forced expiratory volume. It was less accurate in patients who could only breathe at tidal volume levels or had pulmonary disease.

By contrast, in patients without respiratory failure seen in the emergency room for a variety of conditions, capnography correlates reasonably with $PaCO_2$. Barton and Wang studied 76 patients and found a close

relationship between $P_{ET}CO_2$ and $PaCO_2$, even when the values were compared during respiratory and non-respiratory acidosis ($r^2 = 0.899$) [17]. Mainstream capnometry appears to provide more accurate $P_{ET}CO_2$ than conventional sidestream capnometry during spontaneous breathing in non-intubated patients [18].

In a prospective observational study of adult patients undergoing procedural sedation in an urban county hospital, patients were monitored for vital signs, and depth of sedation was monitored by the Observer's Assessment of Alertness/Sedation scale (OAA/S), pulse oximetry, and nasal-sample $P_{ET}CO_2$ [19]. There was no correlation between $P_{ET}CO_2$ and the OAA/S score. Using the criteria of a $P_{ET}CO_2 > 50$ mm Hg, an absolute change > 10 mm Hg, or an absent waveform, the investigators suggested the $P_{ET}CO_2$ may add to the safety of procedural sedation not readily assessed by other means in the emergency department by quickly detecting hypoventilation.

Finally, Takano *et al.* determined the utility of portable capnometry in general wards and in-home care in 41 spontaneously breathing patients [20]. The mean difference between $PaCO_2$ and vital capacity $P_{ET}CO_2$ (VC-$et CO_2$) was 0.5 mm Hg, and was not statistically significant. Regression analysis showed a close correlation between VC-$et CO_2$ and $PaCO_2$ ($r = 0.91$, $P < 0.0001$). Thus, VC-$et CO_2$ was highly correlated with $PaCO_2$, a finding similar to that of Plewa *et al.* [16]. This high correlation was also seen in patients with compromised pulmonary function ($FEV_1 < 70\%$ [$r = 0.88$, $P < 0.0001$]). In contrast, tidal volume $P_{ET}CO_2$, and $PaCO_2$ differed by an average of 9 mm Hg. The investigators concluded that VC-$et CO_2$ measured by portable capnometry can be useful to evaluate the respiratory condition of spontaneously breathing patients receiving general ward and in-home care.

Pediatric sedation

Recent technological advances in patient monitoring have contributed to decreased mortality for individuals receiving general anesthesia in operating room settings. Patient safety has not been similarly targeted for the several million children annually in the United States who receive moderate sedation without tracheal intubation. Critical event analyses have documented that hypoxemia secondary to depressed respiratory activity is a principal risk factor for near-misses and deaths in this population. Current guidelines for monitoring pediatric patient safety during moderate sedation call for continuous pulse oximetry and visual assessment, which may not detect alveolar hypoventilation until arterial oxygen desaturation has occurred. Microstream capnography appears to provide an "early warning system" by generating real-time waveforms of respiratory activity in non-intubated patients.

In a study of 163 children undergoing 174 elective endoscopic procedures with moderate sedation, investigators documented poor ventilation in 3% of all procedures and no apnea. Capnography indicated alveolar hypoventilation during 56% of procedures and apnea during 24%, and allowed early detection of arterial oxygen desaturation because of alveolar hypoventilation, even in the presence of supplemental oxygen [21]. The results of this controlled trial suggest that microstream capnography improves the current monitoring of sedated children, thereby allowing early detection of respiratory compromise and prompting intervention to minimize hypoxemia.

Prehospital use

Capnography is used outside the hospital to confirm tracheal intubation. Such use promotes appropriate ventilation of the patient, with improved outcomes and decreased mortality [10–12]. Pulse oximeters are prone to malfunction because of motion artifacts and hypothermia. Capnography added to oximetry during patient transport reduced the total duration of malfunction and the number of alerts per patient significantly for the capnometer compared to the pulse oximeter [22]. The investigators suggested that having a mode of monitoring ventilation in addition to the oxygenation would be beneficial. Some emergency ambulance services have been equipped with capnographs, and emergency medical personnel have been provided with training to enable them to utilize capnographic data. This number is likely to increase, and capnography is likely to become a routine monitoring device for emergency medical personnel.

Detection of occult hyperventilation in syncope and chronic fatigue syndrome

Capnography has also been utilized as a part of diagnostic maneuvers in the evaluation of syncope in children and adolescents [23,24]. Spontaneous hyperventilation is thought to play a relevant role in the pathophysiology of pediatric neurocardiogenic syncope, and it could identify a specific subtype of response to orthostatic stress in susceptible patients. Inclusion of capnography in tilt-test protocols may improve the assessment

of syncope in children. The capnography head-up tilt test (CHUTT) was found to be predictive of associated psychogenic hyperventilation, one of the main reasons for syncope in 6% of cases.

Similar findings were reported in the chronic fatigue syndrome (CFS) [25]. Thirty-two consecutive patients with CFS and 32 healthy volunteers were evaluated with the aid of the CHUTT. The main outcome measures were blood pressure (BP), heart rate (HR), respiratory rate (RR), and $P_{ET}CO_2$ recorded during recumbence and tilt. Patients with CFS developed significantly lower systolic and diastolic BP and $P_{ET}CO_2$, and a significant rise in HR and RR ($P < 0.01$) during tilt. The postural tachycardia syndrome occurred in 44%, vasodepressor reaction in 41%, cardioinhibitory reaction in 13%, and hyperventilation in 31% of cases in CFS patients. One or more end points of the CHUTT were reached in 78% of patients with CFS but in none of the controls.

Respiratory status during pediatric seizures

To determine the reliability and clinical value of $P_{ET}CO_2$ by oral/nasal capnometry for monitoring pediatric patients presenting postictal or with active seizures, investigators studied 166 patients (105 patients with active seizures, 61 postictal patients) [26]. End-tidal CO_2 was measured by oral/nasal sidestream capnometry, together with RR, SpO_2, and HR every 5 min until 60 min had elapsed. The correlation between $P_{ET}CO_2$ and capillary PCO_2 was significant ($r^2 = 0.97$; $P < 0.0001$). Investigators concluded that dependable $P_{ET}CO_2$ values could be obtained in pediatric seizure patients using an oral/nasal cannula capnometry circuit and that continuous $P_{ET}CO_2$ monitoring provided a reliable assessment of pulmonary status to assist with decisions to provide ventilatory support.

Adult endoscopy

Outpatient endoscopy procedures often require significant sedation, and unrecognized respiratory depression is a constant risk. Apnea or disordered respiration occurs commonly during therapeutic upper endoscopy and frequently precedes the development of hypoxemia, with disastrous outcomes reported. Forty-nine patients undergoing therapeutic upper endoscopy were monitored with pulse oximetry, automated BP measurement, and visual assessment [27]. Graphic assessment of respiratory activity with sidestream capnography was performed in all patients. Episodes of apnea or disordered breathing detected by capnography were documented and compared with the occurrence of hypoxemia, hypercapnia, hypotension, and abnormal respiratory activity recognized by endoscopy personnel.

Simultaneous respiratory rate measurements obtained by capnography and by auscultation with a pretracheal stethoscope verified that capnography was an excellent indicator of respiratory rate when compared with auscultation ($r = 0.967$, $P < 0.001$). Fifty-four episodes of apnea or disordered respiration occurred in 28 patients (mean duration 70.8 s.). Only 50% of apnea or disordered respiration episodes were eventually detected by pulse oximetry, and none were detected by visual assessment. Potentially important abnormalities in respiratory activity are undetected with pulse oximetry and visual assessment. Similar findings later were noted in pediatric patients undergoing endoscopic procedures [21]. The American Society of Gastrointestinal Endoscopy has issued guidelines suggesting that continuous CO_2 monitoring is a useful adjunct for endoscopic procedures that utilize deep sedation [28].

Enteral feeding tube placement

Enteral feedings are an integral part of care for many hospitalized patients. Accessing the gastrointestinal tract safely and in a timely manner can be challenging. Various techniques and devices to enhance the safety of bedside feeding tube placement are available for clinicians. The colorimetric CO_2 detector is applied to detect the presence or absence of CO_2, thus assisting in correct placement of the feeding tube tip into the gastrointestinal tract rather than the airway [29].

Conclusions

Capnography has potential applications as a tool for evaluation of the respiratory system outside of the operating room. Uses include the evaluation and monitoring of patients who present with a variety of conditions in the emergency department, including respiratory failure and reactive airways disease, and in a variety of outpatient or diagnostic settings (pediatric syncope, CFS). Current evidence suggests that capnography generally correlates well with $P_{ET}CO_2$. It is less reliable in patients with significant $\dot{V}/\dot{Q}$ mismatch who are unable to produce forced exhalations. In the opinion of some investigators, the technology should

be employed in all cases requiring sedation in or out of the operating room [28,30]. Without capnography, significant delays in the detection of apnea are demonstrable [31].

However, despite general feelings concerning the value of capnography, its role outside the operating room in sedation/analgesia when utilized by non-anesthesiologists is not fully established. In its practice guidelines for sedation/analgesia in the hands of non-anesthesiologists, The American Society of Anesthesiologists Task Force on sedation and analgesia by non-anesthesiologists states that consultants "were equivocal regarding the ability of capnography to decrease risks during moderate sedation, while agreeing that it may decrease risks during deep sedation. In circumstances in which patients are physically separated from the caregiver, the Task Force believes that automated apnea monitoring (by detection of exhaled carbon dioxide or other means) may decrease risks during both moderate and deep sedation …" [32]. The final analysis suggests that when patients have significant comorbidities (myocardial infarction, severe obstructive pulmonary disease, congestive heart failure), and when the risk of deep sedation to the point of unresponsiveness is likely, non-anesthesiologists should consult anesthesiologists whenever possible.

References

1. American Society of Anesthesiologists. *Standards for Basic Anesthetic Monitoring*. Approved by the House of Delegates October 21, 1986 and last amended on October 15, 2003. Park Ridge, IL: ASA, 2003. Available online at http://www.asahq.org/publicationsAndservices/.
2. Romero PV, Lucangelo U, Lopez Aguilar J, Fernandez R, Blanch L. Physiologically based indices of volumetric capnography in patients receiving mechanical ventilation. *Eur Respir J* 2000; **10**: 232–3.
3. American Heart Association Guidelines for Cardiopulmonary Resuscitation and Emergency Cardiovascular Care. Part 7.1: Adjuncts for airway control and ventilation. *Circulation* 2005; **112**: IV-51–7.
4. Puntervoll SA, Soreide E, Jacewicz W, Bjelland E. Rapid detection of oesophageal intubation: take care when using colorimetric capnometry. *Acta Anaesthesiol Scand* 2002; **46**: 455–7.
5. Eipe N, Tarshis J. A system of classification for the clinical applications of capnography. *J Clin Monit Comp* 2007; **21**: 341–4.
6. Tobias JD, Flanagan JFK, Wheeler, TJ, Garrett JS. Noninvasive monitoring of end-tidal CO_2 via nasal cannulas in spontaneously breathing children during the perioperative period. *Crit Care Med* 1994; **22**: 1805–8.
7. Frieson RH, Alswang M. End-tidal PCO_2 monitoring via nasal catheter in pediatric patients: accuracy and sources of error. *J Clin Monit* 1996; **12**: 155–9.
8. Liu SY, Lee TS, Bongard F. Accuracy of capnography in nonintubated surgical patients. *Chest* 1992; **102**: 1512–15.
9. Schmmitz BD, Shapiro B. Capnography. *Respir Care Clin N Am* 1996; **1**: 107–17.
10. Bhavani-Shankar K, Kumar AY, Moseley HSL, Ahyee-Hallsworth R. Terminology and the current limitations of time capnography: a brief review. *J Clin Monit* 1995; **11**: 175–82.
11. Strömberg NOT, Gustafsson PM. Ventilation inhomogeneity assessed by nitrogen washout and ventilation–perfusion mismatch by capnography in stable and induced airway obstruction. *Pediatr Pulmonol* 2000; **29**: 94–102.
12. You B, Peslin R, Duvivier C, Vu VD. Expiratory capnography in asthma: evaluation of various shape indices. *Eur Respir J* 1994; **7**: 318–23.
13. Yaron M, Padyk P, Hutsinpiller M, Cairns CB. Utility of the expiratory capnogram in the assessment of bronchospasm. *Ann Emerg Med* 1996; **28**: 403–7.
14. Schafer T. Methodik der Atmungsmessung im Schlaf: Kapnographie zur Beurteilung der Ventilation. *Biomed Tech (Berlin)* 2003; **48**: 170–5.
15. Giner J, Casan P. Lung cancer pulse oximetry and capnography in lung function laboratories. *Arch Bronconeumol* 2004; **40**: 311–14.
16. Plewa MC, Sikora S, Engoren M, *et al*. Evaluation of capnography in nonintubated emergency department patients with respiratory distress. *Acad Emerg Med* 1995; **2**: 901–8.
17. Barton CW, Wang ESJ. Correlation of end-tidal CO_2 measurements to arterial $PaCO_2$ in nonintubated patients. *Ann Emerg Med* 1994; **23**: 560–3.
18. Casati A, Gallioli R, Passaretta R, *et al.* End tidal carbon dioxide monitoring in spontaneously breathing, nonintubated patients. *Minerva Anestesiol* 2001; **67**: 161–4.
19. Miner JR, Heegaard W, Plummer D. End-tidal carbon dioxide monitoring during procedural sedation. *Acad Emerg Med* 2002; **9**: 275–80.
20. Takano Y, Sakamoto O, Kiyofuji C, Ito K. A comparison of the end-tidal CO_2 measured by portable capnometer and the arterial PCO_2 in spontaneously breathing patients. *Respir Med* 2003; **97**: 476–81.

21. Lightdale JR, Goldmann DA, Feldman HA, Nardo JA, Fox VL. Microstream capnography improves patient monitoring during moderate sedation: a randomized, controlled trial. *Pediatrics* 2006; **117**: 1170–8.

22. Kober A, Schubert B, Bertalanffy P, *et al*. Capnography in nontracheally intubated emergency patients as an additional tool in pulse oximetry for prehospital monitoring of respiration. *Anesth Analg* 2004; **98**: 206–10.

23. Naschitz JE, Hardoff D, Bystritzki I, *et al*. The role of the capnography head-up tilt test in the diagnosis of syncope in children and adolescents. *Pediatrics* 1998; **101**: 1–6.

24. Martinon-Torres F, Rodriguez-Nunez A, Fernandez-Cebrian S, *et al*. The relation between hyperventilation and pediatric syncope. *J Pediatr* 2001; **138**: 894–7.

25. Naschitz JE, Rosner I, Rozenbaum M, *et al*. The capnography head-up tilt test for evaluation of chronic fatigue syndrome. *Semin Arthritis Rheum* 2000; **30**: 79–86.

26. Abramo TJ, Wiebe RA, Scott S, Goto CS, McIntire DD. Noninvasive capnometry monitoring for respiratory status during pediatric seizures. *Crit Care Med* 1997; **25**: 1242–6.

27. Vargo JJ, Zuccaro G Jr., Dumot JA, *et al*. Automated graphic assessment of respiratory activity is superior to pulse oximetry and visual assessment for the detection of early respiratory depression during therapeutic upper endoscopy. *Gastrointest Endosc* 2002; **55**: 826–31.

28. Standards and Practice Committee, American Society for Gastrointestinal Endoscopy. Sedation and anesthesia in GI endoscopy. *Gastrointest Endosc* 2008; **68**: 815–26.

29. Roberts S, Echeverria P, Gabriel SA. Devices and techniques for bedside enteral feeding tube placement. *Nutr Clin Prac* 2007; **22**: 412–20.

30. Srinivasa V, Kodali BS. Capnometry in the spontaneously breathing patient. *Curr Opin Anaesthesiol* 2004; **17**: 517–20.

31. Pino RM. The nature of anesthesia and procedural sedation outside of the operating room. Review. *Curr Opin Anaesthesiol* 2007; **20**: 347–51.

32. American Society of Anesthesiologists. Practice Guidelines for sedation and analgesia by non-anesthesiologists: an updated report by the American Society of Anesthesiologist Task Force on sedation and analgesia by non-anesthesiologists. *Anesthesiology* 2002; **96**: 1004–17.

Section 1
Chapter
3

Ventilation

Airway management in the out-of-hospital setting

C. C. Zuver, G. A. Ralls, S. Silvestri, and J. L. Falk

Introduction

The ability to safely and effectively manage the airway is among the most fundamental and challenging aspects of out-of-hospital (OOH) emergency medical treatment. Maintaining the integrity of the airway while providing oxygenation to the brain is critical to a successful outcome. Toward this end, various techniques and a wide array of airway devices are available to Emergency Medical Service (EMS) personnel. Commonly used devices to facilitate OOH airway management encompass a spectrum from basic means, such as the bag-valve mask (BVM), to more advanced and invasive means, such as the esophageal–tracheal combitube, laryngeal mask airway (LMA), laryngeal tube airway (LT), endotracheal tube (ET), and, ultimately, emergency surgical airways.

Airway devices in the out-of-hospital setting

Although the trend in OOH airway management has generally migrated towards more technically advanced means, maintaining oxygenation and ventilation using adjuncts, such as the pocket mask or BVM, remains the most common initial maneuver following simple airway opening. Use of the BVM has been in existence since the advent of early OOH advanced life-support systems. The BVM is still the definitive airway management method used by basic life-support providers in many regions. Throughout the years, numerous airway devices have been introduced to OOH providers in an effort to accomplish oxygenation and ventilation, and to better protect the airway from aspiration of gastric contents.

Even in the early stages of the EMS system, endotracheal intubation (ETI) was recognized as the most ideal method of airway management; however, the level of training and experience necessary to acquire the requisite skill was not available to many EMS personnel. Early airway devices, such as the esophageal obturator airway (EOA) and the esophageal gastric tube airway (EGTA), sought to bridge the gap in airway skills for basic life-support systems by providing lower-tech alternatives to ETI. A less emphasized role of these early "alternative airway devices," yet one that would ultimately define the role of their successors, was that of being "rescue" devices to be used by advanced practitioners who failed in their attempts to accomplish ETI. The use of the EOA and EGTA would ultimately fall out of favor after a succession of publications that focused on their relatively high complication rates and questionable efficacy [1,2].

The esophageal–tracheal combitube, a popular and notable successor to the early alternative airway devices, incorporates the benefits of blind insertion, supraglottic ventilation ports, and some protection from regurgitated gastric contents; however, the slight chance that the tube may pass blindly into the trachea because of its double-lumen design should be noted. Although this device is still widely used in EMS, it requires advanced skills for proper use, and cannot be utilized in patients less than 4½ ft (1.35 m) tall, which makes it unsuitable for most pediatric patients. Additionally, skill retention after a 6-month period following initial training on the combitube was shown to be significantly lower than that following training with an LMA [3]. Other concerns related to the combitube include aspiration, tongue injury, tracheal and esophageal injury, and the inherent risk that the wrong port could be used for ventilation [4–7].

More recently, supraglottic airway devices, such as the LMA, LT, and the Cobra perilaryngeal airway (Cobra PLA), have made their debut in the OOH arena. These devices share similar advantages, such as rapid insertion, ease of skill, low complication

Capnography, Second Edition, ed. J. S. Gravenstein, Michael B. Jaffe, Nikolaus Gravenstein, and David A. Paulus. Published by Cambridge University Press. © Cambridge University Press 2011.

Table 3.1 Comparison of alternative airway devices

Performance task	Combi	LMA	LT
Rate of insertion	1+	2+	3+
Stability during patient movement	3+	1+	3+
Skill retention	1+	2+	3+
Ease of insertion during cardiopulmonary resuscitation	1+	1+	3+
Effectiveness of ventilation	3+	3+	3+
Student or training opportunities	0–1+	3+	0–1+
Pediatric use	0+	3+	3+

Performance scale: 0 = contraindicated; 1+ = average; 2+ = above average; 3+ = excellent.
Combi, esophageal–tracheal combitube; LMA, laryngeal mask airway; LT, laryngeal tube airway.

rates, and efficient ventilation. The LMA and LT have both been shown to have a significantly shorter time to establishing ventilation than the ET or combitube [8,9]. Studies comparing supraglottic devices have not consistently shown one device to be superior to the others. In a study by Gaitini *et al.*, the LMA (ProSeal) and LT were shown to achieve comparable clinical and physiologic parameters during mechanical ventilation in adult patients [10]. Another study by Wiese that focused on the time interval of interrupted chest compressions during airway placement showed the LT to be superior to the LMA in reducing "no-flow time" (104 vs. 124 s) [11]. A cadaver study by Bercker *et al.*, which simulated the pressure in the esophagus with increasing gastric distention and pressure, showed the esophageal occlusive capabilities to be better with the intubating LMA than the LT [12]. Another study by Cook concluded that the LMA (ProSeal) was quicker to insert, and efficacy of ventilation was significantly better, than the LT [13]. Although a conclusive study defining the best supraglottic device for OOH use does not exist, strong support for their use has led some EMS systems to advance the status from their traditional role as a "rescue" airway to that of a primary airway device, representing a fundamental change in emergency airway management. Table 3.1 is a subjective comparative analysis of OOH use of advanced airway devices.

Airway devices such as the BVM, combitube, LMA, LT, and Cobra PLA provide safe and effective options for providers not trained in ETI, and for patients in whom ETI cannot be accomplished.

Endotracheal intubation in the out-of-hospital setting

Despite the evolving presence of alternative airway devices in the OOH setting, and the mounting evidence supporting their use, ETI remains a widely accepted technique for addressing respiratory failure in the OOH setting. When properly performed, ETI affords the combination of oxygenation, ventilation, and airway protection. Endotracheal intubation remains the most definitive means of airway control and is consistently thought of as the "gold standard" [13–16]. The indications for ETI in the OOH setting are similar to those in other clinical settings, and include the patient's inability to oxygenate, inability to ventilate, or inability to protect his/her airway. The American Heart Association (AHA) considers ETI to be the ventilatory adjunct of choice in cardiac arrest since it maintains airway patency, facilitates suctioning of secretions, permits delivery of concentrated oxygen mixtures, provides a route of administration for certain medications, allows delivery of a selected tidal volume, and protects the stomach from insufflation and the trachea from aspiration [17].

Recently, questions have arisen as to the appropriateness of the "gold standard" label assigned to ETI for the management of OOH respiratory failure. A 2008 systematic review article by Lecky *et al.* [18] identified only three randomized control trials performed in urban settings that specifically focused on the true clinical benefit of emergency ETI. Two trials involved adults with non-traumatic, OOH cardiac arrest. One of these trials found a non-significant survival disadvantage in patients randomized to receive a physician-operated intubation versus a combitube (relative risk [RR] 0.44, 95% confidence interval [CI] 0.09 to 1.99) [19]. The second trial detected a non-significant survival disadvantage in patients randomized to paramedic intubation versus an esophageal gastric airway (RR 0.86, 95% CI 0.39 to 1.90) [20]. The third study involved a trial of children requiring airway intervention in the OOH environment [21]. The results indicated no difference in survival (odds ratio [OR] 0.82, 95% CI 0.61 to 1.11) or neurologic outcome (OR 0.87, 95% CI 0.62 to 1.22) between paramedic intubation versus bag-valve mask ventilation and later hospital intubation by emergency physicians. The authors of

the review concluded that "in trauma and pediatric patients, the current evidence base provides no imperative to extend the practice of prehospital intubation in urban systems." They further commented on the need for a large randomized control trial of emergency ETI versus simple airway maneuvers in OOH non-traumatic cardiac arrest [18].

The emerging challenge to the role of ETI in the field is further attributed to concerns such as the high skill level needed to perform intubation successfully, the few live patient experiences available to most EMS personnel, and the difficulties in securing ongoing training for the large volume of advanced providers who need it. The extensive training and experience required for competence to be achieved becomes even more critical when one considers the added difficulties of performing this skill in the OOH environment.

Wang *et al*. demonstrated that greater than 40% of paramedics in a regional EMS setting had no OOH intubations during a 12-month study period, and that almost 70% had two or fewer OOH-ETIs [22]. The study concluded that most rescuers "performed few or no clinical ETI during the study period" and that the infrequency with which providers utilize this skill may hinder their ability to achieve and maintain competency [22].

A study of anesthesia residents performing initial intubations in the operating room under attending supervision showed that a mean of 57 intubations were necessary to achieve a 90% success rate, and over 90 intubations were needed for a success rate greater than 95% to be achieved [23]. Most paramedics are not afforded anywhere near this comparable volume of intubations on live patients. To make matters worse, there is a significant trend towards less operating room time for paramedics due to competition from other healthcare professionals, concerns about liability, and the use of techniques other than ETI in the operating room [24]. As a result, a large proportion of paramedic airway training is performed utilizing simulation on manikins. Although simulation training is an important adjunct, scenarios do not typically reflect the spectrum of patients and the difficult environmental conditions encountered in true field airway emergencies, such as a noisy environment, poor patient positioning, cervical spine immobilization, lack of ancillary personnel to assist in the procedure, lack of neuromuscular blocking agents, intoxicated and combative patients, and blood and vomitus in the airway.

Unrecognized esophageal intubation

Given the difficulties and complexity of performing ETI in the field, it is not unexpected that complications might arise. Complications that can and do occur during intubation attempts in the OOH setting are no different from those that occur in any other clinical setting: oropharyngeal and dental trauma; laryngeal and vocal cord injury; unrecognized esophageal intubation; mainstem bronchus intubation; and extended hypoxic intervals during repeated intubation attempts [17,25]. An additional indirect complication of intubation attempts during cardiac arrest is the delay in, or interruption of, performing chest compressions [17,25].

The most disastrous and concerning complications of intubation are those that can lead to the long-term sequelae of anoxic brain injury or death. As such, unrecognized misplaced intubation (UMI) represents one of the greatest dangers in OOH airway management [17,25]. In the operating room, UMI (esophageal) was found to account for 15% of all catastrophic injuries to patients, including brain damage and death, making it the single, most critical anesthetic incident associated with injuries of this type [26–28]. One can reasonably assume that the risk to patients managed with ETI in the field would be no less significant if no reliable method of detecting an, otherwise, UMI was consistently used.

In one of the first studies, in which the primary objective was to determine the UMI rate for OOH intubations, Katz and Falk reported that an alarming 25% of ETs were not in the trachea at the time of emergency department (ED) arrival [29]. This study, which relied on a systematic ED confirmation algorithm, ushered in an era of heightened concern about the true scale of this problem. An important caveat is that this study was performed at a time when end-tidal CO_2 monitoring – and more specifically, capnography – was not widely available to the EMS systems studied. More recent studies using the same methodology have reported substantially, lower – but still very concerning – UMI rates of 7–10% [30–32]. While the precise incidence of UMI likely varies from system to system based on multiple, complex factors, these studies confirm that UMI represents a significant risk to patients.

Direct visualization

For decades, EMS providers have relied heavily on direct visualization of the endotracheal tube passing

through the cords during intubation for confirming proper placement. Indeed, if the clinician sees the tube pass through the vocal cords, he or she should feel reasonably confident that the tube is in the correct position. However ideal, it is not always possible to achieve direct visualization, particularly in the OOH setting where airways are often contaminated with blood or vomitus. Moreover, even after confirming correct tube placement, the tube can become dislodged at any time during securement and transport.

Chest rise and fall

Another step for confirming tube placement frequently referenced in EMS practice is observing signs such as chest rise with ventilation, auscultation of the chest and epigastrium, and condensation in the endotracheal tube during exhalation. These signs have long been used and taught as reassuring indicators of tracheal tube location. It is, however, clear that these techniques are not foolproof, and additional techniques of confirmation are needed [33]. Lack of clearly observed chest rise in correctly intubated patients may occur in patients with obesity, obstructive or restrictive lung disease, and women with large breasts [33]. Even more concerning, observation of chest rise and fall has been witnessed in the setting of esophageal intubation; the stomach distends with ventilation, causing upward movement of the chest, and gas then escapes up the esophagus, causing the chest wall to fall [33].

Auscultation of breath sounds

Auscultation of breath sounds also can be misleading, and is made ever more difficult in the noisy OOH setting [33]. A study conducted in the controlled setting of an operating room demonstrated that when breath sounds were the only means of identification, anesthesiologists incorrectly identified tube location 15% of the time [34]. Auscultation of the epigastrium fares no better. In thin patients, tracheal breath sounds may be transmitted to the epigastric area, simulating gastric insufflation [33]. However, studies in both dogs and humans reveal that condensation in the endotracheal tube occurs in the majority (approximately 85%) of esophageal intubations [34–35].

Pulse oximetry

Similar to the clinical assessment of tube placement, pulse oximetry has been shown to be inadequate in assuring that ventilation is occurring following an intubation attempt. It may take several minutes for oxygen desaturation to take place in patients with misplaced endotracheal tubes, especially in cases of adequate preoxygenation [33,36]. By the time desaturation occurs, the deleterious consequences of hypoxia to the brain and heart may already be manifest. This is not to suggest that clinical assessment and pulse oximetry after intubation are without use, but, rather, more dependable additional confirmatory techniques are needed to determine and monitor the location of the endotracheal tube if the goal is to reliably avoid complications.

Other confirmatory methods

Additional confirmatory methods for assuring proper endotracheal tube placement have evolved over time. Besides clinical assessment and pulse oximetry, the most common confirmatory methods used by EMS personnel are the esophageal detector device (EDD) and CO_2 measurement by a semiquantitative colorimetric device or, more ideally, digital capnography.

The EDD consists of either a self-inflating bulb or a syringe that is attached to the endotracheal tube, and it exploits the differences in the anatomical and physical properties of the esophagus and trachea to distinguish between the two [17,37]. By using either a bulb or syringe, suction is applied to the endotracheal tube. If the tube is in the esophagus, the suction will cause the floppy esophageal walls to collapse and prevent free aspiration of air through the device [17,37]. If the tube is placed in the trachea, however, the rigid cartilaginous rings will prevent collapse of the airway and permit air movement into the device [17,37]. The EDD has a good performance record in the operating room and in the emergency department, with reported sensitivities and specificities in the 95%+ range [37–40]. The device does have noteworthy limitations, however. An EDD cannot provide continuous, breath-to-breath monitoring of endotracheal tube position, a function of critical importance in the OOH setting due to the potential for tube movement during transport. Additionally, inaccurate results in patients with morbid obesity, pulmonary edema, bronchospastic disease, or endotracheal tube obstruction, as in the case of an airway contaminated with blood or vomitus, have been reported [41,42].

The role of end-tidal CO_2 monitoring in the field

End-tidal carbon dioxide ($PETCO_2$) monitoring has emerged as the technology that can best confirm

endotracheal or endobronchial location of an endotracheal tube. In contradistinction to pulse oximetry, expired CO_2 monitoring can identify problems immediately after intubation, before critical hypoxemia becomes manifest. This gives the clinician an opportunity to rectify the problem before the patient suffers adverse consequences [43]. The trend towards the standardized use of CO_2 monitoring after intubation in the OOH setting has mirrored the trend in hospital-based practice.

The concept of end-tidal CO_2 monitoring is easily taught and well understood by EMS personnel. The concentration of CO_2 expired by the lungs is determined by three processes: (1) cellular CO_2 production, based on the body's metabolic state; (2) transport or delivery of CO_2 to the lungs influences $P_{ET}CO_2$ values significantly and varies with pulmonary perfusion (cardiac output); (3) CO_2 elimination plays a role and is dependent on an intact airway and functioning respiratory mechanism (ventilation). The net result of these processes yields a concentration of exhaled CO_2 that is approximately 100 times greater than the concentration of CO_2 in ambient air [44,45]. Hemodynamically normal adults with normal respiratory function have a sustained exhaled CO_2 concentration of approximately 4–5% (35–45 mm Hg) with a normal minute ventilation as opposed to the CO_2 concentration in the esophagus, which measures less than 0.3% [46–47]. By sampling and measuring the $P_{ET}CO_2$ value of the gas coming from the endotracheal tube, one can determine its location to be within the airway – or not – assuming there is pulmonary blood flow. In the setting of cardiopulmonary resuscitation (CPR), where pulmonary blood flow is much lower, one would expect the $P_{ET}CO_2$ to be much lower also [48] (see Figure 3.1). In a prospective observational study of 153 patients intubated in the OOH setting, Figure 3.2 depicts the difference between the UMI rate with and without the use of continuous end-tidal CO_2 monitoring which is quite remarkable [30].

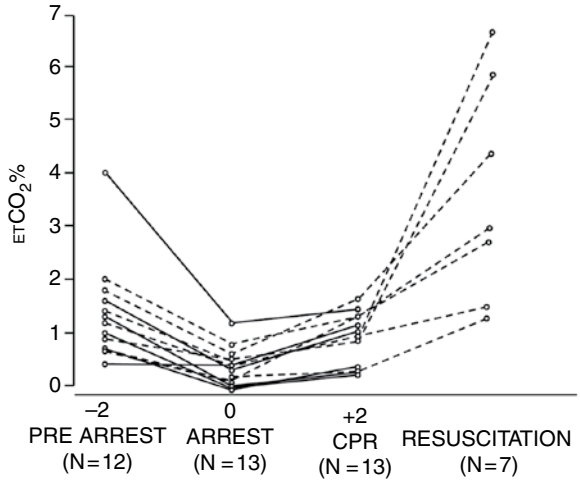

Figure 3.1 End-tidal CO_2 concentration ($ETCO_2$) before cardiac arrest, at the onset of arrest but before precordial compression, 2 min after the start of CPR, and immediately after successful resuscitation in 10 patients on 13 occasions. Solid lines represent non-resuscitated patients, and broken lines resuscitated patients. [From: Falk JL, Rackow EC, Weil MH. End-tidal carbon dioxide concentration during cardiopulmonary resuscitation. *N Engl J Med* 1988; **318**: 607–11.]

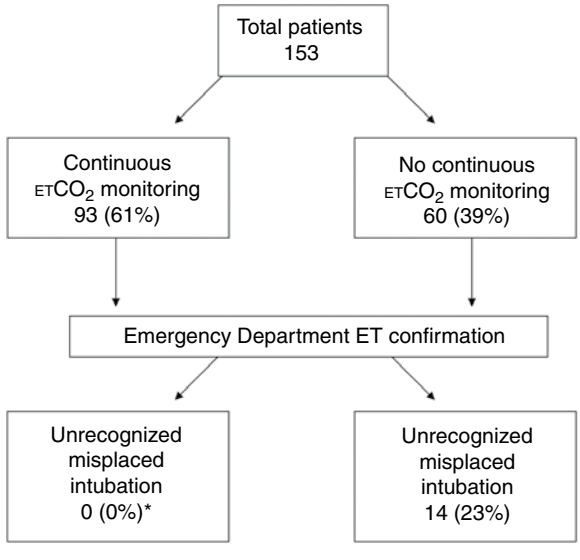

Figure 3.2 Prehospital ET placement and $ETCO_2$ use. *Misplaced intubation rate greater for no $ETCO_2$ monitoring group vs. $ETCO_2$ monitoring group by 23.3% (95% CI: 13.4%, 36.0%). [From: Silvestri S, Ralls GA, Krauss B, *et al.* The effectiveness of out-of-hospital use of continuous end tidal carbon dioxide monitoring on the rate of unrecognized misplaced intubation within a regional EMS system. *Ann Emerg Med* 2005; **45**: 497–503.]

Definitions

Capnometry represents the measurement (quantitative) and *numerical* display of CO_2 concentration, or partial pressure, at the patient's airway. Capnography represents the measurement (quantitative) and *graphical* display of CO_2 concentration, or partial pressure, at the patient's airway. Figure 3.3 demonstrates a typical alveolar waveform in an OOH tracing from an intubated and underventilated patient.

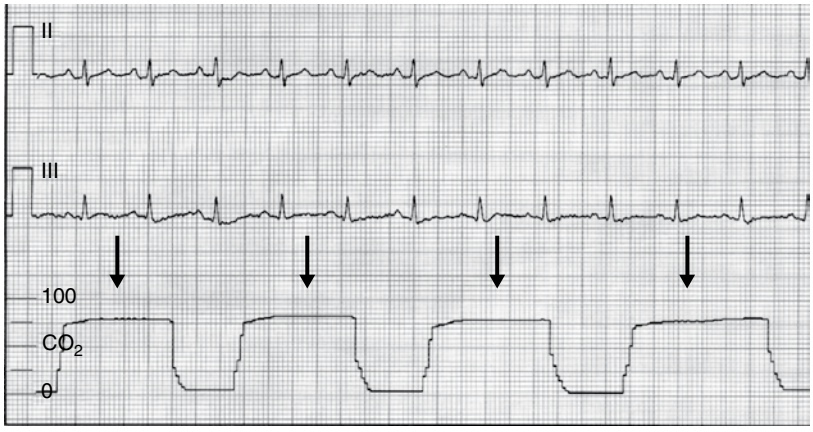

Figure 3.3 Prehospital (LifePak-12®) tracing of characteristic CO_2 waveforms (arrows) in an intubated patient being ventilated via a BVM status-post successful resuscitation.

Semiquantitative colorimetric CO_2 detectors

A semiquantitative colorimetric device is the most basic capnometer, and consists of a clear dome overlying a piece of litmus paper that changes color when CO_2 is detected [44]. A typical device would have the capacity to produce one of three readings: A reading (purple) – exhaled $CO_2 \leq 2.28$ mm Hg (≤0.3%); B reading (beige) – exhaled CO_2 of 3.8–7.6 mm Hg (0.5–1.0%); and C reading (yellow) – exhaled CO_2 >15.2 mm Hg (>2.0%) [49]. These devices are low cost, easy to use, and generally provide reliable confirmation of tube placement, significantly enhancing any clinical assessment possible in the field. Semiquantitative colorimetric devices are limited by their inability to provide reliable information in very low perfusion states (e.g., prolonged cardiac arrest), short function duration, and their lack of a printed record to substantiate correct tube placement if questions arise.

Studies of semiquantitative colorimetric devices in cardiac arrest patients have reported sensitivities and specificities of 69–72% and 100%, respectively [26,50]. While all esophageal intubations were correctly identified by the reading on the device remaining purple (low CO_2), some tracheally placed tubes did not result in a color change to beige or yellow. This could have prompted paramedics to remove a correctly placed endotracheal tube. In cardiac arrest patients, the low CO_2 may result from markedly diminished pulmonary blood flow despite endotracheal placement of the tube. These resultant low CO_2 values may be insufficient to cause a color change in colorimetric devices. In a study by Hayden *et al.* on patients undergoing OOH cardiac arrest, a sensitivity of 95.6% was demonstrated with the colorimetric CO_2 device [47]. In this study, a large number of the positive results were in the intermediate (beige) range on the detector, not a surprising finding since, in addition to a low pulmonary blood flow during CPR, there is also a tendency to hyperventilate during CPR with manual ventilation [47].

Even in cardiac arrest, colorimetric CO_2 devices provide useful information. When a positive result is obtained, the clinician can be assured that the endotracheal tube has been placed correctly [17]. When a negative result is obtained, the situation is more complex, and several things must be considered. Failure to obtain a color change during cardiac arrest can be an indicator of prolonged arrest time with poor pulmonary perfusion (low cardiac output), severe ventilation–perfusion mismatch as in a massive pulmonary embolus, or a misplaced endotracheal tube [51]. If a negative result is obtained with a colorimetric device during cardiac arrest, a second method of detection is recommended such as the esophageal detector device or repeat direct visualization [17,25]. The algorithm in Figure 3.4 describes a suggested management pathway for OOH providers that utilizes qualitative (colorimetric) CO_2 airway confirmatory devices.

Capnography in the out-of-hospital setting

Quantitative devices typically utilize infrared absorption spectroscopy, since – of the exhaled gases – only CO_2 strongly absorbs infrared light [50]. The sensor unit may be placed in different locations, depending on the method of sampling of exhaled gases. Mainstream sampling, often used for intubated patients in the prehospital setting, uses a sensor attached directly to the airway, permitting exhaled gases to pass directly through it [44]. The sidestream technique aspirates gas

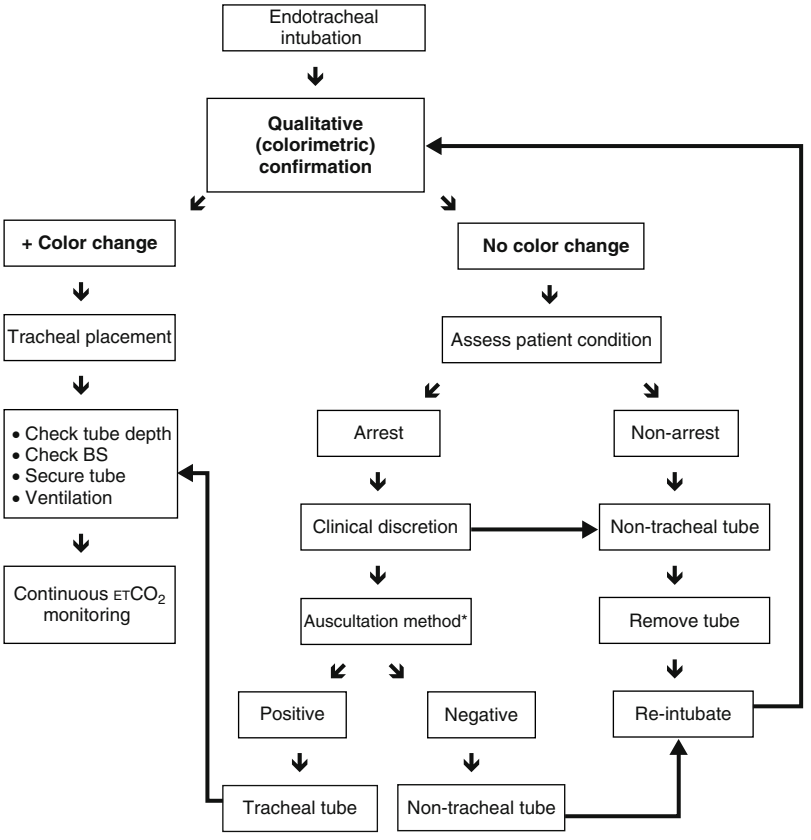

Figure 3.4 Out-of-hospital airway confirmation algorithm utilizing qualitative (colorimetric) $ET CO_2$ confirmation.
*Clinical maneuvers, such as auscultation (chest, epigastric) and direct laryngoscopy may be utilized at provider discretion, but clinicians must be aware of their limitations in discriminating between esophageal and tracheal intubation.

Figure 3.5 Prehospital (LifePak-12®) tracing of waveforms (arrows) during an OOH asystolic patient undergoing CPR and attempted resuscitation. Note that although the amplitude of the waveform is low (corresponding to an $ET CO_2$ <10 mm Hg), the characteristic waveform is still present and indicative of endotracheal location of the tube.

from the airway and delivers it to the remote sensor [44,50]. These devices provide a digital $PET CO_2$ concentration expressed either in millimeters of mercury (mm Hg) or in percent CO_2 of expired air.

Continuous "waveform" capnography represents an advance in CO_2 monitoring technology that offers improved reliability, particularly with respect to utilization in patients in cardiac arrest. This technology is readily available in many OOH systems and, in some regions, is considered a mandatory device for Advanced Life Support units [52]. The threshold for detection of exhaled CO_2 is significantly lower for capnometry and capnography as opposed to colorimetric devices [38]. Additionally, the tracing produced during measurement of CO_2 from a properly placed endotracheal tube is characteristic and recognizable, even when the quantitative $PET CO_2$ value is quite low (see Figure 3.5). The reliability of the capnographic waveform during

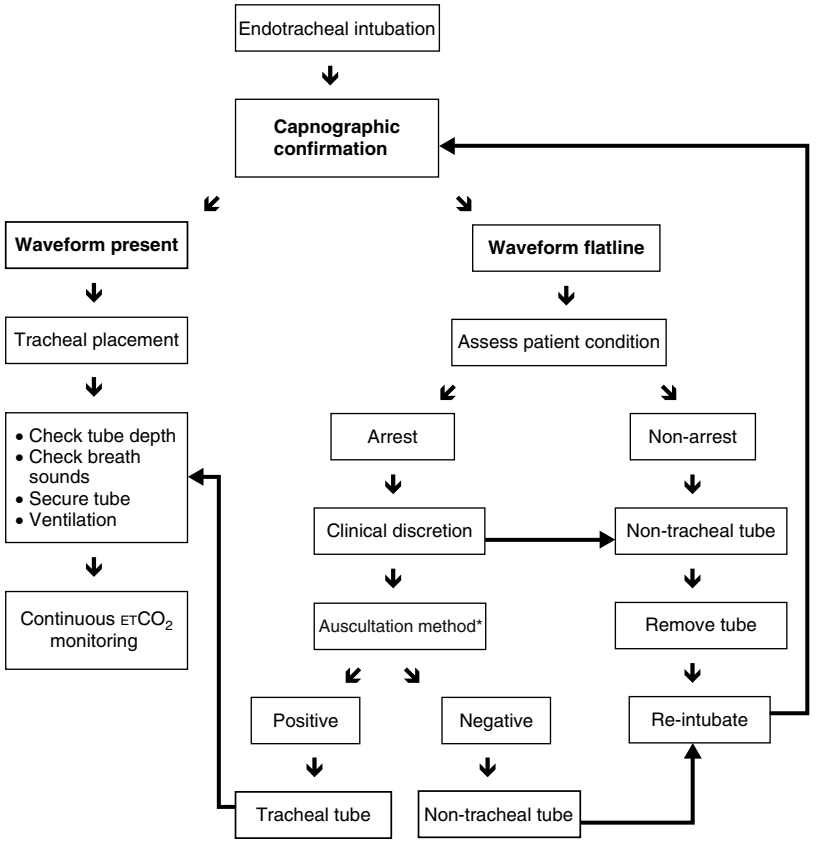

Figure 3.6 Out-of-hospital airway confirmation algorithm utilizing quantitative (capnography) $ETCO_2$ confirmation.
*Clinical maneuvers, such as auscultation (chest, epigastric) and direct laryngoscopy may be utilized at provider discretion, but clinicians must be aware of their limitations in discriminating between esophageal and tracheal intubation.

cardiac arrest and resuscitation has been verified in both animal and human models [48,53]. If the proper waveform is present, regardless of its amplitude, tube placement can be confidently judged to be correct, although endobronchial intubation cannot be differentiated from endotracheal [25,54]. Every major study, either evaluating the efficacy of capnography in arrest and non-arrest patients or comparing it to other methods of detection, has demonstrated the superiority of continuous waveform capnography in this setting. Knapp *et al.* revealed capnography to have a 0% error rate in a study on non-arrest intensive care unit (ICU) patients, clearly performing better than auscultation, a self-inflating esophageal detector device, or a lighted stylet [46]. A study by Singh *et al.* showed capnography to also be superior to the semiquantitative colorimetric device in an OOH setting in both arrest and non-arrest patients [55]. This was further verified in a very convincing study by Grmec of 345 OOH intubations in which capnography had a 100% sensitivity and specificity in both arrest and non-arrest patients compared to capnometry, which had 88% sensitivity and 100% specificity in the arrest population [54]. A study by Silvestri confirmed that capnography was a reliable indicator of both endotracheal and esophageal intubation in cardiac arrest patients by demonstrating that, when employed appropriately, capnography virtually eliminates the problem of UMI [56]. The algorithm in Figure 3.6 describes a suggested management pathway for OOH providers utilizing quantitative (capnographic) $PETCO_2$ confirmation.

In addition to the ability to confirm accurately endotracheal tube location, capnography has additional clinical applications for EMS. In cardiac arrest, the return of spontaneous circulation corresponds to an increase in pulmonary gas exchange and, subsequently, $ETCO_2$ levels. Thus a sudden increase in $ETCO_2$ levels serves as a surrogate indicator to assess for a pulse, thereby decreasing the need for interrupting chest compressions during resuscitation (see Figure 3.7). Capnography has also proven to be useful in acute bronchospasm as a gauge of severity and response to treatment [57]. In spontaneously breathing patients, capnography devices can be configured to provide an immediate signal of hypoventilation or apnea via an "apnea alarm." Table 3.2 summarizes

Table 3.2 Comparison of esophageal detector device (EDD), colorimetric $ETCO_2$ detection (capnometry), and waveform capnography (capnography)

Conditions	EDD	Capnometry	Capnography
Use in patients with adequate perfusion	3+	4+	4+
Use in patients with cardiac arrest (static evaluation)	3+	2–3+	4+
Ability to monitor continuously	1+	2–3+	4+
Use in pediatric patients (<5 y/o)	1+	2–3+	4+
Use in pregnancy	0	2–3+	4+

scale: 0, contraindicated; 1, least useful, to 4+, most useful.

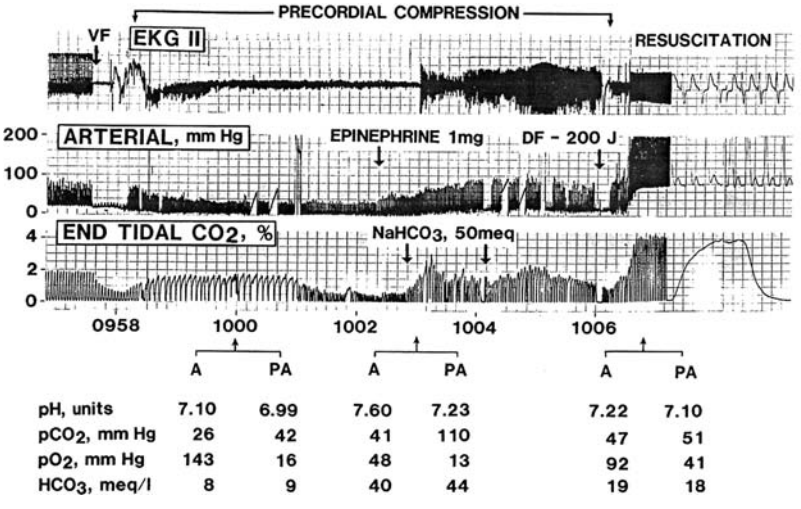

Figure 3.7 Serial changes in the $ETCO_2$ concentration and arterial (A) and mixed venous (PA) blood gases in a representative patient before and immediately after cardiac arrest, during precordial compression, and after defibrillation (DF) and resuscitation. The transient increase in the $ETCO_2$ after the administration of sodium bicarbonate ($NaHCO_3$) is also demonstrated. The original tracing has been modified because of space limitations. [From: Falk JL, Rackow EC, Weil MH. End-tidal carbon dioxide concentration during cardiopulmonary resuscitation. *N Engl J Med* 1988; **318**: 607–11.]

a subjective comparative analysis of the esophageal detector device, capnometry, and capnography.

Conclusion

Out-of-hospital airway management is an evolving topic that requires careful evaluation of the risks and benefits associated with the currently available options. The optimal technique is one that maximizes patient oxygenation and ventilation, while minimizing the risk of hypoxic brain injury and other serious complications. Alternative airways, once relegated to the role of rescue or back-up devices, now play a primary role in facilitating expeditious, effective ventilation and oxygenation.

When performed by skilled and experienced providers, ETI remains the most effective method for the management of OOH respiratory failure. Provider skill level, frequency of live patient intubation experiences, the availability of ongoing training, and clinical necessity may significantly vary from one EMS setting to another. Although ETI has been long regarded as the best option for OOH management of respiratory failure, a more progressive view in the era of modern alternative airway devices may continue to challenge this assumption.

Due to the limitations of OOH clinical assessment after intubation, a compulsory method of determining proper tube location is an essential component of EMS airway management protocols. Capnography is shown to be the most useful modality for determining tube location, both with and without cardiac arrest. (See Figures 3.4 and 3.6 for sample airway confirmation algorithms utilizing qualitative and quantitative $ETCO_2$.)

The use of capnography for OOH airway management enhances patient safety and can prevent the problem of UMI and should be a mandatory component of OOH airway management.

Airway Management - Adult

Basic Life Support

- If suspicion of trauma, maintain C-spine immobilization
- Suction all debris, secretions from airway
- Supplemental 100% oxygen, then BVM ventilate if indicated

Advanced Life Support

- Monitor end-tidal CO_2 (capnography) and oxygen saturation continuously
- Follow algorithm if invasive airway intervention is indicated (ET or LTA):
  - Apnea
  - Decreased level of consciousness with respiratory failure (i.e. hypoxia [O_2 sat < 90] not improved by 100% oxygen, and/or respiratory rate < 8)
  - Poor ventilatory effort (with hypoxia not improved by 100% oxygen)
  - Unable to maintain patent airway
- Following placement of ET or LTA, confirm proper placement:
  - Assess epigastric sounds, breath sounds, and chest rise and fall
  - Observe for presence of alveolar waveform on capnography
  - Record tube depth and secure in place using a commercial tube holder
  - Utilize head restraint devices (i.e., "head-blocks") or rigid cervical collar and long spine board immobilization as needed to help secure airway device in place

Capnography/$ET CO_2$ Monitoring

- Digital capnography (waveform) is the system standard for $ETCO_2$ monitoring
- With the exception of on-scene equipment failure, patients should not be routinely switched from digital capnography (e.g., LifePak 12) to a colorimetric device for monitoring $ETCO_2$
- In the event digital capnography is not possible due to on-scene equipment failure, continuous colorimetric monitoring of $ETCO_2$ is an acceptable alternative
- Continuous $ETCO_2$ monitoring is a mandatory component of invasive airway management
  - If $ETCO_2$ monitoring cannot be accomplished by either of the above methods, the invasive device must be removed, and the airway managed non-invasively
  - If an alveolar waveform is not present with capnography (i.e., flatline), remove the ET, and proceed to the next step in the algorithm

Briefly check filter-line coupling to assure it is securely in place

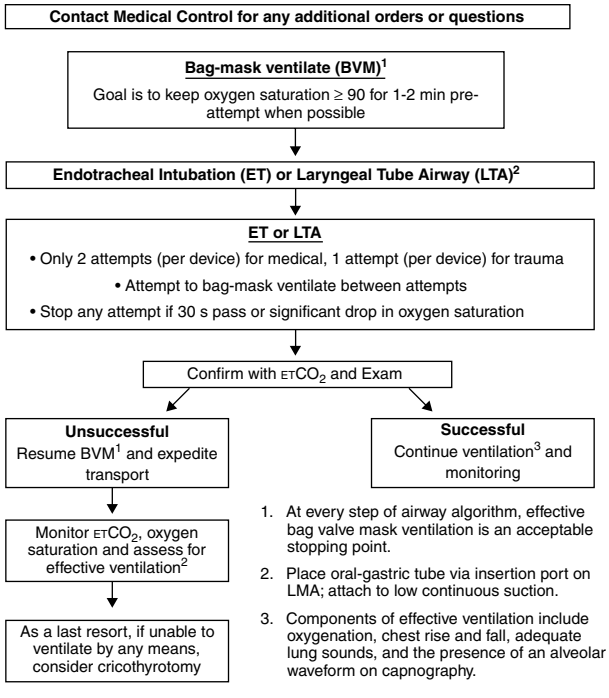

1. At every step of airway algorithm, effective bag valve mask ventilation is an acceptable stopping point.
2. Place oral-gastric tube via insertion port on LMA; attach to low continuous suction.
3. Components of effective ventilation include oxygenation, chest rise and fall, adequate lung sounds, and the presence of an alveolar waveform on capnography.

Figure 3.8 Example protocol for OOH airway management.

How can we combine these concepts of airway management?

A sample OOH airway management protocol is detailed in Figure 3.8. This protocol includes utilization of advanced airway devices as well as airway confirmation and monitoring.

References

1. Hankins DG, Carruthers N, Frascone RJ, Long LA, Campion BC. Complication rates for the esophageal obturator airway and endotracheal tube in the prehospital setting. *Prehosp Disaster Med* 1993; **8**: 117–21.
2. Smith JP, Bodai BI, Seifkin A, Palder S, Thomas V. The esophageal obturator airway: a review. *JAMA* 1983; **250**: 1081–4.
3. Vertongen VM, Ramsay MP, Herbison P. Skills retention for insertion of the Combitube and laryngeal mask airway. *Emerg Med (Fremantle)* 2003; **15**: 459–64.
4. Calkins TR, Miller K, Langdorf MI. Success and complication rates with prehospital placement of an esophageal–tracheal combitube as a rescue airway. *Prehosp Disaster Med* 2006; **21**(2 Suppl 2): 97–100.
5. Vézina MC, Trépanier CA, Nicole PC, Lessard MR. Complications associated with the esophageal–tracheal Combitube in the pre-hospital setting. *Can J Anaesth* 2007; **54**: 124–8.
6. McGlinch BP, Martin DP, Volcheck GW, Carmichael SW. Tongue engorgement with prolonged use of the esophageal–tracheal Combitube. *Ann Emerg Med* 2004; **44**: 320–2.
7. Stoppacher R, Teggatz JR, Jentzen JM. Esophageal and pharyngeal injuries associated with the use of the esophageal–tracheal Combitube. *J Forensic Sci* 2004; **49**: 586–91.
8. Hoyle JD Jr., Jones JS, Deibel M, Lock DT, Reischman D. Comparative study of airway management techniques with restricted access to patient airway. *Prehosp Emerg Care* 2007; **11**: 330–6.
9. Russi CS, Miller L, Hartley MJ. A comparison of the King-LT to endotracheal intubation and Combitube in a simulated difficult airway. *Prehosp Emerg Care* 2008; **12**: 35–41.
10. Gaitini LA, Vaida SJ, Somri M, *et al.* A randomized controlled trial comparing the ProSeal Laryngeal Mask Airway with the Laryngeal Tube Suction in mechanically ventilated patients. *Anesthesiology* 2004; **101**: 316–20.
11. Wiese CH, Bartels U, Bergmann A, *et al.* Using a laryngeal tube during cardiac arrest reduces "no flow time" in a manikin study: a comparison between laryngeal tube and endotracheal tube. *Wien Klin Wochenschr* 2008; **120**: 217–23.
12. Bercker S, Schmidbauer W, Volk T, *et al.* A comparison of seal in seven supraglottic airway devices using a cadaver model of elevated esophageal pressure. *Anesth Analg* 2008; **106**: 445–8.
13. Cook TM, Cranshaw J. Randomized crossover comparison of ProSeal Laryngeal Mask Airway with Laryngeal Tube Sonda during anaesthesia with controlled ventilation. *Br J Anaesth* 2005; **95**: 261–6.
14. Clinton JE, McGill JW. Basic airway management and decision-making. In: Roberts JR, Hedges JR (eds.) *Clinical Procedures in Emergency Medicine*, 3rd edn. Philadelphia, PA: WB Saunders, 1998; 1–15.
15. Nolan JD. Prehospital and resuscitative airway care: should the gold standard be reassessed? *Curr Opin Crit Care* 2001; **7**: 413–21.
16. Pennant JH, Walker MB. Comparison of the endotracheal tube and laryngeal mask airway management by paramedic personnel. *Anesth Analg* 1992; **74**: 531–4.
17. American Heart Association. Guidelines 2005 for Cardiopulmonary Resuscitation and Emergency Cardiovascular Care, Part 7.1: Adjuncts for airway control and ventilation. *Circulation* 2005; **112**(Suppl IV): IV-51.
18. Lecky F, Bryden D, Little R, Tong N, Moulton C. Emergency intubation for acutely ill and injured patients. *Cochrane Database Syst Rev* 2008; **16**: CD001429.
19. Rabitsch W, Schellongowski P, Staudinger T, *et al.* Comparison of a conventional tracheal airway with the Combitube in an urban emergency medical services system run by physicians. *Resuscitation* 2003; **57**: 27–32.
20. Goldenberg IF, Campion BC, Siebold CM, McBride JW, Long LA. Esophageal gastric tube airway vs. endotracheal tube in prehospital cardiopulmonary arrest. *Chest* 1986; **90**: 90–6.
21. Gausche M, Lewis RJ, Stratton SJ, *et al.* Effect of out-of-hospital pediatric endotracheal intubation on survival and neurological outcome: a controlled clinical trial. *JAMA* 2000; **283**: 783–90.
22. Wang HE, Kupas DF, Hostlet D, *et al.* Procedural experience with out-of-hospital endotracheal intubation. *Crit Care Med* 2005; **33**: 1718–21.
23. Konrad C, Schüpfer G, Wietlisbach M, Gerber H. Learning manual skills in anesthesiology: is there a recommended number of cases for anesthetic procedures? *Anesth Analg* 1998; **86**: 635–9.
24. Johnston BD, Seitz SR, Wang HE. Limited opportunities for paramedic student endotracheal

intubation training in the operating room. *Acad Emerg Med* 2006; **13**: 1051–5.

25. Falk JL, Sayre MR. Confirmation of airway placement. *Prehosp Emerg Care* 1999; **3**: 273–8.
26. MacLeod BA, Heller MB, Gerard J, Yealy DM, Menegazzi JJ. Verification of endotracheal tube placement with colorimetric end-tidal CO_2 detection. *Ann Emerg Med* 1991; **20**: 267–70.
27. Goldberg JS, Rawle PR, Zehnder JL, Sladen RN. Colorimetric end-tidal carbon dioxide monitoring for tracheal intubation. *Anesth Analg* 1990; **70**: 191–4.
28. Cheney FW, Posner K, Caplan RA, Ward RJ. Standard of care and anesthesia liability. *JAMA* 1989; **261**: 1599–633.
29. Katz SH, Falk JL. Misplaced endotracheal tubes by paramedics in an urban emergency medical services system. *Ann Emerg Med* 2001; **37**: 32–7.
30. Silvestri S, Ralls GA, Krauss B, *et al.* The effectiveness of out-of-hospital use of continuous end tidal carbon dioxide monitoring on the rate of unrecognized misplaced intubation within a regional EMS system. *Ann Emerg Med* 2005; **45**: 497–503.
31. Jemmett ME, Kendall KM, Fourre MW, Burton JH. Unrecognized misplaced endotracheal tubes in a mixed urban to rural setting. *Acad Emerg Med* 2003; **10**: 961–5.
32. Jones JH, Murphy MP, Dickson RL, Somerville GG. Emergency physician verified prehospital intubation, missed rates by ground paramedics [abstract]. *Acad Emerg Med* 2003; **10**: 448–9.
33. Birmingham PK, Cheney FW, Ward RJ. Esophageal intubation: a review of detection techniques. *Anesth Analg* 1986; **65**: 886–91.
34. Andersen KH, Hald A. Assessing the position of the tracheal tube: the reliability of different methods. *Anaesthesia* 1989; **44**: 984–5.
35. Kelly JJ, Eynon CA, Kaplan JL, de Garavilla L, Dalsey WC. Use of tube condensation as an indicator of endotracheal tube placement. *Ann Emerg Med* 1998; **31**: 575–8.
36. Guggenberger H, Lenz G, Federle R. Early detection of inadvertent oesophageal intubation: pulse-oximetry vs. capnography. *Acta Anaesthiol Scand* 1989; **33**: 112–15.
37. Bozeman WP, Hexter D, Liang HK, Kelen GD. Esophageal detector device versus detection of end-tidal carbon dioxide level in emergency intubation. *Ann Emerg Med* 1996; **27**: 595–9.
38. O'Connor RE, Swor RA. Verification of endotracheal tube placement following intubation. National Association of EMS Physicians Standards and Clinical Practices Committee. *Prehosp Emerg Care* 1999; **3**: 248–50.
39. Pelucio M, Halligan L, Dhindsa H. Out-of-hospital experience with the syringe esophageal detector device. *Acad Emerg Med* 1997; **4**: 563–8.
40. Kasper CL, Deem S. The self-inflating bulb to detect esophageal intubation during emergency airway management. *Anesthesiology* 1998; **88**: 898–902.
41. Lang DJ, Wafai Y, Salem MR, *et al.* Efficacy of self-inflating bulb in confirming tracheal intubation in the morbidly obese. *Anesthesiology* 1996; **85**: 246–53.
42. Coontz DA, Gratton M. Rules of engagement: how to reduce the incidence of unrecognized esophageal intubations. *JEMS* 2002; **27**: 44–59.
43. Vaghadia H, Jenkins L, Ford R. Comparison of end-tidal carbon dioxide, oxygen saturation, and clinical signs for detection of oesophageal intubation. *Can J Anaesth* 1989; **36**: 560–4.
44. Krauss B. Capnography in EMS: a powerful way to objectively monitor ventilatory status. *JEMS* 2003; **28**: 28–41.
45. Vukmir RB, Heller MB, Stein KL. Confirmation of endotracheal tube placement: a miniaturized infrared qualitative CO_2 detector. *Ann Emerg Med* 1991; **20**: 726–9.
46. Knapp S, Kofler J, Stoiser B, *et al.* The assessment of four different methods to verify tracheal tube placement in the critical care setting. *Anesth Analg* 1999; **88**: 776–80.
47. Hayden SR, Sciammarella J, Viccello P, Thode H, Delagi R. Colorimetric end-tidal CO_2 detection for verification of endotracheal tube placement in out-of-hospital cardiac arrest. *Acad Emerg Med* 1995; **2**: 499–502.
48. Falk JL, Rackow EC, Weil MH. End-tidal carbon dioxide concentration during cardiopulmonary resuscitation. *N Engl J Med* 1988; **318**: 607–11.
49. Wayne MA, Slovis CM, Pirrallo RG. Management of difficult airways in the field. *Prehosp Emerg Care* 1999; **3**: 290–6.
50. Sanders AB. Capnometry in emergency medicine. *Ann Emerg Med* 1989; **18**: 1287–90.
51. Ornato JP, Shipley JB, Racht EM, *et al.* Multicenter study of a portable, hand-size, colorimetric end-tidal carbon dioxide detection device. *Ann Emerg Med* 1992; **21**: 518–23.
52. Chapter 64J-1, Florida Administrative Code, Emergency Medical Services. Department of Health, Tallahassee, Fl 32399. December 25, 2008. Available online at http://www.doh.state.fl.us/demo/ems/RulesStatutes/RulesPDFS/64J-1EmergencyMedicalServices-Final10–31–08.pdf. (Accessed June 10, 2009.)
53. Sayah AJ, Peacock WF, Overton DT. End-tidal CO_2 measurement in the detection of esophageal

intubation during cardiac arrest. *Ann Emerg Med* 1990; **19**: 857–60.

54. Grmec S. Comparison of three different methods to confirm tracheal tube placement in emergency intubation. *Intens Care Med* 2002; **28**: 701–4.
55. Singh A, Megargel RE, Schnyder MR, O'Connor RE. Comparing the ability of colorimetric and digital waveform end tidal capnography to verify endotracheal tube placement in the prehospital setting [abstract]. *Acad Emerg Med* 2003; **10**: 466–7.
56. Silvestri S, Ralls G, Papa L, *et al.* Emergency department capnographic confirmation of endotracheal tube position in out-of-hospital cardiac arrest patients [abstract]. *Ann Emerg Med* 2007; **50**: S4.
57. Yaron M, Padyk P, Hutsinpiller M, Cairns CB. Utility of the expiratory capnogram in the assessment of bronchospasm. *Ann Emerg Med* 1996; **28**: 403–7.

Section 1
Chapter
4

Ventilation

Airway management in the hospital setting

A. G. Vinayak and J. D. Truwit

In the hospital setting, patients in the emergency room and intensive care units are at high risk for complications. Many of these adverse events are related to perturbations in respiration. Difficult airway intubation, incorrect placement or dislodgement of an endotracheal tube, and inappropriate intubation of the trachea with an enteral tube are common culprits leading to respiratory morbidity. An array of invasive and noninvasive strategies is available for monitoring these situations in the hospital. We will review the specific role of capnography in the successful airway management of the hospitalized patient.

Confirmation of airway intubation

Significant morbidity and mortality is associated with adverse respiratory events that occur during attempts to achieve endotracheal intubation [1]. Initiating airway intubation in the emergency room or in the intensive care unit allows significant opportunity for miscalculations that can take the form of esophageal intubations, delays in securing ventilation due to a difficult airway, and inadequate ventilation due to inappropriate settings. Failure to establish airway control promptly appears to occur at higher rates in emergent situations such as the intensive care and emergency room settings [2].

Detection of end-tidal carbon dioxide ($P_{ET}CO_2$) can help confirm that endotracheal tubes have been placed in the major airways, and not in the esophagus. This process is often accomplished by attaching a single-use, colorimetric capnometer to the tube after an airway intubation attempt. The color change allows a semiquantitative assessment of the presence of carbon dioxide (CO_2). Additional quantitative information may be obtained by continuous displays of the capnogram waveforms and/or numerical values. The most common technology used is that of infrared absorption.

Commercially available, disposable devices for CO_2 monitoring have been available for over 20 years. Usually the devices have inlet and outlet ports that allow connection to standard bag-mask devices and endotracheal tube adaptors. Within the small plastic housing, a chemically impregnated mesh can be observed through a clear viewing window. The chemical indicator is a base, metacresol purple, which, when exposed to CO_2, undergoes a color change from purple to yellow. On the window frame is a color-coded comparison chart to determine semiquantitatively the fraction of exhaled CO_2 that has chemically reacted [3].

Three ranges of the CO_2 value can be assessed with this device. The mesh indicator will remain purple between 0.03% and 0.5% CO_2. A darker taupe to beige appearance is seen when CO_2 is between 0.5% and 2.0%. Finally, exposure to 2.0% to 5.0% CO_2 levels will produce pale yellow colors. When fresh gas is inspired or delivered, the color will revert to its initial purple appearance. The absence of any appreciable color change is highly suggestive of esophageal intubation.

Confirmation of CO_2 in the airway occurs quickly with this device. The mesh indicator can be stored for over a year in its individually wrapped foil case and, once used, it will produce color changes for up to 15 min when exposed to humidified gases [4]. Disposable, colorimetric capnometers are available in several sizes, including a pediatric device for children older than 6 months of age and over 15 kg, and are designed to decrease the larger deadspace introduced by their adult counterparts [5].

In clinical practice, colorimetric semiquantitative capnometers are highly sensitive and specific after emergent intubation in the pre-hospital and hospital settings [6,7]. The efficacy of this type of capnometry

Capnography, Second Edition, ed. J. S. Gravenstein, Michael B. Jaffe, Nikolaus Gravenstein, and David A. Paulus. Published by Cambridge University Press. © Cambridge University Press 2011.

is greater than auscultation alone [6]. In another comparison of tube placement verification, observers were separated into two groups based on level of airway experience [8]. The least error occurred in both the novice and experienced groups when using CO_2 evaluation rather than auscultation, tracheal transillumination, and self-inflating bulb tests. Given the ease, reliability, and cost-effectiveness of rapid CO_2 detection, recent Advanced Cardiac Life Support (ACLS) recommendations strongly suggest that CO_2 assessment be used for validating successful airway intubation in adult patients [9]. While similar data are supportive of this technique, routine application in the pediatric population requires further evaluation, especially in the resuscitation of neonates and infants [10].

A truly competent CO_2 assessment of airway intubation mandates the awareness of conditions and events that can lead to false-positive and false-negative results. The most important cause of a false-negative result (the lack of CO_2 detection with successful airway intubation) occurs when readings are obtained in the patient prior to adequate restoration of circulation immediately following cardiac arrest. In this situation, inadequate systemic circulation correlates with deficient pulmonary circulation. Ineffective transfer of tissue-generated CO_2 to the lungs leads to insufficient alveolar CO_2 elimination. The minimum CO_2 required to produce a color change is >0.54% (4.1 mm Hg) [11]. End-tidal fraction ($FETCO_2$) values between 0.5% and 2.5% have been demonstrated during effective cardiopulmonary resuscitation (CPR) for cardiac arrest [12].

Given the strong emphasis on airway and breathing in the ABCs of CPR (**A**irway, **B**reathing, **C**irculation), it is not surprising that clinical trials suggest that the lack of circulation is a significant cause of error when using colorimetric CO_2 tube verification postarrest. False-negative rates as high as 23% to 31% have been reported when arrested patients were included in the studies of this airway confirmation test [13]. Furthermore, improper cuff inflation postintubation may add to these rates [14]. Recent consensus updates that emphasize uninterrupted CPR during resuscitation attempts may help avoid these errors [15].

Additional causes of false-negative CO_2 assessment of endotracheal tube positioning include the following situations: tube malfunction (kinked or obstructed tubing); apparatus disconnection; markedly increased deadspace; and pulmonary vascular obstruction. If quantitative capnography is being utilized, any of these conditions can lead to a significant lowering of CO_2 readings that may make tracheal tube position appear equivocal [4]. Excessive positive end-expiratory pressure (PEEP), either administered with a PEEP valve or a result of generated auto-PEEP in the obstructed patient, can lead to increases in deadspace, or even cardiovascular collapse, and can similarly interfere with CO_2 measurement [16].

The inaccurate detection of CO_2 when the tube is actually not positioned in the trachea – a false positive – can lead to serious consequences as well. If the tube were located in the pharynx, CO_2 would be expectedly present. Though not common, CO_2 can be detected even when the esophagus is fully intubated. The recent ingestion of carbonated beverages and/or antacids have been associated with false positivity due to CO_2 release [17].

The most frequent cause of a false-positive result occurs when a large amount of expired gas is forced into the esophagus during bag-mask ventilation. In these cases, CO_2 concentrations in the esophagus, while usually lower than 0.7% [18,19], can be as high as 2.0% or greater [20], and produce semiquantitative colorimetric assessment identical to tracheal estimations. Capnography, in this scenario, has exhibited CO_2 waveforms in up to one-third of esophageal intubations. As would be predicted, subsequent washout of CO_2 occurs with delivery of each successive breath. As a generally accepted rule, several breaths, ideally six, should be administered before attaching a CO_2 detector. If waveform capnography is available, washout may be readily observed with each breath after initial esophageal intubation (see Figure 4.1).

It is important to note that successful airway intubation and correct identification of $PETCO_2$ does not remove the possibility of an endobronchial mainstem intubation. Capnography can produce waveforms that are normal in appearance and end-tidal values within normal limits [21]. Endobronchial intubation is commonly associated with subsequent arterial oxygen desaturation [22]. In addition, increased airway pressures, lung field auscultation, and radiographic correlation remain the diagnostic elements crucial in identifying this morbidity.

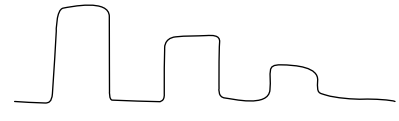

Figure 4.1 Schematic depiction of sequential capnography waveform from esophageal intubation with an initial false-positive $ETCO_2$.

Despite these pitfalls, capnographic assessment – either semiquantitative colorimetric or waveform capnography after airway intubation – remains the most reliable and immediate mode for assessment of successful intubation. Expert knowledge in colorimetric and graphical output interpretation will facilitate the resolution of false-positive and false-negative assessments.

Maintenance of airway

In subsequent chapters, a variety of roles of capnography will be described, including identifying pulmonary embolism, adjusting ventilator settings in response to airflow obstruction or excessive PEEP, and recognizing cardiovascular instability and assuring adequacy of resuscitation efforts. As it relates to airway maintenance, continuous capnography provides graphical and numerical assurance of airway patency. Sudden dramatic drops in waveform values can indicate mucus plugging, tube kinking, apnea, or unplanned extubation. More subtle declines in $P_{ET}CO_2$ can be seen with ventilator–patient dyssynchrony, the development of a cuff leak, and even migration of the endotracheal tube from the trachea to a bronchial location [23]. Any of these capnographic alerts can occur well before changes in heart rate, blood pressure, or oximetry are evident.

Capnography is also valuable during transport to a different location, such as for diagnostic testing. Significant endotracheal tube movement can also occur from neck flexion and extension [24]. Given its ease in application, capnography is a reliable monitoring tool to assess an intact airway.

Assisting with the difficult airway

The utility of capnometry as an adjunct for securing the difficult airway is significant. Blind nasal intubation may be required on occasion when faced with a difficult airway. When upper airway anatomy precludes a clear laryngoscopic evaluation prior to intubation, this technique may be applied. In-line capnometry, combined with airway stethoscopy, has been described in one emergency medicine study as a possible guide to successful nasal intubation [25].

An even more novel technique, combining fiberoptic bronchoscopy and capnography, has been described to help successfully intubate difficult airway patients while awake [26,27]. In a group of patients with previous damage or occlusion to the airway, successful tracheal intubation utilizing a fiberoptic bronchoscope was confirmed in all patients. This procedure was accomplished by inserting a modified suction catheter through the suction port of the bronchoscope, whereby a capnogram was obtained. After at least four consecutive normal capnographic waveforms were obtained, the bronchoscope was then advanced into the airway over this suction catheter. Median time to intubation in these patients was 3 min, although the process in some patients took up to 15 min. While use of this technique has only been described in the anesthesia arena, it has potential applications in the acute care setting in other patients with difficult airway anatomy.

Avoiding airway intubation with enteric tubes

During routine intensive care radiographic evaluations, inappropriate enteral tube placement has been identified as often as endotracheal tube malposition [28]. The overall incidence of tracheal placement of enteral tubes confirmed by radiography has been documented to be 2% [29]. Airway-associated complications from enteral tubes include pneumothorax, pneumonia, bronchopleural fistula, and hemorrhage. These events lead to increased morbidity and mortality, as well as increased hospital length of stay and cost [30].

While radiography of the chest and/or abdomen is the mainstay for confirmation of enteral tube positioning, rapid bedside assessments are performed routinely; these include gastric pH testing, insufflations of air at the proximal site while auscultating the epigastrium, listening for air movement at the proximal site, and pressure manometry [31]. Unfortunately, none of these methods have been consistent with preventing inadvertent tracheal intubation that is diagnosed radiographically. Endoscopically or fluoroscopically-guided placement for enteral access is certainly more successful, but adds significant costs and may be quite time-consuming.

Another alternative involving a two-step radiographic assessment during placement [32] has been utilized. With this method, the tube is partially inserted (30 cm), and, after correct placement is confirmed by imaging, positioning of the tube is completed. Burns *et al.* [33] and Kindopp *et al.* [34] reported that the two-step method can be circumvented by demonstrating that capnography can successfully and sensitively identify when enteral tube placement is in the airway. In a follow-up study by Burns *et al.*, colorimetric assessment of CO_2 presence was as reliable as continuous capnography [33].

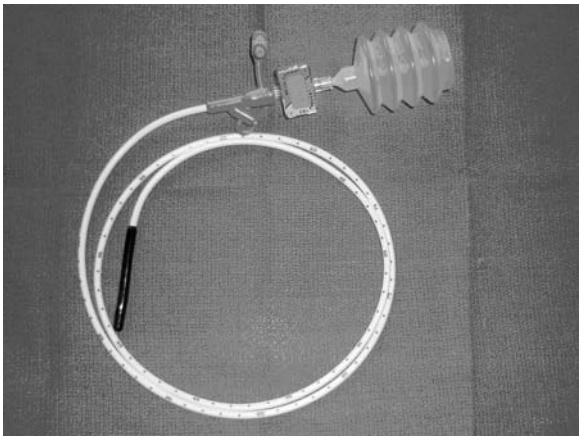

Figure 4.2 Set-up used for colorimetric capnometer attached to a small-bore feeding tube. Alternatively capnography with a numerical output could be used. Both techniques are equally applicable to use with a Salem sump.

Employing capnographic techniques during enteral tube placement reveals that 10–27% of placements are, at some point, complicated by airway intubation, and include false negatives associated with occlusion of ports and stomach acid contamination of the colorimetric indicator which can result in a false positive [35]. While tube type (Salem sump versus smaller soft-bore feeding tube) showed no difference in the incidence of accidental airway placement, nasal insertion was more likely to access the airway as compared to the oral route. Capnography and colorimetric capnometry are successful techniques for helping to safely place tubes into the gut, and may decrease the complications associated with enteral tube placement (Figure 4.2).

Conclusion

Capnography is a valuable tool in providing safe care to the critically ill patient. Its significance in airway management (insertion and maintenance of endotracheal tubes) and its utility in providing safer passage of feeding tubes has been established.

References

1. Caplan RA, Posner KL, Ward RJ, Cheney FW. Adverse respiratory events in anesthesia: a closed claims analysis. *Anesthesiology* 1990; **72**: 828–33.
2. Schwartz DE, Matthay MA, Cohen NH. Death and other complications of emergency airway management in critically ill adults: a prospective investigation of 297 tracheal intubations. *Anesthesiology* 1995; **82**: 367–76.
3. Rosenberg M, Block CS. A simple, disposable end-tidal carbon dioxide detector. *Anesth Prog* 1991; **38**: 24–6.
4. Salem MR. Verification of endotracheal tube position. *Anesthesiol Clin N Am* 2001; **19**: 813–39.
5. Kovacs G, Law JA. *Airway Management in Emergencies*. New York: McGraw-Hill Medical, 2008.
6. Grmec S. Comparison of three different methods to confirm tracheal tube placement in emergency intubation. *Intens Care Med* 2002; **28**: 701–4.
7. Ornato JP, Shipley JB, Racht EM, *et al.* Multicenter study of a portable, hand-size, colorimetric end-tidal carbon dioxide detection device. *Ann Emerg Med* 1992; **21**: 518–23.
8. Knapp S, Kofler J, Stoiser B, *et al.* The assessment of four different methods to verify tracheal tube placement in the critical care setting. *Anesth Analg* 1999; **88**: 766–70.
9. Part 1: Introduction to the International Guidelines 2000 for CPR and ECC : a consensus on science. *Circulation* 2000; **102**(8 Suppl): I1–11.
10. Wyllie J, Carlo WA. The role of carbon dioxide detectors for confirmation of endotracheal tube position. *Clin Perinatol* 2006; **33**: 111–19.
11. Dorsey MJ, Jones BR. An inexpensive, disposable adapter for increasing the safety of blind nasotracheal intubations. *Anesth Analg* 1989; **69**: 135.
12. Garnett AR, Ornato JP, Gonzalez ER, Johnson EB. End-tidal carbon dioxide monitoring during cardiopulmonary resuscitation. *JAMA* 1987; **257**: 512–15.
13. Vukmir RJ. *Airway Management in the Critically Ill*. New York: Parthenon, 2001.
14. Goldberg JS, Rawle PR, Zehnder JL, Sladen RN. Colorimetric end-tidal carbon dioxide monitoring for tracheal intubation. *Anesth Analg* 1990; **70**: 191–4.
15. ECC Committee, Subcommittees and Task Forces of the American Heart Association. 2005 American Heart Association Guidelines for Cardiopulmonary Resuscitation and Emergency Cardiovascular Care. *Circulation* 2005; **112**(24 Suppl): IV1–203.
16. Dunn SM, Mushlin PS, Lind LJ, Raemer D. Tracheal intubation is not invariably confirmed by capnography. *Anesthesiology* 1990; **73**: 1285–7.
17. Sum Ping ST, Mehta MP, Symreng T. Accuracy of the FEF CO_2 detector in the assessment of endotracheal tube placement. *Anesth Analg* 1992; **74**: 415–19.
18. Puntervoll SA, Soreide E, Jacewicz W, Bjelland E. Rapid detection of oesophageal intubation: take care when using colorimetric capnometry. *Acta Anaesthesiol Scand* 2002; **46**: 455–7.
19. Linko K, Paloheimo M, Tammisto T. Capnography for detection of accidental oesophageal intubation. *Acta Anaesthesiol Scand* 1983; **27**: 199–202.

20. Sum-Ping ST, Mehta MP, Anderton JM. A comparative study of methods of detection of esophageal intubation. *Anesth Analg* 1989; **69**: 627–32.
21. Gandhi SK, Munshi CA, Coon R, Bardeen-Henschel A. Capnography for detection of endobronchial migration of an endotracheal tube. *J Clin Monit* 1991; **7**: 35–8.
22. Szekely SM, Webb RK, Williamson JA, Russell WJ. The Australian Incident Monitoring Study. Problems related to the endotracheal tube: an analysis of 2000 incident reports. *Anaesth Intens Care* 1993; **21**: 611–16.
23. Zwerneman K. End-tidal carbon dioxide monitoring: a VITAL sign worth watching. *Crit Care Nurs Clin N Am* 2006; **18**: 217–25.
24. Conrardy PA, Goodman LR, Lainge F, Singer MM. Alteration of endotracheal tube position: flexion and extension of the neck. *Crit Care Med* 1976; **4**: 7–12.
25. Harris RD, Gillett MJ, Joseph AP, Vinen JD. An aid to blind nasal intubation. *J Emerg Med* 1998; **16**: 93–5.
26. Huitink JM, Buitelaar DR, Schutte PF. Awake fibrecapnic intubation: a novel technique for intubation in head and neck cancer patients with a difficult airway. *Anaesthesia* 2006; **61**: 449–52.
27. Huitink JM, Balm AJ, Keijzer C, Buitelaar DR. Awake fibrecapnic intubation in head and neck cancer patients with difficult airways: new findings and refinements to the technique. *Anaesthesia* 2007; **62**: 214–19.
28. Hall JB, Schmidt GA, Wood LDH. *Principles of Critical Care*, 3rd edn. New York: McGraw-Hill, 2005.
29. Rassias AJ, Ball PA, Corwin HL. A prospective study of tracheopulmonary complications associated with the placement of narrow-bore enteral feeding tubes. *Crit Care* 1998; **2**: 25–8.
30. Tornero C, Herrejon A, Salcedo M. [Pneumothorax, atelectasis, and pleural effusion secondary to the placement of an enteral feeding tube.] *Rev Clin Esp* 1992; **191**: 286–7.
31. Araujo-Preza CE, Melhado ME, Gutierrez FJ, Maniatis T, Castellano MA. Use of capnometry to verify feeding tube placement. *Crit Care Med* 2002; **30**: 2255–9.
32. Roubenoff R, Ravich WJ. Pneumothorax due to nasogastric feeding tubes: report of four cases, review of the literature, and recommendations for prevention. *Arch Intern Med* 1989; **149**: 184–8.
33. Burns SM, Carpenter R, Truwit JD. Report on the development of a procedure to prevent placement of feeding tubes into the lungs using end-tidal CO_2 measurements. *Crit Care Med* 2001; **29**: 936–9.
34. Kindopp AS, Drover JW, Heyland DK. Capnography confirms correct feeding tube placement in intensive care unit patients. *Can J Anaesth* 2001; **48**: 705–10.
35. Burns SM, Carpenter R, Blevins C, *et al.* Detection of inadvertent airway intubation during gastric tube insertion: capnography versus a colorimetric carbon dioxide detector. *Am J Crit Care* 2006; **15**: 188–95.

Section 1
Chapter
5

Ventilation

Airway management in the operating room

D. G. Bjoraker

Introduction

Respiratory events constitute the largest class of injury in the American Society of Anesthesiology Closed Claims Study (522 of 1541 cases; 34%) [1]. Three-fourths of the adverse respiratory events were due to inadequate ventilation (196 cases; 38%), esophageal intubation (94 cases; 18%) and difficult tracheal intubation (87 cases; 17%) [1]. In 48% of the esophageal intubations, auscultation of breath sounds was described and documented. In the pediatric age group (age 15 years or younger), respiratory events were more common than for adults (43%) [2]. Reviewers judged that the vast majority (89%) of the inadequate ventilation claims in pediatrics could have been prevented with pulse oximetry and/or capnography [2].

Unrecognized esophageal intubation was identified as an important cause of cardiac arrest, and was attributed solely to anesthesia at one institution [3]. Over a period of 15 years, 4 of 27 cardiac arrests in 163 240 anesthetic cases were attributed to esophageal intubation. In a study of malpractice claims brought against anesthesiologists in Washington State from 1971 to 1982, esophageal intubation was a significant cause of cardiac arrest, brain damage, and death [4]. Of the 192 claims, 7 were brought for esophageal intubation, and, again, several cases documented successful chest auscultation. In an American Society of Anesthesiologists' Committee on Professional Liability survey, 18 of 29 cases of unrecognized esophageal intubation that caused injury included documentation of auscultation of the chest [5]. There is clearly a recurring theme of breath sound auscultation not reliably predicting tracheal intubation.

Confirmation of tracheal intubation with capnography

The usually more controlled circumstances of airway management in the operating room (OR) often provide better conditions, better monitoring, and more experienced personnel, particularly when a problem occurs, than is available in other critical care environments or the emergency department. The obvious reliability of being able to directly visualize placement of an endotracheal tube into the trachea would seem to make it the "gold standard" of successful intubation. However, direct visualization is often either not possible or the observations made may be incorrectly interpreted. Also, misplacement of the tube while or prior to securing it, or during changes in the patient's position, may result in esophageal intubation subsequent to a correct initial placement. Radiographic examination of head and neck flexion and extension demonstrate tube movement by as much as 5 cm which can readily result in extubation [6]. In infants and neonates, the problem of accidental extubation – and, conversely, mainstem intubation – by changing head position is even more critical because of the much smaller dimensions involved [7].

The ideal method of confirming endotracheal intubation has become an enduring search since the first reports of tracheal tube placement nearly a century ago. Knapp *et al.* [8], in a critical care setting of non-cardiac arrest patients, found capnography to be the most reliable method for rapid evaluation of endotracheal tube position, with no failures in 152 examinations. Murray and Modell [9] demonstrated in dogs that disconnection, obstruction, removal, and esophageal placement of the endotracheal tube was evident in a single respiratory cycle. Partial extubation of the trachea and intermittent kinking or obstruction of the endotracheal tube created a recognizable, erratic capnogram pattern, although not greatly changing the maximum expired carbon dioxide (CO_2) concentration. Tobias and Higgins [10] found capnography to be a useful adjunct when performing cricothyrotomy puncture both for transtracheal jet ventilation and for

Capnography, Second Edition, ed. J. S. Gravenstein, Michael B. Jaffe, Nikolaus Gravenstein, and David A. Paulus. Published by Cambridge University Press. © Cambridge University Press 2011.

Table 5.1 Capnography confirmation of endotracheal intubation

False-negative results
Gas sampling problems
Disconnection
Apnea
Equipment failure
Kinked or obstructed tracheal tube
Unintentional PEEP through a loosely fitted or uncuffed tube
Dilution of proximal sampling by fresh gas flow in Mapleson D system
Low sampling flow rates
Gas sampling line leaks
Patient problems
Severe upper- or lower-airway obstruction
Very large alveolar deadspace
Low cardiac output, severe hypotension
Obstruction of pulmonary circulation
Embolism, pulmonary atresia, or stenosis; surgical interruption
Severe lung disease
Cardiac arrest
False-positive results
Bag-and-mask ventilation before intubation
After ingestion of antacids or carbonated beverages (e.g., cola, beer, carbonated mineral water)
Tube in pharynx

PEEP, positive end-expiratory pressure.
Source: Modified from: Salem MR, Wafai Y. Practical confirmation of endotracheal intubation in the trauma patient. *Anesthesiol News* 1997; **23**: 4, 9–11, 12, 30–3.

anesthetic injection. Although airway management in the OR may be more controlled than in the emergency department, Salem and Wafai's list [11] of false positives and false negatives when using capnography to confirm intubation is still applicable (Table 5.1). Their list concentrates on the generally used technique of time-based capnography with sidestream expiratory gas sampling.

While the detection of CO_2 by capnography after completion of a difficult intubation procedure may suggest success, it may more precisely indicate only that the tube tip is somewhere in the respiratory path, although perhaps not exactly where the intubationist desires. Deluty and Turndorf [12] described the blind nasal placement of an Endotrol® tube that resulted in a normal-time capnogram and end tidal partial pressure of CO_2 ($PETCO_2$), but was associated with high inspiratory pressure, a large cuff inflation volume, and the inability to pass a fiberscope into the trachea through the Endotrol® tube. Subsequently, the tube was found to be at a 90° angle to the glottic opening, with the tip imbedded in pharyngeal mucosa. The Murphy eye was located over the vocal cords, thus accounting for the normal capnogram. Deluty and Turndorf's successful recognition of this malpositioned endotracheal tube was based on vigilance in being able to identify atypical clinical features and their persistence in seeking an explanation – both valuable principles in management of the airway. Other methods that are helpful in confirming intubation have been extensively reviewed elsewhere [13,14].

Esophageal CO_2 detection

As the management of the difficult airway in the OR is usually associated with a patient who is producing CO_2 (i.e., not cardiac arrest), the assumption that CO_2 will be detected in the respiratory tract is usually valid. The converse, namely that respiratory levels of CO_2 will *not* be detected in the esophagus is also usually valid, but not always. Sum-Ping *et al.* [15] found esophageal $PETCO_2$ levels of 0.6 ± 0.6% compared with tracheal levels of 4.9 ± 0.7%. Seven of their 21 patients had capnograms similar to tracheal waveforms, but greatly reduced in amplitude. One patient had an end-expired esophageal CO_2 level of 2.0%. Volumetric capnography, rather than time capnography, would have further amplified the notable differences between the tracheal and esophageal CO_2 levels that Sum-Ping *et al.* detected [16].

When mask ventilation is difficult over a prolonged period, the partial pressure of CO_2 in arterial blood ($PaCO_2$) may rise substantially, and the CO_2 tension of exhaled gas entering the hypopharynx will also be increased. A subsequent ventilation effort may return this ventilatory deadspace gas not just to the trachea, but also to the esophagus and stomach [17]. Not surprisingly, later esophageal intubation would yield CO_2. The clinical scenario becomes more complicated if the gastroesophageal sphincter is particularly incompetent, and to-and-fro gastric ventilation is as easily – or more easily – achieved than pulmonary ventilation. If esophageal intubation then occurs, initial breaths may contain substantial CO_2, potentially exceeding 5% if

prolonged hypercarbia has occurred. A capnography pattern indicating declining CO_2 in each subsequent breath over several breaths will help identify esophageal intubation [17].

Prior ingestion of carbonated beverages or antacids may cause intragastric release of large amounts of CO_2 perhaps greater than 20% [18]. In an experiment in swine, Sum-Ping *et al.* [18] demonstrated that esophageal capnography could detect $P_{ET}CO_2$ levels as high as 5.3% after intragastric administration of a carbonated beverage. It is an oversimplification to assume that the decline of esophageal CO_2 with each subsequent breath will behave as a classic single-compartment washout curve. Variables affecting the CO_2 decay will include the quantity of material ingested, the volume of liquid within the stomach, the release of CO_2 from the ingested solution, the excretion of CO_2 via mucosal absorption, the volume of gas within the stomach, the mixing of gastric ventilation with gas in the stomach, and the volume of gastric ventilation entering and exiting the stomach. The volume of gastric inspired and expired gas may change as intragastric volumes and pressures, and esophageal pressures, change with each ventilation.

Endobronchial tube placement recognition

If ventilation is initiated through an endotracheal tube inadvertently placed into an endobronchial position, no substantially unusual capnography or ventilatory parameters may be immediately evident. However, if a properly positioned endotracheal tube migrates into an endobronchial position, and the ventilator settings are unchanged, several observations may alert the anesthesiologist to tube malposition. The $P_{ET}CO_2$ concentration will decrease, and the peak inspiratory pressure will increase (Figure 5.1) [19]. Alveolar ventilation and $PaCO_2$ are inversely related. When the endotracheal tube slips into a bronchial position, the entire ventilation is delivered to that lung, approximately doubling the ventilation/perfusion ($\dot{V}/\dot{Q}$) ratio and reducing the alveolar CO_2 tension in the ventilated lung [20]. Since capnography reflects only the CO_2 tension of the ventilated lung, a sudden decrease in $P_{ET}CO_2$ is observed. If the endobronchial position persists, over time, the arterial blood gases will indicate a decreased pH and oxygen tension, and an increase in CO_2 tension. If the resistance to ventilation through the malpositioned tube becomes extremely high, and the delivery of alveolar ventilation is prevented, the underventilation could then result in an unchanged or increased observed $P_{ET}CO_2$ [20–22].

Ezri *et al.* [23] noted frequent endobronchial migration of the tube tip in morbidly obese patients undergoing laparoscopic gastroplasty. Oxygenation was not impaired, and the $P_{ET}CO_2$ did not change in any of the affected patients; direct fiberoptic examination was the single indicator of malposition. These observations are not necessarily in conflict with the circumstances discussed above where the $P_{ET}CO_2$ concentration decreases and the peak inspiratory pressure increases. Anatomical tube tip migration beyond the carina does not always mean that the tube is completely sealed in the bronchus and initiating one-lung ventilation.

In the Australian Incident Monitoring Study (AIMS) of the first 3947 cases reported, 154 were for accidental bronchial intubations [24]. The capnogram, which was monitored in 122 patients, remained normal or unremarkable 87% of the time, with the remaining cases split between decreasing and increasing $P_{ET}CO_2$ (Table 5.2). In only one case was endobronchial intubation suspected based only on capnography; in an

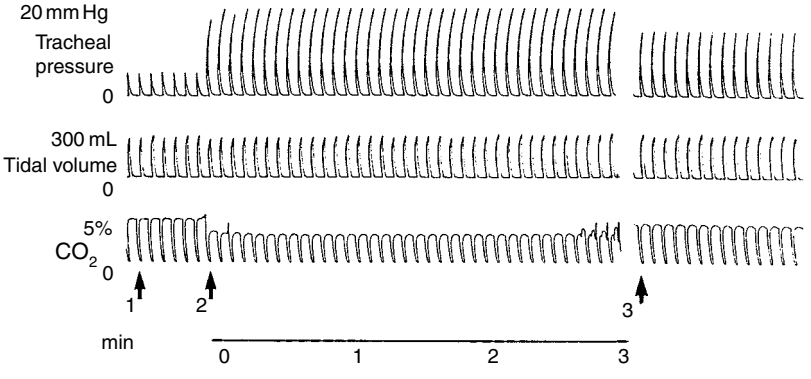

Figure 5.1 Tracheal pressure, tidal volume, and $P_{ET}CO_2$ tension in an experimental study in dogs. (1) Endotracheal tube in trachea. (2) Tip of endotracheal tube pushed down into bronchus. (3) Tip of endotracheal tube pulled back into trachea. [Reproduced with permission from: Gandhi SK, Munshi CA, Coon R, Bardeen-Henschel A. Capnography for detection of endobronchial migration of an endotracheal tube. *J Clin Monit* 1991; **7**: 35–8.]

Table 5.2 Response of $P_{ET}CO_2$ during accidental bronchial intubation in patients monitored with capnometry

$P_{ET}CO_2$ response	Number of cases ($n = 122$)	Total number of cases ($n = 122$)
Normal	23	18.9
Decreased	9	7.4
Increased	7	5.7
Not reported	83	68.0

Source: Modified from: McCoy EP, Russell WJ, Webb RK. Accidental bronchial intubation: an analysis of AIMS incident reports from 1988 to 1994 inclusive. *Anaesthesia* 1997; **52**: 24–31.

additional six cases, capnography contributed to the diagnosis.

Biphasic capnographic waveforms

The time capnogram is an expression of the $\dot{V}/\dot{Q}$ ratio. Initially, with exhalation, the anatomical deadspace gas is assessed (infinite $\dot{V}/\dot{Q}$, zero CO_2 concentration). This is followed by gas delivery from well-ventilated, low-resistance regions of the lung (relatively high $\dot{V}/\dot{Q}$, low CO_2 concentration). Later, the poorly ventilated, high-resistance regions of the lung (relatively low $\dot{V}/\dot{Q}$, high CO_2 concentrations) are delivered. Often, a positive slope (upward to the right) of the alveolar "plateau" portion of the waveform is evident. If a biphasic waveform occurs, the usual continuum of rising CO_2 concentrations has been disrupted because a biphasic separation of the pulmonary ventilation into a low-resistance, high $\dot{V}/\dot{Q}$ region and a high-resistance, low $\dot{V}/\dot{Q}$ region has occurred. Alternatively, this can also be seen with an incompletely sealed mainstem intubation where the non-intubated side exhales more slowly because of the partially occluded path.

Unilateral pathophysiologic conditions that cause unilateral hypoventilation or high airway resistances would result in a biphasic waveform. For example, obstruction of a mainstem bronchus by an external or internal tumor, congenital stenosis, secretions, or a malfunctioning or malpositioned endotracheal tube could result in a biphasic waveform. Similarly, unilateral compression of a lung by air, blood, or fluid could produce a biphasic capnogram. Clinical scenarios include ventilation in the lateral decubitus position, with the non-dependent lung having a relatively high $\dot{V}/\dot{Q}$ ratio and a low airway resistance relative to the dependent lung, or unilateral lung compression by severe kyphoscoliosis. Gilbert and Benumof [25] reported a case in which transient endobronchial advancement of the tube tip during part of each ventilatory cycle produced a biphasic capnogram, which was easily remedied by pulling back the endotracheal tube. Of course, intervening spontaneous breaths during controlled ventilation, a much more common circumstance, must be ruled out.

Positioning of double-lumen tubes

The measurement and comparison of $P_{ET}CO_2$ for each lung during double-lumen tube ventilation may identify or confirm any pathophysiologic defects within each lung. For example, Bhavani-Shankar *et al.* [26] identified an unexpected pulmonary artery thrombus in the putatively normal lung prior to planned contralateral pneumonectomy upon detecting an unexpectedly large $PaCO_2$–$P_{ET}CO_2$ gradient when attempted unilateral ventilation resulted in hypoxemia. After embolectomy $P_{ET}CO_2$ sampling via the working lumen of a fiberscope, with its tip placed distal to the carina, confirmed the correction of the prior large $PaCO_2$– $P_{ET}CO_2$ gradient. However, others did not note any significant alteration in $P_{ET}CO_2$ or in the capnogram when a double-lumen tube was malpositioned [27,28].

Blind endotracheal tube placement with capnography

Many techniques to facilitate blind nasal tracheal intubation use the detection of significant exhaled gas flow from a spontaneously breathing patient to indicate the proximity of the tube tip to the glottic opening. Connecting the breathing circuit to the tube permits oxygen delivery to the pharynx during placement, and facilitates sidestream capnometry. While King and Wooten [29] recommended closure of the mouth and occlusion of the contralateral nares, dilution of the exhaled CO_2 concentration – unless the tube tip is immediately at the vocal folds – is actually desirable. The capnogram (Figure 5.2) initially is triangular in shape with a low maximum concentration, attenuated phase II, and a severely down-sloping phase III [30,31]. As the tube approaches the glottic opening, the maximum CO_2 concentration increases, and the waveform is that commonly seen with leakage around the endotracheal tube from cuff deflation where phase III rapidly decays. Finally, when a tracheal position is achieved, and the airway is sealed by cuff inflation, the idealized phase III plateau or an ascending phase III is

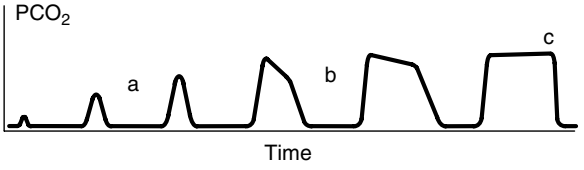

Figure 5.2 A hypothetical capnogram during blind nasal intubation of the trachea in a spontaneously breathing patient. (a) Initially, the waveform is triangular in shape with a low maximum CO_2 concentration, an attenuated phase II, and a severely downsloping phase III. (b) As the tube approaches the glottic opening, the maximum CO_2 concentration increases but the waveform still shows phase III decay. (c) Finally, when a tracheal position is reached and the airway sealed by cuff inflation, the idealized phase III plateau or an ascending phase III is seen.

seen. Omoigui *et al.* [32] found that viewing the capnogram during the procedure was inconvenient, and attached a voltage-controlled oscillator that generates an audio tone increasing in pitch with greater $P_{ET}CO_2$ concentration. A similar method, termed *fibercapnic intubation* by Huitink *et al.* [33] aspirates exhaled gas via a suction catheter passed through the lumen of a fiberscope when the fiberscope view is obscured. When a capnogram is obtained, the scope is advanced over the catheter, and the process is repeated until tracheal rings are viewed. An antisialagogue is helpful in minimizing the aspiration of secretions into the capnometer sampling line.

When accidental partial extubation occurs in a spontaneously breathing patient, the reverse of the above procedure may be evident on the capnogram. If the endotracheal tube tip slowly migrates out of the glottic opening and further from the glottis, the gas sampled by the capnograph is progressively diluted. The progression of waveforms illustrated in Figure 5.2 may be seen, but in right-to-left order.

References

1. Caplan RA, Posner KL, Ward RJ, Cheney FW. Adverse respiratory events in anesthesia: a closed claims analysis. *Anesthesiology* 1990; **72**: 828–33.
2. Morray JP, Geiduschek JM, Caplan RA, *et al.* A comparison of pediatric and adult anesthesia closed malpractice claims. *Anesthesiology* 1993; **78**: 461–7.
3. Keenan RL, Boyan CP. Cardiac arrest due to anesthesia: a study of incidence and causes. *JAMA* 1985; **253**: 2373–7.
4. Solazzi RW, Ward RJ. The spectrum of medical liability cases. In: Pierce EC, Cooper JB (eds.) *International Anesthesiology Clinics*, vol. 22. Boston, MA: Little, Brown, 1984; 43–59.
5. Birmingham PK, Cheney FW, Ward RJ. Esophageal intubation: a review of detection techniques. *Anesth Analg* 1986; **65**: 886–91.
6. Conrady PA, Goodman LR, Lainge F, Singer MM. Alteration of endotracheal tube position: flexion and extension of the neck. *Crit Care Med* 1976; **4**: 71–2.
7. Bosman YK, Foster PA. Endotracheal intubation and head position in infants. *S Afr Med J* 1977; **52**: 71–3.
8. Knapp S, Kofler J, Stoiser B, *et al.* The assessment of four different methods to verify tracheal tube placement in the critical care setting. *Anesth Analg* 1999; **88**: 7667–70.
9. Murray IP, Modell JH. Early detection of endotracheal tube accidents by monitoring carbon dioxide concentration in respiratory gas. *Anesthesiology* 1983; **59**: 344–6.
10. Tobias JD, Higgins M. Capnography during transtracheal needle cricothyrotomy. *Anesth Analg* 1995; **81**: 1077–8.
11. Salem MR, Wafai Y. Practical confirmation of endotracheal intubation in the trauma patient. *Anesthesiol News* 1997; **23**: 4, 9–11, 12, 30–3.
12. Deluty S, Turndorf H. The failure of capnography to properly assess endotracheal tube location. *Anesthesiology* 1993; **78**: 783–4.
13. Salem MR. Verification of endotracheal tube position. *Anesthesiol Clin N Am* 2001; **19**: 8133–9.
14. DeBoer S, Seaver M, Arndt K. Verification of endotracheal tube placement: a comparison of confirmation techniques and devices. *J Emerg Nurs* 2003; **29**: 4445–50.
15. Sum-Ping ST, Mehta MP, Anderton JM. A comparative study of methods of detection of esophageal intubation. *Anesth Analg* 1989; **69**: 627–32.
16. Anderson CT, Breen PH. Carbon dioxide kinetics and capnography during critical care. *Crit Care* 2000; **4**: 2071–5.
17. Sum-Ping ST. Esophageal intubation. *Anesth Analg* 1987; **66**: 483.
18. Sum-Ping ST, Mehta MP, Symreng T. Reliability of capnography in identifying esophageal intubation with carbonated beverage or antacid in the stomach. *Anesth Analg* 1991; **73**: 333–7.
19. Gandhi SK, Munshi CA, Coon R, Bardeen-Henschel A. Capnography for detection of endobronchial migration of an endotracheal tube. *J Clin Monit* 1991; **7**: 35–8.
20. Gandhi SK, Munshi CA, Kampine JP. Early warning sign of accidental endobronchial intubation: a sudden drop or sudden rise in PACO2? *Anesthesiology* 1986; **65**: 114–15.

21. Riley RH, Marcy JH. Unsuspected endobronchial intubation: detection by continuous mass spectrometry. *Anesthesiology* 1985; **63**: 203–4.
22. Riley RH, Finucane KE, Marcy JH. Early warning sign of accidental endobronchial intubation: a sudden drop or sudden rise in PACO2? In reply. *Anesthesiology* 1986; **65**: 115.
23. Ezri T, Hazin V, Warters D, Szmuk P, Weinbroum AA. The endotracheal tube moves more often in obese patients undergoing laparoscopy compared with open abdominal surgery. *Anesth Analg* 2003; **96**: 278–82.
24. McCoy EP, Russell WJ, Webb RK. Accidental bronchial intubation: an analysis of AIMS incident reports from 1988 to 1994 inclusive. *Anaesthesia* 1997; **52**: 24–31.
25. Gilbert D, Benumof JL. Biphasic carbon dioxide elimination waveform with right mainstem bronchial intubation. *Anesth Analg* 1989; **69**: 829–32.
26. Bhavani-Shankar K, Russell R, Aklog L, Mushlin PS. Dual capnography facilitates detection of a critical perfusion defect in an individual lung. *Anesthesiology* 1999; **90**: 302–4.
27. de Vries JW, Haanschoten MC. Capnography does not reliably detect double-lumen endotracheal tube malplacement. *J Clin Monit* 1992; **8**: 236–7.
28. Cohen E, Neustein SM, Goldofsky S, Camunas JL. Incidence of malposition of polyvinylchloride and red rubber left-sided double-lumen tubes and clinical sequelae. *J Cardiothorac Vasc Anesth* 1995; **9**: 122–7.
29. King HK, Wooten DJ. Blind nasal intubation by monitoring end-tidal CO2. *Anesth Analg* 1989; **69**: 412–13.
30. Linko K, Paloheimo M. Capnography facilitates blind nasotracheal intubation. *Acta Anesthesiol Belg* 1983; **34**: 117–22.
31. Bhavani-Shankar K, Philip JH. Defining segments and phases of a time capnogram. *Anesth Analg* 2000; **91**: 973–7.
32. Omoigui S, Glass P, Martel DLJ, *et al*. Blind nasal intubation with audio-capnometry. *Anesth Analg* 1991; **72**: 392–3.
33. Huitink JM, Buitelaar DR, Schutte PF. Awake fibrecapnic intubation: a novel technique for intubation in head and neck cancer patients with a difficult airway. *Anaesthesia* 2006; **61**: 449–52.

Section 1
Chapter
6

Ventilation

Capnography during anesthesia

Y. G. Peng, D. A. Paulus, and J. S. Gravenstein

Introduction

The practice of anesthesia involves the administration of drugs that can interfere with the central control of ventilation (inhalation and local anesthetics, narcotics, sedatives, anxiolytic drugs), the transmission of impulses from and to the muscles of breathing (subarachnoid and epidural blocks), and the integrity of the neuromuscular junction (neuromuscular blocking drugs). The surgeon's manipulations can hinder breathing by interfering with the airway or the lungs. The position of the patient during an operation or examination can hamper gas exchange. Finally, the vicissitudes of breathing equipment and anesthesia machines can cause problems or result in malfunction. It is, therefore, no wonder that many disasters in anesthesia can be traced to problems with respiration. Consequently, anesthesiologists monitor their patients' breathing by listening to the lungs or auscultating over the trachea, counting the respiratory rate, watching chest movement and tidal volume, and employing pulse oximetry and capnography. While pulse oximetry generates invaluable data related to oxygen (O_2) content in arterial blood, it fails to offer breath-by-breath information of basic respiratory gas exchange. In this chapter, we focus on issues related to capnography specific to anesthesia and the operating room.

The importance of capnography in anesthesia is illustrated by the fact that the American Society of Anesthesiologists (ASA) in its *Standards for Basic Anesthetic Monitoring* [1] states: "During all anesthetics the patient's oxygenation, ventilation, circulation and temperature shall be continually evaluated." It continues with a discussion on oxygenation, and then states the following about ventilation:

To ensure adequate ventilation of the patient during all anesthetics.

Methods

1. Every patient receiving general anesthesia shall have the adequacy of ventilation continually evaluated. Qualitative clinical signs such as chest excursion, observation of the reservoir breathing bag and auscultation of breath sounds are useful. Continual monitoring for the presence of expired carbon dioxide shall be performed unless invalidated by the nature of the patient, procedure or equipment. Quantitative monitoring of the volume of expired gas is strongly encouraged.*
2. When an endotracheal tube or laryngeal mask is inserted, its correct positioning must be verified by clinical assessment and by identification of carbon dioxide in the expired gas. Continual end-tidal carbon dioxide analysis, in use from the time of endotracheal tube/laryngeal mask placement, until extubation/removal or initiating transfer to a postoperative care location, shall be performed using a quantitative method such as capnography, capnometry or mass spectroscopy.* When capnography or capnometry is utilized, the end-tidal CO_2 alarm shall be audible to the anesthesiologist or the anesthesia care team personnel.*
3. When ventilation is controlled by a mechanical ventilator, there shall be in continuous use a device that is capable of detecting disconnection of components of the breathing system. The device must give an audible signal when its alarm threshold is exceeded.
4. During regional anesthesia and monitored anesthesia care, the adequacy of ventilation shall be evaluated by continual observation of qualitative clinical signs and/or monitoring for the presence of exhaled carbon dioxide.

[**Under extenuating circumstances, the responsible anesthesiologist may waive the requirements marked with an asterisk*]

We draw attention to point 4 of the ASA- approved methods of monitoring ventilation. Capnometry will

Capnography, Second Edition, ed. J. S. Gravenstein, Michael B. Jaffe, Nikolaus Gravenstein, and David A. Paulus. Published by Cambridge University Press. © Cambridge University Press 2011.

be particularly valuable when patients receive supplemental oxygen. The following, all-too-common clinical scenario makes the point. During a painful procedure under local anesthesia, or early in the postoperative period, a sedated patient is given a narcotic analgesic for pain. As minute ventilation is reduced, the patient's SpO_2 decreases. In response, a well-meaning nurse or physician enriches the patient's air with oxygen. The SpO_2 returns to baseline, but the respiratory depression has not been affected, and, gradually, the $PaCO_2$ increases until it depresses ventilation, occasionally even to the point of apnea or until respiratory acidosis triggers arrhythmias. Pulse oximetry has proven to be an excellent monitor of ventilation as long as the patient is breathing room air. When oxygen is administered, changes in end-tidal carbon dioxide tensions can reveal the presence of respiratory depression even in the face of high SpO_2 values.

Equipment

The use of capnography in anesthesia practice was officially recognized by the Food and Drug Administration (FDA), which published check-out procedures to be followed by anesthesiologists before administering anesthesia. The FDA lists capnography under "relevant standards." The FDA also states that alarms should be incorporated in the equipment. It is good practice to set the alarm levels close to the gas concentration that will be used. Assume that you are planning to give 50% O_2 and that the O_2 alarm default value is 25%. It would be unsafe to wait for the O_2 concentration to drop from 50% to 25% before the alarm sounds. Set the alarm level to, for example, 40% to get an early warning. Similarly, the upper and lower limits of CO_2 alarms should ideally, be set with the low alarm a little lower than the target and the high alarm a little higher (e.g., ±5 of the intended target) during an anesthetic or in the intensive care unit when a patient requires mechanical or assisted ventilation.

The FDA document also addresses the CO_2 absorber. It is often impossible to verify, by inspection, that the CO_2 absorbent is adequate because the color indicator can fail to show exhausted absorbent. However, if CO_2 is detected in the inspired gas, the differential diagnoses of exhausted absorbent versus valve incompetence must be ruled out, as well as the possibility of gas channeling through a non-exhausted absorber or monitor failure. When circle systems are used, the exhaled CO_2 must either be vented to the outside or be absorbed. Consequently, when a high fresh gas flow matches the inspired volume, all exhaled gas will be delivered to the scavenging system, and the CO_2 absorber will essentially sit idle. When the fresh gas flow supplies only enough gas to match the patient's uptake of gas (e.g., 300 mL/min O_2 for the average adult at rest), the patient will rebreathe all exhaled gas unless an absorbent removes the CO_2. Assuming a respiratory quotient (RQ) of 1, our patient would generate 300 mL/min CO_2. Every 100 g of absorbent (typically either soda lime or Baralyme) removes approximately 20 L of CO_2. Absorbers come in different sizes, but most will "scrub" the respired gas for many hours (longer when higher fresh gas flows are used) before inspired CO_2 values begin to appear on the capnogram (Figure 6.1). Estimating the life expectancy of the CO_2 absorbent is not feasible, as too many unknown variables can complicate the calculation such as the age of the absorbent

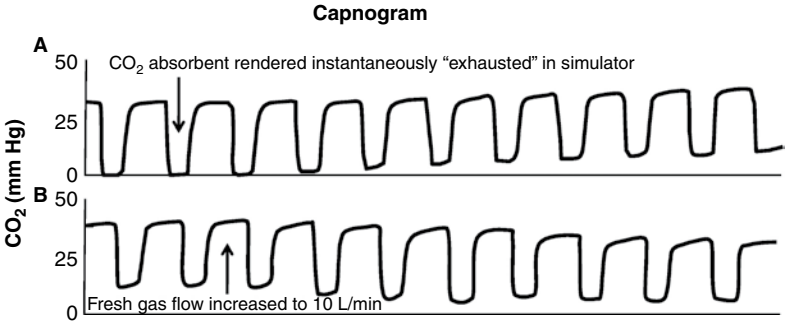

Figure 6.1 Simulation of CO_2 absorbent exhaustion in a circle system. (A) Normal functioning system experiencing acute absorbent exhaustion and manifesting a progressive increase in inspired CO_2 (rebreathing). (B) Increased fresh gas flow reverses the rise in inspired CO_2 with absorbent exhaustion (unlike with expiratory valve incompetence). [Modified from: Goldman JM, Ward DR, Daniel L. BreathSim, a mathematical model-based simulation of the anesthesia breathing circuit, may facilitate testing and evaluation of respiratory gas monitoring equipment. *Biomed Sci Instrum* 1996; **32**: 293–8.]

and its ability to regenerate during idle time, the RQ and CO_2 production of the patient, and the variable fresh gas flow in relation to the patient's minute ventilation. Instead, the inspired CO_2 concentration is monitored. If it increases, it is time to exchange the CO_2 absorber, increase the fresh gas flow, or fix an incompetent valve.

Breathing circuit

A simple diagram can help to identify potential trouble spots of anesthesia equipment (Figure 6.2). The breathing circuit is comprised of hoses that can be disconnected from the machine or patient. The ventilator can be disconnected from the breathing circuit and the fresh gas supply from the breathing circuit. Figure 6.2 shows arrows indicating the different sites of potential disconnection. The consequences of a disconnection will depend on whether the patient can breathe spontaneously and on the location of the disconnect. If it is at the airway, an anesthetized patient – now breathing room air – might wake up while, if the disconnection is at the anesthesia machine, one would observe the significant presence of inspired CO_2. If the patient is dependent on mechanical ventilation, a disconnection will interrupt ventilation of the patient's lungs. Such disconnections have led to many deaths in operating rooms and intensive care units; thus, multiple alarms (that sense tidal volume and pressures, and CO_2) are now incorporated in modern anesthesia and mechanical ventilators to help identify disconnections.

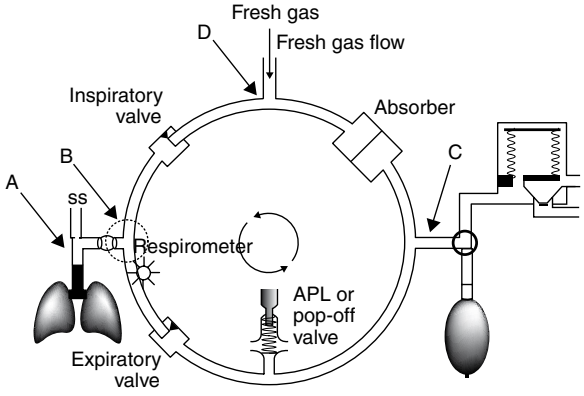

Figure 6.2 Basic concept of an anesthesia circle system. The patient's lungs are shown on the left. As the patient's exhaled gas passes the sampling site (ss), a sample (often as much as 200 mL/min) is aspirated and carried to the sidestream gas analyzer where a time-based capnogram will be generated. An alternative is to let the gas pass through a mainstream cuvette that contains a CO_2 sensor and a flowmeter, thus collecting the information necessary for a volume-based capnogram. The gas then enters the breathing circuit. The exhaled gas will now pass the respirometer where the expired volume can be measured (if it had not been measured already). On its way to the breathing bag or ventilator bellows the exhaled gas passes the adjustable pressure-limiting or pop-off valve. When the system is connected to the ventilator (as shown here), the adjustable pressure-limiting valve will be closed. Otherwise it will be adjusted to enable excess gas to escape late in expiration – as long as the patient is breathing spontaneously, or with manual ventilation, during inspiration. The ventilator bellows shows an escape valve that opens late in expiration should enough pressure develop to overcome the small resistance offered by the valve. When the ventilator compresses the bellows with the beginning of inspiration, the expiratory valve will close and the inspiratory valve open. The gas now passes through the CO_2 absorber, receives fresh gas (which may contain anesthetic gases) on its way to the patient, thus concluding the circle. However, it must pass once again past sensors, which can now analyze the inspired gas. The arrows show common sites for leaks in the system. (A) Between endotracheal tube and breathing circuit. The CO_2 sensors have also been disconnected. (B) Between Y-piece (identified by the stippled circle) and breathing circuit. The CO_2 sensors are still connected to the patient but disconnected from the breathing circuit. (C) Between ventilator and breathing circuit. (D) Between fresh gas inlet and breathing circuit.

Disconnections with mechanical ventilators

Capnography is the best monitor to identify complete disconnection of the breathing circuit. Depending on the make and model of the anesthesia machine, some ventilators (piston-driven or bellows descending on expiration) continue to work after a disconnection. During the expiratory cycle, they will aspirate room air and then deliver inspiratory tidal volumes through the disconnection instead of to the patient. When a complete disconnection occurs adjacent to the CO_2 sampling port (usually located at the endotracheal tube), not only will there be no capnographic tracing, but the capnogram will show a zero baseline. Time- and volume-based instruments will be equally effective in detecting the existence of such a disconnection. The capnometer may not easily identify partial disconnections that reduce tidal volume. Unless the leak is between the patient and sampling port, capnographic evidence will reflect hypoventilation by showing increasing end-tidal PCO_2 ($PETCO_2$). Exhaled tidal volume is a sensitive indicator of leaks and partial disconnects during mechanical ventilation.

It is rare, indeed, that the capnogram can mislead in cases of disconnection. However, one such example was presented by Ginosar and Baranov [2] who observed prolonged "phantom" square-wave capnographic tracings after a patient was disconnected from a Siemens Servo 900c (MEDECO Inc., Boise, ID, USA) ventilator, which had not been turned off. The gas analyzer

aspirated CO_2-containing gas from the expiratory tube, and the continuous operation of the ventilator interrupted the plateau of the capnogram, thus generating a series of rapidly diminishing phantom square-wave capnographic tracings.

Patient disconnection during spontaneous ventilation

Capnography will continue to detect expired CO_2 (and thus miss the disconnection) as long as the patient's exhaled tidal volume passes sidestream or mainstream (Figure 6.2) sampling ports. In such a case, the patient will be breathing room air without the anesthetic agents that would be delivered by the anesthesia machine.

Leaks during mechanical ventilation

The most common leak occurs at the endotracheal tube around an incompletely inflated endotracheal tube cuff (arrow A in Figure 6.2), and thus cannot be blamed on a machine fault. Other leaks, usually small, can develop with defective breathing tubes or leaks in the CO_2 absorber canister. Canister leaks are usually caused by misalignment of the canister housing after replacement of the absorbent or when CO_2 absorber granules cause the canister not to fit tightly. During the build-up of inspiratory pressure, some of the tidal vo1ume will be delivered to the room and the rest to the patient. However, most of the patient's expired volume (low pressure during expiration) will still pass through the sampling site (time-based capnography) or the capnographic sensor (on airway or volumetric capnography), regardless of the position of the leak. The time-based capnogram can appear normal or present low $P_{ET}CO_2$ values should the expired volume be too low to deliver adequate alveolar gas. The volumetric capnogram will reveal a reduced expired volume. If both inhaled and exhaled volumes are recorded, and if the leak is in the breathing circuit rather than between a bidirectional in-line flow sensor and the patient, the differences between the inhaled and exhaled volume will become apparent and more telling than the reduced tidal volumes alone.

Leaks during spontaneous ventilation

These are difficult to detect because the low pressure generated by spontaneous ventilation may not force much gas through the leak.

Inspiratory valve incompetence

A portion of the expired gas will enter the inspiratory breathing hose. While the ventilator will deliver the desired inspiratory volume to the patient (assuming the expiratory valve is working normally), the first part of the inspired gas will contain CO_2, resulting in a characteristic – and easily overlooked – slurred inspiratory slope (Figure 6.3).

Expiratory valve incompetence

The expiratory hose is normally filled with CO_2-rich gas, up to half of which can be pushed back into the patient with the next inhalation should the valve be incompetent. Capnograms will show CO_2 in the inspired gas (Figure 6.4). The volume-based capnogram will show normal inspired and expired volumes but elevated inspired CO_2 tensions (Figure 6.5). It is difficult to demonstrate whether an exhausted CO_2

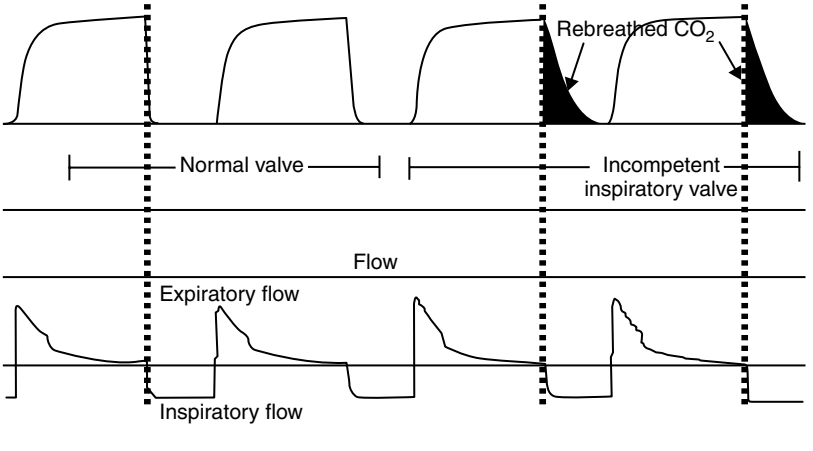

Figure 6.3 Inspiratory valve incompetence capnogram and flow waveforms. Note the downstroke slur/extension that occurs when the inspiratory valve is incompetent and the associated delay in the capnogram returning to baseline. Because the capnogram returns to baseline inspiratory even though there is rebreathing (shaded area, upper panel), the inspired CO_2 will be reported as zero. [Modified from: Goldman JM, Ward DR, Daniel L. BreathSim, a mathematical model-based simulation of the anesthesia breathing circuit, may facilitate testing and evaluation of respiratory gas monitoring equipment. *Biomed Sci Instrum* 1996; **32**: 293–8.]

absorber, which allows rebreathing of exhaled CO_2, or an incompetent expiratory valve is responsible for CO_2 elevating the inspiratory part of the capnogram. A clinically useful maneuver can be used to distinguish between an exhausted CO_2 absorber and an incompetent expiratory valve: if an exhausted absorber is the culprit, increasing the fresh gas flow to exceed the minute ventilation is enough to prevent rebreathing and will correct the problem, but it will not correct the abnormal capnogram should an incompetent expiratory valve have led to the appearance of CO_2 in the inspired gas. Incidentally, increasing the fresh gas flow may also affect the capnogram when the inspiratory valve has become incompetent, although not significantly.

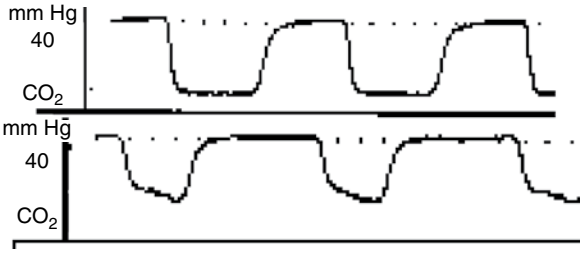

Figure 6.4 Incompetent expiratory valve leads to rebreathing of CO_2 in this time-based capnogram. Observe that the capnogram does not return to baseline, indicating the presence of CO_2 in the inspired gas. In the circle breathing system, all exhaled gas is directed down the expiratory limb. An incompetent expiratory valve allows expiratory limb gas to flow backward and mix with inspiratory limb gas at the Y-piece and CO_2 sampling site. Note that rebreathing of expired limb gases elevates the baseline of the capnogram throughout the inspiratory period. The appearance of the capnogram cannot be distinguished from one generated when the CO_2 absorber is exhausted. However, in modern anesthesia machines, a flow sensor will notice two-way gas flow in the expiratory tube and will issue an appropriate rebreathing alarm.

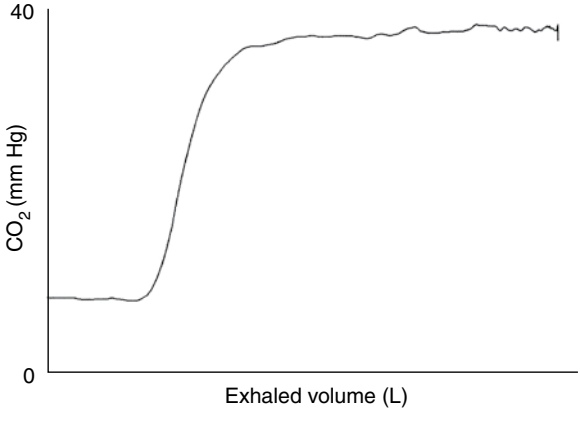

Figure 6.5 Volume-based capnogram with an incompetent expiratory valve. Observe the presence of CO_2 in the deadspace, that is, the last inhaled gas and first exhaled gas. Inhaled and exhaled tidal volumes will not differ.

Sidestream versus mainstream capnography

The most common instrumentation-related capnography problems are caused by blocked and leaking gas sampling catheters in sidestream systems. Blockages are usually caused by filtration systems that are designed to trap water and other liquids before they can be aspirated into the instrument, and produce costly damage. Fortunately, blockages usually generate an alarm or warning message, and may be easily corrected (i.e., by placing spare filters near the instrument). Leaking sample catheters will usually produce abnormal capnogram morphologies.

Figure 6.6 shows a "church steeple" appearance of the capnogram, which can sometimes be seen during mechanical ventilation with fairly high peak inspiratory pressures [3]. A leak in the sampling tube, usually between the sampling tube and the gas analyzer, enables aspiration of room air during low pressure in the breathing circuit (during expiration). This dilutes the exhaled CO_2 and generates the "roof of the church." With the onset of mechanical inspiration, the positive pressure in the sampling tube prevents aspiration of air, and end-tidal CO_2 reaches the analyzer ("steeple of the church"), which quickly gives way to fresh inspiratory gas. The abnormal capnogram shown in Figure 6.6a was caused by room air entrainment through a cracked sample tubing connector. Replacement of the water trap/filter assembly corrected the capnogram (Figure 6.6b).

A large body of capnography-related literature is devoted to diagnosing problems with older generations of anesthesia machines. The classic or traditional pneumatic anesthesia machine is slowly being replaced by more complex electromechanical and pneumatic anesthesia "workstations." The newer systems rely on electronic flow sensing and other technologies to improve the reliability and precision of pulmonary ventilation and delivery of anesthetic agents. However, we are still learning about the subtleties of gas flow patterns, and hence capnographic patterns, in some of these new systems. As we continue to gain experience with these new anesthesia systems, we will have to expand our understanding of the scope of machine-generated capnographic abnormalities.

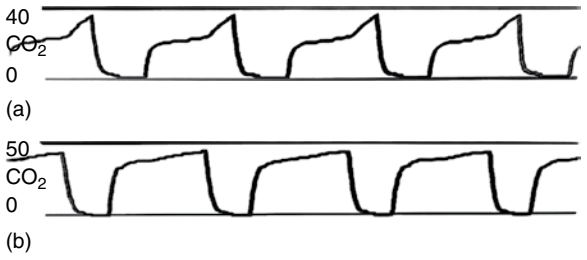

Figure 6.6 (a) A time-based capnogram obtained during mechanical ventilation. The upswing (the "steeple of the church") is generated by a leak, usually between the sampling capillary and the capnograph. The leak enables the gas analyzer to aspirate room air during exhalation (that is when the pressure in the breathing circuit and the sampling capillary is low), thus diluting the sampled CO_2 and generating the "roof of the church." The positive pressure generated early during inspiration stops the aspiration of air and pushes the last CO_2 in the sampling tube towards the analyzer, generating the "steeple." (b) A time-based capnogram after the leak was removed. The volume-based capnogram deprives us of such interesting shapes as it does not remove gas from the breathing circuit and thus cannot be affected by leaks in a sampling tube.

Position- and anesthesia-related problems

In a world of gravity, ventilation falls under its spell. When we stand, abdominal contents and the diaphragm are pulled down, and the lower levels of the lungs receive the lion's share of perfusion while the upper lung fields excel in ventilation. These ventilation/perfusion $\dot{V}/\dot{Q}$ inequalities tend to cancel out, resulting in a reasonably close, overall ventilation-to-perfusion of 1. Upon lying supine, the distribution shifts, the diaphragm no longer travels downward as much and the total functional residual capacity (FRC) can be substantially reduced. With spontaneous breathing, we manage to compensate for these conditions. However, once we paralyze the diaphragm and impose mechanical ventilation, conditions change markedly. Now the upper segments of the lungs receive a disproportionate share of ventilation, resulting in an overall increase of ventilation over perfusion. The addition of anesthetic drugs and, with it, a decrease in pulmonary blood flow, exaggerate the problem, leading to a varying degree of deadspace ventilation (areas of the lung ventilated but not adequately perfused). If we add to these conditions mechanical ventilation with large tidal volumes and slow respiratory rates, deadspace ventilation becomes even more pronounced. Spontaneous breathing causes very minor changes in pressures in the lung. With mechanical ventilation, sizable inspiratory pressures are needed to expand the lung. These pressures compress some capillaries more than others, leading to shunting of blood to the spared capillaries. To make matters worse, anesthetics can interfere with the physiologic hypoxic pulmonary vasoconstriction, which ordinarily causes blood to be diverted to well-ventilated areas. Certain positions used for surgical procedures can aggravate the situation; face-down, lateral, steep head-down, or the infamous kidney support all can further hamper normal pulmonary blood flow and ventilation. It is against this background that blood gases and comparisons of arterial and end-tidal CO_2 values need to be evaluated during anesthesia.

Establishment of an airway

As outlined in the ASA's minimal monitoring standards, capnography is the best method for demonstrating that continued gas exchange is taking place, whether the patient is breathing spontaneously or ventilated by bag and mask, or has a supralaryngeal (or supraglottic) airway, an endotracheal tube, or a tracheostomy. Remember that the stomach can deliver some CO_2 from a gastric bubble, for example, after drinking a carbonated beverage. However, such a bubble is soon exhausted, and CO_2 will disappear from the ventilated stomach. Subsequent capnograms of normal size indicate ongoing ventilation of the lungs.

Pulmonary pathology

Patients with chronic obstructive pulmonary disease or asthma exhibit typical capnograms with upsloping expired values brought about by the slow emptying of partially obstructed segments of the lungs. The differences between PCO_2 in arterial blood ($PaCO_2$) and PCO_2 in end-expired gas ($PETCO_2$) increase. It is essential to be aware of these potentially large differences in the presence of increased airway resistance. Figure 6.7a demonstrates a falsely low $PETCO_2$ produced when mechanical inspiration terminates expiration. Note the marked rise in $PETCO_2$ revealing the presence of hypercarbia when expiration is allowed to continue for several seconds longer. In contrast, Figure 6.7b illustrates the flat, stable alveolar plateau present in a healthy patient. Halogenated anesthetic vapors tend to relax the smooth muscles of the respiratory tract, after which an improvement is often seen in the capnographic pattern.

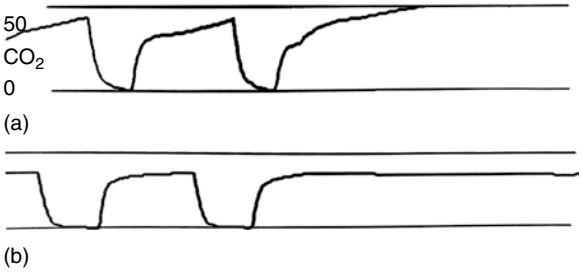

Figure 6.7 Capnogram with steep alveolar plateau. (a) In the presence of a steep alveolar plateau, the displayed $P_{ET}CO_2$ of 38 mm Hg markedly underestimates the $PaCO_2$. Pausing the ventilator for a few seconds provided additional time for slower-emptying alveoli to contribute their CO_2 to the measured gas sample. (b) Normal control with ventilator pause.

One-lung ventilation

When the anesthesiologist inserts a double-lumen endotracheal tube for a thoracotomy, and the patient is put into a lateral position, $\dot{V}/\dot{Q}$ abnormalities will be introduced as the lower lung receives more blood flow and the upper lung more ventilation. Once ventilation to the upper lung is discontinued, its perfusion may not decrease in a coordinated manner. As hypoxic vasoconstriction sets in – provided this mechanism is not depressed by anesthetics – $\dot{V}/\dot{Q}$ abnormalities will tend to improve. Nevertheless, we usually see the expected increase in the difference between arterial and end-tidal CO_2 tensions.

If the endotracheal tube slips into a mainstem bronchus, tidal volume – originally matched for ventilation of two lungs – will suddenly be directed into only one lung, and peak inspiratory pressure will increase. Pulmonary blood delivery of CO_2 into this large tidal volume will cause a particularly flat alveolar plateau and end-tidal values to be reduced, at least temporarily.

Special anesthesia problems

Laparoscopy

In the setting of laparoscopic surgery, the surgeons use peritoneal insufflation with gas in order to provide a view of the anatomic structures. The gas chosen is CO_2 due to its non-flammable character and because it is absorbed relatively promptly. This constant insufflation (usually at pressures not exceeding 15 mm Hg) presents challenges to the anesthesiologist. On the one hand, with insufflation of about 4 L of CO_2 into the abdominal cavity, the diaphragm is pushed up, and compliance and FRC decrease. On the other hand, the addition of absorbed CO_2 to the metabolically generated gas imposes an extra burden on gas exchange. On average, the anesthesiologist will need to increase minute ventilation 1.5-fold in order to maintain a relatively constant $PaCO_2$. At the end of CO_2 insufflation, it takes about 8 min for a return to baseline, and over 16 h before the CO_2 exhaled is solely due to metabolic production [4,5].

When end-tidal values decrease in the face of increased CO_2 load, we ask: is the decrease a consequence of a drop in pulmonary blood flow – for example, secondary to elevated ventilatory pressures or dissection of CO_2 into the mediastinum with compression of intrathoracic veins and a decrease in preload – or is it the result of CO_2 gas embolism? Based on anecdotal evidence and case reports, the consequences of CO_2 gas emboli seem to have a lower mortality rate than air emboli due to the rapid absorption of CO_2 emboli. Many studies have shown that transesophageal echocardiography, or even transthoracic Doppler, are more sensitive tools than capnography for detecting small emboli of minimal clinical consequence. The capnograph remains the best non-invasive tool for the detection of a major embolus. Gas emboli occur not only during laparoscopic procedures, but have also been detected by transesophageal echocardiography during endoscopic vein harvesting for coronary artery bypass grafting [6–8]. Of course, air embolism (see Chapter 21: Capnography and pulmonary embolism) can occur with many different operations in which veins that lie above the level of the right heart are opened. Again, capnography will be helpful in demonstrating the increase in deadspace.

Neurosurgical anesthesia

Several factors affect cerebral blood flow; among them are CO_2 and anesthetics. Halothane has the worst reputation of allowing an increase in cerebral blood flow while thiopental and etomidate have the dual advantage of decreasing O_2 consumption and cerebral blood flow. Other factors are shown in Figure 6.8, a well-known diagram depicting the acute effects of hyper- and hypocarbia on cerebral blood flow. It shows that cerebral perfusion pressure (i.e., mean arterial pressure minus intracranial or cerebral venous pressure) does not lead to changes in cerebral blood flow (and thus changes in intracranial volume) as long as the perfusion pressure falls somewhere between 70 and 150 mm Hg. In chronically hypertensive patients, these values are likely to be higher. A very low partial pressure of

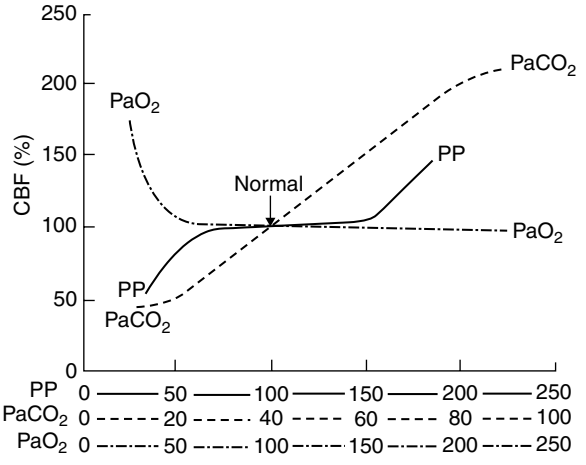

Figure 6.8 The acute effects of hyper- and hypocarbia on cerebral blood flow (CBF). PP, perfusion pressure. All pressures in mm Hg.

oxygen (PO_2) leads to a homeostatic attempt to bring more blood into the brain, thus causing swelling of the brain. While autoregulation works spectacularly well over a considerable range of perfusion pressures, it fails to compensate for the acute effects of changing CO_2 tensions. Observe the almost linear increase of cerebral blood flow with increasing $PaCO_2$. In years gone by, many patients were routinely hyperventilated during anesthesia. Today, we recognize the benefit of normal CO_2 levels and normal cerebral perfusion [9].

The picture is importantly changed in patients with intracranial pathology, which can cause the affected tissue to lose its autoregulation. Hence, in neurosurgical anesthesia, we strive to maintain a normal $PaCO_2$, but attempt to lower it should the brain swell and the patient be at risk of suffering herniation of the brain with its devastating effects. Capnography plays an important role in neurosurgical anesthesia; however, the clinician must be aware of circumstances that might lead to $\dot{V}/\dot{Q}$ disturbances and, thus, to increased differences between end-tidal and arterial PCO_2 values. Therefore, analysis of arterial blood gases may still be necessary to ensure an accurate determination of $PaCO_2$ in the presence of elevated intracranial pressure.

Cardiovascular operations

When cardiac surgery interferes with pulmonary blood flow, end-tidal CO_2 will be proportionally reduced. Indeed, this phenomenon has been used to assess pulmonary blood flow by monitoring end-tidal CO_2 pressures [10]. In Figure 6.9, the authors observed a reasonably good correlation until the $PETCO_2$ values

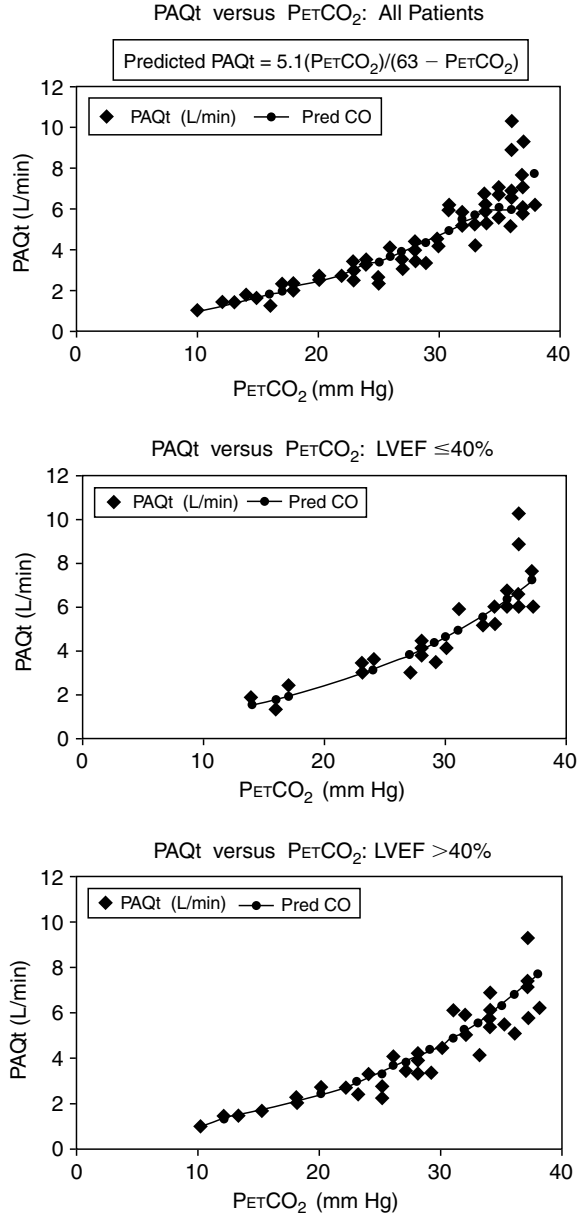

Figure 6.9 End-tidal CO_2 and pulmonary artery blood flow (PAQt). The line shows the calculated pulmonary flow. Observe the good fit of low $PETCO_2$ values and pulmonary flow. See text for explanation. $PAQt = 5.1(PETCO_2)/(63 - PETCO_2)$. Regression analysis revealed an r value of 0.88 ($P < 0.0001$). When data obtained from patients with left ventricular ejection fraction (LVEF) ≤ 40% and > 40% were plotted separately, statistical relationships were similar. [Reproduced with permission from Maslow A, Stearns G, Bert A, *et al*. Monitoring end-tidal carbon dioxide during weaning from cardiopulmonary bypass in patients without significant lung disease. *Anesth Analg*, 2001; **92**: 306–13.]

exceeded about 35 mm Hg. They assumed that, with even better perfusion, areas of deadspace ventilation were now opened up and, thus, the elimination of CO_2 increased with improved pulmonary blood flow. Thus, when minute ventilation and CO_2 production remain constant, end-tidal CO_2 can become a clinically useful indicator of changes in cardiac output. Boccara *et al.* [11] suggest that end-tidal CO_2 can be used to predict unclamping hypotension if end-tidal CO_2 decreases by more than 15% while the aorta is clamped.

During aortic surgery, clamping of the aorta leads to complex cardiovascular adjustments and decrease of cardiac output, as well as a concomitant decrease in CO_2 delivery to the lungs. If ventilation remains unchanged, end-tidal CO_2 values will decline, only to rise again with unclamping of the aorta and with reperfusion of ischemic vascular beds and liberation of acidic metabolites that accumulate during the cessation of peripheral perfusion [12]. During cardiopulmonary bypass with the cessation of pulmonary blood flow, capnographic tracings from the breathing circuit will cease, as no CO_2 is being delivered during this period.

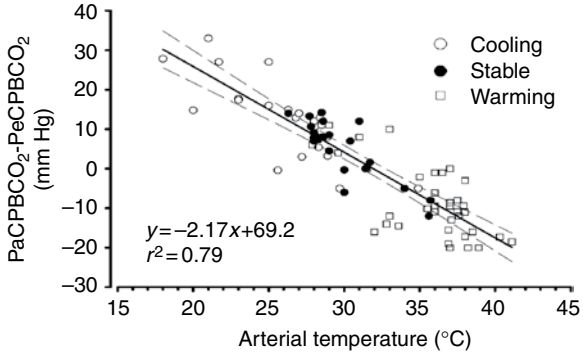

Figure 6.10 Linear regression analysis of temperature and the gradient between arterial carbon dioxide (Pa CPB CO_2) and cardiopulmonary bypass exhaust carbon dioxide (Pe CPB CO_2) in humans ($n = 29$) undergoing temperature changes during cardiopulmonary bypass. Shown are individual data points with the best fitted line (solid line) to $y=mx+b$ along with 95% confidence intervals (dashed lines). The legend depicts the status of temperature management during cardiopulmonary bypass when the data point was observed. [From: Peng YG, Morey TE, Clark D, *et al.* Temperature-related differences in mean expired pump and arterial carbon dioxide in patients undergoing cardiopulmonary bypass. *J Cardiothorac Vasc Anesth* 2007; **21**: 57–60.]

Utilization of capnography during cardiopulmonary bypass

Cardiac surgery with cardiopulmonary bypass (CPB) often involves moderate (28 °C) or deep (18 °C) hypothermic conditions. Hypothermia increases the solubility of CO_2 in blood, and thereby decreases the partial pressure of CO_2 for a given CO_2 content of blood [13].

Current practice does not include the routine monitoring of expired CO_2 from the CPB oxygenator. Peng *et al.* [14] studied the relationship between arterial PCO_2 during bypass (Pa CPB CO_2) and mean cardiopulmonary bypass pump-expired CO_2 (Pe CPB CO_2) during CPB in the cooling, steady state and rewarming phases. A hollow fiber, membrane oxygenator (Gish Biomedical Inc., Rancho Santa Margarita, CA) was used for the study. An α stat acid–base regimen was applied during CPB. The mean expired pump PCO_2 was measured by an infrared multigas analyzer (Capnomac, Datex-Ohmeda Inc., Madison, WI), with the sampling catheter connected to the scavenging port of the oxygenator. Values for Pa CPB CO_2 from the arterial outflow to the patient and Pe CPB CO_2 during CPB at various oxygenator arterial temperatures were collected and compared. The mean difference between Pa CPB CO_2 and Pe CPB CO_2 was positive 12.4 ± 10.0 mm Hg during the cooling phase and negative 9.3 ± 9.9 mm Hg during the rewarming phase, respectively. The cooler the blood temperature, the greater the difference between Pa CPB CO_2 and Pe CPB CO_2 (up to 33 mm Hg). The difference between Pa CPB CO_2 and Pe CPB CO_2 demonstrates a good correlation with the change in temperature (Figure 6.10). During CPB, arterial CO_2 can be approximated by the formula:

$$\mathrm{PaCPBCO_2} = (-2.17 + 69.2) + \mathrm{PeCPBCO_2}x$$

where x is temperature in degrees C.

Intermittent $PaCO_2$ determination has been used as a routine parameter for acid–base management during CPB. The value for Pe CPB CO_2 can be adjusted by proper setting of the CPB sweep flow rate to help optimize cerebral blood flow.

Capnographic changes after tourniquet release

Release of a lower-extremity tourniquet will increase venous PCO_2 as tissue acids enter the blood. In patients who are breathing spontaneously, minute ventilation increases noticeably until $PaCO_2$ normalizes. When mechanically controlled ventilation is kept constant, $P_{ET}CO_2$ will increase and track the changes in $PaCO_2$. Upon release of a tourniquet, some clinicians increase

minute ventilation to facilitate elimination of the acid load [15].

High-frequency jet ventilation

In high-frequency jet ventilation (HFJV), very small tidal volumes at respiratory rates ≥100 breaths/min are employed. No normal capnogram can be produced under these circumstances. However, it is usually possible to interrupt high-frequency ventilation and interpose a few slow breaths that enable the capnographic display of end-tidal CO_2 pressures.

A clinical perspective

Assuming that artifacts from faulty valves or leaks or equipment malfunction have been ruled out, and assuming that the collection of end-tidal gases proceeds without problems, capnographic data can exhibit low, normal, or high end-tidal values. The clinician will need to examine the patient and these data, but, whether low, normal, or high, the adequacy of ventilation is of foremost importance. Given the patient's weight and temperature, we can estimate a desired tidal volume × respiratory rate (Table 6.1). Volumetric capnography facilitates this assessment by providing deadspace ventilation assessment, thereby enabling the calculation of effective alveolar ventilation. There are essentially three scenarios to be considered (with many gray areas between them).

(1) **Low (<34 mm Hg) $P_{ET}CO_2$.** While hyperventilation will lower $P_{ET}CO_2$, we must resist the impulse to decrease minute ventilation until other causes of low $P_{ET}CO_2$ have been excluded. These include a reduced pulmonary blood flow (≈ low cardiac output) secondary to cardiovascular depression from deep anesthesia, low preload (hypovolemia or increased venous capacitance and reduced venous return), compression of vessels (e.g., surgeon compressing the vena cava, etc.), pneumothorax, pulmonary embolism, or cardiac disease. Hypocapnia is one of the most important signals of trouble during anesthesia, and deserves a careful and systematic differential diagnosis and rapid correction.

(2) **Normal (34 to 44 mm Hg) $P_{ET}CO_2$.** A normal capnogram with normal respiratory parameters is reassuring, indeed, but only if the effective alveolar ventilation is, in actuality, appropriate for the patient. The patient's lungs may be hyperventilated, and an arterial blood gas may show a much higher than expected $PaCO_2$, as can occur with deadspace ventilation – with or without a pulmonary shunt. If a large $PaCO_2$–$P_{ET}CO_2$ difference is noted, once again a cause must be determined. The factors responsible for an increased difference between $PaCO_2$ and $P_{ET}CO_2$ will also affect oxygen and anesthetic vapors, although maybe not to the same degree, depending on their individual venous-to-arterial differences. A normal capnogram is a positive finding, but it should not lull the clinician into a false sense of security.

(3) **High (> 44 mm Hg) $P_{ET}CO_2$.** Again, first check if ventilation is adequate. This is very important because automatically increasing ventilation to correct hypercarbia can obscure, for a period of time, the early and best evidence of malignant hyperthermia, or other hypermetabolic syndrome. Due to the critical nature of malignant hyperthermia, it is imperative that it be diagnosed at its earliest stages. Tachycardia, often the first symptom of malignant hyperthermia, should prompt the anesthesiologist to examine differential diagnoses. Minutes before a change in temperature can be detected, end-tidal CO_2 will increase dramatically. This is the pathognomonic sign of increased CO_2 production by hypermetabolic muscle tissue. Therefore, end-tidal CO_2 monitoring is an important non-invasive device that can point to the early stages of malignant hyperthermia [16]. Carbon dioxide production and malignant hyperthermia, and other much rarer conditions are covered extensively in subsequent chapters.

Table 6.1 Average respiratory values for resting, healthy patients

Parameter	Adult range	Neonatal range
Respiratory rate	10–15 breaths/min	30–40 breaths/min
Tidal volume	6–10 mL/kg	5–7 mL/kg
Minute ventilation	4–10 L/min	200–300 mL/kg/min

References

1. American Society of Anesthesiologists. *Standards for Basic Anesthetic Monitoring*. Park Ridge, IL: ASA, 2003.

Available online at http://www.medana.unibas.ch/eng/educ/standard.htm#anchor51776457. (Accessed November 18, 2010.)

2. Ginosar Y, Baranov D. Prolonged "phantom" square wave capnograph tracing after patient disconnection or extubation: potential hazard associated with the Siemens Servo 900c ventilator. *Anesthesiology* 1997; **86**: 729–35.
3. Tripathi M, Pandey M. Atypical "tails-up" capnograph due to breach in the sampling tube of side-stream capnometer. *J Clin Monit Comput* 2000; **16**: 17–20.
4. Kazama T, Ikeda K, Kato T, Kikura M. Carbon dioxide output in laparoscopic cholecystectomy. *Br J Anaesth* 1996; **76**: 530–5.
5. Gandara MV, de Vega DS, Escriu N, *et al*. Respiratory changes during laparoscopic cholecystectomy: a comparative study of three techniques. *Rev Esp Anestesiol Reanim* 1997; **44**: 177–81.
6. Mann C, Boccara G, Fabre JM, Grevy V, Colson P. The detection of carbon dioxide embolism during laparoscopy in pigs: a comparison of transesophageal Doppler and end-tidal carbon dioxide monitoring. *Acta Anaesthesiol Scand* 1997; **41**: 281–6.
7. Bhavani-Shankar K, Steinbrook RA, Brooks DC, Datta S. Arterial to end-tidal carbon dioxide pressure difference during laparoscopic surgery in pregnancy. *Anesthesiology* 2000; **93**: 370–3.
8. Lin SM, Chang WK, Tsao CM, *et al.* Carbon dioxide embolism diagnosed by transesophageal echocardiography during endoscopic vein harvesting for coronary artery bypass grafting. *Anesth Analg* 2003; **96**: 683–5.
9. Brian JE Jr. Carbon dioxide and the cerebral circulation. *Anesthesiology* 1998; **88**: 1365–86.
10. Maslow A, Stearns G, Bert A, *et al*. Monitoring end-tidal carbon dioxide during weaning from cardiopulmonary bypass in patients without significant lung disease. *Anesth Analg* 2001; **92**: 306–13.
11. Boccara G, Jaber S, Eliet J, Mann C, Colson P. Monitoring of end-tidal carbon dioxide partial pressure changes during infrarenal aortic cross-clamping: a non-invasive method to predict unclamping hypotension. *Acta Anaesthesiol Scand* 2001; **45**: 188–93.
12. Johnston WE, Conroy BP, Miller GS, Lin CY, Deyo DJ. Hemodynamic benefit of positive end-expiratory pressure during acute descending aortic occlusion. *Anesthesiology* 2002; **97**: 875–81.
13. Sitzwohl C, Kettner SC, Reinprecht A, *et al*. The arterial to end-tidal carbon dioxide gradient increases with uncorrected but not with temperature-corrected $PaCO_2$ determination during mild to moderate hypothermia. *Anesth Analg* 1998; **86**: 1131–6.
14. Peng YG, Morey TE, Clark D, *et al*.Temperature-related differences in mean expired pump and arterial carbon dioxide in patients undergoing cardiopulmonary bypass. *J Cardiothorac Vasc Anesth* 2007; **21**: 57–60.
15. Deen L, Nyst CL, Zuurmond WW. Metabolic changes after tourniquet release. *Acta Anaesthesiol Belg* 1982; **33**: 107–14.
16. Baudendistel L, Goudsouzian N, Cote C, Strafford M. End-tidal CO_2 monitoring: its use in the diagnosis and management of malignant hyperpyrexia. *Anaesthesia* 1984; **39**: 1000–3.

Section 1
Chapter
7

Ventilation

Monitoring during mechanical ventilation

J. Thompson and N. Craig

Clinical applications of end-tidal carbon dioxide monitoring

Continuous monitoring of end-tidal carbon dioxide ($PETCO_2$) is a long-established standard of care in the operating room (OR). The exhaled CO_2 in conjunction with its associated capnogram provides early detection of potentially dangerous clinical changes in the patient. Continuous monitoring of CO_2 has been responsible for the prevention of adverse events including displacement of the endotracheal tube, hypoventilation, and the disruption of the integrity of the ventilator circuit [1]. Although it is not yet mandated for all patients receiving mechanical ventilatory support outside of the OR, its use in the intensive care unit (ICU) and emergency room setting has become more widespread [2,3]. Carbon dioxide can be useful to monitor the mechanically ventilated patient when used in conjunction with other monitors of the patient's clinical status. The American Association for Respiratory Care has published guidelines for the use of capnography in the clinical settings during mechanical ventilation (Table 7.1) [4].

The level of $PETCO_2$ is a reflection of alveolar CO_2 (partial pressure of carbon dioxide in alveolar gas), and thus represents arterial CO_2 (partial pressure of CO_2 in arterial blood, $PaCO_2$). In contrast to arterial blood gas (ABG) measurement, CO_2 monitoring is non-invasive, less costly, and is a real-time continuous measurement of exhaled CO_2. However, CO_2 monitoring is affected by changes in metabolism or CO_2 production, cardiovascular function, respiratory function, and monitor limitations.

Metabolic changes and CO_2 production

Changes in the metabolic rate of the patient result in a change in CO_2 production and, thus, CO_2 elimination. Monitoring of CO_2 can be used as an indicator of CO_2 production provided that circulation and ventilation are relatively stable [5]. Conditions that increase metabolism include fever, sepsis, pain, and seizures. In the presence of these conditions, CO_2 production will increase, resulting in an elevation in $PETCO_2$. A decrease in metabolism occurs in patients who are hypothermic or patients who are sedated and paralyzed. These conditions lower CO_2 production and can cause a decrease in the $PETCO_2$ if minute ventilation does not increase in parallel. In patients who are mechanically ventilated and unable to alter minute ventilation in response to changes in CO_2 production, an increase in $PETCO_2$ serves to alert the clinician of the need to make adjustments in ventilation.

Cardiovascular function

Transport of CO_2 to the lungs is dependent on adequate cardiovascular function. Any factor that alters cardiovascular function can affect CO_2 transport to the lungs. In the absence of changes in the respiratory status of the patient, $PETCO_2$ changes may serve to suggest changes in the cardiovascular function of the patient. Hypovolemia, hypotension, and pulmonary hypertension can all decrease pulmonary blood flow, and thereby cause a gradual decrease in $PETCO_2$. Cardiac arrest will result in an abrupt rapid decline, and then disappearance of monitored $PETCO_2$. Under conditions of complete cardiovascular collapse, the $PETCO_2$ tracing will disappear until circulation is restored by either chest compressions or return of spontaneous ventilation. Studies have suggested that monitoring $PETCO_2$ is useful in evaluating the effectiveness of cardiopulmonary resuscitation (CPR) (see Chapter 20: Cardiopulmonary resuscitation). With the initiation of effective CPR and the restoration of pulmonary blood flow, a rise in $PETCO_2$ should be noted. It has also been suggested that

Capnography, Second Edition, ed. J. S. Gravenstein, Michael B. Jaffe, Nikolaus Gravenstein, and David A. Paulus. Published by Cambridge University Press. © Cambridge University Press 2011.

Table 7.1 Indications for capnography during mechanical ventilation

Section	Indication
4.1	Evaluation of the exhaled (CO_2), especially $P_{ET}CO_2$, which is the maximum partial pressure of CO_2 exhaled during a tidal breath (just prior to the beginning of inspiration) and is designated $P_{ET}CO_2$.
4.2	Monitoring severity of pulmonary disease and evaluating response to therapy, especially therapy intended to improve the ratio of deadspace to V_D/V_T and the matching of $\dot{V}/\dot{Q}$, and possibly, to increase coronary blood flow
4.3	Use as an adjunct to determine that tracheal rather than esophageal intubation has taken place (low or absent cardiac output may negate its use for this indication); colorimetric CO_2 detectors are adequate devices for this purpose
4.4	Continued monitoring of the integrity of the ventilatory circuit, including the artificial airway
4.5	Evaluation of the efficiency of mechanical ventilatory support by determination of the difference between the arterial partial pressure for CO_2 ($PaCO_2$) and the $P_{ET}CO_2$.
4.6	Monitoring adequacy of pulmonary, systemic, and coronary blood flow
4.6.1	Estimation of effective (non-shunted) pulmonary capillary blood flow by a partial rebreathing method
4.6.2	Use as an adjunctive tool to screen for pulmonary embolism (evidence for the utility of deadspace determinations as a screening tool for pulmonary embolism is at present not conclusive)
4.6.3	Monitoring the matching of $\dot{V}/\dot{Q}$ during independent lung ventilation for unilateral pulmonary contusion
4.7	Monitoring inspired CO_2 when CO_2 gas is being therapeutically administered
4.8	Graphic evaluation of the ventilator–patient interface: evaluation of the shape of the capnogram may be useful in detecting rebreathing of CO_2, obstructive pulmonary disease, waning neuromuscular blockade (curare cleft), cardiogenic oscillations, esophageal intubation, cardiac arrest, and contamination of the monitor or sampling line with secretions or mucus
4.9	Measurement of the volume of CO_2 elimination to assess metabolic rate and/or alveolar ventilation

Source: Reproduced with permission from: AARC Clinical Practice Guideline. Capnography/capnometry during mechanical ventilation – 2003 revision and update. *Respir Care* 2003; **48**: 534–9.

the $P_{ET}CO_2$ measurement may decrease when chest compressions are less effective [6].

Respiratory function

Changes in respiratory function will affect the removal of CO_2 from the lungs to the environment. Obstructive lung diseases, pneumonia, neuromuscular disorders, and central nervous system disorders with impaired respiratory function will alter the $P_{ET}CO_2$ value. Levels of $P_{ET}CO_2$ and $PaCO_2$ are generally closely matched in lungs with low ventilation and perfusion ($\dot{V}/\dot{Q}$) mismatching. In some patients admitted to the ICU for mechanical ventilatory support, there may be no access for arterial sampling, and $P_{ET}CO_2$ monitoring may be the only available guide for establishing adequate ventilation. The $P_{ET}CO_2$ value and its associated capnogram serve as a useful guide for determining the ventilation requirements of the patient. Capnometry without the associated capnogram in this setting is of somewhat limited utility in assessing adequacy of ventilation. Variations from a normal capnogram not only help in diagnosing an underlying clinical or technical problem, they also alert to a potentially larger than usual difference in the $PaCO_2$–$P_{ET}CO_2$ gradient. In a normal appearing capnograph, there is a steep rise in CO_2, followed by a near-horizontal plateau which represents alveolar gas. The absence of a plateau suggests changes in physiologic condition, mechanical problems, or monitoring problems.

Even with arterial access, blood gas sampling does not provide the instantaneous information needed when acute events arise. This is particularly true in patients with cerebral hypertension as a result of trauma. These patients are typically managed with some degree of hyperventilation, as increases in the $PaCO_2$ of the patient with head trauma cause cerebral vasodilation, with an associated increase in intracranial pressure [7]. Optimal management of head-injured patients at risk for intracranial hypertension requires close and continuous monitoring of $P_{ET}CO_2$ to detect sudden changes in $PaCO_2$. The gradient between $PaCO_2$ and

$P_{ET}CO_2$ will widen with impairment of lung function. The wider the gradient is, the more impaired the lung function is likely to be.

Mechanical ventilatory support using the $PaCO_2$–$P_{ET}CO_2$ gradient

In normal individuals, the gradient between arterial and alveolar CO_2 ($PaCO_2$–P_ACO_2) varies between 2 and 5 mm Hg [8]. Comparison of the gradient between arterial and end-tidal CO_2 ($PaCO_2$–$P_{ET}CO_2$) can offer valuable information regarding a patient's clinical status. The gradient is widened by abnormalities in the ratio (normally 0.8), and is altered by deadspace (VD/VT) ventilation or shunt perfusion.

Deadspace ventilation is characterized by an increased $\dot{V}/\dot{Q}$ ratio. In deadspace ventilation, alveoli are ventilated but not well perfused. If there is abnormal perfusion in well-ventilated areas of the lung, the $P_{ET}CO_2$ will decrease. Deadspace ventilation may be caused by physiologic conditions such as pulmonary emboli, hypovolemia, and hemorrhage, as well as excessive continuous positive airway pressure (CPAP). Therapy may be initiated to improve systemic perfusion and, thereby, also pulmonary circulation. As pulmonary circulation improves, the $PaCO_2$–$P_{ET}CO_2$ gradient should narrow, which suggests a positive response to therapy.

Shunt perfusion is characterized by a low $\dot{V}/\dot{Q}$ ratio. Shunt occurs when alveoli have normal perfusion but are not adequately ventilated. Examples of increasing shunt include many pulmonary disease states, such as pneumonia, atelectasis, and acute respiratory distress syndrome (ARDS). Mechanical ventilation strategies aimed at optimizing lung function and decreasing the widened gradient include positive end-expiratory pressure (PEEP). The shunt effect on the $PaCO_2$–$P_{ET}CO_2$ gradient is generally much smaller than the deadspace effect.

The $PaCO_2$–$P_{ET}CO_2$ gradient can be a useful tool for optimizing PEEP in patients with increasing lung disease. At the appropriate level of PEEP, the $PaCO_2$–$P_{ET}CO_2$ gradient should be at its most narrow point. The phenomenon of alveolar overdistension can occur when the optimal PEEP is exceeded. A gradient that has narrowed while PEEP has been gradually increased may widen once optimal PEEP has been exceeded [9]. One drawback of this technique is the frequency of arterial sampling required to assess the gradient.

Diseases such as asthma may produce a widened gradient because airway obstruction can lead to uneven or incomplete emptying of alveoli, gas trapping, and, potentially, auto-PEEP. In this disease state, the capnograph provides useful information about the patient's responses to therapy [10]. The $P_{ET}CO_2$, as a number on its own, does not confer adequate information regarding the physiologic state of the patient. The abnormal appearing slope of the curve may change toward a more normal one with bronchodilator therapy or changes in mechanical ventilation tailored to providing optimal emptying times. Auto-PEEP can lead to increased deadspace, as overdistention can alter perfusion and lead to an increase in deadspace ventilation.

Monitoring the integrity of the airway and breathing circuit

The $P_{ET}CO_2$ tracing in the ICU setting can be used to monitor continuously the position and patency of the endotracheal tube. In patients who are mechanically ventilated and moving spontaneously, there is an ever-present risk of dislodging the endotracheal tube, resulting in inadequate ventilation. Changes in head position, especially with neck flexion or extension, can dramatically change the position of the endotracheal tube. This is particularly important in the neonatal or pediatric patient, in whom the distance between the vocal cords and the carina is much shorter. Likewise, moving a patient who is chemically paralyzed for procedures such as a radiograph can put the patient at risk for endotracheal tube displacement. In this situation, the capnogram will acutely flatten.

Continuously monitoring CO_2 can also alert the clinician to a partial or total occlusion of the endotracheal tube. Although CO_2 monitoring should not take the place of the alarms on the mechanical ventilator, changes in the capnograph may alert the clinician to the need for an early intervention such as suctioning. Another condition that may produce an acute fall in $P_{ET}CO_2$ in an otherwise stable patient is the partial or complete kinking of the endotracheal tube. In addition to problems with the endotracheal tube, any disruption of the integrity of the ventilator circuit will result in an immediate change in the $P_{ET}CO_2$ value [11] (see Figure 7.1).

Transport of the mechanically ventilated patient

Monitoring CO_2 during transport of intubated patients has proven useful in the inter- or intrahospital setting

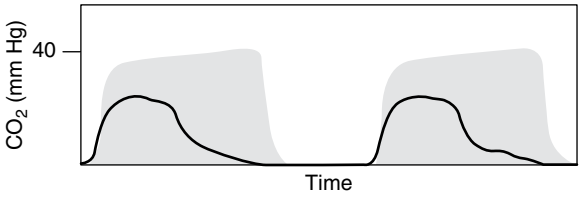

Figure 7.1 Acute change in capnogram from normal (shaded area). The endotracheal tube was in the right main bronchus. [From: Thompson JE, Jaffe MB. Capnographic waveforms in the mechanically ventilated patient. *Respir Care* 2005; **50**: 100–8.]

[12]. When transport is required, inadvertent extubation can occur at any point in the process, during transfer to and from the bed, and during any procedure. In addition to monitoring the position of the airway, often access to arterial blood gas sampling and the laboratory is not as feasible as in the ICU, and thus CO_2 becomes an even more important tool for monitoring the adequacy of ventilation. When patients are transported, they are often manually ventilated. With this mode of ventilation, maintenance of the pre-transport ventilatory parameters is difficult. The $PETCO_2$ trend during transport often alerts the clinician to changes in ventilation or clinical condition of the patient. This is particularly important to the patient with pulmonary hypertension or cerebral hypertension for whom steady hyperventilation is critical. Monitoring $PETCO_2$ provides information on the adequacy of ventilation and rapid detection of hypoventilation.

Recent recommendations of the American Heart Association for Pediatric Advanced Life Support include monitoring exhaled CO_2 of intubated patients, especially during transport and diagnostic procedures that require patient movement [13].

Weaning from mechanical ventilation

Monitoring CO_2 alone may not be adequate for weaning a patient from mechanical ventilation. When the $PaCO_2$–$PETCO_2$ gradient is unknown, a patient weaning from mechanical ventilatory support with a consistent $PETCO_2$ may have an underappreciated increase in deadspace [14]. In the patient with a stable or improving respiratory status, it may be useful, provided it is compared with the $PaCO_2$–$PETCO_2$ gradient at the start of weaning. Monitoring $PETCO_2$ has been shown to correlate well with $PaCO_2$ in postoperative patients without parenchymal lung disease [15]. Other measures of patient status, including vital signs, respiratory rate, and SpO_2, must be closely followed. It should be noted that in patients with cyanotic congenital heart disease, $PETCO_2$ significantly underestimates $PaCO_2$, and may produce a variable gradient depending on the current cardiovascular function of the patient (Figures 7.2–7.4) [16].

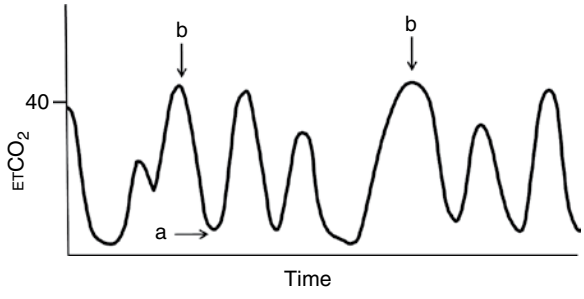

Figure 7.2 Capnogram indicating weaning failure. There is chaotic, rapid breathing, with rebreathing (a). Spontaneous breaths (b) during mandatory (ventilator-delivered) breaths. [Modified from: Carlon GC, Ray C Jr., Miodownik S, Kopec I, Groeger JS. Capnography in mechanically ventilated patients. *Crit Care Med* 1988; **16**: 550–6.]

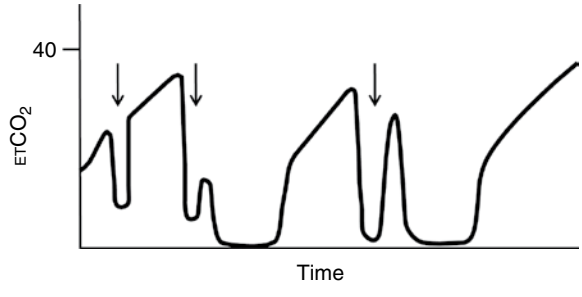

Figure 7.3 Capnogram indicating patient–ventilator asynchrony during intermittent mandatory ventilation. The arrows indicate spontaneous breaths. [Modified from: Carlon GC, Ray C Jr., Miodownik S, Kopec I, Groeger JS. Capnography in mechanically ventilated patients. *Crit Care Med* 1988; **16**: 550–6.]

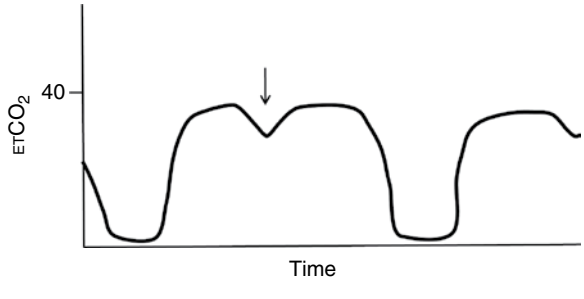

Figure 7.4 Capnogram in which the arrow points to a small spontaneous inspiratory effort that did not trigger the ventilator. [Modified from: Carlon GC, Ray C Jr., Miodownik S, Kopec I, Groeger JS. Capnography in mechanically ventilated patients. *Crit Care Med* 1988: **16**: 550–6.]

Special procedures: monitoring the therapeutic administration of CO_2

In newborns, the therapeutic administration of CO_2 in the ventilator circuit has been used in the preoperative management of hypoplastic left heart syndrome. In this patient population, maintaining a balance between pulmonary and systemic blood flow is critical. Excessive pulmonary blood flow can lead to a compromise of systemic perfusion, resulting in hypoperfusion and metabolic acidosis. One treatment strategy is aimed at increasing pulmonary vascular resistance by the addition of inspired CO_2. It is added to the inspiratory limb of a continuous flow ventilator to produce a respiratory acidosis in order to increase pulmonary vascular resistance while minute ventilation and Vt are maintained at constant levels [17,18]. The level of $PetCO_2$ is monitored, and an alarm set, to maintain a specific range of $PaCO_2$ and avoid significant respiratory acidosis. Sudden changes in $PetCO_2$ will alert the clinician to changes in the clinical status of the patient. Additionally, inspired CO_2 concentrations should be monitored and alarmed to avoid inadvertent alterations of the inspired CO_2.

Use of CO_2 in patients without an artificial airway

Continuous CO_2 monitoring may play a role in the spontaneously breathing patient without an artificial airway. The use of sidestream technology and sampling via a nasal cannula make it possible to monitor patients who are not mechanically ventilated [19]. The use of CO_2 has expanded to the pediatric setting, as advances in technology have allowed for lower sampling flow rates in patients with small tidal volumes and faster respiratory rates. It may provide a tool to monitor respiratory function in a variety of disease conditions, and may limit the need for invasive measurement of $PaCO_2$ by arterial puncture in the awake patient. The disease states may include a variety of conditions, including asthma, bronchiolitis, and neuromuscular diseases. The relationship of the $PetCO_2$ to the $PaCO_2$ value may be difficult to determine, depending on the degree of pulmonary disease or the cardiovascular status of the patient. Therefore, the clinician must be aware of the effect on the measured $PetCO_2$ caused by conditions of hypoventilation, mouth breathing, or low Vd/Vt that may produce a lower $PetCO_2$ reading. It may serve as a trend monitor in patients without arterial access to compare the $PaCO_2$–$PetCO_2$ gradient. It can alert the clinician to impending respiratory failure when used in conjunction with other tools of physical assessment, such as vital sign measurements including SpO_2.

In the patient with asthma or other diseases with changes in airway resistance, $PetCO_2$ and the capnogram can be helpful in evaluating the response to bronchodilator therapy. Decreases in the terminal slope of the curve suggest a positive response to bronchodilator therapy [20]. Capnography may also be a more objective mode that can be used for predicting the need for hospitalization in acute childhood asthma [21].

The pediatric patient, with diseases such as bronchiolitis, may be monitored for response to therapy and adequacy of ventilation. In addition to airway obstruction and atelectasis, patients with bronchiolitis are often at risk for developing apnea. Monitoring CO_2 can rapidly detect the cessation of breathing [22].

Patients with neuromuscular disease who develop muscle fatigue may benefit from CO_2 monitoring. Complaints of fatigue and sleepiness in patients with neuromuscular disease may be a result of nocturnal hypercapnia. Capnography can be used to detect respiratory insufficiency, as pulse oximetry alone does not provide adequate monitoring of the patient with respiratory insufficiency receiving supplemental oxygen. A rising $PetCO_2$ can indicate the onset of muscle fatigue and suggest the need for increased respiratory support such as non-invasive ventilation. Patients who are already receiving non-invasive ventilatory support may be monitored for adequacy of assisted ventilation [23].

Another application of CO_2 monitoring may be as a diagnostic tool for patients with obstructive sleep apnea. Apnea *and obstruction* will cause an immediate reduction in $PetCO_2$; when spontaneous respirations return, $PetCO_2$ will reappear (see Figure 11.2 in Chapter 11: Capnography in sleep medicine) [24].

Continuous CO_2 monitoring may be advantageous in the management of acutely ill patients with diabetic ketoacidosis. Patients with this condition hyperventilate to lower $PaCO_2$ and lessen the severity of acidosis. Capnography may be useful in continuously monitoring the degree of respiratory compensation and response to therapy (Figures 7.5 and 7.6) [25].

Garcia and colleagues have suggested that $PetCO_2$ might approximate $PaCO_2$ and thus serves as an important tool to guide therapy [26]. Note in

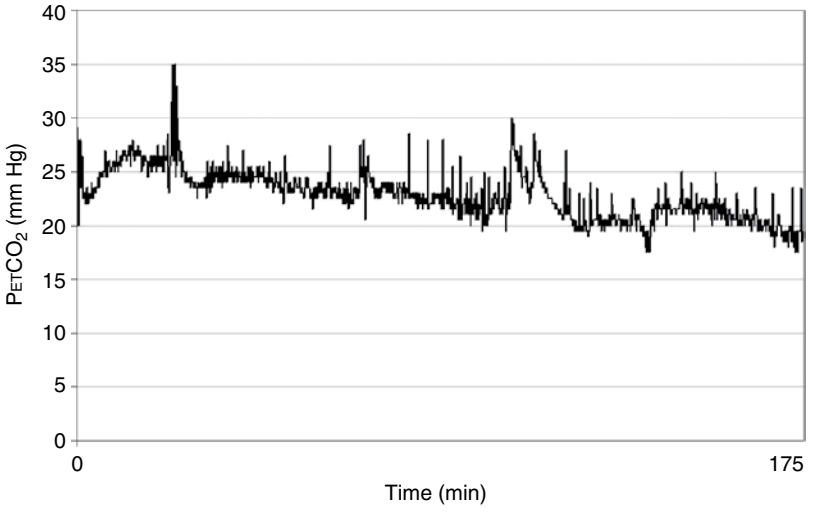

Figure 7.5 Time plot of end-tidal CO_2 for LoFlo C5 sensor in a male patient with diabetic ketoacidosis. [Adapted from: Respironics. Clinical testing of the LoFlo C5 Module: inter-device comparisons. *Respironics* 2008; **4**: 1–5.]

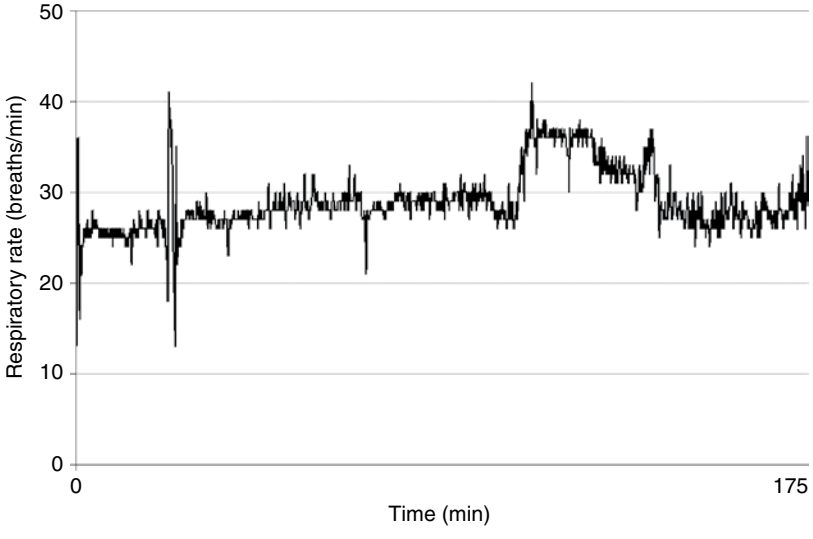

Figure 7.6 Time plot of respiratory rate for LoFlo C5 sensor in a male patient with diabetic ketoacidosis. [From: Respironics. Clinical testing of the LoFlo C5 Module: inter-device comparisons. *Respironics* 2008; **4**: 1–5.]

Figure 7.5, the decrease in $P_{ET}CO_2$, associated with mechanical ventilation at settings of A/C f 12, Vt 590, PEEP12, $FiO_2 = 70\%$), which achieved the compensatory hyperventilation required for the severe metabolic acidosis. Figure 7.6 illustrates the dynamic change in the patient's respiratory rate, which increased to a high level (minute 125) until mechanical ventilation partially relieved patient effort (after minute 150).

There is growing interest in the use of CO_2 monitoring to prevent adverse events during moderate sedation for diagnostic and/or therapeutic procedures outside of the OR. The early detection of alveolar hypoventilation in patients undergoing moderate or deep sedation may be valuable in avoiding significant morbidity and mortality [27].

Clinical applications of volumetric CO_2

Volumetric capnography or volumetric CO_2 ($\dot{V}CO_2$) is the measurement of CO_2 as a function of volume as opposed to time. Three important parameters provided by volumetric CO_2 measurement are CO_2 production, $\dot{V}CO_2$, or more accurately CO_2 elimination, alveolar ventilation (V_A), and physiological dead-space ($V_D/V_{T_{phys}}$). With the Enghoff-modified Bohr equation, $V_D/V_{T_{phys}}$ can be calculated, assuming that alveolar and arterial levels are equal. In the future, methods to extrapolate alveolar PCO_2 from the volumetric capnogram may obviate the need for arterial sampling. All three parameters can offer important

information on the physiologic state of the patient. The use of volumetric capnography has become more widespread in evaluating the adequacy of ventilation and determining optimal ventilator support, as well as potentially useful in weaning patients from mechanical ventilation. In one study, measurements of V_D/V_T and $\dot{V}CO_2$ by volumetric capnography in patients with ARDS correlated with those obtained by the more traditional metabolic monitor method of measuring V_D/V_T [28].

Carbon dioxide production

Changes in $\dot{V}CO_2$ reflect changes in $\dot{V}/\dot{Q}$ and, thus, can serve as a sensitive indicator of changes in the patient's condition. When CO_2 production increases with constant minute ventilation, $PaCO_2$ will increase. As CO_2 elimination equals CO_2 production during steady state conditions, monitoring $\dot{V}CO_2$ on a breath-to-breath basis provides the clinician instantaneous feedback on ventilator adjustments [29]. If increasing minute ventilation (VE) has resulted in the increased elimination of CO_2, then $\dot{V}CO_2$ will increase until a new steady state has been reached. In patients with asthma, changes in minute ventilation that result in an increase in CO_2 elimination will be reflected as an increase in $\dot{V}CO_2$. If an increase in $\dot{V}CO_2$ is not observed, the ventilator adjustments made by the clinician have not improved the elimination of CO_2, and may suggest an increase in air trapping. The surveillance of $\dot{V}CO_2$ may guide the determination of optimal PEEP. Optimizing PEEP in the patient with significant lung disease should be accomplished without compromising pulmonary perfusion; CO_2 removal is compromised when perfusion is compromised. The $\dot{V}CO_2$ level can be observed while the PEEP level is incrementally increased. When a decrease in $\dot{V}CO_2$ is noted, perfusion is compromised, and optimal PEEP has been exceeded.

Predicting ventilatory requirements

Alveolar minute ventilation can be used as a guide for predicting the $PaCO_2$ that may result from adjusting ventilation parameters. Using the equation

$$\text{desired } PaCO_2 = (V_A \times PaCO_2)/\text{adjusted } V_A,$$

one can predict the change in alveolar minute ventilation needed to reach a specific goal for $PaCO_2$. This formula is useful in finely controlling the $PaCO_2$ in patients with intracranial hypertension in whom a very tight range of $PaCO_2$ is necessary when maintaining hyperventilation to limit cerebral vasodilation. Likewise, in the patient in whom the ventilation plan is to employ a strategy of permissive hypercapnia, gradually altering ventilation to a precise $PaCO_2$ permits a gradual elevation in PCO_2 to allow time for the body to buffer pH and prevent significant respiratory acidosis.

Monitoring $\dot{V}CO_2$ during weaning from mechanical ventilation

Observing the $\dot{V}CO_2$ during weaning from mechanical ventilation helps to clinically determine the patient's ability to take over the work done by the mechanical ventilator. As ventilatory support is withdrawn, if the patient can successfully maintain the alveolar minute ventilation necessary to sufficiently remove CO_2, then the $\dot{V}CO_2$ should remain consistent. A stable $\dot{V}CO_2$ will confirm that the $\dot{V}/\dot{Q}$ relationship has not changed.

During the weaning process, if the patient is unable to maintain adequate alveolar ventilation, the $\dot{V}CO_2$ will decrease, indicating an inability to remove CO_2. An improvement in V_D/V_T indicates improvement in pulmonary disease and readiness to wean from mechanical ventilation. Although work of breathing is an important factor in patients who are being weaned from ventilatory support, it is a subjective indicator. A more objective indicator of work of breathing is the V_D/V_T. If ventilator support is withdrawn, and the patient continues to maintain the same minute ventilation and V_D/V_T increases, it indicates that the ability to remove CO_2 is being compromised; this is often associated with a more rapid shallow breathing pattern. The use of V_D/V_T as a predictor for successful extubation has been the subject of many studies. One study by Hubble *et al.* in the pediatric setting determined that a V_D/V_T of < 0.5 is a predictor of successful extubation [30]. A V_D/V_T of 0.65 was associated with the need for additional respiratory support after extubation. The value of V_D/V_T as a predictor of mortality has been studied in patients with congenital diaphragmatic hernia who required extracorporeal membrane oxygenation (ECMO) support. A V_D/V_T of 0.6 was associated with an increase in mortality rate [31]. The use of continuous volumetric capnography, combined with routine clinical management, has been shown to shorten the duration of mechanical ventilation when compared to routine ventilation in a heterogeneous group of pediatric ICU patients [32].

The utility of V_D/V_T as a predictive value is an area of ongoing investigation. The measurement of V_D/V_T within several hours of the onset of respiratory failure

has been shown to predict mortality in ARDS patients [33]. In addition, there may be an association between disease severity and V_D/V_T in infants with acute bronchiolitis who are mechanically ventilated [34].

Summary

Continuous CO_2 and volumetric CO_2 monitoring have become important clinical tools for managing the ICU patient. They have improved our ability to assess complicated patients on various ventilator strategies, and provide us with a better understanding of the relationship between the ventilator and the patient.

References

1. Cote CJ, Liu LM, Szyfelbein SK, *et al*. Intraoperative events diagnosed by expired carbon dioxide monitoring in children. *Can Anaesth Soc J* 1986; **33**: 315–20.
2. Society of Critical Care Medicine: Task Force on Guidelines. Recommendations for services and personnel for delivery of care in a critical care setting. *Crit Care Med* 1988; **16**: 809–11.
3. American College of Emergency Physicians. Expired carbon dioxide monitoring. *Ann Emerg Med* 1995; **25**: 441.
4. AARC Clinical Practice Guideline. Capnography/capnometry during mechanical ventilation – 2003 revision and update. *Respir Care* 2003; **48**: 534–9.
5. Hess D. Capnometry and capnography: technical aspects, physiologic aspects, and clinical applications. *Respir Care* 1990; **35**: 557–76.
6. Kalenda Z. The capnogram as a guide to the efficacy of cardiac massage. *Resuscitation* 1978; **6**: 259–63.
7. Kerr ME, Zempsky J, Sereika S, Orndoff P, Rudy E. Relationship between arterial carbon dioxide and end-tidal carbon dioxide in mechanically ventilated adults with severe head trauma. *Crit Care Med* 1996; **24**: 785–96.
8. Nunn JF. *Applied Respiratory Physiology*, 3rd edn. London: Butterworth, 1969.
9. Blanch L, Fernandez R, Benito S, Mancebo J, Net A. Effects of PEEP on the arterial minus end-tidal carbon dioxide gradient. *Chest* 1987; **92**: 451–4.
10. Sabato K, Hanson JH. Mechanical ventilation for children with status asthmaticus. *Respir Care Clin N Am* 2000; **6**: 171–88.
11. Palmon S, Maywin L, Moore L, Kirsch J. Capnography facilitates tight control of ventilation during transport. *Crit Care Med* 1996; **24**: 608–11.
12. Williamson JA, Webb RK, Cockings J, Morgan C. The capnograph: applications and limitations:- an analysis of 2000 incident reports. *Anaesth Intens Care* 1993; **21**: 551–7.
13. American Heart Association. *Pediatric Advanced Life Support*. Dallas, TX: AHA, 2006.
14. Morley TF, Giaimo J, Maroszan E, *et al*. Use of capnography for assessment of the adequacy of alveolar ventilation during weaning from mechanical ventilation. *Am Rev Respir Dis* 1993; **148**: 339–44.
15. Healey CJ, Fedullo AJ, Swinburne AJ, Wahl GW. Comparison of non-invasive measurements of carbon dioxide tension during withdrawal from mechanical ventilation. *Crit Care Med* 1987; **15**: 764–7.
16. Short JA, Paris ST, Booker PD, Fletcher R. Arterial to end-tidal carbon dioxide tension difference in children with congenital heart disease. *Br J Anaesth* 2001; **86**: 349–52.
17. Bradley SM, Simsic JM, Atz AM. Hemodynamic effects of inspired carbon dioxide after the Norwood procedure. *Ann Thorac Surg* 2001; **72**: 2088–94.
18. Tabbutt S, Ramamoorthy C, Montenegro LM, *et al*. Impact of inspired gas mixtures on preoperative infants with hypoplastic left heart syndrome during controlled ventilation. *Circulation* 2001; **104**: I-159–64.
19. Flanagan JF, Garrett JS, McDuffee A, Tobias JD. Non-invasive monitoring of end-tidal carbon dioxide tension via nasal cannulas in spontaneously breathing children with profound hypocarbia. *Crit Care Med* 1995; **23**: 1140–2.
20. You B, Peslin R, Duvivier C, Vu VD, Grilliat JP. Expiratory capnography in asthma: evaluation of various shape indices. *Eur Respir J* 1994; **7**: 318–23.
21. Kunkov S, Pinedo V, Silver E, Crain ER. Predicting the need for hospitalization in acute childhood asthma using end-tidal capnography. *Pediatr Emerg Care* 2005; **21**: 574–7.
22. Toubas PL, Duke JC, Sekar KC, McCaffree MA. Microphonic versus end-tidal carbon dioxide nasal airflow detection in neonates with apnoea. *Pediatrics* 1990; **6**: 950–4.
23. Kotterba S, Patzold T, Malin JB, Orth M, Rasche K. Respiratory monitoring in neuromuscular disease. *Clin Neurol Neurosurg* 2001; **103**: 87–91.
24. Magnan A, Philip-Joet F, Rey M, *et al.* End-tidal CO_2 analysis in sleep apnea syndrome: conditions for use. *Chest* 1993; **103**: 129–31.
25. Agus MS, Alexander JL, Mantell PA. Continuous non-invasive end-tidal CO_2 monitoring in pediatric inpatients with diabetic ketoacidosis. *Pediatr Diabetes* 2006; **7**: 196–200.
26. Garcia E, Abramo TJ, Okada P, *et al*. Capnometry for non-invasive continuous monitoring of metabolic

status in pediatric diabetic ketoacidosis. *Crit Care Med* 2003; **31**: 2539–43.

27. Lightdale JR, Goldmann DA, Feldman HA, *et al*. Microstream capnography improves patient monitoring during moderate sedation: a randomized controlled trial. *Pediatrics* 2006; **117**: 1170–8.
28. Kallett RH, Daniel BM, Garcia O, Matthay MA. Accuracy of physiologic deadspace measurements in patients with acute respiratory distress syndrome using volumetric capnography: comparison with the metabolic monitor method. *Respir Care* 2005; **50**: 462–7.
29. Taskar V, John J, Larsson A, Wetterberg T, Jonson B. Dynamics of carbon dioxide elimination following ventilator resetting. *Chest* 1995; **108**: 196–202.
30. Hubble CL, Gentile MA, Tripp DS, *et al*. Deadspace to tidal volume ratio predicts successful extubation in infants and children. *Crit Care Med* 2000; **28**: 2034–40.
31. Arnold JH, Bower LK, Thompson JE. Respiratory deadspace measurements in neonates with congenital diaphragmatic hernia. *Crit Care Med* 1995; **23**: 371–5.
32. Cheifetz IM, Myers TR. Respiratory therapies in the critical setting: should every mechanically ventilated patient be monitored with capnography from intubation to extubation? *Respir Care* 2007; **52**: 423–42.
33. Nuckton TJ, Alonso JA, Kallet RH, *et al*. Pulmonary deadspace fraction as a risk factor for death in the acute respiratory distress syndrome. *N Engl J Med* 2002; **346**: 1281–6.
34. Almeida AA, Nolasco da Silva MT, Almeida CC, Ribeiro JD. Relationship between physiologic deadspace/tidal volume ratio and gas exchange in infants with acute bronchiolitis on invasive mechanical ventilation. *Pediatr Crit Care Med* 2007; **8**: 372–7.

Section 1
Chapter
8

Ventilation

Capnography during transport of patients (inter/intrahospital)

M. A. Frakes

Introduction

Both interhospital and intrahospital transport add a variable, and often a difficulty, to the care of critically ill patients. In addition to non-interruption of treatment by continuing it during transport, attention must be paid to the logistics of moving the patient and equipment, the physiologic stressors of the move on the patient and providers, and the barriers presented by the transport milieu.

The potential for unplanned events and patient deterioration during transport is well documented. Approximately two-thirds of patients experience adverse physiological changes during intrahospital transit, and equipment failures complicate up to 13.4% of transports [1–5]. Some of the physiologic changes are likely related to the patient's illness, as changes also occur with similar frequency in acuity-matched patients not undergoing transport. The effect on outcomes, however, is not clear. While mortality is higher for intensive care unit (ICU) patients experiencing intrahospital transport compared with APACHE-score-matched non-transported patients, that increase does not exceed predicted mortality [2,6]. Similar comparisons for interhospital transport are difficult to make because transport generally brings the patient to therapeutic services that would otherwise be unavailable. The use of specially trained transport teams may reduce the incidence of unplanned events, particularly those related to equipment issues [1,7–10].

Respiratory changes are especially common during the transport of artificially ventilated patients, particularly changes in arterial CO_2 tension and pH [11–17], which are associated with worsened patient outcomes [11,17–29]. The transport environment itself, especially interhospital transport, further contributes to the opportunity for mishap. Transport necessarily involves an increased number of patient movements. Each increases the risk for unplanned removal of medical devices, particularly those related to the airway. The transport environment and vehicle noise complicate patient assessment. Lung sound intensity is generally between 22 and 30 decibels, while transport vehicle noise levels can be as high as 100 decibels in helicopters and 84 decibels in ground ambulances [30–32]. Breath sound assessments in ground transport vehicles have been demonstrated to be barely half as accurate as in a traditional environment, and only 0.09% sensitive as an examination tool [33]. Helicopter medical teams are, in all likelihood, unable to evaluate even the simple presence or absence of lung sounds during flight [32].

Capnography and capnometry provide useful information that may help improve decision-making and reduce complications during transport (Figure 8.1). This chapter will review specific clinical applications of that technology: assuring proper endotracheal tube placement, monitoring airway circuit integrity, monitoring the consistency of mechanical ventilation, improving safety in procedural sedation, assessing cardiac output, and evaluating patients in cardiac arrest.

Endotracheal tube placement

Transport personnel are often called upon to intubate patients. Esophageal intubation and detected tube misplacements are not uncommon during transport; undetected esophageal intubation is a clinical catastrophe, with the potential for anoxic injury and death. Even experienced intubators can overlook an esophageal endotracheal tube placement, with these cases accounting for approximately 7% of closed anesthesia malpractice claims [34]. In stark contrast, the incidence of undetected endotracheal tube misplacement during transport has been reported to be as high as 25% [9,35–40].

Capnography, Second Edition, ed. J. S. Gravenstein, Michael B. Jaffe, Nikolaus Gravenstein, and David A. Paulus. Published by Cambridge University Press. © Cambridge University Press 2011.

Figure 8.1 Capnography with a nasal cannula in the ambulance setting.

Capnometry and capnography aid in the confirmation of correct endotracheal tube placement. End-tidal CO_2 ($ETCO_2$) measurement can accurately detect esophageal intubation because CO_2 is exhaled through the trachea, and not the esophagus [41,42]. Because of the relationship between $ETCO_2$ tension and cardiac output, $ETCO_2$ measurement is better in patients with good cardiac output. Overall, capnometry is 93% sensitive and 97% specific in detecting tracheal intubation [43–45]. Colorimetric and quantitative detection methods are equally reliable, and work equally well in patients at the extremes of age and weight [46–49]. However, only frank misplacements are detected by capnographic monitoring; of those, capnography suggests bronchial intubation in only about 4% of patients, and does not detect hypopharyngeal placement when gas exchange is good [50,51].

Of note, false-positive readings are possible from a patient who is esophageally intubated, whose stomach may contain CO_2 from carbonated beverages or artificial respiration. Such errors can be avoided by using a reading obtained after six ventilations have been given through the endotracheal tube and by evaluating the capnogram shape [52–54].

Postintubation capnography is the standard of care for monitoring patients who are intubated. The American Heart Association recommends a non-invasive technique, such as $ETCO_2$ detection, for confirming endotracheal tube placement [55]. Similarly, the American Society of Anesthesiologists describes capnometry as essential for evaluating endotracheal tube or laryngeal mask placement from the time of placement to removal [56]. The use of continuous $ETCO_2$ monitoring reduces the rate of undetected esophageal intubation during transport, perhaps even to zero [9,24,40]. The National Association of Emergency Medical Services Physicians, the group with perhaps the greatest medical oversight of transport providers, also recommends the use of capnography in association with out-of-hospital intubation [57].

Monitoring of ventilation

Circuit integrity

Once an airway device is in place, continuous monitoring is important to assure ventilator circuit patency, including that of the endotracheal tube, and to assure consistent levels of ventilation.

Unplanned extubation is a known complication in critical care, both in and out of the hospital [35,36,58–60]. Even when lung sounds cannot be evaluated, capnography will rapidly demonstrate an unplanned extubation by a sudden $PETCO_2$ decrease and loss of the characteristic waveform shape [42]. Although most commonly considered for monitoring the integrity of endotracheal tube placement, capnography is equally effective in assessing placement of supraglottic airway devices [56,61].

Disconnection of the ventilator circuit poses the same risk for catastrophe as an undetected esophageal intubation or unplanned extubation, especially in a patient with inadequate spontaneous ventilation. A change in the capnogram frequency may signal a disconnection, depending on the patient's spontaneous breathing pattern, and will likely demonstrate a $PETCO_2$ change. End-tidal changes in hypoventilating patients precede pulse oximetry changes, and can provide sufficient advance warning to prevent patient deterioration [42,62,63].

The capnogram and $P_{ET}CO_2$ values will reflect other abnormalities in the mechanical ventilation circuit as well. Any consistent abnormality in the capnogram should prompt a careful evaluation of the ventilator circuit, from gas source to the patient. There have been case reports of a number of interesting abnormalities, but relatively common situations include [42,64,65]:

- *Partial obstruction of the endotracheal tube* can be detected early by waveform changes. The waveform changes from the characteristic square shape to one with a prolonged expiratory up-slope or an increasingly sloped alveolar plateau as expiratory resistance increases. These changes will precede alterations in the $P_{ET}CO_2$ value itself, which requires that the tube be occluded by at least 50%.
- *An expiratory leak in the circuit or the endotracheal tube cuff* will result in a premature return of the exhaled waveform to the baseline, as well as loss of the expected square shape.
- *Minute ventilation lost via a leak* will increase $P_{ET}CO_2$, but will show a normal waveform, while machine failures causing CO_2 rebreathing will increase $P_{ET}CO_2$ and display a rising capnogram baseline.

Consistency of ventilation

Because both arterial CO_2 tension and $etCO_2$ tension are measures of ventilation, and their normal values are similar, the use of $etCO_2$ measurements as a substitute for arterial CO_2 tension is often considered. If this were actually possible, the advantages of breath-to-breath measurement, avoidance of an arterial puncture, and cost savings would be dramatic. However, the use of capnometry in that manner is ill advised.

The alveolar $etCO_2$ gradient ($PaCO_2$–$P_{ET}CO_2$) is generally 3–5 mm Hg. Changes in pulmonary deadspace and other factors affect the difference. Physiologic deadspace is anatomical space other than the pharynx, trachea, and bronchi that is ventilated but not perfused. The ($PaCO_2$–$P_{ET}CO_2$) gradient is an almost perfect measure of that space, widening as deadspace increases. The relationship is so effective that it can be used to modify the Bohr equation for the deadspace fraction to:

$$V_D/V_T = (P[a\text{-}ET]CO_2 / PaCO_2)$$

[41,43,66].

When pulmonary blood flow decreases for any reason, deadspace increases. Cardiac output is directly related to pulmonary blood flow, so decreased cardiac output increases pulmonary deadspace and, therefore, the arterial-to-end-tidal CO_2 gradient. Causes for decreased pulmonary blood flow include cardiac dysfunction, the application of positive end-expiratory pressure (PEEP), and hypovolemia, but it can also be decreased by non-cardiac sources, such as pulmonary emboli and patient positioning [43,45,66].

Other factors, some likely related to pulmonary blood flow alterations and some with a less clear physiology, also change the gradient. Age, smoking, general anesthesia, and major systemic disease increase the alveolar-to-end-tidal difference. It may be as high as 20 mm Hg in patients with severe pulmonary disease. The gradient can also be negative in some cases, especially in supine pregnant women and in exercising individuals. More importantly, in the context of critical care transport, a negative gradient has been found in 8.1% of postcardiac surgery patients and 4% of multiple trauma patients [66–70]. Worsening acuity seems to downgrade the correlation between arterial and $etCO_2$ tensions, and patients being monitored during transport generally trend toward higher acuity [71–77]. When studied specifically in patients experiencing interhospital transport, the correlation was poor ($r = 0.59$), the mean gradient was 12.9, and relationships worsened in patients with underlying disease [71,72,77].

Single-patient correlations vary over time [74,78,79]. However, for the relatively short duration of inter- or intrahospital transport, capnometry is a useful part of a constellation of patient monitors. Over the course of a transport, a number of variables potentially affecting $PaCO_2$–$P_{ET}CO_2$ are minimized; patients are generally maintained in the same position, and transport duration is generally too short for a substantial metabolic change or the progression of major systemic disease. Accordingly, $etCO_2$ changes during transport are most likely related to changes in pulmonary blood flow or minute ventilation. If the patient is transported with careful monitoring of blood pressure and an electrocardiogram as measures of pulmonary blood flow, continuous capnometry should appropriately reflect minute ventilation. If blood pressure and the cardiogram are stable, a change in $P_{ET}CO_2$ probably indicates a minute ventilation change. It is for these reasons that capnometry can be useful in maintaining consistent ventilation.

Changes in arterial CO_2 tension and pH during transport occur in 70–100% of manually ventilated patients. Manual ventilation without minute

ventilation monitoring seems to provide the least ventilatory stability, although changes have even been observed in patients on transport ventilators [11–17]. These ventilatory changes are associated with physiologic changes, and can affect patient outcomes. It is well established that hypocapnia is detrimental to cerebral perfusion [18,19]. Similar adverse physiological effects from overventilation have been observed in patients with low cardiac output states, cardiac arrest, and shock [20–22]. Warner and colleagues reported that intubated trauma patients transported to a tertiary care center and arriving with normocapnia were 43% less likely to die than were patients with hyper- or hypoventilation [11]. Deakin *et al.* reported a similar association in another group of multiple trauma patients [80]. Patients with traumatic brain injury fare even worse at the extremes of ventilation, with up to 70% greater mortality than brain-injured patients with normal ventilation [11,17,26,27]. Similar iatrogenic mortality increases have been observed in non-trauma patients [28,29].

The concerns are not theoretical, as Warner's series also showed that under one-third of intubated trauma patients brought to a tertiary care center had an arrival PCO_2 in the physiologic target range [11]. Other reviews of patients with severe head injuries note that between 19% and 43% of patients arrive with normocapnia [81–83]. A survey of air-medical transport records revealed that one-third of patients with severe head injury had $etCO_2$ values under 25 mm Hg and two-thirds had at least one value under 30 mm Hg [84].

The use of continuous capnometry has been convincingly shown to reduce the frequency of in-transport ventilation alterations [14,23,85,86].

Procedural sedation

Transport teams often provide analgesia and sedation to their patients [87,88]. Although the reported complication rate is low, these medications do depress respiration and mental status [89]. The literature on in-hospital procedural sedation identifies the incidence of hypoventilation in 11–33% of patients undergoing such sedation in the emergency department. The use of continuous capnography detects hypoventilation minutes before either the clinical examination or pulse oximetry changes, especially in patients who receive supplemental oxygen during the course of their sedation [63,90–94]. Even when sedation is delivered by anesthesia professionals, better monitoring was judged as a factor that would have prevented harm in nearly half of closed malpractice claims associated with monitored anesthesia care (sedation care in non-intubated patients) [95].

Evaluation of cardiac output and arrest

Another role for capnometry as a supplemental patient assessment tool is the ability to reflect pulmonary blood flow as an indicator of cardiac output. As described earlier, if ventilation is consistent, capnometry provides a gross breath-to-breath indicator of cardiac output. If a patient does not have continuous blood pressure monitoring, but has minute ventilation monitoring and pulse oximetry, capnometry can indicate a change in pulmonary blood flow and, thus, cardiac output between non-invasive blood pressure determinations.

At the extremes of this group are patients in arrest. A number of patients with so-called pulseless electrical activity (PEA), likely more than two-thirds, actually have cardiac activity, and over 40% have a measurable aortic pulse pressure [96–99]. Another feature of capnometry is that it can distinguish between PEA and very low cardiac output arrest states.

Survival rates from out-of-hospital cardiac arrests remain low, and the cost of futile resuscitation is high [100]. End-tidal CO_2 measurements are useful in assessing resuscitation efforts. During the course of the arrest, worsening end-tidal values may, among other things, be a sign of rescuer fatigue and indicate that chest compressions should be optimized, likely a key factor in improving resuscitation success [101].

Several studies have demonstrated a relationship between $etCO_2$ measurements and outcomes of arrest [102,103]. Sanders *et al.* showed that arrest survivors had an average $PetCO_2$ of 18 mm Hg 20 min into the arrest, while non-survivors averaged 6 mm Hg by the same time. There were no survivors with a value under 10 mm Hg [104]. Another study found that survivors averaged a $PetCO_2$ of 19 mm Hg, while non-survivors averaged 5 mm Hg. A value of 15 mm Hg had the best sensitivity and specificity, with a 91% positive and negative predictive value. However, four of the patients resuscitated had values under 10 mm Hg [105]. A large study evaluated 150 arrests, and showed that, with constant minute ventilation, a $PetCO_2$ of 10 mm Hg or less at 20 min into the resuscitation was 100% sensitive and specific for non-survival [106]. In making decisions with the use of capnometry, bear in mind that resuscitation chemistry can change $PetCO_2$ values. Sodium

Table 8.1 Selected potential complications during transport

Physiologic	Technical
CARDIOVASCULAR	
Hyper- or hypotension (typically from stimulation or increased intrathoracic pressure, respectively)	ECG lead disconnect or artifact
Decreased cardiac output	Monitor failure
Ischemia/infarction	Arterial /central venous catheter disconnect
	Vasoactive drug infusion error or disconnect
	Pacer malfunction
	IABP malfunction
RESPIRATORY	
Hypoxemia/desaturation (relatively uncommon)	Loss of unprotected airway
Hyper- or hypocapnia (relatively common)	Extubation/endotracheal tube obstruction
Loss of FRC	Loss of oxygen gas supply
Increased airway pressures with hemodynamic compromise	Inability to match bedside ventilator mode
Pneumothorax	Ventilator malfunction
	Chest tube occlusion or loss
NEUROLOGIC	
Increased ICP	ICP monitor loss or malfunction
Decreased CPP	Inability to maintain adequate head-up positioning
Inadequate or excessive CBF	Difficulty in temperature control
Herniation	
OTHER	
	Pulled tube (e.g., nasogastric or feeding) or catheter (e.g., Foley, surgical drain)
	Tangled infusion and monitoring catheters
	Loss of hyperalimentation source
	Bed malfunction
	Transport elevator malfunction

ECG, electrocardiogram; IABP, intraaortic balloon pump; ICP, intracranial pressure; CPP, cerebral perfusion pressure; CBF, cerebral blood flow; FRC, functional residual capacity.
Source: Adapted from: Mohammedi I. Intrahospital transport of critically ill patients. In: Gabrielli A, Layon AJ, Yu M (eds.) *Civetta, Taylor, Kirby's Critical Care*, 4th edn. Philadelphia, PA: Lippincott Williams and Wilkins, 2009; 143–9.

bicarbonate both contains and produces CO_2, causing a transient $P_{ET}CO_2$ rise, usually lasting under 2 min [107], whereas high-dose epinephrine administration decreases $P_{ET}CO_2$ [97].

Potential measurement errors

When using capnography for any clinical decision, the user must be aware of possible sources of error. Of the potential errors that can occur with capnography, two are particularly important in the transport environment: oxygen concentration and altitude.

High oxygen concentrations falsely lower the $P_{ET}CO_2$ reading by up to 10%, as interactions between CO_2 and the greater number of oxygen molecules change the infrared absorption of the gas sample. This problem can be avoided by recalibrating the detector with an appropriate reference gas, or by activating a compensatory mode available on some machines.

Changes in atmospheric pressure can also be important [108]. Pressure changes vary the intermolecular forces between CO_2 molecules, increasing infrared absorption by about 0.5% for every 1% change in pressure. The error is usually insignificant, as weather-related atmospheric pressure changes are generally under 20 mm Hg, or approximately 2% at sea level. However, pressure-induced variation is a greater possibility outside the hospital, particularly during air transport. A fixed-wing aircraft cabin pressurized to 5000 ft (1500 m) represents a pressure change of about 17% from sea level, and would result in a measurement change of approximately 9%. Transport over mountainous terrain in a non-pressurized cabin could also cause a notable change. This error can be avoided by recalibrating the capnometer at the appropriate altitude, or by using a unit that automatically measures and adjusts for the ambient pressure.

Conclusion

In the complicated transport environment, whether transport between adjacent units in a hospital or transport between facilities thousands of miles apart, capnography and capnometry provide useful information that may help to improve decision-making and reduce complications. Capnography is the gold standard for monitoring patients on airway appliances and ventilator circuits, and there are useful roles for the technology during procedural sedation and evaluating patients in the time surrounding arrest states (Table 8.1).

References

1. Orr R. Unplanned events in pediatric critical care transport. *Pediatrics* 1999; **104**: S687.
2. Hurst J, Davis K, Johnson D. Cost and complications during in-hospital transport of critically ill patients: a prospective cohort study. *J Trauma* 1992; **33**: 582–5.
3. Evans A, Winslow E. Oxygen saturation and hemodynamic response in critically ill, mechanically ventilated adults during intrahospital transport. *Am J Crit Care* 1995; **4**: 106–11.
4. Indek M, Peterson S, Smith J, Brotman S. Risk, cost, and benefit of transporting ICU patients for special studies. *J Trauma* 1988; **28**: 1020–5.
5. Waydhas C, Schneck G. Deterioration of respiratory function after intrahospital transport of critically ill surgical patients. *Intens Care Med* 1995; **21**: 784–9.
6. Szem J, Hydo L, Fischer E. High risk intrahospital transport of critically ill patients. *Crit Care Med* 1995; **23**: 1660–6.
7. Stearley H. Patient outcomes: intrahospital transportation and monitoring of critically ill patients by a specially trained ICU nursing staff. *Am J Crit Care* 1998; **7**: 282–7.
8. Edge W, Kanter R, Weigle C, Walsh R. Reduction in morbidity in interhospital transport by specialized pediatric staff. *Crit Care Med* 1994; **22**: 1186–91.
9. Frakes M. Flight team management of in-place endotracheal tubes. *Air Med J* 2002; **21**: 29–31.
10. Gebermichael M. Interhospital transport of the extremely ill patient. *Crit Care Med* 2000; **28**: 79–85.
11. Warner K, Cuschieri J, Copass M, Jurkovich G, Bulger E. The impact of prehospital ventilation on outcome after severe traumatic brain injury. *J Trauma* 2007; **62**: 1330–8.
12. Gervais H, Eberle B, Konietzke D. Comparison of blood gases of ventilated patients during transport. *Crit Care Med* 1987; **15**: 761–3.
13. Becker A, Ipekoglu Z, Tureyen K. Secondary insults during intrahospital transport of neurosurgical intensive care patients. *Neurosurg Rev* 1998; **21**: 98–101.
14. Braman S, Dunn S, Amico C, Millman R. Complications of intrahospital transport in critically ill patients. *Ann Intern Med* 1987; **107**: 469–73.
15. Martin S, Agudelo W, Schner M. Monitoring hyperventilation in patients with closed head injury during air transport. *Air Med J* 1997; **16**: 15–18.
16. Hurst J, Davis K, Branson R, Johannigman J. Comparison of blood gases during transport using two methods of ventilatory support. *J Trauma* 1989; **29**: 1637–40.
17. Davis D, Dunford J, Poste J. The impact of hypoxia and hyperventilation on outcome after paramedic rapid sequence intubation of severely head injured patients. *J Trauma* 2004; **57**: 1–8.
18. Stochetti N, Maas A, Chieregato A, van der Plas A. Hyperventilation in head injury: a review. *Chest* 2005; **127**: 1812–27.
19. Brain Trauma Foundation Guidelines for prehospital management of traumatic brain injury. *Prehosp Emerg Care* 2007; **12**(1 Suppl): S1–52.
20. Manley G, Hemphill J, Morabito D, *et al*. Cerebral oxygenation during hemorrhagic shock: perils of hyperventilation. *J Trauma* 2000; **48**: 1025–32.
21. Manley G, Pitts L, Morabito D. Brain tissue oxygenation during hemorrhagic shock, resuscitation, and alterations in ventilation. *J Trauma* 1999; **46**: 261–7.
22. Pepe P, Roppolo L, Fowler R. The detrimental effects of ventilation during low blood-flow states. *Curr Opin Crit Care* 2005; **11**: 212–18.

23. Davis D, Dunford J, Ochs M, Park K, Hoyt D. The use of quantitative end-tidal capnometry to avoid inadvertent severe hyperventilation in patients with head injury after paramedic rapid sequence intubation. *J Trauma* 2004; **56**: 808–14.
24. Davis D, Fisher R, Buono C, *et al*. Predictors of intubation success and therapeutic value of paramedic airway management in a large, urban EMS system. *Prehosp Emerg Care* 2006; **10**: 356–62.
25. Davis D, Patel R. Noninvasive capnometry for continuous monitoring of mental status: a tale of two patients [letter]. *Am J Emerg Med* 2006; **24**: 752–4.
26. Davis D, Stern J, Sise M, Hoyt D. A follow-up analysis of factors associated with head injury mortality after paramedic rapid sequence intubation. *J Trauma* 2005; **59**: 486–90.
27. Poste J, Davis D, Ochs M, *et al*. Air medical transport of severely head injured patients undergoing paramedic rapid sequence intubation. *Air Med J* 2004; **23**: 36–40.
28. Aufderheide T, Lurie K. Death by hyperventilation: a common and life-threatening problem during cardiopulmonary resuscitation. *Crit Care Med* 2004; **32**: S345–51.
29. Aufderheide T, Sigurdsson G, Pirrallo R. Hyperventilation-induced hypotension during cardiopulmonary resuscitation. *Circulation* 2005; **109**: 1960–5.
30. Patel S, Callahan T, Callahan M. An adaptive noise reduction stethoscope for auscultation in high noise environments. *J Acoust Soc Am* 1998; **103**: 2483–91.
31. Price T, Goldsmith L. Changes in hearing acuity in ambulance personnel. *Prehosp Emerg Care* 1998; **2**: 308–11.
32. Hunt R, Bryan D, Brinkley S. Inability to assess breath sounds during air medical transport by helicopter. *JAMA* 1991; **265**: 1982–4.
33. Brown L, Gough J, Bryan-Bert D, Hunt R. Assessment of breath sounds during ambulance transport. *Ann Emerg Med* 1997; **29**: 228–31.
34. Caplan R. The closed claims project. *ASA Newsl* 1999; **63**: 7–9.
35. Katz S, Falk J. Misplaced endotracheal tubes by paramedics in an urban emergency medical services system. *Ann Emerg Med* 2001; **37**: 32–7.
36. Gausche M, Lewis R, Stratton S. Effect of out-of-hospital pediatric endotracheal intubation on survival and neurological outcome. *JAMA* 2000; **283**: 783–90.
37. Jones J, Murphy M, Dickson R. Emergency physician verified out of hospital intubation: miss rates by paramedics. *Acad Emerg Med* 2004; **11**: 707–9.
38. Jemmett M, Kendal K, Fourre M. Unrecognized misplacement of endotracheal tubes in a mixed urban to rural emergency medical services setting. *Acad Emerg Med* 2003; **10**: 961–5.
39. Dunford J, Davis D, Ochs M. Incidence of transient hypoxia and pulse rate reactivity during paramedic rapid sequence intubation. *Ann Emerg Med* 2003; **42**: 721–6.
40. Silvestri S, Ralls G, Krauss B, *et al*. The effectiveness of out-of-hospital use of continuous end-tidal carbon dioxide monitoring on the rate of unrecognized misplaced intubation within a regional emergency medical services system. *Ann Emerg Med* 2005; **45**: 497–503.
41. Guyton A, Hiall J. *Textbook of Medical Physiology*, 10th edn. Philadelphia, PA:WB Saunders, 2000.
42. Krauss B, Hess D. Capnography for procedural sedation and analgesia in the emergency department. *Ann Emerg Med* 2007; **50**: 172–81.
43. Anderson C, Breen P. Carbon dioxide kinetics and capnography during critical care. *Crit Care* 2000; **4**: 207–15.
44. Li J. Capnography alone is imperfect for endotracheal tube placement confirmation during emergency intubation. *J Emerg Med* 2001; **20**: 223–9.
45. Falk J, Rackow E, Weil M. End-tidal carbon dioxide concentration during cardiopulmonary resuscitation. *N Engl J Med* 1988; **318**: 607–11.
46. Salthe J, Ristianssen S, Sollid S, Oglend B, Sorede E. Capnography rapidly confirmed correct endotracheal tube placement during resuscitation of extremely low birthweight babies. *Acta Anaesthesiol Scand* 2006; **50**: 1033–6.
47. Langham M, Chen L. Current utilization of continuous end-tidal carbon dioxide monitoring in pediatric emergency departments. *Pediatr Emerg Care* 2008; **24**: 211–13.
48. Singh S, Allen W, Venkataraman S, Bhende M. Utility of a novel quantitative handheld microstream capnometer during transport of critically ill children. *Am J Emerg Med* 2006; **24**: 302–7.
49. Bhende M, Thompson A, Cook D. Validity of a disposable end-tidal CO_2 detector in verifying endotracheal tube placement in infants and children. *Ann Emerg Med* 1992; **21**: 142–5.
50. Deluty S, Trundorf H. Failure of capnography to properly assess ET tube location. *Anesthesiology* 1993; **78**: 783–4.
51. Werman H, Falcone R. Glottic positioning of the ET tube tip: a diagnostic dilemma. *Ann Emerg Med* 1998; **31**: 643–6.

52. Zbinden S, Schupfer G. Detection of esophageal intubation: the cola complication. *Anesthesia* 1989; **44**: 81.
53. Sum-Ping S, Mehta M, Anderton J. A comparative study of methods of detection of esophageal intubation. *Anesth Analg* 1989; **69**: 627–32.
54. Kramer-Johansen J, Droph E, Steen P. Detection of carbon dioxide in expired air after oesophageal intubation: the role of bystander mouth-to-mouth ventilation. *Acta Anaesthesiol Scand* 2008; **52**: 155–7.
55. American Heart Association. Guidelines for emergency cardiac care: adjuncts for airway control and ventilation. *Circulation* 2005; **112**: IV51–7.
56. American Society of Anesthesiologists. *Standards for Basic Anesthetic Monitoring*. Park Ridge, IL: ASA. Available online at http://www.asahq.org/publicationsAndServices/standards/02.pdf. (Accessed January 18, 2009.)
57. Wang H, Davis D, O'Connor R. Drug-assisted intubation in the prehospital setting. *Prehosp Emerg Care* 2006; **10**: 261–71.
58. Cheifetz I, Myers T. Should every mechanically ventilated patient be monitored with capnography from intubation to extubation? *Respir Care* 2007; **52**: 426–42.
59. da Silva P, de Aguilar V, Neto H, de Carvalho W. Unplanned extubation in a pediatric intensive care unit: impact of a quality improvement programme. *Anesthesia* 2008; **63**: 1209–16.
60. Richmond A, Jaron D, Hanson V. Unplanned extubation in adult critical care. *Crit Care Nurse* 2004; **24**: 32–7.
61. Lee J, Chang C, Han D, Lee Y, Shin C. Relationship beween arterial and end-tidal carbon dioxide pressures during anesthesia using a laryngeal tube. *Acta Anaesthesiol Scand* 2005; **49**: 759–62.
62. Lightdale J, Goldmann D, Feldman H, *et al*. Microstream capnography improves patient monitoring during moderate sedation: a randomized controlled trial. *Pediatrics* 2006; **117**: 1170–8.
63. Burton JH, Harrah JD, Germann CA, Dillon DC. Does end-tidal carbon dioxide monitoring detect respiratory events prior to current sedation monitoring practices? *Acad Emerg Med* 2006; **13**: 500–4.
64. Jaffe R, Talavera J, Hah J, Brock-Utne J. The dromedary sign: an unusual capnograph tracing. *Anesthesiology* 2008; **109**: 149–50.
65. Stevenson G, Gibbs T, Sursh S. An unusual capnogram in a pediatric patient [letter]. *Anesth Analg* 2006; **102**: 1907–8.
66. Kline J, Meek S, Buoudrow D. Use of the alveolar deadspace fraction and plasma d-dimers to exclude acute pulmonary embolism in ambulatory patients. *Acad Emerg Med* 1997; **4**: 856–63.
67. Wahba R, Tesler M. Misleading end-tidal CO_2 tensions. *Can J Anaesth* 1996; **43**: 862–6.
68. Shankar K, Moseley H, Kumar Y. Arterial to end tidal carbon dioxide tension difference during cesarean section anesthesia. *Anesthesia* 1986; **41**: 698–702.
69. Shankar K, Moseley H, Kumar Y. Arterial to end tidal carbon dioxide tension difference during anesthesia for tubal ligation. *Anesthesia* 1987; **42**: 482–6.
70. Jones N, Robertson D, Kane J. Difference between end-tidal and arterial CO_2 in exercise. *J Appl Physiol* 1979; **47**: 954–60.
71. Prause G, Hetz H, Lauda P. A comparison of end-tidal CO_2 documented by capnometry and the arterial pCO_2 in emergency patients. *Resuscitation* 1997; **35**: 145–8.
72. Belpomme V, Ricard-Hibon A, Devoir C, *et al*. Correlation of arterial PCO_2 and $PETCO_2$ in prehospital controlled ventilation. *Am J Emerg Med* 2005; **23**: 852–9.
73. Russell G, Graybeal J, Strout J. Stability of arterial to end tidal carbon dioxide gradients during postoperative cardiorespiratory support. *Can J Anaesth* 1993; **40**: 206–10.
74. Seguia P, Bleichner J, Branger B. The measurement of end-tidal carbon dioxide is not a significant parameter to monitor in patients with severe traumatic brain injury. *Can J Anaesth* 2001; **48**: 396–400.
75. Hardman J, Airkenhead A. Estimating alveolar deadspace from the arterial to end tidal CO_2 gradient: a modeling analysis. *Anesth Analg* 2003; **97**: 1846–51.
76. Drew K, Brayton M, Ambrose A, Bernard G. End-tidal carbon dioxide monitoring for weaning patients. *Dimens Crit Care Nurs* 1998; **17**: 127–34.
77. Remond C, Jimeno M, Dubouloz F. Measurements of endtidal carbon dioxide in extrahospital transport. *Eur J Emerg* 1998; **4**: 179–86.
78. Healey C, Fedullo A, Swinburne A. Comparison of non-invasive measurement of carbon dioxide tension during withdrawal from mechanical ventilation. *Crit Care Med* 1987; **15**: 764–8.
79. Niehoff J, DelGuercio C, LaMorte W, *et al*. Efficacy of pulse oximetry and capnometry in postoperative weaning. *Crit Care Med* 1988; **16**: 701–5.
80. Deakin C, Sado D, Coats T, Davies G. Prehospital end-tidal carbon dioxide concentration and outcome in major trauma. *J Trauma* 2004; **57**: 65–8.
81. David J, Cresta M, Souab A. Severe head injuries: effects of pre-hospital mechanical ventilation on capnia. *Ann Fr Anesth Reanim* 1999; **18**: 398–402.

82. Rouxel J, Tazaourte K, Le Moigno S. Medical prehospital rescue in head injury. *Ann Fr Anesth Reanim* 2004; **23**: 6–14.
83. Helm M, Hauke J, Lampl L. A prospective study of the quality of prehospital emergency ventilation in patients with severe head injury. *Br J Anaesth* 2002; **88**: 345–59.
84. Thomas S, Orf J, Wedel S, Conn A. Hyperventilation in traumatic brain injury patients: inconsistency between consensus guidelines. *J Trauma* 2002; **42**: 47–52.
85. Helm M, Schuster R, Hawke J. Tight control of prehospital ventilation by capnography in major trauma victims. *Br J Anaesth* 2003; **90**: 327–32.
86. Macready N. Flexible monitoring: mobilizing critical care. *Am J Crit Care* 1997; **6**: 1–13.
87. Frakes M, Lord W, Kociszewski C, Wedel S. Factors associated with unoffered trauma analgesia in critical care transport. *Am J Emerg Med* 2009; **27**: 49–54.
88. Sheldon P, Day M. Sedation issues in transportation of acutely and critically ill patients. *Crit Care Nurs Clin N Am* 2005; **17**: 205–10.
89. Kanowitz A, Dunn T, Kanowitz E, Dunn W, VanBuskirk K. Safety and effectiveness of fentanyl administration for prehospital pain management. *Prehosp Emerg Care* 2006; **10**: 1–7.
90. Anderson J, Junkins E, Pribble C, Guenther E. Capnography and depth of sedation during propofol sedation in children. *Ann Emerg Med* 2007; **49**: 9–13.
91. Deitch K, Chudnofsky C, Dominici P. The utility of supplemental oxygen during emergency department procedural sedation with propofol. *Ann Emerg Med* 2008; **52**: 1–8.
92. Lightdale J, Goldmann D, Feldman H, *et al*. Microstream capnography improves patient monitoring during moderate secation. *Pediatrics* 2006; **117**: 1170–6.
93. Fanning R. Monitoring during sedation given by non-anesthetic doctors. *Anesthesia* 2008; **63**: 370–4.
94. Fu ES, Downs JB, Schweiger JW, Miguel RV, Smith RA. Supplemental oxygen impairs detection of hypoventilation by pulse oximetry. *Chest* 2004; **126**: 1552–8.
95. Bhananker S, Posner K, *et al*. Injury and liability associated with monitored anesthesia care. *Anesthesiology* 2006; **104**: 228–34.
96. Bayhahn C, Muller E, Walcher F, Seegar F, Breitkreutz R. Prehospital echocardiography in pulseless electrical activity victims. *Anesthesiology* 2006; **105**: A1735.
97. Cantineau J, Merck P, Lambert Y. Effect of epinephrine on end-tidal carbon dioxide pressure during prehospital cardiopulmonary resuscitation. *Am J Emerg Med* 1994; **12**: 267–70.
98. Paradis NA, Martin GB, Goetting MB, *et al*. Aortic pulse pressure during human cardiac arrest: identification of pseudo-electromechanical dissociation. *Chest* 1992; **101**: 123–8.
99. Bocka J, Overton D, Hauser A. Electromechanical dissociation in human beings: an echocardiographic evaluation. *Ann Emerg Med* 1988; **17**: 450–2.
100. Bobrow BJ, Zuecher M, Ewy GA, *et al*. Gasping during cardiac arrest in humans is frequent and associated with improved survival. *Circulation* 2008; **118**: 2250–4.
101. American Heart Association. Adult basic life support. *Circulation* 2005; **112**: IV19–34.
102. Grmec S, Lah K, Tusek-Bunc K. Differences in end-tidal CO_2 between asphyxia cardiac arrest and ventricular fibrillation pulseless ventricular tachycardia cardiac arrest in prehospital setting. *Crit Care* 2003; **7**: R139–44.
103. Grmec S, Krizmaric M, Mally S, *et al*. Utstein style analysis of out of hospital cardiac arrest, bystander CPR, and expired carbon dioxide. *Resuscitation* 2007; **72**: 404–14.
104. Sanders A, Kern K, Otto C, Milander M, Ewy G. End-tidal carbon dioxide monitoring during cardiopulmonary resuscitation. *JAMA* 1989; **262**: 1347–51.
105. Callahan M, Barton C. Prediction of outcome of cardiopulmonary resuscitation from end-tidal carbon dioxide concentration. *Crit Care Med* 1990; **18**: 358–62.
106. Levine R, Wayne M, Miller C. End-tidal carbon dioxide and outcome of out-of-hospital cardiac arrest. *N Engl J Med* 1997; **337**: 301–6.
107. Niemann J. Effects of acidemia and sodium bicarbonate therapy in Advanced Cardiac Life Support. *Ann Emerg Med* 1984; **13**: 781–2.
108. Blumen I, Callejas S. Transport physiology. In: Blumen I (ed.) *Principles and Direction of Air Medical Transport*. Salt Lake City, UT: Air Medical Physicians Association, 2006; 357–69.

Section 1
Chapter
9

Ventilation

Capnography as a guide to ventilation in the field

D. P. Davis

Introduction

End-tidal carbon dioxide ($P_{ET}CO_2$) monitoring is a necessary tool for guiding the ventilation of patients in the prehospital setting. The unique challenges of the field environment dictate the requirements for an ideal $P_{ET}CO_2$ monitor. Recent data suggest that hyperventilation may be at least as detrimental as hypoxia in patients with severe traumatic brain injury (TBI) [1,2]. Clearly, the device must be rugged and lightweight, with a long battery life. Displays must be equally visible in bright sun and at night, and the ideal device should be portable enough to remove from the ambulance or aircraft and carry to and with the patient. The limited training and experience of many field providers necessitate simplicity. Lastly, the cost of such a device becomes an important issue. In an intensive care unit or operating room, $P_{ET}CO_2$ monitoring is performed on a daily basis, justifying the cost of a sophisticated monitor. In contrast, for a prehospital system, in which each ambulance or aircraft must be supplied with a device, the relatively infrequent event of an intubation results in a lower "bang for the buck."

Throughout this chapter, it is important to keep in mind the differences between $P_{ET}CO_2$, alveolar CO_2, and arterial PCO_2 ($PaCO_2$) as extremes of temperature and altitude, and the potential for sensor interference by condensation or various body fluids, may significantly affect the performance of these devices [3]. Here, we present the evidence for use of $P_{ET}CO_2$ monitoring to guide ventilation in the field and review each type of device available, discussing the advantages and disadvantages of each.

Justification for prehospital $P_{ET}CO_2$ monitoring

Avoiding hyperventilation

Perhaps the best justification for $P_{ET}CO_2$ monitoring in the out-of-hospital environment is to avoid the detrimental effects of hyperventilation, especially in the setting of brain injury. The ability of hyperventilation to decrease intracranial pressure (ICP) was recognized several decades ago, leading to its routine use in treating intracranial hypertension [4–7]. Unfortunately, the lowering of ICP from a decrease in cerebral blood volume comes at the expense of an even greater decrease in cerebral blood flow, potentially leading to ischemia [8–11]. While global measures of cerebral perfusion may or may not fall below the ischemic threshold during hyperventilation, regional and local ischemia has been documented even with a moderate degree of hyperventilation [12–17]. More importantly, a randomized trial documented an increase in mortality with the routine use of hyperventilation ($PaCO_2$ target of 25 mm Hg) in patients with severe TBI [18]. This finding has led to recommendations against the routine use of hyperventilation in severe TBI, except with refractory ICP elevation or impending herniation [19]. If hyperventilation is performed over the first 5 days of admission, the significance of a relatively brief period of prehospital hyperventilation is unclear [18]. Recent evidence indicates that hyperventilation leads to ischemia almost immediately, with a decrease in cerebral perfusion below ischemic levels, and a rise in extracellular glutamate and lactate within the first half-hour [11,13,20]. In addition, current models of ischemic and traumatic brain injury suggest an immediate postinjury period during which the brain is especially vulnerable to secondary insults [10,13,21], underscoring the importance of avoiding hyperventilation in the field environment.

The San Diego Paramedic Rapid Sequence Intubation (RSI) Trial evaluated the impact of paramedic use of neuromuscular blocking agents on outcome in patients with severe TBI [22–24]. Over 98% of trial patients were successfully intubated with either an endotracheal (ET) tube or a Combitube, and fewer than

Capnography, Second Edition, ed. J. S. Gravenstein, Michael B. Jaffe, Nikolaus Gravenstein, and David A. Paulus. Published by Cambridge University Press. © Cambridge University Press 2011.

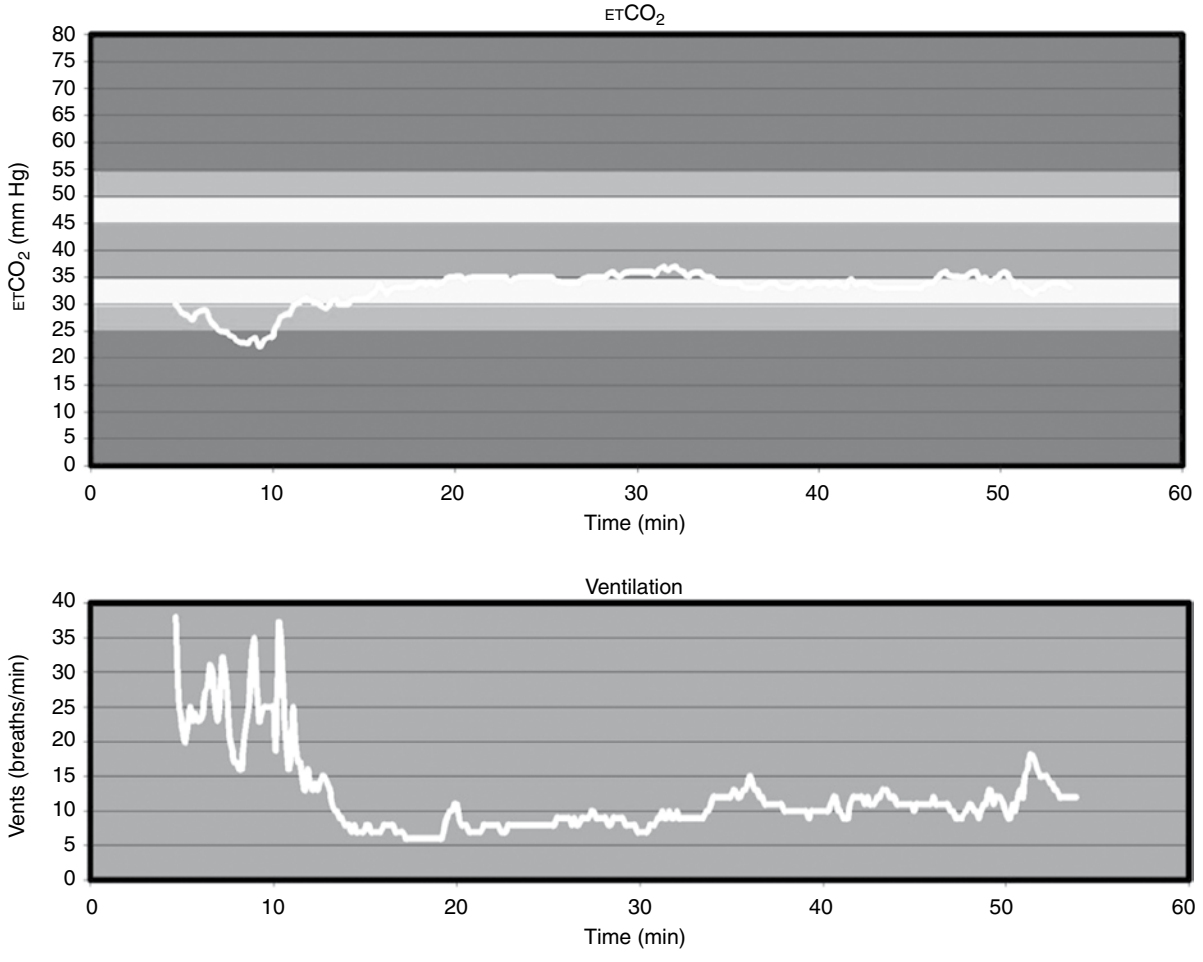

Figure 9.1 Sample capnometry–respiratory rate graph from patient with severe head trauma undergoing rapid sequence intubation by paramedics. Intubation occurred at the appearance of $P_{ET}CO_2$ values. Note the frequent occurrence of hyperventilation immediately following intubation.

1% of patients were hypoxic upon arrival. Nevertheless, the mortality in trial patients was 32% versus only 24% for matched controls [22–24]. Two of the most important clues as to the potential cause of this mortality increase with paramedic RSI were revealed through analysis of data downloaded from handheld capnometer/oximeter devices. Most paramedics were given standardized ventilation parameters (800 mL tidal volume at 12 breaths/min), and were allowed to practice with a spirometer and stopwatch during the training session. One agency instituted the use of capnometry/oximetry during the trial period, with paramedics instructed to target a $P_{ET}CO_2$ value of 30–35 mm Hg and avoid values below 25 mm Hg. Data from these devices revealed a high incidence of desaturation during the RSI procedure and routine hypocapnia despite the target parameters [1,23–25]. Logistic regression analysis revealed a strong association between low $P_{ET}CO_2$ and mortality. A matched-controls analysis revealed an adverse effect of low $P_{ET}CO_2$ values and severe desaturations ($SpO_2 < 70\%$) (Figure 9.1). Subsequent analyses have documented an association between arrival $PaCO_2$ and outcome, confirming the importance of maintaining proper prehospital ventilation parameters in brain-injured patients [26,27].

Does $P_{ET}CO_2$ monitoring avoid hyperventilation?

In theory, monitoring of $P_{ET}CO_2$ data should lead to a low incidence of hyperventilation, regardless of whether manual or mechanical ventilation is used. Thus, the high incidence of hyperventilation we observed, despite the use of capnometry to guide

ventilation, has led to concerns that these devices do not prevent hyperventilation [23,24]. Indeed, multiple investigators have noted a high incidence of hypocapnia in the prehospital environment, especially with manual ventilation [28–33]. In a separate analysis, however, a lower incidence of arrival hypocapnia was documented ($PaCO_2$ <25 mm Hg) in patients monitored with capnometry [2]. Furthermore, the lowest rates of arrival hypocapnia were documented in patients transported by aeromedical crews, who have been using capnometry for many years. The cohort of patients intubated by ground paramedics but transported by aeromedical crews was the only group with improved outcomes versus matched controls [34], which indicates that $PETCO_2$-guided ventilation requires some degree of experience, but also that hyperventilation can be avoided with the use of capnometry.

By inspecting the ventilation patterns obtained by paramedics with the use of capnometry, we obtained useful information [23,24]. A linear relationship was observed between the respiratory rate and $PETCO_2$ value. The mean value for the maximum ventilation rate was quite elevated, at 36 breaths/min, with a mean minimum $PETCO_2$ value of 23.6 mm Hg. A sample graph demonstrating hyperventilation is displayed in Figure 9.2. Hypocapnic patients were more significantly injured, with lower $PETCO_2$ values associated with higher head/neck abbreviated injury score (AIS), lower arrival systolic blood pressure, and lower postintubation SpO_2 values [2]. This may indicate that the excitement and anxiety of caring for critical patients leads to excessively high ventilation rates of these patients. A similar analysis in air transport patients suggested that episodes of hyperventilation were related to impending hypoxemia [35]. It is also possible that the tendency toward hyperventilation despite $PETCO_2$ monitoring reflects the residual belief in its therapeutic benefits on the injured brain. The occurrence of prehospital hyperventilation also reflects a failure of the scientific community to recognize the importance of optimal ventilation in the immediate postinjury period. Additional research and education should help overcome these problems.

Other ventilation effects

While $PETCO_2$-guided ventilation may appear to have the most direct impact on avoiding the reflex cerebral vasoconstriction in response to hypocapnia, it is possible that lower $PETCO_2$ values are a surrogate marker for injurious ventilation patterns that may ultimately play a greater role in patient outcomes. Positive pressure ventilation leads to a rise in mean intrathoracic pressure, which may decrease cerebral perfusion by obstructing venous return and lowering cardiac output [36]. In addition, an elevated mean intrathoracic pressure can be transmitted in a retrograde way via the jugular venous system, leading to a paradoxical rise in ICP. Hyperventilation, especially when produced by high respiratory rates, can quickly raise intrathoracic pressure and exacerbate hypocapnia-driven ischemia. Our mathematical models indicate that

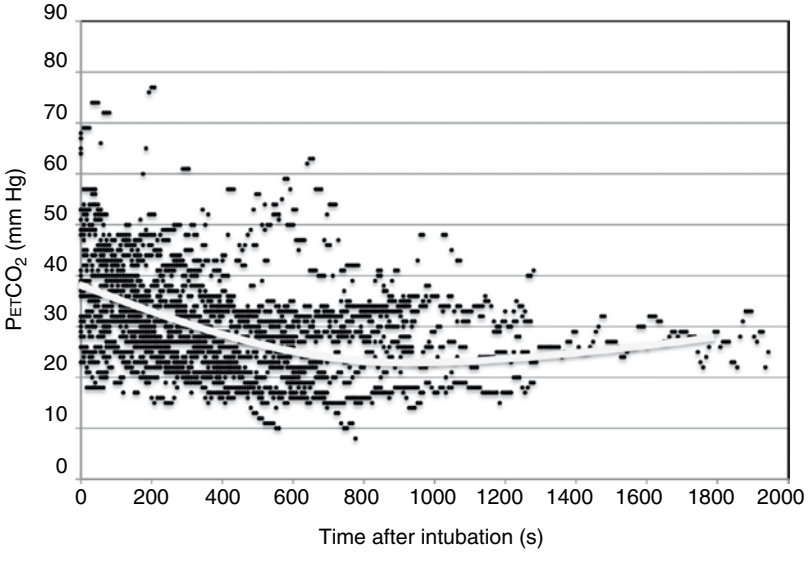

Figure 9.2 Combined data for all patients undergoing capnometry as part of the San Diego Paramedic RSI Trial. Hypocapnia was extremely common, with $ETCO_2$ values below 25 mm Hg in over half of all patients. Note the upswing in $ETCO_2$ values at the end of the prehospital course.

mean intrathoracic pressure may routinely approach 15 mm Hg with ventilation patterns observed by prehospital providers [37].

In addition to its effects on cerebral and systemic hemodynamics, overaggressive ventilation can be detrimental to the critically ill patient through proinflammatory cytokine release and pulmonary endothelial cell apoptosis [38–45]. Data from the intensive care unit document an increase in multiorgan dysfunction syndrome and deaths with high tidal volumes and absence of positive end-expiratory pressure (PEEP) [38]. An observation of significance to field providers is that the most profound rise in injurious cytokines occurs in the first hour of ventilation. While $P_{ET}CO_2$ is not a substitute for airway pressure monitoring, it is likely that the high ventilation rates and low $P_{ET}CO_2$ values observed in our study represent injurious ventilation patterns, especially without PEEP.

Available devices

Colorimetric capnometry

Qualitative capnometry is the simplest form of $P_{ET}CO_2$ monitoring available, with a limited ability to guide ventilation. Qualitative capnometers rely on the tendency of CO_2 to form acid in solution. A paper filter impregnated with dyes that change color with lower pH values is the basis for this technology. When exhaled gases pass through this filter, the resultant color change indicates the presence of CO_2, confirming tracheal (or bronchial) positioning of the ET tube. Although the intensity of color change provides an estimate of the CO_2 concentration, albeit crude, the inability to determine an accurate value for $P_{ET}CO_2$ and the poor sensitivity in detecting breath-to-breath changes prohibit the use of this device to guide ventilation. However, should misplacement of the ET tube become a concern, the qualitative capnometer can be used to reconfirm tracheal placement, keeping in mind that the absence of color change could also indicate that the qualitative capnometer is no longer functional. Details regarding the use of qualitative capnometry to confirm ET tube placement are provided elsewhere in this book.

Semiquantitative capnometry

In recent years, several semiquantitative capnometers that provide a rough estimate of $P_{ET}CO_2$ have been developed for use in the field. Rather than provide an actual $P_{ET}CO_2$ value, however, a series of stacked bars is used, with each bar representing an approximate range of $P_{ET}CO_2$ values. The manufacturers recommend a target number of bars as reflective of an optimal $P_{ET}CO_2$ range; additional bars represent hypercapnia, while a lower number of bars represents hypocapnia. These devices are rugged, lightweight, relatively inexpensive, and simple to use.

Semiquantitative capnometry can be used to confirm initial tracheal positioning of an ET tube. It remains to be seen, however, whether use of these devices will lead to optimized ventilation and better outcomes. The technology by which CO_2 concentration is measured is not as accurate, and hypo- and hypercapnia are a possibility even if the target number of bars is achieved. In addition, field providers may not find the system of stacked bars as useful in guiding ventilation as an actual number. Nevertheless, their affordability could lead to widespread use. Future research should determine their utility in helping healthcare providers avoid the extremes of ventilation.

Quantitative capnometry

The most accurate method of measuring $P_{ET}CO_2$ concentration involves continuous infrared spectrophotometric analysis of expired gases, either with a diverting (sidestream) or non-diverting (mainstream) method. Quantitative capnometry has great potential for guiding ventilation in the prehospital arena. An end-tidal value is provided for each breath, with multiple studies demonstrating reasonable clinical accuracy. It is important to understand, however, the physiological limitations to this method, especially with use of a sidestream sampling port. The most physiologically pertinent estimate of $P_{ET}CO_2$ is derived from a sample of expired gas taken at the end of expiration, as this represents the closest approximation to alveolar gas. This becomes increasingly important in the setting of auto-PEEP, either from intrinsic airway constriction or resistance to expiration created by the airway circuit itself. With greater obstruction to flow, the expiratory phase is prolonged, delaying the point at which the measured expired value comes closest to reflecting alveolar CO_2 concentration. While this delay does not significantly affect the interpretation of capnography, by which this phenomenon is easily recognized, it may underestimate the true alveolar CO_2 concentration with use of a capnometer, depending on clinical circumstances. Particularly in patients with obstructive lung disease (discussed extensively elsewhere in this book), the reported $P_{ET}CO_2$ might not reflect alveolar

concentration of CO_2, resulting in a large, undetected arterial to $PETCO_2$ difference.

More sophisticated capnometry also allows for the capture of volumetric data, combining measurements of $PETCO_2$ and respiratory rate with those of tidal volume and minute ventilation. The combined data should allow optimal control of ventilation, potentially minimizing the adverse effects of both hypocapnia and barotrauma. These devices are currently more expensive and less portable, thus limiting their application in the field. As a result, there are, to date, few data on their out-of-hospital use.

Using the waveform

Capnography, the graphical representation of the CO_2 concentration throughout the breath, provides the most continuous information currently available with regard to adequacy of ventilation. In addition, specific patterns can be easily recognized, allowing for early diagnosis of certain conditions and potential problems with ventilation. Perhaps the most important application of capnography in this regard is the early recognition of auto-PEEP from a variety of etiologies. "Stacking" of breaths due to a combination of patients with a prolonged expiratory phase and excessively high respiratory rates can be identified.

Several capnography patterns can provide valuable clues as to the underlying pathophysiology. A tension pneumothorax or rigid chest wall from significant burns can produce a characteristic pattern of a shortened expiratory phase in combination with a decrease in compliance or increase in peak airway pressures. A cuff leak will result in a gradual down-slope, replacing the expiratory plateau. A right mainstem intubation can lead to a relatively high, narrow expiratory complex. Most concerning is a sudden absence or truncated expiratory complex, indicating proximal migration of the ET tube into the hypopharynx. Examples of these waveforms are displayed elsewhere in this text.

Recommended use of $ETCO_2$ monitoring in the field

Guiding the application of ventilation

The primary role for $PETCO_2$ monitoring in an Emergency Medical Service is to guide ventilation during transport. Applications, such as $PETCO_2$ monitoring for ET tube confirmation and cardiopulmonary resuscitation, are discussed in other chapters. Although the optimal target $PETCO_2$ value has not yet been defined, among the most important considerations is avoiding hypocapnia. The measured value for $PETCO_2$ appears to typically underestimate $PaCO_2$ by approximately 5 mm Hg, depending upon the metabolic state, dilution of $PETCO_2$ by deadspace gases with higher respiratory rates, and degree of underlying lung disease in a given patient. Thus, a target $PETCO_2$ value of 35 mm Hg is recommended. This also appears to be a physiologic threshold for the initiation of brain ischemia [12]. Improved outcomes versus matched controls have been observed with a higher $PETCO_2$ and arrival $PaCO_2$ values, a pattern that continued into the range of hypercapnia [1,2,23,24]. This observation is consistent with recent evidence indicating that permissive hypercapnia may lead to increased cerebral perfusion and improved outcomes [46]. These data may reflect higher $PETCO_2$ and $PaCO_2$ values as surrogate markers for non-injurious ventilation patterns.

Strategies must be developed to modify ventilation parameters in response to capnometry data. The propensity of field providers to use excessively high respiratory rates suggests that the number of breaths per minute should be decreased first in response to hypocapnia [23,24]. The mounting evidence against tidal volumes in excess of 10 mL/kg, especially in the absence of PEEP, would indicate that hypocapnia be ameliorated by lowering volume ventilation [38–45]. Our mathematical models suggest that the hemodynamic impact of lower volume ventilation may outweigh inflammatory considerations in the undifferentiated prehospital patient [37]. This provides some justification for volumetric capnometry, which will allow optimal tidal volume and respiratory rate parameters to be achieved in association with eucapnia.

The application of $PETCO_2$-guided ventilation by field providers represents a fundamental departure from traditional ventilation strategies, which were either undefined or incorporated the use of estimated tidal volumes and respiratory rates. Thus, significant education must accompany the introduction of field $PETCO_2$ monitoring. As discussed above, there appears to be a learning curve associated with this ventilation strategy [2]. In addition, the increased vigilance required for optimal capnometry-guided ventilation may exceed the capabilities of a small team of field providers, or require the use of alarms with implementation of high and low $ETCO_2$ alarm parameters. Thus, it remains to be seen whether further experience with these devices will result in normocapnia and

improved patient outcomes, or if transport ventilators will ultimately be required to achieve target ventilation parameters.

A lower target $P_{ET}CO_2$ may be justified in a patient with suspected transtentorial herniation. Clinical evidence that could justify a target $P_{ET}CO_2$ value as low as 25 mm Hg includes a non-reactive pupil or hypertension with bradycardia, suggesting markedly elevated ICP. It is doubtful, however, that a patient with signs of herniation in the immediate postinjury period will be salvageable with or without hyperventilation. In addition, other strategies for ICP control, such as the use of hypertonic saline or mannitol, may have more benefit without the associated risk of ischemia.

Troubleshooting

Sudden changes in either the $P_{ET}CO_2$ value or the expiratory complex on capnography can indicate an immediate problem, such as tension pneumothorax or misplacement of the ET tube. Unusual expiratory complex morphology may indicate an underlying lung disease or a problem with the airway circuit, such as a ruptured ET tube cuff or excessive airway resistance.

$ET CO_2$ monitoring with ventilators

Transport ventilators offer several advantages to the prehospital provider, and will likely play a larger role in the future of out-of-hospital medicine [47]. Ventilators are far more precise and consistent with regard to the delivered tidal volume and desired respiratory rate. Thus, capnometers can be most useful when determining optimal parameters upon initiation of mechanical ventilation. Any subsequent change in $P_{ET}CO_2$ should then initiate a search for problems with the patient or the airway circuit. In addition, ventilators allow for hands-free airway management, allowing more attention to be given to patient care and monitoring. Finally, mechanical ventilators allow more sophisticated modes of ventilation, including spontaneous respirations that can restore the negative intrathoracic pressure that accompanies inspiration, augmenting venous return, and preventing the rise in ICP associated with positive pressure ventilation [47]. In this situation, $P_{ET}CO_2$ monitoring can be used to determine whether an undersedated patient is "over-breathing" on the ventilator. In addition to the specific capnographic patterns noted, an erratic pattern of normal expiratory complexes intercalated with small, narrow complexes indicate a patient who is coughing, "bucking" against the ventilator, or merely adding spontaneous breathing effort. A change in ventilator mode, the administration of a sedative, or neuromuscular blockade can reverse this pattern. However, use of the latter two must be done in association with good clinical judgment.

Summary

A growing body of literature suggests that the ability to obtain and assess ventilation patterns in the field is of utmost importance in the management of the critically ill patient. The detrimental effects of hyperventilation on the injured brain, the hemodynamic compromise that accompanies positive pressure ventilation, and injurious ventilation strategies are all potential contributors to outcome in intubated patients. Furthermore, management of the initial resuscitation period is extremely important in this regard. Advances in the technology for $P_{ET}CO_2$ monitoring, including capnometry and capnography, have allowed these devices to be small and durable enough to be carried into the field, where they can help avoid hyperventilation and injurious ventilation patterns.

References

1. Davis DP, Dunford JV, Hoyt DB, *et al*. The impact of hypoxia and hyperventilation on outcome following paramedic rapid sequence intubation of patients with severe traumatic brain injury. *J Trauma* 2004; **57**: 1–10.
2. Davis DP, Dunford JV, Ochs M, Park K, Hoyt DB. The use of quantitative end-tidal capnometry to avoid inadvertent severe hyperventilation in head-injured patients following paramedic rapid sequence intubation. *J Trauma* 2004; **56**: 808–14.
3. Bhende MS, LaCovey DC. End-tidal carbon dioxide monitoring in the prehospital setting. *Prehosp Emerg Care* 2001; **5**: 208–13.
4. Johnston IH, Johnston JA, Jennett B. Intracranial-pressure changes following head injury. *Lancet* 1970; **2**: 433–6.
5. Rossanda M. Prolonged hyperventilation in treatment of unconscious patients with severe brain injuries. *Scand J Clin Lab Invest Suppl* 1968; **102**: XIII:E.
6. Whitwam JG, Boettner RB, Gilger AP, Littell AS. Hyperventilation, brain damage and flicker. *Br J Anaesth* 1966; **38**: 846–52.
7. Cruz J. Combined continuous monitoring of systemic and cerebral oxygenation in acute brain injury: preliminary observations. *Crit Care Med* 1993; **21**: 1225–32.

8. Stringer WA, Hasso AN, Thompson JR, Hinshaw DB, Jordan KG. Hyperventilation-induced cerebral ischemia in patients with acute brain lesions: demonstration by xenon-enhanced CT. *AJNR Am J Neuroradiol* 1993; **14**: 475–84.
9. Skippen P, Seear M, Poskitt K, *et al*. Effect of hyperventilation on regional cerebral blood flow in head-injured children. *Crit Care Med* 1997; **25**: 1402–9.
10. Forbes ML, Clark RS, Dixon CE, *et al*. Augmented neuronal death in CA3 hippocampus following hyperventilation early after controlled cortical impact. *J Neurosurg* 1988; **88**: 549–56.
11. Bao Y, Jiang J, Zhu C, *et al*. Effect of hyperventilation on brain tissue oxygen pressure, carbon dioxide pressure, pH value and intracranial pressure during intracranial hypertension in pigs. *Chin J Traumatol* 2000; **3**: 210–13.
12. Coles JP, Minhas PS, Fryer TD, *et al*. Effect of hyperventilation on cerebral blood flow in traumatic head injury: clinical relevance and monitoring correlates. *Crit Care Med* 2002; **30**: 1950–9.
13. Marion DW, Puccio A, Wisniewski SR, *et al*. Effect of hyperventilation on extracellular concentrations of glutamate, lactate, pyruvate, and local cerebral blood flow in patients with severe traumatic brain injury. *Crit Care Med* 2002; **30**: 2619–25.
14. Imberti R, Bellinzona G, Langer M. Cerebral tissue PO_2 and $SjvO_2$ changes during moderate hyperventilation in patients with severe traumatic brain injury. *J Neurosurg* 2002; **96**: 97–102.
15. McLaughlin MR, Marion DW. Cerebral blood flow and vasoresponsivity within and around cerebral contusions. *J Neurosurg* 1996; **85**: 871–6.
16. Ausina A, Baguena M, Nadal M, *et al*. Cerebral hemodynamic changes during sustained hypocapnia in severe head injury: can hyperventilation cause cerebral ischemia? *Acta Neurochir Suppl* 1998; **71**: 1–4.
17. Schneider GH, Sarrafzadeh AS, Kiening KL, *et al*. Influence of hyperventilation on brain tissue-PO_2, PCO_2, and pH in patients with intracranial hypertension. *Acta Neurochir Suppl* 1998; **71**: 62–5.
18. Muizelaar JP, Marmarou A, Ward JD, *et al*. Adverse effects of prolonged hyperventilation in patients with severe head injury: a randomized clinical trial. *J Neurosurg* 1991; **75**: 731–9.
19. Brain Trauma Foundation. The American Association of Neurological Surgeons. The Joint Section on Neurotrauma and Critical Care. Initial management. *J Neurotrauma* 2000; **17**: 463–9.
20. Sarrafzadeh AS, Sakowitz OW, Callsen TA, Lanksch WR, Unterberg AW. Detection of secondary insults by brain tissue pO_2 and bedside microdialysis in severe head injury. *Acta Neurochir Suppl* 2002; **81**: 319–21.
21. van Santbrink H, vanden Brink WA, Steyerberg EW, *et al*. Brain tissue oxygen response in severe traumatic brain injury. *Acta Neurochir (Wien)* 2003; **145**: 429–38.
22. Davis DP, Hoyt DB, Ochs M, *et al*. The effect of paramedic rapid sequence intubation on outcome in patients with severe traumatic brain injury. *J Trauma* 2003; **54**: 444–53.
23. Davis DP, Heister R, Dunford J, *et al*. Ventilation patterns in patients with severe traumatic brain injury following paramedic rapid sequence intubation. *Neurocrit Care* 2005; **2**: 165–71.
24. Davis DP, Stern J, Ochs M, Sise MJ, Hoyt DB. A follow-up analysis of factors associated with head-injury mortality following paramedic rapid sequence intubation. *J Trauma* 2005; **59**: 486–90.
25. Dunford JV, Davis DP, Ochs M, Doney M, Hoyt DB. The incidence of transient hypoxia and heart rate reactivity during paramedic rapid sequence intubation. *Ann Emerg Med* 2003; **42**: 721–8.
26. Davis DP, Idris AH, Sise MJ, *et al*. Early ventilation and outcome in patients with moderate-to-severe traumatic brain injury. *Crit Care Med* 2006; **34**: 1202–8.
27. Warner KJ, Cuschieri J, Copass MK, Jurkovich GJ, Bulger EM. The impact of prehospital ventilation on outcome after severe traumatic brain injury. *J Trauma* 2007; **62**: 1336–8.
28. Braman SS, Dunn SM, Amieo CA. Complications of intrahospital transport in critically ill patients. *Ann Intern Med* 1987; **107**: 469–73.
29. Thomas SH, Orf J, Wedel SK, Conn AK. Hyperventilation in traumatic brain injury patients: inconsistency between consensus guidelines and clinical practice. *J Trauma* 2002; **52**: 47–53.
30. Gervais HW, Eberle B, Konietzke D, Hennes HJ, Dick W. Comparison of blood gases of ventilated patients during transport. *Crit Care Med* 1987; **15**: 761–3.
31. Hurst JM, Davis K, Branson R, Johannigman JA. Comparison of blood gases during transport using two methods of ventilatory support. *J Trauma* 1989; **29**: 1637–40.
32. Tobias JD, Lynch A, Garrett J. Alterations of end-tidal carbon dioxide during the intrahospital transport of children. *Pediatr Emerg Care* 1996; **12**: 249–51.
33. Helm M, Hauke J, Lampl L. A prospective study of the quality of pre-hospital emergency ventilation in patients with severe head injury. *Br J Anaesth* 2002; **88**: 345–9.
34. Poste JC, Davis DP, Ochs M, *et al*. Air medical transport of severely head-injured patients undergoing paramedic rapid sequence intubation. *Air Med J* 2004; **23**: 36–40.

35. Davis DP, Douglas DJ, Koenig W, *et al.* Hyperventilation following aero-medical rapid sequence intubation may be a deliberate response to hypoxemia. *Resuscitation* 2007; **73**: 354–61.
36. Pepe PE, Raedler C, Lurie KG, Wigginton JG. Emergency ventilatory management in severe hemorrhagic states: elemental or detrimental? *J Trauma* 2003; **54**: 1048–55.
37. Davis DP, Davis PW. A mathematical model of ventilation, perfusion, and oxygenation in low-flow states [abstract]. *Circulation* 2007; **116**(II): 932–3.
38. Acute Respiratory Distress Syndrome Network. Ventilation with lower tidal volumes as compared with traditional tidal volumes for acute lung injury and the acute respiratory distress syndrome. *N Engl J Med* 2000; **342**: 1301–8.
39. Tremblay L, Valenza F, Ribeiro SP, Li J, Slutsky AS. Injurious ventilatory strategies increase cytokines and c-fos m-RNA expression in an isolated rat lung model. *J Clin Invest* 1997; **99**: 944–52.
40. Slutsky AS, Ranieri VM. Mechanical ventilation: lessons from the ARDSNet trial. *Respir Res* 2000; **1**: 73–7.
41. Zhang H, Downey GP, Suter PM, Slutsky AS, Ranieri VM. Conventional mechanical ventilation is associated with bronchoalveolar lavage-induced activation of polymorphonuclear leukocytes. *Anesthesiology* 2002; **97**: 1426–33.
42. Uhlig S. Ventilation-induced lung injury and mechanotransduction: stretching it too far? *Am J Physiol Lung Cell Mol Physiol* 2002; **282**: L892–6.
43. Imai Y, Parodo J, Kajikawa O, *et al*. Injurious mechanical ventilation and end-organ epithelial cell apoptosis and organ dysfunction in an experimental model of acute respiratory distress syndrome. *JAMA* 2003; **289**: 2104–12.
44. Wilson MR, Choudhury S, Goddard ME, *et al.* High tidal volume upregulates intrapulmonary cytokines in an in vivo mouse model of ventilator-induced lung injury. *J Appl Physiol* 2003; **95**: 1385–93.
45. Chiumello D, Pristine G, Slutsky AS. Mechanical ventilation affects local and systemic cytokines in an animal model of acute respiratory distress syndrome. *Am J Respir Care Med* 1999; **160**: 109–16.
46. Manley GT, Hemphill JC, Morabito D, *et al*. Cerebral oxygenation during hemorrhagic shock: perils of hyperventilation and the therapeutic potential of hypoventilation. *J Trauma* 2000; **48**: 1025–33.
47. Austin PN, Campbell RS, Johannigman JA, Branson RD. Transport ventilators. *Respir Care Clin* 2002; **8**: 119–50.

Section 1
Chapter
10

Ventilation

Neonatal monitoring

G. Schmalisch

Introduction

The pioneering work of Karlberg *et al.* [1], Cook *et al.* [2], and Nelson *et al.* [3] helped to set the stage for new insights into neonatal pulmonary pathophysiology. The first measurements of carbon dioxide (CO_2) in the expired gas were performed using breathing bags for gas collection [3]. However, in the 1960s, commercial capnographs developed for adults were adapted for measurements in neonates. These first capnographs were bulky, and the mainstream airway adaptors were heavy and could easily displace or kink a neonatal endotracheal tube (ET). The main problem was the deadspace of the airway adaptors, which could easily exceed the tidal volume of a preterm infant. This made long-term measurements possible only by using a sidestream device. This problem was magnified if a pneumotachograph was used in series to measure airflow and volume during volumetric capnography.

New, lightweight infrared (IR) mainstream sensors with a deadspace of <1 mL enable reliable measurements even in preterm infants [4,5]. Some manufacturers offer sensors to measure CO_2 and airflow simultaneously so that the transition from time-based capnography to volume-based capnography is not burdened by an increased apparatus deadspace. For deadspace-free measurements in neonates, special low-flow sidestream capnographs were developed which made long-term monitoring possible [6]. Despite this rapid technological progress, neonatology capnography has not been embraced by neonatologists for the assessment of alveolar gas exchange and airway deadspace because of several remaining technical and methodological problems.

Capnography techniques in neonates

Devices

The range of measurements for the CO_2 fraction (FCO_2) or the corresponding partial pressure (PCO_2) in the breathing gas is identical in neonates and adults. However, CO_2 production in neonates (about 15 mL/min) is much lower than in adults (about 200 mL/min). The much lower amount of exhaled CO_2 makes capnography in neonates more difficult, because there are objective limits for the size of the analyzer chamber or the magnitude of suction flow used with sidestream devices.

Measurements of CO_2 are distinguished between continuous and discontinuous. The oldest method of measuring CO_2 is based on the collection of exhaled gas in a large breathing bag (Douglas bag). In spontaneously breathing infants, special deadspace-reduced exhalation valves are necessary. Nelson *et al.* [3] developed a special valve (Rhan sampler) with a deadspace of 1.3 mL for neonates. Significant problems with such valves are the required opening pressure and the increased expiratory resistance that hampers breathing. Lum *et al.* [7] have shown that in ventilated infants, the Douglas bag method for deadspace measurement is simple but cumbersome. The method failed if there was an unknown bias flow through the ventilator. In neonates, this collection technique provides accurate CO_2 measurements and is used as a reference method to validate new techniques [7]. Fast and continuous CO_2 measurements that enable us to analyze the exhaled CO_2 during the breathing cycle are much better for diagnostic purposes. Therefore, in neonates, they are now used exclusively for clinical and research purposes.

Infrared spectrography is the most frequently used technique because the miniaturized, low-cost mainstream and sidestream sensors are optimal for measurements in neonates. An alternative and expeditious method that could be used is molar mass measurement of the breathing gas by ultrasound spirometry, but, besides technical difficulties, complex mathematical corrections are necessary to extract the CO_2 signal from the molar mass of the breathing gas [8].

Capnography, Second Edition, ed. J. S. Gravenstein, Michael B. Jaffe, Nikolaus Gravenstein, and David A. Paulus. Published by Cambridge University Press. © Cambridge University Press 2011.

Mainstream and sidestream measurements

Several studies in infants have shown that, from a technical point of view, mainstream measurements are superior to sidestream measurements. Mainstream sensors have a faster response time so that reliable, single breath CO_2 measurements, even at high respiratory rates, are possible. In infants who are not intubated, mainstream measurements are difficult.

Figure 10.1 displays the mainstream measurement in a spontaneously breathing newborn using a face mask connected to a CO_2 sensor with an integrated pneumotach for volumetric capnography. The main problem with this technique is the additional equipment deadspace (i.e., face mask and CO_2 analyzer chamber). The apparatus deadspace leads to rebreathing of the exhaled CO_2, which must be considered, especially in very small infants. Due to its influence on ventilatory pattern and gas exchange, this technique can only be used for short-term measurements in neonates [9].

Sidestream measurements without a face mask (e.g., by nasal tubes) are deadspace-free and therefore enable long-term measurements. Their accuracy is commonly less than that of mainstream measurements, particularly at high respiratory rates. In neonates with a minute ventilation of only about 200 mL/min/kg body weight, the suction flow must be low to prevent dilution by surrounding air, which will occur when the expiratory gas flow rate falls below the suction flow rate. However, a low suction flow means a long delay time and a distortion of the CO_2 signal as a consequence of gas mixing in the tube; thus, the sampling tube should be as short as possible. In neonates with high respiratory rates, the technical limitations of sidestream capnometers can lead to an unacceptable under-recording of the alveolar CO_2 [10].

A microstream capnometer, using a suction flow of 30 mL/min and a miniaturized small sample chamber, has been developed and improves the measurement accuracy in intubated and spontaneously breathing patients [6]. For precise synchronized measurements with other respiratory signals, this technique is not ideal because the delay time of the suction tube is affected by pressure changes in the system and changes in the resistance of the tube so that numerical compensations provide only approximations.

The technique to be used in neonates depends on the clinical situation. Provided that the additional apparatus deadspace is tolerable, mainstream measurements have uncontested advantages. However, the clinical setting often causes us to accept sidestream measurements:

- if the apparatus deadspace is not tolerable (e.g., measurements in ventilated preterm infants or small animals with a tidal volume <5 mL) or long-term investigations (e.g., sleep studies);

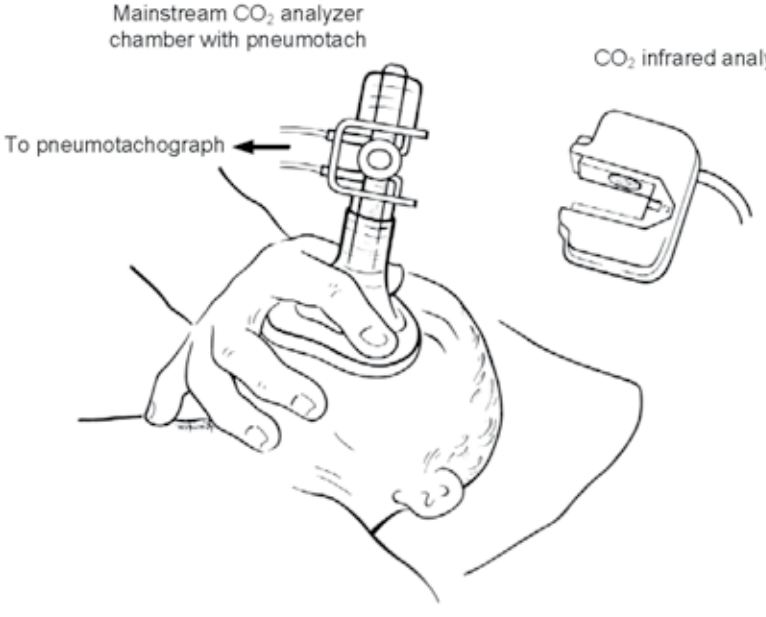

Figure 10.1 Volumetric capnography in a newborn using a face mask connected to a mainstream sensor.

- if there is a need for a direct access to the airways (e.g., for endoscopy);
- if, simultaneously, other devices with high deadspace are already used in-line with the ET (e.g., mainstream gas analyzers of tracer gases); or
- if sidestream gas sampling is already in use (e.g., the frequently used nasal spectacle).

Time-based and volume-based capnograms

The measured CO_2 signal can be recorded as a function of time (time-based capnography) or volume (volumetric capnography) as discussed in Chapter 1 (Clinical perspectives). The informative potential of both presentations differs considerably, as shown in Figure 10.2.

In the past, only time-based capnograms were recorded. Several investigators have described the changes in the waveform of the time-based capnogram that are characteristic of specific clinical situations [4,11]. Some typical patterns measured in neonates are displayed in Figure 10.3.

An important factor is the presence of a more or less steep alveolar plateau at the end of expiration. Only if the capnogram displays a plateau can we then assume that $P_{ET}CO_2$ reflects the alveolar CO_2 pressure. In ventilated patients, the ventilator-imposed expiratory pause can exceed the actual expiratory flow. Diffusion of CO_2 from the lungs or dilution of gas in the ventilator then makes any interpretation of "end-tidal" values doubtful (Figure 10.4).

These pitfalls in time-based capnography can be avoided by volumetric capnography. As shown in Figure 10.2, the volumetric capnogram is divided into three phases. The disadvantage of volumetric capnography is the higher technical expense of simultaneous ventilatory measurements and the necessity for exact compensation of any time delay between airflow and CO_2 signals. In the past, volumetric capnography in the mainstream was only possible with a CO_2 analyzer and a pneumotachograph placed in series, which considerably increases the apparatus deadspace [12]. Meanwhile, combined low-deadspace sensors have become available (deadspace <1 mL), making use of this technique possible in ventilated and spontaneously breathing neonates.

The advantage of volumetric capnography comes with a price: the two respiratory signals (CO_2 and respiratory gas flow) have to be measured in-phase and without artifacts. Experience has demonstrated that the acquisition of artifact-free data requires extra efforts, and the correlative evaluation of two respiratory signals is more difficult than one signal. If they cannot be correctly measured, then reverting back to time-based capnography is necessary.

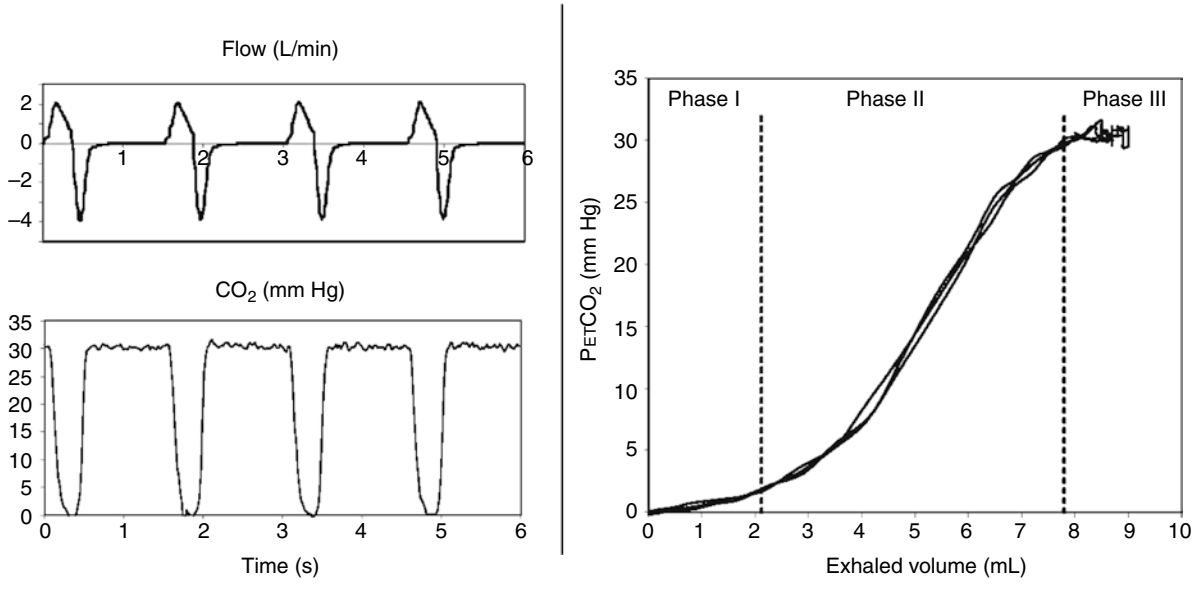

Figure 10.2 Time-based (left) and volume-based capnogram (right) of a ventilated preterm newborn. Note that the exhalation time of the infant is distinctly lower than the adjusted expiratory time, but, in this measurement, the expiratory pause does affect the $P_{ET}CO_2$. The volumetric capnogram shows the typical pattern of a preterm infant with a wide phase II and a very short phase III.

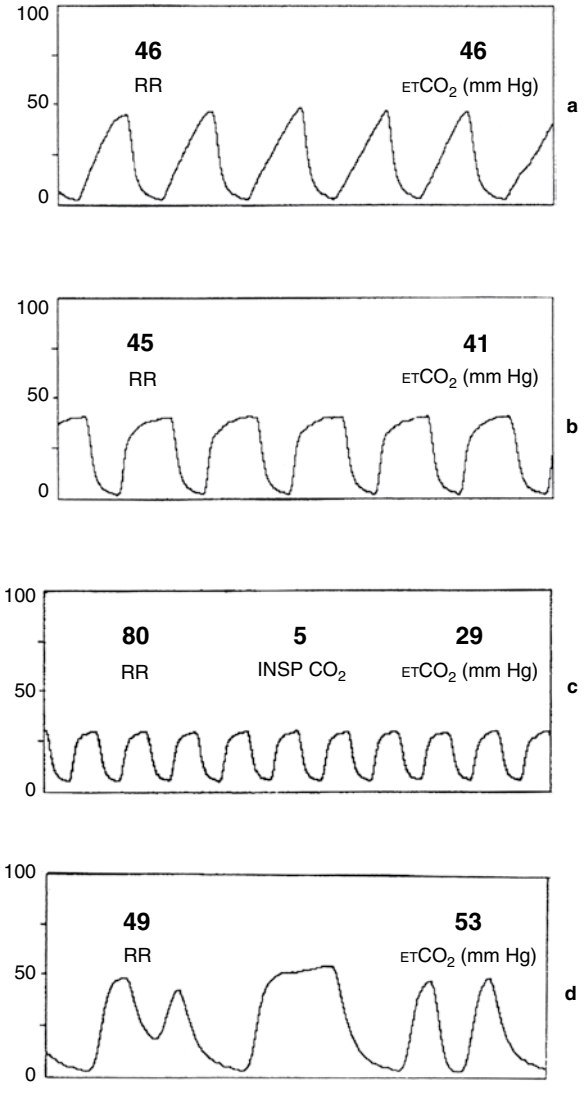

Figure 10.3 Typical pattern of time-based capnograms in ventilated newborns. (a) Capnogram of a premature baby with respiratory distress syndrome before and (b) after administration of surfactant. (c) Rebreathing due to high respiratory rate (RR) and too-large apparatus deadspace. (d) Superimposition of the respiratory cycles of the ventilator by spontaneous breathing. $ETCO_2$, end-tidal CO_2. [From: Arsowa S, Schmalisch G, Wauer RR. Techniques and clinical application of capnography in newborn infants. *Padiatr Grenzgeb* 1993; **31**: 295–331.]

End-tidal carbon dioxide pressure

In infants with normal pulmonary function and matching ventilation-to-perfusion ratio ($\dot{V}/\dot{Q}$), $PETCO_2$ can provide a good estimation of the PCO_2 in arterial blood ($PaCO_2$) [13], even in extremely low-birth-weight infants [5]. Nonetheless, several physiologic factors (e.g., high respiratory rate, incomplete expiration, pulmonary inhomogeneities, disturbed $\dot{V}/\dot{Q}$ ratio), technical factors (e.g., too slow response time, gas dilution by surrounding air), and diseases can affect the $PETCO_2$ and make it unreliable for blood gas replacement.

It appears that in neonatology, $PETCO_2$ measurement may not substitute for arterial or transcutaneous blood gases, but can be helpful in monitoring trends or detecting technical artifacts (e.g., unintended extubation). Nevertheless, the continuous measurement of $PETCO_2$ in spontaneously breathing infants can help us recognize hypoventilation, hyperventilation, and apnea. In mechanically ventilated infants, a sudden decrease in $PETCO_2$ can indicate disconnection, endotracheal leaks, obstructions of the ET, or ventilator malfunction, and even cardiac arrest.

The difference between $PaCO_2$ and $PETCO_2$ ($PaCO_2$–$PETCO_2$) in infants is normally <6 mm Hg if ventilation and perfusion are almost evenly matched. However, when the alveoli are not properly ventilated (shunt perfusion), or the perfusion of the lungs is decreased or regionally interrupted (deadspace ventilation), the $PaCO_2$–$PETCO_2$ difference will increase. An increase of the $PaCO_2$–$PETCO_2$ is one of the most sensitive indicators of acute pulmonary embolism [14].

Alveolar ventilation and deadspaces

Only one part of the total ventilated gas – the alveolar ventilation – takes part in gas exchange with pulmonary capillary blood. The difference between minute ventilation and alveolar ventilation is the deadspace ventilation in which gas exchange is negligible. Deadspace consists of conducting airways (anatomic deadspace), non-perfused or underperfused alveoli (alveolar deadspace), and the apparatus deadspace. In neonates, the deadspace fraction (V_D/V_T) is higher than in adults, which impairs both the alveolar ventilation and the lung clearance index [15].

The first calculations of alveolar ventilation and airway deadspace in neonates from the breathing gas were performed using the chemical CO_2 absorption method by Haldane and Scholander (see Chapter 40: Brief history of time and volumetric capnography), assuming that alveolar CO_2 can be approximated by the arterial CO_2. Chu *et al.* [16] were the first to use a rapid capnograph to measure the $PETCO_2$ in neonates and to calculate the anatomic and physiologic deadspace using the Bohr equation:

Figure 10.4 Capnogram of a ventilated tracheotomized piglet in which $P_{ET}CO_2$ was falsified by CO_2 washout of the sample cell during the expiratory pause. [Graphic display of the CO_2SMO+, Novametrix, USA.]

$$V_{D_{ana}} = V_T \frac{P_{ET}CO_2 - P_{mean}CO_2}{P_{ET}CO_2}$$

or the Bohr–Enghoff equation by substituting arterial CO_2 for $P_{ET}CO_2$:

$$V_{D_{phys}} = V_T \frac{PaCO_2 - P_{mean}CO_2}{PaCO_2}$$

where mean PCO_2 is the CO_2 tension of the mixed expired air. The difference of both deadspaces represents the alveolar deadspace:

$$V_{D_{alv}} = V_{D_{phys}} - V_{D_{ana}}$$

Fletcher *et al.* [17] were the first to calculate the different deadspaces from the CO_2-volume plot from a single breath (see Chapter 42: The early days of volumetric capnography). This single breath CO_2 test ($SBCO_2$ test) is now commercially available and is used for capnography in neonates [18] and older infants [19,20].

The determination of deadspaces by the $SBCO_2$ test can be foiled if there is no alveolar plateau or if the transition from phase II to III cannot be clearly identified. In contrast, the deadspace calculations by the Bohr or the Bohr–Enghoff equations are independent of the shape of the capnogram; that means that the calculated deadspaces, as well as the failure rate of capnography to determine airway deadspaces, depends on the method used [18].

Clinical applications

Operating room

For intraoperative monitoring, time-based capnography is commonly used, and the shape of the capnogram provides robust qualitative data [21] and the $P_{ET}CO_2$ [22]. Anesthesiologists strongly recommend the use of capnography in every newborn requiring tracheal intubation because capnography can instantly identify life-threatening conditions before irreversible damage is done. Widely discussed in the literature are failed intubation [23,24], failed ventilation [25], and failure of the respirator or respiratory circuit [21,26].

What information can the capnogram offer? First, if end-expiratory CO_2 is not present, failure to ventilate the patient's lungs must be assumed. Table 10.1 presents typical causes of absent CO_2.

Second, independent of whether time- or volume-based capnography is used, the shape of the capnogram must be compared with a typical pattern by examining the inspiratory CO_2 baseline, the steepness of phase II and the alveolar plateau of phase III, and the decline of the capnogram at the beginning of the next inspiration. Third, depending on the capnograph used, characteristic parameters derived from the capnogram

Table 10.1 Differential diagnostic causes of absent end-expiratory CO_2

Immediately after intubation, CO_2 only minimal or absent
Inadvertent esophageal intubation
Exhaled CO_2 present, then suddenly absent
Accidental tracheal extubation
Disconnection of breathing circuit
Apneic spells
Cardiac arrest
Severe bronchospasm
Complete obstruction of endotracheal tube
Disconnection of the CO_2 sample catheter
Water condensation or secretions in the sampling tube
Failure of the capnograph

are sought; for example, $P_{ET}CO_2$, CO_2 production, $PaCO_2$–$P_{ET}CO_2$, and the deadspaces.

Inspiratory baseline

During inspiration, fresh CO_2-free gas flows through the mainstream sensor or is aspirated at the sample port. The CO_2 level should be zero; otherwise, there is a rebreathing of CO_2 from the patient (high apparatus deadspace, valve malfunction or exhausted CO_2 absorber). Rebreathing of CO_2 can occur if the tidal volume is relatively low compared to the apparatus deadspace (see Figure 10.3c). This is mainly a problem in very small infants or in non-intubated infants during mask ventilation.

The expiratory CO_2 increase (phase II)

During expiration, the first gas comes from the CO_2-free anatomic deadspace. Subsequently, in healthy lungs, the CO_2 curve rises with a steep upward slope. Phase II can be prolonged when the delivery of CO_2 from the lung is delayed; for example, due to pulmonary inhomogeneities, high resistances of the small airways, and mechanical obstructions, such as a blocked or kinked ET. In neonates, a prolonged phase II can also be caused by technical problems related to the response time of the capnograph.

The alveolar plateau (phase III)

Theoretically, the shape of the alveolar plateau is one of the most interesting parts of the capnogram, because the steepness of the slope is a function of morphometric structure and respiratory mechanics [27]. Phase III contains, at first, gas from the well-ventilated, low-resistance regions of the lung. Later, gas from poorly ventilated, high-resistance regions is exhaled, which causes a slope of the alveolar plateau. Thus, the steepness of the alveolar plateau is commonly used as an indicator for inhomogeneities in the alveolar time constants and $\dot{V}/\dot{Q}$ ratio [19]. In neonates, this interpretation should be used with caution, because the plateau (if it exists at all) is often small, and the steepness is also a function of lung growth [19]. Therefore, the diagnostic value of a phase III analysis is often limited. Nevertheless, the appearance of a phase III in the capnogram indicates that alveolar gas was sampled.

The decrease of CO_2 at the beginning of inspiration

After expiration, the fresh gas from the breathing circuit rinses out the CO_2 from the previous exhalation, and a rapid decrease of the end-expiratory CO_2 at the beginning of inspiration should follow. In the past, several techniques (e.g., tracheal gas insufflation [28]) were developed to reduce rebreathing and deadspace ventilation so that the tidal volume was more efficiently used for gas exchange. A delayed decrease of CO_2 may be caused by a leaking inspiratory valve or a respiratory circuit with a low flow, so that CO_2 can be accumulated in the inspiratory limb. Technical failures resulting in the artifactual presence of inspired CO_2 can represent a slow response time of the CO_2 analyzer, and are not uncommon, especially when using a sidestream device in neonates.

Emergency medicine and transport

In emergency medicine, critically ill infants often require tracheal intubation before transportation to the hospital. The intubation must be done quickly, and the ET must be positioned correctly. Failure to recognize an unintentional esophageal intubation may be catastrophic, and can lead to severe hypoxia and permanent neurologic injury. Such intubation failure can occur, even in the hands of the most experienced personnel.

As stated above, CO_2 monitoring and the measurement of the $P_{ET}CO_2$ can detect esophageal intubation or displacement of the ET at a later stage. Roberts *et al.* [29] investigated the time for correct placement of the ET. A clinical assessment of the position of the endotracheal tube took 97 s, but only 1.6 s using capnography. Especially in extremely low-birth-weight neonates (<1000 g), capnography is strongly recommended during all endotracheal intubations [23].

Due to the vicissitudes of transport, inadvertent extubation can occur at any time. The vibrations and noisy environments of the ambulance or helicopter make assessment of tube positions difficult. In these situations, when the patient is in critical condition, and time is of the essence, the use of capnography is most valuable. The use of portable CO_2 monitors during transport provides an effective visual check of ET position and indirectly gives information about the ventilatory status and circulation. In neonatology, pulse oximetry is widely used for monitoring during transport, but CO_2 measurements of the exhaled gas can also alert clinicians to airway problems before hypoxemia occurs.

Finally, capnography is a useful monitor during transport of intubated, critically ill patients, and may aid the management of patients in whom hypercapnia is detrimental, such as those with head injury and raised intracranial pressure and pediatric patients with pulmonary hypertension.

Intensive care

In contrast to the operating room or during transport, the duration of mechanical ventilation in the intensive care unit (ICU) is usually prolonged. Variables monitored subserve not only ventilator adjustments, but also diagnosis and prognosis (e.g., optimal time of weaning [30]). Ventilatory support in newborn infants must carefully balance the amount of support (oxygen and pressure/volume) and its toxicities [31]. Therefore, monitoring of blood gases plays an essential part in optimizing respiratory support or mechanical ventilation. In neonates, a low $PaCO_2$ can contribute to the development of chronic lung diseases and periventricular leukomalacia, whereas high levels can cause enhanced cerebral blood flow and increase the risk of periventricular hemorrhage. Although arterial blood gas analysis provides the most accurate data, the number of arterial samplings must be limited to prevent excess blood loss. Alternative non-invasive methods are transcutaneous PCO_2 ($PtcCO_2$) measurement or end-tidal CO_2 measurement.

Patient safety

As already stated, capnography can identify disconnections in the ventilatory circuit instantaneously before O_2 and CO_2 levels change in the blood, and corrective measures can be taken before irreversible damage is caused by prolonged hypoxia. An alarm is commonly activated if $PetCO_2$ falls to zero; however, during mechanical ventilation, patients often also breathe spontaneously, generating a measurable $PetCO_2$ (see Figure 10.3d). Circuit disconnections between the CO_2 sampling site and the patient can be identified instantaneously as CO_2 concentration falls to zero, whereas circuit disconnection between the sampling site and ventilator may not be detected due to spontaneous breathing. If spontaneous breathing is adequate, the $PetCO_2$ can reach normal values. High $PetCO_2$ values will alert the clinician to potentially inadequate spontaneous ventilation. In addition to end-tidal CO_2 monitoring, the shape of the capnogram is also examined in the ICU to detect partially kinked or obstructed ETs, which are characterized by prolonged phase II and steeper phase III, and irregular height of the CO_2 tracings. Because accidental kinking or displacement of the ET can easily occur in the ICU during positioning, bathing, or while changing the bed, the capnograph should never be turned off during these activities.

Monitoring CO_2

Measurement of $PetCO_2$ provides a non-invasive estimation of $PaCO_2$ without the time delay associated with arterial blood gas analysis. Monitoring of $PetCO_2$ has several advantages for patients requiring intensive care [31,32]:

- decreased blood loss by arterial sampling
- lower risk of infection
- decreased costs.

In intubated neonates with normal respiratory and cardiovascular physiology, $PetCO_2$ values approximate $PaCO_2$ values. In critically ill patients, the ventilation and pulmonary perfusion ratio is often abnormal so that the $PaCO_2$–$PetCO_2$ difference is increased. Nevertheless, McDonald *et al.* [32] and Wu *et al.* [13] have shown, in large clinical studies in critically ill, mechanically ventilated infants, that $PetCO_2$ correlates with $PaCO_2$ and provides a clinically relevant, reliable estimation of ventilation for most infants. Similar results were found by Rozycki *et al.* [31] investigating 45 newborn infants receiving mechanical ventilation. They suggest that capnography may be useful for trending or screening patients for abnormal arterial CO_2 values. In contrast, Tobias and Meyer [33] found, in intubated infants, that $PetCO_2$ does not accurately predict $PaCO_2$ and that $PtcCO_2$ measurements are more accurate. Similar results were found by Tingay *et al.* [10] during neonatal transport because there was an unacceptable under-recording of the $PaCO_2$ likely due to technical limitations of the

sidestream capnometer used. Their study suggests that $PtcCO_2$ should currently be the preferred method of CO_2 monitoring. However, $PtcCO_2$ measurements are not well tolerated in tiny infants with fragile skin and are affected by acidosis and hypoxia. Low cardiac output, hypothermia, size of tidal volume, and lung disease can adversely affect the $PaCO_2$–$PETCO_2$ difference. McDonald *et al.* [32] showed that, in most of the patients, $PaCO_2$–$PETCO_2$ is small enough so that $PETCO_2$ monitoring enables the clinician to monitor ventilation provided that suitable equipment is used. This means that changes in $PaCO_2$ can be assumed to occur in parallel with those of $PETCO_2$, thus, avoiding repeated blood gas measurements. If the goal of mechanical ventilation is to avoid hypocapnia or hypercapnia, rather than achieving a specific level or range of $PaCO_2$, then continuous $PETCO_2$ measurements may be pertinent to clinical treatment [31]. A new concept of mechanical ventilation in neonates is permissive hypercapnia, which employs lower tidal volumes and, thus, decreases the potential for lung injury [34], although it is important to note that this technique requires careful $PaCO_2$ monitoring to prevent unintentional side effects. Based on this approach, Rozycki *et al.* [31] demonstrated that mainstream CO_2 monitoring can identify a $PaCO_2$ within prescribed parameters ($PaCO_2$ between 34 and 55 mm Hg) 91% of the time. Furthermore, the arterial–alveolar CO_2 difference can be used as a minimally invasive monitor of pulmonary blood flow. A reduction in the cardiac output causes a decrease in pulmonary blood flow, which, in turn, produces a high $\dot{V}/\dot{Q}$ ratio and an increased alveolar deadspace, resulting in a lower $PETCO_2$ and an increased $PaCO_2$–$PETCO_2$ difference. As pulmonary blood flow increases, thereby improving $\dot{V}/\dot{Q}$ ratio, the $PETCO_2$ increases and $PaCO_2$–$PETCO_2$ is diminished. Sanders *et al.* [35] showed that end-tidal CO_2 monitoring can advantageously be used to predict successful resuscitation after cardiac arrest. During cardiac arrest, circulation is compromised and $PETCO_2$ gradually disappears; an increase in the $PETCO_2$ indicates effective cardiopulmonary resuscitation. Recently, Berg *et al.* [36] confirmed these observations in an animal model.

Weaning

In long-term, mechanically ventilated infants, weaning from the respirator presents a critical situation. Weaning from mechanical ventilation often requires multiple blood gas analyses. The practice is not only invasive, but also means that the blood loss incurred can lead to anemia in premature infants. For these infants, non-invasive capnography can be helpful. In addition to the $PETCO_2$ and the occasional $PaCO_2$–$PETCO_2$, capnography also provides information about the breathing pattern and, importantly, the rate of breathing before extubation [30]. Monitoring the capnogram enables us to gradually reduce ventilatory support to the lowest point compatible with comfortable breathing and adequate alveolar ventilation. The stability of the $PETCO_2$ and the proper shape of the capnogram indicate the patient's ability to be weaned from mechanical ventilation. If the patient becomes distressed or the alveolar gas exchange is insufficient, ventilatory support can be returned immediately to the previous settings.

Recently, Hubble *et al.* [30] showed that capnogram-derived parameters are of high diagnostic value in predicting successful extubation in infants and children. In a clinical study of 45 pediatric patients, they found that the ratio of physiologic deadspace and tidal volume ($V_{D_{phys}}/V_T$) <0.5 reliably predicts a successful extubation, whereas ($V_{D_{phys}}/V_T$) >0.65 identifies patients at risk for respiratory failure following extubation. This finding agrees well with previous modeling studies in ventilated newborns, which showed that for $V_{D_{phys}}/V_T$ >0.5, the lung clearance index increased dramatically, indicating a poor alveolar gas exchange [15]. Hubble *et al.* [30] suggest that the calculation of the pulmonary deadspaces in ventilated patients may permit earlier extubation and reduce unexpected extubation failures.

Arnold *et al.* [37] investigated the predictive value of deadspace in neonates with congenital diaphragmatic hernia. Using capnographic measurements in 30 neonates, they found that the respiratory deadspace can be easily quantified in these infants by the Bohr–Enghoff method, and that a physiologic deadspace fraction of >0.60 is associated with a 15-fold increase in mortality rate. In infants treated with extracorporeal membrane oxygenation (ECMO), the survivors manifested a significant decrease in $V_{D_{phys}}/V_T$ before ECMO decannulation.

Lung-function testing

Capnography is a simple, non-invasive technique used to obtain information on alveolar ventilation and the deadspaces of the respiratory system. The shape of the capnogram (mainly the steepness of phase III) provides information about airway obstructions and pulmonary inhomogeneities [27]. For these reasons, capnography

has become an integral component of modern equipment for infant respiratory function testing (e.g., Spiroson, ECO MEDICS, Dürnten, Switzerland).

In spontaneously breathing neonates, volumetric capnography requires an airtight face mask (see Figure 10.1), which has its disadvantages:

- the exact apparatus deadspace after application of the face mask (approximately 50% of the mask volume [38]) is unknown;
- the measured anatomic deadspace includes the apparatus deadspace, which varies with the type of equipment in use; and
- especially in infants with low tidal volume, the apparatus deadspace of the face mask leads to significant CO_2 rebreathing, which affects blood gases and the PCO_2 of the breathing air as well as the breathing pattern. This imposes limits on the duration of the measurement [9,39].

Morris [38] described an in vivo technique used for neonates to determine the effective deadspace of a face mask by water displacement. The disadvantage of this technique is that it is too cumbersome for clinical use, making it of limited value for lung-function testing in spontaneously breathing neonates. More informative is the alveolar deadspace determined by Fletcher's method and the shape of the capnogram. Severe airway obstruction, such as bronchial asthma and laryngotracheobronchitis, can affect the shape of the capnogram, resulting in a prolongation of phase II and increased steepness of phase III.

Similar to other tidal breathing measurements in neonates, capnography for lung-function testing is hampered by the absence of reference values. Unfortunately, despite repeated efforts over the last 50 years to establish reference values for capnographic parameters in healthy infants [2,3], these values are highly specific to the equipment used and the behavioral state of the specific population studied, and cannot be recommended for general use.

Knowledge of the biological development (i.e., the influence of growth and maturation) and clinical/diagnostic value of most of the parameters remains sparse, making it difficult to compare capnographic parameters from different laboratories.

Sleep laboratory

Isolated measurements of lung function are only brief snapshots, and may be of limited value if disturbed lung function is dependent on the behavior of the infant. The extensive sequence of changes in sleep organization during the perinatal period, the length and time spent in sleep by the neonates, and the fact that many respiratory disorders are sleep-related indicate the need for sleep studies in this age group.

In neonates, many cardiorespiratory disorders are caused by apnea. Apnea is defined as the cessation of respiration originating from the central nervous system, or obstruction of the airway [40]. In premature infants, apnea is a very common phenomenon, and its incidence is inverse to the gestational age. Cerebral hemodynamics can be affected if apnea is associated with hypoxia and/or bradycardia. Therefore, the quantification of apnea during sleep and the detection of hypoxia or bradycardia is an essential goal of sleep studies in this age group.

Capnography is used in the sleep laboratory to identify the apnea type (central versus obstructive) and its duration. Transthoracic impedance measurements or breathing belts are commonly used to monitor breathing by chest wall movements; however, they can only detect central apnea. Obstructive apnea (i.e., breathing efforts without airflow) can only be recognized by simultaneous airflow measurements with the help of a pneumotachograph, nasal thermistor, or CO_2 measurements. As face masks are unsuitable for long-term measurements in neonates, sidestream capnography has been shown to be reliable in the detection of central and obstructive apnea during sleep. Capnography can be used as a reliable monitor to detect sleep apnea syndromes characterized by excessive daytime somnolence, tiredness, episodes of asphyxia during the night, or non-refreshing sleep.

For use in the sleep laboratory, the capnograph has to fulfill special requirements:

- the device must be quiet so as not to disturb sleep;
- CO_2 measurement via the nasal prongs should not affect the sleeping infant or respiration by increased airway resistance, and should be insensitive to head movements;
- sidestream gas sampling must have long-term reliability (no collection of condensation in the tube during the duration of measurement); and
- the capnograph must be compatible with commonly used polysomnographic measurement equipment.

Blood gas sampling is not practical during sleep, because it would disturb sleep. The use of $PtcCO_2$ measurement may be more accurate in predicting true

$PaCO_2$, but capnography has better long-term stability and is simpler to perform during sleep [40]. Both techniques have methodological limitations; $PetCO_2$ is affected by changes in pulmonary perfusion and deadspace ventilation, whereas $PtcCO_2$ is subject to changes in peripheral perfusion. Thus, neither technique can reliably predict true $PaCO_2$, but both are useful for trend monitoring. Furthermore, capnography is the only technique fast enough to detect breath-to-breath changes in the expired gases and, hence, presumably, blood gases. Vos *et al.* [41] have shown that nocturnal $PetCO_2$ recording detects obstructive apnea and hypopnea, and is especially helpful in identifying hypopnea that is accompanied by only small dips in oxygen saturation.

Current methodological and technical limitations of capnography in neonates

Technical limitations

The technical requirements of the capnograph for use in neonates are high:

- minimal deadspace of mainstream sensors because of the low tidal volume;
- low suction flow of sidestream monitors due to low breathing flow;
- fast response time of the CO_2 analyzer because of the short exhalation times, especially in preterm neonates with stiff lungs; and
- the high instrument frequency response required to get a sufficient graphic resolution of the capnogram, especially in infants with high respiratory rates.

Deadspace

In the past, the importance of the apparatus deadspace on the breathing pattern and on the measuring results themselves was often underestimated in neonates, although it had been documented in several studies [9,39]. The apparatus deadspace is of particular interest for capnographic measurements because it can lead to rebreathing of exhaled CO_2, with the potential of generating false inspiratory and expiratory CO_2 measurements. This was a significant problem in the past when using volumetric capnography by serial connection of a CO_2 analyzer and a pneumotachograph, where the resulting deadspace was often at least 30% of the tidal volume [18]. Even though combined sensors for volumetric capnography have become available (e.g., neonatal sensor of the CO_2SMO+, Respironics-Novametrix, Wallingford, CT, USA) for deadspaces of about 1 mL, the deadspace problem in neonates remains. If the tidal volume is lower than 5 mL (e.g., ventilated preterm newborn <1000 g), a deadspace of 1 mL is an undesirable burden. Technical limitations in the miniaturization of mainstream sensors compel us to use deadspace-free measuring techniques. To prevent rebreathing in neonates, Evans *et al.* [42] used a bias flow of 3 L/min, similar to deadspace-free ventilatory measurements by the flow-through technique [9]. However, the bias flow reduces the CO_2 concentration of the analyzed breathing gas and can cause a loss in the precision of CO_2 measurements.

Sidestream sampling

Recently, microstream technology (e.g., NBP-75, Nellcor Puritan Bennett, Pleasanton, CA, USA) has been developed for sidestream measurements in neonates. It utilizes low aspiration sampling flows and rapid response time. Hagerty *et al.* [6] showed, in 20 ventilated neonates without pulmonary disease, that this microstream capnography correlates well with the $PaCO_2$, as demonstrated by normal $PaCO_2$–$PetCO_2$ differences. Casati *et al.* [43] demonstrated in 20 spontaneously breathing adults that a microstream capnometer provides a more accurate $PetCO_2$ measurement than conventional sidestream capnometers.

When a sidestream capnograph is used, the sampling tube needs special care to prevent measuring errors. During mechanical ventilation, water droplets and secretions can accumulate in the breathing circuit. Depending on the site of the sample port, the contaminant can enter the sampling tubes and increase flow resistance in the tubing, thus significantly affecting the accuracy of the CO_2 measurement. In extreme circumstances, the sample port or the sampling tube can be completely occluded. Some capnographs either increase the sampling flow or, to clear the contaminant from the tube, reverse the flow (purge) when they sense a drop in pressure from a flow restriction. If this fails, the sampling port and/or the tube has to be replaced.

Occasionally, liquids enter the CO_2 analyzer chamber despite the presence of a water trap. This can affect the performance of the CO_2 monitor and produce abnormal capnograms. Cleaning the CO_2 analyzer chamber is often difficult. Positioning of the sampling site upwards away from the patient

decreases the risk of liquids in the tubes and the analyzer chamber.

When capnograms are abnormal, the clinician should ensure that there is not a system fault. In clinical practice, a common, but less accurate, bedside method to check the capnograph is to record a normal CO_2 tracing (e.g., one's own) to confirm the proper functioning of the capnometer [26].

Response time

It is an essential prerequisite of all physiologic measurements that the response time of the measuring and recording system be sufficiently high so that the magnitude and shape of the signal are not falsified. Thus, especially for measurements in neonates, a capnograph should have a short response time for accurate measurements. The delay time of a capnograph has two components: the transit time and rise time [44]. In sidestream measurements, the transit time is the time taken by the gas sample to travel from the sample port to the CO_2 analyzer, and is dependent on the suction flow, and the length and diameter of the tube. The transit time can be numerically corrected provided that it is nearly constant. The rise time is defined as the time required by the CO_2 analyzer to change from 10% to 90% of the final value. Unfortunately, the possibilities of improving the rise time by signal filtering are marginal, and limited by the rapid increase of the noise in the signal [45].

The effect of an increased rise time on the time-based and volume-based capnogram is shown in Figure 10.5. In this figure, the CO_2 signal of a ventilated newborn with a short exhalation time was low-pass filtered to simulate an increase in the rise time of the analyzer. Even though the errors in the $PETCO_2$ are relatively low, an already low time constant of the low-pass filter leads to a distinct shift of the volumetric capnogram to the right, which results in an overestimation of the calculated deadspaces. This means that in neonates with low exhalation times, deadspace measurements are much more sensitive to the rise time of the CO_2 analyzer than $PETCO_2$ measurements.

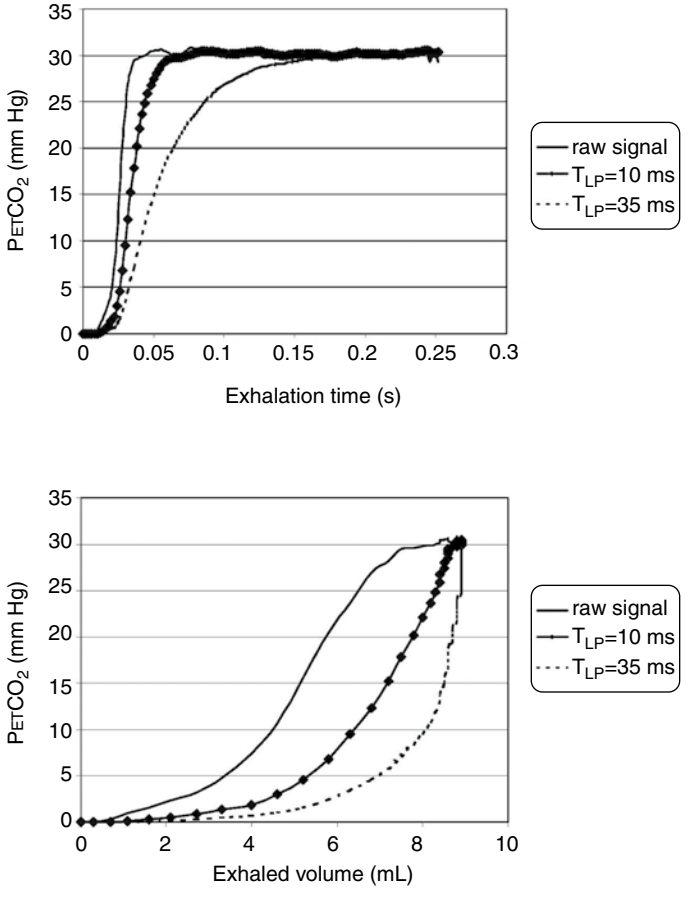

Figure 10.5 Computer simulation to illustrate the effect of low-pass filtering of the CO_2 signal (time constant of the low-pass filter 10 ms and 35 ms, respectively) on the time-based (top) and volume-based capnogram (bottom). Raw data were taken from a ventilated newborn with a 8.9 mL tidal volume and 250 ms exhalation time.

Mainstream capnographs are generally faster than sidestream capnographs because they are not affected by the dynamic problems of the sampling tube. Capnographs currently used in neonates have rise times $T_{10–90\%}$ of about 50–80 ms, depending on the airflow used for testing. For preterm neonates with low expiratory flow and respiratory rates of 60/min and higher (this means expiratory times TE <500 ms), it is doubtful that this rise time is sufficiently accurate to reflect the capnogram (especially the volumetric capnogram) in these small infants. Because low-flow CO_2 sensors with rise times <10 ms are still not available, it is difficult to verify the dynamic errors of the current CO_2 sensors for measurements in neonates. In the past in preterm infants, sidestream devices often did show sinusoidal capnograms without a clear alveolar plateau or inspiratory baseline. Sinusoidal shapes may be due to several factors, such as too high a sampling flow for the volume of CO_2 produced, signal distortions by turbulence produced by gas sampling and transport, long sampling tubes, and CO_2 sampling from an unsuitable site. It is very likely that, in the past, the rise time of the CO_2 analyzers was too long for accurate interpretation of the capnogram in neonates; therefore, older published capnometry results from neonates should be viewed with reservation.

The recently developed ultrasonic flowmeters to measure airflow and the molar mass of the breathing gas have a very short response time and do not have any time delay between signals. Theoretically, they are well suited for deadspace measurements; however, the molar mass is a surrogate signal, and it is difficult to distinguish the CO_2 signal [8].

Sampling rate

The use of equipment developed for measurements in adults has often been shown to be inappropriate for measurements in neonates. This is particularly true for capnography. The relatively low sampling rate translates into insufficient digital resolution. Special technical features are required to deal with the challenges presented by the signals from neonates. These include optimized digital signal processing thresholds for breath detection and dead bands to stabilize the volume integration to deal with the signal-to-noise ratio when using capnography in neonates.

A sampling rate of 50 Hz for CO_2 and gas flow may be sufficient for adults with an expiratory time of several seconds. However, that would provide only 25 sample values in a preterm newborn with an expiratory time of 500 ms, which would put into doubt the ability to clearly distinguish phase I, II, and III of volumetric capnograms. We have to consider that, in contrast to a time-based CO_2 curve, the distances between sampling points in the volume-based CO_2 curve are not equidistant. For tidal breathing signals in neonates, a sampling rate of at least 200 Hz is required, as this is necessary for a precise evaluation and for an accurate graphic presentation of the signals or loops presented in suitable scales.

As already shown, the graphic assessment of a capnogram is an essential prerequisite for valid interpretation of capnogram-derived parameters. The small size of the displays of current monitors (which often have only a low number of sampling points) may be helpful for monitoring purposes. However, the commonly offered hard copy of small diagrams are mostly insufficient for a quantitative evaluation. For a manually quantitative evaluation, a printout on A4 size paper is necessary, which requires high digital resolution in the amplitudes and the time.

Peculiarities of capnography in small lungs

The developing lung and the breathing pattern of neonates differ in many respects from adults. This may influence CO_2 measurements significantly. It is essential to understand these age-related deviations to minimize misleading interpretations of the capnogram.

Small airways

In healthy adult lungs, there is a rapid rise of CO_2 concentration during phase II and only a negligible contribution of the upper airways to the gas exchange. In neonates, the diameter of the airways is much smaller; and the smaller the airway diameter, the higher the impact on the exhaled CO_2. This may explain an exaggerated phase II and a reduced, or even missing, phase III in neonates.

The effect of the airway diameter on the capnogram has been investigated in small animals. Despite the morphological differences between animal and human lungs, Weiler *et al.* [46] showed that in small guinea pigs with an airway diameter <2 mm, no anatomic deadspace was measured, whereas in large guinea pigs with airways >3 mm, an anatomic deadspace could be measured. Obviously, with a larger airway diameter, the ratio between inner surface and volume suffices to prevent a rapid CO_2 exchange between gas and tissue. In much smaller airways at the end of inspiration,

a nearly complete equilibration is possible between the inner bronchial PCO_2 and the PCO_2 of the tissue. Consequently, phase I disappears because the gas exchange is very fast.

Lung growth during infancy also affects phase III (if it is present) of the capnogram [19]. This may explain the steeper slope of phase III in small infants compared to adults. It should be noted that the steeper phase III is, the more difficult it is to distinguish between phase II and III, and the more difficult is the calculation of the deadspaces from the volumetric capnogram by Fletcher's method.

Fletcher's method, developed for adults, requires a clear subdivision of the capnogram into phases I, II, and III. It is, therefore, often difficult to apply Fletcher's method to measurements in small lungs. The Bohr and Bohr–Enghoff equations can be used independently of the shape of the volumetric capnogram; however, the more the capnogram differs from a step function, the more unreliable will be the calculated deadspaces. Currently, there are no special techniques for capnograms in which the three phases cannot be clearly distinguished.

Missing alveolar plateau

Fletcher's method fails if there is no distinct phase III in the volumetric capnogram. A missing alveolar plateau may indicate that the measured $P_{ET}CO_2$ does not reflect alveolar PCO_2. Tirosh *et al.* [47] have shown, in spontaneously breathing preterm infants, that with decreasing gestational age, the number of capnograms without alveolar plateau increased significantly. The influence of the stiffness of the lungs on the incidence of capnograms without alveolar plateau was investigated by Proquitté *et al.* [48] in 21 ventilated newborn piglets (body weight 560–1435 g). Mainstream capnographic measurements were performed in healthy lungs and in surfactant-depleted lungs after lung lavage by saline. As illustrated in Figure 10.6, before lavage, 10% of all capnograms did not show an alveolar plateau, whereas in the surfactant-depleted lungs, the incidence was about 50%. In this study, it was also observed that the incidence of capnograms without alveolar plateau increased considerably with decreasing exhalation time (Figure 10.6). If the exhalation time was shorter than 200 ms, an alveolar plateau was not seen in more than 75% of all recorded files.

This high rate of missing plateaus in Figure 10.6 illustrates the current problems of capnography in small, stiff lungs. The explanations of the observation remain speculative. Likely, it is caused by both the technical limitations of the current technique (mainly the lengthy response time) and the physiological peculiarities of CO_2 exchange in small lungs. For further

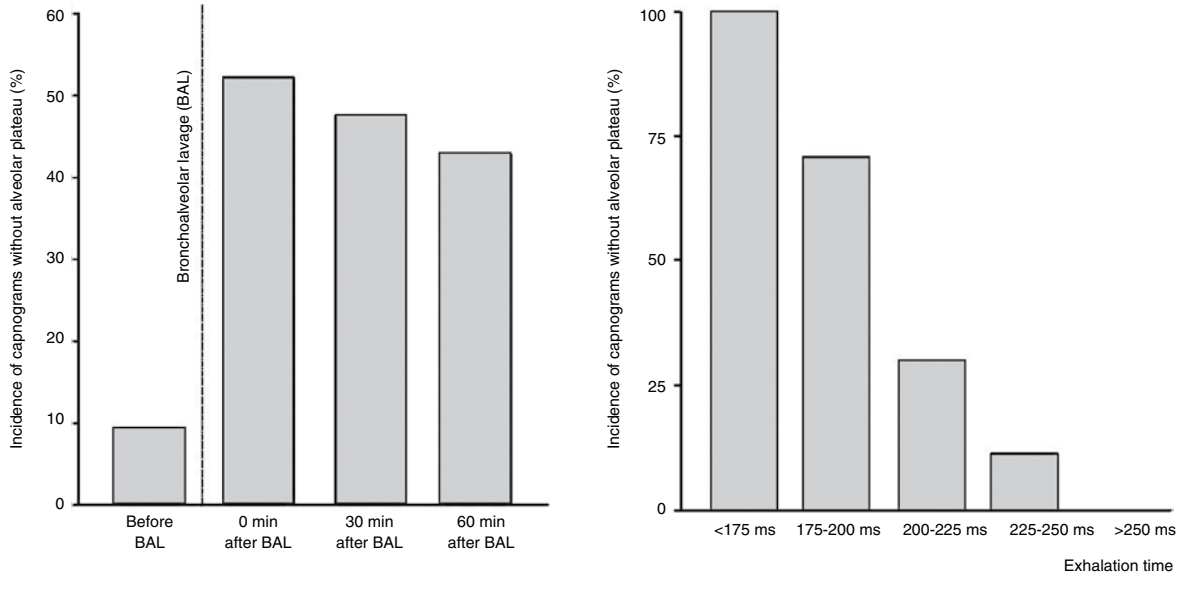

Figure 10.6 Effect of surfactant depletion by bronchoalveolar lavage (BAL) on the incidence of capnograms without an alveolar plateau in newborn piglets (left) and increase of the drop-out rate with decreasing exhalation time (right). [From: Proquitté H, Krause S, Rüdiger M, Wauer RR, Schmalisch G. Current limitations of volumetric capnography in surfactant-depleted small lungs. *Pediatr Crit Care Med* 2004; **5**: 75–80.]

capnographic investigations in small stiff lungs, it is crucial to avoid the current technical limitations and shorten the response time of the sensor, to improve the time resolution of the signals.

Incomplete expiration

Besides morphological differences between adult and newborn lungs, there are also significant differences in the breathing process. Adults and older infants breathe from an end-expiratory lung volume determined by the opposing recoil of the lungs and chest wall. Neonates have a highly compliant chest wall that can cause several problems during breathing, among them a small end-expiratory lung volume, low oxygen stores, and high risk for airway occlusion and atelectasis. Infants compensate for this mechanical disadvantage by actively maintaining lung volume above the resting volume. Kosch and Stark [49] have shown that flow braking and an early onset of inspiration before the complete expiration provide a breathing strategy for the neonate that increases lung volume dynamically.

Using tidal breathing measurements, Schmalisch *et al*. [50] reported that about half of 99 neonates had an incomplete expiration due to a premature onset of inspiration. There was no statistically significant difference between healthy neonates and neonates with chronic lung diseases. An incomplete expiration shortens or even suppresses mainly phase III of the capnogram, and, thus, hampers capnographic measurements in this age group. In mechanically ventilated infants, the expiratory time can be adapted easily to the exhalation time of the patient so that an incomplete expiration can be avoided. In contrast, during spontaneous breathing, the investigator cannot influence the tidal breathing pattern, which must be considered in the interpretation of capnographic measurements.

Conclusion and outlook

Currently, the most important clinical application of capnography in neonates is to monitor mechanical ventilation. Several clinical studies have shown its value in confirming correct positioning of the endotracheal tube, in addition to the early detection of accidental tracheal extubation and disconnection of the breathing circuit. Thus, capnography is a valuable aid in preventing irreversible damage by prolonged hypoxia secondary to hypoventilation.

Compared with the more simple, time-based capnography, volumetric capnography measurements have a much higher informative potential, and enable the calculation of the different airway deadspaces. The technique requires accurate and artifact-free volume measurements. Volumetric capnography in spontaneously breathing neonates is more expensive and only possible with the help of a face mask. Due to the relatively high apparatus deadspace of a face mask, only short-term measurements can be performed.

Mainstream and flow-reduced sidestream capnographs are currently in clinical use. Mainstream capnographs are more accurate than sidestream capnographs, but in neonates with very small tidal volumes, the additional apparatus deadspace of the mainstream sensor can result in unacceptable rebreathing. Deadspace-free CO_2 measurements (e.g., for long-term studies in spontaneously breathing infants) are currently only possible using sidestream measurements.

Despite continuous technological progress, we still face technical limitations in correctly measuring the rapidly changing CO_2 signals of neonates for whom fast CO_2 sensors with an integrated pneumotach for volumetric capnography will be needed. Mainstream capnography, even in very small neonates, calls for the virtual elimination of the apparatus deadspace by a background flow similar to deadspace-free ventilatory measurements by the flow-though technique [9]. The gas exchange in small lungs may differ from adult lungs due to the greater impact of the small airways on gas exchange. Particularly for neonates or small animals in which phase II is prolonged and phase III shortened or absent, we need imaginative physiological concepts to help with the interpretation of such capnograms.

Finally, after improvements in the technical and methodological prerequisites for volumetric capnography, more clinical research is, nevertheless, necessary to demonstrate the clinical value and the diverse diagnostic possibilities of this new technique.

References

1. Karlberg P, Cook CD, O'Brien D, Cherry RB, Smith CA. Studies of respiratory physiology in newborn infants. II. Observations during and after respiratory distress. *Acta Paediatr* 1954; **43**(Suppl. 100): 387–411.
2. Cook CD, Cherry RB, O'Brien D, Karlberg P, Smith CA. Studies of respiratory physiology in the newborn infant: observations on normal and full-term infants. *J Clin Invest* 1955; **34**: 975–82.
3. Nelson NM, Prod'hom LS, Cherry RB, Lipsitz PJ, Smith CA. Pulmonary function in the newborn infant.

I. Methods: ventilation and gaseous metabolism. *Pediatrics* 1962; **30**: 963–74.

4. Arsowa S, Schmalisch G, Wauer RR. Techniques and clinical application of capnography in newborn infants and infants. *Padiatr Grenzgeb* 1993; **31**: 295–311.
5. Amuchou SS, Singhal N. Does end-tidal carbon dioxide measurement correlate with arterial carbon dioxide in extremely low birth weight infants in the first week of life? *Indian Pediatr* 2006; **43**: 20–5.
6. Hagerty JJ, Kleinman ME, Zurakowski D, Lyons AC, Krauss B. Accuracy of a new low-flow sidestream capnography technology in newborns: a pilot study. *J Perinatol* 2002; **22**: 219–25.
7. Lum L, Saville A, Venkataraman ST. Accuracy of physiologic deadspace measurement in intubated pediatric patients using a metabolic monitor: comparison with the Douglas bag method. *Crit Care Med* 1998; **26**: 760–4.
8. Thamrin C, Latzin P, Sauteur L, *et al.* Deadspace estimation from CO_2 versus molar mass measurements in infants. *Pediatr Pulmonol* 2007; **42**: 920–7.
9. Schmalisch G, Foitzik B, Wauer RR, Stocks J. Effect of apparatus deadspace on breathing parameters in newborns: "flow-through" versus conventional techniques. *Eur Respir J* 2001; **17**: 108–14.
10. Tingay DG, Stewart MJ, Morley CJ. Monitoring of end tidal carbon dioxide and transcutaneous carbon dioxide during neonatal transport. *Arch Dis Child Fetal Neonatal Ed* 2005; **90**: F523–6.
11. Thompson JE, Jaffe MB. Capnographic waveforms in the mechanically ventilated patient. *Respir Care* 2005; **50**: 100–8.
12. Wenzel U, Rudiger M, Wagner MH, Wauer RR. Utility of deadspace and capnometry measurements in determination of surfactant efficacy in surfactant-depleted lungs. *Crit Care Med* 1999; **27**: 946–52.
13. Wu CH, Chou HC, Hsieh WS, *et al*. Good estimation of arterial carbon dioxide by end-tidal carbon dioxide monitoring in the neonatal intensive care unit. *Pediatr Pulmonol* 2003; **35**: 292–5.
14. Napolitano LM. Capnography in critical care: accurate assessment of ARDS therapy? *Crit Care Med* 1999; **27**: 862–3.
15. Schmalisch G, Proquitte H, Roehr CC, Wauer RR. The effect of changing ventilator settings on indices of ventilation inhomogeneity in small ventilated lungs. *BMC Pulm Med* 2006; **6**: 1–20.
16. Chu J, Clements JA, Cotton EK, *et al*. Neonatal pulmonary ischemia. I. Clinical and physiological studies. *Pediatrics* 1967; **40**: 709–82.
17. Fletcher R, Jonson B, Cumming G, Brew J. The concept of deadspace with special reference to the single breath test for carbon dioxide. *Br J Anaesth* 1981; **53**: 77–88.
18. Wenzel U, Wauer RR, Schmalisch G. Comparison of different methods for deadspace measurements in ventilated newborns using CO_2-volume plot. *Intens Care Med* 1999; **25**: 705–13.
19. Ream RS, Schreiner MS, Neff JD, *et al*. Volumetric capnography in children: influence of growth on the alveolar plateau slope. *Anesthesiology* 1995; **82**: 64–73.
20. Riou Y, Leclerc F, Neve V, *et al*. Reproducibility of the respiratory deadspace measurements in mechanically ventilated children using the CO_2SMO monitor. *Intens Care Med* 2004; **30**: 1461–7.
21. Benumof JL. Interpretation of capnography. *AANA J* 1998; **66**: 169–76.
22. Domsky M, Wilson RF, Heins J. Intraoperative end-tidal carbon dioxide values and derived calculations correlated with outcome: prognosis and capnography. *Crit Care Med* 1995; **23**: 1497–503.
23. Salthe J, Kristiansen SM, Sollid S, Oglaend B, Soreide E. Capnography rapidly confirmed correct endotracheal tube placement during resuscitation of extremely low birthweight babies (< 1000 g). *Acta Anaesthesiol Scand* 2006; **50**: 1033–6.
24. Wyllie J, Carlo WA. The role of carbon dioxide detectors for confirmation of endotracheal tube position. *Clin Perinatol* 2006; **33**: 111–19.
25. Hsieh KS, Lee CL, Lin CC, *et al*. Quantitative analysis of end-tidal carbon dioxide during mechanical and spontaneous ventilation in infants and young children. *Pediatr Pulmonol* 2001; **32**: 453–8.
26. Bhavani-Shankar K, Moseley H, Kumar AY, Delph Y. Capnometry and anaesthesia. *Can J Anaesth* 1992; **39**: 617–32.
27. Schwardt JD, Gobran SR, Neufeld GR, Aukburg SJ, Scherer PW. Sensitivity of CO_2 washout to changes in acinar structure in a single-path model of lung airways. *Ann Biomed Eng* 1991; **19**: 679–97.
28. Davies MW, Woodgate PG. Tracheal gas insufflation for the prevention of morbidity and mortality in mechanically ventilated newborn infants. *Cochrane Database Syst Rev* 2002; **2**: CD002973.
29. Roberts WA, Maniscalco WM, Cohen AR, Litman RS, Chhibber A. The use of capnography for recognition of esophageal intubation in the neonatal intensive care unit. *Pediatr Pulmonol* 1995; **19**: 262–8.
30. Hubble CL, Gentile MA, Tripp DS, *et al.* Deadspace to tidal volume ratio predicts successful extubation in infants and children. *Crit Care Med* 2000; **28**: 2034–40.
31. Rozycki HJ, Sysyn GD, Marshall MK, Malloy R, Wiswell TE. Mainstream end-tidal carbon dioxide

monitoring in the neonatal intensive care unit. *Pediatrics* 1998; **101**: 648–53.

32. McDonald MJ, Montgomery VL, Cerrito P, *et al.* Comparison of end-tidal CO_2 and $PaCO_2$ in children receiving mechanical ventilation. *Pediatr Crit Care Med* 2002; **3**: 244–9.
33. Tobias JD, Meyer DJ. Noninvasive monitoring of carbon dioxide during respiratory failure in toddlers and infants: end-tidal versus transcutaneous carbon dioxide. *Anesth Analg* 1997; **85**: 55–8.
34. Thome UH, Carlo WA. Permissive hypercapnia. *Semin Neonatol* 2002; **7**: 409–19.
35. Sanders AB, Kern KB, Otto CW, Milander MM, Ewy GA. End-tidal carbon dioxide monitoring during cardiopulmonary resuscitation. A prognostic indicator for survival. *JAMA* 1989; **262**: 1347–51.
36. Berg RA, Henry C, Otto CW, *et al*. Initial end-tidal CO_2 is markedly elevated during cardiopulmonary resuscitation after asphyxial cardiac arrest. *Pediatr Emerg Care* 1996; **12**: 245–8.
37. Arnold JH, Bower LK, Thompson JE. Respiratory deadspace measurements in neonates with congenital diaphragmatic hernia. *Crit Care Med* 1995; **23**: 371–5.
38. Morris MG. A simple new technique to measure the effective deadspace of the face mask with a water volumeter in infants. *Eur Respir J* 1999; **14**: 1163–6.
39. Emralino F, Steele AM. Effects of technique and analytic conditions on tidal breathing flow volume loops in term neonates. *Pediatr Pulmonol* 1997; **24**: 86–92.
40. Morielli A, Desjardins D, Brouillette RT. Transcutaneous and end-tidal carbon dioxide pressures should be measured during pediatric polysomnography. *Am Rev Respir Dis* 1993; **148**: 1599–604.
41. Vos PJ, Folgering HT, van Herwaarden CL. Nocturnal end-tidal PCO_2 to detect apnoeas and hypopnoeas in sleep-disordered breathing. *Physiol Meas* 1993; **14**: 433–9.
42. Evans JM, Hogg MI, Rosen M. Correlation of alveolar PCO_2 estimated by infra-red analysis and arterial PCO_2 in the human neonate and the rabbit. *Br J Anaesth* 1977; **49**: 761–4.
43. Casati A, Gallioli G, Scandroglio M, *et al.* Accuracy of end-tidal carbon dioxide monitoring using the NBP-75 microstream capnometer: a study in intubated ventilated and spontaneously breathing nonintubated patients. *Eur J Anaesthesiol* 2000; **17**: 622–6.
44. Tang Y, Turner MJ, Baker AB. Effects of lung time constant, gas analyser delay and rise time on measurements of respiratory deadspace. *Physiol Meas* 2005; **26**: 1103–14.
45. Wong L, Hamilton R, Palayiwa E, Hahn C. A real-time algorithm to improve the response time of a clinical multigas analyser. *J Clin Monit Comput* 1998; **14**: 441–6.
46. Weiler N, Barnikol WK, Burkhard O. Simultane quasi kontinuierliche Bestimmung des Bronchialvolumens des Meerschweinchens mit Hilfe des O_2- und CO_2-Bronchialplateaus Atemzug für Atemzug. *Prax Klin Pneumol* 1987; **41**: 537–8.
47. Tirosh E, Bilker A, Bader D, Cohen A. Capnography in spontaneously breathing preterm and term infants. *Clin Physiol* 2001; **21**: 150–4.
48. Proquitté H, Krause S, Rüdiger M, Wauer RR, Schmalisch G. Current limitations of volumetric capnography in surfactant-depleted small lungs. *Pediatr Crit Care Med* 2004; **5**: 75–80.
49. Kosch PC, Stark AR. Dynamic maintenance of end-expiratory lung volume in full-term infants. *J Appl Physiol* 1984; **57**: 1126–33.
50. Schmalisch G, Foitzik B, Wauer RR, Patzak A. Influence of preterm onset of inspiration on tidal breathing parameters in infants with and without CLD. *Respir Physiol Neurobiol* 2003; **130**: 101–8.

Section 1
Chapter
11

Ventilation

Capnography in sleep medicine

P. Troy and G. Gilmartin

Sleep is a state clear and distinct from that of wakefulness. It is not the intent of this chapter to define fully the neurobiology of sleep/wake regulation, but to focus on the importance of the potential role of capnography during sleep, and provide a clear definition of the unique changes in ventilation that accompany the sleep state and its various components. Once this knowledge is achieved, the capacity to apply capnography to disorders that are uniquely or significantly characterized by alterations in the patient's ventilation during sleep will be realized. Before we advance to the clinical discussion, we must first consider the important technical aspects in the evaluation of ventilation during sleep.

Technical aspects

Polysomnography

The polysomnogram is the "gold standard" diagnostic approach for evaluating sleep and its related ventilatory abnormalities. The test originated during the 1950s, when the focus was on changes in electrocortical activity as a primary method of assessing sleep itself, with only a minor interest in monitoring breathing or ventilation during sleep. With the evolution of significant clinical interest in sleep-related breathing disorders, the use of polysomnography has been expanded to include more detailed assessment of breathing during sleep. Currently, the standard montage for conducting polysomnography includes bilateral electroencephalogram (EEG) monitoring of frontal, temporal, occipital regions, and chin electromyogram (EMG) tone to allow accurate staging of sleep, as well as airflow and respiratory effort. In a standard recording, airflow is assessed by thermistor measurements, typically at the oropharynx, and pressure measurements are taken at the nasopharynx. Thermistor (or thermocouple) measurements assess temperature changes due to either inspiratory (cool) or expiratory (warm) airflow. Thermistor measurements do retain a capacity to evaluate for the presence or absence of airflow but, given their purely qualitative nature, add little to the understanding of quantitative changes in airflow or ventilation. Nasal pressure recordings have become a standard part of polysomnographic recordings. By utilizing a nasal cannula connected to a pressure transducer, a respiratory waveform can be generated from the pressure fluctuations that accompany inspiration and expiration. Nasal pressure monitoring, therefore, has allowed the generation of a respiratory signal (pressure change) that is truly proportional to airflow [1]. Although proportional, the measurement is uncalibrated and not truly quantitative. This leaves the "gold standard" monitoring of breathing during sleep with significant limitations.

Ventilation during sleep: alternatives?

Pneumotachometers allow quantitative measurement of inspiratory and expiratory tidal volume, as well as respiratory rate. This allows true quantification of ventilation in a given subject. These devices have a disadvantage, however, in that measurement requires a leak-proof patient interface, amplification of the signal generated by the pneumotachometer via a dedicated device, and a quantified calibration of the signal before each individual recording. Due to the complexity of calibrating the quantified signal and the lack of a practical method for establishing a leak-proof interface with the sleeping patient during the entire period of sleep, this method has not proven to be practical in the clinical setting.

Measurement of arterial PCO_2 provides a quantified assessment of ventilation. In the setting of stable CO_2 production, which is reasonable to expect during a single night of sleep in the absence of a dynamic metabolic state or active illness, changes in arterial PCO_2

Capnography, Second Edition, ed. J. S. Gravenstein, Michael B. Jaffe, Nikolaus Gravenstein, and David A. Paulus. Published by Cambridge University Press. © Cambridge University Press 2011.

reflect changes in effective ventilation. Continuous measurements of arterial PCO_2 are simply not practical, and even frequent arterial PCO_2 measurements would require placement of an indwelling catheter, which is by no means a standard of care for outpatient testing. Transcutaneous CO_2 measurements can be obtained, but have a significant lag time relative to actual changes in ventilation and thus provide very limited data on a breath-to-breath basis. Single arterial PCO_2 measurements can be acquired via arterial puncture; however, single measurements are limited in providing a dynamic picture of the patient's ventilatory changes across a given night of sleep.

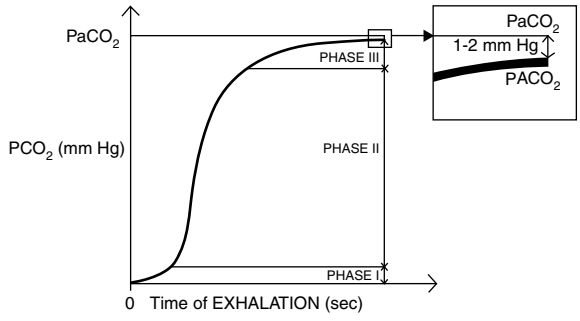

Figure 11.1 Partial pressure of carbon dioxide (PCO_2). Capnography from the expiratory phase of a single breath. Phase I represents anatomic deadspace; phase II represents rapid emptying of alveolar spaces characterized by rapid rise in CO_2; and during phase III, a plateau is ideally achieved, representing true end-tidal CO_2. [From: Soubani AO. Noninvasive monitoring of oxygen and carbon dioxide. *Am J Emerg Med* 2001; **19**: 141–6.]

The argument for capnography during sleep

Capnometry is the measurement of CO_2 concentration in a gas mixture denoted by a continuous waveform display. There are several methods by which concentration can be determined (see Chapter 37: Carbon dioxide measurement). Infrared spectrometry is most commonly used.

Gas can be analyzed with a mainstream or sidestream device. The mainstream approach requires placement of the analyzer within a leak-free ventilatory circuit that can capture all of the exhaled gas to allow truly precise measurements. Similar to the issues raised for pneumotachometry, mainstream sampling has significant technical limitations in the sleeping and spontaneously breathing patient. Sidestream analyzers aspirate a continuous flow of gas through small-bore tubing, and pull this stream of gas into a chamber that is independent of the location at which the sample is obtained. This method can be easily integrated into the polysomnogram by using a split nasal cannula system, allowing one port for nasal pressure recording and another port for sidestream sampling of end-tidal CO_2 levels ($PETCO_2$).

Sidestream measurement of $PETCO_2$ therefore allows quantitative measurement on a breath-to-breath basis of effective ventilation in the sleeping patient. This potentially adds significant information to that obtained with polysomnography. Before moving to a discussion of potential clinical applications, we must first consider the specific aspects of interpreting the signal obtained.

Capnography interpretation

Simply put, without adequate signal quality, capnography during sleep provides only confusing and ultimately largely meaningless information. With appropriate training and education provided to sleep technicians, however, capnography during sleep can substantially – and at times critically – expand our understanding of an individual patient's ventilatory changes during sleep under both healthy and disease conditions. With proper placement of the nasal cannula sidestream sensor, an adequate signal can be achieved that can be confirmed by an appropriate display of the waveform. This waveform must include all three phases of the normal capnograph, with phase I representing anatomic deadspace, phase II representing emptying of alveolar gas with increasing concentrations of CO_2, and phase III (the plateau phase of the curve) representing the alveolar plateau. It is the furthest end point of this alveolar plateau, just prior to inspiration, that represents a true $PETCO_2$. This value, which traces approximately 1–2 mm Hg below arterial CO_2, must be obtained with a true plateau. It is this value and curve integrity that should be tracked to allow adequate monitoring and clinical conclusions to be made (Figure 11.1) [2].

With this understanding, we turn to a definition of the normal changes in ventilation during sleep, as well as relevant clinical disorders, for which capnography during sleep adds significantly to their clinical evaluation and treatment.

Ventilation during sleep

Sleep serves multiple functions in humans, including biochemical (anabolic hormone secretion, protein synthesis, energy conservation), physiologic (restorative function), and neurological (brain development

and consolidation of new learning). The sleep state is divided into two phases: non-rapid eye movement (NREM) and rapid eye movement (REM); NREM is further separated into three stages that occur in progression, and are associated with progressively deeper sleep states. Normal sleep architecture reveals a cyclical pattern, with early sleep consisting of NREM sleep and the late sleep period associated with increased periods of REM sleep. The process of ventilation during sleep is fundamentally altered compared to the awake state. Sleep modifies the chemical (pH, PaO_2, and $PaCO_2$) and mechanical processes (lung volume and upper airway muscle tone), modulating ventilation in addition to removing the conscious control of ventilation. Furthermore, sleep is associated with a decrease in ventilation that becomes more pronounced during the progression of NREM to REM [3].

NREM is characterized by a normal respiratory pattern, with a decrease in ventilation stemming primarily from reduced minute volume. These events are followed by a corresponding increase in $PaCO_2$ by 2–3 mm Hg and an increase in the threshold for responding to this rise in CO_2 that is progressive through the stages of NREM sleep. Corresponding with the decrease in ventilation is diminished chest wall muscle and diaphragm activity. Upper airway resistance is increased during these conditions compared to the awake state [4].

Upon reaching REM sleep, a further decrease in ventilation is marked by an irregular respiratory rate, along with an additional decrease in minute ventilation and additional increase in $PaCO_2$ of 1–2 mm Hg compared to NREM sleep. Although metabolic activity is reduced, which, in theory, should decrease $PaCO_2$, the decline in alveolar ventilation is greater than the reduction in metabolic activity. This leads to the net increase in end-tidal CO_2 that is observed. In addition, there is further blunting of the ventilatory response to hypercapnia compared to what is observed in NREM sleep. During REM sleep, near-complete skeletal muscle atonia ensues, with the exception of the diaphragm, the movement of which is required almost exclusively for ventilation during this phase. Additionally, muscle activity is retained in the muscles controlling eye movement and the muscles of the middle ear. The atonia extends to the muscles of the upper airways as well, leading to a further increase in airway resistance [4].

In summary, the sleep state is characterized by a progressive decrease in minute volume, with a rise in $PaCO_2$, and a blunted capacity to respond to this increase.

Clinical applications

Obstructive sleep apnea and capnography

Sleep-disordered breathing occurs in approximately 2% of children and at least 4% of adults, with an increased prevalence in men over women [5]. Obstructive sleep apnea (OSA) is characterized by repetitive closure of the upper airway during sleep, leading to arousal out of sleep and repetitive desaturation during and following these respiratory events. This is a disease that is not characterized simply by its presence or absence, but, rather, by its development along a spectrum of severity. *Primary snoring* (loud nightly snoring) has a reported prevalence of approximately 20% and was initially considered to be benign. More recently, upper airways resistance syndrome (UARS) has been described in which persistent partial upper airway obstruction occurs without the traditional criteria for OSA (apnea or hypoxemia during sleep), and contributes to both sleep disruption and daytime symptoms [6]. It is, therefore, likely that snoring, UARS, and OSA exist in children and adults along a clinical spectrum of sleep-disordered breathing.

Capnography can add significant information to the definition of frank obstructive events, as the end-tidal CO_2 signal is completely lost during obstructive events and returns with recovery of upper airway patency (Figure 11.2). Changes in $PETCO_2$ secondary to partial airway obstruction, and elevations in $PETCO_2$ in the setting of obstructive hypoventilation or persistent alterations in upper airway resistance, can also be defined through capnography. In addition to providing an important supplemental tool in the clinical setting, capnography is widely applied in the research setting as a means to assess the ventilatory control mechanisms in patients with sleep apnea and understand the effects of continuous positive airway pressure (CPAP) therapy on ventilatory control in OSA [7]. Finally, capnography has practical applications as a diagnostic tool in patients with stroke and other related disorders who may be at increased risk for OSA, but who would likely tolerate polysomnography poorly [8].

Patients undergoing evaluation within the sleep laboratory environment may benefit from the specific application of capnography. It should also be considered in patient populations with more subtle forms of upper airway resistance, including obstructive hypoventilation and UARS, and patients with altered ventilatory responsiveness or conditions for which in-laboratory polysomnography may not be practical.

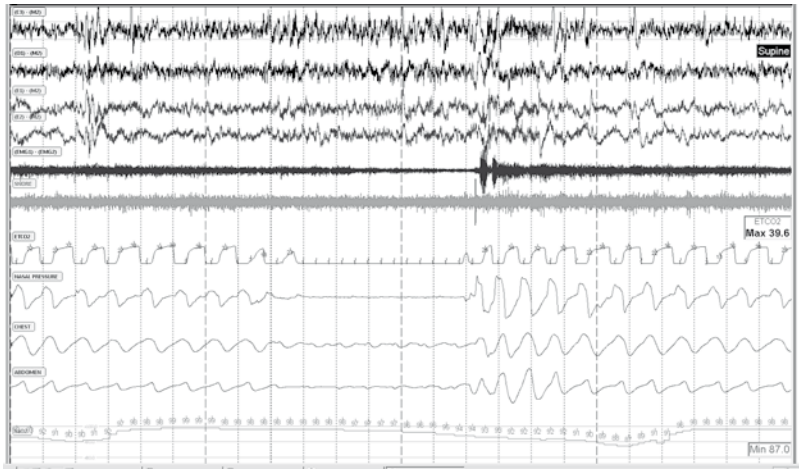

Figure 11.2 Polysomnographic recording from an individual patient with obstructive sleep apnea. With upper airway closure, complete loss of capnograph is demonstrated, with return only upon airway opening and resumption of ventilation following arousal. Actual end-tidal CO_2 is displayed in the box at the right of the screen display. SaO_2, oxygen saturation; Abdomen, abdominal belt to assess abdominal wall movement; Chest, thoracic belt to assess chest wall movement; Nasal pressure, airflow sensor; $P_{ET}CO_2$, end-tidal volume CO_2 monitor; snore, detects snore activity; EMG, electromyogram; E1/E2/C3/O1, electroencephalogram leads.

Obesity hypoventilation syndrome and capnography

The obesity hypoventilation syndrome (OHV) is defined as obesity (BMI > 30 kg/m^2) accompanied by daytime hypercarbia ($PaCO_2$ > 45 mm Hg) in the absence of cardiopulmonary, neuromuscular, or chest wall pathology that can independently impair ventilation. Patients with OHV demonstrate decreased lung compliance and increased resistance that is exacerbated by the recumbent position [9], and leads to increased work of breathing and oxygen consumption ($\dot{V}O_2$) [10]. Given that CO_2 production ($\dot{V}CO_2$) is directly proportional to $\dot{V}O_2$, patients with OHV have a propensity for a higher baseline CO_2, a condition exacerbated by an impaired ventilatory response to hypercapnia compared to normal controls and obese patients without OHV [11]. In addition, most patients with OHV have OSA associated with periods of reduced (hypopnea) or absent (apnea) ventilation during sleep, with resultant CO_2 loading. The fragmented sleep pattern consequently culminates in sleep deprivation, which can further blunt the response to hypercapnia [12]. In OHV, CO_2 loading during periods of apnea, in combination with a blunted capacity to respond to hypercapnia and impaired baseline ventilatory function, leads to a state of chronic hypercapnia. Hypercapnia is further maintained through renal compensatory mechanisms, including bicarbonate retention. The net result of this pathophysiologic process is chronic hypercapnia sustained during wakefulness.

Differentiating OHV from conventional OSA, either as a separate disorder or an additional insult, has significant clinical importance. Capnography can be used to aid in this decision-making. Hypoventilation, regardless of cause, can easily be identified by using capnography during polysomnography. In this setting, upper airway patency (nasal pressure and thermistor measurements) and respiratory effort appear preserved; however, due to ineffective alveolar ventilation, end-tidal CO_2 remains remarkably elevated (Figure 11.3). Finally, capnography during titration of therapeutic interventions, such as bi-level support during sleep to facilitate ventilation, may allow real-time indication of achieving a clinical end point, such as improvement in $P_{ET}CO_2$ to a desired target. Recently, $P_{ET}CO_2$ has been used in this capacity, in patients with OHV, to assess the efficacy of volume-targeted, bi-level positive pressure ventilation in controlling nocturnal hypoventilation [13–15].

Neuromuscular and chest wall disorders and capnography

Respiratory muscle failure is inevitable in many neuromuscular and chest wall disorders. The resulting hypoventilation, as respiratory muscle failure progresses, occurs first during sleep, and particularly during REM sleep. There are established clinical guidelines for management based upon evaluations performed during the wake cycle in this patient population with documented clinical benefit to quality of life and, in many cases, also to duration of life [16]. However, waiting until ventilatory failure actually manifests during the wake cycle may simply be "waiting too long," thus allowing important opportunities for clinical intervention to pass during the early stages of these diseases.

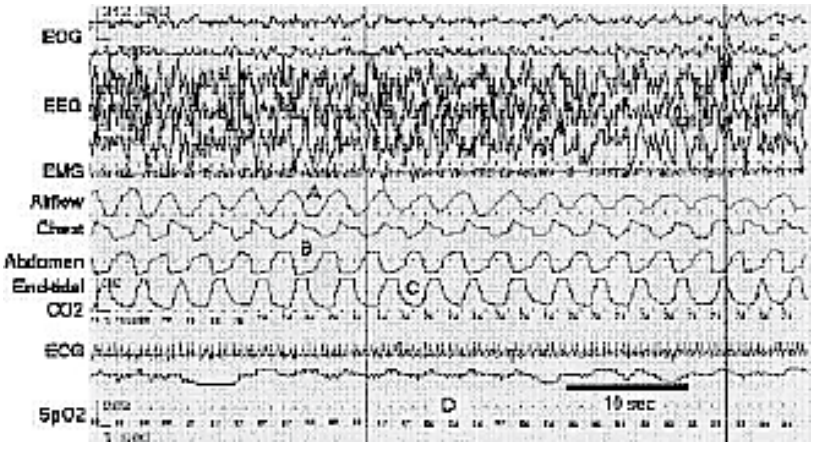

Figure 11.3 Polysomnographic recording from an individual patient with hypoventilation. End-tidal CO_2 remains remarkably elevated in the setting of otherwise apparently preserved measures of upper airway patency and respiratory effort. Decreased oxygen saturations are also noted secondary to severe hypoventilation. SpO_2, oxygen saturation; ECG, electrocardiogram tracing; Abdomen, abdominal belt to assess abdominal wall movement; Chest, thoracic belt to assess chest wall movement; Nasal pressure, airflow sensor; $ETCO_2$, end-tidal volume CO_2 monitor; EMG, electromyogram; EEG, electroencephalogram; EOG, electro-oculogram detecting eye muscle activity. [From: Carroll JL. Obstructive sleep disordered breathing in children: new controversies, new directions. *Clin Chest Med* 2003; **24**: 261–82.]

Careful use of capnography in the clinical arena during sleep will allow the assessment of patients with neuromuscular and chest wall disorders for significant hypercapnia relatively early in the course of the disease. This concern has been most clearly addressed by Ward *et al.* [17] in a population of patients with significant disease but daytime normocapnia; 48 patients with congenital neuromuscular disease and chest wall disorders were studied with overnight polysomnography and transcutaneous CO_2 monitoring. Patients with nocturnal hypoventilation and daytime normocapnia were randomized to either non-invasive ventilation or control conditions. Patients who were treated with non-invasive ventilation for isolated nocturnal hypoventilation had a significant improvement in arterial PCO_2, SaO_2, and quality of life measures when compared with the control group [17].

Given the potential for significant clinical benefits from early intervention, patients with substantial neuromuscular and chest wall disease should certainly be considered for capnography assessment during sleep as part of their clinical management.

Conclusions

Polysomnography remains the most comprehensive approach for evaluation of changes in breathing during sleep in clinical practice. It is extensive in its monitoring capacity, but retains significant limitations in its capability to evaluate changes in ventilation and breathing outside of frank OSA for which it was designed. Capnography is not a standard component of clinical sleep monitoring, but can be used to supplement the clinical assessment. Comprehensive incorporation of capnography into clinical practice has great potential for enhancing the sleep evaluation in many patients. Future directions for practice may include formulating clinical guidelines for use, improving the automated analysis of the recording, and developing caregiver education in potential clinical applications.

References

1. Ayappa I, Norman RG, Krieger AC, *et al.* Non-invasive detection of respiratory event related arousals (reras) by a nasal cannula/pressure transducer system. *Sleep* 2000; **23:** 763–71.
2. Soubani AO. Non-invasive monitoring of oxygen and carbon dioxide. *Am J Emerg Med* 2001; **19:** 141–6.
3. Bulow K. Respiration and wakefulness in man. *Acta Physiol Scand Suppl* 1963; **59**: 1–110.
4. Shneerson J. *Sleep Medicine,* 2nd edn. Malden, MA: Blackwell, 2005.
5. Young T, Peppard PE, Gottlieb DJ. Epidemiology of obstructive sleep apnea: a population health perspective. *Am J Respir Crit Care Med* 2002; **165:** 1217–39.
6. American Academy of Sleep Medicine Task Force. Sleep-related breathing disorders in adults: recommendations for syndrome definition and measurement techniques in clinical research. *Sleep* 1999; **22:** 667–89.
7. Spicuzza L, Bernardi L, Balsamo R, *et al.* Effect of treatment with nasal continuous positive airway pressure on ventilatory response to hypoxia and

hypercapnia in patients with sleep apnea syndrome. *Chest* 2006; **130:** 774–9.

8. Dziewas R, Hopmann B, Humpert M, et al. Capnography screening for sleep apnea in patients with acute stroke. Neurol Res 2005; 27: 83–7.
9. Naimark A, Cherniack RM. Compliance of the respiratory system and its components in health and obesity. J Appl Physiol 1960; 15: 377–82.
10. Kress JP, Pohlman AS, Alverdy J, Hall JB. The impact of morbid obesity on oxygen cost of breathing at rest. Am J Respir Crit Care Med 1999; 160: 883–6.
11. Burki NK, Baker RW. Ventilatory regulation in eucapnic morbid obesity. *Am Rev Respir Dis* 1984; **129:** 538–43.
12. Cooper KR, Phillips BA. Effect of short-term sleep loss on breathing. *J Appl Physiol* 1982; **53:** 855–8.
13. Janssens JP, Metzger M, Sforza E. Impact of volume targeting on efficacy of bi-level non-invasive ventilation and sleep in obesity-hypoventilation. *Respir Med* 2009; **103**: 165–72.
14. Storre JH, Seuthe B, Fiechter R. Average volume-assured pressure support in obesity hypoventilation: a randomized cross-over trial. *Chest* 2006; **130:** 815–21.
15. Carroll JL. Obstructive sleep disordered breathing in children: new controversies, new directions. *Clin Chest Med* 2003; **24:** 261–82.
16. Bourke SC, Bullock RE, Williams TL, Shaw PJ, Gibson GJ. Noninvasive ventilation in ALS: indications and effect on quality of life. *Neurology* 2003; **61:** 171–7.
17. Ward S, Chatwin M, Heather S, Simonds AK. Randomized controlled trial of non-invasive ventilation (NIV) for nocturnal hypoventilation in neuromuscular and chest wall disease patients with daytime normocapnia. *Thorax* 2005; **60:** 1019–24.

Section 1
Chapter
12

Ventilation

Conscious sedation

E. A. Bowe and E. F. Klein, Jr.

Introduction

Although ubiquitous during general anesthesia, capnography has not been utilized to a similar degree during sedation for interventional procedures, regional anesthesia, etc. Despite the fact that no regulatory agency or professional society currently mandates capnography during sedation, documented efficacy, improved sampling techniques, and decreased implementation costs have combined to increase the utilization of this modality in patients undergoing sedation.

Procedural sedation

Apparently based on reports of increased morbidity and mortality in children receiving sedation outside the classic operating room setting [1,2], the *Guidelines for the Elective Use of Conscious Sedation, Deep Sedation, and General Anesthesia in Pediatric Patients*, drafted by the Committee on Drugs of the American Academy of Pediatrics (AAP), were adopted by the AAP and the American Academy of Pediatric Dentistry in 1985 [3]. The term *conscious sedation* was a source of confusion almost since its introduction by the American Dental Association [4]. The first widely accepted definitions were those proposed by the AAP Committee on Drugs (Table 12.1).

The initial intent of the AAP Committee on Drugs was to have the term *conscious sedation* define a state of minimal sedation in which the patient responds appropriately to verbal commands and would cry "Ouch" in response to a painful stimulus [5]. Because the AAP definitions have been misinterpreted to imply that "conscious sedation" is present when the patient manifests only a reflex withdrawal to pain, the AAP recommended adoption of the terminology proposed by the American Society of Anesthesiologists (ASA) (Table 12.2) [6]. The ASA definitions are also currently used by the Joint Commission (formerly the Joint Commission on Accreditation of Healthcare Organizations) [7].

Sedation guidelines

In October 2002, the American Dental Association adopted the *Guidelines for the Use of Conscious Sedation, Deep Sedation and General Anesthesia for Dentists* [8]. These guidelines recommend monitoring of $ETCO_2$ or auscultation of breath sounds for all patients undergoing any form of parenteral sedation. In 2007, this guideline was changed to recommend capnography as an alternative for monitoring ventilation only in conjunction with either "moderate sedation" or "deep sedation or general anesthesia." The American Academy of Pediatric Dentistry *Guidelines on the Elective Use of Conscious Sedation, Deep Sedation and General Anesthesia in Pediatric Dental Patients* (reviewed/revised in May, 1998) [9] include the statement: "There shall be continual monitoring of … expired carbon dioxide concentration via capnography…" and describes a capnograph as "required" for children undergoing "Deep sedation." (*Deep sedation* is defined as a "deeply depressed level of consciousness" and the patient is described as responding only to intense stimulus.)

The 2006 revision of the AAP *Guidelines for Monitoring and Management of Pediatric Patients During and After Sedation for Diagnostic and Therapeutic Procedures* states that capnometry is "valuable" in detecting airway obstruction and apnea, and encourages its use in all children undergoing sedation [10].

The American College of Emergency Physicians *Clinical Policy for Procedural Sedation and Analgesia in the Emergency Department* does not recognize any evidence-based standards regarding capnometry during sedation, and makes no specific recommendations regarding capnometry for any level of sedation, but does state that "There is an excellent correlation

Capnography, Second Edition, ed. J. S. Gravenstein, Michael B. Jaffe, Nikolaus Gravenstein, and David A. Paulus. Published by Cambridge University Press. © Cambridge University Press 2011.

Table 12.1 American Academy of Pediatrics definitions of sedation

Conscious sedation A medically controlled state of depressed consciousness that (1) allows protective airway reflexes to be maintained; (2) retains the patient's ability to maintain a patent airway independently and continuously; and (3) permits appropriate response by the patient to physical stimulation or verbal command, e.g., "Open your eyes."
Deep sedation A medically controlled state of depressed consciousness or unconsciousness from which the patient is not easily aroused. It may be accompanied by partial or complete loss of protective reflexes including the ability to maintain a patent airway independently and respond purposefully to physical stimulation or verbal command.

Source: American Academy of Pediatrics [3].

Table 12.2 Continuum of depth of sedation: definition of general anesthesia and levels of sedation/analgesia

	Minimal sedation anxiolysis	Moderate sedation/analgesia ("conscious sedation")	Deep sedation/ (analgesia)	General anesthesia
Definition	A drug-induced state during which patients respond normally to verbal commands. Although cognitive function and coordination may be impaired, ventilatory and cardiovascular functions are unaffected.	A drug-induced depression of consciousness during which patients respond purposefully[a] to verbal commands, either alone or accompanied by light tactile stimulation. No interventions are required to maintain a patent airway, and spontaneous ventilation is adequate. Cardiovascular function is usually maintained. "Monitored anesthesia care" does not describe the continuum of depth of sedation, rather it describes "a specific anesthesia service in which an anesthesiologist has been requested to participate in the care of a patient undergoing a diagnostic or therapeutic procedure."	A drug-induced depression of consciousness during which patients cannot be easily aroused but respond purposefully[a] following repeated or painful stimulation. The ability to independently maintain ventilatory function may be impaired. Patients may require assistance in maintaining a patent airway, and spontaneous ventilation may be inadequate. Cardiovascular function is usually maintained.	A drug-induced loss of consciousness during which patients are not arousable, even by painful stimulation. The ability to independently maintain ventilatory function is often impaired. Patients often require assistance in maintaining a patent airway, and positive pressure ventilation may be required because of depressed spontaneous ventilation or drug-induced depression of neuromuscular function. Cardiovascular function may be impaired.
Responsiveness	Normal response to verbal stimulation	Purposeful response[a] to verbal or tactile stimulation	Purposeful response[a] following repeated or painful stimulation	Unarousable even with painful stimulus
Airway	Unaffected	No intervention required	Intervention may be required	Intervention often required
Spontaneous ventilation	Unaffected	Adequate	May be inadequate	Frequently inadequate
Cardiovascular function	Unaffected	Usually maintained	Usually maintained	May be impaired

Note: Because sedation is a continuum, it is not always possible to predict how an individual patient will respond. Hence, practitioners intending to produce a given level of sedation should be able to rescue[b] patients whose level of sedation becomes deeper than initially intended. Individuals administering "Moderate sedation/analgesia ('conscious sedation')" should be able to rescue[b] patients who enter a state of "Deep sedation/analgesia," while those administering "Deep sedation/analgesia" should be able to rescue[b] patients who enter a state of "General anesthesia."

[a] Reflex withdrawal from a painful stimulus is *not* considered a purposeful response.

[b] Rescue of a patient from a deeper level of sedation than intended is an intervention by a practitioner proficient in airway management and advanced life support. The qualified practitioner corrects adverse physiologic consequences of the deeper-than-intended level of sedation (such as hypoventilation, hypoxia, and hypotension) and returns the patient to the originally intended level of sedation.

Source: From: American Society of Anesthesiologists. *Continuum of Depth of Sedation: Definition of General Anesthesia and Levels of Sedation/ Analgesia*. Approved by the ASA House of Delegates on October 13, 1999, and amended on October 27, 2004. Available online at http://www.asahq.org/publicationsAndServices/standards/20.pdf.

between $PaCO_2$ and $PETCO_2$ even when the $PETCO_2$ is measured through a nasal cannula while the patient is receiving oxygen," and notes that "capnometry may be helpful when managing cases where the patient's [*sic*] ventilatory efforts cannot be visualized," but states that there is no evidence to substantiate an advantage for its use [11]. The guidelines proposed by the Canadian Association of Emergency Physicians, *Procedural Sedation and Analgesia in the Emergency Department*, make no mention of capnography, recommending only that, "the adequacy of spontaneous ventilations" should be assessed during the procedure, and noting that supplemental oxygen administration "may increase oxygen saturation in the face of hypoventilation, and that undetected CO_2 retention may occur" [12].

The ASA *Standards for Basic Anesthetic Monitoring* state that, for patients receiving regional anesthesia or monitored anesthesia care, "the adequacy of ventilation shall be evaluated by continual observation of qualitative clinical signs and/or monitoring for the presence of exhaled carbon dioxide." [13].

Historical statistics

Although there is a paucity of data, the impression is that the use of sedation for diagnostic or therapeutic procedures, now most commonly termed *procedural sedation*, has dramatically increased in frequency [14, 15]. Clearly, most patients would choose to be analgesic and/or amnestic for painful procedures. In many settings, this sedation is provided by individuals with minimal training in sedation techniques, often working under the direction of a physician who is engrossed in performing the procedure.

In some states, significant adverse patient events during anesthesia must be reported to a regulatory agency; similarly, most hospitals carefully track the number of anesthetics provided in an operating room environment. Comparable reporting of either complications or frequency of sedation, commonly performed in an office setting, is generally lacking. In fact, in the United States, office-based surgery facilities may be credentialed by three different regulatory agencies (Joint Commission, Accreditation Association for Ambulatory Health Care, or American Association for Accreditation of Ambulatory Surgery Facilities) [15], and many states have minimal or no regulations regarding office-based surgery [16]. Even in most hospital settings, tracking the number of patients who receive some form of sedation for a diagnostic or therapeutic procedure is less rigorous and reliable than tracking the number of patients who receive an anesthetic in an operating room.

Differing terminology, voluntary (incomplete) reporting of complications, inability to quantitate the number of procedures performed, and failure to determine preexisting patient status combine to preclude an accurate determination of morbidity and mortality statistics relating to sedation. A 1992 attempt to review morbidity and mortality data for dental patients undergoing sedation or general anesthesia determined that only nine states maintained data regarding these occurrences [17]. Excluding cases of local anesthetic toxicity, death occurred in 81% of 43 incidents. State boards had ruled that misconduct by the practitioner occurred in over 66% of cases with catastrophic outcomes (death, hypoxic brain injury). Inadequate monitoring and inexperienced resuscitators were deemed to have contributed to the adverse outcomes. Anesthetic-related morbidity during dental office procedures was reviewed in a closed-claim analysis [18]. Again, in the absence of data regarding the total number of anesthetics administered, the incidence cannot be determined. Ventilatory depression or airway obstruction leading to hypoxia was primarily responsible for the majority of catastrophic complications. In over 75% of cases, the outcome was described as "avoidable," with "timely monitoring and effective response to adverse occurrences."

Under-reporting of complications was recognized by the authors of two retrospective studies involving patients receiving sedation for endoscopy [19,20]. A non-randomized retrospective analysis of data on 19 363 procedures performed in conjunction with the administration of midazolam or diazepam noted "serious cardiac or respiratory complications" occurring in 5.4 per 1000 procedures [21]. The fact that the reported incidence of complications varied by a factor of 15 between institutions is strong evidence for a reporting bias, and suggests that the true incidence is probably substantially higher than reported. A retrospective study from England reviewing 11 998 gastroscopies noted that approximately 4% of patients required the administration of an antagonist to reverse ventilatory depression and that cardiorespiratory distress occurred in approximately 2.5 per 1000 patients [22]. Twice as many deaths were attributed to complications of sedation than to the procedures themselves, although the authors did comment that because these numbers rely on voluntary reporting,

they "are probably an underestimate." The American Society of Gastrointestinal Endoscopy developed a Clinical Outcomes Research Initiative (CORI) to assess the outcomes of endoscopic procedures. This group developed a database that relied on voluntary reporting of outcomes and few specific definitions. In 5 years (1997–2002), the CORI database included data on 247 889 of 324 737 procedures performed under conscious sedation. They reported 28 deaths due to cardiopulmonary problems (8/100 000) but did not specify which of those deaths were attributable to sedation; however, it was noted that the use of supplemental oxygen was associated with a greater incidence of cardiopulmonary problems [23]. (In the absence of protocols for oxygen administration, it is possible that patients perceived to be at higher risk for cardiorespiratory complications were more likely to receive supplemental oxygen.) In a prospective study involving endoscopic procedures on patients with comorbid diseases, even when the endoscopists had access to measurements of transcutaneous CO_2 ($PtcCO_2$), 4 of 101 patients developed hypercarbia ($PtcCO_2$ > 70 mm Hg) [24]. The authors state that access to values for $PtcCO_2$ likely resulted in greater than usual restraint in the administration of sedatives. A prospective study of 74 patients undergoing sedation for procedures in the emergency department documented ventilatory depression ($etCO_2$ > 50 mm Hg, absent capnograph waveform, or $etCO_2$ increased by more than 10 mm Hg over baseline) in 45% of patients and a need for assisted ventilation in 15% [25].

Children constitute a large percentage of patients who are sedated for procedures. A quality assurance form with voluntary reporting of complications was used to review retrospectively 1140 sedation outcomes in hospitalized children [26]. Sixty-three (5.5%) of children developed hypoxemia: most of these episodes were attributable to respiratory depression, seven (0.6%) occurred as a consequence of upper airway obstruction, and two (0.2%) as a result of apnea. A prospective study of 20 children receiving ketamine for sedation in the emergency department reported maximum $etCO_2$ values during sedation of 47 mm Hg (no attempt was made to correlate $etCO_2$ with $PaCO_2$), and noted that one patient (5%) developed upper airway obstruction and required intervention [27]. Also in the emergency department setting, another study of 106 children receiving sedation for painful procedures demonstrated increases in $etCO_2$ by as much as 22 mm Hg [28]. Perhaps most importantly, this study noted that the highest $etCO_2$ values "invariably occurred after the completion of the procedure," – a time during which most patients in other studies did not have $etCO_2$ monitoring. A study of 21 pediatric oncology patients undergoing sedation for procedures reported that five patients (23.8%) experienced sedation failure (unable to perform the procedure) and three patients (14.3%) experienced significant cardiorespiratory problems (one became apneic; one required two doses of naloxone for ventilatory depression; and one [4.7%] became hypoxic and bradycardic, with a subsequent requirement for supplemental oxygen and physical stimulation for over three hours following the procedure) [29]. A similar study of 50 children receiving sedation for painful procedures documented increases in $etCO_2$ to 53 mm Hg and one episode (2%) of airway obstruction [30].

From these studies, it is apparent that ventilatory depression is a common problem during sedation [13,31,32]. In many instances, this constitutes a greater risk to the patient than the actual procedure being performed [22,33]. Additionally, most studies involving capnography during sedation report that airway obstruction and apnea were detected first (or solely) as a result of that monitoring modality. Accordingly, it seems imperative that these complications be minimized and that any effort that reduces sedation-associated complications will ultimately produce a marked increase in patient safety. Capnography is a relatively inexpensive, non-invasive monitor with documented efficacy in detecting hypercarbia, airway obstruction, and apnea during sedation.

Capnometry sampling devices

Almost as soon as capnography became widely utilized for patients undergoing general anesthesia in an operating room setting, clinicians began seeking a way to monitor exhaled CO_2 in unintubated, spontaneously ventilating patients. While possible with a tight-fitting face mask or laryngeal mask airway, the objective was to have a non-invasive system that could be used on patients receiving supplemental oxygen during sedation. Sampling exhaled gases from spontaneously breathing, unintubated patients presents additional problems not encountered when samples are taken from a "closed" system (e.g., cuffed endotracheal tube). Factors that have been postulated to influence the accuracy of the sample are presented in Table 12.3.

Suggestions included placing an intravenous catheter [34] or capnometry sampling tubing [35] under

Table 12.3 Factors postulated to decrease precision of $ETCO_2$ monitoring using modified nasal cannulae

Patient secretions
Partial airway obstruction
Small tidal volumes
Tachypnea
Large volume of sampling line
Large diameter of nasal prong tips
High sampling flow rate
Dilution of sample by supplemental oxygen administration
Mouth breathing

an oxygen mask, or partially obstructing one of the prongs on a standard nasal cannula with a capnometer sampling tube [36,37], intravenous catheter [38,39], or blunt metal needle [40]. Although these adaptations provide the ability to determine the presence of CO_2 in the sampled gas, the resulting values were deemed "less reliable" than those obtained in intubated patients [41,42].

A variety of sampling systems were proposed which involved the use of a nasal airway. Authors reported using coaxial systems involving the insertion of capnometer sampling tubing [43], a pediatric feeding tube [44], suction catheters [45,46], or other tubing [47] into a nasal airway. Although one study evaluating the accuracy of samples obtained with one of these devices noted that the $PaCO_2$–$PETCO_2$ increased over time in the postoperative period [46], others documented a narrow $PaCO_2$–$PETCO_2$ difference (2.8 ± 2.6 mm Hg in one study [45], 3.6 ± 6.8 mm Hg in another [44]) with these devices. Whatever the efficacy of these sampling techniques, the need to place a nasal airway into an awake or lightly sedated patient will often be unacceptable to the patient, and no recent literature has reported using modifications of a nasal airway to sample exhaled gases in spontaneously breathing, unintubated patients.

A relatively unique suggestion has been to apply two sets of nasal cannulas simultaneously – one for oxygen administration and the other for sampling exhaled gases [48].

Modified nasal cannula

The first sampling system with documented ability to obtain samples, while permitting the quantitative determination of $ETCO_2$ in spontaneously breathing, unintubated patients receiving supplemental oxygen, relied on the complete isolation of one prong of a standard set of nasal cannula, thereby insufflating oxygen into one nostril while sampling exhaled gas from the other nostril [49]. The $PaCO_2$–$PETCO_2$ difference was similar during spontaneous ventilation with supplemental oxygen in the preoperative period (2.1 ± 2.1 mm Hg) to that achieved during general endotracheal anesthesia with positive pressure ventilation (3.1 ± 2.8 mm Hg). The efficacy of this basic design has been repeatedly documented in studies demonstrating a $PaCO_2$–$PETCO_2$ difference generally comparable to that obtained in intubated patients (Table 12.4). Variations of a modified nasal cannula are now used extensively to obtain samples of exhaled CO_2 in patients undergoing sedation.

One study compared $PtcCO_2$ measurements with those obtained using the Microstream® oral/nasal cannula, and reported that despite the theoretic advantage of a lower sampling flow rate, the $ETCO_2$ measured with this device significantly underestimated $PaCO_2$ ($PaCO_2$–$PETCO_2$ = 14.1, SD = 7.4 mm Hg) while the $PtcCO_2$ slightly overestimated $PaCO_2$ ($PaCO_2$–$PtcCO_2$ = −5.6, SD = 3.4 mm Hg).

Small tidal volumes, high respiratory rates, and high sampling flow rates theoretically decrease the accuracy of exhaled gas samples obtained with modified nasal cannulae. However, numerous studies have documented the efficacy of this sampling technique with infants and children (in whom small tidal volumes, high respiratory rates, and high sampling flow rates relative to expiratory flow are the rule rather than the exception)[27,28,30,50–53]. Divided nasal cannulas have been successfully used on children to assess: syncope related to hyperventilation [50]; the presence of hypoventilation during the postictal period [51]; severity of metabolic acidosis associated with diabetic ketoacidosis [54]; the presence of hypercarbia during sedation in the emergency room [28] and dental office [55–57]; ventilatory response during ketamine sedation [27]; the respiratory depression associated with different sedation protocols [30]; and the presence of hypoventilation in the postoperative period [58]. Perhaps most impressive, a study evaluating the significance of patient position on $ETCO_2$ generated adequate data in neonates (age as low as 30 weeks post-conceptual age, weight as low as 1464 g) by using appropriately sized divided nasal cannulae with a sampling flow rate of 150 mL/min [59]. One study using divided nasal cannulas reported that $PaCO_2$–$PETCO_2$ increased when oxygen flow rates were 3 L/min or greater. Inspection of the data indicates that

Table 12.4 Efficacy of different sampling devices

Reference	Patient age (mean)	No. of patients (samples)	Supplemental O_2 admin	Device	$P_{ET}CO_2$ (mm Hg) mean ± SD (range)	$PaCO_2$–$P_{ET}CO_2$ (mm Hg) mean ± SD (range)	Comments
Abramo *et al.* [51]	6.5 yrs	58 (58)	Not described	DNC	34.0 ± 4.26 (22–42)	2.0 ± 2.6 (Range not given)	Reliability not affected by age or respiratory rate
Abramo *et al.* [84]	6.8 yrs	166 (166)	Not described	DNC	42.0 ± 11.8 (Range not given)	0.3 ± 2.1 (Range not given)	Reliable
Bongard *et al.* [45]	Adults	41 (82)	Face mask, "when necessary"	NTA	39.7 ± 5.1 (Range not given)	2.8 ± 2.6 (Range not given)	Accurate estimate of $PaCO_2$
Casati *et al.* [85]	69 yrs	30 (120)	Not described	DNC	31 (SD not given) (18–44)[a]	4.4 (SD not given) (0–28)[a]	
					33 (SD not given) (22–45)[b]	7 (SD not given) (0–22)[b]	
Casati *et al.* [86]	70 yrs	20 (60)	No	DNC	No values given	6.5 ± 4.8 (Range not given)	
Liu *et al.* [44]	Adults	25 (25)	Not described	NTA	34.5 ± 8 (20–52)	3.6 ± 6.8 (–4.7–25.1)	
Tobias *et al.* [58]	7.8 yrs	30 (55)	Not described	DNC	39.7 ± 3.8 (Range not given)	2.2 ± 0.9 (Range not given)	Accurate and reliable
Bowe *et al.* [49]	67 yrs	21 (21)	3 L/min	DNC	36.5 ± 4.7 (28–44)	2.1 ± 2.2 (Range not given)	
Stein *et al.* [87]	NR	30 (150)	4 L/min	Microcap	27.9 ± 7.0 (Range not given)	14.1 ± 7.4 (Range not given)	Poor assessment of $PaCO_2$

DNC, divided nasal cannula; NR, not reported; NTA, nasotracheal airway.
[a] Values when analysis performed with microstream capnometer
[b] Values when analysis performed with standard capnometer

$PaCO_2$–$P_{ET}CO_2$ was unchanged in four of six patients and that the statistical increase in the difference could be attributed to reductions in E_TCO_2 (approximately 15 mm Hg) which occurred in the two remaining patients [52]. Sampling by nasal cannula is not foolproof; most authors report that mouth-breathing results in a low but finite incidence of spuriously low values for E_TCO_2 [10,60,61].

Role of pulse oximetry

Acknowledgment of the risks inherent with sedation requires consideration of practice modifications that

can reduce these risks. Pulse oximetry is considered by many clinicians to be an adequate monitor of ventilation during sedation. Hypoxemia secondary to central ventilatory depression and/or airway obstruction occurs when increases in alveolar CO_2 ($PaCO_2$) produce decreases in alveolar O_2 (PaO_2). Pulse oximeters measure oxygen saturation (SpO_2) instead of the partial pressure of oxygen in arterial blood (PaO_2). The shape of the oxyhemoglobin dissociation curve dictates that PaO_2 will be significantly below 100 mm Hg before desaturation is detected. In patients breathing room air, this occurs with only modest increases in $PaCO_2$. In the presence of supplemental O_2, however, SpO_2 may be maintained at >90% despite truly spectacular increases in arterial carbon dioxide tension ($PaCO_2$), as is readily demonstrated in the interactive website of the Center for Simulation, Safety, Advanced Learning, and Technology at the University of Florida College of Medicine (http://vam.anest.ufl.edu/simulations/alveolargasequation.php). The fact that even minimal increases in inspired oxygen concentration blunt the ability of pulse oximetry to detect hypoventilation has been demonstrated under controlled conditions when minute ventilation was decreased by 50% in intubated, ventilated patients and the presence of decreased oxygen saturation was detected by pulse oximetry. While patients receiving $FiO_2 = 0.21$ manifested decreased SpO_2 (half had SpO_2 <90% within 5 min of initiation of hypoventilation), all patients receiving $FiO_2 > 0.25$ maintained SpO_2 >90% throughout a 10-min period of decreased minute ventilation [62]. Several studies have documented the clinical applicability of this physiology [14,56,60,63–67]. Recognition of this relationship has led to the recommendation that supplemental oxygen should not be administered during sedation in order to enhance the ability of pulse oximetry to detect hypoventilation. While this may be effective, it occurs at the expense of increasing the incidence of hypoxic episodes and decreasing the total body oxygen content present at the time of a problem. Since monitoring exhaled CO_2 is feasible, relatively inexpensive, and non-invasive, it is logical to directly monitor a factor that reflects ventilatory depression.

Ventilatory compromise during sedation

Essentially all drugs used for sedation are ventilatory depressants. Drug combinations typically have a synergistic, rather than simply additive, effect on ventilation. Experienced practitioners recognize that the response of a given individual to a particular dosing regimen is unpredictable; doses with minimal effect on one patient may cause profound ventilatory depression in another [68]. Attempting to categorize sedation into specific levels tends to obscure the fact that even minimal sedation (anxiolysis) is the first step along a path of pharmacologic depression of the central nervous system to general anesthesia [14]. It is also important to note that, in many instances, it is desirable that a patient's level of sedation change during the course of a procedure: deep sedation/analgesia during episodes of increased painful stimulation, and moderate sedation during less stimulating intervals. Numerous studies have reported the frequency of desaturation and airway obstruction/apnea during sedation without the use of capnometry (Table 12.5). Not surprisingly, when capnometry is used, the reported incidence of each of these problems is increased.

Airway obstruction, apnea, hypoventilation detected with capnometry

Numerous studies have used capnometry in an effort to assess procedural sedation. In some studies, the intent is to evaluate the incidence of respiratory compromise using a specific drug regimen; others have compared the detection of airway compromise (hypoxemia, airway obstruction) by using capnometry with other monitoring modalities (trained observers, oximetry) (Table 12.6). Most authors indicate that monitoring with capnometry results in the ability to detect hypoventilation and/or apnea earlier than any other monitoring modality, including observation by dedicated observers (Table 12.7) [31,60,66–71]. The exception appears to be studies conducted with a dedicated observer assessing ventilation with a pretracheal stethoscope [66,72]. Studies conducted with that monitoring technology report no difference between the ability of capnometry and a dedicated observer to recognize apnea. In some studies, dedicated observers failed to detect any form of respiratory compromise (hypercarbia, airway obstruction, apnea) in the absence of hypoxemia [73]. Some authors have gone as far as indicating that there is indisputable evidence that capnometry is effective in detecting alterations in ventilation *prior* to the development of apnea or complete airway obstruction [14,61].

Table 12.5 Frequency of ventilatory compromise

Reference	Patient age	O_2 admin[a]	SpO_2 <90%[b]	Apnea/ obstruct[c]	Comments
Bailey *et al.* [88]	Adults	No	92%	50%	Apnea >15 s
Wright [89]	Adults	No	33%	4%	Apnea >30 s
Iwasaki *et al.* [56]	2–5 y/o	No	50%	10%	Obstruction
Croswell *et al.* [63]	2–4 y/o	Yes	20%	23%	Apnea >15 s
Litman *et al.* [68]	1–3 y/o	Yes	0%	0%	

Source: Modified from Vascello LA and Bowe EA
[a] O_2 admin, whether supplemental O_2 was routinely administered.
[b] SpO_2 <90%, incidence of S_pO_2 <90% during procedure.
[c] Apnea/obstruct, incidence of apnea or airway obstruction detected during the procedure.

Table 12.6 Incidence of hypoxemia, airway obstruction, and apnea in patients undergoing procedural sedation with capnometric monitoring

Reference	No. of patients	Age in yrs: mean (range)	O_2 admin	% Patients with hypoxemia	% Patients with obstruction	% Patients with apnea (duration)
Anderson *et al.* [53]	125	8 (2–17) y/o	Yes	4.8	24.8	11.2 (30 s)
Burton *et al.* [60]	60	Adults	Yes	33	28.3[a]	NR
Coll-Vincent *et al.* [90]	32	Adults	Yes	21.8	NR	25 (20 s)
Deitch *et al.* [73]	80	36 (2–77) y/o	Yes/no[b]	13.6/ 14.3[c]	35	17.5[d]
Mensour *et al.* [79]	160	33.6 y/o[e]	Yes	1	22.5	10 (20 s)
Kim *et al.* [27]	20	6.5 (1.7–13) y/o	No	5	5	0
Lightdale *et al.* [91]	163	14.4[f]	Yes	18	NR	24.5 (15 s)
Miner *et al.* [25]	74	Adults	NR	14.9	14.9	NR
Miner *et al.* [92]	108	Adults	87%[g]	12.9	13.9	NR
Miner *et al.* [93]	62	Adults	NR	4.8	1.6	NR
Miner *et al.* [94]	103	Adults	NR	10.7	5.8	NR
Frank *et al.* [95]	50	Adults	Yes	8	NR	4
Soto *et al.* [65]	39	Adults	Yes	2.6	NR	25.5 (20 s)
Vargo *et al.* [66]	49	Adults	No	25.9	NR	NR
Vargo *et al.* [67]	75	Adults	No	46.7	NR	34.7[h]
Yildizdas *et al.* [96]	126	8.3 (2–17) y/o	NR	3.2	NR	0

[a] Capnography performed on 30 patients; no reports of obstruction in group without capnography.
[b] Study to evaluate impact of supplemental O_2 on incidence hypoxemia during sedation; 44 received O_2, 36 received compressed air.
[c] Incidence of hypoxemia with/without supplemental O_2.
[d] Threshold for duration of apnea not defined.
[e] Age range not specified but noted that 32.3% of patients were "pediatric" patients.
[f] Age range not reported.
[g] Decision to provide supplemental O_2 left to treating physician.
[h] A total of 47 apneic episodes were detected in 26 patients.
NR, not reported

Table 12.7 Capnography versus observation in detection of respiratory events during sedation

Reference	No. of patients	O_2 admin	Detected by observers: *no. of patients (%)*	Detected by capnography: *no. of patients (%)*	Difference (*P* value)
Deitch *et al.* [73]	80	yes	13 (16.2)[a]	35 (43.8)	NR
Lightdale *et al.* [91]	163	yes	6 (3.8)	116 (71.1)	NR
Soto *et al.* [65]	39	yes	0 (0)	10 (25.5)	NR
Vargo *et al.* [66]	49	no	0 (0)	54 (100)[b]	<0.001
Anderson *et al.* [53]	125	yes	4 (3.2)	15 (12)	NR

[a] Physicians did not detect airway compromise in any patient who did not have decreased oxygen saturation.
[b] Some patients experienced more than one episode.
NR, not reported

Hypercarbia

The definition of hypercarbia varies between studies; some authors have not considered hypercarbia to occur until $ETCO_2$ exceeds 70 mm Hg while others consider a 10 mm Hg increase over baseline to constitute hypercarbia. It should be recognized that the authors of most of these studies are attempting to document the safety and efficacy of sedation in the particular circumstances under study. Given these complicating factors, the incidence of hypercarbia was reported to range from 0% to 57.7% (Table 12.8).

Acceptance by specialty societies and regulatory agencies

As evidenced by the disparity in guidelines from different specialty societies, opinions on the value of capnometry vary widely based on the venue and specialty of the sedating physician. Interestingly, the guidelines of most anesthesiology specialty societies [6,74] do not comment on the use of capnography during sedation outside the operating room environment. Many opinion papers advocate capnography for patients undergoing sedation, terming it "the gold standard in the near future" [75], advocating that capnometry be recommended by the ASA as a standard for all patients undergoing procedural sedation [76], and describing capnometry as "quite probably, the most useful assessment tool *not* being used on a daily basis in ambulances throughout the world" [77].

Even authors who argue against adopting capnography as a monitoring standard during sedation usually base their objections on the absence of documented improvements in outcomes [11,69,78–80]. This appears to contradict the results of a study of 4846 patients undergoing sedation for endoscopic procedures. These authors reported that oversedation (necessitating administration of reversal agents or bag-mask ventilation) occurred in 14 of 4246 procedures performed without capnometry, but when capnometry was used in 600 procedures, no cases of oversedation occurred. Surprisingly, and despite these findings, the authors concluded that "capnography does not provide significantly increased safety during moderate sedation" [81]. A study of 163 children undergoing gastrointestinal procedures documented that the use of capnometry resulted in patients being significantly less likely to experience an episode of decreased saturation (SpO_2 <95%) during the procedure. Some evidence suggests that the mortality rate of children undergoing sedation is far greater than that for children receiving a general anesthetic. Even if the mortality rate is 100-fold greater, a statistically valid comparison of outcomes between those sedated with and without capnographic monitoring would require many tens of thousands of patients in each group.

Adoption by providers

In a 2008 survey of 140 physicians in Dublin, Ireland who were trained in sedation techniques, 111 responded and none indicated they used capnometry during procedural sedation. Also, in 2008, a survey of all directors of accredited pediatric emergency medicine fellowships in the United States and Canada revealed that only 53% of respondents had access to capnometry for unintubated patients and that only 20% used capnometry "always" or "often" when performing moderate sedation [82]. On the other hand, some emergency

Table 12.8 Reported incidence of hypercarbia detected by capnometry during sedation

Reference	No. of patients	Age in yrs: mean (range)	Hypercarbia (% of patients)	Definition
Anderson *et al.* [53]	125	8 (2–17)	24.8	>50 mm Hg or 10 mm Hg increase
Burton *et al.* [60]	60	Adults	8.3	>50 mm Hg or 10 mm Hg increase
Deitch *et al.* [73]	80	36 (2–77)	43.8	>50 mm Hg or 10 mm Hg increase
Kim *et al.* [27]	20	6.5 (1.7–13)	0	>50 mm Hg
Lightdale *et al.* [91]	163	14.4	57.7	Not specified
Miner *et al.* [25]	74	Adults	44.6	>50 mm Hg
Miner *et al.* [92]	108	Adults	37.9	>50 mm Hg
Miner *et al.* [93]	62	Adults	50.0	>50 mm Hg
Miner *et al.* [94]	103	Adults	48.5	>50 mm Hg
Yildizdas *et al.* [96]	126	8.3 (2–17) y/o	20.6	>50 mm Hg

departments consider capnometry to be a standard of care during sedation and use it for all patients receiving procedural sedation, and some gastroenterologists use it for all patients undergoing endoscopic retrograde cholangiopancreatography [83].

Conclusion

Available data indicate that divided nasal cannulae are non-invasive, well tolerated by most patients (including children), and capable of providing samples which produce $PaCO_2$–$PETCO_2$ differences comparable to those obtained during general endotracheal anesthesia with positive pressure ventilation. Most studies also document that capnography is more effective in detecting episodes of apnea or airway obstruction than clinical observation or pulse oximetry. Under these circumstances, and in light of the fact that sedation may be associated with more severe complications than the procedure itself, the risk–benefit ratio would clearly seem to favor the routine use of capnography during regional anesthesia, as well as sedation either inside or outside of the operating room.

References

1. Coté CJ. Pediatric premedication: from disasters to guidelines. *Am J Anesth* 1997; **24:** 6–9.
2. Coté CJ, Alderfer RJ, Notterman DA, Fanta KB. Sedation disasters: adverse drug reports in pediatrics – FDA, USP, and others [abstract]. *Anesthesiology* 1995; **83:** A1183.
3. American Academy of Pediatrics, Committee on Drugs, Section on Anesthesiology. Guidelines for the elective use of conscious sedation, deep sedation, and general anesthesia in pediatric patients. *Pediatrics* 1985; **76:** 317–21.
4. Sa Rego MM, Watcha MF, White PF. The changing role of monitored anesthesia care in the ambulatory setting. *Anesth Analg* 1997; **85:** 1020–36.
5. American Academy of Pediatrics, Committee on Drugs. Guidelines for monitoring and management of pediatric patients during and after sedation for diagnostic and therapeutic procedures: addendum. *Pediatrics* 2002; **110:** 836–8.
6. American Society of Anesthesiologists. *Continuum of Depth of Sedation: Definition of General Anesthesia and Levels of Sedation/Analgesia*, Approved by the ASA House of Delegates on October 13, 1999, and amended on October 27, 2004. Available online at http://www.asahq.org/publicationsAndServices/standards/20.pdf. (Accessed July 6, 2009.)
7. Joint Commission on Accreditation of Healthcare Organizations. Standards and Intents for Anesthesia and Anesthesia Care. In: *Revisions to Anesthesia Care Standards: Comprehensive Accreditation Manual for Hospitals*. Oakbrook Terrace, IL: JCAHO, 2009.
8. American Dental Association. *Guidelines for the Use of Conscious Sedation, Deep Sedation and General Anesthesia for Dentists*. (2002) Available online at http://www.ada.org/prof/ed/guidelines/guidedent.doc. (Accessed June 30, 2003.)
9. American Academy of Pediatric Dentistry. Guidelines on the elective use of conscious sedation, deep sedation and

general anesthesia in pediatric dental patients. In: *AAPD Reference Manual 2004–2005*. Chicago, IL: AAPD, 2004; 74–80.

10. Coté CJ, Wilson S. Guidelines for monitoring and management of pediatric patients during and after sedation for diagnostic and therapeutic procedures: an update. *Pediatrics* 2006; **118:** 2587–602.
11. American College of Emergency Physicians. Clinical policy for procedural sedation and analgesia in the emergency department. *Ann Emerg Med* 1998; **31**: 663–77.
12. Innes G, Murphy M, Nijssen-Jordan C, Ducharme J, Drummond A. Procedural sedation and analgesia in the emergency department: Canadian consensus guidelines. *J Emerg Med* 1999; **17:** 145–56.
13. American Society of Anesthesiologists. *Standards for Basic Anesthetic Monitoring*. 2005. Available online at http://www.asahq.org/publicationsAndServices/standards/02.pdf. (Accessed July 3, 2009.)
14. Mandt MJ, Roback MG. Assessment and monitoring of pediatric procedural sedation. *Clin Pediatr Emerg Med* 2007; **8:** 223–31.
15. Pershad J, Kost S. Emergency department based sedation services. *Clin Pediatr Emerg Med* 2007; **8:** 253–61.
16. Fanning RM. Monitoring during sedation given by nonanaesthetic doctors. *Anaesthesia* 2008; **63:** 370–4.
17. Anesthesia Patient Safety Foundation. 3 different organizations can accredit OBA sites. 2000. Available online at http://www.apsf.org/resource_center/newsletter/2000/spring/07-Accredit.htm. (Accessed November 29, 2008.)
18. Twersky RS. Standards for office anesthesia vary widely or do not exist. 2000. Available online at http://www.apsf.org/resource_center/newsletter/2000/spring/05-Twersky.htm. (Accessed November 29, 2008.)
19. Krippaehne JA, Montgomery MT. Morbidity and mortality from pharmacosedation and general anesthesia in the dental office. *J Oral Maxillofac Surg* 1992; **50:** 691–8.
20. Jastek JT, Peskin RM. Major morbidity or mortality from office anesthetic procedures: a closed-claim analysis of 13 cases. *Anesth Prog* 1991; **38:** 39–44.
21. Arrowsmith JB, Gertsman BB, Fleischer DE, Benjamin SB. Results from the American Society for Gastrointestinal Endoscopy/US Food and Drug Administration collaborative study on complication rates and drug use during gastrointestinal endoscopy. *Gastrointest Endosc* 1991; **37:** 421–7.
22. Quine MA, Bell GD, McCloy RF, *et al.* Prospective audit of upper gastrointestinal endoscopy in two regions of England: safety, staffing, and sedation methods. *Gut* 1995; **36:** 462–7.
23. Sharma VK, Nguyen CC, Crowell MD, *et al.* A national study of cardiopulmonary unplanned events after GI endoscopy. *Gastrointest Endosc* 2007; **66**: 27–34.
24. Freeman ML, Hennessy JT, Cass OW, Pheley AM. Carbon dioxide retention and oxygen desaturation during gastrointestinal endoscopy. *Gastroenterology* 1993: **105:** 331–9.
25. Miner JR, Heegaard W, Plummer D. End-tidal carbon dioxide monitoring during procedural sedation. *Acad Emerg Med* 2002; **9:** 275–80.
26. Malviya S, Voepel-Lewis T, Tait AR. Adverse events and risk factors associated with the sedation of children by nonanesthesiologists. *Anesth Analg* 1997; **85:** 1207–13.
27. Kim G, Green SM, Denmark TK, Krauss B. Ventilatory response during dissociative sedation in children: a pilot study. *Acad Emerg Med* 2003; **10:** 140–5.
28. McQuillen KK, Steele DW. Capnography during sedation/analgesia in the pediatric emergency department. *Pediatr Emerg Care* 2000; **16:** 401–4.
29. Marx CM, Stein J, Tyler MK, *et al.* Ketamine-midazolam versus meperidine-midazolam for painful procedures in pediatric oncology patients. *J Clin Oncol* 1997; **15:** 94–102.
30. Tobias JD. End-tidal carbon dioxide monitoring during sedation with a combination of midazolam and ketamine for children undergoing painful, invasive procedures. *Pediatr Emerg Care* 1999; **15:** 173–5.
31. Doyle L, Colletti JE. Pediatric procedural sedation and analgesia. *Pediatr Clin N Am* 2006; **53**: 279– 92.
32. Pitetti RD, Singh S, Pierce MC. Safe and efficacious use of procedural sedation and analgesia by nonanesthesiologists in a pediatric emergency department. *Arch Pediatr Adolesc Med* 2003; **157:** 1090–6.
33. Galandiuk S, Ahmad P. Impact of sedation and resident teaching on complications of colonoscopy. *Dig Surg* 1998; **15**: 60–3.
34. Huntington CT, King H. A simpler design for mass spectrometer monitoring in the awake patient. *Anesthesiology* 1986; **65:** 565–6.
35. Kempem P. Cost-efficient end-tidal carbon dioxide monitoring via Hudson-style mask. *Anesthesiology* 1999; **91:** 1176–7.
36. Ibarra E, Lees DE. Mass spectrometer monitoring of patients with regional anesthesia. *Anesthesiology* 1985; **63:** 572–3.
37. Langer RA. Simple modification of a medium concentration (Hudson type) oxygen mask improves patient comfort and respiratory monitoring with capnography. *Anesth Analg* 1996; **83**: 202.
38. Goldman JM. A simple, easy, and inexpensive method for monitoring $ETCO_2$ through nasal cannulae. *Anesthesiology* 1987; **67**: 606.

39. Shah MG. Measurement of carbon dioxide at both nares and mouth using standard nasal cannula. *Anesthesiology* 1994; **81:** 779–80.
40. Kempen P. Cost-efficient carbon dioxide monitoring via nasal cannula. *Anesthesiology* 1999; **90:** 633–4.
41. Urmey WF. Accuracy of expired carbon dioxide partial pressure sampled from a nasal cannula. I. *Anesthesiology* 1988; **68:** 959–60.
42. Dunphy JA. Accuracy of expired carbon dioxide partial pressure sampled from a nasal cannula. II. *Anesthesiology* 1988; **68**: 960–1.
43. Norman EA, Zeig N, Ahmad I. Better designs for mass spectrometer monitoring of the awake patient. *Anesthesiology* 1986; **64**: 664.
44. Liu SY, Lee TS, Bongard F. Accuracy of capnography in nonintubated surgical patients. *Chest* 1992; **102:** 1512–15.
45. Bongard F, Wu Y, Lee TS, Klein S. Capnographic monitoring of extubated postoperative patients. *J Invest Surg* 1994; **7**: 259–64.
46. Cheng KI, Tang CS, Tsai EM, Wu CH, Lee JN. Correlation of arterial and end-tidal carbon dioxide in spontaneously breathing patients during ambulatory gynecologic laparoscopy. *J Formos Med Assoc* 1999; **98:** 814–19.
47. Hou WY, Sun WZ, Susceto L, *et al.* Validity and feasibility of nasopharyngeal end-tidal carbon dioxide tension monitoring: a novel approach in spontaneously breathing patients. *J Formos Med Assoc* 1993; **92:** 553–7.
48. Desmarattes R, Kennedy R, Davis DR. Inexpensive capnography during monitored anesthesia care. *Anesth Analg* 1990; **71:** 100–1.
49. Bowe EA, Boysen PG, Broome JA, Klein EF. Accurate determination of end-tidal carbon dioxide during administration of oxygen by nasal cannulae. *J Clin Monit* 1989; **5:** 105–10.
50. Martinón-Torres F, Rodriguez-Nuñez A, Fernández-Cebrián S, *et al.* The relation between hyperventilation and pediatric syncope. *J Pediatr* 2001; **138:** 894–7.
51. Abramo TJ, Cowan MR, Scott SM, *et al.* Comparison of pediatric end-tidal CO_2 measured with nasal/oral cannula circuit and capillary PCO_2. *Am J Emerg Med* 1995; **13:** 30–3.
52. Kaneko Y. Clinical perspectives on capnography during sedation and general anesthesia in dentistry. *Anesth Prog* 1995; **42:** 126–30.
53. Anderson JL, Junkins E, Pribble C, Guenther E. Capnography and depth of sedation during propofol sedation in children. *Ann Emerg Med* 2007; **49:** 9–13.
54. Fearon DM, Steele DW. End-tidal carbon dioxide predicts the presence and severity of acidosis in children with diabetes. *Acad Emerg Med* 2002; **9**: 1373–8.
55. Primosch RE, Buzzi IM, Jerrell G. Monitoring pediatric dental patients with nasal mask capnography. *Pediatr Dent* 2000; **22:** 120–4.
56. Iwasaki J, Vann WF Jr., Dilley DCL, Anderson JA. An investigation of capnography and pulse oximetry as monitors of pediatric patients sedated for dental treatment. *Pediatr Dent* 1989; **11:** 111–17.
57. Anderson JA, Vann WF. Respiratory monitoring during pediatric sedation: pulse oximetry and capnography. *Pediatr Dent* 1988; **10:** 94–101.
58. Tobias JD, Flanagan JF, Wheeler TJ, Garrett JS, Burney C. Non-invasive monitoring of end-tidal CO_2 via nasal cannulas in spontaneously breathing children during the perioperative period. *Crit Care Med* 1994; **22:** 1805–8.
59. Kugelman A, Bilker A, Bader D, Cohen A, Tirosh E. Sidestream end-tidal capnometry as related to infant's position and maturation. *Acta Paediatr* 2002; **91:** 869–73.
60. Burton JH, Harrah JD, Germann CA, Dillon DC. Does end-tidal carbon dioxide monitoring detect respiratory events prior to current sedation monitoring practices? *Acad Emerg Med* 2006; **13:** 500–4.
61. Green SM. Research advances in procedural sedation and analgesia. *Ann Emerg Med* 2007; **49:** 31–6.
62. Fu ES, Downs JB, Schweiger JW, Miguel RV, Smith RA. Supplemental oxygen impairs detection of hypoventilation by pulse oximetry. *Chest* 2004; **126:** 1552–8.
63. Croswell RJR, Dilley DC, Lucas WJ, Vann WF. A comparison of conventional versus electronic monitoring of sedated pediatric dental patients. *Pediatr Dent* 1995: **17**: 332–9.
64. Hart LS, Berns SD, Houck CS, Boenning DA. The value of end-tidal CO_2 monitoring when comparing three methods of conscious sedation for children undergoing painful procedures in the emergency department. *Pediatr Emerg Care* 1997; **13:** 189–93.
65. Soto RG, Fu ES, Vila H, Miguel RV. Capnography accurately detects apnea during monitored anesthesia care. *Anesth Analg* 2004; **99:** 379–82.
66. Vargo JJ, Zuccaro G, Dumot JA, *et al.* Automated graphic assessment of respiratory activity is superior to pulse oximetry and visual assessment for the detection of early respiratory depression during therapeutic upper endoscopy. *Gastrointest Endosc* 2002; **55:** 826–31.
67. Vargo JJ, Zuccaro G, Dumot JA, *et al.* Gastroenterologist-administered propofol versus meperidine and midazolam for advanced upper endoscopy: a prospective, randomized trial. *Gastroenterology* 2002; **123:** 8–16.
68. Litman RS, Berkowitz RJ, Ward DS. Levels of consciousness and ventilatory parameters in young

children during sedation with oral midazolam and nitrous oxide. *Arch Pediatr Adolesc Med* 1996; **150**: 671–5.

69. Krauss B, Hess DR. Capnography for procedural sedation and analgesia in the emergency department. *Ann Emerg Med* 2007; **50:** 172–81.
70. Pino RM. The nature of anesthesia and procedural sedation outside of the operating room. *Curr Opin Anaesthesiol* 2007; **20:** 347–51.
71. Miner JR, Burton JH. Clinical practice advisory: emergency department procedural sedation with propofol. *Ann Emerg Med* 2007; **50:** 182–7.
72. Lazzaroni M, Porro GB. Preparation, premedication and surveillance. *Endoscopy* 2003; **35**: 103–11.
73. Deitch K, Chudnofsky CR, Dominici P. The utility of supplemental oxygen during emergency department procedural sedation and analgesia with midazolam and fentanyl: a randomized, controlled trial. *Ann Emerg Med* 2007; **49:** 1–8.
74. Association of Anaesthetists for Great Britain and Ireland. *Recommendations for Standards of Monitoring during Anaesthesia and Recovery*, 2007. Available online at http://www.aagbi.org/publications/guidelines/docs/standardsofmonitoring07.pdf. (Accessed July 3, 2009.)
75. Golnick JM, Mandeville M. Considerations for monitoring pediatric sedation. *J Mich Dent Assoc* 2002; **84**: 34–6.
76. Sandlin D. Capnography for nonintubated patients: the wave of the future for routine monitoring of procedural sedation patients. *J Perianesth Nurs* 2002; **17:** 277–81.
77. Whitehead S. The capnography revolution begins. *JEMS* 2003; **28**: 130.
78. Bennett J. A case against capnographic monitoring as a standard of care. *J Oral Maxillofac Surg* 1999; **57:** 1348–52.
79. Mensour M, Pineau R, Sahai V, Michaud J. Emergency department procedural sedation and analgesia: a Canadian Community Effectiveness and Safety Study (ACCESS). *Can J Emerg Med* 2006; **8:** 94–9.
80. Walker BH Jr. Is capnography necessary for propofol sedation. *Ann Emerg Med* 2004; **44:** 549–50.
81. Koniaris LG, Wilson S, Drugas G, Simmons W. Capnographic monitoring of ventilatory status during moderate (conscious) sedation. *Surg Endosc* 2003; **17**: 1261–5.
82. Langhan ML, Chen L. Current utilization of continuous end-tidal carbon dioxide monitoring in pediatric emergency departments. *Pediatr Emerg Care* 2008; **24:** 211–13.
83. Wilson S, McCluskey A. Use of capnography during endoscopic retrograde cholangio-pancreatography. *Anaesthesia* 2008; **63:** 1010–26.
84. Abramo TJ, Wibee RA, Scott S, Goto CS, McIntire DD. Noninvasive capnometry monitoring for respiratory status during pediatric seizures. *Crit Care Med* 1997; **25**: 1242–6.
85. Casati A, Gallioli G, Passaretta R, *et al.* End tidal carbon dioxide monitoring in spontaneously breathing, nonintubated patients. *Minerva Anestesiol* 2001; **67**: 161–4.
86. Casati A, Gallioli G, Scandroglio M, *et al.* Accuracy of end-tidal carbon dioxide monitoring using the NBP-75 microstream capnometer: a study in intubated ventilated and spontaneously breathing patients. *Eur J Anaesth* 2000; **17**: 622–6.
87. Stein N, Matz H, Schneeweiss A, *et al.* An evaluation of a transcutaneous and an end-tidal capnometer for noninvasive monitoring of spontaneously breathing patients. *Respir Care* 2006; **51**: 1162–6.
88. Bailey PL, Pace NL, Ashburn MA, *et al.* Frequent hypoxemia and apnea after sedation with midazolam and fentanyl. *Anesthesiology* 1990; **73**: 826–30.
89. Wright SW. Conscious sedation in the emergency department: the value of capnography and pulse oximetry. *Ann Emerg Med* 1992; **21**: 551–5.
90. Coll-Vincent B, Sala X, Fernandez C, *et al.* Sedation for cardioversion in the emergency department: analysis of effectiveness in four protocols. *Ann Emerg Med* 2003; **42**: 767–72.
91. Lightdale JR, Goldmann DA, Feldman HA, *et al.* Microstream capnography improves patient monitoring during moderate sedation: a randomized, controlled trial. *Pediatrics* 2006; **117**: e1170–8.
92. Miner JR, Biros MH, Heegaard W, Plummer D. Bispectral electroencephalographic analysis of patients undergoing procedural sedation in the emergency department. *Acad Emerg Med* 2003; **10**: 638–43.
93. Miner JR, Martel ML, Meyer M, Reardon R, Biros MH. Procedural sedation of critically ill patients in the emergency department. *Acad Emerg Med* 2005; **12**: 124–8.
94. Miner JR, Biros MH, Krieg S, *et al.* Randomized clinical trial of propofol versus methohexital for procedural sedation during fracture and dislocation reduction in the emergency department. *Acad Emerg Med* 2003; **10**: 931–7.
95. Frank LR, Strote J, Hauff SR, Bigelow SK, Fay K. Propofol by infusion protocol for ED procedural sedation. *Am J Emerg Med* 2006; **24**: 599–602.
96. Yildizdas D, Yapicioglu H, Yilmaz HL. The value of capnography during sedation or sedation/analgesia in pediatric minor procedures. *Pediatr Emerg Care* 2004; **20**: 162–5.

Section 1
Chapter
13

Ventilation

Capnometry monitoring in high- and low-pressure environments

C. W. Peters, G. H. Adkisson, M. S. Ozcan, and T. J. Gallagher

Introduction

Mankind lives, works, and plays within an extensive range of high- and low-pressure environments. Human populations are found extending from the low-lying deserts of the Middle East to the high-altitude plateaus of South America, Africa, and Asia. Beyond these "normal" environments, mankind has extended its exposure to high- and low-pressure environments through a multitude of commercial and recreational activities. High-pressure exposures are normally related to some form of diving, whether commercial or recreational, but may also include exposure in a hyperbaric chamber for therapeutic purposes or from occupational exposure in high-pressure caissons used for bridge and tunnel construction or for mining. Low-pressure exposures occur primarily due to high-altitude excursions, including airline flights, and skiing and mountain climbing adventures. These supra- and subatmospheric exposures are normally short term, but may be of a more prolonged nature, such as an extended dive under saturation conditions, a climb to Mount Everest, or an assignment to the orbiting Space Station. Regardless of duration, these extremes of environmental exposures can have significant effects on human physiology, and carry significant risks of injury or death if undertaken without an understanding of these effects and without taking appropriate measures to deal with them. One of the key elements of managing these exposures and minimizing the subsequent risk is to understand and monitor the environmental gases. Of these, two of the most significant are oxygen and carbon dioxide.

Altitude exposure

Prior to a discussion of physiologic changes secondary to altitude exposure, it is important to understand how altitude affects atmospheric pressure and subsequent alveolar oxygen availability. At sea level, the atmospheric pressure is 760 mm Hg, equivalent to 14.7 psia, or 1 atmosphere absolute (ATA). As altitude increases from mean sea level (msl) to approximately 30 000 ft (9150 m), the pressure changes in a nearly direct linear relationship (Table 3.1). The major constituents of dry air, expressed as approximate volume percentages and partial pressures, are shown in Table 13.2.

Excursions to high altitudes mean that the partial pressure of O_2 (PO_2) in air decreases in a linear manner along with atmospheric pressure. At sea level, PO_2 is about 159 mm Hg. At 5000 ft (1524 m) above msl, atmospheric pressure drops to 632 mm Hg, and the PO_2 drops to 132 mm Hg. At 12 000 ft (3658 m), atmospheric pressure drops to 483 mm Hg and the PO_2 will be 101 mm Hg.

Although the PO_2 changes in a linear fashion with altitude, of more concern is that the alveolar partial pressure of oxygen (PAO_2) changes in a non-linear fashion. During normal ventilation, the alveolar partial pressure of CO_2 ($PACO_2$) remains relatively constant at 40 mm Hg, but will begin to drop as hyperventilation attempts to compensate for the reduced PAO_2. Alveolar gas is 100% humidified at normal temperature (37 °C), and alveolar water vapor pressure remains relatively constant at 47 mm Hg [1]. A $PACO_2$ of 40 mm Hg and a water vapor pressure of 47 mm Hg change the alveolar mixture of gases and the alveolar availability of oxygen at all altitudes. For example, alveolar gas measured at sea level shows a decrease from a PO_2 of 159 mm Hg (20.9% of the air mixture) to a PAO_2 of 101 mm Hg, or 13.3% of the gas mixture secondary to the presence of CO_2 and water vapor at the alveolar level. This effect is magnified at higher altitudes. At 18 000 ft (5486 m), atmospheric pressure will drop to 380 mm Hg, or 0.5 ATA. The percentage of oxygen in the air remains constant at 20.9%, but PO_2 is now 79 mm Hg. Water vapor remains constant despite altitude changes. Ideal alveolar gas, without hyperventilation, would show a

Capnography, Second Edition, ed. J. S. Gravenstein, Michael B. Jaffe, Nikolaus Gravenstein, and David A. Paulus. Published by Cambridge University Press. © Cambridge University Press 2011.

Table 13.1 Relationship between altitude and pressure

Altitude		Pressure		
Feet	**Meters**	**mm Hg**	**psia**	**ATA**
0	0	760	14.7	1
6 000	1829	609	11.8	0.83
12 000	3658	483	9.34	0.64
18 000	5486	380	7.35	0.5
24 000	7315	295	5.7	0.39
30 000	9144	226	4.37	0.30

Table 13.2 Major constituents of dry air

Component	Volume percentage	Partial pressure (mm Hg)
Nitrogen (N_2)	78.08	593.4
Oxygen (O_2)	20.95	159.2
Argon (Ar)	0.93	7.1
Carbon dioxide (CO_2)	0.03	0.2
	99.99	759.9

drop in P_AO_2 to a significantly lower level (22 mm Hg) than expected, and would be a significantly lower percentage of the available alveolar gas mixture (5.9%). Although the relative change in atmospheric pressure seems small compared to the changes encountered while diving, the effect on available alveolar O_2 is significant.

Altitude and human physiology

As many as 140 million people inhabit regions of the earth at altitudes of 8000 to 17 000 feet (2438–5182 m) [2]. Ambient pressures at these altitudes range from 565 mm Hg (0.74 ATA) down to 396 mm Hg (0.52 ATA). Additionally, over 30 million people travel each year to high altitudes for recreational or commercial purposes. Air travel is the single, most common altitude exposure for most people each year, with an exposure of short duration. Commercial airliners typically pressurize their cabins to avoid exposing passengers to extreme pressure changes so, while a flight may occur at 30 000 ft (9150 m) or more, the cabin normally remains pressurized to an altitude equivalent of 6000–8000 ft (1829–2438 m). Maintaining a lower pressure reduces the plane's structural requirements, but the pressure must be kept sufficiently high to prevent pressure-related illness among the passengers. The altitude equivalent of 8000 ft is a trade-off to satisfy both of these requirements [3]. Additional aspects of the aircraft environment are controlled during flight, and significant medical problems due to airline travel are relatively uncommon. The remainder of the section, therefore, will focus more on recreational or occupational exposure to high altitudes, particularly mountain climbing, which, given the extreme and prolonged exposures typically encountered, poses a far greater risk to the individuals involved.

In addition to pressure-related changes, there are multiple environmental stresses that occur during high-altitude exposures that amplify potential dangers. Extremes of climate, ranging from the hot burning sun during the day to freezing temperatures at night, often compounded by low humidity and high winds, leads to a state of dehydration [4]. Loss of appetite is common. Heavy work and limited caloric intake can lead to marked weight loss [5]. The limiting factor, however, for most altitude exposures is the reduction in PO_2 due to the reduced ambient pressure and the subsequent reduction in P_AO_2 resulting in hypoxia.

Physiologic changes at high altitude

Indigenous populations living in the Andean Altiplano in South America, the Tibetan Plateau in Asia, and at the highest elevations of the Ethiopian Highlands in east Africa have evolved three distinctly different biological adaptations for surviving in the oxygen-deficient air found at high altitude [6].

Andeans have developed an ability to carry more oxygen in their systems by having higher hemoglobin concentrations. Their resting respiratory rate is the same as people living at sea level, but they are able to deliver oxygen to their tissues more effectively. Tibetans compensate for reduced PO_2 much differently. They increase their O_2 intake by taking more breaths per minute than people who live at sea level. Additionally, they appear to have an increased production of systemic nitric oxide that dilates their blood vessels, again allowing them to deliver O_2 more effectively due to an increased blood flow. The mechanism by which Ethiopian highlanders compensate is less clear. Despite living at 11 580 ft (3530 m), they do not breathe more rapidly, nor do they produce excess nitric oxide as the Tibetans; neither do they have increased hemoglobin counts as the Andeans. Despite the absence of these adaptive processes, they maintain relatively normal oxygen levels. While the mechanisms by which indigenous peoples compensate for reduced PO_2 at altitude are important, we are more concerned in this

Table 13.3 Alveolar pressure changes with altitude

Altitude		Pressure			
Feet	**Meters**	**Ambient PO_2**	**Alveolar PO_2**	**Alveolar PCO_2**	**Alveolar PH_2O**
0	0	159.21	103.0	40.0	47
6 000	1829	127.60	76.8	37.0	47
12 000	3658	101.26	54.3	33.8	47
18 000	5486	79.55	37.8	30.4	47
24 000	7315	61.78	31.2	27.4	47
30 000	9144	47.36			

chapter with the non-acclimatized individual who ventures to altitude.

Physiologic responses to altitude exposure

Early hypoxic response

The most serious complications of altitude exposure are associated with a syndrome known as acute mountain sickness (AMS). Prior to that extreme, the non-acclimatized individual will begin to experience significant physiologic changes to compensate for the reduced pressures at higher altitudes. There are both early and late responses primarily associated with the proportional decrease in available alveolar oxygen and subsequently reduced PaO_2. Symptoms increase in severity depending upon the rapidity of change in altitude and the duration of exposure.

Early hypoxic symptoms usually begin with the inability to do normal physical activities, but may involve more subtle changes. The most sensitive individuals will experience a decline of night vision, first apparent at ambient pressures of approximately 0.8 ATA (6000 ft or 1829 m), a response not readily appreciated by many private pilots [7]. At 0.6 ATA (13 500 ft or 4115 m), perioral numbness, tingling of the fingers, or dizziness might be encountered. A portion of this response may reflect an altitude-related hyperventilatory response that mimics standard symptoms of hyperventilation. More sensitive individuals can lose consciousness at around 15 000 ft (4572 m), and almost everyone will become unconscious upon sudden exposure to the atmosphere at altitudes above 20 000 ft (6096 m). The time to loss of consciousness becomes exponentially shorter the lower the pressure drops. While individual variations occur, sudden exposure to an ambient pressure near 0.3 ATA (the summit of Mount Everest) results in unconsciousness in 2 min or less.

Hypoxic respiratory stimulation

Exposure to high altitude results in a significant increase in ventilatory rate and minute ventilation. The principle driving force evolves from hypoxemia sensed at the carotid and aortic bodies. These small nerve clusters have very high metabolic rates and large blood supplies, properties that make them extremely sensitive to a decrease in arterial oxygen tension, regardless of the cause [8,9]. As ventilation increases, it also initiates a negative feedback loop. Hyperventilation results in an acute decrease in $PaCO_2$, the displacement of which permits an increase of PaO_2, as predicted by the alveolar gas equation. The net increase in PaO_2 results in an increase in PaO_2 values and a partial blunting of the hypoxic ventilatory drive. As altitude increases and available PO_2 decreases, this compensatory mechanism allows for survival that would otherwise not be possible (Table 13.3).

Alveolar hyperventilation due to hypoxemia is activated when the PaO_2 is between 40 and 80 mm Hg. This occurs as early as an altitude of 5000–6000 ft (1524–1829 m), and becomes more pronounced as the ambient PO_2 approaches 100 mm Hg, which corresponds to an altitude close to 12 000 ft (3658 m). At this altitude, the PaO_2 has dropped into the 50 mm Hg range. At sea level, a PaO_2 of 60 mm Hg equates to room air saturation near 90%, and lies at the beginning of the steep portion of the oxyhemoglobin dissociation curve. Further changes in ventilation will be directly related to subsequent decreases in PaO_2, and will be more pronounced.

The process of acclimatization

The hypoxic drive appears to be biphasic. After acclimatization at a specific altitude, it may be blunted, but will once again respond should a further decrease in PaO_2 occur, such as during excursions to higher altitudes

[10]. Long-time residents, or those born at high altitudes, appear to have a blunted or absent response to hypoxemia. However, unlike non-responsive lowlanders or experimental animals with a denervated carotid body, this blunted response does not seem harmful, and certainly does not interfere with the quality of performance.

In acclimatized individuals, the more brisk the response to hypoxia, the better the physical performance, at least at the mid-altitude range [11]. Few data have been collected at the higher altitudes, but some authorities believe that these same brisk responders may actually do worse at more extreme altitudes. Brisk responders also fare poorly in most cognitive studies carried out at altitude. It has been postulated that hyperventilation, with its attendant decreased cerebral blood flow and possible cellular ischemia, plays a role.

True acclimatization occurs as a gradual process, and may never actually be complete. Studies have clearly demonstrated that continued exposure to altitude, and the resulting hypoxemia, causes a significant decline in higher cognitive functions [12]. Skill tests at high altitudes are poorly performed, and memory may be altered for as long as 6 months after return to sea level. Many of the most powerful telescopes are located at high altitudes (greater than 12 000 ft or 4000 m above msl) to improve clarity. Various attempts at acclimatization have been undertaken with minimal success. To combat these known decrements in performance, some facilities enrich the environment with O_2 up to 26% [13], with a significant improvement reported in cognitive function and fewer problems with headaches and other effects of high altitude.

Carbon dioxide respiratory stimulation

Receptors in the medulla are sensitive to changes in PCO_2 while peripheral receptors play a secondary role [14]. The brain responds to changes in hydrogen ion [H^+] concentration which is altered by the levels of CO_2. Carbon dioxide reacts in the blood to form carbonic acid and bicarbonate. As arterial PCO_2 ($PaCO_2$) increases, acidosis ensues and cerebrospinal fluid (CSF) PCO_2 increases. The consequence of these events causes the [H^+] levels in the brain to rise. The increased [H^+], in turn, stimulates neural receptors in the brainstem to increase hyperventilation. Studies at altitude have demonstrated reduced CSF bicarbonate levels in both acclimatized and non-acclimatized subjects. Since lowered CSF bicarbonate values mean higher brain [H^+] levels, hyperventilation is increased more than would normally occur for a similar $PaCO_2$ at sea level. Three mechanisms have been proposed. One theory focuses on the development of CSF acidosis secondary to hypoxia. A second proposes equilibration by the kidney, with reduced CSF bicarbonate leading to elevated brain [H^+] levels. The third is from studies of Severinghaus *et al.* [15] and West [16], both of which point to an active transport mechanism to reduce the CSF bicarbonate values.

Table 13.4 Values of PCO_2 and PO_2 at altitude in acclimatized and non-acclimatized individuals

Altitude (msl)		PCO_2	PO_2
Feet	Meters	(mm Hg)	(mm Hg)
10 000	3048	36 (23)	67 (92)
20 000	6096	24 (10)	40 (53)
30 000	9144	24 (7)	18 (30)

The values in parentheses represent acclimatized individuals; this helps explain their impaired tolerance to higher altitudes.

The initial response to PCO_2 changes occurs within the first 24 h, accounting for about 50% of the ventilatory response. The remainder takes place over approximately 2 weeks, provided the individual remains at altitude. These changes in CO_2 become important because the increased time at altitude minimizes the hypoxic response. With acclimatization, the ventilatory response increases by a factor of 5 [17]. Table 13.4 compares the ventilatory response in the non-acclimatized to the acclimatized individual. Without this CO_2 effect, hyperventilation would be inadequate. Hyperventilation in the acclimatized individual ultimately results in a higher PaO_2. The ability to hyperventilate does not appear to be associated with age, gender, or physical conditioning [18], and may be genetically driven (Table 13.4).

Other respiratory changes

At altitude, decreased ambient pressure results in increased lung volume that facilitates the delivery of oxygen and carbon dioxide; diffusion capacity increases by approximately 20–30% (see also Table 13.3) [19]. Proposed mechanisms involve the known increase in pulmonary blood flow, which recruits capillaries and small vessels that were not previously open. The expanded capillary surface area provides an increased alveolar surface area for diffusion, and ultimately aids in the transfer of O_2. Pulmonary hypertension that results with altitude exposure and hypoxemia further helps to increase blood flow (Table 13.5).

Table 13.5 Thoracic volume in native high-altitude dwellers

Altitude (m)	Thoracic volume (mL)
1500	10 500
3260	11 000
4000	12 200

The increased lung volumes contribute to improve diffusion in high-altitude natives who also generally have smaller body masses, which contributes to efficient O_2 utilization.

Cardiopulmonary system

Significant changes take place within the cardiopulmonary system upon ascent to high altitude, with an increased risk of heart failure due to the added stress placed on the lungs, heart, and arteries at high altitudes [20]. The same chemoreceptors that stimulate hyperventilation also play an important role in the cardiac response to hypoxemia. The most important compensatory mechanism is an increase in cardiac output, initially related to increased heart rate. For the same imposed work, increases in cardiac output are identical, whether at sea level or altitude. As cardiac output increases, the amount of oxygen extracted from any given quantity of blood decreases, and venous oxygen tension and the amount of saturated hemoglobin increase [21]. This response also minimizes any shunt effect that may be present because, as venous oxygen tension rises, the shunt becomes less critical. Additionally, PaO_2 remains higher at the tissue level. Predictably, and most likely because of hypoxemia, the pulmonary vascular bed undergoes significant vasoconstriction. Hypoxemia-induced hyperventilation partially blocks this response, but almost all individuals, acclimatized or not, experience some degree of pulmonary hypertension at altitude. Breathing supplemental O_2 can temporarily shift pulmonary pressures toward normal, but prolonged exposure without supplemental O_2 leads to chronic pulmonary hypertension that cannot be reversed with supplemental O_2 therapy [22]. The muscularis layer of the pulmonary artery is minimal so vasoconstriction must be a fairly sensitive and intense response. Beyond vasoconstriction, anatomic changes involve additional layers, including the intima in chronically exposed individuals. Over time, these increased pressures will lead to right ventricular hypertrophy. Stroke volume ultimately decreases, possibly linked to decreased intravascular volume from dehydration and diuresis.

Additional cardiac effects include different types of arrhythmias, including premature atrial and premature ventricular contractions, which have been noted in high-altitude dwellers [23]. Although not well documented, some arrhythmias may represent a consequence of alkalemia secondary to hyperventilation. The periodic breathing often experienced by mountaineers and other high-altitude dwellers is often seen in conjunction with atrial arrhythmias. Over time, hematologic changes develop and help alter cardiac output towards previous levels.

Hematologic changes

Hematologic changes at altitude primarily involve an increase in red blood cells. Various studies have demonstrated that, with the initial exposure to the hypoxemic environment, erythropoietin begins to rise [24] within 2 to 3 days; however, red blood cell numbers take up to 6 months to reach peak levels. Additional capillary beds may also develop to assist in the distribution of blood.

Within 3 weeks, if there is no further change in altitude, the erythropoietin level returns to normal. Subsequent excursions to even higher altitudes will once again stimulate erythropoietin production. Return from altitude causes a reduction to sea level values within 24 h, with the red blood cell increase usually lasting about 6 weeks. Polycythemia develops to compensate for a reduced ambient PO_2 and helps increase O_2 delivery at the tissue level. Concomitant with the blood changes, a diuresis-induced loss of salt and plasma volume leads to a decrease in intravascular volume. Increased levels of exercise can stimulate aldosterone, which helps to restore intravascular volume as blood shifts into the central circulation. These changes are usually well tolerated, and cardiac output stabilizes.

Many athletes move to high altitudes to improve their physical conditioning. The primary benefit seems to be an increase in hemoglobin concentration. However, acclimatization rarely results in the same level of physical and mental fitness that was typical of altitudes near sea level. Strenuous exercise and tasks involving memorization remain more difficult, and the ultimate athletic performance depends on the benefits of polycythemia, coupled with training at reduced altitudes where increased work levels can be achieved, resulting in a higher degree of fitness levels [25]. Because of this temporary advantage in training, the USA and several other nations maintain Olympic

Training Centers at high altitudes. Once the athlete returns to lower altitudes, the physiological changes reverse themselves, and the body returns to normal within a relatively short period.

Neurologic responses

Central nervous system changes begin to take place upon exposure to altitude [26]. Initially, various cognitive functions may deteriorate because of acute hypoxemia. Hyperventilation helps counteract the acute hypoxemia, but can also result in a decrease in cerebral blood flow from vasoconstriction. If significant hyperventilation takes place, $PaCO_2$ values in the range of 20 mm Hg or below can result in pathologic vasoconstriction and, at least temporarily, brain cell ischemia. Long-term central nervous system problems, such as memory loss and difficulty with concentration, may be attributed to the combined effects of hypoxemia and intense vasoconstriction. These changes may persist for significant periods of time, and some evidence suggests that some changes may be of a permanent nature [27].

Serious complications of altitude exposure

Acute mountain sickness

The most serious complication that develops in high-altitude exposures is AMS [28]. Typical symptoms include headache, nausea, anorexia, insomnia, and, occasionally, vomiting. Symptoms generally develop within 6 to 12 hours of arrival at altitude, and are more likely to appear when changes in altitude are more abrupt and greater. The condition can be unpredictable, sometimes developing in individuals who have previously made multiple excursions without difficulty. Although hypoxia has often been ascribed as the cause, it does not appear to be the critical part of the etiology. Acute mountain sickness may be more likely to occur in those who are unable to hyperventilate to the same degree as unaffected individuals at a particular altitude. It may also be associated with abrupt increases in pulmonary artery pressures. Prevention of AMS by gradual ascent with intermittent periods of acclimatization is preferable to treatment of the established syndrome or its potentially lethal subcategories. For example, limiting an altitude excursion to 5000–6000 ft (about 1500–1800 m) above msl in the first 24 h seems to provide some protection.

Acute mountain sickness may progress into two syndromes that can prove lethal if not managed aggressively. High-altitude cerebral edema (HACE) is manifested by altitude-related neurologic symptoms, including altered mental status, ataxia, and eventual deterioration to a comatose state; high-altitude pulmonary edema (HAPE), normally seen at altitudes in excess of 11 000 ft (~3350 m), is manifested by the onset of non-productive cough, shortness of breath, tachypnea, pulmonary crackles, and frothy sputum. Management of both syndromes includes the administration of oxygen, and exposure to increased ambient pressure, either by descent or with the temporary use of a portable hyperbaric chamber.

Pharmacologic treatment

A variety of medications may impact the course of these conditions. The sulfa-based, carbonic anhydrase inhibitor diuretic, acetazolamide, induces metabolic acidosis, stimulating ventilation and thereby mimicking the natural respiratory response to altitude, which may assist in hastening acclimatization. Dexamethasone stabilizes central nervous system membranes, and may temporarily delay or lessen the mental status changes seen in HACE until descent can be accomplished. In certain individuals, heightened pulmonary vasoconstriction induces capillary endothelial leak into the extravascular space, further compromising gas exchange. Dexamethasone, phosphodiesterase inhibitors, and beta-agonists have a physiologic basis for treating HAPE and are often used, but no definitive studies have established their efficacy. The calcium channel blocker, nifedipine, may be used for both prophylaxis of HAPE in sensitive people and as a temporizing measure when rapid descent is not immediately possible [29]. The greatest number of altitude-related deaths are caused by HAPE; temporization with oxygen and continuous positive airway pressure (CPAP) while rapidly increasing ambient pressure are mandatory first steps in its treatment.

Hyperbaric exposure

Exposure to increased barometric pressure is an inherent part of commercial and sport diving. Tunnel or bridge construction that employs pressurized caissons, as will some types of mining, also involves working at increased environmental pressures. Hyperbaric chambers, commonly used for treatment of diving injuries, carbon monoxide poisonings, or wound care, are

Table 13.6 Change in pressure with increasing depth

Depth		Pressure		
Feet	**Meters**	**mm Hg**	**lb/in²**	**ATA**
0	0	760	14.7	1
33	10	1520	29.4	2
66	20	2280	44.1	3
99	30	3040	58.8	4
132	40	3800	73.5	5
165	50	4560	88.2	6
198	60	5320	102.9	7

examples of the therapeutic benefits of elevated pressures and subsequent hyperoxia.

In contrast to barometric changes that occur with increases in altitude (from 760 mm Hg or 1 ATA to near 0 mm Hg/0 ATA), pressure changes that occur within the hyperbaric community can be tremendous. Each 33 ft (10.1 m) of seawater (fsw) represents one additional atmosphere of pressure, or 14.7 lb/in² (34 ft ≈ 10.4 m for fresh water). Divers commonly exceed 100 fsw (30.5 m of seawater [msw]), and experimental dives have been conducted to depths in excess of 2000 fsw (610 msw), with pressures exceeding 60 ATA. Table 13.6 illustrates pressure changes seen within the normal range of hyperbaric exposures; as would be expected, significant physiologic adjustments take place.

Basic gas laws

To understand the physiologic changes that can occur under such pressure changes, it is first necessary to understand the physics of the basic gas laws. The behavior of all gases is affected by three primary factors: gas temperature, gas pressure, and gas volume. The interaction of these three factors has been defined in a set of laws known as the *gas laws*. Five of these play a key role within the hyperbaric environment and are detailed below.

(1) *Dalton's Law of Partial Pressure* states that the total pressure exerted by a mixture of gases is equal to the sum of the pressures that would be exerted by each of the gases if it alone were present and occupied the total volume. In a gas mixture, the portion of the total pressure contributed by a single gas is called the partial pressure (Pp) of that gas.

$$P_{Total} = Pp_1 + Pp_2 + \cdots + Pp_n$$

(2) *Boyle's Law of Pressure and Volume* states that, at a constant temperature, the volume of a gas varies inversely with its absolute pressure, while the density of a gas varies directly with absolute pressure.

$$P_1V_1 = P_2V_2 = \text{constant}$$

Boyle's Law is critical because it relates changes in the volume of a gas to changes in diving depth (pressure), and defines the relationship between pressure and volume in breathing gases.

(3) *Charles' Law of Temperature* states that at a constant pressure, the volume of a gas varies directly with absolute temperature. For any gas at a constant volume, the pressure of a gas varies directly with absolute temperature. Simply stated:

$$\frac{P_1}{P_2} = \frac{T_1}{T_2} \qquad \frac{V_1}{V_2} = \frac{T_1}{T_2}$$

At constant volume — At constant pressure

A change in temperature significantly affects the pressure and volume of a gas. When diving in an open environment, water temperature may vary significantly from ambient air temperature, a factor that may have a significant effect on the available gas supply.

(4) *Henry's Law of Solubility* states that the amount of any given gas that will dissolve in a liquid at a given temperature is a function of the partial pressure of the gas and the solubility coefficient of the gas in that particular liquid. As the partial pressure of a gas increases with depth, more gas per unit volume will dissolve into the blood and body tissues. Over time, a new steady state or "saturation" will occur, a process that normally takes 24 h or more.
Henry's law is critical because the additional gas driven into solution by increased pressure at depth must be released in a controlled fashion during the reduction of pressure that occurs during a diver's ascent. It is essential that the body "decompress" at a controlled rate, or gas bubbles can form within the tissues or bloodstream, leading to the development of decompression illness or arterial gas embolism (AGE).

(5) *The General Gas Law* combines the concepts expressed in Boyle's and Charles' laws as follows:

$$\frac{P_1V_1}{T_1} = \frac{P_2V_2}{T_2}$$

Pulmonary effects

Elevated ambient pressure in the absence of a compensatory increase in breathing gas density compresses lung volumes, and occurs during breath-hold dives, but is relatively insignificant in shallow-water diving. In deeper dives, however, such as practiced in the sport of freediving, depths in excess of 200 m have been attained [30], and lung compression becomes a significant factor. In most hyperbaric exposures, the subject continues to breathe and, as depth increases, inspired and expired gas densities increase, thereby compensating for changes in volume, and no lung collapse actually occurs. As gas density increases, however, so does the work of breathing. Divers use demand valves with high flow rates to help overcome the higher resistance, but at greater depths, even this is not sufficient. Nitrogen in the breathing mixture becomes so dense that normal breathing becomes impossible. For these dives, helium is substituted due to its decreased density and ease of breathing.

In accordance with the gas laws, as depth increases, both the total pressure and partial pressure of any individual gas rise. Nitrogen, in a standard diving mixture, begins to produce feelings of elation and euphoria at a depth around 30 msw. It produces a condition known as *nitrogen narcosis* and, at deeper depth, poses a significant hazard to the diver. Even oxygen becomes toxic at high concentrations. Oxygen, at normal concentrations, does not usually pose a hazard in sport diving at depths less than 120 fsw. However, as divers go deeper, stay longer, or use increased concentrations of oxygen to minimize their decompression requirements, they begin to enter the realm of oxygen toxicity. In addition to long-term pulmonary changes that can be induced by increased oxygen exposures, acute exposure to sufficiently high levels of O_2 can induce toxicity-related seizures, often preceded by nausea, chewing motions, vision disturbances, and altered mental status [31]. In these situations, the patient should be removed from the high O_2 environment. With immediate care, these symptoms are self-limited and have no long-term effects.

For example, the simplified alveolar gas equation [$P_AO_2 = FiO_2 (P_{atm} - pH_2O) - (P_ACO_2/RQ)$] would predict that 100% O_2 at sea level (1 ATA) would imply a P_AO_2 of about 663 mm Hg, calculated as (760–47)–(40/0.8), where 47 mm Hg equals water vapor at 37 °C, 40 mm Hg equals P_ACO_2, and 0.8 equals the respiratory quotient (RQ).

At a depth of 99 fsw, the ATA is 4. Assuming that neither water vapor pressure nor PCO_2 change significantly, the equation then becomes [$P_AO_2 = (3040 - 47) - (40/0.8)$], or an oxygen partial pressure of 2943 mm Hg. Breathing 100% oxygen at depth is very hazardous, and both depth and time exposures must be limited. Certain military groups use closed circuit diving equipment to prevent the escape of bubbles that might give away the swimmer's presence or pinpoint his position under water. In addition to reusing oxygen, the rig is designed to monitor and eliminate CO_2 through the use of specially designed and efficient CO_2 monitoring and elimination systems. Failure of these systems could lead to high levels of CO_2 in the circuit and the development of a wide range of symptoms, ranging from simple headache and confusion to complete disorientation, unconsciousness, and even death. Sport divers most often use an open circuit breathing apparatus, simply exhaling CO_2 into the water; although there are a number of commercially available diving rigs that are being used by more adventurous sport divers.

Decompression sickness and arterial gas embolism

Both decompression sickness (DCS) and AGE are forms of barotrauma and are treated in a similar fashion, but the underlying pathologies are quite different. Arterial gas embolism tends to be more rapid in onset and more severe in its initial presentation while DCS tends to develop more slowly and be less severe. Severe forms of DCS, however, may develop quite rapidly, and mimic a major embolism. Additionally, it is possible to suffer from both DCS and AGE at the same time.

Decompression sickness (DCS)

DCS is an illness resulting from the precipitation of gases previously dissolved in the blood or tissues into bubbles that escape into various tissue compartments upon depressurization. In keeping with Henry's law of solubility, an increase in ambient pressure will increase the solubility of all inhaled gases in tissue and blood. If ambient pressure is reduced too rapidly, excess gas bubbles out of solution, and cannot exit the body through the normal route of elimination.

Consider air, with nitrogen and oxygen as our primary example. Although nitrogen is inert, more will be dissolved in blood and tissues at the higher pressures experienced by the diver. The amount taken up during

the dive depends on the depth, duration, and activity level. With ascent from depth, nitrogen must move from the tissues, back into the blood, before it can be moved to the lungs and exhaled. Failure to follow prescribed ascent rates and decompression stops can result in the nitrogen coming out of solution too rapidly, thereby forming microbubbles [32]. Depending upon the amount of nitrogen dissolved into the tissues and the rate at which a diver ascends in excess of the body's ability to eliminate it, varying amounts of gas will escape from tissues and form bubbles. These bubbles can occlude flow to various structures and lead to specific symptoms, depending upon the anatomical structures involved, resulting in more or less severe patterns of illness.

DCS is usually classified as simple or non-neurologic (Type 1), involving joint pain, mottling of the skin, or lymphatic symptoms, or as the more serious neurologic (Type II) DCS involving the central nervous system. The distinction may be moot, as many have argued that it is a continuum with varying expression of symptoms [33]. Blood flow to the lung is usually not affected, and any change in P_ACO_2 normally results from specific breathing patterns. The exception is a severe form of pulmonary DCS, known as the "chokes," which results from a sudden, massive blocking of the pulmonary arterial circulation by bubbles. The breathing pattern becomes rapid and shallow, and cyanosis may develop as the disorder rapidly progresses to right-sided heart failure and cardiovascular collapse.

Air embolism (AGE)

AGE refers to an overpressurization accident. At depth, a diver breathes gas at an increased density. In keeping with Boyle's law of pressure and volume, as the diver ascends, ambient pressure drops, and the volume of gas in the lungs begins to increase. The increased volume must be exhaled to prevent overpressurization of the pulmonary tissues. If a diver ascends too rapidly, or attempts to ascend while holding his or her breath, the expanding gas will rupture an internal structure such as a bronchiole or alveolus, introducing gas bubbles directly into the vascular system. The resulting blockade of various regions of blood flow produces a variety of symptoms.

Air embolisms may also occur in the clinical setting, primarily during the placement of central venous lines, or during open heart surgery. Introduction of air directly into the central circulation, regardless of its origin, poses a significant risk to the patient. It is in such clinical situations where capnography may play a significant role, as an AGE can affect expired CO_2 [34]. A sudden loss or reduction of the monitored end-tidal CO_2 ($P_{ET}CO_2$) may be the first indication that a significant amount of air was introduced into the vascular system; at this point, it is affecting pulmonary flow.

Definitive treatment for both DCS and AGE consists of placing the patient in a hyperbaric chamber and pressurizing to a specified depth. Treatment consists not only of repressurization, but also of intermittent periods where the patient breathes high partial pressures of oxygen. Depending upon the severity of the DCS, different tables may be used, but for a known AGE, initial recompression to a depth of 165 fsw (6 ATA), with a slow and gradual decompression, is normally recommended. This volume is considered sufficient to reduce any discrete bubbles to a size that allows passage through the capillary beds. Ultimately, these highly compressed bubbles will dissolve and be exhaled.

While in the chamber, intermittent periods of breathing 100% O_2 provide a secondary benefit [35,36]. The high blood oxygen levels stimulate vasoconstriction, which in turn reduces blood flow to tissue, particularly to neural tissue. This mechanism may reduce edema in important structures such as the spinal cord, often contributing to a better outcome.

Carbon dioxide elimination

Carbon dioxide is the main chemical stimulus to breathing, and is closely regulated to keep blood and brain acidity at normal levels. Indeed, ventilatory failure is defined as the condition in which the lungs are unable to meet the metabolic demands of the body as far as CO_2 homeostasis is concerned [37]. If CO_2 in the lungs increases by only 0.2%, minute ventilation may be doubled. Humans can tolerate acute increases in PCO_2 up to 80 mm Hg and chronic elevations up to 140 mm Hg [38]. The signs and symptoms of toxic PCO_2 relate first to respiratory acidosis. Profound vasodilation ensues and, ultimately, an anesthesia-like state of narcosis may develop.

The elimination of CO_2 can be a major problem in a closed hyperbaric environment; thus, monitoring for and maintaining normal levels of ambient CO_2 in any enclosed environment becomes critical.

Depending upon their design, hyperbaric chambers may rely on continuous ventilation to maintain a safe CO_2 level, or have complex CO_2 monitoring and removal systems. In a standard hyperbaric chamber,

ambient CO_2 levels are controlled by periodic or continuous flushing of the atmosphere while carefully maintaining desired depth. During periods where the divers are breathing oxygen by mask, an overboard dump of exhaled gases is provided, which avoids the need for venting during these periods.

Saturation diving systems and other enclosed environmental systems, such as submarines and small submersibles, are more complex and rely on a number of oxygen generators and high capacity CO_2 scrubbers to maintain a breathable atmosphere. These will be discussed in Chapter 27 (Atmospheric monitoring outside the healthcare environment and within enclosed environments: a historical perspective).

Carbon dioxide monitoring and ambient pressure

Depending on the type of technology selected, CO_2 monitoring may be affected by ambient pressure. Infrared analysis and mass spectroscopy are the most common technologies used to monitor end-tidal CO_2. Differences in methods of measurement and units displayed by different commercial monitors (volume percent versus partial pressure) complicate the interpretation of data at varying ambient pressures. To meet the standards published by the International Organization for Standardization (2004) [39], a capnometer should either provide automatic compensation for barometric pressure, or the accompanying documents should explain that the readings in "concentration units" are correct only under the pressure at which the device is calibrated.

Capnometers measure either partial pressures (infrared analyzers) or percent volumes (mass spectroscopes) of gases. Clinicians are accustomed to CO_2 levels expressed as partial pressures; therefore, monitors that measure percent volumes of gases usually display the partial pressure calculated by the following formula:

$$PCO_2 = (\%\ \text{volume}\ CO_2) \times (\text{barometric pressure} - 47\ \text{mm Hg})$$

where 47 mm Hg = water vapor pressure at 37 °C.

Monitors that measure partial pressures are calibrated using a sample gas with a known concentration of CO_2. For example, a monitor calibrated at sea level against a sample gas containing 5% of CO_2 by volume might be set to read 38 mm Hg by using the following formula:

$$PCO_2 = 0.05 \times 760\ \text{mm Hg}.$$

To clarify the effect of ambient pressure on partial pressure and concentration of CO_2, imagine a hypothetical subject who is breathing 100% O_2 at steady minute ventilation. Assume that the end-tidal breath has 5% CO_2, and that a unit volume of end-tidal gas has 100 molecules, of which 5 molecules are CO_2 and 95 molecules are O_2 and water vapor. If the ambient pressure is reduced to 0.50 ATA, there will only be a total of 50 molecules in the same unit volume of end-tidal gas. Since CO_2 production is unaffected by changes in ambient pressure, 5 molecules of CO_2 will still be present in the end-tidal gas sample. The ratio, however, becomes 5 of 50 (or 10%). If the same subject is then compressed to an ambient pressure of 2 ATA, a total of 200 molecules will be present in the same original unit volume. There will be 195 molecules of O_2 and water vapor combined, while the same 5 molecules of CO_2 will be produced. The ratio of CO_2 in the end-tidal gas becomes 5 of 200 (or 2.5%).

Altitude

Capnometers with infrared analyzers report PCO_2 values [40]. If the end-tidal gas sample with a CO_2 concentration of 5% reaches an instrument that is calibrated at sea level, it would display a PCO_2 of 38 mm Hg. In this regard, it would display the correct PCO_2 regardless of ambient pressure. If, however, the device was set to display the *fraction* of CO_2 instead of *partial pressure*, the actual ambient pressure must be known and would directly affect the accuracy of the result [41]. For example, at 0.5 ATA in the previous example, the concentration of CO_2 would read 10%. It is important to note that this *is* an accurate value, physiologically equivalent to an end-tidal CO_2 concentration of 5% at sea level. However, clinicians do not ordinarily think of physiologic values in relation to the barometric pressure.

To avoid errors in clinical management, one of the following steps can be taken. In order of preference, these are:

(1) Adjust the device to read partial pressure instead of concentration; after calibration, it will be accurate at any altitude.
(2) Calibrate the device at altitude with a known gas CO_2 concentration; the device will then display the percentage of CO_2 as it would be measured at sea level.
(3) Interpret the displayed CO_2 concentration in accordance with the actual barometric pressure, which should prompt the clinician to regard 10% of CO_2 at 0.5 ATA equal to 5% at sea level (1 ATA).

We do not encourage this last option because it could lead to confusion and misinterpretation among different members of a healthcare team.

Mass spectrometers measure the volume percent of dry gases. Therefore, the partial pressure of end-tidal CO_2 ($PETCO_2$) is computed and displayed by the machine using the following formula:

PCO_2 = volume ratio of CO_2 × barometric pressure.

It is obvious that a capnometer using mass spectroscopy must allow altitude compensation, displaying accurate values in ambient pressures other than 1 ATA.

Hyperbaric chamber

As long as the monitoring device shares the same ambient pressure as the patient (i.e., in the chamber), the logic discussed above for altitude remains valid in hyperbaric chambers with increased ambient pressures [42,43]. However, many chambers place the analyzer outside the chamber, complicating data interpretation. Let us return to the example of the hypothetical 5 molecules of CO_2 and 95 molecules of O_2 and water combined in the same unit volume of gas. As this volume exits the chamber – accompanied by ambient pressure changes to atmosphere – the unit volume *expands* to twice its original volume, yielding a final CO_2 concentration of 2.5% at the measurement site. Therefore, although the subject still has a $PETCO_2$ of 38 mm Hg *inside* the chamber, it is measured as 17.5 mm Hg by the capnometer *outside* the chamber. The actual PCO_2 inside the chamber can be calculated using the following formula:

$$\text{Actual } PCO_2 = PCO_2 \times (\text{chamber pressure/ambient pressure})$$

In summary, end-tidal CO_2 can be reliably and accurately monitored at altitude or in the hyperbaric setting by any of the available techniques provided that the basic physical properties of the gas mixtures and the principles of the chosen technique are recognized.

References

1. Shapiro BA, Harrison RA, Cane RD, Kozlowski-Templin BA. *Clinical Application of Blood Gases*, 4th edn. Chicago, IL: Year Book Medical Publishers, 1989.
2. Moore LG. Human genetic adaptation to high altitude. *High Alt Med Biol* 2001; **2:** 257–79.
3. Aerospaceweb. Airline cabin pressure. Available online at http://www.aerospaceweb.org/question/atmosphere/q0206a.shtml. (Accessed February 16, 2010.)
4. Palomar College, San Marcos, CA. Adapting to high altitude. Available online at http://anthro.palomar.edu/adapt/adapt_3.htm. (Accessed February 16, 2010.)
5. Westerterp-Plantenga MS. Effects of extreme environments on food intake in human subjects. *Proc Nutr Soc* 1999; **58:** 791–8.
6. National Geographic News. Three high-altitude peoples, three adaptations to thin air. Available online at http://news.nationalgeographic.com/news/2004/02/0224_040225_evolution.html. (Accessed February 16, 2010.)
7. Pretorius HA. Effect of oxygen on night vision. *Aerosp Med* 1970; **41:** 560–2.
8. Lambertsen C. Chemical control of respiration at rest. In: Mountcastle V (ed.) *Medical Physiology*. St Louis, MO: CV Mosby, 1968; 713–63.
9. Mcdonald D. Peripheral chemoreceptors. In: Hornbein T (ed.) *Regulation of Breathing*. New York: Marcel Dekker, 1981; 305–19.
10. Weil JV. Ventilatory control at high altitude. In: Cherniack NS, Widdicome JG (eds.) *Handbook of Physiology*. Bethesda, MD: American Physiologic Society, 1986; 703–27.
11. Schoene RB, Lahiri S, Hackett PH, *et al.* Relationships of hypoxic ventilatory response and exercise performance on Mt. Everest. *J Appl Physiol* 1984; **56**: 1478–83.
12. Kennedy RS, Dunlap WP, Banderet LE, Smith MG, Houston CS. Cognitive performance and deficits in a simulated climate of Mount Everest: operation Everest II. *Aviat Space Environ Med* 1989; **60**: 99–104.
13. Gerard AB, McElroy MD, Taylor MJ, *et al.* 6% oxygen enrichment of room air at simulated 5000 m altitude improves neuropsychological function. *High Alt Med Biol* 2000; **1**: 51–61.
14. Hultgren H. *High Altitude Medicine*. San Francisco, CA: Hultgren Publications, 1997; 5–32, 212–55.
15. Severinghaus JW, Mitchell RA, Richardson BW, Singer MM. Respiratory control at high altitude suggesting accurate transport regulation of cerebral spinal fluid pH. *J Appl Physiol* 1963; **18**: 1155–66.
16. West JB. Diffusing capacities of lung for carbon monoxide high altitude. *J Appl Physiol* 1962; **17**: 421–6.
17. Wren X, Robbins PA. Ventilatory responses to hypercapnia and hypoxia after six hours past the hyperventilation in humans. *J Appl Physiol* 1999; **514**: 885–94.

18. Ward MP, Milledge JS, West JB. *High Altitude Medicine and Physiology*, 3rd edn. New York: Oxford University Press, 2000; 50–64.
19. West JB. Diffusing capacities of the lung for carbon monoxide at high altitude. *J Appl Physiol* 1962; **17**: 421–6.
20. Maggiorini M, Leon-Velarde F. High-altitude pulmonary hypertension: a pathophysiological entity to different diseases. *Eur Respir J* 2003; **22**: 1019–25.
21. Shapiro BA, Harrison RA, Cane RD, Kozlowski-Templin BA. *Clinical Application of Blood Gases*, 4th edn. Chicago, IL: Year Book Medical Publishers, 1989; 74.
22. Etozzi CA, Poiani GJ, Harangozo AM, Boyd CD, Riley DJ. Pressure-induced connective tissues synthesis in pulmonary artery distal segments is dependent on intact endothelium. *J Clin Invest* 1989; **84**: 1005–12.
23. Bärtsch P, Simon J, Gibbs R. Effect of altitude on the heart and the lungs. *Circulation* 2007; **116:** 2191–202.
24. Reynafarje C, Ramos J, Faura J, Villavivencio D. Humoral control of the erythropoietic activity in man during and after altitude exposure. *Proc Soc Exp Biol Med* 1964; **116**: 649–50.
25. Gore CJ, Hahn AG, Watson DB, *et al.* VO_2 max and arterial oxygen saturation at sea level and at 610 m [abstract]. *Med Sci Sport Exerc* 1996; **27** (Suppl): 42.
26. Hornbein TF, Townes BD, Schoene RB, Sutton JR, Houston CS. The cost to the central nervous system of climbing to extremely high altitude. *N Engl J Med* 1989; **321**: 1714–19.
27. Fields DR. Into thin air: mountain climbing kills brain cells – the neural cost of high altitude mountaineering. *Scientific American Mind* 2008; April issue. Available online at http://www.scientificamerican.com/article.cfm?id=brain-cells-into-thin-air. (Accessed February 16, 2010.)
28. Hackett PH, Bertman J, Rodriguez G. Pulmonary edema fluid protein in high altitude pulmonary edema. *JAMA* 1986; **256**: 36.
29. Dietz TE. An Altitude Tutorial: International Society for Mountain Medicine. Available online at http://www.ismmed.org/np_altitude_tutorial.htm. (Accessed February 16, 2010.)
30. Haas C. Current Freediving World Records. Impulse Adventure. Available online at http://www.impulseadventure.com/freedive/world-record.html. (Accessed February 16, 2010.)
31. Butler FK, Thalmann ED. Central nervous system oxygen toxicity in closed-circuit scuba divers II. *Undersea Bio Med Res* 1986; **13**: 193–223.
32. Vann RD, Thalmann ED. Decompression physiology and practice. In: Bennett PB, Elliott DH (eds.) *Physiology of Diving in Compressed Airwork*, 4th edn. London: WB Saunders, 1993; 376–432.
33. Adkisson GH, Macleod MA, Hodgson M, *et al.* Cerebral perfusion deficits in dsybaric illness. *Lancet* 1989; **2**: 119–22.
34. Schaffer KE, McNulty WP Jr., Carey C, Liebow AA. Mechanisms in development of intrastitial emphysema and air embolism on decompression from depth. *J Appl Physiol* 1958; **13**: 15–29.
35. Moon RE. Treatment of decompression sickness and arterial gas embolism. In: Bove AA, Davis JC (eds.) *Diving Medicine*. New York: WB Saunders, 1990; 184–204.
36. Wolf HK, Moon RE, Mitchell PR, Burger PC. Barotrauma and air embolism in hyperbaric oxygen therapy. *Am J Forensic Med Pathol* 1990; **11:** 149–53.
37. Shapiro BA, Harrison RA, Cane RD, Kozlowski-Templin BA. *Clinical Application of Blood Gases*, 4th edn. Chicago, IL: Year Book Medical Publishers, 1989; 49.
38. Hicking KG, Walsh J, Henderson S, Jackson R. Low mortality rate in adult respiratory distress syndrome using low-volume, pressure-limited ventilation with permissive hypercapnia: a prospective study. *Crit Care Med* 1994; **22**: 1568–78.
39. International Organization for Standardization. *ISO 2164: Medical Electrical Equipment: Particular Requirements for the Basic Safety and Essential Performance of Respiratory Gas Monitors*. Geneva: ISO, 2004.
40. Dorsch JA, Dorsch SE. Gas monitoring. In: Dorsch JA, Dorsch SE (eds.) *Understanding Anesthesia Equipment*, 5th edn. Philadelphia, PA: Lippincott Williams and Wilkins, 2008; 685–726.
41. James MFM, White JF. Anesthetic considerations at moderate altitude. *Anesth Analg* 1984; **63**: 1097–105.
42. Arieli R, Daskalovic Y, Eynan M, *et al.* Use of a mass spectrometer for direct respiratory gas sampling from the hyperbaric chamber. *Aviat Space Environ Med* 2001; **72**: 799–804.
43. Mummery HJ, Stolp BW, del Dear G, *et al.* Effects of age and exercise on physiological deadspace during simulated dives at 2.8 ATA. *J Appl Physiol* 2003; **94**: 507–17.

Section 1
Chapter
14

Ventilation

Biofeedback

A. E. Meuret

Hypocapnia and the role of capnometry as a therapeutic tool

Hypocapnia has been experimentally linked to organ injury and a number of other organic illnesses and mental disorders. Reversing hypocapnia, with the goal of achieving normocapnic levels, has been hypothesized to be beneficial for these conditions [1].

In the following text, we describe several conditions that have been associated with hypocapnia and in which capnography biofeedback may present a viable biobehavioral treatment option.

Panic disorder

Based on patient reports and on a variety of other clinical and experimental observations, abnormalities in respiration have been postulated as a central component in anxiety disorders for several decades. Shortness of breath, together with palpitations and faintness, has been found to be one of the most commonly reported symptoms of panic [2,3]. Dyspnea, accompanied by hyperventilation, may contribute to the development and maintenance of panic disorder (PD) [4]. A biological vulnerability due to an abnormal brainstem respiratory control mechanism may trigger a false suffocation alarm, resulting in compensatory hyperventilation and panic attacks [5]. In addition, hyperventilation may not be limited to the attack itself, but may precede and follow it, giving rise to moderate sustained hypocapnia [6]. According to this hypothesis, the cause of seemingly spontaneous panic attacks is often chronic or episodic hyperventilation, of which the patient is generally not aware.

Hypocapnia has repeatedly been identified as distinguishing PD patients from other groups during baseline assessment [7,8]. Standardized voluntary hyperventilation generally increases anxiety, and produces symptoms similar or identical to panic attacks [9]; however, it remains uncertain whether hyperventilation causes panic attacks or is merely an accompanying phenomenon in some panic patients [10]. Other provocation tests such as lactate infusions [11], inhalation of CO_2 [12], and administration of respiratory stimulants, such as doxapram (Dopram®) [13], produce panic attacks that are often accompanied by hypocapnia.

It may seem obvious that therapy that provides continues feedback and monitoring of $P_{ET}CO_2$ would be the most viable option to reverse hypocapnia; however, the majority of treatment studies do not use objective measurements of $P_{ET}CO_2$. Exceptions are studies such as the one by Salkovskis *et al.* [14]. The authors used repeated $P_{ET}CO_2$ measurements to test whether patients suffering from panic attacks had lower resting $P_{ET}CO_2$ levels before treatment, and whether these levels increased during treatment. Psychological outcome variables (panic attack frequency and self-report of anxiety and avoidance) showed a marked improvement compared to baseline. Levels of $P_{ET}CO_2$ increased from 35 mm Hg at baseline to approximately 41.5 mm Hg during the course of the therapy. The authors concluded that respiratory training can restore a patient's $P_{ET}CO_2$, and may thus reduce their previously heightened vulnerability to psychological stressors. More recent studies exploring the effectiveness of a novel capnometry-assisted biofeedback respiratory training for PD are discussed below.

Asthma

Ventilatory changes exacerbate asthmatic symptoms. Breathing patterns with deep inspirations, increased minute ventilation, increased respiratory drive, or decreased $P_{ET}CO_2$ are linked to airway obstruction in

Capnography, Second Edition, ed. J. S. Gravenstein, Michael B. Jaffe, Nikolaus Gravenstein, and David A. Paulus. Published by Cambridge University Press. © Cambridge University Press 2011.

asthma [15,16]. Hypocapnic breathing can also play a key role in exacerbations of asthma during episodes of stress, anxiety, or panic [17]. The increase in respiratory drive through excessive deep breathing also leads to a subjective experience of dyspnea [18]. Asthmatics respond with excessive increases in respiratory drive to challenges such as physical exercise [19,20] and added resistance to airflow [21]. Increased respiratory drive or minute ventilation puts patients at risk for becoming hypocapnic. Using ambulatory monitoring of respiration, we found that RR increased and $PETCO_2$ decreased in asthma patients compared to healthy controls [22]. Similarly, others have observed statistically significant reductions in $PETCO_2$ in mild chronic asthmatics, with no accompanying symptoms of hyperventilation [23]. The level of $PETCO_2$ was negatively correlated with airway hyperreactivity to methacholine provocation. Thus, a deep breathing pattern with high minute volume and/or lowered $PETCO_2$ can lead to subjective and physiologic changes contributing to exacerbations of asthma.

Breathing training and biofeedback have long been advocated as adjunctive treatment in asthma [24,25]. The Buteyko breathing technique is suggested as a tool to improve the asthma patient's quality of life. Patients are taught to breathe slowly and shallowly to increase their $PETCO_2$ levels. The basic assumption is that decreased $PETCO_2$ leads to a number of autonomic, endocrine, and metabolic disturbances that contribute to the pathophysiology of asthma [26].

Three controlled trials of asthmatics demonstrated increases in quality of life as measured by standardized questionnaires and/or a reduction in bronchodilator use [27–29]. Bowler *et al.* reported significant decreases in minute ventilation in the Buteyko breathing training group, but parameters of mechanical lung function and $PETCO_2$ levels remained constant [27]. The two other studies did not incorporate measures of $PETCO_2$, and thus were not able to test the main treatment rationale. A recent study exploring the effectiveness of capnometry-assisted biofeedback training for asthma will be discussed below.

Epilepsy

Cerebral hypoxia accompanying hypocapnic breathing has been hypothesized as a possible cause of seizures in epilepsy [30]. A successful strategy of seizure control would be normalization of the $PaCO_2$ level. Particularly in patients intolerant to the physiologic effects of respiratory alkalosis, the restoration of acid–base balance could be crucial in controlling seizure thresholds. Fried *et al.* developed a method to train idiopathic seizure sufferers to self-regulate $PaCO_2$ levels through diaphragmatic breathing techniques [31]. They used stationary equipment to measure RR and $PETCO_2$. Visual feedback of both parameters was provided on a video monitor, and the goal for adequate breathing was set at 5% $PETCO_2$ and 12–14 breaths/min. Following at least 7 months of diaphragmatic breathing training supported by feedback of $PETCO_2$, a group of 18 patients showed significant decreases in RR and seizure frequency; however, they showed no significant long-term change in $PETCO_2$. Therefore, the hypothesized mechanism of seizure control by CO_2 levels was not supported by the study, and the potential benefits of stable long-term increases in $PETCO_2$ levels could not be investigated. Further, due to incomplete description of the treatment protocol (e.g., no information on duration, number, and frequency of training sessions), data analysis, and the lack of a treatment-control group, the results must be interpreted with caution.

Hyperventilation syndrome

The clinical literature abounds with observations of patients presenting with complaints for which no organic origin is apparent. One group of hyperventilation patients, for example, complain of feeling dyspneic, breathless, dizzy, and light-headed, and report chest pain, heart racing, and/or sweating. It has been proposed that hypocapnia and disturbance of the acid–base balance are the underlying origin of these symptoms [6]. Hyperventilation syndrome (HVS) has become a common designation for the constellation of complaints of these patients. It exists in at least 5–10% of general medical outpatients [32]. The breathing pattern of these patients is typically described as disorganized, with rapid respiratory rates, frequent sighing, low $PaCO_2$ levels, and an emphasis on thoracic rather than abdominal breathing. Patients often feel anxious and depressed. In rare cases, fear of losing consciousness or dying is reported [33].

Earlier therapeutic approaches considered the utility of measuring $PETCO_2$ levels during therapy sessions. Folgering *et al.* [34] and van Doorn *et al.* [35] were among the first to use feedback of $PETCO_2$ levels as a therapeutic tool in HVS. In therapy sessions over the course of 7 weeks, patients were taught to increase $PETCO_2$ levels. Feedback was provided through a two-channel chart recorder while the patients breathed into

a face mask. Compared to patients receiving breathing training without feedback, the feedback training group improved symptomatically and showed significant, sustained increases in $P_{ET}CO_2$ (from approximately 32 to 39 mm Hg). Similarly, in a study by Grossman *et al.*, a stationary CO_2 infrared gas analyzer was used during clinical sessions [36]. The authors demonstrated improvement in both symptom reports and physiological measures.

Agreement about criteria for HVS as a distinct diagnostic entity has never been reached [37]. Furthermore, recent research has questioned the validity of HVS by demonstrating a lack of psychological and physiological specificity of the purported signs and symptoms [38]. For these reasons, no attempts have been made to replicate or extend early innovative interventions in treating chronic hypocapnic breathing.

Novel biobehavioral treatment applications for ambulatory capnometry

Capnometry-assisted respiratory training for panic disorder

Rationale

Given the assumed central role of hypocapnia in panic development and maintenance, capnometry-assisted respiratory training (CART) was developed as a novel, non-pharmacological treatment to counteract the respiratory abnormalities observed in PD. This technique targets respiratory dysregulation, in particular hypocapnia [39–41]. The treatment is a brief 4-week training period that uses immediate feedback of $P_{ET}CO_2$ to teach patients how to raise their subnormal levels of $P_{ET}CO_2$ (hypocapnia/hyperventilation), and thereby gain control over dysfunctional respiratory patterns and associated panic symptoms (e.g., shortness of breath, dizziness). Patients use a portable capnometer for targeting and directly monitoring $P_{ET}CO_2$, the essential feature of hypocapnia.

CART is different from traditional breathing retraining because it focuses directly on the critical variable, $P_{ET}CO_2$ (for a review, see Meuret *et al.* [42]). As discussed earlier, previous breathing training studies have rarely included measurements of $P_{ET}CO_2$ levels, and were thus unable to address the validity of their main underlying rationale for change in therapy. Slow breathing, as is taught in most traditional breathing retraining approaches [43,44], is likely to lead to compensatory deeper breathing that exacerbates hyperventilation [42,45,46], and further intensifies hypocapnic symptoms. We assumed that lasting modifications in breathing behavior and $P_{ET}CO_2$ levels would require intensive breathing retraining combined with close monitoring of relevant breathing parameters. Because sufficiently frequent practice sessions were not practical in a clinic environment, training and monitoring methods had to be adapted to a home environment. Training at home also facilitates the transfer of learned breathing behavior to everyday life situations. The advent of small hand-held capnometers with electronic memory has been a major step towards the implementation of $P_{ET}CO_2$ home training protocols.

Methodology

This capnometry-assisted respiratory therapy is aimed at regulating respiration – and thus reducing symptoms – in PD. Patients use a light, hand-held, battery-operated capnometry device to monitor and modify their $P_{ET}CO_2$. When activated, the instrument continuously displays and records $P_{ET}CO_2$, RR, heart rate, and oxygen saturation (O_2). It stores this information, along with the exact time and date of the measurement. Stored data can be downloaded to a computer through an interface module.

To increase their $P_{ET}CO_2$, patients learned to breathe abdominally and regularly at a decreased rate. Prerecorded audiotapes with pacing tones were used to guide the breathing exercises. Increasing tones indicated inspiration; decreasing tones, expiration; and silence indicated a pause between expiration and inspiration. Respiratory rate was successively decreased across the 4 weeks of training. The tone pattern was modulated to correspond to a RR of 13 breaths/min in the first treatment week, and rates of 11, 9, and 6 breaths/min in the successive weeks. Patients were instructed to practice this highly standardized breathing twice a day for 17 min. Each exercise consisted of three parts: (A) a baseline period during which patients sat in a relaxed and quiet state with their eyes closed for 2 min; (B) a 10-min paced breathing period during which patients monitored their $P_{ET}CO_2$ and RR; and (C) a 5-min transfer phase without pacing tones during which patients maintained the previous breathing pattern in the absence of timing information, but with continued $P_{ET}CO_2$ and

RR feedback. Timing of these phases and instructions were announced on the tape guiding the exercises. During the second and third exercise period, patients were instructed to aim for increased $P_{ET}CO_2$ levels by changing their breathing rhythm, pace, and depth of inspiration.

In addition to the twice-daily home exercises, patients attended five individual training sessions over four weeks. The initial session was mainly educational, while later sessions served to review progress in the daily exercises. Using a docking station for the portable capnometry device, the therapist downloaded the physiological data of the exercises recorded during the previous week, and presented the data in graphical printouts to the patient (Figure 14.1)[40]. These were discussed in conjunction with the patient's self-reported physical and emotional symptoms. The application of new breathing skills during difficult situations was also planned and reviewed.

Figure 14.1 illustrates $P_{ET}CO_2$ and RR at three different times in therapy. The upper panel displays the first home breathing exercise. As can be seen, $P_{ET}CO_2$ levels fluctuate around hypocapnic ranges, and RR is increased and irregular. Overall breathing patterns are irregular in pace and rhythm, being interrupted by frequent sighs as indicated by the spikes in momentary RR. The center panel (Figure 14.1b) displays $P_{ET}CO_2$ and RR after a few days of training. The patient is more able to follow the instructions to breathe at a rate of 13 breaths/min. Nevertheless, $P_{ET}CO_2$ decreases markedly to hypocapnic levels (<25 mm Hg) with the onset of the paced breathing phase. At this early stage in therapy, such seemingly paradoxical effects represent the compensatory breathing efforts of the patient: the slowing of RR and the patient's efforts to keep it regular lead to compensatory increases in tidal volume, thus decreasing $P_{ET}CO_2$ levels. According to the patient's diary, the patient often experiences shortness of breath. While this shortness of breath typically increases throughout the 15-min exercise, it gradually abates over the 4 weeks of training. The lower panel of Figure 14.1 shows the progress documented towards the end of the 4-week training. In addition to decreased RR and increased $P_{ET}CO_2$ at baseline, the patient is able to reach and maintain baseline levels of $P_{ET}CO_2$ and RR throughout paced breathing. Overall, the patient breathes regularly in terms of speed and depth.

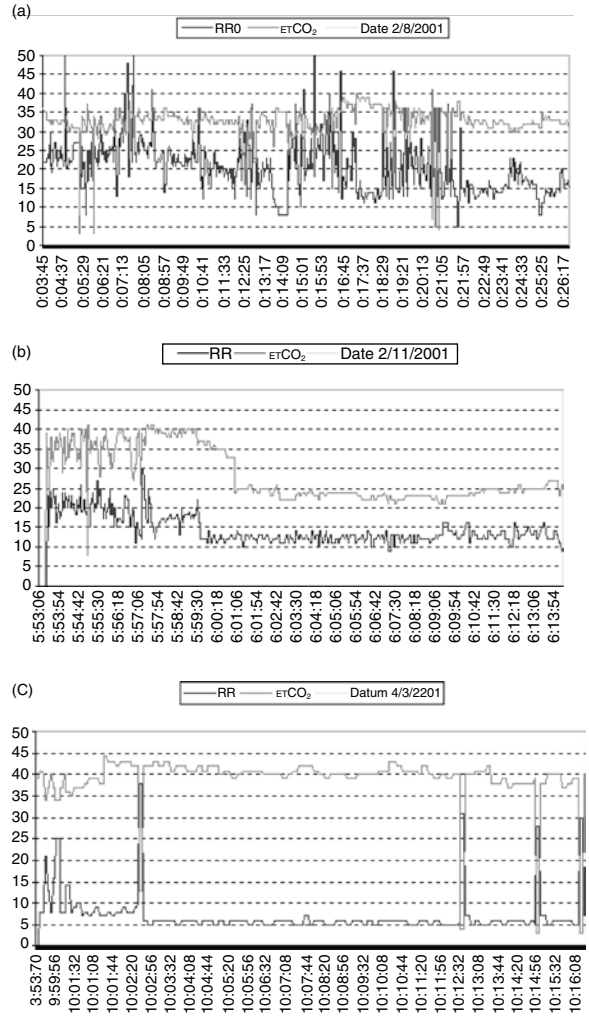

Figure 14.1 Breath-by-breath $P_{ET}CO_2$ and respiratory rate (RR) printouts of exercises performed in the first (upper and middle panel) and last treatment week (lower panel) over the course of the biofeedback breathing exercise for PD. Upper line represents $P_{ET}CO_2$ and lower line represents RR. (a): baseline; (b): paced breathing tones with $P_{ET}CO_2$ feedback; (c): only $P_{ET}CO_2$ feedback.

Results

In two randomized controlled trials (RCT), 4 weeks of CART led to sustained increases in $P_{ET}CO_2$ levels and reduced panic severity and frequency [41,47]. Reductions observed in panic symptoms were comparable to standard cognitive–behavioral therapy (e.g., Barlow *et al.* [48]).

The first RCT was aimed at testing the feasibility and effectiveness of CART. Thirty-seven patients with PD – with or without agoraphobia (PDA) – were

assigned to CART or to a delayed-treatment control group [41]. Clinical status, RR, and $PetCO_2$were assessed throughout treatment and at 2-month and 12-month post-study follow-up assessments. Mean $PetCO_2$ levels were in the hypocapnic range before treatment. Compared to the delayed-treatment control, the CART group improved on all clinical and respiratory measures, with a $PetCO_2$ level increase of approximately 5 mm Hg. Improvements were maintained through follow-up. With 68% achieving panic-free status (as defined by the criteria of the *Diagnostic and Statistical Manual of Mental Disorders* [DSM-IV] [49]) at 12 months follow-up, results were comparable to those achieved in cognitive–behavioral therapy for PDA. Attrition was very low, with no drop-out during the active phase of treatment, two drop-outs (2.8%) at 2-month follow-up, and four (12.1%) at 12-month follow-up. This study offers evidence that raising $PetCO_2$ by means of capnometry feedback is therapeutically beneficial for PDA.

In a follow-up analysis, we further examined the relationship between changes in respiration and changes in self-reported fear of bodily sensations. The results revealed that $PetCO_2$, but not RR, was a partial mediator of changes in bodily symptoms [50]. Results were supported by cross lag panel analyses, a technique for assessing the direct effects of one variable on another over time. The results indicated that, at any assessment time point, levels of $PetCO_2$ predicted level of bodily symptoms at the next assessment point, but not vice versa. Overall, the results suggest that using CART to monitor $PetCO_2$ reduced the fear of bodily sensations, but provided little support that changes in fear of bodily sensations lead to changes in respiration.

In the second RCT, 41 patients diagnosed with PD with agoraphobia were randomly assigned to either 4 weeks of CART or 4 weeks of cognitive training (CT) [47]; only CART led to correction of pretreatment hypocapnia to normocapnic levels. In CART, changes in $PetCO_2$ mediated changes in panic-related cognitions, perceived control, and panic severity, but not vice versa. Cross lag panel analyses supported the mediation results: earlier levels of $PetCO_2$ led to later changes in panic-related cognitions and perceived control, and not vice versa. In CT, changes in misappraisal were associated with – but did not precede nor cause – changes in perceived control (nor vice versa), indicating that the relationship between misappraisal and perceived control was due to unmeasured third variables or to non-specific factors. This was the first study to examine mechanisms of change in the core aspects of panic symptoms in theoretically different interventions. Changes in $PetCO_2$ confirmed the importance of respiratory pathways in our CART treatment for PD.

In summary, there is strong theoretical and clinical evidence to suggest that hypocapnia plays a crucial role in symptom production and maintenance in panic disorder. Capnometry-assisted biofeedback offers viable biobehavioral treatment for patients suffering from panic disorder.

Capnometry-assisted respiratory training as adjunctive treatment for asthma

Rationale

To overcome the deficiencies of earlier hypoventilation training studies in asthma, CART has successfully been adapted to asthma patients [51,52]. Patients with predominantly mild persistent-to-moderate asthma volunteered for breathing training intervention, which was presented as adjunctive behavioral training to supplement their existing medical treatment. They were encouraged to reduce their bronchodilator use, but to keep their other asthma medication constant.

The techniques and protocol followed largely those outlined previously for PD patients. The therapy consisted of five individual sessions of respiratory control training over the course of 4 weeks, with additional homework assignments of two 17-min breathing exercises each day. The therapy rationale outlined the general and asthma-specific adverse effects of overbreathing or hypocapnia. In addition to using the capnometer, patients monitored their lung function and symptoms using a hand-held electronic spirometer, with diary functions for recording ratings of symptoms and mood. Measurements of lung function and symptoms were scheduled before and after each exercise, and during the five therapist-guided sessions.

Results

In this study [50], the first to target $PetCO_2$ levels directly, the feasibility and potential benefits of CART for achieving sustained increases in $PetCO_2$ levels in asthma patients was evaluated. Twelve asthma patients were randomly assigned to either an immediate 4-week treatment group or a waiting-list control group. Patients were instructed to modify their respiration in order to change levels of $PetCO_2$ using the hand-held capnometer. Treatment outcome was

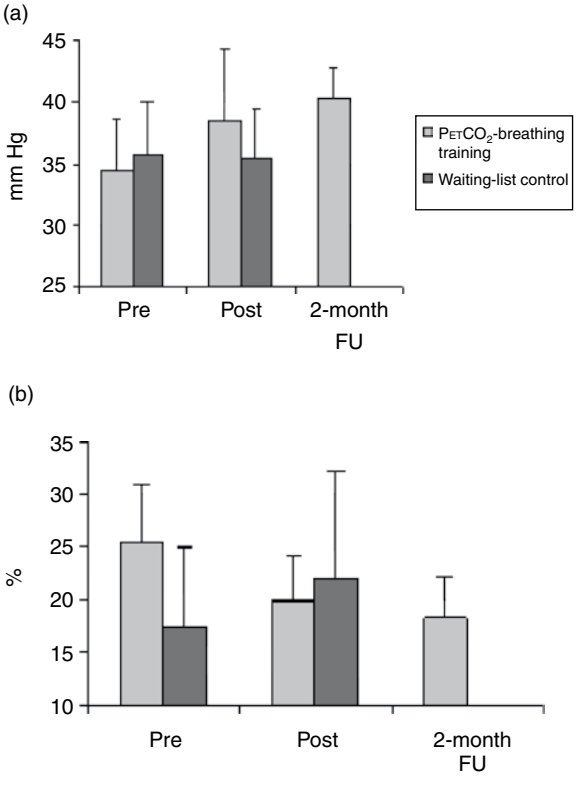

Figure 14.2 Results of a pilot evaluation of the PCO_2-biofeedback training for asthma: (a) $P_{ET}CO_2$; (b) peak expiratory flow (PEF) variability in asthma patients across 4 weeks of $P_{ET}CO_2$-feedback-assisted breathing training ($n = 8$) vs. waiting-list control ($n = 4$). FU = follow-up.

assessed by the following factors: frequency and distress of symptoms, self-reported asthma control, perceived control of asthma, lung function (interrupter resistance, spirometry), and variability of peak expiratory flow (PEF). Following 4 weeks of training with five guided training sessions and twice-daily, 15-min home training, patients in the treatment group showed stable increases in $P_{ET}CO_2$ (Figure 14.2a,) and reductions in RR. These changes were sustained at a 2-month follow-up visit. Mean $P_{ET}CO_2$ levels had increased from a hypocapnic to a normocapnic range, and RR had decreased at follow-up (within-subject effect sizes d = 1.83 and 0.81). Frequency and distress of symptoms were reduced (d = 1.29 and 0.89), and reported asthma control increased (d = 1.01). In addition, mean diurnal PEF variability, which is related to airway hyperreactivity, decreased significantly in the treatment group (d = 0.78) (Figure 14.2b). Little change was found in parameters of basal lung function, although values in respiratory resistance (by interrupter technique) suggested improvements (d = 0.51), although these may have been non-significant due to the small pilot sample size. As in the described RCT studies for PD, credibility and acceptance of the training was very high. Patients reported that the training gave them greater voluntary control over their asthma symptoms, particularly over coughing. Thus, this pilot intervention provided initial evidence for the feasibility and benefits of $P_{ET}CO_2$-biofeedback training in asthma patients.

Capnometry biofeedback: principles and perspectives

Panic and asthma patients in the above-described studies showed clear clinical benefits from using a portable capnometer as a behavioral therapy tool. Patients were able to measure their RR and $P_{ET}CO_2$, as well as O_2 saturation levels at different times of the day and during various situational and emotional states. They not only were better able to understand the mechanism of different breathing maneuvers on symptoms and emotions, but were gradually able to influence and modify these parameters willingly. The direct feedback further allowed the re-evaluation of bodily misconceptions, such as fear of suffocation. This can be particularly important in chronic diseases such as asthma where introspective awareness may be altered and patients are no longer able to detect deteriorations in their physiological state.

Portable capnometry devices facilitate the patient's home training efficiency, self-modification efforts, and treatment compliance by immediate, objective feedback of respiratory parameters. Until recently, a patient's homework compliance and progress outside the therapist's office have rarely been measured systematically because of the lack of affordable and portable devices. Ambulatory capnometry devices with electronic data storage allow the therapist to track a patient's progress without having to rely exclusively on retrospective self-reporting. Self-modification of physiological parameters require more than in-session "snapshots." Monitoring throughout therapy can help health professionals tailor the treatment to the patient's individual needs. It also allows data to be downloaded directly, analyzed, and presented to the patient in therapy sessions. Ambulatory capnometry has the potential to change significantly the behavioral treatment of mental disorders and organic diseases that are linked to respiratory disturbances and hypocapnic breathing. The ongoing development of lighter, less expensive, and user-friendly ambulatory capnometry devices opens

up new possibilities for using capnography as a therapeutic device. However, more research into the application of hypercapnic breathing in clinical therapy is needed before the general therapeutic goal of treating patients can be expressed as "keep the $PaCO_2$ high; if necessary, make it high; and above all, prevent it from being low" [53].

References

1. Laffey JG, Kavanagh BP. Hypocapnia. *N Engl J Med* 2002; **347**: 43–53.
2. McNally RJ, Hornig CD, Donnell CD. Clinical versus nonclinical panic: a test of suffocation false alarm theory. *Behav Res Ther* 1995; **33**: 127–31.
3. Meuret AE, White KS, Ritz T, *et al*. Panic attack symptom dimensions and their relationship to illness characteristics in panic disorder. *J Psychiatr Res* 2006; **6**: 520–7.
4. Ley R. Agoraphobia, the panic attack and the hyperventilation syndrome. *Behav Res Ther* 1985; **23**: 79–81.
5. Klein DF. False suffocation alarms, spontaneous panics, and related conditions: an integrative hypothesis. *Arch Gen Psychiatry* 1993; **50:** 306–17.
6. Lum LC. Hyperventilation syndromes in medicine and psychiatry: a review. *J R Soc Med* 1987; **80:** 229–31.
7. Hegel MT, Ferguson RJ. Psychophysiological assessment of respiratory function in panic disorder: evidence for a hyperventilation subtype. *Psychosom Med* 1997; **59**: 224–30.
8. Munjack DJ, Brown RA, Cabe DD, McDowell DE, Baltazar PL. A naturalistic follow-up of panic patients after short-term pharmacologic treatment. *J Clin Psychopharmacol* 1993; **13:** 156–8.
9. Maddock RJ, Carter CS. Hyperventilation-induced panic attacks in panic disorder with agoraphobia. *Biol Psychiatry* 1991; **29**: 843–54.
10. Garssen B, Buikhuisen M, van Dyck R. Hyperventilation and panic attacks. *Am J Psychiatry* 1996; **153**: 513–18.
11. Gorman J, Battista D, Goetz R, *et al.* A comparison of sodium bicarbonate and sodium lactate infusion in the induction of panic attacks. *Arch Gen Psychiatry* 1989; **46**: 145–50.
12. Papp LA, Martinez JM, Klein DF, *et al.* Respiratory psychophysiology of panic disorder: three respiratory challenges in 98 subjects. *Am J Psychiatry* 1997; **154:** 1557–65.
13. Abelson J, Nesse R. Pentagastrin infusions in patients with panic disorder. I. Symptoms and cardiovascular responses. *Biol Psychiatry* 1994; **36**: 73–83.
14. Salkovskis PM, Jones DR, Clark DM. Respiratory control in the treatment of panic attacks: replication and extension with concurrent measurement of behaviour and PCO_2. *Br J Psychiatry* 1986; **148:** 526–32.
15. Gayrard P, Orehek J, Grimaud C, Charpin J. Bronchoconstrictor effects of a deep inspiration in patients with asthma. *Am Rev Respir Dis* 1975; **111:** 433–9.
16. van den Elshout FJJ, van Herwaarden CLA, Folgering HTM. Effects of hypercapnia and hypocapnia on respiratory resistance in normal and asthmatic subjects. *Thorax* 1991; **46**: 28–32.
17. Knapp PH. Psychosomatic aspects of bronchial asthma: a review. In: Cheren S (ed.) *Psychosomatic Medicine: Theory, Physiology, and Practice*, vol. 2. Madison, CT: International University Press, 1989; 503–64.
18. Mahler DA, Faryniarz K, Lentine T, *et al.* Measurement of breathlessness during exercise in asthmatics: predictor variables, reliability, and responsiveness. *Am Rev Respir Dis* 1991; **144**: 39–44.
19. Ritz T, Dahme B, Wagner C. Effects of static forehead and forearm muscle tension on total respiratory resistance in healthy and asthmatic participants. *Psychophysiology* 1998; **35:** 549–62.
20. Varray A, Prefaut C. Importance of physical exercise training in asthmatics. *J Asthma* 1992; **29**: 229–34.
21. Kelsen SG, Fleegler B, Altose MD. The respiratory neuromuscular response to hypoxia, hypercapnia, and obstruction to airflow in asthma. *Am Rev Respir Dis* 1979; **120**: 517–27.
22. Ritz T, Meuret A, Wilhelm F, Roth WT. End-tidal PCO_2 levels in asthma patients in the laboratory and at home [abstract]. *Biol Psychol* 2003; **62**: 233–4.
23. Osborne CA, O'Connor BJ, Lewis A, Kanabar V, Gardner WN. Hyperventilation and asymptomatic chronic asthma. *Thorax* 2000; **55**: 1016–22.
24. Ritz T, Roth WT. Behavioral interventions in asthma: breathing training. *Behav Modif* 2003; **27:** 710–30.
25. Ritz T, Dahme B, Roth WT. Behavioral interventions in asthma: biofeedback techniques. *J Psychosom Res* 2004; **56**: 711–20.
26. Stalmatski A. *Freedom from Asthma: Buteyko's Revolutionary Treatment.* London: Kyle Cathie, 1999.
27. Bowler SD, Green AG, Mitchell CA. Buteyko breathing techniques in asthma: a blinded randomised controlled trial. *Med J Aust* 1998; **169**: 575–8.
28. Cooper S, Oborne J, Newton S, *et al.* Effects of two breathing exercises (Buteyko and Pranayama) in asthma: a randomized controlled trial. *Thorax* 2003; **58**: 674–9.

29. Opat AJ, Cohen MM, Bailey MJ, Abramson MJ. A clinical trial of the Buteyko breathing technique in asthma as taught by video. *J Asthma* 2000; **37:** 557–64.
30. Riley TI. Epilepsy: or merely hyperventilation? *Emerg Med* 1982; **14**: 162–7.
31. Fried R, Rubin SR, Carlton RM, Fox MC. Behavioral control of intractable idiopathic seizures: self-regulation of end-tidal carbon dioxide. *Psychosom Med* 1984; **46**: 315–31.
32. Magarian GJ. Hyperventilation syndrome: infrequently recognized common expressions of anxiety and stress. *Medicine (Baltimore)* 1982; **61**: 219–36.
33. Howell JB. The hyperventilation syndrome: a syndrome under threat? *Thorax* 1997; **52** (Suppl 3): S30–4.
34. Folgering H, Lenders J, Rosier I. Biofeedback control of $PaCO_2$, a prospective therapy in hyperventilation. In: Herzog H, *et al.* (eds.) *Asthma.* Basel: Karger, 1980; 26–30.
35. van Doorn P, Folgering H, Colla P. Control of the end-tidal PCO_2 in the hyperventilation syndrome: effects of biofeedback and breathing instructions compared. *Bull Eur Physiopathol Respir* 1982; **18**: 829–36.
36. Grossman P, de Swart JC, Defares PB. A controlled study of a breathing therapy for treatment of hyperventilation syndrome. *J Psychosom Res* 1985; **29**: 49–58.
37. Bass C. Hyperventilation syndrome: a chimera? *J Psychosom Res* 1997; **42**: 421–6.
38. Hornsveld HK, Garssen B, Dop MJ, van Spiegel PI, de Haes JC. Double-blind placebo-controlled study of the hyperventilation provocation test and the validity of the hyperventilation syndrome. *Lancet* 1996; **348**: 154–8.
39. Meuret AE, Wilhelm FH, Roth WT. Respiratory biofeedback-assisted therapy in panic disorder. *Behav Modif* 2001; **25**: 584–605.
40. Meuret AE, Wilhelm FH, Roth WT. Respiratory feedback for treating panic disorder. *J Clin Psychol* 2004; **60:** 197–207.
41. Meuret AE, Wilhelm FH, Ritz T, Roth WT. Feedback of end-tidal PCO_2 as a therapeutic approach for panic disorder. *J Psychiatr Res* 2008; **42:** 560–8.
42. Meuret AE, Wilhelm FH, Ritz T, Roth WT. Breathing training for treating panic disorder: useful intervention or impediment? *Behav Modif* 2003; **27**: 731–54.
43. Craske MG, Rowe M, Lewin M, Noriega-Dimitri R. Interoceptive exposure versus breathing retraining within cognitive–behavioural therapy for panic disorder with agoraphobia. *Br J Clin Psychol* 1997; **36:** 85–99.
44. Schmidt NB, Woolaway-Bickel K, Trakowski J, *et al.* Dismantling cognitive–behavioral treatment for panic disorder: questioning the utility of breathing retraining. *J Consult Clin Psychol* 2000; **68:** 417–24.
45. Ley R. The efficacy of breathing retraining and the centrality of hyperventilation in panic disorder: a reinterpretation of experimental findings. *Behav Res Ther* 1991; **29**: 301–4.
46. Conrad A, Müller A, Doberenz S, *et al.* Psycho-physiological effects of breathing instructions for stress management. *Appl Psychophysiol Biofeedback* 2007; **32**: 89–98.
47. Meuret AE, Rosenfield D, Seidel A, Bhaskara L, Hofmann SG. Respiratory and cognitive mediators of treatment change in panic disorder: evidence for intervention specificity. *J Consult Clin Psych* (in press).
48. Barlow DH, Gorman JM, Shear MK, Woods SW. Cognitive-behavioral therapy, imipramine, or their combination for panic disorder: a randomized controlled trial. *JAMA* 2000; **283**: 2573–4.
49. American Psychiatric Association. *Diagnostic and Statistical Manual of Mental Disorders – DSM-IV*, 4th edn. Washington, DC: American Psychiatric Association, 1994.
50. Meuret AE, Rosenfield D, Hofmann SG, Roth WT. Changes in respiration mediate changes in fear of bodily sensations in panic disorder. *J Psychiatr Res* 2009; **43**: 634–41.
51. Meuret AE, Ritz T, Wilhelm FH, Roth WT. Targeting pCO_2 in asthma: pilot evaluation of a capnometry-assisted breathing training. *Appl Psychophysiol Biofeedback* 2007; **32:** 99–109.
52. Ritz T, Meuret AE, Roth WT. Weekly changes in PCO_2 and lung function of asthma patients by paced breathing and capnometry-assisted breathing training in asthma. *Appl Psychophysiol Biofeedback* 2009; **34:** 1–6.
53. Laffey JG, Kavanagh BP. Carbon dioxide and the critically ill: too little of a good thing. *Lancet* 1999; **354**: 1283–6.

Section 1
Chapter
15

Ventilation

Capnography in non-invasive positive pressure ventilation

J. A. Orr, M. B. Jaffe, and A. Seiver

Introduction

Non-invasive positive pressure ventilation (NPPV) – in contrast to invasive positive pressure ventilation (mechanical ventilation with an endotracheal tube) – has been available to treat respiratory failure for over a century [1]. The application of NPPV to the care of acutely ill patients has benefited from the technological progress made in software (e.g., continuous positive airway pressure [CPAP], bi-level) and pneumatics (e.g., blowers) developed for treatment of obstructive sleep apnea (OSA) and obesity hypoventilation syndrome (OHS). In particular, the widespread adoption of bi-level CPAP to treat OSA at home has facilitated the application of NPPV to respiratory failure in the hospital. Technological developments in microprocessors and graphic displays as embodied in the latest generation of non-invasive ventilators (Figure 15.1), improvements in mask design, and more widely available training and education have further encouraged clinician adoption of in-hospital use of NPPV [2–5]. At the same time, technological improvements seen in time-based and volumetric carbon dioxide (CO_2) monitoring have increased the adoption of capnography. This chapter reviews the current status of combining the new evolving technologies of CO_2 monitoring and NPPV, exploring the advantages as well as the challenges that prompt further research.

Figure 15.1 Philips V60 non-invasive ventilator. [Courtesy of Philips-Respironics].

Relevance and clinical value of time-based and volumetric capnography

The non-invasive character of both NPPV and capnography make the combination attractive for the clinical management of acute and chronic respiratory failure. The evidence supporting the use of NPPV in different clinical scenarios continues to expand (Table 15.1). Table 15.2 presents guidelines for the use of NPPV [6–7]. The American Association for Respiratory Care 2003 Update similarly summarizes indications for the use of CO_2 monitoring during mechanical ventilation [8]. These include indications that are particularly relevant to a patient receiving NPPV therapy:

- 4.2 Monitoring severity of pulmonary disease and evaluating response to therapy, especially therapy intended to improve the ratio of deadspace to tidal volume (V_D/V_T) and the matching of ventilation to perfusion (V/Q), and, possibly, to increase coronary blood flow
- 4.5 Evaluation of the efficiency of mechanical ventilatory support by determination of the difference between the arterial partial pressure for CO_2 ($PaCO_2$) and end-tidal CO_2 ($P_{ET}CO_2$)
- 4.9 Measurement of the volume of CO_2 elimination to assess metabolic rate and/or alveolar ventilation

Capnography, Second Edition, ed. J. S. Gravenstein, Michael B. Jaffe, Nikolaus Gravenstein, and David A. Paulus. Published by Cambridge University Press. © Cambridge University Press 2011.

Table 15.1 Non-invasive ventilation for various types of acute respiratory failure (ARF): evidence for efficacy and strength of recommendation

Type of ARF	Level of evidence[a]	Strength of recommendation[b]
Hypercapnic respiratory failure		
COPD exacerbation	A	Recommended
Asthma	C	Option
Facilitation of extubation (COPD)	A	Guideline
Hypoxemic respiratory failure		
Cardiogenic pulmonary edema	A	Recommended
Pneumonia	C	Option
ALI/ARDS	C	Option
Immuno-compromised	A	Recommended
Postoperative respiratory failure	B	Guideline
Extubation failure	C	Guideline
Do-not-intubate status	C	Guideline
Preintubation oxygenation	B	Option
Facilitation of bronchoscopy	B	Guideline

COPD, chronic obstructive pulmonary disease; ALI, acute lung injury; ARDS, acute respiratory distress syndrome.

[a] A, multiple randomized controlled trials and meta-analyses; B, more than one randomized controlled trial, case control series, or cohort studies; C, case series or conflicting data.

[b] Recommended, first choice for ventilatory support in selected patients; Guideline, can be used in appropriate patients but careful monitoring advised; Option, suitable for a very carefully selected and monitored minority of patients.

Source: From: Hill NS, Brennan J, Garpestad E, Nava S. Non-invasive ventilation in acute respiratory failure. *Crit Care Med* 2007; **35**: 2402–7.

One of the important concerns for clinicians using NPPV therapy is identifying when the therapy is failing and providing alternative support (such as invasive ventilation), as further delay will cause patient harm. Measurements of $PaCO_2$ and pH from arterial blood gas samples are generally used to assess the severity of respiratory failure and the response to ventilator support. As respiratory failure progresses, $PaCO_2$ rises. If support is successful, $PaCO_2$ will decrease as the ventilator facilitates respiratory excretion of CO_2. With the current technology, arterial blood samples are drawn and analyzed with a blood gas analyzer, typically located in a laboratory remote from the patient. These measurements are discontinuous and delayed, as well as invasive, requiring arterial access or an arterial puncture. A non-invasive alternative to arterial blood gas measurement is done by monitoring end-tidal CO_2 concentration in the expired gas. The end-tidal CO_2 level is generally considered the CO_2 level measured at the end of the expired breath, but is often better reflected by the highest CO_2 concentration observed during the breath. The partial pressure of end-tidal CO_2 ($PETCO_2$) may serve as a surrogate for the arterial partial pressure of carbon dioxide ($PaCO_2$). In the normal lung, $PETCO_2$ monitoring is well established to be 2–7% less than directly measured $PaCO_2$ [8]. This difference may increase or decrease in the clinical environment, depending on patient factors, such as the degree of abnormality in patient gas exchange (ventilation–perfusion matching), as well as measurement factors, such as whether the breath is large enough to clear the physiologic deadspace, and the extent to which there is dilution by room air and/or supplemental oxygen. Advances in technology have reduced the effect of the measurement factors.

With respect to patient factors that affect the difference between $PETCO_2$ and $PaCO_2$, patients with respiratory failure often take small breaths. Additionally, the underlying disease process may be associated with a mismatch of ventilation and perfusion that impairs gas exchange between the alveoli and the pulmonary capillaries. This can create a significant gradient between the concentration of CO_2 in the systemic artery and that in the alveolar air sacs. Measurements of $PETCO_2$ and $PaCO_2$ will reflect this pathophysiology, with the $PETCO_2$ being less than the $PaCO_2$. The lower the $PETCO_2$ is compared to the $PaCO_2$ (greater difference), the less efficient the lung is as an "exhaust" or elimination system for CO_2 [9]. Patients with acute respiratory failure and effectively increased deadspace ventilation will have a $PaCO_2$–$PETCO_2$ difference that is greater than 2–4 mm Hg. This can confound interpretation of changes in $PETCO_2$ because changes in its value may reflect changes in either the underlying $PaCO_2$ or gas exchange, or both.

Nevertheless, over intervals where clinical assessment and judgment suggest deadspace is not changing, the trend in the $PETCO_2$ values may serve as a marker for changes in arterial values, and are useful to indicate whether NPPV is successfully treating the respiratory failure. For example, if a patient on NPPV has an

Table 15.2 General guidelines for selection of patients for non-invasive ventilation (NIV)

(1) Need for ventilatory assistance?	(2) Contraindications for NIV
Moderate to severe dyspnea	Respiratory arrest
Tachypnea (> 24 for hypercapnic, > 30 for hypoxemic)	Medically unstable
Accessory muscle use	Unable to protect airway
Abdominal paradox	Excessive secretions
$PaCO_2$ > 45 mm Hg, pH < 7.35	Agitated, uncooperative
PaO_2/FiO_2 < 200	Recent upper gastrointestinal or airway surgery Unable to fit mask

Source: From: Hill NS, Brennan J, Garpestad E, Nava S. Non-invasive ventilation in acute respiratory failure. *Crit Care Med* 2007; **35**: 2402–7.

initial $P_{ET}CO_2$ of 60 mm Hg that progressively falls to 50 mm Hg during the first hour of NPPV therapy, it may be reasonable to conclude (if other clinical observations also suggest patient improvement) that NPPV therapy is succeeding [10]. However, if the patient's $P_{ET}CO_2$ starts at 60 mm Hg and rises to 70 mm Hg during the first few hours of treatment, one concludes that endotracheal intubation should not be delayed, or that (at least) an arterial blood gas should be obtained. Thus, trends in end-tidal CO_2 obtained through non-invasive capnographic monitoring during NPPV may help clinicians make judgments about the need for and timing of blood gases and/or endotracheal intubation.

Interfaces

Several different types of patient interfaces are available for the delivery of non-invasive ventilation [11], including "full face" masks (that cover the mouth and nose), "complete face masks" (that cover the entire face), nasal masks, sealed helmets, nasal pillows or plugs, mouthpieces and custom-fabricated masks. Complete face masks, such as the PerforMax™ face mask (Philips-Respironics, Carlsbad, CA, USA) (Figure 15.2), seal around the perimeter of the face, where patients have less pressure sensitivity and smoother facial contours. Complete face masks improve comfort, minimize skin breakdown, and eliminate the nasal bridge seal challenges often associated with full face and nasal masks. The advantages and disadvantages of face and nasal mask types are given in Table 15.3. Mask use in acute and chronic respiratory failure is listed in Table 15.4.

A significant issue to be considered when clinicians use a mask for NPPV is apparatus deadspace. It is important to note that the static deadspace, i.e., the actual volume of the mask, is not an accurate measure of the deadspace experienced physiologically by the patient. The term "dynamic apparatus" deadspace has therefore been introduced [12]. Saatci used a lung model to study the influence of different face mask designs and different non-invasive ventilator modes on total dynamic apparatus deadspace [12]. He concluded that the use of NPPV, together with mask valves, creates flow during expiration that clears the mask deadspace of CO_2, and thus reduces effective (dynamic apparatus) deadspace to a value that is substantially less than mask volume.

Fraticelli *et al.* [13] evaluated four interfaces (three masks and one mouthpiece), and noted the lack of a

Figure 15.2 PerforMax™ Face Mask. [Courtesy of Philips-Respironics.]

Table 15.3 Mask selection

	Complete face mask	Full face mask	Nasal mask
Immediate seal for ventilation required	•		
Mouth breather	•	•	
Claustrophobia	•	•	
Facial abnormalities	•		•
Eye irritation	•		
Lack of teeth	•		
Anxiety	•	•	
Access to mouth			•
Long-term NPPV		•	•

Table 15.4 Mask use in acute and chronic respiratory failure

Mask type	Acute	Chronic
Facial	63%	6%
Nasal	31%	73%
Nasal pillows	6%	11%
Mouthpieces	-	5%

Source: Based on data from: Elliott MW. The interface: crucial for successful non-invasive ventilation. *Eur Respir J* 2004; **23**: 7–8.

$PaCO_2$ increase with the larger *static* deadspace mask configurations: "the most important clinical implication of these results is the possibility to choose different interfaces in the acute patient, based on the patient's physiognomy and mask tolerance, with the aim to limit air leaks regardless of the deadspace."

Sidestream versus mainstream sampling

A capnometer, by definition, is either diverting (i.e., sidestream) or non-diverting (i.e., mainstream). Sidestream gas measurement offers a number of sampling locations, including: (1) inside the mask, (2) at the mask outlet, or (3) with the nasal cannula at or near the patient's nostrils. Sidestream sampling methods generally employ a nasal cannula, which, when used with a mask, reduces the impact of the exhalation port location unless flow is quite large. However, the choice of a sampling site raises additional technical and physiologic issues that must be considered, including condensation and water removal, and waveform distortion.

Methods have evolved to address some of these issues, including the use of filters and alternative tubing designs. Mainstream monitoring can only be effectively performed in circuits where the exhalation port is located distal to the sampling location because the position of the exhalation port relative to the measurement site for $PETCO_2$ can greatly alter the measured values (Figure 15.3). Ports located in the mask will generally flush out the exhaled CO_2 gas prior to its reaching the mainstream sampling port location. This limits the choices of the sampling site, particularly during non-invasive ventilation in which there is only a single limb, placing additional constraints on mask design and fit. This is an area in which future technological developments in both equipment and mask design (e.g., less mixing and lower leaks) may make mainstream gas measurement clinically viable.

Challenges of measurement

Non-invasive measures of $PaCO_2$, such as $PETCO_2$, have been broadly characterized by some authors as not sufficiently accurate surrogates of $PaCO_2$ for clinical use. For example, in one study often cited, Sanders *et al.* [14] evaluated $PETCO_2$ accuracy in 41 patients using three conditions: (1) 19 spontaneously breathing room air; (2) 13 receiving supplemental oxygen; and (3) 22 receiving positive pressure ventilatory assistance via mask. Patients were considered eligible if they were undergoing polysomnographic evaluation for suspected OSA or nocturnal hypoventilation in the presence of awake hypercapnia or neuromuscular/chest wall disease. $PETCO_2$ was measured with a sidestream capnograph with a catheter suspended in a loose-fitting aerosol mask for the first two groups, and either within the mask or attached to port on the mask for the support group. The study concluded that $PETCO_2$ did not adequately reflect $PaCO_2$. However,

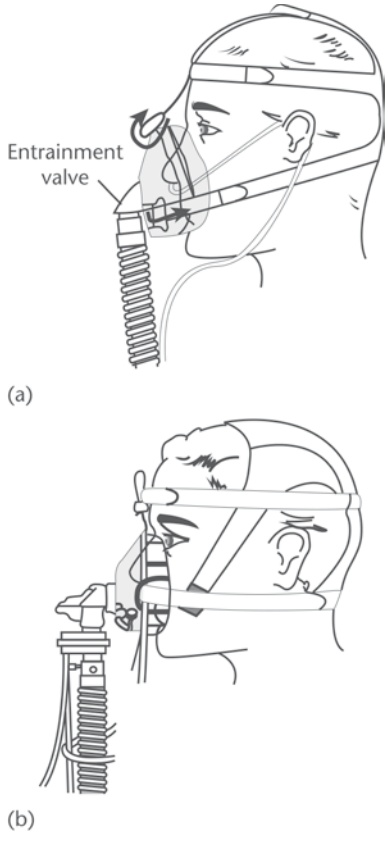

Figure 15.3 Disposable full face mask applied to subject with (a) nasal cannula and (b) mainstream gas sensor and airway adapter. [Courtesy of Philips-Respironics.]

the authors compared the average values of $P_{ET}CO_2$ to those of $PaCO_2$ at three "conditions" using different subjects [15]. Given that clinical evaluation of the effectiveness of ventilator support often relies on evaluation of changes in CO_2 excretion in response to therapeutic interventions, an intra-subject comparison of $P_{ET}CO_2$ changes to changes in $PaCO_2$ would have been a more useful assessment of the clinical utility of $P_{ET}CO_2$.

For $P_{ET}CO_2$ monitoring of NPPV to be successful, the technology must address leaks, mouth-breathing, and the passive exhalation port location. For example, if a nasal mask is used on a mouth-breather, there may be occasions when $P_{ET}CO_2$ values do not reflect exhaled gases, because gas will exit the mouth and bypass the $P_{ET}CO_2$ sensor at the nose. Other factors to consider when selecting an interface for use with NPPV (and thus the location and design of the capnography sensor) include the anticipated duration of NPPV and patient claustrophobia, dentition, and glaucoma.

Obtaining a sample for CO_2 measurement is technically straightforward in the intubated patient because the expired gas flows entirely through an airway adapter where it can be directly analyzed (mainstream technique), or drawn for analysis with a sampling tube (sidestream technique) (see below for further discussion of mainstream and sidestream technologies). However, in the spontaneously breathing, non-intubated subject, obtaining a representative alveolar gas sample is more difficult because the gas exits through both the nostrils and mouth where it can be passively diluted by the surrounding air and/or supplemental oxygen gas flows. A mouthpiece or a sampling cannula that has sampling prongs placed within the nares may resolve this problem. During non-invasive ventilation, however, obtaining a sample of alveolar gas is complicated by the fact that the ventilator actively dilutes the alveolar gas sample during expiration. During expiration, the ventilator, in a bi-level mode, delivers flow to the mask as soon as the expiratory pressure falls below the set expiratory positive airway pressure (EPAP) limit. In most cases, this pressure limit is reached very early following the end of inspiration. Obtaining an accurate end-tidal CO_2 measurement requires enough expired gas volume to fill the gas sample line before EPAP gas from the ventilator arrives to dilute the sample.

When the tidal volume is small or the EPAP is high, the flow from the ventilator is larger than the flow of alveolar gas coming from the lungs; consequently, the end-tidal gas sample is diluted by flow coming from the ventilator, and the measured $P_{ET}CO_2$ value will thus be lowered. Another confounding factor is the leak between the mask and face. This leak increases the amount of flow from the ventilator needed to maintain pressure in the mask. When there is a leak at the skin-to-mask interface close to the gas sample site, such as a nasal cannula used for sidestream gas sampling, gas flow from the ventilator will dilute the sample and thereby dilute the measurement.

Figure 15.4 illustrates the effect of dilution on the capnogram and the end-tidal CO_2 value with waveforms from a computer model, and an example of low and high levels of dilutions. Figure 15.5 schematically illustrates the problem of gas sampling during the end-expiratory phase of NPPV. The capnometer sample is drawn from somewhere in the gas compartment formed by the face and the mask wall, with the source of the alveolar gas shown on the right and the ventilator hose connection to the mask shown on the left. The volume on the right of the compartment includes the

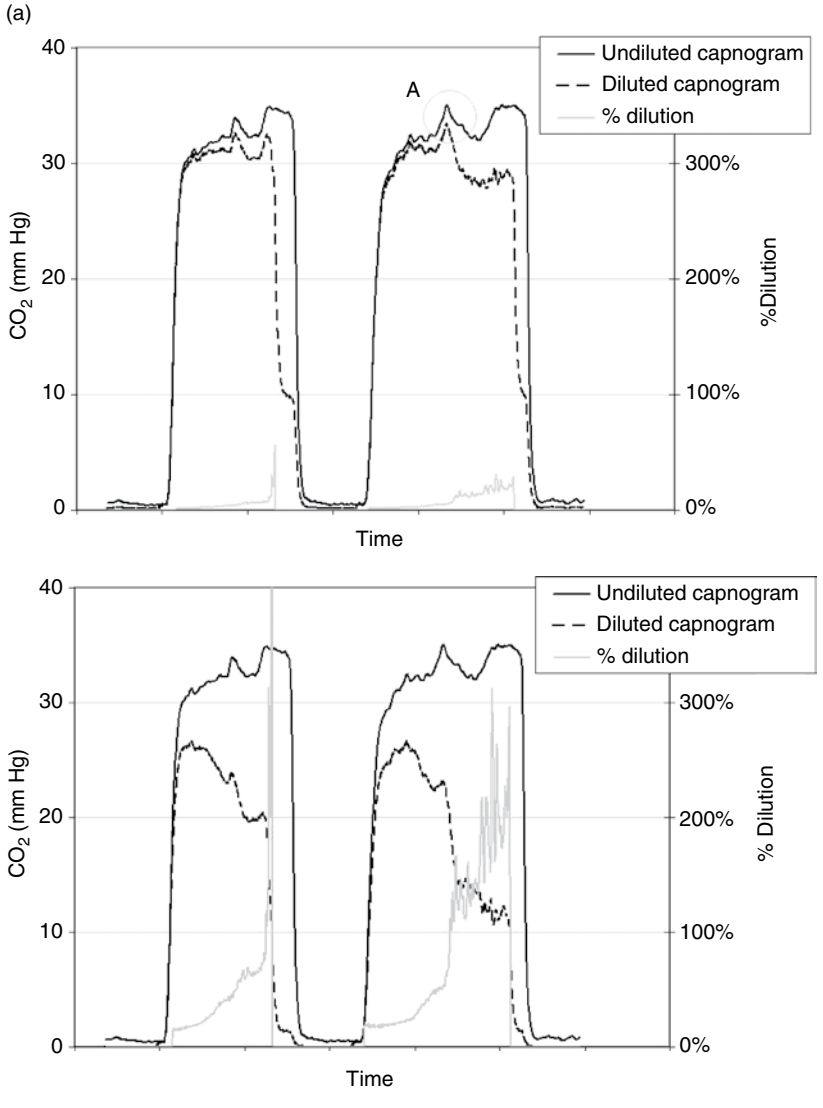

Figure 15.4 Effect of dilution on capnogram created by computer modification of actual patient data. (a) Dilution (EPAP) flow during expiration low relative to the patient's expiratory flow. Note the capnogram is only partially distorted and the measured end-tidal CO_2 value (A) is relatively close in value to the undiluted value. Note that the effect of dilution is increased as the flow from the patient approaches zero during the end-expiratory pause. (b) Dilution flow is large relative to the patient's peak expiratory flow (order of magnitude larger). Note the capnogram is significantly distorted throughout the expiratory period and the measured end-tidal CO_2 is not reliable.

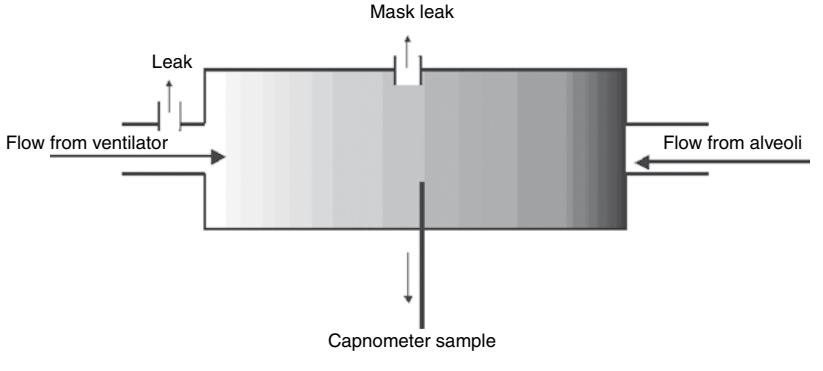

Figure 15.5 Schematic model of the gas sampling during the end-expiratory phase of NPPV. The shaded box represents the volume between the mask and the alveoli where the gas originates. The dark shading represents gas that is purely expired from the alveoli of the lungs and therefore contains an alveolar CO_2 concentration. The light shading represents gas supplied by the ventilator that is void of CO_2.

anatomic deadspace volume, comprising the mouth, nasal cavities and sinuses, and the trachea and large airways in the bronchiolar tree. During expiration, gas flows either exclusively from the patient or exclusively from the ventilator, or is simultaneously supplied by both the patient and the ventilator, depending on the location and magnitude of the leak(s) in the interface.

Note that even when gas is supplied exclusively from the patient, a sufficient volume of gas from the alveolus is needed to flush the non-alveolar gas in the anatomic deadspace that was left from the previous inspiration from the chamber. If the expired volume is too small, the sample may not represent alveolar gas even in the absence of flow from the ventilator. In the ideal setting, there is no flow from the ventilator during expiration, but only flow from the patient so that a gas sample taken from anywhere between the patient and mask wall will represent alveolar gas. Under ideal conditions for gas sampling, the expired tidal volume is sufficient to completely flush all inspired gas from the anatomic deadspace and the chamber while there is no flow from the ventilator. In this situation, where the capnometer sample is drawn makes little difference, since the entire volume is filled with alveolar gas. However, if the tidal volume is not sufficient to completely fill the volume with alveolar gas, the location of the sampling point is critical.

In some cases, alveolar gas cannot fill the sampled volume because it is flushed out by gas from the ventilator. This situation is typical of non-invasive ventilation, where there is almost always a small leak between the mask and face. Flow from the ventilator flows out through the mask leak and dilutes the alveolar gas during expiration. In this case, the concentration of CO_2 at the sampling point may be much lower than it is in the alveoli. Note that the closer the location of the gas sampling site to the source of alveolar gas, the more accurate the measurement. If it were possible to draw a gas sample from within the trachea, there is no doubt that the gas sample would reflect alveolar CO_2 concentration. However, as the sampling point moves further from the source of alveolar gas, the more likely the sample will be diluted by residual inspired gas and EPAP flow.

During bi-level ventilation, the expiratory gas flow from the lungs and the EPAP gas flow from the ventilator compete to fill the sampled volume. If flow from the lungs substantially dominates, capnography will be reliable. On the other hand, if the tidal volume is large, the expiratory flow from the lungs will be higher. This increases the volume from the lungs that is contributed to the gas sample, and also increases the expiratory pressure so that there is less flow from the ventilator.

Obtaining a "valid" end-tidal CO_2 sample becomes even more difficult when the EPAP setting is high and the tidal volume is low. Under these conditions, flow from the ventilator out through the mask leak becomes larger, making the amount of alveolar gas dilution greater. If the tidal volume is low, there is less alveolar gas in the chamber, and consequently, the effect of dilution is more severe. In this situation, there is little relationship between the concentration of CO_2 measured by the capnometer and the concentration in the alveolar gas.

This relationship, as a function of tidal volume, was evaluated in a simulated patient, consisting of a test lung connected via a tube to a model of a patient's face [16]. End-tidal CO_2 measured with a sampling cannula placed under the mask, such that the sample is drawn between the nose and mouth of the simulated patient, was compared to $P_{ET}CO_2$ measured directly in the simulated trachea at various settings of inspiratory positive airway pressure (IPAP) and EPAP. Figure 15.6 is a plot of the difference between measured and true $P_{ET}CO_2$, and demonstrates the dependency of this difference on tidal volume. Standard capnography using a gas sampling cannula placed under the mask during non-invasive ventilation can be unreliable in patients with small or variable tidal volume.

Therefore, the keys to acquiring a technically valid $P_{ET}CO_2$ measurement during NPPV include:

(1) Place the sampling port to acquire the expired gas sample as near the source (nares or mouth) as possible. Sampling the gas from within the nares or mouth is best. This is impossible to do with an on-airway capnometer. The options for sample port placement are on the connector between the ventilator and mask, at some point on the surface of the mask (sampling port), and within, or close to, the nares and mouth. Nuccio demonstrated that valid capnographic data were possible using a nasal/oral sampling cannula placed under the mask at various NPPV settings in a healthy volunteer [17].

(2) Ensure that the expired tidal volume is sufficiently large to overcome the EPAP gas flow during the start of expiration for a period long enough that a valid sample can be acquired. Note that the shape of the capnogram will likely be altered when CO_2 is measured under an NPPV mask. In traditional capnography, there is a protracted plateau period

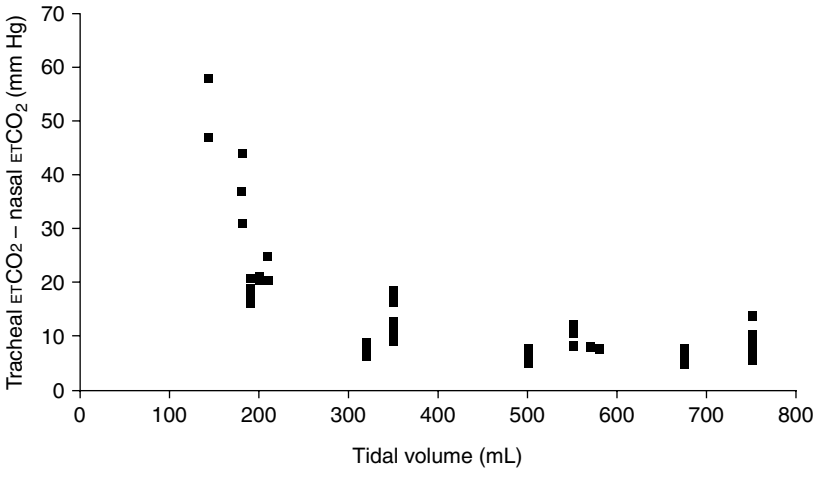

Figure 15.6 Plot of average $P_{ET}CO_2$ error vs. tidal volume. The average error in measured $P_{ET}CO_2$ was 14 ± 10 mm Hg across all test conditions. The average error was 19.5 ± 12.5 mm Hg when the tidal volume was less than 500 mL and was 8.3 ± 2.4 mm Hg when the tidal volume was greater than 500 mL. [From: Orr JA, Brewer LM, Pinkston J. Limitations of capnometry for non-invasive ventilation using under-mask gas sampling. *Crit Care Med* 2007; **35** (Suppl): A234.]

at the end of expiration, during which there is little expiratory flow carrying the alveolar gas. When CO_2 is measured under an NPPV mask, the capnogram plateau is shortened by the dilution caused by ventilator gas during EPAP. The end-tidal gas concentration is observed earlier during expiration. Even if no plateau is observed for a brief period, the gas sample likely does not represent alveolar gas.

(3) Minimize the leaks at the interface between the mask and patient so that the flow from the ventilator that dilutes the expired sample is small.

(4) Ensure that the response time of the capnometer is sufficient to analyze the gas sample, even when the duration of expiration is very short. During conventional capnography, the alveolar gas sample is available for analysis during the end-expiratory pause. During NPPV, the alveolar gas sample is only available while expired gas is flowing from the lungs. During the pause, the ventilator dilutes the sample. The capnometer must have a sufficiently short rise time (see Chapter 36 for definition) to analyze the gas sample, even when the duration of expiratory gas flow is short.

Rebreathing

Rebreathing has been considered a potential cause of failure of NPPV therapy, and may be qualitatively assessed by increased end-tidal values over time as well as observation of capnogram's shape for an upward shift of the plateau and changes to the slope of the expiratory to inspiratory edge of the capnogram over time. The potential for CO_2 rebreathing during bi-level ventilation has been noted in the past with certain home bi-level ventilators with a single limb circuit and not a true exhalation valve [18–20], but its clinical significance has not been established and "has not been shown to be deleterious in any way" [21,22].

Schettino and colleagues used a bench model to investigate the impact of face mask design on CO_2 rebreathing [21]. They reported rebreathing to be associated with less than a 4 mm Hg CO_2 difference. According to Hill [22], such a difference may not be important:

> Indeed, some of the observations (by Schettino) are of doubtful clinical significance. For example, most of the rebreathing in this model system was attributable to the deadspace in the mannequin's upper airway and not to the masks themselves. Furthermore, it is difficult to conceive of how a difference as small as 2–3 ml in the amount of CO_2 rebreathed per breath between the masks could be clinically significant, even if it is statistically significant.

Consistent with Hill's position, Samolski has investigated CO_2 rebreathing in non-invasive ventilation, and found that in healthy volunteers, nasal and facial masks with expiratory valves prevent rebreathing [23].

Other technical considerations

Short-term vs. longer-term use

A patient in respiratory distress requires an interface device that can be applied quickly and easily. Therefore, a mask that covers the nose, mouth, and eyes (i.e., complete face mask) is useful for emergency situations [24,25]. Mainstream sensing technology may not work well with conventional NPPV masks because they utilize exhalation ports to prevent rebreathing of CO_2. These

ports also prevent exhaled gas from reaching the mainstream sampling location at the elbow. Consequently, sidestream sensors are applied when the patient uses an NPPV mask with an exhalation port. Full face masks and nasal masks do not require the exhalation port and, hence, can be used with mainstream capnography.

Leak management

While many non-invasive ventilators are capable of compensating for substantial leaks, many require operator adjustments. In a recent bench study [26], the Vision (Respironics, Carlsbad, CA, USA) and Servo I (Maquet, Sweden) were the only ventilators that required no manual adjustments with increasing leaks. It is generally recommended by manufacturers to have some level of leak to assure that the interface has not been applied too tightly. However, too large a leak will cause both the capnogram and the $P_{ET}CO_2$ values to be dampened. If the leak cannot be minimized, care must be taken when using sidestream monitoring through a cannula to reduce the impact of the leak on the measurement.

Future directions

For CO_2 monitoring to be widely accepted and used routinely with NPPV, the following factors need to further mature.

(1) Greater acceptance and use of time-based and volumetric capnography in invasively ventilated patients.

(2) Improved understanding of the variations of $P_{ET}CO_2$ relative to $PaCO_2$ difference in different disease states and at varying levels of ventilatory support. Ideally, $P_{ET}CO_2$ and a–$ADCO_2$ should be measured and monitored in individual patients over the course of their ventilatory management before the $P_{ET}CO_2$ can be used reliably as an indicator of $PaCO_2$ and the effectiveness of ventilatory support. Research with volumetric capnography and physiologic modeling may be helpful in making this approach applicable to NPPV.

(3) Improved understanding of $P_{ET}CO_2$ monitoring with NPPV as a qualitative tool. In particular, it is important to better understand the changes in these values throughout the various phases of non-invasive ventilatory management. The $P_{ET}CO_2$ to $PaCO_2$ difference will need to be understood in the context of the patient with acute respiratory insufficiency or failure, and the impact of pressure support ventilation upon the reduction of this gradient assessed.

(4) Addressing the use of end-tidal CO_2 with NPPV and active ventilatory failure in light of important considerations when using NPPV, including the education of all the care team members, the patient interface, the importance of mask fit, leak management, and humidity [27]. Plant and colleagues stress the importance of providing training to the healthcare staff specifically focused on the optimal administration of NPPV throughout the hospital [28]. The addition of a supplemental monitoring modality adds a new level of complexity to patient management that will require further specialized training in its application and usefulness.

(5) Application of CO_2 excretion (VCO_2) as a modality of monitoring during NPPV. If leaks are minimized or accurately quantitated, it may be possible to determine the volume of CO_2 that is excreted by the patient rather than just the concentration. Changes in the volume of CO_2 excreted are proportional to changes in effective alveolar ventilation.

Conclusion

Non-invasive positive pressure ventilation and CO_2 monitoring are powerful non-invasive technologies for the management of patients with acute or chronic respiratory failure. Experience with $P_{ET}CO_2$ monitoring with NPPV is still preliminary. Nevertheless, $P_{ET}CO_2$ monitoring for patients requiring NPPV will likely evolve into an important clinical tool, possibly in conjunction with transcutaneous CO_2 monitoring [29]. It is plausible that the synergies between NPPV and time/volumetric capnography will help the clinician to more rapidly identify therapeutic pressure levels that optimize CO_2 elimination and patient work of breathing – key objectives for non-invasive ventilation.

References

1. Hill NS. *Noninvasive Positive Pressure Ventilation: Principles and Applications.* Armonk, NY: Futura Publishing, 2001.
2. Brochard L, Isabey D, Piquet J, *et al.* Reversal of acute exacerbations of chronic obstructive lung disease by inspiratory assistance with a face mask. *N Engl J Med* 1990; **323:** 1523–30.

3. Meduri GU, Abou-Shala N, Fox RC, *et al.* Noninvasive face mask mechanical ventilation in patients with acute hypercapnic respiratory failure. *Chest* 1991; **100:** 445–54.
4. Kramer N, Meyer TJ, Meharg J, Cece RD, Hill NS. Randomized, prospective trial of noninvasive positive pressure ventilation in acute respiratory failure. *Am J Respir Crit Care Med* 1995; **151:** 1799–806.
5. Scala R, Naldi M. Ventilators for noninvasive ventilation to treat acute respiratory failure. *Respir Care* 2008; **53:** 1054–80.
6. Mehta S. Noninvasive ventilation. *Am J Respir Crit Care Med* 2001; **163:** 540–77.
7. Hill NS, Brennan J, Garpestad E, Nava S. Noninvasive ventilation in acute respiratory failure. *Crit Care Med* 2007; **35:** 2402–7.
8. American Association for Respiratory Care. Clinical practice guideline: Capnography/capnometry during mechanical ventilation–2003 revision and update. *Respir Care* 2003; **48:** 534–9.
9. Hoffman RA, Krieger BP, Kramer MR, *et al.* End-tidal carbon dioxide in critically ill patients during changes in mechanical ventilation. *Am Rev Respir Dis* 1989; **140**: 1265–8.
10. Antón A, Güell R, Gómez J, *et al.* Predicting the result of noninvasive ventilation in severe acute exacerbation of patients with chronic airflow limitation. *Chest* 2000; **117:** 828–33.
11. Schönhofer B, Sortor-Leger S. Equipment needs for noninvasive mechanical ventilation. *Eur Respir J* 2002; **20:** 1029–36.
12. Saatci E, Miller DM, Stell IM, Lee KC, Moxham J. Dynamic deadspace in face masks used with non-invasive ventilators: a lung model study. *Eur Respir J* 2004; **23:** 129–35.
13. Fraticelli A, Lellouche F, Taille S, Qader S, Brochard, L. Comparison of different interface during NIV in patients with acute respiratory failure. *Am J Respir Crit Care Med* 2003; **167**: A389.
14. Sanders MH, Kern NB, Costantino JP, *et al.* Accuracy of end-tidal and transcutaneous PCO_2 monitoring during sleep. *Chest* 1994; **106:** 472–83.
15. Woolley A, Hickling K. Errors in measuring blood gases in the intensive care unit: effect of delay in estimation. *J Crit Care* 2003; **18:** 31–7.
16. Orr JA, Brewer LM, Pinkston J. Limitations of capnometry for noninvasive ventilation using under-mask gas sampling. *Crit Care Med* 2007; **35** (Suppl): A234.
17. Nuccio PF, Jackson MR. End tidal CO_2 measurements with noninvasive ventilation. Society for Technology in Anesthesia (STA), January 13–14, 2009, San Antonio, TX.
18. Ferguson GT, Gilmartin M. CO_2 rebreathing during BiPAP ventilatory assistance. *Am J Respir Crit Care Med* 1995; **151:** 1126–35.
19. Lofaso F, Brochard L, Touchard D, *et al.* Evaluation of carbon dioxide rebreathing during pressure support ventilation with airway management system (BiPAP) devices. *Chest* 1995; **108:** 772–8.
20. Renaghan, D. Capnometric analysis of carbon dioxide rebreathing during noninvasive positive pressure ventilation with BiPAP. *Crit Care Med* 2000; **28**: A177.
21. Schettino GP, Chatmongkolchart S, Hess DR, Kacmarek RM. Position of exhalation port and mask design affect CO_2 rebreathing during noninvasive positive pressure ventilation. *Crit Care Med* 2003; **31:** 2178–82.
22. Hill N. What mask for noninvasive ventilation: is deadspace an issue? *Crit Care Med* 2003; **31:** 2247–8.
23. Samolski D, Calaf N, Güell R, Casan P, Antón A. Carbon dioxide rebreathing in non-invasive ventilation: analysis of masks, expiratory ports and ventilatory modes. *Monaldi Arch Chest Dis* 2008; **69:** 114–18.
24. Liesching TN, Cromier K, Nelson D, *et al.* Total face mask vs standard full face mask for noninvasive therapy of acute respiratory failure. *Am J Respir Crit Care Med* 2003; **167**: A996.
25. Criner GJ, Travaline JM, Brennan KJ, Kreimer DT. Efficacy of a new full face mask for noninvasive positive pressure ventilation. *Chest* 1994; **106:** 1109–15.
26. Ferreira JC, Chipman DW, Hill NS, Kacmarek RM. Bilevel vs ICU ventilators providing noninvasive ventilation: effect of system leaks: a COPD lung model comparison. *Chest* 2009; **136:** 448–56.
27. Kacmarek R. Noninvasive positive-pressure ventilation: the little things do make the difference! *Respir Care* 2003; **48:** 919–21.
28. Plant P, Owen J, Elliott M. A multicentre randomized controlled trial of the early use of non-invasive ventilation for acute exacerbations of chronic obstructive pulmonary disease. *Lancet* 2000; **355:** 1931–5.
29. Chhajed PN, Heuss LT, Tamm M. Cutaneous carbon dioxide monitoring in adults. *Curr Opin Anaesthesiol* 2004; **17:** 521–5.

Section 1
Chapter
16

Ventilation

End-tidal carbon dioxide monitoring in postoperative ventilator weaning

J. Varon and P. E. Marik

Introduction

Premature extubation after general anesthesia significantly increases postoperative morbidity. The evaluation of the suitability for weaning and extubation includes a clinical examination that assesses the patient's alertness, and the ability to follow commands and lift his/her head off the bed. These simple steps are the best method for assessing the level of consciousness and muscle strength. Many medical centers continue to utilize arterial blood gas analysis for weaning despite the lack of data supporting its use [1]. Clinical and experimental studies have repeatedly demonstrated that a clinical evaluation lacks the sensitivity for detecting potentially life-threatening events, such as major changes in oxygen arterial saturation (SaO_2), alveolar ventilation, and esophageal intubation [2–4]. Pulse oximetry is now regarded as the standard of care for patients undergoing anesthesia, given that it provides a continuous, non-invasive method of estimating arterial oxygenation. Some authors have suggested that end-tidal CO_2 monitoring should be a part of routine vital sign measurements [5]. A number of methods are available to monitor the adequacy of ventilation, each with its own utility and limitations.

Assessing ventilation adequacy

Several laboratory techniques are commonly used as adjuncts to clinical assessment of the adequacy of ventilation. The most direct is the measurement of the partial pressure of carbon dioxide in arterial blood ($PaCO_2$). However, blood gas analysis requires an arterial puncture, which is expensive, and provides only intermittent $PaCO_2$ data. A variety of devices are available to accomplish these measurements [6]. Transcutaneous measurement of CO_2 tension can provide continuous data, but requires adequate cardiovascular function and peripheral perfusion to be well correlated with $PaCO_2$ [7]. Other disadvantages include its long warm-up and slow response time, and the risk of skin burns.

Under normal conditions, $PaCO_2$ is related to mixed venous partial pressure of CO_2 ($P\bar{v}CO_2$); $PaCO_2 = 0.8\ P\bar{v}CO_2$. However, mixed venous blood sampling requires invasive hemodynamic monitoring, and is, therefore, not practical. Another method that can be used to assess the adequacy of ventilation is capnometry.

Under normal conditions, there is a small difference of <6 mm Hg between $PaCO_2$ and partial pressure of CO_2 at end-tidal ($PETCO_2$). At sea level (atmospheric pressure = 760 mm Hg), the normal value for $PETCO_2$ is about 38 mm Hg. The most important determinants of $PETCO_2$ are alveolar ventilation, pulmonary perfusion (i.e., cardiac output), and CO_2 production [8].

The assessment of $PETCO_2$ may be misleading if not considered in the context of changing hemodynamics and ventilatory pattern. In the mechanically ventilated patient, alterations in ventilation and perfusion ($\dot{V}/\dot{Q}$) can occur due to changes in the deadspace to tidal volume ratio (V_D/V_T), positive end-expiratory pressure (PEEP), the development of atelectasis or pulmonary edema, or patient repositioning. Morley observed that $PETCO_2$ was useful as a predictor of $PaCO_2$ only in patients without significant parenchymal lung disease [9]. Prause and colleagues found that $PETCO_2$ was useful for the adjustment of ventilatory parameters in prehospital emergency care patients only if they had no major cardiopulmonary disease [10]. In a 1985–91 literature review of the efficacy on non-invasive blood gas monitoring in the adult critical care unit, the Technology Subcommittee of the Working Group on Critical Care (Ontario Ministry of Health) concluded that changes in $PETCO_2$ should be interpreted with extreme caution [11].

Capnography, Second Edition, ed. J. S. Gravenstein, Michael B. Jaffe, Nikolaus Gravenstein, and David A. Paulus. Published by Cambridge University Press. © Cambridge University Press 2011.

Clinical applications of end-tidal CO_2 in weaning of postoperative patients

The important role played by capnometry in verification of endotracheal tube placement is discussed in detail elsewhere (Chapter 3: Airway management in the out-of-hospital setting). This chapter focuses on the procedures that are utilized for weaning patients from the ventilator. Successful weaning during the postoperative period requires the assurance that the patient is clinically stable and without clinically significant residual effects of the anesthetic agents utilized during surgery [12]. A number of ventilatory parameters have been evaluated to predict the success of weaning. Some of the standard indices that predict weaning success are depicted in Table 16.1.

The Tobin index, as an indicator of rapid shallow breathing (RSBI), is commonly used to predict weaning success and is calculated as follows:

$$\text{Tobin index} = \frac{f}{V_T}$$

where f = frequency (breaths/min) and V_T = tidal volume (liter). Successful weaning is usually accomplished if the Tobin index is <105 [13]. When $P_{ET}CO_2$ values are considered in combination with the standard parameters to assure adequate ventilation prior to extubation, the chance of successful extubation increases. In a prospective study, Morley and associates studied the reliability of end-tidal CO_2 ($etCO_2$) monitoring as a reflection of arterial CO_2 tension during weaning from mechanical ventilation [9]. Capnographic monitoring of their patients provided reasonable estimates of arterial CO_2 tension during weaning. Saura and colleagues, in a prospective study to evaluate the relationship between $PaCO_2$ and $P_{ET}CO_2$ before and during weaning with continuous positive airway pressure ventilation, found that $P_{ET}CO_2$ could detect clinically relevant hypercapnic episodes [14]. However, in this particular trial, there was a high incidence of false positives that led to arterial blood gas sampling; in general, it is unusual to find a $P_{ET}CO_2$ value higher than that of a $PaCO_2$. Withington *et al.* found that, after a difference between $PaCO_2$ and $P_{ET}CO_2$ was established, $P_{ET}CO_2$ was a useful parameter in weaning otherwise stable post-cardiac surgery patients [15].

Some clinicians utilize $P_{ET}CO_2$ as a marker of the metabolic rate and, therefore, as a way of determining optimal ventilator settings during the weaning process [16]. Patients with high metabolic rates (e.g., sepsis) may be difficult to wean under these conditions, often making it otherwise difficult to predict the success of weaning.

Table 16.1 Standard indices for weaning success

Index	Value suggesting success
Minute ventilation ($\dot{V}_E$)	≤10 L/min
Tidal volume (V_T)	≥5 mL/kg
Vital capacity (V_C)	$2 \times V_T$
Maximal voluntary ventilation (MVV)	$2 \times (\dot{V}_E)$
Rapid shallow breathing index (RSBI)	<105

Special considerations of $P_{ET}CO_2$ in critically ill patients

Cardiopulmonary bypass weaning

The level of $P_{ET}CO_2$ has been used as a surrogate marker for pulmonary blood flow [17]. When used in these circumstances, a $P_{ET}CO_2$ that exceeds 30 mm Hg under conditions of normal minute ventilation is usually associated with a cardiac output greater than 4.0 L/min.

Conclusion

Monitoring $P_{ET}CO_2$ serves as a useful adjunct in weaning postoperative patients from mechanical ventilation. A variety of different devices are available to the practitioner caring for these patients. Data from $P_{ET}CO_2$ monitoring should be used in conjunction with information derived from a clinical evaluation of the patient.

References

1. Salam A, Smina M, Gada P, *et al.* The effect of arterial blood gas values on extubation decisions. *Respir Care* 2003; **48**: 1033–7.
2. Semmes BJ, Tobin MJ, Snyder V, Grenvik A. Subjective and objective measurement of tidal volume in critically ill patients. *Chest* 1985; **87**: 577–9.
3. Vaghadia H, Jenkins LC, Ford RW. Comparison of end-tidal carbon dioxide, oxygen saturation and clinical signs for the detection of oesophageal intubation. *Can J Anaesth* 1989; **36**: 560–4.

4. Cote CJ, Rolf N, Liu MN, *et al.* A single-blind study of combined pulse oximetry and capnography in children. *Anesthesiology* 1991; **74**: 980–7.
5. Zwerneman K. End-tidal carbon dioxide monitoring: a VITAL sign worth watching. *Crit Care Nurs Clin N Am* 2006; **18**: 217–25.
6. Bhende MS, Thompson AE, Howland DF. Validity of a disposable end-tidal carbon dioxide detector in verifying endotracheal tube position in piglets. *Crit Care Med* 1991; **19**: 566–8.
7. Johnson DC, Batool S, Dalbec R. Transcutaneous carbon dioxide pressure monitoring in a specialized weaning unit. *Respir Care* 2008; **53**:1042–7.
8. Adrogue HJ, Rashad MN, Gorin AB, Yacoub J, Madias NE. Assessing acid–base status in circulatory failure: differences between arterial and central venous blood. *N Engl J Med* 1989; **320**: 1312–16.
9. Morley TF, Giaimo J, Maroszan E, *et al.* Use of capnography for assessment of the adequacy of alveolar ventilation during weaning from mechanical ventilation. *Am Rev Respir Dis* 1993; **148**: 339–44.
10. Prause, GH, Hetz P, Lauda H, *et al.* A comparison of the end-tidal CO_2 documented by capnometry and arterial PCO_2 in emergency patients. *Resuscitation* 1997; **35**: 145–8.
11. Ontario Ministry of Health. Technology Subcommittee of the Working Group on Critical Care, Ontario Ministry of Health. *Can Med Assoc J* 1992; **146**: 703–12.
12. Carlon GC, Ray C Jr., Miodownik S, Kopec I, Groeger JS. Capnography in mechanically ventilated patients. *Crit Care Med* 1988; **16**: 550–6.
13. Yang KL, Tobin MJ. A prospective study of indexes predicting the outcome of trials of weaning from mechanical ventilation. *N Engl J Med* 1991; **324**: 1445–50.
14. Saura P, Blanch L, Lucangelo U, *et al.* Use of capnography to detect hypercapnic episodes during weaning from mechanical ventilation. *Intens Care Med* 1996; **22**: 374–81.
15. Withington DE, Ramsay JG, Saoud AT, Bilodeau J. Weaning from ventilation after cardiopulmonary bypass: evaluation of a non-invasive technique. *Can J Anaesth* 1991; **38**: 15–19.
16. Taskar V, John J, Larsson A, Wetterberg T, Johnson B. Dynamics of carbon dioxide elimination following ventilator resetting. *Chest* 1995; **8**: 196–202.
17. Maslow A, Stearns G, Bert A, *et al.* Monitoring end-tidal carbon dioxide during weaning from cardiopulmonary bypass in patients without significant lung disease. *Anesth Analg* 2001; **92**: 306–13.

Section 1
Chapter
17

Ventilation

Optimizing the use of mechanical ventilation and minimizing its requirement with capnography

I. M. Cheifetz and D. Hamel

Optimizing mechanical ventilation

This chapter focuses on the use of capnography to optimize and minimize the length of mechanical ventilation. The sophistication of modern mechanical ventilators enables clinicians with a myriad of options for providing mechanical ventilation. Clinicians can individualize ventilatory strategies to meet specific patient needs. No one would dispute the fact that these ventilatory options have greatly enhanced the delivery of mechanical ventilation; however, the complexity of some of the newer ventilatory parameters makes monitoring of the cardiorespiratory status of critically ill patients even more crucial. Continuous monitoring of capnography provides clinicians with instant feedback on the effects of ventilatory choices. Capnography can also provide continuous monitoring for potentially life-threatening situations.

Advances in capnography

Time-based capnometry is most commonly referred to as *end-tidal carbon dioxide ($ETCO_2$) monitoring*. Capnography, when used without qualification, refers to time-based values displayed over time. Volume-based capnography (i.e., volumetric capnography) uses a combination of a CO_2 sensor and a pneumotachometer, and graphically displays CO_2 elimination in relation to the exhaled volume of gas. This permits the calculation of the net quantity of CO_2 expired by the subject (i.e., the difference between expired and inspired CO_2, although normally inspired CO_2 is negligible), and is expressed as a volume of gas rather than a partial pressure or gas fraction.

An essential role for capnography is to assess the appropriate placement of the endotracheal tube. Although time-based capnography is an effective tool for validating correct placement of the endotracheal tube in the trachea [1–4], volumetric capnography may be even more effective for this purpose. [5,6]. Time-based capnography may provide a false-positive reading (i.e., endotracheal tube not in trachea and monitor displays an end-tidal CO_2 value) in patients who (1) have antacids or carbonated beverages in the stomach, (2) recently received prolonged bag-valve mask ventilation prior to intubation, or (3) have the endotracheal tube tip placed in the pharynx. A false-negative time-based result (i.e., endotracheal tube is in trachea and monitor does not display an end-tidal CO_2 value) may occur in patients with severe airway obstruction, poor cardiac output, pulmonary emboli, or pulmonary hypertension.

Time-based and volume-based capnography display immediate responses to changes in ventilatory strategies and cardiac function. Both $ETCO_2$ and $\dot{V}CO_2$ can be used to determine alterations in gas exchange in response to changes in mechanical ventilatory support. Traditionally, it has been taught that the end-tidal CO_2 value is useful for managing mechanical ventilation only if a normal plateau phase of the capnogram is present. However, if physiologic deadspace is not significantly elevated, end-tidal CO_2 measurements can, in fact, serve to reliably track changes in $PaCO_2$ in many intensive care unit (ICU) patients [7]. One would expect that volumetric capnography would be an even better marker for dynamic changes in gas exchange than capnometry alone or time-based capnography [8,9].

Advances in technology have greatly improved respiratory monitoring capabilities over the past two decades [10–12]. These technologic advances provide essential data concerning cardiorespiratory interactions. Modern respiratory monitors offer clinicians the ability to monitor and accurately quantify CO_2 elimination ($\dot{V}CO_2$) and deadspace ventilation continuously and non-invasively using volumetric capnography. Theoretically, the ability to monitor these parameters non-invasively should lead to improvements in patient

Capnography, Second Edition, ed. J. S. Gravenstein, Michael B. Jaffe, Nikolaus Gravenstein, and David A. Paulus. Published by Cambridge University Press. © Cambridge University Press 2011.

care, a reduction in the duration of mechanical ventilation, and a resultant reduction in the length of ICU admission. A reduced period of mechanical ventilation should, in turn, result in a decrease in the number of arterial blood gas analyses and chest radiographs performed and mechanical ventilator-related charges, thereby producing an overall reduction in hospital costs. Randomized, prospective controlled trials are needed to formally validate these speculations.

Overall, valuable clinical information can be gained with the use of non-invasive CO_2 monitoring [13]. Non-invasive CO_2 monitoring has been shown to be more effective than clinical judgment alone in the early detection of adverse respiratory events, such as hypoventilation, esophageal intubation [4,14–16], and ventilator circuit disconnections, thus potentially preventing patient injury [17].

Proper clinical interpretation of capnographic waveforms is essential to optimize mechanical ventilation [18,19]. Characteristic waveforms and deviations suggest abnormalities that require recognition and imply potential corrections [10,18,19].

Conditions in which there is a significant alteration of physiologic deadspace, such as severe lung injury and impaired cardiac output, often weaken the correlation between $ETCO_2$ and $PaCO_2$. Given that cardiac output may be reduced by elevated mean airway pressure (generally as a result of a significant increase in positive end-expiratory pressure, PEEP) and other ventilatory manipulations, capnography is a valuable tool to assist with optimizing mechanical ventilation, including PEEP management (as discussed below).

The shape of the time-based capnogram can be very helpful in the management of ventilated patients. For example, a delayed upstroke of the expiratory plateau is seen with severe bronchospasm. Any significant failures in circulation, such as decreased cardiac output, cardiac arrest, or hypotension, will be seen as a decrease in the height of the plateau of the time-based capnogram.

Time-based capnography can also be very useful in assessing changes in a patient's cardiovascular status. In the extreme, increases in $ETCO_2$ and $\dot{V}CO_2$ during cardiopulmonary resuscitation indicates an increase in cardiac output as spontaneous circulation returns [20].

Phases of mechanical ventilation

Mechanical ventilation can be divided into three phases: acute stabilization, pre-weaning, and weaning/extubation readiness testing. The acute stabilization phase is the stage at which mechanical ventilation is initiated, and the patient is acutely resuscitated and stabilized from a cardiorespiratory standpoint. During this phase, ventilation strategies are geared toward stabilization of the patient, with little thought of weaning. The duration of this phase is extremely variable and dependent on both the clinician and the patient. Regardless of the condition necessitating mechanical ventilation, ideally this phase should be short and possibly non-existent in many patients. Ventilator parameters are generally at their maximum levels during this phase. High mean airway pressures may be necessary to provide adequate oxygenation, and optimal CO_2 elimination may require high alveolar minute ventilation. Once the patient's condition is stabilized, the patient is deemed to be in the pre-weaning stage.

The underlying condition that led to the requirement for mechanical ventilation need not be resolved for the patient to advance into the pre-weaning stage. The amount of time the patient spends in this phase will again depend on the underlying condition that led to the initiation of ventilation. It is in the pre-weaning phase when the goals of ventilation shift from stabilization to lung protection. Ideally, lung protective ventilation should begin immediately upon intubation. However, during acute stabilization, the focus is on life-saving maneuvers, and lung protective strategies may need to be briefly delayed. Once the patient's cardiorespiratory status is acutely stabilized, the emphasis shifts to lung protection. Lung protective strategies that may be employed include, but are not limited to, any combination of the following: low tidal volume ventilation [21], high-frequency ventilation [22–26], exogenous surfactant [27], and permissive hypercapnia [28–30]. Prone positioning [31–33] and inhaled nitric oxide [34,35] have not been demonstrated to improve outcomes for patients with acute lung injury. Once the patient has demonstrated no need for further increases in ventilator settings and hemodynamic stability for approximately 6 h, the active weaning phase is initiated [36], unless the patient passes an extubation readiness test [37,38]. A discussion of the advantages/disadvantages of extubation readiness testing and spontaneous breathing trials is briefly included later in this chapter.

When a patient enters the weaning phase, the clinician decelerates the ventilator settings in an effort to move toward extubation. While it is important to decrease ventilator support as rapidly as possible,

doing so too aggressively may have deleterious effects. Inadequate PEEP and/or delivered tidal volume can lead to atelectasis and, consequently, deterioration of gas exchange. On the other hand, weaning too cautiously can result in patients remaining intubated longer than necessary. While capnography is of great assistance during all phases of ventilation, it is especially useful during weaning as described below. Preliminary data from our institution indicate that the overall length of ventilation may be reduced with the use of continuous volumetric capnography. (I. M. Cheifetz *et al.* unpublished data).

Tidal volume delivery

During positive pressure ventilation, the quantity of CO_2 expired is routinely controlled by adjusting the total minute ventilation (delivered tidal volume and/or respiratory rate). Since lung protective strategies require low tidal volume ventilation, an accurate determination of the tidal volume delivered to a patient's lungs is essential. Although this seems to be an obvious concept, the question really is: do the tidal volumes displayed by the mechanical ventilator actually reflect the volume of gas delivered to the lungs? For infants and small children, the tidal volumes displayed by the ventilators may not accurately represent the gas volume delivered to the lungs. Many conventional ventilators measure tidal volume at the expiratory valve, i.e., substantially remote from the airway. However, secondary to multiple variables, such as circuit compliance, heaters, in-line suction devices, secretions, and condensation, tidal volumes measured at the expiratory valve of a ventilator do not accurately reflect the true tidal volume delivered to the patient's lungs [39]. Significant differences exist in expiratory valve-determined tidal volumes compared to pneumotachometer-determined tidal volumes at the endotracheal tube. Calculated effective tidal volumes are, thus, obviously affected [39]. The algorithms to calculate the effective delivered tidal volume by the more modern ventilators are much improved over older models; however, most of these algorithms have not been systematically studied in the ICU, especially for infants and young children. Furthermore, some algorithms are not utilized by the ventilators for the infant population, in which these concepts are most important. Considering the overall small tidal volumes used in ventilating infants and young children, even relatively small inaccuracies in tidal volume determination may result in significant adverse conditions. For example, a 10-mL discrepancy represents at least a 33% tidal volume measurement error in a 3-kg infant.

Tidal volume determination at the endotracheal tube is a more accurate representation of the actual tidal volume delivered to the patient's lungs than tidal volume measured at the expiratory valve of the ventilator. When tidal volumes are measured using a pneumotachometer positioned between the ventilator circuit and the endotracheal tube, the ventilator circuit compliance and the confounding circuit variables are no longer pertinent factors.

Many important patient management decisions are based on tidal volume determination [40–42]. If the decision to wean is based on inaccurate tidal volume measurements, then patients ready to be weaned may be assessed as unable; whereas patients assessed as ready may, in fact, not be. When delivered tidal volumes are inadequate despite an appropriate tidal volume reading on a ventilator (based on an expiratory valve measurement), a compensatory increase in respiratory rate often follows, potentially resulting in a false assumption that the patient is not able to be weaned. Again, this is especially true when mechanically ventilating infants and small children.

Alternatively, the clinician may attempt to compensate for the expected discrepancy in tidal volume measurements (expiratory valve versus endotracheal tube) by increasing the ventilator's set delivered tidal volume. However, without an accurate determination of the tidal volume at the endotracheal tube, the risk for overcompensation exists. When overcompensation occurs, the patient is at risk for overdistention, resulting in volutrauma and secondary lung injury [21,30,43].

Therefore, with proximal gas flow monitoring at the endotracheal tube, continuous assessment of the tidal volume delivered to the airways is easily achieved. However, these volumes represent the quantity of gas moving in and out of the lungs but do not provide information as to the portion of the total ventilation that actually participates in gas exchange at the alveolar level.

Alveolar minute ventilation

Minute ventilation values displayed on mechanical ventilators represent the amount of gas moving in and out of the lungs per minute (respiratory rate times tidal volume). This calculated or measured value is the sum of alveolar and deadspace ventilation. Alveolar ventilation is the volume of air that reaches the alveoli and participates in gas exchange at the capillary level

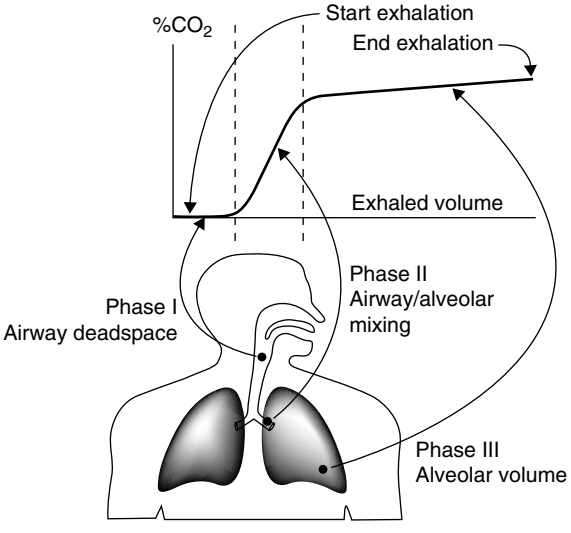

Figure 17.1 Volumetric capnogram. The initial portion of the volumetric capnogram (phase I) represents the quantity of CO_2 eliminated from the large airways. Phase II is the transitional zone which represents ventilation from both large and small airways. Phase III of the capnogram represents $\dot{V}CO_2$ from the alveoli and, thus, the quantity of gas involved with alveolar ventilation. [Image courtesy of Respironics, Inc., Murrysville, PA.]

(minute ventilation less deadspace ventilation) [44]. To determine the quantity of gas that reaches the alveoli and actively participates in gas exchange, it is important to determine the alveolar minute ventilation (MV_{ALV}). Alveolar minute ventilation is determined from the volumetric capnogram (see Figure 17.1). Phase III of the waveform represents the quantity of gas exhaled from the alveoli. Thus, alveolar minute ventilation becomes the volume of this gas per breath summated over 1 min.

In preliminary data from our institution, a linear regression analysis was utilized to compare total minute ventilation with alveolar minute ventilation in a heterogeneous group of 30 ventilated pediatric ICU patients. Data were collected every minute for 24 h (average number of data points per patient = 1440). A poor correlation, defined as r^2 less than 0.70, was noted in 37% (11/30) of the patients. Thus, the traditional determination of minute ventilation does not accurately represent the actual volume of gas involved in gas exchange at the alveolar level. Volumetric capnography provides clinicians with a continuous determination of MV_{ALV} to optimize ventilator management strategies. As deadspace ventilation approaches zero, alveolar minute ventilation approaches total minute ventilation.

Volume of carbon dioxide elimination: volumetric capnography

Volumetric capnography allows the continuous monitoring of the volume of CO_2 eliminated per unit time ($\dot{V}CO_2$). This is the net volume of CO_2 eliminated through the lungs each minute (mL/min). Since $\dot{V}CO_2$ is affected by ventilation, circulation/perfusion, and, to a lesser degree, diffusion, it is a valuable marker for changes in the cardiorespiratory status of a ventilated patient. The value of $\dot{V}CO_2$ signals future changes in $PaCO_2$. The volumetric capnogram has been utilized successfully in the measurement of anatomical deadspace, pulmonary capillary perfusion, and effective ventilation [45]. Monitoring devices that measure $\dot{V}CO_2$ and display volumetric capnograms provide clinicians with a breath-to-breath indicator of patient gas exchange in response to ventilator settings [46] and the effects of cardiorespiratory interactions.

Carbon dioxide production is determined by metabolism. Therefore, the quantity of CO_2 normally produced is dependent on the patient's body weight and level of activity. For a normal, healthy, resting person with a normal respiratory quotient (RQ = 0.8), an estimated minute production can be calculated by using Brody's formula ($\dot{V}CO_2 = 8 \times wt^{0.75}$). At rest, an average-sized adult produces about 200–250 mL of CO_2 per minute [44]. However, for a ventilated patient, it is difficult to determine the "normal" $\dot{V}CO_2$, as Brody's formula does not apply, because a ventilated patient does not represent "a normal, healthy, resting person." Hence, it is important to stress that the usefulness of $\dot{V}CO_2$ in managing ventilated patients is based more on changes over time (i.e., trends and patterns) than absolute values. There are several conditions that do predictably increase or decrease CO_2 production. Carbon dioxide production decreases with a decrease in metabolic activity, and increases with an increase in metabolic activity. For example, CO_2 production increases with agitation, fever, shivering, and caloric intake, and decreases with sedation/sleep and hypothermia (except if shivering occurs).

Carbon dioxide balance (production versus elimination) in the body is dependent on four main factors: production, transportation (cells to blood and blood to lungs), storage (skeletal muscle, fat, and bone), and elimination. In a normal, healthy individual, the amount of CO_2 produced from metabolism rapidly equilibrates with the amount of CO_2 eliminated by the lungs. Since areas of deadspace (anatomic

and physiologic) do not participate in gas exchange, all expired CO_2 derives from alveolar gas. As with oxygen consumption, CO_2 production and elimination ($\dot{V}CO_2$) is a continuous process. Therefore; $\dot{V}CO_2$ rapidly reflects changes in ventilation and perfusion regardless of the etiology. Additionally, $\dot{V}CO_2$ reflects the body's physiologic response to changes in mechanical ventilator settings. Capnography is a very sensitive clinical tool and, thus, useful for reflecting changes in the cardiorespiratory status and metabolic state of the patient [9,47].

By analyzing the volumetric capnogram slopes, clinicians can quickly and easily assess clinical issues of concern. In Figure 17.1, phase I represents gas exhaled from the upper airways (i.e., gas exhaled from anatomical deadspace), which generally is void of CO_2 [8]. Therefore, an increase in phase I indicates an increase in anatomic deadspace ventilation ($V_{D_{ana}}$). Phase II is the transitional phase from upper to lower airway ventilation, and tends to depict changes in perfusion. For example, a decrease in phase II slope would be indicative of reduced perfusion. Phase III is the area of alveolar gas exchange, and represents changes in gas distribution. For example, an increase in the slope of phase III is indicative of increased maldistribution of gas delivery. This topic is discussed in more detail elsewhere (Chapter 34: Capnography and the single-path model applied to cardiac output recovery and airway structure and function).

When weaning from mechanical ventilation, it is important to assure that the volume of gas delivered actually participates in gas exchange. The monitoring of $\dot{V}CO_2$ provides objective data that not only assist in the management of mechanical ventilation, but facilitate weaning.

Successful weaning using volumetric capnography is demonstrated in Figure 17.2a. In the top portion of this figure, alveolar minute ventilation is displayed. Over time, spontaneous ventilation (as displayed by the black bars) increases while total minute ventilation

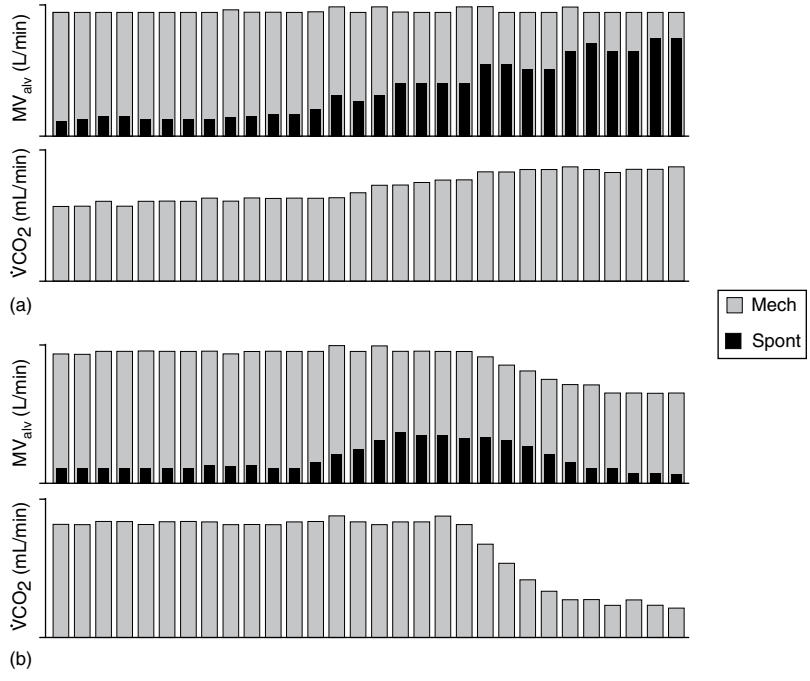

Figure 17.2 Volumetric capnography and weaning from mechanical ventilation. (a) Successful weaning. The top panel represents total MV_{alv} as divided between mechanical breaths and spontaneous breaths. In this graph, the patient's spontaneous ventilation (Spont) is increasing as mechanical ventilator (Mech) support (i.e., synchronized intermittent mandatory ventilation, SIMV, rate) is weaned. In the bottom panel, $\dot{V}CO_2$ slightly increases over time. Thus, the patient is able to tolerate the transition to spontaneous breathing. The mild increase in $\dot{V}CO_2$ represents increased CO_2 production related to the expected increased work of breathing. (b) Failure weaning. The top panel represents total MV_{alv} as divided between mechanical breaths and spontaneous breaths. In this graph, the patient's Spont initially increases as Mech support is weaned. However, over time the patient's respiratory effort deteriorates and minute ventilation falls. In the bottom panel, $\dot{V}CO_2$ decreases over time. Thus, the patient is unable to tolerate the transition to spontaneous breathing. Arterial blood gas analyses would reveal an increasing $PaCO_2$. $\dot{V}CO_2$ in mL/min and MV_{alv} in L/min. [Image courtesy of Respironics, Inc., Murrysville, PA.]

remains stable. Thus, during this period of time, mechanical ventilatory support is being weaned, and the patient assumes the additional work of breathing. In this case of successful weaning, $\dot{V}CO_2$ (see Figure 17.2b) remains stable and then slightly increases, representing increased CO_2 production. This demonstrates that the patient is tolerating the increased spontaneous respiratory effort, and is able to continue to expire CO_2; an arterial blood gas would demonstrate a stable $PaCO_2$.

The slight increase in $\dot{V}CO_2$ in Figure 17.2a represents an increase in CO_2 production as the patient's work of breathing increases in association with the decrease in ventilator support. This minimal increase in $\dot{V}CO_2$ is typical of successful weaning. A more dramatic increase in $\dot{V}CO_2$ would suggest excessive work of breathing and the potential for impending respiratory decompensation. This scenario would be consistent with a visual assessment of increasing respiratory distress (e.g., retractions, tachypnea, and potentially agitation).

Weaning failure is demonstrated in Figure 17.2b. In this case, as the ventilator settings are decreased, the patient is no longer able to maintain an adequate degree of spontaneous ventilation, and, hence, total minute ventilation falls. This decrease in minute ventilation is associated with a decrease in CO_2 elimination. An arterial blood gas would reveal an elevated $PaCO_2$. Volumetric capnography enables the clinician to identify weaning failure and increase mechanical ventilator support promptly, without the requirement for an arterial blood gas determination [48].

Positive end-expiratory pressure management

Determining an appropriate PEEP level is essential for optimal management of the mechanically ventilated patient with acute lung injury or acute respiratory distress syndrome (ARDS). Controversy does exist concerning the best method for achieving the appropriate PEEP level for an individual patient. The best PEEP level for a specific patient is the value that provides the optimal lung volume and, thereby, the highest oxygenation for the lowest fraction of inspired oxygen (FiO_2), the greatest pulmonary compliance, and the highest cardiac output. No PEEP level generally achieves all of these goals for a specific patient at a given time. It is the clinician's responsibility to determine the PEEP level that most optimally balances each of these cardiorespiratory goals.

Maintaining an appropriate level of PEEP may prevent lung derecruitment and the development of atelectasis. Use of excessive PEEP may further exacerbate the presence of overdistention and adversely affect cardiac performance [49]. Titration of PEEP levels can be effectively achieved by monitoring $\dot{V}CO_2$ and the volumetric capnogram. The value of $\dot{V}CO_2$ is more informative than $etCO_2$ during changes in PEEP [8,9].

Monitoring $\dot{V}CO_2$, as well as analyzing the slope of the waveform, provides information regarding the management of PEEP. For example, an increase in $V_{D_{ana}}$ is often present when high PEEP levels are applied [50]. This increase in $V_{D_{ana}}$ is most likely secondary to the restriction of an intact chest wall, thus limiting the expansion of the airways [47]. An increase in $V_{D_{ana}}$ can be quickly recognized by an increase in phase I of the capnogram. When this condition is present, a reduction in PEEP should improve alveolar minute ventilation.

Decreased $\dot{V}CO_2$ with a decline in the phase II slope of the waveform is also indicative of excessive PEEP levels. This decrease, however, is caused by reduced pulmonary perfusion [50–52]. The reduced perfusion secondary to excessive PEEP levels is generally caused by an increase in the mean intrathoracic pressure, in turn creating a decrease in systemic venous return (i.e., decreased right ventricular preload) and possibly an increase in pulmonary vascular resistance (i.e., increased right ventricular afterload) depending on the changes in overall lung volume [49]. These physiologic changes in loading conditions adversely affect right ventricular function and, thereby, cardiac output [49]. The decrease in pulmonary blood flow reduces the amount of CO_2 that is transported from the tissues to the vasculature of the lung [8], and subsequently reduces CO_2 elimination.

Phase III of the waveform represents gas distribution at the alveolar or distal airway level. An elevation in the phase III slope depicts maldistribution of gas, which can be caused by inappropriate PEEP levels and/or small airways restrictive disease. When PEEP levels are inadequate, alveolar collapse can occur, resulting in various degrees of atelectasis.

Importance of rapid and successful liberation from mechanical ventilation

Minimizing the duration of mechanical ventilation is crucial in the management of critically ill infants, children, and adults. Mechanical ventilation is, without

question, a life-sustaining therapy; however; it is not without real risk [53–60].

The application of mechanical ventilation places the patient at risk for many adverse pulmonary, cardiac, and neuromuscular effects. The risks are increased when mechanical ventilation is prolonged. Prolonged mechanical ventilation is associated with increased ventilator-induced lung injury (VILI), airway injury, nosocomial pneumonia, excessive use of pharmacologic sedation, prolonged length of ICU and hospital stay, increased costs, increased physiologic stress, and, potentially, even increased mortality [55–60].

High peak airway pressure, inadequate PEEP, repeated alveolar collapse and expansion, and repetitive de-recruitment can create a stress-activated signaling cascade (see Figure 17.3). The ultimate result of this cascade is VILI and its sequelae. The effects of mechanical ventilation on the body's immune system and organ function are extremely complex [61,62]. The consequences of barotrauma, volutrauma, atelectotrauma, and biotrauma can be significant. Multiple lung protective strategies have been proposed in the medical literature. The best method to minimize VILI and its consequences is to minimize the length of mechanical ventilation.

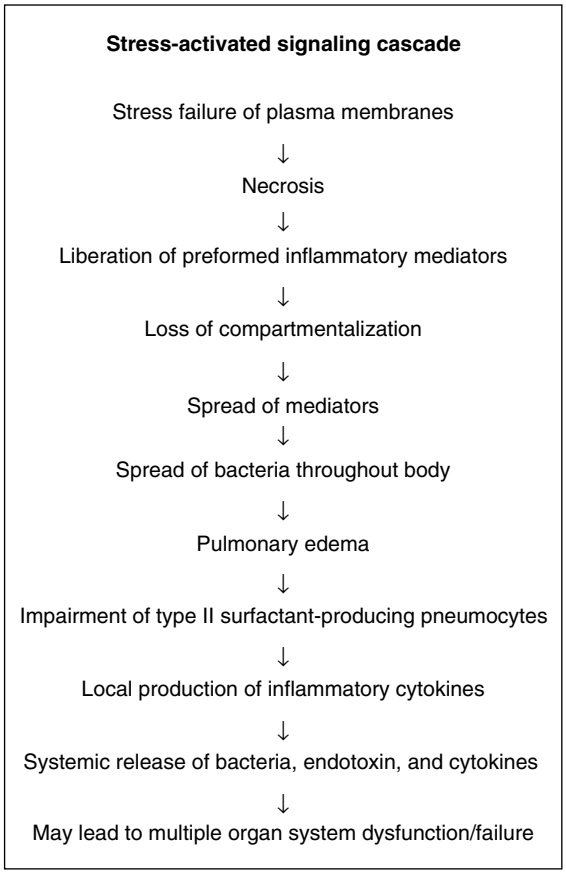

Figure 17.3 Ventilator-induced lung injury (VILI). The stress-activated signaling cascade in response to mechanical ventilation can be extremely complex. This cascade results in VILI and possibly multiorgan system dysfunction/failure.

Clinical debate continues as to whether a patient should be "weaned" or "liberated" from mechanical ventilation (i.e., spontaneous breathing trials/extubation readiness testing). Weaning denotes a gradual reduction in the amount of ventilatory support provided to the patient. *Liberation* from mechanical ventilation implies the use of an extubation readiness test to withdraw mechanical ventilation as soon as the patient meets extubation criteria regardless of the level of ventilatory support. No matter what terminology is used, the goal must be to minimize the length of mechanical ventilation for each patient to the shortest possible time. The clinical difficulty lies in achieving the balance between minimizing the length of ventilation while maintaining an acceptable extubation failure rate. A relative consensus concerning the timing of intubation and the initiation of mechanical ventilation has existed for some time, but the management, weaning, and extubation of mechanically ventilated patients has been primarily subjective and determined by institutional and/or individual practices and preferences [40,63,64]. A myriad of adversities make weaning and liberation from mechanical ventilation an extremely important clinical issue.

Weaning

Weaning from mechanical ventilation is a process requiring ongoing clinical assessment and planning by multidisciplinary members of the patient care team [65]. The contributions made by physicians, nurses, and respiratory care practitioners provide a comprehensive evaluation of the strategy, as well as patient response. Complications result from mechanical ventilation even under the best of circumstances; therefore, ventilator management strategies should be implemented, with weaning geared toward prompt and successful extubation as a primary goal. Careful consideration must be given to initiate optimal weaning and extubation strategies on the first day that success is considered likely [41]. With recent technological advances in capnography, clinicians are provided with measurable and consistent data, thus allowing for a more objective approach to total ventilator management.

Potentially even more complex than the act of weaning is the accurate identification of patients who can be successfully extubated. This is an everyday challenge in ICUs. Patients are at risk for continued VILI if their ability to breathe unassisted is not recognized. However, the ideal timing for extubating a patient with acute lung injury remains elusive, and the techniques utilized have traditionally been more art than science. Although prolonged mechanical ventilation has significant risks, failed extubation also potentially increases morbidity and mortality. Reintubation results in prolonged intubation, increased risk for VILI and nosocomial pneumonia, prolonged ICU and hospital stay, increased costs, and increased mortality [66–78]. Predicting successful extubation presents unique challenges to clinicians. Since mechanical ventilation poses significant risks that increase over time, minimizing the duration of mechanical ventilation, as well as the risk of reintubation, is crucial in the management of critically ill patients [79,80].

It is for these reasons that the development of patient assessment and monitoring techniques, which easily and safely distinguish those patients ready for discontinuation of ventilatory support from those patients who require continued support, is essential [79,80].

Extubation

The final stage in mechanical ventilation is the point at which the patient is likely to tolerate discontinuation of mechanical ventilation. Preparing for extubation begins with the assessment of the patient's ability to breathe effectively without the ventilator and the subsequent ability to continue to maintain adequate gas exchange without an artificial airway. Predicting successful extubation remains a daunting challenge for every clinician involved in the care of mechanically ventilated patients, especially for those working with infants and children. While many measures have been suggested as reliable predictors of successful liberation from mechanical ventilation, few, except for extubation readiness testing, have been proven [37,38,64].

With as many as 20% of recently extubated patients requiring reintubation, great emphasis has been placed on accurately predicting extubation readiness [77,81]. Many discrepancies still exist when evaluating extubation success. Because of the increased risks to patients requiring reintubation [60,70–76,78,82,83], extubation must be timed carefully. Without objective criteria, the variability between clinician thresholds poses a significant clinical dilemma. A particular strategy may be superior in a setting where clinician threshold for extubation is low but fail in a setting where clinician threshold is high. For example, it may appear that clinicians with low extubation failure rates are doing the best job; when, in fact, the low rates of extubation failure may come at the cost of prolonged ventilation and associated complications [56–60,68,69]. Extubation failure rates must be assessed in relation to length of ventilation and patient acuity data.

While many extubation failure predictors exist [84–89], there is only a limited number of studies showing effective success indicators. This is especially true in the case of infants and children. In adult and pediatric patients, the spontaneous breathing trial (SBT) has come into favor in many centers [37,38,64,85,90]. Using the SBT method, patients are assessed at least daily for their ability to breathe spontaneously. Once it is determined a patient can maintain effective ventilation without the assistance of the ventilator, the patient is extubated.

The classic approach to extubation in all age groups – to decrease assisted ventilation to minimal settings – is based more on tradition and subjective assessments than data. With the advent of advanced technology, the clinician has objective data for assessing the ability of patients to be liberated from mechanical ventilation. The physiologic deadspace ratio ($V_D/V_{T_{phys}}$) has long been utilized as a marker of lung disease in adult intensive care [91]. While $V_D/V_{T_{phys}}$ greater than 0.60 has been used in the past as an indication for intubation, it was not until more recently that $V_D/V_{T_{phys}}$ has been studied as a guide for extubation readiness [88]. Until the improvements in CO_2 monitoring technology, measuring the physiologic V_D/V_T ratio was not a simple clinical task. With the present technological advances, V_D/V_T can now be obtained quickly, accurately, and non-invasively at the bedside. Using a modified Bohr equation, volumetric capnography can rapidly calculate and display V_D/V_T values. Additionally, an increase from baseline of phase I of the volumetric capnogram can be seen in the presence of an increase in $V_{D_{ana}}$ (Figure 17.1).

While there are no studies to date on the effectiveness of physiologic V_D/V_T as a predictor of extubation success in adults, V_D/V_T less than 0.5 has been shown to be predictive of extubation success in infants and children [88]. The SBT used in adults assesses the ratio of frequency to tidal volume (f/V_T) to determine extubation readiness. An increase in deadspace would lead

to a decrease in effective tidal volume and a compensatory increase in frequency; hence, the result would be an increased f/Vt. Additionally, alveolar deadspace is increased in the presence of excessive PEEP, intrinsic lung disease, and airway obstruction. Therefore, an increased Vd/Vt warrants investigation prior to an extubation trial.

Summary

With the majority of ICU patients requiring mechanical ventilation, minimizing the duration of mechanical ventilation while optimizing the potential for successful extubation is crucial in the management of critically ill patients. A number of differing opinions exists as to the best mode of weaning from mechanical ventilation. To date, there is little evidence proving one mode is superior to another. Whatever ventilator mode is utilized, weaning from mechanical ventilation should begin as soon as the patient stabilizes. A clear-cut, organized plan, based on objective criteria and adjusted to meet changes in patient status, is clearly recommended.

Capnography, both time-based and volumetric, allows mechanical ventilatory strategies to be designed with clear, precise, objective criteria. With the data provided by capnography, adequate gas delivery, optimal PEEP, and effective ventilation can be established while using the least amount of mechanical assistance, regardless of clinician or institutional preferences.

References

1. Holland R, Webb RK, Runciman WB. The Australian Incident Monitoring Study. Oesophageal intubation: an analysis of 2000 incident reports. *Anaesth Intens Care* 1993; **21**: 608–10.
2. Birmingham PK, Cheney FW, Ward RJ. Esophageal intubation: a review of detection techniques. *Anesth Analg* 1986; **65**: 886–91.
3. Knapp S, Kofler J, Stoiser B, *et al.* The assessment of four different methods to verify endotracheal tube placement in the critical care setting. *Anesth Analg* 1999; **88**: 766–70.
4. American Heart Association. 2005 American Heart Association (AHA) Guidelines for Cardiopulmonary Resuscitation (CPR) and Emergency Cardiovascular Care (ECC) of Pediatric and Neonatal Patients: pediatric advanced life support. *Pediatrics* 2006; **117**: e1005–28.
5. Sum-Ping ST, Mehta MP, Anderton JM. A comparative study of methods of detection of esophageal intubation. *Anesth Analg* 1989; **69**: 627–32.
6. Grmec S. Comparison of three different methods to confirm tracheal tube placement in emergency intubation. *Intens Care Med* 2002; **28**: 701–4.
7. Schmitz BD, Shapiro BA. Capnography. *Respir Care Clin N Am* 1995; **1**: 107–17.
8. Johnson JL, Breen PH. How does positive end-expiratory pressure decrease pulmonary CO_2 elimination in anesthetized patients? *Respir Physiol* 1999; **118**: 227–36.
9. Breen PH, Serina ER, Barker SJ. Measurements of pulmonary CO_2 elimination must exclude inspired CO_2 measured at the capnometer sampling site. *J Clin Monit* 1996; **12**: 231–6.
10. Weingarten M. Respiratory monitoring of carbon dioxide and oxygen: a ten-year perspective. *J Clin Monit* 1990; **6**: 217–25.
11. Lain D. Transcutaneous and end-tidal capnometry. *Respir Care* 2007; **52**: 340–1.
12. Jaffe MB. Infrared measurement of carbon dioxide in the human breath: "breathe-through" devices from Tyndall to the present day. *Anesth Analg* 2008; **107**: 890–904.
13. Kupnik D, Skok P. Capnometry in the pre-hospital setting: are we using its potential? *Emerg Med J* 2007; **24**: 614–17.
14. Kannan S, Manji M. Survey of use of end tidal carbon dioxide for confirming tracheal tube placement in intensive care units in the UK. *Anaesthesia* 2003; **58**: 476–9.
15. Katz SH, Falk JL. Misplaced endotracheal tubes by paramedics in an urban emergency medical services system. *Ann Emerg Med* 2001; **37**: 32–7.
16. Repetto JE, Donohue PK, Baker SF, Kelly L, Nogee LM. Use of capnography in the delivery room for assessment of endotracheal tube placement. *J Perinatol* 2001; **21**: 284–7.
17. Aherns S. Capnography application in acute and critical care. *AACN Clin Issues* 2003; **14**: 123–32.
18. Ansermino JM, Dosani M, Amari E, Choi PT, Schwarz SK. Defining rules for the identification of critical ventilatory events. *Can J Anaesth* 2008; **55**: 702–14.
19. Thompson JE, Jaffe MB. Capnographic waveforms in the mechanically ventilated patient. *Respir Care* 2005; **50**: 100–8.
20. Isserles SA, Breen PH. Can changes in end-tidal PCO_2 measure changes in cardiac output? *Anesth Analg* 1991; **73**: 808–14.
21. ARDS Network. Ventilation with lower tidal volumes as compared with traditional tidal volumes for acute lung injury and the acute respiratory distress syndrome. *N Engl J Med* 2000; **342**: 1301–8.

22. Arnold JH, Hanson JH, Toro-Figuero LO, *et al.* Prospective, randomized comparison of high-frequency oscillatory ventilation and conventional mechanical ventilation in pediatric respiratory failure. *Crit Care Med* 1994; **22**: 1530–9.
23. Clark RH, Gerstmann DR, Null DM Jr., deLemos RA. Prospective randomized comparison of high-frequency oscillatory and conventional ventilation in respiratory distress syndrome. *Pediatrics* 1992; **89**: 5–12.
24. Froese AB. High-frequency oscillatory ventilation for adult respiratory distress syndrome: let's get it right this time! *Crit Care Med* 1997; **25**: 906–8.
25. Arnold JH, Anas NG, Luckett P, *et al.* High frequency oscillatory ventilation in pediatric respiratory failure: a multicenter experience. *Crit Care Med* 2000; **28**: 3913–19.
26. Derdak S, Mehta S, Stewart TE, *et al.* Multicenter Oscillatory Ventilation for Acute Respiratory Distress Syndrome Trial (MOAT) Study Investigators. High-frequency oscillatory ventilation for acute respiratory distress syndrome in adults: a randomized, controlled trial. *Am J Respir Crit Care Med* 2002; **166**: 801–8.
27. Willson DF, Thomas NJ, Markovitz BP, *et al.* Pediatric Acute Lung Injury and Sepsis Investigators. Effect of exogenous surfactant (calfactant) in pediatric acute lung injury: a randomized controlled trial. *JAMA* 2005; **293**: 470–6.
28. Hickling KG. Permissive hypercapnia. *Respir Care Clinic N Am* 2002; **8**: 155–69.
29. Hickling KG, Walsh J, Henderson S, Jackson R. Low mortality rate in adult respiratory distress syndrome using low-volume, pressure-limited ventilation with permissive hypercapnia: a prospective study. *Crit Care Med* 1994; **22**: 1568–78.
30. Hickling KG, Walsh J, Henderson S, Jackson R. Low mortality associated with low lung volume pressure limited ventilation with permissive hypercapnea in severe respiratory distress syndrome. *Intens Care Med* 1990; **16**: 372–7.
31. Curley MA, Hibberd PL, Fineman LD, *et al.* Effect of prone positioning on clinical outcomes in children with acute lung injury: a randomized controlled trial *JAMA* 2005; **294**: 229–37.
32. Guerin C, Gaillard S, Lemasson S, *et al.* Effects of systematic prone positioning in hypoxemic acute respiratory failure: a randomized controlled trial. *JAMA* 2004; **292**: 2379–87.
33. Gattinoni L, Tognoni G, Pesenti A, *et al.* Prone-Supine Study Group. Effect of prone positioning on the survival of patients with acute respiratory failure. *N Engl J Med* 2001; **345**: 568–73.
34. Dobyns EL, Cornfield DN, Anas NG, *et al.* Multicenter randomized controlled trial of the effects of inhaled nitric oxide therapy on gas exchange in children with acute hypoxemic respiratory failure. *J Pediatr* 1999; **134**: 406–12.
35. Dellinger RP, Zimmerman JL, Taylor RW, *et al.* Inhaled Nitric Oxide in ARDS Study Group. Effects of inhaled nitric oxide in patients with acute respiratory distress syndrome: results of a randomized phase II trial. *Crit Care Med* 1998; **26**: 15–23.
36. Cook D, Meade M, Guyatt G, Griffith L, Booker L. *Criteria for Weaning from Mechanical Ventilation Summary*. Rockville, MD: Agency for Healthcare Research and Quality, 2000.
37. Chavez A, de la Cruz R, Zaritsky A. Spontaneous breathing trial predicts successful extubation in infants and children. *Pediatr Crit Care Med* 2006; **7**: 324–8.
38. Randolph AG, Wypij D, Venkataraman ST, *et al.* Effect of mechanical ventilator weaning protocols on respiratory outcomes in infants and children: a randomized controlled trial. *JAMA* 2002; **288**: 2561–8.
39. Cannon ML, Cornell J, Tripp-Hamel DS, *et al.* Tidal volumes for ventilated infants should be determined with a pneumotachometer placed at the endotracheal tube. *Am J Respir Crit Care Med* 2000; **162**: 2109–12.
40. Soo Hoo GW, Park L. Variations in the measurement of weaning parameters: a survey of respiratory therapists. *Chest* 2002; **121**: 1947–55.
41. Manthous CAM. The anarchy of weaning techniques. *Chest* 2002; **121**: 1738–40.
42. Hatzakis GE, Davis GM. Fuzzy logic controller for weaning neonates from mechanical ventilation. *Proc AMIA Symp* 2002; 315–19.
43. Dreyfuss D, Soler P, Basset G, Saumon G. High inflation pressure pulmonary edema. *Am Rev Respir Dis* 1988; **137**: 1159–64.
44. Lawrence M. *The Essentials for Patient Care and Evaluation: Pulmonary Physiology in Clinical Practice*. St Louis, MO: CV Mosby, 1987.
45. Romero PV, Lucangelo U, Lopez Aguilar J, Fernandez R, Blanch L. Physiologically based indices of volumetric capnography in patients receiving mechanical ventilation. *Eur Respir J* 1997; **10**: 1309–15.
46. Taskar V, John J, Larsson A, Wetterberg T, Jonson B. Dynamics of carbon dioxide elimination following ventilator resetting. *Chest* 1995; **108**: 196–202.
47. Breen PH, Mazumdar B, Skinner SC. Comparison of end-tidal PCO_2 and average alveolar expired PCO_2 during positive end-expiratory pressure. *Anesth Analg* 1996; **82**: 368–73.
48. Boynton JH, O'Keefe G. The use of VCO_2 in predicting successful liberation from mechanical ventilation. *Respir Care* 1999; **44**: 1243.

49. Cheifetz IM, Craig D, Quick G, *et al.* Increasing tidal volumes and pulmonary overdistention adversely affect pulmonary vascular mechanics and cardiac output in a pediatric swine model. *Crit Care Med* 1998; **26**: 710–16.
50. Coffey RL, Albert RK, Robertson HT. Mechanisms of physiological deadspace response to PEEP after acute oleic acid lung injury. *J Appl Physiol* 1983; **55**: 1550–7.
51. Dueck R, Wagner PD, West JB. Effects of positive end-expiratory pressure on gas exchange in dogs with normal and edematous lungs. *Anesthesiology* 1977; **47**: 359–66.
52. Nieman GF, Paskanik AM, Bredenberg CE. Effect of positive end-expiratory pressure on alveolar capillary perfusion. *J Thorac Cardiovasc Surg* 1988; **95**: 712–16.
53. DeRobertis ES, Servillo G, Tufano R, Jonson B. Aspiration of deadspace allows isocapnic low tidal volume ventilation in acute lung injury: relationships to gas exchange and mechanics. *Intens Care Med* 2001; **27**: 1496–503.
54. Meade M, Guyatt G, Sinuff T, *et al.* Stress distribution in lungs: a model of pulmonary elasticity. *J Appl Physiol* 1970; **28**: 596–608.
55. Suematsu Y, Sato H, Ohtsuka T, *et al.* Predictive risk factors for delayed extubation in patients undergoing coronary artery bypass grafting. *Heart Vessels* 2000; **15**: 214–20.
56. Tobias JD, Deshpande JK, Gregory DF. Outpatient therapy of iatrogenic drug dependency following prolonged sedation in the pediatric intensive care unit. *Intens Care Med* 1994; **20**: 504–7.
57. Orlowski JP, Ellis NG, Amin NP, Crumrine RS. Complications of airway intrusion in 100 consecutive cases in a pediatric ICU. *Crit Care Med* 1980; **8**: 324–31.
58. Benjamin PK, Thompson JE, O'Rourke PP. Complications of mechanical ventilation in a children's hospital multidisciplinary intensive care unit. *Respir Care* 1990; **35**: 873–8.
59. Pierson DJ. Complications of mechanical ventilation. In: Simmons DH (ed.) *Current Pulmonology,* vol. 9. Chicago, IL: Yearbook Medical Publishers, 1990; 19–46.
60. Manthous CA, Schmidt GA, Hall JB. Liberation from mechanical ventilation: a decade of progress. *Chest* 1998; **114**: 886–901.
61. Margolin G, Groeger JS. Ventilator-induced lung injury and its relationship to recruitment maneuvers. *Crit Care Med* 2002; **30**: 2161–2.
62. Zhang, H, Gregory P, Suter PM, *et al.* Conventional mechanical ventilation is associated with bronchoalveolar lavage-induced activation of polymorphonuclear leukocytes: a possible mechanism to explain the systemic consequences of ventilator-induced lung injury in patients with ARDS. *Anesthesiology* 2002; **97**: 1426–33.
63. Sinha SK, Donn SM. Weaning from assisted ventilation: art or science? *Arch Dis Child Fetal Neonatal Ed* 2000; **83**: F64–70.
64. Esteban AF, Tobin MJ, Alia I, *et al.* The Spanish Lung Failure Collaborative Group. A comparison of four methods of weaning patients from mechanical ventilation. *N Engl J Med* 1995; **332**: 345–50.
65. Henneman E, Dracup K, Ganz T, Molayeme O, Cooper C. Effects of a collaborative weaning plan on patient outcome in the critical care setting. *Crit Care Med* 2001; **29**: 297–303.
66. Whitehead TS, Slutsky AS. The pulmonary physician in critical care: ventilator induced lung injury. *Thorax* 2002; **57**: 635–42.
67. Hess DR. Liberation from mechanical ventilation: weaning the patient or weaning old-fashioned ideas? *Crit Care Med* 2002; **30**: 2154–5.
68. Meade M, Guyatt G, Cook D, *et al.* Predicting success in weaning from mechanical ventilation. *Chest* 2001; **120**(6 Suppl): 400S–24S.
69. Meade M, Guyatt G, Sinuff T, *et al.* Trials comparing alternative weaning modes and discontinuation assessments. *Chest* 2001; **120**(6 Suppl): 425S–37S.
70. Torres A, Gatell JM, Aznar E, *et al.* Re-intubation increases the risk of nosocomial pneumonia in patients needing mechanical ventilation. *Am J Respir Crit Care Med* 1995; **152**: 137–41.
71. Epstein SK, Ciubotaru RL, Wong JB. Effect of failure extubation on the outcome of mechanical ventilation. *Chest* 1997; **112**: 186–92.
72. Esteban A, Alia I, Gordo F, *et al.* The Spanish Lung Failure Collaborative Group. Extubation outcome after spontaneous breathing trials with T-tube or pressure support ventilation. *Am J Respir Crit Care Med* 1997; **156**: 459–65.
73. Daley BJ, Garcia-Perez F, Ross SE. Reintubation as an outcome predictor in trauma patients. *Chest* 1996; **110**: 1577–80.
74. Epstein SK, Ciubotaru RL. Independent effects of etiology of failure and time to reintubation on outcome for patients failing extubation. *Am J Respir Crit Care Med* 1998; **158**: 489–93.
75. Rady MY, Ryan T. Perioperative predictors of extubation failure and the effect on clinical outcome after cardiac surgery. *Crit Care Med* 1999; **27**: 340–7.
76. Demling RH, Read T, Lind LJ, Flanagan HL. Incidence and morbidity of extubation failure in surgical intensive care patients. *Crit Care Med* 1988; **16**: 573–7.

77. Epstein SK. Decision to extubate. *Intens Care Med* 2002; **28**: 535–46.
78. Kurachek SC, Newth CJ, Quasney MW, *et al.* Extubation failure in pediatric intensive care: a multiple-center study of risk factors and outcomes. *Crit Care Med* 2003; **31**: 2657–64.
79. MacIntyre NRM, Cook DJ, Guyatt GH. Evidence-based guidelines for weaning and discontinuing ventilatory support. *Chest* 2001; **120**: 375S–395S.
80. Cook D, Meade M, Guyatt G, *et al.* Trials of miscellaneous interventions to wean from mechanical ventilation. *Chest* 2001; **120**(6 Suppl): 438S–44S.
81. Epstein SK. Extubation. *Respir Care* 2002; **47**: 483–92.
82. Hilbert G. Difficult to wean chronic obstructive pulmonary disease patients: avoid heat and moisture exchangers. *Crit Care Med* 2003; **31**: 1580–1.
83. Baisch SD, Wheeler WB, Kurachek SC, Cornfield DN. Extubation failure in pediatric intensive care incidence and outcomes. *Pediatr Crit Care Med* 2005; **6**: 312–18.
84. Khan N, Brown A, Venkataraman ST. Predictors of extubation success and failure in mechanically ventilated infants and children. *Crit Care Med* 1996; **24**: 1568–79.
85. Kollef MH, Shapiro SD, Silver P, *et al.* A randomized, controlled trial of protocol-directed versus physician-directed weaning from mechanical ventilation. *Crit Care Med* 1997; **25**: 567–74.
86. Goldstone J. The pulmonary physician in critical care. X. Difficult weaning. *Thorax* 2002; **57**: 986–91.
87. Venkataraman ST, Khan N, Brown A. Validation of predictors of extubation success and failure in mechanically ventilated infants and children. *Crit Care Med* 2000; **28**: 2991–6.
88. Hubble CL, Gentile MA, Tripp DS, *et al.* Deadspace to tidal volume ratio predicts successful extubation in infants and children. *Crit Care Med* 2000; **28**: 2034–40.
89. Newth CJL, Venkataraman S, Willson DF, *et al.* National Institute of Child Health and Human Development Collaborative Pediatric Critical Care Research Network. Weaning and extubation readiness in pediatric patients. *Pediatr Crit Care Med* 2009; **10**: 1–11.
90. Ely EW, Meade M, Haponik EF, *et al.* Mechanical ventilator weaning protocols driven by non-physician health-care professionals: evidence-based clinical practice guidelines. *Chest* 2001; **121**: 1947–55.
91. Pontoppidan H, Hedley-Whyte J, Bendizen HH, Laver MB, Radford EP Jr. Ventilation and oxygenation requirements during prolonged artificial ventilation in patients with respiratory failure. *N Engl J Med* 1965; **273**: 401–9.

Section 1
Chapter
18

Ventilation

Volumetric capnography for monitoring lung recruitment and PEEP titration

G. Tusman, S. H. Böhm, and F. Suarez-Sipmann

Introduction

Gas exchange, the lung's main function, depends on a tight matching of the distribution of ventilation and perfusion within any single acinus. Despite the fact that such processes are naturally distributed inhomogeneously, the lungs actively promote matching in areas with different ventilation and perfusion rates in order to keep the ventilation/perfusion ratio ($\dot{V}/\dot{Q}$) within the normal range. This particular task has an anatomic basis since the partitioning of airways and vessels becomes more asymmetric as these pulmonary structures branch downward, finally terminating in the alveoli [1–2]. The fractal nature of the lungs explains almost all of the heterogeneity in the distribution of ventilation and perfusion beyond the known effects of gravity [3].

The lungs are formed by a finite number of units with different $\dot{V}/\dot{Q}$ ratios, and the mean of these ratios will determine the overall status of gas exchange. Therefore, any defect in ventilation and/or perfusion of one particular acinus will produce a local mismatch that can affect lung function in general. A simplistic but easy-to-understand approach to this part of lung physiology is to consider that each acinus is represented by only two possible conditions related to gas exchange: open (functional) or collapsed (non-functional).

Lung collapse: a pressure-dependent mechanism

Due to the high surface tension between intra-alveolar air and tissue at the alveolar–capillary membrane, the lung is highly unstable. Pulmonary acini maintain their normal morphology by two main mechanisms. First, the surfactant tends to stabilize lung units by decreasing the alveolar surface tension. Second, the transpulmonary pressure (Ptp) is the pressure gradient between the airways and the pleural space that constitutes the "force" that normally maintains the lung expanded.

Gravity produces a gradient of pleural pressure within the chest, thereby creating a different Ptp along a gravitational vector. The more dependent pulmonary areas have a lower Ptp compared to their non-dependent counterparts. Thus, these dependent areas are more prone to collapse at the end of expiration. Each lung unit has a *closing* and an *opening* pressure that depends highly on its spatial localization within the lung. Dependent units will have low closing but high opening pressures because their Ptp is minimal at this level.

Mechanical ventilation, per se, may also be a cause of lung collapse, even in patients with normal lungs, since 90% of patients undergoing general anesthesia develop atelectasis and bronchiolar closure in as much as 16–20% of their lung tissue [4,5]. Acute lung injury (ALI) and acute respiratory distress syndrome (ARDS) represent the other extreme of the spectrum, since these pulmonary diseases are associated with the highest amounts of lung collapse [6].

Lung recruitment maneuvers

Lung recruitment is defined as a maneuver that "opens up" any "closed" lung unit [7]. *Lung recruitment maneuvers* in anesthesia and critical care medicine refer to ventilatory maneuvers that are aimed at opening collapsed lung areas. The main goal of recruitment is to restore ventilation and perfusion in such collapsed zones and, thus, move their $\dot{V}/\dot{Q}$ ratio into the normal range. These ventilatory strategies have shown physiologic and clinical improvements in patients with anesthetized normal lungs [8–10] and in sick lungs [11].

Lung recruitment is a pressure-dependent phenomenon. It is induced by raising airway pressures

Capnography, Second Edition, ed. J. S. Gravenstein, Michael B. Jaffe, Nikolaus Gravenstein, and David A. Paulus. Published by Cambridge University Press. © Cambridge University Press 2011.

incrementally until the opening pressure of all lung units is reached. Irrespective of how the recruitment maneuver is being performed, it must respect two main principles to be successful: (1) it must reach the opening pressure of lung units and (2) it should keep *all* lung units above their closing pressure. If these simple rules are adapted to mechanical ventilation, the lung opens with the plateau pressure during *inspiration* and is kept open by applying enough positive end-expiratory pressure (PEEP) during *expiration*.

Alveolar recruitment strategy

The alveolar recruitment strategy (ARS) is a cyclic recruitment maneuver that consists of the following phases (Figure 18.1) [8–10]:

(1) ***Hemodynamic preconditioning***. By applying pressure control ventilation with a constant driving pressure that results in a VT of ≤8 mL/kg (approximately 10–15 cm H_2O in normal lungs), PEEP is increased in steps of 5, from 5 to 20 cm H_2O. Hemodynamics can be closely assessed at a PEEP of 10 and 15 cm H_2O in order to diagnose states of occult hypovolemia. The maneuver is terminated if mean arterial pressure changes by more than 15–20%, or if it decreases below 55 mm Hg and PEEP reduced to previously safe values. Any detected hypovolemia is treated by infusion of saline solution before the maneuver is reinstituted.

(2) ***Recruitment***. Once PEEP levels have reached 20 cm H_2O, the drive pressure will be increased to 20 cm H_2O in order to reach the lung's opening pressures (40 cm H_2O of plateau pressure for normal lungs) [12]. This setting is maintained for 10 breaths. In sick lungs, recruitment pressures can be as high as 50 or 60 cm H_2O [13].

(3) ***Decremental PEEP titration***. During the PEEP titration phase, PEEP is decreased by increments of 2 cm H_2O to determine the lung's closing pressure. Once this pressure has been determined, a new recruitment maneuver is applied to recover any lung tissue that might have collapsed during the PEEP titration process. Baseline ventilation is then resumed, but, at this point, at a level of PEEP that is 2 cm H_2O above the closing pressure.

The maneuver can be adapted for patients suffering from ALI and ARDS, taking into account that the opening and collapsing pressures of the lungs may be considerably different from those found in anesthesia. The plateau pressure required to open up the collapsed lungs in these patients is approximately 50 cm H_2O, and is increased up to 60 cm H_2O in very severe ARDS [13]. The recruitment maneuver should be maintained for approximately 2 min in ALI–ARDS patients in order to accomplish a maximal recruitment effect. The level of PEEP needed to prevent the lung from recollapse after the recruitment maneuver is also higher in patients with pulmonary diseases, with values commonly ranging from 10 to 20 cm H_2O.

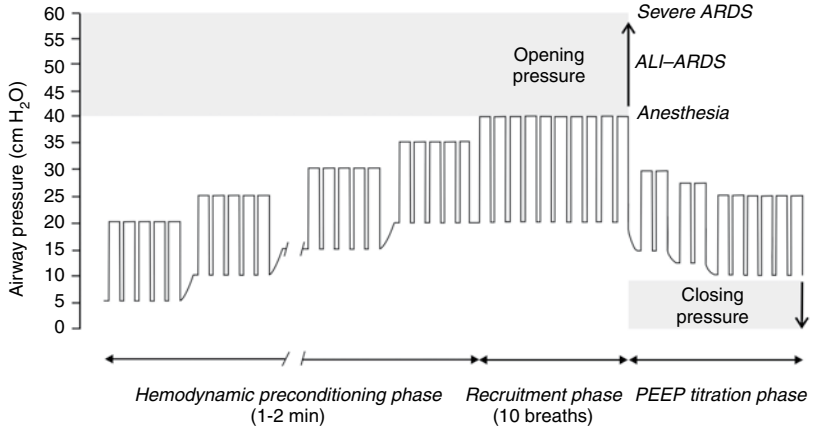

Figure 18.1 Schematic representation of the alveolar recruitment strategy as a cycling recruitment maneuver, with each rectangle representing one respiratory cycle. The opening pressure needed to fully expand the lungs and the pressures needed to keep them open depend on the lung's condition. As PEEP is increased in steps of 5 cm H_2O – from 5 to 20 cm H_20 – in lungs of anesthetized normal subjects, or a PEEP between 25 and 30 cm H_2O in ALI–ARDS patients, the plateau pressure should reach at least 40 cm H_2O and 50 to 60 cm H_2O in normal and pathological lung conditions, respectively. The maneuver is divided into three main phases: (1) the hemodynamic preconditioning; (2) the actual recruitment; and, (3) finally, the PEEP titration phase (see text for more details).

The effect of lung recruitment on CO_2 kinetics

Several chapters in this book refer to the effect of ventilation and perfusion on CO_2 kinetics. Carbon dioxide is a good marker of these two processes because each acinus needs both ventilation and perfusion for CO_2 to be eliminated adequately. Lung recruitment improves CO_2 elimination by increasing the area of the alveolar–capillary membrane available for gas exchange. On one side of this membrane, the alveolar surface increases because the airway pressure surpasses the lung's opening pressure in the collapsed zones, thereby re-aerating previously collapsed units. On the other side, capillaries are opened mainly by the immediate release of the hypoxic pulmonary vasoconstriction reflex (HPV) as O_2 enters into the recruited areas.

Given that diffusion is the mechanism of gas transport through the alveolar–capillary membrane, any increase in the surface area will augment the passage of CO_2 molecules into the alveolar compartment. Fick's law of diffusion contemplates this fact:

$$J = \frac{D \cdot A \cdot d\mathrm{CO}_2/dx}{T}$$

where J = the instantaneous flux of CO_2, D = the gas blood solubility of CO_2, A = the area of the alveolar–capillary membrane, $d\mathrm{CO}_2/dx$ = the gas concentration gradient for CO_2 between blood and gas compartments, and T = the membrane thickness. This law tells us that any decrement (lung collapse) or increment (lung recruitment) of the alveolar–capillary area will have a crucial impact on CO_2 exchange.

Once the CO_2 molecules reach the alveolar compartment, they are transported through the airway to be eliminated to the atmosphere. There are two main mechanisms of CO_2 transport within the airways: (1) diffusion, from the alveolar–capillary membrane to a point within the respiratory bronchiole; and (2) convection, further from these small airways, all the way to the airway opening. Thus, diffusion plays a role also in the transport of CO_2 within the acini, and beyond in gas transport through the alveolar–capillary membrane. The general principles of Fick's first law of diffusion can also be adapted to describe the diffusional flux of CO_2 through the small airways as follows:

$$J/D = A \cdot d\mathrm{CO}_2/dx,$$

where J/D represents the gas-phase molecular diffusivity of CO_2 in air, A = the cross-sectional area of the small airways, and $d\mathrm{CO}_2/dx$ = the axial gas concentration gradient for CO_2. The value of $d\mathrm{CO}_2/dx$ varies inversely with the total cross-sectional area of the small airways at a constant J/D.

Diffusive transport is converted into convective transport at the bronchiolar level. Referring to the basic mechanisms of CO_2 transport within the lung, lung collapse decreases not only the alveolar–capillary area, but also the total cross-sectional area of the small airways, and thus increases the resistance to diffusive as well as convective transport. Lung recruitment thus exerts an opposite effect on both mechanisms due to its strong impact on area A.

Monitoring of recruitment maneuvers

The processes of pulmonary collapse and recruitment are very dynamic [14] due to the unstable nature of lung tissue regarding its three-dimensional morphology. Lung units change from open to closed and from a closed to an open state very quickly. Thus, monitoring of lung collapse and recruitment at the bedside is not an easy task. In theory, this monitoring must be performed in real time, and non-invasively, in order to detect the very moment when the lungs open up and when they start to collapse during a PEEP titration trial. As the pulmonary opening and closing pressures vary between different zones of the lungs and among patients, monitoring of these pressures becomes a prerequisite in tailoring ventilator treatment.

Imaging techniques have the advantage over conventional lung function testing in that they allow the caregiver to directly observe the lung tissue's reaction in response to the therapeutic intervention; thus, these observations can be used to adjust the ventilatory setting. Computed tomography (CT) is considered as the reference method for determining the state of aeration, as well as to diagnose and quantify lung collapse and assess the effect of lung recruitment maneuvers [6,15]. However, this technique can neither be applied at the bedside during prolonged periods of mechanical ventilation, nor does it accommodate the dynamics of lung function. Therefore, electrical impedance tomography seems to be the functional imaging solution of choice for monitoring the physiological effects of mechanical ventilation non-invasively. This technology visualizes changes in regional lung aeration at a high temporal

and a reasonable spatial resolution based upon changes in local tissue resistivity [16].

Lung recruitment maneuvers improve gas exchange and lung mechanics. Their effects can be assessed clinically by the following pattern: increased arterial oxygenation [17] and respiratory compliance [18], reduced expiratory time constant [19], or decreased deadspace [20]. Consequently, these variables have been used for monitoring the phenomenon of lung collapse and recruitment.

The special role of volumetric capnography for monitoring lung recruitment

Volumetric capnography (VC) represents all aspects of CO_2 kinetics, i.e., its production, transport, and elimination. Lung recruitment affects the last two processes, mainly as a consequence of opening previously collapsed pulmonary capillaries and alveoli (assuming that metabolism remains constant during the short time of the maneuver). Volumetric capnography can dynamically reflect such effects using CO_2 as the marker of lung perfusion and ventilation. Lung units without perfusion ($\dot{V}/\dot{Q} = \infty$) and/or ventilation ($\dot{V}/\dot{Q} = 0$) are naturally excluded from such an analysis since their CO_2 molecules do not reach the CO_2 sensor at the airway opening. Therefore, VC is an attractive, non-invasive tool for assessing lung collapse–recruitment physiology because it provides real-time bedside information of the lung status in the context of a cycling recruitment maneuver.

The VC can be interpreted in two ways: (1) information obtained *during* the recruitment maneuver; where the VC-derived variables change according to the induced *nonsteady-state* of CO_2; (2) information obtained *after* the recruitment maneuver and the return to baseline ventilation when the VC-derived variables have reached a new *steady-state* condition that can easily be compared with the ventilation *before* recruitment.

Data from VC during lung recruitment can be grouped and analyzed in four principal ways according to CO_2 kinetics: (1) lung perfusion; (2) gas exchange; (3) lung ventilation; and (4) gas transport within the airways.

Lung perfusion

Volume of CO_2 per breath ($VTCO_{2,br}$) is a variable that depends directly on lung perfusion [21,22]. We have shown a close correlation between $VTCO_{2,br}$ and lung perfusion in patients during weaning from cardiopulmonary bypass. At constant ventilation and metabolism, the amount of CO_2 eliminated per breath paralleled the progressive increase of pulmonary blood flow [22]. This explains why $VTCO_{2,br}$, as well as the end-values of tidal CO_2, are simple online qualitative monitors of lung perfusion in those mechanically ventilated patients whose ventilatory settings and metabolism remain stable (Figure 18.2).

The main effect of lung recruitment maneuvers on lung perfusion is the concomitant recruitment of pulmonary capillaries within the previously atelectatic areas. The presence of O_2 molecules in the newly recruited lung units abolishes the HPV reflex and restores blood flow within these areas. Thus, reperfusion to these newly opened lung areas occurs as a transient increase in $VTCO_{2,br}$, which leads to a more homogeneous distribution of the global pulmonary blood flow (Figure 18.3).

Gas exchange

The difference between arterial and end-tidal partial pressure of CO_2 ($PaCO_2$–$PETCO_2$) is a VC-derived variable that evaluates the efficiency of gas exchange at the alveolar–capillary level, analogous to the A–aO_2 index for oxygenation. Values around 3–5 mm Hg are considered normal, and any number beyond this range is a sign of $\dot{V}/\dot{Q}$ mismatch.

During recruitment, $PaCO_2$–$PETCO_2$ behaves differently from $VTCO_{2,br}$ because it depends more exclusively on the exchange of gases. The difference is reduced

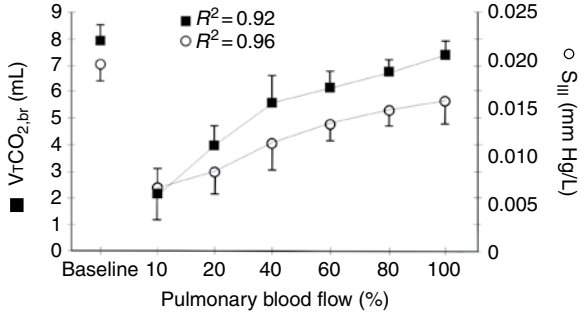

Figure 18.2 Relationship between the elimination of CO_2 per breath ($VTCO_{2,br}$), the slope of phase III (S_{III}), and pulmonary blood flow (PBF) in 14 mechanically ventilated patients undergoing cardiac surgery. At constant ventilation, stepwise weaning from cardiopulmonary bypass was used to control PBF. As pump flow decreased progressively, from a maximum of 100% to 0%, the resulting blood flow through the lungs increased from 0% to 100%. Baseline data were taken before the start of cardiopulmonary bypass. R^2 is the adjusted Pearson's correlation coefficient related to PBF (for further discussion on this topic, refer to Ref. 22).

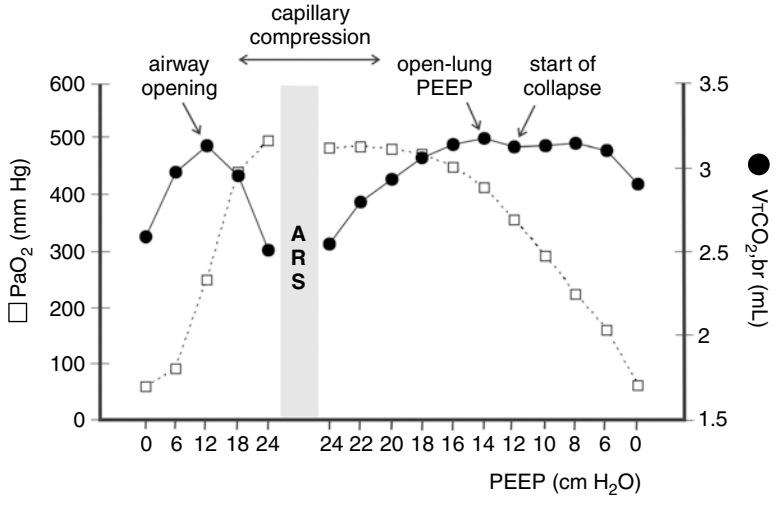

Figure 18.3 Lines represent mean values of eight animals with acute lung injury (ALI) in which recruitment maneuvers and PEEP titrations were performed. Using a volume-controlled mode of ventilation at an $FiO_2 = 1.0$, $VTCO_{2,br}$ as the mean value of the area under the curve of the volumetric capnogram and PaO_2 are shown during the nonsteady-state condition of a recruitment maneuver. PaO_2 is used as a reference method to determine the opening and closing pressures of the lungs based on the following definition: the opening pressure is reached when PaO_2 exceeds 450 mm Hg. The closing pressure is the pressure at which PaO_2 drops below 90% of its maximum value during a decremental PEEP titration. An individual's open-lung PEEP, thus the minimum PEEP to prevent the lungs from collapsing, was defined as the PEEP level with the highest CO_2 elimination per breath. $VTCO_{2,br}$ shows characteristic changes during the protocol sequence. In these animals, collapse occurred at PEEP values between 12 and 16 cm H_2O.

by recruitment and kept low as the lung remains open. $PaCO_2$–$PETCO_2$ starts to increase as soon as lung derecruitment occurs, i.e, when PEEP falls below the pressure needed to stabilize the lung. This variable showed a high sensitivity (0.95) and specificity (0.93) to detect lung derecruitment during a PEEP titration trial in an experimental model of ALI [20].

Gas exchange is a dynamic process that can be reflected by the $VTCO_{2,br}$. Figure 18.3 describes how $VTCO_{2,br}$ can be affected by changes of the effective area of the alveolar–capillary membrane or, in other words, by the relationship between perfusion and ventilation at the alveolar level. The absence of either ventilation (atelectasis or airways closure) or perfusion (capillary compression or HPV) decreases $VTCO_{2,br}$ according to the extent of such defects with respect to the overall alveolar–capillary membrane. Values of $VTCO_{2,br}$ increase after lung recruitment because more CO_2 molecules reach the alveolar compartment via an increased surface area for interchange.

A combination of $VTCO_{2,br}$ with variables derived from lung mechanics may be useful to describe the clinical effects of lung recruitment and to detect the best level of PEEP needed after the maneuver. Recently, the authors described a new variable, the *Tau-CO_2*, or the time-constant for eliminating CO_2 during one breath [19,23]:

$$Tau\text{-}CO_2 = C_{dyn} \cdot R_{aw} \cdot VTCO_{2,br} \text{ (in mL/s)},$$

where C_{dyn} = dynamic compliance (mL/cm H_2O), R_{aw} = airway resistance (cm H_2O/mL/s), and $VTCO_{2,br}$ = carbon dioxide per breath (mL/breath).

The rationale behind the *Tau-CO_2* is the following: lung recruitment increases the expiratory time-constant (E_{tc}), i.e., the product of C_{dyn} and R_{aw}. The E_{tc} describes how fast the passive respiratory system expels the tidal volume during expiration. A short or long E_{tc} indicates that it will take either a short or long time, respectively, until a new equilibrium of the respiratory system is attained after any perturbation of the system. Lung collapse decreases C_{dyn}, whereby a new equilibrium is reached very quickly because the tidal volume is distributed within a smaller lung, with considerable stretch in some normal zones. After lung recruitment, the opposite mechanism is observed: a higher lung volume is present with a higher C_{dyn}, allowing for a slower and more homogeneous expiratory flow. Although R_{aw} may become lower, the overall E_{tc} increases due to a more than proportional increment in C_{dyn}. In simple terms, what *Tau-CO_2* is measuring is the amount of CO_2 excreted in one expiratory time-constant. This amount is increased by recruitment. Again, CO_2 is used as marker for the global mechanical behavior of the lung units.

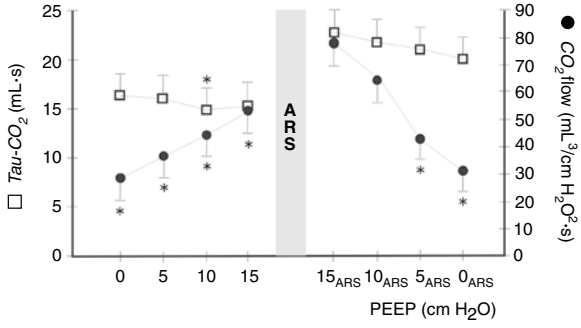

Figure 18.4 Data of 11 morbidly obese patients (BMI 51 ± 10 kg/m^2) undergoing bariatric surgery (from Ref 19). Both *Tau-CO_2* and *CO_{2flow}* indicate that the amount of CO_2 eliminated per unit of time increases after recruitment. This increase in the efficiency of CO_2 elimination is progressively lost as the lung recollapses at lower PEEPs. *$P < 0.05$ compared with value at 15_{ARS}.

As lung recruitment decreases R_{aw}, we modified the initial *Tau-CO_2* formula by moving R_{aw} to the denominator of the above equation in order to emphasize the final and global effect of lung recruitment maneuvers on both lung mechanics and CO_2 elimination. The modified Tau formula, now called *CO_{2flow}*, reads as follows:

$$CO_{2flow} = C_{dyn} \cdot V_T CO_{2,br} / R_{aw} \text{ (in mL/cm } H_2O^2/s).$$

In other words, *CO_{2flow}* indicates that any improvement in the convective transport of CO_2 within the airways due to a decreased R_{aw} will increase the amount of CO_2 eliminated per unit of time.

Figure 18.4 illustrates the behavior of both of the above parameters during the PEEP titration process. Despite stable hemodynamics, these variables showed that the amount of CO_2 eliminated in one respiratory time-constant was highest after lung recruitment; a condition related to the most favorable lung condition, as witnessed by improved oxygenation and deadspace [19,23]. The *CO_{2flow}* variable showed an even more pronounced profile as compared to *Tau-CO_2*, and may be more suitable for monitoring the effects of lung recruitment and PEEP titration.

Ventilation

When commencing mechanical ventilation in a patient, adequate minute ventilation is estimated as the product of V_T and respiratory rate, setting it in relation to the patient's weight. However, a more accurate method to adjust ventilation is to calculate alveolar ventilation (V_A), the portion of inspired gas that actually reaches the gas-exchanging compartment of the lung. It can be calculated non-invasively using VC as:

$$V_A = (V_T - V_{D_{aw}}) \cdot \text{respiratory rate}.$$

The effect of lung recruitment on V_A may vary with the extent of changes in airway deadspace ($V_{D_{aw}}$) induced by P_{aw}. In general, V_A increases due to decrements in $V_{D_{aw}}$; however, sometimes V_A is not significantly affected by recruitments, as is explained further.

By definition, calculating deadspace is the correct way to assess the ineffectiveness of ventilation. One of the effects of lung recruitment on ventilation is a decrement in deadspace, whereby the ineffective portion of the tidal ventilation is reduced. Analyzing the deadspace subcomponents *during* and *after* the recruitment maneuvers provides useful information on the effect that positive pressure ventilation has on the airways and alveolar compartments [9,10,20].

The $V_{D_{alv}}$ always decreases after recruitment because the shunt through the atelectatic areas is minimized by the maneuver. Shunt causes an apparent alveolar deadspace defect (called *V_D shunt*), which can be calculated using the Bohr–Enghoff formula [24]. The "real" $V_{D_{alv}}$ (i.e., ventilated areas without perfusion) is also decreased after lung recruitment because lung compliance improves, plateau pressure decreases, and ventilation distributes more homogeneously within the lungs. Of all deadspace variables $V_{D_{alv}}$ is the most meaningful since it reflects any overdistension developed *during* the highest alveolar pressure at maximal recruitment.

The effect of recruitment and PEEP on $V_{D_{aw}}$ is variable, depending on airway compliance, the degree of airway collapse, and the level of PEEP needed to keep the lungs open. The value of $V_{D_{aw}}$ is decreased – and sometimes it is not – depending on the balance between these factors. In anesthetized patients with normal lungs and high degrees of airway collapse, low levels of PEEP after lung recruitment can decrease $V_{D_{aw}}$ [25]. When the level of PEEP needed exceeds 6 cm H_2O, the increasing diameters of the main airways parallel the increases in $V_{D_{aw}}$ despite the predictable decrements in $V_{D_{alv}}$ commonly observed after the recruitment maneuver [20,25]. This imbalance between the main airway and the alveolar compartment is due to differences in the shape and compliance of these structures. As a consequence, the most commonly used global deadspace variable – the V_D/V_T – sometimes does not represent the effect of lung recruitment because of the opposing directions of $V_{D_{aw}}$ and $V_{D_{alv}}$. The ratio of $V_{D_{alv}}/V_{T_{alv}}$ avoids this abovementioned influential effect of $V_{D_{aw}}$ on V_D/V_T, and can be used as a rather

ideal monitoring tool for lung collapse–recruitment physiology. Therefore, $V_{D_{alv}}$ and $V_{D_{alv}}/V_{T_{alv}}$ are the most sensitive deadspace variables for monitoring the effects of the collapse–recruitment phenomenon on the alveolar level (sensitivity of 0.89 and 1 and specificity of 0.89 and 0.82, respectively) [20]. The advantage of deadspace over PaO_2 is due to the fact that the former also adequately reflects the effects of lung overdistention caused by inadequately high levels of PEEP while PaO_2 proves to be insensitive (Figure 18.3) [26].

Gas transport within the lung

The shape of the VC curve is determined by the way CO_2 is transported through the lungs. This shape is represented by the slopes of phases II and III. Of these VC-derived variables, the phase III slope (S_{III}) has been the most extensively studied because it represents a phenomenon occurring at the gas-exchanging portion of the lung (the alveolar compartment). The value of S_{III} is almost always positive. The reason is the cause of ongoing debate. Both ventilation and perfusion inhomogeneities within the lung play a main role. There is evidence that lung perfusion accounts for only approximately 20% of changes in S_{III} (Figure 18.2); therefore, S_{III} is mainly influenced by the natural non-homogeneous distribution of ventilation within the lungs due to the asymmetry of the airways. This ventilatory maldistribution depends on the interaction between diffusive and convective CO_2 transports within the lungs [27,28].

A bronchospasm crisis in an asthmatic patient is a clear example that ventilation maldistribution is an important factor in the genesis of S_{III}. An increasing inhomogeneity in the distribution of ventilation caused by an asymmetric increment in R_{aw} among lung units produces steeper sloping on S_{III}, while its successful treatment with bronchodilators tends to decrease S_{III} towards more normal values [29].

The clinical and theoretical evidence indicate that the more inhomogeneous the lung, the higher the S_{III}, and vice versa. In other words, S_{III} is related to the global $\dot{V}/\dot{Q}$ relationship, and can be qualitatively assessed in real time and non-invasively at the bedside. The close relationship between S_{III} and $\dot{V}/\dot{Q}$ turns this slope into an interesting tool for assessing the effect of ventilator treatments such as lung recruitment maneuvers and PEEP.

Lung recruitment *decreases* S_{III} as a surrogate for an improved global $\dot{V}/\dot{Q}$ by (1) abolishing HPV in collapsed areas, which results in a more homogeneous and effective distribution of blood flow within the lungs; (2) conducting CO_2 through an increased alveolar–capillary functional membrane; (3) decreasing inhomogeneities in convective and diffusive transport of CO_2 due to more normal lung mechanics; and (4) increasing the expiratory time-constant of lung units according to point 3, mainly by improving the lung's C_{dyn} while peak expiratory flow decreases due to lowered R_{aw}. In this manner, the profile of the expiratory flow becomes more homogeneous as shown by the *Tau-CO_2* concept (Figure 18.4).

The recruitment maneuver and optimum level of PEEP using pressure control modes of ventilation increase V_T due to an increment in lung compliance. The negative correlation between tidal volume and S_{III} is well known, and is attributed to the fact that high tidal volumes are more homogeneously distributed within the lungs than low V_T [30].

Our previous studies in elderly patients support the above conclusions. Under steady-state conditions (constant metabolism, hemodynamics, and ventilation), S_{III} showed lower values after lung recruitment as compared to lungs suffering from anesthesia-induced atelectasis [9]. The same was found during one-lung ventilation [10] and after cardiopulmonary bypass [25].

During nonsteady-state conditions, such as during recruitment and PEEP titration process, S_{III} changes in parallel with changes in $\dot{V}/\dot{Q}$ and lung mechanics. Figure 18.5 shows the effect of lung recruitment on S_{III} in a patient with lung edema after cardiac surgery. Initially, S_{III} decreases because the increasing P_{aw} is able to recruit the collapsed airways. At the highest PEEP before total lung recruitment, S_{III} increases due to mixed effects on lung mechanics, the distribution of ventilation and perfusion. Later, during the PEEP titration trial, S_{III} decreases, reaching the lowest value just *before* lung derecruitment takes place. Afterwards, S_{III} increases continuously as a consequence of an impaired $\dot{V}/\dot{Q}$ due to a progressive lung recollapse.

Summary

Volumetric capnography provides valuable insights into lung collapse–recruitment physiology in a non-invasive and real-time manner, and thus lends itself to monitoring cyclic recruitment maneuvers at the bedside. The information obtained can be separated into the particular effects that lung recruitment exerts on lung perfusion, gas exchange, ventilation, and gas transport, whereby each VC variable carries a particular

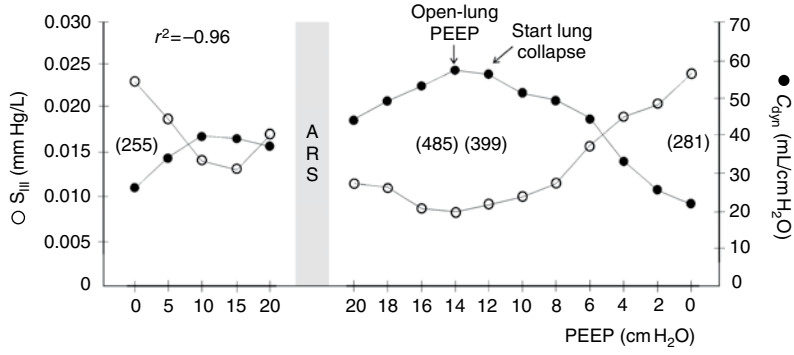

Figure 18.5 The effect of lung recruitment on the slope of phase III (S_{III}) in a patient after cardiac surgery is shown. Dynamic compliance (C_{dyn}) reflects the effects of the lung recruitment procedure on lung mechanics and was thus used to determine both open-lung PEEP and the start of lung collapse during a decremental PEEP titration [18]. The curve of S_{III} shows the effects of lung recruitment on gas exchange. The lines of S_{III} and C_{dyn} almost perfectly mirror each other, and demonstrate a strong inverse correlation in this patient. Values of PaO_2 (mm Hg) for the most important PEEP steps are provided within parentheses.

physiological meaning. The sensitivity and specificity of non-invasive VC can be enhanced by supplemental invasive measurements of gas exchange.

References

1. Altermeier WA, McKinney S, Glenny RW. Fractal nature of regional ventilation distribution. *J Appl Physiol* 2000; **88:** 1551–7.
2. Glenny RW, Bernard SL, Robertson HT. Pulmonary blood flow remains fractal down to the level of gas exchange. *J Appl Physiol* 2000; **89:** 742–8.
3. Hlastala MP, Glenny RW. Vascular structure determines pulmonary blood flow distribution. *News Physiol Sci* 1999; **14**: 182–6.
4. Brismar B, Hedenstierna G, Lundquist H, *et al.* Pulmonary densities during anaesthesia with muscular relaxation: a proposal of atelectasis. *Anesthesiology* 1985; **62:** 422–8.
5. Reber A, Engberg G, Sporre B, *et al.* Volumetric analysis of aeration in the lungs during general anaesthesia. *Br J Anaesth* 1996; **76:** 760–6.
6. Puybasset L, Cluzel P, Chao N, *et al.* A computed tomography scan assessment of regional lung volume in acute lung injury. *Am J Respir Crit Care Med* 1998; **158:** 1644–55.
7. Lachmann B. Open up the lung and keep the lung open. *Intens Care Med* 1992; **18:** 319–21.
8. Tusman G, Böhm SH, Vazquez de Anda GF, do Campo JL, Lachmann B. Alveolar recruitment strategy improves arterial oxygenation during general anaesthesia. *Br J Anaesth* 1999; **82:** 8–13.
9. Tusman G, Böhm, SH, Suárez Sipmann F, Turchetto E. Alveolar recruitment improves ventilatory efficiency of the lungs during anesthesia. *Can J Anaesth* 2004; **51:** 723–7.
10. Tusman G, Böhm, SH, Suárez Sipmann F, Maisch S. Lung recruitment improves the efficiency of ventilation and gas exchange during one-lung ventilation anesthesia. *Anesth Analg* 2004; **98:** 1604–9.
11. Amato MBP, Barbas CSV, Medeiros DM, *et al.* Effect of a protective-ventilation strategy on mortality in the acute respiratory distress syndrome. *N Engl J Med* 1998; **338:** 347–54.
12. Rothen HU, Sporre B, Wegenius G, *et al.* Re-expansion of atelectasis during general anaesthesia: a computed tomography study. *Br J Anaesth* 1993; **71:** 788–95.
13. Borges JB, Okamoto VN, Matos GFJ, *et al.* Reversibility of lung collapse and hypoxemia in early acute respiratory distress syndrome. *Am J Respir Crit Care Med* 2006; **174:** 268–78.
14. Rothen HU, Neumann P, Berglund JE, *et al.* Dynamic of re-expansion of atelectasis during general anaesthesia. *Br J Anaesth* 1999; **82**: 551–6.
15. Gattinoni L, Caironi P, Pelosi P, Goodman LR. What has computed tomography taught us about the acute respiratory distress syndrome? *Am J Respir Crit Care Med* 2001; **164**: 1701–11.
16. Victorino JA, Borges JB, Okamoto VN, *et al.* Imbalances in regional lung ventilation: a validation study on electrical impedance tomography. *Am J Respir Crit Care Med* 2004; **169:** 791–800.
17. Lachmann B, Jonson B, Lindroth M, Robertson B. Modes of artificial ventilation in severe respiratory distress syndrome: lung function and morphology in rabbits after wash-out of alveolar surfactant. *Crit Care Med* 1982; **10:** 724–32.
18. Suarez Sipmann F, Böhm SH, Tusman G, *et al.* Use of dynamic compliance for open lung positive end-expiratory pressure titration in an experimental study. *Crit Care Med* 2007, **35:** 214–21.

19. Suarez Sipmann F, Böhm SH, Tusman G, Borges JB, Hedenstierna G. Tau-CO_2: a novel variable to help optimizing PEEP. *Intens Care Med* 2007; **33**(Suppl 2): S143.
20. Tusman G, Suarez Sipmann F, Böhm SH, *et al.* Monitoring deadspace during recruitment and PEEP titration in an experimental model. *Intens Care Med* 2006, **32:** 1863–71.
21. Schwardt JD, Neufeld GR, Baumgardner JE, Scherer PW. Non-invasive recovery of acinar anatomic information from CO_2 expirograms. *Ann Biomed Eng* 1994; **22**: 293–306.
22. Tusman G, Areta M, Climente C, *et al.* Effect of pulmonary perfusion on the slopes of single-breath test of CO_2. *J Appl Physiol* 2005; **99**: 650–5.
23. Böhm SH, Maisch S, von Sandersleben A, *et al.* The effects of lung recruitment on the phase III slope of volumetric capnography in morbidly obese patients. *Anesth Analg* 2009; **109**: 151–9.
24. Enghoff H. Volumen inefficax: Bemerkungen zur Frage des schädlichen Raumes. *Upsala Läkareforen Forhandl* 1938; **44**: 191–218.
25. Tusman G, Böhm SH, Suarez Sipmann F, Acosta C, Turchetto E. Efecto del reclutamiento pulmonar sobre la capnografía volumétrica después de la circulación extracorpórea. *Rev Arg Anest* 2004; **62:** 240–8.
26. Maisch S, Reissmann H, Fuellekrug B, *et al.* Compliance and deadspace fraction indicate an optimal level of positive end-expiratory pressure after recruitment in anesthetized patients. *Anesth Analg* 2008; **106:** 175–81.
27. Crawford ABH, Makowska M, Paiva M, Engel LA. Convection- and diffusion-dependent ventilation misdistribution in normal subjects. *J Appl Physiol* 1985; **59**: 838–46.
28. Verbank S, Paiva M. Model simulations of gas mixing and ventilation distribution in the human lung. *J Appl Physiol* 1990; **69:** 2269–79.
29. Blanch LL, Fernandez R, Saura P, Baigorri F, Artigas A. Relationship between expired capnogram and respiratory system resistance in critically ill patients during total ventilatory support. *Eur Respir J* 1999; **13:** 1048–54.
30. Schwardt JF, Gobran SR, Neufeld GR, Aukburg SJ, Scherer PW. Sensitivity of CO_2 washout to changes in acinar structure in a single-path model of lung airways. *Ann Biomed Eng* 1991; **19:** 679–97.

Section 1
Chapter
19

Ventilation

Capnography and adjuncts of mechanical ventilation

U. Lucangelo, F. Bernabè, and L. Blanch

Introduction

Mechanical ventilation is a life-saving treatment for patients with acute respiratory failure. The objectives of mechanical ventilation are to relieve acute severe hypoxemia and/or hypercarbia, and perform the action of the respiratory muscles in situations of acute ventilatory or cardiocirculatory failure. Over the past decade, there has been interest in finding other therapeutic options or adjuncts that, together with mechanical ventilation, can improve our understanding of the pathophysiology of respiratory failure and how it affects patient outcome.

The CO_2 tension difference between pulmonary capillary blood and alveolar gas is usually small in normal subjects in whom end-tidal PCO_2 ($PETCO_2$) approximates alveolar ($PACO_2$) and arterial ($PaCO_2$). Physiologic deadspace is the primary determinant of the differences in CO_2 partial pressure measured at these three sites. Patients with cardiopulmonary diseases have altered ventilation to perfusion ($\dot{V}/\dot{Q}$) ratios that produce abnormalities of both deadspace and intrapulmonary shunt that may also affect the difference between these measurements. Differences between arterial and end-tidal PCO_2 (ΔPCO_2) beyond 5 mm Hg are attributed to abnormalities in physiologic deadspace and/or an increase in venous admixture (the fraction of the cardiac output that passes through the lungs without exchanging oxygen) [1–5]. The advanced technology combination of airway gas flow monitoring and mainstream capnography allows breath-by-breath bedside calculation of pulmonary deadspace and CO_2 elimination [2,6]. The use of capnography as a monitoring tool in the course of acute respiratory failure may thereby provide clinicians with this important physiologic information at the bedside.

The purpose of this chapter is to highlight the role of capnography as a monitoring tool with the different adjuncts to mechanical ventilation that are currently used in critically ill patients.

Positive end-expiratory pressure

Acute respiratory distress syndrome (ARDS) is characterized by increased membrane permeability, decreased oncotic pressure, and augmented transvascular hydrostatic pressure gradients that cause noncardiogenic pulmonary edema, atelectasis, and loss of lung volume. As a result of these alterations, ventilation/perfusion heterogeneity and intrapulmonary shunt increase, and oxygenation is severely impaired. Mechanical ventilation is a supportive, life-saving therapy, but can produce further damage to the lungs that is indistinguishable from the pulmonary alterations attributable to ARDS [7,8]. It is, therefore, useful to know the internal mechanism of the heterogeneous distribution of regional atelectasis, lung tissue damage, edema formation, and inflammatory response in ARDS patients undergoing mechanical ventilation. Many studies have attempted to explain the effects of the ventilator on regional lung structure and mechanical function in ARDS patients. In ARDS, the entire lung volume is considerably reduced and the distribution of regional atelectasis is irregular, thus reinforcing the idea that many areas of an injured lung are derecruited [9–13].

The application of positive end-expiratory pressure (PEEP) is used to increase lung volume and improve oxygenation in patients with acute lung injury (ALI). Using a chest computed tomography (CT) scan during a progressive increase in PEEP from 0 to 20 cm H_2O, Gattinoni *et al.* [10] reported that tidal volume distribution in the lungs decreases significantly in the upper lung level (non-dependent areas), does not change in the middle levels, and increases significantly in the lower levels (dependent areas) in supine patients diagnosed with ARDS. In other words, PEEP

Capnography, Second Edition, ed. J. S. Gravenstein, Michael B. Jaffe, Nikolaus Gravenstein, and David A. Paulus. Published by Cambridge University Press. © Cambridge University Press 2011.

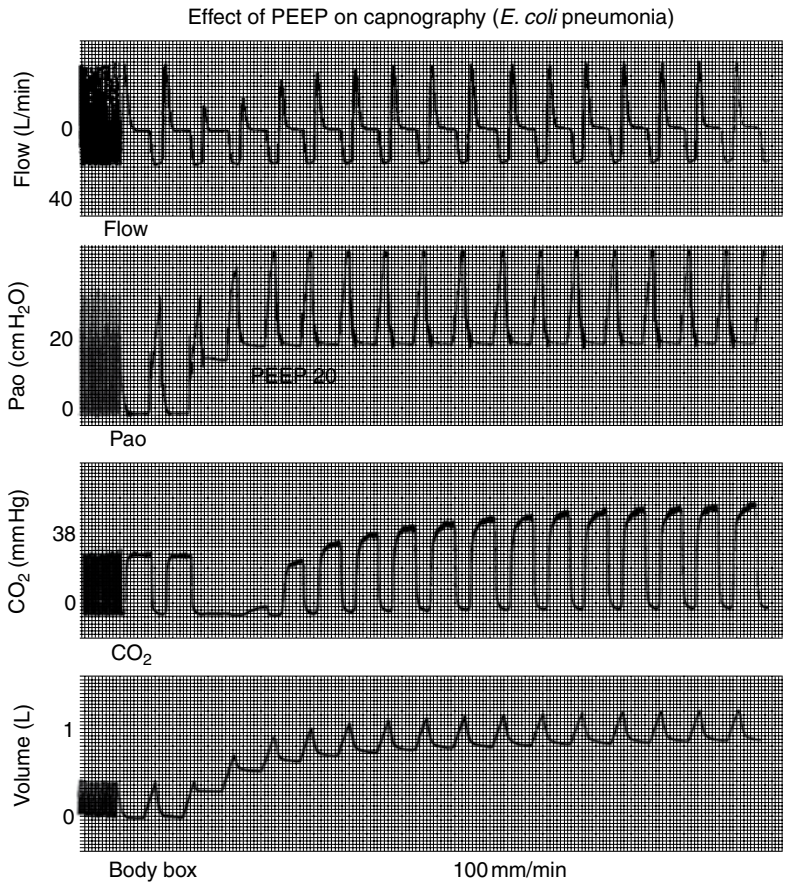

Figure 19.1 Tracings of airflow (Flow), airway pressure (Pao), expired capnograms (CO_2) and tidal volume in an experimental animal with acute lung injury due to *E.coli* pneumonia. Increasing positive end-expiratory pressure (PEEP) from 0 to 20 cm H_2O induces an increase in lung volume. Absence of the capnogram for several breaths after PEEP indicates absence of expired volume until cumulative tidal volume exceeds lung volume expansion induced by PEEP. [Figure courtesy of Dr. Avi Nahum, St. Paul, MN.]

reduces the reopening–collapsing tissue, keeping the lung tissue recruited at end-inspiration open. If a moderate/high PEEP level is used in an attempt to keep all alveoli open, the level of tidal volume should not reach high end-inspiratory plateau pressures (>35 cm H_2O) because additional lung recruitment is insignificant, and hyperinflation may be produced, as demonstrated by CT scan [11,14]. Therefore, alveolar recruitment and overdistension coexist in different parts of the lung after PEEP application in patients with ARDS [15].

The increase in physiologic deadspace in normal anesthetized patients may be attributed to the introduction of muscle paralysis and positive pressure breathing, which causes a reduction of lung volume and alters the normal distribution of ventilation and perfusion across the lung [2]. Alveolar deadspace is significant in acute lung injury and does not vary systematically with PEEP [16–18]). However, when PEEP is administered to recruit collapsed lung units, resulting in improved oxygenation, alveolar deadspace may decrease unless PEEP-induced overdistension increases alveolar deadspace (Figure 19.1) [17,19–21]. In fact, recruitment in ARDS is associated with a decreased arterial minus end-tidal CO_2 gradient [22].

The relationship between the effects of PEEP on volumetric capnography and respiratory system mechanics have been studied in a series of patients with normal lungs, moderate ALI, and severe ARDS. Blanch *et al.* [16] found that respiratory system compliance was markedly decreased, and total respiratory system resistance increased in ARDS compared with similar measurements in control patients. Total physiologic deadspace and expired CO_2 slope were higher in ALI patients compared with control patients, as well as in ARDS patients compared with ALI patients (Figure 19.2). Alveolar ejection volume was lowest in ARDS. The almost rectangular shape of the expired capnogram depends on the homogeneous gas distribution and alveolar ventilation [1,23,24]. Lung heterogeneity creates regional differences in CO_2 concentration, and gas from high $\dot{V}/\dot{Q}$ regions appears first in the upper airway during exhalation. This sequential emptying

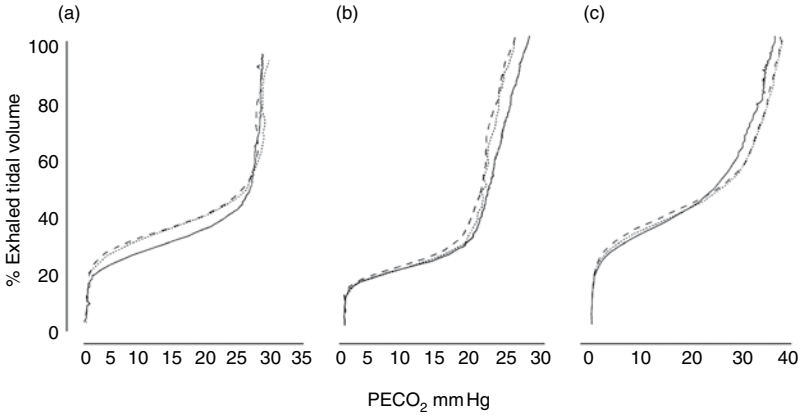

Figure 19.2 Tracings of expiratory CO_2 tension ($PECO_2$) as a function of expired tidal volume (V_T, %) obtained in representative patients at different positive end-expiratory pressures (PEEP): 0, 10, and 15 cm H_2O for a normal subject (a), a patient with acute lung injury (b), and a patient with acute respiratory distress syndrome (c), respectively. Application of PEEP had little effect on CO_2 elimination. [Modified from: Blanch L, Lucangelo U, Lopez-Aguilar J, Fernandez R, Romero P. Volumetric capnography in patients with acute lung injury: effects of positive end-expiratory pressure. *Eur Respir J* 1999; **13**: 1048–54.].

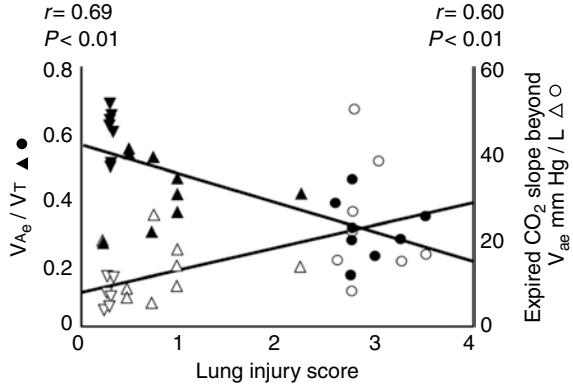

Figure 19.3 Relationship between indices of volumetric capnography (alveolar ejection volume, V_{ae}/ V_T, and phase III expired CO_2 slope) and lung injury score at zero end-expiratory pressure in different groups of patients (invert triangle, control subjects; triangle, acute lung injury; circle, acute respiratory distress syndrome). [Modified from: Blanch L, Lucangelo U, Lopez-Aguilar J, Fernandez R, Romero P. Volumetric capnography in patients with acute lung injury: effects of positive end-expiratory pressure. *Eur Respir J* 1999; **13**: 1048–54.]

contributes to the rise of the alveolar plateau [24,25]; the greater the $\dot{V}/\dot{Q}$ heterogeneity, the steeper the expired CO_2 slope. Accordingly, the slope of the alveolar plateau correlates with the severity of airflow obstruction [26,27].

A significant correlation was found between capnographic indices and the lung injury score, suggesting that the severity of disease affects volumetric capnographic indices and the mechanical properties of the respiratory system (Figure 19.3) [16]. Characteristic features of ALI are alveolar and capillary endothelial cell injuries that result in alterations of the pulmonary microcirculation. Consequently, adequate pulmonary ventilation and blood flow across the lungs are compromised, and physiologic deadspace increases. Since a high deadspace fraction represents an impaired ability to excrete CO_2 due to any $\dot{V}/\dot{Q}$ mismatch [3], Nuckton *et al.* [28] postulated and demonstrated that the measurement of increased physiologic deadspace in standard conditions was independently associated with an increased risk of death in patients diagnosed with ARDS.

The increase in PEEP improved respiratory mechanics in normal subjects and worsened lung tissue resistance in patients with respiratory failure; however, it did not affect volumetric capnographic indices [16]. The same findings have been reported by other authors. Smith and Fletcher [18] found that PEEP did not modify CO_2 elimination in patients immediately after heart surgery. Beydon *et al.* [17] studied the effect of PEEP on deadspace and its partitions in patients with ALI. They found a large alveolar deadspace that resulted unmodified after raising PEEP from 0 to 15 cm H_2O. Patients in whom oxygenation improved with PEEP showed a concurrent decrease in alveolar deadspace and vice versa. Experimentally, Coffey *et al.* [19] found, in oleic-acid-induced ARDS, that low PEEP reduced physiologic deadspace and intrapulmonary shunt. Conversely, and in the same animals, high PEEP increased the fraction of ventilation delivered to areas with high $\dot{V}/\dot{Q}$, resulting in increased physiologic deadspace. Variations in deadspace and their partitions with the application of PEEP largely depend on the type, degree, and stage of lung injury. Moreover, the results of the abovementioned studies also suggest that the ARDS lung, independent of the location of the lung densities, is globally affected by the disease. At present, recording capnographic indices in individual patients may be useful as a way to track physiologic changes related to manipulations of the ventilator, such as modifications in PEEP level.

Unilateral lung injury

Studies of unilateral lung injury demonstrate that the consolidated lung regions do not expand to total lung capacity during inflation [29,30]. Impaired mechanical properties of the consolidated lung are associated with very poor ventilation. The resulting hypoxemia is due to both increased shunt and $\dot{V}/\dot{Q}$ mismatch in the injured regions, and local hypoxic vasoconstriction, in most instances, appears to be ineffective in directing blood flow away from the consolidated lobe. Kanarek *et al.* [31] and Mink *et al.* [29] demonstrated these contentions in a case report and in a canine model of pneumonia, respectively, showing that PEEP increases fractional perfusion to the infected lobe, and may thus actually deteriorate gas exchange. However, the effect of global PEEP on regional lung volume remains controversial. In patients with asymmetric lung injury, tidal volume is unfavorably distributed: healthy lung regions exhibiting normal compliance tend to hyperinflate, whereas affected lung regions with decreased compliance tend to remain collapsed. In a canine model of unilateral lung edema, Blanch *et al.* [32] demonstrated that PEEP and tidal volume ventilation can improve oxygenation despite redistribution of blood flow towards the damaged lung and decreased respiratory system compliance of the healthy lung. An increase in lung volume to near total lung capacity of the healthy lung flattens the pressure–volume relationship, thus decreasing healthy lung compliance and contributing to the redistribution of the tidal volume to the injured lung. Whether PEEP worsens or improves gas exchange depends on the relative magnitude of regional lung mechanical changes [33].

In the setting of unilateral lung injury, measurement of global respiratory system mechanics does not provide clinically useful information for setting ventilator parameters, as the mechanical impairment of the injured parts of the lung cannot be specifically assessed [31,32,34]. In several cases, using independent lung ventilation, Carlon *et al.* [33] showed that selective PEEP improved respiratory failure when conventional therapy failed. In a canine lobar pneumonia model, Light *et al.* [35] clearly demonstrated that unilateral PEEP improved oxygenation and intrapulmonary shunt. In patients with unilateral thoracic trauma, Cinella *et al.* [36] found that the use of independent lung ventilation, with tidal volume and PEEP set to keep plateau airway pressure below 26 cm H_2O in both lungs, improved oxygenation and $\dot{V}/\dot{Q}$ mismatch. Early in the course of the disease, the affected lung exhibited decreased CO_2 elimination compared with the non-affected lung. Equal CO_2 elimination from both lungs was used as a criterion to stop independent lung ventilation and resume conventional mechanical ventilation.

Tracheal gas insufflation

Tracheal gas insufflation (TGI) is an adjunct to mechanical ventilation that allows ventilation with small tidal volumes while CO_2 is satisfactorily eliminated. Pioneering studies demonstrated, in healthy experimental animals and in humans with respiratory failure, that expiratory flushing of the proximal deadspace decreased minute ventilation with no change in $PaCO_2$. Recent work demonstrates that conventional mechanical ventilation aided by TGI may represent a novel ventilatory strategy that succeeds in limiting both the distending forces acting on the lung and the level of $PaCO_2$ elevation that invariably occurs during permissive hypercapnia. Because the anatomic deadspace remains relatively constant as tidal volume is reduced during conventional mechanical ventilation, low tidal volumes are associated with a high deadspace to tidal volume ratio. Tracheal gas insufflation, applied together with conventional mechanical ventilation, effectively reduces the size of the deadspace compartment and improves overall CO_2 elimination by replacing the anatomic deadspace, normally laden with CO_2 during expiration, with fresh gas. As a consequence, less CO_2 is recycled to the alveoli during the next inspiration, and the ventilatory efficiency of each tidal respiration is improved. Therefore, TGI reduces anatomic deadspace and increases alveolar ventilation for a given frequency and tidal volume combination [37–43]. The efficacy of TGI on $PaCO_2$ diminishes when an increased alveolar component dominates the total physiologic deadspace. Nahum *et al.* [44] demonstrated that allowing $PaCO_2$ to rise to supranormal levels (a permissive hypercapnia strategy) counteracted the detrimental effect of increased alveolar deadspace on the CO_2 removal efficacy of TGI.

The main effect of TGI is to flush the deadspace from the carina to the Y of the ventilator circuit. However, TGI has also a distal effect that contributes to remove CO_2; the region affected consists of a jet area extending from the catheter tip – and a turbulent region extending beyond the jet – towards the alveoli. The extent of the jet and turbulent region is related to flow velocity at the catheter tip. The velocity is directly related to flow rate and inversely related to the internal diameter of the TGI

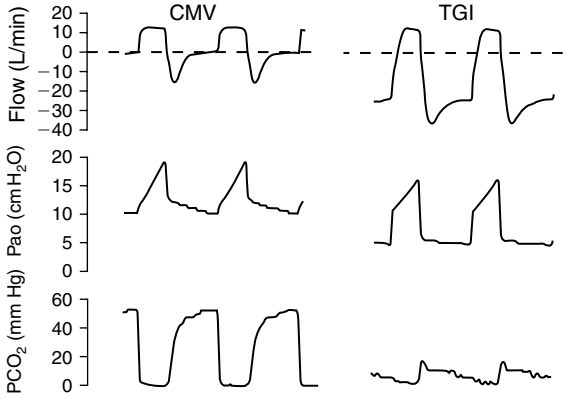

Figure 19.4 Tracings of airflow, airway pressure (Pao) and expired capnogram obtained with and without tracheal gas insufflation (TGI) in an experimental animal. Application of TGI without changing tidal volume improved CO_2 clearance and allowed ventilation at lower airway inspiratory and end-expiratory airway pressures. (CMV, conventional mechanical ventilation.) [From: Blanch L. Clinical studies of tracheal gas insufflation. *Respir Care* 2001; **46**: 158–66.]

catheter [38]. Although the distal effect enhances CO_2 removal, the presence of the catheter and the jet effect oppose expiratory flow, favoring auto-PEEP [42,45].

The efficacy of TGI may be monitored by capnography. The observation of exhaled capnograms provides an indicator of the effect of TGI on the CO_2 concentration of the gas remaining in the proximal anatomic deadspace compartment at the onset of inspiration (Figure 19.4). Although, in patients with respiratory failure, $PETCO_2$ is a poor estimate of $PaCO_2$ [46], changes in $PETCO_2$ induced by TGI correlated significantly with changes in $PaCO_2$, justifying the routine measurement of $PETCO_2$ during TGI application as a marker of its effectiveness [39,47,48].

High-frequency and percussive ventilation

High-frequency ventilation (HFV) was introduced into clinical practice in the early 1970s [49]. Many HFV techniques have been used since, all characterized by a breathing frequency higher than 1 Hz (60 breaths/min), tidal volume lower than deadspace volume, and low peak pressure. These techniques have three essential elements in common: a high-pressure flow generator, a valve for flow interruption, and a circuit for connection to the patient. Depending on the frequencies used, we will refer to various modes of ventilation: "high-frequency jet ventilation" (HFJV), and a variant of this mode (high-frequency flow interruption – HFFI); "high-frequency oscillation" (HFO); and "high-frequency positive pressure ventilation" (HFPPV). Lower frequencies (60–300 cycles/min) are normally used in HFPPV, whereas higher values are typical of HFO (60–2400 cycles/min). If HFO uses low operating frequences, there is an overlap of frequency bands [50,51].

Two studies [52,53] demonstrated a significant improvement in gas exchange in ARDS patients by using HFO. These studies revealed that chances for survival are not only related to the initial disease, but also to early treatment, and that the HFO technique must be considered as life-saving in cases that do not respond to conventional mechanical ventilation. Other HFV modes, such as HFJV and HFPPV, have been widely used as well, mostly during diagnostic examinations of the upper airways (laryngo- and bronchoscopic imaging, tracheal surgery, etc.) [54]. The main advantage of these techniques is the limited cyclic displacement of thoracic and pulmonary structures, with better exposure of the operating region.

Independent of the disease, HFV can result in dynamic lung hyperinflation caused by the decrease in expiration time (Te), as well as by the rapid increase in lung volume and intrathoracic pressure due to the high administration flow speed. This occurs mainly with ventilation techniques that employ passive expiration, such as HFJV and HFPPV, although it has also been described with HFO, which employs active expiration. For all these reasons, HFV techniques, in particular HFJV, are avoided in patients with airway obstruction or with increased airways resistance [55]. Furthermore, negative hemodynamic effects have also been evidenced, neither related to the type of HFV technique nor to the high frequencies used, but to the effect of the high mean airway pressure on thoracic and pulmonary compliance.

Another important clinical aspect concerning HFV is CO_2 monitoring. All these techniques employ subtidal breath volumes that cannot be directly measured. The difficulty in assessing the adequacy of ventilation and CO_2 washout is one of the most important technical problems associated with these techniques. Recently, Kil *et al.* [56] measured capnographic curves and $PETCO_2$ during brief alternation from HFJV (100 cycles/min) to five to six single breaths of conventional mechanical ventilation. They observed, in 40 ASA-1 patients undergoing laryngeal microsurgery, that, by using this periodic interruption of HFJV technique, the $PETCO_2$ level could closely reflect that of $PaCO_2$

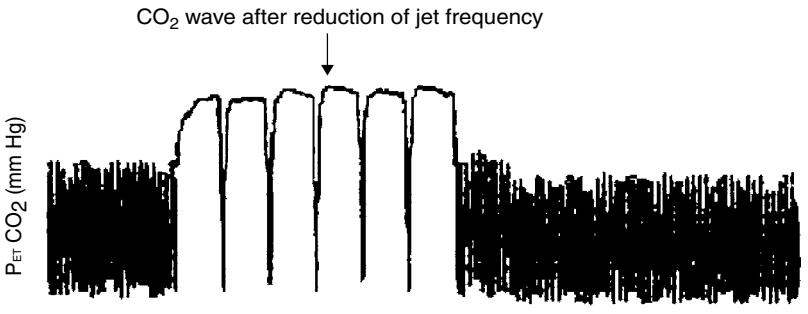

Figure 19.5 Capnography during high-frequency jet ventilation. Large single waves indicate the CO_2 waves after decreasing jet frequency. [From: Kil HK, Kim WO, Choi HS, Nam YT. Monitoring of $P_{ET}CO_2$ during high frequency jet ventilation for laryngomicrosurgery. *Yonsei Med J* 2002; **43**: 20–4.]

(Figure 19.5). An alternative method to determine adequate ventilator settings during HFV is by using a transcutaneous PCO_2 monitoring device [57]. Along the same line, Frietsch *et al.* [58] found that monitoring HFJV during prolonged rigid bronchoscopy is easily performed by capnography via the light channel of the rigid bronchoscope, although the reliability of capnography was lost with flooded airways, and is of limited value during endoscopic instrumentation, resulting in significant airway obstruction. Non-invasive CO_2 monitoring represents a useful adjunct to the periodic analysis of arterial blood gases, and can reduce the number of arterial blood gases during HFJV.

A different HFV technique is high-frequency percussive ventilation (HFPV), introduced by F. M. Bird as a rhythmic cyclic ventilation with flow regulation that produces a controlled pressure. This technique incorporates the positive aspects of conventional mechanical ventilation (CMV) with those of HFV. High-frequency percussive ventilation is delivered by a ventilatory circuit with a high-frequency flow supplier. The real peculiarity of this ventilation technique is a switch valve, which is an interface between the device and the simulator. This unit is called Phasitron® (Percussionaire Corp, Sandpoint, ID, USA). This device operates on the basis of the Venturi principle and delivers mini-bursts of gas, with frequency and duration set by the operator [51,59]. In the case shown in Figure 19.6, percussive frequency is 720 cycles/min, and CMV frequency is 14 cycles/min, with an inspiratory/expiratory (I/E) ratio of 1/1. In clinical practice, the expiratory phase may be completely passive, or may present a percussive oscillatory trend (Figure 19.7).

Initially HFPV was used for the treatment of acute respiratory diseases caused by burns and smoke inhalation [51,60–64], as well as for treatment of the newborn affected by hyaline membrane disease or infant respiratory distress syndrome [65]. Later, its application increased to include other cases of severe gas exchange compromise, where CMV failed. Multiple reports in the literature attest to its effectiveness and safety in several cases affecting the respiratory system (e.g., ARDS, chest trauma) [66], or in head trauma [67] and multiple trauma patients [68] in whom the effects of CMV might compromise other organ functions. The peculiarity of this hybrid technique is that it allows a normal $P_{ET}CO_2$ and CO_2 tracing when the expiratory phase is completely passive (Figure 19.6). Also, when the expiratory phase presents a low pressure percussive oscillatory trend (Figure 19.7), the CO_2 curve is still present without evident geometric modifications. In this case, a consideration of the correlation between $PaCO_2$ and $P_{ET}CO_2$ cannot be formulated because of the presence of expiratory pulsatility flow. The capnographic trace stability allows proper monitoring of the HFPV ventilator setting at the bedside [69,70]. In this situation, a combined transducer (mainstream capnograph plus a pneumotachograph) has been used at a sampling frequency of 100 Hz (CO_2SMO Plus, Respironics-Novametrix, Wallingford, CT, USA).

Capnography and treatment evaluation

Drug delivery via the airways during mechanical ventilation is a common practice and, for some medications, is the preferred route. In these patients, several medications with different properties may be given by direct instillation or via aerosol-generating devices. Among these therapies are bronchodilators, perfluorocarbons, vasoactive drugs, surfactant, antibiotics, anti-inflammatory drugs, mucolytics, inmunomodulating substances, and gene therapy.

Bronchodilator drugs act by relaxing the airway smooth muscle and decreasing resistance to airflow. During mechanical ventilation, inhaled bronchodilator drugs significantly decrease inspiratory airway resistance in patients with chronic obstructive

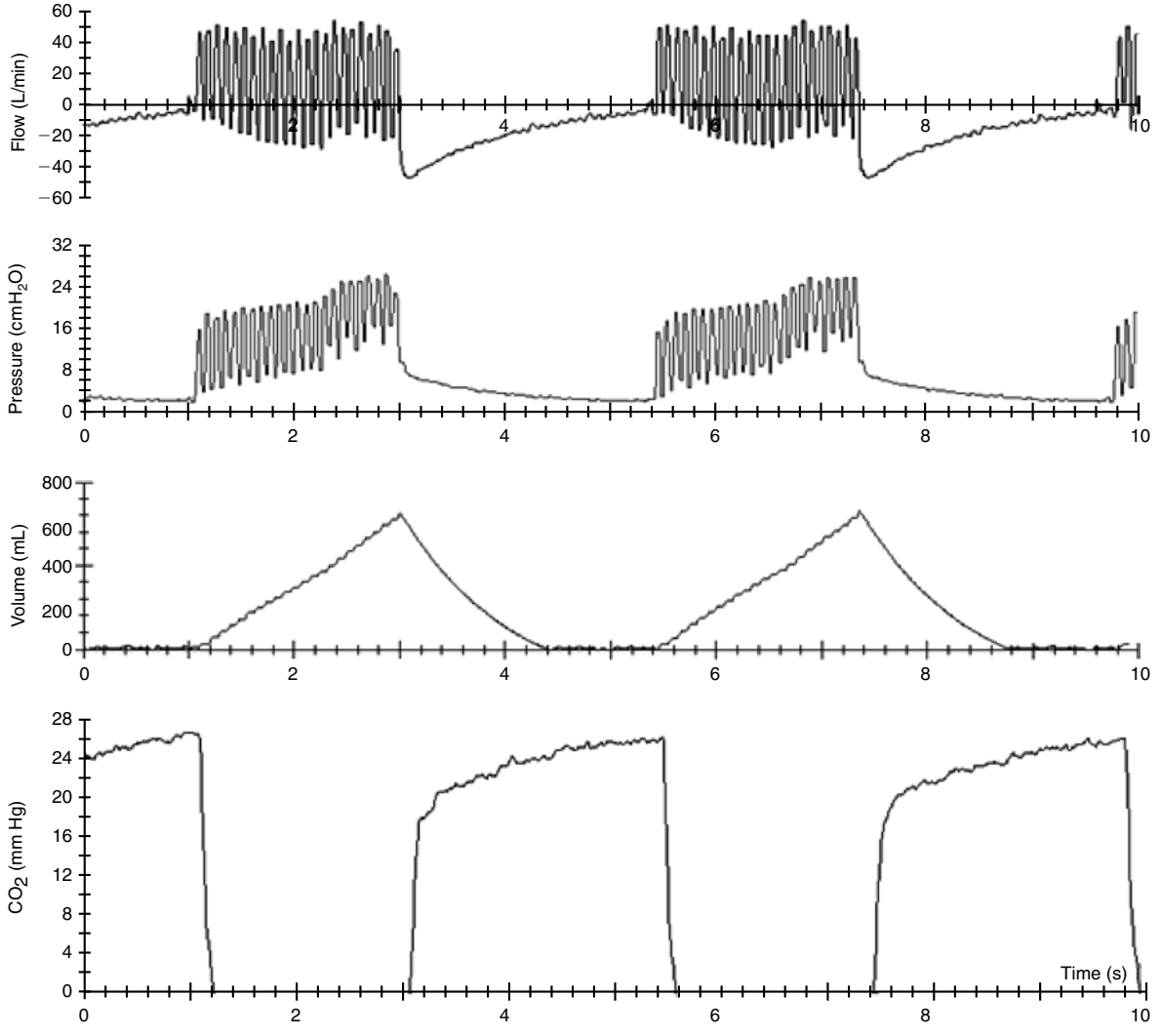

Figure 19.6 Flow, airway pressure, volume, and CO_2 tracings during high-frequency percussive ventilation (HFPV). Percussions are applied only during inspiratory phase and CO_2 waveform remains unaltered.

pulmonary disease (COPD) and in patients with acute asthma [71]. Decreased resistance is associated, at a given tidal volume, with reduced ventilator inspiratory pressure. Moreover, since resistance to expiratory flow might also be reduced, dynamic hyperinflation is lower, thus favoring CO_2 elimination. You *et al.* [26] demonstrated significant correlations between spirometry and several capnographic indices, and concluded that the capnogram shape is a quantitative method for evaluating the severity of bronchospasm. Yaron *et al.* [72] found significant changes in peak expiratory flow rates and in the plateau phase of the expiratory capnogram in asthmatic subjects after inhaled beta-agonist therapy. In fact, a correlation of spirometry or lung mechanics with capnographic indices is usually seen as bronchospasm is relieved or when dynamic hyperinflation is improved [46].

Partial liquid ventilation (PLV) with perfluorocarbons [73–75] has been proposed as a modality to recruit lung units in acute lung injury. Perfluorocarbon, due to its low surface tension and high density (1.91 g/cm^3), may facilitate opening of collapsed, non-compliant dependent lung segments. Consequently, perfluorocarbon may function as "liquid PEEP," preventing complete collapse of unstable alveoli even at low airway pressures, and thereby improves oxygenation and decreases the shear forces acting on the lung parenchyma. The amount of PEEP needed to optimize gas

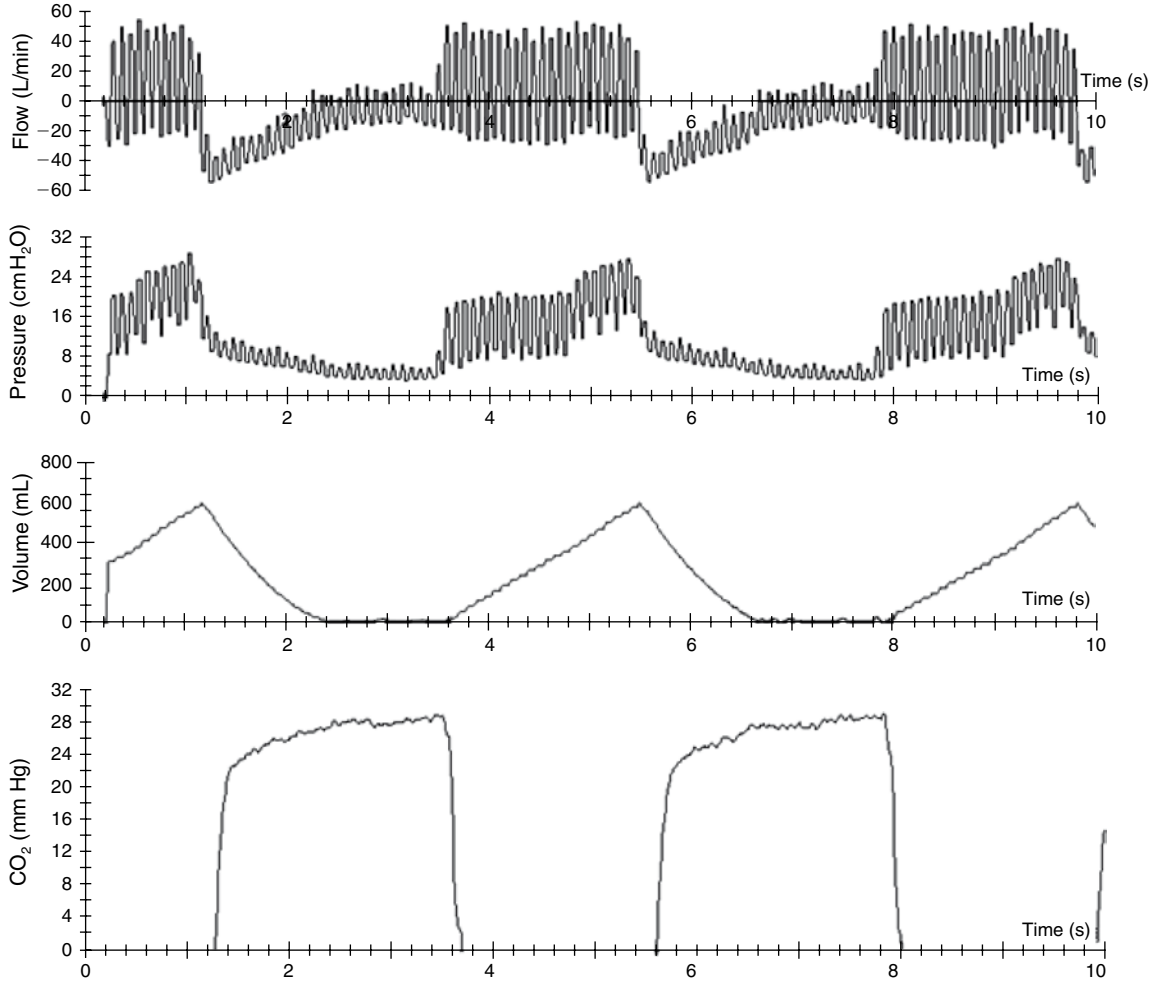

Figure 19.7 Flow, airway pressure, volume, and CO_2 tracings during high-frequency percussive ventilation (HFPV). Percussions are applied during both inspiratory and expiratory phases. Note that percussion does not affect expired capnogram despite low-pressure percussive oscillatory trend.

exchange during PLV in a lung lavage model of ALI has been found to be approximately 10 cm H_2O [43,76]. The impact of PLV on CO_2 elimination has been studied. Mates *et al.* [77] found that PLV resulted in CO_2 retention and an increased arterial–alveolar CO_2 difference at similar ventilator settings. Moreover, negative phase III slopes of CO_2 expirograms occurred during PLV when perfluorocarbon was heterogeneously distributed and flooded lung regions, characterized by prolonged emptying times and low alveolar PCO_2, emptied late in expiration (Figure 19.8).

In patients with sudden pulmonary vascular occlusion due to pulmonary embolism, the resultant high $\dot{V}/\dot{Q}$ mismatch produces an increase in $V_{D_{alv}}$. Several human studies [78,79] have reported the use of CO_2 monitoring in the clinical setting of suspected pulmonary embolism. However, these studies differ in terms of patient selection, types of tests for pulmonary embolism diagnosis, type of capnograph, deadspace calculation, and mode of breathing (assisted or spontaneous). Using volumetric capnography as a bedside technique, the combination of a normal D-dimer level result and a normal $V_{D_{alv}}$ is a highly sensitive screening test that can rule out the diagnosis of pulmonary embolism [80]. In patients with clinical suspicion of pulmonary embolism and elevated D-dimer levels, calculations derived from volumetric capnography, such as late deadspace fraction, had a statistically better diagnostic performance in suspected pulmonary embolism than the traditional measurement of $PaCO_2$–$PETCO_2$ gradient [79]. Finally, volumetric capnography has proven to be an excellent tool to

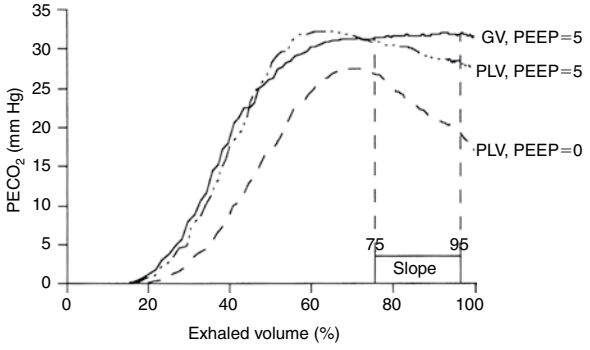

Figure 19.8 Expired CO_2 ($PECO_2$) as a function of exhaled volume (mean of eight breaths) during gas ventilation at PEEP of 5 cm H_2O (GV), during partial liquid ventilation (PLV) at PEEP 0 and 5 cm H_2O. A negative slope of exhaled CO_2 is observed during PLV + PEEP and magnified after PEEP removal. See text for explanation. [From: Mates EA, Tarczy-Hornoch P, Hildebrandt J, Jackson JC, Hlastala MP. Negative slope of exhaled CO_2 profile: implications for ventilation heterogeneity during partial liquid ventilation. *Adv Exp Med Biol* 1996; **388**: 585–97.]

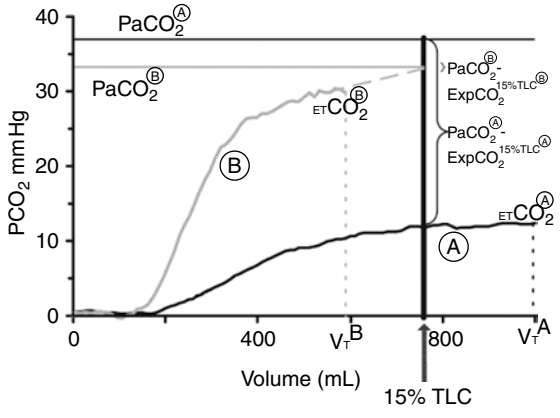

Figure 19.9 Course of volumetric capnography measurement in a patient from beginning (curve A) to 24 h post-thrombolysis (curve B). Arrow value for 15% of the predicted total lung capacity (TLC) (765 mL) used for late deadspace fraction (Fd_{late}) calculation. Fd_{late} reduced from 64.4% at the beginning of thrombolysis to 1.1% on the day after, almost crossing the horizontal $PaCO_2$ line at the 15% of predicted TLC vertical line. [From: Verschuren F, Heinonen E, Clause D, *et al.* Volumetric capnography as a bedside monitoring of thrombolysis in major pulmonary embolism. *Intens Care Med* 2004; **30**: 2129–32.]

monitor thrombolytic efficacy in patients with major pulmonary embolism (Figure 19.9) [81].

Prognostic value of diverse deadspace indices

Acute lung injury is an entity characterized by diffuse alveolar injury, alveolar collapse or consolidation, severe vascular damage, protein-rich lung edema, surfactant inactivation, and inflammation. Due to severe alveolar and vascular damage, the lungs of patients with ALI or ARDS have regions with low $\dot{V}/\dot{Q}$ and high $PaCO_2$ that usually coexist with other areas with high $\dot{V}/\dot{Q}$ and low $PaCO_2$. The combination of these two conditions results in increased pulmonary deadspace [82]. Other causes of pulmonary deadspace are shock, systemic and pulmonary hypotension, and obstruction of pulmonary vessels by pulmonary embolism or microthromboses. It is difficult to evaluate deadspace at the bedside in intensive care unit (ICU) patients, given that artificial ventilation can substantially affect deadspace measurements. Levels of PEEP that recruit collapsed lung can reduce deadspace primarily by reducing intrapulmonary shunt. In contrast, overdistension from PEEP promotes the development of high $\dot{V}/\dot{Q}$ regions with increased deadspace. In both cases, PEEP-associated reductions in cardiac output due to increased intrathoracic pressure also affect pulmonary deadspace (V_D) [19,20].

In ARDS patients, pioneering studies have shown that increased deadspace [20] and its evolution during the first days of the disease was associated with poorer survival [83]. Only in the last decade have deadspace measurements regained researchers' attention, with Nuckton *et al.*'s study [28] being the most successful in suggesting that a high $V_{D_{phys}}/V_T$ is independently associated with an increased risk of death in ARDS patients. Recently, slight improvements in mortality prediction have been reported by serial measurements of V_D during the first week of disease [84], which confirms previous data on the prognostic value of deadspace. More interestingly, it shows that deadspace measured without ventilator adjustments is also associated with mortality in patients ventilated with a non-aggressive ventilatory strategy. This concurs with previous studies showing that deadspace in patients with severe lung damage is barely affected by changes in V_T and PEEP [16–18].

The ratio, V_A/V_T, is an index of alveolar dishomogeneity. It correlates with the severity of lung injury, and is not influenced by the ventilatory settings in mechanically ventilated patients with ALI and ARDS [6,16]. In a recent study aimed to evaluate the utility of these non-invasive capnographic indices to predict outcome at ICU admission and after 24–48 h of treatment in mechanically ventilated patients with ALI or ARDS, Lucangelo and coworkers [85] found that V_A/V_T was the best predictor at admission (V_A/V_T -adm) and after 48 h (V_A/V_T -48h), with a sensitivity

of 82% and specificity of 64%. The capability of VA/VT for predicting outcome has been evaluated in subpopulations of ARDS and ALI patients. A 100% specificity has been demonstrated in predicting outcome in ARDS patients (no false-negative results) [85]. The same authors found an 86% specificity in predicting outcome in ALI patients (one false-negative result in seven cases). The difference between VA/VT -48h and VA/VT -adm (ΔVA/VT) showed a sensitivity of 73% and specificity of 93%, and an area under ROC curve of 0.83. Moreover, interaction between PaO_2/FiO_2 and VA/VT -adm also predicted survival with an area under ROC curve of 0.84. Again, physiologic deadspace after 48 h ($V_{D_{phys}}$/VT 48-h) predicted survival with an area under ROC curve of 0.75. Therefore, capnographic-derived, non-invasive measures of deadspace and VA/VT at admission and after 48 h of mechanical ventilation, associated with PaO_2/FiO_2, provided useful information on outcome in critically ill patients with ALI.

Conclusion

The advanced technology combination of airway flow monitoring and mainstream capnography allows bedside breath-by-breath calculation of the pulmonary deadspace and CO_2 elimination. For these reasons, the use of volumetric capnography is, clinically, of more utility than simple time capnography. Measurement of deadspace fraction early in the course of acute respiratory failure may provide clinicians important physiologic and prognostic information. Further studies are warranted to assess whether the continuous measurement of various derived capnographic indices is useful for risk identification and stratification, and to track the effects of a therapeutic intervention during the course of the disease in critically ill patients.

References

1. Fowler WS. Lung function studies. II. The respiratory deadspace. *Am J Physiol* 1948; **154**: 405–10.
2. Fletcher R, Jonson B, Cumming G, Brew J. The concept of deadspace with special reference to the single breath test for carbon dioxide. *Br J Anaesth* 1981; **53**: 77–88.
3. Feihl F. Respiratory deadspace and survival in the acute respiratory distress syndrome. In: Gullo A (ed.) *Anesthesia, Pain, Intensive Care, and Emergency Medicine.* New York: Springer, 2003; 275–87.
4. Hess D. Capnometry and capnography: technical aspects, physiologic aspects, and clinical applications. *Respir Care* 1990; **35**: 557–76.
5. Piiper J, Scheid P. Diffusion and convection in intrapulmonary gas mixing. In: Fishman AP, Farhi LE, Tenney SM, Geiger SR (eds.) *Handbook of Physiology*. Bethesda, MD: American Physiological Society, 1987; 51–69.
6. Romero PV, Lucangelo U, Lopez-Aguilar J, Fernandez R, Blanch L. Physiologically based indices of volumetric capnography in patients receiving mechanical ventilation. *Eur Respir J* 1997; **10**: 1309–15.
7. Amato MBP, Barbas C, Medeiros DM, *et al.* Effect of a protective-ventilation strategy on mortality in the acute respiratory distress syndrome. *N Engl J Med* 1998; **338**: 347–54.
8. Acute Respiratory Distress Syndrome Network. Ventilation with lower tidal volumes compared with traditional tidal volumes for acute lung injury and the acute respiratory distress syndrome. *N Engl J Med* 2000; **342**: 1301–8.
9. Pelosi P, Crotti S, Brazzi L, Gattinoni L. Computed tomography in adult respiratory distress syndrome: what has it taught us? *Eur Respir J* 1996; **9**: 1055–62.
10. Gattinoni L, Pelosi P, Crotti S, Valenza F. Effects of positive end-expiratory pressure on regional distribution of tidal volume and recruitment in adult respiratory distress syndrome. *Am J Respir Crit Care Med* 1995; **151**: 1807–14.
11. Vieira SRR, Puybaset L, Lu Q, *et al.* A scanographic assessment of pulmonary morphology in acute lung injury: significance of the lower inflection point detected on the lung pressure-volume curve. *Am J Respir Crit Care Med* 1999; **159**: 1612–23.
12. Pelosi P, Cereda M, Foti G, Giacomini M, Pesenti A. Alterations of lung and chest wall mechanics in patients with acute lung injury: effects of positive end-expiratory pressure. *Am J Respir Crit Care Med* 1995; **152**: 531–7.
13. Puybasset L, Cluzel P, Chao N, *et al.* A computed tomography scan assessment of regional lung volume in acute lung injury. *Am J Respir Crit Care Med* 1998; **158**: 1644–54.
14. Crotti S, Mascheroni D, Caironi P, *et al.* Recruitment and derecruitment during acute respiratory failure: a clinical study. *Am J Respir Crit Care Med* 2001; **164**: 131–40.
15. Puybasset L, Gusman P, Muller JC, *et al.* Regional distribution of gas and tissue in acute respiratory distress syndrome. III. Consequences for the effects of positive end-expiratory pressure. *Intens Care Med* 2000; **26**: 1215–27.

16. Blanch L, Lucangelo U, Lopez-Aguilar J, Fernandez R, Romero P. Volumetric capnography in patients with acute lung injury: effects of positive end-expiratory pressure. *Eur Respir J* 1999; **13**: 1048–54.
17. Beydon L, Uttman L, Rawal R, Jonson B. Effects of positive end-expiratory pressure on deadspace and its partitions in acute lung injury. *Intens Care Med* 2002; **28**: 1239–45.
18. Smith RPR, Fletcher R. Positive end-expiratory pressure has little effect on carbon dioxide elimination after cardiac surgery. *Anesth Analg* 2000; **90**: 85–8.
19. Coffey RL, Albert RK, Robertson HT. Mechanisms of physiologic deadspace response to PEEP after acute oleic acid lung injury. *J Appl Physiol* 1983; **55**: 1550–7.
20. Suter PM, Fairley HB, Isenberg I. Optimum end-expiratory pressure in patients with acute pulmonary failure. *N Engl J Med* 1975; **292**: 284–9.
21. Bowie JR, Smith RA, Downs JB. Absence of a capnogram after positive end-expiratory pressure. *J Clin Monit* 1993; **9**: 78–80.
22. Blanch L, Fernandez R, Benito S, Mancebo J, Net A. Effect of PEEP on the arterial minus end-tidal carbon dioxide gradient. *Chest* 1987; **92**: 451–4.
23. Ream RS, Screiner MS, Neff JD, *et al.* Volumetric capnography in children: influence of growth on the alveolar plateau slope. *Anesthesiology* 1995; **82**: 64–73.
24. Engel LA. Intraregional gas mixing and distribution. In: Engel LA, Paiva M (eds.) *Gas Mixing and Distribution in the Lung*. New York: Marcel Dekker, 1985; 287–358.
25. Meyer M, Mohr M, Schulz H, Piiper J. Sloping alveolar plateaus of CO_2, O_2, and intravenously infused C_2H_2 and $CHClF_2$ in the dog. *Respir Physiol* 1990; **81**: 137–52.
26. You B, Peslin R, Duvivier C, Dang Vu V, Grilliat JP. Expiratory capnography in asthma: evaluation of various shape indices. *Eur Respir J* 1994; **7**: 318–23.
27. Blanch L, Fernandez R, Artigas A. The effect of autoPEEP on the $PaCO_2$–$PetCO_2$ gradient and expired CO_2 slope in critically ill patients during total ventilatory support. *J Crit Care* 1991; **6**: 202–10.
28. Nuckton TJ, Alonso JA, Kallet RH, *et al.* Pulmonary deadspace fraction as a risk factor for death in the acute respiratory distress syndrome. *N Engl J Med* 2002; **346**: 1281–6.
29. Mink SN, Light RB, Wood LHD. Effect of PEEP on gas exchange and pulmonary perfusion in canine lobar pneumonia. *J Appl Physiol* 1981; **50**: 517–23.
30. Craven KD, Oppenheimer L, Wood LDH. Effects of contusion and flail chest on pulmonary perfusion and oxygen exchange. *J Appl Physiol* 1979; **47**: 729–37.
31. Kanarek DJ, Shannon DC. Adverse effect of positive end-expiratory pressure on pulmonary perfusion and arterial oxygenation. *Am Rev Respir Dis* 1975; **112**: 457–9.
32. Blanch L, Roussos C, Brotherton S, Michel RP, Angle MR. Effect of tidal volume and PEEP in ethclorvynol-induced asymmetric lung injury. *J Appl Physiol* 1992; **73**: 108–16.
33. Carlon GC, Ray C Jr., Klein R, Goldinger PL, Miodownik S. Criteria for selective positive end-expiratory pressure and independent synchronized ventilation of each lung. *Chest* 1978; **74**: 501–7.
34. Blanch L, Fernández R, Baigorri F, *et al.* Efecto del volumen corriente y de la posición sobre la oxigenación y la mecánica pulmonar en pacientes afectos de neumonía unilateral ventilados mecanicamente. *Med Intensiva* 1992; **16**: 318–23.
35. Light RB, Mink SN, Wood LDH. The effect of unilateral PEEP on gas exchange and pulmonary perfusion in canine lobar pneumonia. *Anesthesiology* 1981; **55**: 251–5.
36. Cinella G, Dambrosio M, Brienza N, *et al.* Independent lung ventilation in patients with unilateral pulmonary contusion: monitoring with compliance and $EtCO_2$. *Intens Care Med* 2001; **27**: 1860–7.
37. Nahum A, Burke WC, Ravenscraft SA, *et al.* Lung mechanics and gas exchange during pressure-control ventilation in dogs: augmentation of CO_2 elimination by an intratracheal catheter. *Am Rev Respir Dis* 1992; **146**: 965–73.
38. Nahum A, Ravenscraft SA, Nakos G, *et al.* Tracheal gas insufflation during pressure-control ventilation: effect of the catheter position, diameter and flow rate. *Am Rev Respir Dis* 1992; **146**: 1411–18.
39. Ravenscraft SA, Burke WC, Nahum A, *et al.* Tracheal gas insufflation augments CO_2 clearance during mechanical ventilation. *Am Rev Respir Dis* 1993; **148**: 345–51.
40. Blanch L. Clinical studies of tracheal gas insufflation. *Respir Care* 2001; **46**: 158–66.
41. Richecoeur J, Lu Q, Vieira SR, *et al.* Expiratory washout versus optimization of mechanical ventilation during permissive hypercapnia in patients with severe acute respiratory distress syndrome. *Am J Respir Crit Care Med* 1999; **160**: 77–85.
42. Blanch L, Van der Kloot TE, Youngblood AM, *et al.* Application of tracheal gas insufflation to acute unilateral lung injury in an experimental model. *Am J Respir Crit Care Med* 2001; **164**: 642–7.
43. Blanch L, Van der Kloot TE, Youngblood AM, *et al.* Selective tracheal gas insufflation during partial liquid ventilation improves lung function in an animal model

of unilateral acute lung injury. *Crit Care Med* 2001; **29**: 2251–7.

44. Nahum A, Shapiro RS, Ravenscraft, SA, Adams AB, Marini JJ. Efficacy of expiratory tracheal gas insufflation in a canine model of lung injury. *Am J Respir Crit Care Med* 1995; **152**: 489–95.
45. Kalfon P, Rao GS, Gallart L, *et al*. Permissive hypercapnia with and without expiratory washout in patients with severe acute respiratory distress syndrome. *Anesthesiology* 1997; **87**: 6–17.
46. Blanch L, Fernandez R, Saura P, Baigorri F, Artigas A. Relationship between expired capnogram and respiratory system resistance in critically ill patients during total ventilatory support. *Chest* 1994; **105**: 219–23.
47. Saura P, Lucangelo U, Blanch L, *et al*. Factores determinantes de la reducción de la $PaCO_2$ con la insuflación de gas traqueal en pacientes con lesión pulmonar aguda. *Med Intensiva* 1996; **20**: 246–51.
48. Kuo PH, Wu HD, Yu CJ, *et al.* Efficacy of tracheal gas insufflation in acute respiratory distress syndrome with permissive hypercapnia. *Am J Respir Crit Care Med* 1996; **154**: 612–16.
49. Oberg PA, Sjostrand U. Studies of blood pressure regulation. I. Common carotid artery clamping in studies of the carotid-sinus baroreceptor control of the systemic blood pressure. *Acta Physiol Scand* 1969; **75**: 276–87.
50. Gioia FR, Rogers MC. High-frequency ventilation of the lungs. In: Atkinson RS, Adams A (eds.) *Recent Advances in Anaesthesia and Analgesia*. New York: Churchill Livingstone, 1985; 63–78.
51. Branson RD. High-frequency ventilators. In: Branson RD, Hess DR, Chatburn RL (eds.) *Respiratory Care Equipment.* Philadelphia, PA: Lippincott Williams and Wilkins, 1995; 458–67.
52. Fort P, Farmer C, Westerman J, *et al.* High frequency oscillatory ventilation for adult respiratory distress syndrome: a pilot study. *Crit Care Med* 1997; **25**: 937–47.
53. Mehta S, Lapinsky SE, Hallett DC, *et al.* Prospective trial of high frequency oscillation in adult with acute respiratory distress syndrome. *Crit Care Med* 2001; **29**: 1360–9.
54. Borg U, Eriksson I, Sjostrand U. High frequency positive-pressure ventilation (HFPPV): a review based upon its use during bronchoscopy and for laryngoscopy and microlaryngeal surgery under anesthesia. *Anesth Analg* 1980; **59**: 594–603.
55. Rouby JJ, Simonneau G, Benhamou D, *et al.* Factors influencing pulmonary volumes and CO_2 elimination during high-frequency jet ventilation. *Anesthesiology* 1985; **63**: 473–82.
56. Kil HK, Kim WO, Choi HS, Nam YT. Monitoring of $PETCO_2$ during high frequency jet ventilation for laryngomicrosurgery. *Yonsei Med J* 2002; **43**: 20–4.
57. Biro P, Eyrich G, Rohling R. The efficency of CO_2 elimination during high frequency jet ventilation for laryngeal microsurgery. *Anesth Analg* 1998; **87**: 180–4.
58. Frietsch T, Krafft P, Becker HD, Buelzebruck H, Wiedemann K. Intermittent capnography during high-frequency jet ventilation for prolonged rigid bronchoscopy. *Acta Anaesthesiol Scand* 2000; **44**: 391–7.
59. Lucangelo U, Fontanesi L, Antonaglia V, *et al.* High frequency percussive ventilation (HFPV): principles and techniques [review]. *Minerva Anestesiol* 2003; **69**: 841–51.
60. Loring WR III, Cioffi WG, Mason AD, McManus WF, Pruitt BA. Improved survival of burned patients with inhalation injury. *Arch Surg* 1983; **128**: 772–80.
61. Rodeberg DA, Housinger TA, Warden GD. Improved ventilation function in burn patients using volumetric diffuse ventilation. *J Am Coll Surg* 1984; **179**: 518–22.
62. Mlcak RP. Ventilation strategies for smoke inhalation. *J Respir Care Pract* 1996; **Feb/Mar**: 103–6.
63. Lentz CW, Peterson HD. Smoke inhalation is a multilevel insult to the pulmonary system. *Curr Opin Pulmon Med* 1997; **3**: 221–6.
64. Reper P, Dankaert R, van Hille F, *et al.* The usefulness of combined high frequency percussive ventilation during acute respiratory failure after smoke inhalation. *Burns* 1998; **24**: 34–8.
65. Campbell PJ, Chilton HW, Garvey PA, Gupta JM. Volumetric diffusive respirator use in neonatal respiratory failure. *J Paediatr Child Health* 1991; **27**: 31–3.
66. Velmahos GC, Chan LS, Tatevossian R, *et al.* High-frequency percussive ventilation improves oxygenation in patients with ARDS. *Chest* 1999; **116**: 440–6.
67. Hurst JM, Branson RD, Davis K. High-frequency percussive ventilation in the management of elevated intracranical pressure. *J Trauma* 1988; **28**: 1363–7.
68. Hurst JM, Branson RD, DeHaven CB. The role of high-frequency ventilation in post-traumatic respiratory insufficiency. *J Trauma* 1987; **27**: 236–41.
69. Lucangelo U, Fontanesi F, Bird FM. High-frequency percussive ventilation. In: Gullo A (ed.) *Anaesthesia, Pain, Intensive Care, and Emergency Medicine.* New York: Springer, 2001; 163–71.

70. Lucangelo U, Fontanesi L, Antonaglia V, *et al.* High frequency percussive ventilation (HFPV): case reports. *Minerva Anestesiol* 2003; **69**: 853–7, 858–60.
71. Dhand R, Tobin MJ. Inhaled bronchodilator therapy in mechanically ventilated patients. *Am J Respir Crit Care Med* 1997; **156**: 3–10.
72. Yaron M, Padyk P, Hutsinpiller M, Cairns CB. Utility of the expiratory capnogram in the assessment of bronchospasm. *Ann Emerg Med* 1996; **28**: 403–7.
73. Tutuncü AS, Faithfull NS, Lachmann B. Intratracheal perfluorocarbon administration combined with mechanical ventilation in experimental respiratory distress syndrome: dose-dependent improvement of gas exchange. *Crit Care Med* 1993; **21**: 962–9.
74. Tutuncü AS, Faithfull NS, Lachmann B. Comparison of ventilatory support with intratracheal perfluorocarbon administration and conventional mechanical ventilation in animals with acute respiratory failure. *Am Rev Respir Dis* 1993; **148**: 785–92.
75. Hirschl RB, Pranikoff T, Wise C, *et al.* Initial experience with partial liquid ventilation in adult patients with the acute respiratory distress syndrome. *JAMA* 1996; **275**: 383–9.
76. Kirmse M, Fujino Y, Hess D, Kacmarek RM. Positive end-expiratory pressure improves gas exchange and pulmonary mechanics during partial liquid ventilation. *Am J Respir Crit Care Med* 1998; **158**: 1550–6.
77. Mates EA, Tarczy-Hornoch P, Hildebrandt J, Jackson JC, Hlastala MP. Negative slope of exhaled CO_2 profile: implications for ventilation heterogeneity during partial liquid ventilation. *Adv Exp Med Biol* 1996; **388**: 585–97.
78. Chopin C, Fesard P, Mangalaboyi J, *et al.* Use of capnography in diagnosis of pulmonary embolism during acute respiratory failure of chronic obstructive pulmonary disease. *Crit Care Med* 1990; **18**: 353–7.
79. Verschuren F, Liistro G, Coffeng R, *et al.* Volumetric capnography as a screening test for pulmonary embolism in the emergency department. *Chest* 2004; **125**: 841–50.
80. Kline JA, Israel EG, Michelson EA, *et al.* Diagnostic accuracy of a bedside D-dimer assay and alveolar deadspace measurement for rapid exclusion of pulmonary embolism. *JAMA* 2001; **285**: 761–8.
81. Verschuren F, Heinonen E, Clause D, *et al.* Volumetric capnography as a bedside monitoring of thrombolysis in major pulmonary embolism. *Intens Care Med* 2004; **30**: 2129–32.
82. Lucangelo U, Blanch L. Dead space. *Intens Care Med* 2004; **30**: 576–9.
83. Shimada Y, Yoshiya I, Tanaka K, Sone S, Sakurai M. Evaluation of the progress and prognosis of adult respiratory distress syndrome: simple respiratory physiologic measurement. *Chest* 1979; **76**: 180–6.
84. Kallet RH, Alonso JA, Pittet JF, Matthay MA. Prognostic value of the pulmonary deadspace fraction during the first 6 days of acute respiratory distress syndrome. *Respir Care* 2004; **49**: 1008–14.
85. Lucangelo U, Bernabè F, Vatua S, *et al.* Prognostic value of different deadspace indices in mechanically ventilated patients with acute lung injury and ARDS. *Chest* 2008; **133**: 62–71.

Section 2

Circulation, metabolism, and organ effects

Section 2
Chapter
20

Circulation, metabolism, and organ effects

Cardiopulmonary resuscitation

D. C. Cone, J. C. Cahill, and M. A. Wayne

Introduction

Sudden cardiac death accounts for approximately 1000 deaths per day in the United States. Sudden cardiac death is not a single clinical entity or disease process; rather, it is a syndrome and the final step in a wide variety of fatal processes. The emergency medical services (EMS) system of the United States and other nations is largely geared toward responding to and attempting to resuscitate victims experiencing out-of-hospital cardiac arrest (OOHCA), despite discouraging statistics indicating that very few of these patients are, in fact, successfully resuscitated. In most EMS systems, OOHCA survival percentages are in the single digits [1–3].

One of the key treatment modalities for cardiac arrest of any cause is cardiopulmonary resuscitation (CPR). This consists of manual (or mechanical) compression of the patient's chest in an effort to create forward blood flow, combined with periodic mouth-to-mouth or mechanically-aided ventilation in an effort to deliver oxygen to the lungs. While having another person attempt to palpate a carotid, femoral, or other pulse during chest compressions may provide some assessment of the effectiveness of the compressions (a palpable pulse accompanying each compression suggests reasonable forward blood flow through the circulatory system), to date, no method has been devised for non-invasively monitoring the effectiveness of CPR in real time. Capnography may provide such a means.

In the majority of cases, CPR and other treatment efforts are unsuccessful, and the patient is eventually pronounced dead either at the scene or at the receiving hospital. A number of clinical indicators can be used to determine when those efforts should be terminated, including degeneration of the electrical rhythm of the heart to asystole despite electrical and chemical treatment [4], or the absence of any cardiac movement on ultrasonographic imaging [5]. The former method requires only a portable electrocardiograph, found on advanced life-support rescue vehicles worldwide, while the latter requires an ultrasound machine, a device that has just started to be employed in the out-of-hospital setting [6–8]. Capnography can likely provide another clinical indicator of death, and, as such, could also be used to guide decisions to terminate resuscitative efforts. This chapter will discuss two roles for capnography in the assessment and treatment of patients in cardiac arrest: evaluation of the efficacy of CPR, and cessation of resuscitation.

Cardiac output, end-tidal carbon dioxide, and CPR

A number of animal studies have shown an excellent correlation between end-tidal carbon dioxide ($P_{ET}CO_2$) and cardiac output during states of low flow [9–11] and during CPR [12–15]. Human studies have noted the same finding [16–19], although one study found this relationship to be logarithmic [17], while others have found it to be linear [16,18]. If CO_2 production and ventilation are relatively constant during CPR [20], one would expect $P_{ET}CO_2$ to reflect the pulmonary blood flow generated by CPR. However, only when ventilation is relatively constant can $P_{ET}CO_2$ accurately reflect circulatory status [11,13,18,21–23]. The interpretation of $P_{ET}CO_2$ in the field must, therefore, always take into account that constant controlled ventilation may be difficult or impossible when manual CPR is being interrupted while the patient is being moved or rescuers change positions. It is also not clear whether changes in the ratio of alveolar deadspace to tidal volume (V_D/V_T) can affect the correlation between $P_{ET}CO_2$ and cardiac output [9,18].

Several researchers have suggested that the close correlation between cardiac output and $P_{ET}CO_2$ readings might be utilized to monitor the effectiveness of CPR in real time [15,22–25]. The first such suggestion appears to have come in 1978, when Kalenda [21],

Capnography, Second Edition, ed. J. S. Gravenstein, Michael B. Jaffe, Nikolaus Gravenstein, and David A. Paulus. Published by Cambridge University Press. © Cambridge University Press 2011.

calling $PETCO_2$ during constant ventilation a "precise and constant mirror of lung perfusion and hence of cardiac output," published a series of three patients being monitored with capnography during CPR. This paper reported a decrease in $PETCO_2$ as the person performing CPR fatigued, followed by an increase in $PETCO_2$ as a new rescuer took over, the latter finding presumably reflecting more effective chest compressions. He also demonstrated a gradual diminution, and then total loss of, $PETCO_2$ in patients not resuscitated, and a significant rise in $PETCO_2$ in a patient who regained a spontaneous pulse. He concludes with a single sentence: "The value of capnography as a guide to the efficacy of cardiac massage is clearly demonstrated."[21].

Other studies have further substantiated Kalenda's conclusion. Falk *et al.* studied 13 cardiac arrests in 10 patients, and found that $PETCO_2$ decreased from a mean of 1.4% pre-arrest to 0.4% after the onset of cardiac arrest [16], with an increase to 1.0% with CPR. Return of spontaneous circulation (ROSC) was heralded with a rapid increase to 3.7% (presumably as forward flow improved abruptly), followed by stabilization at 2.4% 4 min later. In those patients who did not achieve ROSC, $PETCO_2$ remained at an average of 0.7%. The authors suggested that routine monitoring of $PETCO_2$ at the bedside, or in any other location including the field, would be preferable to palpation of the carotid pulse in monitoring the effectiveness of CPR.

An animal study tested the feasibility of using the volume of CO_2 excreted (CO_2ex) in the airway as a non-invasive measure of CPR efficacy [23], and found that cardiac output accounted for greater than 65% of the variability seen in CO_2ex during CPR. These authors indicated that despite the ability of their method to carefully control alveolar ventilation, other variables, such as tissue perfusion, could not be controlled. Changes in regional blood flow during cardiac arrest and CPR can affect the amount of viable tissue (tissue that is still producing CO_2) and mobile CO_2 stores being perfused. Without a better understanding of changes in the stores of CO_2 in the body during low-flow and no-flow states [26], the ability to precisely interpret $PETCO_2$ values during CPR will remain limited. Despite this limitation, the authors believe that the monitoring of CO_2 excretion does provide a reasonable overall picture of the level of perfusion achieved by CPR.

It should be noted that at least one study has found the relationship between cardiac output and $PETCO_2$ to be unreliable. In an animal model, while performing open-chest cardiac massage and delivering a constant cardiac output (as measured by a flow probe in the ascending aorta), $PETCO_2$ decreased over the first 5 min after the induction of ventricular fibrillation, but then gradually, and continuously, increased with CPR for the 50-min duration of the protocol [27]. This occurred despite a constant cardiac output, and was due primarily to an increase in CO_2ex, which the authors postulate might be due to an increase in pulmonary capillary blood flow over time, or an increase in CO_2 production representing factors not directly measured. The authors believe that $PETCO_2$ readings may change over time during CPR, even if cardiac output is constant. These changes may complicate estimating the effectiveness or prognostic value of CPR. A 1989 study by Sanders *et al.* showed a similar finding of a gradual, but significant, increase in $PETCO_2$ over time in patients who were unable to be resuscitated. However, there was significantly less control of the CPR technique, and thus of cardiac output, in this study [28].

A recent animal study found an excellent relationship ($r = 0.88$, $P < 0.001$) between $PETCO_2$ and stroke volume, as measured with transesophageal echocardiographic (TEE) imaging [29]. The authors of this study suggest that indicator dilution techniques, generally used to measure cardiac output, are less reliable under conditions of very low flow, as occurs with CPR [30–32]. The TEE approach allowed investigators to confirm that $PETCO_2$ is quantitatively predictive of the stroke volume index. The loss of reliability under low-flow conditions may explain some of the inconsistencies mentioned. TEE has yet to be introduced in human studies.

Several studies have used the relationship between $PETCO_2$ and cardiac output to test a third variable. Ward *et al.* in a series of 15 patients who had failed initial resuscitation attempts, provided either manual CPR or mechanical CPR, delivered by the Thumper® device (Michigan Instruments, Grand Rapids, MI, USA) while monitoring $PETCO_2$ to determine which mode provided a greater cardiac output [25]. The mean $PETCO_2$ with manual CPR was 6.9 mm Hg versus a mean of 13.6 mm Hg with mechanical CPR ($P < 0.001$). While noting that the reasons for the apparently better cardiac output with the mechanical device were unclear, the authors suggested that monitoring $PETCO_2$ might help optimize chest compressions during CPR. In another study using the Thumper® device, Ornato *et al.* tested blood flow delivered by various CPR compression forces [33]. They used radial artery pressure and $PETCO_2$ as determinants of blood flow.

Berg *et al.* used $PETCO_2$ to test the effect of audio-prompted rate guidance on the quality of pediatric CPR

[34]. Although a somewhat higher $PETCO_2$ was measured during rate-prompted 100 compression/min CPR as compared to the baseline CPR, the difference was not significant (11 mm Hg versus 4 mm Hg, $P = 0.08$). However, $PETCO_2$ was significantly higher during rate-prompted 140 compression/min CPR than at baseline (12 mm Hg versus 4 mm Hg, $P < 0.05$). A similar study in adults found mean $PETCO_2$ values of 8.7 mm Hg during baseline CPR versus 14.0 during rate-prompted CPR at either 80 or 120 compressions/min ($P < 0.01$) [20].

Coronary and cerebral perfusion pressure during CPR

Using a canine cardiac arrest model, good correlation ($r = 0.78$, $P < 0.01$) between $PETCO_2$ and coronary perfusion pressure was found in a 1985 study by Sanders *et al.* [35]. Another study by the same group, using slightly different techniques, found somewhat better results ($r = 0.91$, $P < 0.01$) [36]. It has been postulated that the higher cerebral perfusion pressure simply reflects better overall vascular tone during CPR, and that better vascular tone results in higher $PETCO_2$ via improved pulmonary blood flow [37]. However, the true physiologic relationship between coronary perfusion pressure and $PETCO_2$ remains unclear.

An animal model with ultrasound flow probes and radioactive microspheres was used to examine the relationships between $PETCO_2$ and cardiac output, cerebral perfusion, and renal perfusion [38]. The correlation (r value) between $PETCO_2$ and cardiac output was 0.90, consistent with other studies discussed above. The correlation between $PETCO_2$ and cerebral blood flow was lower, but still significant ($r = 0.64$, $P = 0.01$). However, when *partial* correlation coefficients were determined to ascertain whether $PETCO_2$ primarily correlated with cardiac output or with cerebral blood flow, values were $r = 0.70$ for cardiac output ($P < 0.05$) and $r = 0.30$ for cerebral perfusion ($P > 0.05$). This suggests that during CPR, $PETCO_2$ follows cardiac output and not cerebral blood flow; thus, cardiac output does not necessarily correlate with cerebral flow. These authors believe that this likely limits the usefulness of $PETCO_2$ as a non-invasive measure of cerebral flow during CPR.

Bicarbonate and epinephrine during CPR

A number of studies have found that $PETCO_2$ values may change transiently after the administration of intravenous epinephrine or sodium bicarbonate. This is not surprising in the case of sodium bicarbonate, which rapidly increases the overall CO_2 difference, and thus the $PETCO_2$ reading [22]. In general, this increase is not as large as is seen with ROSC, and is transient. In one study, for example, the readings increased from a mean of 0.8% to a mean of 2.1% (roughly 6–16 mm Hg) after sodium bicarbonate was administered into the central circulation, but returned to baseline in the next 2 min [16]. Another study mentions a similar observation, where $PETCO_2$ increases with the administration of bicarbonate were also observed, but with a return to baseline within 5 min. These data were not presented as part of that study, but appear to be observations that prompted them to discard $PETCO_2$ values obtained in the first 5 min after the administration of sodium bicarbonate [28].

The case with epinephrine is more complex. Having anecdotally noted a decrease in $PETCO_2$ following epinephrine administration [39], and taking into consideration similar findings from animal studies [40,41], Callaham and colleagues prospectively studied these issues [42]. The $PETCO_2$ readings were taken on arrival at the emergency department (ED), and 4 min (or as close to 4 min as possible) after the administration of the largest dose of intravenous (IV) epinephrine. The $PETCO_2$ increased in 28% of the 64 subjects, decreased in 39%, and did not change in 33%. The average change was a decrease of 0.3 mm Hg (not significant).

In a similar study, 20 OOHCA patients were examined [43]. The $PETCO_2$ decreased from a mean of 16.7 mm Hg prior to epinephrine administration to a mean of 12.6 mm Hg 3 min after peripheral IV injection of 2 mg of epinephrine ($P < 0.0001$). The value of $PETCO_2$ decreased in 14 patients, and did not change in six. The authors acknowledge that the mechanism of the observed decrease is not known, and they postulated that the redistribution of blood flow resulting from the vasoconstriction of non-myocardial and non-cerebral vascular beds is associated with an increased afterload, likely altering pulmonary perfusion. A decrease in mixed venous CO_2 concentration may also be involved, although support for this mechanism is not compelling. Redistribution of blood flow within the lungs may also be responsible [44]. Regardless of the mechanism, Cantineau *et al.* recommend caution when interpreting $PETCO_2$ readings collected soon after epinephrine administration [43].

A more recent study of this phenomenon was conducted by Lindberg *et al.* [45]. In an animal model, the investigators found an *increase* in coronary perfusion

pressure after the administration of either epinephrine or norepinephrine, but a *decrease* in $P_{ET}CO_2$. The authors believe that the increase in coronary perfusion pressure reflects overall vasoconstriction, with redistribution of blood flow away from non-vital organs to selectively perfuse vital organs, including the heart. At the same time, they believe that overall cardiac output is reduced due to increased afterload, causing the decrease in $P_{ET}CO_2$ they observed. Others have suggested that a decrease in $P_{ET}CO_2$ after vasopressor administration may be a marker of vasomotor responsiveness, a good prognostic sign [42].

End-tidal CO_2 and prognosis during cardiac arrest

A number of studies in both animals and humans have examined the prognostic capabilities of capnography for patients undergoing CPR. The first such animal study, by Sanders *et al.*, monitored $P_{ET}CO_2$ continuously during resuscitation from an induced cardiac arrest, and the mean $P_{ET}CO_2$ for each animal after the resuscitation interval was determined [36]. They found that this mean $P_{ET}CO_2$ was significantly higher for animals that were resuscitated using high-pressure 80-lb (36-kg) chest compressions than for those animals that could not be resuscitated using 40-lb (18-kg) low-pressure compressions (mean of 9.6 mm Hg versus 3.2 mm Hg, $P < 0.01$).

In a particularly interesting study, Blumenthal and Voorhees examined CO_2 excretion in an animal model by measuring the partial pressure of CO_2 in the airway, and calculating total CO_2 excretion in mL/kg/min [19]. The study found no differences before CPR (mean 13.81 mL/kg/min for survivors, 13.06 for non-survivors, $P = 0.57$), but a significant difference after 3 min of ventricular fibrillation and 13 min of CPR (mean 6.74 mL/kg/min for survivors, 4.88 for non-survivors, $P < 0.0001$). These values represent calculated CO_2 excretion, not raw $P_{ET}CO_2$ values; however, they do seem to support the findings of other studies: better values during CPR suggest a better prognosis. A "cut-off" value for survival of 7.0 mL/kg/min had a positive predictive value of 0.83, and a negative predictive value of 0.73. No animal with a CO_2 excretion rate of less than 5.0 mL/kg/min survived.

Unfortunately, in examining the few available human studies, it quickly becomes clear that differences in inclusion criteria (pulseless electrical activity versus all arrest rhythms), outcome measures (ROSC versus survival), setting (field versus ED versus in-hospital), and measures of central tendency (median versus mean $P_{ET}CO_2$ values) limit our ability to draw firm conclusions or to establish a consensus "cut-off" or threshold value for terminating resuscitation efforts. Differing methodologies, in terms of types of $P_{ET}CO_2$ readings, compound the issue: some studies report the maximum reading obtained, and some report a reading taken after 1 or 2 min of capnographic monitoring. Table 20.1 summarizes the results of several of the human studies that are discussed here.

The first human study to examine the role of capnometry in the prediction of cardiac arrest survival was conducted in 1987 [22]. In an observational series of 23 patients who sustained OOHCA and were brought to the ED still in arrest, Garnett *et al.* calculated the mean of the $P_{ET}CO_2$ readings taken on five consecutive ventilator-assisted breaths 3–5 min after ED arrival. They found no difference between the mean value for the 10 patients who obtained ROSC (1.7%) versus the 13 patients who did not obtain ROSC (1.8%). The authors contrast these findings to those of Sanders *et al.* [36], and postulate that the underlying chronic heart and lung disease found in typical OOHCA patients may cause them to differ significantly in terms of arrest physiology from the canines in the Sanders model.

The next human study of the prognostic value of $P_{ET}CO_2$ in cardiac arrest resuscitation involved 35 cardiac arrests in 34 patients [28]. The nine patients who survived the resuscitation attempt (defined as having a stable blood pressure when the resuscitation team was dismissed by the physician in charge) had higher average $P_{ET}CO_2$ readings during CPR than the 26 who did not, with means of 15 mm Hg versus 7 mm Hg ($P < 0.001$). The initial, final, maximum, and minimum readings were also all higher in the successfully resuscitated patients. No patient with an average $P_{ET}CO_2$ reading of less than 10 mm Hg was successfully resuscitated. The three patients who survived to hospital discharge had higher average of $P_{ET}CO_2$ readings than the 32 who did not leave the hospital, with means of 17 mm Hg versus 8 mm Hg ($P < 0.05$). Perhaps due to the small number of survivors, the initial, final, and maximum $P_{ET}CO_2$ values did not differ between these groups, although the minimum was higher in survivors than non-survivors.

Two additional studies confirmed these findings in ED patients [39,46]. It should be noted, however, that in the first of these studies, while a cut-off of 15 mm Hg yielded the best sensitivity and specificity for survival

Table 20.1 Mean $ET CO_2$ levels for successful and unsuccessful cardiac arrest resuscitation

Study	Setting	*n*	Outcome measure	Reading taken	Success	No success	*P* value	Threshold value proposed	Sensitivity	Specificity	PPV	NPV
Garnett *et al.* (1987)	ED	23	ROSC	Mean of	1.7%	1.8%	Not given					
				5 breaths								
Voorhees *et al.* (1980)	ED and	35	ROSC	Mean	15	7	< 0.001	10	1.00	0.77	0.60	1.00
	hosp											
Callaham and Barton (1990)	ED	55	ROSC	1 min	19	5.2	< 0.0001	15	0.71	0.98	0.91	0.91
Steedman and Robertson	ED	12	ROSC		2.63%	1.64%	< 0.001					
(1990)												
Kern *et al.* (1992)	ED and hosp	23	ROSC	Mean	17.9	10.4	< 0.01					
Callaham *et al.* (1992)	ED	64	ROSC					5	0.93	0.47	0.36	0.96
								10	0.40	0.87	0.50	0.82
								15	0.07	0.98	0.50	0.77
Asplin and White (1995)	EMS	27	ROSC	1 min	23.0	13.2	0.0002					
				2 min	26.8	15.4	0.0019					
				Max	30.8	22.7	0.0154					
Cantineau *et al.* (1996)	EMS	24	ROSC	Initial	18.4	10.2	< 0.01					
				Min	13.9	7.5	< 0.01					
				Max	29.9	18.1	< 0.01					
	EMS	96						10	1.00	0.67		

Table 20.1 *(cont)*

Study	Setting	*N*	Outcome measure	Reading taken	Success	No success	*P* value	Threshold value proposed	Sensitivity	Specificity	PPV	NPV
Wayne et al. (1995)	EMS	90	ROSC	Initial	11.7	10.9	0.672					
				20 min	3.9	31	< 0.0001	10	0.973	1.00	1.00	0.889
Levine et al. (1997)	EMS	150	adm to hosp	Initial	12.3	12.2	0.93					
				20 min	4.4	32.8	< 0.001	10	1.00	1.00	1.00	1.00
Salen et al. (2001)	ED	53	adm to hosp	Peak	35[a]	13.7[a]	< 0.01	16				
Grmec and Klemen (2001)	EMS	139	adm to hosp	Initial				10	1.00	0.90		
Grmec and Kupnik (2003)	EMS	246	adm to hosp	Initial	2.12 kPa	1.09 kPa	0.035	10	1.0	0.74		
			d/c from ICU	Initial	2.63 kPa	1.21 kPa	< 0.01	10	1.0	0.80		

[a] Median value; all others are means. All readings are in mm Hg, except where % or kPa is shown. PPV, positive predictive value; NPV, negative predictive value; EMS, out-of-hospital emergency medical services; ED, emergency department; hosp, hospital; ROSC, return of spontaneous circulation; adm, admission; d/c, discharge; ICU, intensive care unit; Max, maximum; Min, minimum.

as determined with a receiver operating characteristics (ROC) curve, four patients who had both initial and later $PetCO_2$ readings of less than 10 mm Hg were resuscitated. This led the authors to caution that a low $PetCO_2$ value might not be an adequate reason, by itself, to end resuscitative efforts [39]. The authors further advise that the ROC curve can allow the individual clinician to choose a threshold with levels of sensitivity and specificity that he or she feels are justified. It has been postulated that these data, and similar reports of ROSC after prolonged resuscitative attempts with low $PetCO_2$ values [43], may account for the reluctance of the scientific community to incorporate $PetCO_2$ monitoring into life-support algorithms [47].

One of the studies discussed above, comparing $PetCO_2$ at different chest compression rates, found that patients with ROSC had a mean $PetCO_2$ level of 17.9 mm Hg compared to a mean of 10.4 mm Hg in those who did not achieve ROSC [20]. One of the studies examining the role of epinephrine explored several threshold values, using the first recorded $PetCO_2$ value upon the patient's arrival at the ED [42]. Values are presented in Table 20.1; not surprisingly, sensitivity decreases and specificity increases as higher thresholds are chosen.

Following a four-patient feasibility case series [48], a study by Asplin and White conducted in the Rochester, Minnesota EMS system examined the role of $PetCO_2$ readings as determined by paramedics on victims of OOHCA, using an early portable capnograph weighing 3.6 kg [37]. Monitoring was begun as soon as possible after endotracheal intubation and, not knowing the optimal time for taking prognostic $PetCO_2$ readings, the authors collected data after 1 and 2 min, and the maximum $PetCO_2$ reading for each patient. The mean 1-min, 2-min, and maximum values were all higher in those patients who demonstrated ROSC in the field than those who did not (P values of 0.0002, 0.0019, and 0.0154, respectively). Due to the small number of survivors (three patients), no attempt was made to compare $PetCO_2$ values for survivors versus non-survivors.

A similar study published by Cantineau *et al.* found that in a derivation set of 24 patients, mean initial, minimum, and maximum $PetCO_2$ values recorded during the first 20 min of resuscitation were all higher in patients who experienced ROSC than those who did not. In a validation follow-up with 96 patients, the authors' proposed threshold of 10 mm Hg provided 100% sensitivity and 67% specificity for ROSC [49]. This contrasts with a study by Varon *et al.* which found a level greater than 2% (roughly 14 mm Hg) in all survivors of both OOHCA and in-hospital cardiac arrests; however, Varon's study involved the use of colorimetric $PetCO_2$ devices, with values based on estimates of color change [50].

A study by Wayne *et al.* in the Whatcom County, Washington EMS system examined 90 patients with OOHCA [51]. No difference in the *initial* $PetCO_2$ was recorded by the paramedics (mean of 11.7 mm Hg for those who did not achieve ROSC in the field, versus 10.9 for those who did, $P < 0.672$), but after 20 min, a significant difference was seen (3.9 versus 31, $P < 0.0001$). Testing a hypothetical threshold of 10 mm Hg for determining the inability to resuscitate, no patient with a value below the threshold was resuscitated.

A follow-up study tested the *a priori* hypothesis that a $PetCO_2$ level of 10 mm Hg or less, sustained for 20 min, would predict failure to survive OOHCA of the pulseless electrical activity type [47]. This study similarly found no difference in the initial $PetCO_2$ (mean of 12.3 mm Hg for non-survivors versus 12.2 for survivors, $P < 0.93$), but a substantial difference at 20 min (mean of 4.4 mm Hg versus 32.8, $P < 0.001$). No patient with a 20-min level of 10 mm Hg or less survived; sensitivity, specificity, positive predictive value, and negative predictive value were all 100%, although an upper 99% binomial confidence limit of 3.9% was reported given the sample size.

One of several studies that examined the active compression/decompression CPR (ACD/CPR) technique used $PetCO_2$ as a marker for cardiac output to compare the hemodynamics generated by the ACD/CPR method to standard CPR in the out-of-hospital setting [52]. The EMS physicians staffing the advanced life-support units in this study from Germany measured $PetCO_2$ immediately upon intubation, and every 2 min afterward until either ROSC was achieved or 10 min had passed. While no difference was found between the ACD/CPR and standard CPR groups, it was noted that median $PetCO_2$ values were higher at 0, 2, 4, 6, and 10 min in the group of patients who achieved ROSC in the field and were admitted to the hospital compared to those who were pronounced dead at the scene. No patient who survived at least 6 h had a $PetCO_2$ level of less than 15 mm Hg; however, sensitivity, specificity, and predictive values are not presented for this resuscitation threshold. It is worth noting that, in calculating their power and sample size, the authors used a reference value of 12 mm Hg, citing the studies by Callaham and Barton, and Sanders *et al.* [28,39]. Additionally,

a rise in $P_{ET}CO_2$ was seen *prior* to a palpable pulse in patients with ROSC.

Salen *et al.* published a two-center study that examined both cardiac ultrasonography and capnography as predictors of survival to hospital admission for patients undergoing ED resuscitation [53]. The median peak $P_{ET}CO_2$ of those who ultimately survived was either 35 or 39 mm Hg, significantly ($P < 0.01$) higher than those who did not survive (13.7 mm Hg). (The paper's abstract, data table, and discussion section report 35 mm Hg, while the results section and the accompanying editorial [54] show 39 mm Hg.) No patient with a $P_{ET}CO_2$ less than 16 mm Hg survived the arrest, although one non-survivor was reported to have had a $P_{ET}CO_2$ of 48 mm Hg. In multivariate logistic regression, each 1 mm Hg increase in $P_{ET}CO_2$ was associated with 16% greater odds of survival. Further, using a stepwise logistic regression model, the area under the ROC curve was 0.91, showing excellent prediction of survival. While not all patients in this study underwent both cardiac ultrasonography and capnography, higher $P_{ET}CO_2$ levels were more strongly associated with survival than was ultrasonographic evidence of cardiac activity.

Another study found that initial, final, maximum, minimum, and mean $P_{ET}CO_2$ values were all higher in patients who were resuscitated than in those who were not [55]. No patient with an initial, mean, and final reading of less than 10 mm Hg survived. A similar study was published [56] in which capnography was added to the Mainz Emergency Evaluation Scoring System [57]. Initial and final $P_{ET}CO_2$ values were higher in those with ROSC versus those without, and in those who survived (defined here as discharge from the intensive care unit) versus those who did not. All patients with ROSC, and all who survived, had initial $P_{ET}CO_2$ values greater than 10 mm Hg. Finally, a 2001 study of 127 intubated cardiac arrest patients (a mix of intensive care unit and air medical services patients) found that all but one patient with a $P_{ET}CO_2$ value <10 mm Hg died [58]. These prehospital data, combined with the findings from Wayne *et al.* [51], provide strong support for a resuscitation threshold of 10 mm Hg in the field.

Finally, it should be noted that none of the above studies included trauma patients; all consisted of only patients with *medical* cardiac arrest. Several studies have examined the use of $P_{ET}CO_2$ in trauma patients, but most have been performed in the operating room, on patients not in cardiac arrest at the time of initial $P_{ET}CO_2$ measurement [59–61]. To date, only one study has been conducted of $P_{ET}CO_2$ as a predictor of survival in critical trauma patients in the out-of-hospital setting; however, as with the operating room studies, none of the 191 patients studied were in cardiac arrest at the time of intubation and initial $P_{ET}CO_2$ measurement [62].

Summary

In summary, it appears that capnography offers an effective tool to assist in evaluating the progress and results of medical cardiopulmonary resuscitation. At present, we lack data to recommend extrapolation to trauma patients. Moreover, international consensus groups, such as the American Heart Association and the International Liaison Committee on Resuscitation, have not made any recommendations for this application, but, however, noted in the 2005 Guidelines that "Ideally a clinical assessment, laboratory test, or biochemical marker would reliably predict outcome during or immediately after cardiac arrest. Unfortunately no such predictors are available" [63]. Perhaps future editions of these guidelines, supported by additional research, may provide a recommendation in this area.

References

1. Becker LB, Ostrander MP, Barrett J, Kondos GT. Outcome of CPR in a large metropolitan area: where are the survivors? *Ann Emerg Med* 1991; **20**: 355–61.
2. Lombardi G, Gallagher J, Gennis P. Outcome of out-of-hospital cardiac arrest in New York City: The Pre-Hospital Arrest Survival Evaluation (PHASE) Study. *JAMA* 1994; **271**: 678–83.
3. International Liaison Committee on Resuscitation. Guidelines 2000 for Cardiopulmonary Resuscitation and Emergency Cardiovascular Care. II. Ethical aspects of CPR and ECC. *Circulation* 2000; **102**(8 Suppl): I12–21.
4. Bailey ED, Wydro GC, Cone DC. National Association of EMS Physicians Standards and Clinical Practice Committee.Termination of resuscitation in the prehospital setting for adult patients suffering nontraumatic cardiac arrest. *Prehosp Emerg Care* 2000; **4**: 190–5.
5. Blaivas M, Fox JC. Outcome in cardiac arrest patients found to have cardiac standstill on the bedside emergency department echocardiogram. *Acad Emerg Med* 2001; **8**: 616–21.
6. Byhahn C, Bingold TM, Zwissler B, Maier M, Walcher F. Prehospital ultrasound detects pericardial tamponade in a pregnant victim of stabbing assault. *Resuscitation* 2008; **76**: 146–8.
7. Busch M. Portable ultrasound in pre-hospital emergencies: a feasibility study. *Acta Anaesthesiol Scand* 2006; **50**: 754–8.

8. Walcher F, Weinlich M, Conrad G, *et al.* Prehospital ultrasound imaging improves management of abdominal trauma. *Br J Surg* 2006; **93**: 238–42.
9. Isserles SA, Breen PH. Can changes in end-tidal pCO2 measure changes in cardiac output? *Anesth Analg* 1991; **73**: 808–14.
10. Idris AH, Staples ED, O'Brien DJ, *et al.* End-tidal carbon dioxide during extremely low cardiac output. *Ann Emerg Med* 1994; **23**: 568–72.
11. Jin X, Weil MH, Tang W, *et al.* End-tidal carbon dioxide as a non-invasive indicator of cardiac index during circulatory shock. *Crit Care Med* 2000; **28**: 2415–19.
12. Trevino RP, Bisera J, Weil MH, Rackow EC, Grundler WG. End-tidal CO_2 as a guide to successful cardiopulmonary resuscitation: a preliminary report. *Crit Care Med* 1985; **13**: 910–11.
13. Weil MH, Bisera J, Trevino RP, Rackow EC. Cardiac output and end-tidal carbon dioxide. *Crit Care Med* 1985; **13**: 907–9.
14. Grundler W, Weil MH, Rackow EC. Arteriovenous carbon dioxide and pH gradients during cardiac arrest. *Circulation* 1986; **74**: 1071–4.
15. Gudipati CV, Weil MH, Bisera J, Deshmukh HG, Rackow EC. Expired carbon dioxide: a non-invasive monitor of cardiopulmonary resuscitation. *Circulation* 1988; **77**: 234–9.
16. Falk JL, Rackow EC, Weil MH. End-tidal carbon dioxide concentration during cardiopulmonary resuscitation. *N Engl J Med* 1988; **318**: 607–11.
17. Ornato JP, Garnett AR, Glauser FL. Relationship between cardiac output and the end-tidal carbon dioxide tension. *Ann Emerg Med* 1990; **19**: 1104–6.
18. Shibutani K, Muraoka M, Shirasaki S, *et al.* Do changes in end-tidal pCO_2 quantitatively reflect changes in cardiac output? *Anesth Analg* 1994; **79**: 829–33.
19. Blumenthal SR, Voorhees WD. The relationship of carbon dioxide excretion during cardiopulmonary resuscitation to regional blood flow and survival. *Resuscitation* 1997; **35**: 135–43.
20. Kern KB, Sanders AB, Raife J, *et al.* A study of chest compression rates during cardiopulmonary resuscitation in humans: the importance of rate-directed chest compressions. *Arch Intern Med* 1992; **152**: 145–9.
21. Kalenda Z. The capnogram as a guide to the efficacy of cardiac massage. *Resuscitation* 1978; **6**: 259–63.
22. Garnett AR, Ornato JP, Gonzalez ER, Johnson EB. End-tidal carbon dioxide monitoring during cardiopulmonary resuscitation. *JAMA* 1987; **257**: 512–15.
23. Blumenthal SR, Voorhees WD. The relationship between airway carbon dioxide excretion and cardiac output during cardiopulmonary resuscitation. *Resuscitation* 1997; **34**: 263–70.
24. Lepilin MG, Vasilyev AV, Bildinov OA, Rostovtseva NA. End-tidal carbon dioxide as a non-invasive monitor of circulatory status during cardiopulmonary resuscitation: a preliminary clinical study. *Crit Care Med* 1987; **15**: 958–9.
25. Ward KR, Menegazzi JJ, Zelenak RR, Sullivan RJ, McSwain NE Jr. A comparison of chest compressions between mechanical and manual CPR by monitoring end-tidal pCO2 during human cardiac arrest. *Ann Emerg Med* 1993; **22**: 669–74.
26. Voorhees WD, Babbs CF, Tacker WA Jr. Regional blood flow during cardiopulmonary resuscitation in dogs. *Crit Care Med* 1980; **8**: 134–6.
27. Morimoto Y, Kemmotsu O, Murakami F, Yamamura T, Mayumi T. End-tidal CO_2 changes under constant cardiac output during cardiopulmonary resuscitation. *Crit Care Med* 1993; **21**: 1572–6.
28. Sanders AB, Kern KB, Otto CW, Milander MM, Ewy GA. End-tidal carbon dioxide monitoring during cardiopulmonary resuscitation: a prognostic indicator for survival. *JAMA* 1989; **262**: 1347–51.
29. Pernat A, Weil MH, Sun S, Tang W. Stroke volumes and end-tidal carbon dioxide generated by precordial compression during ventricular fibrillation. *Crit Care Med* 2003; **31**: 1819–23.
30. van Grondelle A, Ditchey RV, Groves BM, Wagner WW Jr., Reeves JT. Thermodilution method overestimates low cardiac output in humans. *Am J Physiol* 1983; **245**: H690–2.
31. Hillis LD, Firth BG, Winniford MD. Comparison of thermodilution and indocyanine green dye in low cardiac output or left-sided regurgitation. *Am J Cardiol* 1986; **57**: 1201–2.
32. Tournadre JP, Chassard D, Muchada R. Overestimation of low cardiac output measured by thermodilution. *Br J Anaesth* 1997; **79**: 514–16.
33. Ornato JP, Levine RL, Young DS, *et al*. The effect of applied chest compression force on systemic arterial pressure and end-tidal carbon dioxide concentration during CPR in human beings. *Ann Emerg Med* 1989; **18**: 732–7.
34. Berg RA, Sanders AB, Milander M, *et al.* Efficacy of audio-prompted rate guidance in improving resuscitator performance of cardiopulmonary resuscitation on children. *Acad Emerg Med* 1994; **1**: 35–40.
35. Sanders AB, Atlas M, Ewy GA, Kern KB, Bragg S. Expired pCO_2 as an index of coronary perfusion pressure. *Am J Emerg Med* 1985; **3**: 147–9.
36. Sanders AB, Ewy GA, Bragg S, Atlas M, Kern KB. Expired pCO2 as a prognostic indicator of successful

resuscitation from cardiac arrest. *Ann Emerg Med* 1985; **14**: 948–52.

37. Asplin BR, White RD. Prognostic value of end-tidal carbon dioxide pressures during out-of-hospital cardiac arrest. *Ann Emerg Med* 1995; **25**: 756–61.
38. Lewis LM, Stothert J, Standeven J, et al. Correlation of end-tidal CO2 to cerebral perfusion during CPR. *Ann Emerg Med* 1992; **21**: 1131–4.
39. Callaham M, Barton C. Prediction of outcome of cardiopulmonary resuscitation from end-tidal carbon dioxide concentration. *Crit Care Med* 1990; **18**: 358–62.
40. Ralston SH, Tacker WA, Showen L, Carter A, Babbs CF. Endotracheal versus intravenous epinephrine during electromechanical dissociation with CPR in dogs. *Ann Emerg Med* 1985; **14**: 1044–8.
41. Martin GB, Gentile NT, Paradis NA, *et al.* Effect of epinephrine on end-tidal carbon dioxide monitoring during CPR. *Ann Emerg Med* 1990; **19**: 396–8.
42. Callaham M, Barton C, Matthay M. Effect of epinephrine on the ability of end-tidal carbon dioxide readings to predict initial resuscitation from cardiac arrest. *Crit Care Med* 1992; **20**: 337–43.
43. Cantineau JP, Merckx P, Lambert Y, *et al*. Effect of epinephrine on end-tidal carbon dioxide pressure during prehospital cardiopulmonary resuscitation. *Am J Emerg Med* 1994; **12**: 267–70.
44. Tang W, Weil MH, Gazmuri RJ, *et al*. Pulmonary ventilation/perfusion defects induced by epinephrine during cardiopulmonary resuscitation. *Circulation* 1991; **84**: 2101–7.
45. Lindberg L, Liao Q, Steen S. The effects of epinephrine/norepinephrine on end-tidal carbon dioxide concentration, coronary perfusion pressure and pulmonary arterial blood flow during cardiopulmonary resuscitation. *Resuscitation* 2000; **43**: 129–40.
46. Steedman DJ, Robertson CE. Measurement of end-tidal carbon dioxide concentration during cardiopulmonary resuscitation. *Arch Emerg Med* 1990; **7**: 129–34.
47. Levine RL, Wayne MA, Miller CC. End-tidal carbon dioxide and outcome of out-of-hospital cardiac arrest. *N Engl J Med* 1997; **337**: 301–6.
48. White RD, Asplin BR. Out-of-hospital quantitative monitoring of end-tidal carbon dioxide pressure during CPR. *Ann Emerg Med* 1994; **23**: 25–30.
49. Cantineau JP, Lambert Y, Merckx P, *et al.* End-tidal carbon dioxide during cardiopulmonary resuscitation in humans presenting mostly with asystole: a predictor of outcome. *Crit Care Med* 1996; **24**: 791–6.
50. Varon AJ, Morrina J, Civetta JM. Clinical utility of a colorimetric end-tidal CO2 detector in cardiopulmonary resuscitation and emergency intubation. *J Clin Monit* 1991; **7**: 289–93.
51. Wayne MA, Levine RL, Miller CC. Use of end-tidal carbon dioxide to predict outcome in prehospital cardiac arrest. *Ann Emerg Med* 1995; **25**: 762–7.
52. Mauer D, Schneider T, Elich D, Dick W. Carbon dioxide levels during pre-hospital active compression: decompression versus standard cardiopulmonary resuscitation. *Resuscitation* 1998; **39**: 67–74.
53. Salen P, O'Connor R, Sierzenski P, *et al.* Can cardiac sonography and capnography be used independently and in combination to predict resuscitation outcomes? *Acad Emerg Med* 2001; **8**: 610–15.
54. Sanders AB, Kern KB, Berg RA. Searching for a predictive rule for terminating cardiopulmonary resuscitation. *Acad Emerg Med* 2001; **8**: 654–7.
55. Grmec S, Klemen P. Does the end-tidal carbon dioxide (EtCO2) concentration have prognostic value during out-of-hospital cardiac arrest? *Eur J Emerg Med* 2001; **8**: 263–9.
56. Grmec S, Kupnik D. Does the Mainz Emergency Evaluation Scoring (MEES) in combination with capnometry (MEESc) help in the prognosis of outcome from cardiopulmonary resuscitation in a prehospital setting? *Resuscitation* 2003; **58**: 89–96.
57. Grmec S, Gasparovic V. Comparison of APACHE II, MEES and Glasgow Coma Scale in patients with nontraumatic coma for prediction of mortality. *Crit Care* 2001; **5**: 19–23.
58. Ahrens T, Schallom L, Bettorf K, *et al.* End-tidal carbon dioxide measurements as a prognostic indicator of outcome in cardiac arrest. *Am J Crit Care* 2001; **10**: 391–8.
59. Wilson RF, Tyburski JG, Kubinec SM, *et al.* Intraoperative end-tidal carbon dioxide levels and derived calculations correlated with outcome in trauma patients. *J Trauma* 1996; **41**: 606–11.
60. Tyburski JG, Collinge JD, Wilson RF, et al. End-tidal CO2-derived values during emergency trauma surgery correlated with outcome: a prospective study. *J Trauma* 2002; **53**: 738–43.
61. Tyburski JG, Carlin AM, Harvey EH, Steffes C, Wilson RF. End-tidal CO2–arterial CO2 differences: a useful intraoperative mortality marker in trauma surgery. *J Trauma* 2003; **55**: 892–6; discussion 896–7.
62. Deakin CD, Sado DM, Coats TJ, Davies G. Prehospital end-tidal carbon dioxide concentration and outcome in major trauma. *J Trauma* 2004; **57**: 65–8.
63. American Heart Association. Guidelines for cardiopulmonary resuscitation and emergency cardiovascular care. *Circulation* 2005; **112**(24 Suppl): IV1–203.

Section 2
Chapter
21

Circulation, metabolism, and organ effects

Capnography and pulmonary embolism

J. T. Anderson

Introduction

Pulmonary embolism (PE) represents a clinical diagnostic dilemma. About 650 000 patients are diagnosed with PE each year in the USA and up to one-third die as a result of PE [1,2]. Pulmonary embolism is most commonly due to blood clots that travel through the venous system and lodge in the pulmonary arterial tree. Alternatively, embolism may be due to gas (i.e., air or carbon dioxide [CO_2]) [3], tumor, fat, or even bone cement [4]. Findings in large autopsy studies showed that PE was not identified premortem in up to 70% of patients who die as a direct result of this condition [1,2,5,6]. Presenting symptoms, i.e., tachypnea and shortness of breath [7], or alterations in arterial oxygen content [8–10] are non-specific. In actuality, these findings are more commonly due to an alternative diagnosis, such as postoperative atelectasis or pneumonia. The majority of deaths from PE occur within the first hour of the embolic event. For patients who survive beyond the first hour, appropriate therapy decreases the death rate from 30% to 2.5–10% [1,11]. Conversely, since only 20–40% of patients with clinically *suspected* PE actually have PE, empirical therapy may unnecessarily subject patients to a risk of bleeding. Unfortunately the common diagnostic techniques of $\dot{V}/\dot{Q}$ scanning, pulmonary angiography, or computed tomography (CT) angiography, are cumbersome, invasive, require transportation of potentially critically ill patients, or involve the use of radiation or nephrotoxic agents. A simple, rapid bedside method to screen, or more importantly, diagnose PE would be of great benefit. To this end, several investigators have assessed respiratory deadspace-based parameters derived from capnography to detect the presence of pulmonary emboli. Advances in technology have brought capnography to the bedside. This chapter describes the pathophysiologic basis and use of capnography in the detection of PE from a variety of causes.

Background

Respiratory deadspace

Appropriate appreciation of the parameters derived from time or volumetric capnography to determine the presence of pulmonary emboli requires a thorough understanding of respiratory deadspace. Pulmonary embolism results in an increase in respiratory deadspace, specifically alveolar deadspace, which can be determined with parameters obtained with capnography.

Respiratory deadspace represents the extent to which the exhaled tidal volume contains alveolar gas. Mathematically, this was expressed by Bohr [12] as:

$$\frac{V_D}{V_T} = 1 - \frac{F\bar{E}CO_2}{FACO_2},$$

where V_D is the deadspace, V_T the tidal volume, and $F\bar{E}CO_2$ and $FACO_2$ are the fractions of CO_2 in mixed exhaled gas and alveolar gas, respectively. Due to difficulties with measurement of alveolar CO_2, Enghoff utilized the partial pressure of CO_2 in arterial blood in the place of $FACO_2$ [13]. The arterial PCO_2 ($PaCO_2$) represented a "physiologic integrator of the CO_2 pressures existing in all parts of the lung" [14]. Expressed mathematically as:

$$\frac{V_D}{V_T} = 1 - \frac{P\bar{E}CO_2}{PaCO_2}$$

This latter equation represents the total or physiologic deadspace. In general, the respiratory system can be thought of as comprised of two components: one involved with transport of respiratory gases and another associated with the exchange of respiratory gases. Inefficiencies in either of these components result in "wasted ventilation," and contribute to overall

Capnography, Second Edition, ed. J. S. Gravenstein, Michael B. Jaffe, Nikolaus Gravenstein, and David A. Paulus. Published by Cambridge University Press. © Cambridge University Press 2011.

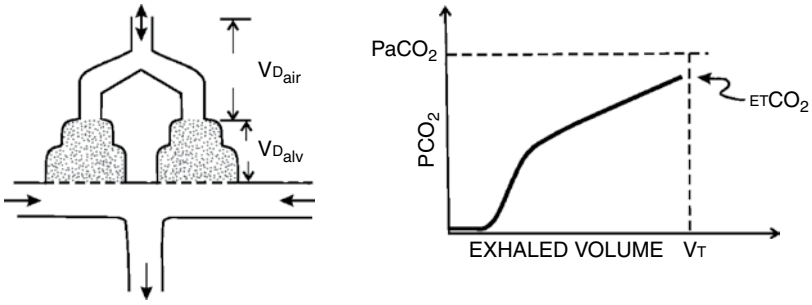

Figure 21.1 Mechanism for increased alveolar deadspace. Two respiratory units with alterations in ventilation/perfusion matching within respiratory units and the resulting capnogram.

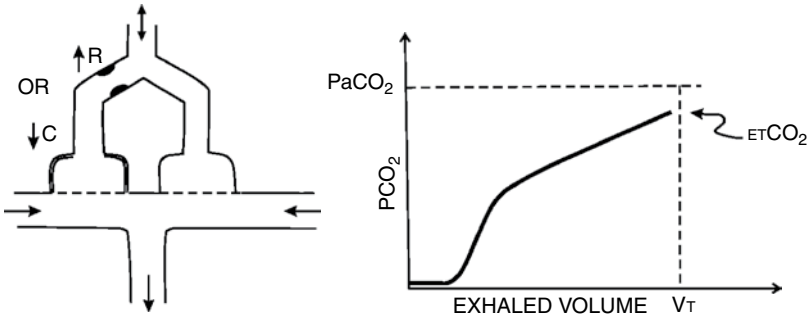

Figure 21.2 Mechanism for increased alveolar deadspace. Two respiratory units with different emptying rates due to differences in airway resistance (R) and compliance (C) and the resulting capnogram. Note increased R or decreased C will result in slower emptying rate.

deadspace. Airway deadspace (or convective deadspace) is the portion of total deadspace due to inefficiencies in the transport component, and alveolar deadspace is the portion due to inefficiencies in the component involved in gas exchange.

The term, *anatomic deadspace,* implies a fixed interface, and therefore a fixed volume. However, the location of the interface and the airway deadspace can also be altered by factors such as inspiratory rate or breath-holding. Generally, factors that favor diffusion or improve convection will shift the interface and decrease airway deadspace. For instance, a prolonged inspiratory phase and end-inspiratory pause will decrease the deadspace [15].

Alveolar deadspace represents inefficiencies in CO_2 and O_2 exchange. Specifically, alveolar deadspace represents inefficiencies distal to the interface of inspired gas and alveolar gas, that is, the interface where convection and diffusion are occurring [15]. Pulmonary embolism alters deadspace, primarily as a result of increased alveolar deadspace. Unfortunately, a number of other pulmonary conditions, such as asthma and chronic obstructive pulmonary disease (COPD), can also alter alveolar deadspace. Differences in the effects of PE on the capnographic waveforms can be exploited to improve the specificity of PE detection. Understanding of these differences requires knowledge of the various forms of alveolar deadspace.

Three general mechanisms can lead to increased alveolar deadspace:

- Alterations within (Figure 21.1) or between respiratory units (Figures 21.2 and 21.3).
- Venous admixture (although use of $PaCO_2$ is a practical representation of the $PACO_2$) (Figure 21.4).
- Incomplete mixing of gases within the respiratory unit (Figure 21.1). This type of alveolar deadspace is decreased by factors that favor more complete mixing or allow increased time for diffusion. For example, a decelerating flow waveform and an end-expiratory pause would decrease alveolar deadspace by facilitating mixing of alveolar gases.

Mismatch between respiratory units results from two basic pathophysiologic mechanisms that can be differentiated with capnography. Spatial differences in gas or blood flow between respiratory units in the lung cause inefficiency in gas exchange that is reflected as increased alveolar deadspace (Figures 21.2 and 21.3). First, alterations in the mechanical properties of the respiratory units, as may occur in chronic bronchitis, increase alveolar deadspace (Figure 21.2). Due

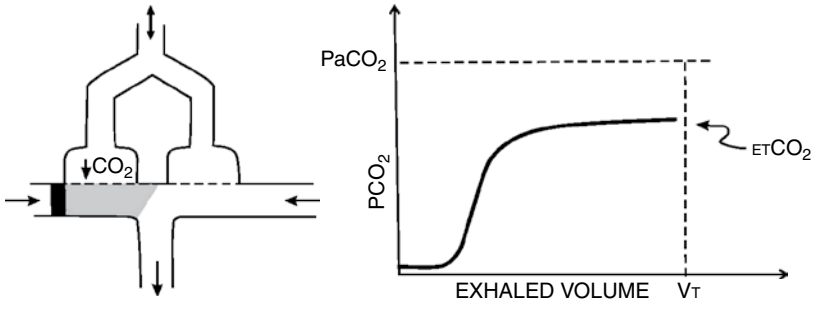

Figure 21.3 Mechanism for increased alveolar deadspace. Two respiratory units with occlusion of pulmonary vasculature with the resulting decrease in the end-tidal value and the resulting volumetric capnogram.

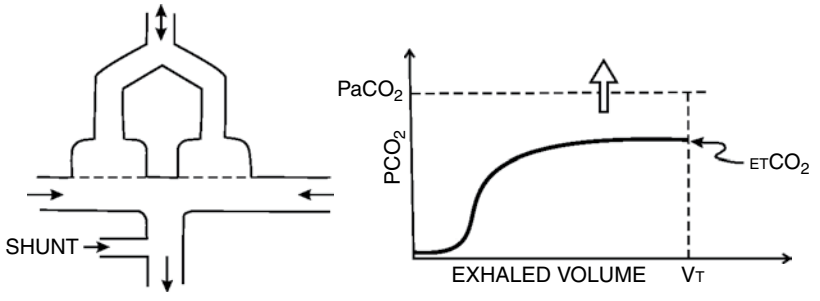

Figure 21.4 Mechanism for increased alveolar deadspace. Two respiratory units with a large shunt and the resulting volumetric capnogram.

to differences in the time constants of the respiratory units, $PaCO_2$ will vary between respiratory units. In this situation, individual respiratory units will empty sequentially at differing rates/times dependent upon mechanical properties. Second, spatial differences between respiratory units may be a consequence of spatial differences in blood flow, as occurs with PE (Figure 21.3). Occlusion of the pulmonary vasculature by an embolism will result in a lack of CO_2 flux to the alveoli in the affected vascular distribution. Because ventilation to the affected alveoli continues unabated, PCO_2 in these alveoli decreases. The mechanical properties may not be affected to a great extent, and, consequently, these alveoli will empty in parallel with other respiratory units with similar time constants. Differences in the emptying time of respiratory units will, as described subsequently, be shown to be of importance to differentiate increased alveolar deadspace from PE from that due to alternative diagnoses.

The last mechanism for increasing alveolar deadspace is a by-product of the method used to calculate deadspace. Arterial PCO_2 is considered a physiologic integrator of $PaCO_2$ present throughout the lung. As such, it is a practical representation of $PaCO_2$ that was substituted into the Bohr equation to calculate deadspace. However, venous admixture may result in increased $PaCO_2$ as CO_2-rich, mixed venous blood effectively bypasses the lung. This effect is minor and can usually be disregarded; however, in the presence of a large shunt, alveolar deadspace may appear increased (Figure 21.4). This mechanism is unaffected by temporal alterations.

Capnographic alterations associated with pulmonary embolism

Distinguishing PE from alternative diagnoses can be accomplished by exploiting the differences in the shape of the volumetric capnogram (Figure 21.5), specifically the slope of phase III, and/or by employing various respiratory maneuvers, including forced exhalations.

In general, the slope of phase III may be essentially horizontal or sloping. Pulmonary embolism will decrease the slope of phase III towards a horizontal orientation (Figure 21.6a). Alternatively, lung disease, such as COPD, will frequently cause an increased slope of phase III (Figure 21.6b). Pulmonary embolism results in an occlusion or limitation of flow in the pulmonary vasculature to respiratory units. The alveoli within the affected respiratory units are cut off from the CO_2 supply in the pulmonary arterial vessels (Figure 21.7). Because ventilation continues, $PaCO_2$ will decrease below the value in similarly ventilated alveoli in perfused respiratory units. Perfusion to peripheral alveoli appears to be especially affected. These alveoli tend to empty later and contribute to

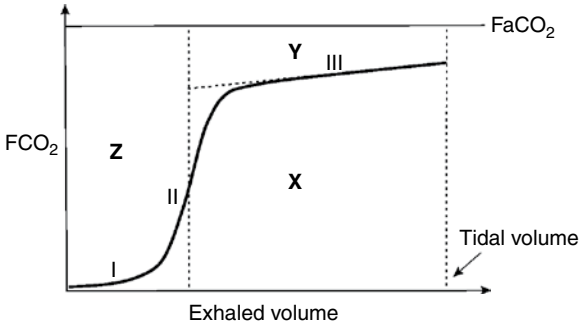

Figure 21.5 Volumetric capnogram. Lines are drawn to divide the curve into three large areas (labeled *X*, *Y*, and *Z*). The vertical line dividing phase II is placed such that the area under the curve equals the area labeled X. By substituting fractional CO_2 values for partial pressure values, calculated areas of the curve correspond to volumes of gas. The total area ($X + Y + Z$) represents the theoretical volume of CO_2 that could be eliminated with an exhaled breath equilibrated with the CO_2 in arterial blood. The area *X* represents the actual volume of exhaled CO_2 per breath (fractional CO_2 × volume exhaled breath). The following calculations are readily obtained:

$$\text{Physiologic deadspace: } \frac{V_{D_{phys}}}{V_T} = \frac{Y+Z}{X+Y+Z}$$

$$\text{Alveolar deadspace: } \frac{V_{D_{alv}}}{V_T} = \frac{Y}{X+Y+Z}$$

$$\text{Anatomic deadspace: } \frac{V_{D_{ana}}}{V_T} = \frac{Z}{X+Y+Z}$$

[Modified from: Anderson JT, Owings JT, Goodnight JE. Bedside non-invasive detection of acute pulmonary embolism in critically ill surgical patients. *Arch Surg* 1999; **134**: 869–75.]

the latter part of phase III. Consequently, the latter part of phase III is depressed out of proportion to the rest of phase III, thereby resulting in a horizontal phase III (Figure 21.6a). In contrast, in the presence of COPD, the peripheral alveoli continue to have a CO_2 supply due to intact perfusion, but ventilation is impaired (Figure 21.8). The $PaCO_2$ in the peripheral alveoli will increase towards the PCO_2 level in mixed venous blood. Because these alveoli tend to empty during the latter part of phase III, the slope is increased (Figure 21.6b).

Methods of pulmonary embolism detection

Physiologic deadspace

Physiologic deadspace is generally assessed using the Enghoff modification [13] of the Bohr equation, which substitutes the $PaCO_2$ value for that of $PACO_2$. Multiple exhaled breaths are collected in a large bag. The PCO_2 of the collected gas represents the mixed exhaled gas. Simultaneously, a blood gas is obtained to determine the $PaCO_2$, and physiologic deadspace is calculated. Alternatively, the physiologic deadspace can be determined from volumetric capnography (Figure 21.5). Pulmonary embolism effects an increase in the physiologic deadspace by increasing alveolar deadspace – a component of the physiologic deadspace. Burki evaluated the utility of physiologic deadspace to diagnose PE [16]. In his study, a threshold of 40% was used to indicate PE. At this cut-off alone, they reported a sensitivity of 100%, though specificity was only 55%. The specificity improved somewhat when spirometry was used. In contrast, Eriksson *et al.* found considerable overlap in the values of physiologic deadspace between patients with and without PE [17]. This was particularly notable in patients with underlying pulmonary disease [17,18]. Further, Anderson *et al.,* in a small group of surgical patients, determined the physiologic deadspace to have a sensitivity of only 60% using a cut-off value of 0.40 [19]. This finding was confirmed in a larger surgical group (J. T. Anderson, unpublished data) (Table 21.1). More recently, Hogg *et al.* evaluated a series of patients who presented to an emergency department with pleuritic chest pain [20]. Over a period of 15 months, 799 patients were assessed, 425 enrolled, and 20 diagnosed with PE. Modifications of the Bohr equation were assessed using end-tidal CO_2, $PaCO_2$, and capillary (fingerstick) PCO_2; optimal deadspace cut-off values were determined as 0.37, 0.32, and 0.32 respectively. The lower value resulted in improved sensitivity (100, 95.3, and 94.4, respectively), though specificity was poor (22.7, 20, and 24, respectively).

Time capnography/end-tidal PCO_2

Time capnography is essentially ubiquitous. It holds immense appeal by virtue of its availability. In the presence of pulmonary emboli, PCO_2 in the affected alveoli decreases. This alveolar gas mixes with the exhaled gas of perfused alveoli and results in a decreased end-tidal PCO_2. Even small clots appear capable of changing the end-tidal CO_2. Carroll simulated a 1-mL embolism by inflating a pulmonary artery catheter balloon [21]. A change in end-tidal PCO_2 was readily apparent in 20 of 24 patients. Several investigators have utilized this technique to non-invasively detect PE either by measurement of the arterial to alveolar CO_2 gradient, or by calculation of the gradient as a fraction of the $PaCO_2$.

Robins *et al.* reported that the difference between CO_2 tension in arterial blood, and that within the end-tidal exhaled breath, was augmented in patients with

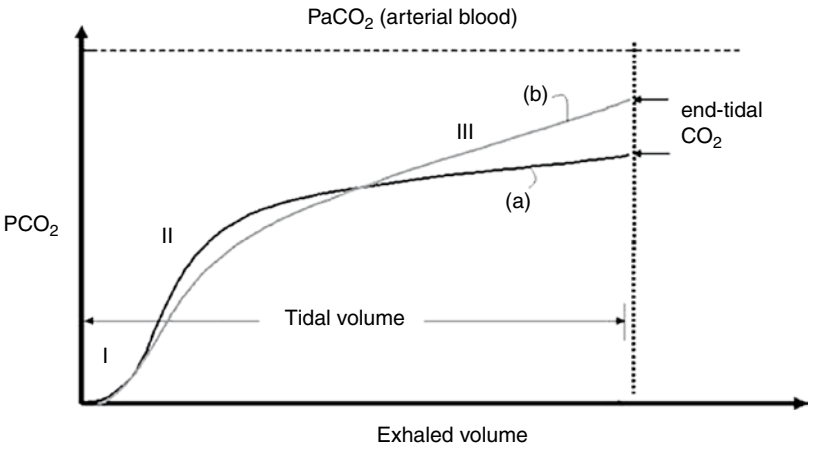

Figure 21.6 Volumetric capnograms with (a) near-horizontal phase III slope but significant arterial to end-tidal gradient (pulmonary embolism) and (b) increased phase III slope (e.g., COPD).

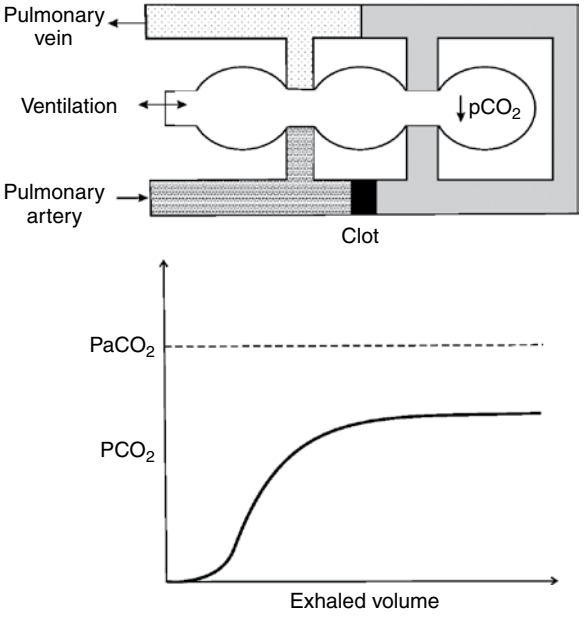

Figure 21.7 Effect of clot (i.e., pulmonary embolus) on ventilated but not perfused peripheral alveoli and resulting capnogram. Upper diagram represents increasing orders of alveolar branching progressing centrally on the left towards the periphery on the right.

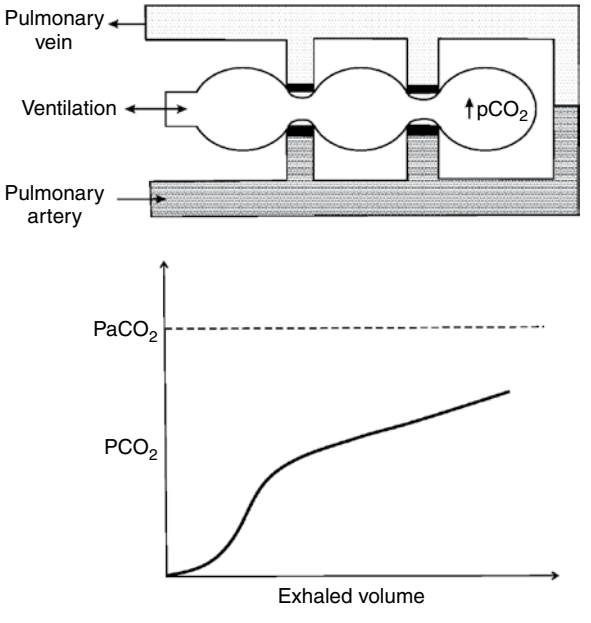

Figure 21.8 Effect of increased ventilation/perfusion mismatching (i.e., COPD) and the resulting capnogram. Upper diagram represents increasing orders of alveolar branching progressing centrally on the left towards the periphery on the right.

PE [22]. He demonstrated an increased gradient in seven of ten patients with clinically suspected PE. The normal arterial to end-tidal CO_2 gradient was considered to be less than 5 mm Hg. Despite the simplicity of measurement of the arterial to end-tidal CO_2 gradient, multiple researchers have questioned its utility in actual practice. Colp and Williams demonstrated an increased arterial to alveolar CO_2 gradient in only three of seven patients with clinically suspected PE [23]. Hatle and Rokseth assessed the utility of the arterial to alveolar CO_2 gradient in several groups of patients with differing diagnoses [24]. Nineteen healthy subjects had a gradient less than 5 mm Hg. All but one of their patients with large pulmonary emboli had gradients exceeding 5 mm Hg. However, 10 of 17 patients with small pulmonary emboli had a normal gradient. The gradient was higher in several patients with various diagnoses, including chronic bronchitis, emphysema, myocardial infarction, primary pulmonary hypertension, and shock. Eriksson *et al.* also demonstrated significant overlap of the gradient in patients with angiographically diagnosed pulmonary

Table 21.1 Comparison of diagnostic modalities to diagnose pulmonary embolism

Test	FDlate (overall)	FDlate (spont)	FDlate (vent)	$V_{D_{phys}}$	$V_{D_{alv}}$	a–$ET CO_2$	$ET CO_2$ VD
Cut-off value	0.06	0.06	0.06	0.40	0.20	5	5
Sensitivity	100	100	100	60	80	70	90
Specificity	87.2	96.6	60	79.5	61.5	71.8	38.5
PPV	66.7	88.9	33.31	42.9	34.8	38.9	27.3
NPV	100	100	100	88.6	92.3	90.3	93.8
LR	7.8	29	2.5	2.92	2.1	2.48	1.46

Sensitivity, specificity, positive predictive value (PPV), negative predictive value (NPV), and likelihood ratio (LR) for cut-off values from literature for FDlate (late deadspace fraction) [18]; $V_{D_{phys}}$ (physiologic deadspace) [16]; $V_{D_{alv}}$ (alveolar deadspace) [32]; arterial end-tidal CO_2 gradient [22]; $ET CO_2$ deadspace (VD) [19,26,30].

emboli and patients with an obstructive lung disease, interstitial lung disease, and even patients with clinically suspected pulmonary emboli who had a negative pulmonary angiogram [18]. More recently, Anderson *et al.,* in a group of postoperative surgical patients, found that measurement of the arterial to alveolar CO_2 gradient had a sensitivity of 70% and specificity of 71.8% using a cut-off value of 0.2 [19]. Sensitivity was improved to 90% when a cut-off value of 0.05 was used, though at the expense of specificity, which was decreased to 38.5%.

Nunn *et al.* described a parameter they termed, *alveolar deadspace fraction* [25], expressed mathematically as:

$$\frac{PaCO_2 - ET CO_2}{PaCO_2}.$$

They believed it to reflect the alveolar deadspace. Fletcher *et al.* pointed out that their assumption was incorrect in concept, and could result in significant errors in the estimation of true alveolar deadspace [15]. Inspection of the volumetric capnogram demonstrates that with a sloping phase III, the end-tidal CO_2 changes significantly, depending on the tidal volume. In the presence of a steeply sloping phase III, as may occur with COPD, true alveolar deadspace (represented by area *Y* divided by the total area encompassed by areas *X*, *Y*, and *Z*: Figure 21.5) would be underestimated by alveolar deadspace fraction. Nonetheless, the alveolar deadspace fraction is readily obtained (generally increased in the presence of increased alveolar deadspace) and can be used as a surrogate to measure changes in alveolar deadspace, although with these limitations.

Multiple investigators have utilized the alveolar deadspace fraction to non-invasively screen for the presence of PE. Kline *et al.* analyzed the efficacy of this fraction in 170 ambulatory emergency room patients with suspected PE [26]. Fifteen percent of patients were diagnosed with PE. Using a cut-off value of 0.2, the overall sensitivity of the test for the detection of PE was 88.5% and specificity was 66%. Further, they determined the test to have a negative predictive value of 96.9%, and a combination of the alveolar deadspace fraction and D-dimer measurement to have a sensitivity of 100%. Johanning *et al.,* in a group of intensive care unit (ICU) patients, found all patients with PE to have an alveolar deadspace fraction that exceeded 0.2 [27]. However, 8 of 14 patients without PE also had an alveolar deadspace fraction exceeding 0.2, though several of these patients were mechanically ventilated. More recently, Rodger *et al.* used the lower cut-off value of 0.15 to evaluate inpatients and outpatients at Ottawa Hospital suspected of having PE [28]. They specifically excluded patients on mechanical ventilation. Using this lower cut-off value, they reported a sensitivity of 79.5%, a specificity of 70.3%, and a negative predictive value of 90.7%. Anderson *et al.,* in a group of surgical patients, including those mechanically ventilated, reported a sensitivity of 60%, a specificity of 76.9%, and a negative predictive value of 88.2% when using a cut-off of 0.2 [19]. Sanchez *et al.* evaluated 270 consecutive inpatients and outpatients with suspected PE who had a positive D-dimer test [29]. With a cut-off of 0.15, they reported a sensitivity of 68.5% and a specificity of 81.5%.

The accuracy of both the arterial to end-tidal CO_2 gradient and alveolar deadspace fraction can be improved with various forced maximal expiration techniques. Inspection of the volumetric capnogram

demonstrates that in the presence of a steep phase III slope (as occurs with COPD or interstitial lung disease) (Figure 21.6b), the end-tidal CO_2 level will vary widely, depending on the depth of exhalation. Following a maximal exhalation, the arterial to end-tidal CO_2 gradient and alveolar deadspace fraction will be less than with normal exhalation. Conversely, in the presence of PE, the slope of phase III is more horizontal (Figure 21.6a), which indicates that the gradient and alveolar deadspace fraction is not significantly altered.

In the presence of lung disease, such as COPD, and maximal exhalation, the decrease in the arterial to end-tidal CO_2 gradient and alveolar deadspace fraction is a product of several mechanisms. Maximal exhalation results in more complete emptying of the lungs, including peripheral alveoli that have a higher PCO_2 level. Further, maximal exhalation is generally preceded with a maximal inhalation, often with a brief inspiratory hold, and produces more even distribution of gases within the alveoli and decreased alveolar deadspace. Emphysema and chronic bronchitis increase alveolar deadspace as a result of incomplete mixing within respiratory units, or regional ventilatory inequalities due to differences in mechanical properties in separate regions of the lung. Both of these mechanisms are ameliorated with prolonged inspiration and an end-inspiratory pause. In contrast, PE is associated with a horizontal phase III. The end-tidal CO_2 level does not vary as much with alterations in exhaled volume. Pulmonary embolism increases alveolar deadspace due to regional variations in perfusion to respiratory units, without significant change in mechanical properties. This mechanism of increased alveolar deadspace is not significantly altered with the respiratory maneuvers described.

Multiple investigators have reported on the utility of forced exhalation to improve the accuracy of measurements based on capnography [26,27,30]. Chopin *et al.* evaluated the ability of a forced exhalation to differentiate patients with an increased deadspace due to COPD from patients with an augmented deadspace due to PE [30]. They derived a value R, which corresponded to the alveolar deadspace fraction calculated at the end of a maximal exhalation. Using a cut-off value of 5%, they achieved a sensitivity and negative predictive value of 100%, a specificity of 65%, and positive predictive value of 74%.

Alveolar deadspace

Alveolar deadspace is increased by PE. Alveolar deadspace is readily measured by assessing the volumetric capnogram using Fowler's method (Figure 21.5) [31]. In a multi-institutional study involving six urban emergency rooms, Kline *et al.* investigated the efficacy of using alveolar deadspace to rapidly exclude the diagnosis of PE [32]. They evaluated a total of 380 patients, in whom 64 (16.8%) had PE. Patients were assessed with a respiratory profile monitor (CO_2SMO Plus!, Respironics-Novametrix, LLC, Wallingford, CT, USA) and their alveolar deadspace was determined. Physiologic and airway deadspace was measured directly; alveolar deadspace was calculated as the difference between physiologic and airway deadspace. Using a cut-off value of 20%, they reported a sensitivity of 67% and a specificity of 76%. When combined with measurement of D-dimer, the sensitivity was improved to 98.4%. Of note, they excluded patients who had clinical evidence of shock, or were unable to breathe room air or be cooperative during the measurement. Anderson *et al.,* in a consecutive series of surgical patients, without exclusion criteria, demonstrated an overall sensitivity of 80% and a specificity of 61.5% [19]. Alveolar deadspace was directly measured utilizing the Fowler's method (Figure 21.5) on a Ventrak Respiratory Monitoring System (Respironics-Novametrix, LLC, Wallingford, CT, USA).

Fdlate (late deadspace fraction)

Bedside screening of PE suffers from two major limitations. First, the patient's baseline respiratory deadspace is generally unknown. Second, respiratory maneuvers such as forced exhalations require patient cooperation that may be limited or inconsistent. Eriksson *et al.* described a derived parameter, Fdlate (late deadspace fraction), which attempts to compensate for these limitations [17,18]. This method takes advantage of differences in the phase III slope between patients with PE and those with other pulmonary diseases. Further, because the value is extrapolated, patient cooperation is less important than methods dependent upon forced exhalation.

Fdlate is determined from fitting the phase III slope portion of the volumetric capnogram (e.g., alveolar plateau) a logarithmic curve of the form:

$$PeCO_2 = a + b\ln(Ve)$$

where PCO_2 = partial pressure CO_2 in the exhaled breath, Ve = exhaled volume (beginning at the start of phase II) (mL), and a and b are constants.

Eriksson *et al.* found that the PCO_2 value of the extrapolated phase III curve reached arterial blood PCO_2 levels at an exhaled volume of approximately

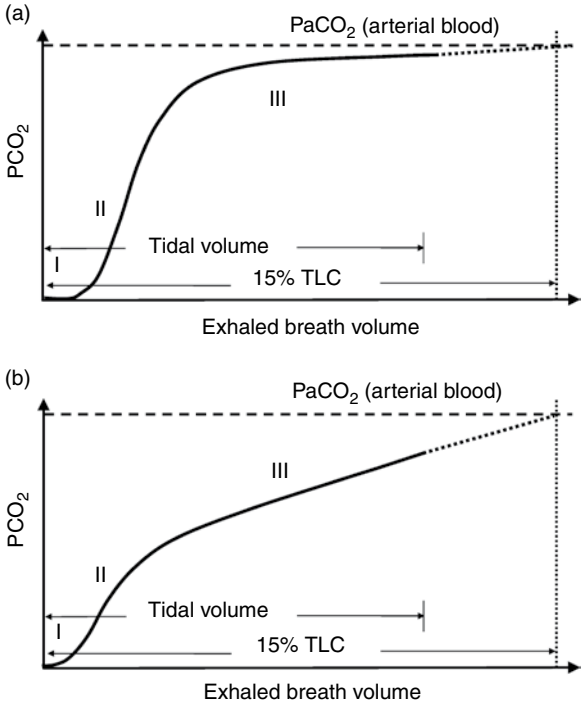

Figure 21.9 Volumetric capnogram illustrating extrapolated phase III slopes for (a) normal patients (b) patients with obstructive and interstitial pulmonary disease. Tidal volume, measured tidal volume; 15% TLC, exhaled volume at 15% total lung capacity; PCO_2, partial pressure of CO_2, $PaCO_2$: arterial partial pressure CO_2. [Adapted from: Anderson JT, Owings JT, Goodnight JE. Bedside non-invasive detection of acute pulmonary embolism in critically ill surgical patients. *Arch Surg* 1999; **134**: 869–75.]

15% total lung capacity (TLC) in normal patients and patients with obstructive and interstitial pulmonary disease [17] (Figure 21.9). However, in patients with pulmonary emboli, the PCO_2 value of the extrapolated phase III curve failed to reach arterial PCO_2 levels at 15% TLC (Figure 21.10). The authors expressed this late deadspace fraction as:

$$F_{D}late = \frac{PaCO_2 - P_{15\%TLC}CO_2}{PaCO_2}.$$

Eriksson *et al.* determined that $F_{D}late$ was effective in the detection and diagnosis of PE [17]. All 39 patients with PE had an increased $F_{D}late$ value. Additionally, the $F_{D}late$ was normal in patients with alternative pulmonary diseases and in normal patients. In a small pilot study, Anderson *et al.* also noted that $F_{D}late$ was able to identify PE in a group of surgical patients [19]. In a follow-up consecutive series of surgical patients, Anderson *et al.* again found $F_{D}late$ effective in the detection of PE in surgical patients (J. T. Anderson, unpublished data).

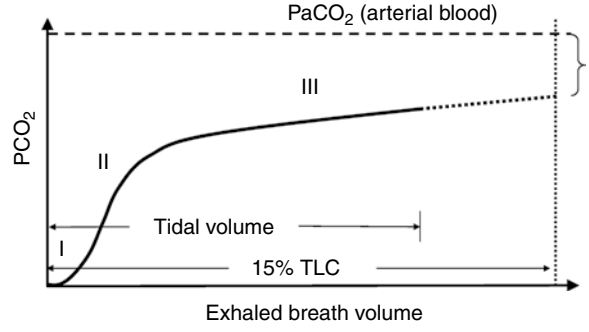

Figure 21.10 Volumetric capnogram illustrating extrapolated phase III slope for patient with pulmonary embolus. Gradient between arterial CO_2 value and extrapolated CO_2 value indicated with bracket. Tidal volume, measured tidal volume; 15% TLC, exhaled volume at 15% total lung capacity; PCO_2, partial pressure of CO_2; $PaCO_2$, arterial partial pressure CO_2. [Modified from: Anderson JT, Owings JT, Goodnight JE. Bedside non-invasive detection of acute pulmonary embolism in critically ill surgical patients. *Arch Surg* 1999; **134**: 869–75.]

When compared to alternative methods based upon deadspace, $F_{D}late$ proved to be superior (Tables 21.1 and 21.2). Overall, when using pulmonary angiography as a gold standard, $F_{D}late$ was found to have a sensitivity of 100%, specificity of 87.2%, negative predictive value of 100%, and positive predictive value of 66.7%. In spontaneously breathing patients (which made up the majority of patients), sensitivity again was 100%, specificity was 96.6%, negative predictive value was 100%, and positive predictive value was 88.9%. $F_{D}late$ performed less well in ventilated patients with a sensitivity of 100%, specificity of 60%, negative predictive value of 100%, and positive predictive value of 33.3%. Remarkably, in this group of patients, a screening algorithm using $F_{D}late$ and D-dimer would have eliminated the need for pulmonary angiography in 70% of patients with clinically suspected PE. Verschuren *et al.* compared the diagnostic performance of parameters obtained from volumetric capnography with the arterial to alveolar CO_2 gradient (obtained from time capnography) in a group of 45 outpatients who presented to an emergency room with suspected PE and findings of a positive D-dimer [33]. Utilizing receiver operating curves (ROC), they determined that $F_{D}late$ outperformed the arterial to alveolar CO_2 gradient as well as various other derived parameters [34].

Limitations of capnographic detection of pulmonary embolism

Bedside tests based on capnography have immense appeal in the evaluation of possible PE. The necessary

Table 21.2 ROC curves: area under curve for various studies

FDlate (late deadspace fraction)	
(All patients)	0.96 ± 0.05
Spontaneous breathing patients	0.99 ± 0.03
Mechanically ventilated patients	0.85 ± 0.18
Physiologic deadspace	0.73 ± 0.10
Alveolar deadspace	0.84 ± 0.08
Arterial–end-tidal CO_2 gradient	0.86 ± 0.08
End-tidal CO_2 deadspace	0.83 ± 0.08

ROC, receiver operating characteristic for various diagnostic modalities to diagnose pulmonary embolism.

equipment is readily available and portable; it is unnecessary to transport the patient, as screening can be done at the patient's bedside. Moreover, ongoing measurements can be readily repeated, and patients can be continuously monitored. Two major hurdles exist, however. The baseline deadspace is generally unknown, and a variety of alternative pathologic states other than PE can increase alveolar deadspace. More liberal use of time and volumetric capnography would allow measurement of baseline deadspace as well as detection of changes in respiratory deadspace in real time. The utility of ongoing capnographic monitoring was evaluated by Johanning *et al.* in a group of ICU patients with suspected PE [27]. In this small cohort, all patients who had an increase in deadspace compared to baseline were later shown to have PE. Patients who did not have PE had a decrease in deadspace.

Increased deadspace due to common pulmonary diseases, such as COPD and interstitial lung disease, can be differentiated from PE by the methods described that exploit differences in the slope of phase III with or without respiratory maneuvers. In contrast, alternative pathologic states, such as pulmonary hypotension or large right-to-left shunt, produce phase III slopes similar to PE. Analogous to PE, pulmonary arterial hypotension may leave some alveoli under- or non-perfused, thereby leading to an increased alveolar deadspace. A variety of clinical situations may lead to pulmonary arterial hypotension, including hemorrhage, sepsis, or cardiogenic shock. Mechanical ventilation with positive pressure exacerbates the effect of pulmonary arterial hypotension on alveolar deadspace. These factors largely explain the decreased accuracy noted in mechanically ventilated ICU patients. Fortunately, in clinical practice, most patients with PE are neither in shock nor mechanically ventilated. In a consecutive series of patients with suspected PE (J.T. Anderson, unpublished data), the majority of the patients were hemodynamically stable and spontaneously breathing. Future refinements and research will likely deal with these limitations. In the series reported by Hatle and Rokseth, one patient with shock, resulting in an elevated arterial to alveolar CO_2 gradient, had a decrease in the arterial to alveolar CO_2 gradient from 24 to 18 mm Hg with maximal exhalation. They noted minimal decrease in the arterial to alveolar CO_2 gradient, a mean of 10.5 to 9 mm Hg, in 11 patients with embolism [24]. Courtney *et al.* demonstrated in an animal model that shock due to PE resulted in a greater deadspace increase than hemorrhagic shock of an equivalent extent [35].

Resolution of pulmonary embolism/ thrombolytic therapy

Occasionally, thrombolytic therapy is utilized to dissolve large pulmonary emboli, particularly in the presence of compromised right ventricular function. As the pulmonary emboli are broken up and previously non-perfused alveoli are perfused, alveolar deadspace decreases. This is reflected by changes in the capnographically derived parameters mentioned earlier. Numerous investigators have demonstrated the ability to track changes in the pulmonary embolic burden with the use of capnography. Wiegand *et al.,* in a group of 12 patients with massive PE requiring mechanical ventilation, analyzed the end-tidal CO_2 before and after thrombolytic therapy [36]. The 10 surviving patients were noted to have a decrease in their arterial to end-tidal CO_2 gradient to a mean of 9.8 to 2.8 mm Hg. Recurrent embolism was detected in two patients, manifested as a sudden reduction in end-tidal CO_2. The ability of volumetric capnography to track the resolution of pulmonary emboli with thrombolytic therapy has also been investigated. Anderson (unpublished data) assessed the utility of alveolar deadspace to track both the resolution and recurrence of pulmonary emboli in a patient who presented with massive PE (Figure 21.11). Verschuren reported two cases of patients who had FDlate measured before and after thrombolytic therapy [34]; FDlate decreased from 0.64 to 0.01 and 0.26 to 0.06, respectively. Of note, echocardiography demonstrated resolution of the right heart dysfunction.

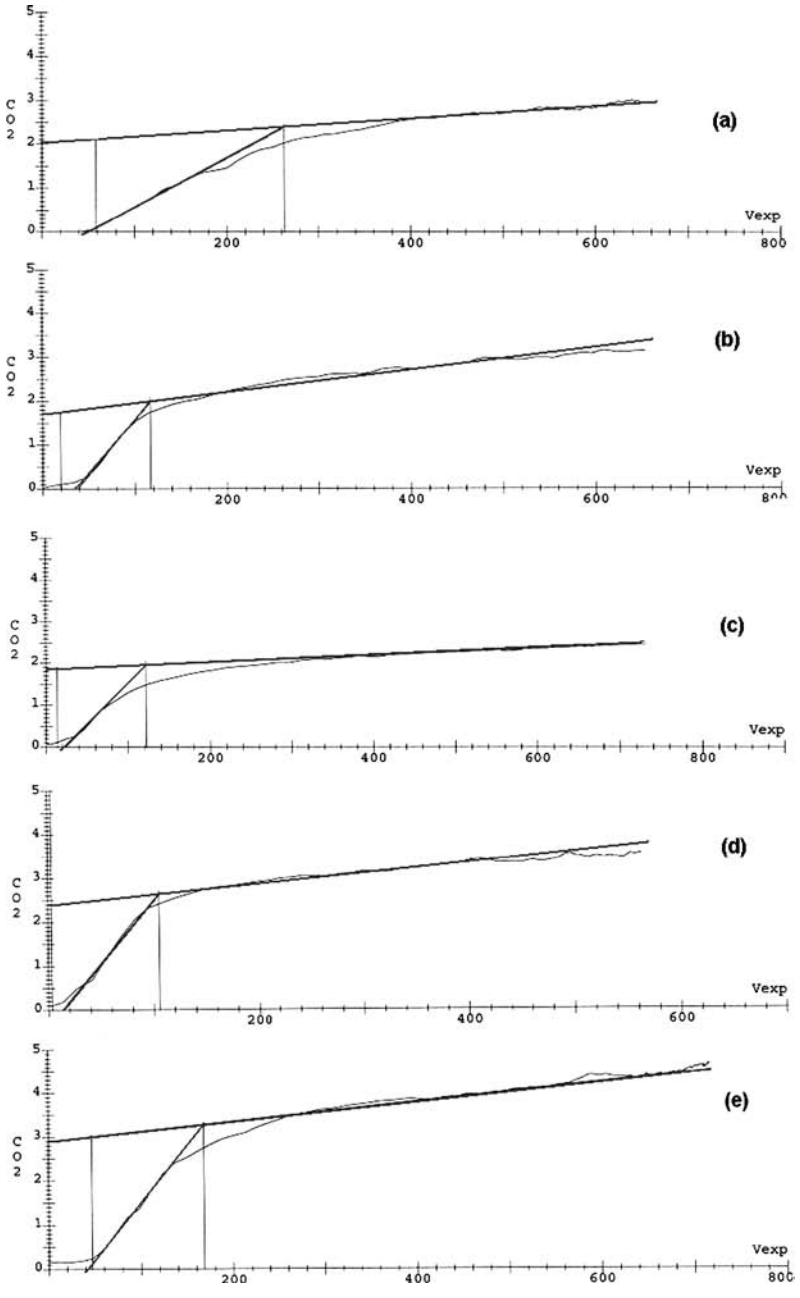

Figure 21.11 (a) A patient who presented in shock as a result of massive pulmonary emboli had a physiologic deadspace of 70% and alveolar deadspace of 60%. (b) After treatment with urokinase and heparin for a period of 12 h, the patient's physiologic and alveolar deadspaces decreased to 54% and 47%, respectively. (c) Shortly thereafter, the patient had a recurrent pulmonary embolism confirmed by pulmonary angiography. Likewise, the physiologic deadspace had increased to 61% and the alveolar deadspace had increased to 55%. (d) After 24 h of treatment with urokinase administered at a higher dose, the physiologic and alveolar deadspaces had decreased to 47% and 40%, respectively. (e) After 48 h of treatment, the physiologic and alveolar deadspaces decreased further to 41% and 30%, respectively. Note the best fit lines for phase II and phase III are overlaid on the curves and vertical lines mark the transition between phases I and II and II and III.

Detection of air or CO_2 embolism

Gas embolism, generally air or CO_2, can arise from a variety of clinical conditions, though two basic mechanisms are primarily responsible. Air may be entrained into the venous system when the venous pressure falls below atmospheric pressure, such as may occur for example during neurosurgical procedures in the upright position or disconnection of a central venous catheter in a spontaneously breathing patient. Alternatively, during laparoscopic procedures, CO_2 under pressure may gain access to the venous system. In either case, massive air or CO_2 embolism can result in obstruction of the pulmonary vascular tree, and impairment of right ventricular and pulmonary function. Compared with a blood clot, gas embolism can cross the capillary system and embolize into the systemic arterial system.

The incidence of gas embolism reported in the literature is variable. Using precordial Doppler measurements (sensitive to as little as 0.05 mL/kg), air embolism has been noted in as many as 58% of patients undergoing craniotomy in the upright position and 25% of patients undergoing craniotomy in the supine or prone position. In other procedures at risk for air embolism, the incidence ranged from 7% for cervical spine surgery to 65% in patients undergoing cesarean section [3]. The incidence of CO_2 embolism is likewise variable. Clinically significant CO_2 embolism is uncommon. One report of 113 253 gynecologic laparoscopies reported only 15 embolisms produced by CO_2 insufflation [37]. More recent studies that utilized echocardiography, which is more sensitive than $PETCO_2$, demonstrated subclinical CO_2 embolism in 11 of 16 patients undergoing laparoscopic cholecystectomy [38].

The tolerated dose of gas depends upon its solubility. A portion of the gas will be excreted in the exhaled breath. Carbon dioxide is much more soluble than air (predominately nitrogen gas), and the level required for clinical manifestation is higher with CO_2 embolism. Rapid embolism of air of approximately 1 mL/kg will produce early symptoms of a gasp and hypotension. Larger volumes of 4 to 7 mL/kg result in death [3,11,39,40]. Generally, the limiting factor for survival is the ability of the right ventricle to pump against the added load. In contrast, Mann *et al.* found in pigs that embolization of approximately 4 mL of CO_2 /kg was required to cause hypotension [41]. The rate of CO_2 insufflation required to maintain a state of pneumoperitoneum is often 1 to 8 mL per second, suggesting a significant potential for the development of a massive CO_2 embolism [11].

Various methods are employed to assess patients for the presence of gas embolism during surgery. Precordial Doppler ultrasound is frequently chosen due to its availability and high sensitivity [3,11]. In the presence of air embolism, a sound resembling a "washing machine" is readily appreciated. The disadvantages of Doppler ultrasound include difficulty with positioning secondary to body habitus, or due to patient positioning at the time of surgery. Transesophageal echocardiography (TEE) is also associated with high sensitivity; however, it is less available and much more invasive [3,11]. Though less sensitive to the presence of small amounts of air or CO_2 embolism, monitoring with capnography has the advantage of being readily available, reliable, and reproducible [3,11]. Capnographic evaluation is more sensitive than monitoring via oxygen saturation or direct visual observation of the patient.

Both air and CO_2 embolism result in increased alveolar deadspace as a consequence of an "airlock" in the vessels in which the gas bubbles lodge. Additionally, the partial pressure of individual gases will differ from that normally present in the blood. In the case of air embolism, an initial increase in end-tidal nitrogen may be identified due to the increased supply of nitrogen to the alveolus and subsequently into the expired breath [3,11]. Generally, CO_2 embolism is manifested acutely with a sudden increase in end-tidal CO_2 [39]. Oppenheimer *et al.* demonstrated a biphasic change in end-tidal CO_2 in dogs undergoing CO_2 embolization [42]. Initially, an increase was noted in the end-tidal CO_2, a consequence of increased excretion of CO_2. As additional bubbles accumulated in the pulmonary artery, alveolar deadspace was increased, resulting in a decreased end-tidal CO_2 level. In both air embolism and CO_2 embolism, there is a "washout curve" during which the end-tidal CO_2 returns to normal as the gases are excreted or dissipated.

Summary

Embolism, in particular the diagnosis of PE, continues to plague the clinician. Early detection and prompt initiation of therapy has been shown to decrease morbidity and mortality. Evaluation of patients with various parameters derived from capnography holds promise for early bedside non-invasive detection of embolism, thereby allowing prompt and effective therapy.

References

1. Olin JW. Pulmonary embolism. *Rev Cardiovasc Med* 2002; **3:** S68–75.
2. Wood KE. Major pulmonary embolism: review of a pathophysiologic approach to the golden hour of hemodynamically significant pulmonary embolism. *Chest* 2002; **121:** 877–905.
3. Souders JE. Pulmonary air embolism. *J Clin Monit Comput* 2000; **16:** 375–83.
4. Fabbri G, Perin S, Coli A, Lari S. Pulmonary embolism associated with use of bone cement during hip arthroplasty. *Chir Organ Mov* 1996; **81:** 347–9.
5. Goldhaber SZ, Hennekens CH, Evans DA, Newton EC, Godleski JJ. Factors associated with correct antemortem diagnosis of major pulmonary embolism. *Am J Med* 1982; **73:** 822–6.
6. Karwinski B, Svendsen E. Comparison of clinical and postmortem diagnosis of pulmonary embolism. *J Clin Pathol* 1989; **42**: 135–9.

7. Bell WR, Simon TL, DeMets DL. The clinical features of submassive and massive pulmonary emboli. *Am J Med* 1977; **62**: 355–60.
8. Stein PD, Goldhaber SZ, Henry JW. Alveolar–arterial oxygen gradient in the assessment of acute pulmonary embolism *Chest* 1995; **107:** 139–43.
9. Stein PD, Henry JW. Prevalence of acute pulmonary embolism among patients in a general hospital and at autopsy. *Chest* 1995; **108:** 978–81.
10. Stein PD, Goldhaber SZ, Henry JW, Miller AC. Arterial blood gas analysis in the assessment of suspected acute pulmonary embolism. *Chest* 1996; **109:** 78–81.
11. Capan LM, Miller SM. Monitoring for suspected pulmonary embolism. *Anesthesiol Clin N Am* 2001; **19**: 673–703.
12. Bohr C. Über die Lungenathmung. *Skand Archiv Physiol* 1891; **2**: 236.
13. Enghoff H. Volumen inefficax: Bemerkungen zur Frage des schädlichen Raumes. *Upsala Lakareforen Forhandl.* 1938; **44**: 191–218.
14. Riley RL, Lilienthal JLJ, Proemmel DD, Frank RE. On the determination of the physiologically effective pressures of oxygen and carbon dioxide in alveolar air. *Am J Physiol* 1946; **147**: 191.
15. Fletcher R, Jonson B, Cumming G, Brew J. The concept of deadspace with special reference to the single breath test for carbon dioxide. *Br J Anaesth* 1981; **53:** 77–88.
16. Burki NK. The deadspace to tidal volume ratio in the diagnosis of pulmonary embolism. *Am Rev Respir Dis* 1986; **133:** 679–85.
17. Eriksson L, Wollmer P, Jonson B, *et al.* SBT-CO2: a new method for the diagnosis of pulmonary embolism? *Clin Physiol* 1985; **5:** 111–15.
18. Eriksson L, Wollmer P, Olsson CG, *et al.* Diagnosis of pulmonary embolism based upon alveolar deadspace analysis. *Chest* 1989; **96**: 357–62.
19. Anderson JT, Owings JT, Goodnight JE. Bedside non-invasive detection of acute pulmonary embolism in critically ill surgical patients. *Arch Surg* 1999; **134**: 869–74; discussion 874–5.
20. Hogg K, Dawson D, Tabor T, Tabor B, Mackway-Jones K. Respiratory deadspace measurement in the investigation of pulmonary embolism in outpatients with pleuritic chest pain. *Chest* 2005; **128**: 2195–202.
21. Carroll GC. Capnographic trend curve monitoring can detect 1-ml pulmonary emboli in humans. *J Clin Monit* 1992; **8:** 101–6.
22. Robins ED, Julian DG, Travis DM, Grump CH. A physiologic approach to the diagnosis of acute pulmonary embolism. *N Engl J Med* 1959; **260**: 586–91.
23. Colp CR, Williams MH Jr. Pulmonary function following pulmonary embolization. *Am Rev Respir Dis* 1962; **85:** 799–807.
24. Hatle L, Rokseth R. The arterial to end-expiratory carbon dioxide tension gradient in acute pulmonary embolism and other cardiopulmonary diseases. *Chest* 1974; **66:** 352–7.
25. Nunn JF, Hill HW. Respiratory deadspace and arterial to end-tidal CO2 tension difference in anesthetized man. *J Appl Physiol* 1960; **15:** 383–9.
26. Kline JA, Meek S, Boudrow D, Warner D, Colucciello S. Use of the alveolar deadspace fraction (VD/VT) and plasma D-dimers to exclude acute pulmonary embolism in ambulatory patients. *Acad Emerg Med* 1997; **4:** 856–63.
27. Johanning JM, Veverka TJ, Bays RA, Tong GK, Schmiege SK. Evaluation of suspected pulmonary embolism utilizing end-tidal CO_2 and D-dimer. *Am J Surg* 1999; **178**: 98–102.
28. Rodger MA, Jones G, Rasuli P, *et al.* Steady-state end-tidal alveolar deadspace fraction and D-dimer: bedside tests to exclude pulmonary embolism. *Chest* 2001; **120:** 115–19.
29. Sanchez O, Wermert D, Faisy C, *et al.* Clinical probability and alveolar deadspace measurement for suspected pulmonary embolism in patients with an abnormal D-dimer test result. *J Thromb Haemost* 2006; **4**: 1517–22.
30. Chopin C, Fesard P, Mangalaboyi J, *et al.* Use of capnography in diagnosis of pulmonary embolism during acute respiratory failure of chronic obstructive pulmonary disease. *Crit Care Med* 1990; **18:** 353–57; erratum *Crit Care Med* 1991; **19**: 450–1.
31. Fowler W. Lung function studies. II. The respiratory deadspace. *Am J Physiology* 1948; **154**: 405.
32. Kline JA, Israel EG, Michelson EA, *et al.* Diagnostic accuracy of a bedside D-dimer assay and alveolar deadspace measurement for rapid exclusion of pulmonary embolism: a multicenter study. *JAMA* 2001; **285:** 761–8.
33. Verschuren F, Heinonen E, Clause D, *et al.* Volumetric capnography as a bedside monitoring of thrombolysis in major pulmonary embolism. *Intens Care Med* 2004; **30**: 2129–32.
34. Verschuren F, Liistro G, Coffeng R, *et al.* Volumetric capnography as a screening test for pulmonary embolism in the emergency department. *Chest* 2004; **125:** 841–50.
35. Courtney DM, Watts JA, Kline JA. End tidal CO_2 is reduced during hypotension and cardiac arrest in a rat model of massive pulmonary embolism. *Resuscitation* 2002; **53:** 83–91.

36. Wiegand UK, Kurowski V, Giannitsis E, Katus HA, Djonlagic H. Effectiveness of end-tidal carbon dioxide tension for monitoring thrombolytic therapy in acute pulmonary embolism. *Crit Care Med* 2000; **28**: 3588–92.
37. Phillips J, Keith D, Hulka J, Hulka B, Keith L. Gynecologic laparoscopy in 1975. *J Reprod Med* 1976; **16**: 105–17.
38. Derouin M, Couture P, Boudreault D, Girard D, Gravel D. Detection of gas embolism by transesophageal echocardiography during laparoscopic cholecystectomy. *Anesth Analg* 1996; **82**: 119–24.
39. Shulman D, Aronson HB. Capnography in the early diagnosis of carbon dioxide embolism during laparoscopy. *Can Anaesth Soc J* 1984; **31:** 455–9.
40. Symons NL, Leaver HK. Air embolism during craniotomy in the seated position: a comparison of methods for detection. *Can Anaesth Soc J* 1985; **32**: 174–7.
41. Mann C, Boccara G, Fabre JM, Grevy V, Colson P. The detection of carbon dioxide embolism during laparoscopy in pigs: a comparison of transesophageal Doppler and end-tidal carbon dioxide monitoring. *Acta Anaesthesiol Scand* 1997; **41**: 281–6.
42. Oppenheimer MJ, Durant TM, Stauffer HM, *et al.* In vivo visualization of intracardiac structures with gaseous carbon dioxide [abstract]. *Am J Physiol* 1956; **186**: 325–34.

Section 2
Chapter
22

Circulation, metabolism, and organ effects

Non-invasive cardiac output via pulmonary blood flow

R. Dueck

Introduction

The need for a non-invasive measurement of cardiac performance has been appreciated for more than a hundred years [1,2]. Routine history and physical examination can usually distinguish a normal from a failing heart. However, differentiation of mild versus moderately impaired cardiac function, or compensated versus compromised diastolic left ventricular dysfunction, requires considerable expertise. Historically, cardiac function measurements were not well suited to trauma, anesthesia and surgery, respiratory failure, or sepsis conditions. The 1970 introduction of the pulmonary artery (PA) catheter for central venous pressure (CVP), PA, and PA wedge pressure (PAWP), followed by the addition of thermal dilution cardiac output (Q_{TD}), were heralded as welcome solutions [3,4]. While these cardiovascular parameters provided valuable clinical information, rising concern over PA catheter risks provided impetus for non-invasive cardiac output (Q_T) monitoring via the Fick principle from pulmonary blood flow [5]. Intermittent or continuous Q_T can be used to help determine the cause of hypotension, e.g., from hypovolemia (low Q_T and high systemic vascular resistance [SVR]), versus sepsis (high Q_T and low SVR), or from a failing right or left ventricle, or both (low Q_T and high CVP/PAWP). Clinical research and experience confirm that non-invasive Fick Q_T can often provide the most critical element for this differential diagnosis.

This chapter reviews the background and theory of complete and partial CO_2 rebreathing Fick Q_T measurement, the literature on clinical testing, and presents examples that demonstrate its utility during acute hemodynamic challenges.

Background and theory

The classic Fick principle was designed to measure pulmonary capillary blood flow (Q_C), which comprises 98% of Q_T in subjects with little or no intrapulmonary or cardiac shunting [2]. The Fick method may employ either O_2 or CO_2 as physiologic tracers, as shown in equations (22.1) and (22.2) below. Both O_2 consumption ($\dot{V}O_2$) and CO_2 elimination ($\dot{V}CO_2$) rate can be measured non-invasively. When O_2 is the physiologic tracer, arterial and mixed venous blood samples are obtained via indwelling arterial and PA catheters. Arterial and mixed venous O_2 content (CaO_2, $C\bar{v}O_2$) are then used to derive Q_C as:

$$Q_C = \frac{\dot{V}CO_2}{CaCO_2 - C\bar{v}CO_2}. \qquad (22.1)$$

When CO_2 is the tracer, the Fick equation becomes:

$$Q_C = \frac{\dot{V}O_2}{C\bar{v}CO_2 - CaCO_2}. \qquad (22.2)$$

A major advantage with CO_2 as the physiologic tracer is that in subjects with normal lungs, both arterial and mixed venous CO_2 content can be determined with non-invasive methods, as described below.

Complete rebreathing CO_2: Fick Q_C method

New technology for less invasive Q_C monitoring was first applied to "complete rebreathing" for a mixed venous PCO_2 estimate, along with inspired, mixed expired, and arterial PCO_2 (via end-tidal CO_2 ([$P_{ET}CO_2$]). For deriving Q_C using equation (22.2), $\dot{V}CO_2$ was determined from:

$$\dot{V}CO_2 = \dot{V}_E \bullet F\bar{E}CO_2, \qquad (22.3)$$

where $\dot{V}_E$ = expired minute volume, and $F\bar{E}CO_2$ = mixed expired CO_2 fraction. Measuring $F\bar{E}CO_2$ required a one-way valve to separate inspired from expired air, and an expired-air collection bag. The value of $C\bar{v}CO_2$ was derived from a large breath $P_{ET}CO_2$ during complete

Capnography, Second Edition, ed. J. S. Gravenstein, Michael B. Jaffe, Nikolaus Gravenstein, and David A. Paulus. Published by Cambridge University Press. © Cambridge University Press 2011.

rebreathing, while arterial CO_2 content required a large non-rebreathing breath $P_{ET}CO_2$, determined with equation (22.4):

$$C_cCO_2 = \left(\left[6.957 \bullet Hg\right] + 94.864\right) \bullet \log\left(1.0 + 0.1933 \bullet P_{ET}CO_2\right) \quad (22.4)$$

where C_cCO_2 = pulmonary capillary CO_2 content (thus C_aCO_2 was determined via equation (22.4) during normal breathing $P_{ET}CO_2$, and $C\bar{v}O_2$ during complete rebreathing $P_{ET}CO_2$, respectively); Hg = hemoglobin concentration (mg/dL); $P_{ET}CO_2$ is assumed equal to alveolar PCO_2.

It was discovered in the 1920s that equilibration of alveolar with mixed venous blood during complete rebreathing is not achieved before mixed venous PCO_2 ($P\bar{v}CO_2$) rises from recirculation of the elevated alveolar PCO_2 [6]. Consequently, Collier developed a rapid infrared analyzer end-tidal gas *equilibrium method* to estimate $P\bar{v}CO_2$ from a brief (<18 s) period of rebreathing into a 1-liter bag charged with CO_2 at 7 mm Hg higher than end-tidal PCO_2 [7]. This provided a $P\bar{v}CO_2$ estimate that was an average of 0.1 mm Hg higher than $P\bar{v}O_2$, as measured by the Van Slyke apparatus. Collier reluctantly concluded that the 3.1 mm Hg standard deviation (SD) was too high for estimating Qc, since the average arterial–venous PCO_2 difference was only 6 mm Hg. Meanwhile, Defares developed an *exponential method* by measuring PCO_2 from end-tidal expired gas samples taken after each of six 1000–2000-mL exhalations into a rebreathing bag [8]. His exponential PCO_2 regression back to time zero provided an average of -0.1 ± 0.2 mm Hg lower $P\bar{v}CO_2$ compared to Haldane analysis of the $P\bar{v}CO_2$ blood sample obtained just prior to rebreathing. Dubois and colleagues found that rebreathing also led to significant lung tissue uptake of CO_2, requiring a lung tissue correction of the $P\bar{v}CO_2$ estimate [9].

In spite of these technical issues and concerns, updated applications of the equilibrium and exponential methods persisted in the literature. Vanhees *et al.* compared the Collier equilibrium and Defares exponential approaches to estimating $P\bar{v}CO_2$ in healthy volunteers at rest and during exercise, using fully automated devices replete with computer software for deriving $P\bar{v}CO_2$, thereby minimizing observer bias [10]. The equilibrium method was employed with high rebreathing bag CO_2 (from 6% to 15%) to assure a rapid equilibration with $P\bar{v}CO_2$, and a high O_2 concentration. With their modified version of the Defares exponential method, 2% CO_2 was placed in the rebreathing bag for rest and 4% CO_2 for exercise conditions. Estimated Qc was higher at rest with the exponential versus equilibrium method (average Qc 9.8 versus 8.4 L/min, respectively, $P < 0.001$), while subjects were more likely to request an end to the exercise study during the equilibrium method. This trend was related to the high rebreathing bag CO_2 content in equilibrium method exercise conditions. However, the Qc difference between these two methods disappeared with exercise, and both methods showed excellent correlation between Qc and $\dot{V}O_2$, ranging from $r^2 = 0.79$ to $r^2 = 0.88$. Thus, the complete CO_2 rebreathing method for obtaining a non-invasive Qc estimate was best suited for studying exercise in subjects with healthy lungs.

Meanwhile, the limitations of complete CO_2 rebreathing led to a series of mathematical and analytical innovations. There was a single-breath CO_2 rebreathing method that was shown to have too high a level of variability [11]. Then came the *one-step rebreathing method* by Farhi *et al.* that avoided the need for estimating mixed venous CO_2 content [12]. In addition, it eliminated the concern for lung tissue uptake of CO_2 during rebreathing, and had the added benefit that it could be used for exercise conditions. However, there were a number of sophisticated technical elements, such as inducing the subject to provide the perfect tidal volume and breathing frequency, as well as determining the appropriate size of rebreathing bag and CO_2 charge for deriving $\dot{V}CO_2$ precisely at the time alveolar PCO_2 recovered back to time zero (prior to the induced increase in minute ventilation). This perfectly timed alveolar PCO_2 requirement clearly made it unreliable for patients with lung disease, while the compliant rebreathing bag and need for patient cooperation made it unsuitable for mechanically ventilated patients.

An innovative approach to avoiding the effect of rising $C\bar{v}CO_2$ during rebreathing was to introduce a non-physiologic tracer for estimating Qc, such as acetylene (C_2H_2) or nitrous oxide (N_2O), since early body uptake of C_2H_2 or N_2O essentially removes them from mixed venous blood during brief rebreathing periods, even during exercise [13,14]. This method also required correction for lung tissue uptake of the tracer gas, while an expensive mass spectrometer was needed for rapid, high precision, breath-to-breath C_2H_2 or N_2O measurements. In addition, tracer gas methods required healthy lungs for accurate Qc estimates.

Partial rebreathing CO_2: Fick Qc method

Gedeon *et al.* were concerned about the Qc error induced by estimates of $P\bar{v}CO_2$ in the denominator of the CO_2 rebreathing method ($C\bar{v}CO_2 - CaCO_2$: equation 22.2), since this difference is small compared to Qc [15]. Consequently, they presented theory and evidence to show that $C\bar{v}CO_2$ could remain unknown and be removed from the equation by adding a second Fick equation, either decreasing or increasing $\dot{V}CO_2$ for a short period with an increase or reduction in deadspace (VD), respectively. In contrast to complete rebreathing, the modest $PaCO_2$ alteration with a brief VD change allowed assumption of a linear CO_2 dissociation curve, and reduced the lung tissue PCO_2 effects. They demonstrated that their Qc measurement could be repeated every 15 min. This method was better suited to sedated mechanically ventilated patients who did not breathe spontaneously during a brief VD alteration. Capek and Roy found that when such a partial rebreathing period was limited to 30 s, $C\bar{v}CO_2$ did not rise significantly; hence, the partial rebreathing method could provide continuous Qc estimates at 3-min intervals [16]. In normal lungs, $PETCO_2$ could be used to estimate arterial PCO_2, making the Qc estimate entirely non-invasive. However, Capek and Roy concluded that this method was sensitive to significant changes in hemoglobin concentration (Hg), e.g., a 30% change in Hg led to a 15% Qc error, while it was less sensitive to modest VD changes and/or shunting. This approach has now been formally designated the *partial CO_2 rebreathing* Qc ($Qc_{,pr}$) method.

De Abreu *et al.* compared the $Qc_{,pr}$ method to thermal dilution cardiac output (QTD), using a PA catheter in sheep with normal versus oleic acid pulmonary edema lungs [17]. They found that the overall correlation of non-shunt pulmonary capillary blood flow between methods was good, $r^2 = 0.73$, $P < 0.0001$. However, the difference between the two methods, $QTD - Qc_{,pr}$, was significantly improved with an intrapulmonary shunt correction during pulmonary edema. In a follow-up sheep study in which hyper- and hypodynamic conditions were induced, as well as increased alveolar deadspace and shunting, associated $PaCO_2$–$PETCO_2$ changes contributed significantly to $QTD - Qc_{,pr}$ [18]. As a result, they recommended using measured $PaCO_2$ for more accurate Qc estimates, especially for high deadspace and low cardiac output conditions. At high cardiac output states, they suspected that $PaCO_2$ measurement error contributed significantly to $Qc_{,pr}$ due to the low $P\bar{v}CO_2$–$PaCO_2$ differences and early $P\bar{v}CO_2$ elevation.

A detailed description of automated continuous $Qc_{,pr}$ methodology was published by Haryadi *et al.* [19]. A differential form of the Fick equation accommodates the increased deadspace in the second equation (to solve for two unknowns, $Qc_{,pr}$ and $C\bar{v}CO_2$):

$$Qc_{,pr} = \frac{\dot{V}CO_{2,1}}{C\bar{v}_{,1}CO_2 - Ca_{,1}CO_2} - \frac{\dot{V}CO_{2,2}}{C\bar{v}_{,2}CO_{2,2} - Ca_{,1}CO_{2,2}}, \quad (22.5)$$

where sample subscripts 1 and 2 ($C\bar{v}_{,1}$, $C\bar{v}_{,2}$) indicate mixed venous values during normal and partial rebreathing, respectively, while $Ca_{,1}CO_2$ and $Ca_{,2}CO_2$ represent the corresponding arterial values, and $\dot{V}CO_{2,1}$ and $\dot{V}CO_{2,2}$ the corresponding $\dot{V}CO_2$ values. Equation (22.5) requires assumption of constant Qc and $C\bar{v}CO_2$ during both normal and partial rebreathing periods. From basic algebra: $X = A/B = C/D = (A-C)/(B-D)$, this differential equation can be rewritten as:

$$Qc_{,pr} = \frac{\dot{V}CO_{2,1} - \dot{V}CO_{2,2}}{(C\bar{v}_{,1}CO_2 - Ca_{,1}CO_2) - (C\bar{v}_{,2}CO_2 - Ca_{,2}CO_2)}, \quad (22.6)$$

The terms in the denominator of equation (22.6) can be rearranged:

$$Qc_{,pr} = \frac{\dot{V}CO_{2,1} - \dot{V}CO_{2,2}}{(C\bar{v}_{,1}CO_2 - C\bar{v}_{,2}CO_2) - (Ca_{,1}CO_2 - Ca_{,2}CO_2)}. \quad (22.7)$$

If the assumptions ($Qc_{,pr}$ and $C\bar{v}CO_2$ do not change) are met, then $C\bar{v}_{,1}CO_2 - C\bar{v}_{,2}CO_2 = 0$, and equation (22.7) collapses to:

$$Qc_{,pr} = \frac{\dot{V}CO_{2,1} - \dot{V}CO_{2,2}}{Ca_{,2}CO_2 - Ca_{,1}CO_2} \text{ or } Qc_{,pr} = \frac{\Delta\dot{V}CO_2}{\Delta CaCO_2}, \quad (22.8)$$

where $\Delta\dot{V}CO_2 = \dot{V}CO_{2,1} - \dot{V}CO_{2,2}$ and $\Delta CaCO_2 = Ca_{,1}CO_2 - Ca_{,2}CO_2$. Inspired and expired tidal volume, along with inspired and expired PCO_2, are measured and integrated to derive $\dot{V}CO_2$ for each breath. A mainstream CO_2 sensor is used for breath-to-breath PCO_2 and $\dot{V}CO_2$ measurements as a means of avoiding errors associated with PCO_2 measurement delay and rise/decay time effects from the gas sampling line

and sensor chamber, respectively. End-tidal PCO_2 and CO_2 solubility are used to measure $Ca,_1CO_2–Ca,_2CO_2$ as $\Delta CaCO_2$ via equation (22.4).

A convenient way of changing ventilation for normal versus partial rebreathing is to introduce a variable-size serial deadspace, especially one that can be automatically included and excluded from the circuit by a pneumatic valve, with computer data acquisition and monitor control software [19]. The partial rebreathing circuit should be expandable and retractable, thus readily adjustable for different tidal volumes or for conditions of relatively high deadspace, such as seen with positive end-expiratory pressure (PEEP). This option is important for preventing $\dot{V}CO_2$ from falling close to zero during partial rebreathing.

De Abreu *et al.* recommended that the Q_T estimate obtained from $Q_{C,pr}$ measurement should incorporate a correction for intrapulmonary shunt or venous admixture [18]. They used measured shunt (anatomic + intrapulmonary) from arterial and mixed venous O_2 content via arterial and PA catheters in animal studies. However, the intent was to avoid placing a PA catheter for mixed venous samples, so a less invasive method was needed. Haryadi *et al.*, therefore, used the iso-shunt lines described by Benator and colleagues to derive a shunt estimate from inspired O_2 fraction (FiO_2) and arterial PO_2 [20]. These shunt isopleths are a series of continuous curves representing the relationship between arterial PO_2 (PaO_2) and FiO_2 for different shunt values, whose mathematical derivations are readily applied online with known FiO_2 and PaO_2. This enabled Haryadi *et al.* to perform shunt correction with the following equation:

$$Q_T = \frac{Q_{C,pr}}{1 - Q_S/Q_T} \quad (22.9)$$

where Q_S/Q_T = shunt fraction.

A measured PaO_2 value is needed for estimating shunt when high FiO_2 leads to PaO_2 values > 100 mm Hg. When PaO_2 is < 100 mm Hg, arterial O_2 saturation by pulse oximetry (SpO_2) may be used to estimate shunt via these isopleths.

Haryadi *et al.* also recommend correcting for $PaCO_2–PETCO_2$ differences in patients with lung disease by using measured $PaCO_2$ values. In addition, they recommend correcting for alveolar deadspace effects during partial rebreathing because unperfused alveoli ($PACO_2 = 0$) delay the equilibration of $PaCO_2$ and $PETCO_2$ during partial rebreathing (see their Appendix)[19].

Partial rebreathing pulmonary blood flow findings

An animal study comparing $Q_{C,pr}$ with Q_{TD} was performed by Haryadi *et al.* in which cardiac output was raised with dobutamine infusion (2.5–15 μg/kg/min) and lowered with halothane (0.5–4.0%) inhalation or inferior vena cava clamping [19]. The continuous cardiac output trend in Figure 22.1 shows a satisfactory

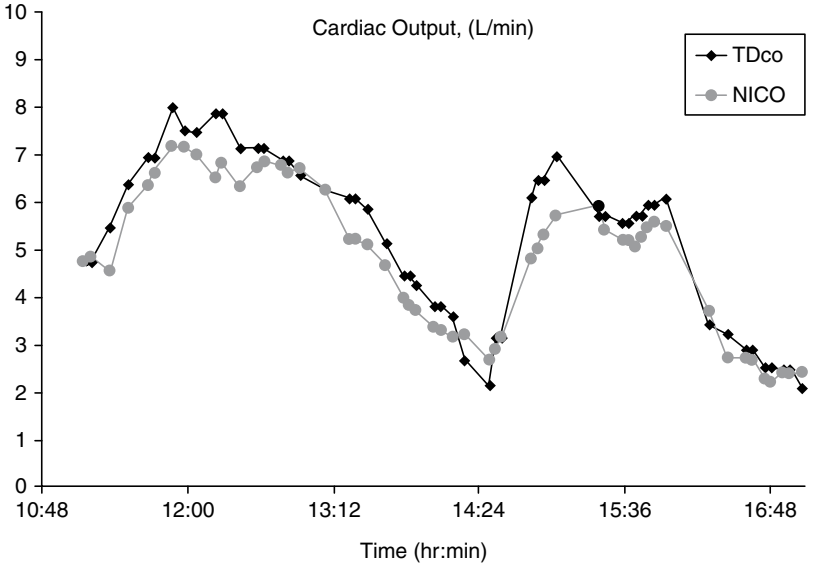

Figure 22.1 This trend plot shows NICO® (Respironics/Novametrix CO_2 monitor) $Q_{C,pr}$ and bolus thermodilution (TDco) Q_T measurements in anesthetized dogs when cardiac output was raised with dobutamine infusion and lowered with halothane inhalation. The weighted correlation coefficient showed $r = 0.93$. [Courtesy of Respironics-Novametrics.]

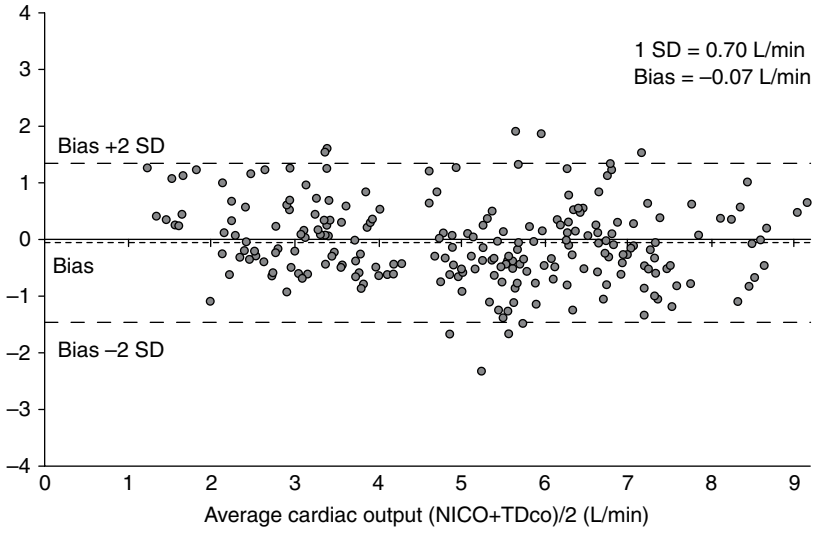

Figure 22.2 Bland–Altman plot: differences between NICO $Q_{C,pr}$ and TDco (Q_{TD}) for the dogs in Figure 22.1 are plotted as bias (average NICO–TD difference) at –0.07 L/min. Precision (SD of the difference) was 0.70 L/min. The dashed lines indicate ± 2 SD from the bias. [Courtesy of Respironics-Novametrics.]

level of agreement between the two methods for cardiac output change, although abrupt up or down changes show brief phase lags by NICO $Q_{C,pr}$. These phase lags are related to buffering of $\dot{V}CO_2$ and $P_{ET}CO_2$ from the relatively large CO_2 storage capacity in body tissues and the smaller CO_2 stores in the lung. The response time of acutely changing $Q_{C,pr}$ for CO_2 is thus limited by the need for stable CO_2 elimination. In spite of these $Q_{C,pr}$ conditions, it is clear that the agreement between $Q_{C,pr}$ and Q_{TD} was very good, as indicated by the weighted correlation coefficient, $r = 0.93$, and by Bland–Altman statistics. The precision (SD of the difference) was 0.70 L/min and bias (mean difference) was –0.07 L/min, as illustrated in Figure 22.2. In addition, the Bland–Altman plot showed no systematic difference for high or low cardiac output values.

Numerous clinical studies in coronary artery bypass graft (CABG) surgery patients comparing partial CO_2 rebreathing with thermal dilution cardiac output have shown a similar level of agreement between the two methods [19].

Tachibana *et al.* assessed the accuracy of NICO $Q_{C,pr}$ compared with Q_{TD} (PA catheter) methods when tidal volume (V_T) was reduced from 12 to 6 mL/kg in intensive care unit (ICU) patients after CABG surgery [21]. The 50% V_T reduction was associated with a significant negative bias for $Q_{C,pr}$, i.e., lower than Q_{TD} values. A follow-up study suggested it was the reduced minute volume (V_E), rather than the reduced V_T, that affected the accuracy of the NICO versus Q_{TD} [22]. A major concern with both of these reports was the insufficient time allowed for mixed venous PCO_2 to stabilize after the large $\dot{V}_E$ reduction. The lengthy period needed to raise the body stores of CO_2 was almost certainly responsible for the significant negative $Q_{C,pr}$ bias. Indeed, Taskar *et al.* reported that the time constant for $\dot{V}CO_2$ recovery (to control) was 17.1 ± 9.9 min for a 10% minute $\dot{V}_E$ increase, and 35 ± 10.7 min for a 10% reduction in $\dot{V}_E$ [23]. This contrasts with Tachibana's 50% $\dot{V}_E$ reduction and a 15-min interval $Q_{C,pr}/Q_{TD}$ measurement.

An interesting clinical contrast is seen with rapid red blood cell (RBC) transfusion. The rapid rise in $\dot{V}CO_2$, in effect, raises $\Delta C\bar{v}CO_2$ more quickly than $\Delta CaCO_2$; hence an abrupt decrease in $Q_{C,pr}$ from the high PCO_2 in blood bank stored RBCs. While this scenario is obviously a non-stable condition, it is distinctly different from an abrupt $\dot{V}_E$ reduction. The rapid RBC infusion, with its rapid increase in $\dot{V}CO_2$, prevents the CO_2 bolus from being stored in the body. Within 3–6 min, the $P_{ET}CO_2$ and $\dot{V}CO_2$ recover to control, while $Q_{C,pr}$ rises above pretransfusion values due to improved blood volume and Hg concentration.

Odenstedt *et al.* performed another comparison of NICO $Q_{C,pr}$ versus Q_{TD} (PA catheter) in 15 operating room and ICU patients [24]. They found a high overall correlation between the two measurements: $Q_{TD} = 0.99Q_{C,pr}$, where $r = 0.96$ over a Q_{TD} range of 2.3–15.7 L/min and $Q_{C,pr}$ range of 2.3–18.1 L/min. The within-subject correlation was also excellent, $r = 0.88$. There was no significant overall bias (Q_{TD}–$Q_{C,pr}$ was 0.04 L/min), and the limits of agreement (bias ± 2 SD) were –1.68 and 1.76 L/min, although there was a small trend towards overestimation by $Q_{C,pr}$ at higher values.

Table 22.1 Bias, precision, and relative error of NICO and CCO against BCO at four operative stages

	Postinduction	Aorta cross-clamp	Iliac reperfusion	Peritoneal closure
Bias ± precision (L/min)				
NICO	−0.1 ± 0.61	−0.52 ± 0.95	−0.99 ± 0.86[a]	−0.72 ± 0.97[a]
CCO	0.23 ± 0.81	0.37 ± 1.05	0.2 ± 1.12	0.72 ± 1.57[a]
Relative error (%)				
NICO	−1.2 ± 18.3	−11.1 ± 23.9	−19.1 ± 15.1	−14.9 ± 15.2
CCO	6.7 ± 23.4	10.9 ± 26.2	3.5 ± 19.6	12.1 ± 22.7

Data by Kotake *et al.* [26] were collected from 28 patients and expressed as bias ± precision (1 SD of bias). Differences against BCO (Bolus Q_{TD}) were statistically analyzed with repeated measures ANOVA. Relative error (%) is defined as [either (NICO or CCO) – BCO]/BCO and expressed in mean ± SD, thus not subject to statistical analysis.

[a] $P < 0.05$ vs. after anesthetic induction. BCO, bolus thermodilution, Q_{TD}, CCO = continuous Q_{TD}, and NICO = non-invasive $Q_{C,pr}$, respectively.

Source: Data from: Kotake Y, Moriyama K, Innami Y, *et al.* Performance of non-invasive partial CO_2 rebreathing cardiac output and continuous thermodilution cardiac output in patients undergoing aortic reconstruction surgery. *Anesthesiology* 2003; **99**: 283–8.

Independent assessment of $\dot{V}CO_2$, using CO_2 insufflation into a lung model, showed a 2–9% underestimation (by the NICO) at a respiratory frequency of 10, and a 5–13% underestimation at a frequency of 15–20. The authors speculated that a high correlation, combined with minimal bias for Q_{TD}–$Q_{C,pr}$, could be due to a small $P_{ET}CO_2$ error balancing a $\dot{V}CO_2$ bias, thus canceling out the error. Intrapulmonary shunt estimates via FiO_2/shunt isopleths were an average of 11% lower compared with shunt values derived from mixed venous and arterial blood O_2 content differences. This shunt difference was not consistent with the high level of agreement between the two Q_T measurements. The authors, therefore, postulated a difference in "effective pulmonary blood flow" based on low ventilation/perfusion ($\dot{V}/\dot{Q}$) ratio. Presumably, the authors meant that the shunt calculations were too high because of the venous admixture effect of low $\dot{V}/\dot{Q}$ areas. However, in the presence of elevated inspired O_2 the effect of areas with low ($\dot{V}/\dot{Q}$) on pulmonary capillary O_2 content, and thus venous admixture or shunt, is minimized. An alternative explanation would be errors in blood gas-derived (rather than direct [cooximeter]) O_2 content values for calculating shunt [25].

The question of a predictable clinical source bias was addressed in an abdominal aortic reconstruction case study by Kotake *et al.* [26]. They measured bolus Q_{TD} with a PA catheter, and compared it with continuous Q_{TD} (CCO) and with NICO $Q_{C,pr}$ during four distinct periods of surgery: (1) after anesthesia induction, (2) during aortic cross-clamp, (3) after reperfusion of the iliac artery, and (4) during peritoneal closure. Overall bias and precision (compared to bolus Q_{TD}) was −0.58 ± 0.9 L/min for the NICO and 0.38 ± 1.17 L/min for the CCO. The NICO bias increased after iliac reperfusion, while the CCO bias increased during peritoneal closure, as shown in Table 22.1. Kotake *et al.* did not determine the reason for the reperfusion NICO bias change, but speculated there may have been modest changes in $\dot{V}CO_2$ and deadspace that were not statistically significant. This explanation suggests that $Q_{C,pr}$ values were not corrected for $PaCO_2$–$P_{ET}CO_2$ and/or shunt changes after iliac reperfusion. Instead, they proposed that $Q_{C,pr}$ with the NICO may be valuable for identifying significant hemodynamic abnormalities, but additional PA catheter data on left ventricular filling pressures and intrapulmonary shunting may be needed when patients have serious cardiac and pulmonary disease. This concern would be most relevant in patients at risk for intrapulmonary shunting with fluid overload, congestive heart failure (CHF), or acute lung injury (ALI).

A computer model study of $Q_{C,pr}$ measurements by Yem *et al.* suggested that the duration of partial rebreathing may be a cause of systematic error [27]. They concluded that for $Q_{C,pr}$ <3 L/min, a rebreathing period >50 s was needed, while for $Q_{C,pr}$ >6 L/min, a rebreathing period of 50 s was excessive. They also suggested that a time constant for CO_2 in an alveolar compartment was inversely proportional to the product of solubility of CO_2 in blood and the $Q_{C,pr}$. This led to their recommendation of applying either a variable period of rebreathing, depending on the latest $Q_{C,pr}$ value, or a proportional correction factor. These suggested modifications will obviously need to be tested

Table 22.2 Cardiac output (Q_T) bias, precision, and limits of agreement

	n	Bias (L/min)	Precision (L/min)	Limits of agreement (L/min)
Before CPB				
UFP vs. NICO	108	0.04	± 1.07	−2.1 to 2.2
UFP vs. Q_{TD}	99	0.18	± 1.01	−1.8 to 2.2
CCO_{TD}	103	0.29	± 1.40	−2.5 to 3.1
After CPB				
UFP vs. NICO	32	−0.46	± 1.06	−2.6 to 1.7
UFP vs. Q_{TD}	32	0.35	± 1.39	−2.4 to 3.1
CCO_{TD}	31	0.36	± 1.95	−3.6 to 4.3

UFP, ultrasonic flow probe; NIC, non-invasive partial CO_2 rebreathing; Q_{TD}, bolus thermodilution Q_T; CCO_{TD}, continuous thermodilution Q_T.
Source: Data from: Botero M, Kirby D, Lobato EB, Staples ED, Gravenstein N. Measurement of cardiac output before and after cardiopulmonary bypass: comparison among aortic transit-time ultrasound, thermodilution, and non-invasive partial CO_2 rebreathing. *J Cardiothorac Vasc Anesth* 2004; **18**: 563–72.

in human subjects prior to incorporation into $Q_{C,pr}$ measurements. Meanwhile, the partial rebreathing period by the NICO has already been reduced to 35 s.

Botero *et al.* compared Q_T measurements via: (1) a sterile, ascending aorta ultrasonic transit-time flow probe (UFP), (2) PA catheter bolus Q_{TD}, (3) continuous Q_{TD} (CCO), and (4) NICO ($Q_{C,pr}$), before and after cardiopulmonary bypass (CPB) in 68 coronary artery bypass (CABP) patients [28]. Measurements by UFP were considered the "gold standard." They found the least bias between UFP and NICO Q_T, with a tendency towards underestimation after CPB, as shown in Table 22.2. The CCO showed the least reproducibility. The authors speculated that increased intrapulmonary shunting and $PaCO_2$–$P_{ET}CO_2$ differences may have altered the UFP/NICO Q_T relationship after CPB. Note that this interpretation suggests that NICO ($Q_{C,pr}$) values in this study may not have been corrected online for acute changes in shunting and/or $P(a–ET)CO_2$ via measured PaO_2 and $PaCO_2$. Alternatively, shunt severity may have been too high (>30% of Q_T) for the designed limits of the shunt correction algorithm.

Shortcuts to pulmonary blood flow assessment

Clinical experience has repeatedly demonstrated that severe acute reduction in pulmonary blood flow during constant ventilation, e.g., due to ventricular fibrillation, is accompanied by a major $P_{ET}CO_2$ reduction. Rapid cardiac output recovery produces a quick $P_{ET}CO_2$ rise. Leigh *et al.* first reported this observation in 1957 [29]. They assumed acute Q_T reduction based on sudden profound hypotension with unilateral pulmonary artery clamping during intrathoracic surgery, whereas it was obvious during ventricular fibrillation. They also observed dramatic $P_{ET}CO_2$ improvement with unclamping of the pulmonary artery and with effective open cardiac massage. More recently, Barton *et al.* found that 14 emergency department patients in cardiac arrest who developed a palpable pulse during resuscitation had a significantly higher $P_{ET}CO_2$ than those who did not ($P_{ET}CO_2$ 19 versus 5 mm Hg, respectively) [30]. Thus, capnometry has potential as a prognostic indicator of lung perfusion and cardiac output during CPR, and has been used to assess the efficacy of different CPR compression rates for improving lung perfusion [31] (see Chapter 20: Cardiopulmonary resuscitation). Similar, though less dramatic, changes can be seen during periods of rapid surgical bleeding and swift resuscitation or transfusion. Note again that the reliability of $P_{ET}CO_2$ as an indicator of pulmonary blood flow might be confounded during rapid stored RBC infusion because of the high PCO_2 in stored blood.

Meanwhile, the availability of volumetric capnometry has enabled measurement of breath-to-breath, online CO_2 production ($\dot{V}CO_2$). An abrupt reduction in Q_C will be accompanied by a reduction in $\dot{V}CO_2$. However, measured $\dot{V}CO_2$ reduction will be more gradual if lung CO_2 content continues to decrease under controlled ventilation until a new stable relationship between CO_2 delivery to the lung and CO_2 elimination is reached [9]. This implies that neither $\dot{V}CO_2$ nor $Q_{C,pr}$ provide immediately accurate reflections of the change in Q_C during a period when $P_{ET}CO_2$ and $\dot{V}CO_2$

are changing rapidly. Thus, reliable estimates of Q_C with $Q_{C,pr}$ measurement are based on the assumption of stable or steady-state gas exchange (Q_C, $C\bar{v}CO_2$, $\dot{V}_E$, and $\dot{V}CO_2$) conditions. Nevertheless, in the absence of an acute pulmonary complication, rapidly decreasing $P_{ET}CO_2$, and $\dot{V}CO_2$ are immediate indicators of compromised tissue perfusion due to reduced Q_T. These indicators, in turn, provide an instantaneous indication for vasopressor intervention, rapid intravenous (IV) fluid infusion, or possibly blood transfusion, as shown in the following sections.

Capnodynamic Q_T monitoring

The most critical need for continuous Q_T measurements is seen in patients with hemodynamic instability. Peyton *et al.* reported the performance of a new prototype "capnodynamic" monitor for breath-by-breath, continuous Q_T via CO_2 compared to ultrasonic flow probe Q_T (Q_{fp}) in anesthetized sheep [32]. Multiple abrupt Q_T elevations and reductions were induced with IV dobutamine and esmolol. Serial six-breath intervals of larger versus smaller tidal volume (V_T, 200-mL difference) were alternated continuously. When Q_C was stable over a 5-min period, a calibration equation was used for the last three of a six-breath period:

$$Q_C = \frac{P_B \bullet [\dot{V}CO_{2i} - \dot{V}CO_{2j}] - VeffCO_2 \bullet \left[\frac{dP_{ET}CO_{2i}}{dt} - \frac{dP_{ET}CO_{2j}}{dt}\right]}{SCO_2 \bullet [P_{ET}CO_{2i} - P_{ET}CO_{2j}]}, \quad (22.10)$$

where P_B = barometric pressure, $\dot{V}CO_{2i}$ and $\dot{V}CO_{2j}$ are CO_2 elimination rates for two breaths, i and j, that are close enough together so $C\bar{v}CO_2$ and Q_C can be assumed equal in a low or high V_T period; $dP_{ET}CO_2/dt$ is the rate of change in $P_{ET}CO_2$ with cyclic V_T alteration; and $VeffCO_2$ is the effective volume of CO_2 in the lung.

The capacitance equation was used for the first three breaths of the six-breath period:

$$VeffCO_2 = \frac{P_B \bullet [\dot{V}CO_{2i+1} - \dot{V}CO_{2j+1}] - Q_C \bullet SCO_2 \bullet [P_{ET}CO_{2i+1} - P_{ET}CO_{2j+1}]}{\left[\frac{dP_{ET}CO_{2i+1}}{dt} - \frac{dP_{ET}CO_{2j+1}}{dt}\right]}. \quad (22.11)$$

A mutual solution to these two equations was obtained iteratively. The lung volume was corrected, as described by Sainsbury *et al.*, using an assumed deadspace of one-third of the V_T [33]. $C\bar{v}CO_2$ was then calculated for breath i (or j):

$$C\bar{v}CO_2 = SCO_2 \bullet \frac{P_{ET}CO_{2i}}{P_B} + \frac{dP_{ET}CO_{2i}}{dt} \bullet \frac{VeffCO_2}{Q_C \bullet P_B} - \frac{\dot{V}CO_{2i}}{Q_C}. \quad (22.12)$$

Where the pattern of change in $P_{ET}CO_2$ between successive cycles was not similar, stable $C\bar{v}CO_2$ and Q_C could not be assumed, thus the continuity equations were used as shown in (22.13) and (22.14). Using Q_C and $C\bar{v}CO_2$ determined from the calibration equation (22.9) at a previous breath i (Q_{C_i} and $C\bar{v}CO_{2i}$), Q_C on a subsequent breath k (Q_{C_k}) was calculated, assuming that metabolic CO_2 production was unchanged:

$$Q_{Ck} = \frac{Q_{Ci}\frac{C\bar{v}CO_{2k}}{C\bar{v}CO_{2i}} \bullet \left[\frac{dP_{ET}CO_{2k}}{dt} \bullet VeffCO_2 - \dot{V}CO_{2k} \bullet P_B\right]}{\frac{dP_{ET}CO_{2i}}{dt} \bullet VeffCO_2 - \dot{V}CO_{2i} \bullet P_B + Q_{C_i} \bullet SCO_2 \bullet \left(P_{ET}CO_2 - \frac{C\bar{v}CO_{2k}}{C\bar{v}CO_{2i}} \bullet P_{ET}CO_{2k}\right)}, \quad (22.13)$$

where

$$C\bar{v}CO_{2k} = SCO_2 \bullet \frac{P_{ET}CO_{2k}}{P_B} + \frac{\frac{dP_{ET}CO_{2i}}{dt} \bullet \frac{VeffCO_2}{P_B} - \dot{V}CO_{2i}}{Q_{C_k}}. \quad (22.14)$$

Equations (22.13) and (22.14) are interdependent functions that were solved iteratively by bisection, with a tolerance of 1% or less. This system of equations allows for changes in Q_C to be followed on a breath-by-breath basis from a series of variables, all of which can be measured non-invasively. The value of Q_T is derived with Q_C, using a shunt estimate, as described by Haryadi *et al.* via iso-shunt lines described by Benator *et al.* and equation (22.9) [19,20].

Peyton *et al.* observed an overall correlation coefficient of $r = 0.79$, $P < 0.001$ for capnodynamic Q_T and ultrasonic flow probe Q_{fp}. Bland–Altman analysis showed a bias of −0.20 and precision of 0.55 L/min for stable periods, compared with a bias of −0.25 and

precision of 0.94 L/min during periods of induced hemodynamic instability. While these overall statistics and subgroup comparisons are favorable, a more critical analysis of QT and Q_{fp} changes showed delay, as well as overshoot and damped QT responses relative to major Q_{fp} swings. In particular, an expanded view of cardiac arrest and dobutamine bolus treatment showed a 2-min delay in QT recovery relative to Q_{fp}. The authors assumed this delay was not due to errors in $C\bar{v}CO_2$ estimates; since they explain that the delay in QT recovery was due to interval lung CO_2 washout with continued ventilation during cardiac arrest, requiring replenishing of lung CO_2 stores with QT recovery. This buffering of CO_2 transport through the lungs is clearly a significant CO_2 capacitance issue for monitoring unstable cardiac output.

Compensation for lung CO_2 capacitance

Kuck and coworkers addressed this issue by developing a mathematical model of lung CO_2 stores to optimize $PETCO_2$ and CO_2 excretion in response to 30-s cycles of partial rebreathing, accompanied by 30-s cycles of recovery with normal breathing [34]. They performed linear regression of $PETCO_2$ and CO_2 excretion using this model (see Figure 1 in Ref [34]). Studies in anesthetized dogs with dobutamine-stimulated increases and halothane-induced reduction of QT showed a correlation coefficient of $r^2 = 0.966$ between NICO $Qc_{,pr}$ and PA catheter thermal dilution QTD over a range of 1 to 11 L/min. Bias was 0.059 and precision 0.58 L/min.

Brewer *et al.* found that the largest component of lung CO_2 capacitance was the functional residual capacity (FRC) [35]. They analyzed the difference in response times between $PETCO_2$ and $\dot{V}CO_2$, and estimated the volume of CO_2 storage in the lung. Estimates of FRC change were then obtained from this CO_2 storage wash-in during partial rebreathing while advancing the endotracheal tube (ETT) in an anesthetized pig sufficiently to isolate one lung, and retracting the ETT for FRC recovery. When compared with the nitrogen (N_2) washout method, FRC showed a correlation coefficient of 0.83.

Incorporation of the observations of Kuck *et al.* and Brewer *et al.* in the updated algorithm for the NICO (version 4.2) was tested independently in a new Kotake *et al.* study of $Qc_{,pr}$ comparison with thermal dilution continuous (CCO) and bolus cardiac output (QTD "gold standard," every 30–45 min) during major vascular surgery [36]. They found a correlation coefficient of 0.83 for CCO and 0.79 for NICO, while bias was 0.19 ± 0.92 for CCO and 0.03 ± 0.97 for NICO. Relative error was 5.1 ± 20.6% for CCO and 4.2 ± 24.8% for NICO. The authors concluded that the accuracy of the NICO was significantly improved with this software update.

Clinical experience with non-invasive pulmonary blood flow monitoring

Muscle relaxant onset time

Ezri *et al.* studied the effects of esmolol 0.5 mg/kg, ephedrine 70 μ/kg, or placebo on NICO QT in 33 patients 30 s before IV rocuronium injection following anesthesia induction [37]. They found that rocuronium onset time (via wrist ulnar nerve train-of-four twitch monitor) was significantly shorter after ephedrine (52.2 ± 16.5 s) compared with esmolol (114.3 ± 11.1 s) and placebo (87.4 ± 7.3 s), $P < 0.0001$. Ephedrine significantly increased QT for 15 min, while esmolol significantly reduced QT for 6 min. These findings support earlier observations of improved intubating conditions consequent to more rapid delivery of the muscle relaxant to the skeletal muscles, with ephedrine given prior to IV paralytics (vecuronium as well as cisatracurium) [38,39].

Hypotension due to vasodilation

There are many routine elective surgery scenarios in which QT monitoring can provide valuable insight and guidance. One such example was an elderly patient without a known history of cardiovascular disease whose systolic blood pressure (BP) fell to the low 80s during general anesthesia for tympanoplasty in spite of an IV fluid challenge and repeated IV phenylephrine bolus doses (personal observation). NICO QT then showed a cardiac index (CI) of 3 L/min/m^2, while systemic vascular resistance (SVR) was 750 dynes • s • cm^{-5}. A continuous 15 μg/min IV phenylephrine infusion produced a stable SVR elevation and maintained systolic BP in the 95–100 mm Hg range with minimal QT reduction from the modestly increased afterload.

A "thready pulse"

A previously healthy, 40-year-old obese female arrived for emergency exploratory laparotomy with "air under the diaphragm"; thus, a presumptive diagnosis of perforated duodenal ulcer was made. She was tachycardic with a heart rate of 110. Because placing a large-bore

IV proved difficult, the emergency surgery was expedited, with IV etomidate anesthesia and phenylephrine vasopressor support, as well as Pentastarch 1000 mL and IV infusion of 3000 mL lactated Ringer's solution. Repeated IV phenylephrine doses were needed in spite of the fluids, while arterial catheter (A-line) placement attempts were unsuccessful. Indeed, the radial artery pulse felt "feeble" at the outset, and, with catheterization attempts, both radial artery pulses became completely non-palpable. The ulnar artery pulse was "thready" and could only be felt during inspiration. Meanwhile, the surgeons reported gross pus from a ruptured appendix. The appendix was removed, and the abdomen was washed out and closed expeditiously. However, since there was no urine output from the indwelling catheter, this thready pulse could mean she was still hypovolemic, so QT measurements were obtained with the NICO. Surprisingly, QT was 7.9 L/min, mean arterial BP was 58 mm Hg (cuff), and SVR was estimated at 465 dynes • s • cm^{-5} (CVP estimate 10 mm Hg). The high QT and low SVR with a ruptured appendix were consistent with a sepsis picture; hence, IV dopamine infusion was started at 3 μg/kg/min. The BP responded well, now making it easy to place the radial artery catheter, which proved critical while treating the fulminant sepsis. However, it is noteworthy that the anesthesiologists were unable to differentiate a hypovolemic, vasoconstricted thready pulse from a septic vasodilated "weak pulse." This example of hemodynamic instability supported the value of QT and SVR monitoring during a "thready pulse" scenario.

Hypovolemia

Significant preoperative hypovolemia remains a common cause of intraoperative hypotension. Blood volume may be low as a consequence of chronic hypertension, dehydration from fasting, and bowel preparation for colon resection, emesis or diarrhea, or from fluid restriction in a patient with impaired renal function. CI can be remarkably low in such patients, but usually responds well to IV fluid loading. A clinical correlate of this scenario is that hematocrit (Hct) decreases precipitously after fluid resuscitation, leaving little margin for further hemodilution from surgical blood loss. Such a patient is likely to receive a blood transfusion. Myocardial O_2 supply may be inadequate to meet the increased O_2 demand because of the reduced blood O_2-carrying capacity, while hemodynamic stability is compromised by hypovolemia. Accordingly, CI monitoring should be considered in patients with limited cardiovascular reserve during moderate- to high-risk surgical procedures. Such procedures include major bowel resection, radical retropubic prostatectomy (RRP), radical cystectomy with ileal diversion, total hip replacement, aortofemoral bypass, and abdominal aortic aneurysm repair. Similar considerations apply to multiple segment spine surgery with metal fixation.

Radical retropubic prostatectomy

A study of CI monitoring during general anesthesia for 40 stable RRP ASA-II–III patients was performed to test the hypothesis that CI would depend on adequate cardiac compensation for acute surgical anemia versus failing compensation due to hypovolemia for RRP. The lowest systolic BP (radial artery catheter), NICO™ CI, and corresponding SVR, $\dot{V}CO_2$, Hct, and blood volume (BV) measurement (indocyanine green dye dilution) were recorded during 500-mL increments of estimated blood loss (EBL). Data are presented for the last 500-mL EBL measurement period prior to transfusion for subjects who were transfused, and for the 500-mL EBL period where it was agreed that transfusion would not be necessary for the remaining subjects, i.e., at the transfusion decision point for both subgroups [40].

We found no BV and CI correlation during control (before blood loss) conditions for all 40 subjects, r^2 = 0.009, P = 0.56. However, correlation increased to r^2 = 0.30, P = 0.001 for the 31 subjects with Hct 21–28% at the transfusion decision point. BV was 61.5 ± 9.6 (mean ± SD) mL/kg lean body mass for subjects with Hct ≤ 28% when CI was ≥ 2.5 L/min/m^2, compared with BV = 50.9 ± 11.1 mL/kg when CI was < 2.5 L/min/m^2, P < 0.01. In contrast, there was no significant difference in low systolic BP for subjects with Hct ≤ 28% whose BV was 61.5 ± 9.6 versus 50.9 ± 11.1 mL/kg, as shown in Table 22.3. Low systolic BP was the lowest value during a 14-min indocyanine green dye decay curve measurement of BV. There was also no correlation between low systolic BP and BV.

We identified four hemodynamic patterns at the transfusion decision point: in group I, nine subjects had sustained BP with Hct >28%; for the remaining 31 subjects with Hct <28%, 17 subjects in group II had normal BV and CI, but low BP due to low SVR; six subjects in group III had low CI, and low normal-to-normal BV; and eight subjects in group IV were hypovolemic with low CI, and reduced BP and pulse pressure. Group I subjects with a higher Hct

Table 22.3 Hemodynamics for subjects with hematocrit 21–28% at the transfusion decision point

	n	BV (mL/kg)	Hct %	CI (L/min/m^2)	SBP (mm Hg)	PP (mm Hg)	SVR (dynes•s•cm^{-5})
CI > 2.5	15	61.5 ± 9.6	25 ± 3	3.02 ± 0.47	97 ± 12	44 ± 8	826 ± 166
CI < 2.5	16	50.9 ± 11.1	25 ± 1	2.11 ± 0.22	97 ± 19	42 ± 12	1195 ± 275
Significance		P < 0.01	NS	N/A	NS	NS	P < 0.01
No transfusion	9	62.7 ± 12.3	27 ± 1	2.88 ± 0.62	109 ± 18	51 ± 13	978 ± 288
Transfusion	22	53.3 ± 10.3	24 ± 2	2.41 ± 0.53	92 ± 12	40 ± 7	1033 ± 301
Significance		*P* < 0.05	*P* < 0.01	*P* < 0.05	*P* < 0.01	*P* < 0.01	NS

BV, blood volume; Hct, hematocrit; CI, cardiac index; SBP, systolic blood pressure; PP, pulse pressure; SVR, systemic vascular resistance. Subjects with Hct 21–28% and low CI < 2.5 L/min/m^2 at the transfusion decision point had >10 mL/kg lower blood volume (BV) and higher systemic vascular resistance (SVR) than subjects who had CI > 2.5, *P* < 0.01. However, Hct, systolic BP, and PP were not significantly (NS) different. Subjects who were transfused had lower BV at the time the decision was made, lower Hct, CI, systolic BP, and PP, while SVR was NS different.
Adapted from: Dueck R, Mitchell M, Albo M, Yi K. Non-invasive cardiac index as a blood volume surrogate to assess the need for transfusion during radical retropubic prostatectomy. *Anesthesiology* 2003; **99**: A180.

Table 22.4 Radical retropubic prostatectomy (RRP) control condition hemodynamics

Group	I: Hct >28%	II: Vasodilate	III: Low CI	IV: Hypovolemia
n	9	17	6	8
Hct	38 ± 3[a]	33 ± 2	33 ± 4	35 ± 5
BV, mL/kg	64.1 ± 14.3	68.6 ± 14.9	70.0 ± 9.4	49.9 ± 7.7[b]
Low CI	2.66 ± 0.46	2.95 ± 0.83	2.44 ± 0.31	2.24 ± 0.40
Mean CI	2.96 ± 0.52	3.27 ± 0.82	2.64 ± 0.25	2.42 ± 0.44[c]
Low SBP	110 ± 9	109 ± 12	104 ± 12	118 ± 19
Low DBP	63 ± 6	62 ± 10	57 ± 8	65 ± 14
Low Mean BP	79 ± 5	77 ± 10	73 ± 8	83 ± 15
Low PP	47 ± 11	47 ± 8	47 ± 11	52 ± 9
Low SVR	1031 ± 286	969 ± 236	1092 ± 103	1292 ± 314[d]
Low $\dot{V}CO_2$ Ind.	98 ± 13	107 ± 16	86 ± 3	84 ± 8[e]
Low $P_{ET}CO_2$	35 ± 2	35 ± 3	33 ± 2	35 ± 2

Hct, hematocrit; CI, cardiac index; SBP, systolic blood pressure; DBP, diastolic blood pressure; SVR, systemic vascular resistance.
[a] Signif. > Group II, *P* < 0.05; [b] Signif. < Group II,III *P* < 0.05; [c] Signif. < Group II, *P* < 0.05;
[d] Signif. > Group II, *P* < 0.05; [e] Signif. < Group II, *P* < 0.01.
Hemodynamic group I subjects (with Hct > 28% at the transfusion decision point) had significantly higher Hct before surgical blood loss, while hypovolemic group IV subjects had significantly lower blood volume (BV) and higher systemic vascular resistance (SVR). Group II subjects (with vasodilation at the transfusion decision point) had normal values during control conditions. Group III (low CI and normal BV) and group IV subjects had significantly lower CO_2 elimination index ($\dot{V}CO_2$, mL/min/m^2) values.

maintained adequate BP in spite of reduced BV; group II had the highest CI, along with the lowest BP and SVR, as shown in Tables 22.4 and 22.5 and Figures 22.3 and 22.4. Group III subjects had low CI in spite of normal or elevated BV after moderate fluid infusion. The seriously hypovolemic group IV had moderate BP and pulse pressure reduction with low CI. Group II subjects' normovolemic hypotension, and normal pulse pressure from vasodilation was therefore distinguishable from group IV subjects' hypovolemic hypotension, higher SVR, low pulse pressure, and low CI. In addition, groups III and IV had very low $\dot{V}CO_2$ during both control and transfusion decision conditions.

These findings demonstrate the complex hemodynamic changes associated with acute surgical

Table 22.5 Transfusion decision hemodynamics

Group	I: Hct >28%	II: Vasodilate	III: Low CI	IV: Hypovolemia
n	9	17	6	8
Hct	32 ± 2[a]	25 ± 2	26 ± 2	25 ± 1
BV, mL/kg	52.8 ± 9.6	61.7 ± 9.7	59.0 ± 7.1	41.7 ± 2.5[b]
Low CI	2.34 ± 0.28	2.93 ± 0.50[c]	2.13 ± 0.13	2.05 ± 0.26
Mean CI	2.66 ± 0.36[d]	3.26 ± 0.57	2.70 ± 0.61	2.35 ± 0.35[d]
Low SBP	117 ± 17	96 ± 12[e]	100 ± 21	98 ± 19
Low DBP	66 ± 7	52 ± 9[e]	56 ± 12	56 ± 15
Low Mean BP	83 ± 9	66 ± 10[e]	71 ± 13	70 ± 16
Low PP	51 ± 15	44 ± 7	44 ± 18	42 ± 9
Low SVR	1212 ± 241	784 ± 131[f]	1210 ± 208	1163 ± 278
Low $\dot{V}CO_2$ Ind	101 ± 16	109 ± 15	85 ± 6 ψ	88 ± 19[g]
Low $PETCO_2$	34 ± 3	36 ± 3	33 ± 2	36 ± 3

BV, blood volume; Hct, hematocrit; CI, cardiac index; SBP, systolic blood pressure; DBP, diastolic blood pressure; PP, pulse pressure; $\dot{V}CO_2$ Ind, CO_2 elimination index; SVR, systemic vascular resistance.
[a] Signif. > Groups II–IV, $P < 0.01$; [b] Signif. < Groups I–III, $P < 0.01$; [c] Signif. > Groups I, III, IV, $P < 0.01$;
[d] Signif. < Group II, $P < 0.01$; [e] Signif. < Group I, $P < 0.05$; [f] Signif. < Groups I, III, IV, $P < 0.01$; [g] Signif. < Group II, $P < 0.01$.
Group I subjects again had significantly higher Hct, while group IV had very low BV. Group II subjects' low CI was in the high normal range, while low CI values for groups I, III, and IV were in the low normal to very low range. In spite of group II subjects' higher CI, they had significantly lower systolic, diastolic, and mean BP due to significantly lower SVR. $\dot{V}CO_2$ index was again significantly lower in groups III and IV, in spite of no difference in $PETCO_2$.

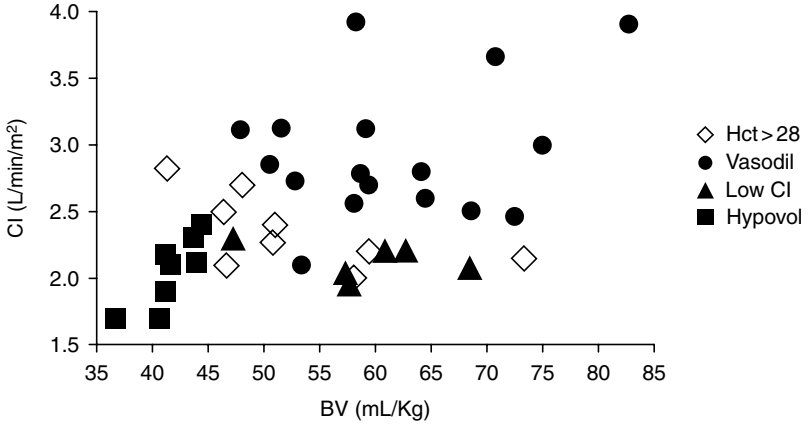

Figure 22.3 Cardiac index (CI) (L/min/m^2) is plotted with respect to BV (mL/kg lean body mass) for hemodynamic groups I, II, III, and IV (with Hct > 28%, vasodilation, low CI, and hypovolemia, respectively) at the transfusion decision point. Note that BV and CI for group I ranged from low to normal, and that group II subjects were in the normal-to-high normal BV and CI range. Group III subjects had low CI in spite of normal BV, thus unable to compensate for acute anemia. Group IV subjects had low CI and very low BV. One group III subject and 3 group IV subjects had CI values in the heart failure (CI < 2.0 L/min/m^2) range.

blood loss and fluid resuscitation. Acute hemodilution results in reduced viscosity, low SVR, and hypotension [40–42]. While normal BV during these conditions may assure normal to high-normal CI, acute anemia, and moderate hypotension is often considered an indication to transfuse RBCs for fear of hypovolemic anemia. In contrast, patients with impaired cardiac function and acute anemia may have compromised cardiac output, even with adequate BP. Meanwhile, acute hypovolemia can be masked by adequate BP due to reflex vasoconstriction, making CI, pulse pressure, and SVR even more valuable for identifying the most hazardous hemodynamic condition: acute hypovolemic anemia. The reduced $\dot{V}CO_2$ with low QT in these patients, as well as in the normovolemic anemic patients with impaired cardiac function, suggested that tissue perfusion might have been compromised by

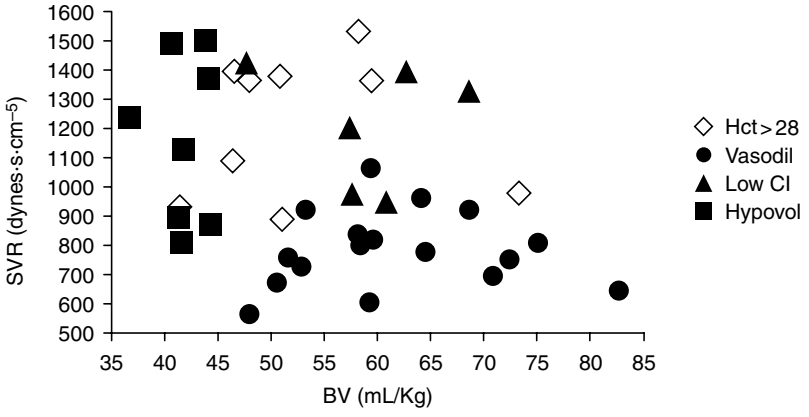

Figure 22.4 Low SVR is plotted with respect to BV (mL/kg) for hemodynamic groups I-IV at the transfusion decision point. Note that SVR was significantly lower for group II. Groups I and III had variable SVR elevation compared to control conditions. Group IV subjects had variable SVR reduction from their high levels before surgical blood loss, in spite of very low BV at the transfusion decision point. SVR reduction was primarily due to acute hemodilution from blood loss and IV fluid infusion.

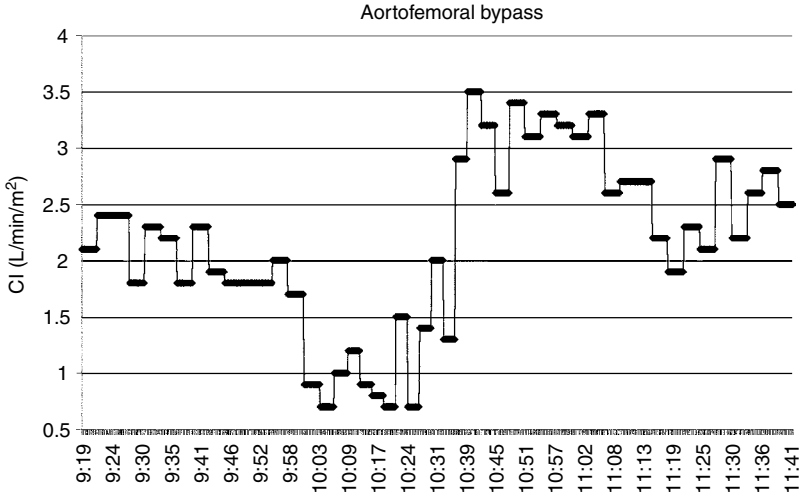

Figure 22.5 A continuous trend of CI versus time is presented in a patient with severe peripheral vascular disease during general anesthesia and surgery for aortofemoral bypass. Note that CI was in the 2.0 L/min/m^2 range prior to infrarenal aortic cross-clamp, then fell to 1.0 L/min/m^2 after cross-clamp after 9:53, indicating acute heart failure. The acute increase in afterload was reflected by systolic BP rising to 180 mm Hg. The delayed CI change was related to the 3-min $Qc_{,pr}$ cycle. CI recovered after release of the aortic cross-clamp at 10:17, then improved to the 3.0 L/min/m^2 range with nitroprusside infusion during the second aortic cross-clamp at around 11:04.

hypovolemia and/or impaired cardiac performance. Failure to compensate for anemia in spite of adequate blood volume may also have been an adverse effect of acute anemia.

Continuous non-invasive $Qc_{,pr}$ monitoring, along with beat-to-beat BP, enabled critical hemodynamic analysis during these acute surgical conditions. The combination of CI, BP, pulse pressure, and SVR readily distinguished adequate versus inadequate cardiovascular compensation for acute anemia due to hypovolemia, while CO_2 elimination rate indicated the adequacy of overall tissue perfusion.

Abdominal aortic cross-clamp

Figure 22.5 presents an example of the effects of abdominal aortic cross-clamping on CI via NICO during aortofemoral bypass surgery. At the beginning of surgery, the CI trend showed a compromised CI in the 2.0 L/min/m^2 range. Five minutes after the 9:53 aortic cross-clamp, there was a 50% CI reduction to the 1.0 L/min/m^2 range, indicating the inability of the heart to compensate for the acute afterload elevation, with systolic arterial BP at 180 mm Hg. This period of stress was relieved by the release of the aortic cross-clamp at 10:17. An IV nitroprusside infusion was then started, and CI recovered to 3.0 L/min/m^2. This allowed the surgeon to resume aortic cross-clamp at 11:04, with a satisfactory BP and CI stabilizing in the 2.0–2.5 L/min/m^2 range.

Figure 22.6 provides an expanded view of the changes induced by the aortic cross-clamp at 9:53, and the recovery after release of the cross-clamp at 10:17. The upper panel shows breath-to-breath changes in $\dot{V}CO_2$ during normal and partial rebreathing periods, while the lower panel shows the corresponding

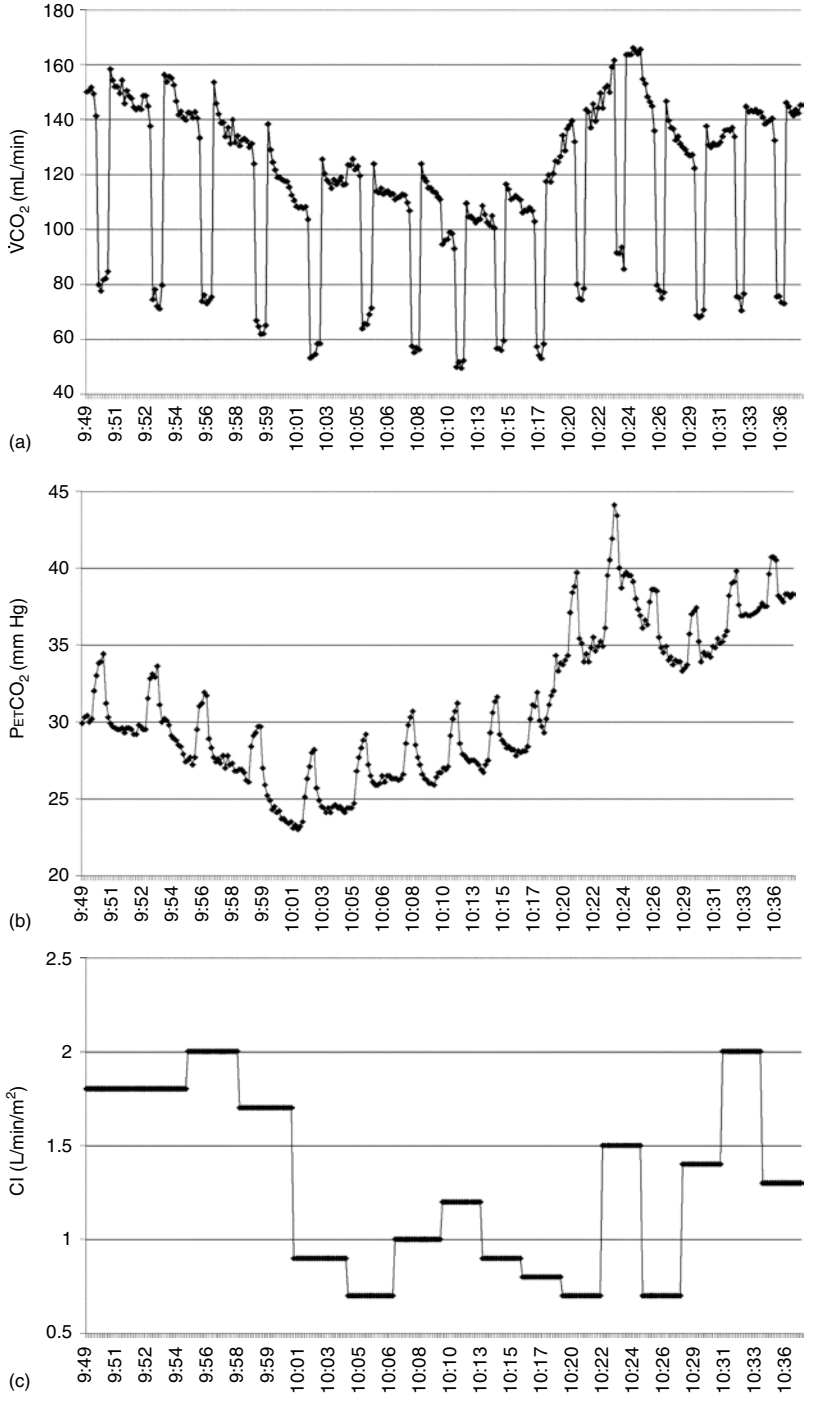

Figure 22.6 An expanded breath-to-breath CO_2 elimination rate ($\dot{V}CO_2$) and end-tidal PCO_2 ($P_{ET}CO_2$) trend is presented for the 3-min normal and partial rebreathing ($Q_{C,pr}$) cycles during the period in which aortic cross-clamp was first applied at 9:52 and then released at 10:16 in the CI trend plot. Note that both $\dot{V}CO_2$ and $P_{ET}CO_2$ trends demonstrated a rapid decrease in CO_2 elimination from the lung after aortic cross-clamp, and a bolus CO_2 delivery after release of the aortic cross-clamp. These acute changes demonstrate the unsteady-state lung CO_2 transport associated with the rapidly decreasing and then improving tissue perfusion after aortic cross-clamp and unclamp maneuvers.

changes in $P_{ET}CO_2$. Note that both $\dot{V}CO_2$ and $P_{ET}CO_2$ recordings show a dramatic reduction soon after 9:52, then an apparent CO_2 bolus from body tissues into the lungs after release of the aortic cross-clamp at 10:16. The fluctuation in $Q_{C,pr}$ (Figure 22.6) during recovery was a reflection of unsteady state CO_2 elimination, representing the limitations of a steady state Fick–CO_2 method of CI monitoring during unstable

lung CO_2 transport. However, the acute directional $\dot{V}CO_2$ and CI trends appropriately reflected critical hemodynamic responses to aortic cross-clamp and unclamping. The CI recovery with nitroprusside infusion provided clear evidence of effective therapy for this patient's compromised heart during abdominal aortic cross-clamp.

Congestive heart failure

Preoperative echocardiographic evaluation of a patient scheduled for RRP showed mild aortic stenosis, moderate concentric left ventricular hypertrophy, with normal ejection fraction but abnormal left ventricular diastolic function. A preoperative Sestamibi cardiac stress test showed inferobasal left ventricular hypokinesis. Perioperative metoprolol therapy for coronary disease was increased from 25 to 50 mg/day for 3 days preoperatively, in compliance with cardiology consult recommendations. Cardiology also suggested that invasive monitoring with a PA catheter was unnecessary.

General anesthesia for RRP was provided with direct radial artery BP and NICO Qт monitoring. Cardiac index was predominantly in the 1.5 L/min/m^2 range. Frequent IV bolus doses of ephedrine and phenylephrine assured adequate arterial BP. In addition, vigorous IV crystalloid and colloid infusion, as well as rapid RBC transfusion, provided two periods where CI temporarily improved into the 2.0 L/min/m^2 range, prior to the sustained improvement after blood loss ended, as shown in Figure 22.7. The IV fluids accumulated to a total of 6 units RBCs, 1000 mL Hetastarch, 3000 mL lactated Ringer's solution and 1000 mL saline, for a total estimated blood loss of 3000 mL. A base deficit was identified through arterial blood gas measurement, which progressed to a nadir of −7. During the last hour of surgery, repeated sighs were needed for low O_2 saturation. A chest radiograph showed pulmonary congestion, even though placement of a PA catheter indicated a PAWP of 10 mm Hg, while thermal dilution CI was in agreement with the 3.5 L/min/m^2 determined by the NICO. The patient received modest dose IV lasix diuretic therapy and mechanical ventilation overnight, then weaned and extubated successfully.

Review of this patient's poor tolerance of anesthesia and surgical blood loss suggests that his left ventricular diastolic dysfunction was more severe than appreciated during preoperative consultation. The initial favorable response to IV fluids before significant surgical bleeding, followed by persistently low CI during two periods of significant blood loss (in spite of rapid IV fluid infusion and blood transfusion), suggest that he may have required a higher left ventricular filling pressure to compensate for acute anemia during rapid surgical bleeding. The increased beta-blockade may have further limited his compensatory cardiac response to acute anemia. The improved cardiac performance, when blood transfusion caught up with blood loss near the end of surgery, supported this impression. However, the decreased oxygenation represented pulmonary congestion, confirmed by chest radiography. It is, thus, reasonable to suggest that the low BP and CI during rapid bleeding would have been more suitably

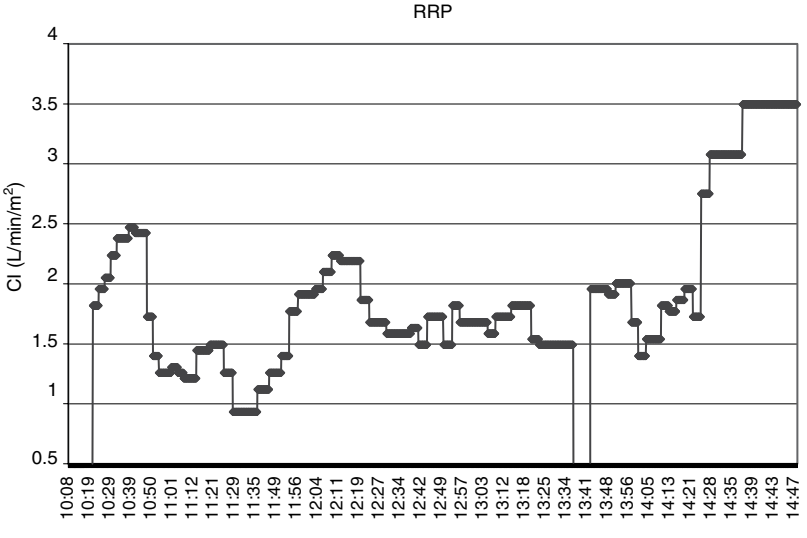

Figure 22.7 The CI trend for this patient during radical retropubic prostatectomy showed significant periods of acute heart failure (CI < 2.0 L/min/m^2) in spite of vigorous IV fluids and blood transfusion, for a total 3000 mL blood loss. A postoperative chest radiograph showed pulmonary congestion, which was treated with IV lasix and overnight assisted ventilation. Acute heart failure indicated the inability to compensate for acute hemodilution during periods of reduced left ventricular filling pressure, with rapid surgical bleeding in a patient with diastolic left ventricular dysfunction and increased perioperative beta-blocker therapy.

managed with an inotropic vasopressor infusion, such as dopamine or dobutamine, rather than the repeated bolus doses of phenylephrine and ephedrine. An inotropic vasopressor infusion should have enabled cardiac output, BP, and SVR to stabilize with IV fluids and blood transfusion, reduced the risk of pulmonary congestion, and avoided the need for overnight ventilatory support.

Summary

Non-invasive cardiac output measurement via the Fick principle for CO_2 has evolved from a theoretical concept in 1870 to an effective clinical application. There is clear evidence that reliable, meaningful pulmonary blood flow (Qc) estimates can be derived from CO_2 elimination and $PETCO_2$ measurements. This technology is well suited to replacing invasive PA catheter and thermal dilution Qt measurements during trauma, surgery, and critical care, thereby reducing the inherent risks associated with invasive methods. A recent prospective study demonstrated that a CI decrease below the 2.5 L/min/m^2 range was associated with reduced blood volume when hematocrit was 22–28%. Patients with limited cardiac reserve, as well as those with very low blood volume, were unable to compensate for acute surgical anemia. Such evidence of cardiac compromise supports the decision to transfuse with RBCs during acute surgical bleeding. Clinical experience with non-invasive cardiac output monitoring has also provided readily recognizable hemodynamic profiles of vasodilation, hypovolemia, sepsis, and acute heart failure. Continuous non-invasive Qt monitoring can, therefore, provide critical cardiovascular information during everyday clinical practice.

References

1. Vandam LD, Fox JA. Adolf Fick (1829–1901), physiologist: a heritage for anesthesiology and critical care medicine. *Anesthesiology* 1998; **88:** 514–18.
2. Fick A. Üeber die Messung des Blutquantums in der Herzenventrikeln. *Sitzung Phys Med Gesell Wurzburg*. July 9, 1870, p 36.
3. Swan HJC, Ganz W, Forrester J, *et al.* Catheterization of the heart in man with use of a flow-directed balloon-tipped catheter. *N Engl J Med* 1970; **283:** 447–51.
4. Ganz W, Donoso R, Marcus HS, Forrester JS, Swan HJ. A new technique for measurement of cardiac output by thermodilution in man. *Am J Cardiol* 1971; **27:** 392–6.
5. Sise CJ, Hollingsworth P, Brimm JE, *et al.* Complications of the flow-directed pulmonary artery catheter: a prospective analysis in 219 patients. *Crit Care Med* 1981; **9:** 315–18.
6. Hamilton WF, Moore JW, Kinsman JM. Delay of blood in passing through the lungs as an obstacle to the determination of the CO2 tension of the mixed venous blood. *Am J Physiol Legacy Content* 1927; **82**: 656–64.
7. Collier CR. Determination of mixed venous CO2 tensions by rebreathing. *J Appl Physiol* 1956; **9:** 25–9.
8. Defares JG. Determination of $PVCO_2$ from the exponential CO_2 rise during rebreathing. *J Appl Physiol* 1958; **13:** 159–64.
9. Dubois AB, Britt AG, Fenn WO. Alveolar CO_2 during the respiratory cycle. *J Appl Physiol* 1952; **4:** 535–48.
10. Vanhees L, Defoor J, Schepers D, *et al.* Comparison of cardiac output measured by two automated methods of CO_2 rebreathing. *Med Sci Sports Exerc* 2000; **32:** 1028–34.
11. Hlastala MP, Wranne B, Lenfant CJ. Single-breath method of measuring cardiac output: a re-evaluation. *J Appl Physiol* 1972; **33**: 846–8.
12. Farhi LE, Nesarajah MS, Olszowka AJ, Metildi LA, Ellis AK. Cardiac output determination by simple one-step rebreathing technique. *Respir Physiol* 1976; **28:** 141–59.
13. Sackner MA, Greeneltch D, Heiman MS, Epstein S, Atkins N. Diffusing capacity, membrane diffusing capacity, capillary blood volume, pulmonary tissue volume, and cardiac output measured by a rebreathing technique. *Am Rev Respir Dis* 1975; **111**: 157–65.
14. Barker RC, Hopkins SR, Kellogg N, *et al.* Measurement of cardiac output during exercise by open-circuit acetylene uptake. *J Appl Physiol* 1999; **87:** 1506–12.
15. Gedeon A, Forslund L, Hedenstierna G, Romano E. A new method for noninvasive bedside determination of pulmonary blood flow. *Med Biol Engin Comput* 1980; **18:** 411–18.
16. Capek JM, Roy RJ. Noninvasive measurement of cardiac output using partial CO_2 rebreathing. *IEEE Trans Biomed Engine* 1988; **35**: 653–61.
17. De Abreu MG, Quintel M, Ragaller M, Albrecht DM. Partial carbon dioxide rebreathing: a reliable technique for noninvasive measurement of nonshunted pulmonary capillary blood flow. *Crit Care Med* 1997; **25:** 675–83.
18. De Abreu MG, Winkler T, Pahlitzsch T, Weismann D, Albrecht DM. Performance of the partial CO_2 rebreathing technique under different hemodynamic and ventilation/perfusion matching conditions. *Crit Care Med* 2003; **31**: 543–51.

19. Haryadi DG, Orr JA, Kuck K, McJames S, Westenskow DR. Partial CO_2 rebreathing indirect Fick technique for noninvasive measurement of cardiac output. *J Clin Monit Comput* 2000; **16**: 361–74 .
20. Benator SR, Hewlett AM, Nunn JF. The use of iso-shunt lines for control of oxygen therapy. *Br J Anaesth* 1973; **45:** 711–18.
21. Tachibana K, Imanaka H, Miyano H, *et al.* Effect of ventilatory settings on accuracy of cardiac output measurement using partial CO_2 rebreathing. *Anesthesiology* 2002; **96:** 96–102.
22. Tachibana K, Imanaka H, Takeuchi M, Takauchi Y, Miyano H. Noninvasive cardiac output measurement using partial rebreathing carbon dioxide rebreathing is less accurate at settings of reduced minute ventilation and when spontaneous breathing is present. *Anesthesiology* 2003; **98**: 830–7.
23. Taskar V, John J, Larsson A, Wetterberg T, Jonson B. Dynamics of carbon dioxide elimination following ventilator resetting. *Chest* 1995; **108:** 196–202.
24. Odenstedt H, Stenqvist O, Lundin S. Clinical evaluation of a partial CO_2 rebreathing technique for cardiac output monitoring in critically ill patients. *Acta Anaesthiol Scand* 2002; **46:** 152–9.
25. Johnson PA, Bihari DJ, Raper RF, *et al.* A comparison between direct and calculated oxygen saturation in intensive care. *Anaesth Intens Care Med* 1993; **21:** 72–5.
26. Kotake Y, Moriyama K, Innami Y, *et al.* Performance of noninvasive partial CO_2 rebreathing cardiac output and continuous thermodilution cardiac output in patients undergoing aortic reconstruction surgery. *Anesthesiology* 2003; **99**: 283–8.
27. Yem JS, Yongquan T, Turner MJ, Baker AB. Sources of error in noninvasive pulmonary blood flow measurements by partial rebreathing. *Anesthesiology* 2003; **98:** 881–7.
28. Botero M, Kirby D, Lobato EB, Staples ED, Gravenstein N. Measurement of cardiac output before and after cardiopulmonary bypass: comparison among aortic transit-time ultrasound, thermodilution, and noninvasive partial CO_2 rebreathing. *J Cardiothorac Vasc Anesth* 2004; **18**: 563–72.
29. Leigh MD, Jenkins LC, Belton MK, Lewis GB. Continuous alveolar carbon dioxide analysis as a monitor of pulmonary blood flow. *Anesthesiology* 1957; **18:** 878–82.
30. Barton CW, Callaham ML. Successful prediction by capnometry of resuscitation from cardiac arrest [abstract]. *Ann Emerg Med* 1988; **17**: 393.
31. Ornato JP, Gonzalez ER, Garnett AR, *et al.* Effect of cardiopulmonary resuscitation compression rate on end-tidal carbon dioxide concentration and arterial pressure in man. *Crit Care Med* 1988; **16:** 241–5.
32. Peyton PJ, Venkatesan Y, Hood SG, Junor P, May C. Noninvasive, automated and continuous cardiac output monitoring by pulmonary capnodynamics: breath-by-breath comparison with ultrasonic flow probe. *Anesthesiology* 2006; **105**: 72–80.
33. Sainsbury MC, Lorenzi A, Williams EM, Hahn CEW. A reconciliation of continuous and tidal ventilation gas exchange models. *Respir Physiol* 1997; **108**: 89–99.
34. Kuck K, Orr JA, Brewer LM. Novel noninvasive cardiac output differential Fick algorithm allows shorter rebreathing times, improved performance versus thermodilution. ASA Annual Meeting October 17–21, 2009, New Orleans, LA, Abstract No. A-611.
35. Brewer LM, Kuck K, Orr JA. Novel functional residual capacity measurement technique based on partial CO_2 rebreathing signals. *Anesthesiology* 2004; **101**: A584.
36. Kotake Y, Ogawa NE, Suzuki T, Morisaki, H, Takeda J. Newer software provides better performance of cardiac output monitoring with partial CO_2 rebreathing (NICO) during major vascular surgery. *Anesthesiology* 2004; **101**: A557.
37. Ezri T, Szmuk P, Warters RD, *et al.* Changes in onset time of rocuronium in patients pretreated with ephedrine and esmolol: the role of cardiac output. *Acta Anaesthesiol Scand* 2003; **47:** 1067–72.
38. Kim KS, Cheong MA, Jeon JW, Lee JH, Shim JC. The dose effect of ephedrine on the onset time of vecuronium. *Anesth Analg* 2003; **96**: 1042–6.
39. Albert F, Hans P, Bitar Y, *et al.* Effects of ephedrine on the onset time of neuromuscular block and intubating conditions after cisatracurium: preliminary results. *Acta Anaesth Belg* 2000; **51:** 167–71.
40. Dueck R, Mitchell M, Albo M, Yi K. Non-invasive cardiac index as a blood volume surrogate to assess the need for transfusion during radical retropubic prostatectomy. *Anesthesiology* 2003; **99**: A180.
41. Weiskopf RB, Viele MK, Feiner J, *et al.* Human cardiovascular and metabolic response to acute, severe isovolemic anemia. *JAMA* 1998; **279:** 217–21.
42. Ickx BE, Rigelot M, Van der Linden PJ. Cardiovascular and metabolic response to acute normovolemic anemia. *Anesthesiology* 2000; **93**: 1011–16.

Section 2
Chapter
23

Circulation, metabolism, and organ effects

$PaCO_2$, $PETCO_2$, and gradient

J. B. Downs

Introduction

Quantitative and/or qualitative analysis of exhaled carbon dioxide (CO_2) has become standard practice in many clinical situations. The rationale for measuring the partial pressure of CO_2 (PCO_2) in exhaled gas is the assumption that end-tidal PCO_2 ($PETCO_2$) is a reflection of alveolar PCO_2 ($PACO_2$). Further, it is assumed that $PACO_2$ is a reflection of the PCO_2 in arterial blood ($PaCO_2$). However, $PaCO_2$, $PACO_2$, and $PETCO_2$ – and their interrelationships – all are affected by multiple variables. This complex set of interactions makes accurate monitoring a complex issue, and is the subject of this chapter.

In order for us to assume that $PETCO_2$ is equivalent to $PACO_2$, certain conditions must apply. First, lung perfusion levels must be consistent throughout the lung. That is, no alveoli must exist with significantly less or greater PCO_2 than others. Unfortunately, this scenario only exists in individuals for whom monitoring of PCO_2 likely would be unnecessary. Second, tidal volume must be of sufficient volume to clear the anatomic deadspace, resulting in an end-tidal gas sample that accurately reflects the composition of alveolar gas. In order for this to occur, tidal volume should equal or exceed three times a volume equivalent to the anatomic deadspace. That is, tidal volume must be at least 6 mL/kg. This seldom is the case in spontaneously breathing patients. Current recommendation by the ARDS Network results in a tidal volume of only 6 mL/kg, or approximately three times the "normal" anatomic deadspace, 2.2 mL/kg ideal body weight. Thus, during most clinical situations, $PETCO_2$ reflects $PACO_2$ with a variable dilution effect from anatomic deadspace. That is, with a V_T of 1 mL/kg, the dilutional effect would be greater than with a V_T of 10 mL/kg. This is because anatomic deadspace is relatively constant and, as V_T increases, the contribution from anatomic deadspace gas to the total will progressively be less.

Carbon dioxide transport to and from the lung

Hemoglobin plays an essential role in CO_2 transport and elimination. Were it not for the avid binding of CO_2 by the hemoglobin molecule, metabolic production of CO_2 would increase venous blood PCO_2 ($PvCO_2$) by nearly 300 mm Hg. Remarkably, $PvCO_2$ is only 5 mm Hg greater than $PaCO_2$. John Scott Haldane described the effect oxygen has on the hemoglobin molecule with regard to CO_2 transport. At the peripheral, capillary, and cellular levels, deoxygenated hemoglobin has a markedly increased affinity for CO_2. The "leftward" shift of deoxygenated hemoglobin permits loading of the hemoglobin molecule with CO_2, with no more than a 5 or 6 mm Hg increase in blood PCO_2. As a result, the CO_2 produced by the body ($\dot{V}CO_2$) can be transported to the lung with a $PvCO_2$ only slightly greater than $PaCO_2$. Conversely, at the pulmonary capillary level, as oxygen binds to the hemoglobin, a "rightward" shift of the CO_2–hemoglobin curve occurs. Thus, CO_2 is delivered to the alveoli, with a resultant decrease in PCO_2 of pulmonary capillary blood of only 5 or 6 mm Hg. As a result, small gradients in PCO_2 permit transport and elimination from the blood of large amounts of CO_2.

Elimination of CO_2 from the lung occurs as a function of gas exchange between the atmosphere and alveoli. This is quantified as alveolar minute ventilation ($\dot{V}A$).

Simplistically, $\dot{V}CO_2$ divided by $\dot{V}A$ closely approximates the fractional concentration of CO_2 at the alveolar level ($FACO_2$). Since oxygen consumption ($\dot{V}O_2$) exceeds $\dot{V}CO_2$ by approximately 20% (respiratory gas exchange ratio of 0.8),

$$FACO_2 = \dot{V}CO_2 / (\dot{V}A - \dot{V}O_2 + \dot{V}CO_2)$$
$$FACO_2 \cdot (PB - PH_2O) = PACO_2,$$

Capnography, Second Edition, ed. J. S. Gravenstein, Michael B. Jaffe, Nikolaus Gravenstein, and David A. Paulus. Published by Cambridge University Press. © Cambridge University Press 2011.

where P_B and P_{H_2O} represent barometric pressure and water vapor pressure, respectively. Assuming equilibrium between PCO_2 at the pulmonary capillary level and the alveoli, we may assume $PaCO_2$ approximately equals P_ACO_2. Thus, we observe that $PaCO_2$ ideally is dependent upon only two variables: $\dot{V}CO_2$ and $\dot{V}_A$.

Since ventilation and pulmonary blood flow are not uniform throughout the lung, the previous analysis is accurate only for areas of the lung where $\dot{V}_A$ and pulmonary perfusion ($\dot{Q}$) are relatively equally matched. When the ratio of ventilation to perfusion ($\dot{V}_A/\dot{Q}$) is increased, due either to increased $\dot{V}_A$ or decreased $\dot{Q}$, less CO_2 will diffuse into the affected alveolar space. The resultant P_ACO_2 in that area of lung will *not* represent overall P_ACO_2. Consequently, $P_{ET}CO_2$ will consist of gas diluted with that from areas of increased $\dot{V}_A/\dot{Q}$, and $P_{ET}CO_2$ will be less than P_ACO_2. If one assumes that P_ACO_2 of well-ventilated alveoli is equivalent to $PaCO_2$, the extent of alveolar "deadspace", alveoli with $\dot{V}_A/\dot{Q}$ = infinity, can be approximated by the following formula:

$$\text{Alveolar deadspace (\%)} = (PaCO_2 - P_{ET}CO_2)/PaCO_2 \times 100.$$

It often is assumed that the difference between arterial and end-tidal PCO_2 ($PaCO_2$–$P_{ET}CO_2$) of 5 mm Hg is "normal." This misconception assumes an alveolar deadspace of approximately 12–15%. Further, it can be calculated that hypoventilation, which results in an increase in $PaCO_2$, will cause a further increase in $PaCO_2$–$P_{ET}CO_2$. For example, if $PaCO_2$ is 40 mm Hg and $P_{ET}CO_2$ is 35 mm Hg, alveolar deadspace = (40 mm Hg – 35 mm Hg)/40 mm Hg × 100 = 12.5%. An increase in $PaCO_2$ to 80 mm Hg, with no change in alveolar deadspace, will increase $P_{ET}CO_2$ only to 70 mm Hg, resulting in a 100% increase in $PaCO_2$–$P_{ET}CO_2$. Therefore, one cannot assume that a single measurement of $PaCO_2$ and calculation of $PaCO_2$-$P_{ET}CO_2$ will permit accurate monitoring of $PaCO_2$ with $P_{ET}CO_2$ measurement over an extended period of time.

Areas of lung with a marked decrease in $\dot{V}_A/\dot{Q}$ will have a minimal effect on $PaCO_2$–$P_{ET}CO_2$. An extremely low $\dot{V}_A/\dot{Q}$, right-to-left intrapulmonary shunting of blood, will result in a transient increase in $PaCO_2$ and increase in $PaCO_2$–$P_{ET}CO_2$. However, within a few circulation times, a resultant increase in $PvCO_2$ will increase $PaCO_2$ and $P_{ET}CO_2$. Therefore, the qualities of the hemoglobin molecule discussed earlier result in a minimal effect of intrapulmonary shunting of blood on the gradient between arterial and end-tidal PCO_2.

Monitoring

Capnography is an exquisite *qualitative* monitor of ventilation. The detection of exhaled CO_2, followed by a decrease in CO_2 in inspired gas, provides evidence of some degree of exchange of gas between the atmosphere and alveoli. Currently, measurement of CO_2 is considered a standard of care for confirming correct placement of a tracheal tube, laryngeal airway, etc. during general anesthesia, in the Emergency Department, and following emergency airway management. Many have suggested that CO_2 analysis may improve the safety of procedures conducted under sedation involving drugs that cause respiratory depression. Clearly, the intermittent fluctuation of PCO_2 in inspired and expired gas of non-intubated patients will ascertain the presence or absence of respiration [1]. Unfortunately, such *qualitative* analyses of exhaled CO_2 is useful primarily only to determine the respiratory rate.

Quantitative exhaled CO_2 analysis

It is widely accepted that $P_{ET}CO_2$ rarely is equivalent to $PaCO_2$. This discrepancy limits use of capnography as an accurate means of assessing ventilation *quantitatively*. In order to gain a greater understanding of the gradient between $PaCO_2$ and $P_{ET}CO_2$, an analysis of the interaction of pulmonary ventilation and perfusion is necessary. Further, the effects of acute changes in ventilation, perfusion, or both, on exhaled CO_2 must be understood in order to accurately utilize $P_{ET}CO_2$ as a valuable monitor.

The alveolar gas equation

The alveolar gas equation (AGE) is used to analyze the effect of ventilation on oxygenation of arterial blood. Any difference between calculated alveolar oxygen tension (P_AO_2) and measured arterial oxygen tension (PaO_2) is presumed to be secondary to a mismatch between alveolar ventilation and perfusion. This widely held perception is based on the analysis of gas exchange that assumes equilibrium conditions are present and that the respiratory gas exchange ratio between CO_2 eliminated from the lung and O_2 extracted from the alveolar space is 0.8. The AGE is represented by the following:

$$P_AO_2 = (P_B - P_{H_2O}) \cdot FiO_2 - PaCO_2 \cdot (FiO_2 + (1 - FiO_2)/R)$$

Clinical application of the AGE assumes $R = \dot{V}CO_2/\dot{V}O_2$, which is accurate when metabolic production of

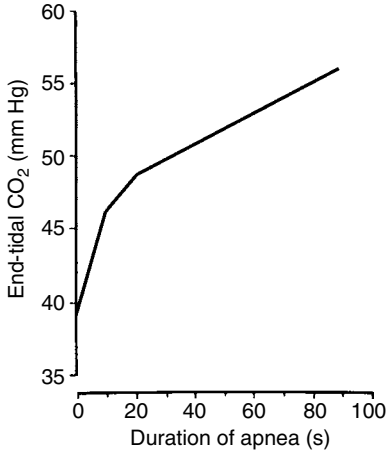

Figure 23.1 Breath-holding from functional residual capacity with a closed glottis results in rapid increase in alveolar PCO_2. [From: Stock MC, Downs JB, McDonald JS, *et al*. The carbon dioxide rate of rise in awake apneic humans. *J Clin Anesth* 1988; **1**: 96–103.]

CO_2 equals excretion of CO_2 from the lung. Such equilibrium is attained when, $\dot{V}CO_2$, $\dot{V}O_2$ and ventilation all are stable, which usually will occur in approximately 1 h following a stepwise decrease in ventilation. In clinical situations where monitoring of gas exchange is appropriate, it is highly unlikely that conditions consistent with equilibrium are present; for example, patients undergoing sleep studies, breathing room air (21% oxygen), often will have a decrease in SpO_2 from a normal level of 98% to levels in the low 70% range, with as little as 30 s of apnea. In this scenario, $PaCO_2$ might increase as much as 8 mm Hg (Figure 23.1) [2]. Application of the AGE would explain a drop in PaO_2 of no more than 10 mm Hg, not even close to the observed decrease of nearly 50 mm Hg that would be associated with a decrease in SpO_2 from 98% to 72%. Classical analysis of the gas exchange based on equilibrium conditions cannot explain many such common clinical observations [3].

Step changes in ventilation

An increase in $\dot{V}_A$ with no change in $\dot{Q}$ will cause an immediate decrease in P_ACO_2, $P_{ET}CO_2$, and $PaCO_2$. Equilibrium will occur within minutes [4]. Conversely, a step *decrease* in ventilation will cause $PaCO_2$, P_ACO_2, and $P_{ET}CO_2$ to rise at a much slower rate. We estimated that halving the respiratory rate, with tidal volume held constant, would cause P_ACO_2 to double in 57 min (Figure 23.2) [5]. This compares very favorably with Nunn's theoretical analysis that $PaCO_2$ would double in 60 min following the halving of $\dot{V}_A$ [4]. When ventilation was decreased, a fall in SpO_2 was apparent in every patient within 3 min, *as long as they breathed 21% oxygen* [5]. This observation cannot be explained by the AGE, as traditionally presented. It *can* be explained, however, as follows. Acute hypoventilation is associated with a sharp decrease in CO_2 exhaled from the lung. As CO_2 stores of the body increase, a gradual, linear rise in PCO_2 will occur in the venous blood, alveolar gas, and arterial blood. Eventually, CO_2 production and CO_2 excretion from the lung, once again, will be equivalent, equilibrium conditions will be reestablished, and the AGE with R = 0.8 again will be applicable. In essence, a step decrease in alveolar ventilation results in an instant change in the respiratory gas exchange ratio (R). The ratio is decreased dramatically and returns to a normal value of 0.8 over a significant period of time following an acute decrease in alveolar ventilation. By substituting a reduced value for R in the AGE, the rapid decline in PaO_2 and SpO_2 can be predicted. The extreme of this scenario occurs with airway occlusion and sudden cessation of alveolar ventilation. The onset of arterial hypoxemia will depend upon the lung volume present at the time of airway occlusion (usually the functional residual capacity) and oxygen consumption. Alveolar CO_2 rapidly will equilibrate with venous PCO_2. As oxygen is extracted at a rate equal to oxygen consumption, it is conceivable that P_ACO_2 may increase to a level exceeding $PaCO_2$; the alveolar CO_2 is concentrated as oxygen is extracted. Following episodes of airway occlusion, $P_{ET}CO_2$ levels exceeding $PaCO_2$ have been observed (Figure 23.3) [6].

Acute increase in $\dot{V}_A/\dot{Q}$

A decrease in overall $\dot{V}_A/\dot{Q}$, inevitably, is a result of regional or global decrease in alveolar ventilation. However, an increase in $\dot{V}_A/\dot{Q}$ may be a result of regional or global change in alveolar ventilation and/or pulmonary blood flow, with variable effects on $PaCO_2$–$P_{ET}CO_2$.

Regional increase in alveolar ventilation

A regional increase in $\dot{V}_A/\dot{Q}$ often occurs during general anesthesia. In fact, it occurs with sufficient frequency that the oft observed $PaCO_2$–$P_{ET}CO_2$ of approximately 5 mm Hg is considered "normal," which is not the case [4]. Induction of general

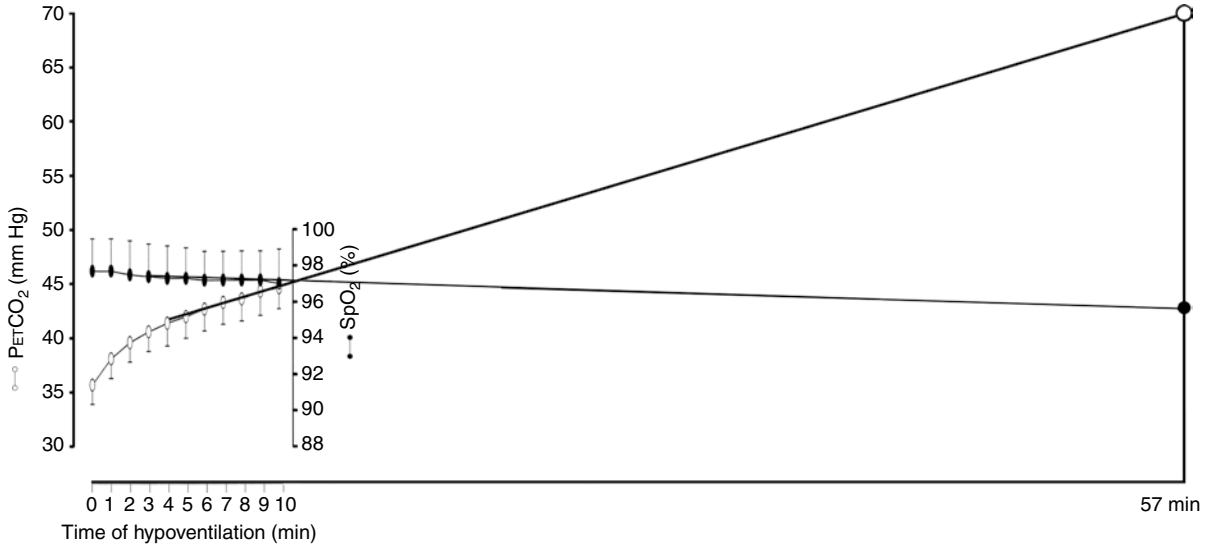

Figure 23.2 A 50% reduction in ventilation results in a linear increase in $PaCO_2$, which will reach equilibration in approximately 57 min. [Modified from: Fu ES, Downs JB, Schweiger JW, Miguel RV, Smith RA. Supplemental oxygen impairs detection of hypoventilation by pulse oximetry. *Chest* 2004; **126**: 1552–8.]

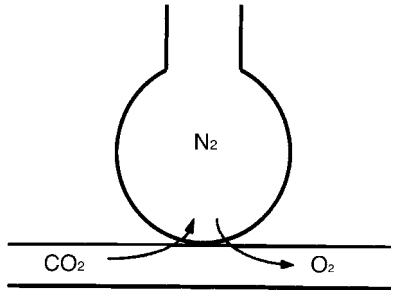

Figure 23.3 Oxygen is extracted from the alveoli at a rate equal to $\dot{V}O_2$. Carbon dioxide diffuses into the alveoli at a rate determined by the $PaCO_2$, which is determined by alveolar ventilation. Thus, R, the respiratory gas exchange ratio, may be altered greatly by changes in alveolar ventilation, resulting in dramatic changes in PaO_2 in short periods of time.

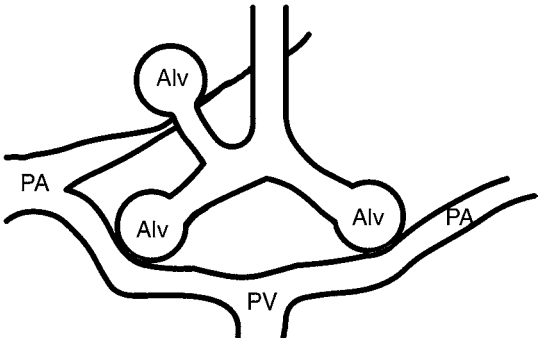

Figure 23.4 Non-dependent alveoli may have decreased perfusion (reduced pulmonary artery [PA] flow) resulting in $PETCO_2$ less than reflected by dependent alveoli and $PaCO_2$.

anesthesia with the onset of positive pressure ventilation will cause an increase in $\dot{V}A/\dot{Q}$ in non-dependent lung regions. This effect is exacerbated by muscle relaxation and loss of spontaneous respiratory effort [7–9]. The lateral position and initiation of one-lung ventilation both produce large discrepancies in $\dot{V}A$ relative to $\dot{Q}$ in dependent vs. non-dependent lung regions. As a result, $PETCO_2$ may be decreased significantly, indicating a large amount of "wasted" ventilation (Figure 23.4). Although a largely iatrogenic pathophysiologic effect, an increase in $\dot{V}A/\dot{Q}$ causing an increase in $PaCO_2$–$PETCO_2$ also can occur secondary to bronchospasm.

Regional increase in $\dot{V}A/\dot{Q}$ secondary to decreased pulmonary blood flow

The capnograph has been used as a monitor during neurologic operative procedures involving the sitting position for more than 30 years, long before CO_2 analyses became the standard of care during all anesthetic procedures. Detection of a significant decrease in regional blood flow with capnography is nearly 100% accurate, whether the etiology is a pulmonary embolus secondary to thrombus, air, amniotic fluid, or even CO_2. The sudden effect of an unperfused, but ventilated, area of lung will cause an instant decrease in $PETCO_2$, alerting

the astute clinician to a significant problem, often before changes in SpO_2 or blood pressure occur or other clinical variables are affected. This effect is secondary to ventilation of unperfused alveoli, as discussed earlier. Clearly, the most common cause of a regional increase in $\dot{V}A/\dot{Q}$ is mechanical ventilation. The effect is exacerbated when patients are paralyzed and spontaneous ventilation is eliminated [7,8]. Lateral body positioning and one-lung ventilation are notorious causes of increased $PaCO_2$–$PETCO_2$. This ubiquitous observation is responsible for the previously mentioned misconception that a $PaCO_2$–$PETCO_2$ of 5 mm Hg is "normal." Further, the larger $PaCO_2$–$PETCO_2$ observed in mechanically ventilated, critically ill patients has caused $PaCO_2$–$PETCO_2$ analysis to be used sparsely in the monitoring of such patients. This is unfortunate, because some mechanical ventilatory patterns have been designed to maximize matching of ventilation and pulmonary perfusion. The comparative efficacy of such patterns have been confirmed by exhaled CO_2 analyses and the multiple gas elimination technique (MIGET) of $\dot{V}A/\dot{Q}$ analyses [9–11]. Currently, popular concepts of mechanical ventilatory support emphasize low tidal-volume ventilation, high respiratory frequency, permissive hypercapnia, etc. All such ventilatory patterns are associated with extremely high $PaCO_2$–$PETCO_2$, secondary to a deadspace-tidal volume ratio often in excess of 0.60. In contrast, ventilatory support techniques based on the use of continuously elevated airway pressure (CPAP) and spontaneous ventilation cause significantly less deadspace ventilation and are much more efficient. This is demonstrated by $PaCO_2$–$PETCO_2$ far less than that observed in most clinical situations (Figure 23.5) [10–12].

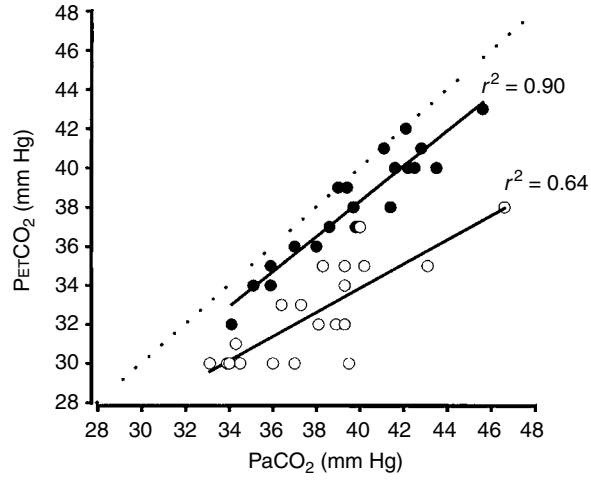

Figure 23.5 By using a ventilation mode that minimized alveolar deadspace, $PETCO_2$ and $PaCO_2$ were nearly the same. In contrast, normal pressure-controlled ventilation caused a significant amount of alveolar deadspace and increased $PaCO_2$–$PETCO_2$. [From: Bratzke E, Downs JB, Smith RA. Intermittent CPAP: a new mode of ventilation during general anesthesia. *Anesthesiology* 1998; **89**: 334–40.]

Global increase in $\dot{V}/\dot{Q}$ (hyperventilation)

An increase in alveolar ventilation and/or decrease in cardiac output (pulmonary blood flow) may cause an increase in global $\dot{V}A/\dot{Q}$. Hyperventilation, for whatever reason, will decrease arterial, alveolar, and end-tidal PCO_2, with no change in $PaCO_2$–$PETCO_2$. In this scenario, $PETCO_2$ will reflect $PaCO_2$ accurately, as long as $PETCO_2 = PaCO_2$. Similarly, a global decrease in cardiac output, with no decrease in perfusion of non-dependent alveoli, will have no effect on $PaCO_2$–$PETCO_2$. However, a decrease in cardiac output infrequently will be distributed evenly throughout the lung. If so, $PaCO_2$–$PETCO_2$ will not be affected. However, since pulmonary blood flow is influenced by gravity, a decrease in pulmonary blood flow caused by decreased cardiac output normally results in a regional decrease in pulmonary perfusion of non-dependent lung regions, and is signaled by a gradual decline in $PETCO_2$ and increase in $PaCO_2$–$PETCO_2$. In this regard, a decrease in cardiac output will present a significantly different pattern of decrease in $PETCO_2$, compared to that occurring with embolic phenomena, with a sudden fall in $PETCO_2$.

Conclusion

End-tidal CO_2 analyses can provide the clinician with information that can be used to guide the monitoring of ventilation and cardiac output. An understanding of the interrelationship between pulmonary perfusion, ventilation, tidal volume, and regional $\dot{V}A/\dot{Q}$ will enhance the utility of capnography as a monitor.

References

1. Soto RG, Fu ES, Vila H, Miguel RV. Capnography accurately detects apnea during monitored anesthesia care. *Anesth Analg* 2004; **99**: 379–82.
2. Stock MC, Downs JB, McDonald JS, *et al.* The carbon dioxide rate of rise in awake apneic humans. *J Clin Anesth* 1988; **1**: 96–103.
3. Gallagher SF, Haines KL, Osterlund L, Murr M, Downs JB. Life-threatening postoperative hypoventilation after bariatric surgery. *Surg Obes Relat Dis* 2010; **6**:102–4.
4. Lumb AB. *Nunn's Applied Respiratory Physiology,* 5th edn. Oxford, UK: Butterworth-Heinemann, 2000; 237–9.

5. Fu ES, Downs JB, Schweiger JW, Miguel RV, Smith RA. Supplemental oxygen impairs detection of hypoventilation by pulse oximetry. *Chest* 2004; **126**: 1552–8.
6. Fletcher R, Jonson B. Deadspace and the single breath test for carbon dioxide during anaesthesia and artificial ventilation. *Br J Anaesth* 1984; **56**: 109–19.
7. Froese AB, Bryan AC. Effects of anesthesia and paralysis on diaphragmatic mechanics in man. *Anesthesiology* 1974; **41**: 242–55.
8. Valentine DD, Hammond MD, Downs JB, Sears NJ, Sims WR. Distribution of ventilation and perfusion with different modes of mechanical ventilation. *Am Rev Respir Dis* 1991; **143**: 1262–6.
9. Wrigge H, Zinserling J, Neumann P, *et al.* Spontaneous breathing with airway pressure release ventilation favors ventilation in dependent lung regions and counters alveolar collapse in oleic acid induced lung injury: a randomized controlled computed tomography trial. *Crit Care Med* 2005; **9**: 780–9.
10. Putensen C, Räsänen J, Lopez F, Downs J. Effect of interfacing between spontaneous breathing and mechanical cycles on the ventilation–perfusion distribution in canine lung injury. *Anesthesiology* 1994; **8**: 921–30.
11. Putensen C, Mutz NJ, Putensen-Himmer G, Zinserling J. Spontaneous breathing during ventilatory support improves ventilation–perfusion distributions in patients with acute respiratory distress syndrome. *Am J Respir Crit Care Med* 1999; **159**: 1241–8.
12. Bratzke E, Downs JB, Smith RA. Intermittent CPAP: a new mode of ventilation during general anesthesia. *Anesthesiology* 1998; **89**: 334–40.

Section 2
Chapter
24

Circulation, metabolism, and organ effects

The physiologic basis for capnometric monitoring in shock

K. R. Ward

Introduction

Shock is a complex entity traditionally defined as a state in which the oxygen utilization or consumption needs of tissues are not matched by the delivery of oxygen. This mismatch commonly results from states of altered tissue perfusion. Common clinical situations that lead to shock include hemorrhage, myocardial infarction, heart failure, trauma, sepsis, and cardiac arrest. In many cases, mixed etiologies can cause tissue perfusion abnormalities. Regardless of the cause, clinicians are better able to treat shock if they understand the underlying mechanisms, shared mechanisms, and physiologic events.

Figure 24.1 represents the basic relationship between oxygen consumption ($\dot{V}O_2$) [1] and oxygen delivery (DO_2) that is pertinent to individual organs and to the whole body [2–4]. Oxygen consumption can remain constant over a wide range of oxygen delivery because most tissue beds are capable of efficiently increasing the ratio of extracted oxygen (OER), resulting in decreasing venous oxygen saturation in each organ. When DO_2 reaches a critical threshold, tissue extraction of oxygen cannot be further increased to meet tissue demands. It is at this point that oxygen consumption ($\dot{V}O_2$) becomes directly dependent on critical DO_2 (DO_2crit), and cells begin converting to greater levels of anaerobic metabolism, as manifested by increases in certain metabolic products such as lactate, nicotinamide adenine dinucleotide, reduced (NADH), and reduced cytochrome oxidase (CtOx). DO_2crit occurs at the point of dysoxia or ischemia where tissue DO_2 cannot meet tissue oxygen demand [2]. Oxygen debt can be defined as the cumulative difference of $\dot{V}O_2$ between baseline and that spent below DO_2 crit. The level of accumulated oxygen debt in shock states is critically linked with both survival and morbidities, such as multisystem organ failure [5,6]. Each

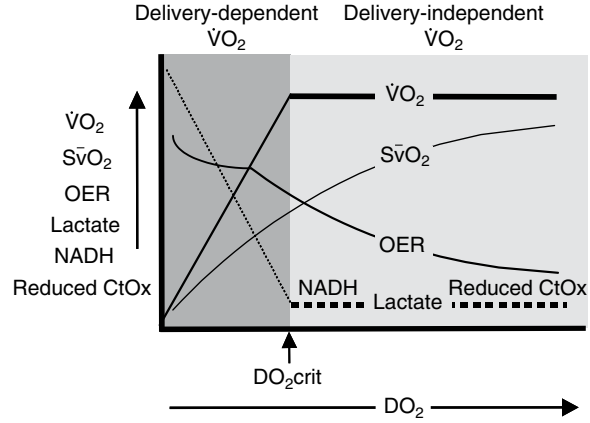

Figure 24.1 Biphasic relationship between DO_2 and $\dot{V}O_2$. The value of OER increases and mixed venous oxygen saturation (SvO_2) decreases in response to decreased DO_2. Below a DO_2crit, $\dot{V}O_2$ becomes delivery-dependent. DO_2 below DO_2crit results in the beginning of anaerobic metabolism as noted by an increase in a variety of cellular products, including lactate, NADH, and reduced CtOx. The DO_2crit of various organ systems can occur at points either above or below whole-body DO_2crit, depending on the metabolic and blood flow regulatory characteristics of the organ system and the rapidity of the reductions in DO_2.

individual organ system has its own biphasic DO_2–$\dot{V}O_2$ relationship. Whole-body measurement of these factors, including surrogates such as systemic lactate, are aggregate measures of all organ systems. Obviously, the more catastrophic the event (e.g., massive hemorrhage or cardiac arrest) the more likely multiple organs will simultaneously reach DO_2crit.

The need for capnometric monitoring in shock

It is the relationship between $\dot{V}O_2$ and carbon dioxide (CO_2) production ($\dot{V}CO_2$) that forms the general foundation for the utility of $\dot{V}CO_2$ and end-tidal PCO_2 ($PETCO_2$) monitoring in shock states. Aerobic

Capnography, Second Edition, ed. J. S. Gravenstein, Michael B. Jaffe, Nikolaus Gravenstein, and David A. Paulus. Published by Cambridge University Press. © Cambridge University Press 2011.

metabolism generates CO_2 and water through its consumption of glucose and other substrates. For the most part, $\dot{V}O_2$ and $\dot{V}CO_2$ are very tightly coupled, and thus parallel to each other. The respiratory quotient (RQ), $\dot{V}CO_2/\dot{V}O_2$, is, on average, 0.85. This quotient is an aggregate measure of the RQ of various organ systems, some of which use mainly glucose such as the brain, and others like the liver which use combinations of substrates, such as glucose, protein, and fat.

The ability of the measurement of the partial pressure of expired carbon dioxide ($P_{ET}CO_2$) monitoring to reflect tissue perfusion lies in its ability to closely reflect alveolar CO_2. Alveolar CO_2 is determined mainly by the combination of $\dot{V}CO_2$, pulmonary capillary blood flow (i.e., cardiac output [CO] minus right-to-left shunt), and alveolar ventilation. As such, alveolar CO_2 and $P_{ET}CO_2$ are linearly related to $\dot{V}CO_2$. The latter, in turn, depends on two different factors: metabolic production and pulmonary excretion of CO_2. In low flow states with steady-state ventilation, $\dot{V}CO_2$ declines secondary to decreased metabolism, decreased delivery of CO_2 to the lungs, and ventilation/perfusion ($\dot{V}/\dot{Q}$) mismatches in the lung. These $\dot{V}/Q$ mismatches result in an enormous increase in the deadspace fraction (up to 0.7) in severe shock and during cardiopulmonary resuscitation (CPR) [7], which produces a widening of the arterial PCO_2 ($PaCO_2$) to $P_{ET}CO_2$ difference, and is further reflected by mixed venous hypercarbia. $\dot{V}CO_2$, which is difficult to measure, also declines secondary to reductions in CO_2 production due to decreases in DO_2 [8–10]. Although sometimes described as a logarithmic relationship, $\dot{V}CO_2$ and thus $P_{ET}CO_2$, have almost the same biphasic relationship with DO_2 as does $\dot{V}O_2$ (Figure 24.2). As such, DO_2crit has been determined by following changes in $\dot{V}CO_2$ and $P_{ET}CO_2$. DO_2crit, as determined by inflective changes of $P_{ET}CO_2$ and $\dot{V}CO_2$ during steady-state ventilation, does not significantly differ compared to determinations made by using changes in $\dot{V}O_2$ or lactate production [10,11].

Although $\dot{V}CO_2$ and $P_{ET}CO_2$ decrease upon reaching DO_2crit, tissue PCO_2 increases (Figures 24.3–24.5). Concomitant with decreases in DO_2 (prior to DO_2crit), increases in tissue CO_2 are produced due to decreased blood flow, which will reduce the amount of aerobically produced CO_2 removed from tissue, creating a tissue respiratory acidosis [12–14]. $\dot{V}O_2$ at the tissue prior to reaching DO_2crit remains constant due to increases in OER, and is reflected by decreased hemoglobin (Hb) oxygen saturation of venous blood from the tissue. Additional tissue CO_2 will be produced after DO_2crit

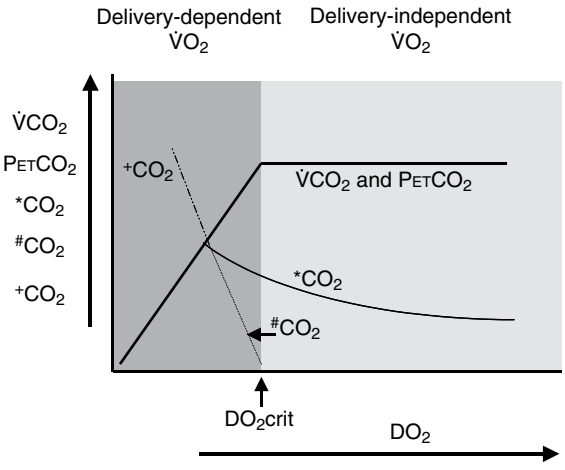

Figure 24.2 Biphasic relationship between DO_2 and $\dot{V}CO_2$. Note the similarities between the relationships as compared to Figure 24.1. When minute ventilation is held constant, DO_2crit can be determined by reductions in $\dot{V}CO_2$, and thus $P_{ET}CO_2$. This corresponds to the point of delivery-dependent $\dot{V}O_2$. $^*CO_2$ represents CO_2 that accumulates as a result of decreased removal of aerobically produced CO_2 secondary to decreases in flow (respiratory acidosis). $^{\#}CO_2$ represents additional tissue CO_2 production and accumulation due to buffering of metabolic acids produced by anaerobic metabolism after DO_2crit is reached, and corresponds to the production of lactate at the point of DO_2crit (see Figure 24.1). $^+CO_2$ represents the combination of aerobically and anaerobically derived CO_2. Overall $\dot{V}CO_2$ is decreased due to decreases in $\dot{V}O_2$. Quantities of CO_2 as depicted on the *y*-axis are not drawn to scale but instead are depicted to demonstrate their temporal relationship to each other in reference to changes in DO_2.

is reached when metabolic acids, such as lactic acid, are produced and then buffered by tissue bicarbonate [15].

Due to these linkages $\dot{V}CO_2$, and thus $P_{ET}CO_2$, are linearly related to DO_2 during states of oxygen-supply-dependent metabolism. In shock states as severe as cardiac arrest where oxygen content does not significantly change, the major component of DO_2 that can be tracked by $\dot{V}CO_2$ or its surrogate marker $P_{ET}CO_2$ is pulmonary blood flow (CO). In this situation, capnometry is definitely advantageous because, almost without exception, CPR is only capable of producing a flow state in which $\dot{V}O_2$ is directly dependent upon DO_2. In other shock states, such as hemorrhage, $\dot{V}CO_2$ and $P_{ET}CO_2$ will still track DO_2 in states of oxygen-supply-dependent metabolism, but in real time, the degree to which each component of DO_2 (CO or oxygen content) is most responsible for the change cannot be ascertained. Regardless of the type of shock, at this DO_2crit level, CO is likely to be significantly reduced, partly because the heart itself is falling below its own DO_2crit, thereby resulting in significant myocardial dysfunction.

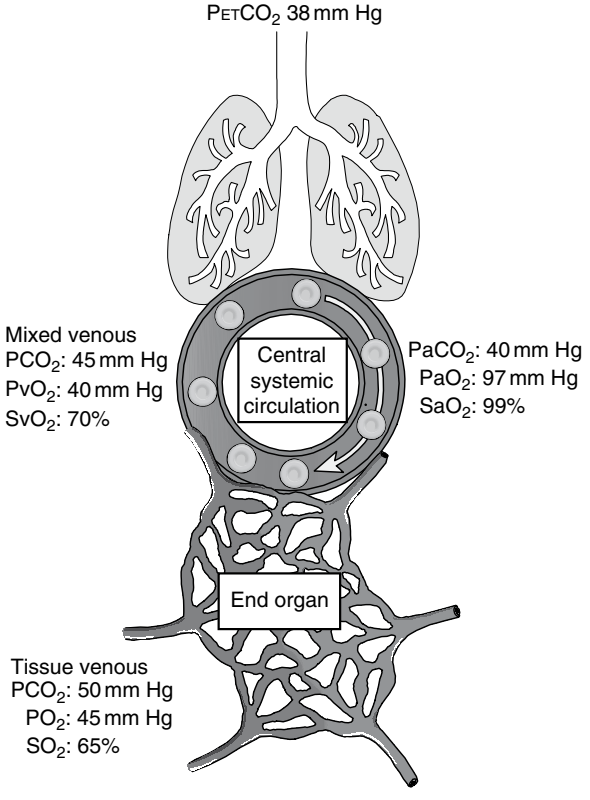

Figure 24.3 Representative blood and tissue gas levels of the normal circulation. Mixed venous values represent aggregate values from all organ systems. Thus, tissue venous values are not necessarily identical to mixed venous values, but can be higher or lower, depending on the individual organ system's level of metabolic activity. The majority of blood volume at the level of the tissue is contained in the venous compartment.

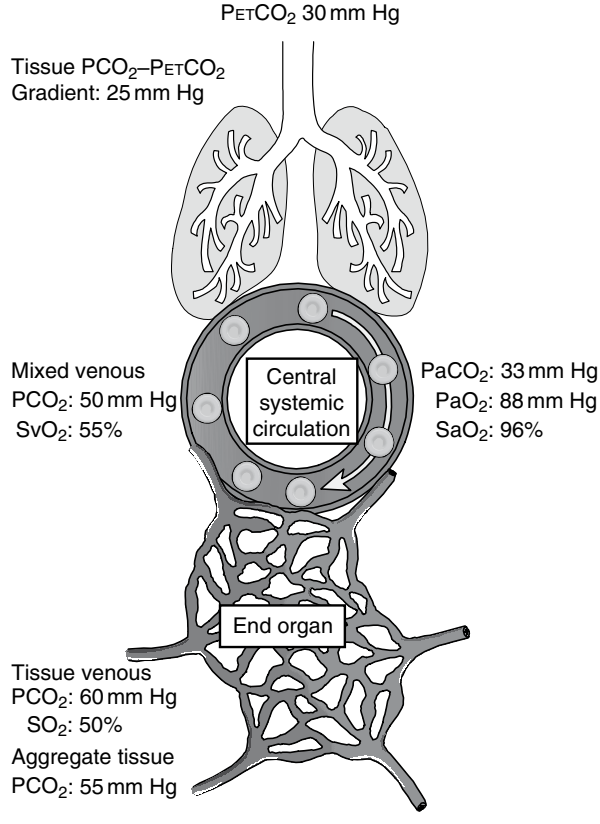

Figure 24.4 Representative blood and tissue gas levels of compensated or early shock states. Note that $P_{ET}CO_2$ and arterial gas levels are not significantly altered despite abnormal values in the tissues. Examination of the $P_{ET}CO_2$ to tissue PCO_2 gradient of a sensitive tissue bed has been demonstrated to be capable of detecting early shock states and ensuring adequate resuscitation, as well as preventing misinterpretation of the tissue PCO_2 due to alterations in minute ventilation. See text for potential tissue PCO_2 measurements. Gradients greater than 11 mm Hg are believed to be abnormal.

In actual practice, neither $\dot{V}O_2$ nor $\dot{V}CO_2$ is commonly monitored in the acute setting for several reasons [3]. To do so would require use of a metabolic cart and indirect calorimetry, or a pulmonary artery catheter and use of derivatives of the Fick method. Neither is currently practical, especially in the prehospital setting or emergency department. However, as the relationship between $P_{ET}CO_2$ and $\dot{V}CO_2$, and hence $\dot{V}O_2$, is sufficiently coupled to allow $P_{ET}CO_2$ to be used as a monitoring tool in shock, there is opportunity to gain insight into the underlying physiologic status of the patient. To accomplish this, both alveolar ventilation (minute ventilation) and $\dot{V}CO_2$ must be relatively constant, in which case changes in $P_{ET}CO_2$ will reflect changes in pulmonary capillary blood flow (PCBF ≈ CO), the major component of DO_2.

Although $\dot{V}CO_2$ production during shock is difficult to measure, wide swings in the RQ to affect the general coupling between $\dot{V}O_2$ and $\dot{V}CO_2$ are not likely. The tissue hypercarbia that occurs during shock states is reflected in venous blood, including that collected from the pulmonary artery (Figures 24.3–24.5). The elevated concentrations of CO_2 in the mixed venous blood pool and increases in alveolar deadspace that routinely occur in severe shock states will ensure that small changes in $\dot{V}CO_2$ do not cause appreciable changes in $P_{ET}CO_2$ [8]. Only greatly enhanced DO_2 will result in a dramatic and sustained increase in $\dot{V}CO_2$, and hence $P_{ET}CO_2$. To make CO_2 monitoring most meaningful in this setting minute ventilation should thus be held relatively constant if $P_{ET}CO_2$ is to be used as an indicator of CO.

Sudden decreases in $P_{ET}CO_2$ when no changes in ventilation have been made can be interpreted as a

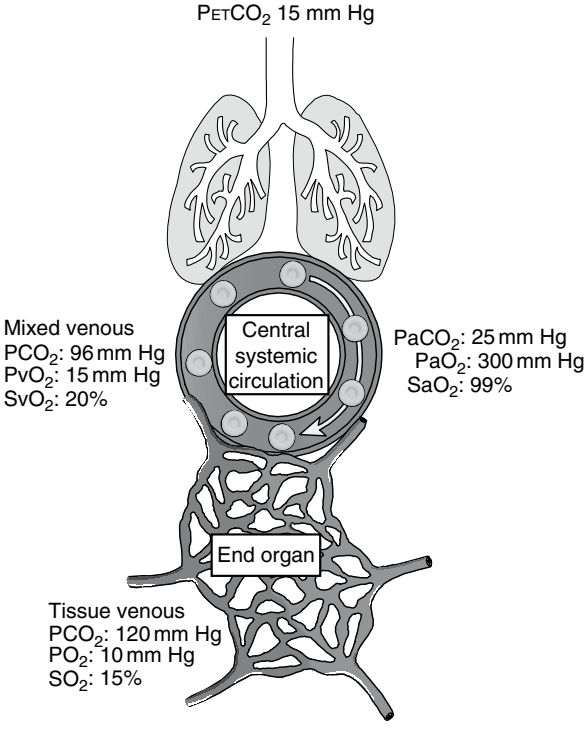

Figure 24.5 Representative blood and tissue gas levels of severe uncompensated shock states such as cardiac arrest or massive hemorrhage. Due to the tremendous reductions in blood flow produced, large deadspace in the lungs is created, thus producing gaps between mixed venous PCO_2, $PETCO_2$, and $PaCO_2$. The severe reductions in DO_2 to each organ system results in very high oxygen extraction at the level of the tissue that produces very low tissue venous PO_2, and thus SO_2 levels. The very high venous PCO_2 levels are due to both decreased removal of aerobically and anaerobically produced CO_2 (see Figure 24.2). As with Figure 24.3, the mixed venous values represent aggregate values of all organ systems.

significant deterioration in CO consistent with returning to a state below DO_2crit [10,11]. In these instances, a state of profound shock is developing, and the patient is sustaining significant levels of oxygen debt. Conversely, utilizing these principles, $PETCO_2$ has even been used to track the progress of patients in cardiogenic shock who are being treated with percutaneous cardiopulmonary assist systems, and has been shown to predict survival and the ability to wean patients from the assist system [16]. Another interesting use of $PETCO_2$ in this regard is the use of the $PaCO_2$–$PETCO_2$ gradient in the immediate post-resuscitation phase of cardiac arrest to assess global heart function. The $PaCO_2$–$PETCO_2$ gradient is, of course, an indicator of alveolar deadspace ventilation [17]. Elevated deadspace ventilation in the post-arrest period indicates a condition of worsened cardiogenic performance, and consequently significantly greater mortality for patients so affected.

Efforts are still under way to use $PETCO_2$ monitoring alone to detect shock and hypoperfusion in spontaneously breathing individuals suspected of hemorrhage or sepsis [18–20]. However, while low $PETCO_2$ values seem to correlate with shock states in spontaneously breathing subjects, they are not specific, as hyperventilation caused by fever, pain, other respiratory problems, or as a physiologic compensation to acid–base abnormalities or hypovolemia, can all present individually or together, and do not necessarily correlate with the patient exceeding the DO_2crit threshold.

Tissue-specific monitoring

Figures 24.1 and 24.2 demonstrate the biphasic relationship between $\dot{V}O_2$ and $\dot{V}CO_2$ with DO_2 not only for the whole body, but also for individual organ systems, which may have DO_2crit values that differ from whole-body DO_2crit. Studies have demonstrated – for example in hemorrhagic and septic shock – that the DO_2crit of the splanchnic bed occurs at a higher global DO_2 than the DO_2crit of the whole body [15,21,22]. Given this factor, DO_2 alterations in an organ system, such as the splanchnic bed or even skin or muscle, could be detected even earlier by monitoring that organ's venous effluent for decreases in Hb oxygen saturation (as OER increases) or increases in the partial pressure of CO_2 in venous blood ($PvCO_2$) because CO_2 is removed less efficiently. In severe and sudden shock states, such as seen following massive hemorrhage or cardiac arrest, profound delivery-dependent $\dot{V}O_2$ is reached so that all organ systems rapidly exceed their DO_2crit values. In this state, each system would demonstrate evidence of profound tissue hypoxia and flow stagnation, represented by very low venous Hb oxygen saturation and elevated venous or tissue CO_2 levels. The advantage of monitoring one tissue over another in this setting is difficult to defend, and likely has no advantage to monitoring $PETCO_2$ alone. In compensated or early states of shock, $PETCO_2$ monitoring will most likely not be capable of detecting changes. The same situation will exist when patients are resuscitated past their whole-body DO_2crit while individual tissue beds still suffer oxygen deficits. Upon increasing CO to levels that restore DO_2 above DO_2crit, $PETCO_2$ levels will transiently increase above baseline levels (35–45 mm Hg), sometimes to levels greater than 80 mm Hg as CO_2 from the tissues is removed and aerobic metabolism is restored. However, simply because $PETCO_2$ has normalized does not mean that tissues are adequately

oxygenated. $P_{ET}CO_2$ monitoring in compensated and post-resuscitation states can be beneficial when combined with measurement of tissue PCO_2.

Tissue CO_2 monitoring and perfusion

Several options to monitor tissue CO_2 in various shock states have been studied, and include transcutaneous CO_2 ($PtcCO_2$) skin monitoring, interstitial fiberoptic PCO_2, gastric mucosal CO_2 via gastric tonometry ($PgCO_2$), and, most recently, sublingual tonometry ($PslCO_2$) [23–31]. Monitoring $PtcCO_2$, $PgCO_2$, and $PslCO_2$ is non-invasive, while interstitial PCO_2 monitoring requires insertion of a probe into the tissue parenchyma. These techniques have been well described [31]. The methods are based on the diffusion of CO_2 from tissue, and reflect the balance between CO_2 supply to the tissue, CO_2 production by the tissue, and CO_2 removal from the tissue; this balance does not mean all tissue compartments contribute equally. The values will be a composite of vascular and interstitial levels in the immediate environment of the sensor. Given that approximately 70% of blood in tissues is venous, tissue CO_2 concentrations will mainly reflect venous PCO_2 [32,33]. The majority of CO_2 accumulation in each tissue will be secondary to the inability to remove aerobically produced CO_2 that was being produced prior to the actual onset of tissue dysoxia or ischemia (Figure 24.2). As mentioned previously, additional CO_2 will be produced in response to metabolic acids (mainly lactate).

Animal and human studies have demonstrated tissue CO_2 levels well over 100 mm Hg in shock states [26,27,34]. Widening of mixed venous to arterial PCO_2 differences reflect changes in tissue DO_2 [8,35]. Access to the mixed venous pool is not always practical and may not be as sensitive as properly selected "peripheral" tissue beds.

All of the above methods of tissue PCO_2 monitoring are sensitive to microcirculatory changes in blood flow not reflected in global DO_2 and $\dot{V}O_2$. Nevertheless, the goal of these measurements is to detect changes in tissue CO_2 as a reflection of changes in DO_2, and therefore, care must be taken not to misinterpret the values influenced by minute ventilation on tissue PCO_2 [36,37]. As normocapnia cannot be ensured in the initial stages of evaluation and resuscitation (especially if the patient is not intubated), use of the tissue CO_2-to-$PaCO_2$ gap is a more sensitive DO_2 measurement related to changes in tissue CO_2 because hypo- or hyperventilation, while affecting tissue CO_2, will not affect the gap [22,30]. Despite this factor, studies investigating approaches of buccal capnometry (tissue CO_2 measurement from the surface of the inner cheek) in settings such as hemorrhage are continuing [38,39]. In controlled laboratory settings, such techniques work extraordinarily well, but animals are mechanically ventilated or lack important injury components, such as significant soft tissue injury and pain.

Figure 24.6 provides a demonstration of these issues. Lower body negative pressure (LBNP) has been used as a hemorrhage mimetic in humans [40]. In this setting, subjects are placed in a chamber sealed around the waist. A typical LBNP protocol consists of a rest period (0 mm Hg), followed by 5 min of chamber decompression of the lower body to −15, −30, −45, and −60 mm Hg, and additional increments of −10 mm Hg every 5 min until subjects become symptomatic (lightheaded). Levels above −60 mm Hg may be associated with as much as 1000 mL of volume displacement from the central circulation into the lower extremities. Subjects are allowed to breathe spontaneously. In this setting, $P_{ET}CO_2$ was measured. $PtcCO_2$ of the skin was measured as an indicator of end-organ perfusion. As Figure 24.6 demonstrates, $P_{ET}CO_2$ decreases during LBNP as subjects begin to hyperventilate. The hyperventilation actually causes $PtcCO_2$ to decrease, but the $PtcCO_2$–$P_{ET}CO_2$ gap widens, indicating tissue hypoperfusion [41]. This is also confirmed using the venous PCO_2 to arterial PCO_2 gap which widens as well (not shown in Figure 24.6). Lactate levels do not change, indicating that the model does not produce a frank state of shock but, instead, provokes compensatory responses to the acute hypovolemia that can be detected with capnography. In this model, the $P_{ET}CO_2$ changes themselves were too variable around baseline values to be of clinical usefulness in detecting hypovolemia [19]. Again, use of the gap appears to be a better strategy.

Given that the arterial-to-alveolar PCO_2 gap is approximately 4 mm Hg, an abnormal tissue-to-$P_{ET}CO_2$ gap of 11 mm Hg to 14 mm Hg suggests perfusion abnormalities [30]. However, this gap has only been studied for gastric tonometry. Gaps for other tissue beds (such as $PtcCO_2$) of the skin or sublingual mucosa will require additional study. Nonetheless, continued elevation of tissue CO_2 resulting from decreases in tissue DO_2 as measured by these methods have been associated with increased mortality [23,26,27,42,43].

Normalization of the tissue CO_2-to-$P_{ET}CO_2$ gap, as a means to maintain adequate resuscitation, will help

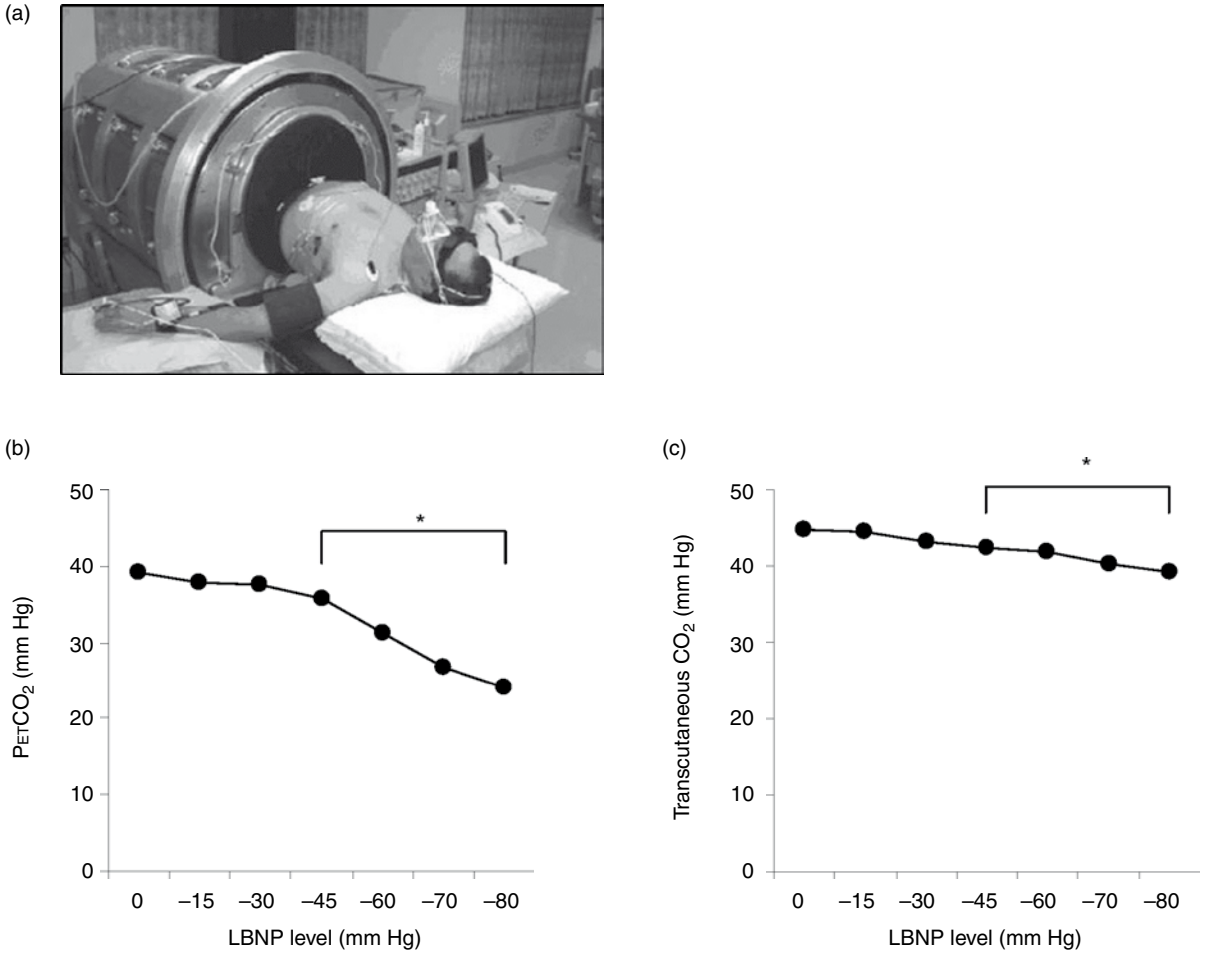

Figure 24.6 (a) Example of a lower body negative pressure (LBNP) device similar to an iron lung that encases the body from the lower thorax to the feet. It can be used to cause a stepwise increase of LBNP that pulls central blood volume into the lower body. (b, c) Changes in $P_{ET}CO_2$ and transcutaneous CO_2 ($PtcCO_2$) during LBNP in 20 subjects. Note the decrease in both $P_{ET}CO_2$ and $PtcCO_2$ during progressive LBNP. The $PtcCO_2$–$P_{ET}CO_2$ gap widens, indicating tissue hypoperfusion; thus the importance of measuring the gap when minute ventilation is not controlled. Brackets with an * represent points of significant change compared to baseline (0 mm Hg) levels.

circumvent occult tissue hypoxia, thereby avoiding further accumulation of oxygen debt and its associated complications. Both mucosal CO_2-to-$P_{ET}CO_2$ gap and mucosal CO_2 to arterial CO_2 gap are independent predictors of outcome in the resuscitation of the septic patient [44]. The major problem with using this strategy may be in patients who have rapidly evolving acute lung injury or who are experiencing significant bronchospasm.

Summary

In shock, oxygen delivery to tissue falls behind oxygen demand and CO_2 production decreases in lockstep. Eventually, metabolic acidosis liberates CO_2. These processes differ in magnitude in different organs and vascular beds, thus complicating the interpretation of global CO_2 data. Nevertheless, monitoring $P_{ET}CO_2$ tensions in shock and during resuscitation can be beneficial to the physician by providing insight into the complexity and evolution of the pathophysiology of shock in a $P_{ET}CO_2$-monitored patient.

References

1. Abraham E, Bland RD, Cobo JC, Shoemaker WC. Sequential cardiorespiratory patterns associated with outcome in septic shock. *Chest* 1984; **85**: 75–80.
2. Schumacker PT, Cain SM. The concept of a critical oxygen delivery. *Intens Care Med* 1987; **13**: 223–9.

3. Chittock DR, Ronco JJ, Russell JA. Monitoring of oxygen transport and oxygen consumption. In: Tobin MJ (ed.) *Principles and Practice of Intensive Care Monitoring*. New York: McGraw-Hill, 1998; 317–43.
4. Vincent JL. Lactate and biochemical indexes of oxygenation. In: Tobin MJ (ed.) *Principles and Practice of Intensive Care Monitoring*. New York: McGraw-Hill, 1998; 369–76.
5. Shoemaker WC, Appel PL, Kram HB. Tissue oxygen debt as a determinant of lethal and nonlethal postoperative organ failure. *Crit Care Med* 1988; **16**: 1117–20.
6. Shoemaker WC, Appel PL, Kram HB. Role of oxygen debt in the development of organ failure sepsis, and death in high-risk surgical patients. *Chest* 1992; **102**: 208–15.
7. Hindman BJ. Sodium bicarbonate in the treatment of subtypes of acute lactic acidosis: physiologic considerations. *Anesthesiology* 1990; **72**: 1064–76.
8. Weil MH, Rackow EC, Trevino R, *et al.* Difference in acid–base state between venous and arterial blood during cardiopulmonary resuscitation. *N Engl J Med* 1986; **315**: 153–6.
9. Relman AS. Difference in acid–base state between venous and arterial blood during cardiopulmonary resuscitation [letter]. *N Engl J Med* 1986; **315**: 1618.
10. Dubin A, Murias G, Estenssoro E, *et al.* End-tidal CO_2 pressure determinants during hemorrhagic shock. *Intens Care Med* 2000; **26**: 1619–23.
11. Guzman JA, Lacoma FJ, Najar A, Kruse JA. End-tidal partial pressure of carbon dioxide as a non-invasive indicator of systemic oxygen supply dependency during hemorrhagic shock and resuscitation. *Shock* 1997; **8**: 427–31.
12. Schlichtig R, Mehta N, Gayowski TJ. Tissue-arterial PCO_2 difference is a better marker of ischemia than intramural pH (pHi) or arterial pH–pHi difference. *J Crit Care* 1996; **11**: 51–6.
13. Jin X, Weil MH, Sun S, *et al.* Decreases in organ blood flows associated with increases in sublingual PCO_2 during hemorrhagic shock. *J Appl Physiol* 1998; **85**: 2360–4.
14. Sato Y, Weil MH, Tang W. Tissue hypercarbic acidosis as a marker of acute circulatory failure (shock). *Chest* 1998; **114**: 263–74.
15. Schlichtig R, Bowles SA. Distinguishing between aerobic and anaerobic appearance of dissolved CO_2 in intestine during low flow. *J Appl Physiol* 1994; **76**: 2443–51.
16. Yoshida T, Watanabe M, Murakami M, Furukawa H, Nakahara H. End-tidal carbon dioxide monitoring indicates recovery from cardiogenic shock in patients receiving percutaneous cardiopulmonary support. *J Artif Organs* 2005; **8**: 63–6.
17. Moon SW, Lee SW, Cho SH, *et al.* Arterial minus end-tidal CO_2 as a prognostic factor of hospital survival in patients resuscitated from cardiac arrest. *Resuscitation* 2007; **72**: 219–25.
18. McGillicuddy DC, Tang A, Cataldo L, Gusev JM, Shapiro NI. Evaluation of end-tidal carbon dioxide role in predicting elevated SOFA scores and lactic acidosis. *Intern Emerg Med* 2009; **4**: 41–4.
19. McManus JG, Ryan KL, Morton MJ, *et al.* Limitations of end-tidal CO_2 as an early indicator of central hypovolemia in humans. *Prehosp Emerg Care* 2008; **12**: 199–205.
20. Whalen BM, Bey T, Wolke BB. Measurement of end-tidal carbon dioxide in spontaneously breathing patients in the pre-hospital setting: a prospective evaluation of 350 patients. *Resuscitation* 2003; **56**: 35–40.
21. Schlichtig R, Kramer DJ, Pinsky MR. Flow redistribution during progressive hemorrhage is a determinant of critical O2 delivery. *J Appl Physiol* 1991; **70**: 169–78.
22. Bowles SA, Schlichtig R, Kramer DJ, Klions HA. Arteriovenous pH and partial pressure of carbon dioxide detect critical oxygen delivery during progressive hemorrhage in dogs. *J Crit Care* 1992; **7**: 95–105.
23. Tremper KK, Mentelos RA, Shoemaker WC. Effect of hypercarbia and shock on transcutaneous carbon dioxide at different electrode temperatures. *Crit Care Med* 1980; **8**: 608–12.
24. Tremper KK, Shoemaker WC, Shippy CR, Nolan LS. Transcutaneous PCO_2 monitoring on adult patients in the ICU and the operating room. *Crit Care Med* 1981; **9**: 752–5.
25. Ivatury RR, Simon RJ, Islam S, *et al.* A prospective randomized study of end points of resuscitation after major trauma: global oxygen transport indices versus organ-specific gastric mucosal pH. *J Am Coll Surg* 1996; **183**: 145–54.
26. McKinley BA, Parmley CL, Butler BD. Skeletal muscle PO_2, PCO_2, and pH in hemorrhage, shock, and resuscitation in dogs. *J Trauma* 1998; **44**: 119–27.
27. McKinley BA, Ware DN, Marvin RG, Moore FA. Skeletal muscle pH, $P(CO_2)$, and $P(O_2)$ during resuscitation of severe hemorrhagic shock. *J Trauma* 1998; **45**: 633–6.
28. Nakagawa Y, Weil MH, Tang W, *et al.* Sublingual capnometry for diagnosis and quantitation of circulatory shock. *Am J Respir Crit Care Med* 1998; **157**: 1838–43.
29. Weil MH, Nakagawa Y, Tang W, *et al.* Sublingual capnometry: a new non-invasive measurement for diagnosis and quantitation of severity of circulatory shock. *Crit Care Med* 1999; **27**: 1225–9.

30. Hurley R, Chapman MV, Mythen MG. Current status of gastrointestinal tonometry. *Curr Opin Crit Care* 2000; **6**: 130–5.
31. Ward KR, Ivatury RR, Barbee RW. Endpoints of resuscitation for the victim of trauma. *J Intens Care Med* 2001; **16**: 55–75.
32. Guyton AC. The systemic circulation. In: Guyton AC (ed.) *Textbook of Medical Physiology,* 6th edn. Philadelphia, PA: WB Saunders, 1981; 219–34.
33. Shepherd JT. Circulation to skeletal muscle. In: Shepherd JT, Abboud FM, Geiger SR (eds.) *Handbook of Physiology*, vol. 3. Bethesda, MD: American Physiology Society, 1983; 319–70.
34. von Planta M, Weil MH, Gazmuri RJ, Bisera J, Rackow EC. Myocardial acidosis associated with CO_2 production during cardiac arrest and resuscitation. *Circulation* 1989; **80**: 684–92.
35. Rackow EC, Astiz ME, Mecher CE, Weil MH. Increased venous–arterial carbon dioxide tension difference during severe sepsis in rats (see comments). *Crit Care Med* 1994; **22**: 121–5.
36. Guzman JA, Kruse JA. Gut mucosal–arterial PCO_2 gradient as an indicator of splanchnic perfusion during systemic hypo- and hypercapnia. *Crit Care Med* 1999; **27**: 2760–5.
37. Pernat A, Weil MH, Tang W, *et al.* Effects of hyper- and hypoventilation on gastric and sublingual PCO_2. *J Appl Physiol* 1999; **87**: 933–7.
38. Cammarata GA, Weil MH, Castillo CJ, *et al.* Buccal capnometry for quantitating the severity of hemorrhagic shock. *Shock* 2009; **31**: 207–11.
39. Pellis T, Weil MH, Tang W, *et al.* Increases in both buccal and sublingual partial pressure of carbon dioxide reflect decreases in tissue blood flows in a porcine model during hemorrhagic shock. *J Trauma* 2005; **58**: 817–24.
40. Cooke WH, Ryan KL, Convertino VA. Lower body negative pressure as a model to study progression to acute hemorrhagic shock in humans. *J Appl Physiol* 2004; **96**: 1249–61.
41. Tiba M, Ryan K, Torres I, *et al.* Oxygen transport characterization of a human model of hemorrhage. *Circulation* 2008; **118**: S1447.
42. McKinley BA, Butler BD. Comparison of skeletal muscle PO_2, PCO_2, and pH with gastric tonometric P(CO2) and pH in hemorrhagic shock. *Crit Care Med* 1999; **27**: 1869–77.
43. Tatevossian RG, Wo CC, Velmahos GC, Demetriades D, Shoemaker WC. Transcutaneous oxygen and CO_2 as early warning of tissue hypoxia and hemodynamic shock in critically ill emergency patients (see comments). *Crit Care Med* 2000; **28**: 2248–53.
44. Poeze M, Solberg BC, Greve JW, Ramsay G. Monitoring global volume-related hemodynamic or regional variables after initial resuscitation: what is a better predictor of outcome in critically ill septic patients? *Crit Care Med* 2005; **33**: 2494–500.

Section 2
Chapter
25

Circulation, metabolism, and organ effects

Carbon dioxide production, metabolism, and anesthesia

D. Willner and C. Weissman

The human body is fueled by nutrients and oxygen (O_2) that are metabolized to energy, carbon dioxide (CO_2), and waste products (see Figure 25.1). The amounts of O_2 consumed and CO_2 produced reflect the rate of body metabolism and the types of nutrients metabolized. The tasks of the respiratory and cardiovascular systems are to ensure that the cells of the body receive sufficient O_2 and adequate amounts of CO_2 are removed. The result of these interactions is tight coupling between the respiratory, cardiovascular, and metabolic systems. Therefore, when interpreting measurements of CO_2 production and O_2 consumption, it is important to consider the interaction of these systems.

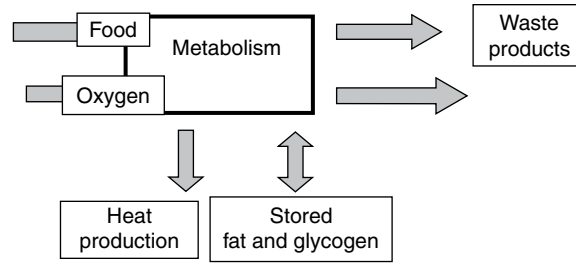

Figure 25.1 Total body metabolism.

Production of CO_2 and consumption of O_2

Biochemistry and physiology

The overall amount of O_2 consumed and CO_2 produced by the human body depends on the rate of metabolism, while the proportion of O_2 consumed to CO_2 produced depends on the type of nutrients being metabolized or synthesized. Each cell type and organ system has a different metabolic function and, as a result, has different metabolic rates and nutrient requirements. Therefore, measurements of *whole-body* O_2 consumption and CO_2 production reflect the sum of the quantity and types of O_2-consuming and CO_2-producing activities of the various cell and organ systems of the body.

Nutrient metabolism: oxidation

The cells of the body metabolize carbohydrates, lipids, and proteins to produce energy in the form of high-energy phosphates (adenosine triphosphate, ATP). This is accomplished through both anaerobic and aerobic metabolism; the latter consumes O_2 and produces CO_2, while the former only produces CO_2. The oxidation of each of these nutrients is unique, resulting in the consumption of different amounts of O_2, the production of differing amounts of CO_2, and an assortment of waste products. The process of producing ATP, called *oxidative phosphorylation*, involves the conversion of these nutrients into acetyl-coenzyme A (acetyl-CoA). Acetyl-CoA then enters the citric acid cycle, which consumes O_2, liberates free energy as ATP, and produces H_2O and CO_2 as waste products.

Ingested carbohydrates are converted to glucose. Glucose oxidation consumes and produces equal numbers of O_2 and CO_2 molecules, respectively:

$$C_6H_{12}O_6 + 6O_2 \rightarrow 6CO_2 + 6H_2O + \text{energy}. \quad (25.1)$$

However, not all the carbohydrates ingested during a meal and converted to glucose are oxidized. Woerle *et al.* [1] reported that in the postprandial period, approximately 44% of the glucose is oxidized, ~45% is converted to glycogen, and the remainder undergoes non-oxidative metabolism to lactate, pyruvate, and alanine [2].

Fats are stored in the body as triglycerides. Triglycerides are hydrolyzed to free fatty acids and glycerol. The glycerol is converted to glucose and metabolized as a carbohydrate. The free fatty acids undergo beta-oxidation in the mitochondria. Unlike glucose oxidation, fatty acid beta-oxidation results in the consumption of more molecules of O_2 than molecules of

Capnography, Second Edition, ed. J. S. Gravenstein, Michael B. Jaffe, Nikolaus Gravenstein, and David A. Paulus. Published by Cambridge University Press. © Cambridge University Press 2011.

CO_2 produced (equation 25.2). The ratio of O_2 consumed to CO_2 produced during long-chain fatty acid oxidation is 0.71. This reaction also produces more than twice the energy (9.4 kcal/g for long-chain triglycerides and 8.3 kcal/g for medium-chain triglycerides) produced by the oxidation of either glucose (3.72 kcal/g) or amino acids/protein (4 kcal/g) [3]:

$$\text{Palmitate} + 23O_2 + 129\text{ADP} + 129\text{P}i \rightarrow 16CO_2 + 145H_2O + 129\text{ATP}. \quad (25.2)$$

Amino acids, the basic components of proteins, can also be used as energy substrates. They undergo deamination, resulting in amino nitrogen being removed and metabolized to urea. The remaining carbon skeletons are oxidized by the citric acid cycle to CO_2 and H_2O. The oxidation of 1 g of protein consumes 0.965 L of O_2 and produces 0.781 L of CO_2, leading to a ratio of CO_2 produced to O_2 consumed of 0.8.

Lipogenesis

De novo synthesis of fatty acids from carbohydrate is called *lipogenesis*, and occurs in humans ingesting carbohydrates in excess of their daily energy expenditure (EE). Glucose is converted to acetyl-CoA and then synthesized to fatty acids. The ratio of CO_2 produced to O_2 consumed is 8.0–8.7, depending on the fatty acid synthesized. This equation approximates lipogenesis:

$$13C_6H_{12}O_6 + 3O_2 \rightarrow C_{55}H_{104}O_6 + 26CO_2 + 29H_2O \quad (25.3)$$

Energy and CO_2 production

Substrate metabolism produces energy and CO_2. The amount of CO_2 produced when 1 kcal is produced from the oxidation of 1 g of CHO is 200 mL, which is greater than that produced when either 1g of lipid (157 mL) or protein (191 mL) is oxidized. Therefore, and importantly, the energy produced from carbohydrates presents a greater respiratory burden since more CO_2 needs to be eliminated [4].

CO_2 stores

The body stores CO_2, but not O_2. Consequently, it is necessary to continuously breathe to provide O_2 to the cells. The body stores about 12–14 L (210 mL CO_2/kg) of CO_2 in a number of locations and forms [4]. A large pool is bound to hemoglobin, and exists as bicarbonate in the extracellular fluid; each liter of aqueous body fluid contains the equivalent of 500 mL of CO_2. CO_2 is also stored as carbonates in bone.

CO_2 production*/elimination**

$$\dot{V}CO_2 = (V_E \times F\bar{e}CO_2) - (V_I \times F\bar{i}CO_2)$$

$$\dot{V}CO_2 = V_E (F\bar{e}CO_2 - F\bar{i}CO_2) \quad \text{(assuming that } V_I = V_E\text{)}$$

where
V_E: expired minute ventilation
V_I: inspired minute ventilation
$F\bar{e}CO_2$: mixed expired CO_2 concentration
$F\bar{i}CO_2$: mixed inspired CO_2 concentration

O_2 consumption*/uptake**

$$\dot{V}O_2 = (V_I \times F\bar{i}O_2) - (V_E \times F\bar{e}O_2)$$

$$\dot{V}O_2 = V_E (F\bar{i}O_2 - F\bar{e}O_2) \quad \text{(assuming that } V_I = V_E\text{)}$$

where
$F\bar{i}O_2$: mixed inspired O_2 concentration
$F\bar{e}O_2$: mixed expired O_2 concentration

Respiratory quotient (RQ)*/respiratory exchange ratio (R)**

$$RQ = \frac{\dot{V}CO_2}{\dot{V}O_2}$$

*Steady-state measurement
**Nonsteady-state measurement

Figure 25.2 Formulae for metabolic calculations.

Production of CO_2 versus elimination of CO_2

Human lungs excrete almost all the CO_2 produced, with only a miniscule amount excreted through the skin [5]. It is, thus, possible to calculate the amount of CO_2 excreted by measuring the difference between the inspired and expired CO_2 contents (see Figure 25.2). Such measurements reflect body CO_2 production only if the subject is in a steady state. In non-steady-state situations, these measurements reflect the pulmonary elimination of CO_2 at that point in time. The eliminated CO_2 may originate from CO_2 produced by metabolism, and released from the CO_2 stores of the body and from the CO_2 in the blood (dissolved or carried by hemoglobin).

To measure true resting/basal CO_2 production, i.e., the amount of CO_2 produced by metabolism, requires that the human subject be in a steady state [6]. A *steady state* is a condition in which the output of the metabolic, cardiovascular, and respiratory systems is stable so that O_2 uptake ($\dot{V}O_2$) and CO_2 excretion/elimination ($\dot{V}CO_2$) by the lungs reflect metabolic activity. To achieve a steady state, a subject should be lying motionless and awake in a comfortable, quiet, thermoneutral

(25 °C) environment while not actively digesting food. *Thermoneutrality* is an environmental temperature in which heat production is not stimulated above baseline values [7]. Measurements are considered steady-state values once the $\dot{V}CO_2$ and $\dot{V}O_2$ values are stable, that is, when they change ≤10% over a period of at least 4–5 consecutive minutes [8,9].

Non-steady-state conditions frequently occur while performing measurements of $\dot{V}CO_2$ and $\dot{V}O_2$ [10]. In such cases, measurements of CO_2 output will not reflect metabolism, but reflect the amount of CO_2 being eliminated through the lungs. A classic example is acute hyperventilation caused by anxiety or discomfort, which results in a transient increase in pulmonary CO_2 excretion and decrease in $PaCO_2$ [11]. Alternately, with the onset of hypoventilation, a transient decrease in CO_2 elimination occurs, but reverses once the alveolar CO_2 concentration rises to a new steady state. Similarly, a decrease in cardiac output transiently decreases the pulmonary elimination of CO_2, which remains low until the CO_2 concentration in the mixed venous blood rises to a new steady state. Changes in mechanical ventilator settings resulting in increases or decreases in minute ventilation in paralyzed and sedated mechanically ventilated patients produce unstable $\dot{V}CO_2$ measurements for at least 120 min [12].

Human metabolism normally operates as a system of supply and demand. Changes in metabolic demand – for example, exercise – require an increase in the O_2 supply to the tissues and the amount of CO_2 removed from them. Therefore when interpreting measurements of $\dot{V}CO_2$ and $\dot{V}O_2$, the present state of activity, conditions of environment, and health status must be considered (Figure 25.1). During all types of exercise, $\dot{V}O_2$ and $\dot{V}CO_2$ increase as the result of increased intramuscular activity. As exercise loads increase, $\dot{V}CO_2$ and $\dot{V}O_2$ increase in parallel until the anaerobic threshold is reached. Above this threshold, $\dot{V}CO_2$ continues to increase, but not $\dot{V}O_2$. Even simple exercise, such as elevating arms to shoulder level in seated subjects, can increase $\dot{V}CO_2$ by 35% [13]; therefore, it is important to observe the activity state of the subjects when measuring $\dot{V}CO_2$ and $\dot{V}O_2$ [14,15]. Similarly, subjects in a cold environment will increase metabolic rate in order to maintain body heat, initially by tensing muscles and then by overt shivering. The latter can increase metabolic rate by up to 400%.

A number of additional factors must be considered when measuring and interpreting CO_2 production/elimination measurements. Another source of CO_2 elimination through the lungs is that produced by colonic bacterial fermentation in the presence of lactulose and similar substances [16,17]. Bicarbonate ions are also produced during the catabolism of glutamine. These ions may then be converted to CO_2 and eliminated by lungs. The contribution of this CO_2 to overall CO_2 production is still unclear [18]. The administration of sodium bicarbonate for the treatment of acidosis will greatly increase the elimination of CO_2 as the bicarbonate is metabolized to CO_2. The infusion of 1.5 mmol/kg of sodium bicarbonate over 5 min caused an acute increase in CO_2 production over 5 min that returned to baseline only after 30 min. The increase in $\dot{V}CO_2$ was dependent on the patient's serum albumin and hemoglobin concentrations, which act as non-bicarbonate buffers of H^+ ions. The higher the blood concentrations of albumin and hemoglobin, the greater the CO_2 release [19].

When measuring CO_2 production, gas leaks around endotracheal tubes, such as occur in the pediatric population, render measurements inaccurate due to loss of expiratory minute ventilation [20]. Leaks in ventilator tubing and its connections cause similar losses of minute ventilation, and render metabolic measurements inaccurate.

CO_2 production and metabolism

Direct versus indirect calorimetry

A subject's metabolic (caloric) expenditure can be directly quantified by measuring whole-body heat loss. Alternately, it can be measured indirectly by measuring O_2 consumption and CO_2 production:

$$\left.\begin{matrix}A\\B\\C\end{matrix}\right\} + O_2 + ADP \rightarrow Heat + CO_2 + H_2O + ATP.$$

A = Lipids; B = Carbohydrates; C = Proteins. (25.4)

Direct calorimetry involves measuring body heat loss by placing the subject in a closed chamber around which water of a known temperature flows. Body heat production is calculated from the increase in water temperature caused by the heat produced by the subject. This method is not practical for clinical use. Consequently, an indirect approach to measuring body EE was developed. The amount of energy used to consume a specific amount of O_2 and produce a given amount of CO_2 was calculated and validated by

simultaneous direct and indirect calorimetry. These simultaneous measurements led Weir [21] to develop an equation (25.5) to calculate EE from measurements of $\dot{V}O_2$ and $\dot{V}CO_2$:

$$EE\ (kcal/day) = 1.44\ (3.9 \times \dot{V}O_2 + 1.1 \times \dot{V}CO_2). \quad (25.5)$$

Simultaneous measurements of nitrogen losses (mainly from the urine and feces), when combined with $\dot{V}O_2$ and $\dot{V}CO_2$ measurements, allow the calculation of substrate utilization, specifically, calculation of the amounts of protein, lipid, and carbohydrates oxidized.

Energy (caloric) expenditure

Energy expenditure is categorized as basal, resting, total, activity, or sleeping, depending upon when the measurements are made. The classic research measurement, the basal metabolic rate, is made at basal steady-state conditions. Basal conditions are defined as lying awake and motionless in a thermoneutral environment immediately upon awakening in the morning, i.e., before breakfast. Such measurements are practical only in research environments and not in the clinical arena. Therefore, most clinical measurements are made at resting conditions: lying in a comfortable (24–26 °C) and quiet environment, 3–4 h after a meal. The exception to the latter are patients receiving continuous enteral or parenteral nutrition, whose resting measurements are made once the nutritional intake has been stable for at least 12 h. Resting EE is about 10% higher than basal expenditure ($\dot{V}CO_2$ is about 2–3 mL/kg and $\dot{V}O_2$ is about 3–4 mL/kg). The measurement for resting EE is obtained 3–4 h after meals due to the phenomenon of diet-induced thermogenesis. After ingesting foodstuffs, $\dot{V}O_2$ and $\dot{V}CO_2$ increase by 15–20% for 1–3 h, generated by the oxidation of food and other factors. The magnitude of diet-induced thermogenesis after a protein meal is greater than one composed of fat or carbohydrates. Medium-chain triglycerides cause greater diet-induced thermogenesis than long-chain triglycerides [22].

Total EE is determined by an individual's basal EE, physical activities, dietary intake, and environment (Figure 25.3) [6]. Sleep, which occupies one-third or more of a normal subject's day, decreases EE by 10–15% from basal values for much of the night; EE then begins to increase towards morning. Some, but not all [23], investigators have reported that O_2 consumption and CO_2 production increase during rapid eye movement (REM) sleep. The degree and type of physical activity performed during the waking hours is a major factor that influences the total daily EE. Individuals with sedentary lifestyles expend much less energy than do physical laborers.

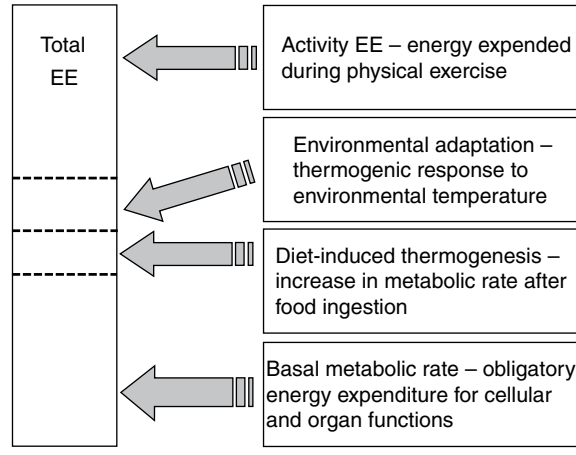

Figure 25.3 Total EE and its components.

CO_2 production and anesthesia

Anesthesia and surgery greatly affect body homeostasis and, consequently, alter the performance of the respiratory, cardiovascular, and metabolic systems, which influences the elimination of CO_2 from the human body. During anesthesia, the principal factors that influence blood CO_2 concentrations are the inspired CO_2 concentration, $\dot{V}CO_2$, and alveolar ventilation. The concentration of CO_2 in the inspired gas is normally close to zero, but may be increased accidentally or intentionally. The level of $\dot{V}CO_2$ may be influenced by anesthesia, type of surgery, and underlying pathologic state.

Minute volume varies widely during anesthesia and surgery. Lower minute volumes occur during spontaneous breathing while under deep anesthesia or partial neuromuscular blockade. Alternately, during mechanical ventilation, very high minute volumes may be attained. In anesthetized, spontaneously breathing patients, surgical stimulation can increase ventilation. At various concentrations of inhalational anesthetics, Eger *et al.* [24] demonstrated that stimulation from the surgical incision produced an increase in alveolar ventilation, resulting in a decrease in resting $PaCO_2$ by as much as 10 mm Hg. In addition, the duration of anesthesia plays a role in CO_2 homeostasis. Anesthesia, similar to sleep, reduces the total-body metabolic rate, causing $\dot{V}CO_2$ to diminish [25]. Fourcade *et al.* [26]

observed that during halothane and enflurane anesthesia, the resting $PaCO_2$ after 6 h was lower than after both anesthesia induction and 3 h of anesthesia. Further indication that anesthesia directly decreases CO_2 production was reported in other studies which found that enflurane caused a 9% decrease in $\dot{V}CO_2$ during anesthesia and surgery, and returned to preoperative values after surgery [27,28]. Similarly, $\dot{V}O_2$ and $\dot{V}CO_2$ decreased 12–15% during halothane and isoflurane anesthesia (with or without surgery). Thus, it appears that anesthesia produced by inhalational agents depresses $\dot{V}CO_2$. Others observed the influence of age, weight, type of surgery, premedication, caudal anesthesia, and different inhalation anesthetics on $\dot{V}CO_2$. Infants weighing 5 kg had decreased $\dot{V}CO_2$ per kilogram during anesthesia. Increased $\dot{V}CO_2$ per kilogram was measured in a body weight up to 10 kg. Above a 10-kg body weight, the amount of $\dot{V}CO_2$ per kilogram decreased, and continued to decrease with increasing age [29]. These findings were supported by other investigators who also observed that children in their teens, although they may have attained adult body weight, had a greater $\dot{V}CO_2$ per kilogram body weight than adults during anesthesia [30].

The proposed mechanism for the age-dependent variation in $\dot{V}CO_2$ per kilogram may result from partial inhibition by halothane of lipolysis in brown adipose tissue [31]. This tissue is rich in blood vessels and consumes more O_2 than other tissues. The amount of brown adipose tissue is greater in younger than older infants. Lipolysis and fat mobilization result in greater $\dot{V}CO_2$ and, therefore, halothane inhibition of lipolysis can explain the decrease in $\dot{V}CO_2$ observed in young infants.

There are few data on the influence of anesthesia and anesthetic drugs on metabolic gas exchange during surgery. Lind [32] examined the influence of different surgical procedures on $\dot{V}O_2$ and $\dot{V}O_2$. He compared emergency laparotomy, elective laparotomy; knee arthroscopy, and gynecological laparoscopy (a propofol infusion was used to maintain anesthesia), and found a significant increase in $\dot{V}O_2$ from the time of pre-skin incision to 5 min after skin incision. The greatest increase in $\dot{V}O_2$ was seen during elective laparotomy. $\dot{V}CO_2$ increased both in the laparoscopy group and, transiently, in the elective laparotomy group, but decreased in the other two groups. In the laparoscopy group, the elevated CO_2 production likely represented CO_2 absorption from CO_2 insufflation of the peritoneal cavity. Pestana *et al.* [33] compared the metabolic gas exchange pattern in patients receiving propofol and midazolam for induction and maintenance of anesthesia. He also compared values in patients anesthetized with midazolam but who were receiving a 10% intralipid infusion (the vehicle for propofol) during the anesthesia to evaluate the direct effect of propofol. $\dot{V}O_2$ increased significantly in all groups at 45 min with respect to basal measurements, and remained elevated throughout the study, possibly due to surgical stress. $\dot{V}CO_2$ decreased gradually during anesthesia. There was a significant decrease in $\dot{V}CO_2$ in all the groups, but largest in the groups receiving propofol or midazolam with intralipid. A plausible explanation is greater lipid oxidation because fat oxidation results in a lower $\dot{V}CO_2$ than the oxidation of proteins or carbohydrates.

A number of studies examined the effects of clonidine, an alpha-2 adrenergic agonist, and midazolam premedication during ketamine anesthesia. Preoperative $\dot{V}O_2$ and $\dot{V}CO_2$ decreased more with clonidine and midazolam premedication than with placebo [34–36]. Intraoperative $\dot{V}O_2$ and $\dot{V}CO_2$ values were increased more in the midazolam group than in the clonidine and placebo groups. Midazolam did not prevent a ketamine-induced increase in catecholamines, nor did it attenuate the catecholamine response to surgery, which probably contributed to the higher observed intraoperative $\dot{V}O_2$ and $\dot{V}CO_2$. Others observed that clonidine was associated with attenuation of the increase in $\dot{V}O_2$ and $\dot{V}CO_2$ commonly observed during recovery from anesthesia [37]. The results regarding midazolam appear to conflict with Harding *et al.* [38] who observed attenuated metabolic, hemodynamic, and ventilatory responses to chest physical therapy after midazolam administration.

Only a few studies have examined the effects of regional and general anesthesia on $\dot{V}O_2$ and $\dot{V}CO_2$. Watters *et al.* [39] compared the effects on EE of combined general and epidural anesthesia, and general anesthesia alone. The study found that $\dot{V}O_2$ and $\dot{V}CO_2$ increased following surgery in both groups for the first two postoperative days despite the visual analog pain scale scores being clearly lower in the patients receiving epidural anesthesia. Similar results were obtained by Tulla *et al.* [40] who found no significant differences in postoperative $\dot{V}CO_2$ and $\dot{V}O_2$ whether hip surgery was performed under general or spinal anesthesia. Diebel *et al.* [41] reported less increase in $\dot{V}O_2$ after major thoracic surgery with epidural plus general anesthesia compared to general anesthesia alone. Viale *et al.* [42] reported only a transient postoperative reduction

in $\dot{V}O_2$ in patients receiving epidural analgesia after major abdominal surgery. These studies appear to indicate that the addition of epidural anesthesia to general anesthesia does not influence $\dot{V}CO_2$. Alternately, $\dot{V}CO_2$ was lower during surgery when 15 mL of 1% lidocaine and 2 mg morphine were administered through lumbar (L1–L2) epidural catheters prior to general anesthesia for laparoscopic hysterectomies than when no epidural medications were administered [43].

The hemodynamic effects of epinephrine, when added to local epidural anesthetics, are well documented. However, little is known about the influence of epinephrine on respiratory gas exchange. Steinbrook and Concepcion [44] observed that the addition of epinephrine, 5 μg/mL, to the epidural injection of 2% lidocaine was associated with a 22% increase in $\dot{V}CO_2$ without a change in $\dot{V}O_2$, despite increases in heart rate and cardiac index. Epidural anesthesia without added epinephrine did not change $\dot{V}O_2$ or $\dot{V}CO_2$. In normal volunteers, there were no differences in the increases in $\dot{V}CO_2$ secondary to glucose infusion (4 mg/kg/min for 3 h) between those who had and did not have a thoracic epidural block with 0.5% bupivacaine from T7 to S1, thereby demonstrating that epidural blockade with local anesthetic in the absence of surgery does not affect fasting protein, or lipid or glucose metabolism [45]. Another study compared metabolic measurements before and after 3 h of feeding with intravenous amino acids and glucose on postoperative day 2 in patients following colectomy. Two groups were studied; one group received patient controlled analgesia and the other received epidural analgesia. Patients in the latter group had smaller increases in $\dot{V}CO_2$ in response to the feedings than those in the former group. This study showed that, postoperatively, epidural analgesia attenuated the $\dot{V}CO_2$ response to nutrients [46].

Neuromuscular blockade

A single dose of succinylcholine, a depolarizing muscle relaxant, significantly increased $\dot{V}CO_2$ 1 and 5 min after succinylcholine-induced fasciculations, but caused no demonstrable changes in $\dot{V}O_2$ [47]. This finding is interesting given that fasciculations produced by succinylcholine presumably increase EE, resulting in increased $\dot{V}O_2$ by skeletal muscle. A continuous infusion of succinylcholine in dogs increased $\dot{V}O_2$ due to increased skeletal activity [48]. Christensen *et al.* [49] observed an increase in $\dot{V}CO_2$ whether succinylcholine was administered as a bolus or as a continuous infusion. However, in patients pretreated with pancuronium, which prevents fasciculations, no increase in $\dot{V}CO_2$ was observed. Similarly, pretreatment with diazepam reduced the increase in $\dot{V}CO_2$ observed with succinylcholine [50]. It appears that the increase in $\dot{V}CO_2$ is a result of succinylcholine-induced muscle fasciculations, and not a direct metabolic effect of the drug.

Vernon and Witte [51] studied sedated, mechanically ventilated children and observed that neuromuscular blockade with non-depolarizing drugs caused a significant reduction in $\dot{V}O_2$ (8.7 vs. 1.7%) and EE (10.3 vs. 1.8%), and, hence, $\dot{V}CO_2$. The patients in this study were sedated, and there was no control group, so it was difficult to assess the exact influence of neuromuscular blockade on $\dot{V}O_2$ and $\dot{V}CO_2$.

CO_2 production/elimination and intraoperative events during anesthesia

Laparoscopy

During laparoscopy, the abdomen is frequently insufflated with CO_2. Therefore, the pulmonary CO_2 output is composed of both metabolically produced and exogenously introduced CO_2 absorbed from the peritoneal cavity. The CO_2 insufflated into the peritoneal cavity diffuses into the abdominal organs and abdominal wall. It is then carried by the blood to the lungs. Kasama *et al.* [52] observed that minute volume during pneumoperitoneum had to be increased by 1.54 times that of the prepneumoperitoneum phase in order to maintain a constant $PaCO_2$. Compared with preinduction values, $\dot{V}CO_2$ and $\dot{V}O_2$ decreased during the period of anesthesia until skin incision. However, with insufflation of CO_2 into the abdominal cavity, a marked (49%) increase in CO_2 output was observed while $\dot{V}O_2$ remained stable. These variables returned to preinduction levels during the recovery period. Consumption of O_2 increased during both gynecologic laparotomy and laparoscopy, while CO_2 production decreased in the laparotomy group and CO_2 output increased during laparoscopy [32]. At 10–20 min after abdominal insufflation with CO_2 in children, 10–20% of expired CO_2 was derived from the absorption of exogenous CO_2. The exogenous CO_2 continues to be eliminated for up to 30 min after desufflation [53]. Younger children warrant close monitoring during and after laparoscopy because they absorb proportionally more CO_2 than older children [54,55]. Other studies [56,57] reported similar results, with $\dot{V}O_2$ remaining stable but

$\dot{V}CO_2$ values increasing more during retroperitoneal than during intraperitoneal CO_2 insufflation, remaining elevated even after exsufflation. However, Kadam *et al.* [58] failed to find any differences in CO_2 elimination between retroperitoneal and transperitoneal donor nephrectomy. Increased CO_2 absorption was also observed in the total extraperitoneal approach to hernioplasty compared to a transabdominal preperitoneal approach [59]. Additionally, Liang *et al.* [60] suggested that intravenous propofol combined with epidural anesthesia for laparoscopic procedures can attenuate the increase in $\dot{V}CO_2$ caused by CO_2 insufflation.

Tourniquet release

Tourniquets are frequently used to provide a bloodless field during orthopedic surgery. Girardis *et al.* [61] examined the effect of tourniquet inflation duration on gas exchange during general anesthesia. During tourniquet inflation, $\dot{V}CO_2$ decreased slightly and $\dot{V}O_2$ remained stable compared to pretourniquet values, a state attributed to lack of arterial blood flow to the limb. Following tourniquet deflation $\dot{V}O_2$ and $\dot{V}CO_2$ increased, with peak values occurring after 5 min. At 15 min after tourniquet deflation, $\dot{V}CO_2$ returned to basal values, but $\dot{V}O_2$ continued to increase. Oxygen is not supplied to the limb during tourniquet inflation and, therefore, the energy for cellular metabolism is provided by anaerobic metabolism. Tourniquet release results in an increase in $\dot{V}O_2$ to replenish cellular O_2 supplies depleted during limb ischemia. These investigators observed that the magnitude of the $\dot{V}O_2$ increase after deflation was dependent on the duration of tourniquet inflation. However, other studies [62,63] seem to contradict these findings, claiming that the increase in $\dot{V}O_2$ and $\dot{V}CO_2$ seen after tourniquet release is related to muscle mass, and not the duration of tourniquet inflation. Takahashi *et al.* [63] studied the effects of tourniquet application in spontaneously breathing patients under epidural anesthesia. Their findings indicate that the changes in metabolic variables with tourniquet release are dependent on body size, i.e., muscle mass, and not the duration of tourniquet application. $\dot{V}O_2$ and $\dot{V}CO_2$ increased after tourniquet release, returning to baseline values 7–10 min after deflation. The increase in $\dot{V}CO_2$ lasted longer than that of $\dot{V}O_2$. Furthermore, men showed a greater increase in $\dot{V}CO_2$ than women due to their greater muscle mass. The increase in $\dot{V}CO_2$ was attributed to the release during limb reperfusion of accumulated metabolites, e.g., lactate, and their subsequent metabolism. Spontaneously breathing patients increased their minute ventilation to compensate for the increased $\dot{V}O_2$ and $\dot{V}CO_2$.

Vascular cross-clamping

Clamping and unclamping of the abdominal aorta during major vascular surgery is associated with major hemodynamic and metabolic consequences. Damask *et al.* [64] examined the metabolic effects of cross-clamping and the effects of narcotic administration during aortic surgery. Three groups of patients were studied:

- Group 1: Abdominal aortic aneurysm resection receiving low-dose morphine
- Group 2: Aorto-iliac bypass graft receiving low-dose morphine
- Group 3: Abdominal aortic aneurysm resection receiving high-dose morphine.

Only Group 1 showed a significant decrease in $\dot{V}O_2$ and $\dot{V}CO_2$ upon aortic cross-clamping and a significant increase in $\dot{V}O_2$ and $\dot{V}CO_2$ after aortic unclamping. The decrease in $\dot{V}O_2$ and $\dot{V}CO_2$ upon cross-clamping appeared to be directly related to the reduction in blood flow to the lower extremities. High-dose morphine did not seem to influence the metabolic rate. The large increases in $\dot{V}O_2$ and $\dot{V}CO_2$ observed in Groups 1 and 3 after unclamping reflect an overall increase in total-body metabolism resulting from renewed flow to the extremities and replenishing of O_2 stores depleted during cross-clamp (O_2 debt). Serum lactate levels increased after unclamping in all groups. Subsequent lactate metabolism can partially explain the increase observed in $\dot{V}CO_2$. The $\dot{V}O_2$ remained elevated until the O_2 debt was replenished. Patients in Group 2 had smaller decreases in, $\dot{V}O_2$, $\dot{V}CO_2$ and lactate upon cross-clamping and after unclamping. This was attributed to the presence of chronic collateral circulation, thereby minimizing the O_2 debt and lactate production. A similar study compared $\dot{V}O_2$ and $\dot{V}CO_2$ in the early postoperative period in patients after coronary artery bypass graft (CABG) surgery and abdominal aortic surgery (AAS) [65]. They observed significantly increased $\dot{V}O_2$ and $\dot{V}CO_2$ values in the early postoperative period in patients after AAS, most likely because of an O_2 debt that was incurred during aortic clamping. The increases in $\dot{V}O_2$ and $\dot{V}CO_2$ extended into the postoperative period because of thermoregulatory vasoconstriction.

Cardiopulmonary bypass

The use of hypothermic cardiopulmonary bypass (CPB) during open-heart surgery causes many changes in body homeostasis. The effects of changes in core body temperature during and after CPB have major influences on $\dot{V}O_2$ and $\dot{V}CO_2$. Boschetti *et al.* [66] observed positive linear correlations between $\dot{V}O_2$ and $\dot{V}CO_2$, and between body temperature and blood flow rate during CPB. Starr [67] also found a direct relationship between CPB flow rate and O_2 consumption. Ranucci *et al.* [68] demonstrated that, while anaerobic metabolism increases during bypass, as evidenced by a serum lactate concentration of greater than 3 mmol/L, $\dot{V}O_2$ decreased, but with little change in $\dot{V}CO_2$, resulting in an increase in respiratory quotient (RQ). The advent of increased anaerobic metabolism is characterized by a decrease in the ratio of oxygen delivery to CO_2 production. Damask *et al.* [69] noted a sharp decrease in $\dot{V}O_2$ and $\dot{V}CO_2$ upon initiation of CPB. $\dot{V}O_2$ and $\dot{V}CO_2$ were lowest during core body temperatures of 21–27 °C. During rewarming and the immediate post-CPB period, increases in $\dot{V}O_2$ and $\dot{V}CO_2$ were observed. Similar results have been described by other investigators [70]. The increase in $\dot{V}O_2$ and $\dot{V}CO_2$ after bypass is ascribed to increased total-body metabolism, replenishment of the O_2 debt incurred during CPB, and metabolism of anaerobic metabolites accumulated during CPB. Hanhela *et al.* [70] reported less increase in $\dot{V}O_2$ and $\dot{V}CO_2$ when patients were rewarmed at the end of CPB to a bladder temperature of over 37 °C, while also being warmed by external passive techniques.

Temperature and CO_2 production

Hypothermia often occurs during and after surgery [71]. It usually results from exposure to a cold operating room environment and anesthetic-impaired thermoregulation. Almost all general anesthetics in clinical use impair autonomic thermoregulatory control and are direct vasodilators. Bacher *et al.* [72] showed that intraoperative hypothermia decreases $\dot{V}O_2$ and $\dot{V}CO_2$. Attempts to prevent hypothermia during open abdominal surgery include intravenous administration of fructose, starting 3 h before anesthesia and continuing for 4 h during surgery. Compared to saline administration, fructose administration prevented hypothermia by increasing energy expenditure secondary to increases in both $\dot{V}CO_2$ and $\dot{V}O_2$ [73]. Similarly, the infusion of amino acids (starting 1–2 h prior to spinal anesthesia) increased $\dot{V}O_2$ and attenuated the extent of intraoperative hypothermia. This increase in metabolic rate is due to amino acid diet-induced thermogenesis [74,75]

Recovery from general anesthesia is very often characterized by shivering, which increases $\dot{V}O_2$ and $\dot{V}CO_2$ and also produces untoward hemodynamic and metabolic changes, such as increased heart rate and cardiac output [76]. Shivering can also occur without hypothermia, likely caused by emergence from anesthesia. Shivering in response to hypothermia can increase $\dot{V}O_2$ by as much as 400–500% [77]. Ralley *et al.* [76] showed markedly increased $\dot{V}O_2$ and $\dot{V}CO_2$ in patients shivering after rewarming from CPB. If ventilation is inadequate to match these increases in $\dot{V}CO_2$, hypercarbia and acidosis can result [78].

Suppression of the shivering response can minimize increases in, $\dot{V}O_2$, $\dot{V}CO_2$, and improve hemodynamic stability [79,80]. A small dose of meperidine can suppress visible shivering and significantly attenuate, but not abolish, the increases in $\dot{V}O_2$ and $\dot{V}CO_2$ [81]. Similar results have been observed when pancuronium and metocurine are administered during postoperative rewarming following coronary revascularization [80]. In a comparison study [82], pancuronium was more effective in suppressing the clinical and metabolic effects of shivering after cardiac surgery than meperidine. Clonidine also decreases shivering and postoperative metabolic demands [37].

Hyperthermia is associated with increased $\dot{V}O_2$ and $\dot{V}CO_2$. De las Alas *et al.* [83] demonstrated in a canine model that $\dot{V}CO_2$ and $\dot{V}O_2$ were early indicators of impending hyperthermia.

Malignant hyperthermia is an uncommon, potentially fatal, autosomal-dominant inherited disorder of skeletal muscle tissue, triggered by halogenated volatile anesthetics and depolarizing muscle relaxants, it is characterized by a hypermetabolic state [84].

Abnormal Ca^{2+} metabolism within the sarcoplasmic reticulum of skeletal muscle cells causes a hypermetabolic response, resulting in increased heat production. The clinical picture includes tachycardia, generalized muscle rigidity, myoglobinuria, and increased end-expiratory CO_2 concentrations. The increase in end-expiratory CO_2 concentrations is the result of increased $\dot{V}CO_2$.

Neuroleptic malignant syndrome is a syndrome with a clinical picture similar to malignant hyperthermia that is induced by chronic use of phenothiazines, butyrophenones, lithium, and other psychoactive

drugs. Little is known regarding $\dot{V}O_2$ and $\dot{V}CO_2$ in this syndrome, but because of a clinical picture comparable to malignant hyperthermia, it is safe to assume that $\dot{V}CO_2$ is increased.

References

1. Woerle HJ, Meyer C, Dostou JM, *et al.* Pathways for glucose disposal after meal ingestion in humans. *Am J Physiol Endocrinol Metab* 2003; **284**: E716–25.
2. Folch N, Peronnet F, Pean M, Massicotte D, Lavoie C. Labeled CO_2 production and oxidative vs nonoxidative disposal of labeled carbohydrate administered at rest. *Metabolism* 2005; **54**: 1428–34.
3. Iapichino G, Radrizzani D, Armani S, *et al*. Metabolic treatment of critically ill patients: energy balance and substrate disposal. *Minerva Anesthesiol* 2006; **72:** 533–41.
4. Armon Y, Cooper DM, Springer C, *et al.* Oral [^{13}C] bicarbonate measurement of CO_2 stores and dynamics in children and adults. *J Appl Physiol* 1990; **69:** 1754–60.
5. Carlson DA, Schreck CE, Brenner RJ. Carbon dioxide released from human skin: effect of temperature and insect repellents. *J Med Entomol* 1992; **29**: 165–70.
6. Weissman C, Kemper M, Damask MC, *et al*. The effect of routine intensive care interactions on metabolic rate. *Chest* 1984; **86**: 815–18.
7. Lowell BB, Speigleman BM. Towards a molecular understanding of adaptive thermogenesis. *Nature* 2000; **404**: 652–60.
8. McClave SA, Spain DA, Skolnick JL, *et al.* Achievement of a steady state optimizes results when performing indirect calorimetry. *J Parenter Enter Nutr* 2003; **27**: 16–20.
9. Reeves MM, Davies PS, Bauer J, Battistutta D. Reducing the time period of steady state does not affect the accuracy of energy expenditure measurements by indirect calorimetry. *J Appl Physiol* 2004; **97:** 130–4.
10. Anderson CT, Breen PH. Carbon dioxide kinetics and capnography during critical care. *Crit Care* 2000; **4:** 207–15.
11. Tobin MJ, Perez W, Guenther SM, D'Alonzo G, Dantzker DR. Breathing pattern and metabolic behavior during anticipation of exercise. *J Appl Physiol* 1986; **60**: 1306–12.
12. Brandi LS, Bertolini R, Santini L, Cavani S. Effects of ventilator resetting on indirect calorimetry measurements in the critically ill surgical patient. *Crit Care Med* 1999; **27:** 531–9.
13. Courser JI Jr., Martinez FJ, Celli, BR. Respiratory response and ventilatory muscle recruitment during arm elevation in normal subjects. *Chest* 1992; **101**: 336–40.
14. Weissman C, Kemper M, Elwyn DH, *et al.* The energy expenditure of the mechanically ventilated critically ill patient: an analysis. *Chest* 1986; **89**: 254–9.
15. Weissman C, Kemper M. The oxygen uptake–oxygen delivery relationship during ICU interventions. *Chest* 1991; **99:** 430–5.
16. Ritz P, Cloarec D, Beylot M, *et al.* Effects of colonic fermentation on respiratory gas exchanges following a glucose load in man. *Metabolism* 1993; **42**: 347–52.
17. Heresbach D, Flourie B, Briet FD, *et al.* Effect of colonic fermentation on respiratory gas exchanges measured in the postabsorptive state. *Am J Clin Nutr* 1995; **62**: 973–8.
18. Wiklund L. Carbon dioxide formation and elimination in man: recent theories and possible consequences. *Ups J Med Sci* 1996; **101**: 35–67.
19. Levraut J, Garcia P, Giunti C, *et al.* The increase in CO_2 production induced by $NaHCO_3$ depends on blood albumin and hemoglobin concentrations. *Intens Care Med* 2000; **26**: 558–64.
20. Dietrich KA, Romero MD, Conrad SA. Effect of gas leak around endotracheal tubes on indirect calorimetry measurements. *J Parenter Enter Nutr* 1990; **12**: 408–13.
21. Weir JB. New methods for calculating metabolic rate with special reference to protein metabolic rate with special reference to protein metabolism. *J Physiol* 1949; **109**: 1–9.
22. Ogawa A, Nosaka N, Kasai M, *et al.* Dietary medium- and long-chain triacylglycerols accelerate diet-induced thermogenesis in humans. *J Oleo Sci* 2007; **56:** 283–7.
23. White DP, Weil JV, Zwillich CW. Metabolic rate and breathing during sleep. *J Appl Physiol* 1985; **59**: 384–91.
24. Eger EI, Dolan W, Steven WC. Surgical stimulation antagonizes the respiratory depression produced by forane. *Anesthesiology* 1972; **36**: 544.
25. Hickey RF, Severinghaus JW. Anesthesia and ventilation. In: Hornbein TF (ed.) *Regulation of Breathing: Lung Biology in Health and Disease*, 2nd edn. New York: Marcel Dekker, 1981; 1251–312.
26. Fourcade HE, Larson CP Jr., Hickey RF, Bahlman SH, Eger EI II. Effects of time on ventilation during halothane and cyclopropane anesthesia. *Anesthesiology* 1972; **36:** 83–8.
27. Carli F, Elia M. The independent metabolic effects of enflurane anaesthesia and surgery. *Acta Anaesthiol Scand* 1991; **35**: 329–32.
28. Carli F, Ronzoni G, Webster J, Khan K, Elia M. The independent metabolic effects of halothane and isoflurane anaesthesia. *Acta Anaesthesiol Scand* 1993; **37:** 672–8.
29. Lindahl, SG, Offord, KP, Johannesson, GP, Meyer DM, Hatch DJ. Carbon dioxide elimination in anaesthetized children. *Can J Anaesth* 1989; **36**: 113–19.

30. Bain JA, Spoerel, WE. Carbon dioxide output and elimination in children under anaesthesia. *Can Anaesth Soc J* 1997; **24:** 533–9.
31. Lindahl SG. Oxygen consumption and carbon dioxide elimination in infants and children during anaesthesia and surgery. *Br J Anaesth* 1989; **62:** 70–6.
32. Lind L. Metabolic gas exchange during different surgical procedures. *Anesthesia* 1995; **50**: 307–7.
33. Pestana D, Garcia-de Lorenzo A, Madero R. Metabolic pattern and lipid oxidation during abdominal surgery: midazolam versus propofol. *Anesth Analg* 1996; **83:** 837–43.
34. Kirvela O, Kanto J. Clinical and metabolic responses to different types of premedication. *Anesth Analg* 1991; **73**: 49–53.
35. Taittonen M, Kirvela O, Aantaa R, Kanto J. Cardiovascular and metabolic responses to clonidine and midazolam premedication. *Eur J Anaesthesiol* 1997; **14**: 190–6.
36. Taittonen M, Kirvela OA, Aantaa R, Kanto JH. The effect of clonidine and midazolam pre-medication on perioperative responses during ketamine anesthesia. *Anesth Analg* 1998; **87**: 161–7.
37. Delaunay L, Bonnet F, Duvaldestin P. Clonidine decreases postoperative oxygen consumption in patients recovery from general anaesthesia. *Br J Anaesth* 1991; **67:** 397–401.
38. Harding J, Kemper M, Weissman C. Midazolam attenuates the metabolic and cardiopulmonary responses to an increase in oxygen demand. *Chest* 1994; **106**: 194–200.
39. Watters JM, March, RJ, Desai D, Monteith K, Hurtig JB. Epidural anaesthesia and analgesia do not affect energy expenditure after major abdominal surgery. *Can J Anaesth* 1993; **40**: 314–19.
40. Tulla H, Takala J, Alhava E, *et al.* Does the anesthetic method influence the postoperative breathing pattern and gas exchange in hip surgery? A comparison between general and spinal anesthesia. *Acta Anaesthesiol Scand* 1992; **30**: 101–5.
41. Diebel LN, Lange MP, Schneider F, *et al.* Cardiopulmonary complications after major surgery: a role for epidural analgesia. *Surgery* 1987; **102**: 660–6.
42. Viale JP, Annat GJ, Tissot SM, *et al.* Mass spectrometric measurements of oxygen uptake during epidural analgesia combined with general anesthesia. *Anesth Analg* 1990; **70:** 589–93.
43. Hong JY. Haemodynamic and ventilatory effects of preoperative epidural analgesia during laparoscopic hysterectomy using NICO. *Singapore Med J* 2008; **49**: 233–8.
44. Steinbrook R, Concepcion M. Respiratory gas exchange and hemodynamics during lumbar epidural anesthesia: effects of lidocaine with and without epinephrine. *Reg Anesth Pain Med* 2000; **25:** 380–4.
45. Schricker T, Klubien K, Wykes L, Carli F. Effect of epidural blockade on protein, glucose, and lipid metabolism in the fasted state and during dextrose infusion in volunteers. *Anesthesiology* 2000; **92:** 62–9.
46. Schricker T, Wykes L, Eberhart L, *et al.* The anabolic effect of epidural blockade requires energy and substrate supply. *Anesthesiology* 2002; **97**: 943–51.
47. Erbguth P, Berguan N. The effect of a single dose of succinylcholine on oxygen consumption and carbon dioxide production in man. *Anesthesiology* 1973, **39**: 447–9.
48. Muldoon SM, Theye RA. The effects of succinylcholine and d-tubocurarine on oxygen consumption. *Anesthesiology* 1969; **31**: 437–42.
49. Christensen KJ, Olsen AS, Jorgensen S. Effects of suxamethonium on CO_2 production. *Acta Anaesthiol Scand* 1985; **29**: 424–6.
50. Schou-Olesen A, Christensen KJ, Hartmann-Anderson F, Jørgensen S. CO2 production after suxamethonium and diazepam. *Acta Anaesthiol Scand* 1986; **30:** 685–8.
51. Vernon DD, Witte MK. Effect of neuromuscular blockade on oxygen consumption and energy expenditure in sedated, mechanically ventilated children. *Crit Care Med* 2000; **28**: 1569–71.
52. Kasama T, Ikeda K, Kato T, Kikura M. Carbon dioxide output in laparoscopic cholecystectomy. *Br J Anaesth* 1996; **76:** 530–5.
53. Pacilli M, Pierro A, Kingsley C, *et al.* Absorption of carbon dioxide during laparoscopy in children measured using a novel mass spectrometric technique. *Br J Anaesth* 2006; **97**: 215–19.
54. McHoney M, Corizia L, Eaton S. Carbon dioxide elimination during laparoscopy in children is age dependent. *J Pediatr Surg* 2003; **38**: 105–10.
55. Mullett CE, Viale JP, Sagnard PE, *et al.* Pulmonary CO_2 elimination during surgical procedures using intra- or extraperitoneal CO_2 insufflation. *Anaesth Analg* 1993; **76:** 622–6.
56. Streich B, Decailliot F, Perney C, Duvaldestin P. Increased carbon dioxide absorption during retroperitoneal laparoscopy. *Br J Anaesth* 2003; **91:** 793–6.
57. Kadam P, Marda M, Shah V. Carbon dioxide absorption during laporoscopic donor nephrectomy: a comparison between retroperitoneal and tranperitoneal approaches. *Transplant Proc* 2008; **40**: 1119–21.

58. Sumpf E, Crozier TA, Ahrens D, *et al.* Carbon dioxide absorption during extraperitoneal and transperitoneal endoscopic hernioplasty. *Anesth Analg* 2000; **91:** 589–95.
59. Liang SW, Lin CS, Xiao J. Effect of intraperitoneal carbon dioxide insufflation on hemodynamics of oxygen consumption during intravenous propofol anesthesia combined with epidural block. *Di Yi Jun Yi Da Xue Xue Bao* 2002; **22**: 166–7.
60. Girardis M, Milesi S, Donato S, *et al.* The hemodynamic and metabolic effects of tourniquet application during knee surgery. *Anesth Analg* 2000; **91**: 727–31.
61. Lee T, Tweed W, Singh B. Oxygen consumption and carbon dioxide elimination after release of unilateral lower limb pneumatic tourniquet. *Anesth Analg* 1992; **75:** 113–17.
62. Takahashi S, Mizutani T, Sato S. Changes in oxygen consumption and carbon dioxide elimination after tourniquet release in patients breathing spontaneously under epidural anesthesia. *Anesth Analg* 1998; **86:** 90–4.
63. Damask MC, Weissman C, Rodriguez J, *et al.* Abdominal aortic cross-clamping: metabolic and hemodynamic consequences. *Arch Surg* 1984; **119**: 1372–7.
64. Hess W, Frank C, Hornburg B. Prolonged oxygen debt after abdominal aortic surgery. *J Cardiothorac Vasc Anesth* 1997; **11:** 149–54.
65. Boschetti F, Perinati G, Montevecchi FM. Factors affecting the respiratory ratio during cardiopulmonary bypass. *Int J Artif Organs* 1998; **21**: 802–8.
66. Starr A. Oxygen consumption during cardiopulmonary bypass. *J Thorac Cardiovasc Surg* 1959; **38**: 46–56.
67. Ranucci M, Isgrò G, Romitti F, *et al.* Anaerobic metabolism during cardiopulmonary bypass: predictive value of carbon dioxide derived parameters. *Ann Thorac Surg* 2006; **81**: 2189–95.
68. Damask M, Weissman C, Askanazi J, *et al.* Do oxygen consumption and carbon dioxide production affect cardiac output after cardiopulmonary bypass? *Arch Surg* 1987; **122**: 1026–31.
69. Hanhela R, Mustonen A, Korhonen I, Salomäki T. The effects of two rewarming strategies on heat balance and metabolism after coronary artery bypass surgery with moderate hypothermia. *Acta Anaesthesiol Scand* 1999; **43:** 979–88.
70. Sessler D. Temperature monitoring in anesthesia. In: Miller R (ed.) *Anesthesia*, 6th edn. Philadelphia, PA: Churchill Livingstone, 2005; 1571–98.
71. Bacher A, Illievich UM, Fitzgerald R, Ihra G, Spiss CK. Changes in oxygen variables during progressive hypothermia in anesthetized patients. *J Neurosurg Anesthesiol* 1997; **9**: 205–10.
72. Mizobe T, Nakajima Y, Ueno H, Sessler DI. Fructose administration increases intraoperative core temperature by augmenting both metabolic rate and the vasoconstriction threshold. *Anesthesiology* 2006; **104:** 1124–30.
73. Widman J, Hammarqvist F, Sellden E. Amino acid infusion induces thermogenesis and reduces blood loss during hip athroplasty under spinal anesthesia. *Anesth Analg* 2002; **95**: 1757–62.
74. Kasai T, Nakajima Y, Matsukawa T, *et al.* Effect of preoperative amino acid infusion on thermoregulatory response during spinal anaestheia. *Br J Anaesth* 2003; **90**: 58–61.
75. Ralley FE, Wynands JE, Ramsay JG, Carli F, MacSullivan R. The effects of shivering on oxygen consumption and carbon dioxide production in patients rewarming from hypothermic cardiopulmonary bypass. *Can J Anaesth* 1988; **35**: 332–7.
76. Eyolfson DA, Tikuisis P, Xu X, Weseen G, Giesbrecht GG. Measurement and prediction of peak shivering intensity in humans. *Eur J Appl Physiol* 2001; **84**: 100–6.
77. Sladen RN. Temperature and ventilation after hypothermic cardiopulmonary bypass. *Anesth Analg* 1985; **64**: 816–21.
78. Rodriguez JL, Weissman C, Damask MC, *et al.* Physiologic requirements during rewarming: suppression of the shivering response. *Crit Care Med* 1983; **11**: 490–7.
79. Zwischenberger JB, Kirsh M, Dechert RE, Arnold DK, Bartlett RH. Suppression of shivering decreases oxygen consumption and improves hemodynamic stability during postoperative rewarming. *Ann Thorac Surg* 1987; **43**: 428–31.
80. Macintyre P, Pavlin E, Duersteg J. Effect of meperidine on oxygen consumption, carbon dioxide production and respiratory gas exchange in postanesthesia shivering. *Anesth Analg* 1987; **66**: 751–5.
81. Cruise C, MacKinnon J, Tough J, Houston P. Comparison of meperidine and pancuronium for the treatment of shivering after cardiac surgery. *Can J Anaesth* 1992; **39**: 563–8.
82. De las Alas V, Voorhees WP, Geddes LA. End tidal carbon dioxide concentration, carbon dioxide production, heart rate and blood pressure as indicators of induced hyperthermia. *J Clin Monit* 1990; **6**: 183–5.
83. Wappler F. Malignant hyperthermia. *Eur J Anaesth* 2001; **18**: 632–52.

Section 2
Chapter
26

Circulation, metabolism, and organ effects

Tissue- and organ-specific effects of carbon dioxide

O. Akça

Background

Carbon dioxide is the major product of cellular respiration. Arterial carbon dioxide partial pressure ($PaCO_2$) between 35 and 45 mm Hg is accepted as a clinically normal range. To best appreciate the dynamics of carbon dioxide, a thorough understanding of acid–base physiology is essential.

Clinically, hypocapnia is induced to treat increased intracranial pressure, diabetic ketoacidosis, near-drowning, congenital diaphragm hernia, and pulmonary hypertension in newborns [1]. Conversely, hypercapnia is induced to insufflate the abdomen in laparoscopic surgery, reverse carbon monoxide poisoning, and augment cerebral perfusion during carotid endarterectomy, as well as to emergently treat central retinal artery occlusion [2,3]. Induced hypercapnia has also been utilized during emergence from anesthesia to stimulate spontaneous breathing. Patients often develop alterations in arterial CO_2 tensions unintentionally from various causes, including narcotic analgesic administration, asthma, pulmonary edema, acute lung injury, excessive/inadequate mechanical ventilation, cardiopulmonary bypass, extracorporeal membrane oxygenation, and high-frequency ventilation.

In an otherwise healthy state, hypocapnia is generally well tolerated, although it may cause paresthesias, palpitations, myalgic cramps, and seizures [4]. The most established indication of its therapeutic use is to mitigate increased intracranial pressure (ICP) with or without neurologic deterioration [5]. Despite many guidelines that suggest otherwise, hyperventilation to induce hypocapnia – as a method to decrease ICP – continues to be widely practiced [6,7]. In the United States, more than one-third of board-certified neurosurgeons [7] and about half of emergency physicians [6] routinely use prophylactic hyperventilation in patients with severe traumatic brain injury regardless of the potential consequences. Before applying or allowing hypocapnia, one needs to consider the full range of pathophysiological effects on patients [1].

Hypercapnia is highly protective in experimental models of acute ischemic myocardial, lung, and brain injury [2,3,8–10]. The potential mechanisms of this protection include alteration of organ oxygen supply-and-demand kinetics, attenuation of free radical activity, improvement in tissue oxygenation, and prevention of ischemia–reperfusion injury. However, because of insufficient data in humans, hypercapnia is not yet used clinically to prevent or treat any organ injury.

The focus of this chapter is on the effects of hypo- and hypercapnia at the organ and tissue level. Because of the broad perspectives of these clinical phenomena, first, carbon dioxide's role in determining acid–base status and tissue oxygenation will be described, followed by its effects on major organ systems.

Carbon dioxide and acid–base basics

The rapid equilibration of CO_2 between the extracellular and intracellular compartments plays a major role in maintaining acid–base status. Low CO_2 partial pressure in tissue (hypocapnia) initiates a biphasic buffering compensation system. In the early phase, equilibration is rapid. As extracellular CO_2 concentration decreases, intracellular CO_2 quickly diffuses into the extracellular space, which then results in the transfer of chloride ions from the intracellular to the extracellular fluid compartment. The transfer of chloride ions from the intracellular to the extracellular compartment, along with the decrease in bicarbonate ions in the extracellular fluid, is known as *tissue buffering* [11]. This early phase is initiated within minutes. The later phase is the inhibition of renal tubular reabsorption of bicarbonate ions, which begins after several hours and can last for days [11].

Capnography, Second Edition, ed. J. S. Gravenstein, Michael B. Jaffe, Nikolaus Gravenstein, and David A. Paulus. Published by Cambridge University Press. © Cambridge University Press 2011.

Table 26.1 Global hemodynamics and tissue oxygenation as a function of target end-tidal PCO_2

Target $PaCO_2$ (mm Hg)	20	30	40	50	60	*P*
Cardiac index (L/min/m^2)	2.7 ± 0.4	2.9 ± 0.4	3.2 ± 0.5	3.6 ± 0.7	3.9 ± 0.2	0.0001
Muscle tissue oxygen saturation (%)*	84.4 ± 7.4	85.8 ± 9.6	86.6 ± 8.1	87.2 ± 8.9	89.0 ± 8.6	0.0004
Laser Doppler flow velocity (U)*	13.6 ± 6.3	13.7 ± 7.7	16.7 ± 6.8	16.2 ± 9.3	17.8 ± 8.5	0.2169
Cerebral oximeter saturation (%)	68.1 ± 10.8	69.1 ± 14.0	78.6 ± 8.6	82.5 ± 10.1	85.4 ± 7.5	< 0.0001
Subcutaneous tissue oxygen tension (mm Hg)	51.9 ± 9.9	57.8 ± 11.2	65.2 ± 14.5	74.0 ± 12.3	82.4 ± 18.6	< 0.0001

Data presented as means ± SDs. See Figure 26.1 for regression analysis. Repeated measure ANOVA was used to analyze normally distributed data. Asterisks (*) indicate non-normally distributed data sets analyzed by Friedman test.
Source: Reproduced with permission from: Akça OA, Doufas AG, Morioka N, *et al*. Hypercapnia improves tissue oxygenation. *Anesthesiology* 2002; **97**: 801–6.

The higher lipid solubility of CO_2 compared to hydrogen ions allows acid–base changes caused by respiratory acidosis and alkalosis to equilibrate between extra- and intracellular fluids much faster than changes caused by metabolic acidosis or alkalosis. As a result, more pronounced effects on both tissue and clinical levels are expected when pH changes are due to respiratory – rather than metabolic – causes. It should be noted that the major determinants of pH are a strong ion difference (sum of the concentrations of sodium, potassium, calcium, and magnesium minus the concentrations of chloride and lactate), the concentration of weak acids (proteins and phosphates), and the arterial partial pressure of CO_2 [12].

Effects of CO_2 on the physiology of tissue oxygenation and perfusion

The primary determinants of tissue oxygen availability are arterial O_2 tension, cardiac output, and local perfusion [13]. Core temperature, pain, smoking, hypovolemia, and supplemental fluid regimen also alter tissue oxygenation in the perioperative setting [14–17]. An additional factor known to influence peripheral tissue perfusion and oxygen delivery is arterial blood CO_2 partial pressure. Hypocapnia decreases the oxygen supply, and thereby may cause tissue ischemia. In contrast, hypercapnia increases tissue perfusion and, thereby, oxygenation [18–22]. The correlation of subcutaneous tissue oxygenation and partial pressure of arterial CO_2 appears to be linear in the range of 20–60 mm Hg $PaCO_2$ (Figure 26.1, Table 26.1) [18]. Although hyperventilation-induced hypocapnia may increase alveolar oxygen tension, other important pulmonary effects of hypocapnic alkalosis, such as attenuation of hypoxic pulmonary vasoconstriction and increased

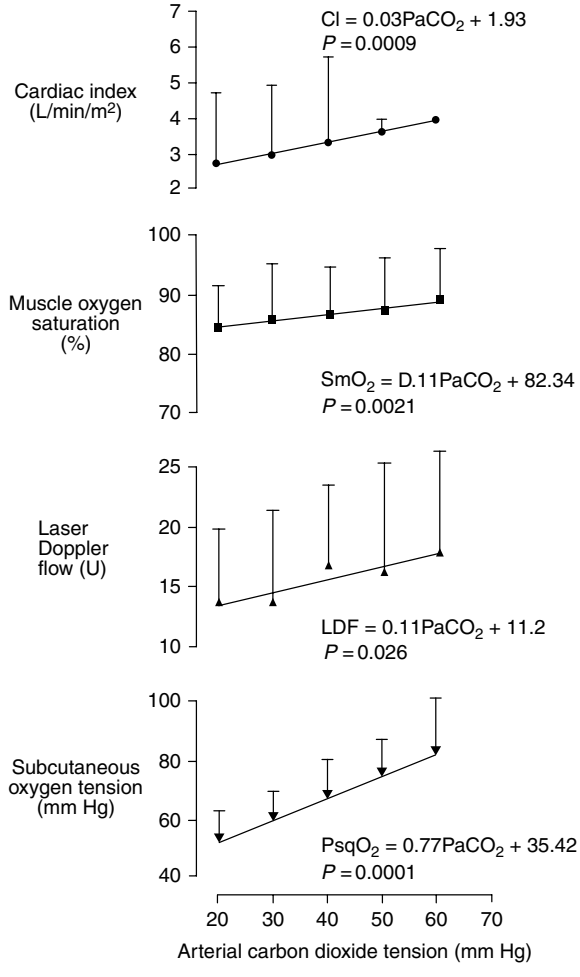

Figure 26.1 Cardiac index (CI), muscle tissue oxygen saturation (SmO_2), skin blood flow (laser Doppler flow velocity, LDF), and subcutaneous tissue oxygen tension ($PsqO_2$) all increased as a linear function of $PaCO_2$. Values of *P* were obtained from linear regression formula. [Reprinted with permission from: Akça OA, Doufas AG, Morioka N, *et al*. Hypercapnia improves tissue oxygenation. *Anesthesiology* 2002; **97**: 801–6.]

intrapulmonary shunting, result in a net decrease in the partial pressure of arterial oxygen [23].

CO_2 and tissue oxygen delivery

Hypocapnia and alkalosis cause a leftward shift of the oxyhemoglobin dissociation curve. Therefore, oxygen off-loading at the tissue level is restricted. Hypocapnia also causes systemic (although not pulmonary) arterial vasoconstriction, decreasing the global and regional oxygen supply and compounding the reduction in the delivery of oxygen to tissue [24]. On the other hand, hypercapnia causes a rightward shift of the oxyhemoglobin dissociation curve, increases cardiac output, decreases systemic vascular resistance and oxygen extraction, and, thus, overall, increases oxygen availability to tissue [25].

CO_2 and splanchnic perfusion

Okazaki *et al.* investigated the effects of CO_2 on the splanchnic visceral organs (liver and kidney) and skeletal muscle in the anesthetized dog [26]. They showed that hyperventilation resulted in a significant decrease in hepatic artery and portal vein blood flow, liver surface PO_2, and kidney surface PO_2 in parallel with the decreased $PaCO_2$; however, these parameters increased dependent on dose when CO_2 was added to the inspired gas (hypercapnic hyperventilation). Ratnaraj *et al.* showed that increasing end-tidal PCO_2 from 30 to 50 mm Hg under general anesthesia improved subcutaneous tissue oxygen tension by ~23% and intramural oxygenation in large and small intestine by 16–45% [20]. In the same study, mild hypercapnia increased cardiac index (30–35%) and stroke volume (~23%), and decreased systemic vascular resistance (~39%) compared to normocapnia. In a follow-up human study done during colon surgery of approximately a 3-h duration, Fleischmann *et al.* showed that, even under high inspired oxygen concentration (FiO_2 of 0.80), in patients who were assigned to undergo mild hypercapnia ($PetCO_2$ of 50 mm Hg), subcutaneous tissue oxygenation increased by 38% and colon intramural oxygenation increased by about 100% compared to the patients who were assigned to normocapnia ($PetCO_2$ of 35 mm Hg) [21]. Recently, Schwartges *et al.* showed in a dog experiment that incremental levels of $PetCO_2$ increased cardiac output and systemic oxygen delivery [22]. When the $PetCO_2$ level was increased from 35 to 70 mm Hg in small increments, investigators noted a concentration-dependent increase in cardiac output (CO), systemic oxygen delivery (DO_2), and gastric mucosal oxygen saturation. The $PaCO_2$ corresponded to changes in tissue oxygenation and appeared to exert significant effects on splanchnic organ perfusion.

Specific organ and tissue effects of CO_2

Central nervous system and brain

Because of the skull's bony structure, when the volume of any of its contents increases regardless of cause – hematoma, edema, inflammation, or mass – it causes an increase in ICP. Increased ICP may result in impaired cerebral perfusion and risk of herniation. To reduce ICP, the volume of the cranial contents must be reduced. Hypocapnic alkalosis decreases cerebral blood volume, owing to its potent cerebral vasoconstriction effect, and, thereby, lowers ICP.

Hypocapnia and brain injury

The beneficial effects of hypocapnia on ICP may be outweighed, however, by the reduced oxygen delivery [27]. Huttunen *et al.* have indicated that hypocapnia potentially even elevates cerebral oxygen demand by increasing neuronal excitability and seizure activity [28]. Additionally, hypocapnia during cardiopulmonary resuscitation may worsen brain injury [29].

During prolonged hypocapnia, extracellular fluid bicarbonate levels decrease, which results in the gradual return of extracellular fluid pH toward normal. In brain tissue, this normalization of local pH also normalizes cerebral blood flow. Therefore, prolonged hypocapnia eventually causes tolerance, and creates a scenario for a rebound increase in ICP when $PaCO_2$ is subsequently normalized. Once $PaCO_2$ returns to normal, the rebound hyperperfusion that ensues triggers an increase in ICP [30].

Hypercapnia and brain injury

Cerebral blood flow is better preserved during hypercapnia than during normocapnia or hypocapnia. Hypercapnia produces greater oxygen delivery, which, in turn, promotes cerebral glucose utilization and induces oxidative metabolism [31]. Increasing CO_2 partial pressure increases oxygenation in the tissues, including the brain [18,32–35]. Most of the effects of CO_2 on cerebroarterial blood flow are maintained by regulating extracellular fluid pH [36].

Vannucci *et al.* studied whether hypercapnia protects against and hypocapnia potentiates hypoxic–ischemic brain damage in the immature rat brain [9]. The investigators allowed the animals to breathe incremental concentrations of inspired carbon dioxide ($FiCO_2$ 0–3–6–9%) for 2 h during the reperfusion phase after 3–4 h of ischemia. They found that hypocapnia was deleterious, and increasing levels of CO_2 were protective. However, the protective effect was saturated at approximately a $FiCO_2$ of 6% ($PaCO_2$ ~54 mm Hg), and further increases appeared to abolish the protection [9]. In a follow-up study, the same group showed that, during hypercapnia, cerebral blood flow was better preserved, and the greater oxygen delivery promoted cerebral glucose utilization and oxidative metabolism for optimal maintenance of tissue high-energy phosphate reserves [31]. Additionally, the concentration of glutamate was decreased in the cerebrospinal fluid during hypercapnia. The reduction of this excitatory neurotransmitter may offer additional protection for the central nervous system. In a recent in-vitro study, hypercapnic preconditioning reduced the damage caused by ischemia and reperfusion in rat brain slices [33].

Mechanisms of increased cerebral blood flow during hypercapnia

A possible mediator responsible for the increase in cerebroarterial blood flow and vasodilatation during hypercapnia is nitric oxide (NO) [37–39]. In many animal (rats, cats, dogs, and rabbits) [38,40,41] and human studies [39], inhibiting NO synthase (the rate-limiting enzyme for NO) attenuated the hypercapnia-induced cerebral hemodynamic effects. For example, cerebral vasodilation in response to hypercapnic acidosis was blocked by L-arginine analogs, such as N^G-nitro-L-arginine (L-NNA) or N^G-monomethyl-L-arginine (L-NMMA) [38], which are NO synthase inhibitors.

There is also evidence that the cerebroarterial vasodilating effects of hypercapnia are mediated through ATP-sensitive potassium (KATP) channels [42]. These channels require L-arginine or L-lysine to maintain an open state [43]; therefore, L-arginine analogs block the KATP channels, as well as NO synthase [43].The KATP channels in the endothelium are pH-sensitive [44]. As the pH decreases from 7.4 to 6.6, the KATP channels shift from a closed to an open state. Because the response to CO_2 is a continuum, it was hypothesized that hypercapnic acidosis triggers KATP channel opening and hypocapnic alkalosis triggers channel closing. This hypothesis was proven by Wei and Kontos [45].

Respiratory system

Hypocapnia and lung injury

Hypocapnia and hypocapnic alkalosis have the potential to worsen lung injury. In an isolated buffer-perfused rabbit lung, Laffey *et al.* showed that hypocapnic alkalosis damaged the uninjured lung [46]. Prolonged ventilation with hypocapnia – which was maintained with lower inspiratory CO_2 concentrations and not by altering ventilation (pH ~7.9, PCO_2 ~12 mm Hg) – increased pulmonary artery pressure, airway pressure, and wet-lung weight [46] (Figure 26.2).

Hypercapnia and ventilator-associated lung injury, acute lung injury, and acute respiratory distress syndrome

The application of high-tidal volume ventilatory techniques causes or potentiates a stretch-induced acute lung injury (ALI), named ventilator-associated lung injury (VALI). Reducing lung stretch means reducing the volumes or pressures applied to the lungs. Unless the respiratory rate is altered, smaller tidal volumes often lead to an elevation of $PaCO_2$, which eventually leads to permissive hypercapnia. The use of smaller tidal volumes in the presence of elevated $PaCO_2$ appears to be beneficial in preventing damage from VALI. These two phenomena – *elevated carbon dioxide* and *smaller tidal volumes* – can be separately controlled by manipulating the respiratory rate. As noted by Laffey and Kavanagh, dissecting these issues may be extremely important to intensivists for a couple of reasons [3]: (1) permissive hypercapnia is associated with improved outcome [47,48]; (2) elevated levels of CO_2 may have beneficial effects other than simply less lung stretch injury [2].

Hypercapnia and endotoxin-induced lung injury

In an endotoxin-induced ALI model, Laffey *et al.* studied the prophylactic and therapeutic effects of hypercapnia on oxygenation, inflammation, and immunological outcomes [49]. They concluded that hypercapnic acidosis protects against lipopolysaccharide-induced lung injury both prophylactically and therapeutically. Hypercapnic acidosis also improved alveolar–arterial oxygen gradients and static compliance, with less neutrophil counts in the bronchoalveolar lavage fluid, and better histological tissue outcomes compared to normo- and hypocapnia.

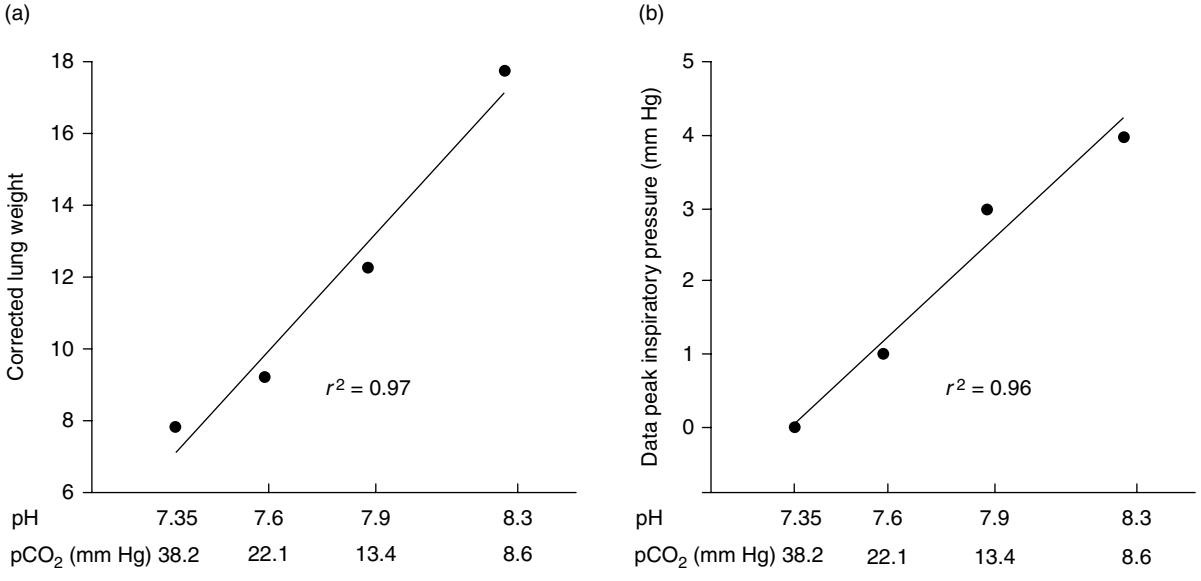

Figure 26.2 (a) Dose–response data for hypocapnic alkalosis versus corrected wet lung weight ($r^2 = 0.97$; $P < 0.02$). (b) Dose–response data for hypocapnic alkalosis versus elevation in airway pressure ($r^2 = 0.96$; $P < 0.02$). [Reprinted with permission from: Laffey JG, Engelberts D, Kavanagh BP. Injurious effects of hypocapnic alkalosis in the isolated lung. *Am J Respir Care Med* 2000; **162**: 399–405.]

In a series of elegant studies, investigators instilled the trachea of rats with *E. coli*, and assessed the progress of pneumonia and pneumonia-induced lung injury in both the acute (6-h) and subacute (48-h) phase with and without antimicrobial treatment [50–52]. In these studies, hypercapnic acidosis (~50–60 mm Hg) mostly preserved peak airway pressures, lung static compliance, and oxygenation. Anti-inflammatory and possibly immunosuppressive effects of hypercapnic acidosis were observed. When the application of hypercapnic acidosis was allowed for 48 h, pneumonia-induced lung injury worsened. However, under antimicrobial treatment, both lung mechanics and histology of lungs were preserved after 48 h of hypercapnic acidosis.

Hypercapnia and ischemia–reperfusion injury

Activation of xanthine oxidase, an important enzyme in ischemia–reperfusion (I/R) injury, has major implications in tissue injury. Shibata *et al.* used I/R and free-radical injury models in isolated buffer-perfused rabbit lungs to demonstrate that hypercapnic acidosis prevented an increase in capillary permeability on an injured lung and cause no microvascular adverse effects on an uninjured lung [10]. The mechanism of this protective effect was through the inhibition of xanthine oxidase by hypercapnic acidosis. In a follow-up study, investigators studied whether hypercapnia would be protective against I/R lung injury in an in-vivo rabbit model. The hypercapnia group ($PaCO_2$ ~100 mm Hg, pH ~7.10) was found to have attenuated protein leakage, reduced pulmonary edema, improved oxygenation, only minimal increases in tumor necrosis factor-alpha (TNF-α) levels, and reduced lung tissue nitrotyrosine (indicating decreased nitration of tissue) [53]. All of these findings support the hypothesis that hypercapnic acidosis preserves lung mechanics, attenuates pulmonary inflammation, and reduces free-radical injury; it might also have attenuated I/R injury-induced apoptosis (Figure 26.3).

Circulatory system, heart, and hemodynamics

Hypocapnia and myocardium

Hypocapnia alters myocardial oxygenation and cardiac rhythm. Acute hypocapnia decreases myocardial oxygen delivery while increasing oxygen demand. Oxygen demand is increased because of the increased myocardial contractility [54] and systemic vascular resistance [55]. Thus, hypocapnia may contribute to clinically relevant acute coronary syndromes.

Hypercapnia and myocardium

Earlier evidence suggested that using fixed acids or buffers to maintain acidotic reperfusion fluids improved recovery of the stunned myocardium

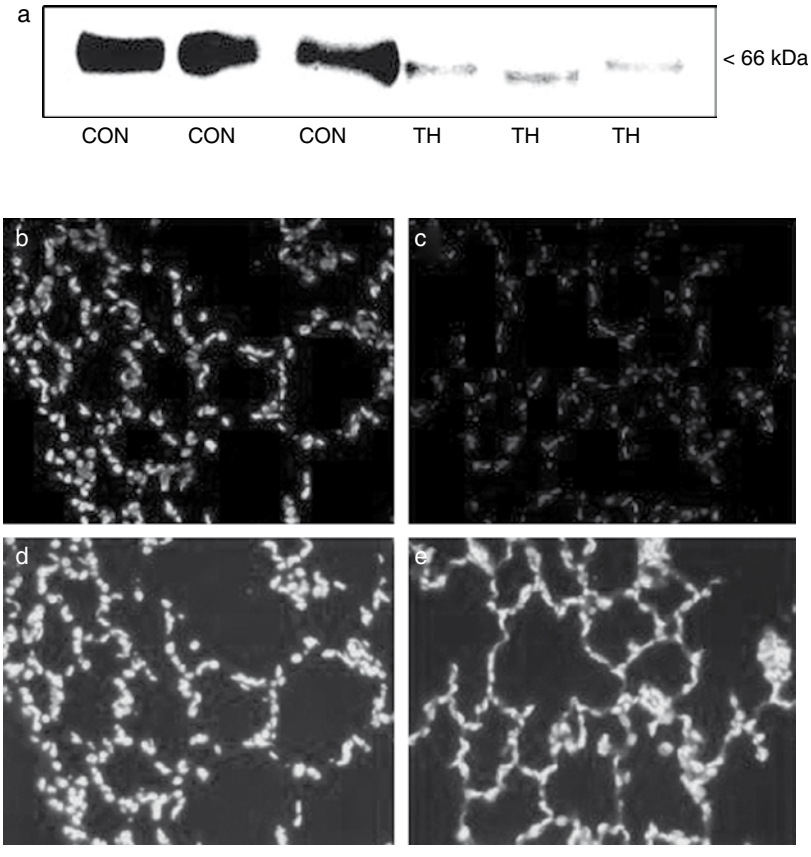

Figure 26.3 (a) Western blot analysis of nitrotyrosine residues from three specimens from each group. A prominent band of nitrotyrosylated protein is demonstrated at approximately 60 kDa. The intensity of the bands is greater in the control (bands 1–3) than in the hypercapnia (bands 4–6) group. (b–e) Examples of apoptosis, demonstrated by TUNEL assay. Fluorescence is greater in the control than in the hypercapnia group (Control Group,[b]; Hypercapnia Group [c]), indicating more apoptosis. Comparable tissue DNA profile is demonstrated in the presence of DAPI (Control Group [d]; Hypercapnia Group [e]). [Reprinted with permission from: Laffey JG, Tanaka M, Engelberts D, *et al.* Therapeutic hypercapnia reduces pulmonary and systemic injury following in vivo lung reperfusion. *Am J Respir Crit Care Med* 2000; **162**: 2287–94.]

[56,57]. Consequently, Nomura *et al.* tested whether hypercapnic acidosis would provide a similar benefit [8]. In blood-perfused neonatal lamb hearts, with cold cardioplegic ischemia at pH 7.4, reperfusion was provided with blood at pH values ranging from 6.8 to 7.8. The pH changes were achieved by altering the $FiCO_2$. In an additional group, hydrochloric acid was used to titrate the pH of the reperfused blood to 6.8 (metabolic acidotic group). The most hypercapnic acidotic group had the best indices of contractility, coronary blood flow, and myocardial oxygen consumption. Conversely, the metabolic acidotic group did not get similar protection [8].

Hypercapnia and cardiac performance

Hypercapnia increases tissue perfusion and oxygenation [18,35], mainly through increased cardiac output. For example, increasing the partial pressure of CO_2 from 20 mm Hg to 60 mm Hg increases the cardiac index about 44% [18]. In a recent study in postoperative cardiac surgery patients, a similar benefit was shown by increasing the partial pressure of CO_2 from 30 to 50 mm Hg. Increasing CO_2 pressure increased the cardiac index, as well as the mixed venous oxygen saturation [58]. Recently, we have shown that, even under constant cardiac output, hypercapnia increases cerebral – but not peripheral – tissue oxygenation [34]. These global oxygenation improvement effects complement the previously mentioned tissue oxygenation effects.

Hashimoto *et al.* presented the effects of CO_2 on myocardial oxygenation during hemorrhagic shock under normocapnic, hypocapnic, and hypercapnic conditions [59]. Hypocapnia decreased coronary flow and myocardial oxygen tension in the outer and inner layers of the myocardium, whereas they were increased by hypercapnia. These finding suggest that hypocapnia might, therefore, compromise the oxygenation of the myocardium during hemorrhagic shock.

Other known effects

Vascular effects of CO_2

Holmes *et al.* investigated the effects of hypercapnia, normocapnia, and metabolic acidosis on the retinal

vasculature of neonatal rats. Those exposed to hypercapnia had pronounced retardation of normal retinal vascular development [60]. Additionally, hypercapnia exacerbated oxygen-induced retinopathy [61]. Similarly, metabolic acidosis induced neovascularization that appeared similar to retinopathy of prematurity [62]. In light of this evidence, one needs to be concerned about allowing permissive hypercapnia in vulnerable neonates [3].

Central sleep apnea and carbon dioxide

Central sleep apnea causes hypoxemia, increased sympathetic nervous system activity, and, in patients with congestive heart failure, increased risk of sudden death [1]. An enhanced ventilatory response to CO_2 may contribute to the development of central sleep apnea in some patients with congestive heart failure [63], and hypocapnia triggers periodic respirations in these patients [64]. One of the mechanisms by which the application of non-invasive positive airway pressure reduces central sleep apnea is by increasing hemoglobin oxygen saturation and increasing $PaCO_2$ toward or above the apneic threshold [64]. In fact, central sleep apnea is predicted by the presence of hypocapnia during waking hours [65]. Hypocapnia is a common finding in patients with sleep apnea, and may be pathogenic.

High altitude and hypocapnia

Sudden exposure to high altitude can result in neurological injury. However, central nervous system impairment seen in previously healthy mountaineers after exposure to extremely high altitudes has been demonstrated to closely correlate with the degree of hypocapnia – not the level of hypoxia – attained [66]. The cause of acute central nervous system symptoms at high altitudes appears to be the alkalosis caused by increased minute ventilation [1].

Summary

Carbon dioxide has many protective effects on organs and tissues. Oxygenation and perfusion are significantly improved at the organ and tissue level due to incremental levels of CO_2 concentration. Perfusion benefits are directly related to increasing CO. However, hypercapnia-related brain oxygenation appears to improve even with constant CO. Hypocapnia induced by hyperventilation is clinically used for treatment of increased ICP, but the compromise in tissue perfusion, and thus the resulting secondary ischemia, should be factored into the risk–benefit equation. Hypercapnia and hypercapnic acidosis, in contrast, appear to offer protection to various organ systems from ischemia–reperfusion injury. Hypercapnia exerts anti-inflammatory effects in lung injury related to ischemia–reperfusion, endotoxins, and mechanical ventilation; nevertheless, increased awareness is required in pneumonia-induced lung injury, and hypercapnia should only be considered under optimum antimicrobial treatment. In conclusion, the active management of CO_2 is a promising strategy to consider for improving tissue perfusion, providing anti-inflammatory effects, and preventing apoptotic injury. In the next decade, we will likely see various phase II and III trials on tissue-organ protective outcomes of hypercapnia in humans.

References

1. Laffey JG, Kavanagh BP. Hypocapnia. *N Engl J Med* 2002; **347:** 43–53.
2. Laffey JG, Kavanagh BP. Carbon dioxide and the critically ill: too little of a good thing? *Lancet* 1999; **354:** 1283–6.
3. Laffey JG, Kavanagh BP. Biological effects of hypercapnia. *Intens Care Med* 2000; **26:** 133–8.
4. Gluck S. Acid–base. *Lancet* 1998; **352:** 474–9.
5. Bullock R, Chesnut RM, Clifton G, *et al.* Brain Trauma Foundation Guidelines for the management of severe head injury. *Eur J Emerg Med* 1996; **3:** 109–27.
6. Huizenga JE, Zink B, Maio R, Hill E. The penetrance of head injury management guidelines into the practice patterns of Michigan emergency physicians. *Acad Emerg Med* 2000; **7:** 1171.
7. Marion DW, Spiegel TP. Changes in the management of severe traumatic brain injury: 1991–1997. *Crit Care Med* 2000; **28:** 16–18.
8. Nomura F, Aoki M, Forbess JM, Mayer JE Jr. Effects of hypercarbic acidotic reperfusion on recovery of myocardial function after cardioplegic ischemia in neonatal lambs. *Circulation* 1994; **90:** 321–7.
9. Vannucci RC, Towfighi J, Heitjan DF, Brucklacher RM. Carbon dioxide protects the perinatal brain from hypoxic–ischemic damage: an experimental study in the immature rat. *Pediatrics* 1995; **95:** 868–74.
10. Shibata K, Cregg N, Engelberts D, *et al.* Hypercapnic acidosis may attenuate acute lung injury by inhibition of endogenous xanthine oxidase. *Am J Respir Crit Care Med* 1998; **158:** 1578–84.
11. Adrogue HJ, Madias NE. Management of life-threatening acid–base disorders. *N Engl J Med* 1998; **338:** 107–11.

12. Kellum J. Determinants of blood pH in health and disease. *Crit Care* 2000; **4:** 6–14.
13. Greif R, Akça O, Horn EP, Kury A, Sessler DI. Supplemental perioperative oxygen to reduce the incidence of surgical wound infection. *N Engl J Med* 2000; **342:** 161–7.
14. Jensen JA, Goodson WH, Hopf HW, Hunt TK. Cigarette smoking decreases tissue oxygen. *Arch Surg* 1991; **126:** 1131–4.
15. Kurz A, Sessler DI, Lenhardt R. Perioperative normothermia to reduce the incidence of surgical-wound infection and shorten hospitalization. *N Engl J Med* 1996; **334:** 1209–15.
16. Akça O, Melischek M, Scheck T, *et al.* Postoperative pain and subcutaneous oxygen tension. *Lancet* 1999; **35**4: 41–2.
17. Arkilic CF, Taguchi A, Sharma N, *et al.* Supplemental perioperative fluid administration increases tissue oxygen pressure. *Surgery* 2003; **133**: 49–55.
18. Akça OA, Doufas AG, Morioka N, *et al.* Hypercapnia improves tissue oxygenation. *Anesthesiology* 2002; **97:** 801–6.
19. Akça O, Liem E, Suleman MI, *et al.* The effect of intraoperative end-tidal carbon dioxide partial pressure on tissue oxygenation. *Anaesthesia* 2003; **58:** 536–42.
20. Ratnaraj J, Kabon B, Talcott MR, Sessler DI, Kury A. Supplemental oxygen and carbon dioxide each increase subcutaneous and intestinal intramural oxygenation. *Anesth Analg* 2004; **99:** 207–11.
21. Fleischmann E, Herbst F, Kugener A, *et al.* Mild hypercapnia increases subcutaneous and colonic oxygen tension in patients given 80% inspired oxygen during abdominal surgery. *Anesthesiology* 2006; **10**4: 944–9.
22. Schwartges I, Schwarte LA, Fournell A, Scheeren TW, Picker O. Hypercapnia induces a concentration-dependent increase in gastric mucosal oxygenation in dogs. *Intens Care Med* 2008; **34:** 1898–906.
23. Domino KB, Lu Y, Einstein BL, Hlastala MP. Hypocapnia worsens arterial blood oxygenation and increases V_A/Q heterogeneity in canine pulmonary edema. *Anesthesiology* 1993; **78:** 91–9.
24. Guzman JA, Kruse JA. Splanchnic hemodynamics and gut mucosal-arterial $PCO_{(2)}$ gradient during systemic hypocapnia. *J Appl Physiol* 1999; **87:** 1102–6.
25. Mas A, Saura P, Joseph D, *et al.* Effects of acute moderate changes in $PaCO_2$ on global hemodynamics and gastric perfusion. *Crit Care Med* 2000; **2**8: 360–5.
26. Okazaki K, Okutsu Y, Fukunaga A. [Effects of carbon dioxide (hypocapnia and hypercapnia) on tissue blood flow and oxygenation of liver, kidney and skeletal muscle in the dog.] *Masui* 1989; **38:** 457–64.
27. Weckesser M, Posse S, Olthoff U, *et al.* Functional imaging of the visual cortex with bold-contrast MRI: hyperventilation decreases signal response. *Magn Reson Med* 1999; **41:** 213–16.
28. Huttunen J, Tolvanen H, Heinonen E, *et al.* Effects of voluntary hyperventilation on cortical sensory responses: electroencephalographic and magnetoencephalographic studies. *Exp Brain Res* 1999; **12**5: 248–54.
29. Safar P, Xiao F, Radovsky A, *et al.* Improved cerebral resuscitation from cardiac arrest in dogs with mild hypothermia plus blood flow promotion. *Stroke* 1996; **2**7: 105–13.
30. Gleason CA, Short BL, Jones MD Jr. Cerebral blood flow and metabolism during and after prolonged hypocapnia in newborn lambs. *J Pediatr* 1989; **115:** 309–14.
31. Vannucci RC, Brucklacher RM, Vannucci SJ. Effect of carbon dioxide on cerebral metabolism during hypoxia-ischemia in the immature rat. *Pediatr Res* 1997; **42:** 24–9.
32. Manley GT, Hemphill JC, Marabito D, *et al.* Cerebral oxygenation during hemorrhagic shock: perils of hyperventilation and therapeutic potential of hypoventilation. *J Trauma* 2000; **48**: 1025–33.
33. Akça O, Payne R, Kehl F, Sessler DI, Schurr A. Hypercapnic acidosis preconditions brain slices to hypoxia. American Society of Anesthesiologists, 2003 Annual Meeting, San Francisco, CA. Available online at http://www.asaabstracts.com/strands/asaabstracts/ (Accessed April 15, 2009.)
34. Akça O, Sessler DI, Delong D, *et al.* Tissue oxygenation response to mild hypercapnia during cardiopulmonary bypass with constant pump output. *Br J Anaesth* 2006; **96:** 708–14.
35. Akça O. Carbon dioxide and tissue oxygenation: is there sufficient evidence to support application of hypercapnia for hemodynamic stability and better tissue perfusion in sepsis? *Intens Care Med* 2008; **34:** 1752–4.
36. Kontos HA, Raper AJ, Patterson JL. Analysis of vasoactivity of local pH, PCO_2, and bicarbonate on pial vessels. *Stroke* 1977; **8:** 358–60.
37. Faraci FM, Breese KR, Heistad DD. Cerebral vasodilation during hypercapnia: role of glibenclamide-sensitive potassium channels and nitric oxide. *Stroke* 1994; **25:** 1679–83.
38. Iadecola C, Pellegrino DA, Moskowitz MA, Lassen NA. Nitric oxide synthase inhibition and cerebrovascular regulation. *J Cereb Blood Flow Metab* 1994; **14:** 175–92.
39. Schmetterer L, Findl O, Strenn K, *et al.* Role of NO in the O_2 and CO_2 responsiveness of cerebral and ocular circulation in humans. *Am J Physiol* 1997; **273**: R2005–12.

40. Faraci FM, Brian JE Jr. Nitric oxide and the cerebral circulation. *Stroke* 1994; **25:** 692–703.
41. Wang Q, Pellegrino DA, Baughman VL, Koenig HM, Albrecht RF. The role of neuronal nitric oxide synthase in regulation of cerebral blood flow in normocapnia and hypercapnia in rats. *J Cereb Blood Flow Metab* 1995; **15:** 774–8.
42. Rosenblum WI, Kontos HA, Wei EP. Evidence for a KATP ion channel link in the inhibition of hypercapnic dilation of pial arterioles by 7-nitroindazole and tetrodotoxin. *Eur J Pharmacol* 2001; **417:** 203–15.
43. Kontos HA, Wei EP. Arginine analogues inhibit responses mediated by ATP-sensitive K channels. *Am J Physiol* 1996; **271:** H1498–506.
44. Xu H, Cui N, Yang Z, *et al.* Direct activation of cloned KATP channels by intracellular acidosis. *J Biol Chem* 2001; **27**6: 12898–902.
45. Wei EP, Kontos HA. Blockage of ATP-sensitive potassium channels in cerebral arterioles inhibits vasoconstriction from hypocapnic alkalosis in cats. *Stroke* 1999; **30:** 851–4.
46. Laffey JG, Engelberts D, Kavanagh BP. Injurious effects of hypocapnic alkalosis in the isolated lung. *Am J Respir Crit Care Med* 2000; **162:** 399–405.
47. Hickling KG, Walsh J, Henderson S, Jackson R. Low mortality rate in adult respiratory distress syndrome using low-volume, pressure-limited ventilation with permissive hypercapnia: a prospective study. *Crit Care Med* 1994; **22:** 1568–78.
48. Amato MB, Barbas CS, Medeiras DM, *et al.* Effect of protective-ventilation strategy on mortality in the acute respiratory distress syndrome. *N Engl J Med* 1998; **338:** 347–54.
49. Laffey JG, Honan D, Hopkins N, *et al.* Hypercapnic acidosis attenuates endotoxin-induced acute lung injury. *Am J Respir Crit Care Med* 2004; **169:** 46–56.
50. Chonghaile MN, Higgins BD, Costello J, Laffey JG. Hypercapnic acidosis attenuates lung injury induced by established bacterial pneumonia. *Anesthesiology* 2008; **109:** 837–48.
51. Ni Chonghaile M, Higgins BD, Castillo JF, Laffey JG. Hypercapnic acidosis attenuates severe acute bacterial pneumonia-induced lung injury by a neutrophil-independent mechanism. *Crit Care Med* 2008; **36:** 3135–44.
52. O'Croinin DF, Nichol AD, Hopkins N, *et al.* Sustained hypercapnic acidosis during pulmonary infection increases bacterial load and worsens lung injury. *Crit Care Med* 2008; **36**: 2128–35.
53. Laffey JG, Tanaka M, Engelberts D, *et al.* Therapeutic hypercapnia reduces pulmonary and systemic injury following in vivo lung reperfusion. *Am J Respir Crit Care Med* 2000; **16**2: 2287–94.
54. Boix JH, Marin J, Enrique E, *et al.* Modifications of tissular oxygenation and systemic hemodynamics after the correction of hypocapnia induced by mechanical ventilation. *Rev Esp Fisiol* 1994; **50:** 19–26.
55. Richardson DW, Kontos HA, Raper AJ, Patterson JL Jr. Systemic circulatory responses to hypocapnia in man. *Am J Physiol* 1972; **223:** 1308–12.
56. Kitakaze M, Weisfeld ML, Marban E. Acidosis during early reperfusion prevents myocardial stunning in perfused ferret hearts. *J Clin Invest* 1988; **82:** 920–7.
57. Matsuda N, Kuroda H, Mori T. Beneficial actions of acidotic initial reperfusate in stunned myocardium of rat hearts. *Basic Res Cardiol* 1991; **86:** 317–26.
58. Ali S, Hahn H, Jacobsohn E, DeWet C, Avidan MS. Therapeutic effects of carbon dioxide administration following cardiac surgery. American Society of Anesthesiologists, 2003 Annual Meeting, San Francisco, CA. Available online at http://www.asaabstracts.com/strands/asaabstracts (Accessed April 15, 2009.)
59. Hashimoto K, Okazaki K, Okutsu Y. [The effect of hypocapnia and hypercapnia on myocardial oxygen tension in hemorrhaged dogs.] *Masui* 1990; **39:** 437–41.
60. Holmes JM, Dufner LA, Kappil JC. The effect of raised inspired carbon dioxide on developing rat retinal vasculature exposed to elevated oxygen. *Curr Eye Res* 1994; **13:** 779–82.
61. Holmes JM, Zhang S, Leake DA, Lanier WL. The effect of carbon dioxide on oxygen-induced retinopathy in the neonatal rat. *Curr Eye Res* 1997; **16:** 725–32.
62. Holmes JM, Zhang S, Leake DA, Lanier WL. Metabolic acidosis-induced retinopathy in the neonatal rat. *Invest Ophthalmol Vis Sci* 1999; **40:** 804–9.
63. Javaheri S. A mechanism of central sleep apnea in patients with heart failure. *N Engl J Med* 1999; **341:** 949–54.
64. Naughton MT, Benard DC, Rutherford R, Bradley TD. Effect of continuous positive airway pressure on central sleep apnea and nocturnal PCO_2 in heart failure. *Am J Respir Crit Care Med* 1994; **150:** 1598–604.
65. Sin DD, Fitzgerald F, Parker JD, *et al.* Risk factors for central and obstructive sleep apnea in 450 men and women with congestive heart failure. *Am J Respir Crit Care Med* 1999; **160:** 1101–6.
66. Hornbein TF, Townes BD, Schoene RB, Sutton JR, Houston CS. The cost to the central nervous system of climbing to extremely high altitude. *N Engl J Med* 1989; **321:** 1714–19.

Section 3

Special environments/populations

Section 3
Chapter
27

Special environments/populations

Atmospheric monitoring outside the healthcare environment and within enclosed environments: a historical perspective

G. H. Adkisson and D. A. Paulus

Introduction

Occupational exposure to contaminant gases and vapors has long been of concern. Historically, specific occupations were known to be hazardous even before the causes of their ailments were understood. Lewis Carroll's Mad Hatter in *Alice in Wonderland*, becoming increasingly deranged from inhaling toxic mercury vapor, was – although a fictional character – only one of a long list of affected workers. He represented hatters who, by trade, used mercury in the process of curing the felt used in hats, and could not avoid inhaling the fumes given off during their workday. Baraboo, Wisconsin's nitroglycerin-inhaling ammunition workers; Eden, Vermont's asbestos-breathing miners; and Harlen, Kentucky's coal dust-coughing miners are but specific examples. *Black Lung* became the bane of coal miners around the world. Mesothelioma afflicted workers in the asbestos industry. Following the invention of dynamite, the cardiovascular and neurological effects of chronic exposure to inhaled nitroglycerin were noted. As long as mankind has developed new industry, new occupational hazards have presented themselves.

More recently, and in addition to specific occupational hazards, we have become increasingly concerned about the environment as a whole. Headlines in the 1970s about global cooling and concerns over an impending ice age [1] have transformed into concerns of global warming and the destruction of the world as we know it. Given the unsettled nature of the science and the uncertainties of how mankind's activities may affect the cycle, climate change has become the term *du jour*. While headlines, along with temperatures, have fluctuated back and forth for over a hundred years, what is important is that we pay greater attention to atmospheric gases, with particular focus on the levels of CO_2 and other potentially harmful trace gases.

Atmospheric gases

The atmosphere is made up of four primary gases (nitrogen, oxygen, argon, carbon dioxide), accounting for over 99% of the total mixture, with trace gases accounting for the remainder. The so-called *greenhouse gases* – water vapor, carbon dioxide, methane, nitrous oxide, ozone, and a host of others (see Figure 27.1) [2] – have taken on new importance as the proponents of human-induced climate change point to the fact that emissions of these greenhouse gases have increased dramatically since the start of the industrial revolution. From 1970 to 2004, total emissions of greenhouse gases increased by 70% and CO_2 increased by about 80%. Carbon dioxide, therefore, represents approximately 75% of the total [3]. (The reader is referred to Figure 1 in the online publication [4].) Production of CO_2 through fossil fuel emissions increased by 29% between 2000 and 2008. Coal contributed about 37% of fossil fuel emissions in 2000, increasing to 40% in 2008. The contribution by oil combustion declined from 41% to 36% over the same period of time. The growth in

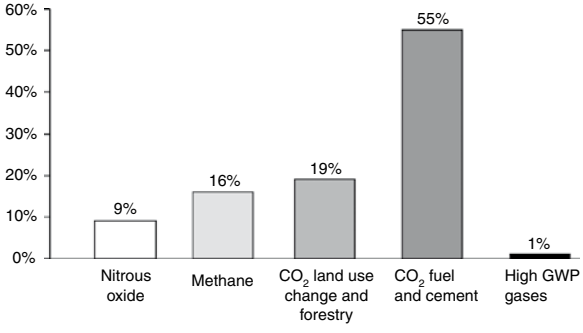

Figure 27.1 Anthropogenic greenhouse gas emissions. [Adapted from: Kruger P, Franklin D. Methane to markets partnership: opportunities for coal mine methane utilization. In: Ramani RV, Mutmansky JM (eds.) Proceedings of the 11th U.S./North American Mine Ventilation Symposium 2006, State College, Pennsylvania, June 5–7, 2006; 3].

Capnography, Second Edition, ed. J. S. Gravenstein, Michael B. Jaffe, Nikolaus Gravenstein, and David A. Paulus. Published by Cambridge University Press. © Cambridge University Press 2011.

fossil fuel emissions is dominated by countries classified as not having non-Annex B emissions limitations in the Kyoto Protocol. The Annex B countries, as an aggregate, have a flat CO_2 emissions record. The increase in international trade and shift of Annex B economies toward service has driven the non-Annex B nations to increase fossil fuel emissions. The land use change contribution has remained rather steady. Perhaps the best approach to view the current concern about greenhouse gases is to revisit the past, particularly through ice core analysis, which can yield a record of thousands of years.

Ice core analysis: a guide to climates of years past

The effect that human activity may be having on climate change is referred to as the *anthropogenic effect*. Given mankind's relatively short time on the Earth, an effort is being made to determine whether current climate changes are part of a natural cycle or whether they are being significantly influenced by the activities of humans, particularly in the areas of energy production and pollution. A number of ways exist to study the Earth's climate history [5]: examination of tree rings, lake and ocean sediments, and trace elements within stalagmites and stalactites [6]. Each of these presents a body of information. Analysis of the dust, snow, and bubbles from ice cores appears to provide a very good proxy for analyzing climate changes over an extended period. Ice cores obtained from Greenland can provide information for the last 100 000 years, and those from the Antarctic can provide information dating back to last 400 000 years [6]. These cores are analyzed for the parameters shown in Table 27.1 [7]. Ratios of the stable isotopes of oxygen (non-radioactive) are used to estimate the temperature at various times. Dust is analyzed for evidence of volcanic activity. Air bubbles are formed as snow under pressure makes a transition into ice. Air is mixed with the snow and, as snow is buried by more snow, it is increasingly compacted, eventually transforming into ice. The accompanying air becomes encapsulated, but until that process is completed, atmospheric gas circulates in and out of the air spaces. This process takes many years. In Greenland, where snow accumulation is rapid, bubbles take about 100 years to become encapsulated. In the Antarctic, where it rarely snows, the same process takes about 2000 years (Figure 27.2) [8].

Samples taken from deep layers of ice are analyzed to determine the transitions that have taken place over thousands of years. For example, the recent

Table 27.1 Atmospheric gas contents in ice core-occluded air

Measure	Climate signal
CO_2 concentration	Biological systems, ocean pump
CH_4 concentration	Wetlands, oceans, biomass, animals, continental shelf hydrates, permafrost
N_2O concentration	Biogeochemical nitrogen cycles from marine and terrestrial activity

Source: Adapted from: Cronin TM. *Principles of Paleoclimatology*. New York: Columbia University Press, 1999; 421.

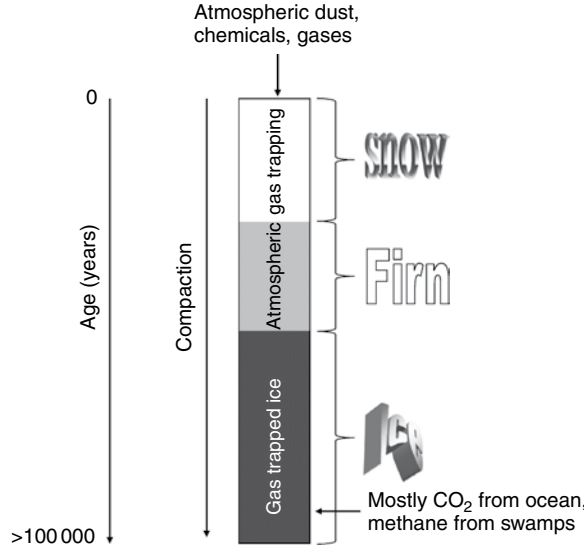

Figure 27.2 Snow-to-ice transition. Over many years, the atmospheric gases become encapsulated in the ice, allowing later ice core analysis. [Adapted from: Raynoud D, Jouzel J, Barnola JM, *et al.* The record of greenhouse gases. *Science* 1993; **259**: 926–34.]

temperature changes occurring alongside changes in CO_2 levels appear to follow each other during the time frame of the industrial revolution (Figure 27.3 [9] and Figure 27.4 [10]). Efforts are now being made to determine whether this is coincidental or whether there is a true cause and effect relationship.

Regardless of our current interest in the broader environment, of more immediate concern is controlling the working environment in various industrial situations to protect the health and well-being of workers. The Occupational Safety and Health Administration (OSHA) is the main federal agency in the United States charged with the enforcement of safety and health legislation. As part of the Centers for Disease Control (CDC), the National Institute of Occupational Safety

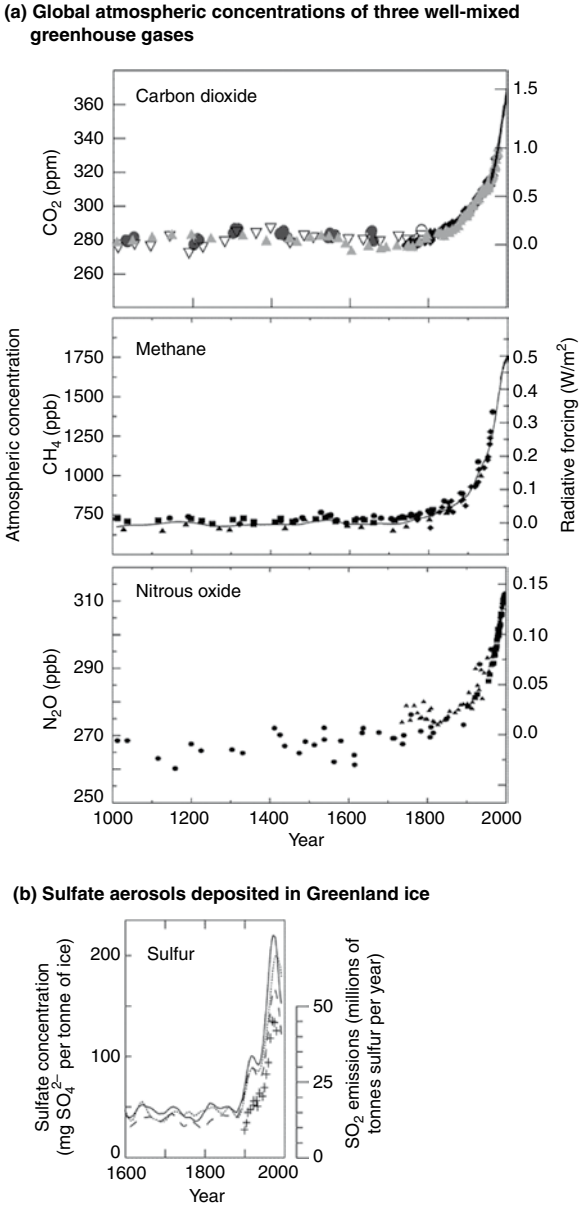

Figure 27.3 Long records of past changes in greenhouse gases show the effects of large and increasing growth in anthropogenic emissions during the industrial era (~1750–present). [From: Indicators of the human influence on the atmosphere during the Industrial Era. *Climate Change 2001. Working Group I: The Scientific Basis*. Intergovernmental Panel on Climate Change Geneva: IPCC.]

and Health (NIOSH) is responsible for conducting research and making recommendations for the prevention of work-related illnesses and injuries. This includes recommendations on acceptable levels of airborne contaminants. Industrial plants have long been of concern, but with proper monitoring and venting of harmful gases, open environments can usually be well controlled. An unfortunate exception to this occurred in Sverdlovsk, Russia in 1979 when the filtering systems failed, and hundreds – possibly thousands – of people were exposed to anthrax. The death toll stands officially at 68, but the true total may never be known [11]. Closed environments present a more complex problem.

Mines

Mines are an example of an environment in which the atmosphere is not strictly enclosed or isolated, but acts in a similar fashion. Airflow is limited, and contaminant gases can easily build up. While mining for coal dates back many centuries, deep shaft mining began in the late eighteenth century and developed along with the industrial revolution as the demand for coal rose. Cave-ins, explosions, and toxic gases all presented significant dangers, particularly given the difficulty of rescuing miners when an incident occurred.

Many hazardous gases are present in mines, including sulfur dioxide (SO_2), nitrogen dioxide (NO_2), carbon monoxide (CO), and methane (CH_4). The first three are products of diesel exhaust. NO_2 also is a product of explosives detonation [12]. Coal miners long ago developed a hazardous gas lexicon. *Firedamp* is a term that refers to a mixture of flammable gases in a mine, primarily composed of CH_4. *Blackdamp* or *chokedamp* is a term for a mixture of unbreathable gases formed when O_2 is removed from an enclosed atmosphere such as following a fire. Chokedamp is sometimes used to refer to CO specifically, while the term *stinkdamp* refers to hydrogen sulfide (H_2S) [13].

Explosions have accounted for most major mining accidents. For example, the Coal Glen Mine disaster in 1925 near Farmville, NC resulted in the death of 53 miners. In West Virginia that same year, a total of 686 mine fatalities were reported. The worst mining disaster in US history occurred in 1907 at Monongah, WV where 361 miners died. Mine safety improved in West Virginia, with only three deaths in 2009 [14]. However, in 2010 an explosion in a coal mine cost 29 miners their lives [15]. The worst mine accident in European history occurred in 1906 at the Courrières Mine in northern France, resulting in 1099 deaths. Furthermore, the worst mining disaster of all time occurred in 1942 at the Benxihu (Honkeiko) Colliery Mine in China where 1549 miners lost their lives [16]. Despite the risk of explosions, open flames were often

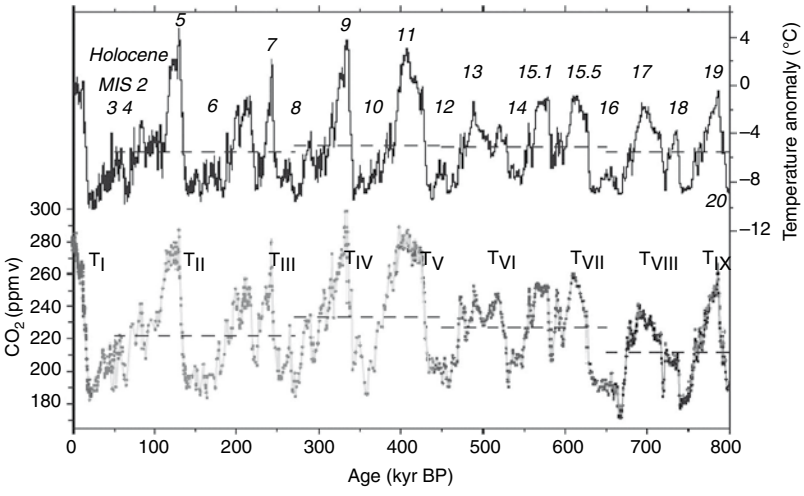

Figure 27.4 Ice core derived levels of temperature and CO_2. Several different ice cores were analyzed to obtain the resultant curves. Note how the curves parallel each other. The horizontal lines represent means for the respective time periods. [From: Lüthi DL, Le Floch M, Bereiter B, *et al.* High-resolution carbon dioxide concentration record 650 000–800 000 years before present. *Nature* 2008; **453**: 379–82.]

used to detect reduced levels of oxygen or the presence of dangerous gases that could develop within the mines. If a flame faltered or went out, it indicated that not enough oxygen was present. Flames, on the other hand, would burn more brightly, or displayed varying colors in the presence of other contaminant gases, such as CH_4 [13]. The Davy safety lamp came into use in the early nineteenth century [17]. It changed how miners checked for certain gases and reduced the risk of explosions. In addition to explosions, asphyxiation from toxic gases was a constant hazard, and newer, better methods of monitoring and protection were required.

One of the earliest methods of detecting gases, such as CH_4 or CO, as well as for the lack of O_2, was the use of birds such as canaries (Figure 27.5) [14]. Canaries were particularly sensitive to CO, and, while mice and presumably other animals were tested for their ability to detect abnormal levels of gas, the canary proved the more practical indicator. As long as the canary continued to sing, or at least continued to live, it was an indication that the atmosphere was breathable. When levels rose, the canary would begin to sway noticeably on its perch and, in the presence of toxic CO levels, would fall off its perch. Starting in 1911, two canaries were used in each British coal mine, a practice that continued until 1986 when the British government announced that 200 canaries would be retired from the mines the following year [18].

Catalytic methods of gas detection have been employed in the past, but, more recently, infrared devices are being used [19]. Modern hand-held devices can detect a range of combustible and toxic gases, as well as alarm in the event of low oxygen situations.

Figure 27.5 Canary with a West Virginia coal miner. [From: West Virginia Office of Miners' Health Safety and Training Photo from West Virginia's Mining History (early 1900s).]

Built-in recording capability can provide a record of individual exposures [20].

Methane is released during the process of coal mining, and detection becomes a dynamic problem. The introduction of the Davy lamp in 1816 improved the ability to detect the presence of CH_4 and any deficiency in O_2 levels. The miners would turn off their lamps, except for one who would hold the Davy lamp up high. In the presence of CH_4, the central yellow flame would become surrounded by a blue tinge. Low oxygen levels were detected if the lamp was lowered to the floor of the mine and a decrease in flame height was noted. The Pieler lamp, introduced in 1883,

improved this method of detection. Methane above 2.5% is explosive in the presence of flame and oxygen; the height of the flame in the Pieler lamp correlated directly with the concentration of methane in the atmosphere [21,22].

Closed environments

The creation of self-contained and somewhat renewable environments has allowed mankind to extend its reach into outer space and into the depths of the oceans. Additionally, the study of completely self-contained and renewable environments was attempted with several closed ecosystem experiments in order to better understand the closed environment of the planet we live on.

Saturation diving habitats

Saturation diving is a technique developed to avoid the lengthy and repeated decompressions required when ascending from deep ocean dives. For example, a single decompression from a 300-ft (92 m), 30-min-long exposure would take up to 3 h to accomplish. Weather conditions were critical, as decompression was made underwater, and thus, the weather above had to be clear enough to allow for stable depth control. Work at depth was limited, and the entire operation was time- and manpower-intensive. After a certain period at depth, in accordance with Henry's law of solubility, the body becomes saturated with gases at a new equilibrium. At that point, decompression time remains constant whether the diver stays one day or for months. A single, controlled decompression from saturated depth is normally accomplished onboard a ship within an environmentally-controlled pressure chamber. Transfer between the shipboard chamber and the working site at depth is accomplished by means of a pressurized transfer capsule handled by a deck crane. Divers, once at depth, leave the transfer capsule, and can work for any number of hours. In addition to acting as a pressurized transport vehicle, the transfer capsule also supplies breathing gas, heat, and communications via cables and hoses linked to the surface. In this manner, divers can go back and forth under a constant pressure, perform useful work and, when the job is completed, undergo a single decompression.

Conditions within the saturation chamber are carefully controlled for gas mixture, humidity, and heat. Dives at saturation depth are normally conducted using a mixture of helium and O_2 (heliox), as nitrogen becomes too dense and work of breathing rises dramatically. Helium is far less dense and allows for reasonable work of breathing, even at great depths. The oxygen content is reduced as depth increases to avoid the risk of O_2 toxicity. A typical mixture at depth may consist of 97–98% He and only 2–3% O_2. Contaminant gases must be carefully controlled, as any toxic effects will be magnified at depth. Carbon dioxide is controlled through the use of CO_2 scrubbers, primarily lithium hydroxide (LiOH), or venting, depending upon the type of chamber.

The SEALAB experiments

SEALABS I, II, and III were the original underwater habitats developed by the United States Navy to prove the viability of saturation diving, and to test the effects of divers living in isolation for extended periods. The first SEALAB was lowered off the coast of Bermuda in 1964 to a depth of 192 ft (58 m), and was planned for a dive of 3 weeks. It was halted after 11 days due to the approach of a major tropical storm. SEALAB II was launched in 1965 off the coast of California at a depth of 203 ft (62 m). Astronaut Scott Carpenter, one of the original seven astronauts from Project Mercury and the second American to orbit the Earth [23], was a member of one of the dive teams, and set a record at the time for staying under saturation for 30 days. In February of 1969, SEALAB III was placed off the coast of San Clemente Island, California at a depth of 610 fsw (186 m). Plagued from the start with a number of problems, the program was halted following the tragic death of one of the aquanauts sent to repair recurrent leaks. It was later discovered that his diving rig was missing baralyme, the chemical used to scrub CO_2 from his breathing circuit [24]. Knowledge gained from the SEALAB expeditions advanced deep ocean diving and rescue methods, and revealed additional insights into the psychological and physiological aspects of humans in isolation.

Closed ecosystems

BIOS-3

BIOS-3 was the first major attempt to create a closed ecosystem [25]. Built between 1965 and 1972 at the Institute of Biophysics in Krasnoyarsk, Siberia, it was a 315-m^3 habitat designed to support up to three people. BIOS-3 facilities were used to conduct ten closed manned experiments, the longest one lasting 180 days. Algae cultivated in tanks under artificial light, was used

to recycle air, absorbing CO_2 and replenishing it with O_2 through the process of photosynthesis. To support a single individual, approximately 86 sq ft (8 sq m) of exposed algae was required. Air was further purified by heating it to 1112 °F (600 °C) in the presence of a catalyst to eliminate other organic compounds. While not a completely closed system, by 1968, system efficiency had reached 85% by recycling water and encouraged further research in the field.

Biosphere 2

Perhaps the most famous attempt to create a closed environment came with the construction of Biosphere 2 in Arizona. Constructed between 1987 and 1991, it covered an area equivalent to two and a half football fields, and remains the largest closed system ever attempted [26]. The structure was effectively sealed, and allowed scientists to monitor virtually every aspect of the changing environment. Two closed missions were conducted: the first from September 26, 1991 to September 26, 1993 and the second from March 6, 1994 through September 6, 1994 when it ended prematurely. Neither mission was without its problems, but a great deal of knowledge was gleaned about closed ecosystems and closed habitat construction.

The first Biosphere project attempted to recreate an entirely closed ecosystem, but our world is far too complex to easily duplicate the delicate balance. One of the many problems encountered was the unexpected loss of habitat O_2 and widely fluctuating CO_2 levels. Most of the vertebrate species and all of the pollinating insects died [27]. Insects flourished, and the local species were accidentally sealed in, upsetting the planned balance.

The oxygen level was preset at 20.9%, but, 16 months into the project, fell steadily until it reached 14.5%. This is equivalent to O_2 availability at an altitude of 13 400 ft (4080 m). Team members became symptomatic, and additional O_2 was added in January and August of 1993. Carbon dioxide fluctuated in the range of 600 ppm on a daily basis. During daylight hours, photosynthesis caused a strong reduction in CO_2 levels that would then rise during night-time hours. In addition to daily fluctuations, there was a strong seasonal variation, with higher levels present during winter (4000–4500 ppm) as compared to summertime levels near 1000 ppm. Various attempts were made to manage the levels through natural methods, but CO_2 scrubbers were required on occasion to preserve a safe atmosphere [28].

Oxygen levels decreased over time as respiratory consumption exceeded available photosynthesis. Carbon dioxide, however, did not increase at a rate that would have been expected given the O_2 consumption. This inconsistency was solved when an isotopic analysis eventually showed that the CO_2 was reacting with exposed concrete surfaces within the biosphere, forming calcium carbonate and binding the additional CO_2 and, secondarily, the O_2 [29]. This was not discovered until the mission was completed and, had Biosphere 2 not been as well-sealed, it is anticipated that the entire imbalance might have gone unnoticed.

Prior to the start of the second mission, a number of system improvements were made. The concrete was sealed to prevent a recurrence of the CO_2 problem, and additional steps were taken to further enhance the ability of the team members to maintain a stable and self-sustaining environment. Unfortunately, due to a management dispute and vandalism by disgruntled members of the staff, the second mission ended prematurely [30]. Both the first and second missions proved, however, that closed ecosystems are extremely complex and vulnerable to multiple unplanned events and unforeseen imbalances.

Space Shuttle

In the complete vacuum of outer space, the Space Shuttle and space stations are enclosed environments in which all aspects of the atmosphere must be managed. For the Space Shuttle, the environmental control and life support system is designed to function for approximately 14 days, and consists of an air revitalization system, water coolant loop systems, atmosphere revitalization pressure control system, active thermal control system, water supply and wastewater system, waste collection system, and an airlock support system (Figure 27.6) [31]. Atmospheric pressure is maintained at 760 mm Hg ± 1.37%, 80% N_2, and 20% O_2. Oxygen and nitrogen tanks are located mid-fuselage of the orbiter. Oxygen is supplied from power-reactant storage and distribution cryogenic tanks, and is maintained in a supercritical state. Oxygen first passes through a series of valves before it reaches fuel cells that have two end products: water and electrical power. Some of the O_2, prior to reaching the fuel cells, is diverted into the cabin to replace what has been consumed [32]. Oxygen consumption rate is approximately 0.84 kg/day per individual, and requires replenishment on a continual basis. The partial pressure of oxygen is constantly

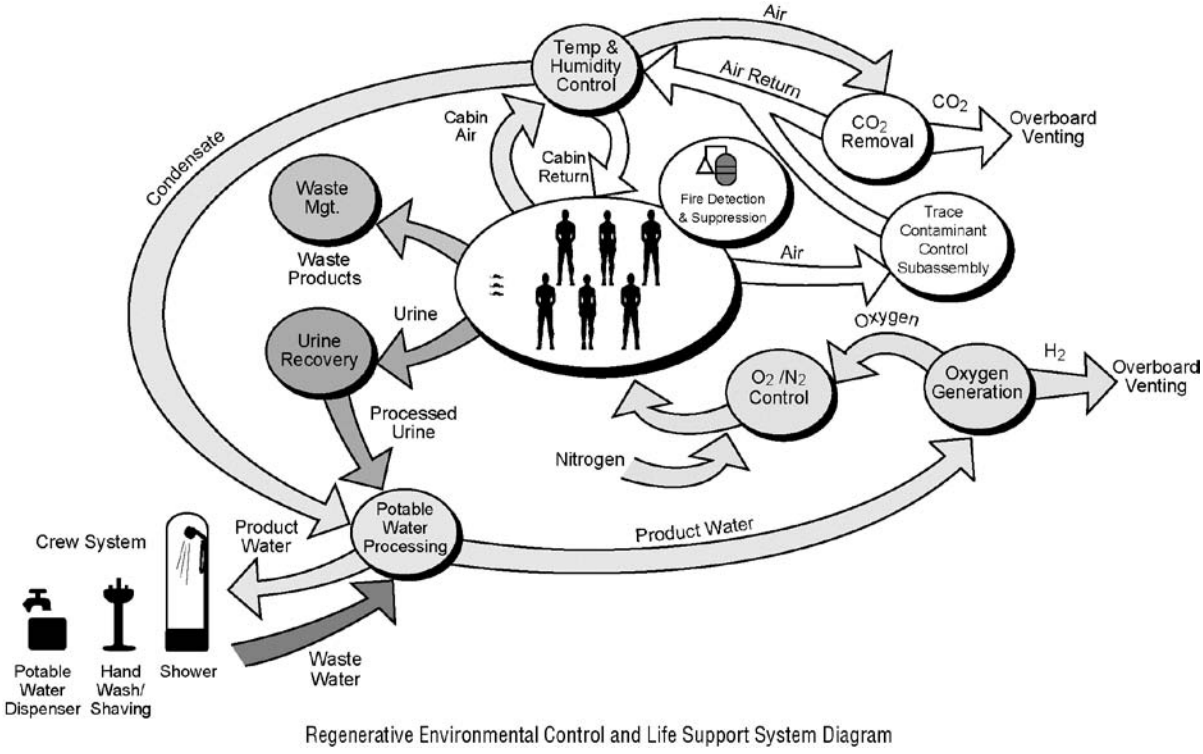

Figure 27.6 The Space Station regenerative environmental control and life support system. [From: *NASA Facts: International Space Station Environmental Control and Life Support System*. FS-202–05–85 MSF, May 2002. Huntsville, AL: NASA.]

monitored. In the automatic mode, the O_2 and N_2 control valves are activated and deactivated to maintain proper balance. An independent gaseous O_2 supply system is available for emergencies, such as failure of the automatic system.

Humidity is controlled between 30% and 75%, while CO_2 and CO are kept at habitable levels [31]. Cabin air is constantly circulated by fan, with about 8.5 air changes per hour. As air circulates, it passes through 300-μm filters and LiOH canisters for CO_2 removal, and through activated charcoal for odor elimination. The reaction of LiOH with CO_2 is: $LiOH + CO_2 \rightarrow LiHCO_3$. The LiOH canisters are changed every 11–12 h [33].

Alarm limits for the Space Shuttle environment are set for:

- Cabin pressure less than 724 mm Hg and greater than 796 mm Hg
- PO_2 less than 145 mm Hg and greater than 186 mm Hg
- Oxygen flow rate greater than 2.3 kg/h
- Nitrogen flow rate greater than 2.3 kg/h.

Hazardous gas detection within the Space Program is exceedingly important. Risks occur during lift-off, in orbit, and on descent. A new method, referred to as the *opto-electronic nose*, has recently been developed for use aboard the Space Shuttle *Endeavor*, and has completed a 6-month test aboard the Space Station [34]. The electronic nose can detect contaminants within a range of 1 to approximately 10 000 parts per million.

International Space Station

Similar environmental considerations present for the International Space Station, although the systems differ slightly. While in orbit, the Space Station system monitors levels of N_2, H_2, O_2, CH_4, CO_2, and water using a system similar to that used by the United States submarine fleet. The environmental control and life-support system aboard the Space Station is designed to function for approximately 180 days, and consists of the following systems: atmosphere control and supply, atmosphere revitalization subsystem, temperature and humidity control, water recovery and management subsystem, and a fire detection and suppression subsystem [35]. Atmosphere and pressure limits are similar to the Space Shuttle, but CO_2 removal is performed in a different manner. Primary removal is by

means of a silica gel with molecular sieves regenerated by vacuum/temperature swings. This is combined with CO_2 reduction by means of a Sabatier reactor that combines hydrogen with CO_2 in the presence of a catalyst to produce methane and water. The reaction is $CO_2 + 4H_2 \rightarrow CH_4 + 2H_20$ [36].

Submarines and submersibles

The first mention of submarines in history is probably Alexander the Great's order to destroy submarine defenses at Tyre. However, it is not clear whether the forces actually possessed submarines. Submarines are essentially enclosed environments designed to enter the hostile environment of the world's oceans. They range from small, privately owned recreational vessels to major strategic naval vessels with an almost unlimited cruising capability. From the earliest designs to today, all submersibles have faced the same basic problems of maintaining a secure internal environment, adequate power, and a breathable atmosphere.

Most submarines are designed as enclosed containers maintained at 1 ATA pressure. The earliest suggestions of a true submarine come from the writings of an Englishman William Bourne who described a craft designed to navigate under water. Despite an elegant description, there is no evidence that he actually constructed a craft [37]. Cornelius van Drebbel, a Dutch alchemist, was the first to actually build and test a submersible vessel. The Drebbel submarine, built around 1620, was made of a wooden frame covered with greased leather. Propulsion was provided by means of oars that extended through watertight grommets at the hull. It was designed to cruise 12–15 ft (4–5 m) below the surface. It could remain submerged for several hours. The air was refreshed by means of snorkel tubes that extended to the surface [38]. It was not until 1944 that a modern snorkel using this principle reappeared [39]. It has been suggested that additional oxygen may have been generated by burning potassium or sodium nitrate while submerged [40]. This reaction also consumes CO_2, and may explain why his crewmen were not affected by the build-up of CO_2 in the atmosphere. This early form of atmospheric regeneration went largely unrecognized for several centuries.

Early submarines sometimes increased pressure internally to balance pressure at their corresponding depth of water. This prevented uncontrolled leakage of water into the hull, but added to the problem of controlling contaminant gases, and increased the effects of CO_2 on the crews. Submarine depth was limited primarily by the amount of external force its hull construction could withstand and the ability to clear the atmosphere. As construction techniques improved, the ability to go to deeper depths increased, but the need for stable power and a clean environment was ever-present. The earliest submarines were literally powered by oars. Moving from manpower to a more reliable source of propulsion was a critical but difficult problem to solve. Even as steam and internal combustion engines were being developed, the problem of placing them into a relatively closed environment proved tricky. Heat became a significant problem in some early designs. Steam and gas engines could operate on the surface, but failed when a craft was sealed for underwater operations. They were simply impractical, as they would use available O_2 and foul the atmosphere unless vented overboard. John Phillip Holland, one of the first providers of submarines to the US Navy, discovered the true dangers of CO poisoning in 1898, when an exhaust leak sickened a number of his crew members. Holland, in a fashion similar to the use of canaries in mines, equipped his submarines with a cage housing several white mice as an early monitoring system [41].

The problem of providing continuous power underwater was eventually solved with the introduction of storage batteries and electric motors. Gasoline engines, and, later, diesel engines driving generators, would charge the batteries and, when submerged, the engines were shut down, and propulsion was by means of battery-driven electric drive motors. Holland was the first to successfully utilize this combination [42,43]. Modern diesel-electric submarines continue to use this basic principle. As technology continued to improve, submarines became a formidable force in the strategic plans of those nations that could afford to build and maintain them. The entire course of submarine warfare changed even more dramatically with the introduction of nuclear power.

The first nuclear submarine was the USS *Nautilus*, commissioned in September 1954 [44]. The advent of nuclear power led to an almost unlimited power supply, negated the requirement of periodic surfacing for recharging batteries, and allowed a boat to remain submerged for extended periods of time. However, the problems of maintaining a breathable and non-toxic atmosphere became even more important. Over time, technology was borrowed from other fields, and new innovations were developed, making it possible in the present day to remain submerged for several months or more.

United States submariners number approximately 30 000, ranging in age from 18 to 48 years. They are generally in good health, as evidenced by a lower morbidity rate than a group of adult males of similar age [45]. Submariners are unique in that they live in their enclosed work environment 24 hours a day, 7 days a week, for months at a time. To facilitate these living conditions, the US Navy developed guidelines based on continuous and emergency short-term exposures to a variety of shipboard contaminants [46–48]. Continuous, long-term exposures are for periods up to 90 days, and the emergency guidelines cover maximum 1-h and 24-h exposure limits.

Sources of atmospheric contamination in a submarine include exhaust from smoking, cooking, the human body, drive train, weapons, sanitation tanks, refrigeration, air conditioning, batteries, and various maintenance activities. The challenge in this setting is to establish safe levels of these contaminants, and monitor and process the various materials.

The Navy Research Laboratory in 1975 developed a central atmosphere monitor (CAMS) for use in submarines and subsequent use in the International Space Station. It uses an infrared CO_2 monitor and a fixed target mass spectrometer. The monitor analyzes the atmosphere for CO, H_2, O_2, water, N_2, and various refrigerant gases. Subsequent improvements allow the system to monitor up to 35 compounds. Complementing the central continuous monitoring system, colorimetric measurements are taken at regular intervals using single-sample tubes. Newer hand-held portable devices are also being utilized for measuring contaminants during certain shipboard activities.

In the modern nuclear submarine, seawater electrolysis provides oxygen to the submarine atmosphere, and the hydrogen byproduct is discharged to the sea. In emergency situations, oxygen can also be generated using a variety of chemical oxygen generators, most commonly through a device known as an *oxygen candle*. This is a cylindrical chemical oxygen generator containing a mixture of iron and sodium chlorate that, when ignited, produces sodium chloride, iron oxide, and approximately 6.5 h of oxygen per kilogram of the mixture. Monoethanolamine scrubbers remove CO_2 from the environment. Carbon monoxide from smoking and hydrogen from battery-charging are removed with a carbon monoxide and hydrogen burner that catalyzes the two gases into CO_2 and water as are other hydrocarbons. Activated carbon filters help remove high-molecular-weight compounds and odors. Electrostatic precipitators remove large particles and aerosols, and vent-fog precipitators remove oil mists in the engine room [48].

Summary

In summary, enclosed and semi-enclosed environments, particularly those in extremely isolated and hostile environments, such as outer space and the deep oceans, present unique challenges in terms of maintaining safe working conditions for the individuals exposed to them. Monitoring and control systems for these environments are highly complex and specialized to meet these unique challenges. As mankind ventures further afield, new and improved techniques will be required to allow us to push the limits of exploration, be it into the depths of our own oceans or into the farthest reaches of outer space.

References

1. Gwynne P. The cooling world. *Newsweek*, April 28, 1975; 64.
2. Kruger P, Franklin D. Methane to markets partnership: opportunities for coal mine methane utilization. In: Ramani RV, Mutmansky JM (eds.) Proceedings of the 11th U.S./North American Mine Ventilation Symposium 2006, State College, Pennsylvania, June 5–7, 2006; 3.
3. Intergovernmental Panel on Climate Change. Summary for policymakers. ln: *Climate Change 2007: Synthesis Report*. Geneva: IPCC, 2007; Available online at http://www.pewclimate.org/docUploads/PewSummary_AR4.pdf. (Accessed May 5, 2010.)
4. Le Quėrė C, Raupach MR, Canadell JG, *et al.* Trends in the sources and sinks of carbon dioxide. *Nature Geosci* 2009; doi:10.1038/NGEO689.
5. Bradley RS. *Reconstructing Climates of the Quaternary,* 2nd edn. San Diego, CA: Academic Press, 1999; 126.
6. Readinger C. Ice core proxy methods for tracking climate change. CSA Discovery Guides, February, 2006. Available online at http://www.csa.com/discoveryguides/discoveryguides-main.php. (Accessed May 5, 2010.)
7. Cronin TM. *Principles of Paleoclimatology*. New York: Columbia University Press, 1999; 421.
8. Raynoud D, Jouzel J, Barnola JM, *et al*. The record of greenhouse gases. *Science* 1993; **259**: 926–34.
9. Intergovernmental Panel on Climate Change. Indicators of the human influence on the atmosphere during the Industrial Era In: *Climate Change* 2001*: The Scientific Basis*. Geneva: IPCC, 2001. Available online

at http://www.grida.no/publications/other/ipcc_tar/?src=/climate/ipcc_tar/. (Accesssed May 4, 2010.)

10. Lüthi DL, Le Floch M, Bereiter B, *et al.* High-resolution carbon dioxide concentration record 650,000–800,000 years before present. *Nature* 2008; **453**: 379–82.
11. Meselson M, Guillemin J, Hugh-Jones M, *et al.* The Sverdlovsk anthrax outbreak of 1979. *Science* 1994; **266**: 1202–8.
12. Dubaniewicz TH, Chilton JE. *Optically Powered Remote Gas Monitor*, Report of Investigations 9558. Washington, DC: Bureau of Mines, 1995.
13. Edwards E. The miners' safety lamp: analysing the English collections at the Pitt-Rivers Museum, July 2009. Available online at http://england.prm.ox.ac.uk/englishness-Miners-lamp.html. (Accessed January 31, 2010.)
14. A Brief History of Coal and Safety Enforcement in West Virginia. West Virginia Office of Miners' Health Safety and Training. Available online at http://www.wvminesafety.org, 2010.
15. Deaths at West Virginia mine raise issues about safety. The *New York Times*. Available at: http://www.nytimes.com/2010/04/07/us/07westvirginia.html. (Accessed May 5, 2010.)
16. Epicdisasters. The ten worst worldwide mining disasters as measured by casualties. Available online at http://www.epicdisasters.com/index.php/site/comments/the_ten_worst_worldwide_mining_disasters/. (Accessed May 5, 2010.)
17. Davy H. On the fire-damp of coal mines and on methods of lighting the mines so as to prevent its explosion. *Phil Trans R Soc London* 1816; **105**: 1–24.
18. BBC News. Coal mine canaries made redundant. In: "On this day, 30 December 1986." Available online at http://news.bbc.co.uk/onthisday/hi/dates/stories/december/30/newsid_2547000/2547587.stm. (Accessed May 2, 2010.)
19. Fowler C, Chalmers D. The application of open path infrared detectors in underground coal mines. In: Ramani RV, Mutmansky JM (eds.) Proceedings of the 11th U.S./North American Mine Ventilation Symposium 2006, State College, Pennsylvania, June 5–7, 2006; 519.
20. MSA The Safety Company. Altair® 5 Multigas Detector. Available online at http://www.msanorthamerica.com/catalog/product503460.html. (Accessed February 8, 2010.)
21. Stutzer M. *The Pieler Methane Detection Lamp*. Available online at http://www.minerslamps.net/homepage/history_of_the_pieler_lamp.htm. (Accessed January 31, 2010.)
22. Hughes HW. *A Textbook of Coal Mining*, 5th edn. London: Charles Griffin, 1904; 485.
23. NASA. Scott Carpenter NASA Astronaut: biographical data. Available online at http://www.jsc.nasa.gov/Bios/htmlbios/carpenter-ms.html. (Accessed May 2, 2010.)
24. Council J. *Original Sealab History*. Available online at http://www.sealab.org/history.html. (Accessed January 31, 2010.)
25. Salisbury FB, Gitelson JI, Lisovsky GM. Bios-3: Siberian experiments in bioregenerative life support. *BioScience* 1997; **47**: 575–85.
26. Biospherics. *Biosphere 2: The Experiment – Invention, Creation and Mission 1 – A Brief Chronology*. Available online at http://www.biospheres.com/experimentchrono1.html. (Accessed April 20, 2010.)
27. Walker E, Carroll D. Biosphere 2: what went wrong? Available online at http://biology.kenyon.edu/slonc/bio3/2000projects/carroll_d_walker_e/biosphere.html. (Accessed May 2, 2010.)
28. Nelson M, Dempster WF, Alvarez-Romo NT, MacCallum NT. Atmospheric dynamics and bioregenerative technologies in a soil-based ecological life support system: initial results from Biosphere 2. *Adv Space Res* 1994; **14**: 417–26.
29. Severinghaus JP, Broecker W, Dempster W, MacCallum T, Wahlen M. Oxygen loss in Biosphere 2. *EOS, Trans Am Geophys Union*, 1994; **75**: 33, 35–7.
30. Poynter J. *The Human Experiment: Two Years and Twenty Minutes Inside Biosphere 2*. New York: Thunder's Mouth Press, 2006; 325–6.
31. NASA. NSTS 1988 *News Reference Manual: Space Shuttle Orbiter Systems, Environmental Control and Life Support System*. Available online at http://science.ksc.nasa.gov/shuttle/technology/sts-newsref/sts_eclss.html#sts_eclss. (Accessed February 6, 2010.)
32. NASA. *Fuel Cell Power Plants*: *NASA Human Space Flight*. Available online at http://spaceflight.nasa.gov/shuttle/reference/shutref/orbiter/eps/pwrplants.html. (Accessed May 2, 2010.)
33. NASA. *Atmosphere Revitalization Overview*. Available online at http://els.jsc.nasa.gov/index.php?intPageId=105. (Accessed February 6, 2010.)
34. NASA/Jet Propulsion Laboratory. Electronic nose to return from space station. *Science Daily*. Available online at http://www.sciencedaily.com/releases/2009/09/090910235638.htm. (Accessed May 2, 2010.)
35. Boeing Inc. *International Space Station: Environmental Control and Life Support System*. Available online at http://www.boeing.com/defense-space/space/spacestation/systems/eclss.html. (Accessed May 2, 2010.)
36. El Sherif D, Knox JC. *International Space Station Carbon Dioxide Removal Assembly (ISS*

CDRA: Concepts and Advancements). Pasadena, CA: NASA Archive 2005–01–2892.

37. Harris B. World submarine history timeline. 1580–1869. Available online at http://www.submarine-history.com/NOVAone.htm. (Accessed February 8, 2010.)
38. Cornelis Drebbel: inventor of the submarine. Dutch Submarines. Available online at http://www.dutchsubmarines.com/specials/special_drebbel.htm. (Accessed February 8, 2010.)
39. Hutchinson R. *Jane's Submarines: War Beneath the Waves from 1776 to the Present Day*. London: HarperCollins, 2001.
40. Clark E. A further note on Drebbel's submarine. *Bull John Rylands Lib* 1941; **26**: 451–5.
41. Parrish T. *The Submarine: A History*. New York: Viking Penguin, 2004; 32.
42. SS-1 Holland. Available online at http://www.globalsecurity.org/military/systems/ship/ss-1.htm. (Accessed August 2, 2010.)
43. Bellis M. *History of the Submarine: The USS* Holland *Submarine*. Available online at http://inventors.about.com/od/hstartinventors/a/JohnHolland.htm. (Accessed February 8, 2010.)
44. Fast attacks and boomers: submarines in the Cold War. Available online at http://www.americanhistory.si.edu/subs/history/subsbeforenuc/revolution/nautilus.html. (Accessed August 2, 2010.)
45. Charpentier P, Ostfeld AM, Hadjimichael OC, Hester R. The mortality of U.S. nuclear submariners, 1969–1982. *J Occup Med* 1993; **35**: 501–9.
46. *Emergency and Continuous Exposure Guidance Levels for Selected Submarine Contaminants*, vol. 1. Committee on Emergency and Continuous Exposure Guidance Levels for Selected Submarine Contaminants, Committee on Toxicology, National Research Council. Washington, DC: National Academies Press, 2007.
47. *Emergency and Continuous Exposure Guidance Levels for Selected Submarine Contaminants*, vol. 2. Committee on Emergency and Continuous Exposure Guidance Levels for Selected Submarine Contaminants, Committee on Toxicology, National Research Council. Washington, DC: National Academies Press, 2008.
48. *Emergency and Continuous Exposure Guidance Levels for Selected Submarine Contaminants*, vol. 3. Committee on Emergency and Continuous Exposure Guidance Levels for Selected Submarine Contaminants, Committee on Toxicology, National Research Council. Washington, DC: National Academies Press, 2009.

Section 3
Chapter
28

Special environments/populations

Capnography in veterinary medicine

R. M. Bednarski and W. Muir

Overview of capnography in veterinary medicine

Capnography as a respiratory monitor and diagnostic tool was not used in clinical veterinary medicine until the early 1980s [1]. Since that time, its use has increased steadily, but it is still underused in clinical veterinary practice. Most veterinarians remain unfamiliar with or are poorly educated regarding the concepts of expired gas monitoring and the relationship between expired carbon dioxide concentrations and ventilation, airway deadspace, and the respiratory component of acid–base balance. Veterinarians familiar with capnography have frequently encountered technical difficulties associated with the use of older or less expensive capnometers, especially when sampling respiratory gas from relatively small (<5 kg), spontaneously breathing, anesthetized animals that frequently demonstrate altered patterns of breathing (apnea, tachypnea, panting) (Figure 28.1). Furthermore, veterinarians often do not access medical technology until it becomes well established in human medicine and is relatively inexpensive. Currently, published veterinary anesthetic monitoring standards do not mandate the use of capnography for the routine monitoring of anesthetized animals [2,3]; nevertheless, time-based capnography is achieving more widespread and routine use in veterinary medicine.

Volumetric capnography, although not commonly used, has recently been used for equine pulmonary function testing [4]. Volumetric capnography simultaneously measures expired CO_2 and tidal volume, facilitating the identification of CO_2 from three sequential compartments: apparatus (anesthetic equipment), anatomic deadspace, and progressively emptying alveoli (alveolar gas). Heterogeneity in lung ventilation–perfusion ($\dot{V}/\dot{Q}$) creates regional differences in CO_2 concentration, and sequential emptying contributes to the rise of the alveolar plateau and the steepness of the expired CO_2 slope. The concept of deadspace accounts for those lung areas that are ventilated but not perfused. In some animals, particularly supine horses, the high $\dot{V}/\dot{Q}$ mismatch produces an increase in alveolar deadspace, often concurrent with an increase in shunt fraction.

Figure 28.1 Anesthetized 1-kg dog. Capnometer airway adaptor volume is equal to 0.5 mL, thus adding minimal deadspace volume to the breathing circuit.

Current methodological and technical limitations of capnography in veterinary medicine

Although mammalian respiratory anatomy and function are remarkably similar among species, there are obvious allometric differences. Regardless of disparate respiratory anatomy and physiology, capnography can be used in both mammalian and non-mammalian species. The concentration of CO_2 in expired gas

Capnography, Second Edition, ed. J. S. Gravenstein, Michael B. Jaffe, Nikolaus Gravenstein, and David A. Paulus. Published by Cambridge University Press. © Cambridge University Press 2011.

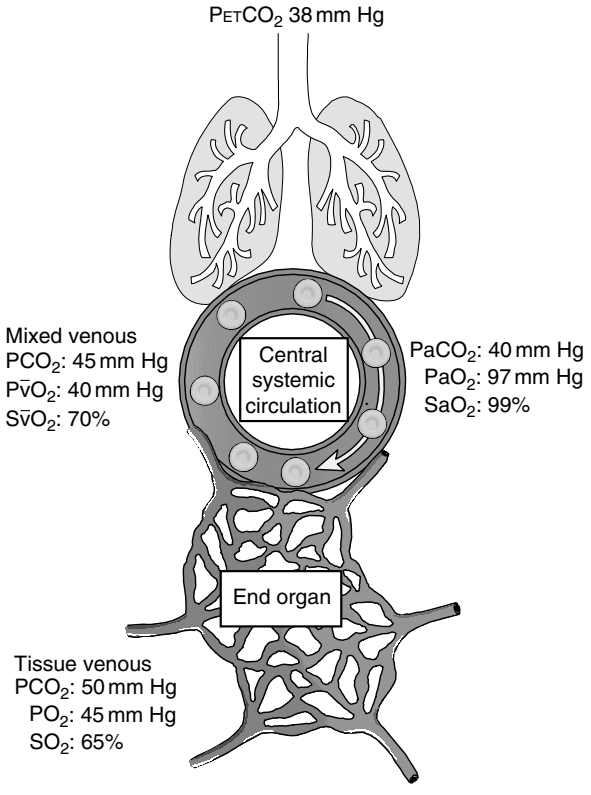

Figure 28.2 Illustration of CO_2 production, transport, and elimination.

is a function of three distinct but interrelated processes: CO_2 production from cellular respiration; CO_2 transport from the tissues to the lungs via the cardiovascular system; and CO_2 elimination from the body by cyclic movement of gases in and out of alveolar (mammals) or non-alveolar lungs (birds and reptiles) (Figure 28.2).

Many limitations of capnography in veterinary medicine are secondary to attempts to use capnometers in smaller domestic and non-domestic species that are designed for use in adult humans. Capnometer limitations related to smaller animal species are similar to those described for human neonates and infants (small tidal volumes, rapid respiratory rates, limited CO_2 production). Additionally, capnography can be challenging, if not impossible, to perform in awake uncooperative animals, thus limiting its use in non-anesthetized animals.

The development of tight-fitting masks, lower sampling rates (50 mL/min), and faster response times makes capnography more useful in smaller and conscious animals. Capnography in animals such as rodents and birds, nevertheless, remains challenging.

Species differences with the use of capnography

A wide range of respiratory volumes exists among animal species (Tables 28.1 and 28.2) [5]. There is remarkable similarity in arterial blood pH and gas values (Table 28.3) [5].

Dogs and cats

Capnography in obtunded, anesthetized, or cooperative dogs and cats is relatively easily performed. The same gas sampling techniques used in anesthetized humans are suitable for use in dogs and cats since the same breathing circuits designed for human adult or pediatric use can be used in these species.

Capnography is less easily performed in non-intubated alert dogs and cats, although a gas sampling tubing from a sidestream analyzer can be inserted into one of the nostrils for intermediate sampling [6]. In this study by Hendricks and King the sampling tubing from a sidestream analyzer was inserted 3–7 mm into one nostril for 30 s, with the alar fold gently closed around the tubing to minimize aspiration of room air. The mouth was held closed when necessary to ensure nasal breathing. End-tidal CO_2 values accurately reflected hypoventilation when compared to simultaneously obtained arterial samples in normal non-panting dogs and cats. The authors concluded that, in this population of awake, non-panting dogs, end-tidal CO_2 was useful in detecting hypoventilation. However, in panting dogs, end-tidal CO_2 did not correlate with $PaCO_2$ ($r = 0.37$, $P = 0.27$), and was of no use in predicting $PaCO_2$.

Few studies have critically compared end-tidal to arterial CO_2 [7,8]. End-tidal and arterial CO_2 were well correlated in supine, closed chest, halothane-anesthetized dogs during spontaneous and controlled ventilation, with a difference between 1.9 and 2.2 mm Hg. The difference was slightly higher during assist mode and intermittent manual ventilation [7]. The correlation of end-tidal and arterial CO_2 was not as good in isoflurane- or halothane-anesthetized dogs undergoing various open-chest surgical manipulations [8]. Dogs were positioned dorsally (supine) or in a left or right lateral recumbent position, depending on surgical need. The authors concluded that end-tidal CO_2 was not a reliable indicator of adequacy of ventilation because it differed greatly from arterial CO_2, and the arterial – end-tidal CO_2 difference was not consistent between dogs or in any given dog over

Table 28.1 Breathing frequency (f), tidal volume (V_T), and minute ventilation (APV_E) of various species

Species	Mean body wt (kg)	*n*	Conditions[b]	f (breaths/min)	V_T		APV_E	
					mL	mL/kg	mL/min	mL/kg/min
Mice	0.02	NS[a]	Awake, prone	163.4	0.15	7.78	24.5	1239
	0.032	NS	Anesthetized	109	0.18	5.63	21.0	720
Rats	0.113	NS	Awake, prone	85.5	0.87	7.67	72.9	646
	0.305	NS	Awake, pleth	103	2.08	6.83	213	701
Cats	3.8	4	Unanesthetized, pleth	22	30	7.9	664	174
	3.7	NS	Anesthetized	30	34	9.2	960	310
Dogs	18.6	6	Awake, prone, chronic trach, intubated	13	309	16.6	3818	205
	18.8	8	Awake, standing, chronic trach, intubated	16.5	314	16.9	4963	264
Sheep	32–37	4	Awake, standing, mask	38	289	8.3	10 400	297
Goats	36.3	3	Awake, standing, mask	13.6	470	12.9	6313	174
	46.4	6	Awake, standing, mask	26	483	10.4	11 900	256
	47.6	6	Awake, standing, mask	17.6	602	12.6	10 540	221
Pigs	12.9	4	Awake, standing	13.1	209	15.9	2731	208
Cows	517 Holstein	7	Awake, standing, mask	23.7	3676	7.1	85 977	166
	405 Jersey	11	Awake, standing, mask	28.6	3360	8.3	94 870	234
Calves	43–73 Hereford	8	4–6 weeks old, standing, sling	26.7	403	15.1	10 290	385
Horses	402	6	Awake, standing, mask	11.8	4253	10.6	49 466	123
	483	6	Awake, standing, mask	15.5	4860	10.1	74 600	154
	486	15	Awake, standing, mask (some sedated) (mask V_D not removed)	10	7300	15.0	79 000	163
Ponies	147	19	Awake, standing, mask	19.0	1370	9.3	26 380	180

[a] Not specified.
[b] Pleth, whole-body plethysmograph; trach, tracheostomy.
Source: McDonell W, Kerr C. Respiratory system. In: Tranquilli W, Thurmon J, Grimm K (eds.) *Lumb and Jones Veterinary Anesthesia and Analgesia*, 4th edn. Ames, IA: Blackwell Publishing, 2007; 117–51.

time. Another study in mechanically ventilated, closed chest, dorsally recumbent, halothane-anesthetized dogs determined a good correlation between end-tidal and arterial CO_2 over a wide range of arterial CO_2 [9]. Arterial CO_2 was manipulated by maintaining a constant tidal volume while varying the respiratory rate. End-tidal CO_2 values differed by 3 ± 5 mm Hg; the bias increased as $PaCO_2$ exceeded 60 mm Hg. In this study, agreement between end-tidal and arterial CO_2 was better for mainstream than sidestream capnography. Studies in cats are lacking, most likely due to their relatively small size.

Horses and cattle

Obtaining accurate and reliable end-tidal CO_2 values from conscious or sedated horses or cattle with conventional capnometric equipment is difficult and oftentimes impossible. Sedating or training horses to accept a tight-fitting mask is necessary. Although volumetric capnography is used for pulmonary function testing in horses, its use has not become widespread [10]. Volumetric capnography in horses has the limitations of high breath-to-breath variability in tidal volumes and flow rates, and requires multiple breaths for accurate interpretation [10,11].

Table 28.2 Arterial blood-gas and acid–base values for various species

Species	Mean body wt {kg}	*n*	Conditions	pH_a	$PaCO^{-}$,	PaO_2	HCO_3^-
Rats	0.207	10	Awake, chronic catheter	7.44	32.7		21.5
	0.305	8	Awake, prone, chronic catheter	7.467	39.8		28.7
Rabbits	3.1	NS[a]	Awake, catheter	7.388	32.8	86	21
	3.5	20	Awake, catheter	7.47	28.5	89.2	20.2
Cats	2.5–5.1	8	Unsedated, chronic catheter, prone	7.41	28.0	108	18
	3–8	10	Unsedated, not restrained, chronic catheter	7.426	32.5	106	22.1
Dogs	18.8	8	Chronic tracheostomy, catheter, unsedated, standing	7.383	39.0	103.8	22.1
	12.2	22	Chronic catheters lateral recumbency	7.40	35	102	21
Sheep	33	NS	Awake, catheter	7.44	40.9	96	27.6
	24.5	11	Unsedated, prone, carotid loop	7.48	33	92	
Goats	18	6	Unsedated, standing	7.46	36.5	101	
	47.6	6	Unsedated, standing, catheter	7.45	35.3	94.5	24.1
	46.6	6	Unsedated, standing	7.45	41.1	87.1	27.6
Calves	31–57	4	Standing, unsedated, aortic catheter	7.39	40	81	24
	48–65	20	Unanesthetized, catheter	7.37	42.8	93.6	23.6
Cows	517	7	Awake, unsedated, standing	7.40	39.6	83.1	24.4
	641	7	Awake, unsedated, standing	7.435	38.7	95.1	25.5
Horses	402	6	Awake, unsedated, standing	7.39	41.1	80.7	24.5
Ponies	147	19	Standing, aortic catheter	7.40	40	88.7	24.4

[a] Not specified.
[b] R. Warren and W. McDonell, unpublished data.
Source: McDonell W, Kerr C. Respiratory system. In: Tranquilli W, Thurmon J, Grimm K (eds.) *Lumb and Jones Veterinary Anesthesia and Analgesia*, 4th edn. Ames, IA: Blackwell Publishing, 2007; 117–51.

Capnometry is more commonly used to monitor ventilation in anesthetized horses. Mainstream capnometers are generally not useful in larger animals (>300 kg) due to the size of their airway and associated large diameter (>2.5 cm) endotracheal tubes and coupling connectors required for mainstream measurements. Sidestream capnometers are used with the sampling tubing attached to an adaptor located on the Y-piece of the anesthetic breathing hoses (Figure 28.3). Alternatively, gas can be sampled through a needle inserted into the endotracheal tube lumen. No measurable difference was found between $P_{ET}CO_2$ values obtained from the proximal and the distal endotracheal tube [12]. The $P_{ET}CO_2$–$PaCO_2$ difference is relatively small in healthy standing horses [13]. However, recumbent anesthetized horses are prone to significant $\dot{V}/\dot{Q}$ mismatch and increased physiologic deadspace [14]. As such, the $P_{ET}CO_2$–$PaCO_2$ difference in anesthetized adult horses, ponies, and neonatal foals can vary widely [12,15–17]. Maintenance of a physiologically normal $P_{ET}CO_2$–$PaCO_2$ difference is better during controlled than during spontaneous ventilation, and is worse in compromised, dorsally recumbent horses [12,17]. During spontaneous ventilation, the $P_{ET}CO_2$–$PaCO_2$ difference is commonly greater than 10 mm Hg, with the disparity increasing with longer anesthetic duration [12,15,16].

Mice and small laboratory animals

Mice and other small laboratory animals are popular biomedical research subjects. Their small size makes

Table 28.3 Lung volumes of various mammalian species: total lung capacity (TLC), functional residual capacity (FRC), and residual volume (RV)

Species	Mean body wt (kg)	*n*	Condition	TLC		FRC (mL/kg)	RV (mL/kg)
				mL	mL/kg		
Mice	0.020	NS[a]	Anesthetized	1.57	78.5	25.0	19.5
Rats	0.31	NS	Anesthetized, prone	12.2	39.4	6.8	4.2
Rabbits	3.14	NS	Anesthetized, supine	111	35.4	11.6	6.4
Cats	3.7	4	Anesthetized			17.8	
Dogs	18.6	6	Awake, prone	2090	112.4	53.6	16.7
	9.2	140	Unsedated, 1 year old			44.8	
Sheep	24.5	4	Unsedated, prone, nasal endotracheal tube			45.3	
Goats	46.4	6	Unsedated, standing, face mask			49.6	
Cows	517	7	Awake, standing			39.4	
	537	5	Anesthetized, prone	45 377	84.5	31.9	16.1
Horses	485		Anesthetized, prone	44 800	92.4	36.3	19.0
	402	6	Awake, standing			51.3	
	394	4	Anesthetized, prone, lung inflated to 35–40 cm H_2O, starved 18 h	45 468	115.4	37.9	
	450–822	6	Conscious, standing			35.6	
Ponies	164–288	8	Conscious, standing			39.9	

[a] Not specified.
Source: McDonell W, Kerr C. Respiratory system. In: Tranquilli W, Thurmon J, Grimm K (eds.) *Lumb and Jones Veterinary Anesthesia and Analgesia*, 4th edn. Ames, IA: Blackwell Publishing, 2007; 117–51.

monitoring of respiratory and cardiovascular variables difficult. Recently, microcapnometry, using very low sampling rates of 5–20 mL/min and fast response times (75 ms to 90% at 20 mL/min), has been described [18]. This completely non-invasive monitoring system produces no monitoring-related morbidity, and is suitable for survival procedures. The sampling tube of the sidestream capnometer is inserted through a predrilled hole at the base of the tracheal catheter to minimize equipment deadspace. Although intubation of small laboratory species is challenging, several techniques have been described [19]. The $P_{ET}CO_2$–$PaCO_2$ difference is small, and can be positive or negative depending on ventilatory rate, tidal volume, and the inspired concentration of CO_2 [18,20].

Birds

The respiratory system of birds differs anatomically and physiologically from that of mammals. The tracheal volume is four times that of comparably sized mammals, mostly due to the bird's relatively long neck [21]. To compensate for these differences, their respiratory rate is relatively slow, with a relatively large tidal volume. The avian lung is fixed to the dorsal rib cage. The lung does not expand and contract, and, therefore, has a minimal functional residual capacity [22]. There is no diaphragm of any sort and no separation of thoracic and abdominal cavities. Gas flow occurs because of a musculoskeletal-induced change in the thoracoabdominal volume (Figure 28.4). Air sacs comprise most of the respiratory volume, and connect to the secondary bronchi via ostia. The nine relatively large air sacs communicate freely with the parabronchial lung, and expand and contract during inspiration and expiration, respectively, acting as a bellows. Air sacs are poorly vascularized and do not directly participate in gas exchange. Gas flows unidirectionally through the avian lung during both phases of the respiratory cycle, from caudal to cranial, via parabronchi that branch from

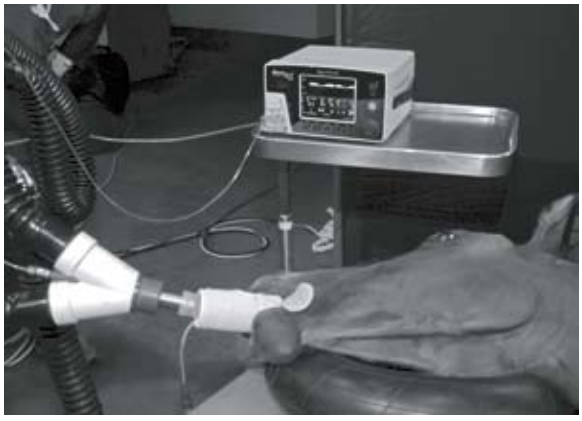

(a)

(b)

Figure 28.3 (a) Adult anesthetized horse with capnometer. (b) Y-piece adaptor and sampling tubing for equine capnometry.

the secondary dorsal and ventral bronchi. The parabronchi lead to air capillaries in which gas exchange occurs. Gas exchange between the air capillaries and pulmonary blood occurs via a cross-current mechanism. During inspiration, gas that has passed through the parabronchial lung and exchanged oxygen and carbon dioxide from the previous respiratory cycle moves into the cranial air sacs. This gas is then expelled from the cranial air sacs during exhalation, mixing with the exhaled gas leaving the lung (Figure 28.5). These anatomic and physiologic entities can result in a negative arterial to end-expired CO_2 gradient [23,24]. Gas flow patterns within the respiratory system can vary, and are controlled by aerodynamic valving [22].

Values of $P_{ET}CO_2$–$PaCO_2$ were closely correlated over a wide range of partial pressures in isoflurane-anesthetized African gray parrots (*Psittacus erithacus*) [25]. This study used a mechanically controlled breathing system with unidirectional valves to ventilate the parrots to three levels of end-tidal CO_2 (<30, 30–40, >40). Throughout the range of end-tidal CO_2 investigated, $P_{ET}CO_2$ consistently overestimated $PaCO_2$ by approximately 5 mm Hg. Another study investigating end-tidal to arterial CO_2 differences in isoflurane-anesthetized raptors demonstrated a strong correlation between $P_{ET}CO_2$ and $PaCO_2$ ($r = 0.94$; $P < 0.0001$) [26]. However, the level of agreement between the two varied significantly at various concentrations of ventilation-induced end-tidal CO_2. Low end-expired CO_2 tensions (18–29 mm Hg) exceeded arterial CO_2 by 6 ± 1.9 mm Hg, and high end-expired tensions (50–63 mm Hg) underestimated arterial CO_2 by 7.6 ± 9.8 mm Hg. In the 30–49 mm Hg range of $P_{ET}CO_2$, the difference between $P_{ET}CO_2$ and $PaCO_2$ was 1 ± 8 mm Hg.

A study in isoflurane-anesthetized Hispaniolan Amazon parrots (*Amazona ventralis*) investigated the relationship of $P_{ET}CO_2$ and $PaCO_2$ during spontaneous and controlled ventilation [27]. The $P_{ET}CO_2$ significantly overestimated $PaCO_2$ during spontaneous ventilation, but, during controlled ventilation, the difference became negligible and reversed over time. Controlled ventilation may alter the pattern of airflow within avian air sacs and parabronchial lung, resulting in a reduced or positive arterial to end-tidal CO_2 gradient. This mechanism is thought to be due to aerodynamic – and not anatomic – valving within the lung–air sac complex [22].

Reptiles

End-expired CO_2 was compared with arterial CO_2 in isoflurane- and sevoflurane-anesthetized and ventilated green iguanas (*Iguana iguana*) [28]. At 10 min, the arterial to end-tidal CO_2 difference was small, but, by 40 min, the arterial to end-expired CO_2 difference significantly increased. The authors attributed this to the relatively greater development of intracardiac shunting during anesthesia, and thus a decrease in end-expired CO_2 values. Amphibia and most reptiles have a three-chambered heart with a common ventricle. The single ventricle functions as two, variably shunting blood from the lungs. Cardiac shunting may also regulate arterial blood gas composition independent of pulmonary ventilation [29]. For these reasons, capnography is not a useful monitor of ventilation in reptiles [30].

Other species

Modern portable capnometers are readily transportable and easy to use. In addition, these units often

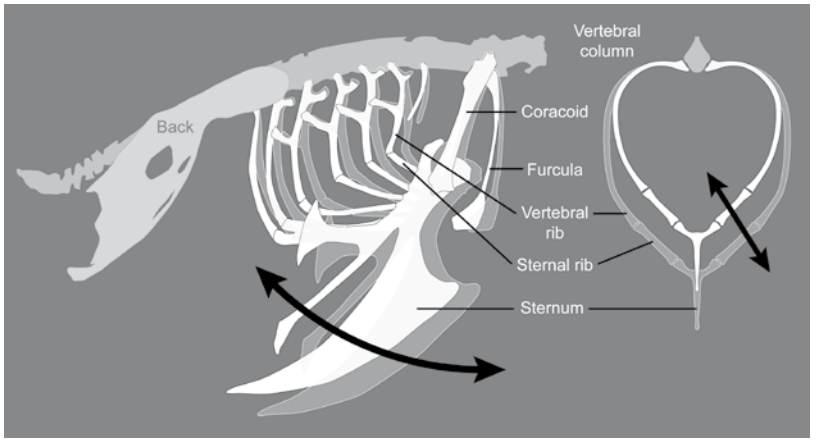

Figure 28.4 Avian skeletal changes that result in gas movement into and out of the thoracoabdominal cavity.

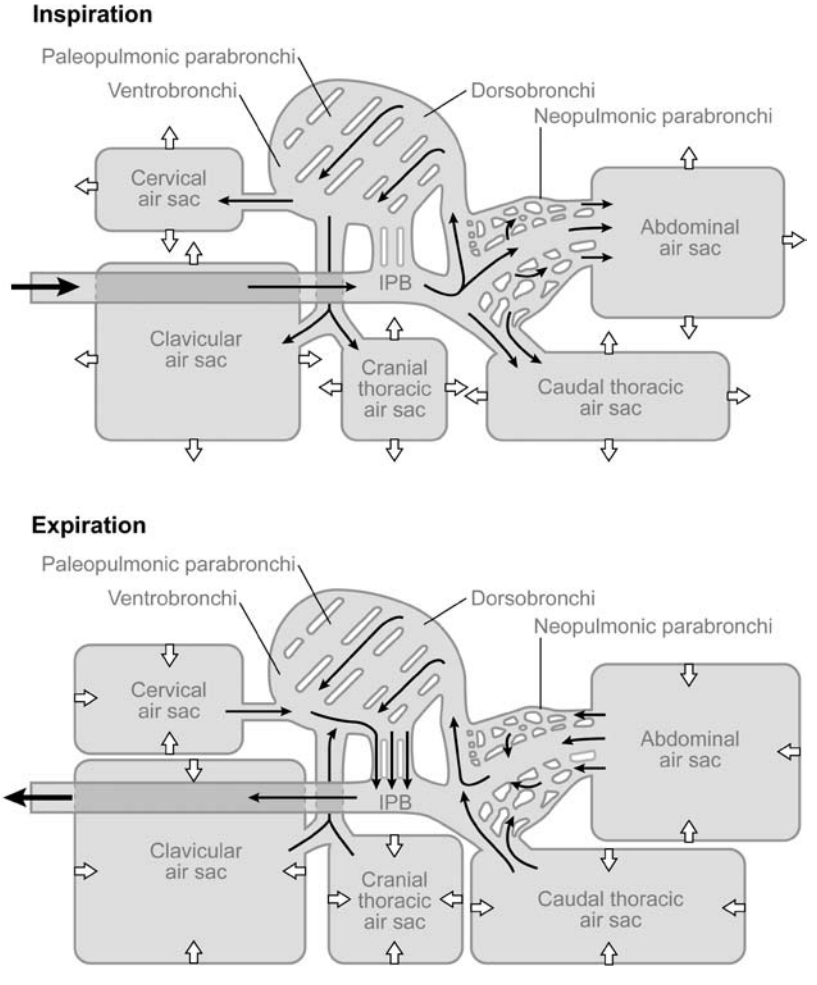

Figure 28.5 Gas flow through the avian air sacs and lung.

have pulse oximetry capability. These characteristics make capnometry one of the most popular monitoring devices used during the immobilization and anesthetizing of wildlife and zoo animals [31]. Potent respiratory depressant drugs, including alpha-2 agonists and superopioids (carfentanil, etorphine), are commonly used in the capture and restraint of "zoo" animals, resulting in significant respiratory depression.

Published reports of capnometry use in these species, however, remain limited.

Harp seals

A study of the $P_{ET}CO_2$–$PaCO_2$ difference in young, intubated, isoflurane-anesthetized harp seals (*Phoca groenlandica*) revealed a strong correlation. The limits of agreement were closer for ventilatory rates greater than 5 per minute compared to slower ventilatory rates [32]. The authors concluded that capnography was a useful monitor of arterial CO_2 at ventilatory rates greater than 5 per minute. End-tidal CO_2 values were measured in freely diving gray seals (*Halichoerus grypus*), and ranged between 28 and 35 mm Hg [33].

Dolphins

Capnography has also been used to evaluate pulmonary function in awake dolphins [34]. In the van Elk *et al.* study, dolphins were trained to accept placement of a human anesthesia mask over their blow-hole and exhale on command. The capnogram morphology of healthy dolphins was similar to that of other mammals. Normal end-expired values were not established in this study, but one dolphin with pneumonia exhibited significantly higher end-tidal CO_2 values and a non-uniform slope to the plateau phase.

References

1. Moens Y, Verstraeten W. Capnographic monitoring in small animal anesthesia. *J Am Anim Hosp Assoc* 1982; **18**: 659–78.
2. American College of Veterinary Anesthesiologists. Recommendations for monitoring anesthetized veterinary patients. Available online at http://www.acva.org/professional/Position/pstn.asp. (Accessed November 25, 2010.)
3. Martinez E, Wagner A, Driessen B, Trim C. *Guidelines for Anesthesia in Horses.* Middleburg, VA: American College of Veterinary Anesthesiologists. Available online at http://www.acva.org/diponly/action/Guidelines_Anesthesia_Horses_041227.htm. (Accessed June 2, 2009.)
4. Herholz C, Gerber V, Tschudi P, *et al.* Use of volumetric capnography to identify pulmonary dysfunction in horses with and without clinically apparent recurrent airway obstruction. *Am J Vet Res* 2003; **64**: 338–45.
5. McDonell W, Kerr C. Respiratory system. In: Tranquilli W, Thurmon J, Grimm K (eds.) *Lumb and Jones Veterinary Anesthesia and Analgesia,* 4th edn. Ames, IA: Blackwell Publishing, 2007; 117–51.
6. Hendricks J, King L. Practicality, usefulness, and limits of end-tidal carbon dioxide monitoring in critical small animal patients. *J Vet Emerg Crit Care* 1994; **4**: 29–39.
7. Hightower C, Kiorpes A, Butler H, *et al.* End-tidal partial pressure of CO2 as an estimate of arterial partial pressure of CO2 during various ventilatory regimens in halothane-anesthetized dogs. *Am J Vet Res* 1980; **41**: 610–12.
8. Wagner A, Gaynor J, Dunlop C, Allen S, Demme W. Monitoring adequacy of ventilation by capnometry during thoracotomy in dogs. *J Am Vet Med Assoc* 1998; **212**: 377–9.
9. Teixeira Neto F, Carregaro A, Mannarino R, Cruz M, Luna S. Comparison of a sidestream capnograph and a mainstream capnograph in mechanically ventilated dogs. *J Am Vet Med Assoc* 2002; **221**: 1582–5.
10. Herholz C, Gerber V, Tschudi P, *et al.* Use of volumetric capnography to identify pulmonary dysfunction in horses with and without clinically apparent recurrent airway obstruction. *Am J Vet Res* 2003; **64**: 338–45.
11. Gallivan G, McDonell W. An evaluation of the multiple-breath nitrogen washout as a pulmonary function test in horses. *Can J Vet Res* 1990; **54**: 99–105.
12. Cribb P. Capnographic monitoring during anesthesia with controlled ventilation in the horse. *Vet Surg* 1988; **17**: 48–52.
13. Littlejohn A. Acid–base and blood gas studies in horses. II. Tracheal end-tidal and arterial blood gas tensions in horses. *Res Vet Sci* 1969; **10**: 263–6.
14. Robinson N. The respiratory system. In: Muir W, Hubbell J (eds.) *Equine Anesthesia Monitoring and Emergency Therapy,* 2nd edn. St Louis, MO: Saunders Elsevier, 2009; 11–36.
15. Geiser D, Rohrbach B. Use of end-tidal CO2 tension to predict arterial CO2 values in isoflurane-anesthetized equine neonates. *Am J Vet Res* 1992; **53**: 1617–21.
16. Meyer R, Short C. Arterial to end-tidal CO2 tension and alveolar deadspace in halothane- or isoflurane-anesthetized ponies. *Am J Vet Res* 1985; **46**: 597–9.
17. Koenig J, McDonell W, Valverde A. Accuracy of pulse oximetry and capnography in healthy and compromised horses during spontaneous and controlled ventilation. *Can J Vet Res* 2003; **67**: 169–74.
18. Thal S, Plesnila N. Non-invasive intraoperative monitoring of blood pressure and arterial pCO2 during surgical anesthesia in mice. *J Neurosci Methods* 2007; **159**: 261–7.
19. Spoelstra EN, Ince C, Koeman A, *et al.* A novel and simple method for endotracheal intubation of mice. *Lab Anim* 2007; **41**: 128–35.
20. Tojima H, Kuriyama T, Fukuda Y. Arterial to end-tidal PCO2 difference varies with different ventilatory

conditions during steady state hypercapnia in the rat. *Jpn J Physiol* 1988; **38**: 445–57.

21. Hinds D, Calde W. Tracheal deadspace in the respiration of birds. *Evolution* 1971; **25**: 429–40.
22. Powell F. Respiration. In: Whittow G (ed.) *Sturkie's Avian Physiology,* 5th edn. Burlington, MA: Academic Press, 2000; 233–64.
23. Piiper J, Drees F, Scheid P. Gas exchange in the domestic fowl during spontaneous breathing and artificial ventilation. *Respir Physiol* 1970; **9**: 234–45.
24. Davies D, Dutton R. Gas–blood PCO2 gradients during avian gas exchange. *J Appl Physiol* 1975; **39**: 405–10.
25. Edling TM, Degernes LA, Flammer K, Horne WA. Capnographic monitoring of anesthetized African gray parrots receiving intermittent positive pressure ventilation. *J Am Vet Med Assoc* 2001; **219**: 1714–18.
26. Desmarchelier M, Rondenay Y, Fitzgerald G, Lair S. Monitoring of the ventilatory status of anesthetized birds of prey by using end-tidal carbon dioxide measured with a microstream capnometer. *J Zoo Wildl Med* 2007; **38**: 1–6.
27. Petifer G, Cornick-Seahorn J, Smith J, *et al.* The comparative cardiopulmonary effects of spontaneous and controlled ventilation by using the hallowell EMC anesthesia work station in Hispaniolan Amazon parrots (Amazona ventralis). *J Avian Med Surg* 2002; **16**: 268–76.
28. Hernandez Divers S, Schumacher J, Stahl S, *et al.* Comparison of isoflurane and sevoflurane anesthesia after premedication with butorphanol in the green iguana (*Iguana iguana*). *J Zoo Wildl Med* 2005; **36**: 169–75.
29. Wang T, Smits W, Burggren W. Pulmonary function in reptiles. In: Gans C, Gaunt A (eds.) *Biology of the Reptilia,* vol. 19*, Morphology of Visceral Organs*. St Louis, MO: Society for the Study of Amphibians and Reptiles, 1998; 297–374.
30. Heard D. Reptile anesthesia. *Vet Clin N Am Exot Anim Prac* 2001; **4**: 83–117.
31. Heard D. Monitoring. In: West G, Heard D, Caulkett N (eds.) *Zoo Animal and Wildlife Immobilization and Anesthesia*. Ames, IA: Blackwell Publishing, 2007; 83–91.
32. Pang D, Rondenay Y, Troncy E, Measures L, Lair S. Use of end-tidal partial pressure of carbon dioxide to predict arterial partial pressure of carbon dioxide in harp seals during isoflurane-induced anesthesia. *Am J Vet Res* 2006; **67**: 1131–5.
33. Reed J, Chambers C, Fedak M, Butler P. Gas exchange of captive freely diving grey seals (*Halichoerus grypus*). *J Exp Biol* 1994; **194**: 1–18.
34. Van Elk C, Epping N, Gans S. Pulmonary function measurements in dolphins using capnography. *Vet Rec* 2001; **149**: 308–9.

Section 4

Physiologic perspectives

Section 4
Chapter
29

Physiologic perspectives

Carbon dioxide pathophysiology

T. E. Morey

Introduction

All mammals require transport of carbon dioxide (CO_2) from the intracellular sites of fuel oxidation to the lungs where elimination occurs. This chapter addresses the clinician, and will discuss reduced and increased CO_2 pressures and outline some of the pathophysiology of CO_2 production and transport, with special reference to capnography. Conditions that reduce the partial pressure of end-tidal (exhaled) CO_2 ($P_{ET}CO_2$) tension include decreases in CO_2 production in mitochondria and its transport by blood that largely depends on functional carbonic anhydrase. In contrast, causes of increased $P_{ET}CO_2$ may encompass intravenous sodium bicarbonate administration and CO_2 absorption from CO_2 insufflated into a body cavity as examples. In addition, capnography has a special use in the assessment of patients for brain death with regard to the apnea test, wherein measurement of CO_2 tensions are a component of assessing the viability of the brainstem.

Reduced CO_2 partial pressures

Mitochondrial disorders

Mitochondria serve as the exclusive site for oxidative phosphorylation, an intricate series of biochemical reactions leading to cellular respiration by producing energy-laden molecules (i.e., adenosine triphosphate [ATP]), water (H_2O), and CO_2 from oxidation of C–C bonds found in various fuel substrates [1]. Any disruption in normal mitochondrial function manifests as diminished energy reserves and CO_2 production, and is most rapidly evident in organs with high-energy requirements such as the brain, heart, kidney, and, especially, the eye [1]. Mitochondrial disorders may be classified as *inherited* or *acquired*. Inheritance and familial pedigree can be particularly complicated to trace because, unlike other organelles, mitochondria carry a genome independent of nuclear DNA that may result in maternal transmittance of disease that does not fit into classic Mendelian autosomal or sex-linked inheritance patterns [2]. Acquired mitochondrial disorders result from exposure of mitochondrial constituents to toxins. Both genetic and acquired mitochondrial disorders are presented herein, with an emphasis on CO_2 production and capnography.

Inherited mitochondrial disorders

Inherited mitochondrial defects result from flaws in either mitochondrial (mtDNA) or nuclear DNA (nDNA) encoding for essential proteins needed to enable mitochondrial bioenergetics. This function of mitochondria depends not only on nDNA, but also on mtDNA that originates solely from ova mitochondria because spermatic mtDNA is quickly degraded following the union of gametes [2]. Each mitochondrion possesses several mtDNA copies that contain 16 569 nucleotide pairs encoding 37 genes. The remaining loci encoding DNA necessary for mitochondrial function are found in the nucleus. Unlike nDNA, mtDNA contains no introns, is rapidly transcribed, and has little ability to self-repair, all of which leads to a one- to twofold magnitude increase in mutation rate [3]. These mutations cause inherited mitochondrial diseases (e.g., carnitine palmitoyltransferase II deficiency, Lebers optic neuropathy, Kearns–Sayre disease), which can be classified using three systems based on (1) defects in substrate transport and utilization, (2) types of genetic mutation, or (3) chief clinical complaints along with associated symptoms. Of course, the usefulness of these schemas generally depends on the medical perspective of the respective practitioner (e.g., medical geneticist, neurologist). Overall, the minimum birth prevalence

Capnography, Second Edition, ed. J. S. Gravenstein, Michael B. Jaffe, Nikolaus Gravenstein, and David A. Paulus. Published by Cambridge University Press. © Cambridge University Press 2011.

of these respiratory chain diseases is estimated to be approximately 1 in 7634 [4]. In perspective to other myopathies, the annual incidences of Duchenne muscular dystrophy and malignant hyperthermia are approximately 1 in 3500 live male births and 1 in 62 000 (with administration of a potent inhalational anesthetic agent and succinylcholine) patients, respectively [4,5].

Although ventilation appears normal in resting patients suffering from inherited mitochondrial disorders, provocative exercise stress unmasks differences in ventilatory patterns compared to age- and sex-matched control subjects. That is, although patients with mitochondrial disease appear to have markedly reduced ventilation at peak exercise ($\dot{V}E_{max}$), this ventilatory rate is abnormally high for the actual amount of work being performed on a cycle ergometer as measured by $\dot{V}E_{max}$ divided by the CO_2 output ($\dot{V}CO_2$). In one study, $\dot{V}E_{max}$ was 71 ± 31 and 104 ± 23 L/min ($P < 0.001$) for diseased and control subjects, respectively, whereas peak $\dot{V}E_{max}/\dot{V}CO_2$ was 55 ± 19 and 41 ± 6 ($P = 0.002$), respectively [6]. Notwithstanding this relative overventilation, the $P_{ET}CO_2$ appears to be only modestly decreased; the $P_{ET}CO_2$ at maximal workloads for diseased and normal subjects was 33 ± 5 and 37 ± 3 mm Hg (not significantly different), respectively [7]. Although the cause of this hyperventilatory response is not known, several hypotheses have been proffered for consideration. One suggestion revolves around a tenet that lactic acid is quickly buffered to CO_2, which would potentially increase the central respiratory drive. However, a recent, well-performed study found no differences in lactate clearance between diseased ($t_{1/2}$: 21.27 ± 6.05 min) and control ($t_{1/2}$: 23.50 ± 5.87 min) subjects [7]. An alternative hypothesis speculates that additional mechanoreceptor stimulation due to poor exercise mechanics secondary to mitochondrial myopathy of respiratory muscles may cause this hyperventilation. Indeed, a decrement in respiratory muscle function is evident in patients with mitochondrial disorders. For example, the maximal inspiratory mouth pressure was determined to be 64 ± 29% and 95 ± 36% predicted ($P = 0.06$) in diseased and normal patients, respectively, whereas the maximal transdiaphragmatic pressure was 61 ± 23 and 115 ± 31 cm H_2O ($P = 0.01$), respectively [6]. For whatever reason, hyperventilation is present during exercise testing of patients suffering mitochondrial disease and is also associated with a hyperdynamic circulatory state.

These abnormal changes in ventilation in response to exercise stress temptingly allude to the possibility that capnography could potentially contribute to the diagnostic testing of patients suspected to suffer mitochondrial disorders. Although pathological diagnosis of tissue (i.e., muscle biopsy with mitochondrial isolation) still endures as the gold standard, a great fraction of the global population has minimal-to-no access to clinical pathology services, especially in medically underserved, Third World nations [8,9]. As such, capnography may serve as a valuable addition to medical diagnostics either as a stand-alone, point-of-care assay or in combination with other testing such as O_2 consumption. However, some of the aforementioned changes in ventilation and circulation observed in patients with mitochondrial disease probably relate to the associated myopathic changes due to mitochondrial dysfunction. As such, other types of myopathies not due to mitochondrial disorders may cause similar ventilation changes in response to provocative exercise stress testing, and will decrease the overall specificity and positive predictive value for this proposed type of testing.

Acquired mitochondrial disorder: cyanide

A number of mitochondrial toxins (e.g., mercury, 1-methyl-4-phenyl-1,2,3,6-tetrahydropyrimidine [MPTP], cyanide) can cause disruption of oxidative phosphorylation and cellular respiration [10]. Some of these poisons are particularly useful during the conduct of medical research, whereas others have little redeeming scientific value. Cyanide intoxication has inspired public fascination, and has been well investigated to uncover its biochemical and physiological effects. In addition, this particular poison may be of interest to clinicians because of a perceived risk of intoxication due to the intravenous administration of sodium nitroprusside. For these reasons, the effects of cyanide on cellular respiration, CO_2 production, and transport are more extensively presented.

Biochemistry

Cyanide is a small molecule (H–C≡N, molecular weight 26.02) that was first identified in 1782 and originates from many natural and artificial sources [11]. Because of its compact, uncharged nature at physiological pH with consequent rapid egress across membranes, this poison is quickly fatal at relatively small concentrations (200 ppm) if aerosolized across pulmonary membranes and rapidly lethal (~5 min) if orally ingested (200 mg). Although cyanide interferes with the activity of many enzymes, its inhibitory effect on mitochondrial energetics is most notable for disruption of the activity of

cytochrome *c* and the resultant abrupt cessation of cellular respiration [11]. Cytochrome *c* is a large lipoprotein bound to the mitochondrial inner membrane and is composed of 13 subunits that catalyze electron transfer in order to convert lactate and O_2 to water and CO_2 with resultant generation of energy as ATP (i.e., Krebs cycle). One critical component of cytochrome *c* is the a_3-subunit, the center wherein electrons and oxygen combine. Because cyanide possesses a stronger affinity for the ferric acid (Fe^{3+}) moiety of the a_3 component of cytochrome *c* than does O_2, this poison does not yield its position to O_2 and, therefore, uncouples oxidative phosphorylation. Consequently, although glycolysis (i.e., anaerobic metabolism) might proceed, aerobic metabolism is halted. Paradoxically, cells suffer asphyxia even in the presence of normal O_2 pressures. Because the Krebs cycle slows or stops, minimal or no CO_2 is produced while O_2 consumption is reduced. As expected, in canine models of sublethal cyanide intoxication, O_2 consumption significantly decreased from 133 ± 19 to 69 ± 21 mL/min, CO_2 production decreased from 128 ± 27 to 103 ± 22 mL/min, and mixed venous lactate concentrations increased from 2.3 ± 0.5 to 7.1 ± 0.7 mM [12,13].

Sources

Cyanide can be derived from several sources, including dietary intake of cyanogens, malicious administration, and iatrogenic production due to administration of sodium nitroprusside.

Cassava Cyanide intoxication may occur from dietary intake of cassava (*Monihot esculanta*). This tropical root is grown within the 30° latitude north or south around the equator, and meets the essential carbohydrate demands of approximately a half billion citizens of underdeveloped nations due to its high starch content and hardy nature [14,15]. For these reasons, the crop is now in global production, and is also called manioc, tapioca, mandioca, and yucca. The uncooked plant possesses inherent cyanide glucosides that may be eaten or contaminate subsequent processed foodstuffs, such as cassava flour, called farofa, which is used to produce bakery goods [16]. The cyanide glucosides are converted to active hydrogen cyanide by linamarase, which is native to cassava. Two resultant diseases associated with acute and chronic cyanide exposure due to cassava ingestion are konzo and tropical ataxic neuropathy, respectively. Konzo means "tired legs" in Zairean, and is an uncharacterized upper motor neuron disease noted for rapidly developing leg paralysis following large ingestions of cassava [17]. Schoolchildren in Mozambique with konzo demonstrate elevated concentrations (225–384 μmol/L) of thiocyanate in the urine [18]. Tropical ataxic neuropathy is typified by presentation with paresthesias, ataxia, visual changes, and other signs. It typically follows a chronic diet of cassava-based foods due to failure of other crops [19]. Other foods potentially laden with cyanogens include almonds, cherry leaves, apricot pits, and other plants [11].

Malicious intent Cyanide's notoriety as a poison in popular culture stems from its criminal use as an agent of suicide and homicide. For example, 913 members of the People's Temple ministered by James Jones allegedly committed coerced suicide in 1978 at Jonestown, Guyana by ingesting a punch contaminated with cyanide [20]. Similarly, laboratory scientists and technicians with ready access to chemicals have employed cyanide salts to achieve rapid suicide [21]. The use of cyanide to achieve homicidal objectives has occurred on both a small and large scale. Several cases of contaminated pharmaceuticals (e.g., acetaminophen) were reported in recent times [22]; of greater magnitude, cyanide gas has been repeatedly deployed in military campaigns since the time of the Napoleonic Wars to dispatch large formations of enemy soldiers [11]. Due to these and other events, cyanide is a chemical well known to the lay public as a potent toxin.

Sodium nitroprusside Of particular concern to medical professionals is the potential for iatrogenic cyanide intoxication following the intravenous administration of sodium nitroprusside. This pharmacological agent is administered intravenously, acts to reduce peripheral blood pressure by causing vascular dilation, and structurally is composed of an iron molecule surrounded by a halo of one NO and five CN moieties. The mechanism whereby blood pressure decreases is due to the release of nitric oxide (NO) from the drug via an enzymatic mechanism that also liberates cyanide molecules. Typically, cyanide is rapidly metabolized by rhodanase to an innocuous product, thiocyanate. However, several conditions (e.g., large or sustained sodium nitroprusside doses, thiosulfate deficiency, renal failure, rhodanase deficiency) may lead to the accumulation of cyanide with resultant systemic toxicity.

The few investigators who have undertaken the task of determining the effects of sodium nitroprusside

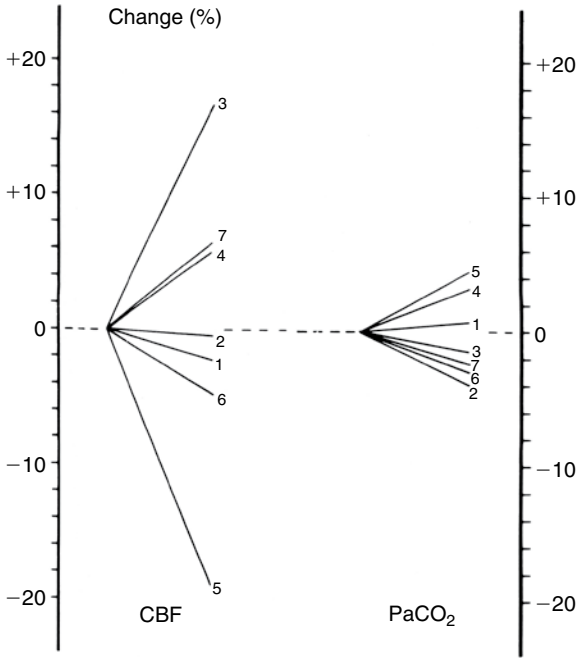

Figure 29.1 The effect of sodium nitroprusside infused intra-arterially in seven awake patients in a dose at the threshold for affecting mean arterial pressure or heart rate. CBF, cerebral blood flow; $PaCO_2$, arterial partial pressure of carbon dioxide. [From: Henriksen L, Paulson OB, Lauritzen M. The effects of sodium nitroprusside on cerebral blood flow and cerebral venous blood gases. I. Observations in awake man during and following moderate blood pressure reduction. *Eur J Clin Invest* 1982; **12**: 383–7.]

on CO_2 production and elimination have published variable findings between and within human studies (Figure 29.1). One group of 26 patients undergoing major otolaryngological surgery and concurrently induced hypotension caused by sodium nitroprusside experienced no change in $PaCO_2$ [23]. In this study of anesthetized, ventilated patients, the $PaCO_2$ was determined to be 38 ± 4 and 38 ± 3 mm Hg before and after infusion of sodium nitroprusside, respectively. In a separate investigation of anesthetized adults undergoing middle ear surgery, with controlled hypotension achieved by sodium nitroprusside infusion, $PETCO_2$ decreased 17%, whereas $PaCO_2$ fell approximately 7% during controlled hypotension, to achieve a mean arterial blood pressure of 60 ± 5 mm Hg [24]. The authors noted that decreases in $PETCO_2$ overestimate reductions in $PaCO_2$. This significant discrepancy between $PaCO_2$ and $PETCO_2$ likely resulted from a large (41.7%) increase in physiological deadspace to tidal volume ratio. Different investigators measured changes in $PaCO_2$ in awake, spontaneously breathing human subjects subjected to graded reductions in blood pressure caused by intravenous sodium nitroprusside [25]. They determined that $PaCO_2$ significantly fell in a dose-dependent manner, with mean values of 4.96, 4.81, 4.78, 4.62, and 4.54 kPa during graduated infusions of sodium nitroprusside to achieve 0, 10, 20, 30, and 40% reductions in mean arterial pressure, respectively.[1]

The investigators, however, attributed this change to hyperventilation in subjects, vis-à-vis cyanide toxicity, although no measurement of pulmonary parameters (e.g., respiratory rate, tidal volume) was noted. In the author's view, sodium nitroprusside likely decreases CO_2 production to some extent, but rarely causes notable decrements in cellular respiration at doses of the drug used in clinical medicine.

Carbonic anhydrase disorders

Carbonic anhydrase comprises a family name for a group of zinc-dependent enzymes that catalyze the reaction of bicarbonate and a proton to form water and CO_2 [26]. The fact that these enzymes originated in deep antiquity (i.e., 3 billion years ago), are ubiquitous, and demonstrate evolutionary convergence between plants and animals attests to their fundamental importance to regulate CO_2 elimination in living organisms [26–28]. The chemical reaction process occurs in two phases, with the first step (equation 29.1) occurring instantaneously and the second step (equation 29.2) facilitated by carbonic anhydrase (CA).

$$CA \bullet Zn - OH^- + H^+ \leftrightarrow CA \bullet Zn - H_2O \qquad (29.1)$$

$$HCO_3^- + CA \bullet Zn - H_2O \leftrightarrow H_2O + CO_2 + CA \bullet Zn - OH^- \qquad (29.2)$$

Only diffusion of H^+ away from the active site limits the reaction rate that has an associated Michaelis–Menten k_{cat} value ~$8{\cdot}10^5$ s^{-1} [26,29]. Conventionally, the perennial summary equation (equation 29.3) remains more familiar to readers of clinical literature, but does not

[1] The chapter author has not modified the units as originally published by the various journals in order to preserve the integrity of the references. For the readers' benefit, however, the conversion factors for units of pressure are as follows: 1 mm Hg = 0.133 kPa or 1 kPa = 7.519 mm Hg; 1 cm H_2O = 0.098 kPa or 1 kPa = 10.204 cm H_2O; 1 mm Hg = 1.357 cm H_2O or 1 cm H_2O = 0.737 mm Hg.

emphasize the need for CA or the absolute requirement for zinc at this enzyme's active site.

$$HCO_3^- + H^+ \xleftrightarrow{CA} H_2O + CO_2 \quad (29.3)$$

From the CA family found in mammals (i.e., α-class vis-à-vis the vegetative β-class), the cytosolic CA II subtype has inspired and received more study than those found in cytosol (CA I, III, VII), membranes (CA IV, IX, XII, XIV), mitochondria (CA V), or secreted (CA VI) [28]. Both mutation and drug-induced inhibition of CA II may lead to changes in CO_2 metabolism and elimination.

Inherited carbonic anhydrase disorders

Disorders in CA II encompass a set of autosomal recessive enzymatic diseases caused by point mutations of the DNA sequence (e.g., TAT→TAG) encoding CA or by splice junction mutations [30]. This rare disease has been reported in several widely dispersed populations of Mediterranean, Arab, and Japanese descent [30–32]. The hallmarks of disease revolve around a clinical triad of renal tubular acidosis, osteoporosis, and cerebral calcification leading to mental retardation [33,34]. As expected, this inherited disorder also modifies CO_2 elimination and alveolar CO_2 concentrations. In Japanese patients suffering CA II due to de novo mutation or consanguineous parents, $P_{ET}CO_2$ was reduced to 35.2 ± 1.3 mm Hg compared to a value of 41.2 ± 2.9 mm Hg measured in a healthy human cohort [35]. In addition, $PaCO_2$ approached the upper limits of normal values in CA II subjects. Taken together, these two observations yielded an increased $PaCO_2$–$P_{ET}CO_2$ difference of 8.3 ± 3.1 mm Hg compared to control values of 1.3 ± 1.3 mm Hg (Figure 29.2). Similarly, data from CA II-deficient mice confirmed by Western blot analysis also showed elevated $PaCO_2$ pressures of 47.4 ± 5.3 mm Hg in homozygous recessive animals, whereas the wild-type value was 38.1 ± 3.4 mm Hg [36]. Furthermore, a sodium bicarbonate challenge (4 mmol/kg) to the mice resulted in an even greater disparity in $PaCO_2$ tensions, and illustrates the importance of CA II in CO_2 elimination. Unfortunately, $P_{ET}CO_2$ was not measured although the animals were anesthetized. Measurement of this parameter is precluded by the fact that currently available capnography technology of either mainstream or sidestream configuration

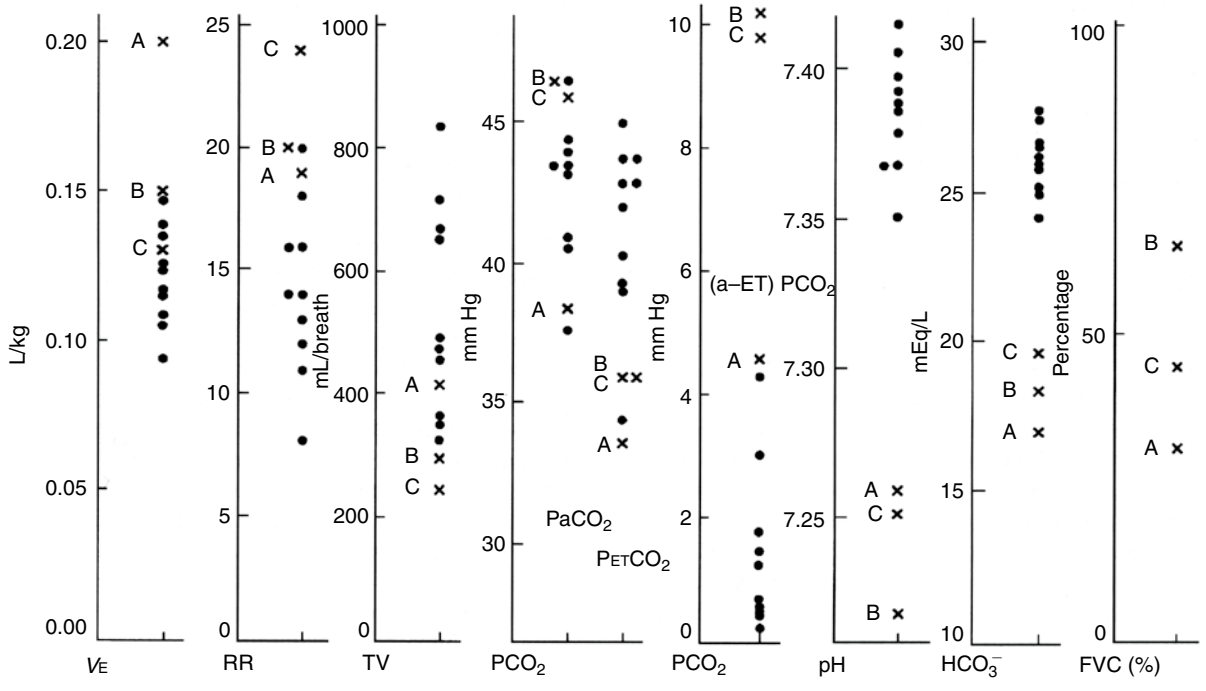

Figure 29.2 Respiratory function parameters in three patients with a deficiency of CA II vs. ten healthy volunteers. V_E, minute ventilation volume per body weight (mL/kg/min); $P_{ET}CO_2$, PCO_2 in end-expiratory gas; pH, $PaCO_2$, and HCO_3^- were shown as the values in arterial blood; $(a–_{ET})PCO_2$, differences between $PaCO_2$ and $P_{ET}CO_2$. [Reprinted with permission from: Taki K, Kato H, Yoshida I. Elimination of CO_2 in patients with carbonic anhydrase II deficiency, with studies of respiratory function at rest. *Respir Med* 1999; **93**: 536–9.]

cannot accommodate extremely rapid respiratory rates (e.g., 160 breaths/min) typical of small rodents, especially when combined with diminutively small tidal volumes (e.g., 0.2 mL/breath). (Similarly, conventional pulse oximetry does not function for small rodents due to extremely high heart rates [e.g., 500 beats/min]. Presumably, this problem has little hope of solution in the near future given the relatively small market of animal research when contrasted to that for clinic medicine.) Nevertheless, these studies suggest that $PaCO_2$ rises in patients suffering this disease, but cannot be overcome by hyperventilation. The contribution of other types of cytosolic CA (e.g., CA I, III, and VII) to CO_2 transfer in the blood and elimination in the lungs likely mitigates the effects of mutant CA II, and allows patients to maintain homeostasis, albeit at abnormal values.

Acquired carbonic anhydrase disorders

Acetazolamide

A sulfanilamide derivative, acetazolamide remains in widespread clinical use in the treatment of open-angle glaucoma recalcitrant to other pharmacological therapies, acute closed-angle glaucoma immediately prior to surgical intervention, and chronic obstructive lung disease with hypoventilation. Similar to those changes observed with inherited CA diseases, acetazolamide therapy also increases the difference between $PaCO_2$ and alveolar CO_2 as shown in Figure 29.3. This finding has been noted in a number of species, including the rabbit, cat, and dog.[2] For example, the gap between $PaCO_2$ and $PETCO_2$ was less than 0.5 kPa, but rapidly widened to 4.9 kPa following treatment with acetazolamide in rabbits [38]. In cats, this difference also increased, but only with intravenous doses of acetazolamide greater than 4 mg/kg of body mass [39]. Similarly, the $PaCO_2$ and $PETCO_2$ measured in anesthetized dogs markedly grew from 0.6 ± 1.0 to 21.9 ± 1.0 mm Hg after carbonic anhydrase inhibition [40]. This effect was observed to be dose-dependent, with additional drug not causing substantial changes in alveolar CO_2 tensions [41]. The location of this "surplus" CO_2 seems to be in tissue. In the presence of significant CA inhibition caused by

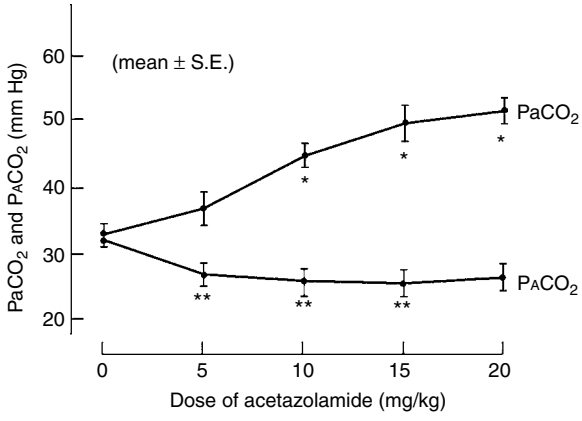

Figure 29.3 The relationship between the dose of acetazolamide and $PaCO_2$ or $PACO_2$. The $PaCO_2$ linearly rises in response to the inhibition rate of the red cell carbonic anhydrase (RCA) activity. However, $PACO_2$ slightly falls by 16% after the administration of 5 mg/kg of acetazolamide, and does not change upon further injections of acetazolamide. *Indicates $P < 0.01$ between control and each value after injection of acetazolamide. **Indicates $P < 0.05$. [Modified from: Taki K, Mizuno K, Takahashi N, Wakusawa R. Disturbance of CO_2 elimination in the lungs by carbonic anhydrase inhibition. *Jpn J Physiol* 1986; **36**: 523–32.]

acetazolamide, tissue PCO_2 was consistently underestimated by venous PCO_2 [42]. Finally, these changes also occur in spontaneously breathing humans receiving the drug for chronic obstructive pulmonary disease [43]. Based on these studies describing the acute use of acetazolamide, anesthesiologists should warily consider the actual relationship between $PETCO_2$ and $PaCO_2$ when administering this drug to anesthetized, ventilated patients.

More recently, a number of inhibitors for isozymes of CA have been developed and proposed as drugs to treat many diverse diseases, such as obesity, seizures, cancer, and infections, from such organisms as *Helicobacter pylori, Mycobacterium tuberculosis*, and others [44]. For example, zonisamide, which has been previously used to treat seizure disorder, has resulted in persistent weight reduction in obese patients, as this drug causes alterations in lipogenesis [45]. The effects of such inhibition on CO_2 production and $PETCO_2$, however, have been under investigated and remain unknown.

Increased CO_2 partial pressures

Bicarbonate infusion

Sodium bicarbonate is sometimes intravenously injected to treat acidemia in patients suffering from metabolic acidosis. This buffer rapidly consumes

[2] No small rodent species were used, which precludes capnographic investigations in many small animal models of disease (e.g., Lesch–Nyhan syndrome, muscular dystrophy, phenylketonuria) including transgenic knockout mice previously subjected to site directed deletion of DNA sequences [37].

hydrogen ions, according to the reaction noted in equation (29.3), in which the reaction was catalyzed very rapidly by carbonic anhydrase. If excess H^+ is present, the quantity of HCO_3^- (i.e., amount of sodium bicarbonate) becomes the limiting factor for CO_2 production; that is, for each HCO_3^- molecule administered, a molecule of CO_2 will be produced. Given that a single adult-sized, syringe of factory-packaged sodium bicarbonate contains 50 mEq of the drug with only a single negative charge, then the mass of bicarbonate may also be expressed as 50 mmol. Avogadro's law stipulates that the volume (V) of a gas is directly proportional to the moles (n) of the gas (i.e., $V \propto n$) for a fixed temperature and pressure [46]. Using this law, the volume of CO_2 produced by a single syringe of sodium bicarbonate can be calculated as follows:

$$V_{50} = V_{1000} \times \frac{n_{50}}{n_{1000}} \tag{29.4}$$

where V_{50} and V_{1000} are the volumes of gas for 50 and 1000 mmol of CO_2, respectively, whereas n_{50} and n_{1000} are the molar masses of 50 and 1000 mmol of CO_2, respectively. Considering gas behavior at standard conditions of temperature (0 °C, 273 K) and pressure (760 mm Hg, 1 atmosphere), the standard molar volume of any gas, including CO_2, is always 22.414 L; that is, 1000 mmol (n_{1000}) of CO_2 occupies 22.414 L (V_{1000}) [46]. Substitution of values yields a calculated volume of 1.121 L of CO_2 for each syringe of bicarbonate injected. However, Spear and colleagues determined that only 80% of expected CO_2 could be recovered from the breath of humans receiving [^{13}C] bicarbonate infusions [47]. The location of the residual 20% CO_2 remains poorly understood, but may enter metabolic pools or bone of finite capacity, as prolonged radiolabeled bicarbonate infusion eventually yields 100% CO_2 recovery. Nevertheless, given this large volume of CO_2 production catalyzed by an extremely rapid, enzyme-facilitated reaction, one would expect to – and, in fact, does – observe changes in $P_{ET}CO_2$ following the injection of sodium bicarbonate.

Although many clinicians have probably noted a $P_{ET}CO_2$ increase following sodium bicarbonate injection, Okamoto and colleagues scientifically investigated this phenomenon in a canine model as illustrated in Figure 29.4 [48]. In control dogs, they determined that the time for a maximal increase in $P_{ET}CO_2$ was 4 ± 0.3 breaths, and that maximal increase in $P_{ET}CO_2$ was 6.4 ± 0.5 mm Hg (0.85 ± 0.006 kPa). However, the time for maximal increase was inversely dependent on cardiac output (Figure 29.5). As such, the latency to maximal increases in $P_{ET}CO_2$ was reduced by increased cardiac output. Furthermore, the maximal increase in $P_{ET}CO_2$ was directly correlated to the hemoglobin concentration (Figure 29.6). This observation most likely can be explained by the absence of carbonic anhydrase in plasma but an abundance in erythrocytes. Similar data in humans note that CO_2 production is dependent on both hemoglobin and albumin concentrations where the albumin serves as a depot for non-bicarbonate buffers in need of titration as shown in Figure 29.7 [49].

CO_2 embolism

CO_2 is commonly used for insufflation of the abdomen during laparoscopy, with open-heart surgery, and occasionally in the thorax during thoracoscopy, because this gas has a number of favorable characteristics, including cost, availability, failure to support combustion, and high blood solubility. However, extremely great CO_2 tensions can occur during laparoscopy such that CO_2 is no longer completely solubilized in blood; embolism of CO_2 occurring during laparoscopy can cause cardiovascular collapse and death [50,51]. It is unclear what changes in $P_{ET}CO_2$ to anticipate during a CO_2 embolus. Theoretically, one would expect a rise in $P_{ET}CO_2$ until a sufficient volume of CO_2 was embolized to cause right ventricular outflow tract obstruction, with subsequent falls in $P_{ET}CO_2$ similar to that caused by air embolus. In fact, Shulman and Aronson noted an abrupt rise in $P_{ET}CO_2$ from 3.8% to 4.2% in women undergoing laparoscopy [52]. Subsequently, the $P_{ET}CO_2$ fell to 4.0% over the course of 30 s, upon which CO_2 insufflation was terminated after diagnosis of CO_2 embolism. In a second case, Diakun also noted a rise in $P_{ET}CO_2$ from 31 to 38 mm Hg in a patient undergoing laparoscopy and suffering CO_2 embolism [53]. In a third report, a Korean woman undergoing laparoscopy for an ovarian cyst suffered a venous CO_2 embolus, with $P_{ET}CO_2$ rising abruptly from 40 to 85 mm Hg, followed by hemodynamic collapse and an $E_{T}CO_2$ of 13 mm Hg [54]. In most case reports, though, a marked reduction in $P_{ET}CO_2$ is first noted and no transient increase in $P_{ET}CO_2$ is reported [51,55]. It is likely that any increase in $P_{ET}CO_2$ is so fleeting and small as to be imperceptible to all but the most fortunate and vigilant anesthesiologist. In addition, one might speculate that an increase or decrease in $P_{ET}CO_2$ depends

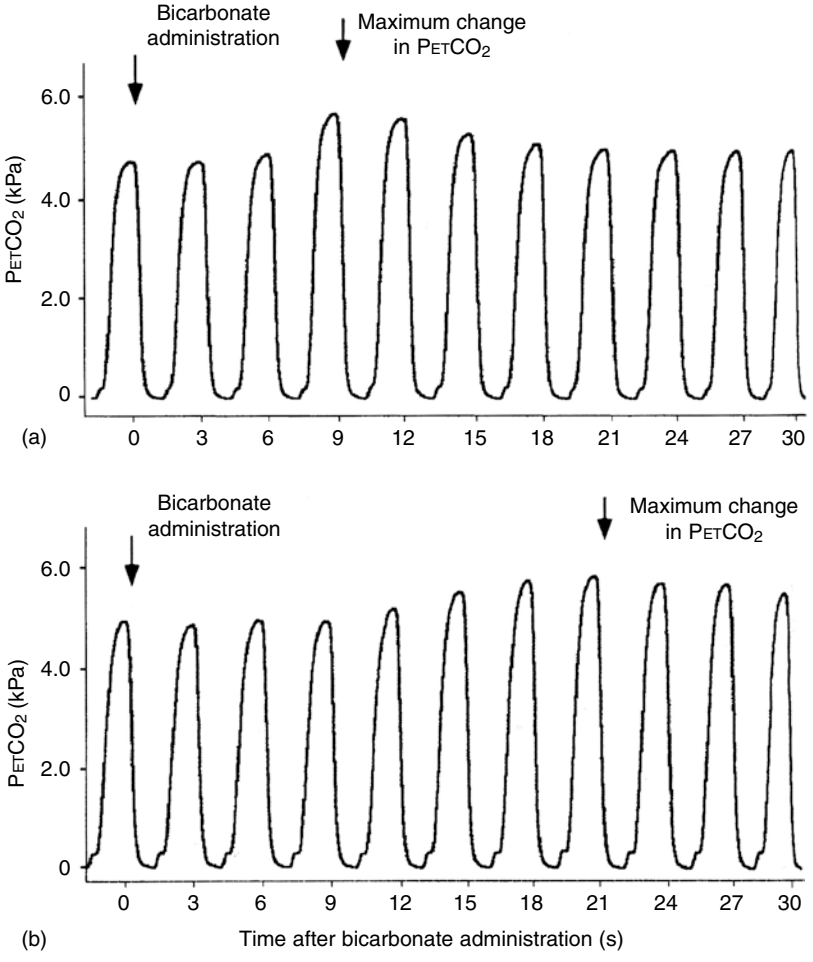

Figure 29.4 Recordings of $P_{ET}CO_2$ following an intravenous administration of sodium bicarbonate (0.2 mmol/kg) at (a) a control state (cardiac output = 1.85 L/min) and (b) at a state of decreased cardiac output (cardiac output = 0.83 L/min) in anesthetized, mechanically ventilated dog. When cardiac output decreased, time-max was prolonged from 3 breaths-time to 7 breaths-time, with no change in ΔCO_2-max. (1 mm Hg = 0.133 kPa). [Reprinted with permission from: Okamoto H, Hoka S, Kawasaki T, Okuyama T, Takahashi S. Changes in end-tidal carbon dioxide tension following sodium bicarbonate administration: correlation with cardiac output and haemoglobin concentration. *Acta Anaesthesiol Scand* 1995; **39**: 79–84.]

on the rate at which CO_2 is introduced into the venous intravascular space; that is, a rapid injection of CO_2 could cause an abrupt decrease in $P_{ET}CO_2$, whereas a small, continuous infusion of CO_2 might lead to transient increases in $P_{ET}CO_2$. However, a porcine model in which CO_2 was intravenously injected at rates as low as 0.01 mL/kg/min noted no significant increase in $P_{ET}CO_2$, whereas the next higher infusion rate (0.05 mL/kg/min) caused a reduction in $P_{ET}CO_2$ from 29 ± 8 to 26 ± 6 mm Hg [56]. In addition, the authors observed that $P_{ET}CO_2$ achieved a nadir value at 40 ± 15 s after injection of CO_2 (0.5 mL/kg/min). Thus, the effects of CO_2 embolus on $P_{ET}CO_2$ probably more closely resemble those caused by other embolic material (e.g., air, clot) in clinical practice, although a momentary window of time on the order of a few seconds may exist in which increased $P_{ET}CO_2$ could be observed with Herculean vigilance.

Apnea testing for brain death

One diagnostic use of increased CO_2 pressures is to establish brain death. The basic principal of this provocative examination is to test the ventilatory response of the respiratory centers of the medulla oblongata to increased pressures of CO_2. If a patient suffering cerebral trauma exerts some respiratory effort with sufficiently increased CO_2 pressures, then the patient is diagnosed with brain injury, but not brain death. Conversely, if no respiratory effort is observed in the absence of other medications that could interfere with breathing, brain death is then established, and subsequent withdrawal of supportive care or consideration of the living remains for organ donation by transplantation professionals is made in consultation with the patient's family members.

The test to establish brain death is performed a number of ways in various hospitals. Some guidelines

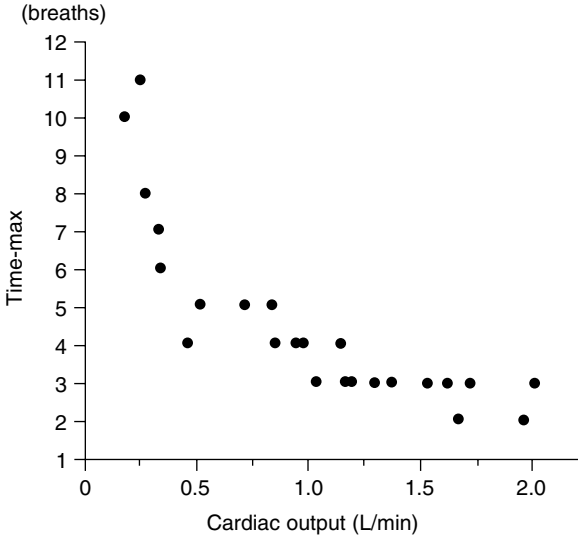

Figure 29.5 Relationship between cardiac output and time-max in anesthetized, mechanically ventilated dog. Cardiac output showed a strong inverse correlation with time-max. ($y = 1.58/x + 1.96$, $r = 0.94$, $P < 0.0001$). [Reprinted with permission from: Okamoto H, Hoka S, Kawasaki T, Okuyama T, Takahashi S. Changes in end-tidal carbon dioxide tension following sodium bicarbonate administration: correlation with cardiac output and haemoglobin concentration. *Acta Anaesthesiol Scand* 1995; **39**: 79–84.]

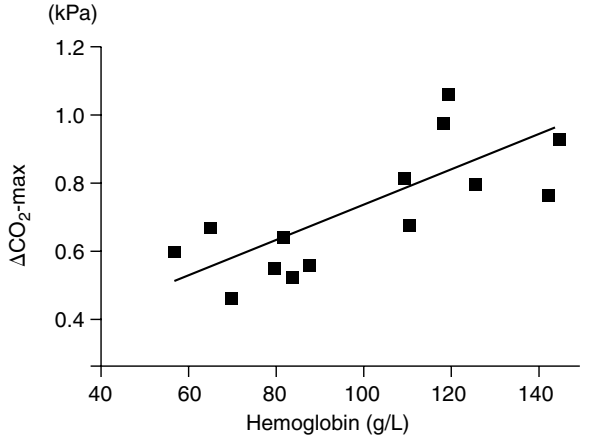

Figure 29.6 Relationship between hemoglobin concentration and ΔCO_2-max in anesthetized, mechanically ventilated dog. A linear correlation was observed ($y = 0.38x + 1.75$, $r = -0.736$, $P < 0.005$) (1 mm Hg = 0.133 kPa). [Reprinted with permission from: Okamoto H, Hoka S, Kawasaki T, Okuyama T, Takahashi S. Changes in end-tidal carbon dioxide tension following sodium bicarbonate administration: correlation with cardiac output and haemoglobin concentration. *Acta Anaesthesiol Scand* 1995; **39**: 79–84.]

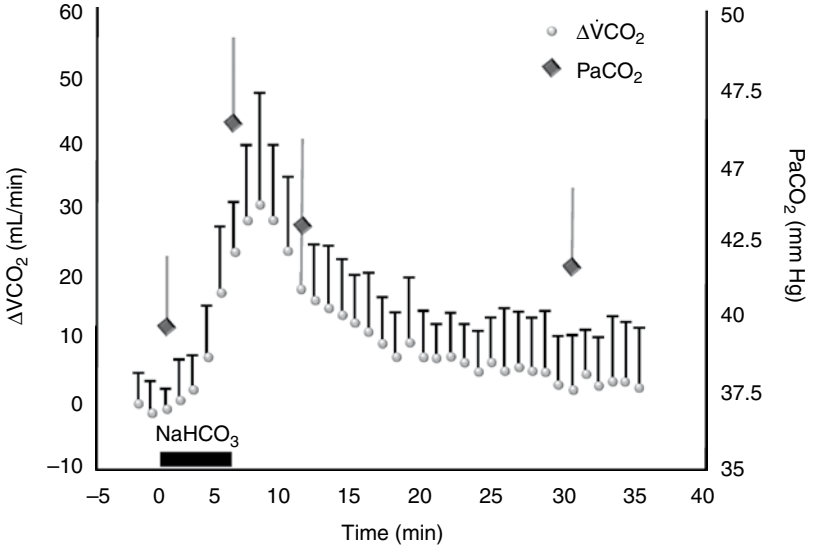

Figure 29.7 Time-course of the changes in $\dot{V}CO_2$ and $PaCO_2$ in 16 artificially ventilated critically ill patients during and after the infusion of 1.5 mmol/kg sodium bicarbonate over 5 min. [Reprinted with permission from: Levraut J, Garcia P, Giunti C, *et al.* The increase in CO_2 production induced by $NaHCO_3$ depends on blood albumin and hemoglobin concentrations. *Intens Care Med* 2000; **26**: 558–64.]

stipulate a minimal duration of 10 min of apnea, with a $PaCO_2$ value in excess of 60 mm Hg [57,58]. In order to maintain clinically acceptable oxygen tensions in the blood over the duration of 10 min, the patient undergoes preoxygenation so that the test can be performed while allowing oxygen delivery to the body via apneic oxygenation. Ventilation is not performed for these patients, as CO_2 elimination is not consistent with performance of the apnea test.

Notwithstanding the years of clinical use for the apnea test, some fundamental problems associated with the examination persist. For example, the rate of rise of CO_2 varies dramatically in patients with various injuries, and depends on a number of factors, including

body temperature and a non-linear rise in CO_2 pressures dependent on preexisting $PaCO_2$ values [58]. In addition, this test can be associated with organ damage, such as hypoxia, hypotension, and arrhythmias that may damage the patient or the patient's potentially life-saving organs for transplantation [59,60]. In some patients, a sufficient CO_2 concentration cannot be achieved before complications ensue [61]. For these reasons, several authors have advocated an alternative test to the apnea examination [60]. In this type of examination, CO_2 is added directly into the inspiratory limb of the airway circuit without any change in ventilatory parameters until the $PaCO_2$ exceeds 60 mm Hg. The benefits of this type of augmentation are that increases in CO_2 tensions are more easily controlled both in terms of time and overall magnitude, and complications due to hypoxia are obviated. Because the patient's lungs remain ventilated, this modified test does not preclude capnography or capnometry. In the author's opinion, measurement of $PETCO_2$ would be a valuable addition to this test. Capnography allows continuous measurement of CO_2 in contrast to spot tests of arterial blood gas samples. As such, capnography would enable more precise and rapid control of CO_2 flow into the airway circuit and provide mutually independent, corroborative evidence for $PaCO_2$ measurement. Given the ubiquitous availability of capnography and the gravity of the decision to be considered by physicians and family members, it seems reasonable to add capnometry to the test and, thus, obtain greater control, flexibility, and quality assurance.

Recently, French investigators reported the use of end-tidal [62] and transcutaneous [63] CO_2 partial pressure to diagnose brain death in intubated and ventilated patients. In the 58 of 60 subjects undergoing this type of apnea, the $PaCO_2$ significantly increased from 40 ± 7 to 97 ± 19 mm Hg, whereas the $etCO_2$ increased from 31 ± 6 to 68 ± 17 mm Hg. Two subjects commenced self-ventilation, as they were not brain-dead. Although an intriguing way to establish brain death and minimize potential organ damage, the larger and highly variable discrepancy in arterial to end-tidal CO_2 gradient (from 9 ± 4 to 29 ± 10 mm Hg) at higher concentrations of $PaCO_2$ during apnea confounded the extrapolation of an individual patient's $etCO_2$ to $PaCO_2$, the relevant specimen upon which the establishment of brain death is based. The same research group determined that a transcutaneous CO_2 pressure during the apnea test greater than 60 mm Hg accurately predicts that a $PaCO_2 > 60$ mm Hg has been achieved [63]. The receiver–operator curve data for transcutaneous CO_2 pressure to predict a $PaCO_2 > 60$ mm Hg demonstrated a positive and negative predictive value of 1.00 and 0.72, respectively. Although promising, additional and repeated investigations would be helpful to determine if real-time CO_2 measurements will ultimately be useful to ascertain brain death in an individual patient.

References

1. Nelson DL, Cox MM. Bioenergetics and metabolism. *Lehninger Principles of Biochemistry*. New York: Worth Publishers, 2000; 485–904.
2. Schon EA. Mitochondrial DNA and the genetics of mitochondrial disease. In: Schapira AH, DiMauro S (eds.) *Mitochondrial Disorders in Neurology*. Oxford, UK: Butterworth-Heinemann, 1994; 31–48.
3. Poulton J. Pathogenesis of mitochondrial disease. In: Applegarth DA, Dimmick JE, Hall JG (eds.) *Organelle Diseases*. London: Chapman and Hall, 1997; 305–35.
4. Skladal D, Halliday J, Thorburn DR. Minimum birth prevalence of mitochondrial respiratory chain disorders in children. *Brain* 2003; **126:** 1905–12.
5. Ording H. Incidence of malignant hyperthermia in Denmark. *Anesth Analg* 1985; **64:** 700–4.
6. Flaherty KR, Wald J, Weisman IM, *et al.* Unexplained exertional limitation: characterization of patients with a mitochondrial myopathy. *Am J Respir Crit Care Med* 2001; **164**: 425–32.
7. Dandurand RJ, Matthews PM, Arnold DL, Eidelman DH. Mitochondrial disease: pulmonary function, exercise performance, and blood lactate levels. *Chest* 1995; **108**: 182–9.
8. Taylor RW, Turnbull DM. Laboratory diagnosis of mitochondrial disease. In: Applegarth DA, Dimmick JE, Hall JG (eds.) *Organelle Diseases*. London: Chapman and Hall, 1997; 341–9,
9. Thomason JA. Quality of health services in Papua New Guinea: what do we know? *PNG Med J* 1993; **36**: 90–8.
10. Sabri MI, Spencer PS, Baggia S, Ludolph AC. Clinical manifestations and mechanisms of action of environmental mitochondrial toxins. In: Sanberg PR, Nishino HN, Borlongan CV (eds.) *Mitochondrial Inhibitors and Neurodegenerative Disorders*. Towota, NJ: Humana Press, 2000; 3–20.
11. Kerns W, Isom G, Kirk MA. Cyanide and hydrogen sulfide. In: Goldfrank LR, Flomenbaum NE, Lewin NA, *et al.* (eds.) *Goldfrank's Toxicologic Emergencies*. New York: McGraw-Hill, 2002; 1498–514.

12. Breen PH, Isserles SA, Westley J, Roizen MF, Taitelman UZ. Effect of oxygen and sodium thiosulfate during combined carbon monoxide and cyanide poisoning. *Toxicol Appl Pharmacol* 1995; **134**: 229–34.
13. Breen PH, Isserles SA, Tabac E, Roizen MF, Taitelman UZ. Protective effect of stroma-free methemoglobin during cyanide poisoning in dogs. *Anesthesiology* 1996; **85**: 558–64.
14. Ravi V, Aked J, Balagopalan C. Review on tropical root and tuber crops. I. Storage methods and quality changes. *Crit Rev Food Sci Nutr* 1996; **36**: 661–709.
15. Kamalu BP. The adverse effects of long-term cassava (*Manihot esculenta Crantz*) consumption. *Int J Food Sci Nutr* 1995; **46:** 65–93.
16. Padmaja G. Cyanide detoxification in cassava for food and feed uses. *Crit Rev Food Sci Nutr* 1995; **35**: 299–339.
17. Sreeja VG, Nagahara N, Li Q, Minami M. New aspects in pathogenesis of konzo: neural cell damage directly caused by linamarin contained in cassava (*Manihot esculenta Crantz*). *Br J Nutr* 2003; **90**: 467–72.
18. Ernesto M, Cardoso AP, Nicala D, *et al.* Persistent konzo and cyanogen toxicity from cassava in northern Mozambique. *Acta Trop* 2002; **82**: 357–62.
19. Oluwole OS, Onabolu AO, Link H, Rosling H. Persistence of tropical ataxic neuropathy in a Nigerian community. *J Neurol Neurosurg Psychiatry* 2000; **69**: 96–101.
20. Lasaga JI. Death in Jonestown: techniques of political control by a paranoid leader. *Suicide Life Threat Behav* 1980; **10**: 210–13.
21. Mueller M, Borland C. Delayed cyanide poisoning following acetonitrile ingestion. *Postgrad Med J* 1997; **73**: 299–300.
22. Dershewitz RA, Levin GS. The effect of the Tylenol scare on parent's use of over-the-counter drugs. *Clin Pediatr (Philadelphia)* 1984; **23**: 445–8.
23. Wildsmith JA, Drummond GB, MacRae WR. Blood-gas changes during induced hypotension with sodium nitroprusside. *Br J Anaesth* 1975; **47**: 1205–11.
24. Ali SS, Dubikaitis A, al Qattan AR. The relationship between end tidal carbon dioxide and arterial carbon dioxide during controlled hypotensive anaesthesia. *Med Princ Pract* 2002; **11**: 35–7.
25. Henriksen L, Paulson OB, Lauritzen M. The effects of sodium nitroprusside on cerebral blood flow and cerebral venous blood gases. I. Observations in awake man during and following moderate blood pressure reduction. *Eur J Clin Invest* 1982; **12**: 383–7.
26. Tripp BC, Smith K, Ferry JG. Carbonic anhydrase: new insights for an ancient enzyme. *J Biol Chem* 2001; **276**: 48615–18.
27. Smith KS, Jakubzick C, Whittam TS, Ferry JG. Carbonic anhydrase is an ancient enzyme widespread in prokaryotes. *Proc Natl Acad Sci USA* 1999; **96**: 15184–9.
28. Potter CP, Harris AL. Diagnostic, prognostic and therapeutic implications of carbonic anhydrases in cancer. *Br J Cancer* 2003; **89**: 2–7.
29. Baird TT, Waheed A, Okuyama T, Sly WS, Fierke CA. Catalysis and inhibition of human carbonic anhydrase IV. *Biochemistry* 1997; **36**: 2669–78.
30. Soda H, Yukizane S, Yoshida I, Aramaki S, Kato H. Carbonic anhydrase II deficiency in a Japanese patient produced by a nonsense mutation (TAT→TAG) at Tyr-40 in exon 2 (Y40X). *Hum Mutat* 1995; **5**: 348–50.
31. Sly WS, Whyte MP, Sundaram V, *et al.* Carbonic anhydrase II deficiency in 12 families with the autosomal recessive syndrome of osteopetrosis with renal tubular acidosis and cerebral calcification. *N Engl J Med* 1985; **313**: 139–45.
32. Fathallah DM, Bejaoui M, Sly WS, Lakhoua R, Dellagi K. A unique mutation underlying carbonic anhydrase II deficiency syndrome in patients of Arab descent. *Hum Genet* 1994; **94**: 581–2.
33. Cumming WA, Ohlsson A. Intracranial calcification in children with osteopetrosis caused by carbonic anhydrase II deficiency. *Radiology* 1985; **157**: 325–7.
34. Whyte MP. Carbonic anhydrase II deficiency. *Clin Orthop* 1993; **294**: 52–63.
35. Taki K, Kato H, Yoshida I. Elimination of CO_2 in patients with carbonic anhydrase II deficiency, with studies of respiratory function at rest. *Respir Med* 1999; **93**: 536–9.
36. Lien YH, Lai LW. Respiratory acidosis in carbonic anhydrase II-deficient mice. *Am J Physiol* 1998; **274**: L301–4.
37. Roemer K, Johnson PA, Friedmann T. Knock-in and knock-out. *New Biol* 1991; **3**: 331–5.
38. Lee TS. End-tidal partial pressure of carbon dioxide does not accurately reflect $PaCO_2$ in rabbits treated with acetazolamide during anaesthesia. *Br J Anaesth* 1994; **73**: 225–6.
39. Wagenaar M, Teppema L, Berkenbosch A, Olievier C, Folgering H. The effect of low-dose acetazolamide on the ventilatory CO_2 response curve in the anaesthetized cat. *J Physiol* 1996; **495**: 227–37.
40. Taki K, Hirahara K, Totoki T, Takahashi N. Retention of carbon dioxide in tissue following carbonic anhydrase inhibition in dogs. *Clin Ther* 1993; **15**: 884–9.
41. Taki K, Mizuno K, Takahashi N, Wakusawa R. Disturbance of CO_2 elimination in the lungs by carbonic anhydrase inhibition. *Jpn J Physiol* 1986; **36**: 523–32.

42. Cardenas V, Heming TA, Bidani A. Kinetics of CO_2 excretion and intravascular pH disequilibria during carbonic anhydrase inhibition. *J Appl Physiol* 1998; **84**: 683–94.
43. Krintel JJ, Haxholdt OS, Berthelsen P, Brockner J. Carbon dioxide elimination after acetazolamide in patients with chronic obstructive pulmonary disease and metabolic alkalosis. *Acta Anaesthesiol Scand* 1983; **27**: 252–4.
44. Supuran CT. Carbonic anhydrases as drug targets: an overview. *Curr Top Med Chem* 2007; **7**: 825–33.
45. Supuran CT, Di FA, De SG. Carbonic anhydrase inhibitors as emerging drugs for the treatment of obesity. *Expert Opin Emerg Drugs* 2008; **13**: 383–92.
46. Silberberg S. Gases and the kinetic-molecular theory. *Chemistry: The Molecular Nature of Matter and Change*. St Louis, MO: Mosby-Year Book Inc, 1996; 172–219.
47. Spear ML, Darmaun D, Sager BK, Parsons WR, Haymond MW. Use of [13C]bicarbonate infusion for measurement of CO_2 production. *Am J Physiol* 1995; **268**: E1123–7.
48. Okamoto H, Hoka S, Kawasaki T, Okuyama T, Takahashi S. Changes in end-tidal carbon dioxide tension following sodium bicarbonate administration: correlation with cardiac output and haemoglobin concentration. *Acta Anaesthesiol Scand* 1995; **39**: 79–84.
49. Levraut J, Garcia P, Giunti C, *et al.* The increase in CO_2 production induced by $NaHCO_3$ depends on blood albumin and hemoglobin concentrations. *Intens Care Med* 2000; **26**: 558–64.
50. Nishiyama T, Hanaoka K. Gas embolism during hysteroscopy. *Can J Anaesth* 1999; **46**: 379–81.
51. Imasogie N, Crago R, Leyland NA, Chung F. Probable gas embolism during operative hysteroscopy caused by products of combustion. *Can J Anaesth* 2002; **49**: 1044–7.
52. Shulman D, Aronson HB. Capnography in the early diagnosis of carbon dioxide embolism during laparoscopy. *Can Anaesth Soc J* 1984; **31**: 455–9.
53. Diakun TA. Carbon dioxide embolism: successful resuscitation with cardiopulmonary bypass. *Anesthesiology* 1991; **74**: 1151–3.
54. Lee Y, Kim ES, Lee HJ. Pulmonary edema after catastrophic carbon dioxide embolism during laparoscopic ovarian cystectomy. *Yonsei Med J* 2008; **49**: 676–9.
55. Beck DH, McQuillan PJ. Fatal carbon dioxide embolism and severe haemorrhage during laparoscopic salpingectomy. *Br J Anaesth* 1994; **72**: 243–5.
56. Couture P, Boudreault D, Derouin M, *et al.* Venous carbon dioxide embolism in pigs: an evaluation of end-tidal carbon dioxide, transesophageal echocardiography, pulmonary artery pressure, and precordial auscultation as monitoring modalities. *Anesth Analg* 1994; **79**: 867–73.
57. Benzel EC, Mashburn JP, Conrad S, Modling D. Apnea testing for the determination of brain death: a modified protocol [technical note]. *J Neurosurg* 1992; **76**: 1029–31.
58. Dominguez-Roldan JM, Barrera-Chacon JM, Murillo-Cabezas F, Santamaria-Mifsut JL, Rivera-Fernandez V. Clinical factors influencing the increment of blood carbon dioxide during the apnea test for the diagnosis of brain death. *Transplant Proc* 1999; **31**: 2599–600.
59. al Jumah M, McLean DR, al Rajeh S, Crow N. Bulk diffusion apnea test in the diagnosis of brain death. *Crit Care Med* 1992; **20**: 1564–7.
60. Melano R, Adum ME, Scarlatti A, Bazzano R, Araujo JL. Apnea test in diagnosis of brain death: comparison of two methods and analysis of complications. *Transplant Proc* 2002; **34**: 11–12.
61. Rudolf J, Haupt WF, Neveling M, Grond M. Potential pitfalls in apnea testing. *Acta Neurochir (Wien)* 1998; **140**: 659–63.
62. Vivien B, Amour J, Nicolas-Robin A, *et al.* An evaluation of capnography monitoring during the apnoea test in brain-dead patients. *Eur J Anaesthesiol* 2007; **24**: 868–75.
63. Vivien B, Marmion F, Roche S, *et al.* An evaluation of transcutaneous carbon dioxide partial pressure monitoring during apnea testing in brain-dead patients. *Anesthesiology* 2006; **104**: 701–7.

Section 4
Chapter
30

Physiologic perspectives

Acid–base balance and diagnosis of disorders

P. G. Boysen and A. V. Isenberg

Introduction

Capnography can provide important clues concerning the acid–base status of patients. For example, an increase or decrease in end-tidal carbon dioxide (CO_2) might indicate a primary respiratory acidosis, or a primary respiratory alkalosis, respectively. Alternatively, increased end-tidal CO_2 tension may be a response to a metabolic alkalosis, and decreased end-tidal CO_2 tension might be due to compensation for a metabolic acidosis. Certain assumptions, which may not be warranted in some cases, must be made to make appropriate evaluations and diagnoses. Global cardiac output and regional perfusion of the lung, as well as deadspace ventilation (VD/VT), should be normal and stable. Under these conditions, end-tidal CO_2 tension and arterial CO_2 tension are proximate. Beyond these initial clues, arterial blood gas analysis is essential to properly evaluate the acid–base status, and diagnose and treat underlying disorders.

Normal acid–base homeostasis

Acids and bases are constantly formed in the body as by-products of metabolism, and are carefully regulated. The normal pH of the blood ranges from 7.36 to 7.44 (Table 30.1). This narrow range is maintained by a complex system of buffering mechanisms, each designed to regulate the amount of hydrogen ion in the body. These mechanisms include intracellular and extracellular chemical buffers, regulation of CO_2 by the respiratory and central nervous systems (CNS), and control of bicarbonate by the kidney.

Chemical buffering

Acids

The metabolic acids produced are classified as volatile and non-volatile. The primary volatile acid is carbonic acid (H_2CO_3); it is produced during CO_2 reactions and exhaled as CO_2. The non-volatile acids are sulfuric acids (produced by the breakdown of sulfur-containing amino acids), organic acids (from the breakdown of carbohydrates and fats), uric acids (from nucleic acid metabolism), and inorganic phosphates. The non-volatile acids are buffered by the blood bicarbonate system.

Bases

Bicarbonate buffers prepare non-volatile acid protons for excretion, a buffer-consuming process. Bicarbonate diffuses freely between interstitial fluid and plasma along a concentration gradient [1], and carries with it about 70% of CO_2 [2]. As bicarbonate is generated, the chloride shift (*Hamberger effect*) serves to maintain ionic equilibrium in the RBCs by moving chloride from the RBCs into the plasma [2]. Renal tubular reabsorption serves to preserve bicarbonate. New bicarbonate production (50–100 mmol/day) occurs during the renal acidification process whereby protons are secreted to form urinary buffers (phosphate and ammonia) that are then eliminated in the urine.

CO_2 regulation

CO_2 is produced by the metabolism of substrate inside cells. It is then transported in blood to the alveolus where it can be excreted in the gas phase. Some CO_2 travels as gas dissolved in plasma, although the majority of CO_2 is transported in RBCs as bicarbonate. Inside the RBCs, CO_2 combines with water to form carbonic acid (or volatile acid), which forms hydrogen ions and bicarbonate as terminal products. The *bicarbonate–carbonic acid equation* is a steady-state reaction that is catalyzed by carbonic anhydrase (acetazolamide inhibits this enzyme):

$$CO_2 + H_2O \rightleftharpoons H_2CO_3 \rightleftharpoons H^+ + HCO_3^-.$$

Capnography, Second Edition, ed. J. S. Gravenstein, Michael B. Jaffe, Nikolaus Gravenstein, and David A. Paulus. Published by Cambridge University Press. © Cambridge University Press 2011.

Table 30.1 Normal acid–base composition

	Low	Mean	High
Arterial blood			
pH	7.36	7.40	7.44
$[H^+]$ (nEq/L)	36	40	44
PCO_2 (mm Hg)	36	40	44
$[HCO_3^-]$ (standard and actual) (mEq/L)	22	24	26
Base excess (BE) (mEq/L)	*–2*	*0*	*2*
Venous blood			
pH	7.34	7.38	7.42
$[H^+]$ (nEq/L)	38	42	46
PCO_2 (mm Hg)	42	46	50
Total CO_2 (mEq/L)	23	26	30

Source: Modified from Adrogue HJ, Madias NE. Arterial blood gas monitoring: acid–base assessment. In: Martin J, Tobin M (eds.) *Principles and Practice of Intensive Care Monitoring*. New York: McGraw-Hill, 1998; 217–41.

Under normal circumstances, CO_2 production and excretion are in equilibrium. The ratio of bicarbonate (HCO_3^-) to H_2CO_3 is maintained at 20 : 1 (mmol/L) by homeostatic processes [3–6]. The plasma arterial CO_2 ($PaCO_2$) is maintained at 40 mm Hg while the venous level is at 46 mm Hg, setting up a gradient for the transport of CO_2 from cells into the blood. *Hypercapnia*, or increased CO_2 levels in the blood, is produced by the underexcretion of CO_2, and *hypocapnia*, or decreased levels of CO_2 in the blood, evolves from the overexcretion of CO_2.

A build-up of CO_2, such as via hypoventilation, will push the bicarbonate–carbonic acid equation to the right, increasing the hydrogen ion concentration, and thereby decreasing the pH (respiratory acidosis). Conversely, a decrease in the CO_2, as in the case of hyperventilation, pushes this equation to the left, diminishing the hydrogen ion concentration and increasing the pH (respiratory alkalosis).

Changes in the bicarbonate will also affect the equilibrium of the bicarbonate–carbonic acid equation. Loss of bicarbonate (through diarrhea or kidney dysfunction) or addition of acid (diabetic ketoacidosis, DKA) will force the reaction to the right, thereby increasing the H^+, producing metabolic acidosis. Likewise, an increased loss of H^+ through the gastrointestinal (GI) tract as a consequence of vomiting or through renal losses will push the equation to the left and increase the pH (metabolic alkalosis).

CO_2 diffuses freely across cell membranes, while HCO_3^- diffuses between the plasma and interstitial fluid in response to concentration gradients. Other buffers, most notably hemoglobin and plasma proteins, are restricted to the vascular compartment.

CO_2 is regulated primarily by the CNS through the medullary chemoreceptors. The $PaCO_2$, therefore, is not normally determined by the rate of CO_2 production, but by neural respiratory center output. Increased $PaCO_2$ is generally caused by hypoventilation, driven by an aberration in the CNS rather than an augmentation of CO_2 production. Aside from CNS regulation, increases or decreases in $PaCO_2$ can be generated by compensation secondary to a primary change in the bicarbonate ion. A volatile acid, CO_2 can be excreted or retained as needed to maintain homeostasis.

Bicarbonate regulation

The kidneys use three mechanisms to regulate plasma bicarbonate. The first method involves reabsorption of filtered bicarbonate, 80–90% of which is reabsorbed in the proximal tubule of the nephron. The kidney filters approximately 4000 mmol of bicarbonate each day; to reabsorb the filtered bicarbonate ion, the renal tubules must secrete 4000 mmol of hydrogen ions. The distal nephron reabsorbs the remaining 10–20% of the bicarbonate, and secretes 40–60 mmol/day of hydrogen ions to maintain the blood pH. The kidney then uses a second regulatory mechanism to take the remaining 40–60 mmol/day of hydrogen ions and form a titratable acid and NH_4. The excess hydrogen ions are then excreted as NH_4 in the urine as the third process of the kidney for bicarbonate regulation. Production and excretion of NH_4 will be increased in a metabolic acidosis with normal renal function but will be impaired in chronic renal failure, hyperkalemia, and renal tubular acidosis (RTA)[7–10].

Henderson–Hasselbalch equation

The sum of the respiratory and metabolic components that drive the blood pH level can be described by the Henderson–Hasselbalch equation:

$$pH = 6.1 + \log\left[\frac{HCO_3^-}{PaCO_2 \times 0.0301}\right]$$

This equation is normally used by clinicians to calculate an expected value of bicarbonate that can be compared to the measured bicarbonate as a way to check the

accuracy of laboratory values while considering the possibility of a mixed acid–base disorder.

Standard HCO_3^- and base excess

The interdependence of the respiratory and metabolic factors that determine the pH described by the Henderson–Hasselbalch equation have led researchers to derive other parameters that can be used to formulate a metabolic component that is independent from the respiratory component [1]. These relationships are only true in vitro, because in vivo, the presence of buffers other than bicarbonate that are restricted to the vascular compartment confounds the in vivo relationship.

The *standard* [HCO_3^-] is a derived parameter corresponding to the plasma bicarbonate concentration (mean is 24 mol/L) in a blood sample fully saturated with oxygen and equilibrated in vitro at 38 °C and having a partial pressure of CO_2 (PCO_2) equal to 40 mm Hg [11]. This standardized blood oxygen factor is necessary because the level of oxygenation of hemoglobin alters the hemoglobin buffer value, that is, when oxygenated hemoglobin releases oxygen, it becomes less acidic, thereby increasing its buffering capacity (and vice versa when hemoglobin picks up oxygen). The standard HCO_3^-, therefore, can be used to quantify alterations in the buffer systems within a blood sample [1].

The blood base excess (BE) is another parameter derived from the Henderson–Hasselbalch relationship. It corresponds to the quantity of acid or alkali that must be added to a liter of fully oxygenated blood exposed in vitro to a PCO_2 of 40 mm Hg at 38 °C to reach a pH of 7.40 [1]. If the initial blood pH is low (acidic), alkali must be added to bring the pH back up to the normal 7.4 value. Thus, the initial blood sample can be said to have a *negative BE* or simply a *base deficit*. With the reverse situation, if a blood sample has a high pH (alkaline), acid must be added to decrease the pH to the normal level, the sample is said to have a *positive BE* or simply a *BE*. The normal value of BE is zero.

Strong ion theory

Traditional acid–base physiology with its basis in the Henderson–Hasselbalch equation has been challenged recently by Peter Stewart's theory, which maintains that hydrogen ion concentration is determined by the dissociation of water ($H_2O \rightarrow H^+ + OH^-$), and not by the addition of hydrogen ions [12,13]. In short, Stewart found that three independent variables determine the hydrogen ion concentration: the strong ion difference (SID), the total concentration of weak acids, and $PaCO_2$. The SID is the net charge balance of all of the "strong ions" in the system; that is, the ions that are essentially inert and completely dissociated (not including water or bicarbonate, because it readily combines with CO_2 or OH^-). The SID discounts the other ions present in low concentrations; one must remember that they are present [14].

$$SID = Na + K + Ca + Mg + PO_4 - (Cl - lactate)$$

Thus, when strong ions are added to a system, neutrality is maintained by altering weak electrolyte dissociation. For example, when sodium bicarbonate is given to a patient, the serum bicarbonate does not increase simply because of giving bicarbonate in the fluid, but because the solution contained the strong cation, sodium, which causes the water dissociation reaction to shift left, resulting in fewer hydrogen ions, and thus a higher pH [15]. The Stewart approach is of aid, particularly when considering the acidosis, especially when of "dilutional" origin and found to be correctable via treatment with the administration of a strong ion, such as chloride [16,17]; it is also useful with mortality prediction in the pediatric intensive care unit (ICU) [18].

Diagnosis of acid–base disorders

Arterial blood gas

Arterial blood gases (ABGs) are thought to provide the best assessment of pulmonary exchange and tissue oxygenation. Central venous and mixed venous blood gases are an additional important means to assess perfusion [19–22]. With circulatory insufficiency, venous pH and $PaCO_2$ have been shown to change earlier and with greater magnitude than arterial values [23]. Further, it has been documented that in patients with circulatory failure, it may be misleading to use only arterial blood samples to monitor acid–base status [3,4]. Severity of the discrepancy between simultaneously sampled arterial and venous blood gas specimens becomes greater with declining circulatory function and extreme during cardiac arrest.

It is important to remember that venous blood HCO_3^- is approximately 2 mEq/L higher than the arterial value because the majority of the metabolically produced CO_2 that is added to venous blood is carried as bicarbonate. Venous blood also has a greater quantity of carbamino compounds and dissolved CO_2 than arterial blood [1].

Capillary blood samples can be used, particularly in children, to measure ABG. Care must be taken to warm the area prior to the procedure (about 5 min) to secure a dilated vascular bed [24]. Acid–base status can also be measured using a peripheral vein in the dorsum of the hand that has been warmed (to 45 °C for 10 min); the resulting values are very close to those from an arterial draw [1]. Lastly, umbilical cord gases should use arterial rather than venous blood, as arterial acidemia may be present with a normal venous pH; the lower range of normal for the arterial pH is 7.10 [25].

The ABGs measure the arterial pH and PCO_2 in the arterial blood. Electrolytes should be drawn simultaneously to obtain a *measured* HCO_3^-, which should be used to compare the *calculated* HCO_3^- from the Henderson–Hasselbalch equation. The two values should agree within 2 mmol/L; otherwise, errors have been introduced in the laboratory, math, or the blood draw itself (commonly a non-simultaneous draw of electrolytes and ABG). Considering that blood sampling is intermittent, transient changes in the acid–base composition that are not detected can exist [1]. Serum albumin should also be measured with a suspected acidosis to aid in consideration of anion gap (AG) issues. A serum creatinine (CR) may be helpful in many cases when considering dysfunction or compensation by the kidneys. Urine pH and osmolar gap are also useful values to consider in the face of their respective acid–base scenarios.

Other important issues to explore when diagnosing an acid–base disorder are patient history and drug use. Chronic renal failure predisposes a patient to metabolic acidosis, as do diarrheal diseases. Vomiting can cause a metabolic alkalosis while patients with pneumonia, sepsis, or cardiac failure frequently have respiratory alkalosis. Air-trapping diseases or sedative overdoses can also induce a respiratory acidosis [10].

Drug history is an important factor. Loop and thiazide diuretics can incite a metabolic alkalosis, while carbonic anhydrase inhibitors can cause a metabolic acidosis. Overdoses of drugs can produce mixed acid–base disorders, such as the combined metabolic acidosis and respiratory alkalosis from a salicylate overdose.

Approach to simple acid–base disorders

Acid–base disorders are shown in Figure 30.1 and Table 30.2.

(1) Thorough history and physical examination.
(2) Draw the arterial blood for ABG. Examine the pH first. If the pH < 7.36, there is acidemia. If the pH is > 7.44, there is alkalemia.
(3) Decide whether the primary disorder is metabolic or respiratory:
   – If acidemia: Respiratory acidosis if $PaCO_2 > 45$
     Metabolic acidosis if $HCO_3^- < 22$

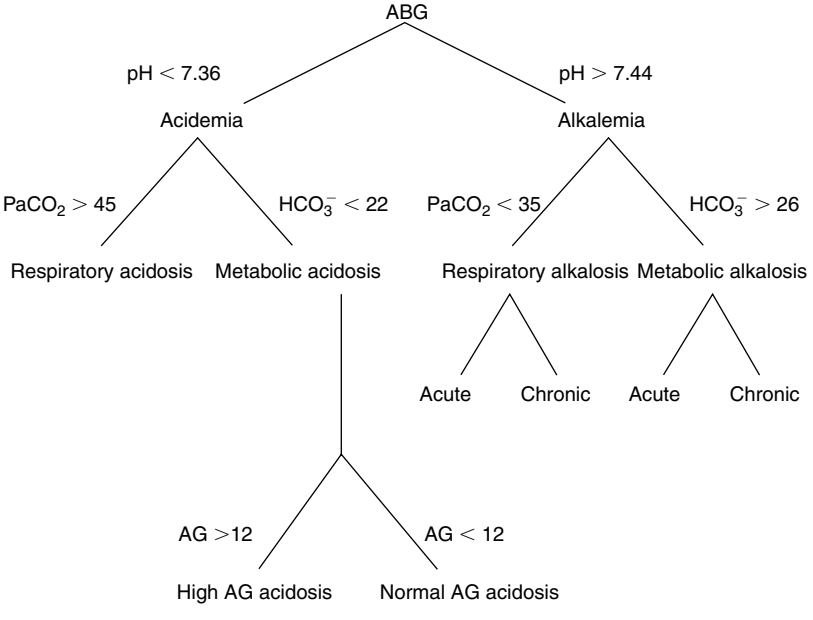

Figure 30.1 Acid–base diagnostic algorithm. [Reproduced with permission from Feibusch KC, Breaden RS, Bader CD, Gomperts SN. *Prescription for the Boards: USMLE Step 2*, 2nd edn. Philadelphia, PA: Lippincott-Raven, 1998.]

Table 30.2 Secondary response to simple acid–base disorders

Metabolic	Acidosis		Alkalosis	
Expected response factor (x) $\Delta PaCo_2 \approx x\,\Delta[HCO_3^-]$	1.2		0.7	
Maximal response (mm Hg)	10		65	
	Acidosis		**Alkalosis**	
Respiratory	**Acute**	**Chronic**	**Acute**	**Chronic**
Expected response factor (x) $\Delta[HCO_3^-] \approx x\,\Delta PaCo_2$	0.1	0.3	0.2	0.4
Maximal response (mEq/L)	30	45	16–18	12–15

Source: Modified from Adrogue HJ, Madias NE. Arterial blood gas monitoring: acid–base assessment. In: Martin J, Tobin M (eds.) *Principles and Practice of Intensive Care Monitoring*. New York: McGraw-Hill, 1998; 217–41.

– If alkalemia: Respiratory alkalosis if $PaCO_2 < 35$
Metabolic alkalosis if $HCO_3^- > 26$

(4) If the primary disorder is metabolic, is there appropriate compensation? (Use the compensation equations; see p. 300). If the primary disorder is respiratory, decide if it is acute or chronic (use the compensation equations).

(5) Consider accuracy of laboratory values (true versus spurious results) and entertain possibility of a mixed acid–base disorder.

(6) Calculate the anion gap (AG):

$$AG = Na - [Cl + HCO_3^-]$$

The normal AG value is 10–12 mEq/L.
If there is a metabolic acidosis and the AG is >12, there is a high AG acidosis. If the AG is 12 or less, there is a normal AG (hypochloremic) acidosis. If the AG is >20, there is an underlying AG acidosis in the face of any other acid–base disturbances present.

(7) If there is an elevated AG, calculate the corrected serum bicarbonate:

$$\text{Corrected bicarbonate} = \text{excess AG} + \text{measured } HCO_3^-$$

If the corrected bicarbonate is low (<24 mEq/L), there is an underlying non-AG acidosis; if high (>24 mEq/L), there is an underlying metabolic alkalosis.

(8) Calculate ancillary laboratory values with respect to suspected diagnosis (albumin, serum/urine osmolar gap, electrolytes [potassium, blood urea nitrogen [BUN], CR, glucose, etc.], blood/urine screens for toxins).

Simple acid–base disorders

Acid–base disorders can be described as *simple*, wherein one acid–base disturbance exists, or *mixed*, where there are two or more acid–base disorders present simultaneously [26–28]. Simple acid–base disorders involve a primary abnormality in either metabolism (change in the bicarbonate) or respiration (change in arterial CO_2) that produces a secondary change, or compensatory response, in the other component. The compensation response serves to ameliorate the primary disturbance in an effort to bring the pH back to baseline [29,30]. Secondary compensation for a primary acid–base disorder, however, does not constitute a mixed acid–base disorder because compensation in itself is not a separate acid–base disturbance.

Compensation

Primary respiratory disturbances will cause secondary changes in the metabolism (renal acid production/secretion alterations), and primary metabolic disturbances will invoke compensatory changes in respiration (increased or decreased ventilation). The amount of compensation can be predicted from the *compensation equations* listed below. If the compensation values differ from predicted values, a mixed acid–base disorder should be considered.

For example, a primary respiratory acidosis will invoke a secondary metabolic alkalosis to compensate for the effects of the excess acid in the system. To illustrate, a comatose victim may develop a respiratory acidosis due to an injured ventilation stimulation pathway (e.g., due to cerebral edema secondary to a head injury), which leads to hypoventilation and CO_2 trapping. The pH will decrease because of the increased $PaCO_2$ and a shift in the carbonic acid equation. The kidneys recognize the acidosis, and effect changes in the acid titration process to secrete less HCO_3^- to compensate for the respiratory acidosis.

The four cardinal simple acid–base disorders are as follows: metabolic acidosis, metabolic alkalosis, respiratory acidosis, and respiratory alkalosis. Secondary responses to each of these four disorders follow a predictable pattern [31]. Classically, the acid–base nomogram (sometimes referred to as the Davenport diagram) can be used to graph a patient's HCO_3^- and pH to determine the type of disorder. The modified acid–base nomogram (Figure 30.2) has shaded intervals that mark the appropriateness of compensation. Values that fall

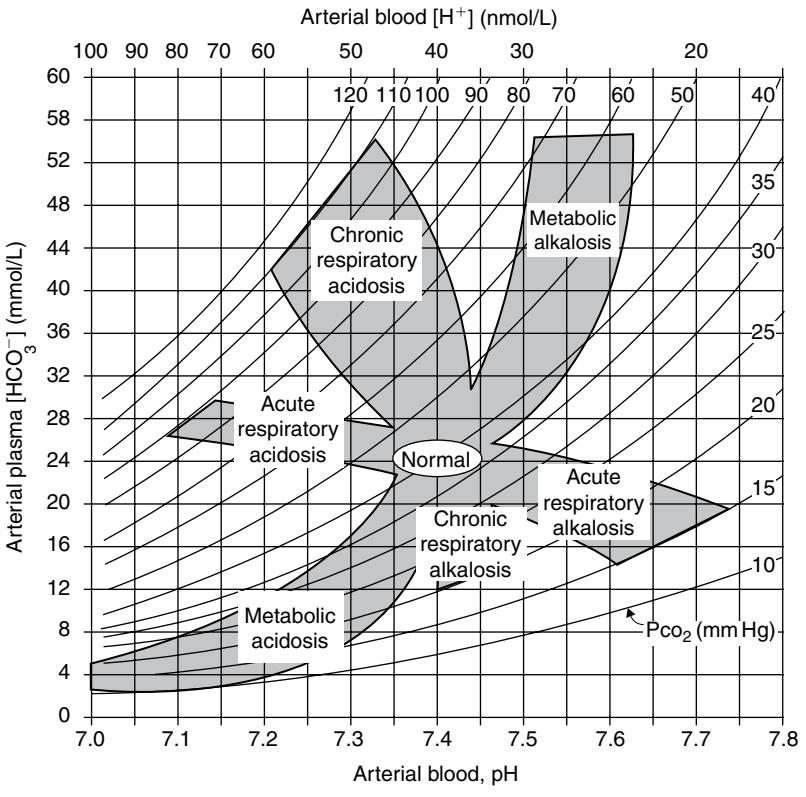

Figure 30.2 Acid–base nomogram. Figure showing the 90% confidence limits of normal respiratory and metabolic compensations for primary acid–base disturbances. Values for mixed disturbances will fall outside of the shaded areas. [Reproduced with permission from: DuBose TD Jr. Acid–base disorders. In: Brenner BM (ed.) *Brenner and Rector's The Kidney*, 6th edn. Philadelphia, PA: WB Saunders, 2000; 925–97.]

outside the shaded areas indicate a mixed disturbance. Further, compensation equations can be used to assess responses to acid–base disorders and to decide whether a mixed acid–base disturbance may be present.

Compensation equations

Disorder	Rule of compensation
Metabolic acidosis	$PaCO_2 = (1.5 \times HCO_3^-) + 8$ or $PaCO_2$ will ↓1.25 mm Hg per mmol/L ↑ in HCO_3^- or $PaCO_2 = HCO_3^- + 15$
Metabolic alkalosis	$PaCO_2$ will ↑ 0.75 mm Hg per mmol/L ↑ in HCO_3^- or $PaCO_2$ will ↑ 6 mm Hg per 10 mmol/L ↑ in HCO_3^- or $PaCO_2 = HCO_3^- + 15$
Respiratory alkalosis	
Acute	HCO_3^- will ↓ 2 mmol/L per 10 mm Hg ↓ in $PaCO_2$
Chronic	HCO_3^- will ↓ 4 mmol/L per 10 mm Hg ↓ in $PaCO_2$
Respiratory acidosis	
Acute	HCO_3^- will ↑ 1 mmol/L per 10 mm Hg ↑ in $PaCO_2$
Chronic	HCO_3^- will ↑ 4 mmol/L per 10 mm Hg ↑ in $PaCO_2$

Mixed acid–base disorders

Mixed acid–base disorders occur when a patient has more than one independent acid–base disorder [1,32]; mixed acid–base disorders are very common in hepatic failure [33,34] and in ICU patients [15,35–37]. Many combinations of acid–base disorders are possible; there

may be pairing of two acidotic disorders (respiratory acidosis with metabolic acidosis), two alkalotic disorders (respiratory alkalosis with metabolic alkalosis), two disorders working towards opposite pH poles that can normalize pH (respiratory acidosis and metabolic alkalosis and vice versa), or even three or more disorders occurring simultaneously.

For example, a person with DKA (a metabolic acidosis) may begin to decrease his/her respirations as he/she becomes more acidemic and less conscious (as a result of the DKA), and can develop a separate respiratory acidosis. Or a person can overdose on sedatives and salicylates and have a mixed acid–base disorder in response to the individual drugs taken (metabolic and respiratory acidosis with sedatives and respiratory alkalosis with salicylates). In the case where a metabolic acidosis and a metabolic alkalosis exist in the same patient, the pH may be normal; and therefore, checking the AG is the next step in the evaluation (an increased AG in this case indicates a metabolic acidosis is present).

Metabolic acidosis

Metabolic acidosis can be caused by an increase in endogenous acid production (lactic or ketoacids in DKA), a decrease in bicarbonate (diarrhea), or an accumulation of endogenous acids (renal failure). A decrease in the pH and in the HCO_3^- will be manifested. The secondary response to metabolic acidosis is hyperventilation, which releases the volatile acid CO_2 from the lungs in an attempt to increase the pH back to baseline, and results in hypocapnia [38–40].

The reduction in pH can produce several effects on the respiratory, cardiac, and nervous systems. Tidal volume increases with increased ventilation, which can lead to Kussmaul respirations. The decreased pH sensitizes the peripheral chemoreceptors, increasing minute ventilation which, within hours, can bring about an almost complete respiratory compensation [15,38].

Metabolic acidosis decreases cardiac contractility, but inotropic activity is maintained because of the sympathetic catecholamine release; cardiac output and heart rate will increase with mild acidemia (pH > 7.2) [41,42]. With a rapidly developing acidosis, left ventricular performance has been noted to decrease. Peripheral arterial vasodilation is common with central venoconstriction[43], a scenario that predisposes the patient to pulmonary edema due to the decrease in vascular compliance. Additionally, acidemia shifts the oxyhemoglobin dissociation curve to the right, unloading oxygen more effectively while an acidemia-induced decrease in 2,3-biphosphoglycerate moves the curve to the left [44].

Metabolic acidosis leads to hyperkalemia as hydrogen ions are exchanged for K^+ or Na^+ on a cellular level. Every pH decrease of 0.10 leads to an increase in plasma potassium of 0.6 mmol/L. Hypokalemia can be caused, in some metabolic acidoses, by urinary wasting of K^+ (RTA, DKA, lactic acidosis, and diarrhea)[10].

Signs and symptoms

Metabolic acidosis produces CNS depression, causing headaches, lethargy, stupor, or coma. Glucose intolerance can also occur. Metabolic acidosis is a particularly common finding in the ICU [15].

Types of metabolic acidosis

There are two types of metabolic acidosis: high AG metabolic acidosis and non-AG (normal AG or hyperchloremic) metabolic acidosis. Both types of metabolic acidosis will have similar capnographic findings; assuming normal cardiac output and pulmonary perfusion, both the end-tidal CO_2 and the $PaCO_2$ will be low.

AG metabolic acidosis

The AG represents the unmeasured anions in plasma, such as anionic proteins, phosphate, sulfate, and other organic anions. Determination of the AG is invaluable in assessing metabolic acidosis [4,45–49]. The normal value is 8–12 mmol/L [50], and can be calculated using the following formula:

$$AG = Na - (Cl + HCO_3^-)$$

A high AG is usually due to an increase in unmeasured anions, such as acetoacetate or lactate – that is, the addition of acid (usually non-volatile), endogenous or exogenous, to the system. It is less commonly due to a decrease in the unmeasured cations (calcium, magnesium, potassium). An increased AG cannot be caused by loss of alkali or by decreased acid excretion by the kidney.

In the case of high AG, typically the loss of bicarbonate is not paralleled by an increase in chloride ions; thus a wide gap is created. With a normal albumin level, a high AG is usually due to non-chloride-containing acids that contain inorganic (phosphate, sulfate), organic (ketoacids, lactate, uremic organic anions), exogenous (salicylate or other ingested toxins which

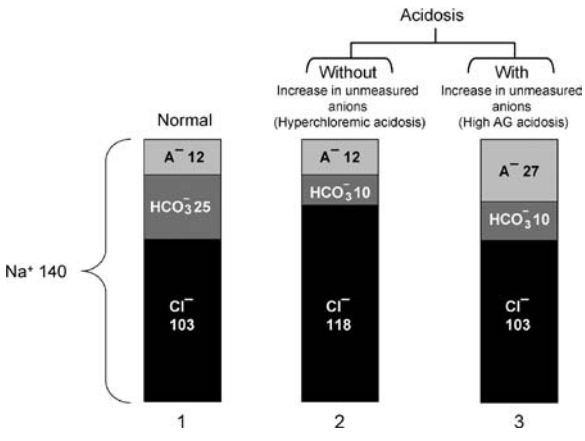

Figure 30.3 Schematic representation of the AG. *Hyperchloremic acidosis* is marked by a decreased serum bicarbonate without an increase in unmeasured anions above normal value; chloride ions are increased to make up the remainder of the negative charge (column 2). In *high AG acidosis* (column 3), increased amounts of fixed acids or other anions (A^-) are present, bicarbonate is decreased, and the level of chloride ions is at its normal value. [Modified from: Brackett NC Jr. An approach to clinical disorders of acid–base balance. *South Med J* 1974; **67**: 1084–101.]

cause organic acid production), or other unidentified anions. A high AG may occur with an increased albumin concentration or alkalosis (alkalosis alters the charge on albumin). Even in the presence of a normal or alkalotic pH, the high AG points to the presence of the addition of excess acid in the body system [15].

A normal AG can be caused by an increase in unmeasured cations or by the addition of atypical cations, such as with lithium overdose. In non-AG acidosis, the loss of base is offset by a rise in chloride that maintains the normal level of anionic charge in the system. A decrease in the albumin concentration can cause a low AG, such as with nephrotic syndrome. Hypoalbuminemia can also lead to a spuriously low AG and mask an acidosis. With acidosis, the anionic charge on albumin can be reduced and cause a low AG. Therefore, it is necessary to correct the serum AG by 2.5–3.0 mEq/L for every g/dL decrease in serum albumin below 4 g/dL [49]. Also, hyperviscosity and severe hyperlipidemia can create a spuriously low AG, and lead to the underestimation of sodium and chloride concentrations (Figure 30.3 and Table 30.3).

High AG metabolic acidosis

There are two mechanisms behind a high AG metabolic acidosis [51]. The first mechanism involves an excessive load of a non-HCl acid (lactate, ketoacid, ingested toxins) that overwhelms the breakdown or excretory processes of the body. The second mechanism involves a diminished capacity of the kidneys to excrete the normal load of endogenous acids typically produced by the body (acute and chronic renal failure).

The three main factors of high AG acidosis that result from an excessive load of non-HCl acid are: (1) lactic acidosis, (2) ketoacidosis, and (3) ingested toxins.

Lactic acidosis

Lactic acidosis (lactate >5 mmol/L, pH <7.25) is most commonly caused by an increase in the plasma L-lactate isomer. L-lactate is produced as a result of decreased tissue perfusion in conditions, such as shock, circulatory failure, severe anemia, mitochondrial enzyme defects, and metabolic inhibitors (carbon monoxide, cyanide), and is commonly monitored on surgical units to check postoperative progress. L-lactate acidosis appears with malignancies, diabetes mellitus, renal or hepatic failure, severe infections, seizures, acquired immune deficiency syndrome, or drugs/toxins (biguanides, ethanol, methanol, isoniazid, azidothymidine analogs, and fructose) [10]. Bowel ischemia or infarction (especially while receiving vasopressors) can also result in increased L-lactate. A D-lactate acidosis can be caused by formation of this isomer by gut bacteria, and is seen in patients with jejunoileal bypass or intestinal obstruction [52], or in patients with impaired D-lactate metabolism [47]; hyperchloremia may also be seen with D-lactate acidosis.

Ketoacidosis

Diabetic ketoacidosis is due to an increase in fatty acid metabolism with the accumulation of ketoacids, acetoacetate, and β-hydroxybutyrate. Lactic acidosis and hyperchloremic acidosis may also occur with uncontrolled diabetes mellitus [53]. Although DKA usually occurs when a patient with type 1 diabetes does not take the required insulin dosage, or has an illness or infection that acutely disrupts insulin requirements, 27% of patients in a series with DKA were type 2 diabetics [54]. Hyperglycemia (glucose >300 mg) occurs as well. In recent studies, end-tidal CO_2 has been used to predict the severity of acidosis in the pediatric population with DKA [55].

Alcoholic ketoacidosis

Alcoholic ketoacidosis occurs in alcoholics who acutely stop drinking, develop nausea and vomiting, and then cease to eat. Glucose is typically low to normal (from

Table 30.3 Causes of metabolic acidosis and alkalosis

Metabolic acidosis		Metabolic alkalosis	
High anion gap (AG)	**Normal anion gap (AG)**	**Chloride-responsive**	**Chloride-resistant**
Endogenous acid load	*Renal diseases*	*Gastrointestinal Cl^- losses*	*Mineralocorticoid excess*
Ketoacidosis	Proximal renal tubular acidosis	Vomiting	Primary aldosteronism
Diabetes	Classic distal tubular acidosis	Nasogastric suction	Cushing syndrome
Alcoholism	Hyperkalemic distal tubular acidosis	Villous adenoma of the colon	Adrenocorticotropic hormone (ACTH)-secreting tumor
Starvation	Interstitial nephritis	*Renal Cl^- losses*	Renovascular disease
Uremia	Urinary tract obstruction	Loop diuretics	Accelerated hypertension
Lactic acidosis	Early renal failure	Furosemide	Renin-secreting tumors
Exogenous toxins	*GI bicarbonate loss*	Bumetanide	*Drugs*
With osmolar gap:	Diarrhea	Ethacrynic acid	Fludrocortisone
Methanol	Small bowel losses	Organomercurials	Corticosterone
Ethylene glycol	Anion exchange resins	Early distal diuretics	Prednisone
Without osmolar gap:	*Drugs*	Thiazides	Prednisolone
Salicylates	Acetaxolamide	Metolazone	Cortisone hydrocortisone
Paraldehyde	Mafenide	Methylprednisolone	Licorice
	Amphotericin B	Indapamide	*Miscellaneous*
	Amiloride	Post-hypercapnic state	Severe K^+ depletion
	Spironolactone	Poorly reabsorbed anions	
	Toluene ingestion	*Alkali administration*	
	Acid infusion	$NaHCO_3^-$	
	HCl	Organic anions: citrate, lactate, acetate	
	Arginine HCl		
	Lysine HCl		

Source: Modified from: Adrogue HJ, Madias NE. Arterial blood gas monitoring: acid–base assessment. In: Martin J, Tobin M (eds.) *Principles and Practice of Intensive Care Monitoring*. New York: McGraw-Hill, 1998; 217–41.

starvation), and the acidosis is incited by elevated ketones, particularly β-hydroxybutyrate. Mild lactic acidosis and low insulin levels may be present, and electrolyte abnormalities are common. Patients with alcoholic ketoacidosis can also present with a metabolic alkalosis from vomiting or respiratory alkalosis from liver disease [56], and may have hypoalbuminemia from liver disease that may further confound the acid–base evaluation.

High AG acidosis from ingested toxins

Salicylates

Salicylate overdose in adults usually results in respiratory alkalosis (panting), a mixed metabolic acidosis–respiratory alkalosis or, less commonly, a pure high AG metabolic acidosis [57,58]. In the latter case, only part of the acidosis is due to salicylates; most is due to increased lactic acid production.

Alcohols

The two main alcohols that are causes of a high AG metabolic acidosis are ethylene glycol and methanol, both of which can induce respiratory depression and coma. If such intoxication is suspected by history, the osmolar gap can be used to identify the presence of extraneous osmolytes.

Osmolar gap

Plasma osmolality is normally determined by sodium, urea, and glucose, and is calculated by:

$$P_{osm} = 2Na + \frac{Glu}{18} + \frac{BUN}{2.8}$$

[Glu and BUN in mg/dL]

The measured and calculated osmolality should agree within 10–15 mmol/kg H_2O.

Decreased kidney function as a factor of high AG metabolic acidosis

Uremic acidosis is a disorder of advanced renal failure; moderate renal insufficiency leads to normal (hyperchloremic) metabolic acidosis. As renal disease progresses, diseased nephrons have a diminished capacity for filtration and reabsorption of organic anions. As the net number of nephrons decreases, organic acids build up. Uremic acidosis is therefore characterized by a reduced rate of NH_4 production and excretion [59,60]; the excess acid (up to 20 mmol/day) is buffered by alkaline salts from bone [61]. As a result of the calcium carbonate buffering, the HCO_3^- rarely falls below 15 mmol/L, and the AG rarely rises above 20 mmol/L.

Non-AG (hyperchloremic) metabolic acidosis

Non-AG (normal or hyperchloremic) metabolic acidosis results from a loss of base (HCO_3^-), as opposed to the addition of acid, as in the case of high AG metabolic acidosis. A non-AG metabolic acidosis occurs primarily through disturbances of the HCO_3^-, either through a primary loss of bicarbonate or failure to replace bicarbonate stores. Excess HCl is another mechanism that produces this condition. A loss of alkali in the system causes reciprocal changes in the HCO_3^- and Cl^- that result in a normal, non-elevated AG. The increased level of chloride (hyperchloremia) that results will approximate the value of the decrease in bicarbonate; the SID theory helps to explain this relationship and the effectiveness of treating hyperchloremic acidosis with sodium bicarbonate [17]. If this relationship is absent, a mixed disorder must be considered.

There are four main groups that cause non-AG metabolic acidosis: (1) gastrointestinal, (2) renal diseases, (3) drugs, and (4) acid infusions.

Gastrointestinal

The primary GI factor of non-AG metabolic acidosis is diarrhea. Diarrheal stools contain a higher level of HCO_3^- than normal stools, and are relatively chloride-poor; along with volume depletion, a metabolic acidosis develops [62]. The urine pH, however, is not acidic as expected with a systemic acidosis. The urine pH will be approximately 6 because the hypokalemia that develops with the metabolic acidosis as a result of intestinal losses increases the renal production and excretion of NH_4 that buffers the normally acidic urine.

Renal disease

Progressive renal disease leads to non-AG metabolic acidosis when the glomerular filtration rate (GFR) is 20–50 mL/min and continues to AG metabolic acidosis (uremic acidosis) as the GFR falls below 20 mL/min. The renal tubular acidoses are a common cause of the non-AG metabolic acidosis.

Drugs

Several drug types can incite a non-AG metabolic acidosis in patients with renal dysfunction: non-steroidal anti-inflammatory drugs (NSAIDs), trimethoprim, pentamidine, and angiotensin-converting enzyme (ACE) inhibitors. A hyperkalemic state will also be present.

Acid infusion

Acid infusions, especially HCl, are occasionally given as treatment for patients with metabolic alkalosis [63,64], particularly when prompt correction of the disturbance is imperative. Other agents that may be used are NH_4Cl and arginine monohydrochloride.

Parenteral nutrition with excess of cationic amino acids (usually the L-amino acid preparations) can lead to a metabolic acidosis [65]. The newer formulas that use protein solutions, rather than the older protein hydrosylate formulations, are thought to be more beneficial [15]. To minimize the possibility of metabolic acidosis, total parenteral nutrition solutions should be buffered with acetate or other organic anions.

Metabolic alkalosis

Metabolic alkalosis is characterized by an elevated blood pH, an increase in HCO_3^-, and later, an augmentation of the $PaCO_2$ secondary to hypoventilation. Metabolic alkalosis is commonly caused by a loss of non-volatile acid from the extracellular fluid (usually HCl via vomiting); it is usually accompanied by hypochloremia and hypokalemia. It can also be induced by hypermineralocorticoid states and severe potassium deficiency [66,67] (Table 30.3).

The development of a metabolic alkalosis involves two stages. In the first stage, a loss of acid invokes the alkalosis. In the second stage, the alkalosis can continue

if the kidneys are unable to compensate by excreting the excess HCO_3^- due to volume contraction, a low GFR, or hypochloremia or hypokalemia [10,68].

The above tetrad increases distal tubule H^+ secretion, and can be treated with NaCl or KCl. However, if the hypokalemia is due to autonomous hypoaldosteronism, the alkalosis must be repaired surgically or pharmacologically [69].

The secondary compensation response to metabolic alkalosis is hypoventilation that serves to retain CO_2 (hypercapnia) and decrease the pH back to baseline [39].

Alkali administration

An increased alkali load in a patient with normal kidney function will not typically cause a metabolic alkalosis. Bicarbonate given in the operating room will generally increase the end-tidal CO_2 to balance the infusion. If there are hemodynamic disturbances, however, alkali excretion may be slowed. Patients administered oral or parenteral citrate loads (transfusions), parenteral hyperalimentation, or exchange resins (polystyrene sulfonate and aluminium hydroxide) should be closely monitored.

Diagnosis

Capnographic findings, in the presence of normal cardiac output and perfusion, will show an increased CO_2 in non-mechanically ventilated patients and increased $PaCO_2$. It is useful to assess the patient's extracellular fluid volume and blood pressure to establish the cause for the metabolic alkalosis; urine electrolytes should also be checked. Additionally, it may be useful to categorize the metabolic alkaloses into those that are chloride-sensitive (responsive to NaCl) and those that are chloride-resistant (not responsive to NaCl) (Table 30.3).

Chloride-sensitive alkalosis

In this type of metabolic alkalosis, chloride depletion is the key factor in the pathogenesis. Urine chloride excretion is decreased with a urine chloride concentration of <10 mEq/L (normal is 10–20 mEq/L); disorders that are chloride-sensitive are typically characterized by a low fluid volume. The paucity of chloride incites a reabsorption of sodium that results in excretion of hydrogen ions and increased production of bicarbonate, which worsens the alkalosis. By treating this disorder with NaCl, the alkalotic cycle can be broken because bicarbonate excretion will be increased.

Gastrointestinal disorders

The chloride-sensitive alkaloses include several GI disorders (vomiting, gastric drainage, villous adenoma of the colon, and chloride-rich diarrhea). Basically, as hydrogen ions are lost through inappropriate GI motility, bicarbonate is retained. The loss of fluid and NaCl in vomitus or by nasogastric suction will cause volume contraction that will invoke the renin/aldosterone system. The GFR will be reduced, and HCO_3^- will be reabsorbed. Chloride is depleted in this process when the HCO_3^- is continually added to plasma in exchange for chloride; this action incites the kidney to conserve chloride. These disorders should be treated by administering fluids for volume expansion, and NaCl, and any potassium depletions should be replenished.

Drugs

Certain diuretics, specifically the thiazides and loops, can produce a chloride-sensitive alkalosis; ethacrynic acid in particular causes a contraction alkalosis. These two classes induce a chloruresis while causing an acute reduction in extracellular fluid volume. Chronic use of these drugs will cause a metabolic alkalosis by increasing distal tubule salt recovery, thereby forcing an increased secretion of hydrogen ions and potassium [10]. Secondary hypoaldosteronism also results. Isotonic saline will correct the deficit.

Other causes

Chloride-sensitive alkalosis has several other inciting factors. Magnesium deficiency results in hypokalemic alkalosis by renal distal tubule acidification with increased action of the renin/aldosterone system. Hypokalemia causes alkalosis by increasing potassium reabsorption at the expense of hydrogen ions – give potassium to correct. After lactic or ketoacidosis presents, the acids that caused the original acidosis are metabolized to bicarbonate. Subsequent to a hypercapnic episode, a surplus of HCO_3^- exists in much the same manner as with other postacidotic episodes. Correct chloride excess, and the alkalosis should subside. Cystic fibrosis, milk-alkali syndrome [70], and excessive loss of NaCl in skin tissues can produce a metabolic alkalosis.

Chloride-resistant alkalosis

A normal level of chloride excretion characterizes this type of metabolic alkalosis; urine chloride concentration is >20 mEq/L. This type of alkalosis includes several mineralocorticoid disorders

(hyperaldosteronism, Cushing syndrome, licorice intake, Bartter syndrome) and profound hyperkalemia. The increased aldosterone will increase acid excretion, leading to alkalosis, particularly with hypokalemia. Excess salts expand extracellular fluid volume, and produce hypertension. The effects of aldosterone resulting in polydipsia, polyuria, and hypo-osmolar urine will continue to increase potassium excretion.

Useful hints

A patient with a high HCO_3^- and a low chloride has either a metabolic alkalosis or chronic respiratory acidosis. Remember that the pH will establish the difference between these two options: high pH with metabolic alkalosis and low pH with the chronic respiratory acidosis.

A patient with alkalosis and chronic hypokalemia suggests mineralocorticoid excess or diuretic use in a hypertensive patient. Low plasma renin activity and normal chloride in a patient who is not taking diuretic medication indicates a primary mineralocorticoid disturbance. Alkalosis and hypokalemia in a normotensive, non-edematous patient suggests Bartter syndrome, Gitelman syndrome, magnesium deficiency, or vomiting. Urine electrolytes should be determined. Alkaline urine with increased sodium suggests vomiting or alkali ingestion. Acidic urine with low sodium, potassium, and chloride can suggest vomiting, a post-hypercapnic state, or prior diuretic ingestion. If urine sodium, potassium, or chloride is not decreased, magnesium level, Bartter or Gitelman syndrome, or current diuretic ingestion should be considered [10].

Respiratory acidosis

Respiratory acidosis is an acid–base disorder in which the primary disturbance is invoked by an increase in the blood CO_2 tension. It is diagnosed by an increase in the $PaCO_2$ and a decrease in blood pH. The secondary compensation response is an increase in HCO_3^-. Acutely, the small increase in HCO_3^- is due to the body's non-HCO_3^- buffers, which promote movement of bicarbonate to the interstitial fluid from the intravascular compartment. This will cause a small decrease in the standard bicarbonate and a somewhat larger decrease in the blood BE. Chronically, renal adaptations lead to much larger increases in HCO_3^-, with a parallel increase in standard bicarbonate and blood BE. Renal acidification processes responding to hypercapnia require 3–5 days to perform maximally [1]. Additionally, hypochloremia is a common finding with respiratory acidosis due to the chloride shift into the RBCs, as well as renal losses from the secondary response.

Using the compensation equations, it can be determined that in the case of an acute respiratory acidosis, the HCO_3^- will increase 1 mmol/L for every 10 mm Hg increase in the $PaCO_2$. With a chronic (24-h duration) respiratory acidosis, renal compensation increases the HCO_3^- at 4 mmol/L for every 10 mm Hg increase in $PaCO_2$. Serum HCO_3^- typically will not increase above 38 mmol/L.

Diagnosis

To diagnose a respiratory acidosis, ABG and electrolyte analyses are performed. History and physical examination should suggest the inciting factor. Nonpulmonary parameters to be assessed include a detailed drug history, hematocrit, upper airway assessment, chest wall rigidity/trauma, and neuromuscular function. Capnographic findings should demonstrate a high end-tidal CO_2 and the ABG will show a high $PaCO_2$.

Clinically respiratory acidosis manifests with symptoms that vary according to the severity and duration of the acidosis, the underlying disease, and whether there is an accompanying hypoxemia. Acute increases in $PaCO_2$ can induce anxiety, dyspnea, confusion, psychosis, hallucinations, and coma (Table 30.4). Chronic increases in $PaCO_2$ cause sleep disturbances, memory loss, daytime somnolence, personality changes, coordination impairment, and motor dysfunctions such as tremor, myoclonic jerks, and asterixis (Table 30.4). Increased $PaCO_2$ may mimic the signs and symptoms of increased intracranial pressure with headaches, papilledema, abnormal reflexes, focal muscle weakness; each of these symptoms is due to vasoconstriction secondary to loss of the vasodilatory effects of CO_2 [10].

Causes

There are several inciting factors of primary respiratory acidosis: (1) central, (2) airway, (3) parenchyma, (4) neuromuscular, and (5) miscellaneous (see Table 30.4).

Central factors

Central causes of respiratory acidosis include drugs, such as anesthetics, alcohol, narcotics, and sedatives. The main mechanism is through the depression of the neural respiratory center (medullary chemoreceptors)

Table 30.4 Causes of acute and chronic respiratory acidosis

	Acute	Chronic
(a) Normal airways and lungs	***CNS depression***	
	General anesthesia Sedative overdose Head trauma Cerebrovascular accident Central sleep apnea Cerebral edema Brain tumor Encephalitis	Sedative overdose Narcotic addiction Primary alveolar hypoventilation Obesity–hypoventilation syndrome (Pickwickian) Brain tumor Bulbar poliomyelitis
	Neuromuscular impairment	
	High spinal cord injury Guillain–Barre syndrome Status epilepticus Botulism Myasthenic crisis Hypokalemic myopathy Familial periodic paralysis Drugs/toxins (paralytics, organophosphates, aminoglycosides)	Poliomyelitis Multiple sclerosis Muscular dystrophy Amyotrophic lateral sclerosis Diaphragmatic paralysis Myxedema Myopathic disease (polymyositis)
	Ventilatory restriction	
	Rib fractures with flail chest Pneumothorax Hemothorax Impaired diaphragmatic function (e.g., ascites)	Kyphoscoliosis Obesity Fibrothorax Hydrothorax
	Iatrogenic events	
	Misplaced/displaced airway Inappropriate mechanical ventilation	-
(b) Abnormal airways and lungs	***Upper airway obstruction***	
	Coma Aspiration/foreign body Laryngospasm Angioedema Obstructive sleep apnea Inadequate intubation	Tonsillar and peritonsillar hypertrophy Paralysis of vocal cords Tumor of the vocal cords or pharynx Airways stenosis after intubation Thymoma, aortic aneurysm
	Lower airways obstruction	
	Bronchospasm Severe asthma Bronchiolitis	COPD (bronchitis, bronchiolitis, emphysema, bronchiectasis)
	Disorders involving alveoli	
	Severe pneumonia or ARDS Severe pulmonary edema	Severe chronic pneumonitis Diffuse infiltrative disease (alveolar proteinosis) Interstitial fibrosis
	Pulmonary perfusion defect	
	Cardiac arrest	-

COPD, chronic obstructive pulmonary disease; ARDS, acute respiratory distress syndrome.
Source: Modified from: Adrogue HJ, Madias NE. Arterial blood gas monitoring: acid–base assessment. In: Martin J, Tobin M (eds.) *Principles and Practice of Intensive Care Monitoring*. New York: McGraw-Hill, 1998; 217–41.

which leads to shallow breathing and CO_2 trapping. Strokes and infections such as encephalitis can also lead to respiratory acidosis through this mechanism.

Airway factors

Several types of airway disturbances can lead to respiratory acidosis. Acute obstruction by foreign body or secretions (pulmonary edema) and asthma can compromise normal breathing and lead to a respiratory acidosis; status asthmaticus may cause metabolic acidosis or respiratory alkalosis. Generalized bronchospasm due to anaphylaxis, inhalational burn, or toxin ingestion will also lead to respiratory acidosis.

Parenchymal factors

Emphysema, pneumoconiosis, and bronchitis will cause a chronic respiratory acidosis as a result of air trapping. Restrictive disorders will lead to a respiratory acidosis because of the high metabolic cost of breathing against stiff lungs and/or chest wall.

Neuromuscular factors

Abnormalities or disease in the motor neurons, neuromuscular junction, and skeletal muscle can incite hypoventilation via respiratory muscle fatigue. Mechanical ventilation may cause respiratory acidosis if it is incorrectly supervised/monitored, if sudden CO_2 production arises (because of fever, agitation, sepsis, or overfeeding), or if pulmonary function suddenly worsens and alveolar ventilation declines.

Miscellaneous factors

High levels of positive end-expiratory pressure in the presence of reduced cardiac output can cause hypercapnia as a result of increases in alveolar deadspace. Permissive hypercapnia is being used with increasing frequency because of studies suggesting lower conventional mechanical ventilation, especially with severe CNS or heart disease.

Respiratory alkalosis

Respiratory alkalosis is an acid–base disorder marked by an elevated pH and a decreased $PaCO_2$. It evolves from hyperventilation, which lowers the $PaCO_2$ and increases the ratio of HCO_3^- to $PaCO_2$, thereby increasing the pH; the hydrogen ion concentration falls because of the reduction of H_2CO_3 in the body [6,28,71]. Acutely, non-bicarbonate cellular buffers, through non-renal mechanisms, respond by consuming HCO_3^- [72–75], a process that takes 5–10 min.

Hypocapnia sustained longer than 2–6 h is further compensated by a decrease in renal ammonium, titratable acid excretion, and a reduction in filtered HCO_3^- reabsorption. Renal adaptation to respiratory alkalosis takes several days (2–3) with normal volume status and normal kidney function. The reduction in bicarbonate with chronic respiratory alkalosis is accompanied by a parallel decrease in the standard bicarbonate and in blood BE; these changes are not observed in acute respiratory alkalosis [1].

In chronic respiratory alkalosis, each 1 mm Hg decrease in $PaCO_2$ causes a 0.4–0.5 mmol/L decrease in the HCO_3^- and a 0.3 mmol/L decrease in the hydrogen ion concentration (0.003 rise in the pH). Additionally, plasma chloride will be increased in chronic respiratory alkalosis to offset the decrease in HCO_3^- [1].

Signs and symptoms

Symptoms of respiratory alkalosis relate primarily to the underlying disease. Typically, with a rapid decrease in the $PaCO_2$, decreased cerebral blood flow can result in dizziness, confusion, and seizures, even without hypoxemia. The cardiovascular effects of respiratory alkalosis in a conscious patient are minimal. In the anesthetized or mechanically ventilated patient, however, cardiac output and blood pressure may fall as a result of the effects of anesthesia and PEEP on heart rate, systemic resistance, and venous return. Arrhythmias may occur in patients with heart disease as a result of changes in oxygen unloading by blood from a left shift in the hemoglobin–oxygen dissociation curve (Bohr effect). Acute respiratory alkalosis causes intracellular shifts of sodium, potassium, and phosphate, and reduces free calcium ion 21 concentration by increasing the protein-bound fraction. Hypocapnia-induced hypokalemia is minor [10]. Capnographic findings will show a reduced end-tidal CO_2 and a reduced $PaCO_2$ (Table 30.5).

Inciting factors

Respiratory alkalosis is the most common acid–base disturbance in critically ill patients. If the alkalosis is severe, prognosis tends to be poor. Respiratory alkalosis is common in mechanically ventilated patients, as well as being a frequent finding in early to moderate heart failure and in the early stages of respiratory failure. Common causes of respiratory alkalosis include mechanical hyperventilation, CNS stimulation, hypoxemia, drugs/hormones, stimulation of chest receptors, and miscellaneous origins (Table 30.6).

Table 30.5 Comparison of acute and chronic respiratory acidosis and alkalosis (mean values)

	Respiratory alkalosis			Respiratory acidosis	
	Acute	Chronic	Normal	Acute	Chronic
$PaCO_2$ (mm Hg)	20	20	40	60	60
pH	7.62	7.52	7.40	7.26	7.30
$[HCO_3^-]$ (mEq/L)	20	16	24	26	29
$[H^+]$ (neq/L)	24	30	40	55	50
$[Na^+]$ (mEq/L)	138	140	140	141	140
$[Cl^-]$ (mEq/L)	104	111	104	104	99
AG (mEq/L)	14	14	12	11	12

Source: Modified from: Adrogue HJ, Madias NE. Arterial blood gas monitoring: acid–base assessment. In: Martin J, Tobin M (eds.) *Principles and Practice of Intensive Care Monitoring*. New York: McGraw-Hill, 1998; 217–41.

Table 30.6 Causes of respiratory alkalosis

Hypoxemia or tissue hypoxia	Stimulation of chest receptors	CNS stimulation	Drugs or hormones	Miscellaneous
Decreased FiO_2	Pneumonia	Voluntary	Doxapram	Sepsis
High altitude	Asthma	Pain/anxiety/ psychosis	Xanthines	Liver failure
Pneumonia	Pneumothorax	Fever	Salicylates	Mechanical hyperventilation
Aspiration/foreign body	Hemothorax	Subarachnoid hemorrhage	Catecholamines	Pregnancy
Laryngospasm	Flail chest	Cerebrovascular accident	Angiotensin II	
Drowning	Acute respiratory distress syndrome	Encephalitis	Vasopressors	
Cyanotic heart disease	Non-cardiogenic pulmonary edema	Tumor	Progesterone	
Severe anemia	Pulmonary embolism	Trauma	Medroxyproges-terone	
Left shift of HbO_2 curve	Pulmonary fibrosis		Dinitrophenol	
Hypotension			Nicotine	
Severe circulatory failure				
Congestive heart failure				

Source: Modified from: Adrogue HJ, Madias NE. Arterial blood gas monitoring: acid–base assessment. In: Martin J, Tobin M (eds.) *Principles and Practice of Intensive Care Monitoring*. New York: McGraw-Hill, 1998; 217–41.

Hyperventilation syndrome

Hyperventilation syndrome occurs as a result of many underlying causes, including episodes of acute anxiety. It includes many neurologic symptoms: paresthesias, circumoral numbness, chest wall tightness or pain, dizziness, inability to take adequate breaths, and tetany. These symptoms themselves may be sufficiently stressful to perpetuate the disorder. ABG analysis demonstrates an acute or chronic respiratory alkalosis, with $PaCO_2$ in the range of 15–30 mm Hg and no hypoxemia.

Central nervous system stimulation

Hyperventilation can be invoked by such stimuli as pain, fear, anxiety, or psychosis, and can lead to respiratory alkalosis if the stimulus is prolonged. Cerebrovascular insult or infection, tumor, or trauma can initiate similar responses. Different patterns of hyperventilation may be produced with $PaCO_2$ at 20–30 mm Hg.

Hypoxemia or tissue hypoxia

Hypoxic states can arise from a variety of conditions induced by high altitudes [76]. Lifelong residents of high altitudes have almost complete pH compensation [75]. Pneumonia, anemia, and asthma are also causes of respiratory alkalosis.

Drugs or hormones

Salicylates are the most common factors of drug-induced respiratory alkalosis [58] because they

directly stimulate the medullary chemoreceptors. Methylxanthines, theophylline, and aminophylline stimulate ventilation and increase the ventilatory response to CO_2. Increased progesterone levels in pregnancy lead to a respiratory alkalosis through the hormonal induction of increased ventilation (arterial $PaCO_2$ is lowered by as much as 5–10 mm Hg).

Stimulation of chest receptors

Hemothorax, flail chest, cardiac failure, and pulmonary embolism can incite a respiratory alkalosis.

Miscellaneous

Respiratory alkalosis is a common finding of hepatic failure, with the severity of failure correlating with the severity of the alkalosis. It is also an early finding in Gram-negative septicemia (prior to the development of fever, hypoxemia, or hypotension)[77], and in the pure form associated with a good prognosis [78].

References

1. Adrogue HJ, Madias NE. Arterial blood gas monitoring: acid–base assessment. In: Martin J, Tobin M (eds.) *Principles and Practice of Intensive Care Monitoring*. New York: McGraw-Hill, 1998; 217–41.
2. Gravenstein JS, Paulus DA, Hayes TJ (eds.) *Capnography in Clinical Practice*. Boston, MA: Butterworth, 1989.
3. Madias NE, Adrogue HJ, Cohen JJ, Schwartz WB. Effect of natural variations in $PaCO_2$ on plasma [HCO_3^-] in dogs: a redefinition of normal. *Am J Physiol* 1979; **236**: F30–5.
4. Madias NE, Adrogue HJ, Horowitz GL, Cohen JJ, Schwartz WB. A redefinition of normal acid–base equilibrium in man: carbon dioxide tension as a key determinant of normal plasma bicarbonate concentration. *Kidney Int* 1979; **16**: 612–18.
5. Madias NE, Ayus JC, Adrogue HJ. Increased anion gap in metabolic alkalosis: the role of plasma-protein equivalency. *N Engl J Med* 1979; **300**: 1421–3.
6. Gennari F, Kassirer JP. Respiratory alkalosis. In: Cohen JJ (ed.) *Acid–Base*. Boston, MA: Little, Brown, 1982; 349–76.
7. Schwartz W, Hall PW, Hays RM, Relman AS. On the mechanism of acidosis in chronic renal disease. *J Clin Invest* 1959; **38**: 39–52.
8. Goodman D, Lemann J, Lennon EJ, Relman AS. Production, excretion, and net balance of fixed acid in patients with renal acidosis. *J Clin Invest* 1965; **44**: 495–506.
9. Wall SM, Knepper MA. Acid–base transport in the inner medullary collecting duct. *Semin Nephrol* 1990; **10**: 148–58.
10. DuBose TD Jr. *Acidosis and Alkalosis*. New York: McGraw-Hill, 2003.
11. Schwartz WB, Relman AS. A critique of the parameters used in the evaluation of acid–base disorders. *N Engl J Med* 1963; **268**: 1382–8.
12. Stewart P. *How to Understand Acid–Base.* New York: Elsevier North Holland, 1981.
13. Kellum JA. Lactate and pHi: our continued search for markers of tissue distress. *Crit Care Med* 1998; **26**: 1783–4.
14. Figge J, Mydosh T, Fencl V. Serum proteins and acid–base equilibria: a follow-up. *J Lab Clin Med* 1992; **120**: 713–19.
15. Gauthier PM, Szerlip HM. Metabolic acidosis in the intensive care unit. *Crit Care Clin* 2002; **18**: 289–308, vi.
16. Waters JH, Miller LR, Clack S, Kim JV. Cause of metabolic acidosis in prolonged surgery. *Crit Care Med* 1999; **27**: 2142–6.
17. Constable PD. Hyperchloremic acidosis: the classic example of strong ion acidosis. *Anesth Analg* 2003; **96**: 919–22.
18. Balasubramanyan N, Havens PL, Hoffman GM. Unmeasured anions identified by the Fencl–Stewart method predict mortality better than base excess, anion gap, and lactate in patients in the pediatric intensive care unit. *Crit Care Med* 1999; **27**: 1577–81.
19. Weil MH, Rackow EC, Trevino R, *et al.* Difference in acid–base state between venous and arterial blood during cardiopulmonary resuscitation. *N Engl J Med* 1986; **315**: 153–6.
20. Benjamin E, Paluch TA, Berger SR, *et al.* Venous hypercarbia in canine hemorrhagic shock. *Crit Care Med* 1987; **15**: 516–18.
21. Bakker J, Vincent JL, Gris P, *et al.* Veno-arterial carbon dioxide gradient in human septic shock. *Chest* 1992; **101**: 509–15.
22. Zhang H, Vincent JL. Arteriovenous differences in PCO_2 and pH are good indicators of critical hypoperfusion. *Am Rev Respir Dis* 1993; **148**: 867–71.
23. Oropello JM, Manasia A, Hannon E, Leibowitz A, Benjamin E. Continuous fiberoptic arterial and venous blood gas monitoring in hemorrhagic shock. *Chest* 1996; **109**: 1049–55.
24. Harrison AM, Lynch JM, Dean JM, Witte MK. Comparison of simultaneously obtained arterial and capillary blood gases in pediatric intensive care unit patients. *Crit Care Med* 1997; **25**: 1904–8.
25. Thorp JA, Rushing RS. Umbilical cord blood gas analysis. *Obstet Gynecol Clin N Am* 1999; **26**: 695–709.

26. Harrington J, Cohen JJ, Kassirer JP. Mixed acid–base disturbances. In: Cohen JJ (ed.) *Acid–Base*. Boston, MA: Little, Brown, 1982; 377–90.
27. Valtin HGF. Approach to the patient: useful tools. In: Valtin HGF (ed.) *Acid–Base Disorders*. Boston, MA: Little, Brown, 1987; 61–86.
28. Valtin HGF. Respiratory alkalosis: clinical examples. In: Valtin HGF (ed.) *Acid–Base Disorders*. Boston, MA: Little, Brown, 1987; 143–57.
29. Giebisch G, Berger L, Pitts RF. The extrarenal response to acute acid–base disturbances of respiratory origin. *J Clin Invest* 1955; **34**: 231–45.
30. Brackett N, Cohen JJ, Schwartz WB. Carbon dioxide titration curve of normal man. *N Engl J Med* 1965; **272**: 6–12.
31. Flenley DC. Another non-logarithmic acid–base diagram? *Lancet* 1971; **1**: 961–5.
32. Narins RG, Emmett M. Simple and mixed acid–base disorders: a practical approach. *Medicine (Baltimore)* 1980; **59**: 161–87.
33. Tyor M, Sieker HO. Biochemical, blood gas and peripheral circulatory alterations in hepatic coma. *Am J Med* 1959; **27**: 50–9.
34. Prytz H, Holst-Christensen J, Korner B, Liehr H. Portal venous and systemic endotoxaemia in patients without liver disease and systemic endotoxaemia in patients with cirrhosis. *Scand J Gastroenterol* 1976; **11**: 857–63.
35. Cohen JJ, Schwartz WB. Evaluation of acid–base equilibrium in pulmonary insufficiency: an approach to a diagnostic dilemma. *Am J Med* 1966; **41**: 163–7.
36. Aberman A, Fulop M. The metabolic and respiratory acidosis of acute pulmonary edema. *Ann Intern Med* 1972; **76**: 173–84.
37. Roncoroni AJ, Adrougue HJ, De Obrutsky CW, Marchisio ML, Herrera MR. Metabolic acidosis in status asthmaticus. *Respiration* 1976; **33**: 85–94.
38. Asch MJ, Dell RB, Williams GS, Cohen M, Winters RW. Time course for development of respiratory compensation in metabolic acidosis. *J Lab Clin Med* 1969; **73**: 610–15.
39. Bone JM, Cowie J, Lambie AT, Robson JS. The relationship between arterial pCO_2 and hydrogen ion concentration in chronic metabolic acidosis and alkalosis. *Clin Sci Mol Med* 1974; **46**: 113–23.
40. Fulop M. A guide for predicting arterial CO_2 tension in metabolic acidosis. *Am J Nephrol* 1997; **17**: 421–4.
41. Wildenthal K, Mierzwiak DS, Myers RW, Mitchell JH. Effects of acute lactic acidosis on left ventricular performance. *Am J Physiol* 1968; **214**: 1352–9.
42. Mehta PM, Kloner RA. Effects of acid base disturbance, septic shock, and calcium and phosphorous abnormalities on cardiovascular function. *Crit Care Clin* 1987; **3**: 747–58.
43. Carrier O, Cowsert M, Hancock J, Guyton AC. Effect of hydrogen ion on vascular resistance in isolated artery segments. *Am J Physiol* 1964; **207**: 168–72.
44. Powell FL Jr. Oxygen and carbon dioxide transport in the blood. In: Johnson L, Byrne JH, Downey JM, *et al.* (eds.) *Essential Medical Physiology*. New York: Raven Press, 1997; 289–98.
45. De Troyer A, Stolarczyk A, De Beyl DZ, Stryckmans P. Value of anion-gap determination in multiple myeloma. *N Engl J Med* 1977; **296**: 858–60.
46. Emmett M, Narins RG. Clinical use of the anion gap. *Medicine (Baltimore)* 1977; **56**: 38–54.
47. Oh MS, Uribarri J, Alveranga D, *et al*. Metabolic utilization and renal handling of D-lactate in men. *Metabolism* 1985; **34**: 621–5.
48. Adrogue HJ, Wilson H, Boyd AE III, Suki WN, Eknoyan G. Plasma acid–base patterns in diabetic ketoacidosis. *N Engl J Med* 1982; **307**: 1603–10.
49. Gabow PA. Disorders associated with an altered anion gap. *Kidney Int* 1985; **27**: 472–83.
50. Winter SD, Pearson JR, Gabow PA, Schultz AL, Lepoff RB. The fall of the serum anion gap. *Arch Intern Med* 1990; **150**: 311–13.
51. Kreisberg RA. Pathogenesis and management of lactic acidosis. *Ann Rev Med* 1984; **35**: 181–93.
52. Uribarri J, Oh MS, Carroll HJ. D-Lactic acidosis: a review of clinical presentation, biochemical features, and pathophysiologic mechanisms. *Medicine (Baltimore)* 1998; **77**: 73–82.
53. Atchley D, Loeb RF, Richards DW, Benedict EM, Driscoll ME. On diabetic acidosis: a detailed study of electrolyte balances following the withdrawal and reestablishment of insulin therapy. *J Clin Invest* 1933; **12**: 297–326.
54. Westphal SA. The occurrence of diabetic ketoacidosis in non-insulin-dependent diabetes and newly diagnosed diabetic adults. *Am J Med* 1996; **101**: 19–24.
55. Fearon DM, Steele DW. End-tidal carbon dioxide predicts the presence and severity of acidosis in children with diabetes. *Acad Emerg Med* 2002; **9**: 1373–8.
56. Wrenn KD, Slovis CM, Minion GE, Rutkowski R. The syndrome of alcoholic ketoacidosis. *Am J Med* 1991; **91**: 119–28.
57. Farber H, Yiengst MJ, Shock NW. The effect of therapeutic doses of aspirin on the acid–base balance of the blood in normal adults. *Am J Sci* 1949; **217**: 256–62.
58. Winters RW, White JS, Hughes MC, Ordway NK. Disturbances of acid–base equilibrium in salicylate intoxication. *Pediatrics* 1959; **23**: 260–85.

59. Litzow JR, Lemann J Jr., Lennon EJ. The effect of treatment of acidosis on calcium balance in patients with chronic azotemic renal disease. *J Clin Invest* 1967; **46**: 280–6.
60. Widmer B, Gerhardt RE, Harrington JT, Cohen JJ. Serum electrolyte and acid–base composition: the influence of graded degrees of chronic renal failure. *Arch Intern Med* 1979; **139**: 1099–102.
61. Pellegrino ED, Biltz RM. The composition of human bone in uremia: observations on the reservoir functions of bone and demonstration of a labile fraction of bone carbonate. *Medicine (Baltimore)* 1965; **44**: 397–418.
62. Watten R, Morgen FM, Songkhla YN, Vanikiati B, Phillips RA. Water and electrolyte studies in cholera. *J Clin Invest* 1959; **38**: 1879–89.
63. Wilson RF, Gibson D, Percinel AK, *et al.* Severe alkalosis in critically ill surgical patients. *Arch Surg* 1972; **105**: 197–203.
64. Harken AH, Gabel RA, Fencl V, Moore FD. Hydrochloric acid in the correction of metabolic alkalosis. *Arch Surg* 1975; **110**: 819–21.
65. Heird WC, Dell RB, Driscoll JM Jr., Grebin B, Winters RW. Metabolic acidosis resulting from intravenous alimentation mixtures containing synthetic amino acids. *N Engl J Med* 1972; **287**: 943–8.
66. Bleich HL, Tannen RL, Schwartz WB. The induction of metabolic alkalosis by correction of potassium deficiency. *J Clin Invest* 1966; **45**: 573–9.
67. Kassirer JP, London AM, Goldman DM, Schwartz WB. On the pathogenesis of metabolic alkalosis in hyperaldosteronism. *Am J Med* 1970; **49**: 306–15.
68. Madias NE, Adrogue HJ, Cohen JJ. Maladaptive renal response to secondary hypercapnia in chronic metabolic alkalosis. *Am J Physiol* 1980; **238**: F283–9.
69. Melby JC. Primary aldosteronism. *Kidney Int* 1984; **26**: 769–78.
70. McMillan DE, Freeman RB. The milk alkali syndrome: a study of the acute disorder with comments on the development of the chronic condition. *Medicine (Baltimore)* 1965; **44**: 485–501.
71. Adrogue HJ, Tobin MJ. Clinical picture of respiratory failure. In: Adrogue HJ, Tobin MJ (eds.) *Blackwell's Basics of Medicine*. Boston, MA: Blackwell Scientific, 1997; 213–308.
72. Kety S, Schmidt CF. The effects of active and passive hyperventilation on cerebral blood flow, cerebral oxygen consumption, cardiac output, and blood pressure of normal young men. *J Clin Invest* 1946; **25**: 107–19.
73. Kazemi H, Shannon DC, Carvallo-Gil E. Brain CO_2 buffering capacity in respiratory acidosis and alkalosis. *J Appl Physiol* 1967; **22**: 241–6.
74. Arbus GS, Herbert LA, Levesque PR, Etsten BE, Schwartz WB. Characterization and clinical application of the "significance band" for acute respiratory alkalosis. *N Engl J Med* 1969; **280**: 117–23.
75. Gledhill N, Beirne GJ, Dempsey JA. Renal response to short-term hypocapnia in man. *Kidney Int* 1975; **8**: 376–84.
76. Lenfant C, Sullivan K. Adaptation to high altitude. *N Engl J Med* 1971; **284**: 1298–309.
77. Simmons D, Nicoloff J, Guze LB. Hyperventilation and respiratory alkalosis as signs of Gram-negative bacteremia. *JAMA* 1960; **174**: 2196–9.
78. Blair E. Acid–base balance in bacteremic shock. *Arch Intern Med* 1971; **127**: 731–9.

Section 4
Chapter
31

Physiologic perspectives

Ventilation/perfusion abnormalities and capnography

N. Al Rawas, A.J. Layon, and A. Gabrielli

Introduction

The lung can be viewed as a simple oxygen (O_2) and carbon dioxide (CO_2) exchanger with both gas and blood flowing in and out (Figure 31.1). When there is equilibrium between these two components, gas exchange will be optimal, assuming that ventilation and perfusion are distributed in the same proportion.

Mismatching of ventilation and blood flow (perfusion) within the diseased lung is the most common cause of hypoxemia and hypercapnia, variations of which can result in both hypoxic and hypercapnic respiratory failure. Despite the great practical importance of this subject, many aspects still remain obscure. Indeed, only a few advances in understanding this concept have been made in the past century.

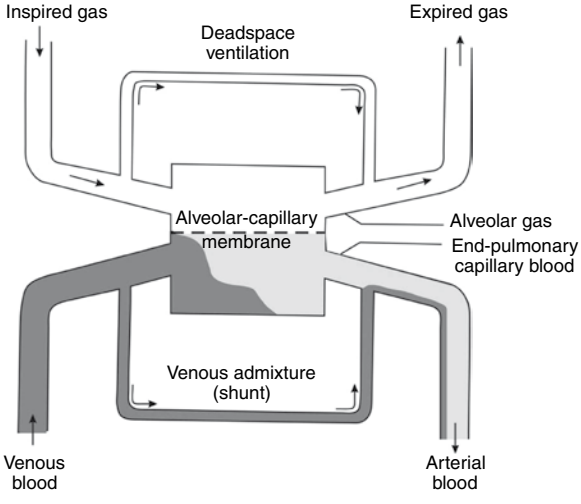

Figure 31.1 Functional representation of gas exchange in the lung. At equilibrium of alveolar gas and pulmonary capillary blood, the resulting end-expiratory gas is the result of venous admixture and deadspace ventilation. [From: Lumb AB. *Nunn's Applied Respiratory Physiology*, 5th edn. Boston, MA: Butterworth-Heinemann, 2000; 164.]

The first was the recognition that the gas exchange taking place in any lung unit is determined by the ratio of ventilation to blood flow. Haldane first recognized that this mechanism was a potential cause of hypoxemia, although he concluded that this mismatching of ventilation and blood flow would not cause CO_2 retention but only hypoxemia, a misconception that still surfaces from time to time [1]. In the mid-portion of the twentieth century, Riley and Cournard clarified the quantitative relationship among ventilation, blood flow, and gas exchange [2]. Not until the mid-1960s did the introduction of computers allow the elucidation of the O_2 and CO_2 dissociation curves.

Ventilation in relation to perfusion

In the last few years, there has been increased interest in considering that the properties of ventilation-perfusion ratio ($\dot{V}/\dot{Q}$) distributions are composed of three alveolar compartments, i.e., those that are: (1) ventilated underperfused; (2) perfused and underventilated; and (3) ideally matched. The breakthrough in understanding the $\dot{V}/\dot{Q}$ ratio occurred when computer methods were applied to analyze the process of distributions originally described by Riley and Cournard [2]. One way of approaching the $\dot{V}/\dot{Q}$ ratio is to examine it from the perspective of distribution of ventilation and blood flow. At rest, an individual of average size has about 4 L of ventilating alveolar volume to accommodate a cardiac output of approximately 5 L, resulting in an "ideal" $\dot{V}/\dot{Q}$ matching of 0.8. In reality, all possible ranges of $\dot{V}/\dot{Q}$ ratios exist within the lungs.

A person's posture and rate of alveolar filling both affect the distribution of inspired gas within the lung. For example, normal tidal breathing in the upright position results in a higher $\dot{V}/\dot{Q}$ ratio at the lung apices than the bases. This relationship changes in the supine position, as it results in preferential perfusion of the posterior portion of the lung as compared with the anterior portion.

Capnography, Second Edition, ed. J. S. Gravenstein, Michael B. Jaffe, Nikolaus Gravenstein, and David A. Paulus. Published by Cambridge University Press. © Cambridge University Press 2011.

The effect of gravity on ventilation seems to be of minor importance compared to its effect on perfusion.

The rate of inflation of the lungs is the result of inflation pressure, compliance, and airway resistance. This concept is summarized in terms of a time constant, defined as the product of the compliance and resistance, and can be interpreted as:

(1) The time required for inflation to 63% of the final volume attained if inflation is prolonged indefinitely.
(2) The time that would be required for inflation of the lungs if the initial gas flow rate were maintained throughout inflation.

If the time constants were equal in all alveoli, the build-up of pressure in the different units would be identical at all times during inflation and therefore:

(1) Distribution of inspired gas would be independent of the rate, duration, and frequency of inspiration.
(2) Compliance would not be affected by changes in frequency.
(3) There would be no redistribution of gas in the lungs.

This "ideal" condition is never encountered in critically ill patients on mechanical ventilation, where time constants vary significantly throughout the lung and are associated with sequential alveolar emptying during exhalation.

In this setting, the alveoli with a higher ventilation rate in relation to perfusion (high $\dot{V}/\dot{Q}$ alveoli) have a resultant lower CO_2 compared to alveoli with a low $\dot{V}/\dot{Q}$ ratio, which would, conversely, have a higher CO_2. The actual overall concentration of CO_2 in the alveoli is determined by the extent of $\dot{V}/\dot{Q}$ in the alveoli ($\dot{V}/\dot{Q}$ ratio) (Figure 31.2a).

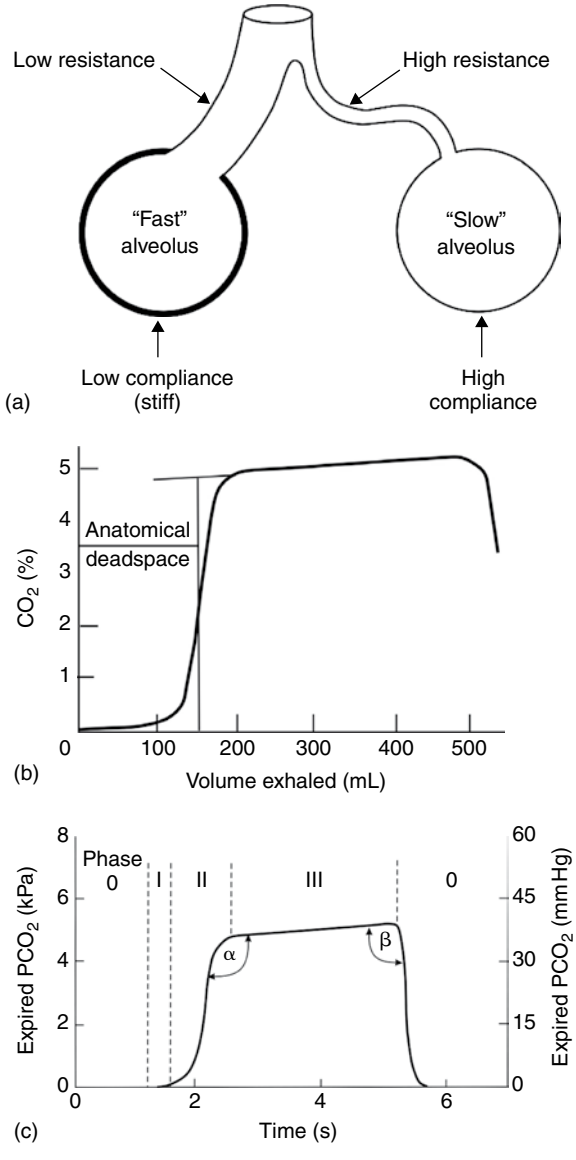

Figure 31.2 (a) Heterogeneous distribution of compliance and resistance resulting in sequential emptying of exhaled gas from different alveoli. (b) Volumetric capnography: CO_2 rise on exhalation is plotted against the volume exhaled. (c) Time capnography: exhalation and inhalation are plotted against time. α, alpha angle; β, beta angle.

Deadspace ventilation

Deadspace may be considered conceptually as areas of ventilation without perfusion. Anatomical deadspace, the volume of the conducting airways, is rarely changed by pathophysiology. Alveolar deadspace can be defined as the portion of the inspired volume that passes through the anatomical deadspace to mix with gas at the alveolar level, but does not take part in gas exchange. The physiologic deadspace is defined as the sum of these two respective components, anatomical and alveolar deadspaces, that represent all parts of the expired tidal volume (V_T) that do not participate in gas exchange. Bohr [3] first calculated the deadspace for a single breath using an equation including:

(1) expired tidal volume (V_T)
(2) mixed expired CO_2 concentration,
(3) alveolar CO_2 concentration, and
(4) physiologic deadspace (V_D).

Generally, the Enghoff-modified Bohr equation is used to calculate physiologic V_D/V_T:

$$\frac{V_D}{V_T} = \frac{PaCO_2 - P_{ET}CO_2}{PaCO_2}$$

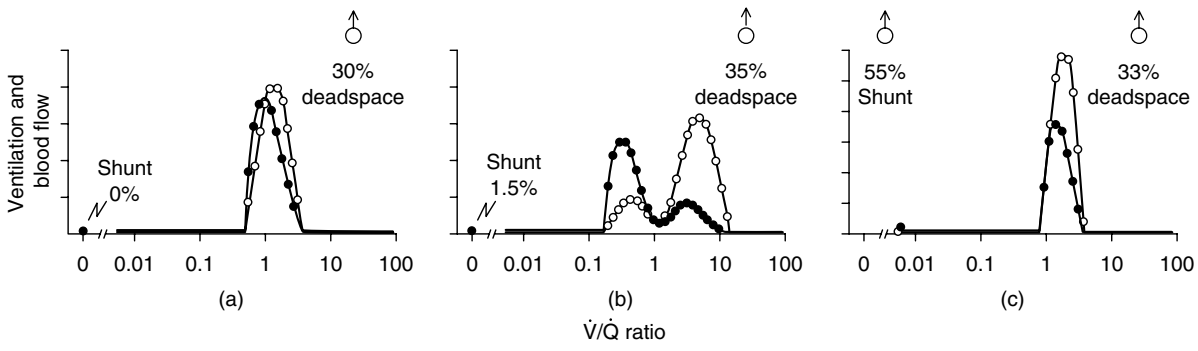

Figure 31.3 Distribution of V̇/Q̇ with the multiple gas elimination technique (MIGET). Open circles represent ventilation; closed circles represent blood flow. (a) Narrow distribution of V̇ and Q̇ in a healthy subject. Note that there is considerable blood flow going to the compartments with V̇/Q̇ ratio between 0.03 and 0.3. There is also an excess of ventilations in lung units with V̇/Q̇ ratio up to 6; however, all ventilation blood flow goes to the compartment closest to normal ventilation ratio, at about 1, and in particular, there is no blood flow to the unventilated compartment. (b) Bimodal distribution of V̇ and Q̇ in a patient with chronic obstructive pulmonary disease (COPD) and V_D/V_T of 35%. Considerable blood flow is going to the compartment with V̇/Q̇ ratio between 0.1 and 1, while relatively low perfusion is noticed above a V̇/Q̇ of 1. (c): Increased shunt in a patient with acute respiratory distress syndrome (ARDS). Late perfusion surge (approximately 0.9–1 V̇/Q̇ ratio) followed by exaggerated ventilations at above a 5 V̇/Q̇ ratio. [From: Roca J, Wagner PD. Contribution of multiple inert gas elimination technique to pulmonary medicine. I. Principles and information content of the multiple inert gas elimination technique. *Thorax* 1994; **49**: 815–24.]

where $PaCO_2$ is partial pressure of carbon dioxide in arterial blood, and $P_{ET}CO_2$ is partial pressure of carbon dioxide at end-tidal.

Several factors can affect the interpretation of this measurement, including:

(1) age
(2) posture
(3) size of individual
(4) position of neck and jaw
(5) lung volume at end inspiration
(6) tracheal intubation or tracheostomy
(7) V_T and respiratory rate
(8) drugs
(9) gender
(10) a variety of clinical conditions include: pulmonary embolism, hypotension, anesthesia, and artificial ventilation.

Volumetric capnography is a plot of CO_2 concentration and expired volume. It has been utilized as a method of real-time calculation of anatomical and physiological deadspace ventilation in patients with V̇/Q̇ mismatch (Figure 31.2b). Given that anatomical deadspace generally does not change over time, alterations of physiological deadspace measured in real time can be used to indicate changes in the alveolar deadspace component. While the information obtained from volumetric capnography can be theoretically useful to titrate ventilator parameters, its use is not yet widespread (see Chapter 18: Volumetric capnography for monitoring lung recruitment and PEEP titration) (Figure 31.3). Alveolar deadspace is a theoretical construct, and CO_2 elimination, as well as the shape of the CO_2 exhalation curve, depend greatly on V̇/Q̇ distribution, as do variables related to oxygenation [4].

Although very similar in shape to volume capnograms, time capnograms provide information in real time, which is useful for determining:

(1) expiratory and inspiratory CO_2
(2) respiratory rate
(3) slope of the exhalation curve
(4) a value for end-expiratory partial pressure of CO_2 ($P_{ET}CO_2$), which may be correlated with the arterial PCO_2 to reveal an arterial–end-expiratory CO_2 difference. This value is useful in the titration of positive end-expiratory pressure (PEEP) or continuous positive airway pressure (CPAP) (Figure 31.2c).

Perfusion in relation to ventilation

Shunt or venous admixture can be seen as the opposite of deadspace (Figure 31.4), and is defined as perfusion without ventilation. Shunt is, by far, the most important cause of hypoxemia in critically ill patients. This is a useful index of V̇/Q̇ inequality, and is related to an alteration in the ideal alveolar–PaO_2 difference caused by blood flow to lung units with an abnormally low V̇/Q̇ ratio. In healthy subjects, a 5% physiologic shunt is normally present, mostly due to emptying of the thebesian and bronchial veins directly into the central circulation. A certain degree of V̇/Q̇ scatter is also

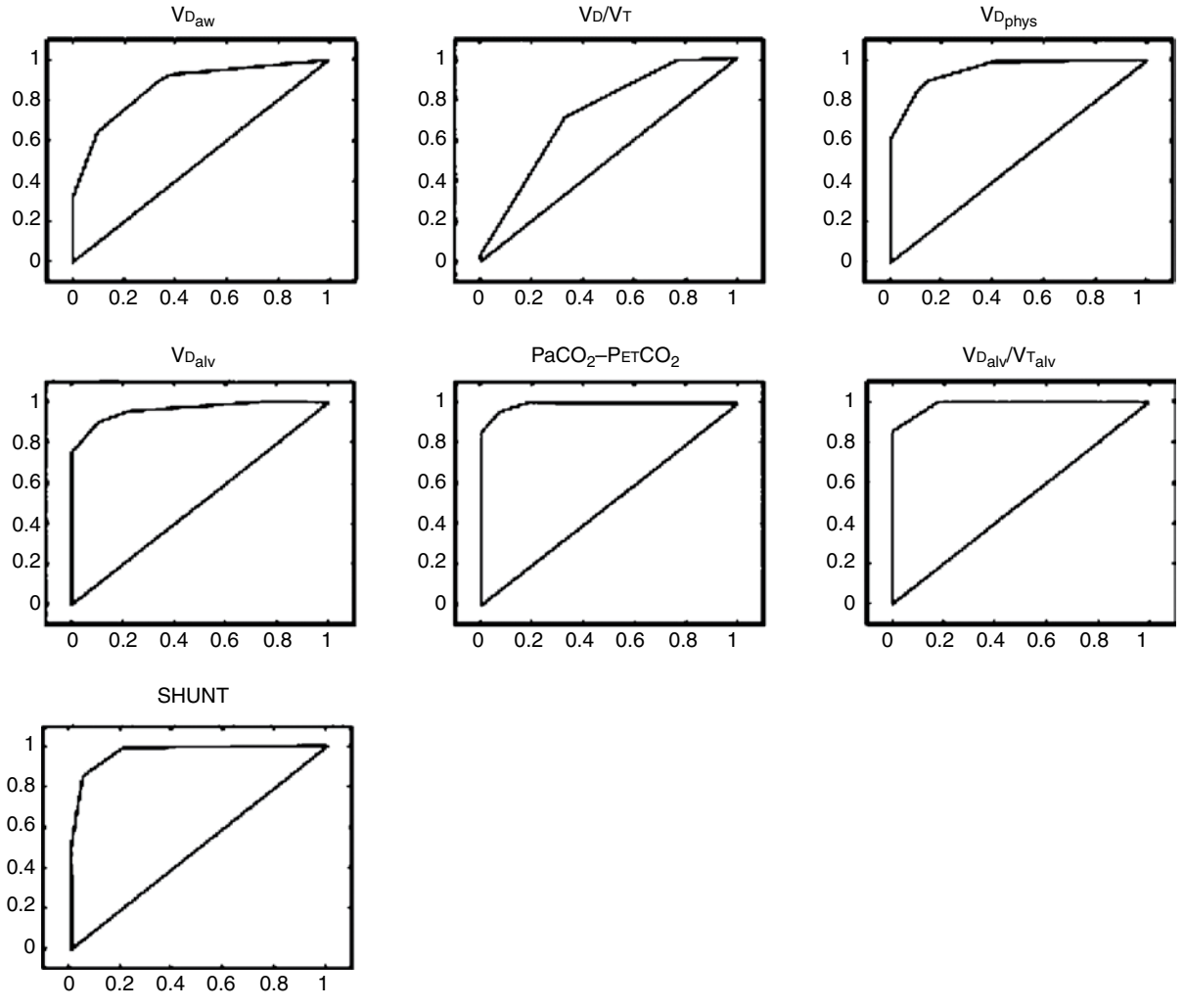

Figure 31.4 Analysis of the receiver operating characteristic curve (ROC) for deadspace variables and lung collapse as defined by the level of PEEP at which the percentage of non-aerated tissue exceeded 5% of the total CT slices. *P* value <0.05 for alveolar deadspace ($V_{D_{alv}}$), alveolar deadspace to alveolar tidal volume ratio ($V_{D_{alv}}/V_{T_{alv}}$), the arterial to end-tidal PCO_2 difference ($PaCO_2$–$P_{ET}CO_2$), and physiological deadspace ($V_{D_{phys}}$). $V_{D_{aw}}$ airway deadspace; V_D/V_T, ratio of physiological deadspace to tidal volume. [From: Tusman G, Suarez-Sipmann F, Böhm SH, *et al*. Monitoring deadspace during recruitment and PEEP titration in an experimental model. *Intens Care Med* 2006; **32**: 1863–71.]

present in healthy individuals. Because the pulmonary circulation operates at low pressure, it is rarely distributed evenly to all parts of the lungs, and the degree of disparity of perfusion is usually greater than that for ventilation.

While absolute distinctions between true shunt and $\dot{V}/\dot{Q}$ scatter are impossible due to the heterogeneous nature of pulmonary diseases, a few methods have been suggested to better define their pathophysiology. In the mid-1970s, the multiple inert gas elimination technique (MIGET) was established as the gold standard to provide qualitative and quantitative information on $\dot{V}/\dot{Q}$ mismatch and pulmonary gas exchange in patients with lung disease [5–7]. The MIGET uses a simultaneous venous infusion of six inert gases in trace concentrations, covering a broad spectrum of partition coefficients to characterize the distribution of the $\dot{V}/\dot{Q}$ within the entire lung.

In summary, mixed expired gas always represents a mixture of ideal alveolar gas, deadspace, and underventilated alveoli. As a result, arterial blood O_2 and CO_2 concentrations represent a mixture of blood with gas tensions of "ideal" alveolar gas and scattered $\dot{V}/\dot{Q}$ ratio blood (Figure 31.5).

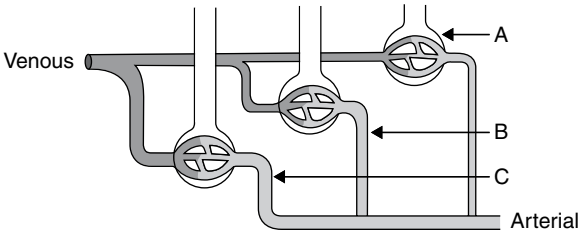

Figure 31.5 Arterial blood O_2 and CO_2 concentration is the average of "ideal" alveolar gas tension (B) and scatter of $\dot{V}/\dot{Q}$ ratios (A and C). (From: Lumb AB. *Nunn's Applied Respiratory Physiology*, 5th edn. Boston, MA: Butterworth-Heinemann, 2000; 187.]

Capnography in patients with $\dot{V}/\dot{Q}$ abnormalities

The use of capnography as a means to monitor "the presence" of exhaled breath has been a monitoring standard of care by the American Society of Anesthesiology for many years. Closed claim analysis studies conducted by anesthesiologists [8] and intraoperative events reviews [9,10] concluded that intraoperative measurement of $P_{ET}CO_2$ provides a warning of potentially catastrophic anesthetic mishaps. In a world of increasingly complex clinical monitoring, capnography has been only recently used as a tool to provide information on pulmonary perfusion, alveolar ventilation, and respiratory patterns. Therefore, its value as a monitor and diagnostic tool in patients with $\dot{V}/\dot{Q}$ mismatch is not yet well defined.

Extensive clinical reviews of the time capnograph are available in other chapters of this book, review articles [11], and websites [12]. In this section, we will briefly review the terminology used to describe different phases of the inspiratory and expiratory capnographic tracing and the physiologic meaning of these waveforms in the setting of a patient with $\dot{V}/\dot{Q}$ abnormalities [11,13].

A time capnogram, a plot of CO_2 vs. time, can be divided into inspiratory and expiratory segments, each one grouped in phases (Figure 31.2c).

Inspiratory segment: The inspiratory phase, phase 0, is usually a flat line overlapping the zero (baseline) CO_2 concentration line, unless rebreathing is present. The later part of the horizontal base line is phase I of the expiratory segment. Phase 0 represents the dynamics of inspiration.

Expiratory segment: The expiratory segment, similar to a single breath CO_2 curve, is divided into phases I, II, and III, and, occasionally, phase IV, which represents the terminal rise in CO_2 concentration.

Phase I: Phase I represents CO_2-free gas from the apparatus and anatomical deadspace.

Phase II: Phase II consists of a rapid S-shaped upswing on the tracing due to mixing of deadspace gas with alveolar gas.

Alpha (α) angle or slope of phase III: The angle between phases II and III, has been referred to as the alpha angle, and increases as the slope of phase III increases. Changes of the alpha angle correlate with sequential emptying of the alveoli, as observed in obstructive lung disease, and seem to be directly proportional to the severity of bronchospasm and inversely proportional to lung recruitment [14]. In general, the more heterogeneous the functional units of the lung, the larger the alpha angle.

Phase III: Phase III is the link between the alpha angle and the $P_{ET}CO_2$. Its slope is the core of $\dot{V}/\dot{Q}$ mismatch abnormalities [15,16]. $\dot{V}/\dot{Q}$ mismatch within the unit may be due either to incomplete gas mixing (alveolar mixing defect) or as a result of late gas distribution to alveoli with low $\dot{V}/\dot{Q}$ ratio (higher PCO_2). Regional variations between respiratory units produce a large spectrum of $\dot{V}/\dot{Q}$ ratios. Under these circumstances, the slope of phase III is determined by the gas-emptying sequence of the alveolar units. If the units empty synchronously, the CO_2 expired results in a smooth flat or slightly up-sloping phase III. In patients with severe $\dot{V}/\dot{Q}$ scatter and longer time constants, CO_2 emptying is sequential, resulting in a steeper rising slope of phase III (Figure 31.6). In general, the more severe the mismatch, the steeper the slope. This attribute makes capnography a useful diagnostic tool to detect abnormalities in $\dot{V}/\dot{Q}$ mismatch of the lung. Factors, such as changes in cardiac output, CO_2 production, airway resistance, and functional residual capacity (FRC), may further affect the $\dot{V}/\dot{Q}$ status of the various units in the lung, and thereby also influence the height or the slope of phase III. Other mechanisms affecting CO_2 mixing that can contribute to the phase III slope are the breathing pattern (breathing frequency [fR]), V_T, and incompetent breathing circuit valves [17].

In hyperventilating subjects, the time for diffusive gas mixing is reduced and localized more peripherally, resulting in a steeper phase III slope of the capnograph that is not representative of $\dot{V}/\dot{Q}$ mismatch in the lung. An incompetent expiratory valve resulting in

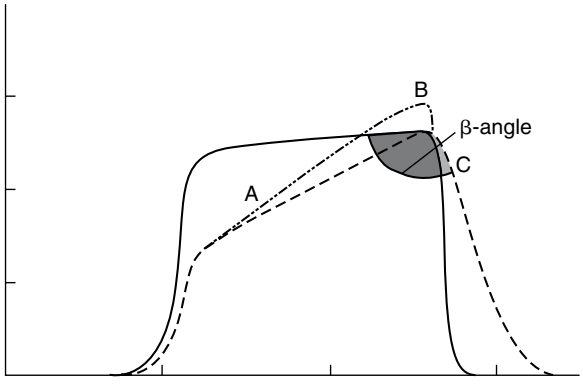

Figure 31.6 (A) Up-sloping of phase III as an index of $\dot{V}/\dot{Q}$ mismatch, variable with inspiratory time and time constant of the lung. (B) Sequential emptying in patients with low lung compliance (decreased functional residual capacity), short inspiratory time (low respiratory rate, large V_T), and severe $\dot{V}/\dot{Q}$ mismatch can result in "reverse" $PaCO_2$–$P_{ET}CO_2$ gradient. The distance between the apex of the phase III B tracing and baseline is phase IV. (C) Increased beta angle as an index of rebreathing. The capnogram may or may not go back to baseline.

rebreathing may affect the alpha angle and up-slope the phase III of the capnogram. A simultaneous recording of flow waveforms measured at the valve can be used to differentiate this technical problem from an abnormal plateau of phase III of the capnogram.

$P_{ET}CO_2$ and $PaCO_2$–$P_{ET}CO_2$ gradient

In healthy adults, the $P_{ET}CO_2$ is lower than $PaCO_2$ (average of all alveoli) by approximately 5 mm Hg. The $PaCO_2$–$P_{ET}CO_2$ difference is due to the $\dot{V}/\dot{Q}$ mismatch in the lungs (alveolar deadspace) as a result of temporal, spatial, and alveolar mixing defects. Healthy infants and children have the best $\dot{V}/\dot{Q}$ matching and lowest alveolar deadspace, resulting in a smaller difference than in adults [18,19]. Reduction in cardiac output and pulmonary blood flow result in a decrease in $P_{ET}CO_2$ and an increase in $PaCO_2$–$P_{ET}CO_2$; the opposite will happen with an increase in cardiac output and pulmonary blood.

The $PaCO_2$–$P_{ET}CO_2$ value is a measure of, and correlates well with, alveolar deadspace. In general, an increase in $PaCO_2$–$P_{ET}CO_2$ suggests an increase in deadspace ventilation as an indirect estimate of $\dot{V}/\dot{Q}$ mismatching of the lung [15].

Despite the widespread use of end-tidal CO_2, the appropriate use of this non-invasive method of assessing blood gases is unclear. In patients with lung disease, $P_{ET}CO_2$ can differ substantially from $PaCO_2$ because of $\dot{V}/\dot{Q}$ mismatching. As a result, changes in $P_{ET}CO_2$ may be seen with a corresponding increase, decrease, or no change in $PaCO_2$, depending on what influences the $\dot{V}/\dot{Q}$ mismatch. However, the $PaCO_2$–$P_{ET}CO_2$ may be the next most appropriate use for $P_{ET}CO_2$ monitoring after using it to verify tracheal intubation.

Under conditions of constant lung ventilation, $P_{ET}CO_2$ monitoring can be used as a monitor of pulmonary blood flow. Increases in cardiac output and pulmonary blood flow result in better perfusion of the alveoli and a rise in $P_{ET}CO_2$. Consequently, alveolar deadspace is reduced as is $PaCO_2$–$P_{ET}CO_2$. The relationship between $P_{ET}CO_2$ and pulmonary artery blood flow was studied during separation from cardiopulmonary bypass [20]. The decrease in $PaCO_2$–$P_{ET}CO_2$ is due to an increase in the alveolar CO_2 with a relatively unchanged arterial CO_2 concentration, suggesting better pulmonary excretion of CO_2. The improved CO_2 excretion is due to better perfusion of the upper parts of the lung [21].

Although, $P_{ET}CO_2$ is related to $PaCO_2$, the difference between the two values may be clinically significant in cases such as acute respiratory distress syndrome (ARDS), patients receiving PEEP, and those being considered for weaning from mechanical ventilation. In general, the difference between $PaCO_2$ and $P_{ET}CO_2$ will increase if there is a contribution of ventilation from high $\dot{V}/\dot{Q}$ ratios. This concept will be more extensively reviewed in the clinical application section.

A phase III variation consisting of an exaggerated increase of $P_{ET}CO_2$ with an up-sloping trend at the very end of the phase III waveform is occasionally referred to as a *terminal rise*, or phase IV (Figure 31.6). The up-slope is primarily linked to an increase in time constants within the lung, and is an indirect indication of the $\dot{V}/\dot{Q}$ status of the lung. A "two lung compartments" theory has been proposed to explain this variant, where two different lung regions with mechanical and $\dot{V}/\dot{Q}$ properties empty in time sequence [22].

A fast alveolar compartment, with high initial expiratory flow rate and rapid emptying of gases, has a somewhat constant CO_2 output, and can be considered responsible for the near-horizontal initial part of phase III trace. A slow alveolar component, when expiratory flow decreases towards the end of expiration, causes a steep rise of exhaled CO_2 and, therefore, a terminal up-slope in the tracing. Normally, a significant portion of the alveolar gases contained in the slow alveolar component remain within the airways and the anatomical deadspace. As such, these

gases are not usually "seen" by the CO_2 sensor at the mouth. However, exaggerated alveolar PCO_2 fluctuations during the respiratory cycle due to decreased FRC, combined with the use of large VT, and low-frequency ventilation increase the chances of higher CO_2-containing exhaled gas reaching the CO_2 sampling site. This has been observed frequently during general anesthesia. Under these circumstances, as the expiratory flow rate decreases towards the end of expiration, low $\dot{V}/\dot{Q}$ areas (alveoli with higher PCO_2) make a more substantial contribution to the gas exchange [23].

In rare circumstances, the slope of phase III increases steadily to a level that reverses the "normal" $PaCO_2$–$PETCO_2$ difference, resulting in a negative $PaCO_2$–$PETCO_2$ value. It goes without saying, but often does not, that more obvious reasons for measurement errors, such as device calibration error or malfunctioning, rebreathing, or inadvertent addition of CO_2 to the inspired gases, and blood gas analysis or sampling error should be ruled out before unnecessarily complicating the interpretation of the finding.

$PETCO_2$ exceeding $PaCO_2$ has been reported in obese and pregnant subjects. Therefore, $PaCO_2$–$PETCO_2$ may not reflect alveolar deadspace when phase III has a steeper slope or when a terminal "step-up knee" of the waveform is appreciated. The $PaCO_2$–$PETCO_2$ difference can be zero or negative, even in the presence of alveolar deadspace ventilation. For example, it has been observed during cardiac surgery that alveolar deadspace increased at the end of cardiopulmonary bypass, but as the slope of phase III was also increased, no change in $PaCO_2$–$PETCO_2$ was noted [24]. In conclusion, changes in alveolar deadspace correlate with $PaCO_2$–$PETCO_2$ only when phase III is flat or has a minimal slope.

The beta (β) angle

Phase III terminates in the beta angle. The descending limb that follows phase III is normally about 90° relative to phase III, and represents the inspiratory phase during which the fresh gases (CO_2-free gases) are inhaled and CO_2 concentration falls rapidly to zero. An increase of the beta angle, and the delay or lack of return of the capnogram to a zero baseline, has been observed during rebreathing (Figure 31.6) [25–27], or as an artifact [28] with defective inspiratory valves and during rapid breathing (especially in infants) when the respiratory rate exceeds the frequency response parameters of the capnograph.

Clinical correlation of $\dot{V}/\dot{Q}$ ratio mismatch and capnography abnormalities

The attention of physiologists and physicians for many years has been focused on how best to assess the quality and quantity of $\dot{V}/\dot{Q}$ inequality. While knowing the actual distribution of $\dot{V}/\dot{Q}$ ratios for each patient would be ideal, in most instances, we must rely on indirect information from arterial blood gas interpretations.

The difference in – and the ratio of – PO_2 between alveolar gas and arterial blood are often useful in assessing the degree of $\dot{V}/\dot{Q}$ inequality. These indices have the advantage of being less sensitive to the patient's level of ventilation than the arterial PO_2 alone.

In the healthy lung, when atmospheric O_2 (21%) has reached the alveoli (i.e., A), the PAO_2 will approximate 100 mm Hg, losing about one-third of the initial partial pressure due to the presence of water vapor and alveolar CO_2. Alveolar O_2 is determined by measuring O_2 in the pulmonary capillary blood, a process in which there is minimal variability at rest with continuous alveolar ventilation. If venous blood enters the arterial system without being ventilated, the admixture is calculated as the shunt fraction:

$$\frac{Q_S}{Q_T} = \frac{CcO_2 - CaO_2}{CcO_2 - C\bar{v}O_2}$$

where Qs is the shunted blood, QT the total blood flow, and CaO_2, $C\bar{v}O_2$, and CcO_2 are the content of the arterial, mixed venous, and capillary blood, respectively.

The most important feature of an absolute shunt is the lack of an increase in the PaO_2 in response to breathing 100% O_2. The PaO_2 is often a useful measure of the degree of $\dot{V}/\dot{Q}$ inequality in a diseased lung. For example, a patient with chronic obstructive pulmonary disease (COPD), with a PaO_2 of 50 mm Hg, likely has more $\dot{V}/\dot{Q}$ inequality than a patient with a PaO_2 of 70 mm Hg, with both inspiring the same FiO_2. The main disadvantage of PaO_2 as a measure of $\dot{V}/\dot{Q}$ inequality is that its value is also affected by the level of ventilation and other causes of hypoxemia.

$\dot{V}/\dot{Q}$ mismatch, absolute shunt, deadspace, and diffusion limitations are the most important intrapulmonary factors regulating the PaO_2. Extrapulmonary factors of importance are:

(1) FiO_2
(2) total ventilation

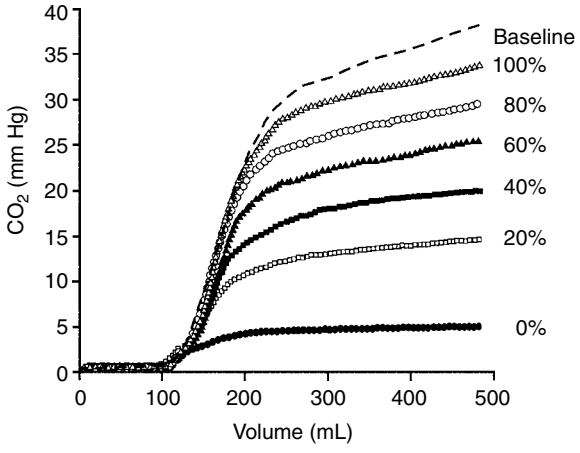

Figure 31.7 Representative SBT-CO_2 curves of patient 7 during the protocol. Dotted line corresponds to baseline SBT-CO_2. Values to the right of each curve express the percentage of total PBF. Note that a SBT-CO_2 curve could also be recorded at 9% of PBF. This is mainly due to CO_2 recovery from bronchopulmonary anastomoses. SBT, single breath test capnogram; PBF, pulmonary blood flow. [From: Tusman G, Areta M, Climente C, *et al.* Effect of pulmonary perfusion on the slopes of single-breath test of CO_2. *J Appl Physiol* 2005; **99**: 650–5.]

(3) cardiac output
(4) O_2 consumption
(5) CO_2 production.

In a single alveolar unit, it is easy to conceptualize the predicted exhaled CO_2 changes during $\dot{V}/\dot{Q}$ mismatch. If blood flow is obstructed, alveolar CO_2 will fall, eventually reaching the composition of inspired gas when blood flow is totally abolished (Figure 31.7). Conversely, if ventilation is abolished, the CO_2 of alveolar gas will be similar to that of mixed venous blood. Predicting mixed venous blood CO_2, to which a very large number of lung units contribute, is more complicated. In general, the blood PCO_2 is unlikely to be raised. In fact, an increase of CO_2 in the pulmonary venous circuit will trigger the chemoreceptors and increase spontaneous ventilation, thereby reducing the PCO_2 of the unshunted blood to normal. If hypoxia greatly increases respiratory drive, the resultant hyperventilation may even result in decreased $PaCO_2$ (hypocapnia), as is typically observed – by arterial blood gas analysis – in spontaneously breathing patients affected by pulmonary emboli. The importance of $\dot{V}/\dot{Q}$ inequality in producing hypercapnia in patients with lung disease has only recently been noted [29]. However, in general, $PaCO_2$ is often of no value in assessing the amount of $\dot{V}/\dot{Q}$ inequality because the gas is highly diffusible and very sensitive to the level of ventilation. As volumetric and time capnography find greater use in clinical and research applications in critically ill patients, our understanding of $\dot{V}/\dot{Q}$ abnormalities will improve.

Capnography during anesthesia

Capnography is considered a standard of care during anesthesia [30], and is strongly recommended by the American College of Emergency Physicians as an adjunctive method to ensure endotracheal tube position [31]. However, how well end-tidal CO_2 reflects changes in $PaCO_2$ is still debated. For example, there is still the belief that the $PaCO_2$–$PETCO_2$ difference may change widely and unpredictably during surgical procedures [32].

Capnography as an index of $\dot{V}/\dot{Q}$ mismatch in obstructive lung disease

Alteration of the slopes of phases II and III of the volumetric capnograph have been extensively studied in patients with obstructive airway diseases as indices of $\dot{V}/\dot{Q}$ alteration, where phase II is due to progressive recruitment of alveoli during gas transit. Furthermore, normal lung models have demonstrated that, during the phase III slope of the time capnogram, CO_2 is continuously excreted into the alveoli, which become progressively smaller as expiration continues. Sequential emptying of the lung occurs with better-ventilated compartments contributing relatively more to the early portion of exhalation, and the more slowly ventilated compartments contributing to the latter part of exhalation [33].

Obstructive airways disease reduces ventilation in some units more than others, causing an increased scatter of $\dot{V}/\dot{Q}$ ratios, and thus, of the range of alveolar PCO_2 values. In small airways obstructive disease, an increased slope is often combined with an indistinct transition from phase II to phase III that is easily recognized, even on the time plot. The slope of phase III is also caused by the continuing evolution of CO_2 from the mixed venous blood into a progressively emptying lung (here, the rate of expiration is crucial: the slower expiration of obstructive lung disease guarantees a steeper slope).

The volumetric capnogram (i.e., single breath test capnogram, SBT-CO_2) typically shows an upward slope of phase III that reflects the changing composition of the alveolar exhaled gas. Two explanations have been proposed. Asynchronous emptying, with low PCO_2 (i.e., high) $\dot{V}/\dot{Q}$, results in regional lung

alveolar inhomogeneity, which is time-dependent. As occurs with airway deadspace, this mixing defect can be reduced by breath-holding or an end-inspiratory pause. A large alveolar deadspace can also be present despite an apparently normal phase III slope in diseases, such as pulmonary embolism and right-to-left intracardiac shunting of blood, as in a patient with a congenital heart defect with cyanosis [34]. This steady increase in alveolar PCO_2 towards the end of expiration explains the mild rising positive slope of phase III as expiration proceeds in normal lung.

Intuitively, phase III in a time capnograph in patients with severe $\dot{V}/\dot{Q}$ mismatch will represent sequential CO_2 release from high $\dot{V}/\dot{Q}$ alveolar units first (low CO_2) and low $\dot{V}/\dot{Q}$ alveolar units last (high CO_2) [17].

Interestingly, the correlation between spirometrically measured exhaled volume and $\dot{V}/\dot{Q}$ ratio in patients with obstructive lung diseases has been poor [35,36], as has been the relationship between forced expiratory volume at 1 s (FEV_1) and gas trapping [37]. When the multiple inert gas washout technique is used to assess ventilation maldistribution in patients with chronic obstruction, it was demonstrated that the $\dot{V}/\dot{Q}$ ratio remains essentially normal until FEV_1 is below 40% of predicted [38]. In these chronically obstructed patients, the capnograph may appear normal.

Conversely, a significantly higher degree of $\dot{V}/\dot{Q}$ mismatch has been found in patients with acute, severe obstruction, in whom compensation for $\dot{V}/\dot{Q}$ inequality (increased cardiac output, hyperventilation, increased hemoglobin, and hypoxic pulmonary vasoconstriction) cannot be readily achieved [35]. This probably explains why treatment with β_2-agonists in acute or chronic severe asthma has been shown to improve FEV_1, but not $\dot{V}/\dot{Q}$ mismatch [39].

In summary, a volumetric-capnographic phase II and III positive slope, and a time-capnographic phase III positive slope are both seen more often in more severe chronic patients and in most patients with acute pulmonary disease. In patients with lung disease, the $PETCO_2$ can differ from $PaCO_2$ because of $\dot{V}/\dot{Q}$ mismatching, and changes in the $PETCO_2$ may be seen with a corresponding increase, decrease, or no change in $PaCO_2$, depending on what happens to the $\dot{V}/\dot{Q}$ mismatch.

Single values of $PETCO_2$ have proven unreliable as differential diagnosis indexes in patients with COPD versus asthma, as well as in patients with increased extravascular lung water [40]. However, $PETCO_2$ during weaning from mechanical ventilation has been used with success to prevent dangerous – and frequently unrecognized – hypercapnia in patients with increased deadspace ventilation [41]. Unfortunately, clinically relevant hypercapnic episodes (change of $PETCO_2$ of greater than 3 mm Hg) can only be detected with a sensitivity of 82% and a specificity of 76%, making arterial sampling during weaning still a frequent necessity. Despite these limitations, capnography may substantially reduce the number of arterial blood gas analyses necessary during weaning from mechanical ventilation [42].

Two different patterns of $\dot{V}/\dot{Q}$ mismatch have been observed with COPD when MIGET was applied [43]. Both depict a bimodal distribution of perfusion or ventilation. Irrespective of the type of COPD (emphysema type A or bronchitis type B), the severity of anatomical emphysema seems to correlate with

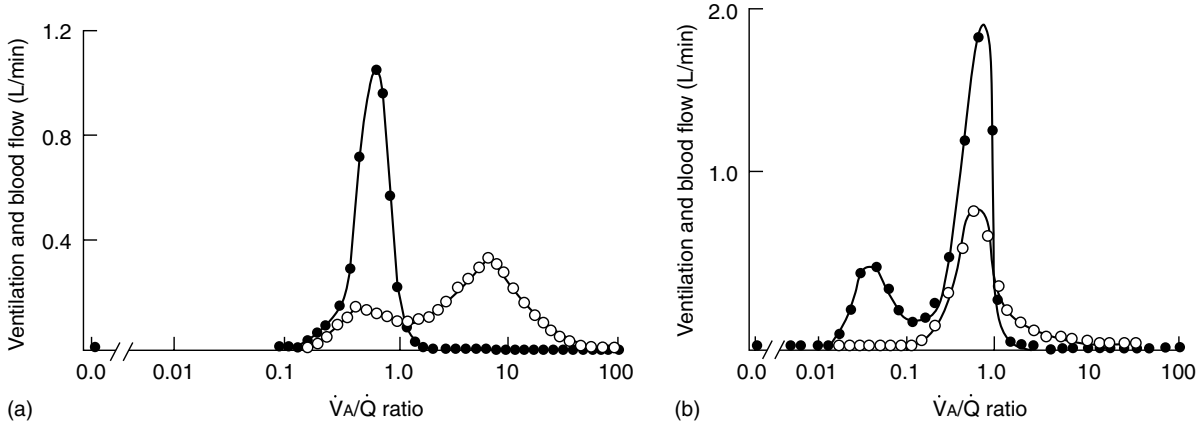

Figure 31.8 Distribution of $\dot{V}/\dot{Q}$ in a patient with: (a) Emphysema-type COPD, (b) Bronchitis-type COPD. Note the different bimodal distribution. Open circles represent ventilation; closed circles represent blood flow. [From: Wagner PD, Dantzker DR, Dueck R, Clausen JL, West JB. Ventilation–perfusion in chronic obstructive pulmonary disease. *J Clin Invest* 1997; **59**: 203–16.]

the dispersion of ventilation and blood flow distribution (Figure 31.8). The relative influence of these two MIGET patterns on deadspace ventilation capnography waveforms and $PaCO_2$–$PETCO_2$ difference is not known.

Capnography as an index of $\dot{V}/\dot{Q}$ mismatch in ARDS

Acute respiratory distress syndrome (ARDS) is an example of severe $\dot{V}/\dot{Q}$ scatter. Low lung compliance and an increase in resistance imply longer time constants and sequential CO_2 emptying, resulting in a steeper rising slope of phase III of a time capnograph (Figure 31.6). Therefore, ventilatory disturbances in ARDS can be monitored with a real-time capnogram.

Ventilatory disturbances in ARDS have also been studied to establish a relationship between volumetric capnography and respiratory system mechanics [44]. Interestingly, a change in VT does not alter capnographic indices in ARDS patients. After adjusting for the breathing pattern, the ratio between alveolar ejection volume to tidal volume (VA_E/VT) exhibited the best correlation with mechanical parameters, suggesting that ventilatory disturbances can be monitored in a patient with ARDS by volumetric capnography to assess lung function and predict outcome.

In a study of patients on the first day of ARDS onset, increased physiological deadspace fraction was an independent and powerful predictor of mortality. The relative risk of death increased by 45% if deadspace was increased by 5%. This feature and poor oxygenation were the most predictive among all severity of illness scores [34].

The $PaCO_2$–$PETCO_2$ difference has been used as a tool for real-time bedside monitoring in ventilated neonates. It has been suggested that this difference can be used to assess improved $\dot{V}/\dot{Q}$ matching when surfactant therapy is used in ARDS patients [45]. Unfortunately, the $PaCO_2$–$PETCO_2$ difference is not always predictable and constant because conditions of both increased and decreased $\dot{V}/\dot{Q}$ ratios are present. Nevertheless, when low $\dot{V}/\dot{Q}$ units are predominant (physiologic shunt), the change in PCO_2 is minimal, and the $PaCO_2$–$PETCO_2$ difference is predicted to be reliable, although occasionally widened. On the contrary, deadspace ventilation can significantly increase the $PaCO_2$–$PETCO_2$ difference, resulting in the measurement becoming progressively less reliable. Direct measurement of deadspace ventilation with volumetric capnography is, therefore, useful to predict the relationship between $PaCO_2$ and $PETCO_2$.

Measurement of deadspace ventilation has also been used to assess the efficacy of therapeutic interventions in patients with acute lung injury and severe $\dot{V}/\dot{Q}$ mismatch. For example, capnography has been used to assess alveolar and physiologic deadspace changes in animal models of ARDS pre- and post-bronchial alveolar lavage and with the use of surfactant [45]. Recent reports in pediatric and adult populations suggest that a VD/VT ratio of 60% is a critical ratio for lack of reliability of $PETCO_2$ in patients with increased extravascular lung water [46]. This observation mirrors our personal experience in adult ARDS patients. (See also Chapter 23: $PaCO_2$, $PETCO_2$, and gradient).

Furthermore, a VD/VT less than 50% seems to have acquired statistical importance in reliably predicting successful extubations, while a VD/VT more than 65% identifies patients at risk for respiratory failure following extubation in the pediatric population [46]. A similar value, VD/VT of 63%, identifies patients at risk of death in adult ARDS [47].

The studies of Hubble *et al.* [46] and Nuckton *et al.* [47] suggest that the direct calculation of deadspace ventilation should be an important parameter to assist with decision-making, and that an increased $PaCO_2$–$PETCO_2$ difference – generally more than 10 mm Hg – might be the trigger to measure this important clinical parameter. Other important causes of a widening gap and decrease in $PETCO_2$ also need to be ruled out. Of particular significance is a low cardiac output state and pulmonary embolism.

In patients with severe $\dot{V}/\dot{Q}$ mismatch, capnography may still be helpful in selecting ventilator settings to achieve a desired $PaCO_2$ or to insure that the $PaCO_2$ is not lowered too rapidly. A sudden change in $PETCO_2$ may indicate a ventilator circuit disconnection, a leak or an obstruction in the circuit, or a malfunctioning ventilator [48]. Another interesting application has been found for the $PaCO_2$–$PETCO_2$ difference in ARDS patients. It has been theorized that narrowing this difference, while PEEP is applied in patients with ARDS, indicates the best possible recruitment of unstable alveoli without overdistension [49]. In other words, calculating VD/VT in patients with a large $PaCO_2$–$PETCO_2$ difference could be strategically useful to optimize PEEP, thereby limiting the promotion of excessive "West zone 1" in the lung (Figure 31.9). Our experience at the University of Florida confirms

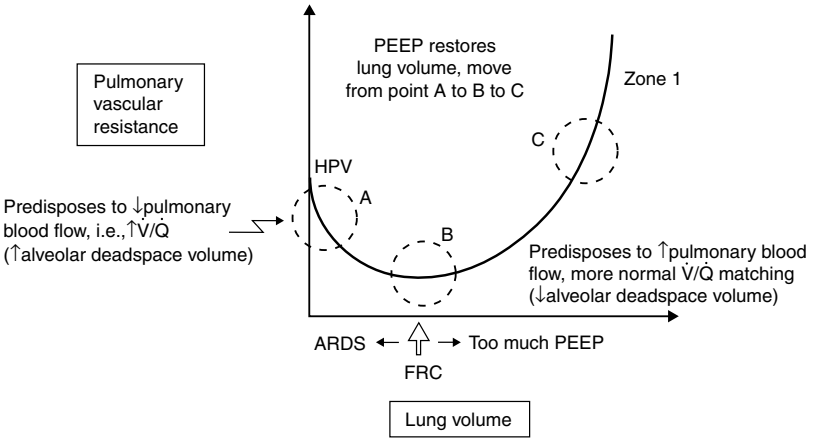

Figure 31.9 Titration of PEEP in patients with low FRC (point A to point B) restores lung volume, decreases pulmonary vascular resistance, *decreases* VD/VT, and improves V̇/Q̇ matching. Excess of PEEP (point B to point C) overdistends the lung, *increases* VD/VT without improving and potentially even deteriorating V̇/Q̇ matching. [Courtesy of M. J. Banner, University of Florida, Gainesville, FL, modified.]

the utility of using VD/VT in titrating PEEP in ARDS patients [50]. Furthermore, we have noted that exhaled CO_2/min (LCO_2), calculated in real time with volumetric capnography, closely correlates with VD/VT ($r^2 = 0.71$), and is another potential means to titrate PEEP to its "best physiologic value" [50]. Nonetheless, this enhanced – although, as yet, theoretical – utility of capnometry in clinical practice has been neither fully validated nor generally accepted [51].

Capnography as an index of V̇/Q̇ mismatch in pulmonary fibrosis

Hypoxemia at rest that worsens during exercise is the hallmark of the respiratory pathophysiology known as *pulmonary fibrosis* [52,53]. In general, the measurement of the diffusing capacity of CO_2 in these patients provides an indication of the degree of gas exchange impairment, and correlates with both V̇/Q̇ mismatch and the degree of vascular reactivity to a high concentration of O_2 and exercise. The effect of V̇/Q̇ mismatch is disproportionate for PCO_2 and O_2. The reason for the difference in behavior between the two gases is the different-shaped dissociation curves of CO_2 and O_2. With an increase in V̇/Q̇ mismatch, the increase of PCO_2 augments the ventilatory drive. As the CO_2 dissociation curve is nearly linear in the physiologic range, increased ventilation will increase CO_2 output in both high and low V̇/Q̇ ratio units. This is not true for O_2, whose relatively flat dissociation curve does not allow an increase of O_2 concentration in the unit with a high V̇/Q̇ ratio. The net result is that the mixed PaO_2 rises only modestly with increased ventilation, and some hypoxemia remains.

In conclusion, the pattern of V̇/Q̇ mismatch in patients with pulmonary fibrosis is highly predictable. There is little clinical experience with the use of capnography in these patients [54].

Capnography as an index of V̇/Q̇ mismatch in one-lung ventilation, lung resection, and lung transplantation

Simplified lung models of one-lung ventilation have demonstrated an up-slope in phase III of the capnogram. This appears to be due to sequential emptying of the lung, with better-ventilated compartments contributing relatively more to the early part of the exhalation while slowly ventilated compartments contribute more to the latter part of exhalation [33]. Delayed alveolar emptying in the phase III capnogram has also been demonstrated by separate bronchospirometry and capnography of the two lungs in a patient with occlusion of the right pulmonary artery [55].

More recently, capnography has been used to evaluate V̇/Q̇ mismatch of a single lung after regional lung surgery, utilizing sequential endobronchial intubation with a fiberoptic bronchoscope [56]. During surgery, gas flow is expected to decrease from the surgical site and increase from the opposite, nonoperative site. Postoperatively, perfusion to the operative site is more severely reduced than ventilation. In these cases, increased V̇/Q̇ mismatch is consistent with a widened $PaCO_2$–$PETCO_2$ gradient, and seems to correlate with hyperinflation of the remaining lobe after resection. A possible vagal nerve denervation-related reduction of blood flow and alveolar wall stretching of the remaining lung seems to correlate with decreased capillary circulation [57].

Capnography has not been reliable during rapid changes of alveolar deadspace ventilation and/or

ischemia–reperfusion lung injury, as may occur immediately after lung transplantation. However, the narrowing of the $PaCO_2$–$PETCO_2$ difference shortly after transplantation may be temporally related to successful readjustment of the recipient pulmonary circulation to the transplanted lung [58].

Capnography as an index of $\dot{V}/\dot{Q}$ mismatch in pulmonary embolism

The recent introduction of bedside volumetric capnography has contributed to the widespread knowledge of the changes that occur in deadspace ventilation during pulmonary embolism. The scientific basis for the use of time capnography for pulmonary embolism has been recognized for over 30 years [59,60]. Pulmonary embolism causes several characteristic clinical symptoms. Among others, the most statistically significant seem to be dyspnea, chest pain, increased minute ventilation, tachycardia, and hypoxemia. The most common physiologic alteration is the development of increased alveolar deadspace. As discussed in the introductory portion of this chapter, pulmonary embolism results in a decrease in blood flow to well-ventilated alveoli [61]. As a result of decreased transport of CO_2 via the pulmonary artery to functional lung units, the expiratory breath content of CO_2 decreases, and the plateau of the CO_2 volume capnogram flattens [62]. Alveolar hypoxia and increased alveolar deadspace results in increased minute ventilation with resultant hypocarbia. A minimal *decrease* of large airway deadspace ventilation is noted, mostly secondary to hypocarbic bronchoconstriction [63]. With ablation of this compensation, as occurs in a patient who is chemically paralyzed, heavily sedated, or anesthetized, the $PaCO_2$ always increases from baseline, and the $PaCO_2$–$PETCO_2$ gap widens [64]. While the pulmonary artery angiogram, spiral chest computerized tomography, and scintillation $\dot{V}/\dot{Q}$ lung scan remain the gold standards for the diagnosis of pulmonary embolism, capnography has the advantage of *not* requiring arterial puncture, and using equipment that is essentially portable, lightweight, and commercially available. Decreased $PETCO_2$ by time capnography has also been noted to correlate quantitatively with lung perfusion defect and pulmonary artery pressure when low perfusion was due to pulmonary embolism [65,66].

A sophisticated neural network has been used to interpret data collected from the capnograms of patients with an established diagnosis of pulmonary embolism. Capnometer and flowmeter measurements were integrated into the network, as were vital signs typically seen in pulmonary embolism; a sensitivity of nearly 100% was achieved, although with a low specificity of about 27% [67].

Pulmonary embolism can significantly affect both volumetric and time capnography. However, in spite of its potential, capnography remains a screening tool only, and cannot be considered a replacement for the gold standard diagnostic techniques discussed.

Capnography as an index of $\dot{V}/\dot{Q}$ mismatch in a low cardiac output state

Decreased cardiac output reduces $PETCO_2$ due to a relative change in the volume of the perfused lung. The percent decrease in $PETCO_2$ showed strong correlation with the percent decrease in cardiac output ($r^2 = 0.82$) in 24 patients undergoing aortic aneurysm surgery with constant ventilation [68]. Additionally, $PETCO_2$ values greater than 30 and 34 mm Hg were invariably associated with a cardiac index greater than 2 L/min/m^2 [21] and 2.5 L/min/m^2, respectively [20]. When cardiac output is severely decreased (Figure 31.7), reduced alveolar blood flow will prevent CO_2 elimination from matching systemic CO_2 production. As a result, $PETCO_2$ will decrease while mixed venous PCO_2 will continue to increase [69]. More sophisticated work in animals showed that end-tidal CO_2 correlates well with left ventricular stroke volume index when transesophageal echocardiographic measurements were used to calculate stroke volume index in a pig model of ventricular fibrillation and resuscitation by chest compression [70]. While the correlation between capnography and cardiac output in subjects with healthy lungs has been encouraging, results in patients with lung disease are still controversial [71].

Capnography as an index of $\dot{V}/\dot{Q}$ mismatch in trauma

The major advantages of capnography are that it does not require collections of arterial blood, is essentially portable and lightweight, and is commercially available. It is, therefore, of no surprise that the use of capnography in monitoring critically ill patients in transport, such as trauma victims, has been extensively described. The following is a short review of the clinical experience of time capnography "in trauma action."

Mismatch of $\dot{V}/\dot{Q}$ is predictably increased in trauma patients. However, the mechanism is thought to be largely secondary to an increase in alveolar deadspace related to blood loss and low cardiac output and, thus, somewhat predictable. Other than endotracheal tube confirmation, the most important clinical use of capnography has been found in "targeting" ventilation during prehospital care of major trauma victims before it is possible to obtain arterial blood gas analysis [72]. The implications of this use should be obvious, as a considerable number of these patients, including those with associated head injuries, can be inadvertently hyperventilated with potentially worsened outcomes from decreased cerebral perfusion. In fact, it is relatively well known that profound and persistent hyperventilation can significantly increase the risk of cerebral ischemia and a subsequent poor long-term outcome [73,74].

Contrasting studies have also been seen in the trauma literature. For example, the incidence of normocapnic ventilation has been increased by following $P_{ET}CO_2$ in trauma victims [72] during transport [75], as long as the patient is maintained in the same position (i.e., supine). Unfortunately, because frequent changes in position alter $\dot{V}/\dot{Q}$ matching, the correlation coefficient of $PaCO_2$ versus $P_{ET}CO_2$ has been disappointingly low ($r = 0.46–0.62$; $P < 0.001$) [76], thus limiting the clinical usefulness of this technique when positioning is not "fixed."

In general, the application of CPAP in these patients decreases shunt and improves $\dot{V}/\dot{Q}$ matching, as long as the patient has been adequately resuscitated and there is no further "West zone 1" produced. The application of CPAP decreased the functional deadspace in a swine model of acute lung injury from chest wall disruption when $\dot{V}/\dot{Q}$ ratio was measured by the MIGET technique [77].

Conclusion

Mismatching of ventilation and blood flow is common, and may be very severe in diseased lungs. The attention of physiologists and physicians has been recently focused on time and volume capnography to monitor the dynamics of CO_2 in critically ill patients. It has been proven that both alveolar deadspace and venous admixture contribute to abnormalities of the capnogram as a single entity, or can coexist [2]. Therefore, capnographic features, such as absolute $P_{ET}CO_2$ value, capnographic waveform interpretation, and $PaCO_2$–$P_{ET}CO_2$ differences, need to be interpreted in view of the presence of $\dot{V}/\dot{Q}$ inequality from lung disease or hemodynamic factors. Despite some limitations, capnography provides significant and clinically useful data that may enable diagnostic and therapeutic interpretation. As capnographic technology improves and clinical experience accumulates, we anticipate even greater use of this monitoring modality.

References

1. Haldane JS, Priestley JG. The regulation of the lung ventilation. *J Physiol* 1905; **32**: 225–66.
2. Riley RL, Cournard A. "Ideal" alveolar air and the analysis of ventilation–perfusion relationships in the lung. *J Appl Physiol* 1949; **1**: 825–47.
3. Bohr C. Über die Lungenathmund. *Skand Arch Physiol* 1891; **2**: 236.
4. Calzia E, Radermacher P, Bein T. Unveiling alveolar recruitment: the fascinating trail between theory and practice. *Intens Care Med* 2006; **32**: 1686–8.
5. Wagner PD, Naumann PF, Laravuso RB. Simultaneous measurement of eight foreign gases in blood by gas chromatography. *J Appl Physiol* 1974; **36**: 600–5.
6. Wagner PD, Saltzman HA, West JB. Measurement of continuous distributions of ventilation–perfusion ratios: theory. *J Appl Physiol* 1974; **36**: 588–99.
7. Evans JW, Wagner PD. Limits on VA/Q distributions from analysis of experimental inert gas elimination. *J Appl Physiol* 1977; **42**: 889–98.
8. Caplan RA, Posner KL, Ward RJ, Cheney FW. Adverse respiratory events in anesthesia: a closed claims analysis. *Anesthesiology* 1990; **72**: 828–33.
9. Tinker JH, Dull DL, Caplan RA, Ward RJ, Cheney FW. Role of monitoring devices in prevention of anesthetic mishaps: a closed claims analysis. *Anesthesiology* 1989; **71**: 541–6.
10. Cote CJ, Rolf N, Liu LM, *et al.* A single-blind study of combined pulse oximetry and capnography in children. *Anesthesiology* 1991; **74**: 980–7.
11. Bhavani-Shankar K, Moseley H, Kumar AY, Delph Y. Capnometry and anaesthesia. *Can J Anaesth* 1992; **39**: 617–32.
12. Capnography. A comprehensive educational website. Available online at http://www.capnography.com. (Accessed June 15, 2009.)
13. Andrew BL, Nunn JF. *Nunn's Applied Respiratory Physiology*, 5th edn. Boston, MA: Butterworth-Heinemann, 2000; 46, 164, 243–5.
14. Tusman G, Areta M, Climente C, *et al.* Effect of pulmonary perfusion on the slopes of single-breath test of CO_2. *J Appl Physiol* 2005; **99**: 650–5.

15. Nunn JF, Hill DW. Respiratory deadspace and arterial to end-tidal carbon dioxide tension difference in anesthetized man. *J Appl Physiol* 1960; **15**: 383–9.
16. Bhavani-Shankar K, Kumar AY, Moseley HS, Ahyee-Hallsworth R. Terminology and the current limitations of time capnography: a brief review. *J Clin Monit* 1995; **11**: 175–82.
17. Strömberg NOT, Gustafsson PM. Ventilation inhomogeneity assessed by nitrogen washout and ventilation–perfusion mismatch by capnography in stable and induced airway obstruction. *Pediatr Pulmonol* 2000; **29**: 94–102.
18. Fletcher R. Invasive and noninvasive measurement of the respiratory deadspace in anesthetized children with cardiac disease. *Anesth Analg* 1988; **67**: 442–7.
19. Rich GF, Sconzo JM. Continuous end-tidal CO_2 difference sampling within the proximal endotracheal tube estimates arterial CO_2 tension in infants. *Can J Anaesth* 1991; **38**: 201–3.
20. Maslow A, Stearns G, Bert A, *et al.* Monitoring end-tidal carbon dioxide during weaning from cardiopulmonary bypass in patients without significant lung disease. *Anesth Analg* 2001; **92**: 306–13.
21. Askrog V. Changes in (a–A)CO_2 difference and pulmonary artery pressure in anesthetized man. *J Appl Physiol* 1966; **21**: 1299–305.
22. Fletcher R, Jonson B, Cumming G, Brew J. The concept of deadspace with special reference to the single breath test for carbon dioxide. *Br J Anaesth* 1981; **53**: 77–88.
23. Fletcher R, Jonson B. Deadspace and the single breath test for carbon dioxide during anaesthesia and artificial ventilation: effects of tidal volume and frequency of respiration. *Br J Anaesth* 1984; **56**: 109–19.
24. Fletcher R, Malmkvist G, Niklason L, Jonson B. On-line measurement of gas-exchange during cardiac surgery. *Acta Anaesthesiol Scand* 1986; **30**: 295–9.
25. Berman LS, Pyles ST. Capnographic detection of anesthesia circle valve malfunctions. *Can J Anaesth* 1988; **35**: 473–5.
26. Podraza AG, Salem MR, Joseph NJ, Brencley JL. Rebreathing due to incompetent unidirectional valves in the circle absorber system. *Anesthesiology* 1991; **75**: A422.
27. Kumar AY, Bhavani-Shankar K, Moseley HS, Delph Y. Inspiratory valve malfunction in a circle system: pitfalls in capnography. *Can J Anaesth* 1992; **39**: 997–9.
28. Badgwell JM, Kleinman SE, Heavner JE. Respiratory frequency and artifact affect capnographic baseline in infants. *Anesth Analg* 1993; **77**: 708–12.
29. West JB. Causes of carbon dioxide retention in lung disease. *N Engl J Med* 1971; **284**: 1232–6.
30. American Society of Anesthesiologists. *Standards for Basic Anesthetic Monitoring*. Approved by the ASA House of Delegates on October 21, 1986, and last amended on October 25, 2005. Available online at http://www.asahq.org/publicationsAndServices/standards/02.pdf. (Accessed June 15, 2009.)
31. American College of Emergency Physicians. Clinical Policies Committee. Verification of endotracheal tube placement. *Ann Emerg Med* 2002; **40**: 551–2.
32. Wahba RW, Tessler MJ. Misleading end-tidal CO_2 tensions. *Can J Anaesth* 1996; **43**: 862–6.
33. van Meerten RJ. Expiratory gas concentration curves for examination of uneven distribution of ventilation and perfusion in the lung: first communication – theory. *Respiration* 1970; **27**: 552–64.
34. Drummond GB, Fletcher R. Deadspace: invasive or not? *Br J Anaesth* 2006; **96**: 4–7.
35. Ballester E, Roca J, Ramis L, Wagner PD, Rodriguez-Roisin R. Pulmonary gas exchange in chronic asthma response to 100% oxygen and salbutamol. *Am Rev Respir Dis* 1990; **141**: 558–62.
36. Wagner PD, Hedenstierna G, Rodriguez-Roisin R. Gas exchange, expiratory flow obstruction and the clinical spectrum of asthma. *Eur Respir J* 1996; **9**: 1278–82.
37. Gustafsson PM, Johansson HJ, Dahlbäck GO. Pneumotachographic nitrogen washout method for measurement of the volume of trapped gas in the lungs. *Pediatr Pulmonol* 1994; **17**: 258–68.
38. Roca J, Wagner PD. Contribution of multiple inert gas elimination technique to pulmonary medicine. I. Principles and information content of the multiple inert gas elimination technique. *Thorax* 1994; **49**: 815–24.
39. Ballester E, Reyes A, Roca J, *et al.* Ventilation–perfusion mismatching in acute severe asthma: effects of salbutamol and 100% oxygen. *Thorax* 1989; **44**: 258–67.
40. Brown LH, Gough JE, Seim RH. Can quantitative capnometry differentiate between cardiac and obstructive causes of respiratory distress? *Chest* 1998; **113**: 323–6.
41. Saura P, Blanch L, Lucangelo U, *et al.* Use of capnography to detect hypercapnic episodes during weaning from mechanical ventilation. *Intens Care Med* 1996; **22**: 374–81.

42. Niehoff J, DelGuercio C, LaMorte W, *et al.* Efficacy of pulse oximetry and capnometry in postoperative ventilatory weaning. *Crit Care Med* 1988; **16**: 701–5.
43. Wagner PD, Dantzker DR, Dueck R, Clausen JL, West JB. Ventilation–perfusion in chronic obstructive pulmonary disease. *J Clin Invest* 1977; **59**: 203–16.
44. Romero PV, Lucangelo U, Lopez-Aguilar J, Fernandez R, Blanch L. Physiologically based indices of volumetric capnography in patients receiving mechanical ventilation. *Eur Respir J* 1997; **10**: 1309–15.
45. Wenzel U, Rudiger M, Wagner MH, Wauer RR. Utility of deadspace and capnometry measurements in determination of surfactant efficacy in surfactant-depleted lungs. *Crit Care Med* 1999; **27**: 946–52.
46. Hubble CL, Gentile MA, Tripp DS, *et al.* Deadspace to tidal volume ratio predicts successful extubation in infants and children. *Crit Care Med* 2000; **28**: 2034–40.
47. Nuckton TJ, Alonso JA, Kallet RH, *et al.* Pulmonary deadspace fraction as a risk factor for death in the acute respiratory distress syndrome. *N Engl J Med* 2002; **346**: 1281–6.
48. Napolitano LM. Capnography in critical care: accurate assessment of ARDS therapy? *Crit Care Med* 1999; **27**: 862–3.
49. Murray IP, Modell JH, Gallagher TJ, Banner MJ. Titration of PEEP by the arterial minus end-tidal carbon dioxide gradient. *Chest* 1984; **85**: 100–4.
50. Rose JT, Banner MJ. Effects of positive end expiratory pressure (PEEP) on physiologic deadspace volume to tidal volume ratio (VD/VT) [abstract]. *Crit Care Med* 2000; **28**: A86.
51. Jardin F, Genevray B, Pazin M, Margairaz A. Inability to titrate PEEP in patients with acute respiratory failure using end-tidal carbon dioxide measurements. *Anesthesiology* 1985; **62**: 530–3.
52. Barbera JA, Ramirez J, Roca J, *et al.* Lung structure and gas exchange in mild chronic obstructive pulmonary disease. *Am Rev Respir Dis* 1990; **141**: 895–901.
53. Crystal RG, Fulmer JD, Roberts WC, *et al.* Idiopathic pulmonary fibrosis: clinical, histological, radiographic, physiologic, scintigraphic, cytologic and biochemical aspects. *Ann Intern Med* 1976; **85**: 769–88.
54. Agusti AGN, Barbera JA. Contribution of multiple inert gas elimination technique to pulmonary medicine. II. Chronic pulmonary diseases: chronic obstructive pulmonary disease and idiopathic pulmonary fibrosis. *Thorax* 1994; **48**: 924–32.
55. van Meerten RJ. Expiratory gas concentration curves for examination of uneven distribution of ventilation and perfusion in the lung: second communication – experiments. *Respiration* 1971; **28**: 167–85.
56. Yoshimasu T, Miyoshi S, Maebeya S, Hirai I, Naito Y. Evaluation of effect of lung resection on lobar ventilation and perfusion using intrabronchial capnography. *Chest* 1996; **109**: 25–30.
57. Schmitz BD, Shapiro BA. Capnography. *Respir Care Clin N Am* 1995; **1**: 107–17.
58. Jellinek H, Hiesmayr M, Simon P, Klepetko W, Haider WA. Arterial to end-tidal CO_2 tension difference after bilateral lung transplantation. *Crit Care Med* 1993; **21**: 1035–40.
59. Robin ED, Julian DG, Travis DM, Crump CH. A physiologic approach to the diagnosis of acute pulmonary embolism. *N Engl J Med* 1964; **260**: 586–91.
60. Burki NK. The deadspace to tidal volume ratio in the diagnosis of pulmonary embolism. *Am Rev Respir Dis* 1986; **133**: 679–85.
61. Dantzker DR, Wagner PD, Tornabene VW, Alazraki NP, West JB. Gas exchange after pulmonary thromboembolization in dogs. *Circ Res* 1978; **42**: 92–103.
62. Schreiner MS, Leksell LG, Gobran SR, *et al.* Microemboli reduce phase III slopes of CO_2 and invert phase II slopes of infused SF_6. *Respir Physiol* 1993; **91**: 137–54.
63. Elliott CG. Pulmonary physiology during pulmonary embolism. *Chest* 1992; **101**: 163S–71S.
64. Nikodymova L, Daum S, Stiksa J, Widimsky J. Respiratory changes in thromboembolic disease. *Respiration* 1968; **25**: 51–66.
65. Eriksson L, Wollmer P, Olsson C, *et al.* Diagnosis of pulmonary embolism based upon alveolar deadspace analysis. *Chest* 1989; **96**: 357–62.
66. Kline JA, Kubin AK, Patel MM, Easton EJ, Seupal RA. Alveolar deadspace as a predictor of severity of pulmonary embolism. *Acad Emerg Med* 2000; **7**: 611–17.
67. Patel MM, Rayburn DB, Browning JA, Kline JA. Neural network analysis of the volumetric capnogram to detect pulmonary embolism. *Chest* 1999; **116**: 1325–32.
68. Leigh MD, Jones JC, Motley HL. The expired carbon dioxide as a continuous guide of the pulmonary and circulatory systems during anesthesia and surgery. *J Thorac Cardiovasc Surg* 1961; **41**: 597–610.
69. Weil MH, Bisera J, Trevino RP, Rackow EC. Cardiac output and end-tidal carbon dioxide. *Crit Care Med* 1985; **13**: 907–9.

70. Pernat A, Weil MH, Sun S, Tang W. Stroke volumes and end-tidal carbon dioxide generated by precordial compression during ventricular fibrillation. *Crit Care Med* 2003; **31**: 1819–23.
71. Pianosi P, Hochman J. End-tidal estimates of arterial PCO_2 for cardiac output measurements by CO_2 rebreathing: a study in patients with cystic fibrosis and healthy controls. *Pediatr Pulmonol* 1996; **22**: 154–60.
72. Helm M, Schuster R, Hauke J, Lampl L. Tight control of prehospital ventilation by capnography in major trauma victims. *Br J Anaesth* 2003; **90**: 327–32.
73. Muizelaar JP, Marmarou A, Ward JD, *et al.* Adverse effects of prolonged hyperventilation in patients with severe head injury: a randomized clinical trial. *J Neurosurg* 1991; **75**: 731–9.
74. Prough DS, Lang J. Therapy of patients with head injuries: key parameters for management. *J Trauma* 1997; **42**: S10–18.
75. Ratnasabapathy U, Allam S, Souter MJ. Apparatus: evaluation of an expired fraction carbon dioxide monitor. *Anaesthesia* 2002; **57**: 900–4.
76. Grenier B, Verchère E, Mesli A, *et al.* Capnography monitoring during neurosurgery: reliability in relation to various intraoperative positions. *Anesth Analg* 1999; **88:** 43–8.
77. Schweiger JW, Downs JB, Smith RA. Chest wall disruption with and without acute lung injury: effects of continuous positive airway pressure therapy on ventilation and perfusion relationships. *Crit Care Med* 2003; **31**: 2364–70.

Section 4
Chapter
32

Physiologic perspectives

Capnographic measures

U. Lucangelo, A. Gullo, F. Bernabè, and L. Blanch

Introduction

Capnography is a graphic display of carbon dioxide (CO_2) during the breathing cycle. Levels of CO_2 may be represented as a trace versus time (time capnography) or expiratory volume (volumetric capnography). In this chapter, clinical data obtained by the morphological analysis of a capnogram and from the derived measurements are studied.

Initially, the morphology of a theoretical capnogram will be examined, with a single alveolus with compliance (C), in series with an airway with resistance (R). Understanding the physiological processes that make up this ideal model allows for correct interpretation of normal and pathologic capnographic waveforms. Time and volumetric capnographic measures will then be compared in a theoretical model and a healthy subject under pathologic conditions.

Time capnography

In time capnography, the whole breathing cycle is analyzed. Figure 32.1 shows a comparison between the capnogram derived by the ideal lung model and that of a healthy subject. In the ideal capnogram, the inspiratory phase (I) may be singled out, where PCO_2 is zero, as external air virtually contains no CO_2, and an expiratory phase (E), which is divided into four segments. At the beginning of the expiratory phase, PCO_2 is still zero (a–b segment), as it comes from airways that are not involved in gas exchange. The b–c segment corresponds to the sharp increase in PCO_2 concentration from the alveoli that produce the gas exchange; the attained value remains constant in time (c–d segment), and then sharply drops again to zero, corresponding with the beginning of the next inspiration. The square waveform of the theoretical capnogram is due to a situation of perfect homogeneity in the model, as the whole system is regulated by both alveolar compliance and airway resistance to the expiratory flow. Hence, CO_2 elimination depends on a single time constant ($\tau = R \times C$) and a single ventilation/perfusion ($\dot{V}/\dot{Q}$) ratio [1]. This is why the b–c and d–e segments are perfectly orthogonal to and the c–d segment is parallel to the time axis, thus forming a 90° angle between them. Basically, the lung is made of approximately 300–400 million alveoli, each having its own τ, and a gravitational variation in the $\dot{V}/\dot{Q}$ ratio [2,3]. Therefore, in the capnogram of a healthy subject, variations in angle width and inclination of its segments may be observed [3,4]. As in the theoretical model, an inspiratory phase (I) and expiratory phase (E) made of three segments may be singled out. The first phase (a–b) represents the beginning of expiration. The analyzed gas fills in the anatomic deadspace (V_D) made of those structures that are not suitable for gas exchange, such as pharynx, larynx, trachea, and bronchi. In mechanically ventilated subjects, the endotracheal or the tracheostomy tube are included in the V_D. Therefore, the concentration of CO_2 from these regions is close to zero up to point b.

From this point on, a second phase starts (wall of the capnogram), which is a mixed air zone. It is a segment with an S-shaped trend and with a sharp upswing due to mixing of gas from the V_D with gas from the alveoli with rapid depletion. The third phase (c–d), the *alveolar plateau*, represents exhalation of pure alveolar gas, and rises slightly due to the mild inhomogeneity of the $\dot{V}/\dot{Q}$ ratio and alveolar CO_2 concentration. Hoffbrand has demonstrated a mean capnograph slope of 1.84 mm Hg/L in normal subjects [5].

The highest value of CO_2 during the alveolar plateau (point d) that is normally present at end expiration is called *end-expiratory partial pressure*, or end-tidal CO_2 ($P_{ET}CO_2$). Once phase III is completed, the capnogram sharply descends towards zero (d–e) due to the negligible amount of CO_2 usually present

Capnography, Second Edition, ed. J. S. Gravenstein, Michael B. Jaffe, Nikolaus Gravenstein, and David A. Paulus. Published by Cambridge University Press. © Cambridge University Press 2011.

in inspiratory gas, thus forming an approximately right angle (beta angle). The descending limb of the capnogram represents the inspiratory phase in which CO_2-free gas from the airways is inhaled, thus producing the rapid fall of PCO_2 to zero. In conclusion, the portion of the capnographic wave from beginning of inspiration to beginning of expiration is termed as phase 0; it consists of the descending limb of the capnogram, and the initial portion of the baseline. Phase 0 represents the inspiratory portion of the breathing cycle [3,6]. The final part of the baseline represents phase I of the expiratory segment.

At the end of phase III, a terminal upswing, called phase IV, may occasionally be seen. In the absence of lung disease, this finding is caused by alveolar characteristics under circumstances such as pregnancy and obesity. In both populations, due to a decrease in lung compliance and functional residual capacity (FRC), two lung compartments are determined, each having different mechanical properties and different $\dot{V}/\dot{Q}$ ratios (fast- and slow-depletion compartments). The action of slower alveoli, richer in CO_2, is more evident in anesthesia and artificial ventilation with high tidal volumes and low breathing frequency.

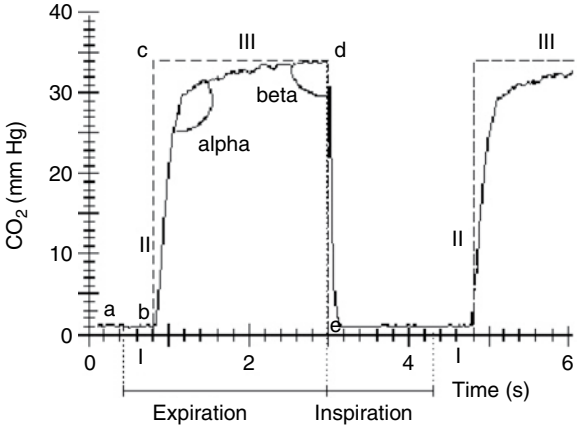

Figure 32.1 Normal time capnogram.

Finally, in the capnogram of a normal subject, it is possible to separate the alpha angle between phases II and III (100°–110°), and the beta angle (≅90°) between phase III and inspiratory phase (Figure 32.1) [3].

Pathologic time capnogram

The main variations in the morphology of the capnographic wave are discussed below.

Phase I (a–b segment)

The length of the a–b segment may be artificially increased via modification of the breathing circuit by addition of airway adapters and antibacterial filters that increase the VD. The main factors that may cause a progressive rise in the baseline are related to the presence of CO_2 in inspiratory gas. This rise may occur with modern ventilators due to a malfunctioning inspiratory valve that, apart from raising the baseline, makes the beta angle more obtuse. When low-flow or closed-circuit anesthesia ventilators are used, the rise in the baseline may be caused by depletion of the CO_2 absorbent system, which occurs in the absence of changes in the beta angle (Figure 32.2) [7–10]. A sharp rise in the baseline is a typical sign of contamination of the device that analyzes gas exhaled in combination with water, mucus, or impurities (Figure 32.3).

Alterations in phases II and III

Bronchial obstruction makes regional alveolar ventilation inhomogeneous, thus altering the normal $\dot{V}/\dot{Q}$ ratio. This produces different readings of alveolar CO_2 that are asynchronously exhaled, flattening the verticality of phase II. As a consequence, phase III increases its slope, and the alpha angle becomes more obtuse. The main clinical causes of obstruction of the expiratory flow are asthma, bronchospasm, and chronic obstructive pulmonary disease (COPD). Even emphysema produces a slanted upstroke of phase II.

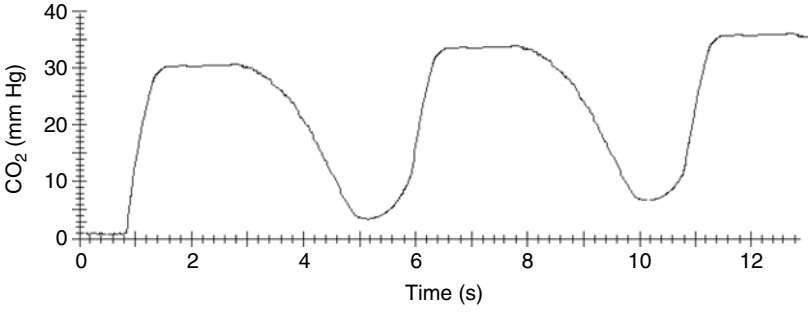

Figure 32.2 Malfunctioning in the inspiratory valve, characterized by a rise in the baseline, by an extension of phase III, and by a widening of the beta angle.

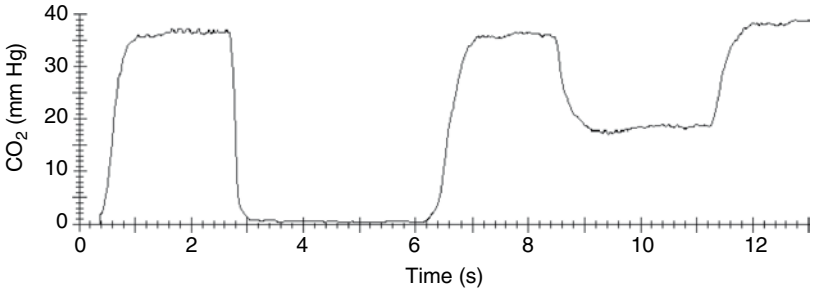

Figure 32.3 Malfunctioning in the cell that analyzes exhaled gas.

Furthermore, obstruction of exhaled gas may be caused by external factors, such as a kinked tracheal tube [11–15].

The variations in phase III slope can be ascribed to the following physiological phenomena [6]:

(1) *Cyclic variation in alveolar CO_2 during ventilation (greater during expiration than during inspiration)*. CO_2 is constantly poured into the alveoli, which progressively reduce their volume as expiration proceeds. The produced effect is a constant increase in alveolar PCO_2 until end expiration, followed by an increase in the slope in phase III.

(2) *Late emptying of the alveoli with the lowest ($\dot{V}/\dot{Q}$) ratio and, thus, with relatively higher PCO_2*. If all the alveoli had the same PCO_2, phase III would be almost horizontal. In effect, this "ideal" situation does not occur even in normal lungs, which have a wide range of $\dot{V}/\dot{Q}$ ratio. Some alveoli have a higher $\dot{V}/\dot{Q}$ ratio (overventilated) than that of "ideal" alveoli and, therefore, have a relatively lower PCO_2. Others have a lower $\dot{V}/\dot{Q}$ ratio (underventilated) than that of ideal alveoli, resulting in a relatively higher PCO_2. Delayed emptying of the alveoli with a low $\dot{V}/\dot{Q}$ ratio (high PCO_2) contributes to the increase in the slope of phase III. The mechanisms by which this effect can be produced are the following:
   (a) *Within the terminal respiratory units*. The difference in $\dot{V}/\dot{Q}$ ratio between units can be caused by both incomplete mixing of the gases (alveolar mixing defect), and by the fact that the maximum ventilation and the maximum perfusion of that unit are out of phase (temporal mismatching – the perfusion is greater during the last part of expiration when ventilation is less).
   (b) *Between the terminal respiratory units*. This mechanism can be the consequence of regional variations in the ventilation per unit of perfusion, which produces a range of $\dot{V}/\dot{Q}$ ratios (spatial mismatching). In this case, the phase III slope is determined by the nature of the alveolar emptying: synchronous or asynchronous. If the alveolar units empty synchronously, the gas from well-perfused and poorly perfused alveoli is exhaled simultaneously, resulting in a horizontal or slightly inclined phase III slope. If the units empty in an asynchronous manner, the units with a higher time constant, and thus a higher PCO_2, empty later (sequential emptying), resulting in a steeper phase III slope.

Other factors such as changes in cardiac output, CO_2 production, airway resistance, and FRC can further influence the $\dot{V}/\dot{Q}$ ratio of the various lung units, affecting the height or slope of the phase III curve. This pattern is evidenced as a normal physiologic variation, even during pregnancy [3].

Deformation of phase II and III: capnographic measures

Because the geometric form of the whole capnographic wave is the result of a continuing process of elimination of alveolar gas, pathologies affecting phase II also affect the alveolar plateau. Lung pathologies globally interact with CO_2 washout, thus altering both convective processes (flow rate, breathing frequency, tidal volume, and conducting airway volume) and diffusive processes (time, and available cross-section and intra-airway concentration gradient) [16]. The shape of the capnogram is modified by airway obstruction [5], and the evaluation of this deformation, using measurable indices, has been previously analyzed as a measurement of bronchial patency. Worth reported on the most important indices applied in the literature for quantitative description of time capnography in patients with

chronic airflow limitation; these indices include phase II and III [17]. These indices have been calculated as the change in partial pressure per second, as percentage of the initial end-tidal amplitude, or as the time interval between 25% and 75% of the inspiratory/end-tidal partial pressure difference. Another index has been proposed that calculates the minimum radius of curvature of the alpha angle as a direct measurement of the time constant. Several studies confirmed that the slope of phase III is connected with asthma, COPD, and respiratory system resistance (Rrs) in intubated and in spontaneously breathing patients [18,19].

The slope of expired CO_2 (mm Hg/s) can be calculated in several ways by linear regression during phase III of the expired capnogram. The initial 25% of the expired capnogram is rejected for calculation, as it consists of gas exhaled in phases I and II [18], or, according to the study by You *et al.* [20], during the half-second preceding the end-expiratory CO_2 peak, or else calculated at 0.36 s before the end of the expirogram [7]. Yaron calculated the derivative (dCO_2/dt) of the alveolar plateau versus time [19]. Both studies proved that there is an increase in the slope in phase III in subjects affected by COPD and/or asthma compared to a control group without lung disease. In particular, in the population studied by Blanch, which included intubated and mechanically ventilated subjects affected by COPD, ischemic heart disease, septic shock, acute respiratory distress syndrome (ARDS), asthma, and coma, the slope in phase III ranged from 0.69 to 12.3 mm Hg/s, with an average of 3.61 ± 0.40 mm Hg/s [18]. Furthermore, the average expired CO_2 slope was 1.62 ± 0.13 mm Hg/s in patients without auto-PEEP and 4.88 ± 0.51 mm Hg/s in patients with auto-PEEP ($P < 0.01$). These findings suggest that a steeper average slope in phase III is associated with a higher degree of alveolar inhomogeneity, confirmed by the presence of high auto-PEEP readings. Although the 41 patients studied were heterogeneous concerning the lung pathologies presented, this study demonstrates a fair overall correlation between auto-PEEP and Rrs ($r = 0.75$; $P < 0.001$), and between auto-PEEP and expired CO_2 slope ($r = 0.74$; $P < 0.001$). Furthermore, as evidence of the importance of total resistances (including the action of the airways, the flow resistance properties of the endotracheal tube, and equipment) in the process of CO_2 elimination, a linear correlation was evidenced between Rrs and the slope in phase III ($r = 0.86$; $P < 0.001$). However, due to the heterogeneity of the patients analyzed and the high prediction interval limits (±7.89 cm H_2O/L/s), Rrs readings cannot be accurately determined. Furthermore, the slope of the alveolar plateau was considered in relation to spirometric readings in asthma patients, expecting to use the capnogram during bronchospasm, and considering its response to bronchodilators that are known to influence spirometric indexes.

You *et al.* studied a group of 24 asthma patients, with an average slope in phase III of 0.3 ± 0.23%/s, with a statistically significant difference from a control group (0.08 ± 0.06%/s) [20]. In asthma patients, a very significant correlation was evidenced between the slope of phase III and forced expired volume in 1 s (FEV_1) ($r = 0.83$; $P < 0.001$). Furthermore, in 13 asthma patients, the effect of bronchodilating therapy was assessed and observed to produce an increase in FEV_1 and a decrease in the slope of phase III ($r = 0.96$; $P < 0.001$).

Similar results were obtained by Yaron, who found an important correlation between the expiratory slope of phase III (dCO_2/dt) and peak expiratory flow rate (PEFR) in spontaneously breathing, asthmatic patients and in normal healthy volunteers [19]. The average dCO_2/dt readings in asthma patients (0.26 ± 0.06) and PEFR readings (274 ± 96 L/min) were significantly different ($P < 0.001$) from readings in normal healthy subjects ($dCO_2/dt = 0.13 \pm 0.06$; PEFR = 527 ± 96 L/min). After bronchodilating therapy in 18 of the asthma patients, the percentage PEFR readings increased from 58% ± 17% to 74% ± 17% of predicted value ($P < 0.001$) in association with a decrease in dCO_2/dt from 0.27 ± 0.05 to 0.19 ± 0.07 ($P < 0.005$). This study suggests that the capnogram is useful in determining the greater effectiveness of inhaled bronchodilating therapy rather than spirometry as an effort-independent, non-invasive method easily performed at the patient's bedside (Figure 32.4). The great disadvantage of these indices is that they are based on a partial pressure–time plot. When expiratory partial pressure is plotted versus time, even in healthy subjects, curve-deforming influences, such as expiratory flow, have to be taken into account [21]. More recently, the volumetric capnogram has been evaluated for use as a PEFR surrogate [22].

Alterations of the inspiratory phase

In instances when the CO_2 exhaled is diluted by external air or by fresh gas flow, $P_{ET}CO_2$ and beta-angle readings may present artifacts (Figure 32.5). If the inspiratory valve in a closed-circuit respiratory cycle is malfunctioning or if the valve is in a sidestream capnograph with a high response time (Figure 32.6), there may be an extension and/or a decrease in the slope of the descending limb [7,9,12,23].

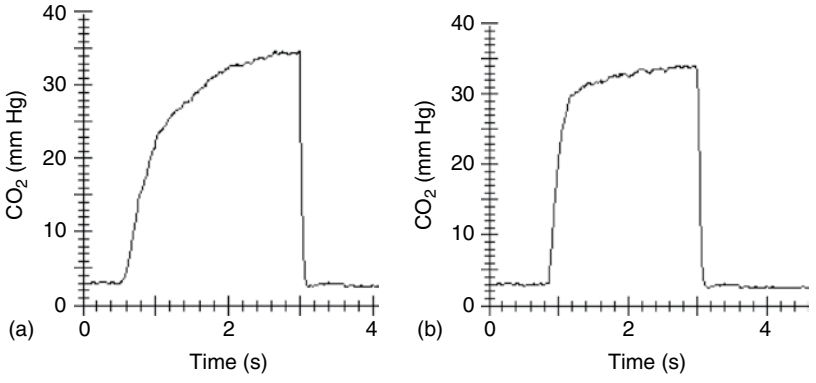

Figure 32.4 Capnogram before (a) and after (b) bronchodilating therapy. Note that in (a) phases II and III are extended, and the alpha angle is wider.

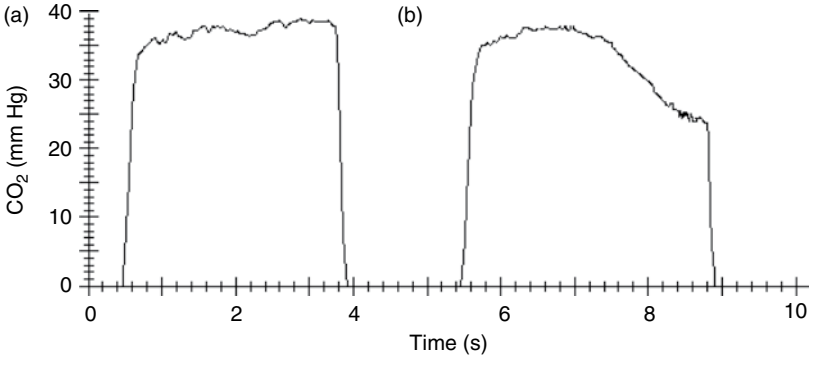

Figure 32.5 In (a) a normal wave is seen; but in (b) the wave presents artifacts due to inadequate sample rate and/or dilution of exhaled gas by the continuing gas flow.

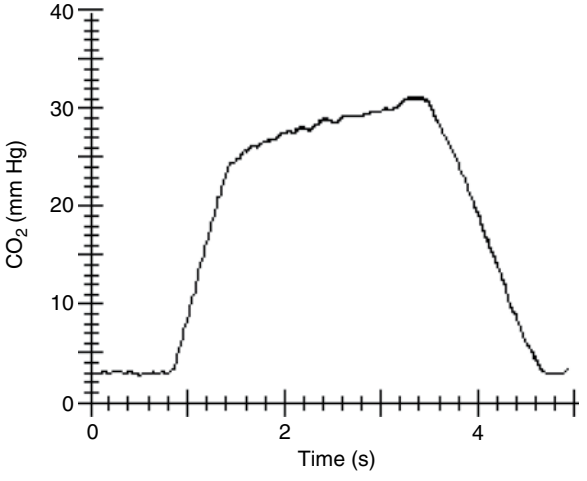

Figure 32.6 Extension of the inspiratory descending limb due to vaporization of gas on the sample line or to the high response time of the analyzer. It occurs in children, who have a shorter breathing cycle.

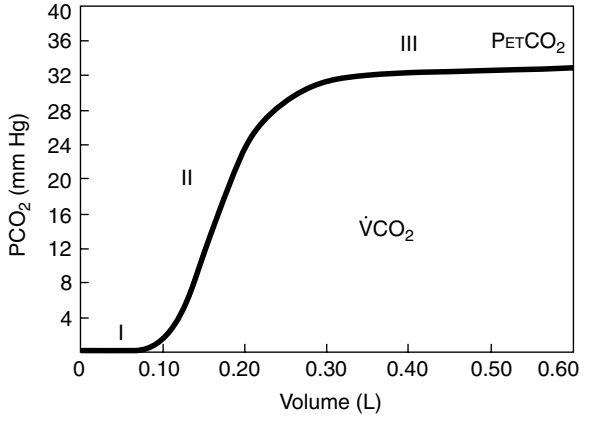

Figure 32.7 Normal volumetric capnogram.

Volumetric capnography

CO_2 may be measured versus volume (volumetric capnogram). The result resembles a single breath test of nitrogen washout (SBT-N_2), which is normally used in pulmonary pathophysiology studies to determine closing volume and anatomical deadspace [24,25]. The physiologic mechanisms responsible for phases I, II, and III in a time capnogram are similar to those responsible for the phases seen in a volumetric capnogram or an SBT-N_2 curve [3].

A typical volumetric capnogram is shown in Figure 32.7, where the three phases that characterize

it can be clearly distinguished [6]. Phase I represents the gas without CO_2 from the airways (anatomical and instrument deadspace). Phase II consists of a rapid S-shaped rise (the result of mixing deadspace gas and alveolar gas). Finally, phase III (alveolar plateau) represents the CO_2-rich gas from the alveoli. Even in this case, phase II forms an alpha angle with phase III.

The study of the phase III slope of the volumetric capnogram provides a more accurate picture of the state of pulmonary $\dot{V}/\dot{Q}$ ratio than the corresponding CO_2 versus time trace [5]. This may occur because a smaller volume of expired gas (approximately the final 15%) occupies half the time available for expiration (Figure 32.8). In this case, CO_2 alterations are distributed over a relatively long period of time, which results in a decrease in the slope of the alveolar plateau

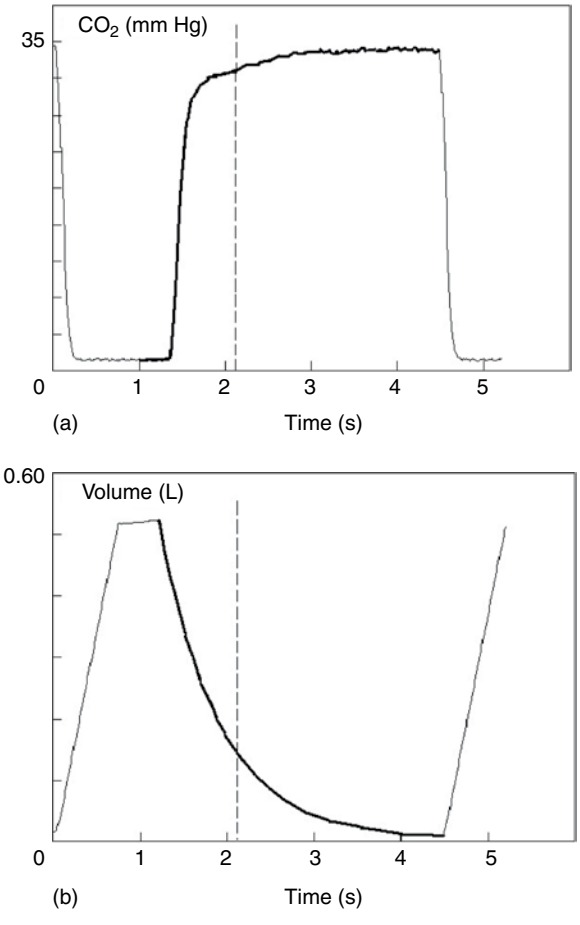

Figure 32.8 CO_2 elimination (a) and expiratory volume (b) are plotted versus time. Alveolar plateau corresponds to the lowest part of expired volume as depicted by the dotted line.

[3]. The advanced technology combination of airway flow monitoring and mainstream capnography allows pulmonary V_D and CO_2 production ($\dot{V}CO_2$) to be calculated. The volumetric capnogram allows breath-by-breath calculation of this and other parameters of ventilatory monitoring. For these reasons, the use of volumetric capnography is, clinically, arguably more relevant than time capnography.

Deformation of phase II: volume capnographic measures

Worth proved that the analysis of phase II versus exhaled volume (ranging from 25–50% to 50–75% of the expiratory CO_2 tension) can distinguish healthy subjects from asthma and emphysema patients [17]. These findings prove that serial inhomogeneity due to different airway morphology may be expressed by the variations in the slope of phase II versus volume. However, the discriminative degree of this index is lower when healthy subjects are compared with emphysema patients with mild airway obstruction [26].

Deformation of phase III: volume capnographic measures

Ream *et al.* analyzed the pattern of the capnographic wave in healthy children, with age ranging from 5 months to 17 years, which evidenced a progressive normalization of the slope of phase III with increasing age [27]. Lung growth involves an increase in the number of acinar cells, which in turn leads to an increase in the alveolar surface and decrease in resistance to gas diffusion. Morphologic lung growth effects a decrease in the arterial alveolar CO_2 gradient, with a flattening and normalization of the slope of phase III. This study reminds us that any interpretation of the capnographic wave must be considered in relation to the patient's age, and a delay in stabilization of the slope of phase III could be a sign of silent pulmonary disease.

Further studies evidenced the role of the slope of phase III, which was correlated with FRC in a surfactant-depleted animal mode [28] and, in another model, separates healthy animals from those with ARDS. Recently, from a global analysis of the volumetric capnogram, it was evidenced that the slope of phase III was one of the most robust predictors of lung volume variations in healthy animals during control ventilation [29] and in a model with acute lung injury [30].

Volume capnography and deadspace evaluation (VD)

From the analysis of volumetric capnogram, it is possible to determine the airway, physiological, and alveolar VD [31] (Figure 32.9). The measurement of Fowler VD (airway VD) is based on the geometric method of equivalent areas ($p = q$), obtained by crossing the back extrapolation of phase III with a vertical line traced so as to have equal p and q areas. Airway VD is then measured from the beginning of expiration to the point where the vertical line crosses the volume axis [24].

Figure 32.10 differs from the previous figure with a line parallel to the volume axis, equal to the CO_2 arterial pressure value ($PaCO_2$). In this case, it is possible to determine the readings from areas Y and Z, which represent the values of alveolar and airway

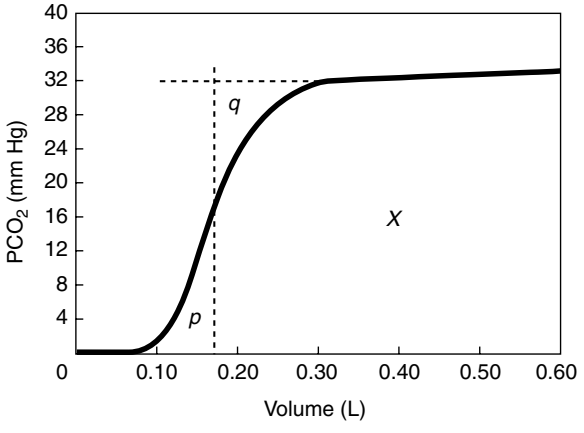

Figure 32.9 Analysis of SBT-CO_2 to determine the airway, physiologic, and alveolar VD.

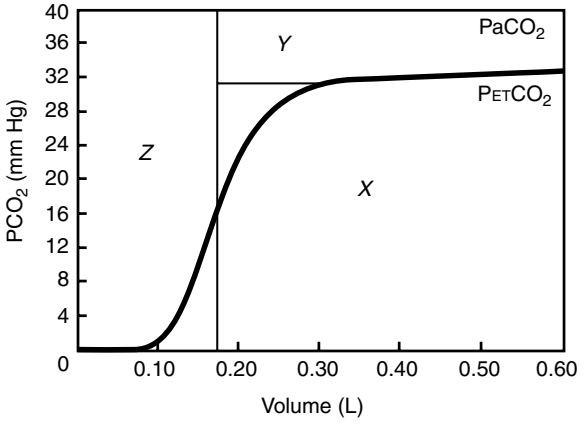

Figure 32.10 This figure differs from Figure 32.9 with a line parallel to the volume axis, equal to the $PaCO_2$.

Table 32.1 SBT-CO_2 parameters and those derived from the added $PaCO_2$ readings

SBT-CO_2 measures the following:	
Airway deadspace	Anatomic deadspace
Tidal alveolar volume	Actual air volume in gas exchange
Alveolar ventilation per minute	Actual air volume in gas exchange per minute
VD/VT	Airway deadspace/tidal volume ratio
CO_2 production	Amount of CO_2 produced by the metabolism
Arterial CO_2 allows to measure the following parameters:	
Physiologic deadspace	Volume of inspired gas, not active in gas exchange (combination of airway and alveolar deadspace)
Alveolar deadspace	Ventilated area not involved in gas exchange
Physiologic VD/VT	Physiologic deadspace/tidal volume ratio

VD, respectively. Table 32.1 summarizes volumetric capnographic parameters and those derived from added $PaCO_2$ readings.

If these values are referred to the tidal volume (VT), it is possible to single out several deadspace components [31]:

$$VD_{phys}/VT = (Y + Z) / (X + Y + Z)$$
$$VD_{alv} / VT = Y / (X + Y + Z)$$
$$VD_{alv} / VT_{alv} = Y / (X + Y)$$
$$VD_{aw}/VT = Z / (X + Y + Z)$$

An alternative method to measure airway deadspace, introduced by Langley, is based on determination of the $\dot{V}CO_2$ value, which corresponds to the area inscribed within the CO_2 versus volume curve (indicated in the figure as X area). Further on, $\dot{V}CO_2$ is plotted versus expired volume (Figure 32.11) [32]. Airway VD can be calculated from the value obtained on the volume axis by back extrapolation of the first linear part of the $\dot{V}CO_2$ versus volume curve [31]. Although these indexes are clinically useful, they are always bound to visual criteria for the definition of phase III. The geometric analysis that establishes the separation between the second and third phases of the capnogram is seldom seen, even in healthy subjects. Another drawback is the morphologic need to represent the third phase

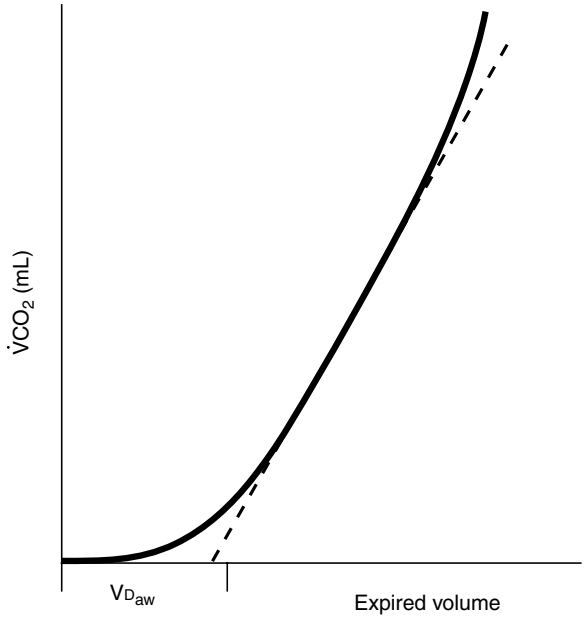

Figure 32.11 The method of Langley and others for estimation of airway deadspace.

as a straight line, ignoring the possibility that a rise in expired PCO_2 may not be linear [33].

Volumetric capnography for non-invasive determination of cardiac output

It is generally known that all situations producing a decrease in lung perfusion (pulmonary embolism, severe hemorrhage, cardiac arrest, etc.) affect the capnographic wave, which exponentially decreases in width. This phenomenon is due to the CO_2 "dilution" effect, caused by a decrease in pulmonary blood flow with constant alveolar ventilation. In this situation, the phases of the capnogram versus time do not vary (except in width) and, in particular, phase III preserves its initial slope. Similarly, the volumetric capnogram undergoes morphological changes during the alterations of the hemodynamic conditions that, as proposed by Arnold *et al.* may be used for a non-invasive determination of cardiac output [34]. In a sheep, the authors analyzed 21 indexes derived from the volumetric capnogram during alterations in cardiac output. After an initial bivariate linear regression analysis, 20 of the 21 analyzed indexes turned out to be connected with cardiac output, thus proving a close association between volumetric capnography and cardiac output measured by ultrasonic flow probe. A stepwise linear regression analysis was used to create a multivariate predictive equation of cardiac output. From the statistical analysis, only two variables were singled out; when these variables were associated, they conveyed a higher predictive value to the experimental model ($r^2 = 0.94$, $P < 0.0001$): the angle between the slope line for phases II and III, divided by the volume of CO_2 per breath (angle/mL CO_2), and the slope of phase II. The equation of predicted cardiac output was the following:

$$\text{cardiac output} = b + (-0.408)X_1 + (0.044X_2),$$

where b represents the baseline cardiac output measure, X_1 = angle/mL CO_2 and X_2 = slope phase II.

It must be emphasized that the only variable not related to cardiac output is the slope of phase III, which is an accurate predictor of lung volume change [34].

The encouraging results of this study suggest a clinical use for volumetric capnography in the field of non-invasive hemodynamic and ventilatory monitoring. Murias *et al.* have shown that using a partial rebreathing method to measure cardiac output, compared to thermodilution, yielded a bias and precision calculation of -0.07 ± 0.91 L/min for lower or intermediate cardiac output values in critical care patients [35]. Therefore, the non-invasive partial CO_2 rebreathing technique may be an alternative method for cardiac output determination in mechanically ventilated critically ill patients.

Alveolar ejection volume and tidal volume

Finally, a different approach to volumetric capnography is that of using the CO_2 elimination curve versus expired volume ($\dot{V}CO_2/V_T$). By using the $\dot{V}CO_2/V_T$ curve, the fraction of volume flow corresponding to alveolar gas exhalation can be calculated.

Alveolar ejection volume (V_{A_e}) can be defined as the fraction of V_T with minimal V_D contamination, which may be inferred from the asymptote of the $\dot{V}CO_2/V_T$ curve at end expiration, whereby V_D is equal to zero. We defined V_{A_e} as the volume that characterizes this relationship, up to a 5% variation [36]. The method of V_{A_e} determination is presented in a normal subject and an ARDS patient in Figure 32.12, where $\dot{V}CO_2(V)$ curves in a representative breath are recorded. After a given volume has been exhaled, $\dot{V}CO_2$ progressively increases to reach a total amount of $\dot{V}CO_2$ elimination in a single expiration ($\dot{V}CO_2$tot). The increase in $\dot{V}CO_2$ is slightly non-linear because of alveolar inhomogeneity,

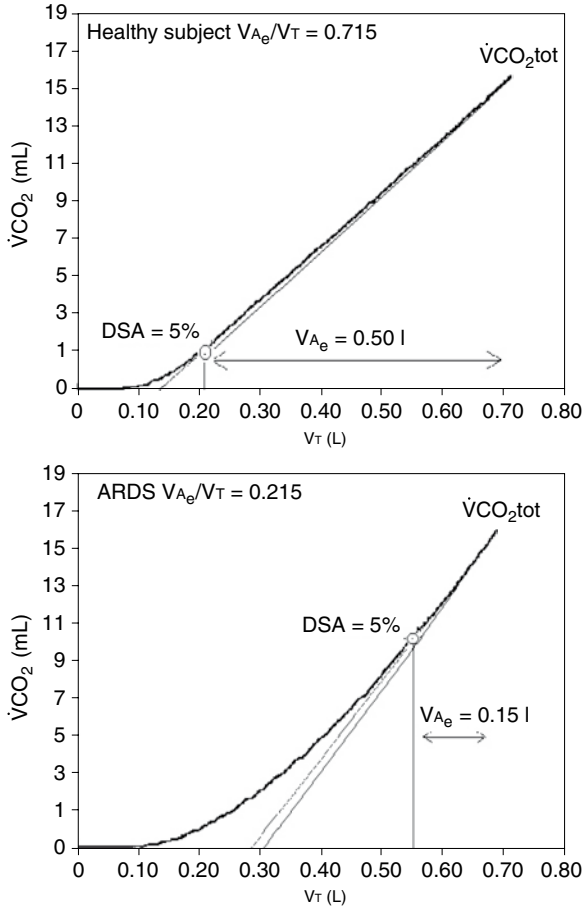

Figure 32.12 Determination of V_{A_e}/V_T in a healthy and an ARDS patient.

i.e., the presence of a certain amount of alveolar gas contaminated by parallel V_D. At the very end of expiration, gas is exhaled only from the alveoli, thus making it pure alveolar gas. Assuming a fixed amount of V_D contamination (V_D allowance [DSA]), we obtained a point on the $\dot{V}CO_2(V)$ curve representing the beginning of the V_{A_e}. The V_{A_e} was then measured from the $\dot{V}CO_2(V)$ curve as follows. First, the slope of the last 50 points of every cycle was obtained by linear fitting, using the least-squares method. Then V_{A_e} was obtained as the value of the volume at the intersection between the $\dot{V}CO_2(V)$ curve and a straight line, with a maximal value at end expiration and a slope equal to 0.95 (1 – DSA) times the calculated slope (Figure 32.12). V_{A_e} is expressed as a fraction of V_T (V_{A_e}/V_T) [36].

The value of V_{A_e}/V_T is a good index in that it demonstrates different behaviors between healthy subjects undergoing general anesthesia and patients with ARDS; it retains this discriminative capacity independent of the tidal volume and positive end-expiratory pressure (PEEP) applied. Finally, apart from the phase III slope, which bears no relation to any index of respiratory mechanics, V_{A_e}/V_T is inversely correlated with resistances and directly correlated with compliance of the respiratory system. It follows that V_{A_e}/V_T can have clinical applications in lung disorders characterized by marked alveolar inhomogeneity [37–38].

The V_{A_e}/V_T prognostic value for outcome was tested in 25 mechanically ventilated patients with acute lung injury [39]. The change in V_{A_e}/V_T between admission and after 48 h (dV_{A_e}/V_T) was greater in patients who died (0.07 ± 0.09) compared to patients who survived (-0.03 ± 0.06, $P < 0.01$), suggesting that dV_{A_e}/V_T can be used to help in predicting mortality in patients with acute lung injury.

Conclusions

Time capnography is universally acknowledged as a safety tool during anesthesia. As an easy-to-use, non-invasive method, capnography is also used in intensive care settings in both intubated and non-intubated patients. With new contributions to the literature, it is evident that volumetric capnography represents a logical evolution from time capnography. Technologic improvements have enabled the use of combined sensors for simultaneous measurement and recording of expiratory flow and CO_2 elimination at the patient's bedside. These recordings establish several parameters for hemodynamic and ventilatory monitoring. A standard for these indices is not yet available, and further clinical studies are required, but the practical and theoretical advantage of volume over time capnography is accumulating.

References

1. Mangalaboyi J, Chopin C, Chambrin MC. Utilisation de la capnographie en réanimation. In: *Monitorage non-invasif en réanimation*. Paris: Masson, 1992; 31–51.
2. Hess D. Capnometry and capnography: technical aspects, physiologic aspects, and clinical applications. *Respir Care* 1990; **35:** 557–76.
3. Bhavani-Shankar K, Kumar AY, Moseley H, Hallsworth RA. Terminology and the current limitations of time capnography: a brief review. *J Clin Monit* 1995; **11:** 175–82.
4. Swedlow DB. Capnometry and capnography: the anesthesia disaster early warning system. *Semin Anesth* 1986; **5:** 194–205.

5. Hoffbrand BI. The expiratory capnogram: a measure of ventilation–perfusion inequalities. *Thorax* 1966; **21:** 518–23.
6. Bhavani-Shankar K, Moseley H, Kumar AY, Delph Y. Capnometry and anaesthesia. *Can J Anaesth* 1992; **39:** 617–32.
7. Kumar AY, Bhavani-Shankar K, Moseley HSL, Delph Y. Inspiratory valve malfunction in a circle system: pitfalls in capnography. *Can J Anaesth* 1992; **39**: 997–9.
8. Pyles ST, Berman LS, Modell JH. Expiratory valve dysfunction in a semiclosed circle anesthesia circuit: verification by analysis of carbon-dioxide waveform. *Anesth Analg* 1984; **63:** 536–7.
9. Berman LS, Pyles ST. Capnographic detection of anesthesia circle valve malfunctions. *Can J Anaesth* 1988; **35:** 473–5.
10. Podraza AG, Salem MR, Joseph NJ, Brencley JL. Rebreathing due to incompetent unidirectional valves in the circle absorber system. *Anesthesiology* 1991; **75:** A422.
11. Leigh MD, Jones JC, Mottley HL. The expired carbon dioxide as continuous guide of the pulmonary and circulatory systems during anaesthesia and surgery. *J Thorac Cardiovasc Surg* 1961; **41:** 597–610.
12. Van Genderingen HR, Gravenstein N, Van der Aa JJ, Gravenstein JS. Computer-assisted capnogram analysis. *J Clin Monit* 1987; **3:** 194–200.
13. Weingarten M. Respiratory monitoring of carbon dioxide and oxygen: a ten-year perspective. *J Clin Monit* 1990; **6:** 217–25.
14. Weingarten M. Anesthetic and ventilator mishaps: prevention and detection. *Crit Care Med* 1986; **14:** 1084–6.
15. Cote CJ, Liu LM, Szyfelbein SK, *et al.* Intraoperative events diagnosed by expired carbon dioxide monitoring in children. *Can Anaesth Soc J* 1986; **33:** 315–20.
16. Neufeld GR, Gobran S, Baumgardner JE, *et al.* Diffusivity, respiratory rate and tidal volume influence inert gas expirograms. *Respir Physiol* 1991; **84:** 31–47.
17. Worth H. Expiratory partial pressure curves in the diagnosis of emphysema. *Bull Eur Physiopathol Respir* 1986; **22:** 191–9.
18. Blanch L, Fernandez R, Saura P, Baigorri F, Artigas A. Relationship between expired capnogram and respiratory system resistance in critically ill patients during total ventilatory support. *Chest* 1994; **105:** 219–23.
19. Yaron M. Utility of the expiratory capnogram in the assessment of bronchospasm. *Ann Emerg Med* 1996; **28:** 403–7.
20. You B, Mayeux D, Rkiek B, *et al.* La capnographie expiratoire dans l'asthme: perspectives d'utilisation chez l'enfant et comme méthode de monitorage. *Rev Mal Respir* 1992; **9:** 547–52.
21. Smidt U. Emphysema as possible explanation for the alteration of expiratory PO_2 and PCO_2 curves. *Bull Eur Physiopathol Respir* 1976; **12:** 605–24.
22. Druck J, Rubio PM, Valley MA, Jaffe MB, Yaron M. Evaluation of the slope of phase III from the volumetric capnogram as a non-effort dependent surrogate of peak expiratory flow rate in acute asthma exacerbation. *Ann Emerg Med* 2007; **50** (3 Suppl): S130–1.
23. Pascucci RC, Schena JA, Thompson JE. Comparison of sidestream and mainstream capnometers in infants. *Crit Care Med* 1989; **17:** 560–2.
24. Fowler WS. Lung function studies. II. The respiratory deadspace. *Am J Physiol* 1948; **154:** 405–16.
25. Comroe JHJ, Fowler WS. Lung function studies. IV. Detection of uneven alveolar ventilation during a breath of oxygen. *Am J Med* 1951; **10:** 408–13.
26. Kars AH, Goorden G, Stijnen T, *et al.* Does phase II of the expiratory PCO_2 versus volume curve have diagnostic value in emphysema patients? *Eur Respir J* 1995; **8:** 86–92.
27. Ream RS, Schreiner MS, Neff JD, *et al.* Volumetric capnography in children: influence of growth on the alveolar plateau slope. *Anesthesiology* 1995; **82**: 64–73.
28. McRae KM, Neufeld GR. Capnogram reflects the severity of acute lung injury in a surfactant depletion model. *Anesthesiology* 1993; **79:** A301.
29. Stenz RI, Grenier BT, Arnold JH. Single breath CO_2 analysis as a predictor of lung volume in a healthy animal model during controlled ventilation. *Crit Care Med* 1998; **26:** 1409–13.
30. Arnold JH, Stenz RI, Grenier B, Thompson JE. Single-breath CO_2 analysis as a predictor of lung volume change in a model of acute lung injury. *Crit Care Med* 2000; **28:** 760–4.
31. Fletcher R, Jonson B, Cumming G, Brew J. The concept of deadspace with special reference to the single breath test for carbon dioxide. *Br J Anaesth* 1981; **53:** 77–88.
32. Langley F, Even P, Duroux P, Nicolas RL, Cumming G. Ventilatory consequences of unilateral pulmonary artery occlusion. In: *Distribution des echanges gaseaux pulmonaires*. Paris: INSERM, 1976; 209–12.
33. You B, Duvivier C, Dang VV, Grilliat JP. Expiratory capnography in asthma: evaluation of various shape indices. *Eur Respir J* 1994; **7:** 318–23.

34. Arnold JH, Stenz RI, Thompson JE, Arnold LW. Noninvasive determination of cardiac output using single breath CO_2 analysis. *Crit Care Med* 1996; **24:** 1701–5.
35. Murias GE, Villagrá A, Vatua S, *et al.* Evaluation of a noninvasive method for cardiac output measurement in critical care patients. *Intens Care Med* 2002; **28:** 1470–4.
36. Romero P, Lucangelo U, Lopez J, Blanch L. Physiologically based indices of volumetric capnography in patients receiving mechanical ventilation. *Eur Respir J* 1997; **10:** 1309–15.
37. Blanch L, Lucangelo U, Lopez J, Fernandez R, Romero P. Volumetric capnography and respiratory system mechanics in patients with acute lung injury: effects of positive end expiratory pressure. *Eur Respir J* 1999; **13:** 1048–54.
38. Romero PV, Lopez-Aguillar J, Lucangelo U, Blanch L. Alveolar ejection ratio elucidated from VCO_2 versus V_T curves. *Intens Care Med* 1995; **21:** S45.
39. Bernabè F, Vatua S, Lucangelo U, *et al.* Alveolar ejection volume predicts death in patients with acute lung injury. *Am J Respir Crit Care Med* 2003; **167:** A934.

Section 4
Chapter
33

Physiologic perspectives

Improving the analysis of volumetric capnograms

G. Tusman, A. G. Scandurra, E. Maldonado, and L. I. Passoni

Introduction

It is well known that the distribution of ventilation within the lungs is heterogeneous due to the sequential filling and emptying of pulmonary units ventilated unevenly both in series and in parallel. This inhomogeneity of ventilation is caused by the anatomical asymmetry of the airways [1,2] and gravity [3].

The analysis of expired gases has been performed for many years, with the goal of achieving a better understanding of the distribution of pulmonary ventilation [2,4–7]. These studies showed that all breathing gases are transported within the lungs by two main mechanisms: *convection* in the conductive airways and *diffusion* at the alveolar level. Thus, inter- and intraregional ventilatory inhomogeneities are highly dependent on gas convection at the macroscopic level of the airway, whereas at its microscopic acinar level, where convection is low and molecular diffusion plays a major role, the asymmetrically branching pulmonary system induces a non-uniformity of gas concentrations due to the interaction of both mechanisms of gas transport [4–7].

Carbon dioxide is considered a good marker of ventilation that can best be analyzed by volumetric capnography (VC; i.e., the plot of expired CO_2 within one tidal breath). Volumetric capnography shows that the interaction of CO_2 convection and diffusion at the bronchiolar level creates a limit or stationary interface between these gas transports, the position of which varies among lung units due to airway asymmetry [7]. At the end of inspiration, these small interfaces are located within the bronchioli, but move mouthward during expiration. Thus, during expiration, the cumulative distribution of these interfaces can be detected at the airway opening, where the mean of this stationary front is represented by the midpoint of the segment of phase II, as can be determined by linear regression.[1]

By convention, this stationary front or interface represents the limit between the airway deadspace ($V_{D_{aw}}$) and alveolar tidal volume ($V_{T_{alv}}$) [8]. Therefore, we elected to call this midpoint of the regression line of phase II the *airway–alveolar interface*.

The precise determination of this airway–alveolar interface has important clinical connotations. First, in mechanically ventilated patients, alveolar ventilation can be adjusted non-invasively if the $V_{T_{alv}}$ is known. Second, the precise location of the airway–alveolar interface is primordial for an accurate calculation of deadspace and its subcomponents [9]. In essence, the most important VC-derived variables depend highly on the unequivocal determination of this interface. Thus, the ability to correctly interpret the essential features and characteristic points of the curve are mandatory for VC to ever reach clinical relevance.

Background

Fowler's method

In 1948, Fowler was the first to describe a practical method to determine the airway–alveolar interface, known today as the *equal area method* [9]. His planimetric technique extrapolates the regression line fitted to phase III, and assumes that a vertical line is placed through the point of phase II, at which both areas *p* and *q* become equal (Figure 33.1). However, such a calculation is difficult to perform, mainly due to the

[1] When the literature mentions "the midpoint of the slope of phase II," it usually refer to "the midpoint of the segment within this phase," which most often is calculated by linear regression.

Capnography, Second Edition, ed. J. S. Gravenstein, Michael B. Jaffe, Nikolaus Gravenstein, and David A. Paulus. Published by Cambridge University Press. © Cambridge University Press 2011.

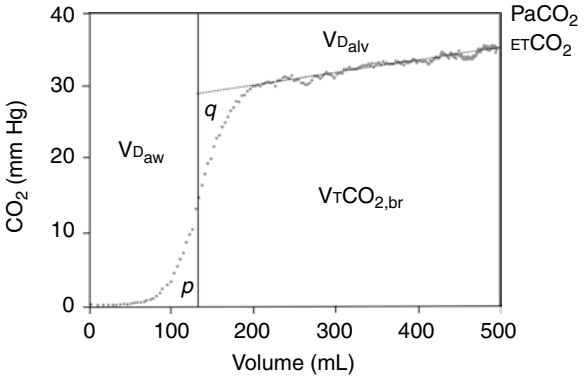

Figure 33.1 Fowler's method and its definition of the airway–alveolar interface (for more details, see text). $V_{D_{aw}}$, airway deadspace; $V_{T_{alv}}$, alveolar tidal volume; $V_TCO_{2,br}$, amount of CO_2 eliminated in one breath (mL).

asymmetry of the CO_2 curve, along with additional complicating factors. The slope of phase III (S_{III}) will have a major impact on the upper wider, and thus most influential, part of area *q*. This point was originally determined by visual inspection, a methodology that is not only imprecise but also highly subjective and non-reproducible.

At that time, Fowler performed his method by hand, but for VC to ever become useful as a clinical tool, VC analysis had to be automated. Below we present the most common computational implementation of Fowler's technique, which consists of the following sequence of steps (Figure 33.1):

(1) Computation of phase III slope (S_{III}) using linear regression from 40% to 80% of the expired volume.
(2) Definition of the start of phase II by finding the first point that rises above the inspired CO_2 baseline.
(3) Finding the maximum slope between the start of phase II and 40% of the expired volume using linear regression around this point to calculate the slope of phase II.
(4) Determining the intersection between the lines of phase II and III on the volume axis (start of phase III).
(5) Determining the position of the airway–alveolar interface by iteratively drawing vertical lines within the limits of phase II, searching for the position at which areas p and q became equal.

There are other factors that can affect the calculation of the airway–alveolar interface by Fowler's method:

- This technique is highly sensitive to noisy airflow and CO_2 raw signals [10].
- A precise measurement of this interface may require an appropriate collection of data points comprising the entire volumetric capnogram. Due to the rapid increase in CO_2 concentration during phase II, a substantial fraction of information is lost if the speed of data acquisition is low. To overcome this situation, local linear interpolation is often used.
- The deformations in VC morphology caused by lung diseases make the determination of the airway–alveolar interface particularly hard to perform since the limit between phase II and III is usually blurred and the slope of phase III becomes highly variable [11–13].

Despite all these limitations, Fowler's method generally appears as the reference method for VC analysis in most publications.

Fitting an appropriate curve to the VC is one approach that would solve most of the limitations discussed above, because it allows the replacement of a mere collection of individual data points over a desired range by a mathematically well-defined curve, especially in regions of sparse data such as phase II. The mathematically unique analytical expression obtained from such a fit permits the calculation of the clinically most relevant parameters with considerably higher precision.

A curve fitting method based on functional approximation using the Levenberg–Marquardt algorithm (FA-LMA) has been described [14]. An analytical function is obtained by a non-linear, least-squares curve fitting. This fitting of VC raw data can be viewed as an optimization problem of the parameters of a proposed function (model function).

The model function proposed is based on the generalized logistic curve

$$f(t,\mathbf{x}) = f_0(t,\mathbf{x}) + f_1(t,\mathbf{x}) + f_2(t,\mathbf{x}),$$

where:

$$f_0(t,\mathbf{x}) = x_1;$$
$$f_1(t,\mathbf{x}) = \frac{(x_2 - x_1)\,x_3}{(1+e^{(-t-x_4)/x_5})};$$
$$f_2(t,\mathbf{x}) = \frac{(x_2 - x_1)\,(1-x_3)}{(1+e^{(-t-x_6)/x_7})}.$$

The first term, $f_0(t,\mathbf{x})$, is the lower asymptote; the second and third terms are logistic curves, whose

parameterization allows the generation of a model of the VC curve, where t is the expired volume and f = concentration of CO_2. This model takes into account the well-known asymmetry of the wave shape. The parameters of the above model were generated by a non-linear least-squares curve fitting optimized by the Levenberg–Marquardt algorithm [15,16]. Figure 33.2 and Table 33.1 show the VC variables and how they were calculated.

When compared with Fowler's method, FA-LMA showed more accuracy and less variability in the calculation of the airway–alveolar interface and S_{III} in simulated and real data from patients [14].

Wolff *et al.* [13] have described the limitations and advantages of five published numerical methods for determining the airway–alveolar interface. These authors pointed out the importance of measuring the interface based on phase II of the capnogram. They showed that the scatter was large and the reproducibility poor, particularly in those techniques where the interfaces were calculated based on phase I [17] or III [18,19] of the VC. This resulted in either an under- or an overestimation of the airway–alveolar interface position. The proposed FA-LMA calculates the airway–alveolar interface focused only on phase II of the VC, thereby avoiding the theoretical problems of under- or overestimation of $V_{D_{aw}}$ and $V_{T_{alv}}$.

Fowler's method has potential pitfalls that make the calculation of the airway–alveolar interface insecure, leaving the measurements of $V_{D_{aw}}$ and $V_{T_{alv}}$ prone to errors. Among the pitfalls to consider are the noise in the data created by artifacts and bounds, the lack of an adequate interpolation of the scarce data obtained during phase II, and the influence that the S_{III} calculation has on the position of the interface. These sources of errors could explain, in part, the differences observed in $V_{D_{aw}}$ and $V_{T_{alv}}$ between Fowler's method and the FA-LMA technique [14].

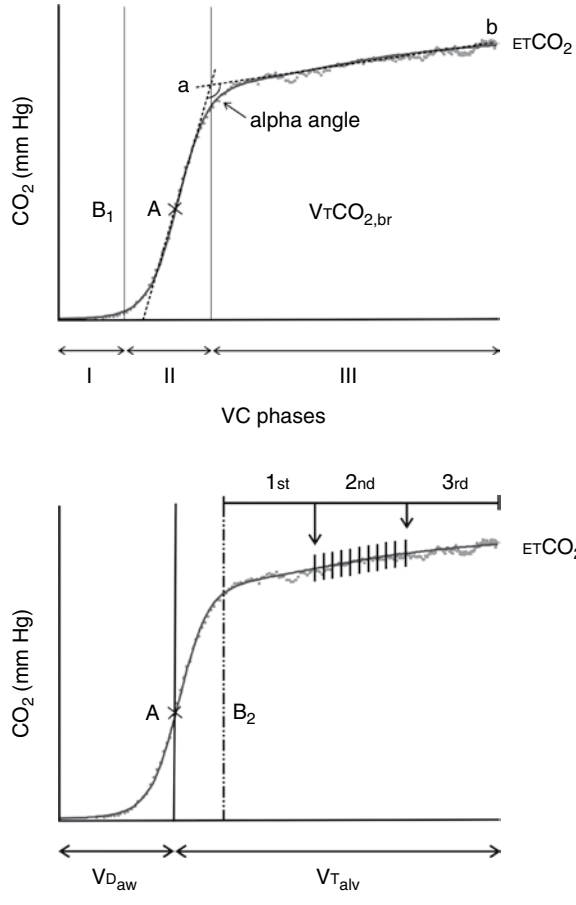

Figure 33.2 Definition of volumetric capnography (VC) variables utilizing the functional approximation using the Levenberg–Marquardt algorithm (FA-LMA). Dotted line is the VC curve as defined by the raw data acquired by the capnograph. Continuous line represents the symbolic function obtained by FA-LMA. A is the airway–alveolar interface placed at the inflection point of the entire VC curve (maximum 1st derivative). B_1 and B_2 correspond to the extremes of the 3rd derivative. B_1 is the left extreme of the 3rd derivative that represents the limit between phase I and II. The intersection between the regression lines of phase II and III determines the limit between phase II and III, and constitutes the alpha angle. The slope of phase III (S_{III}) is calculated between line B_2 and the $ET CO_2$. This portion of the VC was divided into three thirds, where the information of the function in the middle third was used to determine S_{III} (see the text for more details). $VTCO_{2,br}$, amount of CO_2 eliminated in one breath (mL); $V_{D_{aw}}$, airway deadspace; $V_{T_{alv}}$, alveolar tidal volume.

VC-derived variables

Tang *et al.* [10] observed that methods of airway–alveolar interface calculation based on the fitting of phase III are more stable, and have less susceptibility to noise as compared to Fowler's method. The lowest bias and susceptibility to noise was found when the authors' modification of Cumming's technique was used [10,20]; which is based on the x-intercept of a second-order polynomial fitted to the integrated VC curve between 40% and 80% of the expired volume. Despite the fact that Tang and coworkers [10] showed elegantly that the integration of the VC reduced noise and stabilized the determination of the interface, their approach cannot overcome the problem of overestimating the airway–alveolar interface inherent in all methods using phase III as a reference.

Table 33.1 Volumetric capnography-derived variables and their definition by functional approximation using the Levenberg–Marquardt algorithm (FA-LMA)

Parameter	Definition	FA-LMA calculation
Phase I (mL)	Portion of the V_T without CO_2.	From the start of expiration to the point of maximum rate of change of the 2nd derivative (left extreme of 3rd derivative).
Phase II (mL)	Phase II receives CO_2 from units with different perfusion and ventilatory rates.	From the point of maximum rate of change of the 2nd derivative (left extreme of 3rd derivative) to the intersection of phase II and III slopes in the volume axis.
Phase III (mL)	Phase III represents the pure alveolar gas.	From the intersection of phase II and III slopes in the volume axis until the end of expiration.
S_{II} (mm Hg/mL)	Slope of phase II.	The slope of phase II is calculated as the value of the 1st derivative at the inflection point (A).
S_{III} (mm Hg/mL)	Slope of phase III.	First, B_2 was defined as the right-hand maximum of the 3rd derivative, from which the line of phase III could be calculated. Second, phase III data on the right side of line B, until the V_T value were divided into three thirds. Third, the middle third, which is far away from potential interferences with the alpha angle and a possible phase IV/V, was used to calculate S_{III}. This third was divided into ten equidistant points, and the slopes of the analytical function at these points were calculated by the 1st derivative.
Airway–alveolar interface	Limit between convective and diffusive transport of CO_2 within the lungs.	It is calculated as the inflection point (maximum of the 1st derivative).
$V_{D_{aw}}$ (mL)	Airway deadspace.	Volume calculated from the start of expiration to the position of the airway–alveolar interface.
$V_{T_{alv}}$ (mL)	Alveolar tidal volume.	Volume derived by subtracting $V_{D_{aw}}$ from V_T.
$V_TCO_{2/br}$(mL)	Amount of CO_2 eliminated in one breath.	Area under the curve of VC calculated by integration of the function.

In our proposed analysis of the VC, the FA-LMA was applied to all raw data of the VC in order to create an analytical function that fits the collected data points optimally. Such an analytical function of curve can be adapted dynamically as changes in the "shape" of the VC are induced by changing lung physiology. Thus, once a unique curve is fitted, VC-derived variables can subsequently be calculated by robust mathematical methods and definitions. With reference to the statements above, it appears to be highly desirable to determine the airway–alveolar interface by a mathematical method such as the FA-LMA. By convention, this interface is placed around the midpoint of the segment of phase II that corresponds to the mathematical definition of the *inflection point* of the overall curve. To date, none of the published literature on VC has defined the position of the airway–alveolar interface by this method. The main advantage of this estimation method is that the airway–alveolar interface can be calculated precisely and independent of any deformation of the VC caused by interventions or diseases.

We have shown, in simulated and data from real patients, how Fowler's method under- or overestimates the positioning of the airway–alveolar interface depending on the kind of deformations in the capnograms. The inflection point determined by the FA-LMA, however, was insensitive to these changes in the shape of capnograms, and thus defined the position of this interface with greater precision [14].

Given that the analysis of deadspace and the other VC-derived variables depends on the accurate determination of the airway–alveolar interface, the proposed FA-LMA methodology has the important advantage of making the determination of VC-derived variables more precise and less sensitive to biological variability and technical noise. Another advantage of this method is that most of the VC-derived variables can be calculated independently of the others. Therefore, the method avoids the

contamination of sequential and cumulative errors in the final calculation; i.e., Fowler's method determines VD_{aw} based on a prior estimation of the slope of phase III, which, per se, is difficult to do with adequate precision.

Slope of phase III (S_{III})

One of the most important VC-derived variables is S_{III} because this slope depends directly on the distribution of ventilation and perfusion within the lungs. Several authors have elevated the role of S_{III} as a non-invasive tool for the estimation of overall ventilation–perfusion ratio ($\dot{V}/\dot{Q}$) [21]. In general, an increment in S_{III} reflects a more heterogeneous distribution of ventilation, as observed in patients with asthma [22], emphysema [12], or atelectasis [23]. In contrast, any decrement in S_{III} is related to a more homogeneous distribution of ventilation and a better matching of ventilation and perfusion, as can be witnessed during an effective treatment of bronchospasm [24], as the lung grows during childhood [25], or after applying a lung recruitment maneuver [26].

However, measurement of S_{III} is hard to perform because this part of the VC is highly affected by noise, such as that induced by any deformation of the entire curve, cardiogenic oscillations, or phases IV–V of capnograms [27,28]. Any error in S_{III} will decrease the potential value this notable variable might have in the clinical scenario. For this reason, methods such as the FA-LMA that eliminate most sources of potential errors in calculating S_{III} due to the curved portion of VC (alpha angle) and phases IV–V are needed. Calculation of S_{III} must be dynamic, and should not depend on a fixed portion of the expired tidal volume. Contrarily, methods with S_{III} measurements based on a fixed portion of the tidal volume could fail in patients with lung diseases like chronic obstructive pulmonary disease where VC curves are highly deformed [12]. This is true also for Fowler's and most of the other methods in which S_{III} is based on a sample of raw data belonging to the section between 40% and 80% of the expired volume. This effect is observed in Figure 33.3 where S_{III} was calculated with Fowler's method and the FA-LMA technique. Note that Fowler's method overestimated the S_{III} value because part of the section curve (alpha angle) extended beyond 40% of the expired tidal volume. Consequently, a curved portion of the section of the alpha angle was included in the slope calculation and, therefore, the real value of S_{III} was overestimated.

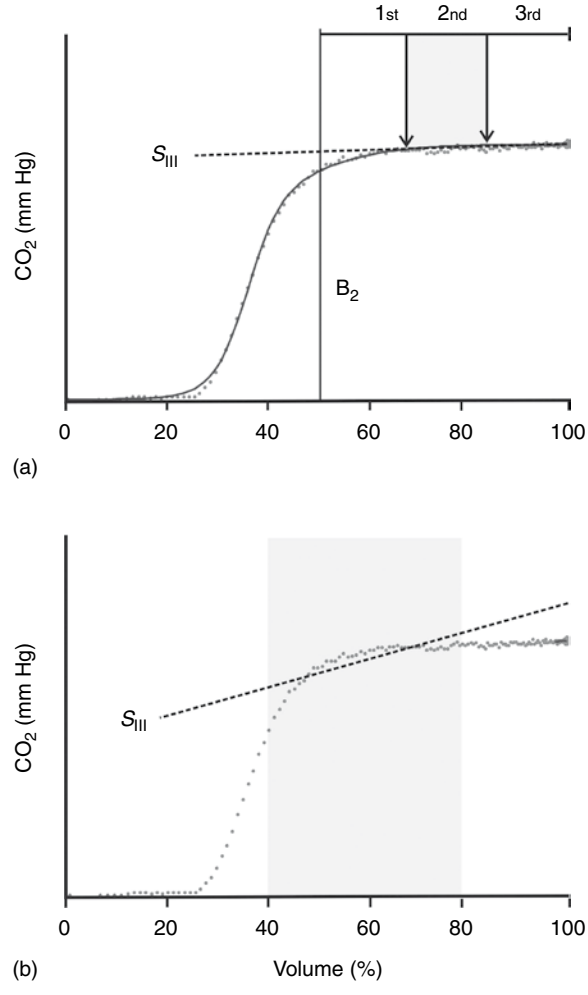

Figure 33.3 Calculation of the slope and the corresponding line of phase III (dotted line) using FA-LMA (a) and the implementation of Fowler's method (b). The same volumetric capnography curve belonging to a patient with a high airway deadspace induced by 10 cm H_2O of positive end-expiratory pressure was analyzed by the two methods. Note that Fowler's method overestimated the slope of phase III (S_{III}) because a section of the curve extends beyond 40% of the expired tidal volume and was thus included in the calculation. The FA-LMA avoided this error in the calculation of S_{III} because line B_2 was dynamically adapted to the curve.

Clinical implications of improved volumetric capnography analysis

Volumetric capnography has proven useful for monitoring ventilation in anesthetized patients [24,29] for:

- diagnosing pulmonary embolism [30] and monitoring its treatment [31];

- determining the optimum level of positive end-expiratory pressure after lung recruitment maneuvers [29]; or
- predicting the outcome of patients with acute respiratory distress syndrome [32].

However, the technical limitations observed in commercial capnographs, the lack of a complete understanding of the meaning of VC-derived variables, and the poor analysis of such curves commonly applied are the main restrictions that prevent VC from becoming an indispensable tool for clinical monitoring and decision-making. A more precise and mathematically robust method of analysis of VC is mandatory for generating more knowledge about the important significance of VC-derived variables. Such standardized analysis of VC could also aid understanding of the physiologic effects that therapies like mechanical ventilation have on a patient's lung.

The application of the more accurate method as presented in this chapter would facilitate continuous bedside monitoring of lung physiology by means of VC-derived variables and improve their quality. In this context, S_{III} is of special clinical value because it noninvasively provides real-time information on the $\dot{V}/\dot{Q}$ relationship of any lung.

Conclusions

The functional approximation of the volumetric capnogram by a Levenberg–Marquardt algorithm provides a new means for determining the airway–alveolar interface in a mathematically robust way. This process, in turn, allows the subsequent measurement of airway deadspace, alveolar tidal volume, and the rest of VC-derived variables, such as S_{III}, with accuracy. This methodology avoids most of the known limitations not only of Fowler's method but also of other techniques. Therefore, FA-LMA can be considered a robust, reproducible, and potentially useful tool for analyzing VC-derived clinical data.

References

1. Altermeier WA, McKinney S, Glenny RW. Fractal nature of regional ventilation distribution. *J Appl Physiol* 2000; **88:** 1551–7.
2. Dutrieue B, Vanholsbeeck F, Verbank S, Paiva M. A human acinar structure for simulation of realistic alveolar plateau slopes. *J Appl Physiol* 2000; **89**: 1859–67.
3. West JB, Dollery CT, Naimark A. Distribution of blood flow in isolated lung; relation to vascular and alveolar pressures. *J Appl Physiol* 1964; **19**: 713–24.
4. Verbank S, Paiva M. Model simulations of gas mixing and ventilation distribution in the human lung. *J Appl Physiol* 1990; **69**: 2269–79.
5. Prisk GK, Guy HJ, Elliot AR, West JB. Inhomogeneity of pulmonary perfusion during sustained microgravity on SLS-1. *J Appl Physiol* 1994; **76**: 1730–8.
6. Crawford ABH, Makowska M, Paiva M, Engel LA. Convection-dependent and diffusion-dependent ventilation maldistribution in normal subjects. *J Appl Physiol* 1985; **59**: 838–46.
7. Engel LA. Gas mixing within acinus of the lung. *J Appl Physiol* 1983; **54**: 609–18.
8. Gomez DM. A physico-mathematical study of lung function in normal subjects and in patients with obstructive pulmonary diseases. *Med Thorac* 1965; **22**: 275–94.
9. Fowler WS. Lung function studies. II. The respiratory dead space. *Am J Physiol* 1948; **154**: 405–16.
10. Tang Y, Turner MJ, Baker AB. Systematic errors and susceptibility to noise of four methods for calculating anatomical deadspace from the CO_2 expirogram. *Br J Anaesth* 2007; **98:** 828–34.
11. Fletcher R, Jonson B. The concept of deadspace with special reference to the single breath test for carbon dioxide. *Br J Anaesth* 1981; **53:** 77–88.
12. Schwardt JD, Neufeld GR, Baumgardner JE, Scherer PW. Noninvasive recovery of acinar anatomic information from CO_2 expirograms. *Ann Biomed Eng* 1994; **22:** 293–306.
13. Wolff G, Brunner JX, Weibel W, *et al.* Anatomical and series deadspace volume: concept and measurement in clinical praxis. *Appl Cardiopulm Pathophysiol* 1989; **2:** 299–307.
14. Tusman G, Scandurra A, Bohm SH, Suarez Sipmann F, Clara F. Model fitting of volumetric capnograms improves calculations of airway deadspace and slope of phase III. *J Clin Monit Comput* 2009; **23:** 197–206.
15. Levenberg K. A method for the solution of certain problems in least squares. *Q Appl Math* 1944; **2:** 164–8.
16. Marquardt D. An algorithm for least-squares estimation of nonlinear parameters. *J Appl Math* 1963; **11:** 431–41.
17. Olsson SG, Fletcher R, Jonson B, Nordstroem L, Prakash O. Clinical studies of gas exchange during ventilatory support: a method using the Siemens-Elema CO_2 analyzer. *Br J Anaesth* 1980; **52:** 491–8.
18. Hatch T, Cook KM, Palm PE. Respiratory deadspace. *J Appl Physiol* 1953; **5:** 341–7.

19. Langley F, Even P, Duroux P, Nicolas RL, Cumming G. Ventilatory consequences of unilateral pulmonary artery occlusion. *Colloques Inst Natl Santé Recherche Med* 1975; **51:** 209–14.
20. Cumming G, Guyatt AR. Alveolar gas mixing efficiency in the human lung. *Clin Sci (London)* 1982; **62:** 541–7.
21. Hofbrand BI. The expiratory capnogram: a measure of ventilation–perfusion inequalities. *Thorax* 1966; **21:** 518–24.
22. You B, Peslin R, Duvivier C, *et al.* Expiratory capnography in asthma: evaluation of various shape indices. *Eur Respir J* 1994; **7:** 318–23.
23. Tusman G, Corrado O, Böhm SH, Melkun F, Nador C. Análisis del espacio muerto durante la cirugía cardíaca. *Rev Arg Anest* 2002; **60:** 75–83.
24. Gustafsson PM, Ljungberg HK, Kjellman B. Peripheral airway involvement in asthma assessed by single-breath SF_6 and He washout. *Eur Respir J* 2003; **21:** 1033–9.
25. Ream RS, Screiner MS, Neff JD, *et al.* Volumetric capnography in children: influence of growth on the alveolar plateau slope. *Anesthesiology* 1995; **82:** 64–73.
26. Tusman G, Böhm, SH, Suárez Sipmann F, Maisch S. Lung recruitment improves the efficiency of ventilation and gas exchange during one-lung ventilation anesthesia. *Anesth Analg* 2004; **98:** 1604–9.
27. Wong EG, Prisk GK, Hastings RH, Dueck R. Capnographic identification of expiratory flow limitation. *Anesthesiology* 2008; **109:** A1230.
28. Nichol GM, Michels DB, Guy HJB. Phase V of the single-breath washout test. *J Appl Physiol* 1982; **52:** 34–43.
29. Scandurra A, Hedenstierna G. Monitoring deadspace during recruitment and PEEP titration in an experimental model. *Intens Care Med* 2006; **32**: 1863–71.
30. Verschuren F, Liistro G, Coffeng R, *et al.* Volumetric capnography as a screening test for pulmonary embolism in the emergency department. *Chest* 2004; **125:** 841–50.
31. Gariani A, Col J, Reynaert M, Liistro G. Volumetric capnography as a bedside monitoring of thrombolysis in major pulmonary embolism. *Intens Care Med* 2004; **30:** 2129–30.
32. Nuckton TJ, Alonso JA, Kallet RH, *et al.* Pulmonary deadspace fraction as a risk factor for death in the acute respiratory distress syndrome. *N Engl J Med* 2002; **346:** 1281–6.

Section 4
Chapter
34

Physiologic perspectives

Capnography and the single-path model applied to cardiac output recovery and airway structure and function

P. W. Scherer, J. W. Huang, and K. Zhao

In the first edition of *Capnography: Clinical Aspects*, we introduced the mathematical single-path model (SPM) of airway gas transport [1] and compared its predictions with experimental data in many clinical and physiological applications. In this second edition, we focus specifically on two of these applications.

Cardiac output and mixed venous PCO_2 recovered non-invasively from single breath volume-based capnograms in goats

Introduction

Cardiac output is a physiological parameter of general clinical value, but especially of importance to physicians managing a patient who requires intensive care. Quantifying the volume of blood ejected per unit time is an important indicator of myocardial function that is affected by a variety of physiologic conditions. The conventional thermodilution method for determining cardiac output requires right heart catheterization. It is a procedure that is associated with increased morbidity and mortality [2], as it requires the insertion of a catheter through the vena cava, atrium, ventricle, and into the pulmonary artery. Serious complications include rupturing of cardiac valves, wall, or vessels in the lung. A non-invasive procedure would permit a more rapid recovery and reduce medical complications. Furthermore, in addition to reduced patient anxiety, the associated healthcare costs may be decreased through improved, but less invasive, cardiac monitoring. We have demonstrated in goats that non-invasive cardiac output determination, using the single-path convection–diffusion model [3,4] as proposed by Scherer *et al.* [5], is a feasible solution to this problem [6]. In this chapter, the SPM-based, non-invasive method for simultaneously estimating cardiac output (Q_B) and mixed venous PCO_2 (C_B), solely from breath-to-breath carbon dioxide ($SBCO_2$) washouts in the form of volumetric capnograms, is presented.

Methods

Volumetric capnogram

The CO_2 washout[1] curve (capnogram or concentration of CO_2 plotted vs. volume expired) is divided into three phases as depicted in Figure 34.1. Phase I consists of gas from the uppermost conducting airways, which has very low CO_2 concentration. Phase II is the rapid rise in CO_2 concentration, which represents the airway concentration gradient between the high CO_2 concentration in the acinar airways and the low CO_2 concentration in the upper conducting airways. Phase III is the alveolar plateau, which represents CO_2 from the alveolated acinar airways, which has evolved from the blood. We mathematically define the phase III slope for a given breath as the segment with a center at 60% of the total expired CO_2 volume and ±35% of the Fowler deadspace,[2] away from that center point. We normalize the phase III slope by dividing it by the mixed expired CO_2 concentration to get the normalized slope (NS), which has units of L^{-1}. This normalization allows the comparison of slopes for breaths taken at different tidal volumes and ventilating frequencies. $\dot{V}CO_2$, the total amount of CO_2 gas exhaled in milliliters per breath, is given by the area under the washout curve.

[1] Washout used to reflect more accurately the underlying physiologic processes.

[2] Volume of the conducting airways at the "midpoint" of the transition from deadspace to alveolar gas determined using method of Fowler [7].

Capnography, Second Edition, ed. J. S. Gravenstein, Michael B. Jaffe, Nikolaus Gravenstein, and David A. Paulus. Published by Cambridge University Press. © Cambridge University Press 2011.

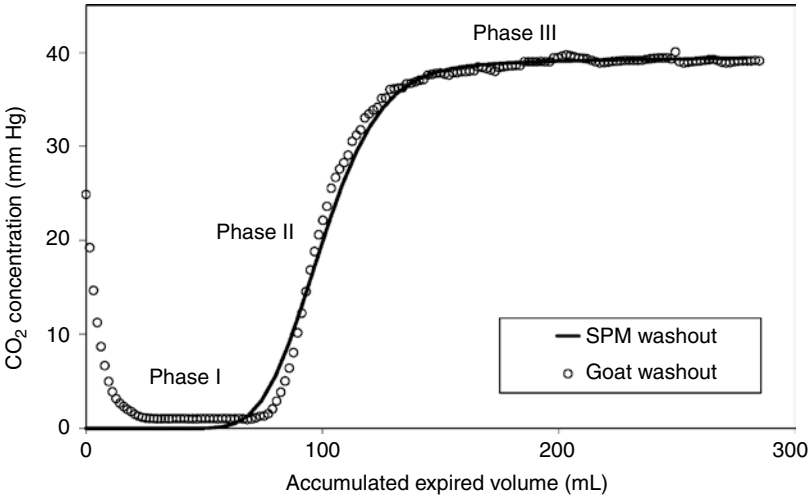

Figure 34.1 A typical CO_2 washout curve obtained from a goat subject (discrete circles) and SPM prediction (continuous line). Phase III is the alveolar plateau toward the end of the curve. The $\dot{V}CO_2$ is the total amount of CO_2 gas exhaled given by the area under the washout curve.

Single-path model

Quantitative analysis of the accumulated expired CO_2 waveform using the SPM, a mathematical model of gaseous convection and diffusion in the mammalian respiratory system [4], allows the calculation of a number of variables relevant to the monitoring of respiratory efficiency and the relationship between ventilation and pulmonary perfusion. The branching three-dimensional structure of the lung airways is approximated by the one-dimensional (spatial) SPM "trumpet bell" model as shown schematically in Figure 34.2. The SPM equation that governs the changes in CO_2 concentration within the airways is:

$$(V + V_A)\frac{\partial c}{\partial t} + Q\frac{\partial c}{\partial z} = \frac{\partial}{\partial z}\left(\frac{DA}{l}\frac{\partial c}{\partial z}\right) + S(z,t) \quad (34.1)$$

where V, A, l, and V_A represent airway volume, total cross-sectional area, length and alveolar volume per generation in a given generation; D is the molecular diffusivity of CO_2 in air; $Q(z,t)$ is airway gas volume flow rate, and z is the continuous non-dimensional generational coordinate; c is the airway concentration of CO_2, and S is a pulmonary blood source term [4,8] for CO_2 having the form

$$S(z,t) = Q_B \cdot \lambda \cdot \frac{N_A(z)}{N_T} \cdot [C_B - c(z,t)] \quad (34.2)$$

where λ is CO_2 solubility, and $N_A(z)/N_T$ is the fraction of total alveoli per generation. The alveolar volume $V_A(z,t)$ expands and contracts to accommodate the tidal volume while $V(z)$ represents the volume of the airways, assumed to be rigid cylindrical tubes with circular cross-sections. In equation (34.1), the four terms – from left to right – represent the accumulation of CO_2 in the airway and alveoli, convective CO_2 transport, longitudinal diffusion of CO_2, and the alveolar evolution of CO_2 from capillary blood.

The SPM consists of the convection–diffusion equation (34.1) applied to the axisymmetric trumpet bell airway model (Figure 34.2), with a source term representing the evolution of CO_2 from the bloodstream [4]. In this longitudinal one-dimensional model, it is assumed that radial mixing occurs instantaneously, a logical assumption in the alveolated airways given the small size of the tubes. The SPM input parameters include tidal volume (VT), breathing frequency (f), functional residual capacity (FRC), C_B, Q_B, gas phase molecular diffusivity in air (D_{mol}), and oropharynx volume (V_{z0}). The boundary conditions used for solving equation (34.1) are $\partial c/\partial z = 0$ at the acinar end ($z = 23$) throughout the breath cycle, $c = c_{insp} = 0$ at the mouth ($z = 0$) during inspiration, and $\partial c/\partial z = 0$ at the mouth during expiration. The initial condition is $c = c_{init}$ throughout the airway, which is set at 4 mm Hg below C_B, the mixed venous PCO_2 concentration. Using these boundary and initial conditions, equation (34.1) is solved to generate the steady-state CO_2 washouts (volumetric capnogram) used in the non-invasive recovery routine. By minimizing the differences between the capnogram obtained from the subject and those produced by the SPM, we can estimate the volume of right ventricular blood ejection to the lung, from which the exhaled CO_2 evolves and the C_B.

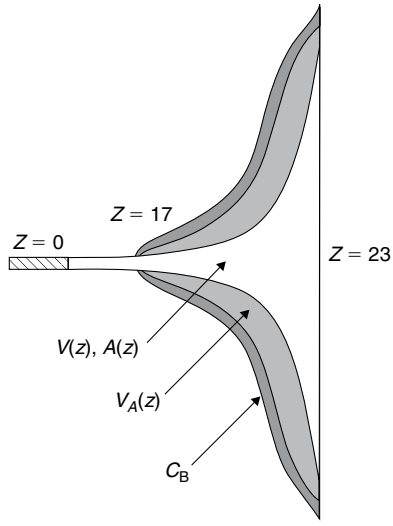

Figure 34.2 Single-path representation of the lung airways used for the numerical SPM. In this symmetrical model, airway length, diameter, and number of alveoli are specified for 23 generations of dichotomous branching airways from the oropharynx ($z = 0$) to the alveolated acinar generations ($z = 17$ to $z = 23$) where pulmonary gas and blood interfaces are located. [From: Schwardt JD, Gobran SR, Neufeld GR, Aukburg SJ, Scherer PW. Sensitivity of CO_2 washout to changes in acinar structure in a single-path model of lung airways. *Ann Biomed Eng* 1991; **19**: 679–97.]

Acinar airway reduction factor β

The NS is very sensitive to the subject's total acinar airway cross-sectional area and, to a lesser extent, the FRC for a given f and VT (see Figure 34.3). The SPM assumes complete 23-generation symmetrical branching of the airway. However, in physiological lungs, airway branching is more randomized, and will cause the actual airway total cross-section at a given inhaled volume to be smaller than that of the symmetrical SPM. In addition, the moving air fronts of the tidal volume into the FRC are parabolic shaped, whereas in the SPM, flat fronts are assumed, which tend to overestimate the cross-sectional area of the true airway at a given inhaled volume. Furthermore, the effectiveness of thoracoabdominal motion during breathing enables airflow to rapidly reach the bottom of the lung, which is especially apparent during smaller tidal volumes. Thus, real lung mechanisms cause the effective airway to appear narrower than the symmetrically defined airway with any tidal volume less than maximal. The structure of the standard symmetric Haefeli-Bleuer and Weibel acinar morphometry [9], coupled with the idealized SPM, therefore, requires conformal scaling in order to provide the best approximated functionality of each individual lung for a given subject.

The degree to which the NS vs. VT curve of the subject differs from that generated numerically by the SPM is adjusted by a uniform acinar area reduction factor β. A uniform reduction in acinar cross-sectional area, characterized by a given value of β, is accompanied by an increase in acinar length L during the SPM computation [10]. This is done to maintain FRC at measured or typical physiological values. The sensitivity of the NS to changes in the total airway cross-sectional area (β in the goat lung) is shown in Figure 34.3. A value of β appropriate for a given subject is found when the subject normalized phase III slope and that from the model simulation calculated with the equivalent parameters (FRC, VT, and f) are equal.

Minimization

When the subject β value for the SPM is set, Q_B and C_B are determined from the SPM simulated values when a simultaneous minimization is achieved in both $\dot{V}CO_2$ and NS between the subject and the model (Figure 34.4). The first step of this process for a goat subject is shown in Figure 34.5a where the absolute differences between the experimental $\dot{V}CO_2$ obtained from a given breath is compared to a series of $\dot{V}CO_2$ generated by the SPM over a range of Q_B and C_B. The darkest area represents the minimal differences between the experimental and the SPM values. The same plot is shown in Figure 34.5b for the absolute differences between experimental NS and a series of NS values generated by the SPM over a range of Q_B and C_B. The best model match between the SPM and the subject is achieved by seeking the simultaneous minimum in both of these two surfaces. The Q_B and C_B values at the simultaneous minimum generated by the SPM will be the final estimation for the subject.

To save time and because the surfaces are smooth, the two surfaces (Figure 34.5a and b) are combined into one single surface (Figure 34.6). Then, a surface minimization algorithm is utilized to seek a global minimum on the combined surface. In order to obtain a simultaneous minimum, the two surfaces must first be normalized and then summed together to obtain a single surface. Normalizing weights are applied in order to achieve a common range. The weight for one surface is the height range of the other surface and vice versa. After summing the normalized $\dot{V}CO_2$ and NS surfaces together, a new surface is obtained, as shown in Figure 34.6. Then a common minimum can be sought by high-definition cubic spline interpolation. Since the surface is smooth, the minimal point is

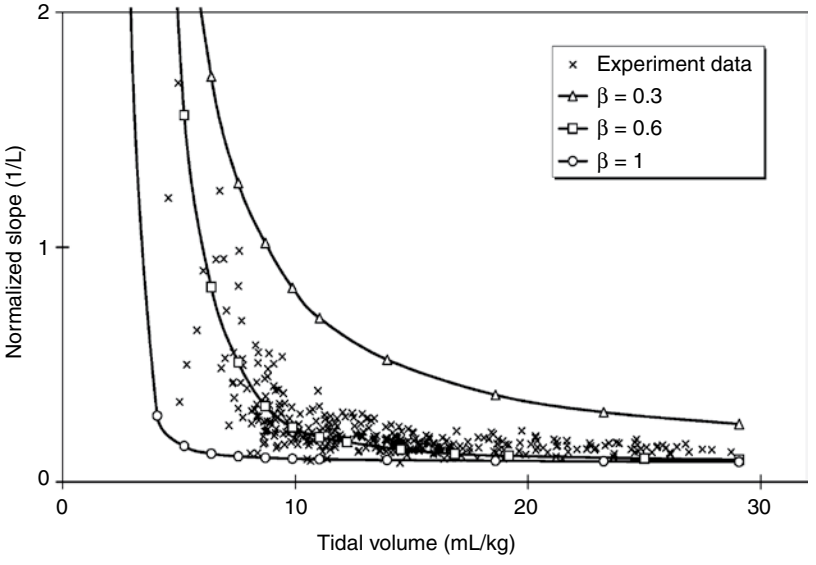

Figure 34.3 Effects of acinar scaling factor β on normalized slope vs. tidal volume. The SPM NS is very sensitive to the β acinar airway reduction factor. In this figure, the goat lung NS was obtained from the SPM with different β while varying the tidal volume. Because of a decrease in acinar cross-sectional area, the NS is higher when β is lowered.

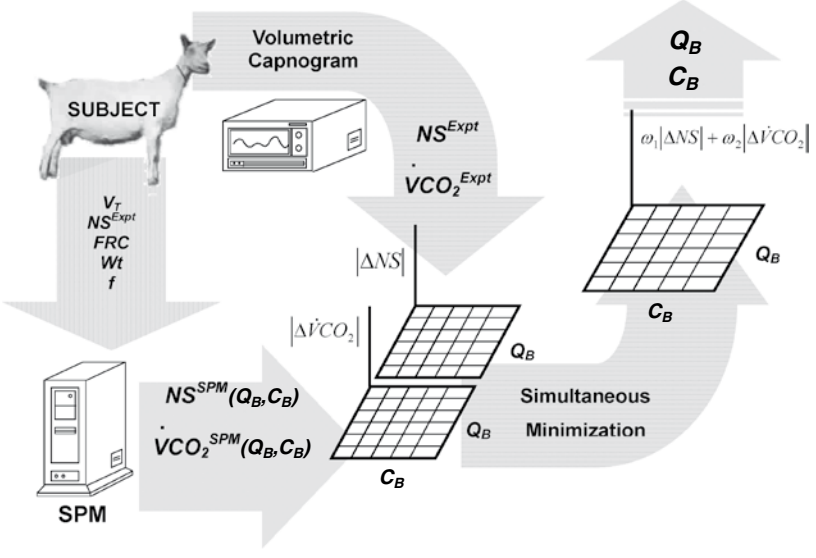

Figure 34.4 Schematic diagram of Q_B and C_B recovery procedure. Iteration to obtain a new β value is not shown.

easily obtained by a simple iteration procedure with a defined step size.

Performance evaluation in goats

The method described for the estimation of Q_B and C_B was applied to 82 data points collected from 21 goats under anesthesia with controlled ventilation. (Six data points were discarded due to invalid physiological conditions.) Ventilation was performed at a targeted tidal volume set by the mechanical ventilator (8, 10, 12, 15, or 18 mL/kg). Each data point consists of averaged hemodynamics, mixed venous and arterial blood samplings of CO_2 gases, and breath-to-breath volumetric capnograms taken over a period of 20 to 40 breaths after steady state has reached.

To model the goat lung, the Weibel human airway morphology [9] was modified since no similar anatomic goat lung data are available. A larger deadspace was added to represent the longer goat trachea, and the FRC was reduced to reflect the smaller lung of the goat compared to the human lung. The model was adjusted with a given set of physiological parameters and β to find a best fit for the phase III region over most of the goats. A typical match of the goat SPM to the experimental capnogram is shown in Figure 34.1. Although it is difficult to obtain a perfect fit, the objective is to seek

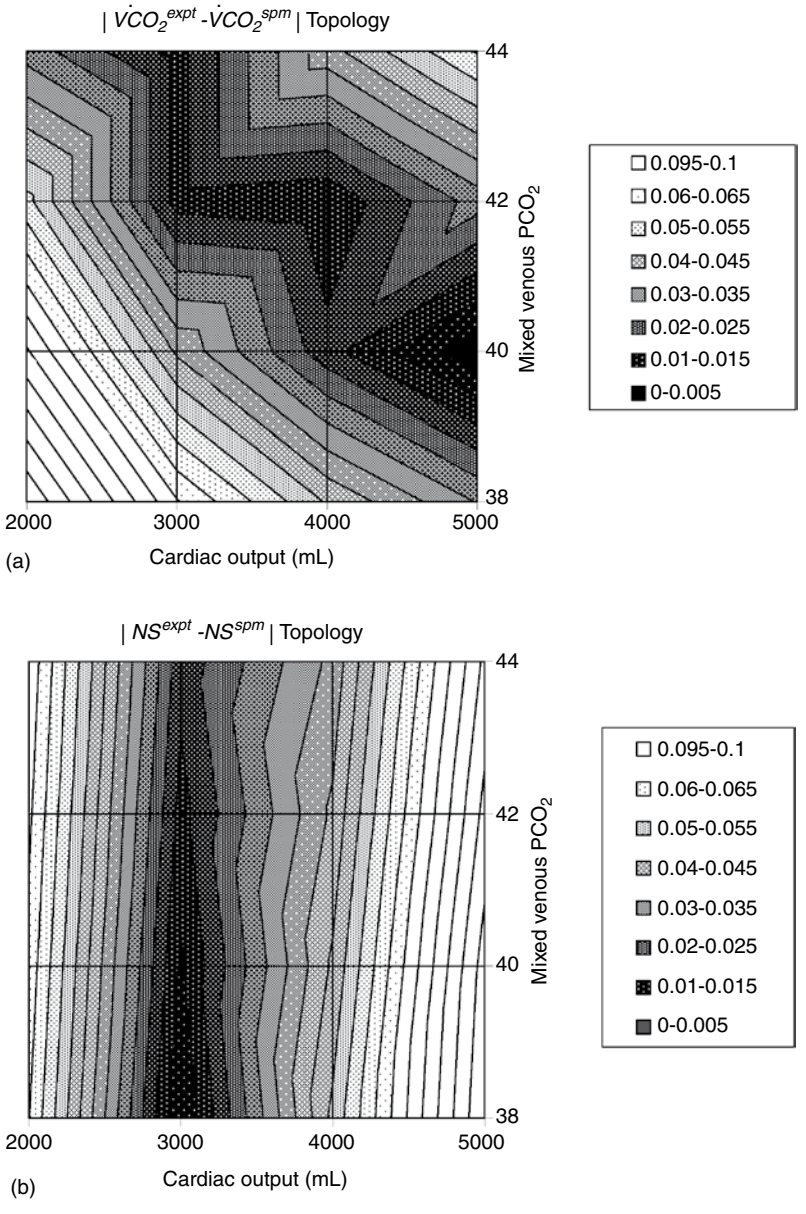

Figure 34.5 (a) The normalized absolute differences between $\dot{V}CO^{expt}$ and $\dot{V}CO_2^{SPM}$ are plotted on a contour plot over a range of cardiac output and mixed venous pCO_2 values. The darker area depicts minimal differences between $\dot{V}CO_2^{expt}$ and $\dot{V}CO_2^{SPM}$. (b) The normalized absolute differences between NS^{Expt} and NS^{SPM} are similarly plotted.

for a reasonable phase III fit with the experimental data for all the goats.

Results

In order to evaluate the accuracy of the SPM method for estimating the cardiac output, the recovered Q_B is compared to that calculated by the mass balance equation for CO_2 based on the Fick principle:

$$\dot{V}CO_2 = Q_B \cdot \lambda \cdot (\sqrt{C_B} - \sqrt{C_{art}}) \quad (34.3)$$

where λ is the CO_2 solubility factor ($\lambda = 2.13$), C_{art} is the arterial PCO_2 concentration, and Q_B is the cardiac output calculated from the other three experimentally measured variables. This cardiac output value is the "gold standard" used to compare the recovered results by the SPM method for the goat data.

In Figure 34.7, the SPM-recovered values of Q_B are compared to the values of Q_B calculated from the mass balance equation as shown by the identity plot. Most estimated data points are within the ±15% error lines. Overall, an absolute averaged error of 16.7% ± 8.6%

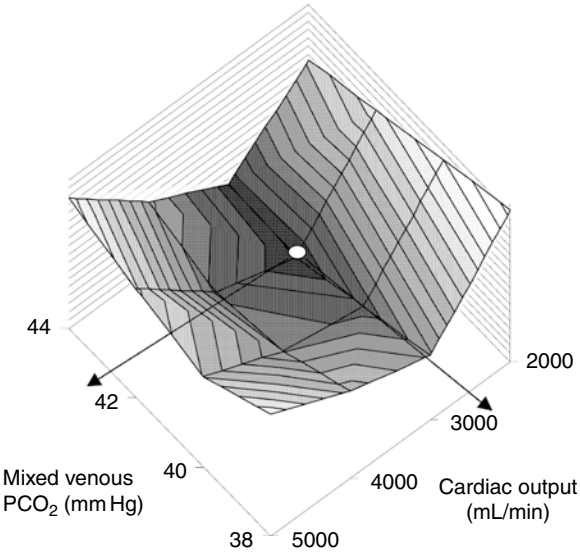

Figure 34.6 NS and VCO_2 combined topology. The combined topology is obtained by normalizing Figure 34.5a and Figure 34.5b, then summing point by point. The minimum point of this surface (white circle) is found by high-definition cubic spline interpolation. [From: Huang J. Non-invasive estimation of cardiac output and mixed venous PCO_2 using the single path model of gas exchange. Ph.D. dissertation, University of Pennsylvania, Philadelphia, PA, 2000.]

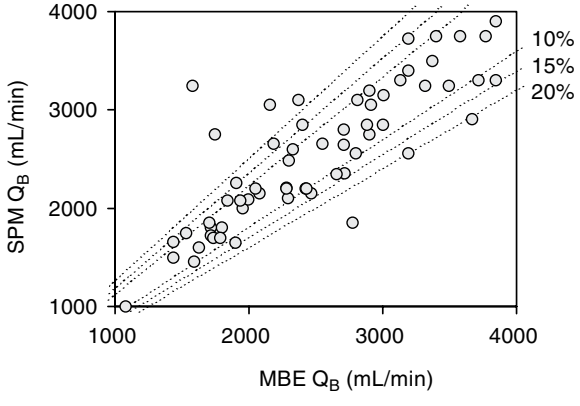

Figure 34.7 Goat Q_B estimation accuracy by the SPM-based method. Comparison of the cardiac outputs (Q_B) recovered from the SPM and the goat experiment data, calculated by the mass balance equation. The three diagonal lines are the error rates of ±10%, ±15%, and ±20%, respectively. Most recovered Q_B were within the ±15% error lines with only a few outliers. [From: Huang J. Non-invasive estimation of cardiac output and mixed venous PCO_2 using the single path model of gas exchange. Ph.D. dissertation, University of Pennsylvania, Philadelphia, PA, 2000.]

was achieved. Most of the outliers tend to have smaller tidal volumes where the NS is extremely sensitive and difficult to estimate for the SPM.

In Figure 34.8, the SPM-recovered C_B is compared to the goat C_B experimentally obtained, as shown by

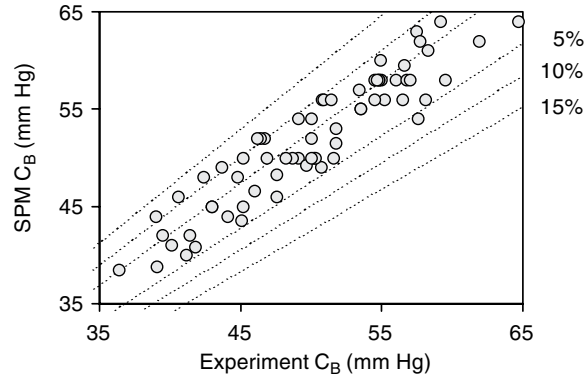

Figure 34.8 Goat C_B estimation accuracy of SPM-based method. Comparison of the mixed venous PCO_2 (C_B) recovered from the SPM and the goat experimental data. The three diagonal lines are the error rates of ±5%, ±10%, and ±15%, respectively. Most recovered C_B were within the ±5% error lines. There is a slight systematic overestimate by the SPM. [From: Huang J. Non-invasive estimation of cardiac output and mixed venous PCO_2 using the single path model of gas exchange. Ph.D. dissertation, University of Pennsylvania, Philadelphia, PA, 2000.]

the identity plot. Most estimated data points are very accurate, i.e., within the ±5% error lines. Overall, an absolute averaged error of 5.6% ± 4.4% was achieved. A slight systematic overestimation was observed. This shift may be due to the site from which the C_B data was collected experimentally and differences in anatomy between the Weibel human and goat lung.

This non-invasive method of cardiac output recovery from the SPM, therefore, gives similar accuracy as the invasive thermodilution method and, in addition, provides a highly accurate value for the mixed venous PCO_2. At present, the method is computer-time-intensive but, in principle, could be speeded up for use in real time by creating a large-scale SPM database.

Discussion and conclusion

Cardiac output is a physiological parameter that tends to have greater intrinsic variation than mixed venous PCO_2, which is tightly controlled by the body. This difference may have contributed to the higher error percentage in Q_B than in C_B recovered by the SPM.

We observed that the accuracy of the recovered Q_B and C_B values depends heavily on the selection of the β airway cross-section reduction factor. For large tidal volumes, the NS is mostly controlled by continued CO_2 evolution, and the NS is fairly constant and reproducible for a given breathing frequency. Therefore, the task of selecting a β reduction factor for a large tidal volume in the SPM is simple.

As tidal volume falls below 10 mL/kg, the NS increases rapidly, as shown in Figure 34.3, which causes the NS to become less predictable as airway cross-sectional area decreases. The large rise in the NS seen for small values of VT is due to the effect of molecular diffusion on CO_2 gas exchange between the VT and the FRC, as the smaller VT penetrates less deeply into the peripheral acinar airways and encounters smaller total airway cross-sectional areas. This makes fitting the β reduction factor very difficult because the NS variance at smaller VT is much larger than at high VT, as shown in Figure 34.3. The difficulty in finding the best β reduction factor for smaller VT degrades the recovery accuracy for data points with VT ≤ 10 mL/kg.

The accuracy of this SPM-based method for cardiac output estimation may be diminished for various physiological condition anomalies. If pulmonary blood shunts are present, parts of the lung will not be perfused evenly, thus causing a derangement of the ventilation–perfusion relationship. The SPM recovery method will not account for the shunted blood that is not ventilated; thus, with the significant shunt fraction, the SPM recovery method may underestimate the true Q_B. The extent of this underestimation can be assessed only when the system is developed and applied to patients with known pulmonary shunt.

Abrupt changes in cardiac output that arise spontaneously or are produced pharmacologically may not be reflected in changes in the capnogram in a timely manner. This delay or possibly complete loss of recovery may occur with the SPM method. However, the proposed method should still be capable of showing the trend in these rapidly changing clinical settings. Since the SPM recovery method does not require re-establishing the baseline, it will automatically provide the most accurate estimation when steady state is re-established. Human or animal testing will be necessary to determine the adequacy of the SPM recovery method in these unsteady cases.

Longitudinal gas diffusive resistance and design of the human acinar airway

Introduction and background

The question of why bronchial airway generations have certain average lengths and diameters [11,12], and what are the gas transport consequences of these dimensions, has received some research attention. It has long been recognized that the upper proximal airways serve to conduct gases, mostly by convection, to the lower acinar airways where transport by molecular diffusion predominates. Wilson showed that for generations 0 to 10, the ratio of average airway diameters between consecutive generations $d_n/d_{n+1} \cong 2^{1/3}$ was consistent with a design that minimizes, for a given alveolar ventilation rate, respiratory muscle metabolism [13]. Using the same argument, Wilson and Lin were less successful in explaining the increase in total airway cross-sectional area with generation, $A(z)$, between generations 12 and 18 where both convection and diffusion of gases occur [14].

The SPM of airway gas diffusion and convection [4] provides new insight into the exchange of respiratory gases between the tidal volume, and the resident FRC during resting breathing. For example, as shown for CO_2 in Figure 34.9, for steady-state breathing of a 750-mL tidal volume, VT, with a sinusoidal period of 5.0 s, the greater part of the flow of CO_2 from the FRC into the VT occurs during the second half of inspiration. At this time in the breath cycle, the VT–FRC interface is, as shown, moving through the acinar airways, and the exchange between the two volumes occurs mostly by longitudinal molecular diffusion. This is confirmed by changes in acinar airways CO_2 concentration, which is seen in Figure 34.9 to drop while this exchange is transpiring, and to rise during expiration when CO_2 is added back into the acinar FRC by pulmonary capillary blood flow.

This picture of longitudinal diffusive gas exchange between the VT and FRC motivates us to hypothesize that the total acinar airway cross-section $A(x)$ function (where x is longitudinal distance along the acinus) is designed to minimize the resistance to this exchange while simultaneously satisfying other constraints. The optimal acinar $A(x)$ function can thus be estimated by standard methods of the calculus of variations [15].

Methods

From Fick's first law of diffusion and its analogy to Ohm's law for the flow of direct current through a resistor, the differential resistance to longitudinal diffusion along the variable $A(x)$ acinus can be defined as:

$$dR = \frac{dx}{AD} \tag{34.4}$$

where D is the molecular diffusivity in air ($DCO_2 \cong 0.17$ cm²/s, $DO_2 \cong 0.2$ cm²/s).

Therefore, cumulative longitudinal acinar airway diffusive resistance $R(x)$ can be estimated by integrating

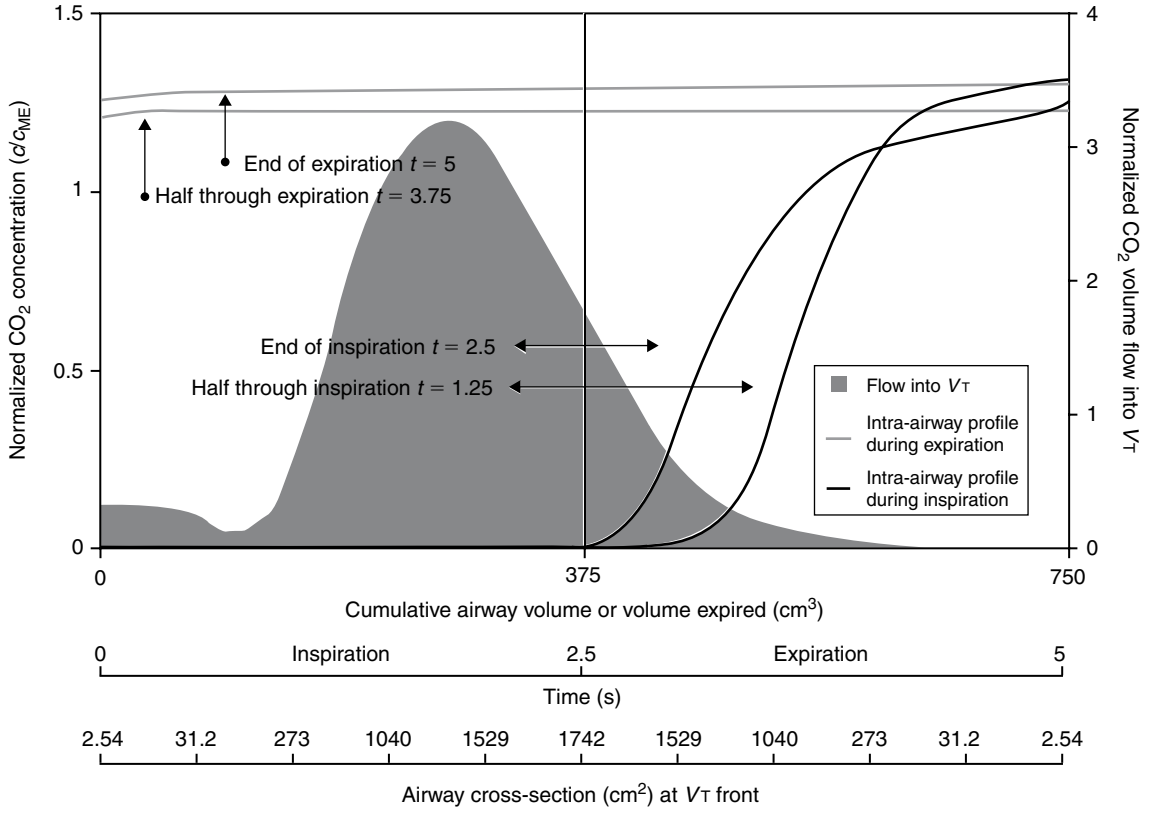

Figure 34.9 Normalized intra-airway CO_2 gas concentration and CO_2 volume flow into the tidal volume as computed by the SPM for sinusoidal breathing in a healthy adult lung. CO_2 volume flow into the V_T is normalized by dividing by the average $\dot{V}CO_2$ per breath. The computation shows that most CO_2 is transferred into the V_T during the second half of inspiration and that CO_2 concentration rises in the acinar airways during expiration due to evolution from the pulmonary capillary blood. [From: Huang J. Non-invasive estimation of cardiac output and mixed venous PCO_2 using the single path model of gas exchange. Ph.D. dissertation, University of Pennsylvania, Philadelphia, PA, 2000.

equation (34.4) between $x = 0$ and any point x along the acinus

$$R(x) = \int_0^x \frac{d\varsigma}{AD} \tag{34.5}$$

while the total longitudinal diffusive resistance is $R(a) = \int_0^a \frac{dx}{AD}$, where a is the total length of the acinus or approximately 8 mm [9,11,12,16]. If one assumes that the $A(x)$ function represents a surface of revolution of local circular radius $y(x)$, then $A(x) = \pi y^2(x)$. The hypothesis cast in the framework of the calculus of variations then becomes:

$$\text{minimize} \int_0^a \left(\frac{1}{\pi y^2 D} \right) dx \tag{34.6}$$

while holding another integral involving y, the constraint, constant.

A constraint that yields good agreement (see Figure 34.10) with acinar anatomic data [9,12,16] is that of constant surface area of the trumpet bell surface of revolution enclosing the airways or

$$\int_0^a 2\pi y ds = \text{constant} = 7130.06 \text{ cm}^2 \tag{34.7}$$

where ds is the differential arc length along the curve $y(x)$. The motivation for this constraint comes from the fact that the lung develops embryologically as a bud off the esophagus. Constraining the surface area of this bud reduces the force necessary for it to push into the surrounding tissue. Other possible constraints are detailed in the discussion section below. The constant in equation (34.7) is produced by adding all the airway cross-sections [9,12,16] and determining the single large tube cross-section and its surface area necessary

to enclose them for each acinar generation. From the anatomic data, this number is found to be 7103.06 cm^2 for the entire healthy adult lung acinus [12].

The function $A(x) = \pi y^2(x)$ is then determined, as an isoperimetric problem in the calculus of variations by simultaneously satisfying equations (34.6 and 34.7), which yields $y(x)$ implicitly as a solution to the Euler–Lagrange equation [15] as

$$x = \frac{\left(C_1 - \frac{1}{\pi y^2 D}\right)^2}{2\pi\lambda\left(C_1 - \frac{2}{\pi y^2 D}\right)} \cdot \cosh^{-1}\left(\frac{2y\pi\lambda}{C_1 - \frac{1}{\pi y^2 D}}\right) - C_2 \quad (34.8)$$

where $C_1 = -0.2437$ s/cm^4, $C_2 = 0.7440$ cm, and $\lambda = -0.1498$ s/cm^5 are constants determined by applying the Weibel values for $A(0)$ and $A(a)$ as boundary conditions on $A(x)$ and satisfying equation (34.7).

A physiologically useful parameter obtained from the $A(x)$ curve is the mean longitudinal acinar airway gas diffusive resistance defined using equation (34.5) as

$$\overline{R} = \frac{1}{a} \cdot \int_0^a R(x)dx. \quad (34.9)$$

A simple equation for $\overline{R}$ can be obtained by using the exponential approximation $A(x) = A_0 e^{kx}$ and equation (34.4) in the form $dR = Pdx/AD$, where P is atmospheric pressure (760 mm Hg) and O_2 gas transfer rate is defined in vol/s and an O_2 concentration in mm Hg, as is customary in respiratory physiology. Using these definitions in equations (34.4 and 34.5) gives

$$\overline{R} = \frac{1}{a} \cdot \int_0^a \left\{ \int_0^x \frac{P \cdot e^{-k\varsigma}}{D \cdot A_0} \cdot d\varsigma \right\} dx = \frac{P}{k \cdot a \cdot D \cdot A_0}\left[a + \frac{e^{-ka}}{k} - \frac{1}{k}\right] \quad (34.10)$$

Results

The resulting acinar $A(x)$ function for the whole lung is shown in Figure 34.10, along with anatomic data [9,12] and the simple exponential function approximation, $A_0 e^{kx}$, where $A_0 = 69.4$ cm^2 and $k = 6.309$ cm^{-1} determined by linear regression using the data shown in Figure 34.10.

Discussion

The constraint applied above in determining the optimal acinar $A(x)$ function forces all the acinar airways, not counting the alveoli, to lie inside a trumpet bell surface of revolution of predetermined surface area. This

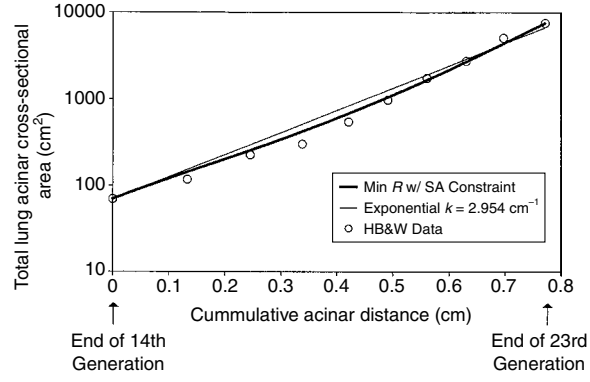

Figure 34.10 Comparison of the optimized $A(x)$ function and an exponential function with acinar anatomic data of Haefeli-Bleuer and Weibel [9], and Weibel [12] (HB&W) (circles) for the total lung acinar cross-sectional area at the end of each generation showing that the optimized $A(x)$ better fits the data. For the optimized $A(x)$ function, the non-linear regression coefficient $R^2 = 0.9882$. For the exponential $A(x)$ function, $R^2 = 0.9596$.

serves to limit the size of $A(x)$, which otherwise, if only equation (34.6) were satisfied with no other limitation, would be found to be infinite. Another constraint that might seem reasonable is to require that the total acinar airway volume $V = \int_0^a A dx$ be held constant while the diffusive resistance is minimized. This leads to a constant value for A (or y) given by

$$\text{A} = \text{constant} = \frac{V}{a} \cong 1825 \text{ cm}^2, \quad (34.11)$$

which does not vary with x, cannot satisfy the boundary conditions at $A(0)$ and $A(a)$, and therefore does not fit the anatomical data shown in Figure 34.10 as well as the solution given by equation (34.8). Another possibility might be to minimize V while holding the enclosing surface area constant. This leads to V approaching zero, which is not physiologically acceptable.

The hypothesis that the acinar airways are designed to minimize longitudinal gas diffusive resistance while holding the enclosing trumpet bell surface area constant is, of course, just an "educated guess." It is possible that other, perhaps more complex, criteria could be found that would also fit the data well. It seems reasonable, however, to propose an acinar design criterion that involves optimizing diffusive transport since molecular diffusion is unquestionably the major mode of gas exchange in the respiratory airways.

The agreement between the optimized $A(x)$ given by equation (34.8) and the anatomic data shown in

Figure 34.10, along with the picture of VT–FRC gas exchange shown in Figure 34.9, suggests that minimization of longitudinal acinar gas diffusive resistance is an important feature of acinar airway design or evolution. In this regard, it is interesting to compute the mean acinar diffusive resistance for O_2 transfer using the exponential approximation $A(x) = A_0 e^{kx}$, and equation (34.10) above. Substituting parameters from Weibel [12] into equation (34.10) for $\overline{R}$ ($a = 0.773$ cm, $k = 6.309\ \text{cm}^{-1}$, $A_0 = 69.4\ \text{cm}^2$, $DO_2 = 0.2\ \text{cm}^2/\text{s}$) gives for a healthy lung

$$\overline{R}^{H}_{O_2} = 0.115\ \text{mm Hg} \bullet \text{min/mL} \qquad (34.12)$$

which is much higher than

$$\frac{1}{D_{Lo_2}} \approx 0.0333\ \text{mm Hg} \bullet \text{min/mL}.$$

Calculating $\overline{R}^{H}_{O2}$, using the optimal $A(x)$ function shown in Figure 34.10, gives a still higher value of 0.411 mm Hg min/mL since the optimal $A(x)$ is always smaller than the exponential approximation.

It is important to note that $1/D_{LO_2}$ is a measure of the resistance to O_2 transport across the alveolar membrane between well-mixed alveolar gas and the pulmonary capillary blood, and does not include the longitudinal diffusive resistance to O_2 exchange between VT and FRC, which, as noted above, occurs along and within the acinar airways during the second half of inspiration similar to the CO_2 exchange shown in Figure 34.9.

Given that averaging over the whole acinus used in equation (34.9) could lead to some overestimation of $\overline{R}$, it still appears that even in healthy lungs, $\overline{R}^{H}_{O2}$ (with a similar value for $\overline{R}^{H}_{CO2}$) is the major component of gas transfer resistance between the tidal volume or atmosphere and the blood.

A second independent, physiological estimate of $\overline{R}^{H}_{O_2}$ and $\overline{R}^{H}_{CO_2}$ can be obtained by using the operational definition $\overline{R}_x = \Delta P_x / \dot{V}_x$, where x indicates the gas of interest, ΔP_x is the partial pressure difference between the atmosphere and the well-mixed alveolar value, and $\dot{V}_x$ is the average gas uptake or evolution rate. Using standard resting values for O_2 and CO_2 [17] gives

$$\overline{R}^{H}_{O_2} = \frac{55\ \text{mm Hg}}{250\ \text{mL/min}} = 0.22\ \text{mm Hg} \bullet \text{min/mL} \quad \text{and}$$

$$\overline{R}^{H}_{CO_2} \cong \frac{40\ \text{mm Hg}}{200\ \text{mL/min}} = 0.2\ \text{mm Hg} \bullet \text{min/mL} \qquad (34.13)$$

values in between the simple exponential and optimized estimates of 0.115 mm Hg min/mL and 0.411 mm Hg min/mL given above.

The fact that all these airway estimates of $\overline{R}^{H}_{O2}$ and $\overline{R}^{H}_{CO2}$ agree in order of magnitude lends support to the idea that airways diffusive gas resistance is significantly larger than the resistance to gas transfer across the alveolar membrane. However, even though acinar airway gas phase diffusive resistance appears to be an order of magnitude larger than gas transfer resistance across the alveolar membrane, in diseases that do not significantly affect the airways, membrane resistance can well be, clinically, the most important since both operate in series.

In the case of diseases, such as emphysema, that destroy acinar airway architecture, $\overline{R}^{D}$ can be much higher than $\overline{R}^{H}$. Figure 34.11, for example, shows capnograms from a healthy and diseased (chronic obstructive pulmonary disease, COPD) lung, computed using the SPM compared to experimental measurements. For the COPD computation, the healthy $A(x)$ function was reduced by a constant factor β, and a was lengthened to keep total acinar airway volume constant [10], giving the exponential $A(x)$ parameters $k^D = 2.73\ \text{cm}^{-1}$, $a^D = 1.72$ cm, and $A_0^D = 31.230\ \text{cm}^2$. For the healthy and diseased lungs shown in Figure 34.11, equation (34.10) then gives

$$\frac{\overline{R}^{D}_{O_2}}{\overline{R}^{H}_{O_2}} \cong 5.1. \qquad (34.14)$$

Lengthening the airways in conjunction with reducing their cross-section by factor β is necessary to maintain FRC at least constant while simulating the anatomical effects of COPD. It is well known that the FRC in severe emphysema is usually increased as the patients develop barrel chests and experience restrictions to expiratory flow. If reduction in acinar airway cross-section by the factor β were not accompanied by simultaneous lengthening, the FRC would decrease, and not increase, as is usually the case.

Large increases in gas phase diffusive resistance in comparison to healthy lungs were also found by Schwardt *et al.* in a study of COPD patients [10]. As shown in Figure 34.11, for these patients, volume-based capnograms show that much less CO_2 (and O_2) is transferred per breath between VT and FRC than in healthy subjects, which is due to an increase in the acinar gas phase $\overline{R}$ associated with lengthening and narrowing of the COPD $A(x)$ trumpet bell. COPD is one

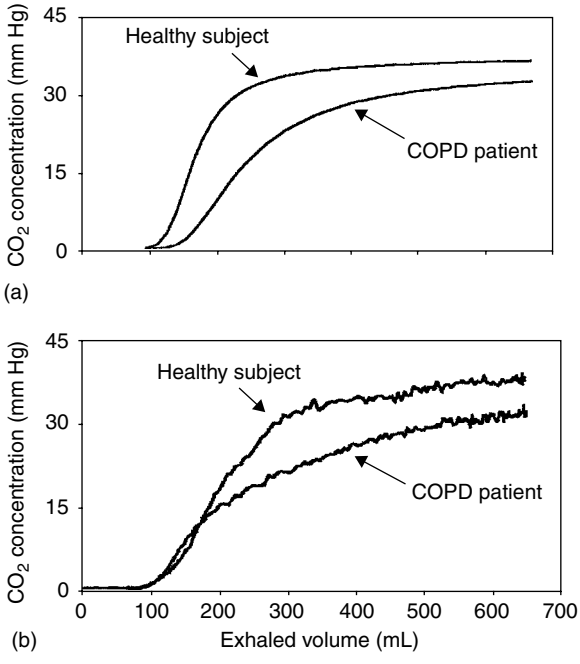

Figure 34.11 Comparison of SPM capnogram simulations for (a) a healthy and (b) a COPD lung with experimental data [10]. Much less CO_2 is evolved per breath in the COPD lung (area under the capnogram) than in the healthy lung. Healthy lung parameters are FRC = 3840 mL, $\beta = 0.72$, $V_T = 690$ mL, mixed venous $pCO_2 = 42$ mm Hg, and cardiac output = 5394 mL/min. COPD lung parameters are FRC = 5210 mL, $\beta = 0.45$, $V_T = 690$ mL, mixed venous $pCO_2 = 36$ mm Hg, and cardiac output = 5123 mL/min. A β value of around 0.7 is necessary in the SPM to accurately model gas exchange in the healthy lung. This is necessary to simulate the effect of asymmetry in the real airways, which is not included in the SPM where Weibel's [12] symmetric airway model is used. [(a) Adapted from: Schwardt JD, Neufeld GR, Baumgardner JE, Scherer PW. Non-invasive recovery of acinar anatomic information from CO_2 expirograms. *Ann Biomed Eng* 1994; **22**: 293–306. (b) This is original.]

disease where acinar airway alteration – replacement of a large number of small airways by a small number of large airspaces – leads to the lengthening of the diffusive path accompanied by reduction in gas phase cross-sectional area. These effects work together to increase $\overline{R}$ as implied in equation (34.4) and shown also in equation (34.14).

It is interesting to note that current efforts to aid emphysema patients through lung volume reduction surgery [18] may be more successful when the patient's acinar $A(x)$ function is altered and returned to a shorter and more rapidly flaring $A(x)$ characteristic of the healthy lung. Although there are many physiological parameters altered by this surgery, it would be interesting to compare patient pre- and postoperative CO_2 washout curves (capnograms) to see if they are shifted as shown in Figure 34.11.

Finally, it is interesting to speculate that alveolar airway smooth muscle may function to change $A(x)$, and thereby change airway $\overline{R}$ as a means of modulating gas exchange between the atmosphere and the alveoli.

Conclusion

The agreement of the optimized acinar $A(x)$ function with anatomic data, and the large values of $\overline{R}_{O_2}$ and $\overline{R}_{CO_2}$ compared to $1/D_{LO_2}$ and $1/D_{LCO_2}$, suggest that longitudinal acinar gas phase diffusive resistance is the major resistance to gas exchange between the atmosphere and the pulmonary capillary blood, and should be recognized as an important concept in respiratory gas exchange, especially in lung disease where acinar airway anatomy is significantly altered.

Acknowledgments

Part I, concerning the recovery of cardiac output from capnograms recorded in goats, is taken mostly from the Ph.D. thesis of John Huang [20], which should be consulted for further details. In Part II, the authors acknowledge valuable discussions of diffusive gas exchange resistance with Dr. William J. Muller. The authors also acknowledge many valuable discussions with Dr. Gordon R. Neufeld.

References

1. Scherer PW, Zhao K. Anatomical and physiological basis of volume capnography studied by the single path model. In: Gravenstein JS, Jaffe MB, Paulus DA (eds.) *Capnography: Clinical Aspects*. Cambridge, UK: Cambridge University Press, 2004; 321–35.
2. Connors AF Jr., Speroff T, Dawson NV, *et al.* The effectiveness of right heart catheterization in the initial care of critically ill patients. *JAMA* 1996; **276**: 889–97.
3. Scherer PW, Shendalman LH, Greene NM. Simultaneous diffusion and convection in single breath washout. *Bull Math Biophys* 1972; **34**: 393–412.
4. Scherer PW, Gobran S, Aukburg SJ, *et al.* Numerical and experimental study of steady-state CO_2 and inert gas washout. *J Appl Physiol* 1988; **64:** 1022–9.
5. Scherer PW, Neff JD, Neufeld GN. Determination of cardiac output from single breath CO_2 washout. Proceedings of Biomedical Engineering Society Fall Meeting, 1995, Boston, MA. v23, S-9.
6. Huang JW, Scherer PW, Neufeld GR. Cardiac output recovered from single breath CO_2 washout in goats. Proceedings of Biomedical Engineering Society Fall Meeting, Cleveland, OH, 1998.

7. Fowler WL. Lung function studies. II. The respiratory deadspace. *Am J Physiol* 1948; **154**: 405–16.
8. Scherer PW, Neff JD, Baumgardner JE, Neufeld GR. The importance of a source term in modeling multibreath inert gas washout. *Respir Physiol* 1996; **103:** 99–103.
9. Haefeli-Bleuer B, Weibel ER. Morphometry of the human pulmonary acinus. *Anat Rec* 1988; **220:** 401–4.
10. Schwardt JD, Neufeld GR, Baumgardner JE, Scherer PW. Non-invasive recovery of acinar anatomic information from CO_2 expirograms. *Ann Biomed Eng* 1994; **22:** 293–306.
11. Weibel ER. *Morphometry of the Human Lung.* Berlin: Springer-Verlag, 1963.
12. Weibel ER. Design of airways and blood vessels considered as branching trees. In: Crystal RG, West JB (eds.) *The Lung*: *Scientific Foundations,* vol. 1. New York: Raven Press, 1991; 711–20.
13. Wilson TA. Design of the bronchial tree. *Nature* 1967; **213:** 668–9.
14. Wilson TA, Lin KH. Convection and diffusion in the airways and the design of the bronchial tree. In: Bouhuys A (ed.) *Airways Dynamics: Physiology and Pharmacology*. Springfield, IL: Charles C. Thomas, 1970; 5–19.
15. Courrant R, Hilbert D. *Methods of Mathematical Physics*. New York: Interscience, 1953.
16. Weibel ER. Lung morphometry and models in respiratory physiology. In: Chang HK, Paiva M (eds.) *Respiratory Physiology: An Analytical Approach.* New York: Marcel Dekker, 1989: 1–560.
17. Guyton AC, Hall JE. *Textbook of Medical Physiology*, 10th edn. New York: WB Saunders, 2000; 454–5.
18. Ware JH. The National Emphysema Treatment Trial: how strong is the evidence? *N Engl J Med* 2003; **348:** 2055–6.
19. Huang J, Yang G, Scherer PW, Neufeld G. Airway cross-section strongly influences alveolar plateau slope of capnograms for smaller tidal volumes. *Respir Physiol* 2000; **119:** 51–5.
20. Huang J. Non-invasive estimation of cardiac output and mixed venous PCO_2 using the single path model of gas exchange. Ph.D. dissertation, University of Pennsylvania, Philadelphia, PA, 2000.

Appendix: list of symbols

Symbol	Definition	Units
a	Total length of the acinus	cm
A_0	Total acinar airway cross-sectional area at beginning of acinus at $x = 0$	cm^2
$A(x)$	Total acinar airway cross-section area versus distance function	cm^2
$A(z)$	Total cross-sectional area per generation in generation z [cm^2]	cm^2
λ	Solubility of CO_2 in blood ($\lambda = 2.13$)	min/breath · mm $Hg^{1/2}$
β	Uniform acinar area reduction factor	dimensionless
$C(z,t)$	Airway concentration of CO_2 in generation z	mm Hg
C_{art}	Arterial PCO_2 concentration	mm Hg
C_B	Mixed venous PCO_2 concentration	mm Hg
D	Molecular diffusivity in air	cm^2/s
Dmol	Gas phase CO_2 molecular diffusivity in air ($DCO_2 = 0.17$)	cm^2/s
$\frac{1}{DLO_2}$	Resistance to O_2 transport across the alveolar membrane between well-mixed alveolar gas and the pulmonary capillary blood—reciprocal of O_2 diffusing capacity	mm Hg · min/mL
$\frac{1}{DLCO_2}$	Resistance to CO_2 transport across the alveolar membrane between well-mixed alveolar gas and the pulmonary capillary blood—reciprocal of O_2 diffusing capacity	mm Hg · min/mL
$ETCO_2$	End-tidal CO_2 concentration	mm Hg
f	Breathing frequency	breath/min
FRC	Functional residual lung capacity	mL
l	Length per generation in a given generation	cm

Symbol	Definition	Units
MBE	Mass balanced equation based on Fick principle	
$\frac{N_A(Z)}{N_T}$	Ratio of alveoli per generation z to total number of alveoli in Weibel lung	dimensionless
NS	Normalized Phase III slope	L^{-1}
$Q(z, t)$	Airway gas volume flow rate in generation z at time t	mL/s
Q_B	Cardiac output	mL/min
$\overline{R}$	Mean longitudinal acinar airway gas diffusion resistance	mm Hg · min/mL
$\overline{R}^{H}_{CO_2}$	Mean longitudinal acinar airway gas diffusion resistance for O_2 in healthy lung	mm Hg · min/mL
$\overline{R}^{H}_{CO_2}$	Mean longitudinal acinar airway gas diffusion resistance for CO_2 in healthy lung	mm Hg · min/mL
$\overline{R}^{D}_{CO_2}$	Mean longitudinal acinar airway gas diffusion resistance for O_2 in diseased (COPD) lung	mm Hg · min/mL
$\overline{R}^{D}_{CO_2}$	Mean longitudinal acinar airway gas diffusion resistance for CO_2 in diseased (COPD) lung	mm Hg · min/mL
S	Pulmonary blood source term for CO_2	mL · mm Hg/s
$SBCO_2$	Single breath CO_2 airway washout	
SPM	Single-path model	
t	Time	s
$V(z)$	Airways volume of generation z	cm^3
V_A	Alveolar volume per generation in a given generation	cm^3
$\dot{V}CO_2$	Exhaled CO_2 volume	mL/breath
V_T	Tidal volume	mL or mL/kg
V_{zo}	Oropharynx volume	mL
x	Longitudinal distance into acinus	cm
$y(x)$	Radius of acinar trumpet bell surface of revolution	cm
ς	Dummy variable of integration	cm
z	Non-dimensional generational coordinate	dimensionless

Section 4
Chapter
35

Physiologic perspectives

Carbon dioxide and the control of breathing: a quantitative approach

M. C. K. Khoo

Introduction

Breathing is controlled by a diverse set of neural, pulmonary, vascular, and muscular components intricately connected through feedforward and feedback elements. For this elaborate system to function as an efficient regulator of gas exchange, it is not sufficient for the individual parts to be fully operational and free of underlying pathology. The flow of sensory and control data among the different components also have to be integrated temporally. Since each component of this system has its own dynamic response characteristics, and because it takes time for data to flow from one structure to another, control is never static. Moreover, the characteristics of many critical respiratory control structures vary over timescales that range from minutes to years. In contrast, much of what has been written about the chemical regulation of ventilation in most texts [1–4] and review chapters [5,6] on respiratory physiology is based on an understanding derived from steady-state or quasi-static measurements. Rather than revisiting old ground, the purpose of this chapter is to present an additional perspective that emphasizes the integrative and dynamic aspects of ventilatory control specifically with respect to CO_2. The dynamic factors affecting the chemoreflex control of ventilation are multifaceted, and their interactions can easily lead to complex behavior. For this reason, a quantitative approach that employs mathematical modeling as a tool enables us to sort out which factor contributes to which facet of the observed behavior.

Respiratory control physiology: an overview

It is useful to begin by reviewing the basic physiological structures and processes that are primarily responsible for mediating the chemoreflex control of ventilation by using a systems perspective. Figure 35.1 presents a schematic overview of ventilatory control relevant to our discussion. The presence of multiple feedback loops is apparent in this diagram. There are two main groups of chemoreceptors. The peripheral chemoreceptors, located in the carotid bodies, were the first to be discovered by Heymans and Heymans in the 1920s [7]. There are also chemoreceptors located in the aortic bodies that lie at the arch of the aorta, but the carotid bodies generally have been known to produce greater responses to chemical stimulation by high arterial PCO_2 and/or low arterial PO_2. Although initially thought to be the only mediators of chemosensitivity, subsequent experiments showed that, in normoxia, the peripheral chemoreceptors could only account for a quarter to one-third of the overall ventilatory response to hypercapnia [8,9]. The "missing" contribution to the total chemoreflex response was discovered in the 1950s and 1960s when areas on the superficial layers of the ventral medulla were found to be sensitive to H^+ ions [10]. Subsequent studies have suggested that central chemoreceptors are not concentrated in one specific place, nor are they confined to the superficial layers of the medulla [11]. As such, the chemosensitivity in the different locations can vary significantly [12]. Although these receptors produce large changes in ventilatory drive, the diffusion of CO_2 across the blood–brain barrier and through brain interstitial fluid from the arterial blood takes time. Hence, the response of the central chemoreflex loop is sluggish, with time constants on the order of about 100 s [5]. In contrast, the carotid chemoreceptors sit in an environment of high perfusion by the arterial blood, and, thus, the response time for peripheral chemoreception to changes in $PaCO_2$ is considerably smaller.

The evidence to date suggests that input from the central and peripheral chemoreceptors or from the higher centers is required to produce oscillatory

Capnography, Second Edition, ed. J. S. Gravenstein, Michael B. Jaffe, Nikolaus Gravenstein, and David A. Paulus. Published by Cambridge University Press. © Cambridge University Press 2011.

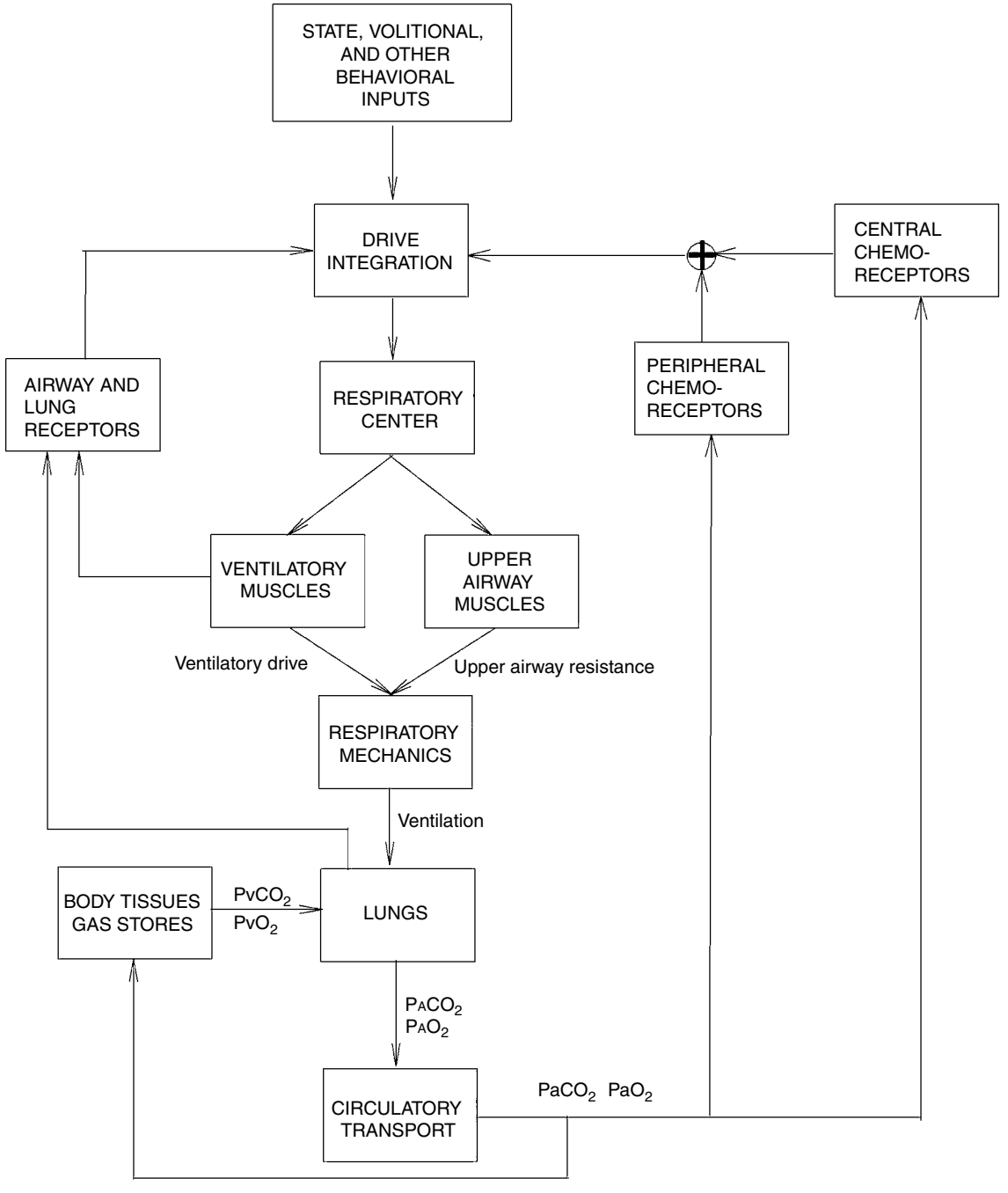

Figure 35.1 Schematic diagram of the key factors affecting control of breathing.

activity in the brainstem respiratory neurons and network [13]. The latter consist of the dorsal respiratory group, located in the ventrolateral nucleus of the tractus solitarius, and the ventral respiratory group, located bilaterally in the retrofacial nucleus, nucleus ambiguous, and the nucleus retroambiguus. Inputs from the pulmonary stretch receptors, the irritant receptors (also known as rapidly adapting pulmonary stretch receptors), airway receptors, juxtapulmonary–capillary (J) receptors, and proprioceptors play a secondary role and contribute primarily by modulating the breathing pattern.

Current methods for assessing CO_2 ventilatory control and their limitations

Hypercapnic ventilatory response

Under normal conditions, ventilation ($\dot{V}E$) and arterial PCO_2 ($PaCO_2$) (and alveolar PCO_2, $PACO_2$) are tightly coupled through the powerful negative feedback loops of the chemoreflexes: any increases in $PaCO_2$ lead to rapid increases in $\dot{V}E$, which acts to partially offset the initial rise in PCO_2. By administering various concentrations of inhaled PCO_2 in a setting of hyperoxia, it is possible to obtain different combinations of $\dot{V}E$ and $PACO_2$ after the corresponding responses have attained a steady state. From these combinations, a steady-state hypercapnic ventilatory response can be derived. The drawback of this very simple method is that it takes 10–15 min to arrive at each combination of $\dot{V}E$ and $PACO_2$; as such, the method is highly time-consuming and impractical.

The rebreathing technique introduced by Read [14] in 1967 is more commonly employed in clinical practice since it can be completed in about 5 min. Here, the subject breathes into and out of a small (4–6 L) rebreathing bag that is filled with an initial gas mixture containing 7% CO_2 in oxygen. After an initial transient phase, an equilibrium in PCO_2 is established between arterial blood, mixed venous blood, the alveoli, the rebreathing bag, and, presumably, brain tissue. Thereafter, the PCO_2 in both blood and gas phases increases linearly with time, and $\dot{V}E$ also increases proportionally without reversing the rise in PCO_2 as one would expect in a closed-loop situation. The rise in PCO_2 in all compartments is proportional to the CO_2 metabolic production rate. Since $\dot{V}E$ also rises linearly, the ratio of the change in $\dot{V}E$ to the change in end-tidal $PETCO_2$, (representing $PACO_2$) produces hypercapnic ventilatory sensitivity. The increasing $\dot{V}E$ is mediated predominantly by the central chemoreflex loop, since the hyperoxic background suppresses the peripheral chemoreceptors. The slope of the rebreathing response line presumably reflects the sensitivity of the medullary chemoreceptors to changes in brain tissue PCO_2. As long as the arterial–cerebral venous CO_2 gradient remains constant, the rebreathing slope should also be similar to the slope derived from the steady-state CO_2 inhalation technique. However, they are, in fact, not quite the same, since cerebral blood flow increases with increasing $PaCO_2$, which reduces the arterial–cerebral venous CO_2 gradient at high PCO_2 [15]. Another limitation of the rebreathing method is that it does not provide any data about the dynamics of the chemoreflex response.

Response to transient CO_2 inhalation

Measuring the ventilatory response to one, two or three breaths of inhaled gas with a high CO_2 concentration (6–20%) in air has been used for determining the contribution of the peripheral chemoreflexes [16–18]. These CO_2 response tests are based on the premise that the transient elevation of $PaCO_2$ is fully sensed by the rapidly responding peripheral chemoreceptors, whereas the stimulus is substantially attenuated and delayed by the time it is sensed by the central chemoreceptors. The large difference in response times, in effect, allows the central and peripheral drives to be functionally partitioned. There are minor variations in the methods used by previous researchers to compute the peripheral chemoreflex gain. In the study by McClean *et al.* [16], baseline ventilation was determined from the five breaths that preceded the inhalation breath. Following exposure to the transient hypercapnia, the breath with the highest ventilation value within 20 s of the stimulus breath was selected. The ratio between the increase in ventilation from baseline to maximum response and the increase in end-tidal $PETCO_2$ was assumed to reflect a peripheral chemoreflex gain. Because of the short duration of the test, multiple runs of the experiment are generally carried out, and the peripheral gains calculated from the different repetitions are averaged.

The single-breath and other transient CO_2 inhalation tests assume that the $PETCO_2$ is representative of $PACO_2$ before, during, and immediately after the stimulus is delivered. Using a simulation model of closed-loop CO_2 ventilatory control, Khoo [19] showed that this assumption may not be true. The $PETCO_2$ at the stimulus breath can be substantially higher than $PACO_2$ due to mixing in the conducting airways between alveolar gas and the CO_2-enriched inhalate. This leads to underestimation of the true peripheral chemoreflex gain. Another assumption is that the central chemoreflex contribution to the estimate of peripheral gain is negligible due to the large difference in response times between the medullary and arterial chemoreceptors. Khoo's simulation study again showed that this assumption may not be valid.

The bolus of CO_2 inhaled during the single-breath test is roughly equivalent to subjecting the respiratory

control system to an impulsive stimulus, which contains a broad range of frequency components. Although most of the higher-frequency components are filtered out by the time the disturbance is sensed by the central chemoreceptors, the low-frequency components persist, which leads to some central chemoreflex contribution. Furthermore, the degree of attenuation may be temporarily reduced as a result of the transient increase in cerebral blood flow after a single-breath inhalation of CO_2. As such, peripheral gain estimated through the single-breath test may be significantly overestimated when the true peripheral chemoreflex gain is low and central chemoreflex gain is high.

Measuring dynamic CO_2 chemoresponsiveness

Dynamic end-tidal forcing

The dynamic end-tidal forcing technique, first introduced by Swanson *et al.* [20] in 1971, employs specially designed hardware and a feedback control algorithm to manipulate the inspired gas concentration so that the resulting $P_{ET}CO_2$ exhibits a time course of one's choosing. The $P_{ET}CO_2$ waveform (assumed to represent P_ACO_2, and thus $PaCO_2$) acts as the forcing function for the ventilatory controller, while breath-by-breath ventilation that occurs is the controller output. This is clearly superior to merely using inhaled PCO_2 as a representation of the true input sensed by the chemoreceptors, since the response to inhaled PCO_2 is the closed-loop response to the system, which includes cardiopulmonary factors related to gas exchange.

If a square wave change in $P_{ET}CO_2$ is applied against a background of normoxia or hypoxia, it is expected that both the central and peripheral chemoreflexes would contribute to the total ventilatory response. In order to distinguish the central from the peripheral component of the response, this hypercapnic ventilatory response test requires the assumption of a mathematical model as well as the application of a robust algorithm for estimation of the model parameters from noisy measurements. An additive two-compartment model was initially proposed by Swanson and Bellville [21], and this took the form given by the three differential equations below:

$$\tau_c \frac{d\dot{V}_c}{dt} + \dot{V}_c = G_c\left[P_{ET}CO_2(t - T_d) - I\right] \quad (35.1)$$

$$\tau_p \frac{d\dot{V}_p}{dt} + \dot{V}_p = G_p\left[P_{ET}CO_2(t - T_d) - I\right] \quad (35.2)$$

$$\dot{V}_E = \dot{V}_c + \dot{V}_p \quad (35.3)$$

In the above equations, τ_c and τ_p represent the characteristic response times of the central and peripheral chemoreflexes, respectively; G_c and G_p represent the corresponding steady-state gains, whereas I is the corresponding apneic threshold (i.e., the contribution of each chemoreflex component becomes zero when the PCO_2 stimulus falls below the threshold value). $P_{ET}CO_2$ is assumed to be equal to P_ACO_2, which in turn is assumed to be equilibrated with end-capillary PCO_2. T_d is the transport delay of blood from the pulmonary capillaries to the chemoreceptors. The above model assumes that chemoreceptors respond to arterial $PaCO_2$ at vascular sites in their vicinity. The response of the carotid body chemoreceptors to a step change in $PaCO_2$ in cats is a rapid overshoot, followed by a decline to the steady state with a time constant between 10 and 30 s [22]. This time constant, τ_p, appears to be of similar magnitude in humans [23]. In contrast, the dynamic ventilatory response mediated by the medullary receptors is highly sluggish, with estimated response time constants that range from 60 to 180 s [23].

Swanson and Bellville used step changes in $P_{ET}CO_2$ to produce ventilatory responses. An optimization algorithm was employed to iteratively adjust the unknown model parameters (τ_c, τ_p, G_c, G_p, T_d, I) so that the fit between the model prediction and measured ventilation was optimized. Subsequently, this model was expanded and refined to improve its predictive capabilities by assuming different time delays for peripheral and central chemoreflexes and by incorporating the dependence of τ_c on $P_{ET}CO_2$, since hypercapnia increases cerebral blood flow [23]. Aside from using square waves as the pattern of stimulation by $P_{ET}CO_2$, sinusoidal patterns have also been used [24], as well as a step change followed by a linear rate of rise in $P_{ET}CO_2$ [15].

Frequency response of the respiratory controller

Rather than thinking in terms of gains and time constants, an alternative means of representing dynamic responses is to consider how the model described in equations (35.1) through (35.3) would respond to sinusoidal fluctuations in $P_{ET}CO_2$ over a broad range

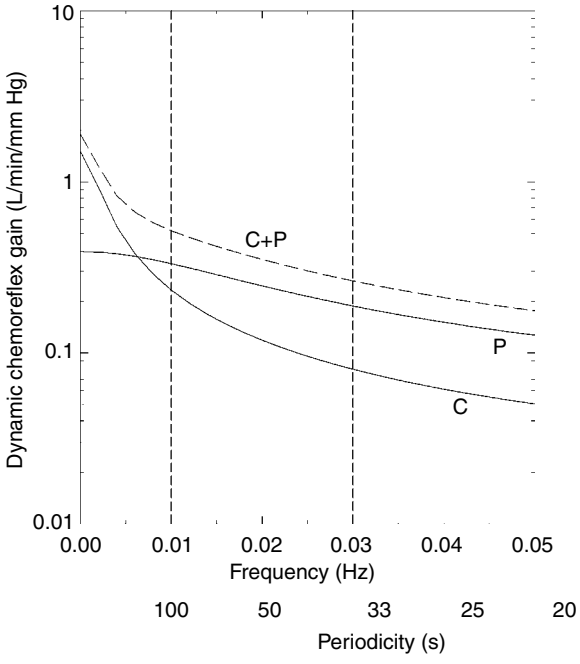

Figure 35.2 Central (C) and peripheral (P) chemoreflex components of dynamic chemoresponsiveness. [Reproduced with permission from Fig. 9 in: Khoo MCK, Yang F, Shin JJW, Westbrook PR. Estimation of dynamic chemoresponsiveness in wakefulness and non-rapid eye movement sleep. *J Appl Physiol* 1995; **78**: 1052–64.]

of frequencies. Since this model is assumed to be linear, the response of each chemoreflex component to a sinusoidal fluctuation of P_ACO_2 would also be sinusoidal at the same frequency, but attenuated and phase-shifted with respect to the input signal. Thus, each sinusoidal frequency will be associated with a corresponding gain (output amplitude/input amplitude) and phase shift. By plotting these gains and phase shifts versus frequency, one obtains the frequency response of the system. The frequency responses of the chemoreflex controller model described by equations (35.1) through (35.3) and its central and peripheral components are displayed in Figure 35.2. Here, we have assumed the central and peripheral chemoreflex CO_2 gains to be 1.8 and 0.6 L/ min/ mm Hg, with time constants assumed to be 100 and 10 s, respectively. Although the steady-state sensitivity of the central chemoreflex to CO_2 is three times as large as the peripheral gain, the slow dynamics create a strong attenuating effect on its response to dynamic blood-gas stimuli that fluctuates over a timescale of several breaths. Over a range of frequencies pertinent to the fluctuations that occur on an inter-breath basis, the dynamic gain of the peripheral chemoreflex is between 75% and 200% larger than the corresponding dynamic central chemoreflex gain, even though the former is one-third the magnitude of the latter in the steady state. It should be noted that the relative contribution of the central chemoreflex to the overall dynamic ventilatory response is still by no means negligible. Indeed, single-breath and other dynamic stimuli have been reported to evoke a small but significant ventilatory response during hyperoxia when the peripheral chemoreceptors presumably have been silenced.

Pseudorandom binary forcing

A pseudorandom binary sequence (PRBS) contains samples that each can take on only one of two possible values – one low and one high. The PRBS is pseudorandom because the time series is actually periodic, with a cycle duration of $n + 1$ samples if n is the total number of points in the sequence. However, within one period of this series, each sample is virtually uncorrelated with other samples, and what value each sample assumes appears random. In PRBS CO_2 forcing, the inhaled CO_2 concentration is switched between 0 (air) and 4–6% over a total duration of 64 or 128 breaths; thus, the entire experimental protocol can be completed within 10 min. The maximum concentrations of CO_2 (<6%) used in this procedure make the test relatively non-intrusive. The random-like nature of the sequence exposes the ventilatory control system to dynamic perturbations that span a broad range of frequencies between 0.01 and 0.05 Hz, consistent with the dynamics of the fluctuations generally observed in spontaneous breathing. Figure 35.3 displays the results of an experiment in which the subject was exposed to a PRBS-modulated inhalate that was switched between air and a mixture containing 5% CO_2/21% O_2/74% N_2 (top panel). Note that, because of mixing in the equipment deadspace, there are single breaths in which the mixture inhaled is less than 5% CO_2. Also, it should be noted that the pattern of ventilation (bottom panel) resembles the time course of $P_{ET}CO_2$ (middle panel) more closely than that of inhaled PCO_2.

The most straightforward method for analyzing the data obtained from PRBS experiments is that of applying the linear systems theory. This approach was adopted by Sohrab and Yamashiro [25] and subsequently by Modarreszadeh and Bruce [26]. Basically, they estimated the impulse response (which may be viewed as the equivalent single-breath ventilatory response to a unit change in inhaled PCO_2) through a deconvolution procedure involving the autocorrelation of

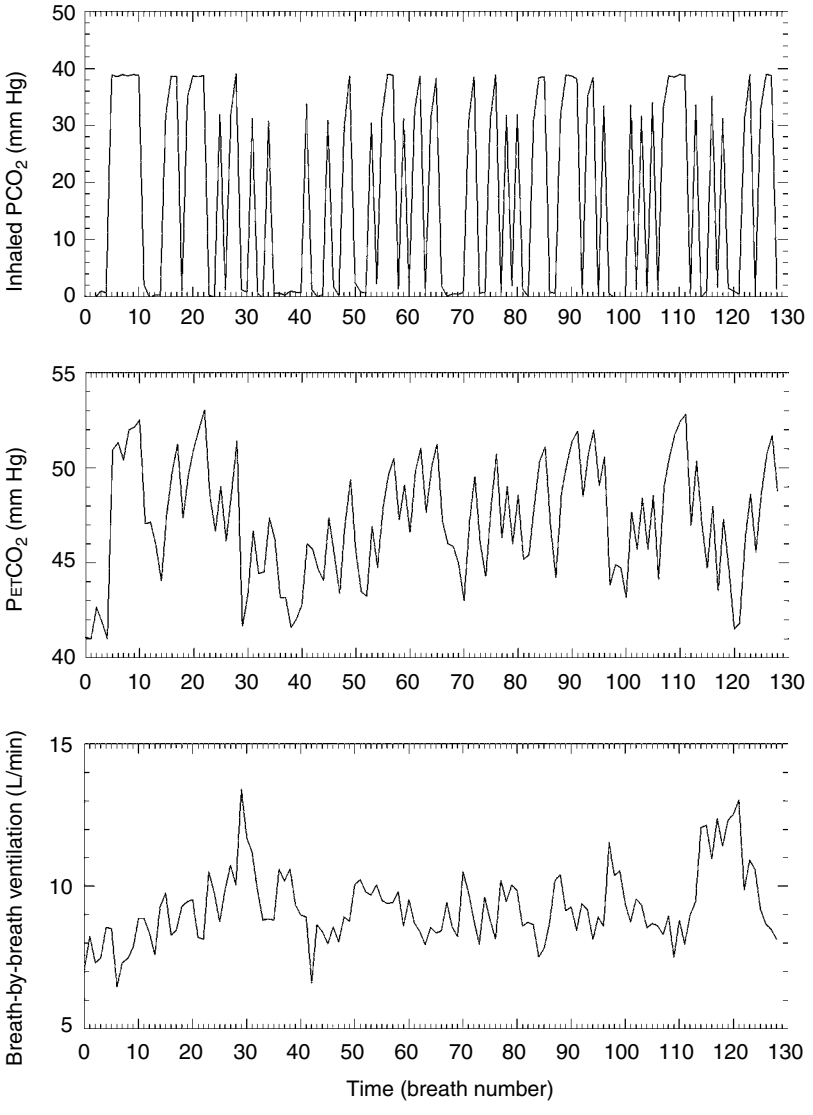

Figure 35.3 An example of the human ventilatory response to pseudorandom binary forcing of inhaled PCO_2.

the inhaled PCO_2 sequence and the cross-correlation between inhaled PCO_2 and ventilation. However, what this calculation produced was the closed-loop impulse response, which incorporates not only the dynamics of the chemoreflexes but also the dynamics of lung CO_2 clearance. In order to delineate the chemoreflex from the dynamics of the controlled system (the "plant"), it was necessary to assume a simple (single compartment) model for the respiratory controller.

We have proposed an alternative approach that produces more robust estimates of dynamic chemoresponsiveness [27]. Here, a linear model is first used to relate the changes in $P_{ET}CO_2$ to changes in ventilation. Assuming $x(n)$ represents the change in $P_{ET}CO_2$ from the mean at breath n, and $y(n)$ the change in ventilation from the mean, we relate $y(n)$ to $x(n)$ through an autoregressive model with an exogenous input (ARX) model:

$$y(n) = -\sum_{k=1}^{L} a_k\, y(n-k) + \sum_{m=0}^{M} b_m\, x(n-k-N_D) + e(n) \tag{35.4}$$

where $e(n)$ represents the residuals between the data and the corresponding model prediction. By minimizing the sum of squares of $e(n)$, the unknown coefficients (a_k, b_m, N_D) and the number of terms (L, M) in equation (35.4) can be estimated. Once the unknown

parameters have been estimated, they are used to generate the following frequency response:

$$H(f) = \frac{\sum_{i=0}^{M} b_i \exp(-j2\pi(i + N_D) fT}{1 + \sum_{k=1}^{L} a_i \exp(-2\pi kfT)} \quad (35.5)$$

where f represents frequency, T the average breath duration, and j is the square root of –1. Having obtained the estimate of $H(f)$, the dynamic gain at any frequency can be calculated as follows:

$$G_D(f) = \sqrt{\mathrm{Re}[H(f)]^2 + \mathrm{Im}[H(f)]^2}. \quad (35.6)$$

Error analyses have shown that, for the PRBS inputs that range from 5 to 10 min in duration, these estimates of G_D are most accurate in the frequency range of 0.01 to 0.03 Hz, which is equivalent to periodicities that range from 30 s to 100 s.

Assessing CO_2 chemoresponsiveness using spontaneous variations in ventilation

The advantage of the input from PRBS over more traditional tests, such as steps or ramps, is that the former has more power over a broader range of frequency components. This capability increases the frequency content of the ensuing ventilatory response, and therefore yields more data on the dynamic characteristics of chemoreflex control. The fluctuations in blood gases that arise from a variety of external inputs to the respiratory system are, for the most part, dynamic and largely stochastic assessments that incorporate dynamic information such as that provided by PRBS forcing, and, thus, are clearly more pertinent to respiratory control. However, the remaining drawback in all CO_2-based tests is that they only permit fluctuations towards hypercapnia and, as such, they only provide information about chemosensitivity in the region *above* the eucapnic set point. On the other hand, recent experiments on both animal preparations and humans receiving ventilatory assistance have suggested that CO_2 sensitivity may be markedly higher below the eucapnic point [28].

An alternative approach for assessing dynamic chemoresponsiveness involves the careful monitoring of $\dot{V}E$ and $PETCO_2$ following natural perturbations to the respiratory control system. For instance, it has been reported that a hyperventilatory sigh can lead to a transient dip in $PETCO_2$, which is subsequently followed by an undershoot in $\dot{V}E$ that, in turn, raises $PETCO_2$ [29,30]. Hence, the sigh may be thought of as a single-breath negative CO_2 pulse. The method [30] that we have proposed for estimating G_D from post-sigh fluctuations in $\dot{V}E$ and $PETCO_2$ is essentially the same as that outlined above (p. 365). An ARX model (equation 35.4) is first used to correlate fluctuations in $PETCO_2$ following the sigh, with subsequent changes in $\dot{V}E$, and then, using the estimated coefficients of the ARX model, the transfer function of the chemoreflex controller can be deduced (equation 35.5). From the corresponding frequency response, G_D can be calculated (equation 35.6). When this method was applied to data produced by model simulation, G_D was found to strongly correlate with peripheral chemoreflex gain, although there was also some degree of dependence on G_c [30]. Further, G_D increased significantly with hypoxia, supporting our results from the simulated data that the estimated G_D is most strongly correlated with peripheral chemoreflex gain.

A variation of the above method is based on the observation that the spontaneous fluctuations in $\dot{V}E$ are usually relatively broadband in frequency content, even if occasional sighs are not included for consideration. A random pause in breathing, for example, may lead to a transient increase in $PETCO_2$, which, in turn, may lead to the generation of a larger-than-normal breath. Thus, ventilatory drive at any given breath may be causally related to a chemical drive component, which reflects ventilatory changes that occurred T_d seconds ago (T_d being the time delay between variations in alveolar gas tensions and their subsequent effect on the chemoreflexes). However, there is a random component as well. We have developed an algorithm in which the impulse response of the chemoreflex controller can be found by solving the inverse problem that relates the cross-correlation between $PETCO_2$ and $\dot{V}E$ to the autocorrelation of changes in $PETCO_2$ [31]. From the estimated impulse responses, G_D can be deduced. As with the method using hyperventilatory sighs, the estimates of G_D here are also highly correlated with peripheral chemoreflex gain and, to a smaller extent, with central chemoreflex gain [32].

CO_2 chemoresponsiveness and ventilatory stability

If the ultimate purpose of determining chemoreflex gain is to arrive at an informed assessment of the relative stability (i.e., how far from instability

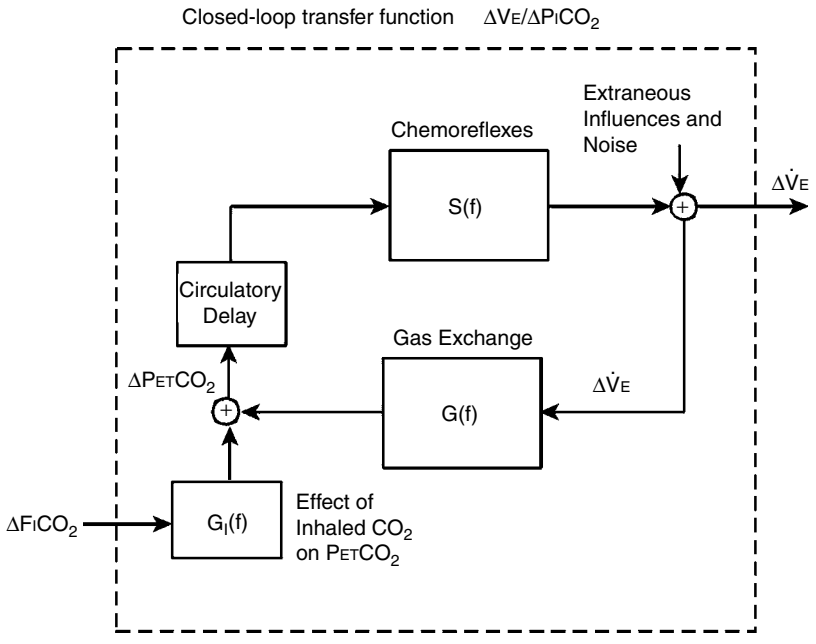

Figure 35.4 Model employed for estimating loop gain from the ventilatory response to PRBS-modulated changes in inhaled PCO_2. [Adapted from Fig. 6 in: Khoo MCK. Determinants of ventilatory instability and variability. *Respir Physiol* 2000; **122**: 167–82.]

is the system?) of respiratory control, then the loop gain should be estimated rather than chemoreflex gain. Loop gain (LG) takes into consideration all the factors that could lead to ventilatory instability. These include plant gain (the degree of amplification or attenuation with which ventilatory changes get translated into changes in blood gases) along with chemoreflex gain. A summary of existing methods for assessing LG has been published in a review article by Khoo [33]. For our purposes here, we will only focus on two of these methods that are aimed at estimating dynamic LG.

The first method [34] is based on measurements of ventilatory response obtained during the administration of PRBS-modulated changes in CO_2 in the inhalate. Thus, the data used in this algorithm are likely similar in form to that displayed in Figure 35.3. Changes in $P_{ET}CO_2$ ($\Delta P_{ET}CO_2$) are assumed to be composed of two parts: (a) the direct effect of the administered change in inhaled PCO_2; and (b) the effect of changes in ventilation ($\Delta\dot{V}_E$.) on CO_2 exchange in the lungs. Following a circulatory delay, $\Delta P_{ET}CO_2$ is sensed by the chemoreceptors, resulting in subsequent $\Delta\dot{V}_E$. A schematic diagram of this model is shown in Figure 35.4. The closed-loop transfer function, $H(f)$, of this model is, by definition, the ratio of the output to the input, i.e., $\Delta\dot{V}_E/\Delta P_ICO_2$. At any frequency, LG is given by the following equation:

$$LG(f) = \frac{1}{\frac{G_1(f)}{G(f)H(f)} - 1} \qquad (35.7)$$

where $G(f)$ is the frequency response of the gas exchange process and $G_1(f)$ represents the direct effect of the inhaled CO_2 on $\Delta P_{ET}CO_2$. By applying this algorithm to data simulated by a respiratory control model, we found that the strongest correlation between the estimated LG magnitude and the model LG magnitude were obtained when model LG magnitude included the product between the plant gain, $G(f)$, and the sum of peripheral gain plus a small fraction (0.08) of central gain. Although there is some bias in the estimation of the absolute values of LG magnitude, relative changes in LG are closely related to changes in the corresponding estimated values.

In the second method, the chemoreflex control system was perturbed by the abrupt and strong increase in ventilation that accompanied an acoustically induced arousal from sleep [35]. The increase in ventilation led, within the same breath, to a substantial drop in $P_{ET}CO_2$, and the latter was sensed after a short delay by the chemoreceptors, which, in turn, reduced ventilatory output. The ventilatory responses to these acoustically induced arousals were similar in form to the responses that follow hyperventilatory sighs, as described earlier. In order to deduce LG from these

responses, the ventilatory drive at a given breath was assumed to depend on the ventilatory drive in past breaths in the form of an ARX model, similar in structure to that displayed above (p. 365). A major limitation with this method is that it was only applied to subjects who were asleep. It might be possible to apply this test to awake subjects, for instance, by having them take occasional hyperventilatory breaths. However, it is unclear to what extent behavioral influences might impact the ventilation that follows the hyperventilatory breath, and consequently, affect the estimation of LG.

Summary

The traditional methods for assessing human CO_2 chemoreflex control in the clinic are inadequate because they do not take into account the fact that the respiratory control system is highly dynamic. Steady-state or quasi-static measurements of the ventilatory response to hypercapnia suggest that the central chemoreflex is the dominant contribution to ventilatory control, with the peripheral chemoreflex playing only a minor role. However, recent studies show that, when dynamic fluctuations in ventilation and $PaCO_2$ are taken into account, the peripheral chemoreflex is, in fact, the principal player. The evidence to date suggests that measures of dynamic chemoresponsiveness are more pertinent to the assessment of respiratory system stability. A variety of tests of dynamic chemoresponsiveness, which require the administration of dynamic changes in inhaled CO_2 or perturbations to ventilation, have been developed. The more complex nature of the stimuli and the resulting responses in ventilation necessitate the application of computational methodologies derived from the realm of signal and system analysis.

Acknowledgments

The original work highlighted in this chapter was supported by various grants from NHLBI, the Biomedical Simulations Resource (RR-01861 and EB-001978), NIH Research Career Development Award (HL-02536), and an American Lung Association Career Investigator Award. The writing of this chapter was supported in part by HL-090451.

References

1. Hornbein TF. *Regulation of Breathing*. New York: Marcel Dekker, 1981.
2. Dempsey JA, Pack AI. *Regulation of Breathing,* 2nd edn. New York: Marcel Dekker, 1995.
3. Crystal RG, West JB, Barnes PJ, Weibel ER (eds.) *The Lung: Scientific Foundations*. New York: Lippincott Williams and Wilkins, 1997.
4. Altose MD, Kawakami Y (eds.) *Control of Breathing in Health and Disease*. New York: Marcel Dekker, 1999.
5. Cunningham DJC, Robbins PA, Wolff CB. Integration of respiratory responses to changes in alveolar partial pressures of CO_2 and O_2 and in arterial pH. In: Fishman AP, Cherniack NS, Widdicombe JG, Geiger SR (eds.) *Handbook of Physiology, The Respiratory System,* Sec.3. *Control of Breathing*, vol. 2, Pt. 1. Bethesda, MD: American Physiological Society, 1986; 475–528.
6. Fitzgerald RS, Lahiri S. Reflex responses to chemoreceptor stimulation. In: Fishman AP, Cherniack NS, Widdicombe JG, Geiger SR (eds.) *Handbook of Physiology, The Respiratory System,* Sec.3. *Control of Breathing*, vol. 2, Pt. 1. Bethesda, MD: American Physiological Society, 1986; 313–62.
7. Heymans JF, Heymans C. Sur les modifications et sur la regulation réflexe de l'activité de centre respiratoire de la tête isolée du chien. *Arch Intern Pharmacodyn* 1927; **33**: 272–370.
8. Edelman NH, Epstein PE, Lahiri S, Cherniack NS. Ventilatory response to transient hypoxia and hypercapnia in man. *Respir Physiol* 1973; **17**: 302–14.
9. Honda Y, Watanabe S, Hashizume I, *et al.* Hypoxic chemosensitivity in asthmatic persons two decades after carotid body resection. *J Appl Physiol* 1979; **46**: 632–8.
10. Mitchell RA, Loeschke HH, Massion WH, Severinghaus JW. Respiratory responses mediated through superficial chemosensitive areas on the medulla. *J Appl Physiol* 1963; **16**: 523–33.
11. Nattie E, Li A. Central chemoreception 2005: a brief review. *Auton Neurosci* 2006; **126:** 332–8.
12. Honda Y, Tani H. Chemical control of breathing. In: Altose MD, Kawakami Y (eds.) *Control of Breathing in Health and Disease*. New York: Marcel Dekker, 1999; 41–87.
13. Remmers JE. Central neural control of breathing. In: Altose MD, Kawakami Y (eds.) *Control of Breathing in Health and Disease*. New York: Marcel Dekker, 1999; 1–40.
14. Read DJC, Leigh J. Blood–tissue PCO_2 relationships and ventilation during rebreathing. *J Appl Physiol* 1967; **23**: 53–70.
15. Berkenbosch A, Bovill JG, Dahan A, DeGoede J, Olievier ICW. The ventilatory CO_2 sensitivities from Read's rebreathing method and the steady state method are not equal in man. *J Physiol (London)* 1989; **411**: 367–77.

16. McClean PA, Phillipson EA, Martinez D, Zamel N. Single breath of CO_2 as a clinical test of the peripheral chemoreflex. *J Appl Physiol* 1988; **64**: 84–9.
17. Leigh J. Evaluation of a two-breath CO_2 test as a measure of arterial chemoreflex sensitivity to CO_2 in man. *J Physiol (London)* 1972; **224**: 28P–9P.
18. Edelman NH, Epstein PE, Lahiri S, Cherniack NS. Ventilatory responses to transient hypoxia and hypercapnia in man. *Respir Physiol* 1973; **17**: 302–14.
19. Khoo MCK. A model-based evaluation of the single-breath CO_2 ventilatory response test. *J Appl Physiol* 1990; **68**: 393–9.
20. Swanson GD, Carpenter TM, Snider DE, Bellville JW. An on-line hybrid computing system for dynamic respiratory response studies. *Comp Biomed Res* 1971; **4**: 205–15.
21. Swanson GD, Bellville JW. Step changes in end-tidal CO_2: methods and implications. *J Appl Physiol* 1975; **39**: 377–85.
22. Lahiri S, Mulligan E, Mokashi A. Adaptive response of the carotid body chemoreceptors to CO_2. *Brain Res* 1982; **234**: 137–47.
23. Bellville JW, Whipp BJ, Kaufman RD, *et al*. Central and peripheral chemoreflex loop gain in normal and carotid body-resected subjects. *J Appl Physiol* 1979; **46**: 843–53.
24. Robbins PA. The ventilatory response of the human respiratory system to sine waves of alveolar carbon dioxide and hypoxia. *J Physiol (London)* 1984; **350**: 461–74.
25. Sohrab S, Yamashiro SM. Pseudorandom testing of ventilatory response to inspired carbon dioxide in man. *J Appl Physiol* 1980; **49**:1000–9.
26. Modarreszadeh M, Bruce EN. Long-lasting ventilatory response of humans to a single breath of hypercapnia in hyperoxia. *J Appl Physiol* 1992; **72**: 242–50.
27. Khoo MCK, Yang F, Shin JJW, Westbrook PR. Estimation of dynamic chemoresponsiveness in wakefulness and non-rapid eye movement sleep. *J Appl Physiol* 1995; **78**: 1052–64.
28. Dempsey JA. Crossing the apneic threshold: causes and consequences. *Exp Physiol* 2004; **90**: 13–24.
29. Fleming PJ, Goncalves AL, Levine MR, Woollard S. The development of stability of respiration in human infants: changes in ventilatory responses to spontaneous sighs. *J Physiol (London)* 1984; **347**: 1–16.
30. Khoo MCK, Marmarelis VZ. Estimation of peripheral chemoreflex gain from spontaneous sigh responses. *Ann Biomed Eng* 1989; **17**: 557–70.
31. Khoo MCK. Noninvasive tracking of peripheral ventilatory response to CO_2. *Int J Biomed Comput* 1989; **24**: 283–95.
32. Khoo MCK. Estimation of chemoreflex gain from spontaneous breathing data. In: Khoo MCK (ed.) *Modeling and Parameter Estimation in Respiratory Control*. New York: Plenum Press, 1989: 91–105.
33. Khoo MCK. Determinants of ventilatory instability and variability. *Respir Physiol* 2000; **122**: 167–82.
34. Ghazanshahi SD, Khoo MCK. Estimation of chemoreflex loop gain using pseudorandom binary CO_2 stimulation. *IEEE Trans Biomed Eng* 1997; **44**: 357–66.
35. Asyali MH, Berry RB, Khoo MCK. Assessment of closed-loop ventilatory stability in obstructive sleep apnea. *IEEE Trans Biomed Eng* 2002; **49**: 206–16.

Section 5

Technical perspectives

Section 5
Chapter
36

Technical perspectives

Technical specifications and standards

D. E. Supkis

Introduction

The performance specifications of a capnograph are discussed in the context of the ISO 21647 standard for respiratory gas monitors (RGMs) [1]. Additionally, alarm systems are discussed with reference to the Alarm Standard [2].

Standards

Clinicians use standards in every aspect of daily life, from which side of the road their automobiles travel to how pharmaceuticals are prescribed. A *standard* is defined by Merriam-Webster as: "something established by authority, custom, or general consent as a model or example." Standards govern the equipment used during various clinical situations (i.e., surgical anesthesia), and how the information provided by the equipment is used. These standards are clinical practice guidelines developed by various clinical organizations, such as the American Society of Anesthesiologists, American Association for Respiratory Care, and others. Equipment standards will be the focus in this section, and clinical practice guidelines are addressed elsewhere in this book.

There are two main developers of standards: governmental agencies, such as the Food and Drug Administration (FDA), and standards development organizations (SDOs) such as the American Society for Testing and Materials (ASTM), Comité Européen pour Normalisation (CEN), British Standards Institute (BSI), International Electrotechnical Commission (IEC), and International Organization for Standardization (ISO). For a standard to be written by a SDO, the need has to be first expressed. This need can be identified by manufacturers, governmental bodies, or users (clinicians). Typically, it is manufacturers that identify the need for a standard. This usually occurs when the device or technology that is the subject of the standard becomes accepted by the clinicians, and as a result, is widely used. In addition, because multiple manufacturers or providers of the technology compete in the marketplace, in the case that a new manufacturer wants to provide the technology, a widely accepted standard is extremely useful. The standard acts as a guideline for development of their product and, with documentation of conformance to the standard, approval by governmental regulatory agencies is expedited. This is especially true if the governmental regulatory agency recognizes the standard.

After the need for a new standard is assessed, usually by a formal balloting process, a SDO will host a working group consisting of clinicians, manufacturers, and interested parties, including representatives of governmental regulatory agencies. While specific details of the standards development process may differ slightly between SDOs, the overall process is the same. The working group of clinicians, manufacturers, and interested parties first develop a working draft of the standard; the draft is then balloted among its members. Once the draft has matured and has been affirmed by the working group ballot process, the draft standard is balloted to the subcommittee in charge of the standard (e.g., for capnography in the USA, it is F29 of ASTM). The committee will discuss the standard and conduct a formal ballot of the draft standard. Most SDOs have strict voting regulations. One of the most important regulations is the requirement that the total number of voting manufacturers cannot outnumber the total number of voting users and interested parties. The draft standard rarely passes on the first ballot, and will need to be balloted several times before passing. The working group reviews the negative votes, and the draft standard is modified as needed. Once the committee has approved the draft standard, it is submitted for society

Capnography, Second Edition, ed. J. S. Gravenstein, Michael B. Jaffe, Nikolaus Gravenstein, and David A. Paulus. Published by Cambridge University Press. © Cambridge University Press 2011.

(e.g., ASTM) balloting. This is a perfunctory step and is rarely disapproved. The entire process, from identifying a need to final approval of the standard, is extremely slow. It is common to take 2–5 years to get a standard approved. Another problem is that the standard process has its own unique vocabulary and procedures. For a newcomer to the world of standards, this new parlance and approach can be quite daunting. It is difficult for users and interested parties to participate in the development of standards due to the limited amount of time they can be away from their primary jobs and their travel budget. Hence, though there are many manufacturers serving as members of the committee, only a few have voting status. Once the standard is approved by the society, governmental agencies may adopt the standard. Some SDOs will adopt and use the approved standard as a basis for their own equipment standard.

Performance measures

Equipment standards are consensus-based standards developed solely for minimum safety and performance of medical equipment. They do not address how and where the equipment is to be used; those decisions are governed by the clinical practice standards at each institution. Equipment standards normally focus on how the equipment functions in the clinical environment, and are not aimed at clinicians and users. These standards are written specifically for manufacturers and governmental regulatory organizations. For example, in the USA, the FDA adopts a consensus standard and uses that standard as a basis for pre-market approval of medical electrical devices. The FDA may choose – and usually does – to add requirements to the consensus standards.

Before performance measures are discussed, a few definitions are in order. Note that standards attempt to define terms in as clear and unambiguous language as possible, often using other already defined terms as part of the definition. The definitions will be translated into many languages, and one must realize that while the "official" language of standards is English, there are many variants of English; thus, what constitutes an RGM must be defined.

An RGM is defined as:

> medical electrical equipment intended to measure the gas level(s) or partial pressure(s) in respiratory gases. NOTE: The RGM consists of a complete monitor including accessories, sensor, and sampling tube (in the case of a diverting RGM) specified by the manufacturer in the accompanying documents for the intended use of the RGM. (Definition 3.15) [1]

This definition is somewhat incomplete in that the scope of this IEC/ISO standard limits the device to use with humans in a continuous monitoring mode. It does not address spot check devices, such as those that measure carbon dioxide (CO_2) with colorimetric techniques.

There are only two types of RGMs:

(1) An RGM in which the sensor or detector is placed within the respiratory gas stream. An electronic cable connects the sensor to the supporting electronics. Such a device is commonly known as a mainstream RGM. For purposes of the standard, a mainstream RGM is defined as a non-diverting RGM.
(2) Sidestream or diverting monitors. The diverting monitors remove a portion of the respiratory gas from the breathing circuit, and transport the respiratory gases via a tube to the sensor located within the housing of the RGM.

The standard clearly defines the distinction between side- and mainstream gas monitors and the terms used within each of these monitor types. Another important term that requires definition is "sampling site," as there may be some confusion about its location in the monitor. For non-diverting monitors, the sample site and sensor are clearly located in the respiratory circuit. The location in diverting monitors is where the confusion lies. Is the sampling site in the housing of the RGM, or could it be the location of where the respiratory gases are sampled by a diverting RGM? The location of the sampling site for a diverting RGM is the "location at which respiratory gases are diverted for measurement to a remote sensor in a diverting RGM" [1].

Measurement accuracy

Measurement accuracy is the ability of an RGM to determine the composition of the respiratory gas mixtures. The resolution appears fairly easy, but is actually quite difficult, with many complicating factors to consider.

First, the composition of respiratory gases is not a binary or a two-part gas mixture (oxygen [O_2] and nitrogen [N_2]), or a three-part gas mixture, (O_2, N_2, and CO_2). There are many different gases involved, such as acetone (diabetic ketoacidosis), ethanol, methane (bowel obstruction), and the ever-present water vapor. Water vapor is disruptive to all current technologies that measure respiratory gases. Diverting or sidestream RGMs are especially susceptible to interference by water. The gas sample with the water vapor

Table 36.1 Measurement accuracy (from ISO 21647, 2004)

Gas	Measurement accuracy (gas levels in % volume fraction)
Halogenated agent	± (volume fraction of 0.2% + 15% of gas level)
CO_2	± (volume fraction of 0.43% + 8% of gas level)
Nitrous oxide	± (volume fraction of 2.0% + 8% of gas level)
O_2	± (volume fraction of 2.5% + 2.5% of gas level)

Source: © International Organization for Standardization (ISO). This material is reproduced from ISO 21647 with permission of the American National Standards Institute on behalf of ISO.

is transported via the sampling tube (which is usually several feet long) from the sample site to the sensor. The water vapor will cool and start to condense. The condensate can cause obstruction to the flow of respiratory gases in the RGM, or can contaminate the sample site, resulting in inaccurate respiratory gas measurements.

An O_2 analyzer can be a very simple device used to measure the fraction of inspired O_2 (FiO_2 meter). Several technologies are currently used that are quite adequate, robust, and inexpensive. Other types of more rapid response O_2 analyzers can measure inspired and expired O_2 concentration on a breath-by-breath basis. The technology used in these analyzers is quite different than the simple FiO_2 meter. The goal of the standard was not to render the simple, but adequate, O_2 analyzers obsolete. Measurement accuracy is specified by the ISO/IEC standard and provided in Table 36.1.

The next major difficulty in measurement accuracy is how to assess the effects of other gases present in the respiratory gas mixtures. Most equipment standards try to emulate clinical situations in their testing procedures, although it is technically difficult given the myriad of clinical conditions. The goal of equipment standards is to develop testing apparatus and test procedures that are representative of clinical situations; otherwise, testing becomes difficult and is subject to interpretation. The gas mixtures required, when measuring accuracy to arrive at the standard, use nitrogen as the carrier gas. Most test gases do not contain O_2 for many reasons. The presence of O_2 degrades the shelf-life of the test gases, and the O_2 reacts with the halogenated agents and the walls of the containment vessel. Thus, over time, the O_2 concentration in the test gas mixtures changes. The test gases were also chosen so that they could be easily obtained in reasonable quantities and transported by customary methods. Moreover, certain combinations of halogenated agents in an O_2 mixture are not stable, and are potentially explosive. The accuracy requirements for halogenated anesthetic agents and nitrous oxide are broad for two reasons: (1) halogenated agents are, chemically, very similar to each other; and (2) historically, clinical practitioners have thought that the ranges were adequate for clinical use.

Another difficulty in obtaining accurate measurement can be illustrated through statements concerning the accuracy for CO_2. In an earlier standard, ASTM F1456–01 [3], the accuracy of CO_2 was stated in confusing language, and accuracy requirements were specified in a different format than other RGMs, namely, anesthetic agents and O_2 analyzers. The accuracy for CO_2 in both ASTM F-1456–01 and ISO 9918 (1993) was stated as "the carbon dioxide reading shall be within ±12% of the test gas value or ±4 mm Hg whichever is greater, over the full measurement range of the capnometer, corrected to one atmosphere."

Measurement accuracy has been defined as the "quality which characterizes the ability of an RGM to give indications approximating to the true value of the quantity measured" [1]. The *maximum inaccuracy* for a capnograph has been defined in the standard as: CO_2 plus or minus (volume fraction of 0.43% plus 8% of gas level) gas levels in volume fraction %.

The offset provided some tightening of the specifications around 0, but was not clinically or technically insurmountable, in addition to some relaxation of the physiologic specifications in a range that was, again, clinically not significant. This can be viewed from Figure 36.1 which plots both the former (ISO 9918, 1993) [4] and current (ISO 21647, 2004) accuracy specifications [1].

Measurement range

Capnometers for clinical use must be able to detect CO_2 in the range of 0–10%, or 76 mm Hg. An extended range to 100 mm Hg and greater can be useful for detection of gross hypercapnia.

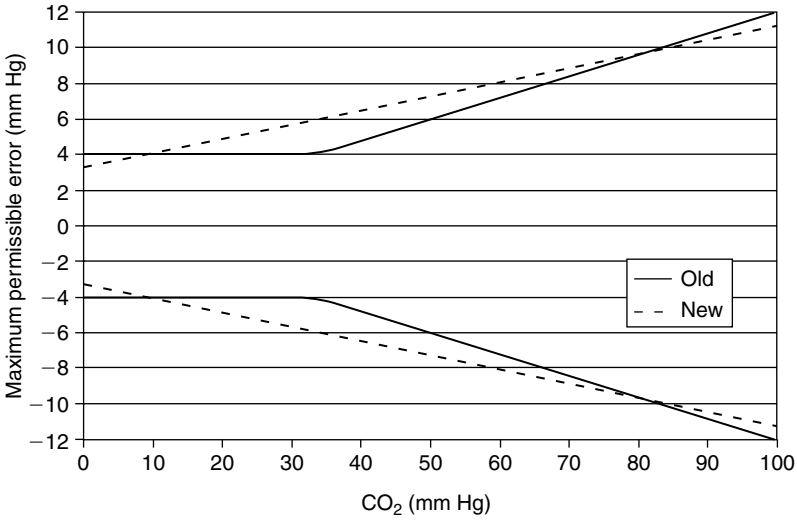

Figure 36.1 Maximum inaccuracy specification per ISO RGM standards.

Measurement drift

An RGM is usually left on for extended periods of time, from weeks to months at a time. When an electronic device, such as a capnograph, is initially powered on, there is an interval of time where the device "warms up." After the warm-up period, the device is ready for use. If the device is used for an extended interval of time, the calibration of the device may wander outside of normal operation: this phenomenon is called *drift*. A capnograph should be able to hold its calibration for a reasonable period of time. The capnograph should not have to be recalibrated – or have its calibration checked – every few hours, a need only required in first-generation machines. The standard of the current RGM refers to it as *drift of measurement*. The monitor is set up in normal operating mode, and is allowed to stabilize for at least 6 h. At the beginning of the test, the RGM is verified for accuracy. After operating for 6 h, it is again tested, and then at 3 h intervals thereafter to ensure that accuracy has been maintained, and that there is no significant drift of measurement.

The gases used in accuracy testing mimic clinical situations, and consist of CO_2, nitrous oxide, O_2, and anesthetic vapors, with a balance of nitrogen. Since test gases that contain O_2 and anesthetic vapors are inherently unstable, this testing is kept to a minimum.

Response time

One of the most important features in an RGM for the clinician is the total system response time. Basically, when there is a change in patient condition, when and how is the clinician alerted to that change? The standard defines *total system response time* as the time from the step function change in gas levels at the sampling site to achieve 90% of a final gas reading. This is often further subdivided into delay time and rise time. *Delay time* is sometimes called lag or transit time. Delay time depends on sampling flow rate, the diameter and length of the sampling tube, and the sample viscosity. In general, faster flows, shorter tubes, and lower viscosity result in shorter delay time. Rise time can be characterized in a number of ways. All relate to the assumption that the 0–100% response is exponential and lengthy. In most applications, the clinician is not interested in how long it takes to obtain a 100% response; 90% or 95% is usually satisfactory (see Figure 36.2). By subjecting a measuring system to an instantaneous change, that is, a change that is very fast compared with the response of the system being measured, we can assess the true response characteristics of the system. This is sometimes referred to as a *step change*. The manufacturers are expected to disclose the total response time to the clinician so that the clinicians can make a reasonable comparison between varieties of devices. Non-diverting capnographs have an advantage in this area, as there is no delay time.

For mainstream or non-diverting RGMs, the total system response time is primarily a function of how fast the respiratory gas starts flowing past the sensor. The RGM standard regulates the flow of gases to a specific velocity so that manufacturers with different sample size cells have a level playing field of total system response time.

It is now possible to compare the performance of pediatric and adult RGMs. For diverting or sidestream

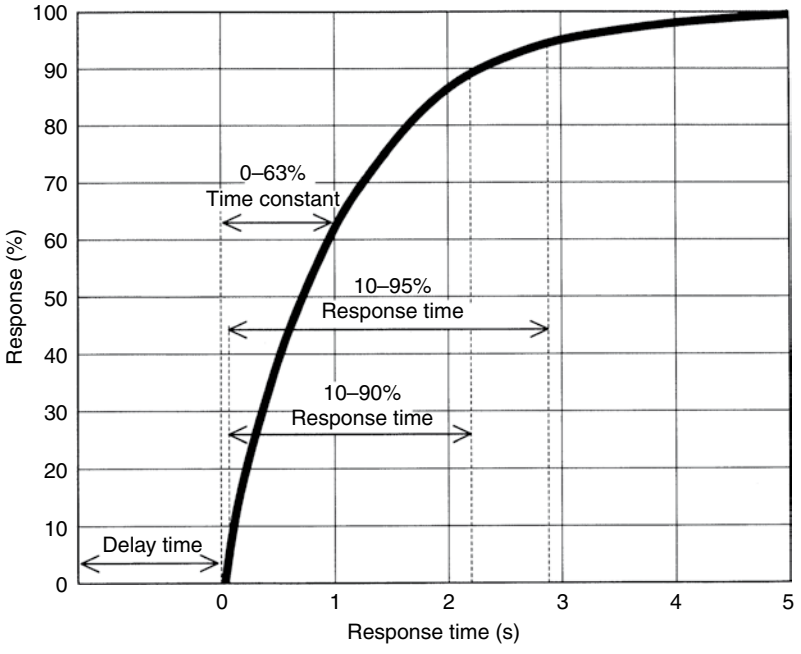

Figure 36.2 For sidestream sampling, total response time is equal to the delay or transit time in the sampling catheter plus the measurement rise time which is expressed different ways. [From: Gravenstein JS, Paulus DA, Hayes TJ. *Capnography in Clinical Practice*, 2nd edn. Boston, MA: Butterworth-Heinemann,1989.]

RGMs, the manufacturer is required to list the total system response time for each sample flow rate that is designed to operate in a specific RGM. In this manner, the clinician can compare a variety of diverting RGMs, as the total system response time is highly dependent on the sample flow rate. For example, with a neonatal respiratory circuit, it would be inappropriate for a sample rate to be 250 mL/min; this sample flow rate would be potentially excessive (>3 mL/s) for an infant, and could render mechanical ventilation inadequate. However, the total system response time would be quite good. On the other hand, a 10 mL/min sample rate in an adult patient would have an inadequate total system response time.

What response time is necessary? The answer to that question has two parts. First, response time must be fast enough to measure both end-tidal and inspiratory gas concentrations accurately. Second, response time should also be fast enough to provide a high-fidelity display of the concentration waveform. Interpretation is valid only when the waveform accurately represents the profile, or at least, accurately enough to detect the events for which the patient is being monitored.

Interfering gas and vapor effects

The quantitative effects (if any) on gas readings caused by the interfering gases (given by the gas levels listed in Table 36.2) are disclosed in the operating instructions of a machine (e.g., users' or service manual). The capnometer can – and usually does – encounter unexpected gases, as well as new anesthetic and therapeutic gases. It is the intent of the standard to require the manufacturer to disclose the effects of these gases on the measurement of CO_2. These unexpected gases may cause the capnometer to display falsely low or high readings. Common gas vapors that interfere with gas readings include ethanol, acetone (e.g., in diabetic ketoacidosis), and methane (e.g., in bowel obstruction). Isopropanol, the primary ingredient in "alcohol wipes," is used as a cleaning agent for medical equipment. During the cleaning of medical equipment, capnographs may inadvertently sample vapors of isopropanol, resulting in a prolonged inaccuracy of capnograph, depending on the technology used. Xenon, a relatively new anesthetic vapor primarily utilized in a research environment, has major technology problems to overcome before it can be widely used. Helium–O_2 mixtures (i.e., heliox) are now quite commonly used in patients with upper respiratory airway obstruction to help bridge the patient with an obstructed airway until definitive management can be completed. The propellants used in metered dose inhalers and frequently in the operating room, intensive care unit, and emergency room settings can cause interference in RGMs.

Table 36.2 Test gas levels of interfering gases and vapors (from ISO 21647, 2004)

Gas or vapor	Gas level (% volume fraction)[a]
Nitrous oxide	60[b]
Halothane	4[b]
Enflurane	5[b]
Isoflurane	5[b]
Sevoflurane	5[b]
Xenon	80[c]
Helium	50[d]
Metered dose-inhaler propellants	Specified by the manufacturer
Desflurane	15[b]
Ethanol	Specified by the manufacturer
Isopropanol alcohol	Specified by the manufacturer
Acetone	Specified by the manufacturer
Methane	Specified by the manufacturer

[a] Test gas levels shall be ±20% of the specified level.
[b] If intended for use with inhalation halogenated agents.
[c] If intended for use with xenon.
[d] If intended for use with helium.
Source: © International Organization for Standardization (ISO). This material is reproduced from ISO 21647 with permission of the American National Standards Institute on behalf of ISO.

Units

As international organizations, both the ISO and IEC normally require all units of measurement to be expressed in the metric system. Unfortunately, medicine has not completely adapted or converted over to the metric system. It is common and easier to use the traditional non-metric units of measure for certain measurements, such as volume percent to express the concentration of anesthetic gases and vapors[1] and millimeters of mercury for measuring CO_2.

Alarm systems

Much progress has been made concerning medical alarms, such as the various types of alarm signals, as well as the ability to define and set alarms to alert the clinician of changing patient conditions (IEC 60601–1-8, 2006, 2nd edn.) [2]. Historically, equipment manufacturers developed alarms as the need materialized and they saw fit. It is common to have a variety of alarm protocols in operating room suites, with protocols often differing from room to room, the postanesthetic care unit (PACU), and the intensive care unit. Large manufacturers could develop a protocol for every product line. This standard has been through many lively discussions, heated drafts, and contentious voting cycles. It has unified the clinical alarm protocols into a single document. Three different types of alarm conditions are defined: high, medium, and low priority, with a variety of alarm signals mandated by the alarm condition. To simplify it, a *low-priority* condition triggers a low-priority alarm, usually a blinking light. A *medium-priority* condition signals a medium-priority alarm, which is a beep and a flashing light. A *high-priority* condition results in a high-priority alarm signal, usually flashing lights and beeping sirens. The respiratory gas alarm condition priorities are listed in Table 36.3. The only high-priority alarm listed in the entire table is for situations when the FiO_2 is less than 18% O_2. This is a life-threatening condition that could be caused by a mechanical failure, and is usually not the result of a clinical intervention. For anesthetic agents, there is a two-tiered alarm system that depends on the ability of the RGM to quantitate a mixture of anesthetic agents.

Luer connections

The Luer connector is the most common connector in the entire hospital. It connects virtually every single piece of intravenous (IV) tubing, every single needle, and a variety of other devices. The *Luer connector* is defined as a 6% conical taper by international standard [5,6]. The Luer connector is a compact, secure, and easily manufactured connector, features that have given rise to its ubiquity within the hospital. Unfortunately, it has created some problems. In Europe, cross-connects between IV and enteral feeding systems and several medication errors have been linked to Luer connectors. The European Committee for Standardization, CEN, commissioned a report by the CEN Healthcare Sector Forum (CEN/CHeF) to examine the validity of problems with the use of Luer connectors. The investigative committee was tasked with reviewing the world's medical literature involving Luer connectors and cross-connects. After an extensive review, the committee found about a dozen reports of cross-connects. These cross-connects occurred mainly in two categories: (1) enteral feeding devices connected

[1] The standard does provide that anesthetic vapors be converted over to minimum alveolar concentration (MAC) values. The manufacturer must either use the standard MAC values of a healthy 40-year-old adult male patient which is published in the package insert mandated by the FDA or disclose how MAC values are derived.

Table 36.3 Alarm priorities for RGM (from ISO 21647, 2004)

	Alarm condition priority[a]	
Gas	**Low gas level**	**High gas level**
Inspired halogenated anesthetic agent	Low priority[b]	Medium priority
Exhaled CO_2	Medium priority	Medium priority
Inspired CO_2	–	Medium priority
Inspired nitrous oxide	Low priority[b]	Medium priority[b]
Inspired O_2	Medium priority	Medium priority[b]
Inspired O_2, 18%	High priority	–
Multiple halogenated anesthetic agents present[c]	Medium priority	Medium priority
Multiple halogenated anesthetic agents, value <3 MAC[d]	Low priority	Low priority
Multiple halogenated anesthetic agents, value >3 MAC[d]	Medium priority	Medium priority

[a] The priorities listed are the minimum priority. Exhaled gas level alarm conditions may also be provided.
[b] This alarm condition is optional.
[c] When the RGM is capable of detecting but not capable of quantifying and displaying the mixture of halogenated anesthetic agents.
[d] When the RGM is capable of detecting, quantifying, and displaying the mixture of halogenated anesthetic agents.
Source: © International Organization for Standardization (ISO). This material is reproduced from ISO 21647 with permission of the American National Standards Institute on behalf of ISO.

to IV systems and (2) pneumatic-powered devices connected to IV systems. Several of the cross-connects were the result of patients mistakenly connecting one system to another. The CEN/CHeF recommended that Luer connectors be limited to the IV systems only, and sought to develop new connectors for all other systems. The task of developing new connector systems for small-bore connectors (connectors with a maximum bore diameter of 8.5 mm) has been assigned to a joint working group under the administrative lead of ISO Technical Committee 210. The family of standards under development (ISO 80369–1 through 7) [7] includes a Part 1 standard for general requirements and Parts 2 through 7 for specific requirements for connectors:

Part 2: Connectors for breathing systems and driving gases applications
Part 3: Connectors for enteral applications
Part 4: Connectors for urethral and urinary applications
Part 5: Connectors for limb cuff inflation applications
Part 6: Connectors for neuraxial applications
Part 7: Luer fittings (ISO 594 replacement).

The risk assessment for harm to the patient as it relates to RGMs is solely related to a cross-connect of the exhaust port of diverting (i.e., sidestream) monitors. Note that the current standard mandates that the exhaust port shall not be a Luer connector and, as such, significantly decreases the risk of the exhaust port being connected to an IV system, which would thereby cause harm to the patient. Cross-connects of the inlet port to the diverting or sidestream RGMs could be a hazard to the patient if the consequence was monitor malfunction or inaccurate reading. The sample tube connection to the breathing circuit is usually a female Luer connection. This is clinically important because inhaled bronchodilator medications are given through this port as well as resuscitative drugs. Unfortunately, an IV or feeding tube can also be attached to this port, although there is a large disparity in size of IV tube connections, which makes it quite obvious that this is not to be connected to either enteral or IV fluids.

The current standard

The current ISO/IEC RGM standard replaces previous standards which were a combination of individual standards of O_2 analyzers, capnographs, and anesthetic agent monitors. The RGM standard is primarily written for manufacturers in order to ensure that all RGMs perform equally in the clinical environment and that regulators have a fail-proof system for accepting or rejecting new RGMs. For clinicians, the standard serves as a basis for comparison of RGMs, ensuring that all RGMs work in a similar function.

Electromagnetic interference and radiation

Noise is an unwanted signal. Electromagnetic interference and radiation have causative factors that are

both external and internal to the measuring system. Noise not only interferes with the ability to get accurate quantitative information but also, in gas analysis, may obscure some details of the waveform that may be important. External sources include electromagnetic radiation in the radio frequency range. Radio transmitters, oscillators, and power lines, for example, transmit noise in a narrow band. Wide-band sources include radiation from the stratosphere, and discharges from various electrical equipment (X-ray machines, motors, pumps, lighting, etc.). Moreover, an electrical conductor can act as an antenna for the reception of this type of signal. Interference can be greatly reduced by proper shielding, which involves enclosing the critical conductors in a conductive material that is grounded. Standards have, therefore, been developed to test medical equipment for their immunity to electromagnetic interferences, as well as to assure that they do not emit electromagnetic interference that might interfere with other equipment. A collateral standard, IEC 60601–1-2 (2007) [8], has been developed and describes these tests.

Calibration

Long-term stability is an important criterion, and determines the frequency of calibration. Even if calibration is automatic, it requires time and may interrupt monitoring. Indeed, to attain the full benefits of capnography, monitoring must be continuous. Automatic zeroing during the inspiratory phase is particularly troublesome because inspiratory gas occasionally contains CO_2 (e.g., when an expiratory valve fails or the CO_2 absorber is exhausted). Lengthy procedures for calibration should be required infrequently and brief procedures no more than once a day. Most modern infrared capnographs are stable for at least 1 month (perhaps longer); some are touted to not need calibration for 1 year. There are various ways to confirm the accuracy of end-tidal values of CO_2 when an instrument generates data that do not match clinical expectations. An optical filter, a beam occluder, or a sample cell containing CO_2, or gas from a cylinder, all produce signals that can confirm the operation of the instrument.

Acknowledgment

The tables in this chapter are from ISO 21647 with permission of the American National Standards Institute on behalf of ISO. No part of this material may be copied or reproduced in any form, electronic retrieval system or otherwise or made available on the Internet, a public network, by satellite or otherwise without the prior written consent of the American National Standards Institute (ANSI) 25 West 43rd Street, New York, NY 10036. Copies of this ISO document may be purchased from the ANSI, (212) 642–4900, http://webstore.ansi.org.

References

1. International Organization for Standardization. ISO 21647 (2004). Medical electrical equipment – particular requirements for the basic safety and essential performance of respiratory gas monitors. Available online at http://www.iso.org/iso/iso_catalogue/. (Accessed November 22, 2010.)
2. International Electrotechnical Commission. IEC 60601–1-8 (2006). (2nd edn). Medical electrical equipment. Part 1–8: General requirements for safety – collateral standard: general requirements, tests and guidance for alarm systems in medical electrical equipment and medical electrical systems. August. Available online at http://www.iso.org/iso/iso_catalogue/. (Accessed November 22, 2010.)
3. American Society for Testing and Materials. ASTM F1456–01 (2001). Standard specification for minimum performance and safety requirements for capnometers. Available online at http://www.astm.org/standard/indexshtml/. (Accessed November 22, 2010.)
4. International Organization for Standardization. ISO 9918 (1993). Capnometers for use with humans – requirements. Available online at http://www.iso.org/iso/iso_catalogue/. (Accessed November 22, 2010.)
5. International Organization for Standardization. ISO 594–1 (1986). Conical fittings with a 6% (Luer) taper for syringes, needles and certain other medical equipment. Part 1: General requirements. Available online at http://www.iso.org/iso/iso_catalogue/. (Accessed November 22, 2010.)
6. International Organization for Standardization. ISO 594–2 (1998). Conical fittings with 6% (Luer) taper for syringes, needles and certain other medical equipment. Part 2: Lock fittings. Available online at http://www.iso.org/iso/iso_catalogue/. (Accessed November 22, 2010.)
7. International Organization for Standardization. ISO/DIS 80369–1 (2006). Small bore connectors for liquids and gases in healthcare applications. Part 1: General requirements. Available online at http://www.iso.org/iso/iso_catalogue/. (Accessed November 22, 2010.)
8. International Electrotechnical Commission. IEC 60601–1-2 (2007). (3rd edn). Medical electrical equipment. Parts 1–2: General requirements for safety – collateral standard: electromagnetic compatibility–requirements and tests. September. Available online at http://www.iec.ch/. (Accessed November 22, 2010.)

Section 5
Chapter
37

Technical perspectives

Carbon dioxide measurement

M. B. Jaffe

In this chapter, we review the technical aspects of carbon dioxide (CO_2) measurement techniques currently available: infrared (IR), acoustic, colorimetric, and mass spectrometry, with a focus on IR-based approaches (Table 37.1). The Raman method is no longer commercially available and therefore not discussed. We also compare mainstream and sidestream approaches. Before discussing the technologies, some interesting properties of CO_2 deserve comment.

Carbon dioxide and its physical properties

Interest in the critical role of CO_2 in such essential phenomena as metabolism, photosynthesis, combustion, and environmental temperature control has furthered the development of a number of methods to detect and quantify CO_2. Carbon dioxide's well-documented physical properties are the key to understanding the relevant analytic techniques. At normal temperatures and pressures, CO_2 is a colorless, odorless gas. Its concentration in air is so small (0.03%) that air is usually treated as if the partial pressure of CO_2 (PCO_2) were zero. This may not be the case in poorly ventilated rooms or encapsulated spaces (submarines) where the PCO_2 can rise above 1% of ambient pressure.

Carbon dioxide has a molecular weight of 44, is very soluble in polar solvents such as water, and reacts with water to form carbonic acid, a weak acid. Also, this molecule is easily fragmented and ionized to form charged species, and has optical absorption bands in the IR spectrum. There is a remarkable similarity between several of the physical properties of CO_2 and nitrous oxide (N_2O). Both deviate from the ideal gas law to the same degree, as indicated by their mole volumes of 22.25 L instead of the ideal mole volume of 22.4 L. Both are soluble in water, which is an advantage physiologically but a disadvantage with online methods of analysis in wet systems where out-gassing in a rapidly changing concentration can be a problem. Nitrous oxide also has absorption bands in the IR spectrum, some of them close to those of CO_2.

Measuring gas concentration in a respired gas requires a continuous, fast response and the ability to distinguish different gases from each other. This technology is very different from that used to measure CO_2 in a sample of gas or blood. The technologies that have been successful rely on the asymmetric modes of molecular vibration to enable CO_2 to absorb IR light, as well as the symmetric modes of vibration to enable CO_2 to scatter light (Raman) and the ability of the molecule to be charged in an electron beam to enable the use of mass spectrometry.

The electromagnetic spectrum can be described by wavelength (λ), wave number ($n = 1/\lambda$), and frequency ($\nu = c/\lambda$), where c is the velocity of light. Infrared spectroscopists use wave number because it is proportional to energy:

$$E = h\nu = hc/\lambda,$$

where h is Planck's constant. This relationship is a reminder that higher-energy quanta have higher frequencies, higher wave numbers, and shorter wavelengths. Some of these frequencies have enough energy to ionize molecules (roentgen and ultraviolet); some are absorbed and cause chemical reactions (ultraviolet and visible); and some influence the vibration and rotation of molecules (IR). The IR spectrum begins just beyond the red part of the visible spectrum (0.4–0.8 μm) and extends to approximately 40 μm (10^{-6} m = 1 μm). The near-ultraviolet begins at 0.2 μm and extends up to the visible. The far-ultraviolet (less than 0.2 μm) and the X-ray region involve high-energy quanta. Generally, the last two have neither been practical nor suitable for online clinical gas monitoring because of safety concerns.

Capnography, Second Edition, ed. J. S. Gravenstein, Michael B. Jaffe, Nikolaus Gravenstein, and David A. Paulus. Published by Cambridge University Press. © Cambridge University Press 2011.

Table 37.1 Selected CO_2 measurement devices used clinically

Technology	Type	Manufacturer	Model(s)[a]	References of interest
Infrared	Mainstream	Philips-Respironics (Wallingford, CT)	Capnostat® III,V	[45,46]
	Mainstream	Protocol (Pryon) (Menomonee Falls, WI)	SC-300	[47]
	Sidestream	Philips-Respironics (Wallingford, CT)	LoFlo™	[48]
	Sidestream	Oridion (Needham, MA; Jerusalem, IL)	Microstream®	[49]
Colorimetric	Indicator-metacresol purple	Nellcor Puritan Bennett (Pleasanton, CA)	EasyCap® II	[50]
Photoacoustic	-	Innova AirTech Instruments (Ballerup, Denmark)	Model 1312	[51]
Mass spectroscopy	Quadrupole	Centronic Limited (Croydon, UK)	MGA 200	-

[a] Monitor or sensor technology/name.
Source: Adapted with data from: Nellcor Puritan Bennett Inc. EASY CAP II brochure, 1997 and Mercury Medical StatCO_2 brochure 2003.

Infrared technology

General description

The IR part of the spectrum has distinct advantages for medical monitoring. Its energy is safe because it causes no permanent changes in the molecule. The absorption of IR light increases molecular rotation and vibration, which increases temperature and pressure, but only modestly. Therefore, IR technology can be used in-line to measure respiratory gases. Blackbody radiators heated to moderate temperatures can be used to radiate IR energy, which can be detected by a host of solid-state devices. Materials that can transmit IR energy are readily available for sample cell windows and filters. In essence, IR instruments are simple and relatively inexpensive.

Carbon dioxide has a strong absorption band in the near-IR region (4.26 μm), which lies between two strong bands for water vapor, and yet is separated enough from the main bands of most other potentially interfering molecules (Figure 37.1).

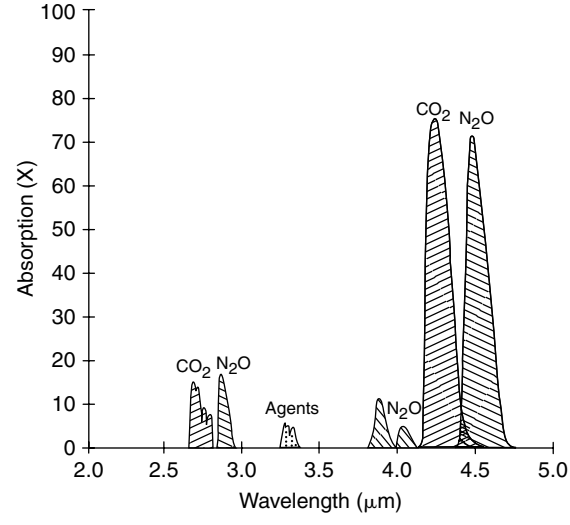

Figure 37.1 The IR absorption spectrum for the gases CO_2 and N_2O and the volatile anesthetic agents. [Reproduced with permission from: Raemer DB, Calalang I. Accuracy of end-tidal carbon dioxide tension analyzers. *J Clin Monit* 1991; **7**: 195–208].

Infrared absorption requirements

In order to absorb IR radiation, a molecule must be both asymmetric and polyatomic. Atoms or molecules such as helium, argon, hydrogen, oxygen, and nitrogen do not satisfy these requirements and, therefore, do not absorb IR radiation, whereas CO_2, N_2O, and water do. However, molecular asymmetry does not simply

mean that different atoms exist in the same molecule. It also means that allowed IR vibrations will cause the centers of electrical charge to be displaced; in other words, an allowed vibration will alter the molecule's dipole moment. A *dipole* consists of two equal and opposite electrical charges that are slightly separated. Its moment is the product of charge and separation distance. Carbon dioxide serves as a good example of the principles involved because it has both symmetric and asymmetric vibrations. The frequency with which these vibrations occur depends on the masses of the atoms, as well as the strength of the bond holding the atoms together. These vibrations occur at frequencies on the order of 10^{13} per second. This corresponds to frequencies found within the IR part of the spectrum. The absorption of IR energy simply increases the amplitude of these vibrations, but does not change their frequencies. Given that a linear molecule with n atoms has $3n - 5$ fundamental vibrations, CO_2 ($n = 3$) must have four fundamental vibrational modes. For CO_2, two IR-active fundamental vibrations are predicted and two are found: one at 2349 cm^{-1} (4.26 μm) and the other at 667 cm^{-1} (14.99 μm). Fortunately, the high-intensity waveband for CO_2 at 4.26 μm lies between two intense bands for water. With carefully characterized, narrow-band pass optical filters, CO_2 can be measured with little interference either from water vapor or from the neighboring band for N_2O [1].

Pressure broadening

As we have described, IR absorption is a measure of the vibrational frequencies of atoms within a molecule. Associated with these vibrational absorption bands are a number of other lines related to the rotation of the molecule. These energy transitions are usually small, and are sometimes called *rotational* or *sidebands*. To summarize, the IR spectra of gases are due to a combination of transitions involving both vibrational and rotational energy levels that combine to produce a band structure. These transitions depend on factors both internal and external to the molecule. Internally, the vibrational frequencies depend on the strength of the bond between atoms and their relative masses. Rotation depends on their moments of inertia. Externally, temperature, spatial arrangement of atoms, intermolecular forces, and collisions between molecules influence these transitions. This external relationship results in absorptions that depend on the other molecules in the gas mixture, as they influence intermolecular forces. Collisional dependence can be seen empirically because sidebands widen as the pressure increases. As pressure decreases (either due to changes in total pressure or the PCO_2), fewer intermolecular collisions occur, and the bandwidth narrows. Similarly, as the pressure increases, more collisions occur, and the bandwidth widens [2]. This dependence on pressure is recognized by the usual terminology – *collision* or *pressure broadening* – and tends not to be device-specific [3]. It is a complex function of the total pressure and the presence of other gases. In effect, the absorption band is spread out, and the use of narrow-band sources or filters fails to correct this result. System software using nominal values typically compensates for this effect.

Consequently, a calibration curve depends not only on total pressure but also on the constituents of the gas mixture. Change the constituents and the curve changes. Correction for this effect is perhaps most important for CO_2 because CO_2 is usually present in relatively low concentrations (5%), along with other gases that can vary greatly and reach high concentrations. In the intensive care unit, for example, CO_2 will be measured in expired gas and in a wide variety of O_2 concentrations; in the operating room, measurements will be made in the presence of highly variable concentrations of N_2O and O_2 as well as low concentrations of volatile anesthetic agents. The accuracy of measurement of N_2O, present in high concentrations, is not expected to be greatly influenced by relatively small amounts of CO_2 and volatile anesthetic agents. Correction for significant concentrations of O_2, however, has not been reported; the effect is probably minimal, and the accuracy requirements for N_2O are not great.

The measured absorption of CO_2 can be altered by cross-interference and collision broadening due to the presence of gases such as N_2O and O_2. Cross-interference, the overlapping of absorption bands of other gases, can occur from N_2O due to the presence of strong absorption bands that slightly overlap both edges of the CO_2 band (Figure 37.1). The impact of this effect can vary significantly between devices. However, the use of narrow-band sources or narrow-band filters in front of a detector with sufficiently small half-power bandwidths can effectively eliminate the effect of cross-interference.

Lambert–Beer law

All IR instruments consist of a radiation source, a cell through which samples of gas flow, and a detector that produces a signal related to the intensity of the

radiation detected. The quantitative aspects of photometric measurement are stated by the Lambert–Beer law as:

$$A = \log (I_0/I) = \varepsilon I_c.$$

Under carefully controlled conditions at a select absorption band, the absorbance of a sample (A) is proportional both to the concentration of sample (c) and the depth of the absorbing layer (I). The molar extinction coefficient (ε) is a wavelength-dependent constant that characterizes the sample. I_0 is the intensity of radiation with no sample in the beam, and I is the intensity with a sample. For solutions, absorbencies are additive. Absorbance can thus also be written as minus the log of the transmittance ($A = -\log T$), which denotes that the relationship between concentration and transmittance is non-linear. Transmittance approaches zero as concentration approaches infinity. However, a part of the range approaches linear.

In the IR region, gases do not follow the Lambert–Beer law because of the pressure-broadening effect. Both total pressure and diluent gases influence the sidebands and, thus, the amount of radiation absorbed. However, under controlled conditions, calibration curves can be constructed, the influence of perturbations studied, and quantitations made.

Non-dispersive IR monitors

Infrared absorption methods of gas measurement can be sensitive and selective, as well as provide a continuous, accurate, precise, and rapid response that is not saturated or damaged by high concentrations of the "target" gases such as CO_2. Most continuous monitors of respiratory gases are of the non-dispersive IR (NDIR) type; they do not have the capacity for dispersing the radiation into its component wavelengths as do dispersive types (i.e., spectrometers). The essential components of nearly all IR gas analyzer are (a) a source of IR radiation with an emission spectrum that includes the absorption bands of the gases to be measured; (b) a sample cell fitted with windows "possessing" suitable transmission properties; (c) an optical or gas filter to limit the wavelength range measured by the detector; (d) a means, either physical in the form of a rotating chopper disk or an electronic circuit, to modulate the IR radiation from the source; and (e) a detector to convert the IR radiation into an electrical signal [4]. NDIR-type devices can be classified into two categories based upon whether or not the device uses a selective or non-selective detector. A selective detector uses a narrow-band filter so that only light within that band can be measured, whereas a non-selective design would not use such filtering. NDIR-type devices can be further divided into *double-beam-in-space* or *double-beam-in-time* (i.e., single path, dual wavelength) [4]. The primary components of an IR system – the source, the detector, and chopper – will be described in greater detail.

Sources

The source of IR radiation may be broad- or narrow-band. It may be electronically pulsed or constant and chopped mechanically. It may be filtered with narrow-band filters either at the source or the detectors. For narrow-band emission, some sidestream monitors use an electric discharge source consisting of a hermetically sealed glass tube containing a gas. The gas is excited by the application of a high-voltage, radio frequency electromagnetic field, which results in the emission of a narrow IR spectrum. Benches with broad-band sources also utilize reliable and stable narrow-band interference filters in front of the detectors to measure in-band signal for CO_2 and separately out-of-band signal as a reference channel. Thus, one can select only a portion of the CO_2 band, effectively eliminating any interference from water vapor or the even closer bands of N_2O. The absorption of the IR radiation by CO_2 is non-linear, affected by the presence of other gases and proportional to gas concentration, path length, and absorption coefficient of the particular gas. The non-linearities, path length, and specifics of the bench design are typically estimated with data from an empirical lookup table that translates the measured signals to a value in CO_2, which is then corrected by most manufacturers for the effects of gases such as O_2 and N_2O.

Detectors

The IR detectors can be a microphone-type or solid state. Microphone-type detectors are filled with IR absorbing gas, which is heated by the radiation it receives, and expands as a consequence. The microphone detector can have a single or dual chamber. The single-chamber type is also called the *Veingerov design* [5], and the dual-chamber type is called the *Luft design* [6]. In the Luft design, a diaphragm separates the two chambers. The single-chamber design has less drift but is more sensitive to vibration. The position of the diaphragm can be detected by capacitance techniques or by measuring the gas flow from one chamber to the other. Another way of designing a respiratory gas detector, common to nearly all current commercial devices, is

to use solid-state sensors that have broad-spectral sensitivity and an optical filter that transmits radiation in the appropriate region. These filters can be made with bandwidths that are quite narrow, e.g., 5% of the peak wavelength at 50% transmission. An excellent detector for gases such as CO_2, with strong absorption peaks in the near-IR range, is lead selenide because of its broad-spectral response in the near-IR region. It is sometimes thermoelectrically cooled to improve signal-to-noise ratio. One limitation of the solid-state detector is its lower sensitivity (relative to the microphone types of the same path length) when the measured concentrations are low. The disadvantages of the microphone designs include vibration sensitivity and higher cost.

Chopper

The use of a chopper, either mechanical or electronic, permits a common source and detector in the double-beam-in-time types, but has the added advantage of producing and alternating signals, one from the sample beam and the other from the reference beam. The PCO_2 is then calculated using the difference of the transmittance of the two measured signals. Also a chopper can be used to modulate the IR source, and a beam splitter can be used so that half of the light is seen by a detector with a filter selective to a strong absorption band for CO_2 and the other half seen by a detector with a filter selective to a region of the IR spectrum where little or no IR radiation is absorbed by CO_2 (Figure 37.2). The CO_2 concentration is then calculated using the ratio of the transmittance of the two measured signals.

Some analyzers use a single beam with a rotating filter wheel. This has the advantage of combining the signal modulation produced by the chopper with multigas monitoring, as well as source and sample cell monitoring with a reference cell. Appropriate optical filters are mounted in the wheel, along with a reference cell. Each revolution provides the necessary optical information to calculate gas concentrations. For greater detail on IR spectroscopy and IR instrumentation, consult any of the excellent references books [1,7].

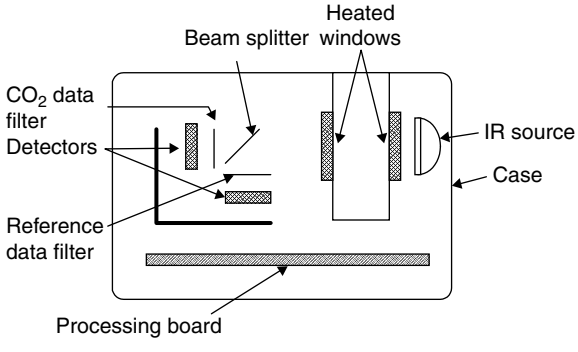

Figure 37.2 Cross-section of representative solid-state mainstream coaxial design.

Other methods

Photoacoustic spectroscopy

Photoacoustic spectroscopy (PAS) combines pulsed excitation of the gas by IR energy and acoustic detection of the pressure changes by a sensitive microphone [8]. Photoexcitation is accomplished by intermittently exposing the gas sample to filtered IR radiation. In this regard, it is much like transmission IR spectrometry in which one needs a source, filter, chopper, and detector (Figure 37.3). The benefits of a chopper in transmission IR technique have been discussed. In this situation, however, the chopper serves a different function. It is an essential part of the signal, not part of a detection strategy. Infrared energy causes changes in the vibrational and rotational energy of the molecule. This energy can be transferred to neighboring molecules through collisions, which increase their translational (kinetic) energy. This results in an increase in collisional frequency, or, in other words, an increase in pressure. All of this occurs very quickly, so that during the dark periods, the collisional frequency decreases and the pressure drops. A hypersensitive microphone detects this cyclical change in pressure. The system is designed so that the frequency of the pressure (sound) wave differs for each gas. The sequence for PAS is:

light → absorption → heating → thermal expansion → pressure wave → acoustic detection,

whereas for transmission IR spectrometry, it is instead:

light → absorption → photo-optical detection.

Colorimetric detectors

Chemical sensors trace their roots to observations made in 1916 and to basic chemistry. The influence of CO_2 on pH is well described by the Henderson–Hasselbalch equation. Increasing CO_2 concentration in an aqueous medium causes the concentration (activity) of the hydrogen ion to increase, and consequently, the pH decreases. This

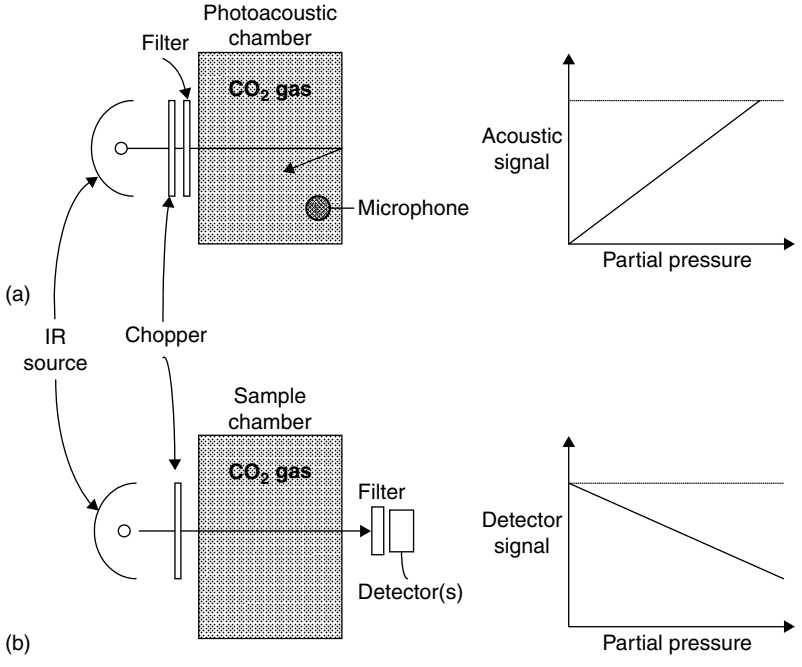

Figure 37.3 Contrast of two methods: (a) photoacoustic spectroscopy and (b) transmission IR spectroscopy.

relationship describes the underlying mechanism of the Stow–Severinghaus $PaCO_2$ electrode, which is part of every blood gas analyzer.

In addition to electrometric detection involving pH electrodes, a change in pH can be followed by a change in color of a dye solution. The yellow–red color change of a phenol sulfonphthalein solution, for example, occurs over a pH range of 6.6–8.0, making it useful for acid–base titrations. Marriott (1916) [9] first explored CO_2's visual detection for medical purposes. Draper (1938) [10] later suggested using bromoscresol purple in a calcium carbonate solution to detect rebreathing. Later, Berman and associates (1984) [11] advocated a cresol red, phenolphthalein solution to confirm placement of the endotracheal tube.

These suggestions did not receive wide acceptance because the methods were inconvenient, requiring the placement of an aqueous solution in the breathing circuit, and they are not fast enough for breath-to-breath detection. In general, an acceptable device should include a stable dye that does not produce toxic fumes, has low airflow resistance and deadspace so as not to compromise the work of breathing, and produces a color change that is fast and not red–green so as not to eliminate the 8% of the population that is color-blind. Also, it should be easily incorporated into the breathing circuit. A number of colorimetric devices have been available over the last several years. Table 37.2 presents the specifications of two representative devices. These disposable detectors, when placed at the endotracheal tube, make possible the viewing of the color of a mesh substrate coated with an indicator dye. Surrounding each detector area is a color chart.

In general, the color change should be observed for at least several breaths before interpreting results. They are not generally affected by N_2O, volatile anesthetic agents, and short exposures to water vapor. The color fades after a period of use measured in hours, so it is not intended for long-term use. Shelf-life up to 24 months is claimed for some devices if the foil package is unopened. Investigators report generally good performance of colorimetric devices, but note their shortcomings: they are semiquantitative; have no alarms; are difficult to read in the dark; and their use is suggested only if quantitative capnometry is not available [12]. Additionally, Puntervoll *et al.* (2002) [13] compared capnography to a colorimetric device, and noted that the latter may falsely indicate correct tracheal intubation when the tube is, in fact, in the esophagus due to the device's sensitivity to low CO_2 values.

Mass spectroscopy

Two types of mass spectrometers have been important medically: the magnetic sector with fixed detectors and the quadrupole. Each has been used either as a

Table 37.2 Representative colorimetric devices

Device name/ manufacturer	CO_2 color changes		Deadspace (mL)	Flow resistance, weight, recommended patient size, max usage time
EASY CAP II[a]	Purple	Room air	25	3 cm H_2O at 60 L/min
Nellcor Inc.	"A" – slight change in color	0.03 to <0.5%		20 g
	"B" – light purple to tan	0.5 to <2%		>15 kg
	"C" – hues of yellow	2–5		Up to 2 h
$StatCO_2^{TM}$	Blue	No CO_2 present	25	3 cm H_2O at 60 L/min
Mercury Medical	Green	1–2% CO_2		22 g
	Yellow	>5%		>15 kg
				Up to 24 h

[a] Introduced to the market as the forced mid-expiratory flow (FEF) end-tidal CO_2 detector by Fenem Inc. and later acquired by Nellcor Inc.
Source: Nellcor Puritan Bennett Inc. EASY CAP II brochure, 1997 and Mercury Medical $StatCO_2$ brochure 2003.

dedicated instrument providing continuous monitoring of single patients or as a shared instrument (multiplexed) providing discontinuous monitoring of several patients in sequence.

Magnetic sector-fixed detector

In the same way that light can be separated into its component wavelengths using a prism or diffraction grating, so, too, can a gas mixture be separated into its component parts by a combined electric and magnetic field. Sample gas is aspirated into a vacuum chamber and, within, is ionized by an electron beam. The charged fragments are accelerated by an electric field into a dispersion chamber where they are separated according to mass by an orthogonal magnetic field. Discrete detectors in the focal plane measure the component gases.

Quadrupole mass filter

The magnetic sector and quadrupole instruments are similar in that both require a high vacuum because the mean free path (distance traveled between collisions) must be long compared with the chamber dimensions, and the separation scheme requires that the particles be charged [14]. The principles used for separation, however, are quite different. The quadrupole is really a mass filter that depends on the influence of a combined direct current (DC) and radio frequency field (Figure 37.4). Four parallel rods are designed so that the tuning of the combined fields will result in particles of only one type traversing the longitudinal axis and ending up at the ion collector. The trajectory of all others is such that they strike one of the four rods and are removed from the ion beam. Changing the voltages in a controlled manner makes it possible to scan the mass spectrum. This can be done in a few milliseconds. Sampling the collector output at appropriate times during the scan makes it possible to measure the component masses. Scanning and sampling repetitively provide continuous monitoring.

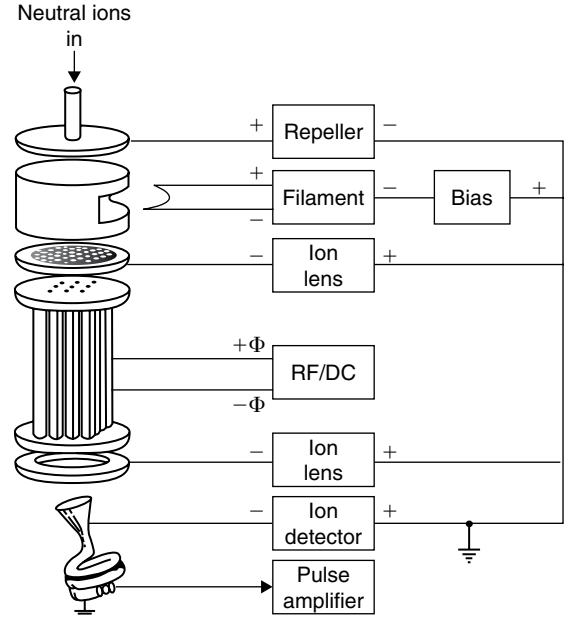

Figure 37.4 Instrumental design of a miniature linear quadrupole array, showing a miniature ionization source, the quadrupole rod array and ceramic jigs for positioning, and an electron multiplier detector. Each quadrupole rod is 25 mm long and has a radius of 1 mm. [Adapted from: Orient OJ, Chutjian A, Garkanian V. Miniature, high-resolution, quadrupole mass-spectrometer array. *Rev Sci Instrum* 1997; **68**: 1393–7.]

Technical challenges

A mass spectrometer presents interesting design challenges. In part, these involve moving a gas sample at atmospheric pressure to a distant measurement chamber that is at a low pressure, and doing so without altering the relative concentrations of the component gases. In effect, gas flow at high and low pressures is influenced by different relationships. These relationships must be understood and appropriate measurement strategies implemented to get reliable results. In the ionization chamber, gas molecules will be charged and split into fragments. These must be identified and traced to their parent molecule. Some overlap of fragments is expected, and corrections must be formulated. Similarly, CO_2 and N_2O present a problem, as each has a molecular weight close to 44. In addition, agents with large molecular weights may be beyond the mass range of most spectrometers, and, therefore, their fragments must be measured.

Advances have been made on the miniaturization of the various component systems of a variety of the mass spectrometer types, including the sample introduction, ion source, mass analyzer, ion detection, data acquisition, and vacuum systems [15]. Badman and Cooks note that miniaturization benefits all types of mass analyzers because the mean free path of the ions is reduced due to the reduction in the distance of travel and the number of collisions with background gases, relative to a larger-sized device operated at the same pressure. The most common miniature mass analyzers are linear quadrupole type (Figure 37.4), which is favored due to demands for size and the desire for an instrument that can operate effectively at relatively high (millitorr range) pressures [15].

Mainstream and sidestream capnography

A capnometer, by definition, is either diverting (i.e., sidestream) or non-diverting (i.e., mainstream). A diverting capnometer transports a portion of the respired gases from the sampling site, through a sampling tube, to the sensor, whereas a non-diverting capnometer does not transport gas away from the sampling site [16,17]. The measurement of the partial pressure of a gas significantly distant from the sampling site requires that a number of "laws of physics" issues be addressed including (1) water removal, (2) different conditions at the sampling site and sample cell in terms of temperature and humidity, (3) mixing of the sample gas as it is drawn to the cell, (4) variable pressure drop across the tubing and the possible misrepresentation of the partial pressure values due to the above and other effects, and (5) dynamic distortions to the waveform. While some of these effects can be compensated for, or corrected by other measurements or by the assumption of nominal values, others cannot.

With mainstream devices, the sensor, consisting of the sample cell and IR bench, is placed at the airway. This location results in a "crisp" capnogram that reflects the PCO_2 in real time within the airway. On the other hand, sidestream devices aspirate a sample of gas from the breathing circuit through a 6–8 foot (1.8–2.4 m) long, small-bore tube (e.g., 1 mm inner diameter). This sample is then often passed through a water trap and drying tubing prior to being analyzed in a sample cell. Using a remote location results in a delay time of up to several seconds and a rise time distortion of perhaps greater than 200 ms.

Mainstream devices, with their limitations on size and weight, have traditionally only offered measurement of a single gas, such as CO_2, whereas sidestream devices can offer measurement of all of the respiratory and anesthesia gases. However, technological developments have seen the recent availability of mainstream devices with CO_2 and O_2, as well as anesthetic agents in lightweight devices.

Water vapor effects can cause cross-interference (absorption band overlap) and collision broadening, but the band at 4.26 μm is relatively free from any water vapor absorption effects, and shows minimal collision broadening effects. Partial pressure dilution effects, on the other hand, are of concern. Mainstream IR analyzers, when located near the patient connection, measure gas near body temperature and pressure, saturated (BTPS) conditions. Water vapor condensate on the windows of the airway adapter has been effectively minimized in mainstream systems by heating its windows above body temperature or by using hydrophobic coatings. How close the exact water vapor pressure is to BTPS conditions depends on factors, including the presence and type of humidification, fresh gas flow, length of time in use, and ambient temperature [18]. Normally, exhaled gas is fully saturated and/or slightly less than 37 °C, which results in a water vapor pressure of 47 mm Hg. In sidestream systems, the temperature of the sampled gases decreases toward room temperature during its transit from the patient connection to the monitor. The result is condensate forming on the walls of the tubing, with

a consequent decrease in the partial pressure of water vapor from the BTPS value of 47 mm Hg. With the inclusion of water-permeable tubing, such as Nafion® brand tubing, the water vapor pressure in the tubing will tend to equilibrate with the water vapor pressure in the room.[1] This decrease in water vapor pressure can cause a small increase in CO_2 concentration [19]. Mainstream capnometers will correctly read the PCO_2 at the conditions in the breathing circuit typically at or near BTPS. Sidestream devices incorporate software that compensates for water vapor removed and, as a result, may introduce errors if assumed conditions are very different from actual conditions [20], which may change over time. In some designs, the use of water traps, particularly in anesthesia, can easily lead to partial failure or blockage of the trap, causing dramatic changes in waveforms and end-tidal values. This is particularly significant in systems that do not display the capnogram.

The limitations of the technologies and design choices, and their performance in the different clinical environments and patient populations must be considered. Capnography as a "front-line" monitor is well established [21], and the different technologies have been extensively evaluated in the literature [18,22]. Aspects of each technology will be reviewed (Table 37.3).

Mainstream capnography: overview

The sample cell, referred to as the *cuvette*, serves as the airway adapter, and is located in the respiratory gas stream, obviating the need for gas sampling and scavenging. It interfaces directly with the IR bench. A source emits IR radiation that includes the absorption band for CO_2. Photodetectors, typically located on the other side of the airway adapter, measure the transmitted radiation. A lightweight, flexible, multiconductor cable transmits the amplified detected signals to the monitor from which the PCO_2 is calculated and displayed graphically in the form of a capnogram. The monitor has traditionally contained only the electronics associated with control and measurement functions of the IR bench. Newer designs with advancements in electronics packaging and components have incorporated these electronics into the measurement head.

Many of the disadvantages of mainstream sensors presented in the past are primarily technological in nature, and often relate to older generations of that technology. These disadvantages are often listed in older reviews [23,24], while more recent reviews note otherwise [25]. Contemporary shortcomings include possible damage during handling, increased mechanical deadspace, issues of weight on airway, and use limited to intubated patients. For example, in the past, the mainstream IR benches have been deemed "vulnerable to costly damage." While earlier IR benches were vulnerable, primarily due to the use of moving parts such as the chopper or filter wheels, some newer mainstream IR benches with all solid-state designs are robust enough to survive repeated drops onto hard floors, and have been in use in high-impact areas such as the emergency room, ambulances, and transport for well over a decade. Historically, the primary concerns of mainstream-based systems have been related to size and weight; however, reduction in both size and weight has alleviated these concerns. Current-generation mainstream devices, besides being relatively light and having decreased deadspace, have generally demonstrated better performance than conventional sidestream systems in terms of signal fidelity and end-tidal measurements, particularly at higher respiratory rates in small children [26]. Careful airway adapter design and advances in technology have reduced the concerns for deadspace and weight. As with any airway adapter used for gas monitoring (either mainstream or sidestream), improper connection to other breathing circuit elements can cause artifacts in the capnogram. For example, a partial disconnection of a mainstream adapter can mimic a "curare-cleft" capnogram [27], but is easily recognizable.

Condensed water or liquid mixtures can affect the windows of the airway adapter. If droplets appear within the cuvette optical path, severe scattering and absorption can occur. However, devices using approaches such as a single-beam ratiometric design can compensate for the contamination if scattering/absorption effects are not spectrum-dependent. Dust and optically opaque particles do not appreciably affect system precision.

Sidestream capnography: overview

Sidestream gas analyzers utilize a long sampling plastic tube connected to an adapter in the breathing circuit (such as a T-piece at the endotracheal tube or mask connector) or a nasal catheter. The sample gas is continuously aspirated from the breathing circuit through

[1] Note that the driving force here is water vapor pressure gradient, not the total pressure.

Table 37.3 Comparison of mainstream and sidestream CO_2 analyzers

Feature	Mainstream	Sidestream
Airway connections		
Location of IR analysis unit ("bench")	At the airway connector	In the monitor
Weight of airway connection	Medium (<2 oz)	Light
Location of airway connector	End of endotracheal tube	End of endotracheal tube (may replace "angle" connector)
Gases available?	CO_2 (O_2, N_2O, agents limited availability)	CO_2, O_2, N_2O, agents widely available
Use on non-intubated patients?	Yes but only with a face mask or mouthpiece. Possible dilution of sample with significant loss of seal	Yes with nasal adapter or oxygen prongs. Probable dilution of sample
Connecting tube or cable?	Cable	Sample tube
Required components to "sample" gas	Airway adapter	Airway adapter, sample tube, filters and/or water trap, water-permeable tubing (for some environments)
Cost of replacing airway connector	Bench expensive to replace; airway adapter inexpensive to moderately expensive	Very inexpensive on a per-sensor basis – but on very wet patients may require hourly changes
Sample volume drawn	None	50–250 mL/min
Deadspace added to airway connector	Low (<1 mL in neonates)	Low
Zeroing and calibration		
Zeroing	Manual – may use gas cell or zero on airway adapter if needed	Automatic – requires internal valving and sometimes external gas tanks
Accuracy of Zeroing	Accurate—may use separate ref cell in place of airway adapter	Accurate—uses sample tubing and adapter that will be used during monitoring
Response and signal fidelity		
Delay between sampling and waveform display	None	Less than 3 s
Bench 10–90% rise time	Typically < 70 ms	200–300 ms (may not include additional effect of accessory)
Accuracy of waveform shape	Excellent. No effect due to variable pressure drop	Variable – depends upon factors including sample rate, mixing, sample cell design, accessory (airway adapter vs. nasal cannula), etc.
Moisture and contamination		
Changes in water vapor pressure	Not affected	Affected due to condensation and drying of sample
Moisture handling	Bench at airway adapter contains a means to prevent condensation, (heating and/or hydrophilic coatings), droplets may condense on window but usually clear rapidly	Water trap – modern water traps can be extremely efficient but tend to clog (some use Nafion® tubing which equilibrates with ambient humidity)

Table 37.3 (*cont.*)

Feature	Mainstream	Sidestream
Potential of cross-contamination between patients	None – disposable or reusable airway adapter can be sterilized and then reused at no risk of contamination	None if sampled gas not returned to breathing circuit airway adapter and sample tubes can be disposed at low cost or sterilized and reused at no risk of contamination provided no purging[a] or return of gas to breathing circuit
Gas scavenging required (with anesthetic agents)?	No	Yes
Compensations		
Airway pressure compensation	Not required	Pressure fluctuations due to sample rate compensated with measurement of pressure

[a] Not permitted per ISO 21647 standard.
Source: Adapted from Philips-Respironics, Inc., Murrysville, PA, with permission.

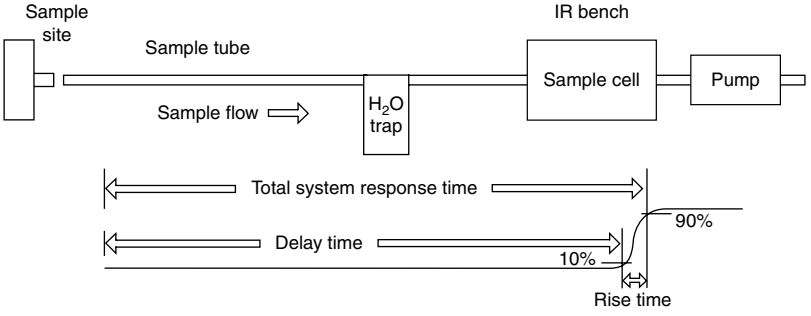

Figure 37.5 Physical components of a gas sampling system with total system response time, delay time, and rise time illustrated. [Image courtesy of Philips-Respironics, Inc., Murrysville, PA.]

the sampling tube and into the sample cell within the monitor (Figure 37.5) at sample flow rates ranging from 50 to 250 mL/min.

The location of the sampling port varies, and may range anywhere from an elbow connected to an endotracheal tube to the Y-piece. For example, it may be placed on the ventilator or patient side of an in-line filter or heat moisture exchanger. Placement on the ventilator side results in a drier sampling tube with the inherent risk of distortion of the capnographic waveform and lower end-tidal values [28,29], whereas placement on the patient side can result in the accumulation of condensate and patient secretions in the sampling system. The sampled gas that is withdrawn from the patient may contain anesthetic gases and, as such, this gas should be routed to a gas scavenging system or, if the hazards of cross-infection have been adequately addressed, returned to the patient breathing system to avoid pollution of the operating room environment [30], costs associated with greater usage of anesthetic [31] gases, and possible exposure risks in underventilated areas [32,33].

Condensation from a humidified sample gas in combination with patient secretions occasionally can block and contaminate the sampling line. To protect the sample cell from condensate, the distal end of the sampling tube is often connected to a water trap and water vapor-permeable tubing, such as Nafion® tubing. The effectiveness of water traps and filter designs varies between manufacturers. Additionally, sources of leaks external to the monitor have been reported as possible causes of artifact in the capnogram, such as loose fittings [34], cracked or slit sampling tubes [35,36], cracked sample filters [37], and cracked airway adapters [38], along with sources of leaks internal to the monitor such as partial disconnection [39]. Leaks and obstructions can occur at connection points and tubes within the sidestream sampling system. More recent designs of airway adapters for sidestream systems have reduced the likelihood of aspirating secretions by using sampling ports that are located in the center of the adapter rather than at the wall, and have reduced

the effect of leaks by including a removable sample cell as part of the sample set.

Even with no leaks or obstructions in the sampling system, significant distortion of the capnogram can occur under some conditions. At the sample tubing–airway interface, expired gas may be diluted with entrained ambient air whenever the gas flow rate falls below the "constant" sample flow rate [40]. The design of the sampling tube and its positioning within the breathing circuit or nares (if a nasal catheter is used) can affect the quantity of surrounding air that is entrained along with the expired gas. Within the sample tube itself, dispersion may occur due to the effects of velocity profile and diffusion [40]. Additionally, the sample flow rate may vary significantly, owing to a variety of factors, including the sample tube length [41], airway pressure, and an occluded exhaust line [42]. Some monitors compensate by either increasing the sampling flow or attempting to purge the sample tubes when an increased pressure drop is sensed across a flow restriction. In spite of the presence of water traps and water-permeable tubing, liquids may be aspirated into the monitor's internal components.

Conventional sidestream capnographs may not be accurate when used in neonatal and pediatric patients because they aspirate a significant portion of the patient's total ventilation [43]. Older sidestream designs used sample rates as high as 250 mL/min, but newer designs have reduced the gas sampling flow rate, the diameter of the sampling tube (1 mm inner diameter), and sample cell volume. This trade-off decreases the ventilation levels that can be monitored and extends the operating life of the filter and/or water trap while, at the same time, potentially increasing the possibility of occlusion.

Artifacts in sidestream CO_2 waveforms can take on many forms. For example, excessive damping of the response (Figure 37.6) can occur. In some circumstances, the artifact may resemble physiologic changes that may be characteristic of diseases, such as a form of restrictive or obstructive lung disease [26]. For example, Pascucci *et al.* note that "a falsely low value for end-tidal CO_2 may incorrectly assure the clinician that alveolar ventilation is adequate when, in fact, it is not." Thus, they further note that "the inability of the capnogram to return to zero baseline on inspiration, a common artifact with sidestream recordings, may suggest rebreathing of CO_2 and prompt unnecessary changes in fresh gas flow or modifications of the patient circuit" [26].

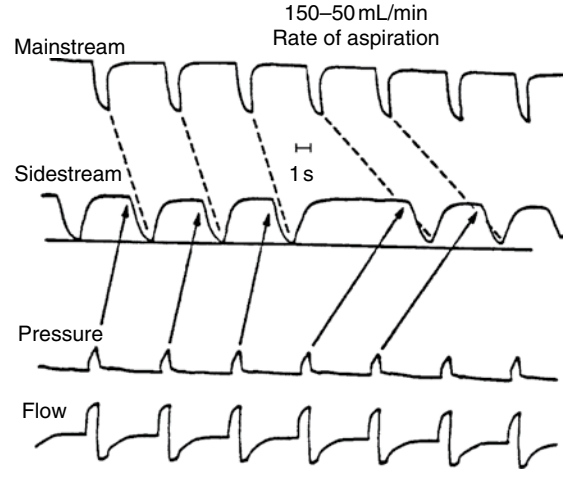

Figure 37.6 Relationship between capnogram (both mainstream and sidestream) and other "pneumatic" parameters of pressure and flow. Note the time delay and dampening effects from reducing the sample flow rate in the sidestream system. [Reproduced with permission from: Gravenstein JS, Paulus DA, Hayes TJ. *Capnography in Clinical Practice*, 2nd edn. Boston, MA: Butterworth-Heinemann, 1989.]

The use of conventional sidestream monitoring requires that careful attention be paid to the physical set-up both external and internal to the monitor. The recent introduction of more robust devices has lessened some of these concerns.

Algorithmic issues

Breath detection

Algorithms to detect and delineate breaths using capnograms often are solely based upon simple thresholds (Figure 37.7). However, such approaches are susceptible to brief swings due to cardiogenic oscillations and noise (Figure 37.8). More sophisticated and robust approaches may use multiple signals, such as flow and/or pressure with the CO_2 waveforms [44], as well as the application of additional criteria.

End-tidal CO_2 determination

Besides breath detection algorithms, the specifics of each manufacturer's algorithm for end-tidal measurements, such as averaging windows, breath-to-breath averaging, and its classification of end-tidal, must be considered when interpreting data. This is particularly important if no waveform is displayed.

Although the end-tidal value should reflect the alveolar value, whether the reported end-tidal value is the PCO_2 at end-expiration (either actual or apparent) or

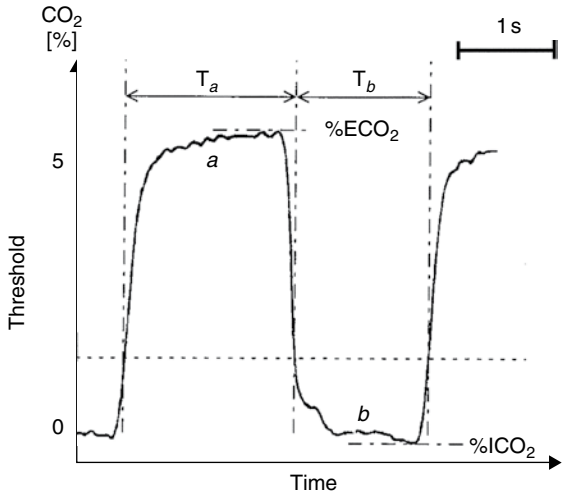

Figure 37.7 Normal capnogram. During expiration, exhaled CO_2 causes a peak in the capnogram at *a*. During the inspiratory phase, fresh gas or room air is sampled, and the capnogram returns to its baseline at *b*. Breaths may be counted and timed by the use of a simple thresholding technique; each crossing of the threshold by the capnogram is noted, allowing calculation of parameters describing each breath. % ECO_2 is the end-tidal level and %ICO_2 is the inspired level. [Reproduced with permission from: Smith TC, Green A, Hutton P. Recognition of cardiogenic artifact in pediatric capnograms. *J Clin Monit* 1994; **10**: 270–5.]

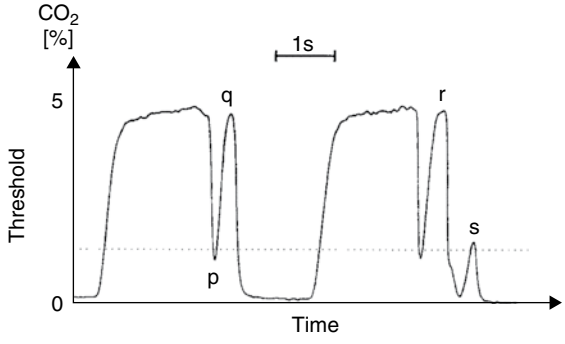

Figure 37.8 Capnogram representing two breaths that could be misclassified as representing five by a simple thresholding algorithm. A cardiogenic oscillation at the end of the first expiration crosses the threshold at p, causing peak q to be misclassified as a new expiratory phase. Similarly, oscillation artifacts r and s are also misclassified. Simultaneous recordings of chest and abdominal movement using respiratory inductance plethysmography were used in this figure to exclude non-cardiogenic causes. [Reproduced with permission from: Smith TC, Green A, Hutton P. Recognition of cardiogenic artifact in pediatric capnograms. *J Clin Monit* 1994; **10**: 270–5.]

the largest value during the "expiratory" period defined by the capnogram (which can be elongated by rebreathing), or something entirely different, depends upon the manufacturer, and often is not disclosed in the product manuals.

Two examples of this difficulty are illustrated in Figures 37.9 and 37.10. Figure 37.9 shows an example of two breaths of patient asynchrony. The end of expiration, as defined by the flow waveform (point A), results in an end-tidal value of 27 mm Hg. However, using the capnogram by itself (i.e., the apparent expiration–inspiratory transition – point C) results in an end-tidal value of 30 mm Hg. On the other hand, if the largest value is used (point B), an end-tidal value of 31 mm Hg is obtained. Figure 37.10a illustrates a phenomenon often seen in neonates with long expiratory pauses due to the inspiration:expiration ratios of 1:8 – 1:10, during which very minor inspiratory efforts are made which result in a capnogram that is difficult to interpret. Determining an end-tidal value with a time-based capnogram is very difficult. However, comparing time- and volumetric-based capnograms allows for some clarity. The ventilation–perfusion relationships of the lung are more accurately reflected in the slope of phase III by a volumetric capnogram than that of a time-based capnogram in which the gradient of the phase III slope is usually less obvious and can be misleading. The phenonemon in Figure 37.10a may occur because a smaller volume of expired gases (approximately the final 15%) often occupies half the time available for expiration, so that a similar change in the CO_2 concentration is distributed over a greater length of time in the time-based capnogram than in the volumetric capnogram. In Figure 37.10b, the plot of the expired volume vs. the partial pressure of CO_2 during expiration clearly shows the plateau from which an end-tidal value may unambiguously be determined, as well as the other parameters associated with volumetric capnography.

Rebreathing

Other than the end-tidal partial pressure of CO_2, only breathing frequency and a measure of inspiratory CO_2 levels are clinically reported because only the apparent transition between the expiratory and inspiratory segments can be reliably delineated from a capnogram. However, only with no airway deadspace does this transition correspond to the time of the actual beginning of inspiration as delineated by the flow waveform. Figure 37.11 illustrates how this transition can shift in time and become rounded with the addition of apparatus deadspace. The transition between inspiration and expiration cannot be discerned because of the presence of anatomic deadspace that fills with inspiratory gas at end-expiration.

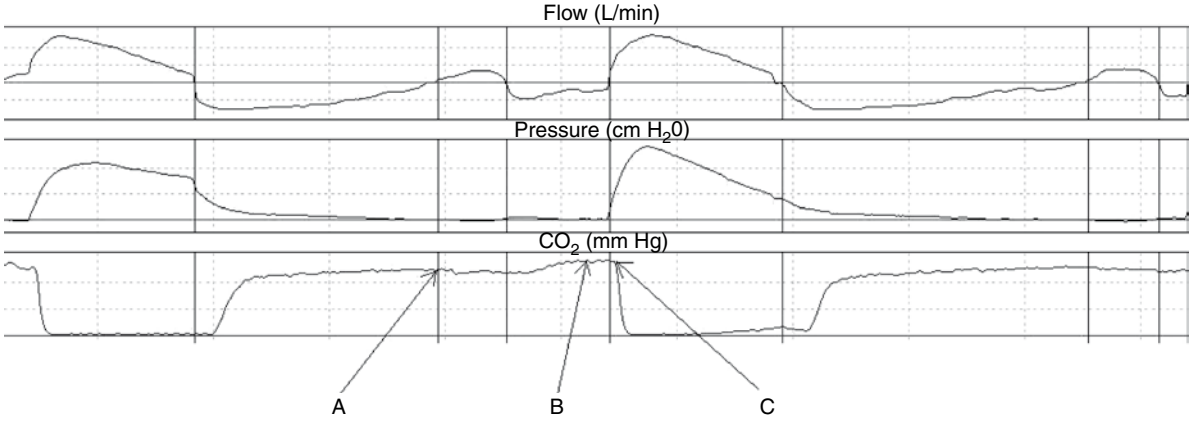

Figure 37.9 Example of patient asynchrony illustrating the variation in end-tidal values depending upon its definition. End-tidal PCO_2 ($P_{ET}CO_2$) at A is 27 mm Hg, at B is 31 mm Hg, and at C is 30 mm Hg. [Image courtesy of Philips-Respironics, Inc., Murrysville, PA.]

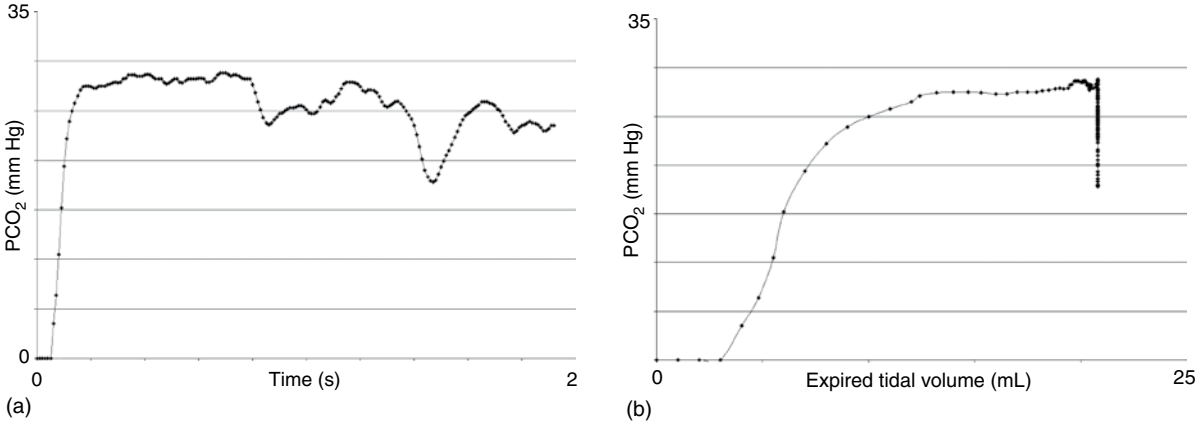

Figure 37.10 Time-based and volumetric capnogram for a neonatal subject with a long expiratory pause. [Image courtesy of Philips-Respironics, Inc., Murrysville, PA.]

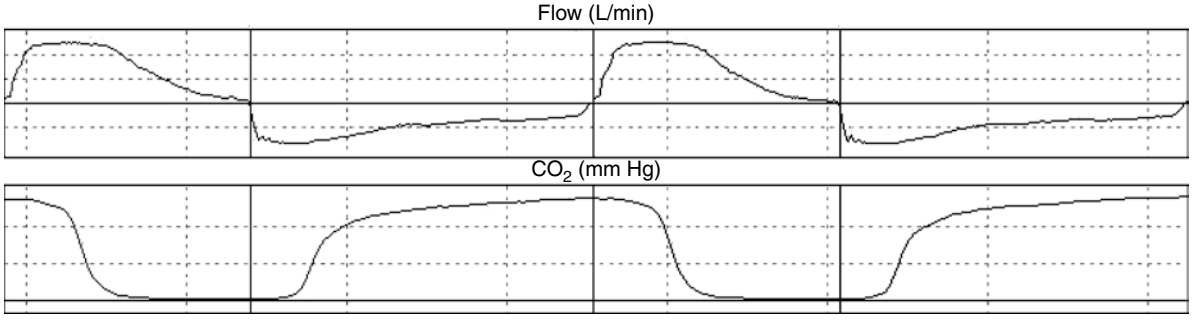

Figure 37.11 Flow and CO_2 waveforms illustrating shift in transition from expiration to inspiration due to rebreathing. [Image courtesy of Philips-Respironics, Inc., Murrysville, PA.]

References

1. Alpert NL, Keiser WE, Szymanski HA. *IR Theory and Practice of Infrared Spectroscopy,* 2nd edn. New York: Plenum Press, 1970.
2. Bergman NA, Rackow H, Frumin MJ. The collision broadening effect of nitrous oxide upon infrared analysis of carbon dioxide during anesthesia. *Anesthesiology* 1958; **19**: 19–26.
3. Kennell EM, Andrews RW, Wollman H. Correction factors for nitrous oxide in the infrared analysis of carbon dioxide. *Anesthesiology* 1973; **39**: 441–3.
4. Hill DW, Powell T. *Non-Dispersive Infra-Red Gas Analysis in Science, Medicine and Industry*. New York: Plenum Press, 1968.
5. Veingerov ML. Eine Methode der Gasanalyse beruhend auf dem optisch-akustischen Tyndall-Röntgeneffekt. *Dokl Akad Nauk SSSR* 1938; **19**: 687–8.
6. Luft K. Über eine neue Methode der registrierenden Gasanalyse mit Hilfe der Absorption ultraroter Strahlen ohne spektrale Zerlegung. *Z Techn Phys* 1943; **24**: 97–104.
7. Kruse DW, McGlauchlin LD, McQuistam RB. *Elements of Infrared Technology: Generation, Transmission and Detection*. New York: John Wiley, 1962.
8. Rosencwaig A. *Photoacoustics and Photoacoustic Spectroscopy*. New York: John Wiley, 1980.
9. Marriott WM. Determination of alveolar carbon dioxide tension by a simple method. *JAMA* 1916; **66**: 1594–6.
10. Draper WB. Means of indicating presence and relative amounts of carbon dioxide in gases for breathing. US Patent 2,136,236, issued November 8, 1938.
11. Berman JA, Furgiuele JJ, Marx GF. The Einstein carbon dioxide detector. *Anesthesiology* 1984; **60**: 613–14.
12. Petroianu GA, Maleck WH, Bergler WF, Altmannsberger S, Rufer R. Preliminary observations on the Colibri CO_2-indicator. *Am J Emerg Med* 1998; **16**: 677–80.
13. Puntervoll SA, Soreide E, Jacewicz W, Bjelland E. Rapid detection of oesophageal intubation: take care when using colorimetric capnometry. *Acta Anaesthesiol Scand* 2002; **46**: 455–7.
14. Barrington AE. *High Vacuum Engineering*. Englewood Cliffs, NJ: Prentice Hall, 1963.
15. Badman ER, Cooks RG. Miniature mass analyzers. *J Mass Spectrom* 2000; **35**: 659–71.
16. ISO 21647: International Organization for Standardization. Medical electrical equipment – particular requirements for the basic safety and essential performance of respiratory gas monitors. Available online at http://www.iso.org/iso/iso_catalogue/.
17. McArthur CD. American Association for Respiratory Care clinical practice guideline. Capnography/capnometry during mechanical ventilation – 2003, revision and update. *Respir Care* 2003; **48**: 534–9.
18. Raemer DB, Calalang I. Accuracy of end-tidal carbon dioxide tension analyzers. *J Clin Monit* 1991; **7:** 195–208.
19. Fletcher R, Werner O, Nordstrom L, Jonson B. Sources of error and their correction in the measurement of carbon dioxide elimination using the Siemens-Elema CO_2 analyzer. *Br J Anaesth* 1983; **55**: 177–85.
20. Severinghaus JR. Water vapor calibration errors in some capnometers: respiratory conventions misunderstood by manufacturers? *Anesthesiology* 1989; **70**: 996–8.
21. Williamson JA, Webb RK, Cockings J, Morgan C. The Australian Incident Monitoring Study. The capnograph: applications and limitations – an analysis of 2000 incident reports. *Anaesth Intens Care* 1993; **21**: 551–7.
22. Lauber R, Seeberger B, Zbinden AM. Carbon dioxide analysers: accuracy, alarm limits and effects of interfering gases. *Can J Anaesth* 1995; **42**: 643–56.
23. Hess D. Capnometry and capnography: technical aspects, physiologic aspects, and clinical applications. *Respir Care* 1990; **35**: 557–73.
24. Block FE Jr., McDonald JS. Sidestream versus mainstream carbon dioxide analyzers. *J Clin Monit* 1992; **8**: 139–41.
25. Ward KR, Yealy DM. End-tidal carbon dioxide monitoring in emergency medicine. Part I. Basic principles. *Acad Emerg Med* 1998; **5**: 628–36.
26. Pascucci RC, Schena JA, Thompson JE. Comparison of a sidestream and mainstream capnometer in infants. *Crit Care Med* 1989; **17**: 560–2.
27. Tripathi M. A partial disconnection at the main stream CO_2 transducer mimics "curare-cleft" capnograph. *Anesthesiology* 1998; **88**: 1117–19.
28. Hardman JG, Curran J, Mahajan RP. End-tidal carbon dioxide measurement and breathing system filters. *Anaesthesia* 1997; **52**: 646–8.
29. Goodman E, Johnson PA. End-tidal carbon dioxide tracing configuration depends on sampling size. *Anesth Analg* 2001; **92**: 1357–8.
30. Lawson D, Jelenich S. Capnographs: a new operating room pollution hazard? *Anesth Analg* 1985; **64**: 378.
31. Boldt J, Jaun N, Kumle B, Heck M, Mund K. Economic considerations of the use of new anesthetics: a comparison of propofol, sevoflurane, desflurane, and isoflurane. *Anesth Analg* 1998; **86**: 504–9.
32. National Institute of Occupational Safety and Health. NIOSH alert: Controlling exposures to nitrous oxide.

DHHS (NIOSH) Publication No. 94–100, 1994. Available online at http://www.niosh.com/.

33. Smith DA. Hazards of nitrous oxide exposure in healthcare personnel. *AANA J* 1998; **66**: 390–3.
34. Zupan J, Martin M, Benumof JL. End-tidal CO_2 excretion waveform and error with gas sampling line leak. *Anesth Analg* 1988; **67**: 579–81.
35. Skeehan TM, Biebuyck JF. Erroneous mass spectrometer data caused by faulty patient sampling tube; case report and laboratory study. *J Clin Monit* 1991; **7:** 313–19.
36. Tripathi M, Pandey M. Atypical "tails-up" capnograph due to breach in the sampling tube of side-stream capnometer. *J Clin Monit Comput* 2000; **16**: 17–20.
37. Body SC, Taylor K, Philip JH. Dual-plateau capnogram caused by cracked sample filter. *Anesth Analg* 2000; **90**: 233–4.
38. Ti LK, Dhara SS. Another cause of a prolonged downstroke on the capnograph. *Anesthesiology* 1998; **89**: 801–2.
39. Healzer JM, Spiegelman WG, Jaffe RA. Internal gas analyzer leak resulting in an abnormal capnogram and incorrect calibration. *Anesth Analg* 1995; **81**: 202–3.
40. Epstein RA, Reznik AM, Epstein MAF. Determinants of distortions in CO_2 catheter sampling systems: a mathematical model. *Respir Physiol* 1980; **41**: 127–36.
41. Schena J, Thompson J, Crone RK. Mechanical influences on the capnogram. *Crit Care Med* 1984; **12**: 672–4.
42. Hussain S, Raphael DT. Analysis of a straight-line capnographic waveform. *Anesth Analg* 1997; **85**: 465.
43. Gravenstein N. Capnometry in infants should not be done at lower sampling flow rates. *J Clin Monit* 1989; **5**: 63–4.
44. Govindarajan N, Prakash O. Breath detection algorithm in digital computers. *Int J Clin Monit Comput* 1990; **7:** 59–64.
45. Knodle DW, Mace LE, Labuda LL. Gas analyzers. US Patent 4,914,720, issued April 3, 1990.
46. Knodle DW, Graham PK, Labuda LL. Infrared source. US Patent 5,369,277, issued November 29, 1994.
47. Knodle DW, Clary TR. Nondispersive infrared radiation source. US Patent 5,602,398, issued February 11, 1997.
48. Rich DR, Pierry AT, Fudge BM, Sandor JL, Triunfo JA. Sidestream gas sampling system with detachable sample cell. US Patent 7,341,563, issued March 11, 2008.
49. Coleman Y, Krauss B. Microstream capnography technology: a new approach to an old problem. *J Clin Monit Comput* 1999; **15**: 403–9.
50. Fehder CG. Carbon dioxide indicator device. US Patent 4,728,499, issued March 1, 1988.
51. Nexo SA, Christensen J, Jorgensen IE. Photoacoustic gas analyzer. US Patent 4,818,882, issued April 4, 1989.

Section 5
Chapter
38

Technical perspectives

Gas flow measurement

M. B. Jaffe

The importance of flow

Gas composition measurements are routine in the operating room, and becoming so in the intensive care unit. At present, most of the technologies have the ability to provide breath-by-breath information, presenting expiratory values and minimum inspiratory values for each of the measured gases. In addition, the shape of the waveform has proven to be of great value, especially when monitoring carbon dioxide (CO_2). The simultaneous measurement of flow adds important information to the measurement of exhaled CO_2.

Volume

In its simplest terms, measuring gas flow makes possible the online determination of inspired and expired volumes. Assuming constant flow velocity (as with an inspiratory square wave common to many ventilators), and knowing the time during which the flow occurs, enables the determination of volume. However, expiratory flow velocity (in contrast to inspiratory) is normally not constant, and volume must be expressed as an integral of flow. Calculations of flow use integration methods, such as the trapezoidal rule or higher-order methods. These integration methods can be used to compare inspiratory and expiratory flow to detect leaks in the breathing circuit. Flow determinations can be made over a single breath, over several breaths, or over a specified time period (e.g., 1 min for minute volume). A second application can compare gas concentration versus volume (instead of time), as is conventional today in volumetric capnography.

Clinical issues: overview

The clinical measurement of respired gas flow on patients, particularly during mechanical ventilation, requires attention to sensor(s) location, gas composition, gas temperature, inlet conditions, humidity, deadspace, effective resistance of breathing circuit, and operating range of the flow sensor(s). All of these factors must be taken into account when comparing flow measured by two different devices. The bandwidth of the flow signal must also be considered. For non-intubated, resting, adult tidal breathing, a bandwidth of at least 4 Hz is required [1]. Others have suggested higher bandwidths, particularly for infants [2]. Recent clinical guidelines suggest sampling rates of 100 or 200 samples/s, depending on the integration methods used to obtain values sufficiently accurate for research purposes in infants [3]. Various technologies have been used clinically to measure airway flow. Many of these techniques were originally developed strictly for precise short-term laboratory measurements, and require meticulous attention to detail, including calibration and operator attendance at all times.

A continuous, bidirectional airway flow measurement used in the clinical environment demands simplicity, reliability, ease of use, and the ability to work in humid/wet circuits without operator intervention. The devices should be relatively inexpensive, add minimal deadspace, and should operate over a wide range of flows, and require minimal or no calibration. Devices typically designed for the pulmonary function testing environment will generally not work well in continuous monitoring applications.

Continuous, accurate, and reliable flow measurements under clinical conditions have been a major technical challenge. The number of solutions that have been proposed reflects the difficulty of the problem, and can be cataloged under principles involving ultrasound detection, hot-wire anemometry, and differential pressure measurements.

Capnography, Second Edition, ed. J. S. Gravenstein, Michael B. Jaffe, Nikolaus Gravenstein, and David A. Paulus. Published by Cambridge University Press. © Cambridge University Press 2011.

Factors affecting flow readings

A number of factors that can affect flow measurement, independent of the technology used, should be considered, including sensor location, gas conditions, gas composition and temperature, inlet conditions, resistance, deadspace, humidity, and operating ranges. Other factors that should also be investigated are lung compliance, presence and nature of secretions, leak (endotracheal tube, ETT), and cuffed versus uncuffed ETTs and degree of inflation of cuff.

Sensor location

Proximal flow measured at the patient's airway can substantially differ from flow measured inside of or at the ventilator, particularly if not adequately compensated. Many ventilators measure flow, not at the proximal airway, but close to the ventilator (Table 38.1). This can result in a substantial difference between the flow volume actually delivered to the patient and the flow volume displayed by the ventilator that includes the "wasted" gas compression and circuit distension volumes. Humidification can also affect the values. This unused portion of the apparent tidal volume (compression/distension volume) does not ventilate the patient's lungs, but remains within the breathing circuit, and tends to elongate and distend the breathing circuit tubing. The compression volume is related to the internal volume of the ventilator, volume of the humidifier (if present), volume and compliance of the circuit tubing, and volume of other components of the breathing circuit, such as the heat and moisture exchanger (HME). The volume due to compression loss that does not reach the patient becomes increasingly important as pressures increase and volume decreases. During the inspiratory phase of a ventilator-delivered breath, compression occurs throughout the breathing circuit, causing the breathing tubing to distend and elongate. During the expiratory phase of a ventilator-delivered breath, the compressed gas and stored energy in the distended and elongated breathing tubes is released; the released volume is measured by sensors at the exhalation port of the ventilator. Unless volume measurements are made directly at the patient's airway, the exhaled volume displayed by the ventilator can overestimate the actual tidal volume due to release of the compressible volume into the exhalation port of the breathing circuit [4]. Some ventilators allow for a correction factor (i.e., compression factor) of the measured volume to arrive at the circuit compression volume. The factor, calculated as compression volume over the corresponding ventilation pressure, allows the compressible volume to be estimated by multiplying this factor by the peak pressure minus positive end-expiratory pressure. Even with this correction applied, the precise estimation of the compression volume is difficult due to variations between individual breathing circuits, breathing circuit length, use of humidifiers, heat and moisture exchangers, and other circuit components. Failure to account for the wasted compression volume can result in hypoventilation in patients on ventilator support. Studies of several ventilators found that the discrepancy between displayed and proximally measured volume was as high as 23% [5], and varied significantly on the same ventilator with different manufacturers' breathing circuits [6].

Table 38.1 Flow sensor location

Ventilator	Site	Flow sensor
Bear 5	Distal to exhalation valve	Vortex shedding
Bird 6500ST	At exhalation valve outlet	Variable orifice
Hamilton Veolar	Proximal airway	Variable orifice
Maquet Servo i	Proximal airway	Fixed orifice
Maquet Servo 900c	Proximal to exhalation valve for expiratory and inspiratory limb for inspiratory	Screen
Philips-Respironics V200	Distal to exhalation valve	Hot-wire
Puritan-Bennett 840	Proximal to exhalation valve	Hot-wire

Source: Modified from: Tobin MJ. *Principles and Practice of Mechanical Ventilation*. New York: McGraw-Hill, 1994.

Gas conditions

Gas volumes may be measured under different conditions. This can lead to confusion. Conventionally, ventilation is reported at BTPS (body temperature of 37 °C, ambient pressure, and saturated with water vapor) while gas volumes associated with CO_2 elimination ($\dot{V}CO_2$) and oxygen (O_2) consumption ($\dot{V}O_2$) are often reported in STPD (standard temperature 0 °C, pressure 760 mm Hg, and dry). To allow conversion

between the two conditions, the ideal gas law, $PV = nRT$ (where P is pressure in absolute terms, V is volume, n moles of non-water molecules, R is 62.3656 liters/mm Hg/mol degree, and T is temperature in absolute terms) is applied. Note that the total pressure consists of the partial pressures of the gases and water vapor. By applying this relationship, where 47 mm Hg is the water vapor pressure at 37 °C (body temperature) and 0 and 760 mm Hg are the standard temperature and pressure, respectively, one obtains the equation below:

$$V_{STPD} = \frac{(P_B - 47)(V_{B\,TPS})(273)}{760(273 + 37)} = \frac{(P_B - 47)(V_{BTPS})}{863}.$$

Using these expressions, the volumes can be calculated at different conditions to demonstrate differences in measured volumes at different points in the breathing circuit.

Gas composition/humidity

The effect of humidification on the measurement of volume is a factor to also consider. Within the airways, respiratory gases are effectively saturated with water vapor. As such, the vapor pressure of water depends entirely on temperature. To calculate water vapor pressure for a saturated system, different equations have been developed, including a precise equation consisting of a logarithmic function [7] and a quadratic equation that provides a reasonable degree of accuracy. Relative humidity, a measure of moisture saturation in air, is calculated as the ratio of partial pressure of water (PH_2O) over the vapor pressure of water (P_{vapor}) at the same temperature. This chapter does not cover the aspects of cooling, rain-out, the associated temperature gradients, and humidity changes that occur in breathing circuits. For more detail, please consult reviews on inspired gas conditioning [8] and humidification and mechanical ventilation [9]). It should be noted that when inspired gas is less than 100% saturated, or has a temperature that is less than body temperature, expired tidal volume will be greater than inspired tidal volume because of the water vapor that is added in the lungs.

Flow sensors should be designed to be unaffected by moisture accumulation in the flow sensing/measurement component. With differential flow sensors, the measurement and generation of the flow-dependent pressure decrease can be affected by the presence of moisture on the walls of the flow sensor. The same applies for hot-wire and ultrasonic flow sensors. Proper breathing circuit maintenance and avoiding gravity-dependent positions within the breathing circuit, however, is still required to avoid pooling of water and sputum in the flow sensor.

Gas composition/temperature

Accurate flow measurement requires that the nominal values for the inspiratory and expiratory gas composition and temperatures be considered. With some devices, the user can choose typical ambient values for O_2, CO_2, and nitrogen if testing with a calibration syringe or typical clinical values. Compensations for additional gases, such as nitrous oxide, helium, or an anesthetic agent, are often available. The consequence of improperly compensating for the gas concentrations can result in a significant change in the reported flow value, depending on the flow measurement technology used. Correction of gas composition assumes that the viscosity can be computed as the linear combination of the product of each individual viscosity and its gas fraction. Gas flow sensors based on thermal measurements, such as hot-wire or hot-film anemometers, are sensitive to the heat capacity of the measured gas, and are thereby influenced by gas composition.

Inlet conditions

Flow sensors should be designed to be insensitive to changes in inlet conditions, and should be carefully considered independent of the measurement technology. For example, changing the proximal connections from a direct ETT connection to a connection via an elbow markedly changes the cross-sectional profile of the flow entering the flow sensor. A robust flow sensor design should produce little change on the measured flow, regardless of the type and geometry of upstream devices. Even small changes in the geometry of the breathing circuit tubing relative to the flow sensor can have a significant effect on the measured flow. For example, it has been demonstrated that Fleisch pneumotachographs connected between the Y-piece and ETT can exhibit a flow rate-dependent error in measured flow up to 10% [10]. If sufficient entrance length is provided in the flow sensor, laminar flow and a consistent flow velocity profile can be achieved. However, this is usually not practical, so entrance length to a flow sensor must be traded for the design requirement of minimal deadspace (Figure 38.1). Obviously, a balance

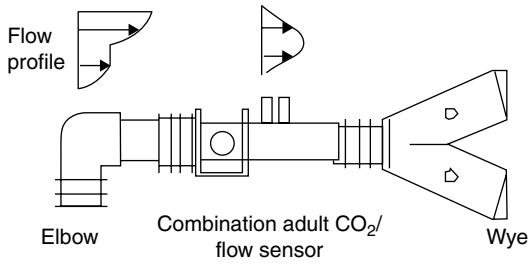

Figure 38.1 Expiratory flow velocity profiles at exit of elbow and at differential pressure sensor illustrating the effect of entrance length. Wye, Y-piece. [Image courtesy of Respironics, Inc., Murrysville, PA.]

must be sought between low deadspace and insensitivity to changes in inlet conditions. Inlet flow conditioners can be designed as part of the flow sensor to mitigate the effects of unknown upstream geometry.

Resistance

The addition of a flow sensor to a breathing circuit should have minimal impact on the measured flow volume. Typically, resistance of a flowmeter in product specifications and standards for pulmonary function testing is stated in terms of a pressure decrease or resistance at a particular flow rate. When reading resistance specifications, it is important to consider both the flow rate at which the pressure decrease is reported and the nature of the flow–pressure relationship. For devices that do not have an inherent linear relationship, consider the relationship of flow–pressure over the expected flows and pressures. For such devices, a more relevant measure would be a flow–pressure plot, or a determination that reports the added work of breathing under specified conditions rather than the pressure decrease at a particular flow rate.

Operating range of flow sensor: choosing the right sensor

While the operating range for flow is constrained by the range of sensors and associated measurement electronics, the operating range of derived parameters, such as volume, must be considered in light of the flow sensor's range and the physiological limits. In all measurement technologies, no *single* sensor will work over the range spanning from neonate to adult. To span this wide range, most manufacturers have used two or more different sensors. The criteria for selecting which sensor to use should include ETT size, patient age, flow/volume values, and acceptable levels of deadspace and resistance.

The use of volume measurements in breathing circuits must consider the effects of gas conditions, compression volumes, and location of the flow sensors so that the values can be properly interpreted. If possible, proximal flow sensors should be used to minimize the problems associated with gas conditions and compression.

Flow measurement technologies

For relatively dry gas, laboratory quality airflow measurements can be made by placing great attention on accuracy, calibration, repeatability, and precision. Flowmeters that perform suitably in these environments include the Fleisch and Lilly style pneumotachometers, hot-wire and hot-film anemometers, rotating vane spirometers, and ultrasonic flowmeters. Hot-wire anemometers (also known as thermal dissipation devices), based upon the convective cooling by the flowing gas, often use heated (300 °C) platinum or a platinum alloy, the properties of which make the use of these devices inappropriate when flammable gases are present [11]. Rotating vane spirometers (which are not discussed in this chapter) tend to underestimate at low flows and overestimate at high flows due to the friction and inertia of the turbine [12,13]. Overall, in respiratory research, the most widely used flow measurement device is the Fleisch-type differential pressure sensor with a heated screen orifice. Differential pressure sensors, hot-wire anemometers, and ultrasonic sensors will each be discussed.

Differential pressure flow sensors

Differential pressure flow sensors incorporate a type of restriction (point orifice, variable flap, vena constriction, annular obstruction, target or linear flow restrictor) that generates a pressure difference across the sensor. Flexible tubing, attached to either side of the flow obstruction, transmits the differential pressure signal to a sensitive pressure sensor located inside a monitor at the bedside. Factors that influence flow measurement for this type of sensor include the molecular weight of gas, temperature, and airway pressure [14,15].

Fleisch type

The popular Fleisch pneumotachograph [16] uses a bundle of capillary tubes that provides a small but fixed resistance to airflow, and is based on Poiseuille's law, in which the laminar flow in a thin tube is proportional to

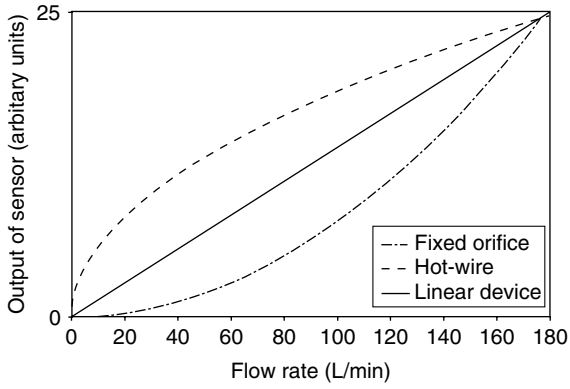

Figure 38.2 Flow versus "output" for a "linear" device (i.e., Fleisch pneumotachograph) and "non-linear" devices (fixed orifice flow sensor) and hot-wire anemometer over the adult flow range. [Image courtesy of Respironics, Inc., Murrysville, PA.]

the pressure loss per unit length. This design ensures laminar flow through the sensor body, thereby producing a nearly linear relationship between the flow and differential pressure. The decrease in pressure across these capillaries is calibrated in terms of flow, and is measured continuously by a differential pressure transducer. A family of pneumotachs is needed to cover the complete physiological range. The Fleisch pneumotach (Figure 38.2) is calibrated to work over a range of laminar flows, which necessitates close attention to breathing circuit details, so that turbulent flow is not inadvertently introduced, which could cause error. While it is an excellent device for short-term monitoring, it is easily contaminated by sputum and water condensate, which may change the flow characteristic of the device. Because of this possibility, heated pneumotachs were introduced. Also, due to its relatively large surface area (deadspace), it is often not suited for continuous respiratory monitoring, and is heavy, costly, and difficult to clean.

Silverman and Whittenberg/Lilly modification

In the 1940s, Silverman and Whittenberg (1950) [17], and also Lilly (1950) [18], suggested a modification to the Fleisch pneumotach, which was intended to reduce the condensation problem. This pneumotach used a fine metal mesh (400 mesh wire screen) that provides airflow resistance, and is protected by two lower-mesh screens on either side. These protective screens condense water vapor, collect particulates, improve laminar flow at high frequencies, and lower deadspace. However, water vapor remained a problem, even with the advent of heaters, so the same problem inherent in the Fleisch pneumotach (monitoring continuous proximal airway flows) was not completely solved.

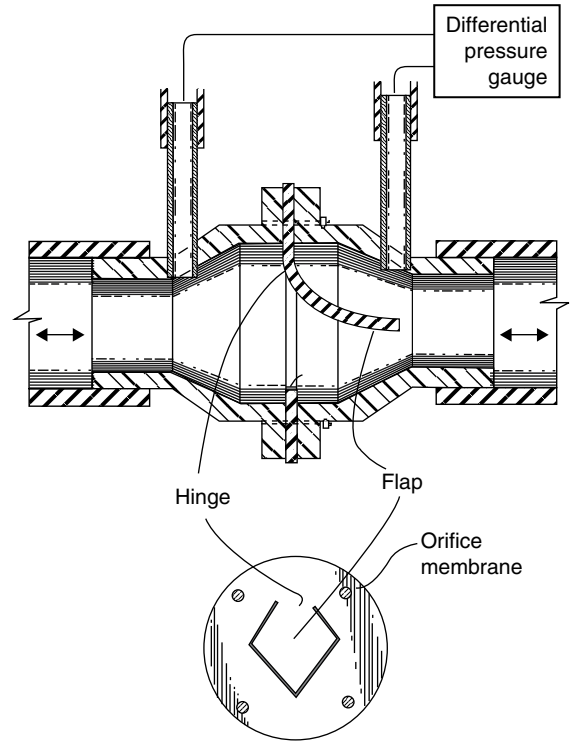

Figure 38.3 Variable orifice pneumotachograph. [Adapted from: Osborn JJ. A flow meter for respiratory monitoring. *Crit Care Med* 1978; **6**: 349–51, and Osborn JJ. Variable orifice gas flow sensing head. US Patent 4,083,245, issued April 11, 1978.]

Variable orifice type

The variable orifice type flow sensors have become popular for long-term monitoring in the critical care environment due to their improved immunity to artifactual flow signals caused by moisture and secretions in the breathing circuit (Figure 38.3) [19,20]. These flow sensors use a flexible sheet (plastic or stainless steel) to create an opening that is small when flow is low and wide as flow increases. This dynamically changing orifice results in a more linear relationship between differential pressure and flow, allowing a larger range of flows to be measured accurately than is traditionally allowed by a fixed orifice type of device. The variable orifice flowmeter works quite well under conditions of moisture and mucous secretions. Its accuracy, however, depends on the consistent stress–strain characteristics of the variable orifice flap, which can be degraded by inter-device variations created during manufacturing or intra-device changes due to fatigue when used long

term. In order to solve this problem, some manufacturers offer sensors with device-specific, factory precalibration parameters stored within a memory chip attached within the flowmeter connector. Variable flap flowmeters can be very susceptible to changes in flow patterns generated by different breathing circuit adapters (inlet configurations) located immediately before the flowmeter.

Fixed orifice type

The pressure decrease across a fixed orifice flow sensor is, in general, proportional to the square of the flow. The relationship between the measured differential pressure to flow (L/min) can be described by the equation:

$$\frac{P_m T_{std}}{P_{std} T_m} K\sqrt{\Delta P},$$

where P_m, P_{std}, T_m, and T_{std} are the measured and standard pressures (in mm Hg) and temperatures (in K), respectively; K is a correction factor that includes gas composition and other factors, and ΔP is the differential pressure (in mm Hg). The $P_m T_{std}/ P_{std} T_m$ is the ideal gas law correction of calculated flow to standard conditions. Microprocessors can be programmed to store the flow sensor parameters, and compensate for the non-linear pressure–flow relationship. In addition, recent advances in differential pressure sensor technology have made it possible to reliably measure very low flows. Some fixed orifice flow sensors use Pitot tubes to measure the velocity of gas flow, and thus are based upon different measurement principles than target flowmeters that measure the disk drag force produced by the reduced annular area. Figure 38.4 illustrates a commercial device.

Turbulent flowmeters

Elliott *et al.* (1977) [21] pursued resistive flow concepts, and investigated a turbulent air flowmeter. Fleisch-type pneumotachs produce linear responses over a range of laminar flows, and are dependent on gas viscosity. Turbulent flowmeters, however, have a powerlaw relationship that depends on dimensions, length, and diameter, as well as viscosity and density. The major advantages of this type of flowmeter are that they are relatively uninfluenced by the wet airways usually found in breathing circuits, and less influenced by changing gas composition. Major disadvantages are poor accuracy at low flows, and the relatively high pressure decrease at high flows. Turbulent flowmeters typically have a higher resistance to flow when compared with laminar-type flowmeters. The turbulent flow approach was further pursued by Saklad *et al.* (1979) [22]. Instead of creating turbulence in a tube, this group created turbulence across a fixed orifice. They claimed as major advantages insensitivity to temperature changes and water vapor.

Hot-wire flow sensors

Earlier studies of heat transfer from a heated wire by Boussinesq (1905) [23] were extended by King (1914) [24] who sought to verify experimentally his theoretical results [25]. The basic "heat balance" relationship can be written as:

heat stored = electrical power in – aerodynamic heat transfer out,

or mathematically as

$$\frac{dc_w}{dt} = P - Q,$$

where c_w is the specific heat of the wire.

From this basic relationship, King obtained an equation for the hot-wire heat loss:

$$Q = L(k_t) + 2\sqrt{(\pi k_t c_p \rho u r_w)(T_w - T_{adw})},$$

where Q is the heat loss per unit time (forced convective heat transfer), T_w the wire temperature, T_{adw} temperature adiabatic wall condition, L characteristic length, k_t heat conductivity at specified temperature, c_p specific heat at constant pressure, ρ density of flowing medium, r_w radius of the wire, and u magnitude of the velocity.

In the above equation, heat loss is a function of the properties of the wire, including its dimensions and

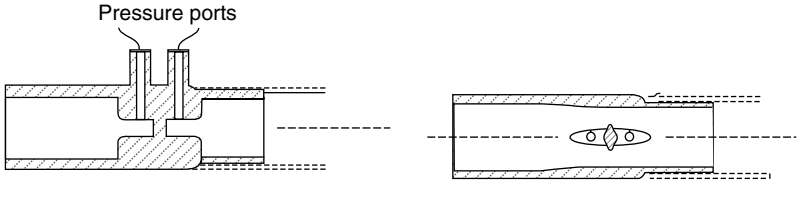

Figure 38.4 Fixed orifice target flow sensor. [Adapted from: Kofoed SA, Orr JA. Differential pressure sensor for respiratory monitoring. US Patent 5,535,633, issued July 16, 1996.]

Table 38.2 Representative commercial flow sensors used clinically

Technology	Type	Manufacturer	Model[a]	Reference
Differential	Screen	Hans Rudolph	3830/4830 adult pneumotach	Rudolph, 1991 [30]
	Variable orifice	Bicore	Varflex® flow transducer	Stupecky, 1991 [31]
	Variable orifice	Bird	Partner® Ili volume monitor	Guillaume *et al*., 1991 [32]
	Fixed orifice (target)	Respironics-Novametrix	Series 3 flow sensors	Kofoed and Orr, 1996 [33]
	Fixed orifice (Pitot)	Datex-Ohmeda	D-lite® flow sensor	Merilainen *et al*., 1993 [34]
	Fixed orifice (Pitot)	Medical Graphics	Prevent™ pneumotach	Porszasz *et al*., 1994 [35]
Hot-wire	CTA	Bear	NVM-1 (neonatal volume monitor)	Cutler, 1993 [36]
Ultrasonic	Time of flight	NDD	Easyone™ spirometer	Harnoncourt *et al*., 1996 [37]; Buess *et al*., 1986, 1989 [29,38]

[a] All trademarks are the property of their respective holders.

heat conductivity, and properties of the fluid, including its specific heat and density. Additionally, note that the nature of the equation is such that the sensitivity of lower flow rates increases and, at higher flow rates, decreases. Thus, the hot-wire sensor tends to be more accurate at low flow rates, but less accurate at high flow rates. Also note that hot-wire anemometers are insensitive to the direction of flow, and, hence, require that two heated wires be placed in series in order to determine the direction of flow.

The two types of hot-wire anemometers primarily used are the constant current anemometer (CCA) and the constant temperature anemometer (CTA). Both designs usually use a bridge circuit (such as the Wheatstone bridge), with one of the legs acting as the hot-wire. By passing a current through the wire ("resistor"), its temperature increases, in essence becoming a "hot-wire." The resistance of a wire (e.g., platinum) is generally proportional to its temperature over the operating range. With the constant current type of hot-wire anemometer, gas flows past the hot-wire, the wire is cooled, and the altered resistance of the wire is measured to indicate the flow rate of the gas passing through the hot-wire resistor. With this type of sensor, the current level is usually low, such that the sensor does not become heated.

Such CTAs are designed to maintain the temperature as reflected by the resistance of the hot-wire anemometer constant. The resistance level is chosen to be higher than the sensor resistance at ambient conditions; consequently, the sensor temperature will be higher than ambient. As the resistance of the wire resistor changes in response to gas flow, the current through the platinum wire resistor is adjusted to maintain its temperature – and, hence, its resistance – constant. The resulting voltage decrease across the resistor indicates the flow rate of the gas (Table 38.2).

In general, hot-wire sensors are typically used for measurements in air and electrically non-conducting fluids. For clinical use, the advantages include high linearity, wide dynamic range, practically negligible influences of temperature and vapor pressure with humidified gases, capability of measuring bidirectional airflow, and ease of operation [11,26]. Problems that have limited the clinical use of this type of sensor include calibration difficulties, influences of barometric pressure, influences of the composition of gases (including anesthetic agents), stability of the sensing element with time, use with nebulizers, hot-wire burning, possibility of producing nitrogen oxides from the catalytic action of the hot-wire, interchangeability of transducers, sterilization, vulnerability to damage (i.e., handle with care), and flammability [11]. Stability may be impaired with foreign materials, such as sputum or dust, or water droplets adhering to the hot-wire and

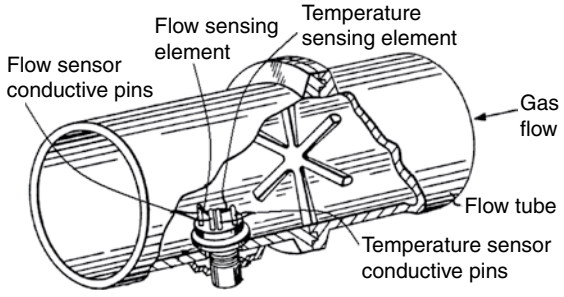

Figure 38.5 Hot-wire sensor assembly mounted in a flow tube. [Adapted from: Cutler CW. Flow sensor system and method. US Patent 5,263,369, issued November 23, 1993.]

altering its temperature coefficient. New designs have improved performance, although the influences of gas composition and barometric pressure are unavoidable. Figure 38.5 illustrates a commercial hot-wire device.

Ultrasonic flow sensors

An ultrasonic sensor, such as that proposed by Blumenfeld *et al.* (1974, 1975) [27,28] does not depend on a Doppler shift in ultrasound frequency, but simply measures the influence of gas flow on the transmission time of pulses between two crystals. The transit time principle is based on the use of transducers to transmit and receive signals through the flow. The signal travels faster when moving with the flow stream rather than against it. The difference between the two transit times is used to calculate the flow rate; thus, transmission time (t_d) is decreased in the direction of flow (downstream) and increased (t_u) in the opposite direction (upstream). It can be shown [29] that,

$$t \cong t_u - t_d = \frac{2Lu \times \cos(\beta)}{c^2}$$

where $u << c$, u = mean flow velocity along the sound path, c = velocity of sound, L = length of the sound transmission path, and β is the angle between the transducer and flow axis (Table 38.2).

Although the mathematical relationships are clear, the potential variability of L and c can introduce considerable complexity. The ultrasound velocity depends on temperature and humidity. The speed of sound, c, also depends on the fractional composition and densities of the gases, as well as their specific heat at constant pressure and constant volume. Buess *et al.* (1986) [29] note that during air-breathing, the maximal changes in

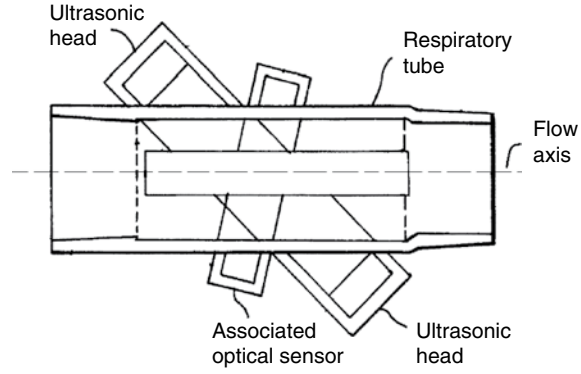

Figure 38.6 Ultrasonic flow sensor. [Adapted from: Harnoncourt K, Guggenbuhl W, Schlegelmilch RM, Buess C. Apparatus for measuring the parameters of respiratory gases. US Patent 5,503,151, issued April 2, 1996.]

c^2 term is limited to 63%. Also, the measured average flow velocity between acoustic sensors does not always represent the required average flow velocity. In essence, composition, temperature, and water vapor dependence require careful control in order to implement corrections and provide accurate flow measurements. Additionally, costs associated with measurement circuitry have traditionally made ultrasonic sensors costly. With the development of application-specific integrated circuits (ASICs) for these sensors, costs have been reduced. Figure 38.6 shows in schematic form a time-of-flight device.

Summary

Advances in technology have impacted all of the flow measurement methods described. Increased performance of piezo-resistive pressure sensors has improved the low-end performance characteristics of differential pressure flow methods, and novel approaches in hot-wire anemometry have overcome some of its shortcomings. Advances in microelectronics, such as the use of ASICs, have decreased the costs of ultrasonic flow sensors. Even while technology has permitted cost and performance improvements to be made on all fronts, the correct sensor type for each application depends on a careful evaluation of each product and how it fits the particular needs.

References

1. Lemen RJ, Gerdes CB, Wegmann MJ, Perrin KJ. Frequency spectra of flow and volume events for forced vital capacity. *J Appl Physiol* 1982; **53**: 977–84.

2. Turner MJ, Davies VA, De Ravel TJ, Rothberg AD, MacLeod IM. Bandwidths of respiratory gas flow and pressure waveforms in mechanically ventilated infants. *Physiol Meas* 1993; **14**: 419–31.
3. Frey U, Stocks J, Coates A, Sly P, Bates J. European Respiratory Society/American Thoracic Society. Specifications for equipment used for infant pulmonary function testing: ERS/ATS Task Force on standards for infant respiratory function testing. *Eur Respir J* 2000; **16**: 731–40.
4. Tobin MJ. *Principles and Practice of Mechanical Ventilation*. New York: McGraw-Hill, 1994.
5. Gammage GW, Banner MJ, Blanch PB, Kirby RR. Ventilator displayed tidal volume: what you see may not be what you get [abstract]. *Crit Care Med* 1988; **16**: 454.
6. Bartel LP, Bazik JR, Powner DJ. Compression volume during mechanical ventilation: comparison of ventilators and tubing circuits. *Crit Care Med* 1985; **13**: 851–4.
7. Goff JA, Gratch S. Low-pressure properties of water from –160 to 212 deg F. *Trans Am Soc Heat Vent* 1946; **52**: 95–122.
8. Shelly MP. Inspired gas conditioning. *Respir Care* 1992; **37**: 1070–80.
9. Branson RD. Humidification for patients with artificial airways. *Respir Care* 1999; **44**: 630–41.
10. Kreit JW, Sciurba FC. The accuracy of pneumotachograph measurements during mechanical ventilation. *Am J Respir Crit Care Med* 1996; **154**: 913–17.
11. Yoshiya I, Shimada Y, Tanaka K. Evaluation of a hot-wire respiratory flow-meter for clinical applicability. *J Appl Physiol* 1979; **47**: 1131–5.
12. Ilsley AH, Hart JD, Withers RT, Roberts JG. Evaluation of five small turbine-type respirometers used in adult anesthesia. *J Clin Monit* 1993; **9**: 196–201.
13. Yeh MP, Adams TD, Gardner RM, Yanowitz FG. Turbine flowmeter vs. Fleisch pneumotachometer: a comparative study for exercise testing. *J Appl Physiol* 1987; **63**: 1289–95.
14. Turner MJ, MacLeod IM, Rothberg AD. Effects of temperature and composition on the viscosity of respiratory gases. *J Appl Physiol* 1989; **67**: 472–7.
15. Sullivan WJ, Peters GM, Enright PL. Pneumotachographs: theory and clinical application. *Respir Care* 1984; **29**: 736–49.
16. Fleisch A. Pneuomotachograph: apparatus for recording respiratory flow. *Arch Ges Physiol* 1925; **209**: 713–22.
17. Silverman L, Whittenberg JL. Clinical pneumotachograph. In: *Methods in Medical Research*, vol. 2. Chicago, IL: Year Book Publishers, 1950; 104–12.
18. Lilly JC. Flow meter for recording respiratory flow of human subjects. In: *Methods in Medical Research*, vol. 2. Chicago, IL: Year Book Publishers, 1950; 113–21.
19. Osborn JJ. A flow meter for respiratory monitoring. *Crit Care Med* 1978; **6**: 349–51.
20. Osborn JJ. Variable orifice gas flow sensing head. US Patent 4,083,245, issued April 11, 1978.
21. Elliott SE, Shore JH, Barnes CW, Lindauer J, Osborn JJ. Turbulent airflow meter for long-term monitoring in patient–ventilator circuits. *J Appl Physiol* 1977; **42**: 456–60.
22. Saklad M, Sullivan M, Paliotta J, Lipsky M. Pneumotachography: a new low deadspace, humidity independent device. *Anesthesiology* 1979; **51**: 149–53.
23. Boussinesq J. An equation for the phenomena of heat convection and an estimate of the cooling power of fluids. *J Mathematique* 1905; **1**: 285–332.
24. King LV. On the convection of heat from small cylinders in a stream of fluid. *Phil Trans R Soc London* 1914; **A214**: 373–432.
25. Stainback PC, Nagabushana KA. Review of hot-wire anemometry techniques and the range of their applicability for various flows. *Electron J Fluid Eng Trans ASME* 1993; **167**: 1–54.
26. Yoshiya I, Nakajima T, Nagai I, Jitsukawa S. A bidirectional respiratory flowmeter using the hot-wire principle. *J Appl Physiol* 1975; **38**: 360–5.
27. Blumenfeld W, Turney SZ, Denman RJ. A coaxial ultrasonic pneumotachometer. *Med Biol Eng* 1975; **13**: 855–60.
28. Blumenfeld W, Wilson PD, Turney S. A mathematical model for the ultrasonic measurement of respiratory flow. *Med Biol Eng* 1974; **12**: 621–5.
29. Buess C, Pietsch P, Guggenbuhl W, Koller EA. Design and construction of a pulsed ultrasonic air flowmeter. *IEEE Trans Biomed Eng* 1986; **33**: 768–74.
30. Rudolph KA. Pneumotach. US Patent 5,060,655, issued October 29, 1991.
31. Stupecky J. Variable area obstruction gas flow meter. US Patent 4,989,456, issued February 5, 1991.
32. Guillaume DW, Norton MG, DeVries DF. Variable orifice flow sensing apparatus. US Patent 4,993,269, issued February 19, 1991.

33. Kofoed SA, Orr JA. Differential pressure sensor for respiratory monitoring. US Patent 5,535,633, issued July 16, 1996.
34. Merilainen P, Hanninen H, Tuomaala L. A novel sensor for routine continuous spirometry of intubated patients. *J Clin Monit* 1993; **9**: 374–80.
35. Porszasz J, Barstow TJ, Wasserman K. Evaluation of a symmetrically disposed pitot tube flowmeter for measuring gas flow during exercise. *J Appl Physiol* 1994; 77: 2659–65.
36. Cutler CW. Flow sensor system and method. US Patent 5,263,369, issued November 23, 1993.
37. Harnoncourt K, Guggenbuhl W, Schlegelmilch RM, Buess C. Apparatus for measuring the paramters of respiratory gases. US Patent 5,503,151, issued April 2, 1996.
38. Buess C, Guggenbuhl W, Koller EA. A pulsed diagonal-beam ultrasonic airflow meter. *J Appl Physiol* 1989; **67**: 2639–42.

Section 5
Chapter
39

Technical perspectives

Combining flow and carbon dioxide

J. A. Orr and M. B. Jaffe

Introduction

The combination of flow and carbon dioxide (CO_2) gas concentration makes possible the continuous assessment of CO_2 production. If CO_2 gas concentration and flow were constant, multiplying the two would provide information on CO_2 elimination for each breath. For example, if the exhalation phase lasts 2 s:

CO_2 (elimination) = concentration × flow × time
= 0.04 (i.e., 4%) × 250 mL/s × 2
= 20 mL/breath.

Gas uptake could be assessed in a similar way using the differences between inspiratory and expiratory values. In a clinical situation, these measurements change instantaneously, and are not constant. Therefore, these multiplications must be made over short periods, and the results added. The challenge is to integrate concentration and flow signals in such a way that the temporal relationship between the two variables is accurate.

Volume of carbon dioxide defined

During normal conditions, the lung will excrete CO_2 at the same rate as the total body production rate, with no net change in body CO_2 stores. The volume of carbon dioxide ($\dot{V}CO_2$) and CO_2 elimination (often incorrectly referred to as CO_2 production) is the net volume of CO_2 measured at the mouth or airway, and is calculated as the difference between expired and inspired CO_2 normalized to a minute. The value of $\dot{V}CO_2$ is computed by summing the dot product of the flow and CO_2 waveforms over the breath cycle. $\dot{V}CO_2$ is usually reported at standard temperature and pressure dry (STPD) conditions. For breath-by-breath measurements, it is calculated as:

$$\dot{V}CO_2 = \sum_{\text{breath}} FCO_2(t) \times \dot{V}(t) \times \Delta t,$$

where $FCO_2(t)$ and $\dot{V}(t)$ are the sampled individual values of the CO_2 and flow waveforms summed over the entire breath, and Δt is the sampling interval. When present, inspired CO_2, if not taken into account, could result in an error in the calculation of $\dot{V}CO_2$ [1]. The resulting per-breath values are summed for all breaths in a minute, or per-breath volume is multiplied by the respiratory rate to convert the volume in a single breath to milliliters per minute. However, in anesthesia and intensive care, components such as filters, heat and moisture exchange filters, connecting tubes, elbows, airway adapters, and suction adapters are placed between the endotracheal tube connector and Y-piece, causing partial rebreathing, and therefore increased amounts of inspired CO_2. Note that this inspired CO_2, if not considered, could result in an error in the calculation of $\dot{V}CO_2$ of several percent [1].

Figure 39.1 illustrates the dot-product multiplication process with the plot of an actual waveform flow and CO_2 versus time of a mechanical breath delivered in a volume control mode. Note that due to the apparatus deadspace from the mainstream sensor, Y-piece, and other circuit components, a small volume of end-expiratory CO_2 (from the previous breath) is rebreathed upon initiation of inspiration. Note that in this patient, the expiratory CO_2 waveform rises rapidly to a plateau, and the CO_2 volume curve follows that of the expiratory portion of the flow waveform. $\dot{V}CO_2$ would then be the difference between the expiratory and inspiratory areas of the dot-products. If PCO_2 and volume are plotted instead, the net volume of CO_2 eliminated can be viewed as the area between the expiratory and inspiratory curves (Figure 39.2). With no rebreathing, the volume of CO_2 eliminated during a breath is the area under the volumetric capnogram. However, the presence of inspiratory CO_2 must be accounted for when reporting and interpreting $\dot{V}CO_2$ [1].

Capnography, Second Edition, ed. J. S. Gravenstein, Michael B. Jaffe, Nikolaus Gravenstein, and David A. Paulus. Published by Cambridge University Press. © Cambridge University Press 2011.

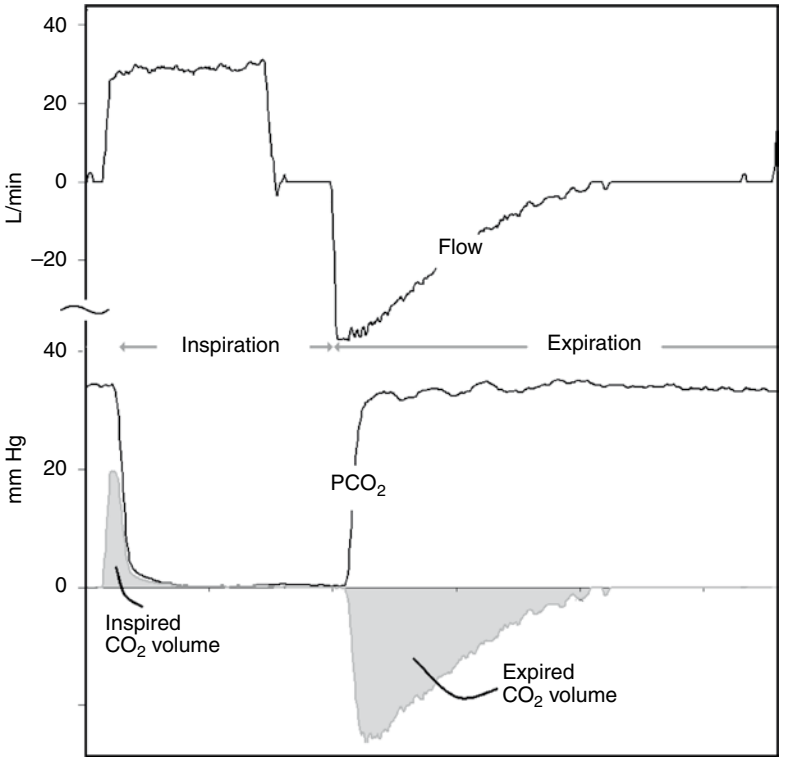

Figure 39.1 Plot of flow and CO_2 waveforms for an individual ventilator-delivered breath, with dot-product showing inspired and expired CO_2 volumes. [Image courtesy of Philips-Respironics, Inc., Murrysville, PA.]

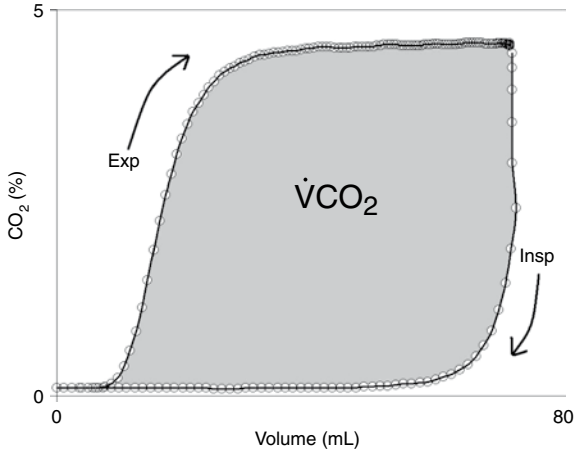

Figure 39.2 Plot of CO_2 (%) versus volume for a pediatric subject illustrating both the expiratory (Exp) and inspiratory (Insp) portions. While often the inspiratory portion is negligible (as in this figure), the net CO_2 volume per breath (shaded) is the difference between the area under the expired and inspired portions of the curve or, similarly, the area within the loop. (Individual data samples shown with sampling rate of 100 samples/s).

The recorded $\dot{V}CO_2$ does not accurately reflect the underlying physiology when there are leaks in the collecting system or when conditions are such that all the gas considered part of the alveolar ventilation volume cannot be measured; that is, pneumothorax with leak or an endotracheal tube cuff leak. Due to the complex interaction between V_D/V_T, physiological deadspace, and alveolar ventilation, the volume of CO_2 excreted by each breath is variable. The results of several breaths are often averaged in an attempt to decrease the effect of normal breath-to-breath changes in volume. Depending on how $\dot{V}CO_2$ is used (metabolic versus ventilator adjustments), a different averaging interval may be required, and includes a range of averaging intervals such as 1 breath, 8 breaths, 1 min, 3 min, and longer.

During steady-state conditions, the lung will excrete CO_2 at the same rate as the total body production rate, and there will be no net change in body CO_2 stores. In this case, $\dot{V}CO_2$ is representative of total body production, and is proportional to metabolic rate. Because the body can store (buffer) a large amount of CO_2 relative to the rate at which CO_2 is produced, eliminated CO_2 can be different from metabolically produced CO_2 for a long time (up to 1 h) following a change in ventilation. However, changes in $\dot{V}CO_2$ can provide an instantaneous indication of changes in alveolar ventilation [2].

Measurement site considerations

With today's compact systems, measurements of flow and gas partial pressure (or concentration) are

undertaken using flow and gas sensors that may or may not be located proximally and in the mainstream flow. Proximal flow measured at the patient's airway can be substantially different from flow measured inside or at the ventilator since the delivered flow in the inspiratory limb of the breathing circuit and the exhaled flow from the expiratory limb are typically measured internally by two separate flow sensors. Gas concentration may be measured at or near the patient's airway, measured distally from the patient's airway, or a portion sampled and measured by a system located a distance from the sample site. The challenge is to combine the concentration and flow signals in such a way that the temporal relationship between these two variables is accurate. Also, given that frequency response differs among sensors, it is important that the frequency response of the flow and CO_2 signal be suitably matched.

As noted, the location of gas sampling and flow measurement varies, and can affect the reliability and accuracy of volumetric gas measurements; this applies to both mainstream and sidestream devices. Placement of the gas sampling site more proximally will potentially allow the end-tidal partial pressure of CO_2 ($P_{ET}CO_2$) value to better reflect the alveolar concentration. Placement of the sampling site adapter as close to the inspiratory limb (or Y-piece) as possible will not eliminate the apparatus deadspace due to the volume of the adapter and connectors [1]. If the inspiratory CO_2 volume is not considered, overestimation of $\dot{V}CO_2$ will increase with decreases in tidal volume (V_D/V_T) and/or increases in apparatus deadspace. Moreover, the last part of the alveolar plateau of the capnogram, normally considered to be $P_{ET}CO_2$, is also the PCO_2 of the alveolar gas in the apparatus deadspace that is rebreathed in the next inspiration, and does not contribute to the overall pulmonary CO_2 elimination. The pros and cons of the different combinations of measurement sites are reviewed.

Proximal flow and gas measurement

With robust mainstream sensors for flow and carbon dioxide located at or very close to the same point in the gas stream (Figure 39.3), the principal issue is one of matching the frequency response of the two sensors. Issues of deadspace and resistance, and robustness to the challenging environment at the airway must also be kept in mind. Devices such as combined CO_2/flow airway adapters (Figure 39.4) minimize the added

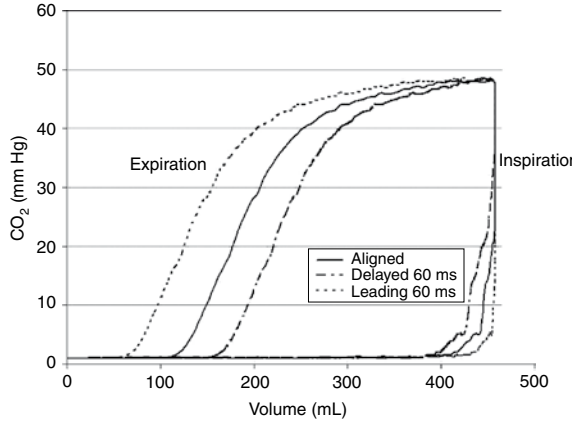

Figure 39.3 Volumetric capnogram showing both expiratory and inspiratory limbs and illustrating the effect of time misalignment. Note if the CO_2 waveform is delayed relative to the volume, the loop gets smaller on both ends; conversely when the CO_2 waveform is advanced relative to volume, the loop gets larger on both ends. [Image courtesy of Philips-Respironics, Inc., Murrysville, PA.]

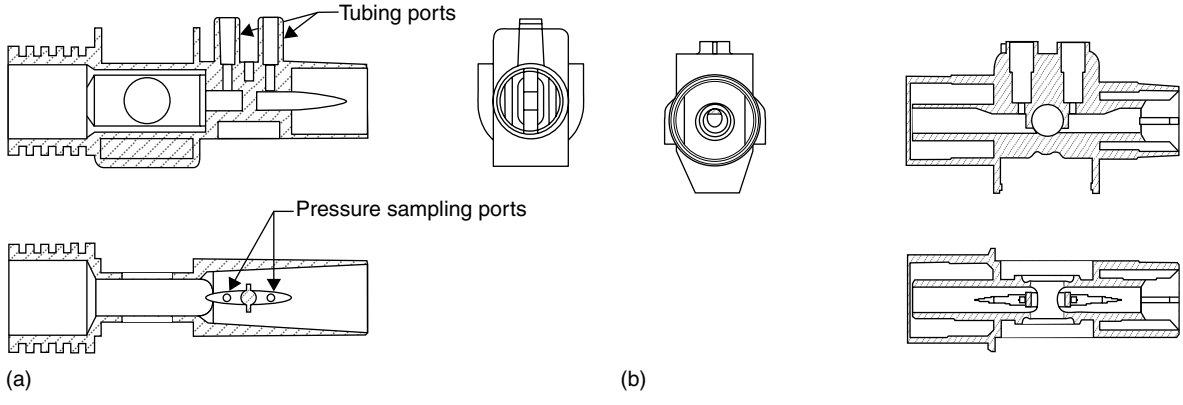

Figure 39.4 (a) Combination adult and (b) combination neonatal CO_2/flow sensors: side, top, and end sections. [Image courtesy of Philips-Respironics, Inc., Murrysville, PA.]

deadspace between the Y-piece and elbow, and permit accurate measurement of carbon dioxide production and volumetric capnogram-derived parameters such as V_D/V_T [3].

Proximal flow and distal gas measurement

Placement of the CO_2 sensor in the expiratory limb eliminates the need to measure inspired CO_2 and accounts for rebreathing; however, standard capnometry is not possible when only expired gas is analyzed. In this configuration, it is not possible to estimate functional anatomic deadspace, or to calculate alveolar tidal and minute volumes. This configuration leads to overestimation of CO_2 elimination because the expired volume is greater due to the water condensation at the Y-piece, and CO_2 reads somewhat higher because it is measured after condensation.

Proximal gas measurement and distal flow measurement

If the sensors are separated, as with a mainstream CO_2 sensor used with separate flow sensors in the inspiratory and expiratory limb of the ventilator, the additional problems – correcting for the effects of different gas characteristics (temperature and humidity) and calibration issues associated with using separate sensors for inspiratory and expiratory flow – must be considered. The delay in CO_2 analysis is more of a problem with sidestream systems, in which proper matching of the signals must be considered. Variations in temperature and the vapor content of expired gases that affect volume correction and the mixed expired fraction of CO_2 is more of an issue with sidestream systems than mainstream systems. Note that while end-tidal values can be determined relatively accurately with proximal gas and distal flow measurements, volumetric capnogram-based measurements are challenging due to signal alignment issues. In addition, manufacturers of such devices occasionally resort to using surrogate measures, such as the expired volume at 50% of the end-tidal value, for estimating airway deadspace.

Mainstream flow and sidestream gas sampling

When trying to combine a signal from a flow sensor (proximal mainstream or within the ventilator) with a sidestream CO_2 signal, the potential for compounding errors increases, and the issues become even more complicated than with other approaches. Investigators have pursued techniques, ranging from simple corrections to more complicated non-linear approaches that include correcting the measured signal with an inverted form of the step response function [4] and a model to correct for time compression due to the effects of airway pressure on sample flow rates in positive pressure breathing systems [5]. These corrections attempt to address some of the above errors, but, while theoretically appealing, are complicated by clinical and manufacturing realities. The breathing circuit, over time, often becomes congested with secretions and other contaminants that are drawn into the sampling tube and measurement system. The specifications of sampling pumps, stated as a nominal flow rate (often with a tolerance of ±10%), varies with time, load, and between units. Increasing airway pressure compresses the gas in the sampling tube and raises the pressure drop across the sampling tube, changing the velocity of the gas in the tube (Figure 39.5). All of these issues contribute to the difficulty in flow and CO_2 signal alignment [6].

Signal processing issues

In order to avoid the undesirable effect of aliasing, an anti-aliasing filter (i.e., low pass) is employed before the analog-to-digital converter. However, it is necessary to know the bandwidth of the signal of interest so that the filter's cut-off frequency is sufficiently high. For example, an anti-aliasing filter with a bandwidth of 10 Hz can be applied to the signal to effectively remove a 13-Hz noise component. Butterworth filters, commonly employed for anti-aliasing, are used for their maximally flat response in the transmission passband, minimal passband ripple, and are best suited for applications requiring preservation of amplitude linearity in the passband region. Methods for determining the frequency response of flow and gas analyzers have been presented in the literature [7], and are referred to the reader for more detailed discussions on the subject. Given that integration of the dot-product of the flow and CO_2 signals over an entire breath generates a significant low-pass filter, there is little need to further low-pass filter the input signals prior to integration.

Calibration issues

The accuracy of these devices can be verified using a simple bench procedure. The procedure requires

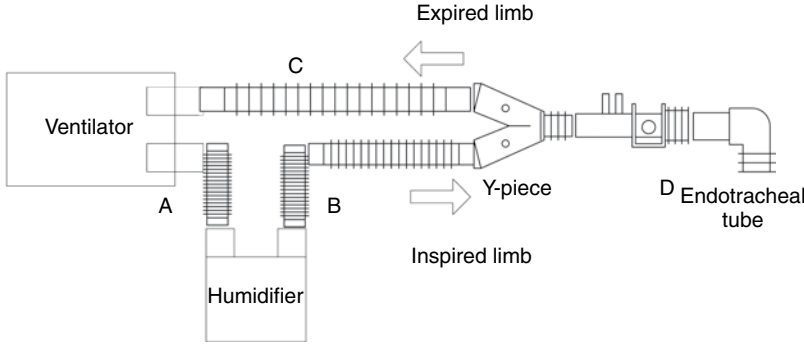

Figure 39.5 Ventilator with breathing circuit, with humidifier on inspiratory limb with proximal mainstream combined CO_2/flow sensor (grayed). Conditions at A through D are described below. (A) Gas from the ventilator inspiratory port consists of room air or an elevated level of oxygen. The gas is typically dry and at room temperature, which is nominally 25 °C. (B) Gas exiting the humidifier is typically at 100% relative humidity (RH) (i.e., saturated) and at a temperature greater than room temperature and less than or equal to 39 °C. (C) Gas returning from the patient has a lower partial pressure of water vapor due to condensation and a lower temperature (such as 33 °C). (The relative humidity is still 100%, but the partial pressure of water vapor is lower.) (D) Gas expired at the patient's mouth is most likely slightly less than body temperature of nominally 37 °C and fully saturated. If an unheated breathing circuit were to be used, the gas inspired at the patient's mouth would be less than the 35 °C due to cooling during transport through as much as 8 ft (2.4 m) of 15-mm internal diameter breathing circuit tubing. (Image courtesy of Philips-Respironics, Inc., Murrysville, PA.]

establishing a bench model of a mechanically ventilated lung. A known flow of pure CO_2 (e.g., 200 mL/min) is infused into a mechanical lung simulator (e.g., Training Test Lung, Michigan Instruments, Grand Rapids, MI, USA) using a precision gas flow controller. When the $\dot{V}CO_2$ measurement device under testing is connected to the test lung, the measured CO_2 elimination should match the CO_2 infusion rate [8]. Care should be taken to ensure that the flow controller used to determine the injection of CO_2 is accurate and not affected by the pressure change in the lung with ventilation. This type of simulation can be used to test the effect of signal alignment and frequency matching of the signals, as well as compensation of inspired CO_2 and other effects.

Conclusions

Clinically acceptable results for volumetric CO_2 measurements may be achieved with all of the configurations reviewed under the right favorable conditions if close attention is paid to the measurement, the equipment set-up, and interpretation of the displayed results. However, as more extremes of ventilator conditions in the critical care setting are encountered, only the proximal mainstream flow and gas measurement solution provides reliable results under the wide spectrum of ranging humidity, pressure, and temperature values that are seen in the clinical environment.

References

1. Breen PH, Serina ER, Barker SJ. Measurement of pulmonary CO_2 elimination must exclude inspired CO_2 measured at the capnometer sampling site. *J Clin Monit* 1996; **12**: 231–6.
2. Taskar V, John J, Larsson A, Wetterberg T, Jonson B. Dynamics of carbon dioxide elimination following ventilator resetting. *Chest* 1995; **108**: 196–202.
3. Kallet RH, Daniel BM, Garcia O, Matthay MA. Accuracy of physiologic deadspace measurements in patients with acute respiratory distress syndrome using volumetric capnography: comparison with the metabolic monitor method. *Respir Care* 2005; **50**: 462–7.
4. Farmery AD, Hahn CE. Response-time enhancement of a clinical gas analyzer facilitates measurement of breath-by-breath gas exchange. *J Appl Physiol* 2000; **89**: 581–9.
5. Farmery AD, Hahn CE. A method of reconstruction of clinical gas-analyzer signals corrupted by positive-pressure ventilation. *J Appl Physiol* 2001; **90**: 1282–90.
6. Fletcher R, Werner O, Nordstrom L, Jonson B. Sources of error and their correction in the measurement of carbon dioxide elimination using the Siemens-Elema CO_2 analyzer. *Br J Anaesth* 1983; **55**: 177–85.
7. Jackson AC, Vinegar A. A technique for measuring frequency response of pressure, volume, and flow transducers. *J Appl Physiol* 1979; **47**: 462–7.
8. Orr JA, Westenskow DR, Bauer A. A prototype gas exchange monitor for exercise stress testing aboard NASA Space Station. *J Appl Physiol* 1989; **66**: 492–7.

Section 6

Historical perspectives

Section 6
Chapter
40

Historical perspectives

Brief history of time and volumetric capnography

M. B. Jaffe

Carbon dioxide and the gas laws

Carbon dioxide (CO_2) is now the fourth most abundant gas (after nitrogen, oxygen, and argon) on Earth. Several billion years ago, before O_2 assumed its present position, CO_2 was much more plentiful. Today, we are concerned that its modest concentration in the atmosphere may rise over its current level of approximately 0.04%.

For most of its history, no one had heard of CO_2. However, even in antiquity, people knew of "evil airs", for example, in the famous Grotto del Cane (Naples). At this site, a poisonous gas lingered at the floor of the grotto, and dogs (and cats and chickens) would be overcome by a gas, while people could survive a trip into the grotto as long as they would stay upright and kept their noses well above the CO_2 that was seeping out of cracks in the bottom of the cave. Given the knowledge that the density of CO_2 is greater than that of air, in hindsight, this makes perfect sense, and is actually seen anytime dry ice is used where the dry ice cloud hugs the floor.

Jan Baptista Van Helmont (1579/80–1644) was the first to recognize the formation of CO_2 gas during fermentation and burning of wood. He called it *gas sylvestre* (Roman deity, Sylvester, a spirit of the woods). However, that title had to be surrendered when, in 1755, J. Black named it *fixed air*, because he had discovered it as a constituent of carbonated alkali. The gas finally yielded to chemical analysis when Antoine-Laurent de Lavoisier (1743–94) demonstrated it to be an oxide of carbon. It took many years before CO_2 could be measured in the exhalation or blood of man and beast [1].

Before measurements of CO_2 gas became possible, measurements of gases had to be developed. Thus, we must mention Otto Guericke (1602–86), who had held many posts, among them mayor in the city of Magdeburg, the capital of Saxony-Anhalt in Germany. The University of Magdeburg now calls itself the Otto-von-Guericke University, in recognition of its famous son. Around 1650, Guericke had evacuated air from two large matching hemispheres, which even a team of eight horses were unable to separate. This demonstration, in part, was used to disprove the adage that "nature abhors a vacuum." Many think of Guericke as having introduced us to the concept of barometric pressure. In doing so, he also showed us how to aspirate gas by means of a vacuum pump.

Next, Robert Boyle (1627–91) deserves mention. He was an aristocrat–experimenter who taught in Oxford and London, and who published several scientific treatises describing his experiments, among them one on *New Experiments … Touching the Spring of the Air …* [2]. Once again, vacuum pumps played a role. We now remember Boyle's law, which states that pressure = k/volume, an important fact when gases are exposed to different pressures during measurements. One of Boyle's assistants at Oxford, Robert Hooke (1635–1703), built a vacuum pump for Boyle. This was not Hooke's most memorable accomplishment, of which there were many, but an important one for the present day.

If pressure affects the volume of gas, so does temperature, expressed as $V = kT$ by the French balloonist–scientist, Jacques Alexander César Charles (1746–1823). Joseph Louis Gay-Lussac (1778–1850), another French balloonist–scientist, contributed details by describing the relationship between pressure and temperature, when volume and amount are held constant, $P/T = k$.[1] In 1834, Émile Clapeyron (1799–1864) combined the laws of Boyle, Charles, and

[1] The law expressing this relationship (isovolumic) was named after Charles at the suggestion of Gay-Lussac, and was intended to give credit to the unpublished work of Charles performed in 1787.

Capnography, Second Edition, ed. J. S. Gravenstein, Michael B. Jaffe, Nikolaus Gravenstein, and David A. Paulus. Published by Cambridge University Press. © Cambridge University Press 2011.

Gay-Lussac into the first formulation of the ideal gas law: $PV = R(T + 267)$ (temperature in degrees Celsius).[2]

At this point, we will break from the string of French balloonists and turn to the British Isles and Professor William Thomson (1824–1907), who later would be knighted in 1892 as Lord Kelvin of Largs – now known as Lord Kelvin. He proposed an absolute scale of temperature in 1848, and wrote the ideal gas law in the well-known form, $PV = nRT$, where n is the number of moles of gas present, R is the universal gas constant, and T is absolute temperature in degrees Kelvin. This terse, mathematical summary, the result of many empirical observations and insight, states that the product of the pressure (P) and volume (V) of an ideal gas is proportional to its absolute temperature (T) and to the number of molecules in it. In 1873, the Dutch physicist, Johannes van der Waals (1837–1923), modified the ideal gas law, and derived a new gas law to account for the actions of real fluids. The van der Waals equation is commonly expressed as: $(P + a/V^2)(V - b) = RT$, where the values for the constants a and b are different for real gases.

The current, frequently used infrared spectrometry-based measurement of CO_2 owes thanks to William Herschel (1738–1822), known primarily as the astronomer who discovered Uranus (1781), but who also discovered infrared radiation (1800). He passed sunlight through a prism, holding a thermometer just beyond the red end of the visible spectrum, and observed the temperature increase. From this observation, Herschel concluded that there must be an invisible form of energy [3].

Pierre Bouguer (1698–1758), in 1729, first expressed the relationship between the absorption of radiant energy and the absorbing medium, noting: "In a medium of uniform transparency the light remaining in a collimated beam is an exponential function of the length of the path in the medium" (from the French) [4]. Johann Heinrich Lambert (1728–77), considered the founder of the theory of light measurement, published the classic tome, *Photometria*, in Latin [5], in which he presented the logarithmic law of the absorption of light, now often known as Beer–Lambert law (after August Beer [1825–63]), or Lambert–Beer law. Later, Anders Angström (1889) described pressure broadening and observed that, by increasing the size of the sample cell with a constant amount of gas, the infrared absorption was reduced, contrary to what was that predicted by Lambert–Beer's law [6].

[2] Note that later work revealed that the number should actually be 273.2, giving: $PV = R(T + 273.2)$

John Tyndall (1820–93) studied the radiative properties of various gases, and constructed the first ratio spectrophotometer (Figure 40.1), which he used to measure the absorption of gases, such as water vapor, "carbonic acid" (now known as CO_2), ozone, and hydrocarbons. He also observed the large differences in the ability of "perfectly colorless and invisible gases and vapors" to absorb and transmit radiant heat. He also found that oxygen, nitrogen, and hydrogen are almost transparent to radiant heat, but that water vapor, CO_2, and ozone are very good absorbers of heat radiation, and that "even in small quantities, these gases absorb much more strongly than the atmosphere itself" [7]. Tyndall is also credited with making some of the first measurements of expired CO_2 in humans [8]. He reported, in his famous Rede Lecture "On radiation" at Cambridge University, perhaps the earliest infrared quantitative measurement of CO_2 in human breath. In the section of the lecture titled, "Influence of vibratory period and molecular form: physical analysis of the human breath," he notes:

> *The presence of the minutest quantity of carbonic acid may be detected by its action on the rays from the carbonic oxide flame. Carrying, for example, the dried human breath into a tube four feet long, the absorption there effected by the carbonic acid of the breath amounts to 50 per cent of the entire radiation. Radiant heat may indeed be employed as a means of determining practically the amount of carbonic acid expired from the lungs. … The absorption produced by the breath, freed from its moisture, but retaining it carbonic acid, was first determined. Carbonic acid, artificially prepared, was then mixed with dry air in such proportions that the action of the mixture upon the rays of heat was the same as that of the dried breath. The percentage of the former being known immediately gave that of the latter. The same breath, analyzed chemically by Dr. Frankland, and physically by Mr. Barrett, gave the following results*:

Percentage of Carbonic Acid in the Human Breath

Chemical Analysis	Physical Analysis
4.66	4.56
5.33	5.22

> *It is thus proved that in the quantity of ethereal motion which it is competent to take up, we have a practical measure of the carbonic acid of the breath, and hence of the combustion going on in the human lungs.*

These measurements were made in the context of demonstrating the sensitivity of different molecules to absorb infrared radiation differently, depending upon the radiation source. Since a human's exhaled breath has a significantly higher percentage of CO_2 than the atmosphere, it

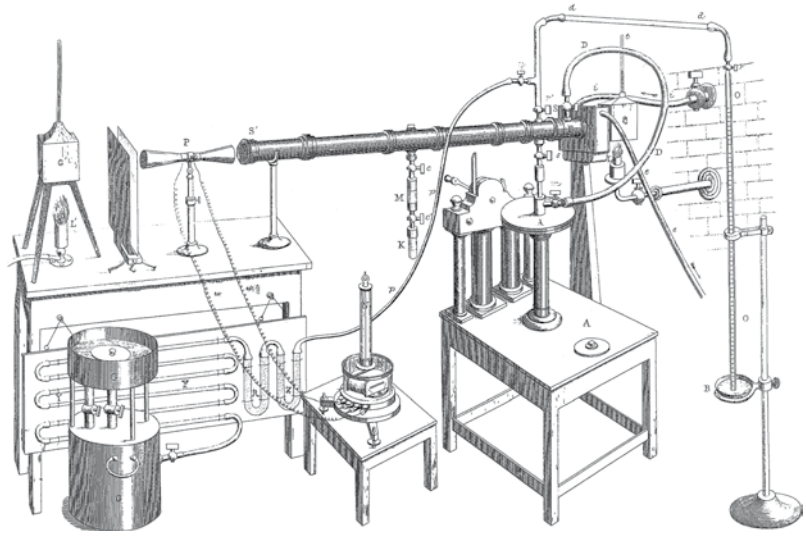

Figure 40.1 Tyndall's experimental apparatus, shown here, consisted of a long tube that he filled with various gases. The ends of the tube were capped with slabs of rock salt crystal, a substance known to be highly transparent to heat radiation. The Leslie cube was heated with a flame, and emitted radiation that traversed the tube and interacted with the gas before entering one cone of a differential thermopile. Radiation from a second Leslie cube passed through a screen and entered the other cone. The common apex of the two cones, containing the differential thermopile junction, was connected in series to a galvanometer that measured small voltage differences. The intensity of the two sources of radiation entering the two cones could be compared by measuring the deflection of the galvanometer, which is proportional to the temperature difference across the thermopile. Different gases in the tube would cause varying amounts of deflection of the galvanometer needle. If the intensity of the reference source of radiation was known, the intensity of the other source (and thus the absorptive power of the gas in the tube) could be calculated. [From: Tyndall J. *Heat: A Mode of Motion*, 6th edn. New York: D. Appleton and Co., 1890.]

provided an easy source of the gas. Given the flux at the time in understanding human metabolism, the conclusion by Tyndall – that the CO_2 in the lung is a result of the "combustion" within that organ – is understandable.

August Krogh (1874–1949), while working in the Laboratory of Medical Physiology under Professor Christian Bohr, was intrigued with problems connected with the gas exchange of the living organism. With his wife, Dr. Marie Krogh, he undertook a series of experiments and concluded – contrary to the views held at the time by Bohr and J. S. Haldane – that diffusion alone was sufficient to explain the gas exchange in the lungs. Krogh's results were later confirmed by others and have become widely accepted. Additionally, Krogh made a number of contributions to the development of physiological instrumentation, including a recording spirometer, an electromagnetic bicycle ergometer, and improved methods for gas analysis [9].

Measurement of carbon dioxide and its volume

Chemical

John Scott Haldane (1860–1936), amongst his many contributions, developed the first version of a gas analyzer that employed chemical absorption. For many years thereafter, it was considered *the* reference method for CO_2, subsequently known as the *Haldane method* [10]. The principle of Haldane's method of gas analysis was to draw a known volume of gas (10 mL) into a graduated burette by raising and lowering a reservoir of mercury held underneath. The gas was then exposed to a series of absorbents (e.g., sodium or potassium hydroxide for CO_2), and the diminution of volume was recorded while the gas was kept at a constant temperature and pressure. The volume of CO_2 in the original sample was computed as the ratio of the change in volume divided by the total volume.

Lloyd (1958) modified the Haldane apparatus and improved its accuracy to within 0.02% vol/vol [11]. However, the method was considered complex, very slow, and highly dependent upon operator skill. Campbell (1960) proposed a simpler version of Haldane's apparatus that was judged to be sufficiently accurate for clinical work [12]. Similarly, a smaller version of the Haldane apparatus was developed by Scholander (1947) which used 0.5 mL instead of 10 mL samples [13]. Apparatus for gas analysis, with gas sample sizes ranging from 35 mL to a fraction of 1 mL and accuracy of 0.005% to 2%, taking from several minutes to hours to analyze, have been described [14]. A variety

of modifications to simplify the method and account for errors, such as those due to the presence of nitrous oxide (N_2O), have been reported [15]. The Van Slyke apparatus, well known to many (by now mature) clinicians, is similar to the Haldane and Scholander apparatus, and was primarily used clinically for blood gas analysis [16].

Various investigators sought to extend these discrete chemical absorption-based measurement methods to "continuous" analysis. Rein (1933) combined the chemical method with a hot-wire flowmeter to obtain a continuous recording of gas concentration by measuring the "imbalance" between two chambers [17]; in one, the gas is absorbed and, in the other, it is not. Bezinger (1938) introduced a rubber bag with a 2–3 L capacity between the subject and measuring device to buffer peaks in flow velocity [18]. Hartmann and Braun, of Frankfurt am Main, Germany, offered a device in the 1950s that automated this analysis.

Physical

August Herman Pfund (1879–1949) developed an early gas analyzer in 1939 that was used at Johns Hopkins Hospital in Baltimore to measure CO and CO_2 [19,20]. Pfund described this thermal method of CO_2 measurement as "mak(ing) possible continuous analysis without disturbing the mixture" in contrast to chemical methods that destroy the material under testing. An electrically heated spiral of nichrome wire and silvered concave mirror served as the radiation source. The radiation passed through an absorption cell and into a detector. The detector consisted of "three bakelite rings with 36 brass studs to which thin wires of iron and constantan (a copper–nickel alloy with high electrical resistance and a low temperature coefficient) are attached to form a thermopile of 33 junctions in series." The detector cell was filled with a mixture of 3% CO_2 and 97% dry air. If no CO_2 was present in the absorption cell, the radiation would be absorbed in the detector cell, and the increase in temperature would be measured by the thermopile. The presence of CO_2 in the absorption cell would cause less radiation to be absorbed in the detector cell, and, therefore, a smaller rise in temperature.

Karl Friedrich Luft (1909–99) is often credited with developing infrared technology using a balanced condenser microphone detector consisting of sealed cells that contained pure CO_2 separated by a diaphragm. This type of detector, now known as the Luft cell, can be traced to the photoacoustic effect first observed by Alexander Graham Bell and later demonstrated by Bell at the Paris Exposition in 1880. Bell (1880) exposed a test tube containing cigar smoke to chopped sunlight – this was the photo part [21]. The test tube was connected to a hearing tube from which emanated sound – the acoustic part. The pitch of the sound waves was controlled by the frequency of the chopped sunlight. John Tyndall (1881) [22] and Wilhelm Röntgen (1881) [23] performed similar experiments after learning of Bell's discovery.

In 1937, Luft joined Badische Anilin und Soda Fabrik (BASF) where he was confronted with a measurement problem [24]. The method of fabricating plastic resulted in a highly explosive mixture of butane and air. In order to avoid the creation of such a volatile mixture, a method to measure low concentrations of butane was sought. It was observed that this chemical had strong absorption properties in the infrared band, but it was known that photometric methods of the time had failed since they were too strongly affected by interfering gases in the mixture, such as CO_2 and water vapor. Luft came up with an idea that a gas could serve as a "radiation receiver" and, as such, might have the necessary selectivity required. He discussed this possibility with Lehrer who had just successfully developed a recording infrared spectrophotometer. This discussion led to their collaboration and development of a device known as the URAS (ultrarot absorptions-Schreiber – infrared absorption writer). It consisted of the three main components – power supply, optics, and amplifiers – packaged in separate, off-the-shelf, electrical switching boxes that were bolted together. Despite using common components, the supply problems – that began shortly before the war – continued throughout the war. The manufacture of these detector cells was considered to be a very tedious and delicate process. In 1943, Luft's oft-referenced paper on these cells was published in *Zeitschrift für technische Physik* [25]. He and Lehrer were awarded a patent (filed in 1938) on the technology [26]. Despite all of the problems, BASF was able to manufacture several hundred units that were mostly used in I.G. Farbenindustrie chemical factories [24]. Additionally, the technique was used for environmental monitoring in submarines. A large number of manufactured devices that were moved into the salt mines were confiscated by the occupational powers and moved to the USA and England after the war [24]. At the end of 1952, Hartmann and Braun acquired the URAS trademark and license to manufacture and

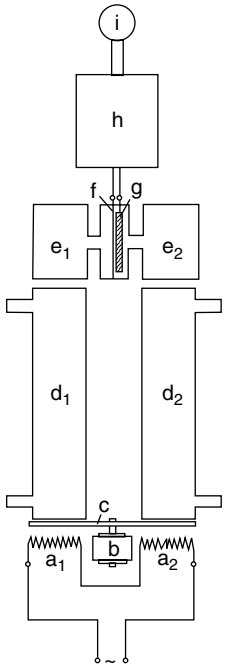

Figure 40.2 Luft's device. The radiation coming from the sources a_1 and a_2 is periodically interrupted through a shutter wheel c that is driven by motor b. The shutter wheel c has slits positioned in such a way that the radiation from both sources can pass through at the same time (or is interrupted at the same time). Behind shutter wheel c, the radiation flows through pipes d_1 and d_2, where d_1 contains the gas to be measured and d_2 is filled with a reference gas (at half atmosphere). The radiation continues its excursion and enters chambers e_1 and e_2, which contain – as a "reception layer" – the gas that is to be determined. Both chambers are separated (in an almost gas-tight fashion) from each other through a thin (metal) membrane f; this membrane forms, together with the insulated counter plate g, an electrical capacitor. If the gas mixture contains the component that is to be determined, chamber e_1 receives a weaker radiation than e_2; as a consequence, and corresponding to the interruptions by the shutter wheel c, there is a periodic pressure difference between chambers e_1 and e_2 which can – through membrane f – be transformed in changes of capacitance. The membrane capacitor is followed by an amplifier h, which allows a readout at the measuring instrument i of the capacitance variations, and thereby the concentration of the gas that is to be determined". [Translated from German, from: Lehrer E, Luft K. Verfahren zur Bestimmung von Bestandteilen in Stoffgemischen mittels Strahlungsabsorption (Process for determining the components of mixtures through radiation absorption.) Patent No. 730,478, issued January 14, 1943.]

distribute the URAS device from BASF [24]. The Luft detector is shown in Figure 40.2 and is depicted as in the original German patent. Concurrently, Veingerov (1938), while at the State Optical Institute of Leningrad under A. A. Lyebyedyev (1893–1969), built early infrared radiation detectors and optoacoustical gas analyzers to study infrared absorption in gases [27].

Concerns about the environment in the 1960s stimulated exploration of photoacoustic spectroscopy, especially when coupled with new light sources and highly sensitive microphones. The technology promised to help with the identification and quantitation of trace amounts of atmospheric pollutants. Today, further development of this technology enables the measurement of several gases simultaneously.

Just as absorption of infrared energy can increase the rotational and vibrational activity of molecules, so can absorption of visible or ultraviolet radiation. Predicted by Smekal (1923) [28] and confirmed by Raman and Krishnan (1928) [29], the phenomenon is called *Raman scattering*. Radiation scattering can occur in several ways. For example, sunrays become visible beams when airborne dust dances in their path. In this case, the particles are large compared to the wavelength of light (*Tyndall effect*). When the scattered particles are small (molecules), two kinds of scattering occur. One is an absorption–reemission phenomenon in which the wavelength does not change (*Rayleigh scattering*). Although wavelength does not change, shorter wavelengths are scattered more efficiently. These factors explain why the sky appears blue; the shorter blue wavelengths in sunlight are preferentially scattered, which increases the intensity of that wavelength as it reaches earth.

A second kind of absorption–reemission scattering can cause a wavelength change. This implies that some of the absorbed radiation is retained, increasing the amplitude of molecular vibrations. The remaining energy is remitted at a longer – or slightly shifted – wavelength (lower frequency), as is required for conservation of energy.

By definition, both the Raman and Rayleigh transitions produce scattered light, and thus, must be measured off the path of incident light, usually at right angles. The intensity is usually very low. A rule of thumb is that only 0.1% of the incident light is scattered. Of that percent, only 0.1% experiences a Raman shift; therefore, about one in a million photons is scattered with a change in wavelength. Consequently, continuous Raman monitoring requires the high photon densities obtainable from lasers and the efficient separation of the relatively high-intensity Rayleigh scattering from low-intensity Raman scattering. Early investigators used mercury vapor lamps and long exposures of fast photographic emulsions. These have given way to high-intensity coherent lasers and extremely sensitive photon detectors.

An additional method of clinical relevance used to quantify gas concentrations is mass spectroscopy. The idea of separating charged particles (ions) by their mass was first proposed and practically applied by J. J. Thompson and F. W. Aston [30], who used the technique in isotope research. The technical evolution of that idea – from a laboratory tool useful in many fields of research to a practical clinical instrument – required 50 years of experience, the prodding and support of the National Aeronautics and Space Administration (NASA), and the vision of early medical users who recognized its potential.

Researchers through the 1950s and 1960s were quick to take advantage of the mass spectrometer to measure several gases simultaneously and to explore basic questions in respiratory physiology [31]. NASA supported the development of mass spectrometry as the appropriate technique for monitoring respiratory gases, planetary atmospheres, and closed environments in outer space. In medicine, mass spectrometry was first used for monitoring patients in the intensive care unit because the gases to be monitored were relatively simple. In the operating room, detecting N_2O and CO_2 presented a problem because both gases have almost identical masses, and a mass spectrometer, with the resolving power to separate them, was considered too expensive. Measuring anesthetic vapors presented several challenges. Techniques had to be developed to accommodate the relatively large mass of the agents to spectrometers with lower mass ranges. In addition, reducing the pressure – from atmospheric to very low pressure – required for mass spectrometers was difficult. By the early 1980s, sampling and detection problems were resolved, and reliability was improved. In 1981, mass spectrometry became established as a cost-effective and reliable monitor for operating room use [32]. In recent years, the enhanced capabilities of infrared devices have challenged what was once the unique position of mass spectrometry as a multigas monitor.

Early clinical applications

John Hutchinson (1811–61) published a paper about a water spirometer and the measurements achieved with it [33]. Hutchinson recorded the vital capacities of over 4000 persons with his spirometer and classified them in such categories as "paupers," "Battalion Grenadier Guards," "pugilists and wrestlers," "giants and dwarfs," "girls," "gentlemen," and "diseased cases." He demonstrated the linear relationship of vital capacity to height, and also showed that vital capacity does not relate to weight at any given height [34]. Volume-measuring devices similar to one originally developed by Hutchinson are still in use today, with only minor alterations. However, volume was easily measured from the integration of flow, which led to the development of devices based upon the pressure drop across capillary tubes [35] and screens [36,37].

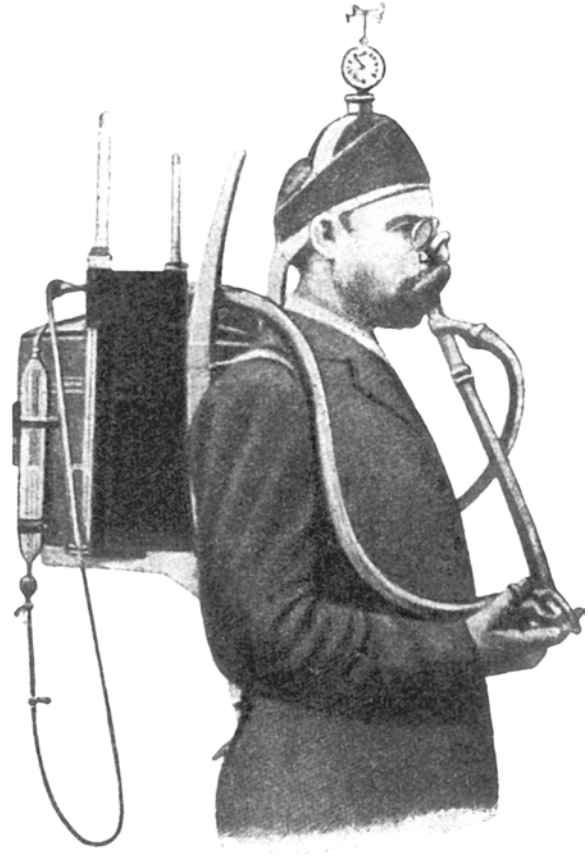

Figure 40.3 Nathan Zuntz and his portable metabolism apparatus. [From: Zuntz N, Loewy A (eds.) *Lehrbuch der Physiologie des Menschen*. Leipzig: F. C. W. Vogel, 1920.]

The first "portable" metabolism apparatus was devised by Nathan Zuntz (1847–1920) (Figure 40.3) [38,39]. In 1892, Zuntz's student, Magnus-Levy, applied this apparatus at the bedside, and embarked on pioneering investigations of metabolism in patients with a variety of medical conditions, including myxedema, hyperthyroidism, obesity, and pregnancy [40].

Since the early 1900s, gas exchange was most often clinically measured by either the "gold standard," the Douglas bag method [41], or with the Tissot spirometer [42]. In fact, it was noted that Douglas, as part of the preparations for an expedition to Pike's Peak in

Colorado, developed the bag method for collection of expired gases [43]. The Douglas bag required the collection of exhaled air in large, impermeable 50-L canvas bags, and subsequent sampling and analysis of the collected gas to measure the mixed gas fractions and the total expired volume by manually "squeezing" the entire contents of the bag through a spirometer. Problems noted with the Douglas bag technique included faulty technique and loss of CO_2 through pores in the bag. Shepard (1955) suggested filling the bag to near capacity within 15 min to minimize loss by diffusion [44], while Balchum *et al.* (1953) recommended using synthetic bags with a lower permeability to CO_2 [45], realizing that the solubility coefficient of rubber with respect to the respiratory gases was the primary problem. With the Tissot-type spirometer, the subject breathes through a two-way respiratory valve, passing all expired gas into a calibrated cylinder, which is sealed from the outside by a water seal in a second cylinder. Ventilation is determined by recording the total volume of gas, time of collection, calibration constant, gas temperature, and barometric pressure [46].

In the 1960s, with the development of the Parkinson-Cowan dry gas meter, the measurement of inspired minute ventilation also became commonplace. The complexity and manual nature of these measurements led to the development of semi-automated methods [47]. Using this approach, the measurement of the expired mixed gas fractions was initially achieved by sampling gas from a mixing chamber into 2-L latex bags for subsequent analysis. It included drawing a continuous sample of exhaled air from a mixing chamber directly into electronic gas analyzers. The voltage output of these gas analyzers and the inspired ventilation meter was converted to digital form, and the calculations for O_2 consumption and CO_2 elimination were performed by a microcomputer. The time lag between the process of drying and the analysis of the gas and measurement of volumes made it necessary to make timing adjustments.

The concept of deadspace was first clearly elucidated by Zuntz in 1882 [48]. In 1890, Christian Bohr introduced his equation for calculating respiratory deadspace in terms of concentrations of alveolar and expired gases (Figure 40.4) [49]. Enghoff (1938) later substituted arterial values to approximate the alveolar values [50]. The earliest description in the literature of the volumetric capnogram and a method to determine "airway" deadspace is that of Aitken and Clark-Kennedy (1928) (Figure 40.5) [51]. Fowler (1948), when describing the single-breath test for nitrogen (SBT-N_2) curve, sought to use uniform terminology to clarify the

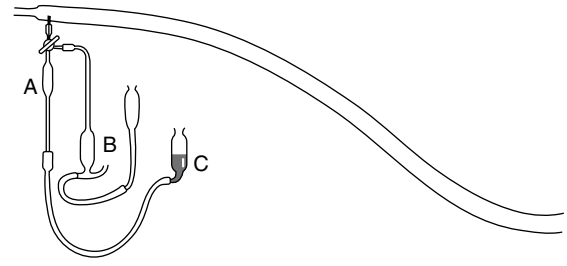

Figure 40.4 Apparatus for obtaining and analyzing alveolar air. [Reproduced with permission from: Haldane JS, Priestley JG. *Respiration*, 2nd edn. London: Oxford University Press, 1935.]

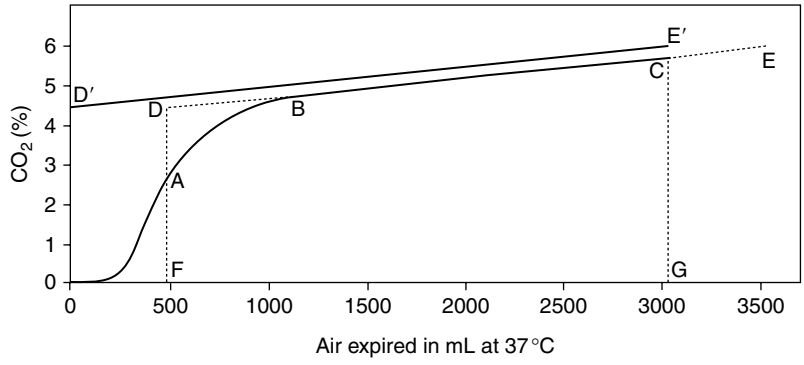

Figure 40.5 Diagram to show the method of deducing the alveolar CO_2 curve and the deadspace from the experimental CO_2 curve. The flat part BC of the experimental curve 0ABC is prolonged to the left to D until the area FDCG equals the area 0ABCG, DF and CG being perpendicular to 0G. 0F then represents the volume of the deadspace. DC is prolonged to the right to E, over a distance equal to 0F (when measured horizontally). The whole line DE then represents the changing concentration of alveolar CO_2 throughout expiration. [Reproduced with permission from: Aitken RS, Clark-Kennedy AE. On the fluctuation in the composition of the alveolar air during the respiratory cycle in muscular capacity. *J Physiol* 1928; **65**: 389–411.]

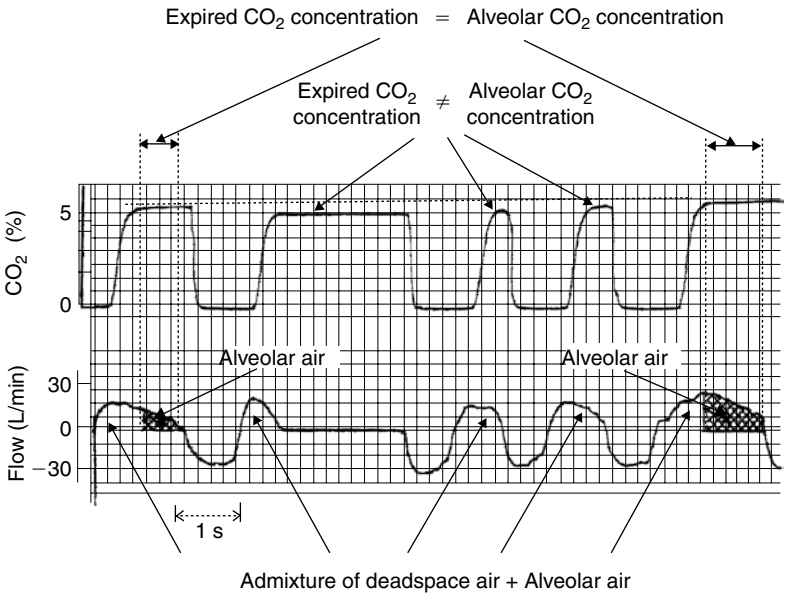

Figure 40.6 Simultaneous CO_2 and flow curve showing criteria for reading alveolar concentration of CO_2 from recorded plateau. [Reproduced with permission from: Elam JA, Brown EL, Ten Pas RH. Carbon dioxide homeostasis during anesthesia. I. Instrumentation. *Anesthesiology* 1955; **16**: 876–85.]

meaning of deadspace, and thus divided this curve into four phases: I, II, III, and IV [52]. Fowler wanted to better understand the magnitude and constancy of deadspace. Krogh and Lindhard (1913) measured deadspace and found it to vary over a narrow range (confirmed by others) [53], whereas Haldane and Priestley suggested that deadspace might increase as much as 800 mL during a maximal inflation.

Krogh (1923) developed an improved kymographic method using a spirometer chamber with CO_2 and moisture absorbents [54]. Krogh recognized that the tables for estimating basal metabolism advanced by Harris and Benedict (1919) had "nothing to do with the biological laws which must be supposed to govern the relations between the metabolism and sex, weight, height, and age, respectively" [55]. Instead, he suggested using actual measurements of metabolism, such as are still practiced today.

Different methods to sample "alveolar" CO_2 gas were developed [56], including single breath methods requiring forced expirations at the end of a normal expiration or inspiration, the collection of gas for analysis, and multiple-breath methods. Continuous analysis permitted gas from "a single expiration to be 'fractionated' into many successive samples" [56]. It was recognized that continuous analysis was relevant to the measurement of intrapulmonary gas mixing and ventilation–perfusion relationship [56], and is "enhanced by simultaneous analysis of gas volumes," but that these instruments "are rather complex and are not generally available" [56].

Elam and colleagues, while working on the problem of CO_2 elimination from closed circuit anesthesia systems under US Army support, published early pioneering work in the field. They were first to publish capnographic profiles of human respiration in the anesthesiology literature [57,58]. Their work on CO_2 homeostasis, published in a series of four papers [59–62], included both normal and abnormal characteristics of the capnographic profile and measurements of deadspace and alveolar ventilation. "As part of this work, Elam built a machine to 'mimic' human respiration, which resulted in an early prototype of a ventilator that worked in either volume or pressure modes" (Figure 40.6) [57]. Additionally, the advent of commercial air travel with pressurized passenger compartments propelled the development of technology to measure CO_2 [63].

Smalhout (1967) [64] and Smalhout and Kalenda (1981) [65] popularized the use of the terms, *capnography*, *capnograph*, and *capnogram*. The publication of their atlas of strip chart recordings of capnograms helped to illustrate many of the applications of capnography [65].[3] However, they noted that this "represent(ed) little more than the surface of a deep pool." (For an account of the early days of time

[3] Termed *infrared CO_2 meters* from the 1950s and into the early 1970s, the term capnograph was derived from the Godart Capnograph.

capnography, see Chapter 41: The first years of clinical capnography.) Weingarten (1990) [66] summarized their contributions by noting that:

> Under their direction, capnography survived a stormy gestational period as it reached maturity in The Netherlands. It was introduced in the US at a small private meeting sponsored by a major instrument manufacturer held in conjunction with the World Congress on Intensive Care Medicine in Washington DC, in May 1978. Five anesthesiologists attended the meeting, two of whom concluded that capnography would prove to be of very little value.

While single breath curves for CO_2 appeared as early as 1961 in the literature [67], it was not until the 1980s that Fletcher – in his doctoral thesis (1980) [68] and later in various publications [69] – presented the concepts of deadspace and CO_2 elimination in a unified framework. His presentation became widely known as the SBT or single breath CO_2 ($SBCO_2$) curve (i.e., the expiratory portion of the volumetric capnogram). (For an account of the early days of volumetric capnography, see Chapter 42: The early days of volumetric capnography.) Also recommended are the contributions of J. S. Gravenstein who, in the first and second editions of *Capnography in Clinical Practice* published in 1989 [70] and 1995 [71], respectively, and in the first edition of this book (2004) [72], summarized the state of the art at the time and helped to further popularize the use of capnography.

Commercial capnography – time and volumetric

Rapidly responding, point-of-care CO_2 analyzers were originally developed for medical use in response to needs expressed by clinicians of the day as part of an effort to understand a problem or so that therapy (e.g., mechanical ventilation) could be more optimally delivered. Mainstream infrared CO_2 analyzers (also termed non-diverting and breathe-through) were introduced in the early 1950s. However, these early devices were physically large and cumbersome to use, and thus were considered impractical for clinical use. Later advancements in both mainstream and sidestream devices were primarily driven by developments in technology. These advancements decreased the size of these devices to allow their incorporation in clinical monitors and address the known technological and related ease-of-use weaknesses of the early devices that limited their clinical application.

A review of the commercialization of infrared CO_2 devices would be incomplete without a discussion of the contributions of Max Liston [73]. In 1950, Max Liston founded the Liston–Becker Company. The early devices included breathe-through (i.e., mainstream) analyzers; the principal products were sidestream sampling, non-dispersive infrared (NDIR) analyzers [74], including Models 16, 28, and 30. Max Liston discusses the transition to sidestream sampling, and how the use of his CO_2 analyzer helped improve the management of patients being ventilated with iron lungs, and thereby reduced mortality:

> *The objection to breathe-through system that we had was the instrument was so large and that it obscured the anesthetist's view of the face that they relied on – color, facial reactions during the surgery – so they objected to that – as far as the surgical application goes. Catheter sampling came as the result of the work of Affeldt and Farr at Rancho Los Amigos in Downey, California. They were working on the polio situation – the mask not suitable – so we developed the catheter approach for them which became the preferred method of sampling* [75]. *In the-mid 1950 they published a very favorable report which noted that the time on Drinker respirators [76] dropped in half after using that [device] to adjust their respirators – the fatality rate dropped by 30% on polio subjects – equipped all 7 of the polio foundation bulbar polio centers with the model 16. (Max Liston, personal communication, 2004)*

The Liston–Becker gas analyzer and its successor designs consisted of a "pickup" unit and "control" unit. The pickup unit, located near the patient's head, was sealed, and could be pressurized with up to 5 lbs (2.25 kg) of air pressure to make it safe for use with explosive anesthetic gas mixtures [77]. This company had already developed a capacitance-based photometer for measuring CO_2 and other heteroatomic gases. The instruments were adapted for medical use, and were also installed on American and NATO nuclear submarines to monitor internal atmospheric CO_2 levels. In 1955, Beckman Instruments acquired the Liston–Becker Company. Beckman Instruments continued the development of NDIR gas analyzers, with Max Liston remaining as director of engineering until 1965. Representative Beckman capnographs included the Beckman Model LB-1 (Figure 40.7) and Beckman LB-2 analyzers.[4]

[4] Beckman Model LB-1, originally marketed by the Spinco (centrifuge) division in Palo Alto, CA, eventually ended up with the advanced technology operations (ATO) division in Anaheim, CA, which was primarily responsible for government contracts, including placing the technology on-board the US nuclear submarine fleet. The ATO divisions focus changed and, in the 1970s, became the physiological measurement operations (PMO) division which was divested by the company shortly after its acquisition by SmithKline in 1982, and became a separate company named Sensormedics. The LB-1 was originally

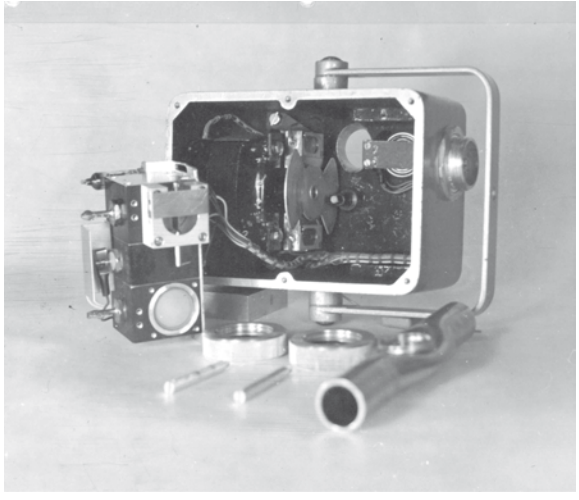

Figure 40.7 Beckman LB-1 sensor head with detector assembly removed. Chopper visible in center of photo.

Representative systems using the Luft detector included the Hartmann and Braun URAS series of instruments, and Godart capnographs (Table 40.1) [78], a modification of the URAS 4 [6]. These systems were widely used for CO_2 measurement in the 1960s and 1970s [79].

In the early 1970s, exercise researchers developed their own systems to automate the tedious steps associated with Douglas bags. This led to the development of commercial metabolic carts with first- and second-generation mixing chambers based on the Beckman metabolic measurement cart (MMC). It used a Monroe calculator for computation and printout [80], and a Beckman MMC Horizon System with an Intel 8085 microprocessor containing 64 Kb of memory, with two floppy disk drives for program and data storage [81]. Sidestream gas was sampled from the mixing chamber and measured by an infrared CO_2 analyzer (Beckman LB-2 head) and polarographic O_2 analyzer (Beckman OM-11 bench). Flow was measured at the exit port of the mixing chamber with a turbine flowmeter. Rates of CO_2 elimination and O_2 consumption were determined using the Haldane equation, which assumes a net N_2 change of zero. While initially developed for studies of exercise physiology, these devices were later adapted for bedside nutritional studies. Macfarlane (2001) published an extensive review of the devices for exercise [82].

In 1988, a Raman scattering instrument was introduced for clinical use. The RAman SCattering AnaLyzer (RASCAL) monitor was originally developed by a group of researchers from the University of Utah who formed a medical instrumentation company (Albion Instruments) to commercialize laser-based Raman scattering technology. This company was subsequently bought by Ohmeda (Louisville, CO). Both the RASCAL and its successor, RASCAL II, monitors were online sidestream monitors for O_2, CO_2, N_2, N_2O, and the three anesthetic vapors: halothane, enflurane, and isoflurane [83]. It used eight discrete optical channels to both identify and quantitate these gases. Each channel employed collection optics to gather the scattered radiation, a rejection filter to eliminate the unshifted Rayleigh light, a Raman line filter, and a narrow band-pass dielectric interference filter which isolated the waveband intensity that quantitated the gas. A photomultiplier tube monitored radiation intensities. This device is no longer marketed.

Early mainstream infrared devices (as those used by Elam) were physically large, cumbersome, and impractical for clinical use. Advancements in both mainstream and sidestream technology decreased the size of these devices to allow their inclusion in clinical monitors. However, it was not until the introduction in the 1970s of devices such as the Hewlett-Packard 47210A (Figure 40.8) [84,85] and Siemens-Elema Model 930 [86] that mainstream devices began to be used in the clinical environment. The Hewlett-Packard device is one of the technologies developed for automotive applications and adapted for medical use [87]. Its airway adapter consisted of a hollow aluminum casting with sapphire windows. The sensor comprised an infrared source (heated broadband black body radiator) and a detector assembly consisting of a rotating filter wheel, a band-pass filter, and a lead–selenide detector. Siemens-Elema introduced a mainstream CO_2 sensor add-on for the Servo 900 series of ventilators: the CO_2 Analyzer 930 (Figure 40.9). Their design used a slightly different approach than Hewlett-Packard: a single detector with a filter specific for CO_2 and a chopper on the detector side. It interfaced with the ventilator, combined the measurements of flow and CO_2, and measured "CO_2 tidal production" in addition to end-tidal CO_2. It

intended for use in operating rooms in which ether and cyclopropane were commonly used anesthetics. This accounts for the separation of the sample head from the rest of the instrument. The head was pressurized (with a bicycle pump) to avoid any in-leakage of ambient gases, and included a pressure switch which disabled power to the head if the pressure dropped. The LB-1 was sold with a separate sample pump, which was also to be used outside the operating room. (Allen Norton, 2003, personal communication.)

Table 40.1 Representative commercial infrared CO_2 analyzers used clinically, from 1950s through present

Manufacturer (location)	Model[a]	Features of interest
	1950s, 1960s, and 1970s	
Hartmann and Braun (Frankfurt, Germany)	URAS 1	Sidestream, Luft cell detector
Liston–Becker (Springdale, CT)	16	Total sampling (i.e., mainstream) using 7/8-inch tubing with 90% response time of 50 ms
Godart-Statham (Utrecht, Holland)	Capnograph Mark I	Sidestream, Luft cell detector, sampling rate 0.25–3 L/min
Beckman Instruments[b] (Pasadena, CA)	LB-1, LB-2, LB-3	Sidestream, different detectors for CO_2, halothane, and N_2O
	1980s	
Hewlett-Packard (Waltham, MA)	M14360A	Mainstream, solid-state source, chopper wheel on detector
Siemens-Elema (Solna, Sweden)	Model 930	Mainstream integrated with 900 series ventilators
Criticare Systems (Waukesha, WI)	Poet®	Sidestream
Cascadia Technology Corporation.[c] (Redmond, WA)	Capnostat®	Mainstream, all solid-state design with thick film source
	1990s	
Andros Analyzers (Berkeley, CA)	Breathwatch™ Model 4210	Mainstream design with IR lamp source
BCI (Waukesha, WI)	Capnocheck®	Sidestream
	Model 8200	
Novametrix Medical Systems (Wallingford, CA)	Capnostat® II, III	Mainstream, smaller versions of previous generations
Pryon Corporation[d] (Menomonee Falls, WI)	SC-300	Mainstream, all solid-state design
Oridion Systems (Needham, MA/Jerusalem, Israel)	MicroCap®	Low-flow sidestream (50 mL/min)
	2000s	
Respironics-Novametrix[e] (Wallingford, CA)	LoFlo™	Low-flow sidestream (50 mL/min), sample cell part of sample set
Respironics-Novametrix (Wallingford, CA)	Capnostat®5	Mainstream, all signal processing in on-airway sensor head

[a] Model name may list either the monitor name or sensor name (if mainstream), also ordering within decades approximate to year of product introduction. Trademarks are property of their respective owners.
[b] In 1950, National Technical Laboratories, Pasadena, CA was changed to Beckman Instruments.
[c] Acquired by Novametrix Medical Systems, Inc.
[d] Acquired by Protocol Systems and Protocol acquired by Welch-Allyn.
[e] Acquired by Philips Healthcare.
Sources include: *Medical Electronics* (various years), medical literature, and company product literature.

introduced in a commercial product the concepts of both effective and ineffective ventilation.

Innovations in mainstream gas sensors of the late 1980s [87] eliminated the mechanical chopper of earlier designs, resulting in smaller, more robust mainstream CO_2 sensors, including pulsed thick film infrared sources [88], and increased its robustness by the use of a coaxial optical design [89].

In the early 1990s, volumetric capnography sensors appeared, which combined mainstream flow and CO_2 into an integrated airway adapter [90], as well as combining mainstream flow and sidestream CO_2 sensors

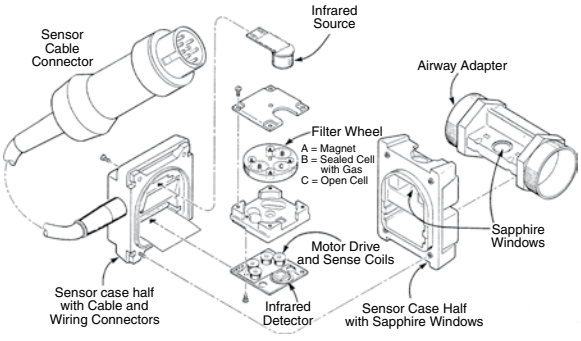

Figure 40.8 "Exploded" view of the assembly for the 14360A sensor. [From: Solomon RJ. A reliable, accurate CO_2 analyzer for medical use. *Hewlett-Packard J* 1981; **32**: 3–21. Copyright (1981), Courtesy of Hewlett-Packard Development Company, L.P.]

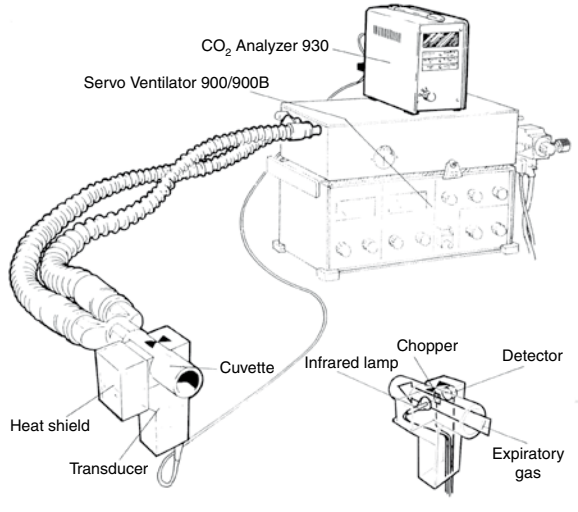

Figure 40.9 CO_2 Analyzer 930 with Servo Ventilator 900. [Reproduced with permission from: CO_2 Analyzer – Model 930 Manual, 1981. Copyright (1981), MAQUET Critical Care AB.]

[91]. Technological advances in sidestream systems continue, with newer source designs [92] and novel configurations with removable sample cells [93], as well as mainstream designs that incorporate digital signal processors and miniaturized optics. Future technological improvements promise even greater robustness, adaptability, and performance.

References

1. Lavoisier A. *Oeuvres de Lavoisier*, vol. 2, *Mémoires de chimie et de physique*. Paris: Imprimerie Imperiale, 1862.
2. Boyle R. *New Experiments Physico-Mechanical, Touching the Spring of the Air and Its Effects*. Oxford, 1660.
3. Herschel W. Investigation of the powers of the prismatic colours to heat and illuminate objects. *Phil Trans R Soc London*1800; **90**: 255–83.
4. Gillispie CC (ed.) *Dictionary of Scientific Biography*. New York: Macmillan, 1980.
5. Lambert JH. *Photometria sive de Mensura et Gradibus Luminis, Colorum et Umbrae*. Augsbourg: Widow of E. Klett, 1760.
6. Cormack R, Powell JN. Improving the performance of the infra-red carbon dioxide meter. *Br J Anaesth* 1972; **44**: 131–41.
7. Burchfield JA. John Tyndall: a biographical sketch. In: *John Tyndall, Essays on a Natural Philosopher*. Dublin: Royal Dublin Society, 1981.
8. Tyndall J. On radiation. The "Rede" Lecture delivered in the Senate House before the University of Cambridge on Tuesday, May 16. London: Longman, Green, Longman, Roberts, 1865.
9. Rehlberg PB. August Krogh. *Yale J Biol Med* 1951; **24**: 83–102.
10. Haldane JS. *Methods of Air Analysis*. London: Griffin, 1912.
11. Lloyd BB. A development of Haldane's gas analysis apparatus. *J Physiol* 1958; **143:** 5–6.
12. Campbell EJM. Simplification of Haldane's apparatus for measuring CO_2 concentration in respired gases in clinical practice. *Br Med J* 1960; **1**: 457–8.
13. Scholander PF. Analyzer for accurate estimation of respiratory gases in one-half cubic centimeter samples. *J Biol Chem* 1947; **167**: 235–50.
14. Comroe JH Jr. V measurements of composition of respired gases. In: *Methods in Medical Research*, vol. 2. Chicago, IL: Year Book Publishers, 1950; 122–31.
15. Nunn JF. Respiratory measurements in the presence of nitrous oxide. *Br J Anaesth* 1958; **30**: 254–63.
16. Van Slyke DD, O'Neill JM. The determination of gases in blood and other solutions by vacuum extraction and manometric measurement. *J Biol Chem* 1924; **61**: 523–9.
17. Rein H. Gas exchange recorder: Attempts at continuous registration of respiratory gas exchange in man and animals. *Arch Exp Pathol Pharmkol* 1933; **171**: 363.
18. Bezinger T. Untersuchungen über die Atmung und den Gasstoffwechel, insbesondere bei Suerstoffmangel und unterdruck, mit fortlaufend unmittelbar aufzeichnenden Methoden. (Studies on respiration and gas exchange with continuous direct recording methods.) *Ergebn Physiol* 1938; **40**: 1–52.
19. Pfund AH. Apparatus for detecting and measuring heteroatomic gases. US Patent 2,212,211, issued August 20, 1940.

20. Pfund AH, Gemmill CL. An infrared absorption method for the quantitative analysis of respiratory and other gases. *Bull Johns Hopkins Hosp* 1940; **67**: 61–5.
21. Bell AG. Upon the production of sound by radiant energy. *Am J Sci* 1880; **20**: 305–24.
22. Tyndall J. Action of an intermittent beam of radiant light upon gaseous matter. *Proc Soc London* 1881; **31**: 307–17.
23. Röntgen WC. Über Tone, welche durch intermittirende Bestralung eines Gases entstechen. *Ann Physik Chemie* 1881; **12**: 155–9.
24. Luft KF, Schaefer W, Wiegleb G. 50 Jahre NDIR-Gasanalyse. (50 years of NDIR gas analysis.) *Tm Technisches Messen* 1993; **60**: 363–71.
25. Luft K. Über eine neue Methode der registrierenden Gasanalyse mit Hilfe der Absorption ultraroter Strahlen ohne spektrale Zerlegung. *Z Techn Phys* 1943; **24**: 97–104.
26. Lehrer E, Luft K. Verfahren zur Bestimmung von Bestandteilen in Stoffgemischen mittels Strahlungsabsorption. Patentschrift. (Process for determining the components of mixtures through radiation absorption.) Patent No. 730,478, issued January 14, 1943.
27. Veingerov ML. Eine Methode der Gasanalyse beruhend auf dem optisch-akustischen Tyndall-Röntgeneffekt. *Dokl Akad Nauk SSSR* 1938; **19**: 687–8.
28. Smekal A. On the quantum theory of dispersion. *Naturwiss* 1923; **11**: 873.
29. Raman CV, Krishnan KS. A new type of secondary radiation. *Nature* 1928; **121**: 501.
30. Hill NC. *Introduction to Mass Spectrometry*. London: Jeyden, 1966.
31. Fowler KT. The respiratory mass spectrometer. *Phys Med Biol* 1969; **14**: 185–99.
32. Ozanne GM, Young WG, Mazzei WJ, Severinghaus JW. Multi-patient anesthetic mass spectrometry: rapid analysis of data stored in long catheters. *Anesthesiology* 1981; **55**: 62–70.
33. Hutchinson J. On the capacity of the lungs, and on the respiratory functions, with a view of establishing a precise and easy method of detecting disease by the spirometer. *Medico-Chirurg Trans (London)* 1846; **29**: 137–61.
34. Petty TL. John Hutchinson's mysterious machine revisited. *Chest* 2002; **121**: 219S–23S.
35. Fleisch A. Pneumotachograph: apparatus for recording respiratory flow. *Arch Ges Physiol* 1925; **209**: 713–22.
36. Silverman L. Respiratory air flow characteristics and their relation to certain lung conditions occurring in industry. *J Indust Hyg Toxicol* 1946; **28**: 183.
37. Lilly JC. Flow meter for recording respiratory flow of human subjects. *Methods in Medical Research*, vol. 2. Chicago, IL: Year Book Publishers, 1950; 113–21.
38. Zuntz N, Loewy A (eds.) *Lehrbuch der Physiologie des Menschen*. Leipzig: F. C. W. Vogel, 1920.
39. Fenn W, Rahn H. *Handbook of Physiology*, Section 3, *Respiration*, vol. 1. Washington, DC: American Physiological Society, 1964.
40. Lusk G. *Nutrition, Clio Medica Series no. 10*. New York: Hoeber, 1933.
41. Douglas CG. A method for determining the total respiratory exchange in man. *Proc Phys Soc* 1911; **18**: 17–18.
42. Tissot J. Nouvelle méthode de mesure et d'inscription du débit et des mouvements respiratoires de l'homme et des animaux. *J Physiol Pathol Gén* 1904; **6**: 688–700.
43. Douglas CG, Haldane JBS, Henderson Y, Schneider EC. Physiological observations made on Pike's Peak, Colorado, with special reference to adaptation to low barometric pressures. *Phil Trans R Soc London* B 1913; **203**: 185–318.
44. Shepard RJ. A critical examination of the Douglas bag technique. *J Physiol* 1955; **127**: 515–24.
45. Balchum OJ, Hartman SA, Slonim NB, Dressler SH, Ravin A. The permeability of the Douglas type bag to respiratory gases. *J Lab Clin Med* 1953; **41**: 268–80.
46. Consolazio CF, Johnson RE, Pecora LJ. *Physiological Measurements of Metabolic Functions in Man*. New York: McGraw-Hill, 1963.
47. Wilmore JH, Costill DL. Semiautomated systems approach to the assessment of oxygen uptake during exercise. *J Appl Physiol* 1974; **36**: 618–20.
48. Haldane JS, Priestley JG. *Respiration,* 2nd edn. London: Oxford University Press, 1935.
49. Bohr C. Über die Lungenathmung. *Skand Arch Physiol* 1891; **2**: 236–68.
50. Enghoff H. Volumen inefficax: Bemerkungen zur Frage des schädlichen Raumes. *Upsala Läkareforen Förhandl* 1938; **44**: 191–218.
51. Aitken RS, Clark-Kennedy AE. On the fluctuation in the composition of the alveolar air during the respiratory cycle in muscular capacity. *J Physiol* 1928; **65**: 389–411.
52. Fowler WS. Lung function studies. II. The respiratory deadspace. *Am J Physiol* 1948; **154**: 405.
53. Krogh A, Lindhard J. The volume of the "deadspace" in breathing. *J Physiol* 1913; **47**: 30–44.
54. Krogh A. Determination of standard (basal) metabolism of patients by a recording apparatus. *Boston Med Surg J* 1923; **189**: 313–17.

55. Harris JA, Benedict FG. *A Biometric Study of Basal Metabolism in Man*. Washington, DC: Institution, Carnegie, 1919.
56. Fowler WS, Comroe JH Jr. Alveolar gas. In: *Methods in Medical Research*, vol. 2. Chicago, IL: Year Book Publishers, 1950; 219–26.
57. Peppriell JE, Bacon DR, Lema MJ, Ament R, Yearley CK. The development of academic anesthesiology at the Roswell Park Memorial Institute: James O. Elam, MD, and Elwyn L. Brown, MD. *Anesth Analg* 1991; **72**: 538–45.
58. Sands RP, Bacon DR. An inventive mind: the career of James O. Elam, M.D. *Anesthesiology* 1998; **88**: 1107–12.
59. Elam JA, Brown EL. Carbon dioxide homeostasis during anesthesia. II. Total sampling for determination of deadspace, alveolar ventilation, and carbon dioxide output. *Anesthesiology* 1955; **16**: 886–902.
60. Elam JA, Brown EL. Carbon dioxide homeostasis during anesthesia. III. Ventilation and carbon dioxide elimination. *Anesthesiology* 1956; **17**: 116–28.
61. Elam JA, Brown EL. Carbon dioxide homeostasis during anesthesia. IV. An evaluation of the partial rebreathing system. *Anesthesiology* 1956; **17**: 129–34.
62. Elam JA, Brown EL, Ten Pas RH. Carbon dioxide homeostasis during anesthesia. I. Instrumentation. *Anesthesiology* 1955; **16**: 876–85.
63. Clamans HG. Continuous recording of oxygen, carbon dioxide and other gases in sealed cabins. *J Aviat Med* 1952; **23**: 330–3.
64. Smalhout B. Capnografie. Ph.D. thesis, University of Utrecht, The Netherlands. (Published by Oosthoek Publishing Co., Utrecht, the Netherlands, 1967.)
65. Smalhout B, Kalenda Z. *An Atlas of Capnography*, 2nd edn. The Netherlands: Kerckebosche Zeist, 1981; 163.
66. Weingarten M. Respiratory monitoring of carbon dioxide and oxygen: a ten-year perspective. *J Clin Monit* 1990; **6**: 217–25.
67. Berengo A, Cutillo A. Single breath analysis of carbon dioxide records. *J Appl Physiol* 1961; **16**: 522–30.
68. Fletcher R. The single breath test for carbon dioxide. Ph.D. thesis. University of Lund, Sweden, 1980.
69. Fletcher R, Jonson B. Deadspace and the single breath test for carbon dioxide during anesthesia and artificial ventilation. *Br J Anaesth* 1984; **56**: 109–19.
70. Gravenstein JS, Paulus DA, Hayes TJ. *Capnography in Clinical Practice*. London: Butterworth-Heinemann, 1989.
71. Gravenstein JS, Paulus DA, Hayes TJ. *Gas Monitoring in Clinical Practice*, 2nd edn. London: Butterworth-Heinemann, 1995.
72. Gravenstein JS, Jaffe MB, Paulus DA (eds.) *Capnography: Clinical Aspects*. Cambridge UK: Cambridge University Press, 2004.
73. Liston MD. Interviews by David C. Brock and Gerald E. Gallwas at Irvine, California and Fullerton, California, February 19, 2002 and January 22, 2003. (Published by Chemical Heritage Foundation, Philadelphia, PA, Oral History Transcript 0252).
74. Liston MD. Apparatus for the analyzation of mixtures. US Patent 2,698,390, issued December 28, 1954.
75. Crane MG, Affeldt JE, Austin E, Bower AG. Alveolar carbon dioxide levels in acute poliomyelitis. *J Appl Physiol* 1956; **9**: 11–18.
76. Drinker F, Shaw LA. An apparatus for the prolonged administration of artificial ventilation. *J Clin Invest* 1929; **7:** 229–47.
77. Siebecker KL, Mendenhall JT, Emanuel DA. Carbon dioxide in anesthetic atmospheres as measured by the Liston-Becker (infra-red absorption) gas analyzer. *J Thorac Surg* 1954; **27**: 468–76.
78. Blackburn JP, Williams TR. Evaluation of the Datex CD-101 and Godart Capnograph Mark II infra-red carbon dioxide analysers. *Br J Anaesth* 1980; **52**: 551–5.
79. Hill DW, Powell T. *Non-Dispersive Infra-Red Gas Analysis in Science, Medicine, and Industry*. New York: Plenum Press, 1968.
80. Beckman Instruments. *Beckman MMC: Operating Instructions – Physiological Measurements Operations*, 2nd edn. Anaheim, CA: Beckman Instruments,1981.
81. Beckman Instruments. *Beckman MMC: Horizon Systems Operating Instructions – Physiological Measurements Operations*. Anaheim, CA: Beckman Instruments, 1983.
82. Macfarlane DJ. Automated metabolic gas analysis systems. *Sports Med* 2001; **31**: 841–61.
83. Westenskow DR, Smith KW, Coleman DL, Gregonis DE, VanWagenen RA. Clinical evaluation of a Raman scattering multiple gas analyzer for the operating room. *Anesthesiology* 1989; **70**: 350–5.
84. Solomon RJ. A reliable, accurate CO_2 analyzer for medical use. *Hewlett-Packard J* 1981; **32**: 3–21.
85. Kinsella SM. Assessment of the Hewlett-Packard HP47210A capnometer. *Br J Anaesth* 1985; **57**: 919–23.
86. Siemens-Elema. *CO_2 Analyzer 930: Operating Manual,* 2nd edn. Solna, Sweden: Siemens-Elema AB Ventilator Division, S-17195, 1981.
87. Jaffe MB. Infrared measurement of carbon dioxide in the human breath: "breathe-through" devices from Tyndall to the present day. *Anesth Analg* 2008;**107:** 890–904.

88. Knodle D, Graham PK, Labuda LL. Infrared source. US Patent 5,369,277, issued November 29, 1994.
89. Knodle DW, Mace LE, Labuda LL. Gas analyzers. US Patent 4,914,720, issued April 3, 1990.
90. Kofoed SA, Orr JA, Rich DR. Multiple function airway adapter. US Patent 5,789,660, issued August 4, 1998.
91. Merilainen PT, Eskelinen K, Hanninen HE. Gas flow restricting and directing device intended for flow measurement. US Patent 5,088,332, issued February 18, 1992.
92. Rosenfeld EZ, Boasson H. Gas analyzer and a source of IR radiation therefor. US Patent 4,755,675, issued 5 July, 1988.
93. Rich DR, Pierry AT, Fudge BM, Sandor JL, Triunfo J. A side-stream gas sampling system with detachable sample cell. Patent Cooperation Treaty Publication, 60/370,002, issued October 16, 2003.

Section 6
Chapter
41

Historical perspectives

The first years of clinical capnography

B. Smalhout

Introduction

The clinical use of capnography had its beginning in World War II. The German Navy had excellent submarines, which could remain submerged for long periods of time. There was oxygen enough on board, but the problem was getting rid of the enormous quantities of carbon dioxide produced by the crew. Each submarine was equipped with CO_2 absorbers, but their capacity was limited. An average crew of 60 men produced, in 24 h, at least 44 000 liters or nearly 10 000 US gallons of pure CO_2, making a longer stay inside the hull of the ship very uncomfortable. Enter German bioengineer, Karl Luft, who was invited to investigate this problem. Luft was already well known for his work on CO_2 detection based on infrared absorption. He had constructed a useful apparatus, named the URAS (Ultra Rot Absorptions Schreiber, translation: infrared absorption writer). At first, it was only used as a measuring device for CO_2, e.g., a capnometer. Later, a one-channel recorder was added. Henceforth, changes in CO_2 contents in the respiratory cycle could be studied online, turning the capnometer into a real capnograph.

After the war, this instrument became available for clinical use, though, at first, mainly for scientific purposes. The Netherlands was one of the first countries where the capnograph was used as a monitoring device for patients with respiratory problems. My first experience with a capnograph was in 1957, when I was working as a young medical officer in the Central Military Hospital of Utrecht, The Netherlands. A comatose soldier with severe brain trauma required artificial ventilation. At that time, no ventilators were available in the hospital, so we had to ventilate the patient manually day and night by squeezing the bag and observing the small indicator on the capnometer. The CO_2 contents of the expired gas were required to be between 4% and 5% (equivalent to 32 and 40 mm Hg). Working in eight 3-h shifts a day, we kept the soldier alive for many weeks until he recovered and resumed spontaneous respiration.

Two years later, I worked as a resident in anesthesiology at the University Hospital of Utrecht. At that time, it was already known that a relationship existed between the PCO_2 and intracranial pressure. The neurosurgical clinic had the first operating room (OR) equipped with a capnograph of the famous brand, Hartmann and Braun. This instrument was typically German-made: heavy, indestructible, but very reliable. It needed a warm-up time of about 2 h; thus, we kept the capnograph connected to the wall plug day and night. It worked faultlessly for nearly 20 years (Figure 41.1).

By means of a one-channel recorder, the Omniascriptor, mounted on top of the machine, an online capnogram could be recorded on paper tape. Two paper speeds were possible: (1) at low speed, the paper was running at 25 mm per minute; (2) at high

Figure 41.1 The first capnograph in the Central Military Hospital, Utrecht, The Netherlands (1962). On top is the one-channel Omniascriptor. [Photo: Ltn. Klunder.]

Capnography, Second Edition, ed. J. S. Gravenstein, Michael B. Jaffe, Nikolaus Gravenstein, and David A. Paulus. Published by Cambridge University Press. © Cambridge University Press 2011.

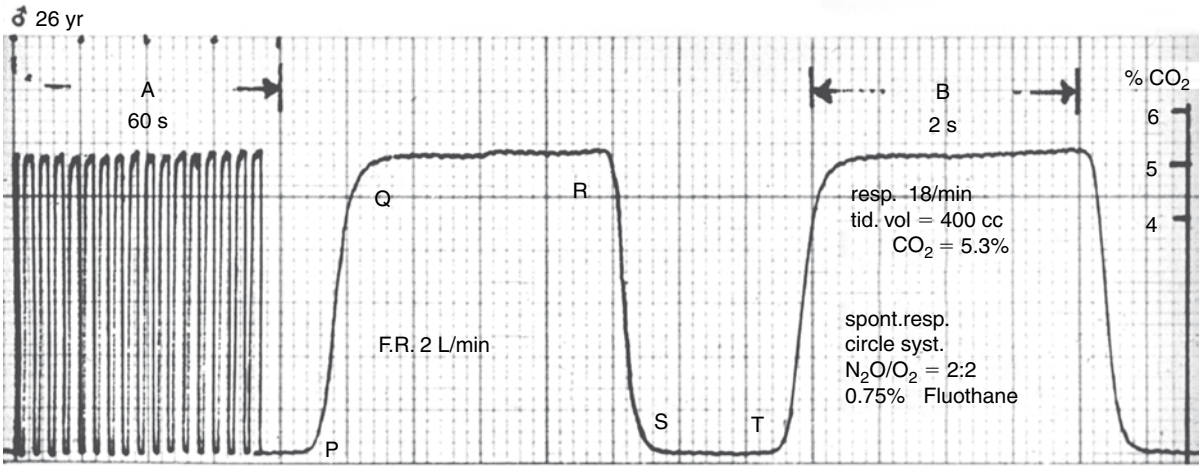

Figure 41.2 The normal capnogram, recorded on the original paper tape of the Omniascriptor (1962).

speed, it was 30 times faster: 25 mm in 2 s. The sampling flow was roughly 500 mm/min via a sidestream system. Figure 41.2 shows an example of such a recording. Every peak represents one respiration. It allows measurement of the respiratory rate by counting the peaks in 1 min. The high-speed recording on the right-hand side shows the classical shape of the capnogram, starting the expiration at P, and rapidly rising to its alveolar plateau (QR). This plateau is slightly sloping upwards to the right. From the point where the alveolar plateau reaches its highest level, the end-tidal CO_2 ($PETCO_2$) can be measured. Under optimal conditions in a patient with adequate blood circulation, patent airways, and normal lung function, the $PETCO_2$ is more or less equivalent to arterial PCO_2 ($PaCO_2$). The next inspiration begins at R. The curve drops steeply downwards, and the ST segment represents the remaining part of the inspiration. Because the inspiratory gas mixture contains practically no CO_2, the capnogram returns to zero or baseline. If this does not occur, it is probably due to rebreathing, just as occurred in the submarines studied by Karl Luft.

There is only one normal shape of the capnographic waveform, but there are many possible variations. At first, little attention was paid to these variations, and the capnograph was mainly used as a capnometer. However, once I was appointed as a neuroanesthesiologist, I operated the Omniascriptor continuously, at low speed, during every operation. Every 10 min, one or two respirations were recorded at high paper speed to study the capnographic waveform. I used about 2.5 m of paper tape per hour. Neurosurgical operations sometimes took more than 8 h; during that time, the Omniascriptor produced about 20 m of paper tape. Every respiration of the patient during the entire anesthetic and surgical procedure was documented.

During seven years, I collected and studied about 6000 capnographic recordings, with a total length of 20 km. From reviewing the paper tapes, which contained the clinical data and surgical events of the patient, I learned that there were many variations in the shape of the capnogram. Each one had clinical significance for denoting specific physiological, technical, or pathological conditions or events. These variations enabled the anesthesiologist to make diagnoses, detect discrepancies, prevent catastrophes, and enabled determination of the patient's clinical condition. In 1967, these findings resulted in a Ph.D. thesis by Smalhout [1], entitled "Capnography: its importance in diagnosis, operations and after-treatment of neurosurgical patients." It was written in Dutch, with a summary in English. In 450 pages, the interpretation of the capnographic waveform regarding dysregulation of respiration and blood circulation, and its role in monitoring neuroanesthesia, was described.

Based on this publication, *An Atlas of Capnography* [2] was published in 1975, and a second, revised edition was printed in 1981. From that year on, I presented more than 100 lectures on capnography in more than 50 cities throughout the USA and Canada. Up to that time, capnography was hardly known in North America, and, although the principles of capnography were better known in Europe, it was not routinely used in clinical practice in most hospitals in European countries. After hundreds of lectures in nearly all the European countries – from Spain to Sweden and from

Great Britain to Russia – the firm of Hewlett-Packard made it possible for me to publish a small booklet for daily use in ORs. It was printed on plastic pages, so it could be washed and cleaned if blood was spilled on the contents. The title was *A Quick Guide to Capnography and Its Use in Differential Diagnosis* [3]. This booklet was distributed all over the world, in several languages, including Japanese and Chinese.

In 1978, the Health Council of the Netherlands published an *Advisory Report on Anaesthesiology* [4] concerning all facets of this specialty. In a chapter about monitoring equipment, the routine use of a capnograph in combination with a recording device was stated as mandatory; since that report, all ORs in the Netherlands have been equipped with capnographs.

The analysis of the capnogram

The capnogram has five qualities:

(1) *Frequency*. This provides information on the respiratory rate or the frequency of the ventilation.
(2) *Maximum height* of the CO_2 wave, which indicates the $PetCO_2$.
(3) *Rhythm*, which can be seen on the slow recording. Especially with spontaneous respiration, it is important to see if the patient's breathing is regular, irregular, or periodic. Many types of irregularities are typical for a brainstem dysfunction, e.g., Cheyne–Stokes breathing. In an artificially ventilated patient, the capnogram offers perfect technical control of the ventilator.
(4) *Shape of the capnographic curve*. The waveform enables the anesthesiologist to make a differential diagnosis between a multitude of medical and technical airway problems.
(5) *Baseline*, or zeroline. The capnogram has to return to baseline after every expiration. If it does not, the patient rebreathes his/her own CO_2.

The origin of the capnogram

The expired CO_2 that is recorded as a waveform undergoes the following stages inside and outside the body:

(1) *Production*. The quantity of CO_2 produced in the body's cells varies with metabolism. If the patient is cooling down, for instance during a medical intervention, or as a result of an accident (nearly drowned in ice-cold water), the metabolism and, hence, the production of CO_2, is diminished. If ventilation remains stable, as in artificial respiration, the $PetCO_2$ decreases. On the other hand, if body temperature is rising, the level of expired CO_2 increases. By demonstrating these changes, the capnogram is the earliest warning system for malignant hyperthermia.
(2) *Transport*. Once the CO_2 is produced, it is transported to the lungs through the bloodstream. Thus, the shape of the capnogram is also dependent on the quality of the circulation. If the ventilation and body temperature are kept stable, the $PetCO_2$ closely follows the variations in blood pressure, or, rather, the perfusion. If blood pressure or perfusion is non-existent, as in cardiac arrest, then no CO_2 is transported to the lungs, and the low-speed capnogram will show a rapid washout pattern, but the efforts and effectiveness of resuscitation attempts are also immediately noted on the waveform.
(3) *Elimination*. After arriving in the lungs, the CO_2 has to be eliminated. This elimination depends on the state of the lungs, airways, the respiratory mechanism, and the limitations of the technical devices used in anesthesia and intensive care.

Capnographic possibilities

To recap, capnography enables monitoring of:

(1) Metabolism
(2) Circulation
(3) Lung perfusion
(4) Lung diffusion
(5) Position of the endotracheal (ET) tube
(6) Patency of the ET tube
(7) Quality of the spontaneous respiration
(8) Patency of the airways
(9) Functioning of the ventilator
(10) State of the connecting tubing
(11) Activity of the CO_2 absorber
(12) Effect of drugs used in anesthesia
(13) Position of the patient on the OR table.

Examples of all these possibilities follow.

The capnograph as a monitor of metabolism

If a patient is cooling down, the metabolism will be lower than normal. If such a patient is ventilated with a respiratory minute volume according to his/her age or weight, he/she will certainly be hyperventilated,

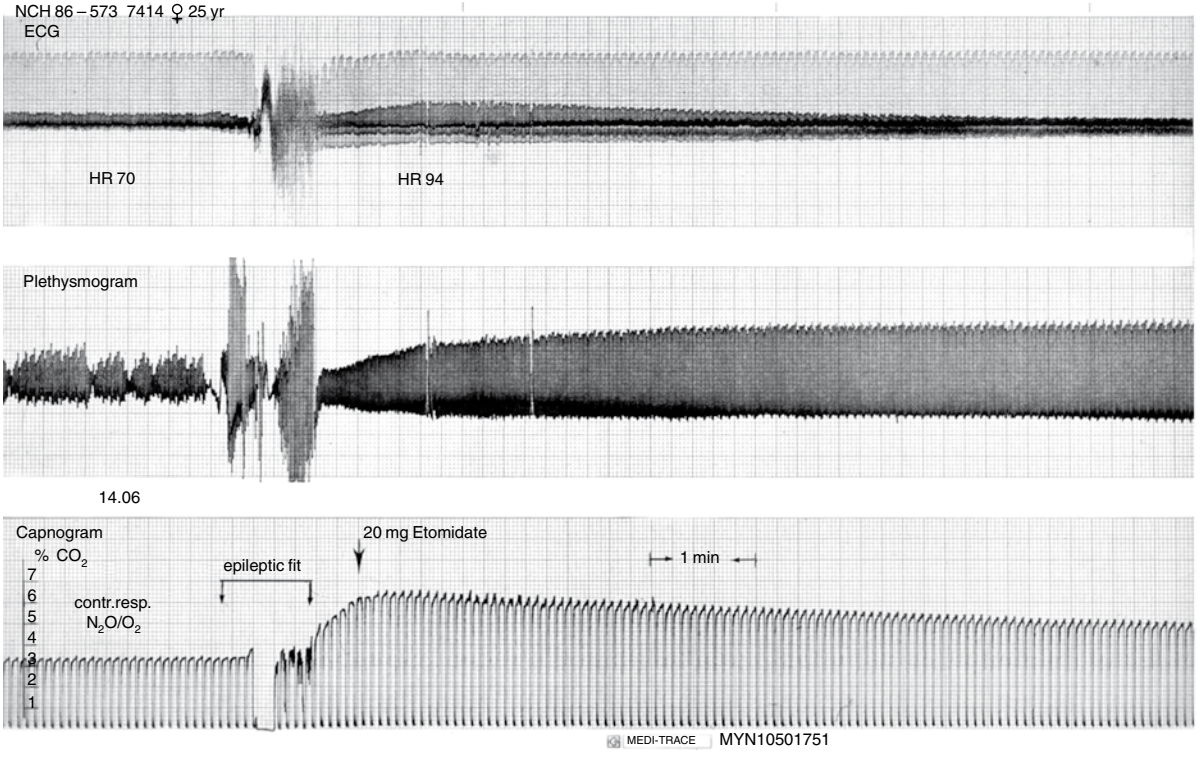

Figure 41.3 Electrocardiogram (ECG), plethysmogram (taken from a fingertip), and capnogram during an epileptic fit (1980). Paper speed, 25 mm/min; $P_{ET}CO_2$ 3.2%.

which can endanger his/her brain function. If the body temperature decreases from 37 to 30 °C, the $P_{ET}CO_2$ will decrease from 5% (40 mm Hg) to 3% (24 mm Hg), assuming that ventilation is unchanged. The $P_{ET}CO_2$ can be a reliable indicator of the correct respiratory volume; hence, when monitoring metabolism, the body temperature should be also considered.

Another factor for increased metabolism is muscular activity. A very good example is an epileptic fit, which is shown in Figure 41.3. The patient was a 26-year-old woman who underwent brain surgery under general anesthesia with muscular relaxation. The patient was connected to a ventilator and slightly hyperventilated to lower the intracranial pressure. Suddenly, the very regular pattern was interrupted by an epileptic fit (indicated by arrows). The ECG and the plethysmogram were suddenly disturbed by the uncontrolled contractions of all the muscles, despite an estimated adequate dose of muscle relaxants. During the 12 s of the tonic phase of the attack, there was no ventilation at all. However, immediately afterwards, the capnogram was rising rapidly. Within 1 min, the $P_{ET}CO_2$ increased twofold because of the muscle contractions. After the epileptic fit, it took a considerable time before CO_2 production returned to normal. As can be seen, the plethysmographic amplitude was also increased due to vasodilatation as a consequence of the higher $PaCO_2$.

The capnograph as a monitor of ventilation

There are at least ten important ventilatory complications possible in a patient during surgery:

(1) Disconnection of the tubing
(2) Leakage in the ventilating system
(3) Ventilator failure
(4) Hypoventilation
(5) Hyperventilation
(6) Obstruction of the ET tube
(7) Obstruction of the airways
(8) Rebreathing
(9) Residual curarization
(10) ET tube in the esophagus.

Figure 41.4, a recording from 1964, shows two fragments from a capnogram of a 3-year-old girl who was breathing spontaneously under general anesthesia

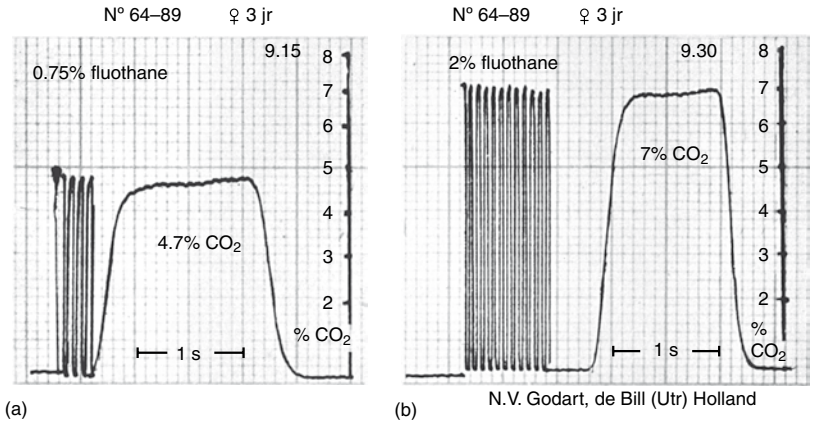

Figure 41.4 Capnogram of normal respiration (a) and during respiratory depression (b). Godart capnograph, 1964.

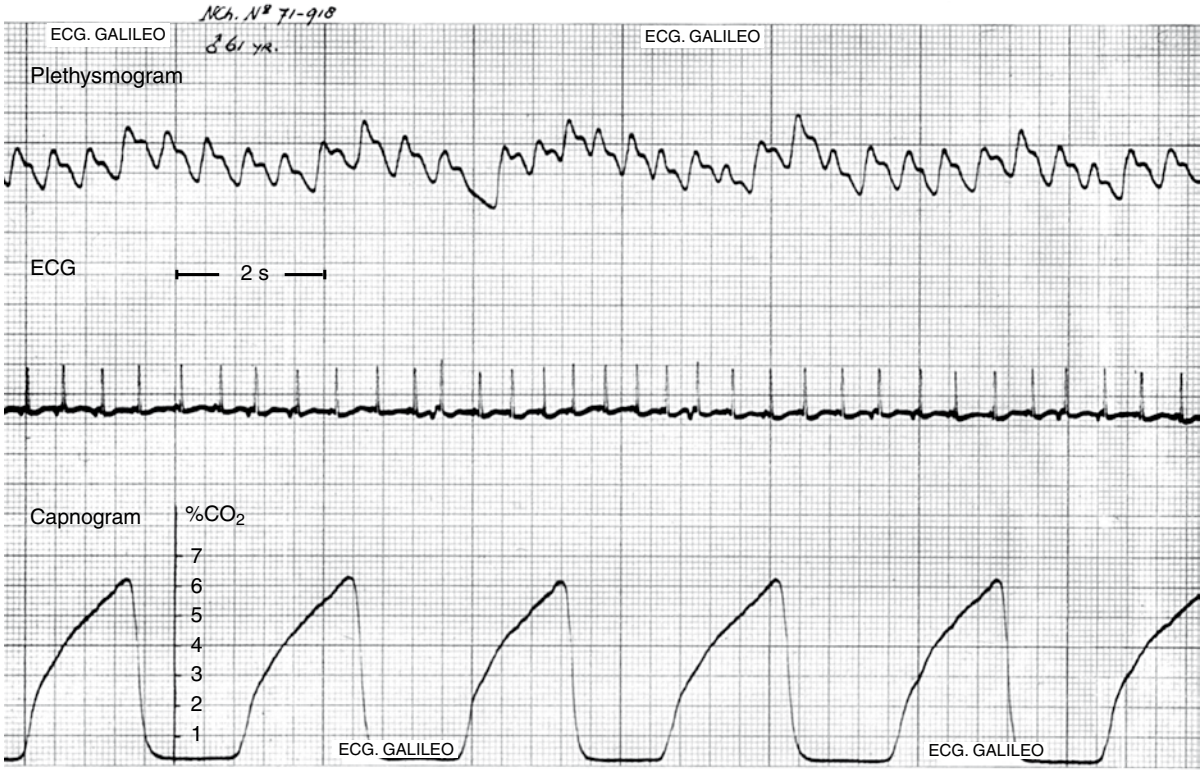

Figure 41.5 Plethysmogram, ECG, and capnogram of a 61-year-old man with chronic obstructive pulmonary disease (COPD) (1971).

with halothane. On the left-hand side, a capnogram is recorded while breathing a gas mixture containing 0.75% halothane. The capnographic waveform is perfectly normal. The plateau is nearly horizontal, the $P_{ET}CO_2$ is 4.7%, and the respiratory rate is 25. After increasing the halothane concentration to 2%, the capnographic waveform changed completely within 15 min. The alveolar plateau became much shorter, because in the interim, the patient had developed tachypnea. The $P_{ET}CO_2$ had risen to 7% (56 mm Hg), indicating a serious respiratory depression – a diagnosis that can be made at a glance.

Figure 41.5 shows a three-channel, high-speed recording of a 61-year-old man with serious chronic obstructive pulmonary disease (COPD). There is no real alveolar plateau. The oblique curve slopes upwards to about 6.4%, and then drops at the next inspiration. The CO_2 level cannot be considered as end-tidal,

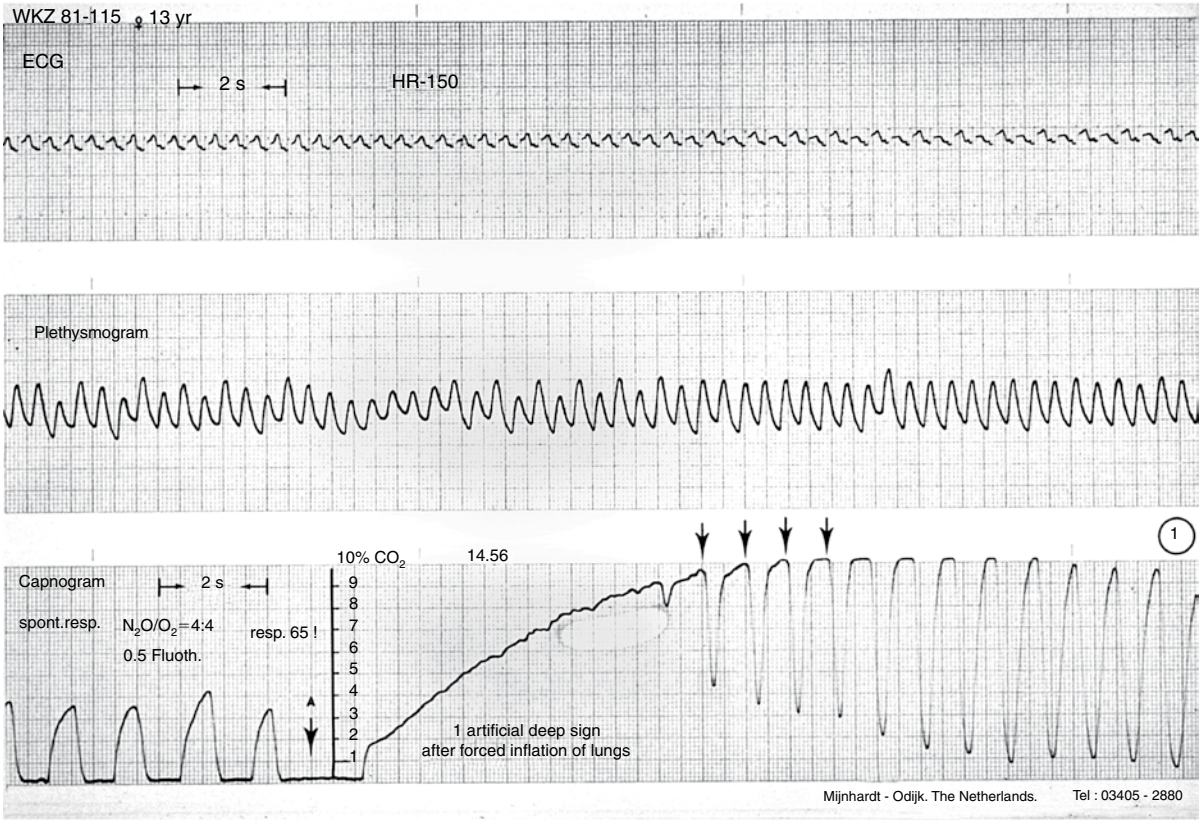

Figure 41.6 ECG, plethysmogram, and capnogram of a 13-year-old girl with cystic fibrosis (1981). Left: spontaneous respiration. Right: during forced expiration.

because an alveolar plateau is lacking. Such patients mostly have a considerable alveolar–arterial CO_2 difference. The shape of the capnogram in Figure 41.5 is typical for an expiratory problem.

Figure 41.6, made in 1981, shows the high-speed three-channel recording of a 13-year-old girl, suffering from cystic fibrosis. The capnogram was taken when the spontaneously breathing girl was just falling asleep. The sampling tube was carefully placed in the nasopharynx. On the left-hand side, four capnographic curves are seen. They are completely lacking an alveolar plateau, and resemble alligator teeth. The CO_2 concentration is seemingly low, about 4%, but the respiratory rate is very high, about 65/min. However, when the thoracic cage was manually compressed, the capnographic curve sloped slowly upwards, and reached a horizontal plateau of more than 10% (80 mm Hg!). This was the actual $P_{ET}CO_2$ value: two and a half times higher than expected. As can be seen, the alveolar plateau is interrupted repeatedly (indicated by arrows), caused by the respiratory attempts of the child, while her thoracic cage was still compressed. In nearly every patient with an expiratory problem, the actual $P_{ET}CO_2$ concentration can be obtained.

Capnography and the effect of muscle relaxants

Often, when a patient is emerging from an anesthetic, he/she may still be under the influence of the muscle relaxants used during the anesthetic procedure. Of course, nowadays, this can be detected by means of electromyography and by obtaining the *train of four*. Still, *residual curarization*, as it was formerly called when curare was used as a muscle relaxant, remains a potential danger. In the early 1960s, it was possible to capnographically judge the patient's respiratory efforts. Even in patients who are awake postoperatively and can breathe and talk, a respiratory disaster caused by muscle relaxants can develop in the recovery room. The typical shape of the capnogram in such a patient can be seen in Figure 41.7. It is derived from

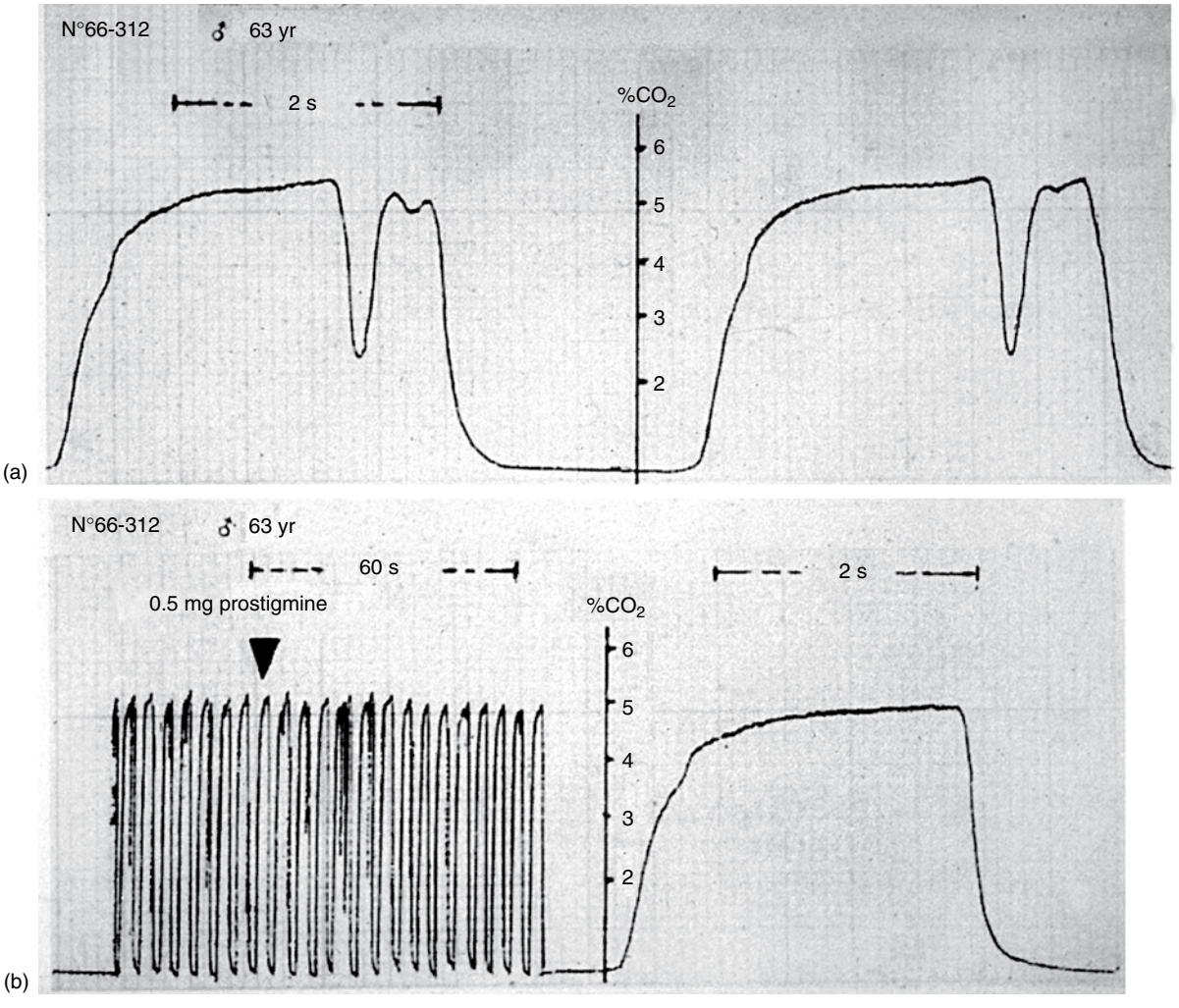

Figure 41.7 (a) "Curare" capnogram of spontaneous respiration of a 63-year-old man: effect of residual muscle relaxants. (b) The effect of an antidote (prostigmine) (1966).

a 63-year-old man breathing spontaneously for more than 2 h after one single dose of 20 mg curare. The first fragment shows the high-speed recording of two consecutive respirations. The curve starts nearly normal, with an alveolar plateau of about 5.4% (43.2 mm Hg), but in the second half of this plateau, a deep incision or cleft can be seen. This cleft is caused by the fact that the thoracic respiratory muscles are more paralyzed than the much stronger diaphragm; thus, the recording consists of two different capnograms. The larger tracing is caused by the diaphragm, and the smaller one by the thoracic muscles. Both waves are partially covering each other.

Such a highly specific capnogram is an absolute indication to administer an antidote. In this case, 0.5 mg prostigmine was given. The effect of this treatment can be seen in the second fragment; the capnographic waveform immediately became normal.

The same type of "curare" capnogram can be seen in spontaneously breathing patients suffering from a (fresh) cervical transverse lesion. They are also breathing mainly with their diaphragm. Of course, these patients do not react to antidotes, but as soon as their sternal bone is stabilized mechanically, the typical cleft in the capnographic plateau disappears.

Since 1970, most capnograms in the Institute of Anaesthesiology of the University Hospital of Utrecht have been recorded on multichannel paper, which runs continuously during the entire anesthetic and surgical procedures (Figure 41.8). All monitors are built into

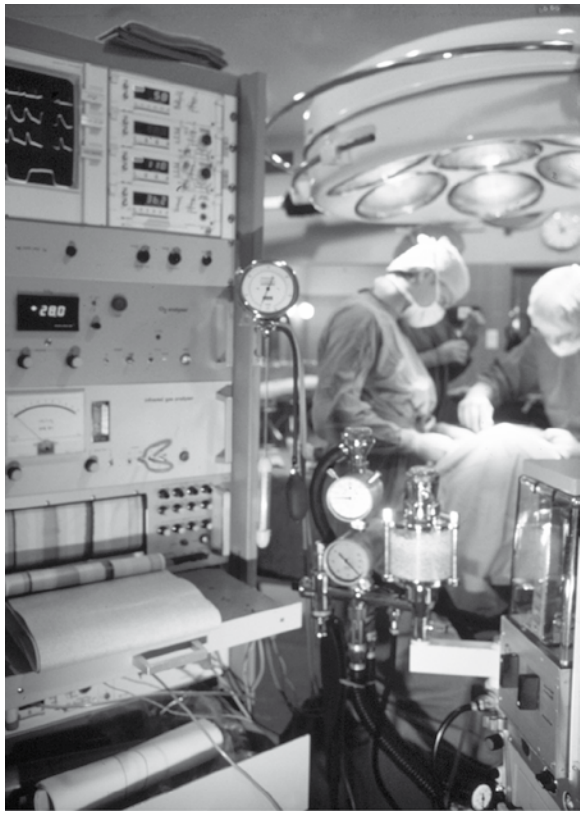

Figure 41.8 Monitor unit of the Institute of Anaesthesiology, with continuously running four-channel recording on paper tape. University Hospital of Utrecht, the Netherlands (1981). [Photo: C. F. Timmers.]

one large unit. Such a unit is available in every OR or induction room.

Cardiogenic oscillations

The following two figures show the effect of an anesthetic drug on the capnographic waveform. Figure 41.9 displays the capnogram and the plethysmogram of a 13-year-old healthy girl. Her capnogram is excellent, with a beautiful alveolar plateau, and a normal $P_{ET}CO_2$ of 5.2% (41 mm Hg). However, after having received 50 µg of fentanyl, this pattern quickly changed (see Figure 41.10). There are fewer respirations, because of a lower respiratory rate. The plateau has disappeared, and, in its stead, secondary peaks are visible, synchronous with the beating of the heart. The $P_{ET}CO_2$ has risen to about 6.5% (52 mm Hg), which is much too high. There are fewer capnographic curves because of the lower respiratory rate. The secondary peaks, indicated by arrows, are called *cardiogenic oscillations*. They are caused by the beating of the heart against the lungs. This can only be seen when either the respiration is very slow, or the tidal volume is small. Cardiogenic oscillations always indicate that the respiration is inadequate.

This can clearly be seen in the 18-year-old boy with severe Duchenne disease (progressive muscular atrophy). Figure 41.11 displays the high-speed, three-channel recording of his ECG, plethysmogram, and capnogram, while he was still breathing spontaneously. The respiratory rate was 24, and his capnogram mainly showed very high cardiogenic oscillations that reached a top level of more than 10% (80 mm Hg) CO_2. Such a capnogram is an absolute indication for artificial or assisted respiration.

The capnograph as a monitor of circulation

The most important circulatory complications are:

(1) Hypotension
(2) Cardiac/circulatory arrest
(3) Air embolism
(4) Hypertension.

When the ventilation is kept stable by means of a ventilator, at a constant speed, volume, and pressure, and the body temperature of the patient remains unchanged, the $P_{ET}CO_2$ follows the variations in blood perfusion closely. The clinical use of this phenomenon was described for the first time by Digby Leigh [5,6].

Hypotension

Figure 41.12 shows a two-channel slow recording of the capnogram and the direct arterial pressure in a 59-year-old man. The fragment covers a period of about 3 min. The patient underwent an operation for an abdominal aortic aneurysm. At the moment indicated by the arrow, the clamp on the left iliac artery was released. Within 30 s, the systolic blood pressure dropped from 145 mm Hg to 70 mm Hg, and was restored after 3 min. The capnogram likewise descended, falling from 3.8% to 3%. When the blood pressure started to rise again, the capnogram rose simultaneously, and even exceeded the original level. The explanation is that when the circulation increased, all the CO_2 that was stored in the tissues during the period of hypotension was quickly transported to the lungs by the improved perfusion.

The variations in the height of the capnogram are not as impressive as those of the blood pressure. This is caused by the fact that, even at a low blood pressure, the blood perfusion, to a great extent, can remain sufficient.

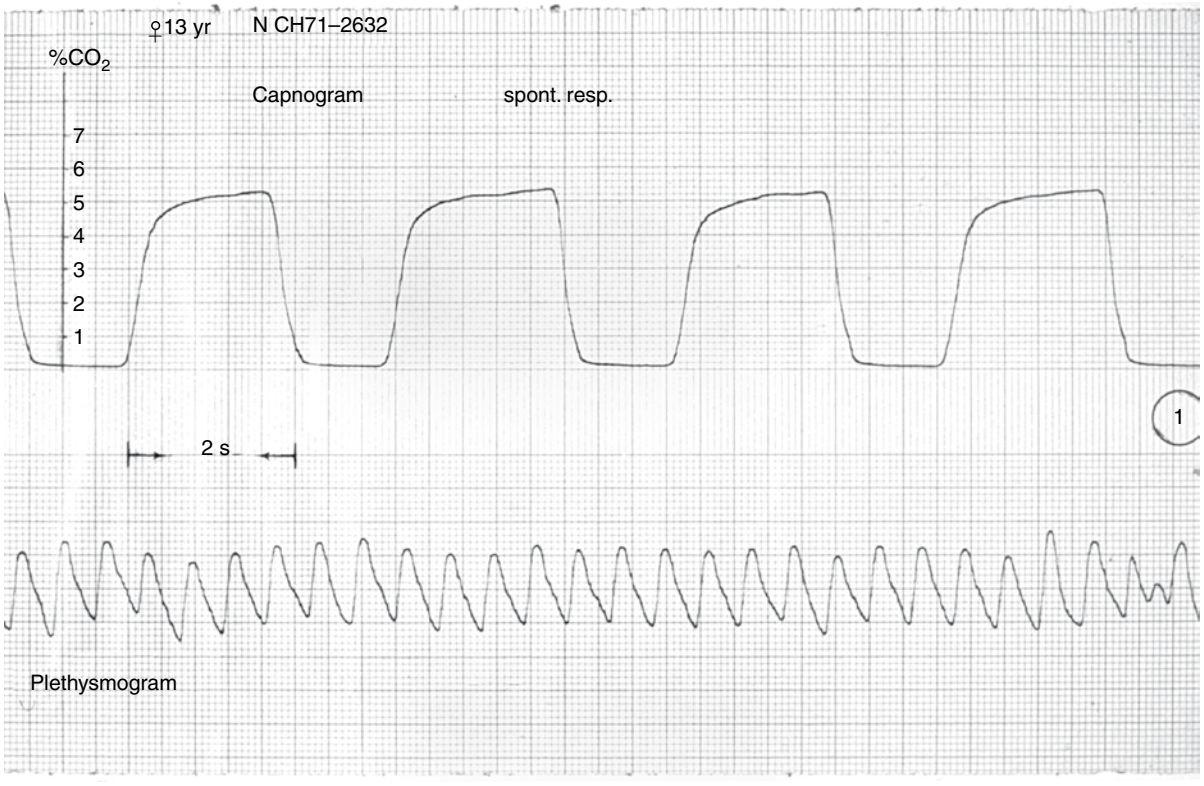

Figure 41.9 Capnogram and plethysmogram of a 13-year-old girl. Spontaneous respiration (1971).

It offers the opportunity to assess whether or not hypotension is life-threatening. This is clearly illustrated by the next two cases.

The first case involves a 76-year-old man. After a right-sided lung resection, complications occurred, making a reintervention inevitable. During this operation, the surgeon accidentally ruptured the right pulmonary artery, causing massive bleeding. In order to stop the hemorrhage, he put a finger in the hole, a typical Dutch habit, as is known worldwide. However, every time when he withdrew his finger in an attempt to close the hole surgically, a gush of blood spurted out of the artery, and the blood pressure decreased in a stepwise fashion. On the four-channel recording in Figure 41.13, this is indicated by arrows. The capnogram showed the same stepwise fall. The lowest blood pressure was 40/20, which is very low for a man 76 years of age. Nevertheless, a reasonable capnogram was visible, not lower than 3.8% (30.4 mm Hg). This meant that the blood perfusion was still sufficient to sustain life; thus, at that moment, it was not a life-threatening situation. On the right-hand side, one can see that the blood pressure again increased due to massive blood transfusion, the improvement of which is visible on the capnogram.

The next case (Figure 41.14) involves a 45-year-old man with a large kidney tumor that had grown through the diaphragm into the right lung. The hemorrhage was so profuse that the blood pressure fell below 20 mm Hg. It is clearly seen that, below a systolic pressure of 40 mm Hg, the capnogram also collapsed, a sign indicating that the patient was in mortal danger. However, as soon as the blood pressure was rising somewhat (up to 40 mm Hg) post transfusion, the $P_{ET}CO_2$ increased. By means of such documentation, it can be proven that the most dangerous period of hypotension (between A and B) lasted no longer than a few minutes.

Cardiac arrest and resuscitation

Figure 41.15 shows probably the first capnographic recording in the world of a cardiac arrest and resuscitation. This capnogram of a 55-year-old man was recorded in 1962, with the one-channel Omniascriptor and a Hartmann and Braun capnograph. The patient was breathing spontaneously. On the left, the washout

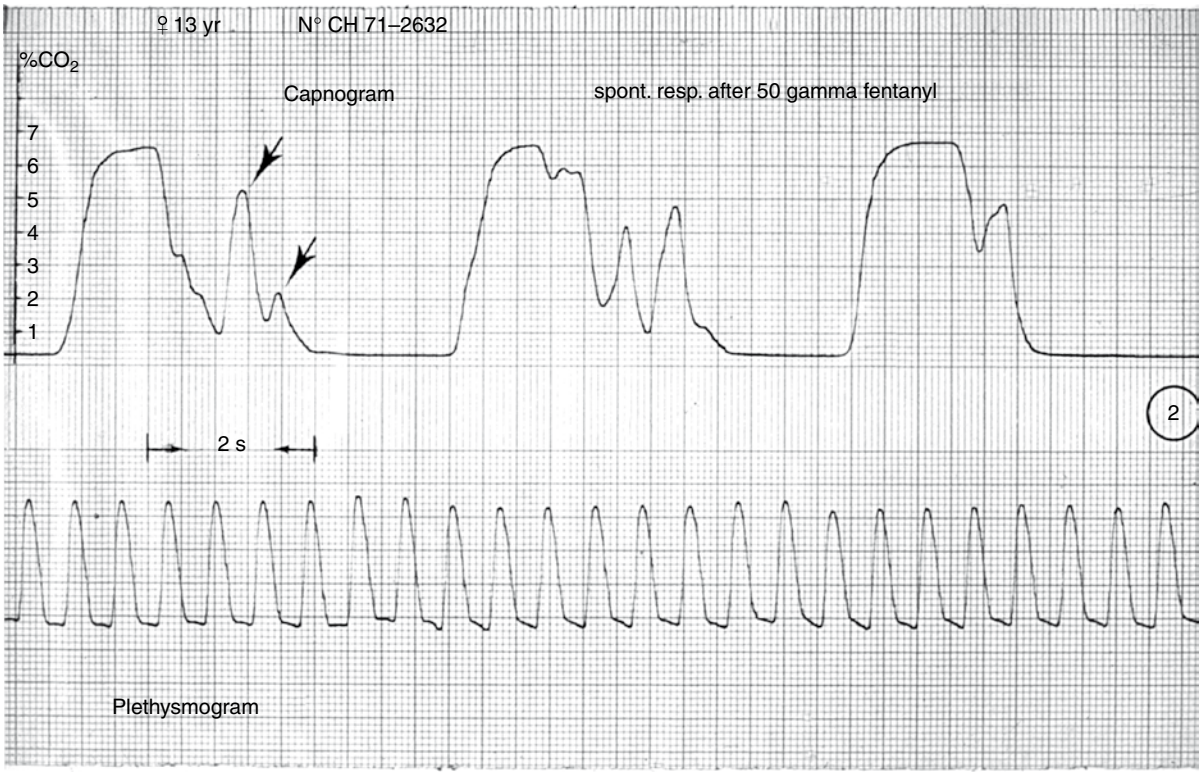

Figure 41.10 The same patient, but after 50 µg of fentanyl: cardiogenic oscillations.

curve, which is so typical for a circulatory arrest, is clearly visible. One minute later, external cardiac massage was started. The effect on the capnogram is visible, and showed the massage to be ineffective. In the meantime, the patient was intubated and ventilated manually. A thoracotomy was performed (indicated by an arrow) 150 s after the cardiac arrest. The CO_2 was rising rapidly, and, soon, the heart resumed its spontaneous activity.

From this recording, we learn that the whole procedure, from diagnosis to recovery, took exactly 5 min. In 1969, it was already clear that capnographic documentation of such events was very precise and legally very important in cases where doubt was cast on the medical conduct.

Because of the knowledge gleaned, since 1970, resuscitations at the Institute of Anaesthesiology of the University Hospital of Utrecht were, whenever possible, monitored with at least a capnograph. An example can be seen in Figure 41.16, a low-speed, two-channel recording of cardiac resuscitation of a 50-year-old man in 1981. The patient was ventilated mechanically with a constant frequency, tidal volume, and pressure; thus, all the variations in $P_{ET}CO_2$ were caused by changes in blood perfusion of the lungs. External cardiac massage was performed, which kept the CO_2, and, hence, lung perfusion, on an acceptable level. However, every one or two minutes, the resuscitator stopped momentarily to glance at the screen of the ECG monitor. During these moments, there was no blood circulation, and the capnogram immediately started to descend, while the plethysmogram showed no pulsations. As soon as the cardiac massage was resumed, the CO_2 once again increased, as clearly indicated by the arrows, although the right-hand side of the recording indicated that the average level of the $P_{ET}CO_2$ was falling down gradually. That meant that the resuscitator had become exhausted and needed to be replaced. The successful effect of a fresh resuscitator can be seen in Figure 41.17.

The capnograph has proven to be an excellent and reliable device to judge the efficiency of the resuscitation technique. The next case, recorded in 1981, is a striking illustration of this statement. It concerned a 39-year-old man who had undergone many laparotomies for nephrectomies and kidney transplants. His transplanted kidney showed signs of rejection and had to be removed. Immediately after induction

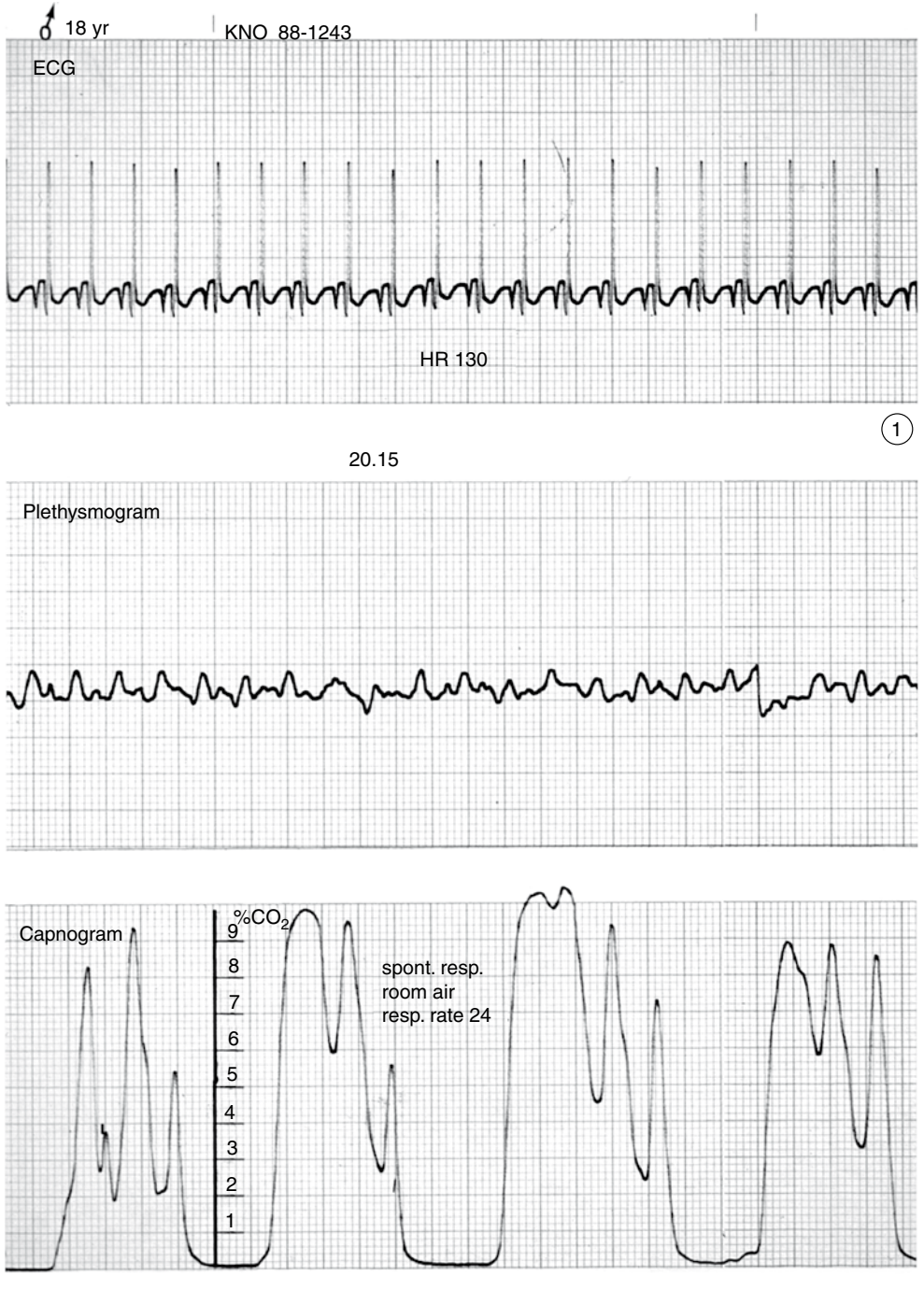

Figure 41.11 ECG, plethysmogram, and capnogram of an 18-year-old boy with Duchenne disease (1988). Spontaneous respiration. Multiple cardiogenic oscillations. Very high $P_{ET}CO_2$.

of general anesthesia, an asystole developed. External cardiac massage was started immediately, but the effect was poor. No blood pressure could be measured and the average level of the $P_{ET}CO_2$ during mechanical ventilation was no higher than 2% (16 mm Hg). His pupils became dilated and did not react to light. His abdomen was extremely flabby, and his abdominal wall represented an old battlefield of surgical scars. When

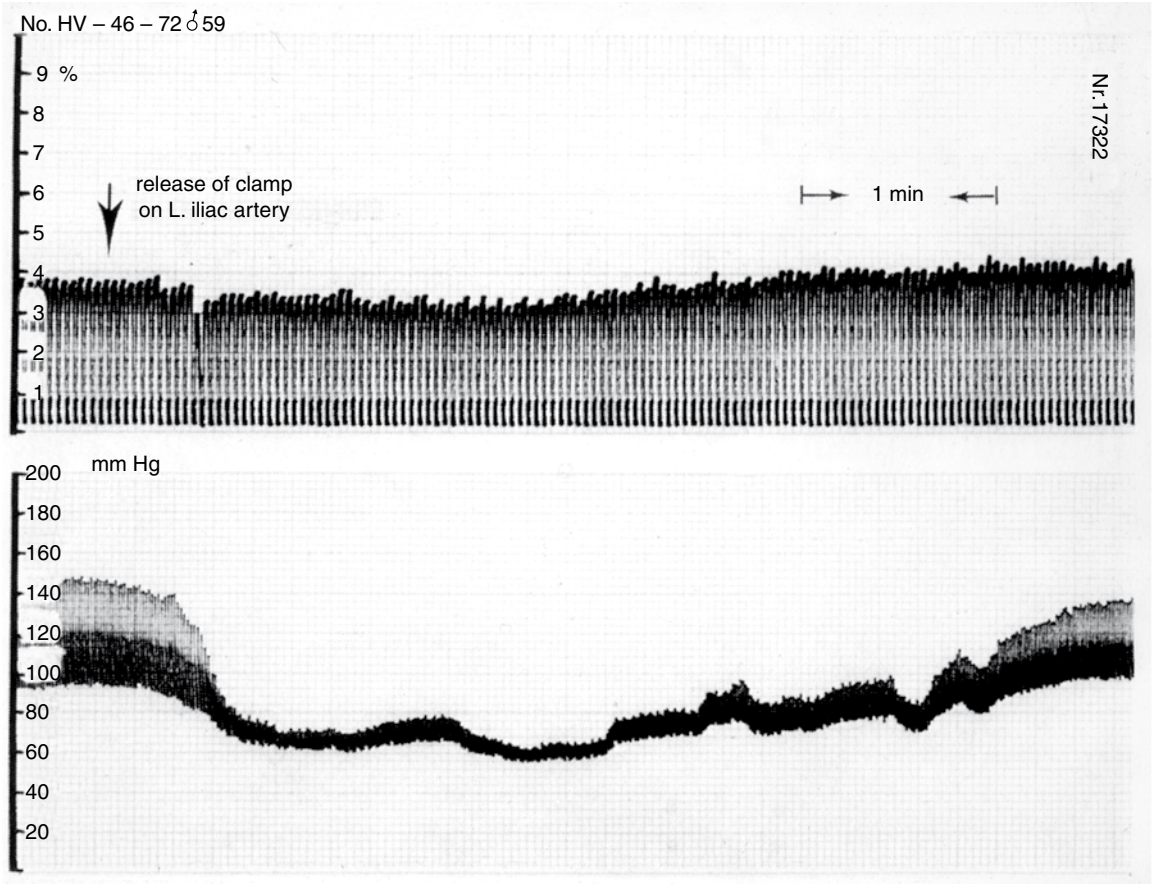

Figure 41.12 Capnogram and arterial blood pressure of a 59-year-old man. Effect of hypotension on the capnogram (1972).

the sternum was pushed downwards during cardiac massage, the abdominal wall bulged forwards, displaying a huge abdominal hernia. Assuming that the heart had escaped our attempts of compression by moving downwards in the direction of the flabby belly, we tried to make the anterior abdominal wall as tight as possible by grasping the skin and underlying muscles in our hands and folding them in creases. The dramatic effect is clearly visible on the capnogram as well as on the plethysmogram and the ECG. Therefore, guided by the capnogram, the patient was resuscitated successfully (Figure 41.18).

The capnograph as a monitor of technical defects

Technical defects in anesthesia machines, connecting tubes, ventilators, valve housings, ET tubes, etc., are life-endangering. In the 1960s, it was already clear that the capnograph was an early-warning device and could prevent disasters, a few examples of which will follow. In Figure 41.19, a fragment of the three-channel recording is seen of a 71-year-old woman who underwent plastic surgery while mechanically ventilated. Her capnogram was absolutely perfect, as can be seen on the high-speed recording on the left. The regular capnographic pattern was abruptly interrupted (indicated by an arrow), and the high-speed capnographic recording at the right shows the typical shape of an expiratory problem, as in COPD (Figure 41.5). Because it is impossible to develop a COPD in a few seconds, the underlying problem can either represent a sudden bronchial spasm or kinking of the ET tube. A quick inspection showed that it was, indeed, the tube, so the problem could be solved at once.

Other technical problems include leakages, disconnection of corrugated tubes, or saturation of the CO_2 absorbers (see Figure 41.20). Leakages and disconnections cause sudden interruptions of the CO_2

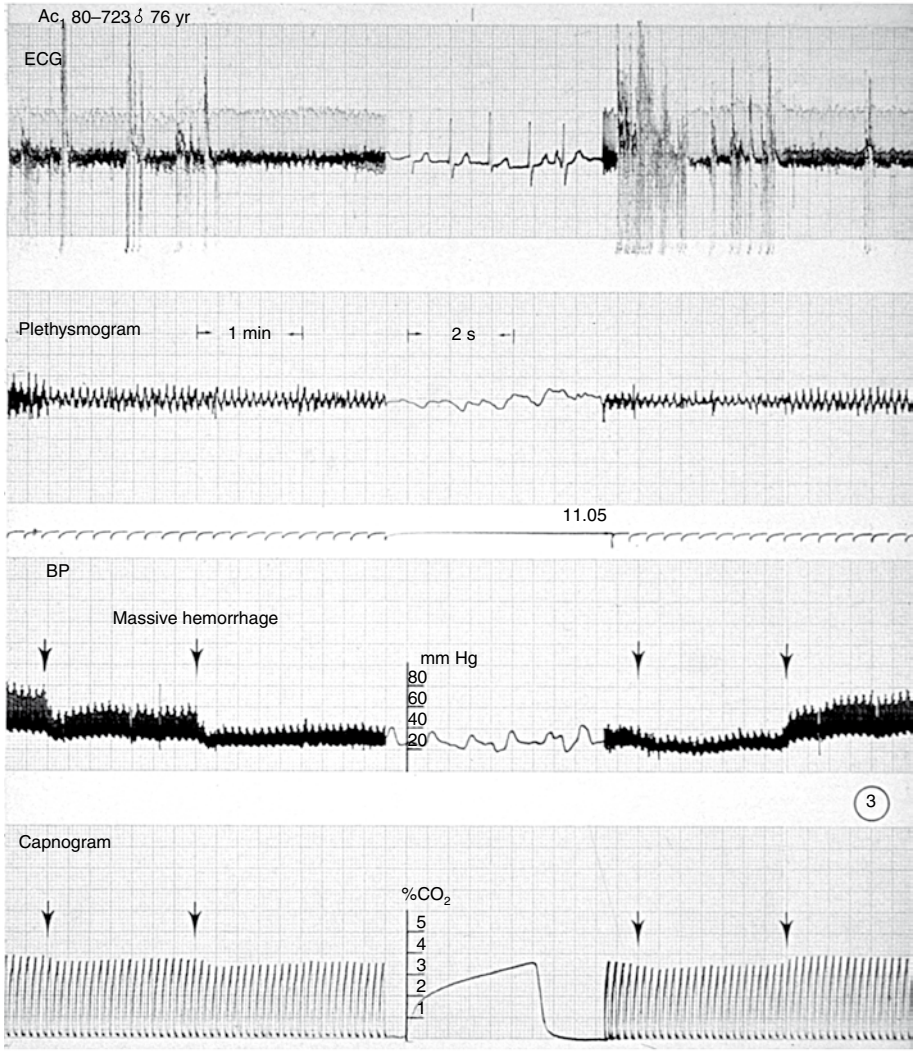

Figure 41.13 ECG, plethysmogram, blood pressure, and capnogram of a 76-year-old man during pulmonectomy, right. Severe loss of blood. Effect on capnogram (1980).

pattern, and inactivity of the CO_2 absorber (recorded on the right) makes the baseline rise, returning to zero as soon as a fresh absorbent canister has been connected.

The capnograph as a monitor of medical errors

Medical errors are still important factors that can endanger the health, or cost the life, of a patient. Such catastrophes can be recorded objectively in this manner, akin to the data flight-recorder (the so-called *black box*) in a commercial airliner. This is important not only for legal reasons, but also for the analysis and reconstruction of anesthetic or surgical accidents. The capnograph offers these possibilities, provided that the device is running continuously during the entire medical procedure.

Nearly fatal pain stimulus

Figure 41.21 shows a 5-min-long fragment of a four-channel recording of a 58-year-old woman (circa 1983). She was suffering from a highly dangerous intracranial aneurysm of the arteria communicans anterior. While awaiting surgery, she was already under anesthesia and mechanically ventilated, being paralyzed by muscle relaxants. She was slightly hyperventilated to a $P_{ET}CO_2$ of 3.7% (29.6 mm Hg) to decrease the intracranial pressure. The blood pressure was lowered to 60/30 mm Hg to prevent spontaneous rupture of the aneurysm during the neurosurgical intervention. Because 40 min had already passed since the induction of anesthesia,

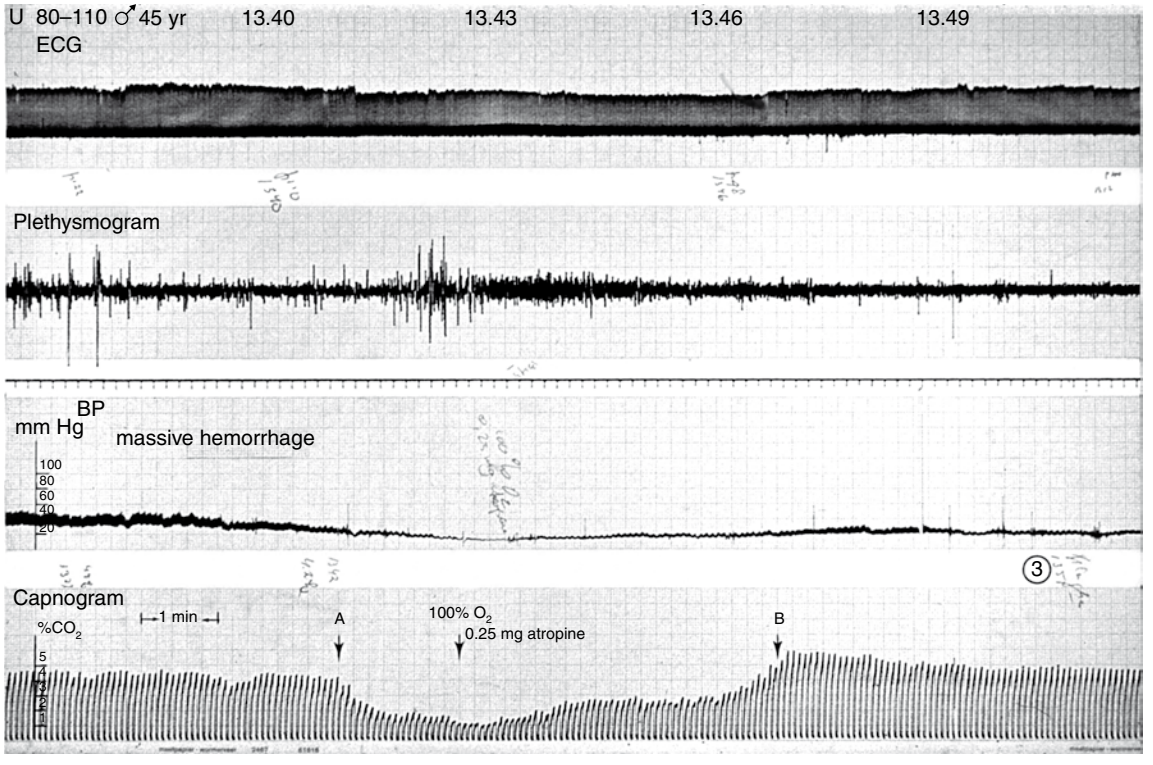

Figure 41.14 ECG, plethysmogram, blood pressure, and capnogram of a 45-year-old man during removal of a large kidney tumor, right. Extreme loss of blood. Systolic blood pressure lower than 20 mm Hg. Effect on capnogram.

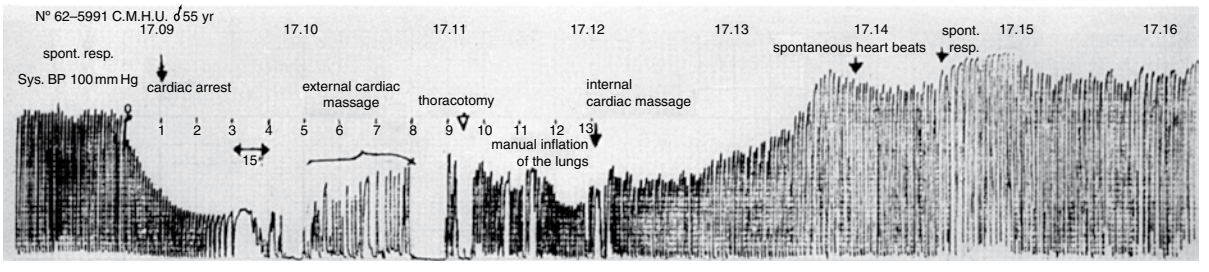

Figure 41.15 The first capnographic recording of a cardiac arrest and resuscitation. The patient was a 55-year-old man, at the Central Military Hospital, Utrecht (1962).

the patient required a new dose of the analgesic, fentanyl, before the start of the operation. However, without any warning or consulting the anesthesiologist, the surgeon made a deep incision in the patient's head (that moment indicated on the left-hand side by an arrow). The woman reacted violently to this painful stimulus. Although she did not move because of the muscle relaxants, within 1 min, her blood pressure rose from 60/30 to 170/90 mm Hg, creating a life-threatening situation. A fatal rupture of the aneurysm could be expected at any moment. The plethysmogram disappeared for almost 10 s due to extreme capillary vasoconstriction caused by the adrenalin from the adrenal glands. After that, the plethysmographic oscillations increased fourfold due to a rise in blood pressure. The capnogram rose from 3.7% (29.6 mm Hg) to 5.2% (41.6 mm Hg). It was an arduous task normalizing the blood pressure once again. Fortunately, no intracranial hemorrhage occurred.

Suppose the action of the neurosurgeon had resulted in a tragedy; then certainly he would have accused the anesthesiologist of causing the fatal

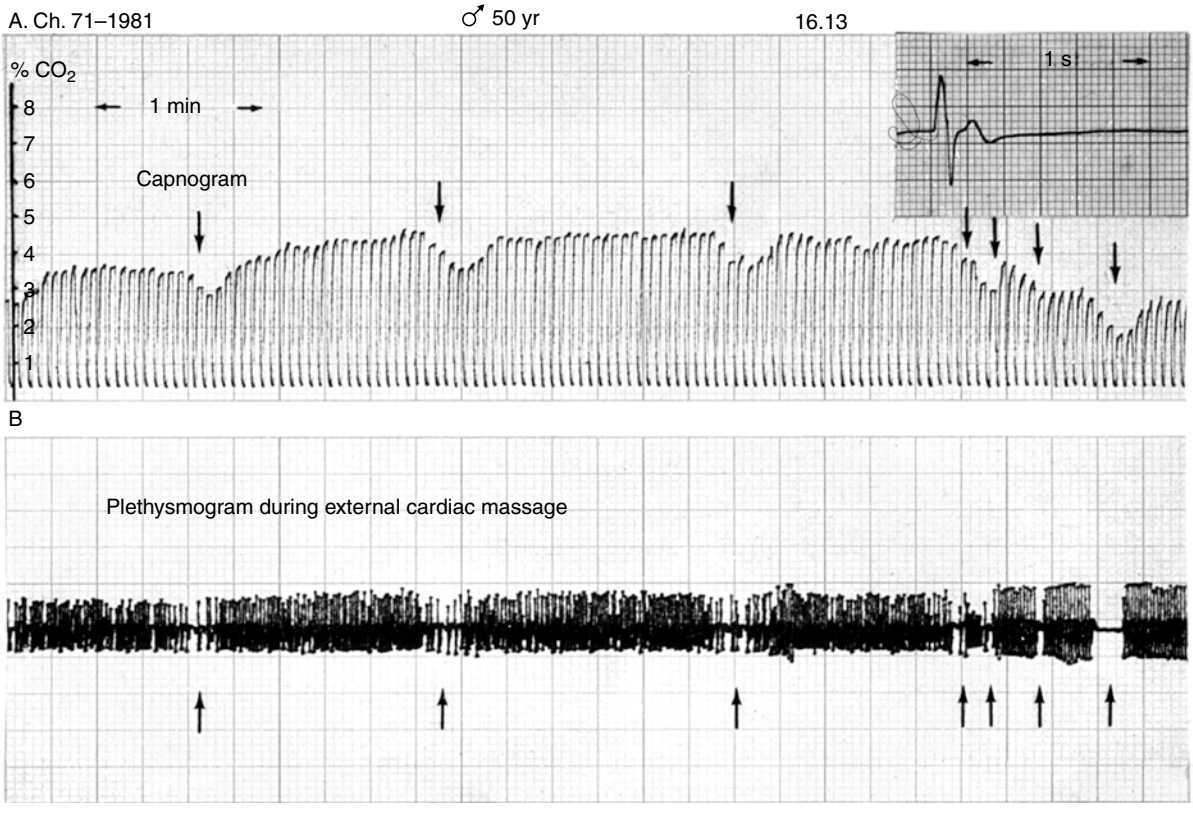

Figure 41.16 Capnogram and plethysmogram of a 50-year-old man during external cardiac massage. At right, the resuscitator becomes exhausted (1981).

outcome, because he would state that no patient could die from a simple skin incision, and thus, would claim that the anesthesia was the cause, and the anesthesiologist would be blamed. With the recording in hand, the anesthesiologist could have proved his innocence.

Compression of the heart

A surgical team performs a lobectomy of the right lung. The thoracic surgeon is busy closing the bronchial stump with staples. His assistant has two hands in the open chest of the patient. At that moment, Figure 41.22 was recorded. As can be seen, indicated by the first arrow, the ECG suddenly changed, the capnogram narrowed considerably, and the blood pressure fell from 130/70 to 45/30 mm Hg. The capnogram closely followed the variations of the blood pressure, and fell from 4.5% (36 mm Hg) to 1% (8.5 mm Hg). This combination is typical for a mechanical compression of the heart. There were simply too many hands and instruments in the thoracic cavity. The surgeons were urgently requested to withdraw as soon as possible, which they did immediately, knowing that everything was being recorded. The favorable effect can be seen directly after the second arrow. The life-threatening situation had lasted exactly 108 s.

The capnograph as a monitor of air embolism

Air embolism is a very dangerous complication, and the diagnosis is often too late. The classic symptom of the *mill-wheel murmur* can only be heard after a considerable amount of air is collected in the heart – and then the situation is already nearly fatal. The capnogram has been proven to be a very reliable and early warning. Even a small bubble of air can be immediately detected. Figure 41.23 shows the four-channel recording of such an event in a 20-year-old man during an orthopedic operation. Typical for air embolism is that the EGG, during the first minutes, remains

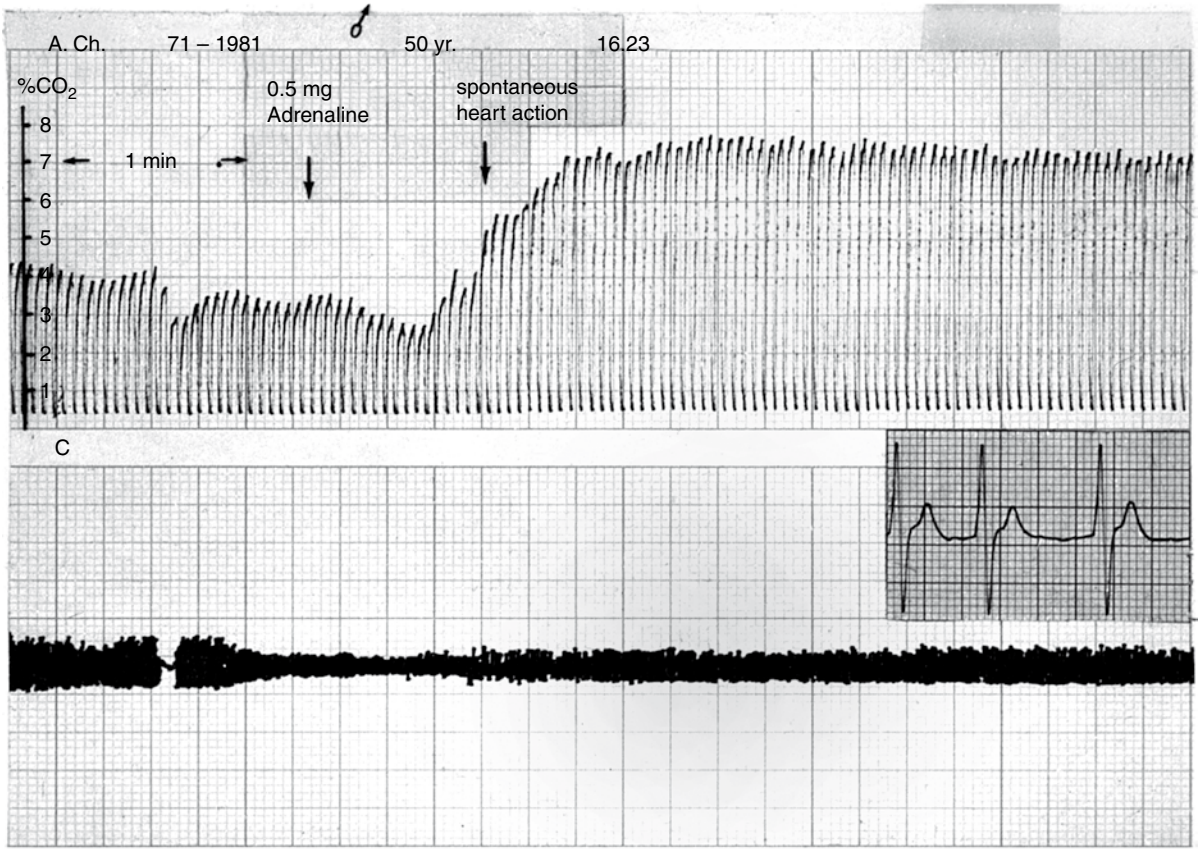

Figure 41.17 The same patient as in Figure 41.16. The capnographic recording of the successful resuscitation (1981).

unchanged, but the plethysmogram narrows immediately, while the capnogram gradually descends synchronously with the blood pressure. When only a few small air bubbles enter the bloodstream, then only the capnogram shows little dips. Air bubbles cause severe vasoconstriction in the lung capillaries, thereby diminishing lung perfusion and, in so doing, lowering the expired CO_2 contents. Such as in the case of a cardiac arrest, the effect of the treatment or resuscitation can clearly be seen on the capnogram (Figure 41.24).

Compression of the inferior vena cava

During a laparotomy of a 68-year-old woman for debulking an ovarian carcinoma, the gynecologists used a vast amount of towels and gauze to keep the bowels away from the surgical field. Suddenly, an impressive change was noted on the four-channel low-speed recording (Figure 41.25). While the ECG did not change, oscillations of the plethysmogram diminished in size, the blood pressure fell from 100/50 to 50/20 mm Hg, and, at the same time, the $PETCO_2$ was decreasing. In principle, there were three diagnostic possibilities:

(1) Severe sudden loss of blood
(2) Air embolism
(3) Compression of the inferior cava vein, preventing the venous return to the heart.

Since there was no blood loss, and the possibility of air embolism was negligible, the most probable diagnosis was compression of the cava vein by the towels and gauzes. The gynecological team was urgently requested to remove all the gauzes from the abdominal cavity as soon as possible. This improved the clinical situation immediately (see Figure 41.26). Because of the continuous capnogram recording, the life-threatening complication was detected, diagnosed, and solved within a few minutes. The adequate capnographic $PETCO_2$, which was never lower than 3% (24 mm Hg),

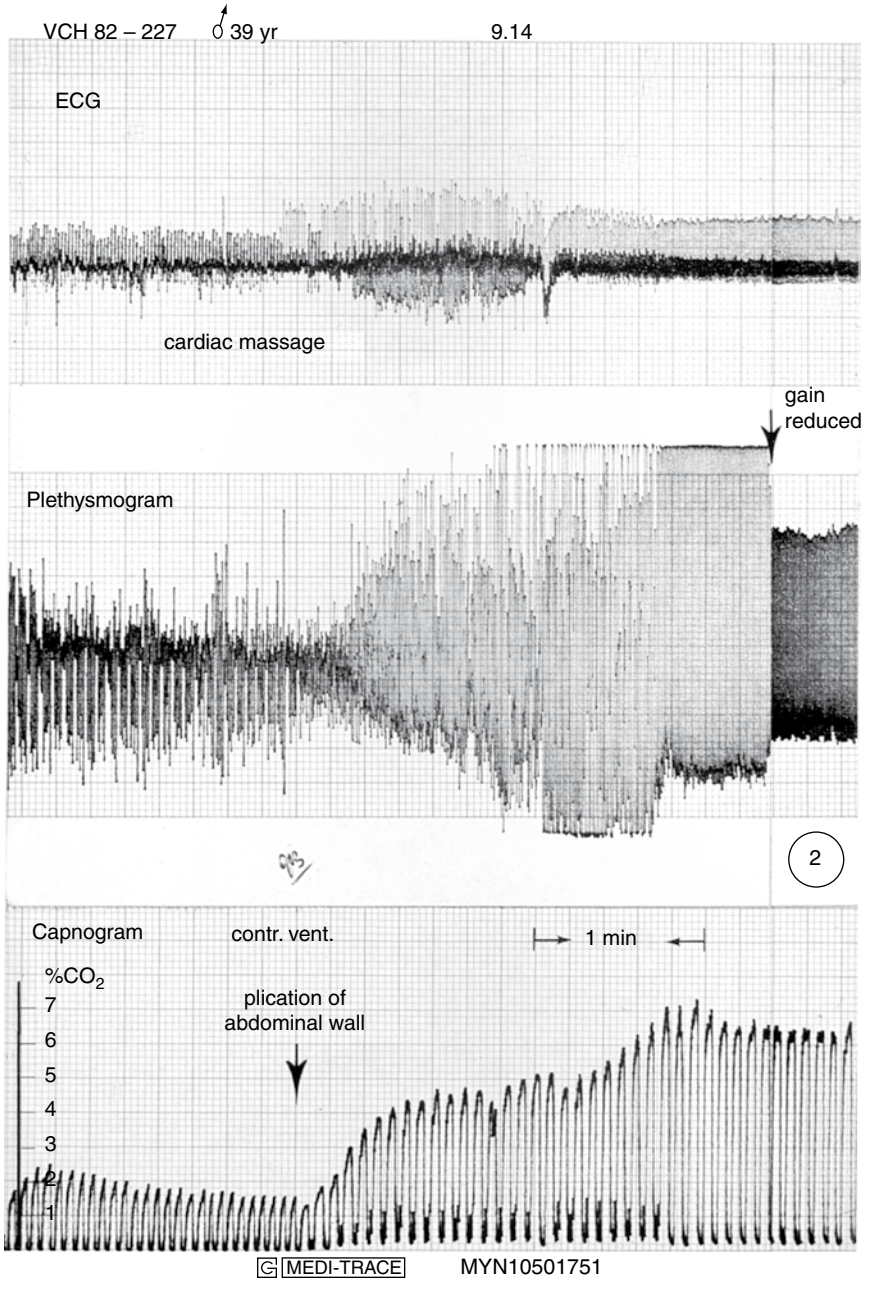

Figure 41.18 ECG, plethysmogram, and capnogram in a 39-year-old patient. Effect of tightening the abdominal wall, leading to successful external cardiac massage.

proved that the blood perfusion during the event was never insufficient.

Is hypotension dangerous or not?

The question always arises whether a certain fall in blood pressure becomes life-threatening. Clinical experience of more than 40 years of capnography has taught us that as long as the $P_{ET}CO_2$ during a period of hypotension is not lower than about 2.5% (20 mm Hg), perfusion of the lung is more or less comparable with that in the other organs, especially the kidneys, heart, and brain. The capnogram can even indicate that during a certain level of hypotension, the perfusion can be improved. In Figure 41.27, this is seen in a 66-year-old male neurosurgical

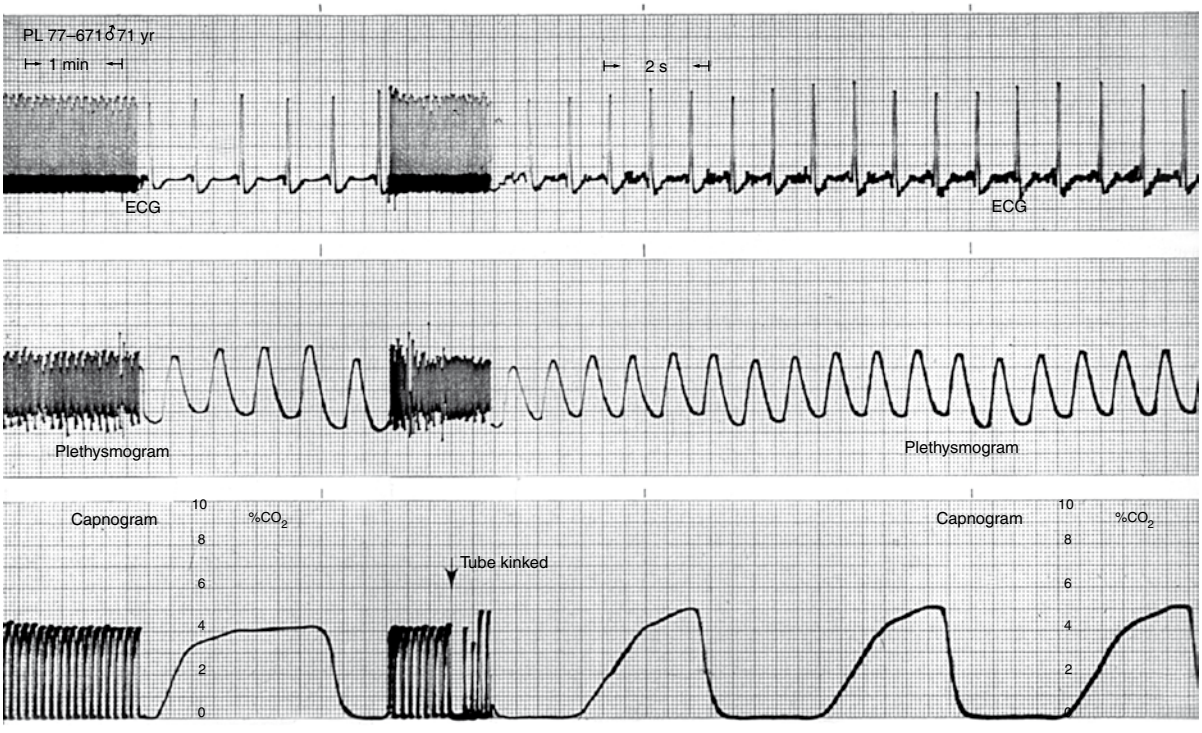

Figure 41.19 ECG, plethysmogram, and capnogram of a 71-year-old woman. Effect on the shape of the capnogram by kinking of the endotracheal tube.

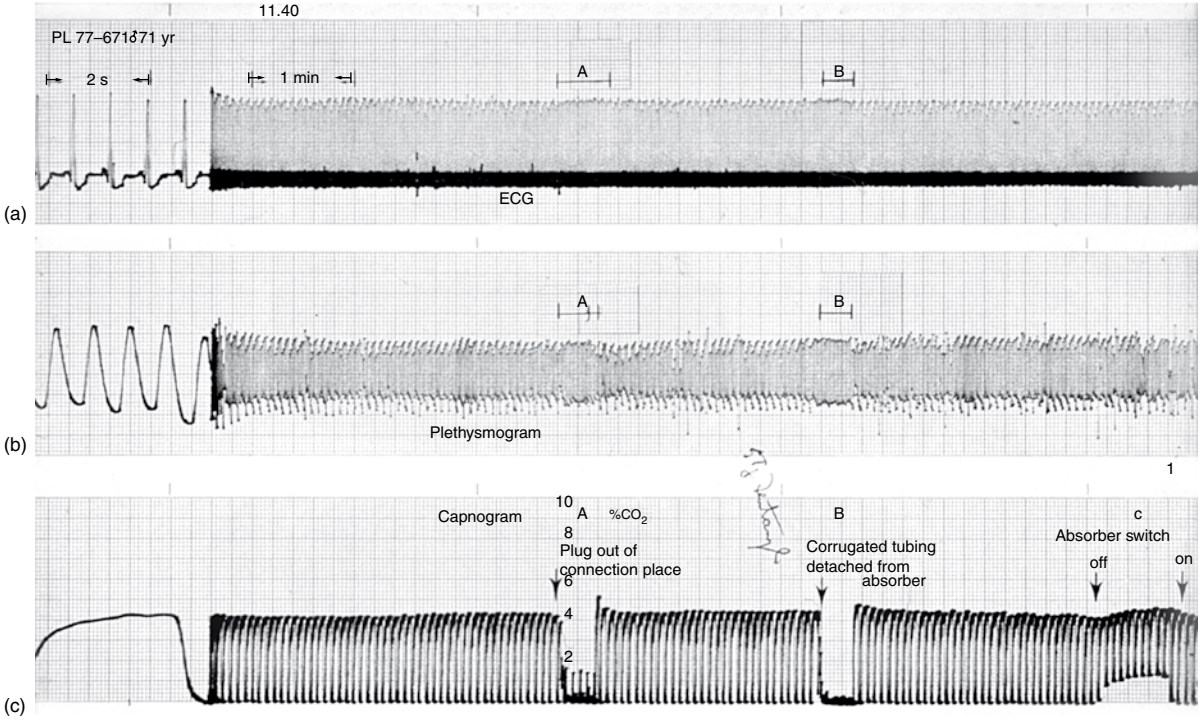

Figure 41.20 The capnographic recording of a leakage (a), a disconnection (b), and switching off and on the soda-lime absorber (c).

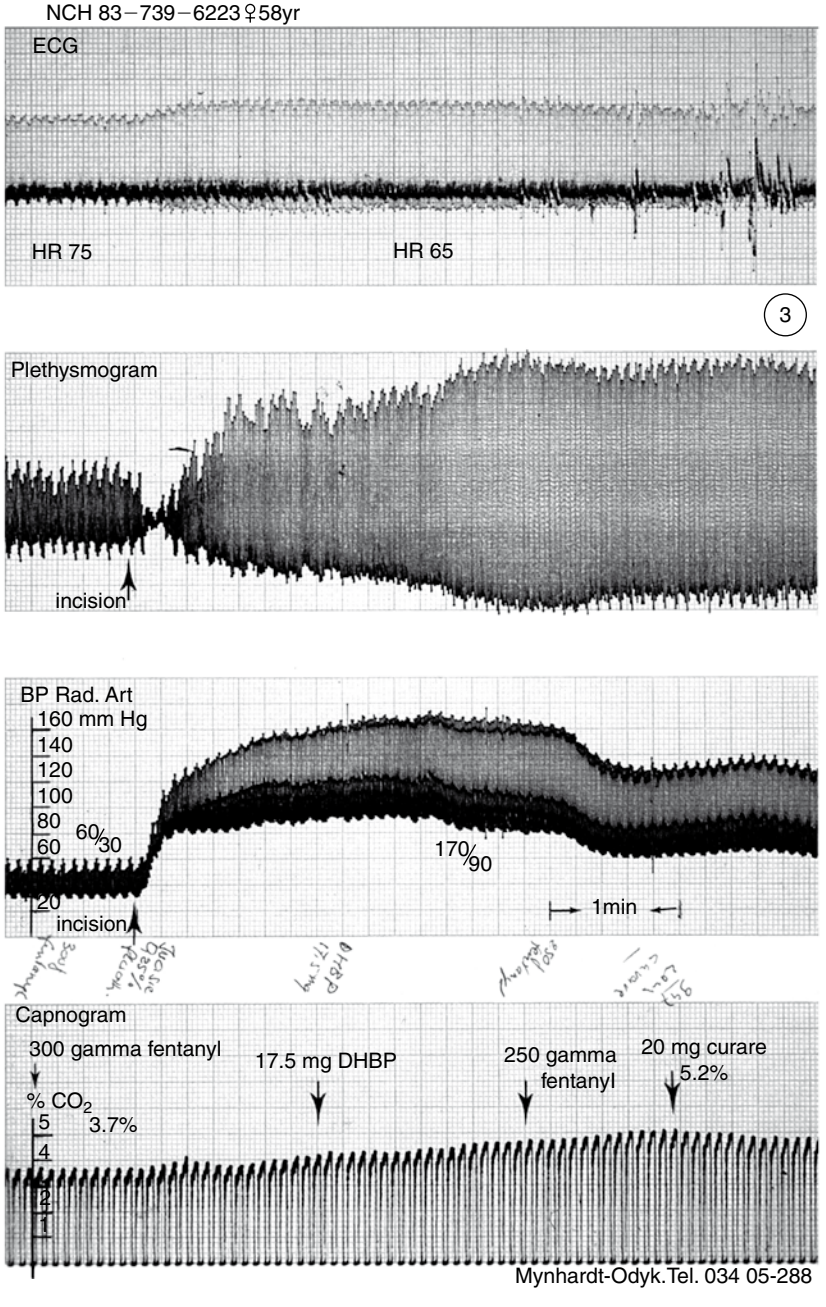

Figure 41.21 ECG, plethysmogram, blood pressure, and capnogram of a 58-year-old woman (1983). The nearly fatal effect of a painful stimulus.

patient. He underwent an extraintracranial bypass operation. His blood pressure of 140/80 mm Hg was purposely lowered to 84/50 mm Hg by means of 12.5 mg dehydrobenzperidol (DHBP). This is a low dose for a man of this age. However, the plethysmogram was broadening considerably, indicating vasodilatation, and the capnogram tracing rose from 3.6% (28.8 mm Hg) to 3.8% (30.4 mm Hg). This proved that although the blood pressure was low, perfusion had improved.

Central neurologic disturbances of spontaneous respiration

Already by the late 1950s, it had become clear that the capnograph was an excellent instrument for

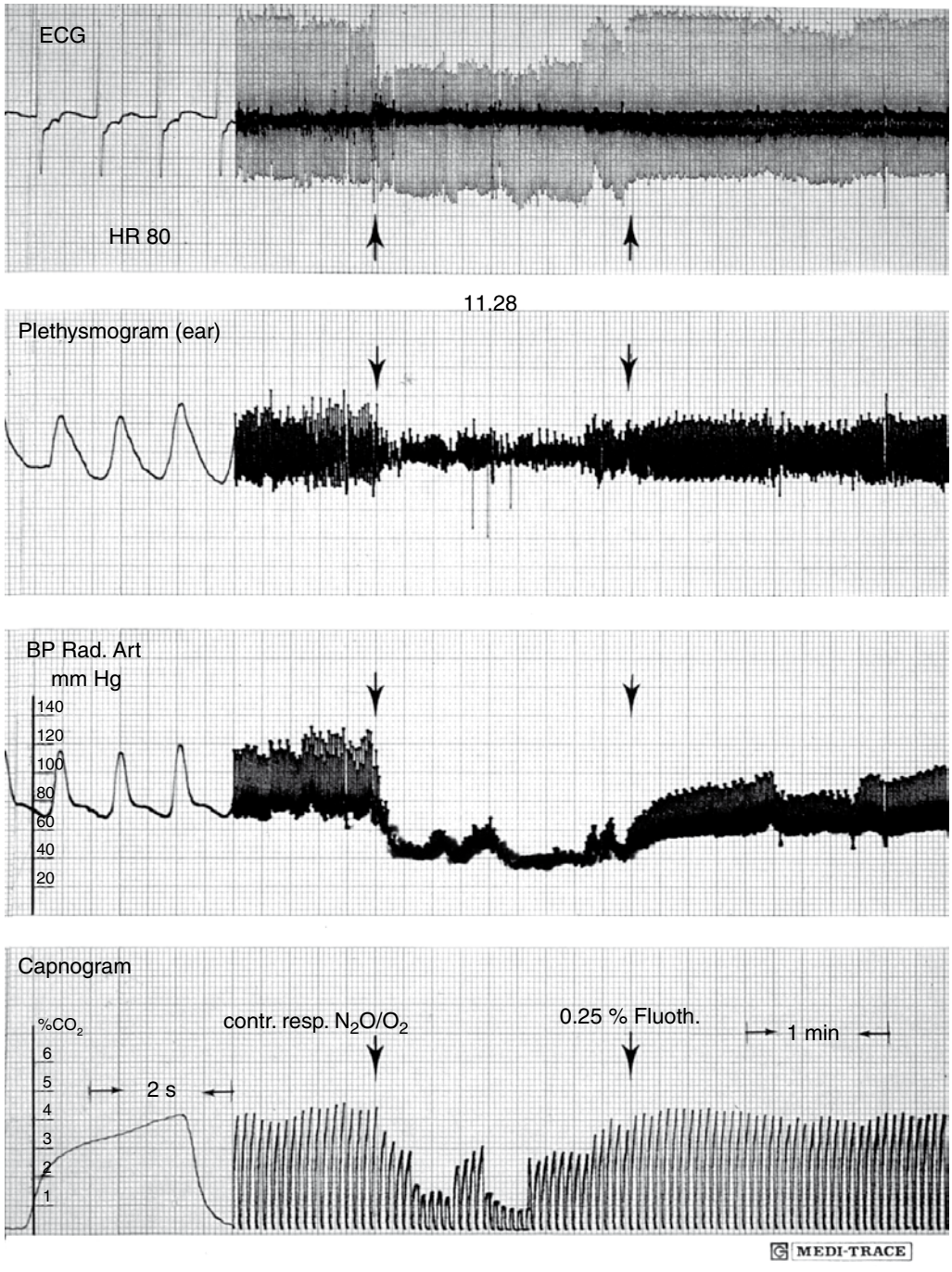

Figure 41.22 ECG, plethysmogram, blood pressure, and capnogram of a patient during lung resection. Effect on all the vital parameters of compression of the heart, followed by withdrawal of hands and instruments.

recording and studying spontaneous respiration, especially in patients with intracranial pathology. There are many variations of the respiratory rhythm caused by neurological disturbances in the brain or brainstem. Strangely enough, they are less well known than cardiac arrhythmias. This book is not the place to describe them all; that has already been extensively covered by Frowein [7].

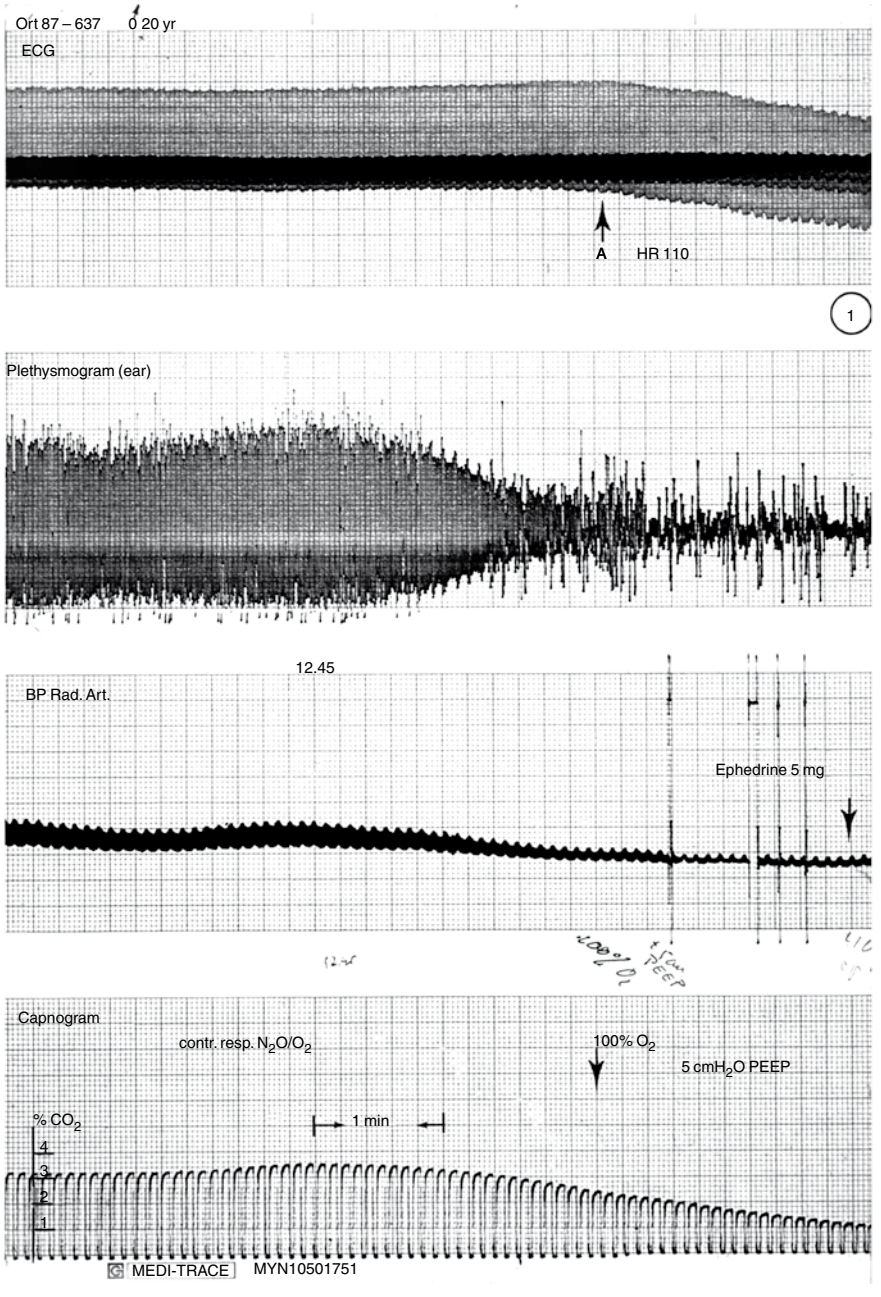

Figure 41.23 ECG, plethysmogram, blood pressure, and capnogram during air embolism in a 20-year-old man (1986).

One example is perhaps enough to illustrate the exceptional value of the capnograph in recording and studying central respiratory problems. Figure 41.28 shows the capnogram of the spontaneous respiration, together with the ECG, blood pressure, and the plethysmogram of a 55-year-old man. He was recovering from an intracranial operation on the trigeminal nerve. Clearly seen is the typical pattern of the classical Cheyne–Stokes breathing, indicating a brainstem disturbance. It is striking that the periodical rhythm of the respiration is also visible in the other vital systems.

Summary

More than 40 years of clinical capnography have shown that the capnograph is one of the most useful monitors in anesthesiology and intensive care. Its

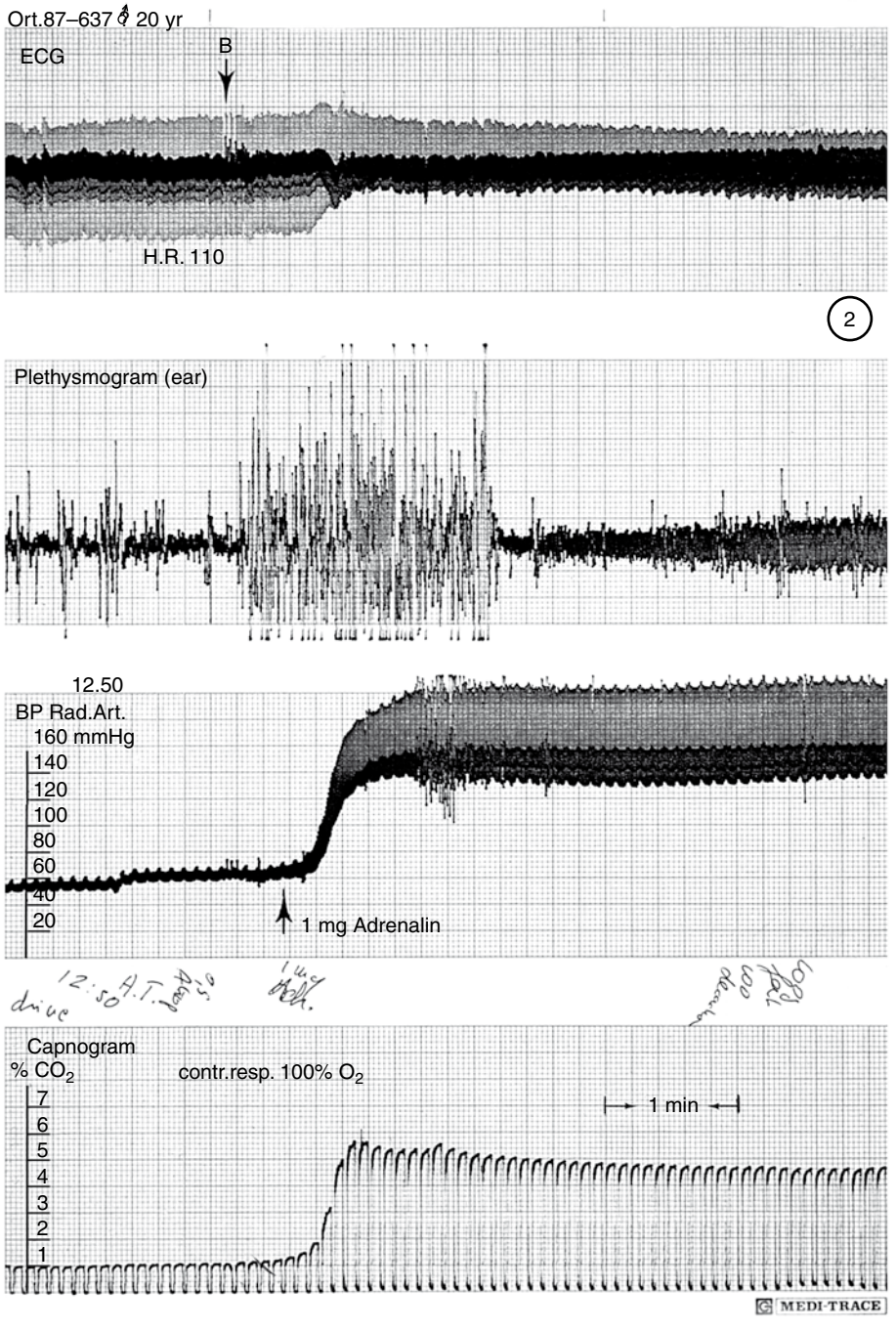

Figure 41.24 The resuscitation of the same patient as in Figure 41.23.

high value is only comparable with that of the ECG and the pulse oximeter. Nearly all the clinical possibilities of the capnograph had already been discovered between 1950 and 1970. All the recordings shown in this chapter were made by the author himself. Taken from his personal archives, and recorded between 1962 and 1982, they reflect the increasing importance of the CO_2 infrared monitor in the first decades of clinical capnography. During the recent World Congress of Anesthesiology, which took place in April 2004 in Paris, a Canadian anesthesiologist told the audience that in his country, the insurance

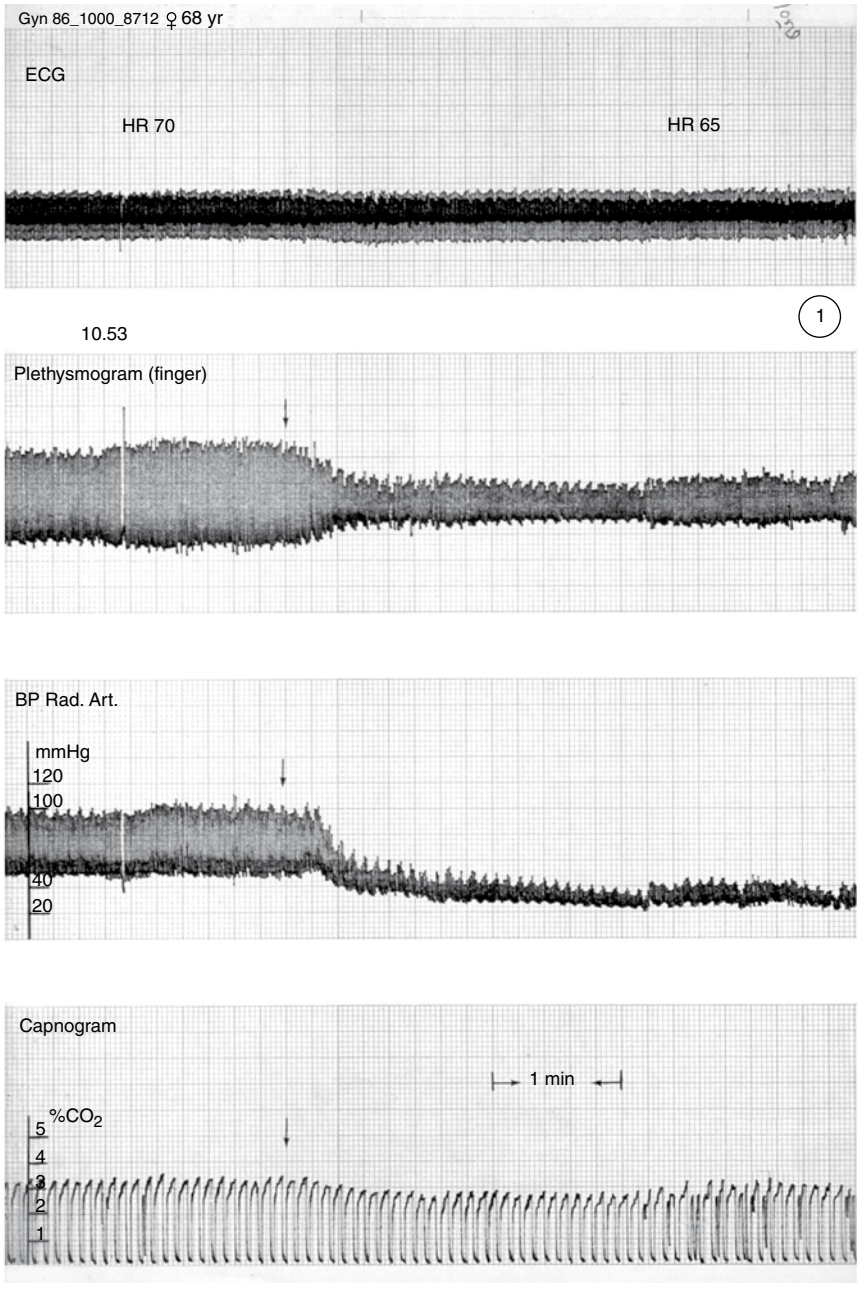

Figure 41.25 ECG, plethysmogram, blood pressure, and capnogram of a 68-year-old female patient during filling of the abdominal wall with gauzes in order to keep the bowels away. Effect on the plethysmogram, the blood pressure, and the capnogram of compression of the vena cava inferior.

companies have lowered the insurance premiums for medical liability by 80% for anesthesiologists who monitor their patients with a capnograph.

The history of clinical capnography has proven that measuring and recording expired CO_2 can prevent catastrophic events. There are only two conditions: the recording must be (a) continuous and (b) simultaneous with other vital parameters. In so doing, the monitor acts like a flight data-recorder in commercial aviation. The recording can be documented on paper or electronically. The paper tape has the advantage in that it is easy to write down quickly additional information, and it contains the entire anesthetic management of even many hours for examination.

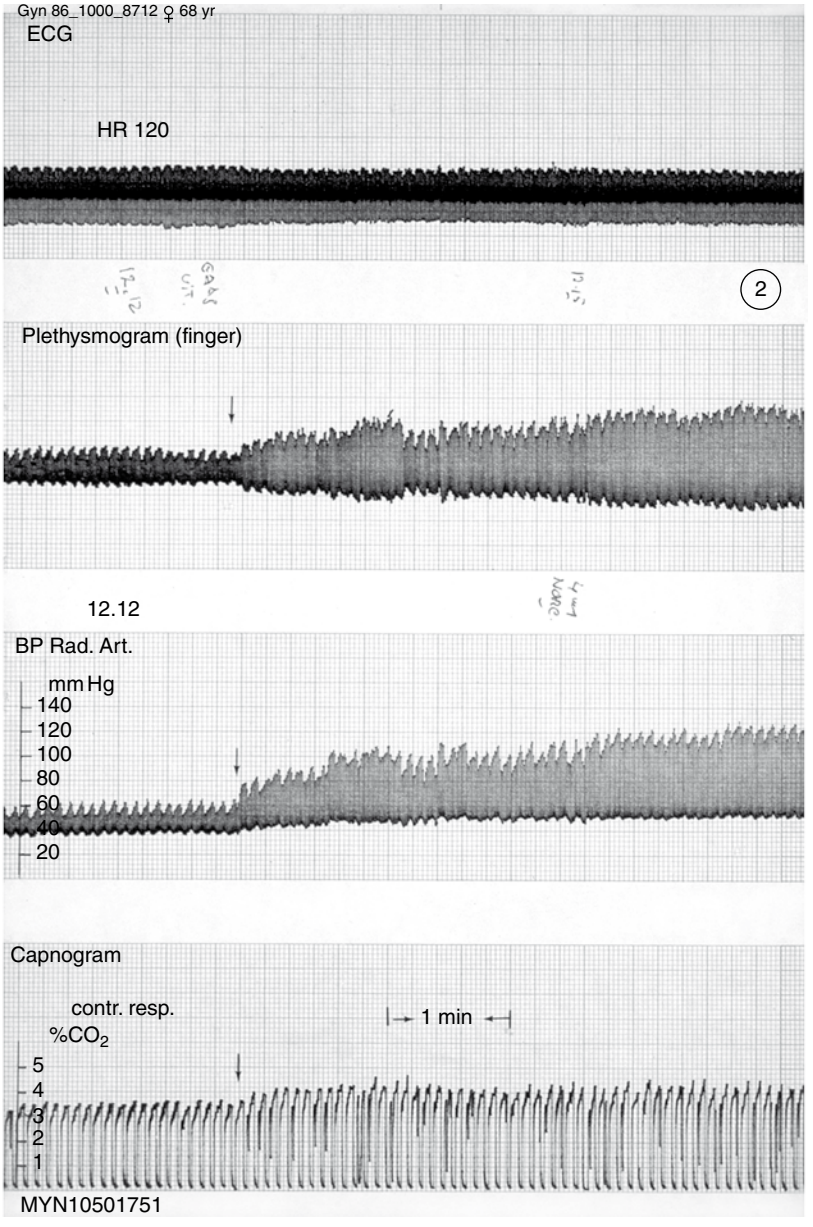

Figure 41.26 Recovery of the vital parameters, in the same patient as in Figure 41.25, after removal of all the gauzes and towels from the abdominal cavity.

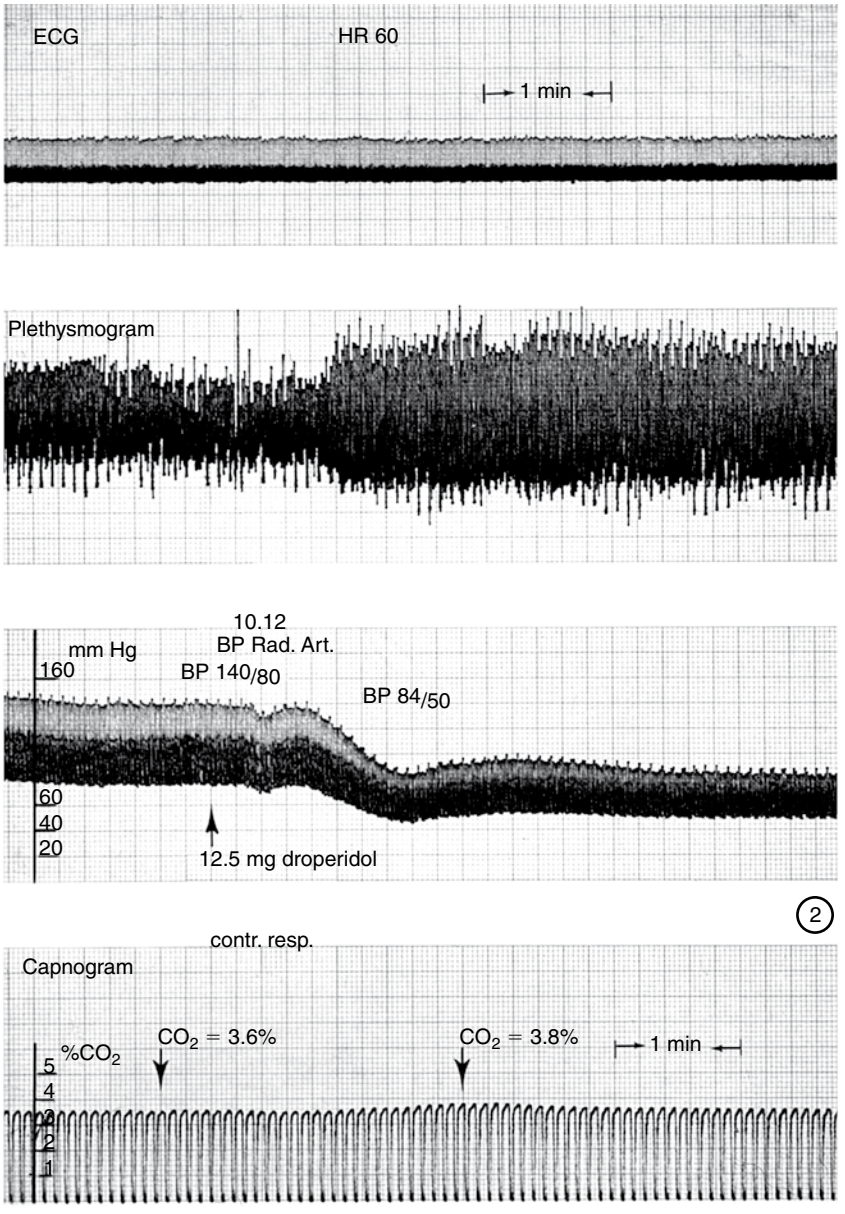

Figure 41.27 ECG, plethysmogram, blood pressure, and capnogram of a 66-year-old man. Blood pressure was lowered after 12.5 mg dehydrobenzperidol (DHBP or droperidol), although the broadening of the plethysmogram and the rising of the capnogram indicate improved perfusion.

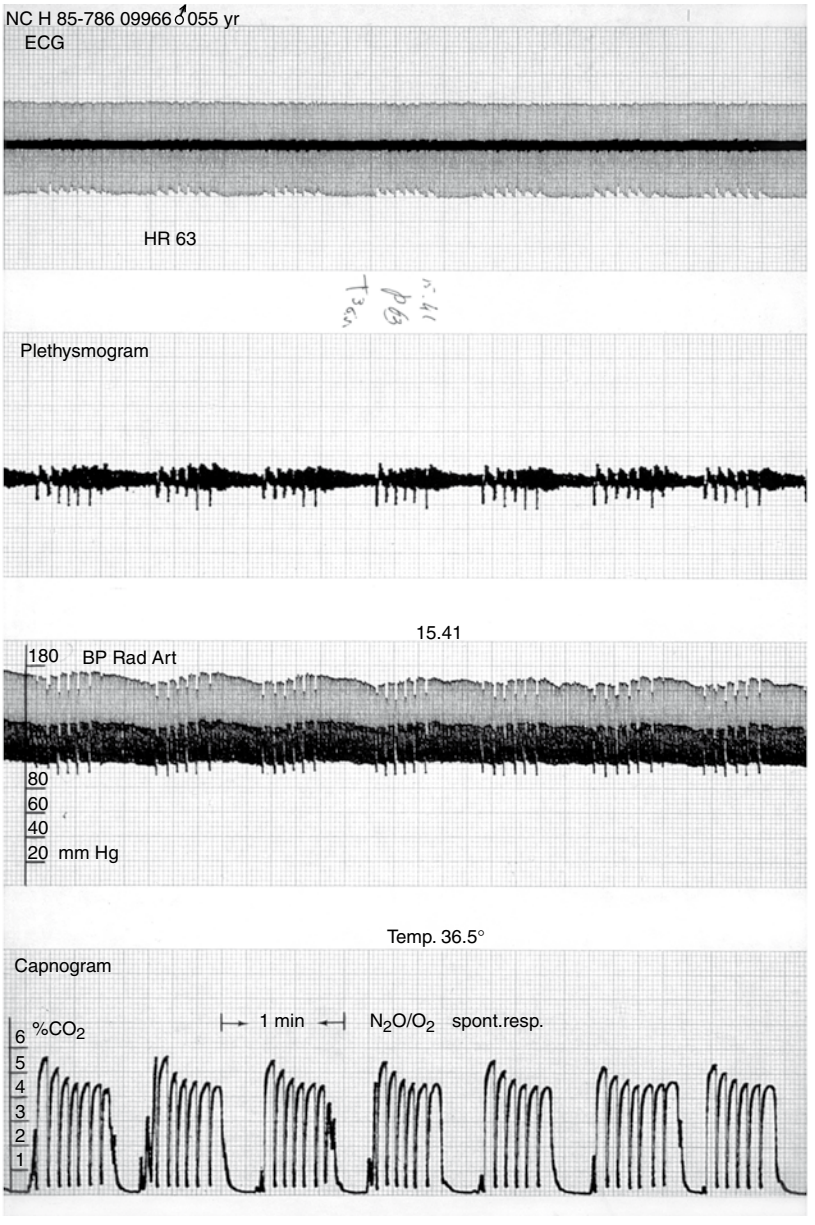

Figure 41.28 ECG, plethysmogram, blood pressure, and capnogram of a 55-year-old man after a craniotomy. Spontaneous respiration, and, typical Cheyne–Stokes breathing.

The disadvantage is the considerable amount of paper tape that has to be stored in the archives. During an 8-h operation, about 20 m of paper tape can be collected. However, the safety of the patient and the judicial security of the anesthesiologist are improved in an impressive way that was never before possible. Thus, it appears that the hell of the German submarine warfare between 1940 and 1945 unexpectedly gave birth to the incredible blessing of capnography that still saves and protects millions of lives all over the world.

References

1. Smalhout B. Capnography: its importance in diagnosis, operations and after-treatment of neurosurgical patients – The interpretation of the capnogram in dysregulation of respiration and blood circulation, and its role in monitoring neuro-anaesthesia.(Published by Oosthoek Publishing Co., Utrecht, the Netherlands, 1967.) Ph.D. thesis, University of Utrecht, the Netherlands.

2. Smalhout B, Kalenda Z. *An Atlas of Capnography*. Zeist, the Netherlands: Kerckebosch Publications, 1975.
3. Smalhout B. *A Quick Guide to Capnography and Its Use in Differential Diagnosis.* Böblingen, Germany: Hewlett-Packard, 1981.
4. Health Council of the Netherlands. *Advisory Report on Anaesthesiology. Part I. Recent Developments in Anaesthesiology*. The Hague: Government Publishing Office, 1978, 1980.
5. Leigh MD, Jenkins LC, Belton MK, Lewis GB Jr. Continuous alveolar carbon dioxide analysis as a monitor of pulmonary blood flow. *Anesthesiology* 1957; **18**: 878–82.
6. Leigh MD, Jones JC, Motley HL. The expired carbon dioxide as a continuous guide of the pulmonary and circulatory systems during anaesthesia and surgery. *J Thorac Cardiovasc Surg* 1961; **41**: 597–610.
7. Frowein RA. *Zentrale Atemstörungen bei Schädel-Hirn Verletzungen und bei Hirntumoren.* Berlin: Springer-Verlag, 1963.

Section 6
Chapter
42

Historical perspectives

The early days of volumetric capnography

R. Fletcher

In 1975, I was a trainee in the department of anesthesia at the University Hospital, Lund, Sweden, when the Siemens-Elema CO_2 analyzer 930 was newly installed in the cardiac surgery operating rooms. The compact and user-friendly 930 was said to owe its technology to the space exploration program. It could only work in conjunction with the Servo ventilator, from which it drew power and timing signals. The rapid response of its Ge–As sensor gave it a vastly superior performance to the previous generation of capnographs. The 50% response time (12 ms) of the original model meant that the CO_2 signal was only slightly delayed compared to the Servo's flow signal (4 ms) [1]. The flow signal made possible volumetric capnography; not only the measurement of expired CO_2 partial pressure or fraction, but also minute expired CO_2 volume ($\dot{V}CO_2$). However, the CO_2 measurement was affected by the presence of N_2O, which, in practice, meant that the 930s used in anesthesia and intensive care had to be separately calibrated.

My mentor was Lars Nordström, a cardiac anesthetist, who had already written his MD thesis on use of the Servo ventilator. He coupled the device to an eight-channel writer, so that in addition to having the capability of an electrocardiogram, and assessment of arterial and venous pressure, we could obtain expired PCO_2 (volume of CO_2 expired per breath), and airway flow and pressure. This was advanced technology for the 1970s, for I do not believe that capnography in any form was in regular clinical use at this time anywhere outside the Netherlands, where Smalhout had pioneered it, *and* certainly not in any cardiac theaters of which I was aware.

The revolution that the 930 brought about in our clinical practice and understanding of gas exchange depended on two aspects of its function. First, by measuring $\dot{V}CO_2$, it became simultaneously a metabolic monitor (what better measure of metabolic activity?), and a monitor of cardiorespiratory integrity. Any interruption in the transport of CO_2-rich blood from the tissues to the airway, whether in perfusion or ventilation, could be detected. Second, the ability to plot expired CO_2 against expired volume allowed us to present CO_2 single breath tests (SBT-CO_2) (Figure 42.1), which yielded diagnostic information. Many pulmonary conditions produce characteristic changes, giving further insight into the gas exchange process. We were able to reconstruct intraoperative events from this information, for instance, protamine anaphylaxis [2].

My doctorate was supervised by Professor Björn Jonson, a pulmonary clinical physiologist, who had also been involved in the development of the Servo ventilator. We obtained data from patients with lung fibrosis, emphysema, obstructive disease, sarcoidosis, and even pulmonary embolism. An existing computer program was adapted by Lisbet Janson to print out the SBT-CO_2 results.

We quantified the single-breath tests using Jonson's *efficiency factor*, which compares the volume of CO_2 eliminated per breath to what would be eliminated by a theoretical square wave, ideal breath (Figure 42.2). This would make the mean *efficiency* of patients with lung fibrosis 82%, whereas emphysema was 75%. Gross obesity added a fourth phase to the tracing, one we ascribed to the influence at end-expiration of slowly emptying, low ventilation/perfusion ($\dot{V}/\dot{Q}$) basal areas. These tests could be combined with a value for arterial blood CO_2 (Figure 42.1). Thus, pulmonary embolism (Figure 42.3) gave a striking picture: a flat single-breath test with a massive alveolar deadspace, a truly parallel deadspace. There were marked cardiogenic oscillations, which we ascribed to cardiac activity affecting the filling and emptying of lung regions with greatly different $\dot{V}/\dot{Q}$ ratios. Capnography is used today in Lund, Sweden as a diagnostic test for pulmonary embolism. I once observed a similar picture intraoperatively

Capnography, Second Edition, ed. J. S. Gravenstein, Michael B. Jaffe, Nikolaus Gravenstein, and David A. Paulus. Published by Cambridge University Press. © Cambridge University Press 2011.

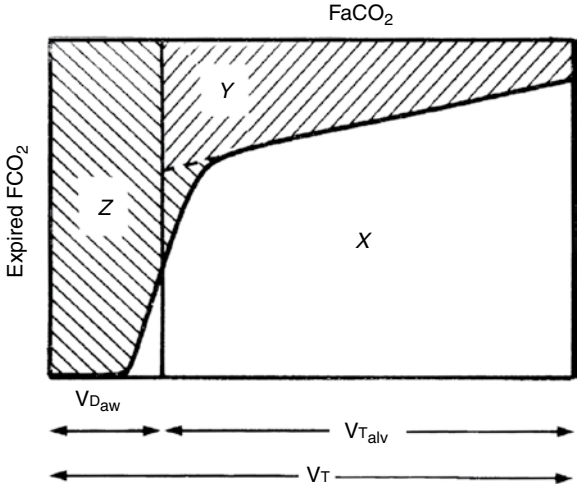

Figure 42.1 Schematic single breath test. $FaCO_2$ represents the FCO_2 of a gas in equilibrium with arterial blood. Area *X* represents the volume of CO_2 in the breath. Area *Y* represents the alveolar deadspace. The alveolar deadspace fraction is given by $Y/(X+Y)$. $V_{T_{alv}}$ is the alveolar tidal volume. The physiological deadspace fraction is represented by areas $(Y+Z)/(X+Y+Z)$. Note that fractions are used, rather than partial pressures, in order that the areas may represent CO_2 volumes, actual or notional.

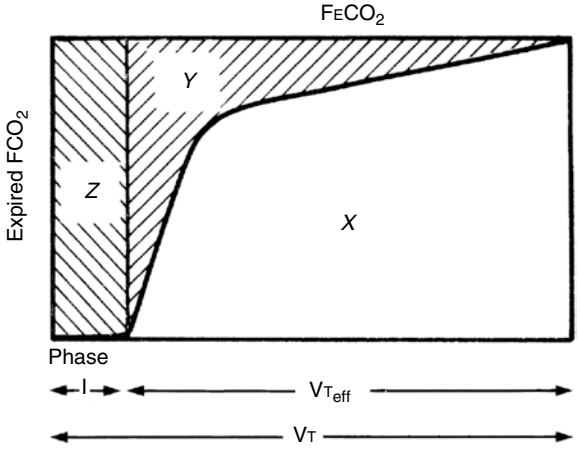

Figure 42.2 Definition of *efficiency*. The breath is divided into phase I, the ineffective part, and $V_{T_{eff}}$, the effective part (which contains phases I and II). *Efficiency* is calculated from 100 x area *X* divided by areas $(X+Y)$. In effect, efficiency is a non-invasive measure of ventilatory efficiency.

during a carcinoid flush. It was the first time I had seen such sudden reductions in $\dot{V}CO_2$ and end-tidal PCO_2, which were too abrupt to be due to metabolic changes. At first, I assumed there had been an equipment malfunction, but the recorded data showed a picture very much like that in Figure 42.3.

Gordon Cumming, then at Midhurst Medical Institute, Sussex, UK, suggested we plot CO_2 cumulative

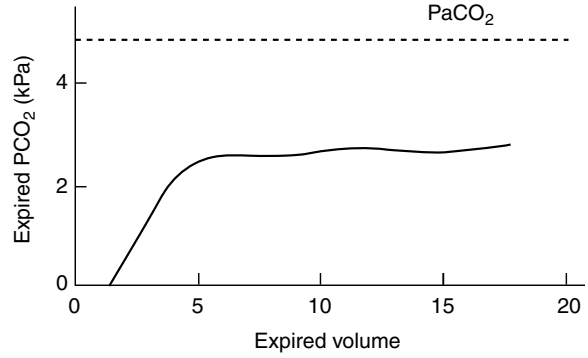

Figure 42.3 Trace of a CO_2 single breath test obtained from a patient with pulmonary embolism. There is a large alveolar deadspace, creating a large arterial–end-tidal CO_2 difference. The fluctuations in alveolar CO_2 are known as cardiogenic oscillations; on the time plot, they can be seen to have the same frequency as the heart rate. A similar picture is seen during a carcinoid flush (see text).

volume against expired volume, as he was doing in his studies with Keith Horsfield on oxygen and nitrogen. Cumming regarded the S-shaped increase in expired CO_2, phase II, as the recruitment of transit times for the different unit pathways. His method gave us an alternative to that of Fowler for measuring "series," anatomical, or *airway deadspace* ($V_{D_{aw}}$), our preferred term. It was preferred because it was clear that anatomical deadspace varied much more than could be accounted for on purely anatomical grounds; time, flow rate, and ventilatory pattern greatly affected it, as exemplified by Nordström's term, *mean distribution time*. However, it became clear that Cumming's method for $V_{D_{aw}}$ was subject to the same constraints as Fowler's. Particularly in obstructive lung disease, it became necessary to find another way of identifying the midpoint of the fresh gas/alveolar gas interface, such as the *point of inflexion* in phase II.

I recorded CO_2 single breath tests from anesthetized, ventilated patients at frequencies of 15–20 (mean tidal volume 0.45 L) and 9 breaths/min (mean tidal volume 0.74 L), and compared the efficiency of gas exchange. Inspiration occupied 25% of the cycle, and the end-inspiratory pause was 10% of the cycle. The value of $V_{D_{aw}}$ was the same at both settings, probably due to more time for the interface to diffuse proximally at the slower rate. The alveolar deadspace fraction and the arterial–end-tidal ($PaCO_2$–$P_{ET}CO_2$) difference were always much less at the large tidal volumes, which we ascribed to a more even spatial distribution of inspired gas. There were no differences in calculated venous admixture [3]. As a result of these observations, we published an article describing our concept of deadspace [4].

Twenty-five years ago, the importance of avoiding hypothermia during anesthesia and surgery was still not well appreciated. Some patients coming to our recovery unit, still intubated after major surgery, were hypothermic and starting to shiver. The 930 showed us that shivering can double CO_2 production, which explained why the patients became hypertensive, tachycardic, and hypercapnic. Clearly, their hypertension could not be fully managed until the shivering and hypercapnia had been treated. Without the 930, these metabolic consequences would have not been picked up until later, exposing the patient to an unnecessary period of instability.

Capnography was an essential part of our monitoring for patients susceptible to malignant hyperpyrexia. An unusual case presented itself: an infant with a myopathy developed malignant hyperpyrexia, and had repeated episodes of increased temperature and CO_2 elimination postoperatively, which responded to dantrolene [5].

In severe lung disease, the 930 reduced the amount of guesswork involved in setting the ventilator. When transferring a patient from volume- to pressure-controlled ventilation, it makes more sense to aim for a given $\dot{V}CO_2$ rather than a particular minute ventilation. Pressure control was always more effective at removing CO_2 for any given peak pressure, as mean distribution time was increased. With the 930, it was also possible to immediately ascertain the effect on $\dot{V}CO_2$ of extending the inspiratory phase, or increasing positive end-expiratory pressure (PEEP). Allied with pulse oximetry, this greatly simplified setting the ventilator in severe lung disease. Internationally, the wisdom gleaned at the time favored large tidal volume and low-rate ventilation. However, my colleagues and I argued, from first principles, that smaller tidal volumes at greater rates, and with a generous PEEP, would better avoid the collapse of unstable units, in addition to avoiding high peak pressures. Experimentation with the 930 showed that such ventilatory patterns were indeed possible without inducing hypercapnia. I was able to show [6] that when compliance is low, as during laparoscopy in the head-down position, the ratio of $\dot{V}CO_2$ to peak airway pressure was greater at 15 and 20 breaths/min than at 10.

The 930 became an essential monitoring tool for cardiac surgery. I used it to get an image of CO_2 elimination as cardiopulmonary bypass was started, producing a family of curves that resembled pulmonary embolism [7]. When surgery for congenital cardiac disease expanded in Lund, I turned my attention to gas exchange in infants, in particular the pattern of CO_2 elimination in intracardiac right-to-left shunting. As expected, normal children, and those with atrial septal defects, had very little alveolar deadspace and a zero $PaCO_2$–$PetCO_2$ difference [8]. Congenital cyanotic heart disease was associated with a lower CO_2 production, reflecting a lesser metabolic rate [9]. However, I realized I had not fully understood the problem when writing my thesis. If one rewrites the shunt equation using CO_2 instead of O_2, it becomes clear that right-to-left shunting causes a significant "apparent" or "virtual" alveolar or parallel deadspace, and thus a significant $PaCO_2$–$PetCO_2$ difference. This effect appeared to be overlooked in the literature; the explanation usually offered for the increased $PaCO_2$–$PetCO_2$ difference in right-to-left shunting was alveolar hypoperfusion. In fact, the shunt equation makes it clear that it is not necessary to postulate this mechanism in order to explain much of the alveolar deadspace observed, although later work [10] suggested that alveolar hypoperfusion might occur.

With the help of Andrew Black, I demonstrated the theoretical relationship between the $PaCO_2$–$PetCO_2$ difference and arterial PO_2 [11]. When pulse oximetry became clinically available, my colleague, Olof Werner, suggested I demonstrate the theoretical relationship between the $PaCO_2$–$PetCO_2$ difference and arterial saturation [12]. Depending on hemoglobin concentration and arterial PCO_2, there is a more or less straight-line relationship between the two.

There were many practical applications in cardiothoracic anesthesia. Work done by Werner and his colleagues in Lund had already shown the benefits of volumetric capnography in pulmonary surgery [13,14]. After surgery designed to palliate cyanotic lesions, $\dot{V}CO_2$ and expired PCO_2 were greater when circulation was restored. In lung transplantation, the use of two ventilators and two capnographs identified the proportion of the total respiratory load performed by each lung. Administering sodium bicarbonate always produced a sharp increase in $\dot{V}CO_2$.

It is a matter of personal regret that the promotion and production of the Siemens-Elema 930 ceased without a successor in view; however, the gauntlet has been taken up elsewhere. The technology will become more sophisticated, and the sensors more compact and robust. Innovative anesthesiologists will find new applications for the information offered by volumetric capnography! Its benefits are, first, the ability to

measure $\dot{V}CO_2$, an assessment of metabolism or cardiorespiratory function, and, second, to provide the results of the CO_2 single breath test, i.e., expired CO_2 plotted against expired volume, as a diagnostic tool. Clearly, the most interest will be in the fields of intensive care and cardiothoracic surgery, but, no doubt, other novel applications will add themselves to those already discovered.

References

1. Fletcher R. The single breath test for carbon dioxide. Thesis, University of Lund, Sweden, 1980.
2. Nordström L, Fletcher R, Pavek K. Shock of anaphylactoid type induced by protamine, a continuous cardiorespiratory record. *Acta Anaesthesiol Scand* 1978; **22**: 195–201.
3. Fletcher R, Jonson B. Deadspace and the single breath test for CO_2 during anaesthesia/IPPV. *Br J Anaesth* 1984; **56**: 109–19.
4. Fletcher R, Jonson B, Cumming G, Brew J. The concept of deadspace with special reference to the single breath test for CO_2. *Br J Anaesth* 1981; **53**: 77–88.
5. Fletcher R, Blennow G, Olsson A-K, Ranklev E, Törnebrandt K. Malignant hyperthermia in a myopathic child: prolonged postoperative course requiring dantrolene. *Acta Anaesthesiol Scand* 1982; **26**: 435–8.
6. Fletcher R, Stannard L. Best ventilator setting for major gynaecological laparoscopic surgery. *Br J Anaesth* 1999; **83**: 184P.
7. Fletcher R. Lung function during reduced pulmonary perfusion. *Br J Anaesth* 1987; **59**: 652P.
8. Fletcher R, Niklason L, Drefeldt B. Gas exchange during controlled ventilation in children with normal and abnormal pulmonary circulation. *Anesth Analg* 1986; **65**: 645–52.
9. Fletcher R. Carbon dioxide production in cyanotic children during anaesthesia with controlled ventilation. *Br J Anaesth* 1988; **56**: 109–19.
10. Short JA, Paris ST, Booker PD, Fletcher R. Arterial to end tidal carbon dioxide tension difference in children with congenital heart disease. *Br J Anaesth* 2001; **86**: 349–53.
11. Fletcher R. The relationship between alveolar deadspace and arterial oxygenation in children with congenital heart disease. *Br J Anaesth* 1989; **62**: 168–76.
12. Fletcher R. The relationship between the arterial to end-tidal PCO_2 difference and hemoglobin saturation in congenital heart disease. *Anesthesiology* 1991; **75**: 210–75.
13. Werner O, Malmkvist G, Beckman A, Stahle S, Nordstrom L. Carbon dioxide elimination from each lung during endobronchial anaesthesia. *Br J Anaesth* 1984; **56**: 995–1001.
14. Werner O, Malmkvist G, Beckman A, Stahle S, Nordstrom L. Gas exchange and haemodynamics during thoracotomy. *Br J Anaesth* 1984; **56**: 1343–9.

Appendix: Patterns of time-based capnograms

Examples of some frequently observed capnographic patterns. The added explanations are not exhaustive. For details, please consult the relevant chapter in the book.

All images used in this Appendix, except those with references separately listed, are derived from Respironics, Inc., Murrysville, PA, Publications.

Normal waveforms and nomenclature

The "normal" capnogram is a waveform that represents the varying carbon dioxide (CO_2) levels throughout the respiratory cycle.

Waveform characteristics:

A–B	Baseline
B–C	Expiratory upstroke
C–D	Expiratory plateau
D	End-tidal concentration
D–E	Inspiration begins

Typically, the timescale (abscissa) for the capnogram is 12.5 mm/s and that of the trend plot 25 mm/min. The ordinate can be calibrated in CO_2 percent (of ambient pressure) or in mm Hg, torr, or kPa where 1 kPa = 7.5 mm Hg and 1 torr = 1 mmHg.

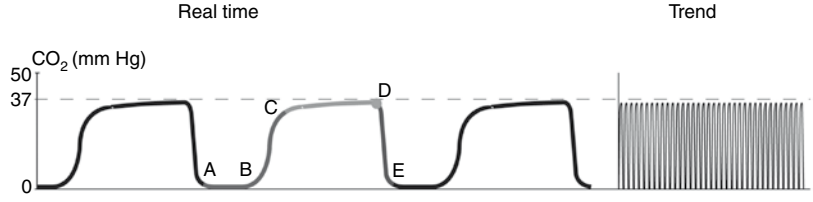

Figure AP1

Time capnogram nomenclature – inspiratory segment (Phase 0) and expiratory segment (divided into phases I, II, and III), alpha angle, angle between phase II and III; beta angle, angle between phase III and descending limb of phase 0 (inspiration). [With permission from: Kodali BS, Philips J. Defining segments and phases of a time capnogram. *Anesth Analg* 2000; **91**: 973–7.]

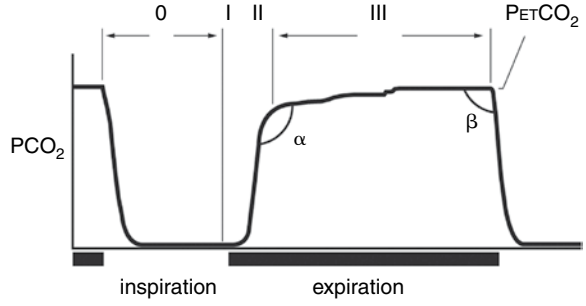

Figure AP2

Waveforms (real-time and trend)

Hypoventilation

Elevated plateau (phase III) and end-expiratory values of the capnogram, as seen, for example, with hypoventilation. Check for malignant hyperthermia. Observe the extended inspiratory slope. Check inspiratory value.

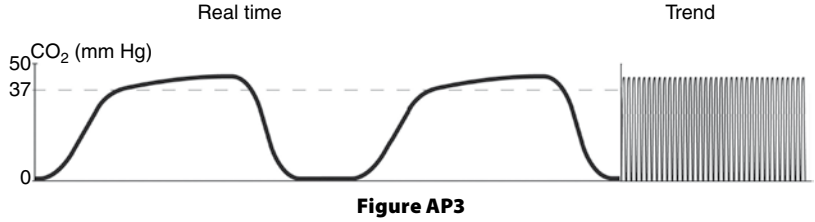

Figure AP3

Rapidly increasing partial pressure of CO_2 (PCO_2) at end-tidal ($PETCO_2$), as might occur with the addition of CO_2 to blood (bicarbonate infusion or laparoscopic CO_2 insufflation) or with improving perfusion of the lungs after a period of low cardiac output. Sepsis and malignant hyperthermia raise CO_2 production, but end-tidal levels increase more slowly than shown here.

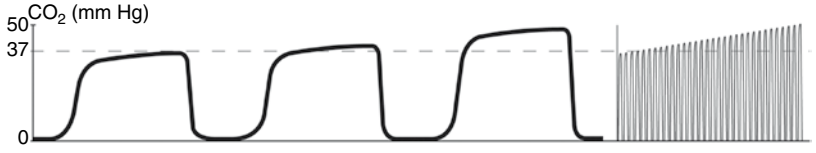

Figure AP4

Hyperventilation

Decreasing $PETCO_2$, as might be seen with hyperventilation or decreasing delivery of CO_2 to the lungs with falling cardiac output or pulmonary embolism.

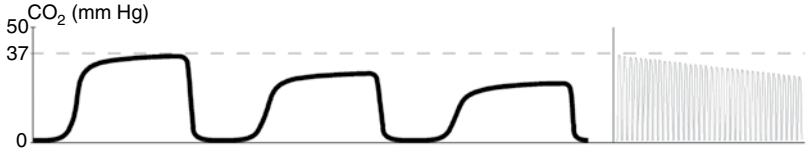

Figure AP5

Non-diagnostic

Damped capnograms (poorly defined phases, no obvious $PETCO_2$) are difficult to interpret, as they might be seen with high fresh gas flows in a spontaneously breathing patient during pre-oxygenation by face mask. It does not enable an estimation of the adequacy of breathing or of arterial PCO_2 ($PaCO_2$).

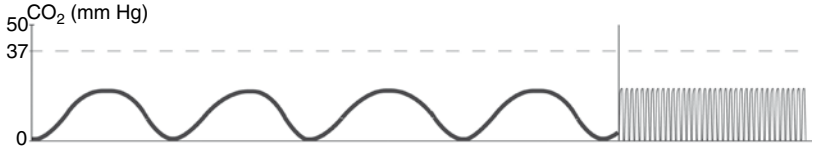

Figure AP6

Rebreathing

Increasing levels of inspired CO_2, as might be seen with the addition of deadspace to the endotracheal tube or exhausted CO_2 absorber.

Figure AP7

Sudden loss of expiratory CO_2

Cessation of ventilation, as might occur with disconnection, extubation, kinking, or obstruction of the endotracheal tube.

Figure AP8

Spontaneous breathing during mechanical ventilation

Interruption of plateau phase of capnogram by a spontaneous breath with a tidal volume large enough to reach zero PCO_2, as might be seen in a patient who takes breaths during mechanical ventilation of the lungs.

Figure AP9

Muscle relaxants (i.e., curare cleft)

Interruption of the plateau phase of the capnogram by small inspiratory efforts of the patient as might be seen in patients on mechanical ventilation. If the patient's $PaCO_2$ is high enough to trigger the respiratory center and if the center is not depressed, a patient weakened by neuromuscular blockade might attempt to take a breath. Other explanations: in a weakened patient, a hiccup or pain (very light anesthesia) might produce these inspiratory efforts. Smalhout calls these "curare clefts" (see Chapter 41: The first years of clinical capnography). Compression of the chest (e.g., by the surgeon) can also cause irregularities of the plateau (both up and down).

Figure AP10

Faulty ventilator circuit valve

Elevated baseline, as might be seen with faulty valves of a circle breathing system.

Figure AP11

Additional waveform patterns

Asthma

Capnograms of data from a normal subject and a subject with asthma (note short plateau phase: either shorter time base than normal or tachypnea). [Adapted with permission from: Yaron M, Padyk P, Hutsinpiller M, Cairns CB. Utility of the expiratory capnogram in the assessment of bronchospasm. *Ann Emerg Med* 1996; **28**: 403–7.]

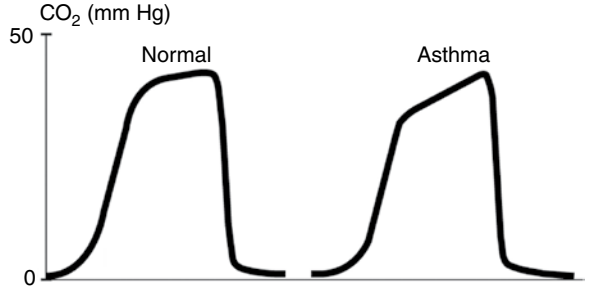

Figure AP12

Cardiogenic oscillations

Cardiogenic oscillations, as might be seen when the action of the heart produces small tidal volumes during prolonged breath-holding in patients with open glottis (or patent endotracheal tube).

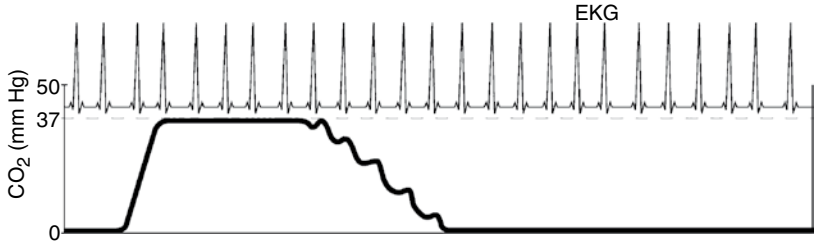

Figure AP13

Cardiopulmonary resuscitation

Serial changes in the PETCO2 concentration in a representative patient before and immediately after cardiac arrest, during precordial compression and after defibrillation and resuscitation. [Adapted with permission from: Falk JL, Rackow EC, Weil MH. End-tidal carbon dioxide concentration during cardiopulmonary resuscitation. *N Engl J Med* 1988; **318**: 607–11.]

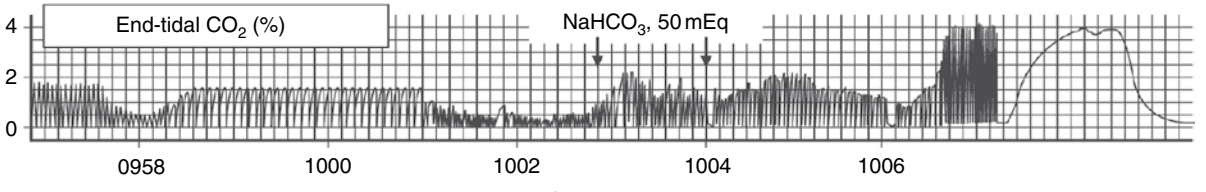

Figure AP14

Index

abbreviated injury score 74
abdominal aortic cross-clamp 220
abdominal aortic surgery 245
acclimatization 117, 119
acetazolamide
  high-altitude complications 120
  respiratory effects 288
acetyl-CoA 239
acetylene tracer 209
acid–base balance 250, 295–310
  chemical buffering 295
  normal 295
acid–base disorders
  approach to 298–99
  compensation equations 299
  diagnosis 297
  mixed 300
  simple 299
acids 295
acinar airway reduction factor 349
acute lung injury 170, 177
acute mountain sickness 120
acute respiratory distress syndrome 153, 160, 318
  alveolar deadspace 177
  mechanical ventilation 169
  ventilation/perfusion mismatch 322
adults
  normal respiratory values 5
air
  constituents of 116
air embolism 4, 204, 444
air travel 116
airway
  anesthesia 48
  difficult 34
  establishment of 48
  integrity 56
  neonates 91
airway devices
  out-of-hospital setting 20
airway maintenance 34
airway management
  hospital setting 32–35
  operating room 37–41
  out-of-hospital setting 19–29
airway obstruction
  conscious sedation 108–09
  monitoring 13
airway–alveolar interface 340
alanine 239
alarm systems 378
alcoholic ketoacidosis 302
aliasing 410
altitude exposure 115
  alveolar pressure changes 117
  and pressure 116
  capnometry 124
  human physiology 116
  hypocapnia 256
  lung volume 119
altitude mountain sickness 117
alveolar CO_2 *See* P_ACO_2
alveolar deadspace 4, 83, 170, 196, 200, 226, 315
  acute respiratory distress syndrome 177
  causes of 177
  increased 196
    gas embolism 205
  pulmonary embolism 201
alveolar deadspace fraction 200
alveolar ejection volume *See* V_{A_e}
alveolar gas equation 122, 226
alveolar hyperventilation 117
alveolar hypoventilation 15
alveolar minute ventilation 150, 152, 233
alveolar O_2 *See* P_AO_2
alveolar plateau 85, 329
  missing 92
alveolar recruitment 161
alveolar ventilation 165
  monitoring 12
  neonates 83
  relationship to $PaCO_2$ 39
American Heart Association 20, 64, 192
American Society for Testing and Materials (ASTM) 373
American Society of Anesthesiologists 43, 64
American Society of Anesthesiology Closed Claims Study 37
American Society of Gastrointestinal Endoscopy
  Clinical Outcomes Research Initiative (CORI) 105
amino acids 240
anatomic deadspace 83, 196
anesthesia 43
  airway establishment 48
  and CO_2 production 242
  atalectasis 166
  breathing circuit 45
  capnography 320
    equipment 44
  cardiovascular surgery 50
  general 103
  intraoperative events
    cardiopulmonary bypass 246
    laparoscopy 244
    temperature 246
    tourniquet release 245
    vascular cross-clamping 245
  laparoscopy 49
  morbidity 104
  neurosurgical 49
  one-lung ventilation 49
  position-related problems 48
  ventilation during 43
anion gap *See* metabolic acidosis
antacids
  false-positive CO_2 estimates 39
anthropogenic effect 262
antisialagogues 41
anxiolysis 103, 108
anxiolytics 43
aortic body 117, 360
aortic pulse pressure 66
aortic surgery 51
APACHE 63
apnea 16, 26, 34, 58
  central sleep 256
  conscious sedation 108–09
apnea test for brain death 290
ARDS *See* acute respiratory distress syndrome
arterial blood gases 297
  analysis 12
arterial carbon dioxide partial pressure *See* $PaCO_2$
arterial CO_2 tension *See* $PaCO_2$
arterial gas embolism 122–23
arterial–alveolar gradient 56
arterial-to-alveolar PCO_2 gap 235

asthma 5, 48, 196, 330, 332
  arterial–alveolar gradient 56
  biofeedback 131
    rationale 131
    results 131
  CO_2 monitoring 58
  hypocapnia 127
  waveforms 465
atelectasis 145
  anesthesia-induced 166
atmospheric gases 261
atmospheric monitoring 261–69
  closed ecosystems 265
  mines 263
  saturation diving 265
  SEALAB experiments 265
atmospheric pressure 115
  changes in 68
ATP 239
Australian Incident Monitoring Study (AIMS) 39
Avogadro's law 289

Badische Anilin und Soda Fabrik (BASF) 418
bag-valve mask 19
Bartter syndrome 306
bases 295
Beckman metabolic measurement cart 424
Beer–Lambert law *See* Lambert–Beer law
bicarbonate 240
  during cardiopulmonary resuscitation 187
  regulation 296
bicarbonate buffers 295
bicarbonate infusion 288
bicarbonate–carbonic acid equation 295
bi-level ventilation 141
biofeedback 127–33
  asthma 127, 131
  epilepsy 128
  hyperventilation syndrome 128
  panic disorder 127, 129
  principles and perspectives 132
Bios-3 265
Biosphere 2 266
birds, capnography 276
Black, Andrew 459
blackdamp 263
Bland–Altman plot 212, 215
blood transfusion
  decision hemodynamics 219
Bohr equation 59, 65, 83, 198
Bohr, Christian 417, 421
Bohr–Enghoff equation 84, 165
Bouguer, Pierre 416
Boyle, Robert 415
Boyle's Law of Pressure and Volume 121
brain
  CO_2 effects 252
brain death
  apnea testing 290
brain injury, traumatic 66, 72
breath detection 392
breath sounds
  auscultation 22
  patients in transit 63
breathing circuit 45
  integrity 56
    during transit 64
breathing, control of 360–68
  dynamic end-tidal forcing 363
  frequency response of respiratory controller 363
  hypercapnic ventilatory response 362
  physiology 360
  pseudorandom binary forcing 364
  response to transient CO_2 inhalation 362
British Standards Institute (BSI) 373
bronchiolitis 58
bronchodilators 174
bronchopleural fistula 34
bronchospasm 26, 330
Buteyko breathing technique 128

calcium metabolism 246
calibration 380
calorimetry
  direct 241
  indirect 241
capacitance equation 215
capnogram
  analysis of 432
  church-steeple appearance 47
  origins of 432
capnography 1, 27, 226, 329–37
  advances in 148
  alpha angle 13
  applications 432
  beta angle 13, 319
  cardiopulmonary resuscitation 185–92
  clinical uses 12
  conscious sedation 105
  definition 23
  endotracheal tube placement 64
  history 455
  monitoring
    air embolism 444
    circulation 437
    medical errors 442
    metabolism 432
    technical defects 441
    ventilation 433
  neonate
    devices 80
    emergency medicine and transport 85
    intensive care 86
    mainstream and sidestream measures 81
    operating room 84
    response time 90
    safety 86
    sampling rate 91
    small airways 91
    technical limitations 89
  out-of-hospital setting 24–27
  patients in transit 63–68
  pulmonary embolism 195–205
  sleep disorders 96–100
  time-based *See* time-based capnography
  veterinary medicine 272–79
  volume-based *See* volume-based capnography
  waveforms
    biphasic 40
    use of 76
capnography head-up tilt test (CHUTT) 16
capnometry 27
  at altitude 124
  colorimetric 75
  conscious sedation
    modified nasal cannula 106
  definition 23
  endotracheal tube placement 64
  quantitative 75
  semiquantitative 75
  sleep disorders 97
capnometry-assisted respiratory training *See* biofeedback
carbohydrate metabolism 239
carbon dioxide 239–47, 415
  absorbers 151
  balance 151, 240
  elimination 151
  embolism 663, 922
  exhaled 11, 226
  increased partial pressures 288
    apnea testing for brain death 290
    bicarbonate infusion 288
  inhalation test 362
  measurement 381–93, 417
    algorithms 392
    chemical 417
    colorimetric detectors 385
    early clinical applications 420
    infrared absorption 382
    mainstream/sidestream capnography 388
    mass spectroscopy 386

photoacoustic spectroscopy 385
physical 418
metabolic changes affecting 54
cardiovascular function 54
respiratory function 55
monitoring 226
and ambient pressure 124
asthma 58
neonates 58
non-invasive 149
spontaneously breathing patients 58
tissue levels 235
pathophysiology 283–86
physical properties 381
production 60, 239–40
anesthesia 242
biochemistry/physiology 239
calorimetry 241
intraoperative events 244
reduced partial pressures
carbonic anhydrase disorders 286
mitochondrial disorders 283
regulation 295
respiratory stimulation 118
stores 240
tissue/organ effects 250–56
central nervous system and brain 252
central sleep apnea 256
circulatory system and heart 254
oxygen delivery 252
respiratory system 253
splanchnic perfusion 252
vascular effects 255
transport 162, 225
volume 407, 417
carbon monoxide 263
carbonated beverages
false-positive CO_2 estimates 39, 64
carbonic acid 295, 416
carbonic anhydrase disorders 286
acquired 288
inherited 287
cardiac arrest 54, 438
out-of-hospital 185, 191
patients in transit 66
$P_{ET}CO_2$ 185–92
and prognosis 188
cardiac arrhythmias 119
cardiac compression 444
cardiac output 65, 208–23, 331
animal models 347–53
capnodynamic monitoring 215
complete rebreathing CO_2 Fick Qc method 208
determination of 336
partial rebreathing CO_2 Fick Qc method 210
findings 211
patients in transit 66
thermal dilution 210
cardiogenic oscillations 3, 7, 437, 465
cardiopulmonary bypass 51, 246
weaning from 146
cardiopulmonary resuscitation 33, 185–92, 465
bicarbonate and epinephrine 187
coronary and cerebral perfusion 187
cardiopulmonary system
high-altitude changes 119
cardiovascular function
and CO_2 54
cardiovascular surgery
anesthesia 50
carnitine palmitoyltransferase II deficiency 283
carotid body 117
carotid pulse 186
cassava, cyanide in 285
cats, capnography 273
cattle, capnography 274
Centers for Disease Control (CDC) 262
central atmosphere monitor 269
central nervous system
CO_2 effects 252
high-altitude changes 120
central sleep apnea 256
central venous pressure 208
cerebral edema
high altitude 120
cerebral perfusion pressure 187
Charles, Jacques Alexander César 415
Charles' Law of Temperature 121
chemical buffering 295
chemoreceptors 360
chemoresponsiveness
measurement of 363
spontaneous variations in ventilation 366
ventilatory stability 366
chest wall disorders 99
children
conscious sedation 105
sedation 15
seizures
respiratory monitoring 16
chokedamp 263
chokes 123
chronic fatigue syndrome
occult hyperventilation 15
chronic obstructive pulmonary disease 48, 196, 201, 319, 330, 356
circulation, monitoring of 437
citric acid cycle 240
Clapeyron, Émile 415
climate
extremes of 116
clonidine
and response to anesthesia 243
closed ecosystems 265
Bios-3 265
Biosphere 2 266
International Space Station 267
Space Shuttle 266
submarines/submersibles 268
Cobra Perilaryngeal Air 19
colorimetric capnometers 11, 32
colorimetric capnometry 75
colorimetric CO_2 detector 16, 385
semi-quantitative 24
Comité Européen pour Normalisation (CEN) 373
compensation equations 299–300
complete rebreathing 208
compliance, pulmonary 11
computed tomography 162
congestive heart failure 222
conscious sedation 103
airway obstruction 108–09
apnea 108–09
capnography 102–11
acceptance by providers 110
acceptance by regulatory agencies 110
vs. observation 110
children 105
definition of 103
guidelines 102
history 104
hypercarbia 110
hypoventilation 108
hypoxemia 109
pulse oximetry 107
sampling devices 107
ventilatory compromise 108–09
ventilatory depression 105
constant current anemometer 403
constant temperature anemometer 403
continuity equations 215
continuous "waveform" capnography 25
convection 162, 340
coronary artery bypass graft 212, 245
coronary perfusion pressure 187
Cumming, Gordon 458
curare cleft 3, 55, 464
Cushing syndrome 306
cyanide 284
biochemistry 284
poisoning 285
sources of 285
cytochrome *c* 285

Dalton's Law of Partial Pressure 121
Davenport diagram 299
Davy Safety Lamp 264
D-dimer test 200

deadspace 89, 195, 421
  alveolar *See* alveolar deadspace
  anatomic *See* anatomic deadspace
  dynamic apparatus 137
  evaluation of 335
  Fletcher's calculation 92
  physiological *See* physiological deadspace ventilation 6, 56, 314
decompression sickness 122
deep sedation 103
dexamethasone
  high-altitude complications 120
diabetic ketoacidosis 58, 250, 296
diaphragmatic hernia 87
difficult airway 34
diffusion 162, 340
diving 122
  saturation 265
dogs, capnography 273
dolphins, capnography 279
double-lumen tube ventilation 40
Douglas bag 80, 421
Duchenne muscular dystrophy 284
dynamic end-tidal forcing 363
dysoxia 231, 235
dyspnea 127

echocardiography
  transesophageal 186, 205
electrical impedance tomography 162
electroencephalography 96
electromagnetic interference 379
electromagnetic radiation 379
electromyography 96
emphysema 330, 356
endobronchial mainstem intubation 33
endobronchial tube
  confirmation of placement 39
endoscopy 16
endotoxin-induced lung injury 253
endotracheal intubation 19
  blind placement 40
  confirmation of 32, 37–38
  out-of-hospital setting 20–21
  patients in transit 63
  positioning
    false-negative CO_2 assessment 33
    false-positive CO_2 assessment 33
    monitoring of 56
endotracheal tube
  kinking of 56
  leaks 65
  occlusion of 56, 65
  placement 148
Endotrol® tube 38
end-tidal CO_2 *See* $PetCO_2$
energy expenditure 242
energy production 240
enteral feeding tubes
  placement 16
enteric tubes
  avoidance of airway intubation 34
epidural anesthesia 243
epilepsy 433
  hypocapnia 128
epinephrine
  and cardiopulmonary resuscitation 187
  and gas exchange 244
equal area method 340
erythropoietin
  high-altitude changes 119
esophageal CO_2 detection 38
esophageal detector device 22, 27
esophageal gastric airway 19–20
esophageal intubation 64
  unrecognized 21–22, 37
    auscultation of breath sounds 22
    chest rise and fall 22
    direct visualization 21
    pulse oximetry 22
esophageal obturator airway 19
esophageal–tracheal combitube 19
ethylene glycol poisoning 303
etomidate 49
Euler–Lagrange equation 355
exercise 241
expiration
  incomplete 93
expiratory positive airway pressure (EPAP) limit 139
expiratory time-constant 164
expiratory valve incompetence 46
extubation 155
  unplanned 64
    neonates 86

face masks 137, 139
  selection of 138
  use of 138
fiberoptic bronchoscope 34
fibrecapnic intubation 41
Fick principle 208
Fick's law of diffusion 162
firedamp 263
Food and Drug Administration (FDA) 44, 373
functional residual capacity 48, 330–31

gas analyzer
  improper calibration 2
gas diffusive resistance 353–57
gas embolism 204
gas exchange 11, 163
  anesthesia effects 243
gas flow 397–404
  calibration 410
  clinical issues 397
  differential pressure flow sensors 400
    fixed orifice type 402
    Fleisch type 400
    hot-wire flow sensors 402
    Silverman and Whittenberg/Lilly modification 401
    turbulent flowmeters 402
    variable orifice type 401
  distal
    and proximal gas measurement 410
  factors affecting readings 398
    gas conditions 398
    humidity 399
    inlet conditions 399
    operating range of flow sensor 400
    resistance 400
    sensor location 398
    temperature 399
  mainstream 410
  measurement site conditions 408
  measurement technologies 400
  proximal
    and gas measurement 409–10
  signal processing 410
  ultrasonic sensors 404
  volume 397
gas laws 121, 415
  Boyle's Law of Pressure and Volume 121
  Charles' Law of Temperature 121
  Dalton's Law of Partial Pressure 121
  General Gas Law 121
  Henry's Law of Solubility 121
Gay-Lussac, Joseph Louis 415
general anesthesia 103
General Gas Law 121
Gitelman syndrome 306
glucose oxidation 239
glutamine, catabolism 241
glycerol 239
glycogen 239
greenhouse gases 261
Guericke, Otto von 415

Haldane, John Scott 417
halothane 49
Hamberger effect 295
harp seals, capnography 279
head injury 66
heart
  CO_2 effects 254
heliox 265
hemodynamic preconditioning 161
Henderson–Hasselbalch equation 296, 385
Henry's Law of Solubility 121, 265
Herschel, William 416

high altitude 116
  acute mountain sickness 120
  cardiopulmonary changes 119
  early hypoxia response 117
  hematologic changes 119
  hypoxic respiratory stimulation 117
  lung volume increase 118
  neurologic changes 120
high-frequency oscillation 173
high-frequency ventilation 173
  jet 52, 173
  percussive 174
  positive pressure 173
high-pressure environments 115–25
history 424–26
  clinical capnography 430–55
  volume-based capnography 457–60
Hooke, Robert 415
horses, capnography 274
hospital setting
  airway management 32–35
hot-wire anemometers 400, 403
  constant current 403
  constant temperature 403
Hutchinson, John 420
hydrogen sulfide 263
hyperaldosteronism 306
hyperbaric chambers 123, 125
hyperbaric exposure 120
  pulmonary effects 122
hypercapnia 11, 250–51, 296
  and brain injury 252
  and cardiac performance 255
  and lung injury 253
    endotoxin-induced 253
  cerebral blood flow 253
  ischemia–reperfusion injury 254
  myocardial effects 254
  nocturnal 58
hypercapnic acidosis 253
hypercarbia 99
  conscious sedation 110
hyperkalemia 306
hyperpyrexia *See* hyperthermia
hyperthermia 246
  malignant 8, 246, 459
hyperventilation 7, 66, 118, 229, 241
  alveolar 117
  avoidance of 72
    $P_{ET}CO_2$ role in 73
  hypercapnic 252
  occult 15
  waveforms 463
hyperventilation syndrome 128, 309
hypocapnia 11, 66, 74, 127, 250, 296, 308
  altitude exposure 256
  and brain injury 252
  and lung injury 253
  asthma 127
  epilepsy 128
  myocardial effects 254
  panic disorder 127
hypocapnic alkalosis 252–53
hypokalemic acidosis 305
hypoplastic left heart syndrome 58
hypotension 54, 437
  dangers of 446
  vasodilation-induced 216
hypothermia 246
hypoventilation 45, 66, 99, 226, 241, 296
  alveolar 15
  and sedation 66
  conscious sedation 108
  nocturnal 100
  waveforms 462
hypovolemia 54, 65, 217, 251
hypoxemia 16, 74
  conscious sedation 109
  in children 15
hypoxic pulmonary vasoconstriction reflex 162

ice core analysis 262
inferior vena cava compression 445
infrared absorption spectroscopy
  See infrared detectors 384
  double-beam-in-space 384
  double-beam-in-time 384
  Luft design 384
  non-dispersive 384
  Veingerov design 384
infrared radiation 382
  absorption 382
  chopper 385
  pressure broadening 383
  sources 384
infrared spectrography 80
inspiration
  decreased CO_2 at start of 85
inspiratory baseline 85
inspiratory valve incompetence 46
intensive care
  neonates 86
International Electrotechnical Commission (IEC) 373
International Liaison Committee on Resuscitation 192
International Organization for Standardization (ISO) 124, 373
International Space Station 267
intracranial pressure, raised 250
ischemia 231, 235
ischemia–reperfusion injury 250, 254
isopropanol
  as contaminant 377

Jonson, Björn 457

Kearns–Sayre disease 283
ketoacidosis 302
  alcoholic 302
  diabetic 193
Konzo 285
Krebs cycle 285
Krogh, August 417
Krogh, Marie 417
Kussmaul respirations 301
Kyoto Protocol 262
kyphoscoliosis 40

lactate 231, 239
lactic acidosis 302
lactulose 241
Lambert, Johann Heinrich 416
Lambert–Beer law 384, 416
laparoscopy 244
  anesthesia 49
laryngeal mask airway 19
laryngeal tube airway 19
late deadspace fraction
  pulmonary embolism 201
Lavoisier, Antoine-Laurent de 415
leaks
  minimization of 142–43
Leber optic neuropathy 283
Lesch–Nyhan syndrome 288
Levenberg–Marquardt algorithm 341
licorice intake, metabolic alkalosis 306
lipogenesis 240
lipolysis 243
Liston, Max 423
Liston-Becker Company 423
loop gain 367
low-pressure environments 115–25
lower body negative pressure 235
Luer connectors 378
Luft, Karl Friedrich 418
lung
  gas transport in 166
lung CO_2 capacitance
  compensation for 216
lung collapse 160
lung function testing
  neonates 87
lung growth 92
lung injury
  endotoxin-induced 253
  hypercapnia 253
  hypocapnia 253
  unilateral 172
Lung Injury Score 171
lung perfusion 163
lung recruitment 340–45
  and CO_2 kinetics 162
  monitoring of 162
lung resection 323

lung transplantation 323
lung volumes 12

magnesium deficiency 306
  hypokalemic alkalosis 305
mainstream capnography 1, 11, 47, 388–89
  analyzers 390
  neonates 81, 91
  non-invasive positive pressure ventilation 138, 463
  sleep disorders 97
Mainz Emergency Evaluation Scoring System 192
malignant hyperthermia 8, 52, 246, 459
mass balance equation 351
mass spectroscopy 386
  magnetic sector-fixed detector 387
  quadrupole mass filter 387
  technical challenges 388
measurement accuracy 374
measurement drift 376
mechanical ventilation 169–78
  acute respiratory distress syndrome 169
  capnography in treatment evaluation 174
  disconnection 45
  extubation 155
  high-frequency/percussive 173
  leaks 46
  lung collapse 160
  minimization of 148–56
  monitoring during 54–61
  optimization 148–56
  patient transport 56
  phases of 149
  tracheal gas insufflation 172
  unilateral lung injury 172
  waveforms 464
  weaning from 57, 60, 154
    failure of 153
    importance of 153
    neonates 87
medical errors 442
  cardiac compression 444
  nearly fatal pain stimulus 442
metabolic acidosis 299, 301
  anion gap 301
  causes 303
  chloride-resistant 305
  chloride-sensitive
    drug-induced 305
  high anion gap 302
    decreased renal function 304
    ketoacidosis 302
    lactic acidosis 302
  non-anion gap (hyperchloremic) 304
    acid infusion 304
    drug-induced 304
    gastrointestinal 304
    renal disease 304
  signs and symptoms 301
metabolic alkalosis 299, 304
  alkali administration 305
  causes 303
  chloride-sensitive 305
    gastrointestinal disorders 305
  diagnosis 305
metabolic demand 241
metabolism 239
  capnographic monitoring 432
methane 263–64
methanol poisoning 303
mice, capnography 275
microcapnometry 276
microstream capnography 15, 81, 106
midazolam
  premedication 243
mill-wheel murmur 444
mines 263
mining accidents 263
minute ventilation 4–5, 52, 60
  alveolar 150, 152
  loss of 65
minute volume
  anesthesia 242
mitochondrial disorders 283
  acquired 284
  inherited 283
monoethanolamine scrubbers 269
morbidity
  anesthesia-related 104
multiple inert gas elimination technique 229, 315–16
muscle relaxants 464
  effects of 435
  onset time 216

NADH 231
narcotics 43
nasal cannula 106
nasal pressure monitoring 96
National Association of Emergency Medical Services Physicians 64
National Institute of Occupational Safety and Health (NIOSH) 263
neonates
  alveolar ventilation 83
  incomplete expiration 93
  lung function testing 87
  monitoring 80–93
  normal respiratory values 5
  $PaCO_2$ 83
  $PETCO_2$ 83
  sleep laboratory 88
  therapeutic CO_2 administration 58
  weaning from mechanical ventilation 87
neuroleptic malignant syndrome 246
neuromuscular blockade 43, 244
neuromuscular disease 58, 99
neurosurgical anesthesia 49
NICO monitor 212–13, 216
nifedipine
  high-altitude pulmonary edema 120
nitric oxide 116, 253
nitrogen dioxide 263
nitrogen narcosis 122
nitrogen washout 12
nitrous oxide 7
nitrous oxide tracer 209
non-invasive positive pressure ventilation 135–43
  acute respiratory failure 136
  patient interfaces 137
  patient selection 137
  $PETCO_2$ monitoring 139
  rebreathing 142
  short-term vs. long-term use 142
  sidestream vs. mainstream sampling 138
  time-based capnography 135
  volume-based capnography 135
Nordström, Lars 457
NPPV *See* non-invasive positive pressure ventilation
nutrient metabolism 239

obesity hypoventilation syndrome 99
Observer's Assessment of Alertness/Sedation scale (OAA/S) 15
obstructive lung disease 320
obstructive sleep apnea 58, 98, 135
Occupational Safety and Health Administration (OSHA) 262
one-lung ventilation 49, 323
operating room
  airway management 37–41
  neonatal monitoring 84
osmolar gap 303
out-of-hospital setting
  airway devices 19–20
  airway management 19–29
  endotracheal intubation 20–21
overventilation 66
oxidation 239
oxidative phosphorylation 239
oxygen 239
oxygen consumption 231, 239
  biochemistry/physiology 239
oxygen delivery 231
  tissues 252
oxygen saturation 14
oxygen toxicity 122

$PaCO_2$ 11, 38, 72, 118, 136, 225–29, 250
  at altitude 118
  changes during transport 65
  measurement challenges 138
  neonates 83
  pulmonary embolism 198
  relationship to alveolar ventilation 39
  sleep disorders 96
  ventilatory adequacy 145
$PaCO_2$–$PetCO_2$ gradient 318
panic disorder 127
  biofeedback 129
    methodology 129
    results 130
PaO_2 115
Parkinson–Cowan dry gas meter 421
partial rebreathing method 210
  findings 211
PCO_2
  mixed venous 347–53
peak expiratory flow rate 332
$PeCO_2$ determination 392
PEEP 56, 65, 75, 169, 211
  management 153
  titration 340–45
percussive ventilation 173
perfluorocarbons, ventilation with 175
performance measures 374
PerforMax™ face mask 137
perfusion
  in relation to ventilation 315
$PetCO_2$ 5, 11, 23, 27, 32, 136, 169, 225–29, 232, 318, 329
  and cardiac arrest 185–92
  as predictor of $PaCO_2$ 14, 58
  avoidance of hyperventilation 73
  clinical applications 54
  critically ill patients 146
  dilution effects 139
  field uses
    guidance of ventilation 76
    troubleshooting 77
  high 52
  low 52
  monitoring with ventilators 77
  neonates 83
  normal 52
  NPPV monitoring 139
  optimization of 216
  out-of-hospital monitoring 22, 72
    justification for 72
  panic disorder 127
  pulmonary embolism 198
  ventilatory weaning
    postoperative 145–46
Pfund, August Herman 418
pH
  changes during transport 65
Phasitron® 174
Philips V60 non-invasive ventilator 135
phosphodiesterase inhibitors
    high-altitude complications 120
photoacoustic spectroscopy 385
physiological deadspace 65, 155, 169
  anesthetized patients 170
  pulmonary embolism 198
Pieler lamp 264
Planck's constant 381
pneumonia 34
pneumoperitoneum 244
pneumotachometry 96, 150
pneumothorax 34
PO_2
  at altitude 118
pocket mask 19
polycythemia 119
polysomnography 96, 100
positive end-expiratory pressure
    See PEEP
positive pressure ventilation 74
prehospital situation 15
  capnography as guide to ventilation 72–77
pressure
  and altitude 116
  and depth 121
pressure broadening 383
pulmonary artery wedge pressure 208
pulmonary blood flow 208–23
  abdominal aortic cross-clamp 220
  assessment shortcuts 214
  congestive heart failure 222
  hypotension due to vasodilation 216
  hypovolemia 217
  muscle relaxant onset time 216
  radical prostatectomy 217–18
  thready pulse 216
pulmonary capillary blood flow *See* Qc
pulmonary edema 145
  high altitude 120
pulmonary embolism 7, 176, 195–205
  alterations associated with 197
  detection
    alveolar deadspace 201
    late deadspace fraction 201
    limitations of capnography 202
    physiological deadspace 198
    time-based capnography 198
  thrombolytic therapy 203
  ventilation/perfusion mismatch 324
pulmonary fibrosis 323
pulmonary hypertension 54
pulse
  thready 216
pulse oximetry 14–15, 44
  conscious sedation 107
  unrecognized esophageal intubation 22
pulseless electrical activity 66
$PvCO_2$ 209
  Collier equilibrium method 209
  Defares exponential method 209
pyruvate 239

Qc 208
  calibration equation 215
  complete rebreathing method 208
  partial rebreathing method 210
Qt *See* cardiac output

radical prostatectomy 217–18
Raman scattering 419, 424
RAman SCattering AnaLyzer (RASCAL) monitor 424
rapid respiration
  damping 2
Rayleigh scattering 419
reactive airway disease 13
rebreathing 142, 393
  waveforms 463
receiver operating characteristics (ROC) curve 191
red blood cell transfusion
  rapid 212
repressurization 123
reptiles, capnography 277
respiration
  central neurologic disturbances 448
respiratory acidosis 251, 299, 306, 309
  causes 306–07
    airway factors 308
    central factors 306
    neuromuscular factors 308
    parenchymal factors 308
  diagnosis 306
respiratory alkalosis 7, 251, 299, 308–09
  causes 309
  inciting factors 308
    CNS stimulation 309
    drugs and hormones 309
    hyperventilation syndrome 309
    hypoxemia/tissue hypoxia 309
    stimulation of chest receptors 310
  signs and symptoms 308
respiratory assessment
  outside operating room 11–17
respiratory deadspace *See* deadspace
respiratory gas monitors
  calibration 380
  definition of 374
  interfering gas/vapor effects 377
  ISO 21647 standard 373
  performance measures 374
    accuracy 374
    drift 376

respiratory gas monitors (*cont.*)
range 375
response time 376
types of 374
respiratory quotient 232
respiratory rate 5, 52
respiratory system resistance 332
response time 376
resuscitation 438
Rhan sampler 80
Röntgen, Wilhelm 418
rotating vane spirometers 400
rotational energy transitions 383

salicylate overdose 303
San Diego Paramedic Rapid Sequence Intubation (RSI) Trial 72
saturation diving 265
SEALAB 265
sedation
conscious 102–11
definitions of 103
patients in transit 66
procedural 102
sedatives 43
seizures
respiratory monitoring 16
shivering 246
shock 231–36
capnometric monitoring 231
tissue CO_2 monitoring and perfusion 235
tissue-specific monitoring 234
shunt perfusion 56
sidebands 383
sidestream capnography 1–2, 47, 388–89
analyzers 390
neonates 81, 89
non-invasive positive pressure ventilation 138
sleep disorders 97
sidestream gas sampling 410
S_{III} 166
single-breath capnography 12
single-path model 353
sleep
non-rapid eye movement (NREM) 98
rapid eye movement (REM) 98
ventilation during 97
sleep disorders 13
capnography 96–100
obesity hypoventilation syndrome 99
obstructive sleep apnea 58, 98, 135
snoring 98
sleep laboratory 98
neonates 88
snoring 98
sodium bicarbonate 241
sodium nitroprusside 285
Space Shuttle 266
spirometry 11
splanchnic perfusion 252
spontaneous breathing trial 155
spontaneous circulation, return of 186, 188
spontaneous ventilation
disconnection 46
leaks 46
standard temperature and pressure dry (STPD) conditions 407
standards development organizations 373
stinkdamp 263
Stow–Severinghaus $PaCO_2$ electrode 386
strong ion theory 297
subarachnoid block 43
submarines/submersibles 268
succinylcholine 244
sudden cardiac death 185
sulfur dioxide 263
sulfuric acid 295
syncope
occult hyperventilation 15
systemic vascular resistance 208

Tau-CO_2 164
technical defects 441
technical specifications 373–80
alarm systems 378
calibration 380
Luer connectors 378
performance measures 374
units 378
technical standards 373, 379
temporal mismatching 331
tension pneumothorax 76
thermistors 96
thermogenesis, diet-induced 242
thermoneutrality 241
thiopental 49
Thomson, William 416
thrombolytic therapy 203
Thumper® device 186
tidal volume 5, 52
at endotracheal tube 150
delivery 150
size of 141
small 139
time-based capnography 1–4, 11, 148, 329
artifacts 2
cardiovascular status 149
history 423
interpretation 4–6
cardiovascular issues 4
pulmonary issues 4
neonates 82
non-invasive positive pressure ventilation 135
pathologic 330
altered inspiratory phase 332
phase I 330
phases II and III 330–31
patterns of 461–65
pulmonary embolism 198
uses 12–16
airway obstruction monitoring 13
alveolar ventilation monitoring 12
deadspace ventilation monitoring 13
endoscopy 16
enteral feeding tube placement 16
evaluation of non-intubated patients 14
occult hyperventilation 15
pediatric sedation 15
pediatric seizure monitoring 16
prehospital 15
sleep disorders 13
ventilated patients 149
Tissot spirometer 421
tissue buffering 250
tissue hypoxia 309
tissue oxygen delivery 252
tissue oxygenation/perfusion 251
Tobin index 146
tourniquet release 51, 245
tracheal gas insufflation 172
transesophageal echocardiography 186, 205
transport of patients
capnography during 63–68
complications 67
mechanical ventilation 56
monitoring of respiration circuit integrity 64
neonates 85
procedural sedation 66
sources of measurement error 67
transpulmonary pressure 160
trauma
ventilation/perfusion mismatch 324
triglycerides 239
Tyndall effect 419
Tyndall, John 416, 418

units 378
unrecognized misplaced intubation *See* esphageal intubation, unrecognized
upper airways resistance syndrome 98
uric acid 295

V_{A_e}/V_T 336
van der Waals, Johannes 416
Van Helmont, Jan Baptista 415
Van Slyke apparatus 418

vascular cross-clamping 245
VCO_2
  age variation 243
  anesthesia effects 242
VD shunt 165
ventilation 165
  adequacy of 145
  consistency of 65
  deadspace 314
  in relation to perfusion 313
  $P_{ET}CO_2$-guided 72, 76
  prehospital
    capnography as guide to 72–77
  step changes 227
  weaning from
    postoperative 145–46
ventilation/perfusion matching 136
ventilation/perfusion mismatch 11, 55, 232, 313–25
  acute respiratory distress syndrome 322
  capnography 317
    clinical correlation 319
  low cardiac output state 324
  obstructive lung disease 320
  one-lung ventilation, lung resection and lung transplantation 323
  pulmonary embolism 324
  pulmonary fibrosis 323
  trauma 324
ventilation/perfusion ratio 11, 40, 160, 169, 226, 330
  acute increase 227
  global increase. *See* hyperventilation
  regional increase 227
    decreased pulmonary blood flow 228
ventilator-associated lung injury 253
ventilator disconnection 64
ventilator-induced lung injury 154
ventilatory failure 123
ventilatory maldistribution 166
ventilatory requirements, prediction of 60
veterinary capnography 272–79
  acid–base values 275
  birds 276
  blood gases 275
  dogs and cats 273
  dolphins 279
  harp seals 279
  horses and cattle 274
  limitations of 272
  lung volumes 276
  reptiles 277
  respiratory parameters 274
  small laboratory animals 275
  species differences 273
volume-based capnography 6–7, 11, 38, 148, 151, 333
  analysis 340–45
    clinical implications 344
    Fowler's method 340
  cardiac output estimation 336, 347
  clinical uses 59
  deadspace evaluation 335
  history of 423, 457–60
  lung recruitment 340–45
  neonates 82
  non-invasive positive pressure ventilation 135
  PEEP titration 340–45
  phase II deformation 334
  phase III deformation 334
  variables 342–43
    S_{III} 344
  veterinary medicine 272
volutrauma 150

wasted ventilation 195
water trap 89
  artifacts 2–3
waveforms
  normal 462
  real time and trend 462
    asthma 465
    cardiogenic oscillations 465
    cardiopulmonary resuscitation 465
    faulty ventilatory circuit valve 464
    hyperventilation 463
    hypoventilation 462
    mechanical ventilation 464
    muscle relaxants 464
    non-diagnostic 463
    rebreathing 463
    sudden loss of expiratory CO_2 464
Wheatstone bridge 403

Zuntz, Nathan 420